ENGIN
TL
501
S43

VOLUME 23 / NUMBER 13
JULY 8, 1985
ACC. NOS. N85-22342 TO N85-23681

THE UNIVERSITY
OF MICHIGAN
JUL 10 1985
ENGINEERING
LIBRARY

STAR

AN ABSTRACT JOURNAL

Scientific and Technical Aerospace Reports

PRODUCED BY THE
SCIENTIFIC AND TECHNICAL
INFORMATION
BRANCH

NASA

NATIONAL AERONAUTICS AND SPACE ADMINISTRATION

WHAT YOU CAN DO FOR *STAR*

All users of this abstract service are urged to forward reports to be considered for announcement in *STAR*. This will aid NASA in its efforts to provide the fullest possible coverage of all scientific and technical publications that might support aeronautics and space research and development. If you have prepared relevant reports (other than those that you will transmit to NASA, DoD, or DOE through the usual contract- or grant-reporting channels), please send them for consideration to the NASA Scientific and Technical Information Facility, P.O. Box 8757, B.W.I. Airport, Maryland 21240.

Reprints of journal articles, book chapters, and conference papers are also welcome. These will be considered for announcement in *STAR's* companion journal, *International Aerospace Abstracts*.

You may specify a particular source to be included in a report announcement if you wish; otherwise the report will be placed on public sale at the National Technical Information Service. Copyrighted publications will be announced but not distributed or sold.

PURCHASE OF *STAR*

The semimonthly issues are available for sale by the Superintendent of Documents, U.S. Government Printing Office, Washington, D.C. 20402.

PUBLISHED BY:

UNITED STATES GOVERNMENT
NATIONAL AERONAUTICS AND SPACE ADMINISTRATION
SCIENTIFIC AND TECHNICAL INFORMATION BRANCH
Scientific and Technical Aerospace Reports, Volume 23, is prepared by the NASA Scientific and Technical Information Facility operated for the National Aeronautics and Space Administration by PRC Government Information Systems.

The Administrator of the National Aeronautics and Space Administration has determined that the publication of this periodical is necessary in the transaction of the public business required by law of this Agency. Use of funds for printing this periodical has been approved by the Director of the Office of Management and Budget through March 22, 1988.

US ISSN 0036-8741

INTRODUCTION

Scientific and Technical Aerospace Reports (STAR) is a major component of a comprehensive National Aeronautics and Space Administration information system covering aeronautics, space, and supporting disciplines. *STAR* is issued on the 8th and 23rd of each month and announces current publications of the following types:

- NASA, NASA contractor, and NASA grantee reports
- Reports issued by other U.S. Government agencies, domestic and foreign institutions, universities, and private firms
- Translations in report form
- NASA-owned patents and patent applications
- Dissertations and theses

THE UNIVERSITY OF MICHIGAN
JUL 10 1985
ENGINEERING LIBRARY

Cumulative index volumes are published annually.

Journal, book, and conference literature, cover-to-cover journal translations, and certain foreign dissertations are announced in a companion journal, *International Aerospace Abstracts (IAA)*, available on subscription from the American Institute of Aeronautics and Astronautics, Technical Information Service, 555 West 57th Street, 12th Floor, New York, New York 10019.

SUBJECT SCOPE

Subject scope of *STAR*, and *IAA* includes all aspects of aeronautics and space research and development, supporting basic and applied research, and applications. Aerospace aspects of earth resources, energy development, conservation, oceanography, environmental protection, urban transportation, and other topics of high national priority are also covered.

OTHER NASA PUBLICATIONS

Other NASA publications and information services are described in the publication, *The NASA Scientific and Technical Information System ... and How to Use It*, available without charge from the NASA Scientific and Technical Information Facility, P.O. Box 8757, B.W.I. Airport, Maryland 21240.

HOW TO USE *STAR* SUBJECT CATEGORIES

STAR is categorized by 10 major subject divisions divided into 74 specific subject categories and one general category/division. The major subject divisions are listed in the Table of Contents, together with a note for each that defines its scope and provides any cross-references. For example:

AERONAUTICS

Includes aeronautics (general); aerodynamics; air transportation and safety; aircraft communications and navigation; aircraft design, testing and performance; aircraft instrumentation; aircraft propulsion and power; aircraft stability and control; and research and support facilities (air).

For related information see also *Astronautics*.

Each major division is further divided into as many as nine specific categories, which are identified by category numbers.

Abstracts in *STAR* are grouped by specific category, the categories appearing in sequential order. Category breaks in the abstract section are identified by the category number and title, and a scope note. Cross-references to other categories are provided as appropriate. For example:

02 AERODYNAMICS

Includes aerodynamics of bodies, combinations, wings, rotors, and control surfaces; and internal flow in ducts and turbomachinery.

For related information see also *34 Fluid Mechanics and Heat Transfer*.

CROSS-REFERENCES

Individual *STAR* abstracts are not ordinarily cross-referenced, except for certain conference reports or book translations that have had separate abstracts written for their component papers or chapters. Citations and abstracts of the components follow immediately after those of the parent document. When the subject content of a component differs sufficiently from the general content of the parent, a cross-reference citation also is printed at the end of the category to which it normally would have been assigned if it were independent.

DOCUMENTS ON MICROFICHE

Documents on microfiche[1] are designated by a pound sign (#) following the accession number. The pound sign is used without regard to the source or quality of the microfiche.

AVAILABILITIES

One or more sources from which a document announced in *STAR* is available to the public is given in each citation. The most commonly indicated sources and their acronyms or abbreviations are listed below. If the publication is available from a source other than those listed, the publisher and his address will be displayed on the availability line or in combination with the corporate source line.

(1) A microfiche is a transparent sheet of film, 105 by 148 mm in size, containing as many as 60 to 98 pages of information reduced to micro images (not to exceed 26:1 reduction).

Avail: NTIS. Sold by the National Technical Information Service. Prices for hard copy (HC) and microfiche (MF) are indicated by a price code following the letters HC or MF in the *STAR* citation. Current values for the price codes are given in the tables on page vii.

Initially distributed microfiche under the NTIS SRIM (Selected Research in Microfiche) is available at greatly reduced unit prices. For this service and for information concerning subscription to NASA printed reports, consult the NTIS Subscription Section, Springfield, Va. 22161.

NOTE ON ORDERING DOCUMENTS: When ordering NASA publications (those followed by the * symbol), use the N accession number. NASA patent applications (only the specifications are offered) should be ordered by the US-Patent-Appl-SN number. Non-NASA publications (no asterisk) should be ordered by the AD, PB, or other *report* number shown on the last line of the citation, not by the N accession number. It is also advisable to cite the title and other bibliographic identification.

Avail: SOD (or GPO). Sold by the Superintendent of Documents, U.S. Government Printing Office, in hard copy. The current price and order number are given following the availability line. (NTIS will fill microfiche requests, as indicated above, for those documents identified by a # symbol.)

Avail: NASA Public Document Rooms. Documents so indicated may be examined at or purchased from the National Aeronautics and Space Adminstration, Public Documents Room (Room 126), 600 Independence Ave., S.W., Washington, D.C. 20546, or public document rooms located at each of the NASA research centers, the NASA Space Technology Laboratories, and the NASA Pasadena Office at the Jet Propulsion Laboratory.

Avail: DOE Depository Libraries. Organizations in U.S. cities and abroad that maintain collections of Department of Energy reports, usually in microfiche form, are listed in *Energy Research Abstracts*. Services available from the DOE and its depositories are described in a booklet, *DOE Technical Information Center - Its' Functions and Services* (TID-4660), which may be obtained without charge from the DOE Technical Information Center.

Avail: Univ. Microfilms. Documents so indicated are dissertations selected from *Dissertation Abstracts* and are sold by University Microfilms as xerographic copy (HC) and microfilm. All requests should cite the author and the Order Number as they appear in the citation.

Avail: USGS. Originals of many reports from the U.S. Geological Survey, which may contain color illustrations, or otherwise may not have the quality of illustrations preserved in the microfiche or facsimile reproduction, may be examined by the public at the libraries of the USGS field offices whose addresses are listed in this Introduction. The libraries may be queried concerning the availability of specific documents and the possible utilization of local copying services, such as color reproduction.

Avail: HMSO. Publications of Her Majesty's Stationery Office are sold in the U.S. by Pendragon House, Inc. (PHI), Redwood City, California. The U.S. price (including a service and mailing charge) is given, or a conversion table may be obtained from PHI.

Avail: BLL (formerly NLL): British Library Lending Division, Boston Spa, Wetherby, Yorkshire, England. Photocopies available from this organization at the price shown. (If none is given, inquiry should be addressed to the BLL.)

Avail: Fachinformationszentrum, Karlsruhe. Sold by the Fachinformationszentrum Energie, Physik, Mathematik GMBH, Eggenstein Leopoldshafen, Federal Republic of Germany, at the price shown in deutschmarks (DM).

Avail: Issuing Activity, or Corporate Author, or no indication of availability. Inquiries as to the availability of these documents should be addressed to the organization shown in the citation as the corporate author of the document.

Avail: U.S. Patent and Trademark Office. Sold by Commissioner of Patents and Trademarks, U.S. Patent and Trademark Office, at the standard price of 50 cents each, postage free. (See discussion of patents and patent applications below.)

Avail: ESDU. Pricing information on specific data, computer programs, and details on ESDU topic categories can be obtained from ESDU International Ltd. Requesters in North America should use the Virginia address while all other requesters should use the London address, both of which are on page vi.

NASA PATENTS AND PATENT APPLICATIONS

Patents and patent applications owned by NASA are announced in *STAR* under appropriate subject categories and are referenced in the *STAR* indexes. In the Report/Accession Number Index, patents are indexed by the NASA Case Number (which appears in lieu of the report number in other indexes), the U.S. Patent Number, the U.S. Patent Application Serial Number, and the U.S. Patent Class. Patent applications for which patents have not yet been issued are indexed by the NASA Case Number and the U.S. Patent Application Serial Number.

NASA *patent application specifications* are sold in paper copy by the National Technical Information Service at price code A02 ($7.00 domestic; $14.00 foreign). Microfiche are sold at price code A01 ($4.50 domestic; $9.00 foreign). The US-Patent-Appl-SN- number should be used in ordering either paper copy or microfiche from NTIS. Printed copies of *patents* (which are not microfiched) are available for purchase at 50 cents per copy from:

Commissioner of Patents and Trademarks
U.S. Patent and Trademark Office
Washington, D.C. 20231

When ordering patents, the U.S. Patent Number should be used, and payment must be remitted in advance, preferably by money order or check payable to the Commissioner of Patents and Trademarks. Prepaid purchase coupons for ordering are also available from the Patent and Trademark Office. The patents and patent applications announced in *STAR* are owned by NASA and are available for royalty-free licensing. Requests for licensing terms and further information should be addressed to:

Assistant General Counsel for Patent Matters/Code GP-1
National Aeronautics and Space Administration
Washington, D.C. 20546

ELIGIBILITY AND REGISTRATION FOR NASA INFORMATION PRODUCTS AND SERVICES

A variety of services is available to organizations of the following types that have registered with NASA to receive specific services or products:

1. NASA offices, research centers, contractors, subcontractors, grantees, and consultants;
2. Other U.S. Government agencies and their contractors;
3. Libraries in the United States that have arrangements with NASA to maintain collections of NASA documents for public reference;
4. Other organizations in the United States having a need for NASA documents in work related to aeronautics and space research;
5. Organizations abroad that have established reciprocal document exchange arrangements with NASA.

Only the central service points or central points of document acquisition and control within qualified organizations are eligible to register for NASA products and services. Domestic organizations that may be eligible to receive various classes of NASA publications and services should address their requests for registration or for further information to:

NASA Scientific and Technical Information Facility
ATTN: Registration Activity
P.O. Box 8757
B.W.I. Airport, Maryland 21240

Organizations abroad should direct requests to the same address, but to the attention of: International Exchange Program.

AVAILABILITY OF *STAR* ABSTRACTS ON MICROFICHE

Microfiche of the abstract sections of this issue and other issues of *STAR* are available on annual subscription from NTIS, Attn: Subscriptions, 5285 Port Royal Road, Springfield, Virginia 22161. Annual subscription rates are $60.00 North America; $120.00 foreign. Abstract sections for previous years retroactive to 1964 are available at the current rates. Microfiche for individual *STAR* issue abstract sections are not available.

PUBLIC COLLECTIONS OF NASA DOCUMENTS

DOMESTIC: NASA and NASA-sponsored documents and a large number of aerospace publications are available to the public for reference purposes at the library maintained by the American Institute of Aeronautics and Astronautics, Technical Information Service, 555 West 57th Street, 12th Floor, New York, New York 10019.

EUROPEAN: An extensive collection of NASA and NASA-sponsored publications is maintained by the British Library Lending Division, Boston Spa, Wetherby, Yorkshire, England for public access. The British Library Lending Division also has available many of the non-NASA publications cited in *Star*. European requesters may purchase facsimile copy or microfiche of NASA and NASA-sponsored documents, those identified by both the symbols # and * from ESA - Information Retrieval Service European Space Agency, 8-10 rue Mario-Nikis, 75738 Paris CEDEX 15, France.

FEDERAL DEPOSITORY LIBRARY PROGRAM

In order to provide the general public with greater access to U.S. Government publications, Congress established the Federal Depository Library Program under the Government Printing Office (GPO), with 50 regional depositories responsible for permanent retention of material, inter-library loan, and reference services. Over 1,300 other depositories also exist. A list of the regional GPO libraries appears on the inside back cover of *STAR*.

ADDRESSES OF ORGANIZATIONS

American Institute of Aeronautics and Astronautics
Technical Information Service
555 West 57th Street, 12th Floor
New York, New York 10019

British Library Lending Division,
Boston Spa, Wetherby, Yorkshire,
England

Commissioner of Patents and Trademarks
U.S. Patent and Trademark Office
Washington, D.C. 20231

Department of Energy
Technical Information Center
P.O. Box 62
Oak Ridge, Tennessee 37830

ESA-Information Retrieval Service
ESRIN
Via Galileo Galilei
00044 Frascati (Rome) Italy

ESDU International, Ltd.
1495 Chain Bridge Road
McLean, Virginia 22101

ESDU International, Ltd.
251-259 Regent Street
London, W1R 7AD, England

Fachinformationszentrum Energie, Physik, Mathematik GMBH
7514 Eggenstein Leopoldshafen
Federal Republic of Germany

Her Majesty's Stationery Office
P.O. Box 569, S.E. 1
London, England

NASA Scientific and Technical Information Facility
P.O. Box 8757
B.W.I. Airport, Maryland 21240

National Aeronautics and Space Administration
Scientific and Technical Information Branch (NIT-1)
Washington, D.C. 20546

National Technical Information Service
5285 Port Royal Road
Springfield, Virginia 22161

Pendragon House, Inc.
899 Broadway Avenue
Redwood City, California 94063

Superintendent of Documents
U.S. Government Printing Office
Washington, D.C. 20402

University Microfilms
A Xerox Company
300 North Zeeb Road
Ann Arbor, Michigan 48106

University Microfilms, Ltd.
Tylers Green
London, England

U.S. Geological Survey Library
National Center – MS 950
12201 Sunrise Valley Drive
Reston, Virginia 22092

U.S. Geological Survey Library
2255 North Gemini Drive
Flagstaff, Arizona 86001

U.S. Geological Survey
345 Middlefield Road
Menlo Park, California 94025

U.S. Geological Survey Library
Box 25046
Denver Federal Center, MS 914
Denver, Colorado 80225

NTIS PRICE SCHEDULES

Schedule A

STANDARD PAPER COPY PRICE SCHEDULE

(Effective January 1, 1993)

Price Code	Page Range	North American Price	Foreign Price
A01	Microfiche	$ 4.50	$ 9.00
A02	001-025	7.00	14.00
A03	026-050	8.50	17.00
A04	051-075	10.00	20.00
A05	076-100	11.50	23.00
A06	101-125	13.00	26.00
A07	126-150	14.50	29.00
A08	151-175	16.00	32.00
A09	176-200	17.50	35.00
A10	201-225	19.00	38.00
A11	226-250	20.50	41.00
A12	251-275	22.00	44.00
A13	276-300	23.50	47.00
A14	301-325	25.00	50.00
A15	326-350	26.50	53.00
A16	351-375	28.00	56.00
A17	376-400	29.50	59.00
A18	401-425	31.00	62.00
A19	426-450	32.50	65.00
A20	451-475	34.00	68.00
A21	476-500	35.50	71.00
A22	501-525	37.00	74.00
A23	526-550	38.50	77.00
A24	551-575	40.00	80.00
A25	576-600	41.50	83.00
A99	601-up	-1	-2

1/ Add $1.50 for each additional 25 page increment or portion thereof for 601 pages up.

2/ Add $3.00 for each additional 25 page increment or portion thereof for 601 pages and more.

Schedule E

EXCEPTION PRICE SCHEDULE

Paper Copy & Microfiche

Price Code	North American Price	Foreign Price
E01	$ 6.50	$ 13.50
E02	7.50	15.50
E03	9.50	19.50
E04	11.50	23.50
E05	13.50	27.50
E06	15.50	31.50
E07	17.50	35.50
E08	19.50	39.50
E09	21.50	43.50
E10	23.50	47.50
E11	25.50	51.50
E12	28.50	57.50
E13	31.50	63.50
E14	34.50	69.50
E15	37.50	75.50
E16	40.50	81.50
E17	43.50	88.50
E18	46.50	93.50
E19	51.50	102.50
E20	61.50	123.50

E-99 - Write for quote

N01	35.00	45.00

VOLUME 23 NUMBER 13 / JULY 8, 1985

TABLE OF CONTENTS

AERONAUTICS

Includes aeronautics (general); aerodynamics; air transportation and safety; aircraft communications and navigation; aircraft design, testing and performance; aircraft instrumentation; aircraft propulsion and power; aircraft stability and control; and research and support facilities (air).

For related information see also *Astronautics*.

01 AERONAUTICS (GENERAL) 1965

02 AERODYNAMICS 1968
Includes aerodynamics of bodies, combinations, wings, rotors, and control surfaces; and internal flow in ducts and turbomachinery.
For related information see also *34 Fluid Mechanics and Heat Transfer*

03 AIR TRANSPORTATION AND SAFETY 1970
Includes passenger and cargo air transport operations; and aircraft accidents.
For related information see also *16 Space Transportation* and *85 Urban Technology and Transportation*.

04 AIRCRAFT COMMUNICATIONS AND NAVIGATION 1970
Includes digital and voice communication with aircraft; air navigation systems (satellite and ground based); and air traffic control.
For related information see also *17 Spacecraft Communications, Command and Tracking* and *32 Communications*.

05 AIRCRAFT DESIGN, TESTING AND PERFORMANCE 1971
Includes aircraft simulation technology.
For related information see also *18 Spacecraft Design, Testing and Performance* and *39 Structural Mechanics*.

06 AIRCRAFT INSTRUMENTATION 1973
Includes cockpit and cabin display devices; and flight instruments.
For related information see also *19 Spacecraft Instrumentation* and *35 Instrumentation and Photography*.

07 AIRCRAFT PROPULSION AND POWER 1973
Includes prime propulsion systems and systems components, e.g., gas turbine engines and compressors; and on-board auxiliary power plants for aircraft.
For related information see also *20 Spacecraft Propulsion and Power, 28 Propellants and Fuels*, and *44 Energy Production and Conversion*.

08 AIRCRAFT STABILITY AND CONTROL 1975
Includes aircraft handling qualities; piloting; flight controls; and autopilots.

09 RESEARCH AND SUPPORT FACILITIES (AIR) 1976
Includes airports, hangars and runways; aircraft repair and overhaul facilities; wind tunnels; shock tube facilities; and engine test blocks.
For related information see also *14 Ground Support Systems and Facilities (Space)*.

ASTRONAUTICS

Includes astronautics (general); astrodynamics; ground support systems and facilities (space); launch vehicles and space vehicles; space transportation; spacecraft communications, command and tracking; spacecraft design, testing and performance; spacecraft instrumentation; and spacecraft propulsion and power.

For related information see also *Aeronautics*

12 ASTRONAUTICS (GENERAL) 1977
For extraterrestrial exploration see *91 Lunar and Planetary Exploration*.

13 ASTRODYNAMICS 1985
Includes powered and free-flight trajectories; and orbit and launching dynamics.

14 GROUND SUPPORT SYSTEMS AND FACILITIES (SPACE) N.A.
Includes launch complexes, research and production facilities; ground support equipment, e.g., mobile transporters; and simulators.
For related information see also *09 Research and Support Facilities (Air)*.

15 LAUNCH VEHICLES AND SPACE VEHICLES 1986
Includes boosters; manned orbital laboratories; reusable vehicles; and space stations.

16 SPACE TRANSPORTATION 1988
Includes passenger and cargo space transportation, e.g., shuttle operations; and rescue techniques.
For related information see also *03 Air Transportation and Safety* and *85 Urban Technology and Transportation*.

17 SPACECRAFT COMMUNICATION, COMMAND AND TRACKING N.A.
Includes telemetry; space communications networks; astronavigation; and radio blackout.
For related information see also *04 Aircraft Communications and Navigation* and *32 Communications*.

18 SPACECRAFT DESIGN, TESTING AND PERFORMANCE 1989

Includes spacecraft thermal and environmental control; and attitude control.
For life support systems see *54 Man/System Technology and Life Support*. For related information see also *05 Aircraft Design, Testing and Performance* and *39 Structural Mechanics*.

19 SPACECRAFT INSTRUMENTATION 1998
For related information see also *06 Aircraft Instrumentation* and *35 Instrumentation and Photography*.

20 SPACECRAFT PROPULSION AND POWER 1998
Includes main propulsion systems and components, e.g., rocket engines; and spacecraft auxiliary power sources.
For related information see also *07 Aircraft Propulsion and Power, 28 Propellants and Fuels*, and *44 Energy Production and Conversion*.

CHEMISTRY AND MATERIALS

Includes chemistry and materials (general); composite materials; inorganic and physical chemistry; metallic materials; nonmetallic materials; and propellants and fuels.

23 CHEMISTRY AND MATERIALS (GENERAL) 2013
Includes biochemistry and organic chemistry.

24 COMPOSITE MATERIALS 2015
Includes laminates.

25 INORGANIC AND PHYSICAL CHEMISTRY 2017
Includes chemical analysis, e.g., chromatography; combustion theory; electrochemistry; and photochemistry.
For related information see also *77 Thermodynamics and Statistical Physics.*

26 METALLIC MATERIALS 2020
Includes physical, chemical, and mechanical properties of metals, e.g., corrosion; and metallurgy.

27 NONMETALLIC MATERIALS 2036
Includes physical, chemical, and mechanical properties of plastics, elastomers, lubricants, polymers, textiles, adhesives, and ceramic materials.

28 PROPELLANTS AND FUELS 2039
Includes rocket propellants, igniters, and oxidizers; storage and handling; and aircraft fuels.
For related information see also *07 Aircraft Propulsion and Power, 20 Spacecraft Propulsion and Power,* and *44 Energy Production and Conversion.*

ENGINEERING

Includes engineering (general); communications; electronics and electrical engineering; fluid mechanics and heat transfer; instrumentation and photography; lasers and masers; mechanical engineering; quality assurance and reliability; and structural mechanics.
For related information see also *Physics.*

31 ENGINEERING (GENERAL) 2041
Includes vacuum technology; control engineering; display engineering; and cryogenics.

32 COMMUNICATIONS 2052
Includes land and global communications; communications theory; and optical communications.
For related information see also *04 Aircraft Communications and Navigation* and *17 Spacecraft Communications, Command and Tracking.*

33 ELECTRONICS AND ELECTRICAL ENGINEERING 2062
Includes test equipment and maintainability; components, e.g., tunnel diodes and transistors; microminiaturization; and integrated circuity.
For related information see also *60 Computer Operations and Hardware* and *76 Solid-State Physics.*

34 FLUID MECHANICS AND HEAT TRANSFER 2091
Includes boundary layers; hydrodynamics; fluidics; mass transfer; and ablation cooling.
For related information see also *02 Aerodynamics* and *77 Thermodynamics and Statistical Physics.*

35 INSTRUMENTATION AND PHOTOGRAPHY 2094
Includes remote sensors; measuring instruments and gages; detectors; cameras and photographic supplies; and holography.
For aerial photography see *43 Earth Resources.* For related information see also *06 Aircraft Instrumentation* and *19 Spacecraft Instrumentation.*

36 LASERS AND MASERS 2095
Includes parametric amplifiers.

37 MECHANICAL ENGINEERING 2098
Includes auxiliary systems (non-power); machine elements and processes; and mechanical equipment.

38 QUALITY ASSURANCE AND RELIABILITY 2100
Includes product sampling procedures and techniques; and quality control.

39 STRUCTURAL MECHANICS 2101
Includes structural element design and weight analysis; fatigue; and thermal stress.
For applications see *05 Aircraft Design, Testing and Performance* and *18 Spacecraft Design, Testing and Performance.*

GEOSCIENCES

Includes geosciences (general); earth resources; energy production and conversion; environment pollution; geophysics; meteorology and climatology; and oceanography.
For related information see also *Space Sciences.*

42 GEOSCIENCES (GENERAL) 2105

43 EARTH RESOURCES 2117
Includes remote sensing of earth resources by aircraft and spacecraft; photogrammetry; and aerial photography.
For instrumentation see *35 Instrumentation and Photography.*

44 ENERGY PRODUCTION AND CONVERSION 2128
Includes specific energy conversion systems, e.g., fuel cells and batteries; global sources of energy; fossil fuels; geophysical conversion; hydroelectric power; and wind power.
For related information see also *07 Aircraft Propulsion and Power, 20 Spacecraft Propulsion and Power, 28 Propellants and Fuels,* and *85 Urban Technology and Transportation.*

45 ENVIRONMENT POLLUTION 2130
Includes air, noise, thermal and water pollution; environment monitoring; and contamination control.

46 GEOPHYSICS 2131
Includes aeronomy; upper and lower atmosphere studies; ionospheric and magnetospheric physics; and geomagnetism.
For space radiation see *93 Space Radiation.*

47 METEOROLOGY AND CLIMATOLOGY 2137
Includes weather forecasting and modification.

48 OCEANOGRAPHY 2140
Includes biological, dynamic and physical oceanography; and marine resources.

LIFE SCIENCES

Includes sciences (general); aerospace medicine; behavioral sciences; man/system technology and life support; and planetary biology.

51 LIFE SCIENCES (GENERAL) 2141
Includes genetics.

52 AEROSPACE MEDICINE 2142
Includes physiological factors; biological effects of radiation; and weightlessness.

53 BEHAVIORAL SCIENCES 2142
Includes psychological factors; individual and group behavior; crew training and evaluation; and psychiatric research.

54 MAN/SYSTEM TECHNOLOGY AND LIFE SUPPORT 2143
Includes human engineering; biotechnology; and space suits and protective clothing.

55 PLANETARY BIOLOGY N.A.
Includes exobiology; and extraterrestrial life.

MATHEMATICAL AND COMPUTER SCIENCES

Includes mathematical and computer sciences (general); computer operations and hardware; computer programming and software; computer systems; cybernetics; numerical analysis; statistics and probability; systems analysis; and theoretical mathematics.

59 MATHEMATICAL AND COMPUTER SCIENCES (GENERAL) 2144

60 COMPUTER OPERATIONS AND HARDWARE 2144
Includes computer graphics and data processing.
For components see *33 Electronics and Electrical Engineering.*

61 COMPUTER PROGRAMMING AND SOFTWARE 2145
Includes computer programs, routines, and algorithms.

62 COMPUTER SYSTEMS 2149
Includes computer networks.

63 CYBERNETICS 2149
Includes feedback and control theory.
For related information see also *54 Man/System Technology and Life Support.*

64 NUMERICAL ANALYSIS 2149
Includes iteration, difference equations, and numerical approximation.

65 STATISTICS AND PROBABILITY 2153
Includes data sampling and smoothing; Monte Carlo method; and stochastic processes.

66 SYSTEMS ANALYSIS 2153
Includes mathematical modeling; network analysis; and operations research.

67 THEORETICAL MATHEMATICS N.A.
Includes topology and number theory.

PHYSICS

Includes physics (general); acoustics; atomic and molecular physics; nuclear and high-energy physics; optics; plasma physics; solid-state physics; and thermodynamics and statistical physics.
For related information see also *Engineering.*

70 PHYSICS (GENERAL) 2154
For geophysics see *46 Geophysics.* For astrophysics see *90 Astrophysics.* For solar physics see *92 Solar Physics.*

71 ACOUSTICS 2154
Includes sound generation, transmission, and attenuation.
For noise pollution see *45 Environment Pollution.*

72 ATOMIC AND MOLECULAR PHYSICS 2156
Includes atomic structure and molecular spectra.

73 NUCLEAR AND HIGH-ENERGY PHYSICS N.A.
Includes elementary and nuclear particles; and reactor theory.
For space radiation see *93 Space Radiation.*

74 OPTICS 2158
Includes light phenomena.

75 PLASMA PHYSICS 2161
Includes magnetohydrodynamics and plasma fusion.
For ionospheric plasmas see *46 Geophysics.* For space plasmas see *90 Astrophysics.*

76 SOLID-STATE PHYSICS 2162
Includes superconductivity.
For related information see also *33 Electronics and Electrical Engineering* and *36 Lasers and Masers.*

77 THERMODYNAMICS AND STATISTICAL PHYSICS 2165
Includes quantum mechanics; and Bose and Fermi statistics.
For related information see also *25 Inorganic and Physical Chemistry* and *34 Fluid Mechanics and Heat Transfer.*

SOCIAL SCIENCES

Includes social sciences (general); administration and management; documentation and information science; economics and cost analysis; law and political science; and urban technology and transportation.

80 SOCIAL SCIENCES (GENERAL) N.A.
Includes educational matters.

81 ADMINISTRATION AND MANAGEMENT 2165
Includes management planning and research.

82 DOCUMENTATION AND INFORMATION SCIENCE 2167
Includes information storage and retrieval technology; micrography; and library science.
For computer documentation see *61 Computer Programming and Software.*

83 ECONOMICS AND COST ANALYSIS N.A.
Includes cost effectiveness studies.

84 LAW AND POLITICAL SCIENCE 2168
Includes space law; international law; international cooperation; and patent policy.

85 URBAN TECHNOLOGY AND TRANSPORTATION 2168
Includes applications of space technology to urban problems; technology transfer; technology assessment; and surface and mass transportation.
For related information see *03 Air Transportation and Safety, 16 Space Transportation,* and *44 Energy Production and Conversion.*

SPACE SCIENCES

Includes space sciences (general); astronomy; astrophysics; lunar and planetary exploration; solar physics; and space radiation.
For related information see also *Geosciences.*

88 SPACE SCIENCES (GENERAL) 2169

89 ASTRONOMY 2169
Includes radio and gamma-ray astronomy; celestial mechanics; and astrometry.

90 ASTROPHYSICS 2170
Includes cosmology; and interstellar and interplanetary gases and dust.

91 LUNAR AND PLANETARY EXPLORATION 2172
Includes planetology; and manned and unmanned flights.
For spacecraft design see *18 Spacecraft Design, Testing and Performance.* For space stations see *15 Launch Vehicles and Space Vehicles.*

92 SOLAR PHYSICS 2205
Includes solar activity, solar flares, solar radiation and sunspots.

93 SPACE RADIATION 2206
Includes cosmic radiation; and inner and outer earth's radiation belts.
For biological effects of radiation see *52 Aerospace Medicine.* For theory see *73 Nuclear and High-Energy Physics.*

GENERAL

99 GENERAL N.A.

Note: N.A. means that no abstracts were assigned to this category for this issue.

SUBJECT INDEX I-1
PERSONAL AUTHOR INDEX I-69
CORPORATE SOURCE INDEX I-81
CONTRACT NUMBER INDEX I-95
REPORT / ACCESSION NUMBER INDEX I-97

TYPICAL CITATION AND ABSTRACT

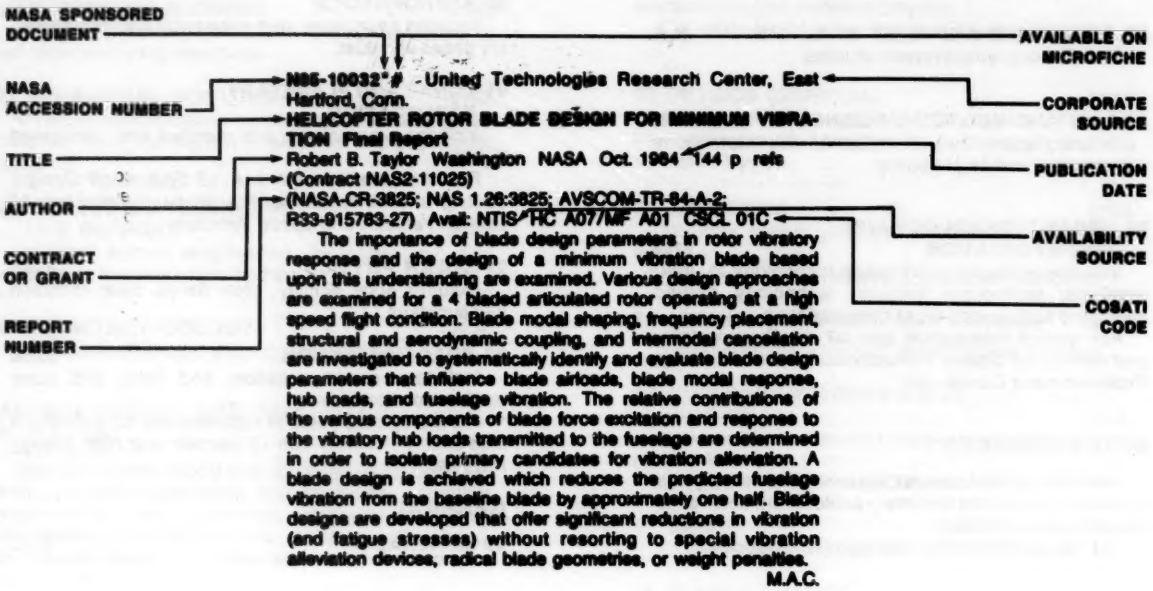
NASA SPONSORED DOCUMENT
NASA ACCESSION NUMBER
TITLE
AUTHOR
CONTRACT OR GRANT
REPORT NUMBER
AVAILABLE ON MICROFICHE
CORPORATE SOURCE
PUBLICATION DATE
AVAILABILITY SOURCE
COSATI CODE
N85-10032*# - United Technologies Research Center, East Hartford, Conn.
HELICOPTER ROTOR BLADE DESIGN FOR MINIMUM VIBRATION Final Report
Robert B. Taylor Washington NASA Oct. 1984 144 p refs
(Contract NAS2-11025)
(NASA-CR-3825; NAS 1.26:3825; AVSCOM-TR-84-A-2; R33-915783-27) Avail: NTIS HC A07/MF A01 CSCL 01C
The importance of blade design parameters in rotor vibratory response and the design of a minimum vibration blade based upon this understanding are examined. Various design approaches are examined for a 4 bladed articulated rotor operating at a high speed flight condition. Blade modal shaping, frequency placement, structural and aerodynamic coupling, and intermodal cancellation are investigated to systematically identify and evaluate blade design parameters that influence blade airloads, blade modal response, hub loads, and fuselage vibration. The relative contributions of the various components of blade force excitation and response to the vibratory hub loads transmitted to the fuselage are determined in order to isolate primary candidates for vibration alleviation. A blade design is achieved which reduces the predicted fuselage vibration from the baseline blade by approximately one half. Blade designs are developed that offer significant reductions in vibration (and fatigue stresses) without resorting to special vibration alleviation devices, radical blade geometries, or weight penalties.
M.A.C.

VOLUME 23 NUMBER 13 / JULY 8, 1985

Scientific and Technical Aerospace Reports

A Semimonthly Publication of the National Aeronautics and Space Administration

01 AERONAUTICS (GENERAL)

N85-22342* National Aeronautics and Space Administration, Washington, D. C.
AERONAUTICAL ENGINEERING: A CONTINUING BIBLIOGRAPHY WITH INDEXES, SUPPLEMENT 185
Mar. 1985 132 p
(NASA-SP-7037(185); NAS 1.21:7037(185)) Avail: NTIS HC $6.00 CSCL 01A

This bibliography lists 462 reports, articles and other documents introduced into the NASA scientific and technical information system in February 1985. Aerodynamics, aeronautical engineering, aircraft design, aircraft stability and control, geophysics, social sciences, and space sciences are some of the areas covered. R.J.F.

N85-22343* National Aeronautics and Space Administration, Washington, D. C.
AERONAUTICAL ENGINEERING: A CUMULATIVE INDEX TO THE 1984 ISSUES OF THE CONTINUING BIBLIOGRAPHY
Jan. 1985 573 p
(NASA-SP-7037(183); NAS 1.21:7037(183)) Avail: NTIS HC $10.00 CSCL 01A

This bibliography is a cumulative index to the abstracts contained in NASA SP-7037(171) through NASA SP-7037(182) of Aeronautical Engineering: A Continuing Bibliography. NASA SP-7037 and its supplements have been compiled through the cooperative efforts of the American Institute of Aeronautics and Astronautics (AIAA) and the National Aeronautics and Space Administration (NASA). This cumulative index includes subject, personal author, corporate source, foreign technology, contract, report number, and accession number indexes. Author

N85-22344*# Sikorsky Aircraft, Stratford, Conn.
EXPERIMENTAL STUDY OF MAIN ROTOR TIP GEOMETRY AND TAIL ROTOR INTERACTIONS IN HOVER. VOLUME 1. TEXT AND FIGURES Progress Report, Aug. 1982 - Nov. 1983
D. T. Balch and J. Lombardi Feb. 1985 94 p refs 2 Vol.
(Contract NAS2-11266)
(NASA-CR-177336-Vol-1; NAS 1.26:177336-Vol-1) Avail: NTIS HC A05/MF A01 CSCL 01A

A model scale hover test was conducted in the Sikorsky Aircraft Model rotor hover Facility to identify and quantify the impact of the tail rotor on the demonstrated advantages of advanced geometry tip configurations. The test was conducted using the Basic Model Test Rig and two scaled main rotor systems, one representing a 1/5.727 scale UH-60A BLACK HAWK and the others a 1/4.71 scale S-76. Eight alternate rotor tip configurations were tested, 3 on the BLACK HAWK rotor and 6 on the S-76 rotor. Four of these tips were then selected for testing in close proximity to an operating tail rotor (operating in both tractor and pusher modes) to determine if the performance advantages that could be obtained from the use of advanced geometry tips in a main rotor only environment would still exist in the more complex flow field involving a tail rotor. The test showed that overall the tail rotor effects on the advanced tip configurations tested are not substantially different from the effects on conventional tips. B.W.

N85-22345*# Sikorsky Aircraft, Stratford, Conn.
EXPERIMENTAL STUDY OF MAIN ROTOR TIP GEOMETRY AND TAIL ROTOR INTERACTIONS IN HOVER. VOLUME 2: RUN LOG AND TABULATED DATA Progress Report, Aug. 1982 - Nov. 1983
D. T. Balch and J. Lombardi Feb. 1985 235 p 2 Vol.
(Contract NAS2-11266)
(NASA-CR-177336-Vol-2; NAS 1.26:177336-Vol-2) Avail: NTIS HC A11/MF A01 CSCL 01A

A model scale hover test was conducted in the Sikorsky Aircraft Model Rotor hover Facility to identify and quantify the impact of the tail rotor on the demonstrated advantages of advanced geometry tip configurations. The existence of mutual interference between hovering main rotor and a tail rotor was acknowledged in the test. The test was conducted using the Basic Model Test Rig and two scaled main rotor systems, one representing a 1/5.727 scale UH-60A BLACK HAWK and the others a 1/4.71 scale S-76. Eight alternate rotor tip configurations were tested, 3 on the BLACK HAWK rotor and 6 on the S-76 rotor. Four of these tips were then selected for testing in close proximity to an operating tail rotor (operating in both tractor and pusher modes) to determine if the performance advantages that could be obtained from the use of advanced geometry tips in a main rotor only environment would still exist in the more complex flow field involving a tail rotor. This volume contains the test run log and tabulated data. B.W.

N85-22346*# Analytical Methods, Inc., Redmond, Wash.
STUDY FOR PREDICTION OF ROTOR/WAKE/FUSELAGE INTERFERENCE, PART 1 Final Report, 1 Jun. 1980 - 1 Nov. 1983
D. R. Clark and B. Maskew Mar. 1985 92 p refs 2 Vol.
(Contract NAS2-10620)
(NASA-CR-177340-Vol-1; NAS 1.26:177340-Vol-1;
Rept-8304-I-Vol-1) Avail: NTIS HC A05/MF A01 CSCL 01A

A method was developed which allows the fully coupled calculation of fuselage and rotor airloads for typical helicopter configurations in forward flight. To do this, an iterative solution is carried out based on a conventional panel representation of the fuselage and a blade element representation of the rotor where fuselage and rotor singularity strengths are determined simultaneously at each step and the rotor wake is allowed to relax (deform) in response to changes in rotor wake loading and fuselage presence. On completion of the iteration, rotor loading and inflow, fuselage singularity strength (and, hence, pressure and velocity distributions) and rotor wake are all consistent. The results of a fully coupled calculation of the flow around representative helicopter configurations are presented. The effect of fuselage components on the rotor flow field and the overall wake structure is detailed and the aerodynamic interference between the different parts of the aircraft is discussed. R.J.F.

N85-22347*# Analytical Methods, Inc., Redmond, Wash.
STUDY FOR PREDICTION OF ROTOR/WAKE/FUSELAGE INTERFERENCE. PART 2: PROGRAM USERS GUIDE Final Report, 1 Jun. 1980 - 1 Nov. 1983
D. R. Clark and B. Maskew Mar. 1985 94 p refs 2 Vol.
(Contract NAS2-10620)
(NASA-CR-177340-Vol-2; NAS 1.26:177340-Vol-2; Rept-8304-I-Vol-2) Avail: NTIS HC A05/MF A01 CSCL 01A

A method was developed which permits the fully coupled calculation of fuselage and rotor airloads for typical helicopter configurations in forward flight. To do this, an iterative solution is carried out based on a conventional panel representation of the fuselage and a blade element representation of the rotor where fuselage and rotor singularity strengths are determined simultaneously at each step and the rotor wake is allowed to relax (deform) in response to changes in rotor wake loading and fuselage presence. On completion of the iteration, rotor loading and inflow, fuselage singularity strength (and, hence, pressure and velocity distributions) and rotor wake are all consistent. The results of a fully coupled calculation of the flow around representative helicopter configurations are presented. The effect of fuselage components on the rotor flow field and the overall wake structure is discussed as well as the aerodynamic interference between the different parts of the aircraft. Details of the computer program are given.
R.J.F.

N85-22348# Air Force Wright Aeronautical Labs., Wright-Patterson AFB, Ohio.
AIR FORCE TECHNICAL OBJECTIVE DOCUMENT, FLIGHT DYNAMICS LABORATORY PLANS FOR FISCAL YEAR 1986. AIR FORCE TECHNICAL OBJECTIVE DOCUMENT Final Report, Oct. 1983 - Aug. 1984
Aug. 1984 68 p Supersedes AFWAL-TR-83-3000
(AD-A149648; AFWAL-TR-84-3000; AFWAL-TR-83-3000) Avail: NTIS HC A04/MF A01 CSCL 01/3

This document presents an overview of the AF Flight Dynamic Lab's technical planning objectives which are described for Structures and Dynamics, Vehicle Equipment, Flight Control, Aeromechanics, and Technology Assessment. Keywords include: active control; ablation and models; aerodynamic characteristics, and flow fields; aerodynamic configurations and control surfaces; aerodynamic heating, convection (heat transfer) & enviroments; Aero-elastic effects, twist; air cushion vehicles and landing; air to air and air to surface; flutter; airframe--interactions and propulsion systems; and military aircraft--survival; ballistics/impact; boost glide vehicles; boundary layer computations; canopies--materials and penetration; test chambers, environments; cockpit --automation/display systems/multipurpose controls/ voice control; composite structures; control--enviroments and simulation; control systems and digital systems; stabilization of unstable aircraft and spacecraft; cost effectiveness and trade off analysis, cost reduction technologies; crews and integrated systems; cryogenics and refrigeration systems; diagnostic equipment and holography; dynamics and structural response; elastic properties, materials, plastic properties and response; energy management; external stores; mechanical failure; fatigue life; fire control; flight control--robust control system architecture, artificial intelligence/fault tolerant; terrain following/terrain avoidance, and in flight simulator; flight testing; fluid flow and lasers, flutter suppression, fly-by-wire controls; fracture (mechanics); geometry and nozzles; heat and sources; landing gear.
GRA

N85-22349# Naval Postgraduate School, Monterey, Calif. Dept. of Administrative Science.
AVIATION MAINTENANCE COMPUTERIZED MANAGEMENT INFORMATION SYSTEMS: PERSPECTIVE FOR THE FUTURE M.S. Thesis
Jerre Floyd Derrick and Theodore Aldred Miller Jun. 1984 89 p
(AD-A150637) Avail: NTIS HC A05/MF A01 CSCL 01/3

The Naval Aviation Logistics Command Management Information System (NALCOMIS) is the next generation solution to the information assimilation gap faced by Naval Aviation maintenance managers. This thesis examines the scope of the problem at the Organizational and Intermediate levels of maintenance, and the intended effect of NALCOMIS and three peripheral information systems. The underlying concepts of the four systems investigated are used to explore Artificial Intelligence as the logical augmentation or follow-on to the NALCOMIS program. Recommendations regarding the implementation of AI and expert systems are made.
GRA

N85-22350# Advisory Group for Aerospace Research and Development, Neuilly-Sur-Seine (France).
GROUND AND FLIGHT TESTING FOR AIRCRAFT GUIDANCE AND CONTROL
Reiner Onken, ed. (DFVLR, Brunswick, West Germany) and Hermann A. Rediess, ed. (Hydraulic Research Textron, Inc., Irving, Calif.) Loughton, England Dec. 1984 195 p refs
(AGARD-AG-262; ISBN-92-835-1482-3) Avail: NTIS HC A09/MF A01

Aircraft guidance and control functions, components, and systems are evaluated with emphasis on specific examples of user oriented test programs rather than descriptions of the facilities. Topics include control handling and active control testing; tests on flight path control; navigation system testing; combat guidance and control evaluation; and testing of flight-crucial digital systems in guidance and control. For individual titles, see N85-22351 through N85-22362.

N85-22351*# National Aeronautics and Space Administration. Ames Research Center, Moffett Field, Calif.
SPACE SHUTTLE PILOT-INDUCED-OSCILLATION RESEARCH TESTING **c05**
Bruce G. Powers *In* AGARD Ground and Flight Testing for Aircraft Guidance and Control Dec. 1984 7 p refs Original language document was announced as N84-20566 (For primary document see N85-22350 13-01)
Avail: NTIS HC A09/MF A01 CSCL 01C

The simulation requirements for investigation of pilot-induced-oscillation (PIO) characteristics during the landing phase are discussed. Orbiters simulations and F-8 digital fly-by-wire aircraft tests are addressed.
Author

N85-22352# Deutsche Forschungs- und Versuchsanstalt fuer Luft- und Raumfahrt, Brunswick (West Germany). Inst. fuer Flugmechanik.
DYNAMIC WIND TUNNEL TESTING FOR ACTIVE CONTROL RESEARCH **c08**
K. Wilhelm and B. Gmelin *In* AGARD Ground and Flight Testing for Aircraft Guidance and Control Dec. 1984 26 p refs (For primary document see N85-22350 13-01)
Avail: NTIS HC A09/MF A01

For the investigation of problems associated with the application of active control systems a technique was developed, which allows a comprehensive treatment of flight mechanics problems including the effects of aerodynamics, aeroelastics and control systems. Since this technique, the dynamic wind tunnel test technique, is a synthesis of both computer simulation and wind tunnel test a variety of information on specific flight mechanical phenomena can be obtained. At DFVLR two experimental devices were developed: the installation for dynamic simulation in wind tunnels for investigation in the field of fixed-wing aircraft; and the rotor test stand for investigation in the field of rotary-wing aircraft. At first a brief description of the test facilities is given, further advantages and special problems associated with the application of this test technique are shown. In addition, test results of completed test programs are presented.
Author

N85-22353*# National Aeronautics and Space Administration. Langley Research Center, Hampton, Va.
DYNAMIC WIND-TUNNEL TESTING OF ACTIVE CONTROLS BY THE NASA LANGLEY RESEARCH CENTER **c08**
Irving Abel, Robert V. Doggett, Jerry R. Newsom, and Maynard Sandford *In* AGARD Ground and Flight Testing for Aircraft Guidance and Control Dec. 1984 23 p refs (For primary document see N85-22350 13-01)

Avail: NTIS HC A09/MF A01 CSCL 01C

Dynamic wind-tunnel testing of active controls by the NASA Langley Research Center is presented. Seven experimental studies that were accomplished to date are described. Six of the studies focus on active flutter suppression. The other focuses on active load alleviation. In addition to presenting basic results for these experimental studies, topics including model design and construction, control law synthesis, active control system implementation, and wind-tunnel test techniques are discussed. Author

N85-22354# Royal Aircraft Establishment, Bedford (England). Operational Systems Div.

CIVIL AVIONICS FLIGHT TESTING WITH THE RAE(B) BAC1-11 **c06**

R. R. Newbery and P. England *In* AGARD Ground and Flight Testing for Aircraft Guidance and Control Dec. 1984 22 p refs Original contains color illustrations (For primary document see N85-22350 13-01)

Avail: NTIS HC A09/MF A01

The BAC 1-11 research aircraft and test flight facility are described. Significant results were achieved in the fields of automatic control, improved accuracy of navigation, the use of CRT flight deck displays, the development of time control maneuvers, and the use of direct voice input. The role of avionics systems in the total air traffic management system is addressed. The development of flight path and time control algorithms will be extended to deal with multiple constraints. Further attention will be paid to the interfaces between the aircraft systems, crew, and air traffic control. B.G.

N85-22355# Deutsche Forschungs- und Versuchsanstalt fuer Luft- und Raumfahrt, Brunswick (West Germany).

GUIDANCE AND CONTROL RESEARCH FLIGHT TESTING WITH HFB 320 TEST AIRCRAFT **c08**

V. Adam and W. Lechner *In* AGARD Ground and Flight Testing for Aircraft Guidance and Control Dec. 1984 13 p refs (For primary document see N85-22350 13-01)

Avail: NTIS HC A09/MF A01

Flight testing is the last and decisive phase in the development process of new aircraft guidance and control methods, procedures and equipment to give evidence of the expected functional performance. No highly elaborated ground-based simulation can replace this phase unless there is complete knowledge of the aircraft system characteristics and no restriction on expenditure. On the other hand there is no doubt that simulation including most of the real system hardware is a necessary phase to pass before flight testing can be started. This is the means for step by step system validation on the ground under reproducible conditions. In-flight simulation, direct lift control, side stick control, fly-by-wire and integrated navigation tests on the German aircraft HFB 320 are reported. Ground-based experimental systems and flight test equipment are also described. B.G.

N85-22356*# National Aeronautics and Space Administration. Langley Research Center, Hampton, Va.

A FLIGHT MANAGEMENT ALGORITHM AND GUIDANCE FOR FUEL-CONSERVATIVE DESCENTS IN A TIME-BASED METERED AIR TRAFFIC ENVIRONMENT: DEVELOPMENT AND FLIGHT TEST RESULTS **c05**

Charles E. Knox *In* AGARD Ground and Flight Testing for Aircraft Guidance and Control Dec. 1984 17 p refs (For primary document see N85-22350 13-01)

Avail: NTIS HC A09/MF A01 CSCL 01C

A simple airborne flight management descent algorithm designed to define a flight profile subject to the constraints of using idle thrust, a clean airplane configuration (landing gear up, flaps zero, and speed brakes retracted), and fixed-time end conditions was developed and flight tested in the NASA TSRV B-737 research airplane. The research test flights, conducted in the Denver ARTCC automated time-based metering LFM/PD ATC environment, demonstrated that time guidance and control in the cockpit was acceptable to the pilots and ATC controllers and resulted in arrival of the airplane over the metering fix with standard deviations in airspeed error of 6.5 knots, in altitude error of 23.7 m (77.8 ft), and in arrival time accuracy of 12 sec. These accuracies indicated a good representation of airplane performance and wind modeling. Fuel savings will be obtained on a fleet-wide basis through a reduction of the time error dispersions at the metering fix and on a single-airplane basis by presenting the pilot with guidance for a fuel-efficient descent. Author

N85-22357# Deutsche Forschungs- und Versuchsanstalt fuer Luft- und Raumfahrt, Brunswick (West Germany). Inst. fuer Flugfuehrung.

AVIONICS FLIGHT EVALUATION SYSTEM (AFES) **c06**

Karlheinz Hurrass *In* AGARD Ground and Flight Testing for Aircraft Guidance and Control Dec. 1984 9 p refs (For primary document see N85-22350 13-01)

Avail: NTIS HC A09/MF A01

New avionic systems require thorough testing. Particularly as far as navigation systems are concerned, very accurate reference trajectories have to be established. For this purpose, DFVLR has developed an Avionics Flight Evaluation System (AFES). A tracking radar, a laser tracker, and an inertial navigation system (INS) on board the test aircraft are used in order to measure flight trajectories. The data of all these sensors are combined by optimal filters. In order to be able to evaluate in real time, computers are used at different locations. All elements of this measurement system are linked together by an efficient data transfer system. Besides the reference system, AFES contains subsystems for artificial traffic loading and measuring multipath effects. Author

N85-22358# Royal Aircraft Establishment, Farnborough (England).

REFERENCE SYSTEMS FOR THE EVALUATION OF DEAD-RECKONING NAVIGATION EQUIPMENT **c04**

R. F. Stokes and S. G. Smith *In* AGARD Ground and Flight Testing for Aircraft Guidance and Control Dec. 1984 17 p Original language document was announced as N84-34406 (For primary document see N85-22350 13-01)

Avail: NTIS HC A09/MF A01

Aircraft dead reckoning navigation systems present particular problems in their assessment, and diagnosis in development where a continuous measurement of their error pattern is required. The need for long range, long duration flights with a continuous high accuracy reference led to the development of an integrated navigation system. The recorded data is processed post-flight in a Kalman filter which is used to estimate the inertial system errors. The final reference is formed by compensating the inertial outputs for these errors and has the properties of high accuracy, low noise, and continuous availability. Although simple in concept the implementation of such a scheme is complex. The major problem lies in constructing suitable mathematical models of the various equipments, and the technique of pre-processing is described. The second difficult area is that of obtaining the statistical information regarding the performance of the equipment in a form suitable for inclusion in the models. Although the reference is produced off-line, it is possible to implement the techniques on-line. R.S.F.

N85-22359# Industrieanlagen-Betriebsgesellschaft m.b.H., Ottobrunn (West Germany).

AIR COMBAT SIMULATION: METHODS, MODELS, TRENDS **c05**

G. Wunderlich and H. P. Fehrenz *In* AGARD Ground and Flight Testing for Aircraft Guidance and Control Dec. 1984 17 p refs (For primary document see N85-22350 13-01)

Avail: NTIS HC A09/MF A01

Various methods are described briefly to evaluate weapon system parameters needed during air combat. The influences and connections between unmanned and manned combat simulation are derived as well as the main differences between 1 vs 1 and m vs n combat including relevant pilot behavior. Finally unmanned and manned m/n air combat simulations are described and it is shown how both methods support each other thus broadening the validity of application and results. Author

N85-22360# Societe Nationale Industrielle Aerospatiale, Marignane (France). Avionics and Systems Group.
GROUND EVALUATION OF HELICOPTER AIR-TO-AIR WARFARE **c05**
G. Catani *In* AGARD Ground and Flight Testing for Aircraft Guidance and Control Dec. 1984 13 p (For primary document see N85-22350 13-01)
Avail: NTIS HC A09/MF A01

Air to air capability has become a necessity for armed helicopters. The simulation models allow theoretical evaluation of given air to air fire controls through a large area of air to air scenarios. During definition phases, they represent a powerful means of building and ground testing every fire control. On the other hand increased efficiency during development phases makes it possible to avoid expensive in-flight tests of non-optimized systems. Simple gun pilot fire control systems and definition and evaluation of complex gun/missile fire control systems were described. B.G.

N85-22361# Messerschmitt-Boelkow-Blohm G.m.b.H., Munich (West Germany). Military Aircraft Div.
TESTING OF THE DIGITAL FLIGHT CONTROL SYSTEM OF THE GERMAN CCV FIGHTER EXPERIMENTAL AIRCRAFT **c08**
Udo Korte *In* AGARD Ground and Flight Testing for Aircraft Guidance and Control Dec. 1984 12 p refs Original language document was announced as N83-22110 (For primary document see N85-22350 13-01)
Avail: NTIS HC A09/MF A01

A quad redundant digital FBW Control System for a highly unstable fighter aircraft has been developed and flight tested by MBB in a a single seater F-104 G which had been modified as a CCV demonstrator. The CCV program was funded by the German MOD. From Dec. 1977 to Nov. 1981 a total of 118 flights has been conducted. During these flights the quadruplex system was successfully tested for five different configurations starting with the highly stable basic aircraft and ending up with the highly unstable canard configuration with a static instability up to 22% mean aerodynamic chord (MAC). Some of the results obtained regarding control system design, handling evaluation and redundancy management with the digital system will be presented. Author

N85-22362*# National Aeronautics and Space Administration. Langley Research Center, Hampton, Va.
AIRLAB: A LABORATORY FOR FLIGHT-CRUCIAL-ELECTRONICS SYSTEM RESEARCH **c05**
H. Milton Holt, Dale G. Holden, and Amy O. Lupton *In* AGARD Ground and Flight Testing for Aircraft Guidance and Control Dec. 1984 12 p refs (For primary document see N85-22350 13-01)
Avail: NTIS HC A09/MF A01 CSCL 01C

A new laboratory, AIRLAB, recently completed at the NASA Langley Research Center was developed as a focus for conducting research on fault-tolerant electronic systems for flight-crucial applications. The laboratory was conceived and implemented to enhance the utilization of aeronautical research for improving the performance of future aerospace vehicles. Advanced vehicles will require highly reliable digital electronic systems to perform flight-crucial functions which if lost, would cause total failure of the vehicle. Techniques to form the basis for a validation methodology that can be used to determine the performance and reliability of advanced digital systems are being developed. Included are the development of analytical models, emulation techniques, and experimental procedures. The techniques and methods are verified using these specimens of fault-tolerant computers and systems and the capabilities of AIRLAB. Author

02 AERODYNAMICS

Includes aerodynamics of bodies, combinations, wings, rotors, and control surfaces; and internal flow in ducts and turbomachinery.

For related information see also *34 Fluid Mechanics and Heat Transfer.*

N85-22363 Princeton Univ., N. J.
AERODYNAMIC BEHAVIOR OF VENTILATED WIND TUNNEL WALLS Ph.D. Thesis
Pong-Jeu Lu 1984 288 p
Avail: Univ. Microfilms Order No. DA8425698

A new approach is developed to study the wall behavior which indicates the mutual interference between wall perforations in the presence of the non-uniform pressure field induced by the model. In the global analysis, the method of matched asymptotic expansions is employed to form and explain the idea of an averaged wall boundary condition. With the use of a wavy wall model problem, the appropriate boundary condition for perforated walls in subsonic flow is derived. The newly obtained perforated wall condition contains an extra term which has not been identified in the classical formulation. A local analysis is also used to study the flow through an isolated hole in the wind tunnel wall. Both inviscid irrotational (potential) and rotational (shear) flows are considered. A value for the cross-flow resistance constant, which takes into account all the geometrical and Mach number effects, is derived, analytically. Dissert. Abstr.

N85-22364*# Auburn Univ., Ala. Dept. of Computer Science and Engineering.
NONLINEAR ROTORDYNAMICS ANALYSIS Final Report
William B. Day 15 Mar. 1985 38 p refs
(Contract NAS8-35992)
(NASA-CR-171425; NAS 1.26:171425) Avail: NTIS HC A03/MF A01 CSCL 01A

The special nonlinearities of the Jeffcott equations in rotordynamics are examined. The immediate application of this analysis is directed toward understanding the excessive vibrations recorded in the LOX pump of the SSME during hot firing ground testing. Deadband, side force and rubbing are three possible sources of inducing nonlinearity in the Jeffcott equations. The present analysis initially reduces these problems to the same mathematical description. A special frequency, named the nonlinear natural frequency is defined and used to develop the solutions of the nonlinear Jeffcott equations as asympotic expansions. This nonlinear natural frequency which is the ratio of the cross-stiffness and the damping, plays a major role in determining response frequencies. Numerical solutions are included for comparison with the analysis. Also, nonlinear frequency-response tables are made for a typical range of values. B.W.

N85-22365*# Tekworld Co., Hampton, Va.
EFFECTS OF LEADING-EDGE DEVICES ON THE LOW-SPEED AERODYNAMIC CHARACTERISTICS OF A HIGHLY-SWEPT ARROW-WING
Samuel J. Scott, Oran W. Nicks, and P. K. Imbrie Feb. 1985 67 p
(NASA Purchase Order L-69215B)
(NASA-CR-172531; NAS 1.26:172531) Avail: NTIS HC A04/MF A01 CSCL 01A

An investigation was conducted in the Texas A&M University 7 by 10 foot Low Speed Wind Tunnel to provide a direct comparison of the effect of several leading edge devices on the aerodynamic performance of a highly swept wing configuration. Analysis of the data indicates that for the configuration with undeflected leading edges, vortex separation first occurs on the outboard wing panel for angles of attack of approximately 2, and wing apex vorticies become apparent for alpha $>$ or $=$ 4 deg. However, the occurrence of the leading edge vortex flow may be postponed with leading edge devices. Of the devices considered, the most promising were a simple leading edge deflection of 30 deg and a leading edge slat system. The trailing edge flap effectiveness was found to be

essentially the same for the configuration employing either of these more promising leading edge devices. Analysis of the lateral directional data showed that for all of the concepts considered, deflecting leading edge downward in an attempt to postpone leading edge vortex flows, has the favorable effect of reducing the effective dihedral. B.W.

N85-22366*# National Aeronautics and Space Administration. Langley Research Center, Hampton, Va.
THE APPLICATION OF SOME LIFTING-BODY REENTRY CONCEPTS TO MISSILE DESIGN
M. Leroy Spearman Mar. 1985 29 p refs Presented at the AIAA 23rd Aerospace Sci. Meeting, Reno, Nev., 14-17 Jan. 1985 Previously announced in IAA as A85-19791
(NASA-TM-86394; NAS 1.15:86394; AIAA-85-0497) Avail: NTIS HC A03/MF A01 CSCL 01A

The aerodynamic characteristics of some lifting-body concepts are examined with a view to the applicability of such concepts to the design of missiles. A considerable amount of research has been done in past years with vehicle concepts suitable for manned atmospheric-entry and atmospheric flight. Some of the concepts appear to offer some novel design approaches for missiles for a variety of missions and flight profiles, including long-range orbital/reentry with transatmospheric operation for strategic penetration, low altitude penetration, and battlefield tactical. The concepts considered include right triangular pyramidal configurations, a lenticular configuration, and various 75-degree triangular planform configurations with variations in body camber and control systems. The aerodynamic features are emphasized but some observations are also made relative to other factors such as heat transfer, structures, carriage, observability, propulsion, and volumetric efficiency. Author

N85-22367*# Kansas Univ., Lawrence. The Flight Research Lab.
CALCULATION OF VORTEX-FLAP AERODYNAMIC CHARACTERISTICS Status Report, 1 Oct. 1984 - 31 Mar. 1985
C. Edward Lan and C. C. Hsing 22 Apr. 1985 7 p refs
(Grant NAG1-396)
(NASA-CR-175624; NAS 1.26:175624) Avail: NTIS HC A02/MF A01 CSCL 01A

The lateral-directional characteristics for configurations with vortex flaps were calculated by the VORSTAB code. In view of the poor correlation between the VORSTABL results and the data, it was decided to examine in detail the reasons behind the discrepancy. After corrections in the data, the characteristics were recalculated. The prediction of dihedral effect is now largely improved. B.G.

N85-22368*# Hamilton Standard, Windsor Locks, Conn.
LARGE-SCALE ADVANCED PROPFAN (LAP) PERFORMANCE, ACOUSTIC AND WEIGHT ESTIMATION, JANUARY, 1984
D. Parzych, A. Shenkman, and S. Cohen Feb. 1985 61 p
(Contract NAS3-23051)
(NASA-CR-174782; NAS 1.26:174782; SP-06A83) Avail: NTIS HC A04/MF A01 CSCL 01A

In comparison to turbo-prop applications, the Prop-Fan is designed to operate in a significantly higher range of aircraft flight speeds. Two concerns arise regarding operation at very high speeds: aerodynamic performance and noise generation. This data package covers both topics over a broad range of operating conditions for the eight (8) bladed SR-7L Prop-Fan. Operating conditions covered are: Flight Mach Number 0 - 0.85; blade tip speed 600-800 ft/sec; and cruise power loading 20-40 SHP/D2. Prop-Fan weight and weight scaling estimates are also included. Author

N85-22369*# Vigyan Research Associates, Inc., Hampton, Va.
METHOD FOR THE PREDICTION OF THE INSTALLATION AERODYNAMICS OF A PROPFAN AT SUBSONIC SPEEDS Final Report, 1 Aug. 1981 - 31 Dec. 1984
B. Chandrasekaran Washington NASA Apr. 1985 124 p refs
(Contract NAS1-16742)
(NASA-CR-3887; NAS 1.26:3887) Avail: NTIS HC A06/MF A01 CSCL 01A

A subsonic flow panel code has been modified to handle the effects of a propeller wake. The effects of the propeller were modelled by a system of ring vortices of constant strength. Principles based on the blade element theory, the vortex theory and the momentum theory were used to evaluate the axial velocity increase, the swirl velocity and the pressure increase across the propeller. Theoretical calculations are compared to experimental results at Mach numbers up to 0.70 over a range of angles of attack. The discrepancies between the theory and the experimental results are analyzed. Suggestions for improvements to enhance the accuracy of the theoretical prediction are indicated. Author

N85-22370*# National Aeronautics and Space Administration. Langley Research Center, Hampton, Va.
AERODYNAMIC HEATING RATE DISTRIBUTIONS INDUCED BY TRAILING EDGE CONTROLS ON HYPERSONIC AIRCRAFT CONFIGURATIONS AT MACH 8
Louis G. Kaufman, II (Grumman Aerospace Corp., Bethpage, N.Y.) and Charles B. Johnson Aug. 1984 186 p refs
(NASA-TM-87453; RM-799; NAS 1.15:87453) Avail: NTIS HC A09/MF A01 CSCL 01A

Aerodynamic surface heating rate distributions in three dimensional shock wave boundary layer interaction flow regions are presented for a generic set of model configurations representative of the aft portion of hypersonic aircraft. Heat transfer data were obtained using the phase change coating technique (paint) and, at particular spanwise and streamwise stations for sample cases, by the thin wall transient temperature technique (thermocouples). Surface oil flow patterns are also shown. The good accuracy of the detailed heat transfer data, as attested in part by their repeatability, is attributable partially to the comparatively high temperature potential of the NASA-Langley Mach 8 Variable Density Tunnel. The data are well suited to help guide heating analyses of Mach 8 aircraft, and should be considered in formulating improvements to empiric analytic methods for calculating heat transfer rate coefficient distributions. Author

N85-22371*# George Washington Univ., Washington, D.C. School of Engineering and Applied Science.
ON THE SOLUTION OF THE THREE-DIMENSIONAL FLOWFIELD ABOUT A FLOW-THROUGH NACELLE Ph.D. Thesis
William Bernard Compton, III 5 May 1985 159 p refs
(NASA-TM-87448; NAS 1.15:87448) Avail: NTIS HC A08/MF A01 CSCL 01A

The solution of the three dimensional flow field for a flow through nacelle was studied. Both inviscid and viscous inviscid interacting solutions were examined. Inviscid solutions were obtained with two different computational procedures for solving the three dimensional Euler equations. The first procedure employs an alternating direction implicit numerical algorithm, and required the development of a complete computational model for the nacelle problem. The second computational technique employs a fourth order Runge-Kutta numerical algorithm which was modified to fit the nacelle problem. Viscous effects on the flow field were evaluated with a viscous inviscid interacting computational model. This model was constructed by coupling the explicit Euler solution procedure with a flag entrainment boundary layer solution procedure in a global iteration scheme. The computational techniques were used to compute the flow field for a long duct turbofan engine nacelle at free stream Mach numbers of 0.80 and 0.94 and angles of attack of 0 and 4 deg. Author

N85-22372# Royal Aircraft Establishment, Farnborough (England).
INVESTIGATIONS INTO THE EFFECTS OF SCALE AND COMPRESSIBILITY ON LIFT AND DRAG IN THE RAE 5m PRESSURISED LOW-SPEED WIND TUNNEL
S. P. Fiddes, D. A. Kirby, D. S. Woodward, and D. H. Peckham Jun. 1984 22 p refs
(RAE-TM-AERO-2006; BR93111) Avail: NTIS HC A02/MF A01

Results from experiments in a 5m low speed wind tunnel capable of operation over pressures from 1 to 3 atm so that the

effects of Mach and Reynolds number may be separated are presented. This decoupling of scale and compressibility effects enables reliable extrapolation of test results to full-scale conditions and gives greater insight into the underlying flow mechanisms. The large size of the tunnel, combined with pressurization to 3 atm enables tests on small combat/trainer aircraft and on bomblike stores to be carried out at full scale. Prediction and improvement of the high-lift performance of specific aircraft; optimization of high-lift devices on generalized research models; and work on the drag of stores carried externally on combat aircraft are discussed. Author (ESA)

N85-22790# Joint Publications Research Service, Arlington, Va.
METHOD FOR PROMPT MODELING OF QUASIPERIODIC-MOVEMENT OF SOLID NEAR-AXISYMMETRICAL BODY IN ATMOSPHERE Abstract Only
V. M. Belokonov, I. V. Belokonov, and Yu. M. Zabolotnov *In its* USSR Rept.: Eng. and Equipment (JPRS-UEQ-85-003) 12 Mar. 1985 p 8 Transl. into ENGLISH from Izv. Akad. Nauk SSSR: Mekhan. Tverdogo Tela (Moscow), no. 2, Feb. 1984 p 43-50 (For primary document see N85-22782 13-31)
Avail: NTIS HC A06

N85-22791# Joint Publications Research Service, Arlington, Va.
FLIGHT DYNAMICS OF AXISYMMETRICAL ROTATING BODIES IN AIR MEDIUM Abstract Only
I. T. Borisenok, B. Ya. Lokshin, and V. A. Privalov *In its* USSR Rept.: Eng. and Equipment (JPRS-UEQ-85-003) 12 Mar. 1985 p 8 Transl. into ENGLISH from Izv. Akad. Nauk SSSR: Mekhan. Tverdogo Tela (Moscow), no. 2, Feb. 1984 p 35-42 (For primary document see N85-22782 13-31)
Avail: NTIS HC A06

N85-22792# Joint Publications Research Service, Arlington, Va.
HYPERSONIC FLOW ABOUT TRIANGULAR AIRFOIL AT LARGE ANGLES OF ATTACK Abstract Only
V. N. Golubkin *In its* USSR Rept.: Eng. and Equipment (JPRS-UEQ-85-003) 12 Mar. 1985 p 9 Transl. into ENGLISH from Prikl. Mat. i Mekhan. (Moscow), v. 48, no. 3, May - Jun. 1984 p 376-382 (For primary document see N85-22782 13-31)
Avail: NTIS HC A06

N85-22793# Joint Publications Research Service, Arlington, Va.
ABSOLUTE STABILITY OF UNSTEADY MOVEMENT OF AXISYMMETRICAL ROTATING FLIGHT VEHICLE Abstract Only
V. I. Skorodinskiy *In its* USSR Rept.: Eng. and Equipment (JPRS-UEQ-85-003) 12 Mar. 1985 p 9 Transl. into ENGLISH from Izv. Akad. Nauk SSSR: Mekhan. Tverdogo Tela (Moscow), no. 3, May - Jun. 1984 p 17-21 (For primary document see N85-22782 13-31)
Avail: NTIS HC A06

03 AIR TRANSPORTATION AND SAFETY

Includes passenger and cargo air transport operations; and aircraft accidents.

For related information see also *16 Space Transportation* and *85 Urban Technology and Transportation.*

N85-22373*# National Aeronautics and Space Administration, Washington, D. C.
AEROSPACE SAFETY ADVISORY PANEL Annual Report, covering calendar year 1984
Jan. 1985 80 p
(NASA-TM-87426; NAS 1.15:87426) Avail: NTIS HC A05/MF A01 CSCL 13L

The following areas of NASA's responsibilities are examined: (1) the Space Transportation System (STS) operations and evolving program elements; (2) establishment of the Space Station program organization and issuance of requests for proposals to the aerospace industry; and (3) NASA's aircraft operations, including research and development flight programs for two advanced X-type aircraft. B.G.

N85-22374# Ametek, Santa Barbara, Calif. Offshore Research and Engineering Div.
AIRCRAFT SKIN PENETRATOR AND AGENT APPLICATOR. VOLUME 1: WORKING MODEL DEVELOPMENT AND CONSTRUCTION Final Report, 17 Sep. 1982 - 15 Mar. 1983
R. H. Cuthbertson Tyndall AFB, Fla. AF Engineering and Services Center Nov. 1984 64 p
(Contract F08635-82-C-0472)
(AD-A150498; AFESC/ESL-TR-84-12) Avail: NTIS HC A04/MF A01 CSCL 01/2

This report covers development of an aircraft skin penetrator device to provide rapid penetration and allow placement of a suitable fire-suppressing agent onto the base of the aircraft fire. Volume 1 discusses in detail the research conducted on the development of the proposed working model of the Aircraft Skin Penetrator/Agent Applicator. The report contains photographs of the different concepts considered. Volume 2 has detailed drawings showing the construction of the working model Penetrator and sketches which show how the Penetrator may be used to fight aircraft fires. GRA

04 AIRCRAFT COMMUNICATIONS AND NAVIGATION

Includes digital and voice communication with aircraft; air navigation systems (satellite and ground based); and air traffic control.

For related information see also *17 Spacecraft Communications, Command, and Tracking* and *32 Communications.*

N85-22375# Lincoln Lab., Mass. Inst. of Tech., Lexington.
TCAS II: DESIGN AND VALIDATION OF THE HIGH-TRAFFIC-DENSITY SURVEILLANCE SUBSYSTEM
William H. Herman and Robert S. Kennedy 12 Feb. 1985 157 p refs
(Contract DOT-FA77-WAI-817)
(DOT/FAA/PM-84/5; ATC-126) Avail: NTIS HC A08/MF A01

Lincoln Laboratory is developing an airborne collision avoidance system (TCAS II), concentrating primarily on the air-to-air surveillance sybsystem. The surveillance functions required are to detect the presence of nearby transponder equipped aircraft, and then generate a surveillance track on each aircraft, issuing range and altitude reports once per second. The development effort from mid-1981 to the present focused on the surveillance problems associated with high aircraft density. A number of surveillance techniques to deal with the high density environment were identified and evaluated mainly through airborne measurements. A TCAS II design was synthesized, and this design was subjected to in-flight testing in the Los Angeles Basin using a Boeing 727. Results indicate that the performance objectives were met. R.J.F.

N85-22376# Federal Aviation Administration, Washington, D.C.
PLANNED OFFICE AND FACILITY CONSOLIDATIONS: TO IMPROVE SYSTEM EFFECTIVENESS AND EFFICIENCY, FY 1985-87
1 Dec. 1984 106 p
(AD-A150441) Avail: NTIS HC A06/MF A01 CSCL 01/5

This revised plan, which was directed by House Report 98-1159 accompanying the FY-1985 Continuing Appropriations Resolution, has the same basic objectives as the FY-1984 effort. Perhaps the most important difference is that the need to implement it is even more compelling. The program outlined below updates the previously published plan for field office and facility consolidations, and encompasses actions through fiscal year 1987. Flight Service Station (FSS) Modernization/Consolidation, Airport Traffic Control Tower (ATCT) Closures, Consolidation of the Functions of the Terminal Radar Approach Control Facilities (TRACON) and

the Air Route Traffic Control Centers (ARTCC), Realignment of the Airway Facilities Sector Offices (AFSO's), Consolidation of Aviation Standards (AVS) Field Offices. GRA

N85-22358# Royal Aircraft Establishment, Farnborough (England).
REFERENCE SYSTEMS FOR THE EVALUATION OF DEAD-RECKONING NAVIGATION EQUIPMENT
R. F. Stokes and S. G. Smith *In* AGARD Ground and Flight Testing for Aircraft Guidance and Control Dec. 1984 17 p Original language document was announced as N84-34406 (For primary document see N85-22350 13-01)
Avail: NTIS HC A09/MF A01

N85-23131# Joint Publications Research Service, Arlington, Va.
USE OF THREE OMEGA RADIONAVIGATION SYSTEM POSITION LINES FOR SOLVING PROBLEMS IN MARINE GEODESY Abstract Only
V. A. Monakhov and I. A. Iordanskiy *In its* USSR Rept.: Earth Sci. (JPRS-UES-85-002) 1 Feb. 1985 p 28 Transl. into ENGLISH from Izv. Vyssh. Ucheb. Zaved.: Geod. i Aerofotosyemka (Moscow), no. 2, Mar. - Apr. 1984 p 26-30 (For primary document see N85-23116 13-42)
Avail: NTIS HC A07/MF A01

05 AIRCRAFT DESIGN, TESTING AND PERFORMANCE

Includes aircraft simulation technology.

For related information see also *18 Spacecraft Design, Testing and Performance* and *39 Structural Mechanics.*

N85-22377 Mississippi State Univ., Mississippi State.
DETERMINATION OF AERODYNAMIC AND PROPULSION PARAMETERS OF GENERAL AVIATION AIRCRAFT USING STEADY STATE FLIGHT TEST DATA Ph.D. Thesis
Mehdi Sabzehbarvar 1984 70 p
Avail: Univ. Microfilms Order No. DA8428151

The feasibility of identifying concurrently an aircraft's propulsive efficiency and aerodynamic drag parameters using the Gradient Search technique along with the application of Lock's propeller model was studied. The primary task was to perform a curve fitting process to represent the propeller blade lift and drag coefficients calculated by the extensive work that Lock conducted during the 1930's and 1940's. It was found that an iterative analysis was useful to reduce all the propeller chart interpolation into a numerical interpolation. The Gradient Search method was used to estimate the performance parameters because of stable convergence and its ability to handle the poor initial value guesses. For the present investigation, initial parameter guesses up to fifty percent off the actual values were tried and convergence was obtained within an accuracy of 2.0 percent in about fifty iterations. This parameter identification technique requires only steady state measurement of propeller blade angle and RPM, aircraft weight, speed, rate of climb, and atmospheric density. Dissert. Abstr.

N85-22378*# Lockheed-California Co., Burbank.
STUDY FOR THE OPTIMIZATION OF A TRANSPORT AIRCRAFT WING FOR MAXIMUM FUEL EFFICIENCY. VOLUME 1: METHODOLOGY, CRITERIA, AEROELASTIC MODEL DEFINITION AND RESULTS Final Report
N. A. Radovcich, D. Dreim, D. A. OKeefe, L. Linner, S. K. Pathak, J. S. Reaser, D. Richardson, J. Sweers, and F. Conner Jan. 1985 356 p refs
(Contract NAS1-16794)
(NASA-CR-172551; NAS 1.26:172551) Avail: NTIS HC A16/MF A01 CSCL 01C

Work performed in the design of a transport aircraft wing for maximum fuel efficiency is documented with emphasis on design criteria, design methodology, and three design configurations. The design database includes complete finite element model description, sizing data, geometry data, loads data, and inertial data. A design process which satisfies the economics and practical aspects of a real design is illustrated. The cooperative study relationship between the contractor and NASA during the course of the contract is also discussed. A.R.H.

N85-22379*# National Aeronautics and Space Administration. Langley Research Center, Hampton, Va.
TWO DEGREE-OF-FREEDOM FLUTTER SOLUTION FOR A PERSONAL COMPUTER
David L. Turnock Feb. 1985 43 p
(NASA-TM-86381; NAS 1.15:86381) Avail: NTIS HC A03/MF A01 CSCL 01C

A computer programmed flutter solution has been written in the BASIC language for a personal computer. The program is for two degree-of-freedom bending torsion flutter applications and utilizes two dimensional Theodorsen aerodynamics. The aerodynamics were modified to include approximations for Mach number (compressibility) effects and aspect ratio (finite span) effects. Input options, user instructions, program listing, and a test case application are included. Author

N85-22380*# National Aeronautics and Space Administration. Langley Research Center, Hampton, Va.
A DESCRIPTION OF THE LANGLEY WIREFRAME GEOMETRY STANDARD (LAWGS) FORMAT
Charlotte B. Craidon Feb. 1985 45 p refs
(NASA-TM-85767; Z-2; NAS 1.15:85767) Avail: NTIS HC A03/MF A01 CSCL 01A

The background leading to the adoption of a Langley Research Center wireframe geometry format standard, a detailed description of the standard, and recommendations for use of the standard is given. The standard chosen is flexible enough to describe almost any complex shape. Author

N85-22381*# National Aeronautics and Space Administration. Langley Research Center, Hampton, Va.
APPROACH FOR SERVICE LIFE EXTENSION OF EXPLOSIVE DEVICES FOR AIRCRAFT ESCAPE SYSTEMS
Laurence J. Bement and Morry L. Schimmel (McDonnell Aircraft Co., St. Louis, Mo.) Feb. 1985 23 p refs
(NASA-TM-86323; NAS 1.15:86323) Avail: NTIS HC A02/MF A01 CSCL 01C

The service life evaluation of explosive devices used in a wide variety of aircraft escape systems is described. The purpose was to develop a service extension approach, supported by tests on candidate devices, to evaluate the effects of service, age, and degradation, and allow responsible, conservative, service life determinations. An overview is given on the recommended approach and experimental procedures for accurate service evaluations with test results on rigid and flexible explosive transfer lines, one-way transfers, and flexible linear shaped charges. Author

N85-22382*# Georgia Inst. of Tech., Atlanta. Center for Rotary Wing Aircraft Technology.
SIMPLE THEORETICAL MODELS FOR COMPOSITE ROTOR BLADES Final Report
R. Rao Valisetty and Lawrence W. Rehfield Nov. 1984 35 p refs
(Grant NAG1-398)
(NASA-CR-175620; NAS 1.26:175620) Avail: NTIS HC A03/MF A01 CSCL 01C

The development of theoretical rotor blade structural models for designs based upon composite construction is discussed. Care was exercised to include a member of nonclassical effects that previous experience indicated would be potentially important to account for. A model, representative of the size of a main rotor blade, is analyzed in order to assess the importance of various influences. The findings of this model study suggest that for the slenderness and closed cell construction considered, the refinements are of little importance and a classical type theory is adequate. The potential of elastic tailoring is dramatically demon-

strated, so the generality of arbitrary ply layup in the cell wall is needed to exploit this opportunity. Author

N85-22383# Nielsen Engineering and Research, Inc., Mountain View, Calif.
PRELIMINARY DEVELOPMENT OF AN APPROXIMATION PROCEDURE FOR SUPERCRITICAL WING DESIGN OPTIMIZATION APPLICATIONS Final Report, 1 Jul. 1981 - 1 Nov. 1984
S. S. Stahara 28 Dec. 1984 47 p
(Contract N00014-81-C-0557)
(AD-A150177; NEAR-TR-337) Avail: NTIS HC A03/MF A01 CSCL 20/4

An investigation was carried out involving the preliminary development of an approximation procedure and associated computational codes for rapidly determining approximations to nonlinear, three-dimensional flow solutions, with the purpose of establishing a method for minimizing the computational work requirements associated with design optimization studies of supercritical wings. The results here concern the extension of a previously-developed successful approximation method for determining accurate approximations to two-dimensional nonlinear transonic flows involving the simultaneous change of multiple geometric and/or aerodynamic parameters. The specific development involves combination of the nonlinear approximation procedure with the FLO22 three-dimensional wing transonic flow solver together with the CONMIN optimization program in a configuration suitable for supercritical wing design/optimization studies. GRA

N85-22384# Joint Publications Research Service, Arlington, Va.
CHINA REPORT: SCIENCE AND TECHNOLOGY
26 Mar. 1984 37 p refs Transl. into ENGLISH from various Chinese articles
(JPRS-CST-84-008) Avail: NTIS HC A03/MF A01

An improved general purpose transport aircraft is described. Other areas of discussion are: Optimal design projects of various sizes in Shanghai; Research in microcirculation; Hemoorhagic fever research; Need for develop research on eugenics; and Organ transplants. For individual titles, see N85-22385 through N85-22386.

N85-22385# Joint Publications Research Service, Arlington, Va.
IMPROVED Y-11 GENERAL-PURPOSE TRANSPORT DESIGNATED Y-12
Xiong Wenjie *In its* Chaina Rept: Sci. and Technol. (JPRS-CST-84-008) 26 Mar. 1984 p 3-8 refs Transl. into ENGLISH from Guoji Hangkong (Beijing, China), no. 12, 5 Dec. 1983 p 2-4 (For primary document see N85-22384 13-05)
Avail: NTIS HC A03/MF A01

After extensive market research and analysis, certain improvements to the 'Y-11' so its performance can meet a wider range of additional requirements were made. This improved model is the 'Y-12' general purpose aircraft. The development plan of the 'Y-12' was finalized, actual design, and manufacturing and assembly of three prototypes began. The first successful flight of the 'Y-12' took place and at the present time, two of the aircraft are being used in full scale flight tests, and small scale production has began. The improved specifications are given and discussed. E.R.

N85-22386# Joint Publications Research Service, Arlington, Va.
OPTIMAL DESIGN EFFORTS IN SHANGHAI DESCRIBED c66
In its China Rept: Sci. and Technol. (JPRS-CST-84-008) 26 Mar. 1984 p 9-18 refs Transl. into ENGLISH from Yunchouxue Zazhi (Shanghai), no. 1, Oct. 1982 p 54-58 (For primary document see N85-22384 13-05)
Avail: NTIS HC A03/MF A01

The main areas affected by optimal design in Shanghai are: machinery, structures, motive power, electrical machinery, radio, optics, textiles, chemical engineering, railways, shipbuilding and construction. The techniques of optimal design are also being applied with excellent results to the solution of problems in biomedical engineering. Establishing an effective, solvable model based on the characteristics of the problem is a critical aspect of optimal design: this requires an analysis of the real problems under consideration. Selecting the proper optimization methods to deal with each specific problem also directly affects the results of optimal design efforts. Therefore, it is extremely important to master the applications nd techniques of all optimization computations. Some typical examples in different areas, involving different methods of solution, in the hope of promoting an exchange of experience are presented. Author

N85-22351*# National Aeronautics and Space Administration. Ames Research Center, Moffett Field, Calif.
SPACE SHUTTLE PILOT-INDUCED-OSCILLATION RESEARCH TESTING
Bruce G. Powers *In* AGARD Ground and Flight Testing for Aircraft Guidance and Control Dec. 1984 7 p refs Original language document was announced as N84-20566 (For primary document see N85-22350 13-01)
Avail: NTIS HC A09/MF A01 CSCL 01C

N85-22356*# National Aeronautics and Space Administration. Langley Research Center, Hampton, Va.
A FLIGHT MANAGEMENT ALGORITHM AND GUIDANCE FOR FUEL-CONSERVATIVE DESCENTS IN A TIME-BASED METERED AIR TRAFFIC ENVIRONMENT: DEVELOPMENT AND FLIGHT TEST RESULTS
Charles E. Knox *In* AGARD Ground and Flight Testing for Aircraft Guidance and Control Dec. 1984 17 p refs (For primary document see N85-22350 13-01)
Avail: NTIS HC A09/MF A01 CSCL 01C

N85-22359# Industrieanlagen-Betriebsgesellschaft m.b.H., Ottobrunn (West Germany).
AIR COMBAT SIMULATION: METHODS, MODELS, TRENDS
G. Wunderlich and H. P. Fehrenz *In* AGARD Ground and Flight Testing for Aircraft Guidance and Control Dec. 1984 17 p refs (For primary document see N85-22350 13-01)
Avail: NTIS HC A09/MF A01

N85-22360# Societe Nationale Industrielle Aerospatiale, Marignane (France). Avionics and Systems Group.
GROUND EVALUATION OF HELICOPTER AIR-TO-AIR WARFARE
G. Catani *In* AGARD Ground and Flight Testing for Aircraft Guidance and Control Dec. 1984 13 p (For primary document see N85-22350 13-01)
Avail: NTIS HC A09/MF A01

N85-22362*# National Aeronautics and Space Administration. Langley Research Center, Hampton, Va.
AIRLAB: A LABORATORY FOR FLIGHT-CRUCIAL-ELECTRONICS SYSTEM RESEARCH
H. Milton Holt, Dale G. Holden, and Amy O. Lupton *In* AGARD Ground and Flight Testing for Aircraft Guidance and Control Dec. 1984 12 p refs (For primary document see N85-22350 13-01)
Avail: NTIS HC A09/MF A01 CSCL 01C

N85-22784# Joint Publications Research Service, Arlington, Va.
REDESIGN OF FUSELAGE COMPARTMENTS BY METHOD OF SPECIAL CONTOURS Abstract Only
F. K. Chistyakov, V. V. Naykhanov, and A. A. Dubanov *In its* USSR Rept.: Eng. and Equipment (JPRS-UEQ-85-003) 12 Mar. 1985 p 1-2 Transl. into ENGLISH from Izv. Vyssh. Ucheb. Zaved.: Aviats. Tekhn. (Kazan, USSR), no. 1, Jan. - Mar. 1984 p 106-108 (For primary document see N85-22782 13-31)
Avail: NTIS HC A06

N85-22817# Joint Publications Research Service, Arlington, Va.
NORMAL MODE CALCULATIONS FOR FUSELAGE TYPE INTRICATE STRUCTURES BY REGARDING THEM AS SYSTEMS WITH SUPERPOSED CONSTRAINTS Abstract Only
V. Borisov *In its* USSR Rept.: Eng. and Equipment (JPRS-UEQ-85-003) 12 Mar. 1985 p 43 Transl. into ENGLISH from Izv. Vyssh. Ucheb. Zaved.: Aviats. Tekhn. (Kazan, USSR), no. 1, Jan. - Mar. 1984 p 102-105 (For primary document see

N85-22782 13-31)
Avail: NTIS HC A06

06 AIRCRAFT INSTRUMENTATION

Includes cockpit and cabin display devices; and flight instruments.

For related information see also *19 Spacecraft Instrumentation* and *35 Instrumentation and Photography.*

N85-22387*# Analytical Mechanics Associates, Inc., Mountain View, Calif.
ANALYSIS OF ESTIMATION ALGORITHMS FOR CDTI AND CAS APPLICATIONS Final Report
Tsuyoshi Goka Apr. 1985 216 p refs
(Contract NAS1-16135)
(NASA-CR-172444; NAS 1.26:172444) Avail: NTIS HC A10/MF A01 CSCL 01D

Estimation algorithms for Cockpit Display of Traffic Information (CDTI) and Collision Avoidance System (CAS) applications were analyzed and/or developed. The algorithms are based on actual or projected operational and performance characteristics of an Enhanced TCAS II traffic sensor developed by Bendix and the Federal Aviation Administration. Three algorithm areas are examined and discussed. These are horizontal x and y, range and altitude estimation algorithms. Raw estimation errors are quantified using Monte Carlo simulations developed for each application; the raw errors are then used to infer impacts on the CDTI and CAS applications. Applications of smoothing algorithms to CDTI problems are also discussed briefly. Technical conclusions are summarized based on the analysis of simulation results.
Author

N85-22388# Royal Signals and Radar Establishment, Malvern (England). Reliability and Environmental Engineering Section.
RELIABILITY PREDICTIONS FOR MILITARY AVIONICS. ROYAL SIGNALS AND RADAR ESTABLISHMENT RELIABILITY PREDICTION METHOD NO. 250
Sep. 1977 18 p
(BR69221) Avail: NTIS HC A02/MF A01

A prediction model for military avionics applications, 18 months after an equipment is first introduced, is presented. Base component failure rates, with maximum stress levels are presented. Factors influencing avionics reliability are outlined. Author (ESA)

N85-22354# Royal Aircraft Establishment, Bedford (England). Operational Systems Div.
CIVIL AVIONICS FLIGHT TESTING WITH THE RAE(B) BAC1-11
R. R. Newbery and P. England *In* AGARD Ground and Flight Testing for Aircraft Guidance and Control Dec. 1984 22 p refs Original contains color illustrations (For primary document see N85-22350 13-01)
Avail: NTIS HC A09/MF A01

N85-22357# Deutsche Forschungs- und Versuchsanstalt fuer Luft- und Raumfahrt, Brunswick (West Germany). Inst. fuer Flugfuehrung.
AVIONICS FLIGHT EVALUATION SYSTEM (AFES)
Karlheinz Hurrass *In* AGARD Ground and Flight Testing for Aircraft Guidance and Control Dec. 1984 9 p refs (For primary document see N85-22350 13-01)
Avail: NTIS HC A09/MF A01

07 AIRCRAFT PROPULSION AND POWER

Includes prime propulsion systems and systems components, e.g., gas turbine engines and compressors; and on-board auxiliary power plants for aircraft.

For related information see also *20 Spacecraft Propulsion and Power, 28 Propellants and Fuels,* and *44 Energy Production and Conversion.*

N85-22389 Defence Research Information Centre, Orpington (England).
OXIDATION RESISTANT MATERIALS FOR HOT GAS TURBINES AND JET ENGINES
K. Hauffe Oct. 1984 58 p refs Transl. into ENGLISH from Metall (West Germany), v. 36, no. 8, 1982 p 882-888 and v. 36, no. 10, 1982 p 1082-1087
(AD-B087399L; DRIC-T-7145; BR93288) Copyright. Avail: NTIS HC A04/MF A01 CSCL 21/5

The use of highly alloyed chromium and chromium-nickel steels in gas turbines operating at high temperatures and jet engines with isothermic and cyclic temperature guidance is discussed. Aluminum-containing nickel-chromium alloys are superior in their oxidation behavior to cobalt-chromium alloys. The presence of small amounts of halides and sulfur compounds in the combustion gases requires addition of compounds to the alloys to protect high-grade alloys against corrosion at high temperatures. To limit the expense of the alloys it is necessary to focus development on oxidation resistant layers coated on the basic alloy. Heat-resistant fiber reinforced composite material combined with oxidation resistant layers is of particular technical importance. The development of nonmetallic materials for high temperature use, particularly silicon nitride, silicon carbide and carbon or graphite, gives interesting results. Author (ESA)

N85-22390*# Oklahoma State Univ., Stillwater. School of Mechanical and Aerospace Engineering.
DEFLECTED JET EXPERIMENTS IN A TURBULENT COMBUSTOR FLOWFIELD Ph.D. Thesis Final Report
G. B. Ferrell and D. G. Lilley Feb. 1985 273 p refs
(Grant NAG3-549)
(NASA-CR-174863; NAS 1.26:174863) Avail: NTIS HC A12/MF A01 CSCL 21E

Experiments were conducted to characterize the time-mean and turbulent flow field of a deflected turbulent jet in a confining cylindrical crossflow. Jet-to-crossflow velocity ratios of 2, 4, and 6 were investigated, under crossflow inlet swirler vane angles of 0 (swirler removed), 45 and 70 degrees. Smoke, neutrally buoyant helium-filled soap bubbles, and multi-spark flow visualization were employed to highlight interesting features of the deflected jet, as well as the tracjectory and spread pattern of the jet. A six-position single hot-wire technique was used to measure the velocities and turbulent stresses in nonswirling crossflow cases. In these cases, measurements confirmed that the deflected jet is symmetrical about the vertical plan passing through the crossflow axis, and the jet penetration was found to be reduced from that of comparable velocity ratio infinite crossflow cases. In the swirling crossflow cases, the flow visualization techniques enabled gross flow field characterization to be obtained for a range of lateral jet-to-crossflow velocity ratios and a range of inlet swirl strengths in the main flow. Author

N85-22391*# Massachusetts Inst. of Tech., Cambridge. Gas Turbine Lab.
STRUCTURAL RESPONSE OF A ROTATING BLADED DISK TO ROTOR WHIRL Final Report
Edward F. Crawley Apr. 1985 140 p refs
(Grant NAG3-200)
(NASA-CR-175605; NAS 1.26:175605) Avail: NTIS HC A07/MF A01 CSCL 21E

A set of high speed rotating whirl experiments were performed in the vacuum of the MIT Blowdown Compressor Facility on the

MIT Aeroelastic Rotor, which is structurally typical of a modern high bypass ratio turbofan stage. These tests identified the natural frequencies of whirl of the rotor system by forcing its response using an electromagnetic shaker whirl excitation system. The excitation was slowly swept in frequency at constant amplitude for several constant rotor speeds in both a forward and backward whirl direction. The natural frequencies of whirl determined by these experiments were compared to those predicted by an analytical 6 DOF model of a flexible blade-rigid disk-flexible shaft rotor. The model is also presented in terms of nondimensional parameters in order to assess the importance of the interation between the bladed disk dynamics and the shaft-disk dynamics. The correlation between the experimental and predicted natural frequencies is reasonable, given the uncertainty involved in determining the stiffness parameters of the system. Author

N85-22392*# Case Western Reserve Univ., Cleveland, Ohio. Dept. of Mechanical and Aerospace Engineering.

DILUTION JET CONFIGURATIONS IN A REVERSE FLOW COMBUSTOR M.S. Thesis Final Report

James Zizelman Apr. 1985 214 p refs

(Grant NsG-3206)

(NASA-CR-174888; NAS 1.26:174888) Avail: NTIS HC A10/MF A01 CSCL 21E

Results of measurements of both temperature and velocity fields within a reverse flow combustor are presented. Flow within the combustor is acted upon by perpendicularly injected cooling jets introduced at three different locations along the inner and outer walls of the combustor. Each experiment is typified by a group of parameters: density ratio, momentum ratio, spacing ratio, and confinement parameter. Measurements of both temperature and velocity are presented in terms of normalized profiles at azimuthal positions through the turn section of the combustion chamber. Jet trajectories defined by minimum temperature and maximum velocity give a qualitative indication of the location of the jet within the cross flow. Results of a model from a previous temperature study are presented in some of the plots of data from this work. Author

N85-22393*# Jet Propulsion Lab., California Inst. of Tech., Pasadena.

LARGE AMPLITUDE FORCING OF A HIGH SPEED 2-DIMENSIONAL JET Interim Report, Jan. 1982 - Dec. 1983

L. Bernal and V. Sarohia 15 Dec. 1984 48 p refs Sponsored in part by Navy

(Contract NAS7-918)

(NASA-CR-175646; JPL-Pub-84-91; NAS 1.26:175646) Avail: NTIS HC A03/MF A01 CSCL 21E

The effect of large amplitude forcing on the growth of a high speed two dimensional jet was investigated experimentally. Two forcing techniques were utilized: mass flow oscillations and a mechanical system. The mass flow oscillation tests were conducted at Strouhal numbers from 0.00052 to 0.045, and peak to peak amplitudes up to 50 percent of the mean exit velocity. The exit Mach number was varied in the range 0.15 to 0.8. The corresponding Reynolds numbers were 8,400 and 45,000. The results indicate no significant change of the jet growth rate or centerline velocity decay compared to the undisturbed free jet. The mechanical forcing system consists of two counter rotating hexagonal cylinders located parallel to the span of the nozzle. Forcing frequencies up to 1,500 Hz were tested. Both symmetric and antisymmetric forcing can be implemented. The results for antisymmetric forcing showed a significant (75 percent) increase of the jet growth rate at an exit Mach number of 0.25 and a Strouhal number of 0.019. At higher rotational speeds, the jet deflected laterally. A deflection angle of 39 deg with respect to the centerline was measured at the maximum rotational speed. M.G.

N85-22394*# National Aeronautics and Space Administration. Ames Research Center, Moffett Field, Calif.

EFFECTS OF INLET DISTORTION ON A STATIC PRESSURE PROBE MOUNTED ON THE ENGINE HUB IN AN F-15 AIRPLANE

Donald L. Hughes, Lawrence P. Myers, and Karen G. Mackall 1985 23 p refs

(NASA-TP-2411; H-1182; NAS 1.60:2411) Avail: NTIS HC A02/MF A01 CSCL 21E

An inlet static pressure (PS2) probe was mounted on the hub of an F100 engine in an F-15 airplane. Flight test results showed that for low distortion conditions, the ratio of engine-face total pressure to static pressure agreed well with previous altitude facility data. Off-schedule operation of the inlet third ramp angle caused increased distortion of the inlet airflow during steady-state flight conditions. Data are shown for inlet third ramp excursions leading to engine stall. The relationships of inlet face total to static pressure ratio as a function of several distortion descriptors are also described. Author

N85-22395*# National Aeronautics and Space Administration. Langley Research Center, Hampton, Va.

IGNITION OF MIXTURES OF SiH SUB 4, CH SUB 4, O SUB 2, AND Ar OR N SUB 2 BEHIND REFLECTED SHOCK WAVES

Allen G. McLain, Casimir J. Jachimowski, and R. Clayton Rogers Apr. 1985 17 p refs

(NASA-TP-2415; L-15881; NAS 1.60:2415) Avail: NTIS HC A02/MF A01 CSCL 21E

Ignition delay times in mixtures of methane, silane, and oxygen diluted with argon and nitrogen were measured behind reflected shock waves generated in the chemical kinetic shock tube at Langley Research Center. The delay times were inferred from the rapid increase in pressure that occurs at ignition, and the ignition of methane was verified from the emission of infrared radiation from carbon dioxide. Pressures of 1.25 atm and temperatures from 1100 K to 1300 K were generated behind the reflected shocks; these levels are representative of those occurring within a supersonic Ramjet combustor. Expressions for the ignition delay time as a function of temperature were obtained from least squares curve fits to the data for overall equivalence ratios of 0.7 and 1.0. The ignition delay times with argon as the diluent were longer than those with nitrogen as the diluent. The infrared wavelength observations at 4.38 microns for carbon dioxide indicated that silane and methane ignited simultaneously (i.e., within the time resolution of the measurement). A combined chemical kinetic mechanism for mixtures of silane, methane, oxygen, and argon or nitrogen was assembled from one mechanism that accurately predicted the ignition of methane and a second mechanism that accurately predicted silane hydrogen ignition. Comparisons between this combined mechanism and experiment indicated that additional reactions, possibly between silyl and methyl fragments, are needed to develop a good silane methane mechanism. M.G.

N85-22396# Shell Research Ltd., Chester (England). Continuous Combustion Fuels Div.

THE INFLUENCE OF FUEL QUALITY UPON FLAME-TUBE TEMPERATURE AND FLAME RADIATION IN A MODEL GAS-TURBINE PRIMARY ZONE

T. T. Bowden and J. H. Pearson Feb. 1984 27 p refs

(Contract MIN-DEF-A45A/578)

(K233; BR91055) Avail: NTIS HC A03/MF A01

Fuels with hydrogen contents varying from 8.66% to 15.16% weight were burned under conditions simulating those occurring in aviation gas turbine engines. Flame-tube temperature and flame radiation were correlated against the inspection properties of hydrogen content, aromatics content and smoke point. All three criteria give good correlation, with hydrogen content providing the best. Results indicate that aromatic content may be an inappropriate specification requirement for fuels containing condensed bicyclic saturated hydrocarbons. Author (ESA)

N85-22397# Massachusetts Inst. of Tech., Cambridge. Gas Turbine Lab.

CURRENT PROBLEMS IN TURBOMACHINERY FLUID DYNAMICS Final Report, 1 Oct. 1981 - 30 Sep. 1984

E. M. Greitzer, J. L. Kerrebrock, W. T. Thompkins, J. E. McCune, and A. H. Epstein 3 Dec. 1984 55 p

(Contract F49620-82-K-0002)
(AD-A150533; AFOSR-85-0016TR) Avail: NTIS HC A04/MF A01 CSCL 21/5

A multiinvestigator program on problems of current interest in turbomachinery fluid dynamics is being conducted at the MIT Gas Turbine Laboratory. Within the scope of this effort, four different tasks, encompassing both design and off design programs, have been identified. These are: (1) Investigation of fan and compressor design point fluid dynamics (including formation of design procedures using current 3-D transonic codes and development of advanced measurement techniques for use in transonic fans); (2) Studies of basic mechanisms of compressor stability enhancement using compressor cassing/hub treatment; (3) Fluid mechanisms of inlet vortex flow distortions in the gas turbine engines; (4) Investigations of 3-D analytical and numerical computations of flows in highly loaded turbomachinery blading. GRA

N85-22823# Joint Publications Research Service, Arlington, Va.
EFFICIENCY OF ALGORITHMS FOR GAS-AIR CHANNEL DIAGNOSTICS IN GAS TURBINE ENGINES BASED ON GAS THERMODYNAMIC PARAMETERS Abstract Only
A. M. Akhmedzyanov and K. F. Galiullin *In its* USSR Rept.: Eng. and Equipment (JPRS-UEQ-85-003) 12 Mar. 1985 p 80 Transl. into ENGLISH from Izv. Vyssh. Ucheb. Zaved.: Aviats. Tekhn. (Kazan, USSR), no. 1, Jan. - Mar. 1984 p 7-13 (For primary document see N85-22782 13-31)
Avail: NTIS HC A06

N85-22825# Joint Publications Research Service, Arlington, Va.
EXERGETICAL ANALYSIS OF TURBOJET ENGINE CYCLE Abstract Only
K. A. Malinovskiy *In its* USSR Rept.: Eng. and Equipment (JPRS-UEQ-85-003) 12 Mar. 1985 p 81-82 Transl. into ENGLISH from Izv. Vyssh. Ucheb. Zaved.: Aviats. Tekhn. (Kazan, USSR), no. 1, Jan. - Mar. 1984 p 32-37 (For primary document see N85-22782 13-31)
Avail: NTIS HC A06

N85-22826# Joint Publications Research Service, Arlington, Va.
ENERGY LOSSES AT LEADING EDGE OF TURBINE BLADE DURING MULTIROW JET COOLING Abstract Only
V. V. Rumyantsev and I. P. Makov *In its* USSR Rept.: Eng. and Equipment (JPRS-UEQ-85-003) 12 Mar. 1985 p 82 Transl. into ENGLISH from Izv. Vyssh. Ucheb. Zaved.: Aviats. Tekhn. (Kazan, USSR), no. 1, Jan. - Mar. 1984 p 37-40 (For primary document see N85-22782 13-31)
Avail: NTIS HC A06

N85-22827# Joint Publications Research Service, Arlington, Va.
EXPERIMENTAL DETERMINATION OF OPTIMUM RATIO OF RUNNER BLADE HEIGHT AT EXIT TO RUNNER BLADE HEIGHT AT ENTRANCE OF RADIAL INWARD-FLOW MICROTURBINES Abstract Only
N. T. Tikhonov, A. N. Tikhonov, and V. N. Matveyev *In its* USSR Rept.: Eng. and Equipment (JPRS-UEQ-85-003) 12 Mar. 1985 p 83 Transl. into ENGLISH from Izv. Vyssh. Ucheb. Zaved.: Aviats. Tekhn. (Kazan, USSR), no. 1, Jan. - Mar. 1984 p 40-44 Original language document previously announced as A84-47559 (For primary document see N85-22782 13-31)
Avail: NTIS HC A06

N85-22828# Joint Publications Research Service, Arlington, Va.
SOME UNIQUE FEATURES IN OPERATION OF TWO-STAGE TURBOJET ENGINE WITH AFTERBURNER Abstract Only
B. D. Fishbeyn *In its* USSR Rept.: Eng. and Equipment (JPRS-UEQ-85-003) 12 Mar. 1985 p 83-84 Transl. into ENGLISH from Izv. Vyssh. Ucheb. Zaved.: Aviats. Tekhn. (Kazan, USSR), no. 1, Jan. - Mar. 1984 p 45-49 (For primary document see N85-22782 13-31)
Avail: NTIS HC A06

N85-22829# Joint Publications Research Service, Arlington, Va.
HYDRODYNAMIC SIMULATION OF TRANSIENT PROCESSES IN INJECTION SYSTEM OF AIRCRAFT ENGINES DURING PUMP UNSWIRLING Abstract Only
V. V. Chervakov, N. S. Yershov, and B. V. Ovsyannikov *In its* USSR Rept.: Eng. and Equipment (JPRS-UEQ-85-003) 12 Mar. 1985 p 84 Transl. into ENGLISH from Izv. Vyssh. Ucheb. Zaved.: Aviats. Tekhn. (Kazan, USSR), no. 1, Jan. - Mar. 1984 p 49-54 Original language document previously announced as A84-47561 (For primary document see N85-22782 13-31)
Avail: NTIS HC A06

N85-22830# Joint Publications Research Service, Arlington, Va.
EFFECT OF WATER INJECTION INTO AIR FOR TURBINE COOLING ON ECONOMY OF OPERATION OF GAS TURBINE ENGINE WITH AFTERBURNING Abstract Only
G. M. Gorelov, V. P. Danilchenko, and V. Ye. Reznik *In its* USSR Rept.: Eng. and Equipment (JPRS-UEQ-85-003) 12 Mar. 1985 p 85 Transl. into ENGLISH from Izv. Vyssh. Ucheb. Zaved.: Aviats. Tekhn. (Kazan, USSR), no. 1, Jan. - Mar. 1984 p 81-83 (For primary document see N85-22782 13-31)
Avail: NTIS HC A06

N85-22832# Joint Publications Research Service, Arlington, Va.
ANNULAR GROOVE IN COMPRESSOR CASING AS DEVICE FOR CONTROL OF AIR STREAM Abstract Only
V. N. Yershov, A. P. Yefimenko, and V. Yu. Nezym *In its* USSR Rept.: Eng. and Equipment (JPRS-UEQ-85-003) 12 Mar. 1985 p 86 Transl. into ENGLISH from Izv. Vyssh. Ucheb. Zaved.: Aviats. Tekhn. (Kazan, USSR), no. 1, Jan. - Mar. 1984 p 85-86 (For primary document see N85-22782 13-31)
Avail: NTIS HC A06

N85-22833# Joint Publications Research Service, Arlington, Va.
EXPERIMENTALLY DETERMINED CHARACTERISTICS OF VORTEX HEATERS Abstract Only
Sh. A. Piralishvili and N. N. Novikov *In its* USSR Rept.: Eng. and Equipment (JPRS-UEQ-85-003) 12 Mar. 1985 p 86-87 Transl. into ENGLISH from Izv. Ucheb. Zaved.: Aviats. Tekhn. (Kazan, USSR), no. 1, Jan. - Mar. 1984 p 93-95 (For primary document see N85-22782 13-31)
Avail: NTIS HC A06

N85-22834# Joint Publications Research Service, Arlington, Va.
MATHEMATICAL MODELING OF TRANSIENT PERFORMANCE OF GAS TURBINE ENGINE Abstract Only
Yu. A. Skortsov *In its* USSR Rept.: Eng. and Equipment (JPRS-UEQ-85-003) 12 Mar. 1985 p 87 Transl. into ENGLISH from Izv. Vyssh. Ucheb. Zaved.: Aviats. Tekhn. (Kazan, USSR), no. 1, Jan. - Mar. 1984 p 96-98 (For primary document see N85-22782 13-31)
Avail: NTIS HC A06

N85-22838# Joint Publications Research Service, Arlington, Va.
ESTIMATION OF GAS TURBINE ENGINE BOOST PROVIDED BY INJECTING WATER BEHIND COMPRESSOR Abstract Only
A. N. Prokofyev *In its* USSR Rept.: Eng. and Equipment (JPRS-UEQ-85-003) 12 Mar. 1985 p 90 Transl. into ENGLISH from Izv. Vyssh. Ucheb. Zaved.: Mashinostr. (Moscow), no. 4, Apr. 1984 p 80-82 (For primary document see N85-22782 13-31)
Avail: NTIS HC A06

08 AIRCRAFT STABILITY AND CONTROL

Includes aircraft handling qualities; piloting; flight controls; and autopilots.

N85-22398*# Stanford Univ., Calif. Electronics Labs.
MODEL REDUCTION FOR CONTROL SYSTEM DESIGN Final Report
Dale Enns Mar. 1985 305 p refs
(Grant NAG2-223)

(NASA-CR-170417; NAS 1.26:170417) Avail: NTIS HC A14/MF A01 CSCL 01C

An approach and a technique for effectively obtaining reduced order mathematical models of a given large order model for the purposes of synthesis, analysis and implementation of control systems is developed. This approach involves the use of an error criterion which is the H-infinity norm of a frequency weighted error between the full and reduced order models. The weightings are chosen to take into account the purpose for which the reduced order model is intended. A previously unknown error bound in the H-infinity norm for reduced order models obtained from internally balanced realizations was obtained. This motivated further development of the balancing technique to include the frequency dependent weightings. This resulted in the frequency weighted balanced realization and a new model reduction technique. Two approaches to designing reduced order controllers were developed. The first involves reducing the order of a high order controller with an appropriate weighting. The second involves linear quadratic Gaussian synthesis based on a reduced order model obtained with an appropriate weighting. Author

N85-22352# Deutsche Forschungs- und Versuchsanstalt fuer Luft- und Raumfahrt, Brunswick (West Germany). Inst. fuer Flugmechanik.

DYNAMIC WIND TUNNEL TESTING FOR ACTIVE CONTROL RESEARCH

K. Wilhelm and B. Gmelin *In* AGARD Ground and Flight Testing for Aircraft Guidance and Control Dec. 1984 26 p refs (For primary document see N85-22350 13-01)
Avail: NTIS HC A09/MF A01

N85-22353*# National Aeronautics and Space Administration. Langley Research Center, Hampton, Va.

DYNAMIC WIND-TUNNEL TESTING OF ACTIVE CONTROLS BY THE NASA LANGLEY RESEARCH CENTER

Irving Abel, Robert V. Doggett, Jerry R. Newsom, and Maynard Sandford *In* AGARD Ground and Flight Testing for Aircraft Guidance and Control Dec. 1984 23 p refs (For primary document see N85-22350 13-01)
Avail: NTIS HC A09/MF A01 CSCL 01C

N85-22355# Deutsche Forschungs- und Versuchsanstalt fuer Luft- und Raumfahrt, Brunswick (West Germany).

GUIDANCE AND CONTROL RESEARCH FLIGHT TESTING WITH HFB 320 TEST AIRCRAFT

V. Adam and W. Lechner *In* AGARD Ground and Flight Testing for Aircraft Guidance and Control Dec. 1984 13 p refs (For primary document see N85-22350 13-01)
Avail: NTIS HC A09/MF A01

N85-22361# Messerschmitt-Boelkow-Blohm G.m.b.H., Munich (West Germany). Military Aircraft Div.

TESTING OF THE DIGITAL FLIGHT CONTROL SYSTEM OF THE GERMAN CCV FIGHTER EXPERIMENTAL AIRCRAFT

Udo Korte *In* AGARD Ground and Flight Testing for Aircraft Guidance and Control Dec. 1984 12 p refs Original language document was announced as N83-22110 (For primary document see N85-22350 13-01)
Avail: NTIS HC A09/MF A01

09 RESEARCH AND SUPPORT FACILITIES (AIR)

Includes airports, hangars and runways; aircraft repair and overhaul facilities; wind tunnels; shock tube facilities; and engine test blocks.

For related information see also *14 Ground Support Systems and Facilities (Space).*

N85-22399 Oklahoma State Univ., Stillwater.

CALIBRATION OF WIND TUNNEL FLOW QUALITY

Ph.D. Thesis

Ayman Said Abu-Mostafa 1984 128 p
Avail: Univ. Microfilms Order No. DA8427638

Preston-tube measurements on a transition cone were corrected and used to derive a calibration procedure for the 11-ft TWT flow quality. This procedure was applied to the corrected laminar data, and an effective freestream unit Reynolds number was defined by requiring a matching of the average Preston-tube pressure in flight and in the 11-TWT. Results show the operating Reynolds number is below the effective value. The distribution of this effective Reynolds number correlates well with the tunnel noise. Analyses of transitional and turbulent data, however, did not result in effective Reynolds numbers that can be correlated with noise since vorticity fluctuations present in transitional and turbulent boundary layers dominate and mask the effects of tunnel noise on Preston-tube measurements. So, in order to calibrate the effects of noise on transonic wind tunnel tests, only laminar data should be used. To calibrate the effects of transonic wind-tunnel noise on drag measurements, the Preston-tube data must be supplemented with direct measurements of skin friction. Such data could be used in the subject procedure to define equivalent flight unit Reynolds numbers which would result in a matching of the average, laminar skin friction. Dissert. Abstr.

N85-22400*# Mechanical Technology, Inc., Latham, N. Y.

DEVELOPMENT OF A MULTIPLANE MULTISPEED BALANCING SYSTEM FOR TURBINE SYSTEMS

Michael R. Martin 19 Jul. 1984 114 p refs
(Contract NAS3-20609)
(NASA-CR-174750; NAS 1.26:174750; MTI-84TR39) Avail: NTIS HC A06/MF A01 CSCL 14B

A prototype high speed balancing system was developed for assembled gas turbine engine modules. The system permits fully assembled gas turbine modules to be operated and balanced at selected speeds up to full turbine speed. The balancing system is a complete stand-alone system providing all necesary lubrication and support hardware for full speed operation. A variable speed motor provides the drive power. A drive belt and gearbox provide rotational speeds up to 21,000 rpm inside a vacuum chamber. The heart of the system is a dedicated minicomputer with attendant data acquisition, storage and I/O devices. The computer is programmed to be completely interactive with the operator. The system was installed at CCAD and evaluated by testing 20 T55 power turbines and 20 T53 power turbines. Engine test results verified the performance of the high speed balanced turbines. B.W.

N85-22401*# National Aeronautics and Space Administration. Langley Research Center, Hampton, Va.

CRYOGENIC WIND TUNNELS: A SELECTED ANNOTATED BIBLIOGRAPHY

Marie H. Tuttle (Vigyan Research Associates, Inc., Hampton, Va.), Robert A. Kilgore, and Peggy D. McGuire Apr. 1985 71 p
(NASA-TM-86346; L-15915; NAS 1.15:86346) Avail: NTIS HC A04/MF A01 CSCL 14B

This selected, annotated bibliography supersedes three previous bibliographies--NASA TM-80168 (Oct. 1979), Supplement to NASA TM-80168 (May 1980), and NASA TM-84474 (Sept. 1982). There are 376 entries, 109 of which have been added in this updated version. Selection for inclusion was made with consideration of usefulness of the document to persons interested in building or using a cryogenic wind tunnel. A cryogenic wind tunnel is defined as one which operates with test gas stagnation temperature below 150 K. Publications of historical interest are included that are directly related to key events in the evolution of the cryogenic wind tunnel. The arrangement is chronological by date of publication in the case of reports and by presentation in the case of papers. B.W.

N85-22849# Joint Publications Research Service, Arlington, Va.

CARD'S LOW-SPEED WIND TUNNEL DESCRIBED

Wang Maoxun and Pan Ruikang *In its* Chinese Rept: Sci. and Technol. (JPRS-CST-85-005) 20 Feb. 1985 p 160-166 refs

Transl. into ENGLISH from Guoji Hangkong (Beijing, China), no. 10, 5 Oct. 1984 p 2-4 (For primary document see N85-22843 13-31)
Avail: NTIS HC A10/MF A01

12 ASTRONAUTICS (GENERAL)

For extraterrestrial exploration see *91 Lunar and Planetary Exploration.*

N85-22402*# National Aeronautics and Space Administration, Washington, D. C.
D-1 REPORT: THE FIRST GERMAN SPACELAB MISSION
Feb. 1985 13 p Transl. into ENGLISH of "D-1 Report Die Erste Deutsche Spacelab Mission" Linder Hoehe, West Germany, no. 1, Oct. 1984 p 1-4 Transl. by Scientific Translation Service, Santa Barbara, Calif. Original doc. prep. by German Res. and Testing Inst. for Aeron. and Astron.
(Contract NASw-4004)
(NASA-TM-77637; NAS 1.15:77637) Avail: NTIS HC A02/MF A01 CSCL 22A

Introduction of a new popular magazine on the DI mission, the first West German Space mission. The DI project office publishes the magazine. The German sponsored astronauts are to study the gravitational effects of reduced gravity on the human generated processes of the environment. Other areas of concern are boundary surface and transport phenomena, physical chemisty and process engineering, metals and composite materials, and single crystals. E.R.

N85-22403# Joint Publications Research Service, Arlington, Va.
USSR REPORT: SPACE
4 Feb. 1985 128 p Transl. into ENGLISH from various Russian articles
(JPRS-USP-85-001) Avail: NTIS HC A07

News items, abstracts, and scientific reports on aspects of space including life sciences; interplanetary sciences; space policy and administration; launch table; space applications; space sciences; and manned mission highlights are discussed. For individual titles, see N85-22404 through N85-22457.

N85-22404# Joint Publications Research Service, Arlington, Va.
TASS UPDATE ON UNMANNED FLIGHT OF SALYUT-7 c54
In its USSR Rept.: Space (JPRS-USP-85-001) 4 Feb. 1985 p 3-10 Transl. into ENGLISH from Izvestiya (USSR), 20 Dec. 1984 p 1 (For primary document see N85-22403 13-12)
Avail: NTIS HC A07

The relationships between man and automation in space are examined. The advantages and disadvantages of all automation, all human control, and a man machine interplay are discussed. Also considered were spacecraft control modes; automation in the first space flights; work on orbital complexed; and the flight control center. B.G.

N85-22405# Joint Publications Research Service, Arlington, Va.
LYAKHOV AND ALEKSANDROV ON 150-DAY FLIGHT
V. A. Lyakhov and A. P. Aleksandrov *In its* USSR Rept.: Space (JPRS-USP-85-001) 4 Feb. 1985 p 11-17 Transl. into ENGLISH from Zemlya i Vselennaya (USSR), no. 3, May-Jun. 1984 p 5-11 (For primary document see N85-22403 13-12)
Avail: NTIS HC A07

During the second expedition aboard the Salyut-7 station more than 300 experiments were carried out in the fields of astronomy, geophysics, medicine, bioengineering, biology, as well as visual observations to study Earth's natural resources. Highlights of the experiments are described. B.G.

N85-22406# Joint Publications Research Service, Arlington, Va.
COMMENTS ON SALYUT-7 150-DAY FLIGHT
K. P. Feoktistov and A. A. Longov *In its* USSR Rept.: Space (JPRS-USP-85-001) 4 Feb. 1985 p 18-24 Transl. into ENGLISH from Zemlya i Vselennaya (USSR), no. 3, May-Jun. 1984 p 10-16 (For primary document see N85-22403 13-12)
Avail: NTIS HC A07

Long orbital space flights require the presence of men onboard to analyze rapidly changing situations, to make unordinary decisions, to change conditions for the implementation of experiments, to regulate equipment, to intervene routinely in transpiring processes, and to carry out repair and preventive maintenance work. All problems to be solved aboard the orbital complex can be arbitrarily broken down into four groups: investigations, experiments, and tests of scientific equipment; industrial production; effects on the human body under spaceflight conditions; and improvement of space technology. The second long term expedition on Salyut-7 station provided work in all four groups. B.G.

N85-22407# Joint Publications Research Service, Arlington, Va.
PLANS FOR INTERBOL SATELLITE EXPERIMENT Abstract Only
Y. Gordeyev *In its* USSR Rept.: Space (JPRS-USP-85-001) 4 Feb. 1985 p 25 Transl. into ENGLISH from Moskovskiy Komsomolets (USSR), 7 Oct. 1984 p 4 (For primary document see N85-22403 13-12)
Avail: NTIS HC A07

In the Interbol project, measurements will be made simultaneously in various regions of near Earth space, and the condition of the solar wind and the magnetosphere is to be monitored. This is expected to shed light on cause and effect relationships among a number of processes which are little understood as yet. These studies will be conducted with the aid of a complex consisting of a satellite of the Prognoz series and a subsatellite of the Magion type, which will fly at a certain distance from the Prognoz. Plans call for the launching of two such complexes, one of which will be placed into the tail of the magnetosphere, where magnetic field energy accumulates and plasma processes take place which convert this energy into electric energy. The second complex will simultaneously conduct measurements in three regions of the magnetosphere where plasma processes occur which give rise to polar auroras in the atmosphere and magnetic disturbances on Earth. Author

N85-22408# Joint Publications Research Service, Arlington, Va.
ALL-UNION CONFERENCE OF RADIO ASTRONOMERS c89
V. M. Kontorovich *In its* USSR Rept.: Space (JPRS-USP-85-001) 4 Feb. 1985 p 28-31 Transl. into ENGLISH from Zemlya i Vselennaya (USSR), no. 3, May-Jun. 1984 p 61-64 (For primary document see N85-22403 13-12)
Avail: NTIS HC A07

The role of radio astronomy in the study of the universe was examined. Topics included galactic models; radio galaxies; interferometer observations, remnants of supernovae; pulsars; interpulse emission at decameter wavelengths; stellar evolution; recombination lines of carbon carried out with the UTR-Z radio telescope; evolution of chemical and isotopic composition of the interstellar medium; red shifts; and radio scanning. B.G.

N85-22409# Joint Publications Research Service, Arlington, Va.
MODERN PROBLEMS IN POLARIMETRY OF SOLID SURFACES OF COSMIC BODIES Abstract Only c89
Y. G. Shkuratov, L. A. Arkimov, and V. P. Tishkovets *In its* USSR Rept.: Space (JPRS-USP-85-001) 4 Feb. 1985 p 32 Transl. into ENGLISH from Astronomicheskiy Vestnik (USSR), v. 18, no. 3, Jul.-Sep. 1984 p 163-178 (For primary document see N85-22403 13-12)
Avail: NTIS HC A07

Optical polarimetry is one of the least developed methods among those which can be employed in remote study of cosmic bodies not having an atmosphere. Recently increased interest in this method has been displayed by planetologists specializing in study of the composition and structure of solid planetary surfaces. Different sections are devoted to the following subjects: negative polarization of light (P sub min, alpha sub inv, alpha sub min parameters) and orientation of polarization plane; phase variation of negative polarization; correlation between negative polarization parameters and other optical characteristics; conditions for appearance of negative polarization (influence of surface structure);

Umov effect applicable to cosmic bodies without atmosphere; positive polarization of light (parameters alpha sub max, delta and h); circular polarization as promising direction in polarimetric study of cosmic bodies without atmosphere. In some cases, it is stressed, the second Stokes parameter should be used instead of the traditional degree of polarization. Various models of negative polarization are subjected to a critical analysis and some new experimental facts are presented. Author

N85-22410# Joint Publications Research Service, Arlington, Va.
EXPANSION OF FUNCTIONS DESCRIBING PLANETARY SURFACE AND GRAVITY FIELD Abstract Only c91
S. G. Valeyev *In its* USSR Rept.: Space (JPRS-USP-85-001) 4 Feb. 1985 p 33 Transl. into ENGLISH from Astronomicheskiy Vestnik (USSR), v. 18, no. 3, Jul.-Sep. 1984 p 208-214 (For primary document see N85-22403 13-12)
Avail: NTIS HC A07

The problem of description of the surface and gravity field of planets is examined using an expansion in spherical and other functions with particular consideration of the problem of expansion of lunar relief in spherical functions. The factors exerting an influence on approximating expressions can be divided into two groups. The first group includes errors generated by observational errors. Errors in the second group, generated by the mathematical description itself are stressed here. The approach used in solving the problem is statistical (regression) modeling. This approach is applied in an expansion of a function describing averaged surface relief by a number of spherical harmonics. The numerical example presented shows that the use of regression modeling makes it possible to obtain expansions with a number of terms approximately half as great as in the ordinary approach with the same or a higher descriptive accuracy. Also examined are the problems caused by the great dimensionality of the problems and the diversity of variants of initial data. The described approach gives adequate but economical models of relief and the gravity field. Author

N85-22411# Joint Publications Research Service, Arlington, Va.
AVERAGING OF EQUATIONS OF COMETARY ORBITAL MOTION WITH ALLOWANCE FOR NONGRAVITATIONAL EFFECTS Abstract Only c91
Y. N. Polyakhova *In its* USSR Rept.: Space (JPRS-USP-85-001) 4 Feb. 1985 p 33-34 Transl. into ENGLISH from Astronomicheskiy Vestnik (USSR), v. 18, no. 3, Jul.-Sep. 1984 p 235-239 (For primary document see N85-22403 13-12)
Avail: NTIS HC A07

A study was made of a Keplerian elliptical cometary orbit experiencing some nongravitational perturbing acceleration with the components S, T, W in an orbital coordinate system. After writing the equations for perturbed motion, the equations are averaged (this requires stipulation of the law of changes of perturbing nongravitational acceleration as a function of heliocentric distance r). A simplified law of continuous change in the components of reactive acceleration is selected and the rates of secular changes in the elements of the cometary orbit under the influence of nongravitational reactive acceleration are determined. Formulas are derived which can be used in predicting cometary orbits. It is shown that the components of relative velocity of gas escape can attain several kilometers per second. The estimates made by the proposed method are consistent with the high velocities of axial rotation of the nucleus of Halley's comet. With rapid rotation of the nucleus the radial gas jet initially directed toward the Sun as a result of thermal inertia continues to rotate together with the escape sector. B.W.

N85-22412# Joint Publications Research Service, Arlington, Va.
CORRELATION OF INTERPLANETARY MEDIUM PARAMETERS IN TRANSITION REGION OF HIGH-VELOCITY SOLAR WIND STREAMS Abstract Only c92
N. V. Mymrina, L. I. Dorman, N. S. Kaminer, and A. Y. Kuzmicheva *In its* USSR Rept.: Space (JPRS-USP-85-001) 4 Feb. 1985 p 34-35 Transl. into ENGLISH from Geomagnetizm i Aeronomiya (USSR), v. 24, no. 3, May-Jun. 1984 p 376-380 (For primary document see N85-22403 13-12)
Avail: NTIS HC A07

Investigations of variations in the intensity of galactic cosmic rays (GCR) during presence of the Earth in high velocity streams (HVS) of the solar wind which are associated with coronal holes have shown that the structure of HVS and characteristics of the medium exert a considerable influence on the distribution of cosmic rays in the interplanetary medium. The transition region between the quiet solar wind and HVS, where a significant anisotropy of cosmic rays arises, is of considerable importance. These phenomena were studied using data from the King catalogue for the period 1973-1974 (declining solar activity) when there was a great number of HVS, of which 62 with a velocity 500-800 km/sec were selected for analysis. This made it possible to obtain a number of relationships between the parameters of the streams. It was discovered that there is a close correlation between the transverse dimensions of the HVS and the maximum velocity of plasma in the stream. This agrees well with the known correlation between the dimensions of coronal holes and the velocity of HVS if it is assumed that the size of the coronal hole and the width of the HVS are closely correlated. B.W.

N85-22413# Joint Publications Research Service, Arlington, Va.
CHARACTERISTICS OF LATITUDE EFFECT ON COSMIC RAY CHARGED COMPONENT IN ATMOSPHERE AT ALTITUDES 3-5 KM Abstract Only c93
A. M. Altukhov, P. N. Ageshin, A. F. Krasotkin, V. A. Rogoshin, V. M. Senchenok, A. N. Charakhchyan, and T. N. Charakhchyan *In its* USSR Rept.: Space (JPRS-USP-85-001) 4 Feb. 1985 p 35-36 Transl. into ENGLISH from Geomagnetizm i Aeronomiya (USSR), v. 24, no. 3, May-Jun. 1984 p 386-392 Original language document announced as A84-40082 (For primary document see N85-22403 13-12)
Avail: NTIS HC A07

Measurements of the charged component of cosmic rays taken from aircraft in the height range 2-10 km over various parts of the Soviet Union are discussed. Reverse latitudinal effects of 5-10 percent in cosmic ray distribution are identified which have been observed for periods of one year and longer. The observed anomalies cannot be explained by thermal or geomagnetic effects or in terms of the anisotropy of galactic cosmic rays and need to be further investigated. V.L. (IAA)

N85-22414# Joint Publications Research Service, Arlington, Va.
HYDROMAGNETIC PRECURSORS OF INTERPLANETARY PLASMA BURST Abstract Only c75
A. V. Gulyelmi and K. G. Ivanov *In its* USSR Rept.: Space (JPRS-USP-85-001) 4 Feb. 1985 p 36 Transl. into ENGLISH from Geomagnetizm i Aeronomiya (USSR), v. 24, no. 3, May-Jun. 1984 p 489-491 Original language document announced as A84-40100 (For primary document see N85-22403 13-12)
Avail: NTIS HC A07

The hydromagnetic precursor hypothesis states that, before a flare stream reaches the magnetosphere, specific magnetic field oscillations are observed which are due to the penetration into the magnetosphere of hydromagnetic waves preceding the flare stream. This paper gives a theoretical description of this phenomenon and examines relevant experimental data. It is noted that flare stream precursors may be sought in geomagnetic pulsations preceding sudden storm commencements. B.J. (IAA)

N85-22415# Joint Publications Research Service, Arlington, Va.
LONGITUDE AND PITCH-ANGLE DISTRIBUTIONS OF STREAMS OF HIGH-ENERGY ELECTRONS UNDER EARTH'S RADIATION BELTS Abstract Only c93
S. A. Averin, A. M. Galper, V. M. Grachev, V. V. Dmitrenko, V. G. Kirillov-Ugryumov, and S. Y. Ulin *In its* USSR Rept.: Space (JPRS-USP-85-001) 4 Feb. 1985 p 37 Transl. into ENGLISH from Geomagnetizm i Aeronomiya (USSR), v. 24, no. 3, May-Jun. 1984 p 494-495 Original language document announced as A84-40102 (For primary document see N85-22403 13-12)
Avail: NTIS HC A07

The results of measurements of fluxes of electrons with energies E sub e = 460MeV in a wide range of longitudes and

pitch angles are given, together with the experimental dependences of the mean fluxes of albedo and quasi-trapped electrons (determined from the pitch-angle and longitude distributions) on the drift shell parameter L and the geomagnetic cutoff rigidity threshold. The measurements were made using the Yelena-F gamma-telescope on the Salyut-6 orbital station with definite spatial orientations of the station and instrument. The station had an orbital inclination of 51.6 deg. There were nine measurement sessions with different telescope positions relative to the station axes. On the basis of the pitch-angle distributions and results of computations of the limiting pitch angle separating electrons into albedo (having reflection points in the Northern and Southern Hemispheres below the altitude h< 60 km) and quasitrapped (by the geomagnetic field (H > 60 km) particles it was possible to determine the fluxes of electrons of both types. G.L.C.

N85-22416# Joint Publications Research Service, Arlington, Va.
LAGRANGIAN SOLUTIONS IN PHOTOGRAVITATIONAL RESTRICTED CIRCULAR THREE-BODY PROBLEM Abstract Only **c90**
L. G. Lukyanov *In its* USSR Rept.: Space (JPRS-USP-85-001) 4 Feb. 1985 p 38 Transl. into ENGLISH from Astronomicheskiy Zh. (USSR), v. 61, no. 3, May-Jun. 1984 p 564-570 (For primary document see N85-22403 13-12)
Avail: NTIS HC A07

Lagrangian solutions in the photogravitational restricted circular three-body problem are obtained. The problem is formulated as follows. It is assumed that the main bodies M sub 1 and M sub 2 with the masses 1-mu and mu(mu<= 1/2) move under the influence of reciprocal attraction in circles with a unit angular velocity, the distance between them being assumed equal to unity. A study was made of the motion of a body M of small mass caused by the main bodies and characterized by the force function U-(Q sub 1(1-mu)/R sub 1) + ((Q sub 2)mu/R sub 2) where R sub 1 and R sub 2 are the distances between the M body and the main bodies M sub 1 and M sub 2 respectively, Q sub 1 and Q sub 2 are some constant parameters. When Q sub 1 = Q sub 2 = 1 the classical restricted three-body problem is obtained. Depending on the characteristics of the emitting body and the size and mass of the M body the Q sub 1 and Q sub 2 values can assume values in the range - infinity to 1. Investigating the existence of linear and triangular libration points in the restricted photogravitational problem of three bodies for any real Q sub 1 and Q sub 2 values from - infinity to + infinity. G.L.C.

N85-22417# Joint Publications Research Service, Arlington, Va.
NONTRADITIONAL METHOD FOR DETERMINING UNPERTURBED ORBITS OF UNKNOWN SPACE OBJECTS USING INCOMPLETE OPTICAL OBSERVATIONAL DATA Abstract Only **c13**
N. I. Perov *In its* USSR Rept.: Space (JPRS-USP-85-001) 4 Feb. 1985 p 39 Transl. into ENGLISH from Astronomicheskiy Zh. (USSR), v. 61, no. 3, May-Jun. 1984 p 571-576 (For primary document see N85-22403 13-12)
Avail: NTIS HC A07

A physical-geometrical method for computing the orbits of earth satellites on the basis of an inadequate number of angular observations (N<3) was developed. Specifically, a new method has been developed for calculating the elements of Keplerian orbits of unidentified artificial satellites using two angular observations (alpha sub k, S sub k, k = 1). The first section gives procedures for determining the topocentric distance to AES on the basis of one optical observation. This is followed by description of a very simple method for determining unperturbed orbits using two satellite position vectors and a time interval which is applicable even in the case of antiparallel AED position vectors, a method designated the R sub 2 iterations method. G.L.C.

N85-22418# Joint Publications Research Service, Arlington, Va.
COMPUTATION OF ELLIPTICAL FUNCTIONS IN PROBLEMS OF CELESTIAL MECHANICS Abstract Only **c90**
I. A. Gerasimov *In its* USSR Rept.: Space (JPRS-USP-85-001) 4 Feb. 1985 p 39-40 Transl. into ENGLISH from Astronomicheskiy Zh. (USSR), v. 61, no. 3, May-Jun. 1984 p 609-610 (For primary document see N85-22403 13-12)
Avail: NTIS HC A07

Elliptical functions are widely used in celestial mechanics in the theory of motion of artificial Earth satellites and resonance asteroids, in qualitative study of the restricted three-body problem and in simple computation of Laplace coefficients. However, advances in computer technology dictate a reexamination of existing algorithms for computing elliptical functions for increasing their accuracy. Having the k modulus, it is usually necessary to find the value of the elliptical function for a stipulated argument u. The easiest way to do this is a changeover to theta functions, which are power series relative to the q parameter with coefficients being trigonometric functions of the argument u. Using expressions of the elliptical functions through the theta function, it is relatively easy to compute the required function. The fundamental problem is therefore a determination of the q parameter on the basis of the known k value. Formulas are derived for computing the theta function with high precision. A numerical example of the computations is given. Author

N85-22419# Joint Publications Research Service, Arlington, Va.
ALGORITHM FOR DETERMINING OPTIMAL THREE IMPULSE POINT-TO-ORBIT TRANSFER WITH LIMITED TRANSFER TIME Abstract Only **c13**
V. V. Ivashkin and A. P. Skorokhodov *In its* USSR Rept.: Space (JPRS-USP-85-001) 4 Feb. 1985 p 40 Transl. into ENGLISH from Kosmicheskiy Issled. (USSR), v. 22, no. 1, Jan.-Feb. 1984 p 3-12 (For primary document see N85-22403 13-12)
Avail: NTIS HC A07

A spacecraft transfers from an initial orbital point in a central Newtonian gravitational field to a final elliptical orbit. The planetocentric distance and the radial and transverse components of the spacecraft velocity are specified at the initial point in time. At the final point in time, only the pericentric and apocentric distances or a focal parameter and energy constant are specified. An algorithm is described for the determination of the space vehicle transfer which is energy optimal when the transfer flight time is constrained and the transfer is accomplished with three impulse maneuvers. The algorithm is based on an indirect optimization technique which derives the optimal trajectory from a single parameter family of trajectories which are optimal given the time constraint and obvious distance limitations. The initial approximation of the relevant boundary value problem is the well known solution of the case of a free transfer flight time. The variable parameters of the boundary value problem are analyzed in detail and the resulting algorithm with 12 main steps is discussed. Author

N85-22420# Joint Publications Research Service, Arlington, Va.
MOTION OF SYMMETRICAL SATELLITE WITH FLEXIBLE VISCOELASTIC RODS ABOUT CENTER OF MASS IN CIRCULAR ORBIT Abstract Only **c15**
N. Y. Bolotina and V. G. Vilke *In its* USSR Rept.: Space (JPRS-USP-85-001) 4 Feb. 1985 p 41 Transl. into ENGLISH from Kosmicheskiy Issled. (USSR), v. 22, no. 1, Jan.-Feb. 1984 p 13-19 (For primary document see N85-22403 13-12)
Avail: NTIS HC A07

A symmetrical satellite moves in a circular orbit in a central Newtonian force field. The satellite has two flexible rods positioned along its axis of symmetry. A system of coordinates is tied to the satellite with the origin at the center of mass of the system in the position when the rods are straight. An additional translationally moving system of coordinates is also used to completely describe the evolution of the rotational motion of the satellite. Approximate equations describing the system dynamics based on an averaging technique using Anduay variables are described. The purely theoretical treatment adduces no applications or sample calculations. Author

N85-22421# Joint Publications Research Service, Arlington, Va.
REJECTION OF ANOMALOUS OBSERVATIONS WHEN DETERMINING SPACECRAFT TRAJECTORIES Abstract Only **c13**

Y. S. Savrasov *In its* USSR Rept.: Space (JPRS-USP-85-001) 4 Feb. 1985 p 41-42 Transl. into ENGLISH from Kosmicheskiye Issled. (USSR), v. 22, no. 1, Jan.-Feb. 1984 p 20-36 (For primary document see N85-22403 13-12)
Avail: NTIS HC A07

The majority of techniques used to reject coarse anomalous observation errors when tracking space vehicles is based on procedures which smooth the observations with a polynomial of some degree. A more economical method which precludes the necessity of preliminary smoothing is possible and eliminates the problem of the optimal choice of the degree of the smoothing polynomial. The major task of processing an observational sample consists in discriminating the set of measurements which does not contain anomalous data. This problem is solved here in three steps, involving the generation of an initial sample of measurement residuals, followed by the discrimination from the remaining residuals of new measurement residuals which can be included in the initial set and then applying particular criteria to split the initial sample into one set of valid measurement residuals and a set of anomalous residuals. Three specific cases considered are: (1) the initial measurement error residuals have uniform distributions; (2) the errors have a normal distribution; and (3) the measurement errors have a normal distribution only in a narrow range. B.W.

N85-22422# Joint Publications Research Service, Arlington, Va.
OPERATIONAL EXPERIENCE WITH ION CONCENTRATION SENSORS IN ORIENTATION SYSTEMS Abstract Only c18
V. P. Legotayev, V. Nikolayev, K. I. Saulin, M. B. Sukhovoy, and Y. G. Ulyanov *In its* USSR Rept.: Space (JPRS-USP-85-001) 4 Feb. 1985 p 42 Transl. into ENGLISH from Kosmicheskiye Issled. (USSR), v. 22, no. 1, Jan.-Feb. 1984 p 37-43 (For primary document see N85-22403 13-12)
Avail: NTIS HC A07

The history of first and second generation ion flow type orientation sensors is reviewed. The following conclusions are made: the detectors and orientation systems which have been developed have working altitudes of more than 1,000 km, determine the direction of an incident ion flow in an angular deviation range of no less than + or - 90 deg and provide information on the position of the incident ion flow for approximately 90% orbital period of the vehicle. The need for a nominal orientation precision as high as 0.1 is responsible for the following approaches to third generation system design: (1) the introduction of variable setting of the ion sensor (the nominal ion concentration) as a function of the working altitude in each phase of the flight; (2) producing a digital output signal from the ion detector, interfacing it with a digital computer and developing the software for the periodic correction of the oriented position; and (3) implementation of automatic testing of the measurement accuracy of ion sensing chamber functioning by means of rocket motor pulses, generation of gas flows in particular directions and rotation of structural elements or other effects on the incident ion flow. G.L.C.

N85-22423# Joint Publications Research Service, Arlington, Va.
PROTONS WITH ENERGIES ABOVE 30 KeV IN EARTH'S RADIATION BELT AT LOW ALTITUDES DURING MAGNETICALLY QUIET TIME CLOSE TO GEOMAGNETIC EQUATOR Abstract Only c46
N. A. Vlasova, B. N. Knyazev, A. S. Kovtyukh, A. G. Kozlov, M. I. Panasyuk, S. Y. Reyzman, and E. N. Sosnovets *In its* USSR Rept.: Space (JPRS-USP-85-001) 4 Feb. 1985 p 43 Transl. into ENGLISH from Kosmicheskiye Issled. (USSR), v. 22, no. 1, Jan.-Feb. 1984 p 53-66 (For primary document see N85-22403 13-12)
Avail: NTIS HC A07

The Molniya-1, Molniya-2 and Cosmos-900 satellites launched between 1970 and 1977 carried differential proton spectrometers (the latter two also carried an alpha particle and proton spectrometer) which measured energies between 31 KeV and 50 MeV. Reduction of these data show: (1) differential energy spectra of protons with energies above 30 KeV close to the geomagnetic equator at middle latitudes are characterized by a maximum in the E layer of hundreds of KeV, which shifts to higher energies as the shell level number L decreases; (2) the near-equatorial proton spectra when $L > or = 4$ can be approximated by a simple exponential function or by the superimposition of the thermal Maxwellian and nonthermal tail in the form of a power function; (3) the change in the characteristic energy of the spectra in the outer radiation belt region ($L > 4$) indicates the existence of a weaker dependence on L than follows from the expression when the energy $E = L$ to the -n power (approx.), where $2.4 < n < 3$, which is characteristic of betatron acceleration with particle transport deep into a radiation belt; (4) the region of proton precipitation is formed at $L > 3$ with a maximum at L approx. = 6 or 7 on the night side. G.L.C.

N85-22424# Joint Publications Research Service, Arlington, Va.
ONE-DIMENSIONAL MODEL OF AURORAL MAGNETIC FORCE WITH LONGITUDINAL CURRENT AND CYCLOTRON HEATING OF IONS Abstract Only c46
M. A. Volkov, A. V. Volosevich, and Y. I. Galperin *In its* USSR Rept.: Space (JPRS-USP-85-001) 4 Feb. 1985 p 44 Transl. into ENGLISH from Kosmicheskiye Issled. (USSR), v. 22, no. 1, Jan.-Feb. 1984 p 67-86 Original language document announced as A84-26982 (For primary document see N85-22403 13-12)
Avail: NTIS HC A07

Characteristic scales and stationarity times are examined for various types of auroral structures. The method of kinetic-equation moments is used to construct a stationary system of drift-kinetic equations for ionospheric ions accelerated along a dipole flux tube, with allowance for temperature anisotropy for specified scales. It is shown that stationary solutions for auroral flux tubes exist only in the presence of a supersonic ascending flow of ionospheric ions. Given realistic values of the field-aligned current density, ions of ionospheric origin are found to be the dominant type of ion at the upper boundary of the acceleration region. It is also shown that the cyclotron heating of ions at the level limited by the broadening of ion resonances leads to a growth in perpendicular temperature of only several tens of eV at a parallel potential difference of 0.1-1 keV, which is insufficient to explain conical beams with a perpendicular temperature of 0.1-1 keV. (IAA)

N85-22425# Joint Publications Research Service, Arlington, Va.
HELIUM ATOMS IN INTERSTELLAR AND INTERPLANETARY SPACE. II: DETERMINATION OF DIRECTION OF INTERSTELLAR GAS MOTION RELATIVE TO SUN Abstract Only c90
V. G. Kurt, Y. N. Mironova, Z. L. Berto, and F. Dalodye *In its* USSR Rept.: Space (JPRS-USP-85-001) 4 Feb. 1985 p 45 Transl. into ENGLISH from Kosmicheskiye Issled. (USSR), v. 22, no. 1, Jan.-Feb. 1984 p 97-102 (For primary document see N85-22403 13-12)
Avail: NTIS HC A07

The far ultraviolet photometer on board the Prognoz-6 satellite measured the brightness distribution in the 584 A line of atomic helium in interplanetary space. Since atoms of neutral helium penetrate deeper into the solar system than neutral hydrogen and are focused by the Sun's gravitational field, it is possible to determine the direction of the vector V sub w, which is the sum of the interstellar gas velocity vector V sub t and the vector -V sub s which is the velocity vector of the Sun relative to several hundreds of the closest stars. The scanning geometry of the photometer system is illustrated graphically and the data from seven observational sessions between 29 Sep. 1977 and 15 Jan. 1978 are summarized in tabular form. The velocity vector projected onto the celestial sphere (V sub s) has a right ascension of 77 plus or minus 2 deg and a declination of 17 plus or minus 2.5 deg. R.J.F.

N85-22426# Joint Publications Research Service, Arlington, Va.
ROCKET BODY CHARGE NEUTRALIZATION PROCESSES IN ARAKS EXPERIMENT (DATA FROM TWO LAUNCHES) Abstract Only c20
G. G. Managadze and S. B. Lyakhov *In its* USSR Rept.: Space (JPRS-USP-85-001) 4 Feb. 1985 p 45-46 Transl. into ENGLISH from Kosmicheskiye Issled. (USSR), v. 22, no. 1, Jan.-Feb. 1984

p 103-109 (For primary document see N85-22403 13-12)
Avail: NTIS HC A07

In the ARAKS experiments, two identical narrow beam (0.02) transducers of the Ushba electron spectrometer scanned an energy range of 1 to 16 KeV every 10 msec from orientation angles of 75 and 120 deg relative to the longitudinal axis of the test rocket in order to determine the nature of the neutralization of the charge built-up on a spacecraft when electrons are injected from the craft given the condition that the neutralization current due to thermal electrons in the unperturbed ionospheric plasma is much less than the injection current (by a factor of about 1,000). The steady-state potential of a rocket body at the moment of electron injection at altitudes over 150 km exceeds 1 KV and is governed by the current from a supplemental neutralization current source. The potential at times briefly become commensurate with the accelerating voltage of the electron injector and leads to the cessation of injection. Western evidence of significant spacecraft charging by an electron accelerator at ionospheric altitudes is also cited. Author

N85-22427# Joint Publications Research Service, Arlington, Va.
COSMOGENIC Na-22 AND Al-26 IN LUNA-24 LUNAR DRILL CORE SOIL SAMPLES Abstract Only **c91**
A. K. Lavrukhina, P. Povinets, and G. K. Ustinova *In its* USSR Rept.: Space (JPRS-USP-85-001) 4 Feb. 1985 p 46 Transl. into ENGLISH from Kosmicheskiye Issled. (USSR), v. 22, no. 1, Jan.-Feb. 1984 p 110-119 Original language document announced as A84-26986 (For primary document see N85-22403 13-12)
Avail: NTIS HC A07

Low-background (beta-gamma-gamma) spectrometry was used to study the Na-22 and Al-26 radioactivity in Luna - 24 drill core samples, and the equilibrium radioactivity of these cosmogenic isotopes is calculated by an analytical method. It is shown that, during the last million years, the regolith surface layer at the Luna-24 landing site has remained practically unchanged; i.e., it has not been subject to the intense effect of any mechanical processes on the lunar surface. The mean intensity of galactic cosmic rays with a rigidity exceeding 0.5 GV remained constant (within 20 percent) during the last million years, and agreed with the present-day mean intensity of 0.24 particles/sq cm s sr. The mean spectrum of the galactic cosmic rays over the last million years agrees approximately with the mean spectrum for 1962 or 1971. (IAA)

N85-22428# Joint Publications Research Service, Arlington, Va.
ROTATIONAL MOTION OF A SATELLITE Abstract Only **c13**
A. A. Khentov *In its* USSR Rept.: Space (JPRS-USP-85-001) 4 Feb. 1985 p 46-47 Transl. into ENGLISH from Kosmicheskiye Issled. (USSR), v. 22, no. 1, Jan.-Feb. 1984 p 130-131 Original language document announced as A84-26988 (For primary document see N85-22403 13-12)
Avail: NTIS HC A07

A solution to the differential equation describing the rotation of a satellite around the normal to the orbit is considered which corresponds to the case when the z axis of the satellite makes one revolution in absolute space for two revolutions of the satellite center of mass in orbit. The solution is stable in the sense of Liapunov in the linear approximation if e is not greater than C.32046 and if e is in the range 0.9004-0.9174, and is unstable for other values of the orbit eccentricity. B.J. (IAA)

N85-22429# Joint Publications Research Service, Arlington, Va.
SATELLITE OSCILLATIONS IN ELLIPTICAL ORBIT Abstract Only **c13**
A. A. Burov *In its* USSR Rept.: Space (JPRS-USP-85-001) 4 Feb. 1985 p 47 Transl. into ENGLISH from Kosmicheskiye Issled. (USSR), v. 22, no. 1, Jan.-Feb. 1984 p 133-134 (For primary document see N85-22403 13-12)
Avail: NTIS HC A07

The planar oscillations of a satellite in an elliptical orbit are described by a system of first order canonical differential equations written in terms of a Hamiltonian function which is analytical in a specified range of eccentricities. With sufficiently small values of the eccentricity this system of equations possesses a single parameter family of hyperbolic solutions which attain equilibrium when the eccentricity is zero. The solution of the equation is found for the case of a coordinate system tied to the satellite center of mass and the effect of the eccentricity on satellite oscillation stability is described mathematically. The conditions for a unique periodic solution of the system are also defined. The purely theoretical analysis adduces neither sample calculations nor applications. R.J.F.

N85-22430# Joint Publications Research Service, Arlington, Va.
OBSERVATION OF COSMIC RAY FLUX VARIATIONS IN STRATOSPHERE Abstract Only **c93**
Y. I. Barannikov, O. A. Barsukov, and P. F. Gavrilov *In its* USSR Rept.: Space (JPRS-USP-85-001) 4 Feb. 1985 p 47-48 Transl. into ENGLISH from Kosmicheskiye Issled. (USSR), v. 22, no. 1, Jan.-Feb. 1984 p 134-136 (For primary document see N85-22403 13-12)
Avail: NTIS HC A07

Studies of cosmic rays in the stratosphere were conducted during 1975-1981 using balloons and high altitude aircraft. The aircraft was flown at altitudes of 16 to 20 km and had equipment for measuring the vertical proton flux with energies of E sub p = 350 to 1,000 MeV, the omnidirectional neutron flux at energies of E sub n = 0.025 eV + 10 MeV and the omnidirectional charged particle flux with energies of E sub e >> 1.3 MeV and E sub p > 20 MeV. The balloons measured the vertical electron flux in an energy range of 50 to 500 KeV. All the data indicated the existence of pulsating cosmic ray flux variations in the auroral region with characteristic pulsation times of 150 to 400 sec. Possible mechanisms generating these pulsations include pulsations of the solar diameter or oscillations of the solar surface which cause pulsations in the density and velocity of the solar wind and consequently the interplanetary magnetic field. It is noted that the natural period of magnetospheric line of force oscillations for latitudes of about 70 deg N is approximately 400 sec. No firm conclusions were drawn though it is indicated that geomagnetic pulsations are related to the preflare situation on the Sun. B.W.

N85-22431# Joint Publications Research Service, Arlington, Va.
INCREASE IN HYDROGEN EMISSION OF UPPER ATMOSPHERE FOLLOWING LAUNCHES OF SPACE VEHICLES Abstract Only **c46**
N. M. Martsvaladze and L. M. Fishkova *In its* USSR Rept.: Space (JPRS-USP-85-001) 4 Feb. 1985 p 48 Transl. into ENGLISH from Kosmicheskiye Issled. (USSR), v. 22, no. 1, Jan.-Feb. 1984 p 136-137 Original language document announced as A84-26992 (For primary document see N85-22403 13-12)
Avail: NTIS HC A07

An increase in the amount of hydrogen in the upper atmosphere is attested by a slight enhancement of the normalized hydrogen-alpha emission intensity observed an average of 2 to 6 days after spacecraft launches. These observations of the 656.3 nm emission line in the nighttime sky spectrum were made at the Abastumani Astrophysical Observatory of the Georgian Academy of Sciences between 1968 and 1978. The analysis is applied only to spacecraft with an apogee above 800 km, starting with the INTELSAT-3C (F-3) in 1969 and concluding with the Navstar-2, DSCS-13 and DSCS-14 in 1979. The deviations in the alpha line intensity from the average season values is plotted as a function of time in terms of days before and after the launch date. There is an increase in the excess hydrogen line emission intensity in the winter, some 3 to 6 days after a launch with a maximum upward deviation 4 to 5 days following the launch. The effect is not observed in the summer. R.J.F.

N85-22432# Joint Publications Research Service, Arlington, Va.
DETERMINATION OF ANGULAR RESOLUTION OF CODED APERTURE GAMMA-RAY TELESCOPE Abstract Only **c89**
Y. D. Kotov, S. A. Lazarev, B. I. Luchkov, Y. V. Smirnov, and V. N. Yurov *In its* USSR Rept.: Space (JPRS-USP-85-001) 4 Feb. 1985 p 49 Transl. into ENGLISH from Kosmicheskiye Issled. (USSR), v. 22, no. 1, Jan.-Feb. 1984 p 141-143 (For primary

document see N85-22403 13-12)
Avail: NTIS HC A07

While the angular resolution of the best modern gamma-ray telescopes using spark chambers is about 2 deg for gamma quanta energies in the 100 MeV range, aperture coding by inserting a coding screen in front of the detector can increase the resolution to 1' to 10' while cutting the effective aperture of the telescope in half. An experiment is described that uses a beam of tagged gamma quanta from the Pakhra accelerator to calibrate second generation gamma-ray telescopes. A one-dimensional coding screen with 19 elements (10 transparent teflon elements and 9 lead absorbing elements) was used. The screen was 15 mm thick. It is shown that high energy gamma ray telescopes using this technique can achieve an angular resolution of a few minutes. This is demonstrated here for a gamma quanta energy of 100 MeV and for the bremsstrahlung spectrum of gamma radiation corresponding to cosmic gamma radiation sources. A low frequency filtering technique employing a discrete Fourier transform was used on the resulting images and is briefly described. R.J.F.

N85-22433# Joint Publications Research Service, Arlington, Va.
VOLCANISM ON VENUS AS CONNECTING LINK Abstract Only c91
L. V. Ksanfomaliti *In its* USSR Rept.: Space (JPRS-USP-85-001) 4 Feb. 1985 p 58 Transl. into ENGLISH from Pisma Astronomicheskiy Zh. (USSR), v. 10, no. 8, Aug. 1984 p 620-630 (For primary document see N85-22403 13-12)
Avail: NTIS HC A07

Investigations of Venus made during recent years revealed a number of phenomena which still remain unexplained. These phenomena include electrical activity of the atmosphere, a bimodal distribution of particles in Venusian clouds and variability of properties of the upper cloud layer as indicated by polarimetric and radiometric methods. The evidence that volcanic activity on the planet can explain all the mentioned phenomena is reviewed. For example, the observed electrical discharges are grouped along definite young mountain regions. The low position of the field sources and their fixed positions relative to the planetary surface strongly suggest that the discharges are related to natural relief, in all probability to volcanic eruptions. Although there is no direct evidence of Venusian volcanism, there appears to be no other explanation for the concentration of sources of electromagnetic pulses detected by instrumentation aboard spacecraft. Other indirect evidence of Venusian volcanism is presented. If the observed changes in haze concentration above the cloud layer are actually related to volcanism, polarimetric measurements from the Earth might be used in monitoring volcanic activity on Venus. R.J.F.

N85-22434# Joint Publications Research Service, Arlington, Va.
INTERPLANETARY SHOCK WAVES DURING APRIL AND MAY OF 1981 Abstract Only c90
G. N. Zastenker and N. L. Borodkova *In its* USSR Rept.: Space (JPRS-USP-85-001) 4 Feb. 1985 p 58-59 Transl. into ENGLISH from Kosmicheskiye Issled. (USSR), v. 22, no. 1, Jan.-Feb. 1984 p 87-96 Original language document announced as A84-26983 (For primary document see N85-22403 13-12)
Avail: NTIS HC A07

Regular measurements performed by the Prognoz-8 satellite of the interplanetary plasma during the XII STIP period (April-May 1981) are examined. Nine intense interplanetary disturbances identified as interplanetary shock waves were detected. The characteristics of plasma flow before and after the arrival of the shock front are examined, and the shock waves are correlated with solar flares. (IAA)

N85-22435# Joint Publications Research Service, Arlington, Va.
ANALYSIS OF SYSTEMATIC ERRORS IN SYSTEMS OF SELENODETIC COORDINATES Abstract Only c91
V. A. Nikonov *In its* USSR Rept.: Space (JPRS-USP-85-001) 4 Feb. 1985 p 59 Transl. into ENGLISH from Astronomicheskiy Vestnik (USSR), v. 18, no. 2, Apr.-Jun. 1984 p 107-116 (For primary document see N85-22403 13-12)
Avail: NTIS HC A07

A selenodetic network, the Apollo system, was developed on the basis of orbital surveys made from the Apollo spacecraft. It is presently the best dynamic selenocentric coordinate system. The random errors in coordinates of control points in this independent system are 2 to 3 times fewer than the random errors of coordinates of points in systems (catalogues) prepared by traditional surface telescopic methods. The Apollo system is used as a basis for studying the selenodetic coordinates and for detecting the systematic errors which may be present in them. The three best selenodetic catalogues were investigated: D. W. Arthur, COMMUN. LUNAR AND PLANETARY LABOR., Vol 7, Part 5, No 130, pp 303-312, 1968; D. L. Meyer, et al., ICARUS, Vol 4, No 5, 6, pp 513-530, 1965; M. Moutsoulas, MOON, Vol 5, pp 302-331, 1972. The analysis presented reveals that there are no systematic errors other than those caused by noncoincidence of the coordinate systems. R.J.F.

N85-22436# Joint Publications Research Service, Arlington, Va.
MICROSTRUCTURE OF VENUS CLOUD LAYER BASED ON SPECTROPHOTOMETRIC DATA FROM VENERA-11 SPACECRAFT Abstract Only c91
D. V. Titov *In its* USSR Rept.: Space (JPRS-USP-85-001) 4 Feb. 1985 p 60 Transl. into ENGLISH from Kosmicheskiye Issled. (USSR), v. 22, no. 1, Jan.-Feb. 1984 p 120-129 Original language document announced as A84-26987 (For primary document see N85-22403 13-12)
Avail: NTIS HC A07

The cloud-particle size distribution at heights of 48-65 km was reconstructed on the basis of Venera-11 data using the Tikhonov regularization method. A combined interpretation of spectrophotometric and nephelometric data made it possible to determine the aerosol refractive index. A value of about 1.33, obtained for the lower part of the cloud layer, points to the possible presence of aspherical particles. (IAA)

N85-22437# Joint Publications Research Service, Arlington, Va.
VISUALIZATION OF RADAR ALTIMETRY DATA FOR VENUS Abstract Only c91
D. G. Stankevich, S. P. Redkin, Y. V. Korniyenko, A. T. Bazilevskiy, and Y. G. Shkuratov *In its* USSR Rept.: Space (JPRS-USP-85-001) 4 Feb. 1985 p 60-61 Transl. into ENGLISH from Kosmicheskiye Issled. (USSR), v. 22, no. 1, Jan.-Feb. 1984 p 138-140 Original language document announced as A84-26993 (For primary document see N85-22403 13-12)
Avail: NTIS HC A07

The visualization and analysis of Pioneer-Venus radar-altimetry data were carried out by the Intercosmos Council of the Soviet Academy of Sciences in collaboration with NASA. This paper briefly describes the representation of relief in the form of a three-dimensional graphic, the two-dimensional representation of the surface in oblique illumination, the representation of the relief in an axonometric projection, and the stereoscopic representation of the relief. A morphological description of the images is given. IAA

N85-22438# Joint Publications Research Service, Arlington, Va.
PRELIMINARY PHOTOMAPS OF VENUS SURFACE IN THE MAXWELL MOUNTAINS AND ADJACENT AREAS Abstract Only c91
A. F. Bogomolov and Y. S. Tyuflin *In its* USSR Rept.: Space (JPRS-USP-85-001) 4 Feb. 1985 p 61 Transl. into ENGLISH from Geodiziya i Kartografiya (USSR), no. 8, Aug. 1984 p 11-16 (For primary document see N85-22403 13-12)
Avail: NTIS HC A07

The results of radar mapping of the surface of Venus by the Venera-15 and Venera-16 spacecraft are discussed. A preliminary photographic map of the Maxwell mountains and adjecent area constructed from these radar images is presented. Twelve panoramas from the Venera-16 spacecraft obtained from 12 through 23 January 1984 were used to produce the images. The Central Scientific Research Institute of Geodosy, Aerial Surveying and Cartography referenced the panoramas and constructed the parallels and meridians on the maps. Coordinate

construction was performed initially for each radar panorama; then, after averaging coordinates at common points, for the entire map. Equations allowing the transition to be made from measured spherical coordinates of points on the radar panorama for known moments in time to venerographic coordinates are presented. All necessary parameters are determined for computation of the coordinates of points on the terrain shown on the radar panoramas. R.J.F.

N85-22439# Joint Publications Research Service, Arlington, Va.
HYPSOMETRIC FEATURES ON VENUS Abstract Only c91
Z. F. Rodionova *In its* USSR Rept.: Space (JPRS-USP-85-001) 4 Feb. 1985 p 62 Transl. into ENGLISH from Astronomicheskiy Vestnik (USSR), v. 18, no. 2, Apr.-Jun. 1984 p 117-127 (For primary document see N85-22403 13-12)
Avail: NTIS HC A07

A cartometric study was made of Venusian relief for ascertaining such morphometric characteristics as the areas and mean elevations of different regions and the surface in general. The measurements were made using the USGS hypsometric map of Venus at 1:50,000,000 in a Mercator projection covering 93.6% of the entire surface; horizontal resolution about 100 km, vertical resolution about 0.1 to 0.2 km. A special technique was used in determining the areas and mean elevations of 22 regions on the planet. Hypsographic curves were plotted for the different regions and a map of Venusian relief averaged for 5 deg grid squares (contours drawn each 0.5 km) was compiled. A table gives the areas and mean elevations of highlands and lowlands on Venus. Mountainous regions occupy 7.4% of the surface; hilly areas -- 54.8%; and low-lands--37.9%. The hypsographic curve for Venus is compared with those for Mars and the Earth, constructed relative to the mean level for each planet. On Venus about 40% of the surface is above the mean level, on Earth about 43% and on Mars about 53%. In the Northern Hemisphere of Venus, plains occupy a greater area (46%) than in the Southern Hemisphere (30%), the same as on the Moon, Mars and Mercury. Author

N85-22440# Joint Publications Research Service, Arlington, Va.
REMOTE SENSING USED FOR STUDY OF FOREST RESOURCES c43
A. Metalnikov, V. Yezhkov, and P. Moroz *In its* USSR Rept.: Space (JPRS-USP-85-001) 4 Feb. 1985 p 67-72 Transl. into ENGLISH from Ekonomicheskaya Gaz. (USSR), no. 34, Aug. 1984 p 16 (For primary document see N85-22403 13-12)
Avail: NTIS HC A07

Remote methods of probing the Earth from space have not only improved the operational efficiency and precision of work on forest management, but have also reduced the costs. The effectiveness of using space photography was demonstrated in the recording and inventory of field and soil protective planting. Ongoing changes in forest resources caused by human activity and natural factors are recorded by measurement of length, width, and areas of forests. Damage done by forest fires and changes in the condition of damaged areas over time are monitored; development of burn areas into centers of forest pathology is predicted and prevented; and steps toward economic incorporation of damaged sectors and restoration of the forests are determined. B.G.

N85-22441# Joint Publications Research Service, Arlington, Va.
EVALUATING ACCURACY IN DETERMINING POSITION OF EARTH'S CENTER OF MASS AND ELEMENTS OF ORIENTATION OF GEODETIC COORDINATE SYSTEM Abstract Only c43
M. M. Mashimov and K. V. Malets *In its* USSR Rept.: Space (JPRS-USP-85-001) 4 Feb. 1985 p 73 Transl. into ENGLISH from Izv. Vysshikh Uch. Zaved.: Geod. i Aerofotosyemka (USSR), no. 1, Jan.-Feb. 1984 p 45-49 (For primary document see N85-22403 13-12)
Avail: NTIS HC A07

Work on the determination of the Earth's center of mass and elements of orientation of a geodetic coordinate system from observations of an artificial Earth satellite is discussed. The initial equations are written for solving this problem. This involves a functional dependence of the measured parameters obtained using the results of rangefinder, Doppler, angular, altimeter and radiointerferometer observations of satellites from surface stations and the sought-for parameters -- the initial conditions, the coordinates of astrogeodetic observatories and the coordinates of the Earth's center of mass and the orientation of the system of geodetic coordinates. The derived system of equations makes it possible to form a covariation matrix for r0 and proceed to an a priori evaluation of the accuracy in determining the position of the Earth's center of mass and the elements of orientation on the basis of the results of satellite observations. This evaluation requires transformation from a geocentric coordinate system to a system in which the x-axis is directed toward the ascending node of the circular orbit. This makes it possible to obtain results in a form convenient for analysis. Correction equations for the measured distances (astrogeodetic observatory-artificial earth satellite) make it possible to obtain the mean square errors in determining the position of the Earth's center of mass and the elements of orientation. Author

N85-22442# Joint Publications Research Service, Arlington, Va.
EVALUATING ACCURACY IN ORIENTATION OF TOPOGRAPHIC PHOTOGRAPH AND SATELLITE-CENTERED DIRECTION FROM STAR PHOTOGRAPH Abstract Only c35
M. I. Shcherbakov *In its* USSR Rept.: Space (JPRS-USP-85-001) 4 Feb. 1985 p 74 Transl. into ENGLISH from Izv. Vysshikh Uch. Zaved.: Geod. i Aerofotosyemka (USSR), no. 1, Jan.-Feb. 1984 p 49-55 Original language document announced as A84-34490 (For primary document see N85-22403 13-12)
Avail: NTIS HC A07

Consideration is given to aspects of the determination and accuracy assessment of the orientation of a topographic photograph and satellite-centric directions at a point on a planetary surface with reference to a star photograph. The linear elements of external orientation are determined by integrating the differential equations of motion of a planetary satellite, and the angular elements of external orientation are determined with reference to a star photograph obtained by a stellar camera aboard the satellite. The stellar camera operates synchronously with the topographic camera which takes photos of the planetary surface. Differential formulas are presented, and modeling results are given. B.J. (IAA)

N85-22443# Joint Publications Research Service, Arlington, Va.
METHOD FOR APPROXIMATING AUTOCORRELATION FUNCTIONS FOR DESCRIBING AREAL PHOTOIMAGE FEATURES Abstract Only c35
V. V. Gavrilov *In its* USSR Rept.: Space (JPRS-USP-85-001) 4 Feb. 1985 p 74-75 Transl. into ENGLISH from Izv. Vysshikh Uch. Zaved.: Geod. i Aerofotosyemka (USSR), no. 2, Mar.-Apr. 1984 p 68-72 (For primary document see N85-22403 13-12)
Avail: NTIS HC A07

The algorithm currently used in the automatic interpretation of features on the Earth's surface on the basis of their photoimages is inadequate due to the procedures used in computing the autocorrelation functions (ACF), a large memory volume being required for the input information. An algorithm is proposed which is advantageous in comparison with the algorithm for computing ACF on the basis of discrete values. Its use in analysis of an image fragment measuring 1 sq cm made it possible to reduce the computer memory volume by a factor of more than 100. Accuracy in computing ACF was increased by noise elimination. The computed values of the two-dimensional ACF form a matrix of 20 x 20 or 30 x 30 elements. The algorithm for approximation of ACF was embodied in the computation block for two-dimensional autocorrelation analysis developed on the basis of an electronic computer. The analyzer was used in two-dimensional autocorrelation processing of half-tone images of cultivated land and forest. The ACF were determined for three angles of image rotation (0, 45, 90 deg). The approximation algorithm was highly effective. The required accuracy was attained with 5 to 7 iterations. Author

N85-22444# Joint Publications Research Service, Arlington, Va.
EXPERIENCE IN AUTOMATED INTERPRETATION OF AEROSPACE PHOTOGRAPHS Abstract Only c35
I. K. Lurye *In its* USSR Rept.: Space (JPRS-USP-85-001) 4 Feb. 1985 p 75-76 Transl. into ENGLISH from Vestnik Moskovskogo Univ., Ser. 5: Geografiya (USSR), no. 4, Jul.-Aug. 1984 p 63-69 (For primary document see N85-22403 13-12)
Avail: NTIS HC A07

A software method for use in automated interpretation of aerospace video information, in particular, from a multizonal aerospace survey is described. The Aerospace Methods Laboratory at Moscow State University developed two algorithms for solving this problem in two stages. The first algorithm is for the preliminary classification of multizonal information and evaluating the uniformity of multizonal data. This algorithm for the rapid discrimination of classes (RDC) is used in the breakdown of initial data into a relatively small number of groups, after which each group is regarded as a single object. Use of this algorithm does not require a priori information on these objects other than a multizonal photograph. The second algorithm is a successive clusterization iteration algorithm (SCIA). In contrast to the RDC algorithm it requires a definite volume of a priori information on the considered objects. It is necessary to stipulate the standard brightness characteristics of these objects. The algorithms is used in identifying the classes formed by the RDC algorithm with standard objects (called clusters), in each iteration evaluating the results on the basis of experimentally determined criteria. The results of automated interpretation of agricultural crops are given as an illustration of the practical use of the method. Author

N85-22445# Joint Publications Research Service, Arlington, Va.
GEOINDICATION METHOD FOR INTERPRETING AERIAL AND SPACE PHOTOGRAPHS: STATUS AND PROSPECTS Abstract Only c35
B. N. Mozhayev and A. G. Zhuchenko *In its* USSR Rept.: Space (JPRS-USP-85-001) 4 Feb. 1985 p 76 Transl. into ENGLISH from Sov. Geologiya (USSR), no. 8, Aug. 1984 p 60-65 (For primary document see N85-22403 13-12)
Avail: NTIS HC A07

The geoindication method as developed in the USSR is reviewed with references to the authors of the earliest studies laying the groundwork for this field and with a discussion of the work done and being done by different individuals and organizations. It is emphasized that the geoindication method for the interpretation of aerial and space photographs in all its variants is directed to the solution of practical problems. It is being used successfully in geological mapping, in the search for minerals, in engineering geology and hydrogeological research, in predictive metallogenetic studies, in investigating anthropogenic and natural processes and in solving other economic problems. The practical introduction of the method is favoring optimization of aerospace geological research, the organization of data and collection of new information on geological structure and patterns of distribution of minerals. Progress is being made in the direction of compilation of geoindication maps and forming of new types of data banks. In a number of organizations of the USSR Geology Ministry geoindication research is being carried out at a high scientific level, with a systemic approach, automated processing of materials from aerial and space surveys, use of computers, and on-the-ground checking of the results. Author

N85-22446# Joint Publications Research Service, Arlington, Va.
NEW METHOD OF RECONSTRUCTING CONDITIONS OF RECENT DIFFERENTIATION OF OIL AND GAS IN THE AMUDARYA BASIN (BASED ON RESULTS OF INTERPRETATION OF SPACE PHOTOGRAPHS) Abstract Only c43
G. I. Amurskiy, N. N. Solovyev, and V. A. Kuzminov *In its* USSR Rept.: Space (JPRS-USP-85-001) 4 Feb. 1985 p 77 Transl. into ENGLISH from Izv. Akad. Nauk SSSR: Ser. Geologicheskaya (USSR), no. 6, Aug. 1984 p 112-122 (For primary document see N85-22403 13-12)
Avail: NTIS HC A07

Results are presented from an experiment on the use of materials provided by satellites to refine the geological structure and recent history of the Dengizkul'-Zevardinskaya zone of oil and gas accumulation in the Amudar'ya oil and gas basin. Three groups of superficially distinct photographic objects are visible on space photographs of this zone, apparently reflecting genetically related geological phenomena and processes, responsible in the final analysis for the formation and specifics of the structure and distribution of accumulations of gas and oil. Middle scale jointing and its significance in the formation of hydrocarbon deposits is discussed. Some specifics of the structure and the nature of depressions with no outlets are analyzed. Concentric photo anomalies are considered as elements reflecting the recent growth of local structure. The data presented confirm the assumptions stated previously by many investigators that gas bearing traps in certain deposits may previously have been filled with oil or vice versa. Author

N85-22447# Joint Publications Research Service, Arlington, Va.
USE OF MOBILE SURFACE STATION FOR SYNCHRONOUS SATELLITE MEASUREMENTS IN SEISMOLOGICAL RESEARCH Abstract Only c46
G. K. Mardirosyn and D. N. Mishev *In its* USSR Rept.: Space (JPRS-USP-85-001) 4 Feb. 1985 p 77-78 Transl. into ENGLISH from Izv. Akad. Nauk Armyanskoy SSR: Nauki o Zemle (USSR), v. 37, no. 3, May-Jun. 1984 p 47-56 (For primary document see N85-22403 13-12)
Avail: NTIS HC A07

The INTERCOSMOS and BOLGARIYA-1300 space programs specialists at the Central Space Research Laboratory, Bulgarian Academy of Sciences, developed a prototype of a mobile surface station for synchronous satellite measurements (MSSSSM). The station consists of primary and secondary electric supply systems, measurement instruments, instrumentation for determining position, precise time system, programming device, data collection system, autonomous recorders, radio communication system and auxiliary devices. The instruments include: devices for measuring spectral reflection characteristics, devices for measuring temperature of surface air layer, surface soil layer and vertical temperature profiles, devices for measuring moisture content of soil surface layer and vertical moisture content distribution, instruments for measuring gradient of soil conductivity, instrumentation for hydrological measurements, seismic detectors, magnetometers, and standard set of meteorological instruments. The type, number, structure and arrangement of seismic detectors and the organization of measurements are dependent on the specific objectives of the work and measurement conditions. Author

N85-22448# Joint Publications Research Service, Arlington, Va.
APPROXIMATE PERTURBING PART OF GEOPOTENTIAL BY POLYNOMIALS OF STIPULATED FORM Abstract Only c46
Y. V. Plakhov and A. V. Paramzin *In its* USSR Rept.: Space (JPRS-USP-85-001) 4 Feb. 1985 p 78-79 Transl. into ENGLISH from Izv. Vysshikh Uch. Zaved.: Geod. i Aerofotosyemka (USSR), no. 3, May-Jun. 1984 p 61-66 (For primary document see N85-22403 13-12)
Avail: NTIS HC A07

The problem examined is the representation of perturbing potential by a series of coefficients of orthogonal polynomials of a particular type. The objective is to combine the merits of the classical expansion in spherical functions and point models for predicting the perturbed motion of geodetic artificial Earth satellites. Although the classical expansion is convenient for analytical integration of the equations of motion, it is very unwieldy in numerical integration, whereas with use of point models the situation is the reverse. The physical validation of the possibility of solving this problem is the adequate smoothness of geopotential at satellite altitudes, characterized by the sum of all the spherical harmonics. A simpler analytical approximation of geopotential is proposed and the mathematical procedures are entirely obvious. Author

N85-22449# Joint Publications Research Service, Arlington, Va.
EXPERIENCE IN COMBINED SPECIAL MAPPING USING SPACE

INFORMATION Abstract Only c43
V. A. Astakhova, V. V. Kozlov, and V. I. Ryabchikova *In its* USSR Rept.: Space (JPRS-USP-85-001) 4 Feb. 1985 p 79-80 Transl. into ENGLISH from Geod. i Kartografiya (USSR), no. 7, Jul. 1984 p 40-44 (For primary document see N85-22403 13-12)
Avail: NTIS HC A07

Several research organizations in the USSR are carrying out experimental work for developing new types of maps for certain regions, including the subarctic region of the Northeastern USSR. In areas such as the latter, inaccessibility and other field work difficulties dictate a heavy reliance on space photographs. The difficulties in visual special interpretation of space photographs peculiar to the investigated area are discussed in relation to the overall objective, i.e., combining the special subject matter maps into one so-called complex mapping and the collating and integration of the special content maps which were initially compiled. The difficulties can be overcome in part by compiling intermediate maps of natural complexes and separate interpretations of key elements, such as hydrography, distribution of Quaternary deposits, geological structure as expressed at the surface, etc. A definite sequence for interpretation of space photographs was worked out. The intricacies of geomorphological, geological and landscape photointerpretation are discussed.
Author

N85-22450# Joint Publications Research Service, Arlington, Va.
COMBINED ANALYSIS OF THE DYNAMICS OF COMPLEX ECOSYSTEMS BASED ON REPEATED REMOTE MEASUREMENTS Abstract Only c43
B. V. Vinogradov, U. A. Shvede, and A. N. Kaptsov *In its* USSR Rept.: Space (JPRS-USP-85-001) 4 Feb. 1985 p 80 Transl. into ENGLISH from Dokl. Akad. Nauk SSSR (USSR), v. 277, no. 6, Aug. 1984 p 1505-1509 Original language document announced as A85-11587 (For primary document see N85-22403 13-12)
Avail: NTIS HC A07

The technique of repeated aerial survey is examined as an effective method for the monitoring of ecosystems and the ecological prediction of their dynamics over large areas. This technique is illustrated by the aerial monitoring of a complex forest-swamp-meadow ecosystem within the middle Latvian declivity during 1956-1974. A spatial balance model of this ecosystem constructed on the basis of the repeated sensings is presented, and a spatial-frequency matrix describing the land dynamics is given. The application of quantitative extrapolational analysis to the data obtained is considered. B.J. (IAA)

N85-22451# Joint Publications Research Service, Arlington, Va.
FEOKTISTOV RECALLS PERIOD LEADING TO GAGARIN SPACEFLIGHT
K. P. Feoktistov *In its* USSR Rept.: Space (JPRS-USP-85-001) 4 Feb. 1985 p 85-89 Transl. into ENGLISH from Sotsialisticheskaya Ind. (USSR), 20 Nov. 1984 p 4 (For primary document see N85-22403 13-12)
Avail: NTIS HC A07

The history of the Soviet space program up to the first manned space flight is described. Elements of the design and manufacture of the first prototype for manned flight are discussed. B.G.

N85-22452# Joint Publications Research Service, Arlington, Va.
FEOKTISTOV SAYS MANNED LUNAR, MARS FLIGHTS LACK JUSTIFICATION
Konstantin P. Feoktistov *In its* USSR Rept.: Space (JPRS-USP-85-001) 4 Feb. 1985 p 90-94 Transl. into ENGLISH from Sotsialisticheskaya Ind. (USSR), 21 Nov. 1984 p 4 (For primary document see N85-22403 13-12)
Avail: NTIS HC A07

Technological assessment of the results from the lunar expeditions in regard to equipment development and utilization by other sectors of space exploration are presented. Also considered is the feasibility of manned flights to Mars. B.G.

N85-22453# Joint Publications Research Service, Arlington, Va.
FEOKTISTOV ARGUES AGAINST U.S. SPACE SHUTTLE DESIGN CONCEPT c16
Konstantin P. Feoktistov *In its* USSR Rept.: Space (JPRS-USP-85-001) 4 Feb. 1985 p 95-99 Transl. into ENGLISH from Sotsialisticheskaya Ind. (USSR), 22 Nov. 1984 p 4 (For primary document see N85-22403 13-12)
Avail: NTIS HC A07

The advantages and disadvantages of the U.S. Space Shuttle design concept are discussed. Topics include cost effectiveness, spacecraft launching, spacecraft landing, orbital servicing, stage separation, maneuverability, and military technology. B.G.

N85-22454# Joint Publications Research Service, Arlington, Va.
FEOKTISTOV DISCUSSES NEED FOR SPACE COLONIZATION
Konstantin P. Feoktistov *In its* USSR Rept.: Space (JPRS-USP-85-001) 4 Feb. 1985 p 100-103 Transl. into ENGLISH from Sotsialisticheskaya Ind. (USSR), 23 Nov. 1984 p 4 (For primary document see N85-22403 13-12)
Avail: NTIS HC A07

Four basic arguments (energy, population, cataclyms, and natural resources) that are advanced by advocates of settling in space are examined. These arguments are then contrasted with the technical assessment of the present achievements. There is no doubt that sooner or later, man will build large objects in space for the purpose of solving various scientific and applied problems. Undoubtedly these will be of great assistance in the solution by mankind of its own terrestrial problems, but whether or not they become the basic place and means for the development of terrestrial civilization remains to be seen. B.G.

N85-22455# Joint Publications Research Service, Arlington, Va.
U.S., SOVIET SPACE PROGRAM AIMS CONTRASTED
G. S. Khozin *In its* USSR Rept.: Space (JPRS-USP-85-001) 4 Feb. 1985 p 104-110 Transl. into ENGLISH from Zemlya i Vselennaya (USSR), no. 2, Mar.-Apr. 1984 p 14-18 (For primary document see N85-22403 13-12)
Avail: NTIS HC A07

International treaties and agreements which establish the principles for research and use of space for peaceful purposes are used to assess the U.S. and U.S.S.R. space programs. B.G.

N85-22456# Joint Publications Research Service, Arlington, Va.
INMARSAT MARINE SATELLITE ORGANIZATION c15
V. Y. Anoshin and K. A. Bekyashev *In its* USSR Rept.: Space (JPRS-USP-85-001) 4 Feb. 1985 p 111-118 Transl. into ENGLISH from Rybnoye Khozyaystvo (USSR), no. 3, Mar. 1984 p 45-48 (For primary document see N85-22403 13-12)
Avail: NTIS HC A07

The policies, organizational structure, financial management, membership, satellite network, and operating procedures of INMARSAT (International Organization of Marine Satellite Communication) are discussed. B.G.

N85-22457# Joint Publications Research Service, Arlington, Va.
LIST OF RECENT SOVIET SPACE LAUNCHES c15
In its USSR Rept.: Space (JPRS-USP-85-001) 4 Feb. 1985 p 119 Transl. into ENGLISH from Tass (USSR), n.d., n.p. (For primary document see N85-22403 13-12)
Avail: NTIS HC A07

The launch schedule for Soviet spacecraft is given with the following orbital parameters: apogee, perigee, period, inclination. Also included is the date and designation. B.G.

13 ASTRODYNAMICS

Includes powered and free-flight trajectories; and orbit and launching dynamics.

N85-22458 Colorado Univ., Boulder.
SATELLITE-TO-SATELLITE ORBIT DETERMINATION USING MINIMUM, DISCRETE RANGE AND RANGE-RATE DATA ONLY Ph.D. Thesis
Chia-Chuan Chow 1984 106 p

Avail: Univ. Microfilms Order No. DA8428642

The problem of determining the orbit of an unknown satellite from another satellite given minimum range and range-rate observations at discrete times is considered. The problem considered is, for concreteness, a geocentric satellite observing another geocentric satellite. The orbit determination goal is for simplicity, the calculation of position and velocity at one of the observation times. It is shown that the unknown position and velocity at the chosen epoch can be obtained by solving a set of six nonlinear algebraic equations in which the position and velocity at other times are computed by using f and g functions. The resulting system of six nonlinear algebraic equations is then solved by iteration with a modified Newton's method. Several sophisticated methods were applied and a hybrid method due to Powell was selected from these. Results obtained from application of the method to a number of examples are examined. Rules for constructing the initial guesses that reduce computation and improve the probability of convergence to the true solution are presented. Dissert. Abstr.

N85-22417# Joint Publications Research Service, Arlington, Va.
NONTRADITIONAL METHOD FOR DETERMINING UNPERTURBED ORBITS OF UNKNOWN SPACE OBJECTS USING INCOMPLETE OPTICAL OBSERVATIONAL DATA Abstract Only
N. I. Perov *In its* USSR Rept.: Space (JPRS-USP-85-001) 4 Feb. 1985 p 39 Transl. into ENGLISH from Astronomicheskiy Zh. (USSR), v. 61, no. 3, May-Jun. 1984 p 571-576 (For primary document see N85-22403 13-12)
Avail: NTIS HC A07

N85-22419# Joint Publications Research Service, Arlington, Va.
ALGORITHM FOR DETERMINING OPTIMAL THREE IMPULSE POINT-TO-ORBIT TRANSFER WITH LIMITED TRANSFER TIME Abstract Only
V. V. Ivashkin and A. P. Skorokhodov *In its* USSR Rept.: Space (JPRS-USP-85-001) 4 Feb. 1985 p 40 Transl. into ENGLISH from Kosmicheskiy Issled. (USSR), v. 22, no. 1, Jan.-Feb. 1984 p 3-12 (For primary document see N85-22403 13-12)
Avail: NTIS HC A07

N85-22421# Joint Publications Research Service, Arlington, Va.
REJECTION OF ANOMALOUS OBSERVATIONS WHEN DETERMINING SPACECRAFT TRAJECTORIES Abstract Only
Y. S. Savrasov *In its* USSR Rept.: Space (JPRS-USP-85-001) 4 Feb. 1985 p 41-42 Transl. into ENGLISH from Kosmicheskiye Issled. (USSR), v. 22, no. 1, Jan.-Feb. 1984 p 20-36 (For primary document see N85-22403 13-12)
Avail: NTIS HC A07

N85-22428# Joint Publications Research Service, Arlington, Va.
ROTATIONAL MOTION OF A SATELLITE Abstract Only
A. A. Khentov *In its* USSR Rept.: Space (JPRS-USP-85-001) 4 Feb. 1985 p 46-47 Transl. into ENGLISH from Kosmicheskiye Issled. (USSR), v. 22, no. 1, Jan.-Feb. 1984 p 130-131 Original language document announced as A84-26988 (For primary document see N85-22403 13-12)
Avail: NTIS HC A07

N85-22429# Joint Publications Research Service, Arlington, Va.
SATELLITE OSCILLATIONS IN ELLIPTICAL ORBIT Abstract Only
A. A. Burov *In its* USSR Rept.: Space (JPRS-USP-85-001) 4 Feb. 1985 p 47 Transl. into ENGLISH from Kosmicheskiye Issled. (USSR), v. 22, no. 1, Jan.-Feb. 1984 p 133-134 (For primary document see N85-22403 13-12)
Avail: NTIS HC A07

N85-22781# Joint Publications Research Service, Arlington, Va.
SPACE INTERCEPTION GUIDANCE WITH UNCERTAIN FACTORS Abstract Only
Sun Shiqing *In its* China Rept: Sci. and Technol. (JPRS-CST-84-030) 10 Oct. 1984 p 44 refs Transl. into ENGLISH from Yuhang Xuebao (Beijing, China), no. 2, 30 Apr. 1984 p 32-42 Original language document previously announced as A84-43355 (For primary document see N85-22777 13-31)
Avail: NTIS HC A03/MF A01

N85-22783# Joint Publications Research Service, Arlington, Va.
PERIODIC MOVEMENTS OF AXISYMMETRICAL SATELLITE ABOUT CENTER OF MASS DUE TO GRAVITATIONAL MOMENT Abstract Only
V. V. Sazonov and M. Ye. Sidoryuk *In its* USSR Rept.: Eng. and Equipment (JPRS-UEQ-85-003) 12 Mar. 1985 p 1 Transl. into ENGLISH from Izv. Akad. Nauk SSSR: Mekhan. Tverdogo Tela (Moscow), no. 3, May - Jun. 1984 p 6-16 (For primary document see N85-22782 13-31)
Avail: NTIS HC A06

N85-22847# Joint Publications Research Service, Arlington, Va.
DEVELOPMENT, PROSPECT OF SATELLITE DYNAMICS DISCUSSED
Huang Kuyi *In its* Chinese Rept.: Sci. and Technol. (JPRS-CST-85-005) 20 Feb. 1985 p 84-95 refs Transl. into ENGLISH from Ziran Zazhi (Shanghai), no. 9, 1984 p 663-667 (For primary document see N85-22843 13-31)
Avail: NTIS HC A10/MF A01

14 GROUND SUPPORT SYSTEMS AND FACILITIES (SPACE)

Includes launch complexes, research and production facilities; ground support equipment, e.g., mobile transporters; and simulators.

For related information see also *09 Research Support Facilities (Air).*

N85-22507*# SRI International Corp., Menlo Park, Calif.
DEVELOPMENT OF A CONTINUOUS BROAD-ENERGY-SPECTRUM ELECTRON SOURCE
R. C. Adamo and J. E. Nanevicz *In* NASA. Lewis Research Center Spacecraft Environ. Interactions Technol., 1983 Mar. 1985 p 465-475 refs (For primary document see N85-22470 13-18)
(Contract DNA001-81-C-0267)
Avail: NTIS HC A99/MF E03 CSCL 14B

15 LAUNCH VEHICLES AND SPACE VEHICLES

Includes boosters; manned orbital laboratories; reusable vehicles; and space stations.

N85-22459*# Boeing Aerospace Co., Huntsville, Ala.
SPACE STATION SYSTEMS TECHNOLOGY STUDY (ADD-ON TASK). VOLUME 1: EXECUTIVE SUMMARY Final Report
Feb. 1985 105 p Prepared in cooperation with Spectra Research Systems, Inc., Huntsville, Ala. 3 Vol.
(Contract NAS8-34893)
(NASA-CR-171415; NAS 1.26:171415; D483-10012-1) Avail: NTIS HC A06/MF A01 CSCL 22B

System concepts were characterized in order to define cost versus benefits for autonomous functional control and for controls and displays for OMV, OTV, and spacecraft servicing and operation. The attitude control topic focused on characterizing the Space Station attitude control problem through simulation of control system responses to structural disturbances. The first two topics, mentioned above, focused on specific technology items that require advancement in order to support an early 1990s initial launch of a Space Station, while the attitude control study was an exploration of the capability of conventional controller techniques. G.L.C.

N85-22460*# National Aeronautics and Space Administration, Washington, D. C.
ADVANCING AUTOMATION AND ROBOTICS TECHNOLOGY

FOR THE SPACE STATION AND FOR THE US ECONOMY. VOLUME 1: EXECUTIVE OVERVIEW
Mar. 1985 36 p 2 Vol.
(NASA-TM-87566-Vol-1; NAS 1.15:87566-Vol-1) Avail: NTIS HC A03/MF A01 CSCL 22B

In response to Public Law 98-371, dated July 18, 1984, the NASA Advanced Technology Advisory Committee has studied automation and robotics for use in the Space Station. The Executive Overview, Volume 1 presents the major findings of the study and recommends to NASA principles for advancing automation and robotics technologies for the benefit of the Space Station and of the U.S. economy in general. As a result of its study, the Advanced Technology Advisory Committee believes that a key element of technology for the Space Station is extensive use of advanced general-purpose automation and robotics. These systems could provide the United States with important new methods of generating and exploiting space knowledge in commercial enterprises and thereby help preserve U.S. leadership in space. Author

N85-22461*# National Aeronautics and Space Administration, Washington, D. C.
ADVANCING AUTOMATION AND ROBOTICS TECHNOLOGY FOR THE SPACE STATION AND FOR THE US ECONOMY, VOLUME 2
Mar. 1985 160 p refs 2 Vol.
(NASA-TM-87566-Vol-2; NAS 1.15:87566-Vol-2) Avail: NTIS HC A08/MF A01 CSCL 22B

In response to Public Law 98-371, dated July 18, 1984, the NASA Advanced Technology Advisory Committee has studied automation and robotics for use in the Space Station. The Technical Report, Volume 2, provides background information on automation and robotics technologies and their potential and documents: the relevant aspects of Space Station design; representative examples of automation and robotics; applications; the state of the technology and advances needed; and considerations for technology transfer to U.S. industry and for space commercialization. Author

N85-22462*# Martin Marietta Corp., Denver, Colo. Space Systems Div.
SELECTED TETHER APPLICATIONS IN SPACE: PHASE 2. EXECUTIVE SUMMARY Final Report
Morris H. Thorson and Lester J. Lippy Feb. 1985 23 p
(Contract NAS8-35499)
(NASA-CR-171421; NAS 1.26:171421; MCR-85-1309) Avail: NTIS HC A02/MF A01 CSCL 22B

The application of tether technology has the potential to increase the overall performance efficiency and capability of the integrated space operations and transportation systems through the decade of the 90s. The primary concepts for which significant economic benefits were identified are dependent on the space station as a storage device for angular momentum and as an operating base for the tether system. Concepts examined include: (1) tether deorbit of shuttle from space station; (2) tethered orbit insertion of a spacecraft from shuttle; (3) tethered platform deployed from space station; (4) tether-effected rendezvous of an OMV with a returning OTV; (5) electrodynamic tether as an auxiliary power source for space station; and (6) tether assisted launch of an OTV mission from space station. A.R.H.

N85-22463*# Martin Marietta Corp., Denver, Colo. Space Systems Div.
SELECTED TETHER APPLICATIONS IN SPACE: PHASE 2 Final Report
Morris H. Thorsen and Lester J. Lippy Feb. 1985 138 p
(Contract NAS8-35499)
(NASA-CR-171422; NAS 1.26:171422; MCR-85-1308) Avail: NTIS HC A07/MF A01 CSCL 22B

System characteristics and design requirements are assessed for tether deployment. Criteria are established for comparing alternate concepts for: (1) deployment of 220 klb space shuttle from the space station; (2) tether assisted launch of a 20,000 lb payload to geosynchronous orbit; (3) placement of the 20,000 lb AXAF into 320 nmi orbit via orbiter; (4) retrieval of 20,000 lb AXAF from 205 nmi circular orbit for maintenance and reboost to 320 nmi; and (5) tethered OMV rendezvous and retrieval of OTV returning from a geosynchronous mission. Tether deployment systems and technical issues are discussed. A.R.H.

N85-22420# Joint Publications Research Service, Arlington, Va.
MOTION OF SYMMETRICAL SATELLITE WITH FLEXIBLE VISCOELASTIC RODS ABOUT CENTER OF MASS IN CIRCULAR ORBIT Abstract Only
N. Y. Bolotina and V. G. Vilke *In its* USSR Rept.: Space (JPRS-USP-85-001) 4 Feb. 1985 p 41 Transl. into ENGLISH from Kosmicheskiy Issled. (USSR), v. 22, no. 1, Jan.-Feb. 1984 p 13-19 (For primary document see N85-22403 13-12)
Avail: NTIS HC A07

N85-22456# Joint Publications Research Service, Arlington, Va.
INMARSAT MARINE SATELLITE ORGANIZATION
V. Y. Anoshin and K. A. Bekyashev *In its* USSR Rept.: Space (JPRS-USP-85-001) 4 Feb. 1985 p 111-118 Transl. into ENGLISH from Rybnoye Khozyaystvo (USSR), no. 3, Mar. 1984 p 45-48 (For primary document see N85-22403 13-12)
Avail: NTIS HC A07

N85-22457# Joint Publications Research Service, Arlington, Va.
LIST OF RECENT SOVIET SPACE LAUNCHES
In its USSR Rept.: Space (JPRS-USP-85-001) 4 Feb. 1985 p 119 Transl. into ENGLISH from Tass (USSR), n.d., n.p. (For primary document see N85-22403 13-12)
Avail: NTIS HC A07

N85-22485*# Systems Science and Software, La Jolla, Calif.
ELECTRIC FIELD EFFECTS ON ION CURRENTS IN SATELLITE WAKES
D. E. Parks and I. Katz *In* NASA. Lewis Research Center Spacecraft Environ. Interactions Technol., 1983 Mar. 1985 p 195-204 refs (For primary document see N85-22470 13-18)
(Contract F19628-82-C-0081)
Avail: NTIS HC A99/MF E03 CSCL 22B

N85-22504*# Jet Propulsion Lab., California Inst. of Tech., Pasadena.
GALILEO INTERNAL ELECTROSTATIC DISCHARGE PROGRAM
Philip L. Leung, Gregory H. Plamp, and Paul A. Robinson, Jr. *In* NASA. Lewis Research Center Spacecraft Environ. Interactions Technol., 1983 Mar. 1985 p 423-433 refs (For primary document see N85-22470 13-18)
Avail: NTIS HC A99/MF E03 CSCL 22B

N85-22508*# Air Force Geophysics Lab., Hanscom AFB, Mass.
AUTOMATIC CHARGE CONTROL SYSTEM FOR SATELLITES
B. M. Shuman and H. A. Cohen *In* NASA. Lewis Research Center Spacecraft Environ. Interactions Technol., 1983 Mar. 1985 p 477-481 refs (For primary document see N85-22470 13-18)
Avail: NTIS HC A99/MF E03 CSCL 22B

N85-22520*# National Aeronautics and Space Administration. Lewis Research Center, Cleveland, Ohio.
PRELIMINARY ASSESSMENT OF POWER-GENERATING TETHERS IN SPACE AND OF PROPULSION FOR THEIR ORBIT MAINTENANCE
Robert E. English and Patrick M. Finnegan *In its* Spacecraft Environ. Interactions Technol., 1983 Mar. 1985 p 637-647 refs (For primary document see N85-22470 13-18)
Avail: NTIS HC A99/MF E03 CSCL 22B

N85-22521*# California Univ., San Diego, La Jolla. Dept. of Physics.
PRELIMINARY INVESTIGATION OF THE ELECTRODYNAMICS OF A CONDUCTING TETHER
W. B. Thompson *In* NASA. Lewis Research Center Spacecraft Environ. Interactions Technol., 1983 Mar. 1985 p 649-662 refs Sponsored in part by Martin Marietta Aerospace Corp. (For primary

document see N85-22470 13-18)
Avail: NTIS HC A99/MF E03 CSCL 22B

N85-22778# Joint Publications Research Service, Arlington, Va.
NATION SAID TO RANK HIGH WITH 15 SATELLITES
In its China Rept: Sci. and Technol. (JPRS-CST-84-30) 10 Oct. 1984 p 27 refs Transl. into ENGLISH from Xinhua (Beijing, China), 5 Sep. 1984 (For primary document see N85-22777 13-31)
Avail: NTIS HC A03/MF A01

16 SPACE TRANSPORTATION

Includes passenger and cargo space transportation, e.g., shuttle operations; and rescue techniques.

For related information see also *03 Air Transportation and Safety* and *85 Urban Technology and Transportation.*

N85-22464*# Jet Propulsion Lab., California Inst. of Tech., Pasadena.
REPORT ON FINAL RECOMMENDATIONS FOR IMPS ENGINEERING-SCIENCE PAYLOAD
Henry B. Garrett 1 Sep. 1984 124 p refs
(Contract NAS7-918)
(NASA-CR-175659; JPL-Pub-84-56; NAS 1.26:175659) Avail: NTIS HC A06/MF A01 CSCL 22B

Six general categories of key scientific and engineering concerns for the interactions measurements payload for shuttle (IMPS) mission are addressed: (1) dielectric charging; (2) material property changes; (3) electromagnetic interference, plasma interactions, and plasma wake effects associated with high-voltage solar arrays and large space structures; (4) radio frequency distortion and nonlinearities due to the enhanced plasma in the shuttle ram/wake; (5) shuttle glow and contamination; and (6) plasma interactions with the space-based radar. Lesser concerns are the interactions associated with EVA; the radiation and SEU effects peculiar to the auroral/polar cap environments; and space debris. The measurements needed to address the concerns associated with the general categories are described and a list of generic investigations capable of making the required measurements, emphasizing the spectrum of measurements necessary to quantize the interactions in the auroral/polar environments are included. A suggested ground-test plan for the IMPS project, a description of proposed follow-on IMPS missions, and a detailed bibliography for each of the interactions discussed are included. Author

N85-22465*# Lockheed Missiles and Space Co., Sunnyvale, Calif.
VIBROACOUSTIC STUDY OF THE NASA GODDARD SPACE FLIGHT CENTER OSS-1 PAYLOAD
Y. A. Lee and W. Henricks Jan. 1985 37 p refs
(Contract NAS5-25156)
(NASA-CR-175320; NAS 1.26:175320; LMSC-D980796) Avail: NTIS HC A03/MF A01 CSCL 22B

A comparative evaluation of shuttle liftoff and ground test random response data obtained from the Office of Space Science-1 (OSS-1) pallet payload flown in the cargo bay of STS-3 is presented. The study was initiated to evaluate the possibility that the payload flight vibration response can exceed that occurred during ground test when the ground test acoustic excitation is normalized to the flight acoustic environment. In addition, the analytically derived response from the Vibroacoustic Payload Environment Prediction System (VAPEPS) is compared with OSS-1 ground test results. M.G.

N85-22466*# Chrysler Corp., New Orleans, La. Data Management Services.
RESULTS OF AEROHEATING DFI AND ET DESIGN-DATA TEST ON A 0.0175-SCALE MODEL 60-OTS CONDUCTED IN THE VON KARMAN GAS DYNAMICS FACILITY (VKF) 40' SUPERSONIC AND THE 50' HYPERSONIC WIND TUNNELS A AND C
J. Marroquin (Rockwell International Corp., Downey, Calif.) and C. R. Leef (Rockwell International Corp., Downey, Calif.) Mar. 1985 169 p refs
(Contract NAS9-17179)
(NASA-CR-167693; NAS 1.26:167693; DMS-DR-2520) Avail: NTIS HC A08/MF A01 CSCL 22B

The 0.0175-scale thin-skin thermocouple Model 60-OTS was tested in the von Karman Gas Facility 40-inch continuous flow supersonic tunnel A and the VKF Tunnel C. Testing was conducted at Mach numbers 2.25 to 4.0, and Reynolds numbers from 0.4 x 10 to the 6th power/ft to 6.6 x 10 to the 6th power/ft. Angle of attack range was from -5.0 to +5.0 degrees, and angle of sideslip range was from -6 to +6 degrees. The primary objective of this test was to provide a valid base for the external tank (ET) and solid rocket booster (SRB) heating prediction methodology for ascent flight by taking heating data at Development Flight Instrumentation (DFI) locations for flight conditions simulating STS-1 through -4. A second objective was to obtain additional aeroheating data to support potential reduction of the thermal protection system (TPS) on the ET. The third phase of the test was funded and conducted by NASA/MSFC for the purpose of establishing confidence in the data base from the lower temperature tunnel A. M.G.

N85-22467*# Chrysler Corp., New Orleans, La. Data Management Services.
RESULTS OF THE AFRSI REWATERPROOFING SYSTEMS SCREENING TEST IN THE NASA/AMES RESEARCH CENTER (ARC) 2 X 2-FOOT TRANSONIC WIND TUNNEL
J. Marroquin (Rockwell International Corp., Downey, Calif.) and R. B. Kingsland (Rockwell International Corp., Downey, Calif.) Mar. 1985 117 p refs
(Contract NAS9-17179)
(NASA-CR-167694; NAS 1.26:167694; DMS-DR-2521) Avail: NTIS HC A06/MF A01 CSCL 22B

An experimental investigation was conducted in the NASA/Ames Research Center 2x2-foot Transonic Wind Tunnel to evaluate two AFRSI rewaterproofing systems and to investigate films as a means of reducing blanket joint distortion. The wind tunnel wall slot configuration influenced on the flow field over the test panel was investigated; primarily using oil flow data, and resulted in a closed slot configuration to provide a satisfactory screening environment flow field for the test. Sixteen AFRSI test panels, configured to represent the test system or film, were subjected to this screening environment (a flow field of separated and reattached flow at a freestream Mach numnber of 0.65 and q = 650 or 900 psf). Each condition was held until damage to the test article was observed or 55 minutes if no damage was incurred. All objectives related to AFRSI rewaterproofing and to the use of films to stiffen the blanket fibers were achieved. Author

N85-22468*# Chrysler Corp., New Orleans, La. Data Management Services.
RESULTS OF A M = 5.3 HEAT TRANSFER TEST OF THE INTEGRATED VEHICLE USING PHASE-CHANGE PAINT TECHNIQUES ON THE 0.0175-SCALE MODEL 56-OTS IN THE NASA/AMES RESEARCH CENTER 3.5-FOOT HYPERSONIC WIND TUNNEL
John Marroquin (Rockwell International Corp., Downey, Calif.) Mar. 1985 31 p ref
(Contract NAS9-17179)
(NASA-CR-167695; NAS 1.26:167695; DMS-DR-2524) Avail: NTIS HC A03/MF A01 CSCL 22B

An experimental investigation was performed in the NASA/Ames Research Center 3.5-foot Hypersonic Wind Tunnel to obtain supersonic heat-distribution data in areas between the orbiter and external tank using phase-change paint techniques. The tests used Novamide SSV Model 56-OTS in the first and second-stage ascent configurations. Data were obtained at a nominal Mach number of 5.3 and a Reynolds number per foot of 5 x 10 to the 6th power with angles of attack of 0 deg, +/- 5 deg, and sideslip angles of 0 deg and +/- 5 deg. M.G.

N85-22469# Florida Univ., Gainesville.
SHUTTLE FLIGHT TEST OF AN ADVANCED GAMMA-RAY

DETECTION SYSTEM Semiannual Technical Report, 1 Jul. - 31 Dec. 1983
A. C. Rester, Jr. 28 Feb. 1984 21 p
(Contract F49620-83-C-0131; ARPA Order 4565; AF Proj. 230-9) (AD-A150316; AFOSR-84-1256TR) Avail: NTIS HC A02/MF A01 CSCL 18/4

In August of 1983 the Gamma-Ray Advanced Detector (GRAD) Project was assigned to the AFP-675 Program for flight on a future Space Shuttle mission. In order to adapt the experiment to the requirements of AFP-675 we are making a number of changes, both in hardware and software. However, the necessity for such changes is more than affected by an expansion in scope of the experiment made possible by the introduction of a Payload Specialist into the operation. The principal changes to be made are in the avionics, as GRAD was originally designed for operation through ground-based telemetry. This complete redesigning of our avionics to accomodate operation by a Payload Specialist from the aft flight deck of the Orbiter allows us to take advantage of very recent findings on radiation-induced microprocessor failure in other space shuttle experiments in order to make the GRAD avionics less vulnerable to such latch-ups. Advances in bismuth germanate (BGO) scintillator technology during the year since construction of the prototype GRAD now make it possible for us to construct a BGO shield with a closed-ended geometry. This improvement will enhance the signal-to-noise ratio. In addition we are experimenting with a new type of decay-vetoed calibration probe using an alpha-rather than a beta-emitting radioactive source. GRA

N85-22453# Joint Publications Research Service, Arlington, Va.
FEOKTISTOV ARGUES AGAINST U.S. SPACE SHUTTLE DESIGN CONCEPT
Konstantin P. Feoktistov *In its* USSR Rept.: Space (JPRS-USP-85-001) 4 Feb. 1985 p 95-99 Transl. into ENGLISH from Sotsialisticheskaya Ind. (USSR), 22 Nov. 1984 p 4 (For primary document see N85-22403 13-12)
Avail: NTIS HC A07

17 SPACECRAFT COMMUNICATIONS, COMMAND AND TRACKING

Includes telemetry; space communications networks; astronavigation; and radio blackout.

For related information see also *04 Aircraft Communications and Navigation* and *32 Communications.*

No abstracts in this category.

18 SPACECRAFT DESIGN, TESTING AND PERFORMANCE

Includes spacecraft thermal and environmental control; and attitude control.

For life support systems see *54 Man/System Technology and Life Support.* For related information see also *05 Aircraft Design, Testing and Performance* and *39 Structural Mechanics.*

N85-22470*# National Aeronautics and Space Administration. Lewis Research Center, Cleveland, Ohio.
SPACECRAFT ENVIRONMENTAL INTERACTIONS TECHNOLOGY, 1983
Washington Mar. 1985 673 p refs Conf. held in Colorado Springs, 4-6 Oct. 1983 Prepared in cooperation with AFGL, Hanscom AFB, Mass.
(NASA-CP-2359; E-2186; NAS 1.55:2359; AFGL-TR-0018) Avail: NTIS HC A99/MF E03 CSCL 22B

State of the art of environment interactions dealing with low-Earth-orbit plasmas; high-voltage systems; spacecraft charging; materials effects; and direction of future programs are contained in over 50 papers. For individual titles, see N85-22471 through N85-22523.

N85-22471*# National Aeronautics and Space Administration, Washington, D. C.
SPACE STATION TECHNOLOGY PLANNING
R. E. Smylie *In* NASA. Lewis Research Center Spacecraft Environ. Interactions Technol., 1983 Mar. 1985 p 1-8 (For primary document see N85-22470 13-18)
Avail: NTIS HC A99/MF E03 CSCL 22B

Technological requirements for Space Station design were discussed. The requirements are discussed in relation to the following areas: high voltage arrays; environmental interactions; energy management; power supplies; architecture; and modularity. B.G.

N85-22472*# National Aeronautics and Space Administration, Washington, D. C.
SUPRATHERMAL PLASMA OBSERVED ON STS-3 MISSION BY PLASMA DIAGNOSTICS PACKAGE c75
W. Paterson, L. A. Frank, H. Owens, J. S. Pickett, G. B. Murphy, and S. D. Shawhan *In* NASA. Lewis Research Center Spacecraft Environ. Interactions Technol., 1983 Mar. 1985 p 13-17 refs Prepared in cooperation with Iowa Univ., Iowa City (For primary document see N85-22470 13-18)
(Grant NAG3-449)
Avail: NTIS HC A99/MF E03 CSCL 20I

Artificially produced electron beams were used extensively during the past decade as a means of probing the magnetosphere, and more recently as a means of actively controlling spacecraft potential. Experimentation in these areas has proven valuable, yet at times confusing, due to the interaction of the electron beam with the ambient plasma. The OSS-1/STS-3 Mission in March 1982 provided a unique opportunity to study beam-plasma interactions at an altitude of 240 km. On board for this mission was a Fast Pulse Electron Generator (FPEG). Measurements made by the Plasma Diagnostics Package (PDP) while extended on the Orbiter RMS show modifications of the ion and electron energy distributions during electron beam injection. Observations made by charged particle detectors are discussed and related to measurements of Orbiter potential. Several of the PDP instruments, the joint PDP/FPEG experiment, and observations made during electron beam injection are described. B.G.

N85-22473*# Stanford Univ., Calif.
VEHICLE CHARGING ON STS-3 MISSION
P. R. Williamson, P. M. Banks, L. R. O. Storey, and W. J. Raitt (Utah State Univ., Logan) *In* NASA. Lewis Research Center Spacecraft Environ. Interactions. Technol., 1983 Mar. 1985 p 19-32 (For primary document see N85-22470 13-18)
(Contract NAS5-24455; Grant NAGw-235)
Avail: NTIS HC A99/MF E03 CSCL 22B

In the Vehicle Charging and Potential experiment on the STS-3 mission, a pulsed electron gun was used to eject known charges and currents from the Shuttle Orbiter, and the resulting perturbations of the surface charge and current densities were studied with appropriate instruments. An ejected current of 100 mA, if maintained for a time sufficiently long for equilibrium to be established, could change the vehicle potential by 50 V or more when the ambient plasma density was low. In general, the observed perturbations could be ordered qualitatively in terms of the plasma density and of the attitude of the shuttle relative to its orbital velocity vector. Author

N85-22474*# National Aeronautics and Space Administration, Washington, D. C.
ELECTRON AND ION DENSITY DEPLETIONS MEASURED IN THE STS-3 ORBITER WAKE
G. B. Murphy (Iowa Univ., Iowa City), J. S. Pickett (Iowa Univ., Iowa City), W. S. Raitt (Utah State Univ., Logan), and S. D. Shawhan

In NASA. Lewis Research Center Spacecraft Environ. Interactions Technol., 1983 Mar. 1985 p 33-42 refs (For primary document see N85-22470 13-18)
(Contract NAG3-449)
Avail: NTIS HC A99/MF E03 CSCL 22B

The third Space Shuttle flight on Columbia carried instrumentation to measure thermal plasma density and temperature. Two separate investigations, the Plasma Diagnostics Package (PDP) and the Vehicle Charging and Potential Experiment (VCAP), carried a Langmuir Probe, and the VCAP also included a Spherical Retarding Potential Analyzer (SRPA). Only those measurements made while the PDP is in the payload bay are discussed here since the VCAP instrumentation remains in the payload bay at all times and the two measurements are compared. The wake behind a large structure (in this case the Space Shuttle Orbiter) flying through the ionospheric plasma is discussed. Much theoretical work was done regarding plasma wakes. The instrumentation on this mission gives the first data taken with a large vehicle in the ionospheric laboratory. First, the PDP Langmuir Probe and its data set will be presented, then the VCAP Langmuir Probe and SRPA with associated data. The agreement between the two data sets is discussed and then followed by some other PDP data which infers an even lower wake density. B.G.

N85-22475*# Air Force Geophysics Lab., Hanscom AFB, Mass.
SHUTTLE ELECTRICAL ENVIRONMENT
M. Smiddy, W. P. Sullivan, D. Girouard, and P. B. Anderson (Regis Coll.) *In* NASA. Lewis Research Center Spacecraft Environ. Interactions Technol., 1983 Mar. 1985 p 43-70 (For primary document see N85-22470 13-18)
Avail: NTIS HC A99/MF E03 CSCL 22B

Part of an AFGL payload flown on the STS-4 mission consisted of experiments to measure in-situ electric fields, electron densities, and vehicle charging. During this flight some 11 hours of data were acquired ranging from 5 minute snapshots up to continuous half-orbits. These experiments are described and results presented for such vehicle induced events as a main engine burn, thruster firings and water dumps in addition to undisturbed periods. The main characteristic of all the vehicle induced events is shown to be an enhancement in the low frequency noise (less than 2 kHz), in both the electrostatic and electron irregularity (delta N/N) spectra. The non-event results indicate that the electrostatic broadband emissions show a white noise characteristic in the low frequency range up to 2 kHz at an amplitude of 10 db above the shuttle design specification limit, falling below that limit above 10 kHz. The vehicle potential remained within the range of -3 to +1 volt throughout the flight which exhibits normal behavior for a satellite in a low equatorial orbit. Author

N85-22476*# Air Force Geophysics Lab., Hanscom AFB, Mass.
MEASURED ELECTRON CONTRIBUTION TO SHUTTLE PLASMA ENVIRONMENT: ABBREVIATED UPDATE
W. McMahon, R. Salter, R. Hills (Tri-Con Associates, Inc., Cambridge, Mass.), and D. Delorey (Boston Coll., Chestnut Hill, Mass.) *In* NASA. Lewis Research Center Spacecraft Environ. Interactions Technol., 1983 Mar. 1985 p 71-80 refs (For primary document see N85-22470 13-18)
Avail: NTIS HC A99/MF E03 CSCL 22B

The differential energy spectra of electrons between 1 and 100 eV were measured by an electron spectrometer flown on an early shuttle. This energy range was scanned in 64 incremental steps with a resolution of 7%. The most striking feature that was observed throughout these spectra was a relatively flat distribution of the higher energy electrons out to 100 eV. This is in contrast to normal ambient spectra which consistently show a rapid decline in quantitative flux beyond 50 to 55 eV. The lower energy (1 to 2 eV) end of these spectra showed steep thermal trails comparable to normal ambient spectral structure. In general, daytime fluxes were significantly higher than those obtained during nighttime measurements. Quantitative flux excursions which may possibly be associated with thruster firing were frequently observed. Spectral structure suggestive of the N2 vibrational excitation energy loss mechanism was also seen in the data from some measurement periods. Examples of these spectra are shown and possible correlations are discussed. Author

N85-22477*# National Aeronautics and Space Administration. Lewis Research Center, Cleveland, Ohio.
LABORATORY STUDIES OF KAPTON DEGRADATION IN AN OXYGEN ION BEAM **c72**
Dale C. Ferguson *In its* Spacecraft Environ. Interactions Technol., 1983 Mar. 1985 p 81-90 refs (For primary document see N85-22470 13-18)
Avail: NTIS HC A99/MF E03 CSCL 18H

Results are presented from a preliminary laboratory investigation of the degradation of the widely used polyimide Kapton under oxygen ion bombardment. Recent space shuttle flights have shown that Kapton and some other materials exposed to the apparent ram flow of residual atmosphere (at orbital velocity in low Earth orbit) lose mass and change their optical properties. It was hypothesized that these changes are caused by chemical interaction with atomic oxygen, aided by the 5-eV impact energy of atmospheric oxygen atoms in the ram. The reaction rate under O(+) bombardment seemed to be independent of incident energy over a wide range of energies. Although the flux of thermal ions in this experiment was much greater than the accelerated flux, the observed Kapton degradation was limited to the beam area and ram flow direction. This is consistent with an activation energy above the thermal energies but well below the beam energies. The results reproduce well the material loss, optical changes, SEM surface structure, and ram directionality of the samples returned by the shuttle. These factors, along with the lack of degradation under argon ion bombardment, are convincing evidence for ram flow oxidation as the mechanism of degradation. B.G.

N85-22478*# National Aeronautics and Space Administration. Lewis Research Center, Cleveland, Ohio.
ELECTRON BEAM CHARGING OF SPACE SHUTTLE THERMAL PROTECTION SYSTEM TILES
John V. Staskus *In its* Spacecraft Environ. Interactions Technol., 1983 Mar. 1985 p 91-102 refs (For primary document see N85-22470 13-18)
Avail: NTIS HC A99/MF E03 CSCL 22B

Six space shuttle reusable surface insulation tiles were tested in the NASA Lewis Research Center's electron bombardment test facility. The 30-cm-square specimens were assembled by using the same materials and techniques used to apply the tiles to the space shuttle and were composed to 15-cm- and 20-cm-square tiles and pieces on 0.6-cm-thick aluminum substrates. There were two specimens of each of three thicknesses. One specimen of each thickness had gaps of less than 0.1 cm between tiles, and the other had gaps of approximately 0.15 cm. The specimens were exposed to monoenergetic electron beams (2 to 25 keV) with nominal fluxes of 0.1 and 1 nA/sq. cm. Tests were conducted with both grounded and floating substrates. The data presented include charging rates, equilibrium potentials, and substrate currents. There is evidence that discharging occurred. Author

N85-22479*# Michigan Univ., Ann Arbor.
SPACECRAFT-ENVIRONMENT INTERACTION: THE ENVIRONMENTAL PLASMA ASPECT
Uri Samir *In* NASA. Lewis Research Center Spacecraft Environ. Interactions Technol., 1983 Mar. 1985 p 103-107 refs (For primary document see N85-22470 13-18)
Avail: NTIS HC A99/MF E03 CSCL 22B

The effects involved in the interaction between an obstacle and a space plasma can be divided into: (1) effects on the obstacle itself (i.e., its charging); and (2) effects on the environmental plasma due to the motion of the obstacle (i.e., the creation of shocks ahead of the obstacle and complicated wakes behind the obstacle). In the wake (or antisolar direction), plasma oscillations are excited and instabilities, wave-particle interactions, turbulence, etc., are believed to take place. The effects on the obstacle and on the environmental space plasma are coupled. Hence, simultaneous solutions to the Vlasov (or Boltzmann) and Poisson equations are sought. To obtain realistic solutions of practical use, three-

dimensional and time-dependent models of the interaction are needed. Achieving the latter is indeed not simple. G.L.C.

N85-22480*# Air Force Geophysics Lab., Hanscom AFB, Mass.
DIRECT MEASUREMENTS OF SEVERE SPACECRAFT CHARGING IN AURORAL IONOSPHERE
W. J. Burke, D. A. Hardy, F. J. Rich, A. G. Rubin, M. F. Tautz (RADEX, Inc.), N. A. Saflekos (Boston Coll., Chestnut Hill, Mass.), and H. C. Yeh (Boston Coll., Chestnut Hill, Mass.) *In* NASA. Lewis Research Center Spacecraft Environ. Interactions Technol., 1983 Mar. 1985 p 109-123 refs (For primary document see N85-22470 13-18)
Avail: NTIS HC A99/MF E03 CSCL 22B

Questions are addressed concerning how large space structures in polar orbit will interact with auroral environments. Because spacecraft charging at ionospheric attitudes does not seriously threaten the operation of today's relatively small polar satellites the subject of environment interactions has not received the widespread attention given to it at geostationary altitude. As a matter of economics it is desirable to apply as much as possible of what was learned about spacecraft interactions at geostationary orbit to low Earth orbits. The environment at auroral latitudes in the ionosphere differs from that encountered at geostationary altitude in at least two major aspects. (1) There is a large reservoir of high-density, cold plasma which tends to mitigate charging effects by providing a large source of charged particles from which neutralizing currents maybe drawn. Significant wake effects behind large structures will introduce new problems with differential charging. (2) Between the magnetic equator and the ionosphere, auroral electrons frequently undergo field-aligned accelerations of several kilovolts. In such environments, fluxes of energetic protons are usually below the levels of instrumentation sensitivity. G.L.C.

N85-22481*# Air Force Geophysics Lab., Hanscom AFB, Mass.
CHARGING OF DMSP/F6 SPACECRAFT IN AURORA ON 10 JANUARY 1983
Arthur L. Besse, Allen G. Rubin, and David A. Hardy *In* NASA. Lewis Research Center Spacecraft Environ. Interactions Technol., 1983 Mar. 1985 p 125-130 refs (For primary document see N85-22470 13-18)
Avail: NTIS HC A99/MF E03 CSCL 22B

Spacecraft charging has been widely observed in geosynchronous orbit on the ATS-5 and ATS-6 pair and on the SCATHA spacecraft. An adequate theory for explaining the observations exist. Neither the data or theory can be exported to low polar orbit and its drastically different environment. Evidence of charging on the DMSP F6 spacecraft is presented. A simple model is set up explaining the observations. Two independent instruments on the spacecraft showed charging to a moderate (44 volts) negative potential. The selection spectrometer showed a flux of 2 billion electrons per sq. cm. sec. ster. peaked at 9.5 keV. This was marginally sufficient to overcome the flux of cold ambient ions. Charging calculations are presented showing where simplications are justified and where serious uncertainties exist. More serious charging is predicted for the Shuttle in polar orbit. G.L.C.

N85-22482*# Air Force Geophysics Lab., Hanscom AFB, Mass.
AVERAGE AND WORST-CASE SPECIFICATIONS OF PRECIPITATING AURORAL ELECTRON ENVIRONMENT
David A. Hardy, William J. Burke, M. S. Gussenhoven, E. Holeman (Emmanuel Coll.), and H. C. Yeh (Boston Coll., Chestnut Hill, Mass.) *In* NASA. Lewis Research Center Spacecraft Environ. Interactions Technol., 1983 Mar. 1985 p 131-153 refs (For primary document see N85-22470 13-18)
Avail: NTIS HC A99/MF E03 CSCL 22B

The precipitation electrons in the auroral environment are highly variable in their energy and intensity in both space and time. As such they are a source of potential hazard to the operation of the Space Shuttle and other large spacecraft operating in polar orbit. In order to assess these hazards both the average and extreme states of the precipitating electrons must be determined. Work aimed at such a specification is presented. First results of a global study of the average characteristics are presented. In this study the high latitude region was divided into spatial elements in magnetic local time and corrected geomagnetic latitude. The average electron spectrum was then determined in each spatial element for seven different levels of activity as measured by K sub p using an extremely large data set of auroral observations. Second a case study of an extreme auroral electron environment is presented, in which the electrons are accelerated through field aligned potential as high as 30,000 volts and in which the spacecraft is seen to charge negatively to a potential approaching .5 kilovolts. G.L.C.

N85-22483*# Southwest Research Inst., San Antonio, Tex.
POLAR PLASMAS AS OBSERVED BY DYNAMICS EXPLORERS 1 AND 2 c75
J. Barfield, J. Burch, C. Gurgiolo, C. Lin, D. Winningham, and N. A. Saflekos *In* NASA. Lewis Research Center Spacecraft Environ. Interactions Technol., 1983 Mar. 1985 p 155-176 refs (For primary document see N85-22470 13-18)
(Contracts NAS5-26363; NAS5-25693; F19628-82K-0024; FY7121-83-N-001)
Avail: NTIS HC A99/MF E03 CSCL 20I

Plasma measurements from the Dynamics Explorer 1 and 2 satellites were used to characterize the polar cap environment. Analysis of numerous polar-cap passes indicate that, in general, three major regimes of plasma exist: (1) polar rain--electrons with magnetosheath-like energy spectra but much lower densities, most intense near the cusp and weakening toward the central polar cap; (2) polar wind--low energy upward flowing ions with both field-aligned and conical distributions; and (3) acceleration events--sporadic events consistent with the acceleration of electrons and positive ions by parallel electric fields. (1) to (3) were observed at high altitudes by Dynamics Explorer 1, while (1) and (3) were also observed at low altitudes by Dynamics Explorer 2. The plasma parameters associated with these plasma regimes are presented and discussed in terms of source and acceleration mechanisms. G.L.C.

N85-22484*# Jet Propulsion Lab., California Inst. of Tech., Pasadena.
AURORAL-POLAR CAP ENVIRONMENT AND ITS IMPACT ON SPACECRAFT PLASMA INTERACTIONS
Henry B. Garrett *In* NASA. Lewis Research Center Spacecraft Environ. Interactions Technol., 1983 Mar. 1985 p 177-193 refs Sponsored in part by AFGL (For primary document see N85-22470 13-18)
(Contract NAS7-918)
Avail: NTIS HC A99/MF E03 CSCL 22B

The high density of the plasma at shuttle altitude is likely to increase greatly the possibility of arcing and shorting of exposed high voltage surfaces. For military missions over the polar caps and through the auoroal zones, the added hazards of high energy auroral particle fluxes or solar flares will further increase the hazard to shuttle, its crew, and its mission. A review of the role that the auroral and polar cap environment play in causing these interactions was conducted. A simple, though comprehensive attempt at modelling the shuttle environment at 400 km will be described that can be used to evaluate the importance of the interactions. The results of this evaluation are then used to define areas where adequate environmental measurements will be necessary if a true spacecraft interactions technology is to be developed for the shuttle. G.L.C.

N85-22485*# Systems Science and Software, La Jolla, Calif.
ELECTRIC FIELD EFFECTS ON ION CURRENTS IN SATELLITE WAKES c15
D. E. Parks and I. Katz *In* NASA. Lewis Research Center Spacecraft Environ. Interactions Technol., 1983 Mar. 1985 p 195-204 refs (For primary document see N85-22470 13-18)
(Contract F19628-82-C-0081)
Avail: NTIS HC A99/MF E03 CSCL 22B

Small currents associated with satellite spin, dielectric conduction, or trace concentrations of H+, can have a substantial effect on the potential of a satellite and the particle currents reaching

its surface. The importance of such small currents at altitudes below about 300 km stems from the extremely small 0+ currents impinging on the wake-side of the spacecraft. The particle current on the downstream side of the AE-C satellite is considered. Theoretical estimates based on a newly described constant of the motion of a particle indicate that accounting for small concentrations of H+ remove a major discrepancy between calculated and measured currents. G.L.C.

N85-22486*# National Aeronautics and Space Administration. Lewis Research Center, Cleveland, Ohio.
THREE-DIMENSIONAL CALCULATION OF SHUTTLE CHARGING IN POLAR ORBIT
D. L. Cooke, I. Katz, M. J. Mandell, J. R. Lilley, Jr., and A. J. Rubin (AFGL) *In* NASA. Lewis Research Center Spacecraft Environ. Interactions Technol., 1983 Mar. 1985 p 205-227 refs (For primary document see N85-22470 13-18)
(Contract F19628-82-C-0081)
Avail: NTIS HC A99/MF E03 CSCL 22B

The charged particles environment in polar orbit can be of sufficient intensity to cause spacecraft charging. In order to gain a quantitative understanding of such effects, the Air Force is developing POLAR, a computer code which simulates in three dimensions the electrical interaction of large space vehicles with the polar ionospheric plasma. It models the physical processes of wake generation, ambient ion collection, precipitating auroral electron fluxes, and surface interactions, including secondary electron generation and backscattering, which lead to vehicle charging. These processes may be followed dynamically on a subsecond timescale so that the rapid passage through intense auroral arcs can be simulated. POLAR models the ambient plasma as isotropic Maxwellian electrons and ions (0+, H+), and allows for simultaneous precipitation of power-law, energetic Maxwellian, and accelerated Gaussian distributions of electrons. Magnetic field effects will be modeled in POLAR but are currently ignored. G.L.C.

N85-22487*# National Aeronautics and Space Administration. Lewis Research Center, Cleveland, Ohio.
POLAR ORBIT ELECTROSTATIC CHARGING OF OBJECTS IN SHUTTLE WAKE
I. Katz, D. E. Parks, D. L. Cooke, M. J. Mandell (AFGL), and A. J. Rubin *In* NASA. Lewis Research Center Spacecraft Environ. Interactions Technol., 1983 Mar. 1985 p 229-234 refs (For primary document see N85-22470 13-18)
(Contract F19628-82-C-0081)
Avail: NTIS HC A99/MF E03 CSCL 22B

A survey of DMSP data has uncovered several cases where precipitating auroral electron fluxes are both sufficiently intense and energetic to charge spacecraft materials such as teflon to very large potentials in the absence of ambient ion currents. Analytical bounds are provided which show that these measured environments can cause surface potentials in excess of several hundred volts to develop on objects in the orbiter wake for particular vehicle orientations. G.L.C.

N85-22488*# Parker (Lee W.), Inc., Concord, Mass.
WAKES AND DIFFERENTIAL CHARGING OF LARGE BODIES IN LOW EARTH ORBIT
Lee W. Parker *In* NASA. Lewis Research Center Spacecraft Environ. Interactions Technol., 1983 Mar. 1985 p 235-252 refs (For primary document see N85-22470 13-18)
Avail: NTIS HC A99/MF E03 CSCL 22B

Highlights of earlier results using the Inside-Out WAKE code on wake structures of LEO spacecraft are reviewed. For conducting bodies of radius large compared with the Debye length, a high Mach number wake develops a negative potential well. Quasineutrality is violated in the very near wake region, and the wake is relatively empty for a distance downstream of about one half of a Mach number of radii. There is also a suggestion of a core of high density along the axis. A comparison of rigorous numerical solutions with in situ wake data from the AE-C satellite suggests that the so called neutral approximation for ions (straight line trajectories, independent of fields) may be a reasonable approximation except near the center of the near wake. This approximation is adopted for very large bodies. Work concerned with the wake point potential of very large nonconducting bodies such as the shuttle orbiter is described. Using a cylindrical model for bodies of this size or larger in LEO (body radius up to 10 to the 5th power Debye lengths), approximate solutions are presented based on the neutral approximation (but with rigorous trajectory calculations for surface current balance). There is a negative potential well if the body is conducting, and no well if the body is nonconducting. In the latter case the wake surface itself becomes highly negative. The wake point potential is governed by the ion drift energy. M.G.

N85-22489*# Air Force Geophysics Lab., Hanscom AFB, Mass.
SHEATH IONIZATION MODEL OF BEAM EMISSIONS FROM LARGE SPACECRAFT
S. T. Lai, H. A. Cohen, K. H. Bhavnani (RADEX, Inc.), and M. Tautz (RADEX, Inc.) *In* NASA. Lewis Research Center Spacecraft Environ. Interactions Technol., 1983 Mar. 1985 p 253-262 refs Previously announced as N84-19463 (For primary document see N85-22470 13-18)
Avail: NTIS HC A99/MF E03 CSCL 22B

An analytical model of the charging of a spacecraft emitting electron and ion beams has been applied to the case of large spacecraft. In this model, ionization occurs in the sheath due to the return current. Charge neutralization of spherical space charge flow is examined by solving analytical equations numerically. Parametric studies of potential large spacecraft are performed. As in the case of small spacecraft, the ions created in the sheath by the returning current play a large role in determining spacecraft potential. Author (GRA)

N85-22490*# Hughes Aircraft Co., El Segundo, Calif.
INTERACTIONS BETWEEN LARGE SPACE POWER SYSTEMS AND LOW-EARTH-ORBIT PLASMAS
N. John Stevens *In* NASA. Lewis Research Center Spacecraft Environ. Interactions Technol., 1983 Mar. 1985 p 263-276 refs (For primary document see N85-22470 13-18)
Avail: NTIS HC A99/MF E03 CSCL 22B

There is a growing tendency to plan space missions that will incorporate very large space power systems. These space power systems must function in the space plasma environment, which can impose operational limitations. As the power output increases, the operating voltage also must increase and this voltage, exposed at solar array interconnects, interacts with the local plasma. The implications of such interactions are considered. The available laboratory data for biased array segment tests are reviewed to demonstrate the basic interactions considered. A data set for a floating high voltage array test was used to generate approximate relationships for positive and negative current collection from plasmas. These relationships were applied to a hypothetical 100 kW power system operating in a 400 km, near equatorial orbit. It was found that discharges from the negative regions of the array are the most probable limiting factor in array operation. Author

N85-22491*# York Univ., Toronto (Ontario).
CALCULATION OF SECONDARY-ELECTRON ESCAPE CURRENTS FROM INCLINED-SPACECRAFT SURFACES IN A MAGNETIC FIELD
J. G. Laframboise *In* NASA. Lewis Research Center Spacecraft Environ. Interactions Technol., 1983 Mar. 1985 p 277-286 refs (For primary document see N85-22470 13-18)
(Contract F19628-83-K-0028)
Avail: NTIS HC A99/MF E03 CSCL 22B

In low Earth orbit, the geomagnetic field B(vector) is strong enough that secondary electrons emitted from spacecraft surfaces have an average gyroradius much smaller than typical dimensions of large spacecraft. This implies that escape of secondaries will be strongly inhibited on surfaces which are nearly parallel to B(vector), even if a repelling electric field exists outside them. This effect is likely to make an important contribution to the current balance and hence the equilibrium potential of such surfaces,

making high voltage charging of them more likely. Numerically calculated escaping secondary electron fluxes are presented for these conditions. For use in numerical spacecraft charging simulations, an analytic curve fit to these results is given which is accurate to within 3% of the emitted current. M.G.

N85-22492*# Kansas Univ., Lawrence.
SELF-CONSISTENT SIMULATION OF PLASMA INTERACTIONS WITH SECONDARY-EMITTING INSULATORS **c75**
S. T. Brandon, R. L. Rusk, T. P. Armstrong, and J. Enoch *In* NASA. Lewis Research Center Spacecraft Environ. Interactions Technol., 1983 Mar. 1985 p 287-303 refs (For primary document see N85-22470 13-18)
Avail: NTIS HC A99/MF E03 CSCL 20I

A cylindrical particle-in-cell (PIC) plasma simulation code applicable to plasma densities encountered in low Earth orbit (LEO) is described. The simulated geometries include that of a plain disk and a disk surrounded by a dielectric. Both configurations are mounted upon a ground plate in contact with a plasma environment. Techniques allowing simulation of dielectric charging using PIC time scales are discussed. Current versus voltage characteristic curves are calculated and the results are compared to experimental data. M.G.

N85-22493*# Systems Science and Software, La Jolla, Calif.
SURFACE INTERACTIONS AND HIGH-VOLTAGE CURRENT COLLECTION
M. J. Mandell and I. Katz *In* NASA. Lewis Research Center Spacecraft Environ. Interactions Technol., 1983 Mar. 1985 p 305-320 refs (For primary document see N85-22470 13-18) (Contract NAS3-23058)
Avail: NTIS HC A99/MF E03 CSCL 22B

Spacecraft of the future will be larger and have higher power requirements than any flown to date. For several reasons, it is desirable to operate a high power system at high voltage. While the optimal voltages for many future missions are in the range 500 to 5000 volts, the highest voltage yet flown is approximately 100 volts. The NASCAP/LEO code is being developed to embody the phenomenology needed to model the environmental interactions of high voltage spacecraft. Some plasma environment are discussed. The treatment of the surface conductivity associated with emitted electrons and some simulations by NASCAP/LEO of ground based high voltage interaction experiments are described. Author

N85-22494*# National Aeronautics and Space Administration. Lewis Research Center, Cleveland, Ohio.
THE PIX-2 EXPERIMENT: AN OVERVIEW **c75**
Carolyn K. Purvis *In its* Spacecraft Environ. Interactions Technol. Mar. 1985 p 321-332 refs (For primary document see N85-22470 13-18)
Avail: NTIS HC A99/MF E03 CSCL 20I

The second Plasma Interactions Experiment (PIX-2) was launched in January 1983 as a piggyback on the second stage of the Delta launch vehicle that carried IRAS into orbit. Placed in a 870 km circular polar orbit, it returned 18 hrs of data on the plasma current collection and arcing behavior of solar arrays biased to +/-1000 V in steps. The four 500 sq cm solar array segments were biased singly and in combinations. In addition to the array segments PIX-2 carried a Sun sensor, a Langmuir probe to measure electron currents, and a hot-wire filament electron emitter to control vehicle potential during positive array bias sequences. The PIX-2 experiment is reviewed from program and operational perspectives. M.G.

N85-22495*# National Aeronautics and Space Administration. Lewis Research Center, Cleveland, Ohio.
PLASMA INTERACTION EXPERIMENT 2 (PIX 2): LABORATORY AND FLIGHT RESULTS **c75**
Norman T. Grier *In its* Spacecraft Environ. Interactions Technol. Mar. 1985 p 333-347 (For primary document see N85-22470 13-18)
Avail: NTIS HC A99/MF E03 CSCL 20I

The Plasma Interaction Experiments 1 and 2 (PIX 1 and 2) were designed as first steps toward understanding interactions between high-voltage solar arrays and the surrounding plasma. The PIX 2 consisted of an approximately 2000-sq cm array divided into four equal segments. Each of the segments could be biased independently and the current measured separately. In addition to the solar array segments, PIX 2 had a hot-wire-filament electron emitter and a spherical Langmuir probe. The emitter was operated when the array segments were biased positively bove 125 V. Thermal electrons from the emitter aided in balancing the electron currents collected by the array. Laboratory and flight results of PIX 2 are presented. At high positive voltages on the solar array segments, the flight currents were approximately an order of magnitude larger than the ground test currents. This is attributed to the tank walls in the laboratory interfering with the electron currents to the array segments. From previous tests it is known that the tank walls limit the electron currents at high voltages. This was the first verification of the extent of the laboratory tank effect on the plasma coupling current. M.G.

N85-22496*# National Aeronautics and Space Administration. Lewis Research Center, Cleveland, Ohio.
RAM-WAKE EFFECTS ON PLASMA CURRENT COLLECTION OF THE PIX 2 LANGMUIR PROBE **c75**
Dale C. Ferguson *In its* Spacecraft Environ. Interactions Technol. Mar. 1985 p 349-357 refs (For primary document see N85-22470 13-18)
Avail: NTIS HC A99/MF E03 CSCL 20I

The Plasma Interaction Experiment 2 (PIX 2) Langmuir probe readings of the same polar magnetospheric regions taken on consecutive orbits showed occasional apparent densities as much as 10 times lower than the average, although each pass clearly showed density structures related to the day/night boundary. At other points in the orbit, Langmuir probe currents varied by as much as a factor of 20 on a time scale of minutes. The hypothesis is advanced that these apparent inconsistencies in Langmuir probe current are the results of the probe's orientation relative to the body of the spacecraft and the velocity vector. Theoretical studies predict a possible depletion in collected electron current by a factor of 100 in the wake. Experimental results from other spacecraft indicate that a wake electron depletion by a factor of 10 or so is realistic. This amount of depletion is consistent with the PIX 2 data if the spacecraft was rotating. Both the Sun sensor and temperature sensor data on PIX 2 show a complex variation consistent with rotation of the Langmuir probe into and out of the spacecraft wake on a time scale of minutes. Furthermore, Langmuir probe data taken when the probe was not in the spacecraft wake are consistent from orbit to orbit. This supports the interpretation that ram/wake effects may be the source of apparent discrepancies at other orientations. M.G.

N85-22497*# National Aeronautics and Space Administration. Lewis Research Center, Cleveland, Ohio.
NASCAP SIMULATION OF PIX 2 EXPERIMENTS **c75**
James C. Roche and Myron J. Mandell (Systems, Science and Software, San Diego) *In its* Spacecraft Environ. Interactions Technol. Mar. 1985 p 359-366 (For primary document see N85-22470 13-18)
Avail: NTIS HC A99/MF E03 CSCL 20I

The latest version of the NASCAP/LEO digital computer code used to simulate the PIX 2 experiment is discussed. NASCAP is a finite-element code and previous versions were restricted to a single fixed mesh size. As a consequence the resolution was dictated by the largest physical dimension to be modeled. The latest version of NASCAP/LEO can subdivide selected regions. This permitted the modeling of the overall Delta launch vehicle in the primary computational grid at a coarse resolution, with subdivided regions at finer resolution being used to pick up the details of the experiment module configuration. Langmuir probe data from the flight were used to estimate the space plasma density and temperature and the Delta ground potential relative to the space plasma. This information is needed for input to NASCAP. Because of the uncertainty or variability in the values of

these parameters, it was necessary to explore a range around the nominal value in order to determine the variation in current collection. The flight data from PIX 2 were also compared with the results of the NASCAP simulation. R.J.F.

N85-22498*# National Aeronautics and Space Administration. Lewis Research Center, Cleveland, Ohio.
AN INVESTIGATION OF ARC DISCHARGING ON NEGATIVELY BIASED DIELECTRIC CONDUCTOR SAMPLES IN A PLASMA **c75**
William L. Miller *In its* Spacecraft Environ. Interactions Technol. Mar. 1985 p 367-377 refs (For primary document see N85-22470 13-18)
Avail: NTIS HC A99/MF E03 CSCL 20I

Proposals are now being developed for the construction of high-power photovoltaic systems for operation in low Earth orbit, where the plasma number density is about 1,000 to 1,000,000 per cubic cm. Existing data indicate that interactions between the plasma and high-voltage surfaces of an orbiting power system will occur. In ground tests, where the applied voltage is increased negatively from ground, the array current collection shows an approximately linear rise until it terminates in arcing at greater than several hundred volts negative. This arcing may reduce the power generation efficiency and could possibly affect the low-level logic circuits of the spacecraft. Therefore it is important that the arcing phenomenon be well understood. This study is a survey of the behavior of different dielectric-conductor samples, including a solar cell module, that were biased negatively in a low-density plasma environment with the intent of defining arc discharge conditions and characteristics. Procedures and results are discussed. Author

N85-22499*# National Aeronautics and Space Administration. Lewis Research Center, Cleveland, Ohio.
DISCHARGES ON A NEGATIVELY BIASED SOLAR CELL ARRAY IN A CHARGED-PARTICLE ENVIRONMENT **c44**
David B. Snyder *In its* Spacecraft Environ. Interactions Technol. Mar. 1985 p 379-388 refs Previously announced as N84-23690 (For primary document see N85-22470 13-18)
Avail: NTIS HC A99/MF E03 CSCL 10A

The charging behavior of a negatively biased solar cell array when subjected to a charged particle environment is studied in the ion density range from 200 to 12,000 ions/sq cm with the applied bias range of -500 to -1400 V. The profile of the surface potentials across the array is related to the presence of discharges. At the low end of the ion density range the solar cell cover slides charge to from 0 to +5 volts independent of the applied voltage. No discharges are seen at bias voltages as large as -1400 V. At the higher ion densities the cover slide potential begins to fluctuate, and becomes significantly negative. Under these conditions discharges can occur. The threshold bias voltage for discharges decreases with increasing ion density. A condition for discharges emerging from the experimental observations is that the average coverslide potential must be more negative than -4 V. The observations presented suggest that the plasma potential near the array becomes negative before a discharge occurs. This suggests that discharges are driven by an instability in the plasma. Author

N85-22500*# National Aeronautics and Space Administration. Lewis Research Center, Cleveland, Ohio.
DESIGN GUIDELINES FOR ASSESSING AND CONTROLLING SPACECRAFT CHARGING EFFECTS Abstract Only
Carolyn K. Purvis, H. B. Garrett (JPL, California Inst. of Tech., Pasadena), A. Whittlesey (JPL, California Inst. of Tech., Pasadena), and N. John Stevens (Hughes Aircraft Co., El Segundo, Calif.) *In its* Spacecraft Environ. Interactions Technol. Mar. 1985 p 389 Previously announced as N84-33452 (For primary document see N85-22470 13-18)
Avail: NTIS HC A99/MF E03 CSCL 22B

The need for uniform criteria, or guidelines, to be used in all phases of spacecraft design is discussed. Guidelines were developed for the control of absolute and differential charging of spacecraft surfaces by the lower energy space charged particle environment. Interior charging due to higher energy particles is not considered. A guide to good design practices for assessing and controlling charging effects is presented. Uniform design practices for all space vehicles are outlined. E.A.K.

N85-22501*# Aerospace Corp., Los Angeles, Calif.
AEROSPACE SPACECRAFT-CHARGING GUIDELINES DOCUMENT Abstract Only
J. F. Fennell, D. F. Hall, H. C. Koons, P. F. Mizera, and A. F. Vampola *In* NASA. Lewis Research Center Spacecraft Environ. Interactions Technol., 1983 Mar. 1985 p 391 (For primary document see N85-22470 13-18)
Avail: NTIS HC A99/MF E03 CSCL 22B

A short summary document on spacecraft charging was prepared for use by engineers in the various Aerospace Corporation program offices that support Air Force Space Division programs. The magnetospheric charging environment at near-geosynchronous altitudes is outlined and the mechanisms of charging and discharging are discussed. Statistical results from the P78-2 (SCATHA) satellite engineering experiments are given. The document is intended to be a layman's source for charging information and for design guidance and criteria. R.J.F.

N85-22502*# Boston Coll., Chestnut Hill, Mass.
EMI CHARACTERISTICS OF A POTENTIAL CONTROL SYSTEM
D. E. Donatelli, H. A. Cohen (AFGL), W. J. Burke (AFGL), and H. C. Koons (Aerospace Corp., Los Angeles) *In* NASA. Lewis Research Center Spacecraft Environ. Interactions Technol., 1983 Mar. 1985 p 393-411 refs (For primary document see N85-22470 13-18)
(Contract F19628-81-K-0011)
Avail: NTIS HC A99/MF E03 CSCL 22B

With the development and use of charged particle sources for controlling spacecraft potentials there is a need to better understand the effects of these systems on spacecraft operations. The emission of charged particles perturbs the spacecraft environment and signals are generated which may interfere with other vehicle functions. In particular, the generated signals are apt to interfere with detectors for observing waves that exist naturally in the space environment. Examples of this type of interference are presented from the SCATHA satellite during a period when the vehicle was highly charged. A plasma source on board the spacecraft succeeded in discharging the vehicle with each of four different operating modes. The VLF broadband receiver on SCATHA detected interference over the entire 0-5 kHz range of both the electric and magnetic field detectors during these charged particle emissions. This frequency range includes the 2 kHz electron gyrofrequency but is below the 9 kHz electron plasma frequency. The observations suggest that interference occurs through introduction of anomalous signals, and through suppression of background field measurements. Author

N85-22503*# California Univ., San Diego, La Jolla.
ANOMALOUSLY HIGH POTENTIALS OBSERVED ON ISEE
E. C. Whipple, I. S. Krinsky, R. B. Torbert, and R. C. Olsen (Alabama Univ., Huntsville) *In* NASA. Lewis Research Center Spacecraft Environ. Interactions Technol., 1983 Mar. 1985 p 413-422 refs Previously announced as N84-17258 (For primary document see N85-22470 13-18)
(Grant NAG-320)
Avail: NTIS HC A99/MF E03 CSCL 22B

Data from two electric field experiments and from the plasma composition experiment on ISEE-1 are used to show that the spacecraft charged to close to -70 V in sunlight at 0700 UT on March 17, 1978. Data from the electron spectrometer experiment show that there was a potential barrier of -10 to -20 V about the spacecraft during this event. The potential barrier was effective in turning back emitted photoelectrons to the spacecraft. The stringent electrostatic cleanliness specifications imposed on ISEE make the presence of differential charging unlikely. Modeling of

this event is required to determine if the barrier was produced by the presence of space charge. Author (ESA)

N85-22504*# Jet Propulsion Lab., California Inst. of Tech., Pasadena.
GALILEO INTERNAL ELECTROSTATIC DISCHARGE PROGRAM **c15**
Philip L. Leung, Gregory H. Plamp, and Paul A. Robinson, Jr. *In* NASA. Lewis Research Center Spacecraft Environ. Interactions Technol., 1983 Mar. 1985 p 423-433 refs (For primary document see N85-22470 13-18)
Avail: NTIS HC A99/MF E03 CSCL 22B

The Galileo spacecraft which will orbit Jupiter in 1988 will encounter a very harsh environment of energetic electrons. These electrons will have sufficient energy to penetrate the spacecraft shielding, consequently depositing charges in the dielectric insulating materials or ungrounded conductors. The resulting electric field could exceed the breakdown strength of the insulating materials, producing discharges. The transients produced from these Internal Electrostatic Discharges (IESD) could, depending on their relative location, be coupled to nearby cables and circuits. These transients could change the state of logic circuits or degrade or even damage spacecraft components, consequently disrupting the operation of subsystems and systems of the Galileo spacecraft during its expected mission life. An extensive testing program was initiated for the purpose of understanding the potential threats associated with these IESD events. Data obtained from these tests were used to define design guidelines. Author

N85-22505*# TRW Space Technology Labs., Redondo Beach, Calif.
CHARACTERISTICS OF EMI GENERATED BY NEGATIVE METAL-POSITIVE DIELECTRIC VOLTAGE STRESSES DUE TO SPACECRAFT CHARGING **c32**
R. C. Chaky and G. T. Inouye *In* NASA. Lewis Research Center Spacecraft Environ. Interactions Technol., 1983 Mar. 1985 p 437-452 refs (For primary document see N85-22470 13-18)
Avail: NTIS HC A99/MF E03 CSCL 20N

Charging of spacecraft surfaces by the environmental plasma can result in differential potentials between metallic structure and adjacent dielectric surfaces in which the relative polarity of the voltage stress is either negative dielectric/positive metal or negative metal/positive dielectric. Negative metal/positive dielectric is a stress condition that may arise if relatively large areas of spacecraft surface metals are shadowed from solar UV and/or if the UV intensity is reduced as in the situation in which the spacecraft is entering into or leaving eclipse. The results of experimental studies of negative metal/positive dielectric systems are given. Information is given on: enhanced electron emission I-V curves; e(3) corona noise vs e(3) steady-state current; the localized nature of e(3) and negative metal arc discharge currents; negative metal arc discharges at stress thresholds below 1 kilovolt; negative metal arc discharge characteristics; dependence of blowoff arc discharge current on spacecraft capacitance to space (linear dimension); and damage to second surface mirrors due to negative metal arcs. R.J.F.

N85-22506*# SRI International Corp., Menlo Park, Calif.
LABORATORY STUDIES OF SPACECRAFT RESPONSE TO TRANSIENT DISCHARGE PULSES
J. E. Nanevicz and R. C. Adamo *In* NASA. Lewis Research Center Spacecraft Environ. Interactions Technol., 1983 Mar. 1985 p 453-463 refs (For primary document see N85-22470 13-18)
Avail: NTIS HC A99/MF E03 CSCL 22B

The in-orbit measurement of spacecraft discharge properties was investigated. The experiments include design and fabrication of appropriate sensors and effects of spacecraft electromagnetic responses on the interpretation of the discharge data. Electric field sensors especially designed to response to high-speed transient signals were installed on a mock-up of a satellite. The simple mock-up was basically a sheet of aluminum rolled to form a cylinder. A movable spark-discharge noise source designed to be electromagnetically isolated from its power supply system was used to induce transient signals at various locations on the spacecraft's outer surface. The measurements and their implications are described. It is concluded that practical orbital measurements to define discharge noise source properties should be possible, and that simple mock-ups of the type described below are useful in sensor system design and data interpretation. E.A.K.

N85-22507*# SRI International Corp., Menlo Park, Calif.
DEVELOPMENT OF A CONTINUOUS BROAD-ENERGY-SPECTRUM ELECTRON SOURCE **c14**
R. C. Adamo and J. E. Nanevicz *In* NASA. Lewis Research Center Spacecraft Environ. Interactions Technol., 1983 Mar. 1985 p 465-475 refs (For primary document see N85-22470 13-18) (Contract DNA001-81-C-0267)
Avail: NTIS HC A99/MF E03 CSCL 14B

The development of a practical prototype, large-area, continuous-spectrum, multienergy electron source to simulate the lower energy (approx = 1 to 30 keV) portion of the geosynchronous orbit electron environment was investigated. The results of future materials-charging tests using this multienergy source should significantly improve the understanding of actual in-orbit charging processes and should help to resolve some of the descrepancies between predicted and observed spacecraft materials performance. E.A.K.

N85-22508*# Air Force Geophysics Lab., Hanscom AFB, Mass.
AUTOMATIC CHARGE CONTROL SYSTEM FOR SATELLITES **c15**
B. M. Shuman and H. A. Cohen *In* NASA. Lewis Research Center Spacecraft Environ. Interactions Technol., 1983 Mar. 1985 p 477-481 refs (For primary document see N85-22470 13-18)
Avail: NTIS HC A99/MF E03 CSCL 22B

The SCATHA and the ATS-5 and 6 spacecraft provided insights to the problem of spacecraft charging at geosychronous altitudes. Reduction of the levels of both absolute and differential charging was indicated, by the emission of low energy neutral plasma. It is appropriate to complete the transition from experimental results to the development of a system that will sense the state-of-charge of a spacecraft, and, when a predetermined threshold is reached, will respond automatically to reduce it. A development program was initiated utilizing sensors comparable to the proton electrostatic analyzer, the surface potential monitor, and the transient pulse monitor that flew in SCATHA, and combine these outputs through a microprocessor controller to operate a rapid-start, low energy plasma source. E.A.K.

N85-22509*# Rome Air Development Center, Hanscom AFB, Mass.
DISCHARGE PULSE PHENOMENOLOGY **c32**
Arthur R. Frederickson *In* NASA. Lewis Research Center Spacecraft Environ. Interactions Technol., 1983 Mar. 1985 p 483-509 refs (For primary document see N85-22470 13-18)
Avail: NTIS HC A99/MF E03 CSCL 20N

A model was developed which places radiation induced discharge pulse results into a unified conceptual framework. Only two phenomena are required to interpret all space and laboratory results: (1) radiation produces large electrostatic fields inside insulators via the trapping of a net space charge density; and (2) the electrostatic fields initiate discharge streamer plasmas similar to those investigated in high voltage electrical insulation materials; these streamer plasmas generate the pulsing phenomena. The apparent variability and diversity of results seen is an inherent feature of the plasma streamer mechanism acting in the electric fields which is created by irradiation of the dielectrics. The implications of the model are extensive and lead to constraints over what can be done about spacecraft pulsing. E.A.K.

N85-22510*# JAYCOR, San Diego, Calif.
DISCHARGE CHARACTERISTICS OF DIELECTRIC MATERIALS EXAMINED IN MONO-, DUAL-, AND SPECTRAL ENERGY ELECTRON CHARGING ENVIRONMENTS **c72**
P. Coakley, M. Treadway, N. Wild, and B. Kitterer *In* NASA.

Lewis Research Center Spacecraft Environ. Interactions Technol., 1983 Mar. 1985 p 511-524 refs (For primary document see N85-22470 13-18)
(Contract F29601-82-C-0015)
Avail: NTIS HC A99/MF E03 CSCL 18H

The effects of midenergy electrons on the charge and discharge characteristics of spacecraft dielectric materials and the data base from which basic discharge models can be formulated is expanded. Thin dielectric materials were exposed to low, mid combined low and mid, and spectral energy electron environments. Three important results are presented: (1) it determined electron environments that lead to dielectric discharges at potentials less negative than -5 kV; (2) two types of discharges were identified that dominate the kinds of discharges seen; and (3) it is shown that, for the thin dielectric materials tested, the worst-case discharges observed in the various environments are similar.
E.A.K.

N85-22511*# Pennsylvania State Univ., University Park.
MASS SPECTRA OF NEUTRAL PARTICLES RELEASED DURING ELECTRICAL BREAKDOWN OF THIN POLYMER FILMS c27
B. R. F. Kendall *In* NASA. Lewis Research Center Spacecraft Environ. Interactions Technol., 1983 Mar. 1985 p 525-535 refs (For primary document see N85-22470 13-18)
(Grant NsG-3301)
Avail: NTIS HC A99/MF E03 CSCL 11G

A special type of time-of-flight mass spectrometer triggered from the breakdown event was developed to study the composition of the neutral particle flux released during the electrical breakdown of polymer films problem. Charge is fed onto a metal-backed polymer surface by a movable smooth platinum contact. A slowly increasing potential from a high-impedance source is applied to the contact until breakdown occurs. The breakdown characteristics is made similar to those produced by an electron beam charging system operating at similar potentials. The apparatus showed that intense instantaneous fluxes of neutral particles are released from the sites of breakdown events. For Teflon FEP films of 50 and 75 microns thickness the material released consists almost entirely of fluorocarbon fragments, some of them having masses greater than 350 atomic mass units amu, while the material released from a 50 micron Kapton film consists mainly of light hydrocarbons with masses at or below 44 amu, with additional carbon monoxide and carbon dioxide. The apparatus is modified to allow electron beam charging of the samples. E.A.K.

N85-22512*# Case Western Reserve Univ., Cleveland, Ohio.
ELECTRON YIELDS FROM SPACECRAFT MATERIALS
K. Yang, W. L. Gordon, and R. W. Hoffman *In* NASA. Lewis Research Center Spacecraft Environ. Interactions Technol., 1983 Mar. 1985 p 537-545 refs (For primary document see N85-22470 13-18)
(Grant NsG-3197)
Avail: NTIS HC A99/MF E03 CSCL 22B

Photoyields and secondary electron emission (SEE) characteristics were determined under UHV conditions for a group of insulating materials used in spacecraft applications. The SEE studies were carried out with a pulsed primary beam while photoyields were obtained with a chopped photon beam from a Kr resonance source with major emission at 123.6 nm. This provides a photon flux close to that of the Lyman alpha in the space environment. Yields per incident photon are obtained relative to those from a freshly evaporated and air oxidized Al surface. Results are presented for Kapton, FEP Teflon, the borosilicate glass covering of a shuttle tile, and spacesuit outer fabric. E.A.K.

N85-22513*# Hughes Research Labs., Malibu, Calif.
KAPTON CHARGING CHARACTERISTICS: EFFECTS OF MATERIAL THICKNESS AND ELECTRON-ENERGY DISTRIBUTION c27
W. S. Williamson, C. R. Dulgeroff, J. Hymann, and R. Viswanathan (Hughes Space and Communications Group, Los Angeles) *In* NASA. Lewis Research Center Spacecraft Environ. Interactions Technol., 1983 Mar. 1985 p 547-558 refs (For primary document see N85-22470 13-18)
Avail: NTIS HC A99/MF E03 CSCL 11G

Charging characteristics of polyimide (Kapton) of varying thicknesses under irradiation by a very-low-curent-density electron beam, with the back surface of the sample grounded are reported. These charging characteristics are in good agreement with a simple analytical model which predicts that in thin samples at low current density, sample surface potential is limited by conduction leakage through the bulk material. The charging of Kapton in a low-current-density electron beam in which the beam energy was modulated to simulate Maxwellian and biMaxwellian distribution functions is measured. E.A.K.

N85-22514*# SRI International Corp., Menlo Park, Calif.
ELECTRICAL CONDUCTION IN POLYMER DIELECTRICS c27
David B. Cotts *In* NASA. Lewis Research Center Spacecraft Environ. Interactions Technol., 1983 Mar. 1985 p 559-569 refs (For primary document see N85-22470 13-18)
(Contract F19628-81-C-0076)
Avail: NTIS HC A99/MF E03 CSCL 11G

The use of polymer dielectrics with moderate resistivities could reduce or eliminate problems associated with spacecraft charging. The processes responsible for conduction and the properties of electroactive polymers are reviewed, and correlations drawn between molecular structure and electrical conductivity. These structure-property relationships led to the development of several new electroactive polymer compositions and the identification of several systems that have the requisite thermal, mechanical, environmental and electrical properties for use in spacecraft.
E.A.K.

N85-22515*# Communications Satellite Corp., Clarksburg, Md. COMSAT Lab.
INVESTIGATIONS OF RADIATION-INDUCED AND CARRIER-ENHANCED CONDUCTIVITY c33
A. Meulenberg, Jr., L. W. Parker (Parker (Lee W.), Inc., Concord, Mass.), E. J. Yadlowski (H-Y Tek Corp., Radford, Va.), and R. C. Hazelton (H-Y Tek Corp., Radford, Va.) *In* NASA. Lewis Research Center Spacecraft Environ. Interactions Technol., 1983 Mar. 1985 p 571-590 refs (For primary document see N85-22470 13-18)
Avail: NTIS HC A99/MF E03 CSCL 09C

A steady-state carrier computer code, PECK (Parker Enhanced Carrier Kinetics), that predicts the radiation-induced conductivity (RIC) produced in a dielectric by an electron beam was developed. The model, which assumes instantly-trapped holes, was then applied to experimental measurements on thin Kapton samples penetrated by an electron beam. Measurements at high bias were matched in the model by an appropriate choice for the trap-modulated electron mobility. A fractional split between front and rear currents measured at zone bias is explained on the basis of beam-scattering. The effects of carrier-enhanced conductivity (CEC) on data obtained for thick, free-surface Kapton samples is described by using an analytical model that incorporates field injection of carriers from the RIC region. The computer code, LWPCHARGE, modified for carrier transport, is also used to predict partial penetration effects associated with CEC in the unirradiated region. Experimental currents and surface voltages, when incorporated in the appropriate models, provide a value for the trap modulated mobility that is in essential agreement with the RIC results. B.W.

N85-22516*# Beers Associates, Inc., Reston, Va.
A SIMPLE MODEL OF ELECTRON BEAM INITIATED DIELECTRIC BREAKDOWN c72
B. L. Beers, R. E. Daniell, and T. N. Delmer *In* NASA. Lewis Research Center Spacecraft Environ. Interactions Technol., 1983 Mar. 1985 p 591-598 refs (For primary document see N85-22470 13-18)
(Contract F19601-82-C-0023)
Avail: NTIS HC A99/MF E03 CSCL 20H

A steady state model that describes the internal charge distribution of a planar dielectric sample exposed to a uniform electron beam was developed. The model includes the effects of

charge deposition and ionization of the beam, separate trap-modulated mobilities for electrons and holes, electron-hole recombination, and pair production by drifting thermal electrons. If the incident beam current is greater than a certain critical value (which depends on sample thickness as well as other sample properties), the steady state solution is non-physical. B.W.

N85-22517*# National Aeronautics and Space Administration. Lewis Research Center, Cleveland, Ohio.
SPACECRAFT ENVIRONMENTAL INTERACTIONS: A JOINT AIR FORCE AND NASA RESEARCH AND TECHNOLOGY PROGRAM
Charles P. Pike (AFGL), Carolyn K. Purvis, and Wayne R. Hudson (NASA, Washington) *In its* Spacecraft Environ. Interactions Technol., 1983 Mar. 1985 p 599-608 (For primary document see N85-22470 13-18)
Avail: NTIS HC A99/MF E03 CSCL 22B

A joint Air Force/NASA comprehensive research and technology program on spacecraft environmental interactions to develop technology to control interactions between large spacecraft systems and the charged-particle environment of space is described. This technology will support NASA/Department of Defense operations of the shuttle/IUS, shuttle/Centaur, and the force application and surveillance and detection missions, planning for transatmospheric vehicles and the NASA space station, and the AFSC military space system technology model. The program consists of combined contractual and in-house efforts aimed at understanding spacecraft environmental interaction phenomena and relating results of ground-based tests to space conditions. A concerted effort is being made to identify project-related environmental interactions of concern. The basic properties of materials are being investigated to develop or modify the materials as needed. A group simulation investigation is evaluating basic plasma interaction phenomena to provide inputs to the analytical modeling investigation. Systems performance is being evaluated by both groundbased tests and analysis. B.W.

N85-22518*# Air Force Geophysics Lab., Hanscom AFB, Mass.
INTERACTIONS MEASUREMENT PAYLOAD FOR SHUTTLE
D. A. Guidice and C. P. Pike *In* NASA. Lewis Research Center Spacecraft Environ. Interactions Technol., 1983 Mar. 1985 p 609-618 (For primary document see N85-22470 13-18)
Avail: NTIS HC A99/MF E03 CSCL 22B

The Interactions Measurement Payload for Shuttle (IMPS) consisted of engineering experiments to determine the effects of the space environment on projected Air Force space systems. Measurements by IMPS on a polar-orbit Shuttle flight will lead to detailed knowledge of the interaction of the low-altitude polar-auroral environment on materials, equipment and technologies to be used in future large, high-power space systems. The results from the IMPS measurements will provide direct input to MIL-STD design guidelines and test standards that properly account for space-environment effects. B.W.

N85-22519*# National Aeronautics and Space Administration. Marshall Space Flight Center, Huntsville, Ala.
SPACE TEST PROGRAM OF HIGH-VOLTAGE SOLAR ARRAY-SPACE PLASMA INTERACTIONS c44
M. R. Carruth, Jr. (NASA. Marshall Space Flight Center, Huntsville, Ala.) and Carolyn K. Purvis *In its* Spacecraft Environ. Interactions Technol., 1983 Mar. 1985 p 619-635 refs (For primary document see N85-22470 13-18)
Avail: NTIS HC A99/MF E03 CSCL 10A

Future spacecraft, notably the proposed Space Station, will require power systems much larger than have previously been flown. It is recognized that at higher voltages, and at the relatively high plasma density present at low Earth orbital altitudes, undesirable interactions between the high voltage solar array and the space plasma will occur. Space experiments on high voltage solar array space plasma interactions in low Earth orbit are an absolute requirement for confident design of a higher voltage solar array. Experiments are presently being identified to provide the necessary space data for calibration of ground testing, validation of analytical models, and development of design guidelines required for confident design of high voltage solar arrays in space. A proposed flight experiment program which is designed to obtain the required data is summarized. B.W.

N85-22520*# National Aeronautics and Space Administration. Lewis Research Center, Cleveland, Ohio.
PRELIMINARY ASSESSMENT OF POWER-GENERATING TETHERS IN SPACE AND OF PROPULSION FOR THEIR ORBIT MAINTENANCE c15
Robert E. English and Patrick M. Finnegan *In its* Spacecraft Environ. Interactions Technol., 1983 Mar. 1985 p 637-647 refs (For primary document see N85-22470 13-18)
Avail: NTIS HC A99/MF E03 CSCL 22B

The concept of generating power in space by means of a conducting tether deployed from a spacecraft was studied. Using hydrogen and oxygen as the rocket propellant to overcome the drag of such a power-generating tether would yield more benefit than if used in a fuel cell. The mass consumption would be 25 percent less than the reactant consumption of fuel cells. Residual hydrogen and oxygen in the external tank and in the orbiter could be used very effectively for this purpose. Many other materials (such as waste from life support) could be used as the propellant. Electrical propulsion using tether generated power can compensate for the drag of a power-generating tether, half the power going to the useful load and the rest for electric propulsion. In addition, the spacecraft's orbital energy is a large energy reservoir that permits load leveling and a ratio of peak to average power equal to 2. Critical technologies to be explored before a power-generating tether can be used in space are delineated.
Author

N85-22521*# California Univ., San Diego, La Jolla. Dept. of Physics.
PRELIMINARY INVESTIGATION OF THE ELECTRODYNAMICS OF A CONDUCTING TETHER c15
W. B. Thompson *In* NASA. Lewis Research Center Spacecraft Environ. Interactions Technol., 1983 Mar. 1985 p 649-662 refs Sponsored in part by Martin Marietta Aerospace Corp. (For primary document see N85-22470 13-18)
Avail: NTIS HC A99/MF E03 CSCL 22B

An introductory study of the properties of an electrically conducting tether flown from the shuttle is presented. Only a single configuration is considered: a vertical conductor moving normally across the Earth's field, connecting the shuttle to a large conducting balloon that passively extracts electrons from the ionosphere. The distortions in the plasma at maximum current collection are described, as are the local and distant wakes. Numerical values are given. B.W.

N85-22522*# Air Force Geophysics Lab., Hanscom AFB, Mass.
ASTRONAUT HAZARD DURING FREE-FLIGHT POLAR EVA c52
William N. Hall *In* NASA. Lewis Research Center Spacecraft Environ. Interactions Technol., 1983 Mar. 1985 p 663-674 refs (For primary document see N85-22470 13-18)
Avail: NTIS HC A99/MF E03 CSCL 06R

Extravehicular Activity (EVA) during Shuttle flights planned for the late 1980's includes several factors which together may constitute an astronaut hazard. Free-flight EVA is planned whereas prior United States Earth orbit EVA has used umbilical tethers carrying communications, coolant, and oxygen. EVA associated with missions like LANDSAT Retrieval will be in orbits through the auroral oval where charging of spacecraft may occur. The astronaut performing free flight EVA constitutes an independent spacecraft. The astronaut and the Shuttle make up a system of electrically isolated spacecraft with a wide disparity in size. Unique situations, such as the astronaut being in the wake of the Shuttle while traversing an auroral disturbance, could result in significant astronaut and Shuttle charging. Charging and subsequent arc discharge are important because they have been associated with operating upsets and even satellite failure at geosynchronous orbit. Spacecraft charging theory and experiments are examined to

evaluate charging for Shuttle size spacecraft in the polar ionosphere. B.W.

N85-22523*# Rice Univ., Houston, Tex.
ARGON ION POLLUTION OF THE MAGNETOSPHERE c46
Ramon E. Lopez *In* NASA. Lewis Research Center Spacecraft Environ. Interactions Technol., 1983 Mar. 1985 p 675-692 refs (For primary document see N85-22470 13-18)
Avail: NTIS HC A99/MF E03 CSCL 04A

Construction of a Solar Power Satellite (SPS) would require the injection of large quantities of propellant to transport material from Low Earth Orbit (LEO) to the construction site at Geostationary Earth Orbit (GEO). This injection, in the form of approx 10 to the 32nd power, 2 KeV argon ions (and associated electrons) per SPS, is comparable to the content of the plasmasphere (approx 10 to the 31st power ions). In addition to the mass deposited, this represents a considerable injection of energy. The injection is examined in terms of a simple model for the expansion of the beam plasma. General features of the subsequent magnetospheric convection of the argon are also examined. Author

N85-22524# Toronto Univ., Downsview (Ontario). Inst. for Aerospace Studies.
A QUANTITATIVE COMPARISON OF ACTIVE AND PASSIVE DAMPING FOR LARGE SPACE STRUCTURES
Francis Shen Feb. 1985 78 p refs
(UTIAS-TN-249; ISSN-0082-5263) Avail: NTIS HC A05/MF A01

A quantitative method for comparing active and passive damping according to weight and positivity criteria is outlined which assumes thruster actuators for active damping and viscoelastic material for passive damping. Each of these damping techniques is implemented by optimizing the damping performance against weight. The Mobile Communications Satellite (MSAT) is used as a model to compare active and passive damping. The results show that, in general, active damping is much more weight-cost effective and possesses better positivity qualities than passive damping. Until the design of the active system incorporates a filter for observation noise that is equal in magnitude to the disturbance noise, passive damping will not be more weight-cost effective than active damping. A.R.H.

N85-22422# Joint Publications Research Service, Arlington, Va.
OPERATIONAL EXPERIENCE WITH ION CONCENTRATION SENSORS IN ORIENTATION SYSTEMS Abstract Only
V. P. Legotayev, V. Nikolayev, K. I. Saulin, M. B. Sukhovoy, and Y. G. Ulyanov *In its* USSR Rept.: Space (JPRS-USP-85-001) 4 Feb. 1985 p 42 Transl. into ENGLISH from Kosmicheskiye Issled. (USSR), v. 22, no. 1, Jan.-Feb. 1984 p 37-43 (For primary document see N85-22403 13-12)
Avail: NTIS HC A07

19 SPACECRAFT INSTRUMENTATION

For related information see also *06 Aircraft Instrumentation* and *35 Instrumentation and Photography.*

N85-22525*# Sperry Rand Corp., St. Paul, Minn. Advanced Materials and Devices Dept.
FEASIBILITY OF SELF-STRUCTURED CURRENT ACCESSED BUBBLE DEVICES IN SPACECRAFT RECORDING SYSTEMS Final Report, 1982 -1985
G. L. Nelson, D. R. Krahn, R. H. Dean, M. C. Paul, D. S. Lo, D. L. Amundsen, and G. A. Stein Apr. 1985 284 p refs
(Contract NAS1-16911)
(NASA-CR-172554; NAS 1.26:172554) Avail: NTIS HC A13/MF A01 CSCL 14B

The self-structured, current aperture approach to magnetic bubble memory is described. Key results include: (1) demonstration that self-structured bubbles (a lattice of strongly interacting bubbles) will slip by one another in a storage loop at spacings of 2.5 bubble diameters, (2) the ability of self-structured bubbles to move past international fabrication defects (missing apertures) in the propagation conductors (defeat tolerance), and (3) moving bubbles at mobility limited speeds. Milled barriers in the epitaxial garnet are discussed for containment of the bubble lattice. Experimental work on input/output tracks, storage loops, gates, generators, and magneto-resistive detectors for a prototype device are discussed. Potential final device architectures are described with modeling of power consumption, data rates, and access times. Appendices compare the self-structured bubble memory from the device and system perspectives with other non-volatile memory technologies. Author

20 SPACECRAFT PROPULSION AND POWER

Includes main propulsion systems and components, e.g., rocket engines; and spacecraft auxiliary power sources.

For related information see also *07 Aircraft Propulsion, 28 Propellants and Fuels,* and *44 Energy Production and Conversion.*

N85-22526# Alabama Univ., Huntsville. Chemical Propulsion Information Agency.
TWENTY-FIRST JANNAF COMBUSTION MEETING, VOLUME 1
Debra Sue Eggleston, ed. Oct. 1984 500 p refs Meeting held at Laurel, Md., 1-4 Oct. 1984 3 Vol.
(Contract N00024-83-C-5301)
(AD-A150981; CPIA-Publ-412-Vol-1) Avail: NTIS HC A21/MF A01 CSCL 21/8

Topics covered include: metallized propellant combustion; metal combustion; flowfield and combined effects of combustion instability; solid propellant performance and combustion; combustion diagnostics; charge phenomenology; advanced propellants; propellant combustion and thermodynamics; propellant combustion and flash; combustion and performance analysis of liquid rocket engines; test and analysis of liquid rocket engine components; nitramine decomposition and modeling; Ramjet instability; and supersonic combustion. For individual titles, see N85-22527 through N85-22564.

N85-22527# Naval Postgraduate School, Monterey, Calif.
SOLID PROPELLANT COMBUSTION DIAGNOSTICS AND AUTOMATED DATA RETRIEVAL FROM HOLOGRAMS c28
J. M. Glenn, K. J. Graham, R. K. Harris, Y. Lee, D. W. Netzer, and J. P. Powers *In* APL 21st JANNAF Combust. Meeting, Vol. 1 Oct. 1984 p 1-14 refs (For primary document see N85-22526 13-20)
(Contract F04611-84-X-0001)
Avail: NTIS HC A21/MF A01 CSCL 21/9

High speed motion pictures, holography, and measurements of scattered laser light are being used to study the behavior of particulate matter in the combustion products of solid rocket propellants. An automated data retrieval system for obtaining particulate data from reconstructed holograms is also under development. Progress on all phases of this continuing effort are discussed. Author

N85-22528# Pennsylvania State Univ., University Park. Dept. of Mechanical Engineering.
STATUS OF BORON COMBUSTION RESEARCH c25
G. M. Faeth *In* APL 21st JANNAF Combust. Meeting, Vol. 1 Oct. 1984 p 15-29 refs (For primary document see N85-22526 13-20)
Avail: NTIS HC A21/MF A01 CSCL 21/2

The potential performance of boron fuels as well as problems encountered during combustion of liquid and solid propellants containing boron are discussed. Current understanding of combustion of boron particles and slurries, and expansion and plume processes of combustion products of boron are described. Research problems suggested include: atomization and secondary breakup of slurries to promote boron particle dispersion and rapid combustion; particle surface properties and treatments, to better

understand flammability limits and promote ignition; heterogeneous and homogeneous B-O-H chemistry, to provide more rational understanding of boron combustion and energy conversion; oxide coating structure, to resolve controversy concerning the mechanism whereby this layer inhibits boron particle ignition; transport properties of particle agglomerates, to determine the extent of transport enhancement by percolation through agglomerates; coalescence and injection of boron particles from solid propellant grains, to help resolve the problems of high particle loadings in boron-containing solid propellants; and turbulent mixing and reaction of boron-particle-laden flows to establish more rational combustion chamber design methods. A.R.H.

N85-22529# Pennsylvania State Univ., University Park.
GASIFICATION OF BORON OXIDE DROPS AND BORON SLURRY AGGLOMERATES IN COMBUSTION GASES **c28**
S. R. Turns, J. T. Holl, A. S. P. Solomon, and G. M. Faeth *In* APL 21st JANNAF Combust. Meeting, Vol. 1 Oct. 1984 p 31-44 refs (For primary document see N85-22526 13-20)
Avail: NTIS HC A21/MF A01 CSCL 21/2

Boron oxide gasification is a relatively slow process with 1000 micron initial diameter drop lifetimes ranging from two minutes to two hours. The presence of water vapor speeds gasification, and probably accounts for the shorter ignition delays observed for the oxidation of boron particles in wet environments. Application of a diffusion-limited equilibrium model provided excellent agreement with oxide drop-life histories at all conditions except for the low-temperature wet environment. In this case, results of a partial-equilibrium analysis suggest chemical kinetics limit gasification rates. Observations of surface morphology of partially-reacted agglomerates suggests that the ignition and combustion process consists of the heat-up of a relatively porous agglomerate composed of individual boron particles covered with a solid oxide coating, followed by oxide melting to form a liquid coating of low porosity. The oxide layer then gasifies, leaving an open, porous structure of reacting boron particles. Finally, the boron melts transforming the agglomerates to a droplet. Measurements of ignition times and burning rates were interpreted in this framework for agglomerates formed from three different slurries. A.R.H.

N85-22530# Rensselaer Polytechnic Inst., Troy, N. Y. Dept. of Chemical Engineering and Environmental Engineering.
COMBUSTION KINETICS OF METAL ATOMS AND METALLIC RADICALS OVER WIDE TEMPERATURE RANGES **c25**
Arthur Fontijn *In* APL 21st JANNAF Combust. Meeting, Vol. 1 Oct. 1984 p 45-52 refs (For primary document see N85-22526 13-20)
(Grant AF-AFOSR-0073-82)
Avail: NTIS HC A21/MF A01 CSCL 21/2

The dependence of the rate coefficients of gas-phase oxidation reactions of metallic species on temperature is discussed. Examples given pertain primarily to Al and B species reactions in the 300 K to 1900 K range. These reactions show a wide variety of log k(T) vs. 1/T behavior patterns. It is argued that, because of this variety, it is not yet possible to make reliable predictions regarding reactions for which no experimental data on temperature dependence are available. However, some guidance is given toward preliminary estimates. Quantitative kinetic data on the reactions are given. The experimental high temperature fast flow reactor (HTFFR) method used to obtain data is reviewed. Author

N85-22531*# Colorado Univ., Boulder.
IGNITION PHENOMENA OF BULK ALUMINUM ALLOY AS A FUNCTION OF OXYGEN PRESSURE **c25**
Ke Nguyen, James W. Bransford (NBS, Washington, D.C.), and Melvyn C. Branch *In* APL 21st JANNAF Combust. Meeting, Vol. 1 Oct. 1984 p 53-61 refs Sponsored in cooperation with NASA. Marshall Space Flight Center and Air Force (For primary document see N85-22526 13-20)
Avail: NTIS HC A21/MF A01 CSCL 21B

An ignition phenomena of 6061 aluminum alloy was investigated as a function of oxygen pressure. Cylindrical aluminum alloy specimens were ignited in a pure oxygen environment by a focused CW CO2 laser beam. The experiments were conducted at oxygen pressures ranging from 0.084 to 2.413 MPa. The temperature history of the entire upper surface of the specimen and of a 0.5 mm diameter spot located initially at the center of the specimen top surface was recorded by using a commercial two-color ratio pyrometer and a fast-response, narrow-band, two-color pyrometer. Mass, brightness, and interior temperatures (for certain experiments) were also recorded throughout the experiment. The results show that the surface temperatures at ignition of the alloy obtained from the temperature curves are below the melting temperature of the aluminum oxide and are slightly dependent on oxygen pressure. The data indicate that the ignition mechanism is complex and probably composed of several phenomena acting both separately and in conjunction with each other. Author

N85-22532# Georgia Inst. of Tech., Atlanta. School of Aerospace Engineering.
COMBUSTION OF ZIRCONIUM CARBIDE **c25**
J. K. Sambamurthi, E. W. Price, R. K. Sigman, R. R. Panyam, and C. J. Park *In* APL 21st JANNAF Combust. Meeting, Vol. 1 Oct. 1984 p 63-70 refs (For primary document see N85-22526 13-20)
(Grant AF-AFOSR-0356-83)
Avail: NTIS HC A21/MF A01 CSCL 21/2

Due to recent interest in zirconium carbide as an ingredient in solid propellants, a variety of tests was run on available ZrC particles including controlled heating and combustion tests. The results appear to show that ZrC particles burn in a complex way with solid or liquid accumulating on the surface; a gaseous oxide leaving the surface; and possibly a reaction between the accumulating oxide and the original ZrC. Test results indicate that ZrC does not concentrate on the burning surface or change the surface details. It ignites as it leaves the surface, burns fast enough to be fully consumed in the motor (fine particles), and the particles change size only slightly during burning. Stabilization of combustion is produced by particle damping. Author

N85-22533# Utah Univ., Salt Lake City. Fluid Dynamics Lab.
NONLINEAR INTERACTIONS BETWEEN VORTICES AND ACOUSTIC WAVES IN A ROCKET COMBUSTION CHAMBER
G. A. Flandro and P. A. Finlayson *In* APL 21st JANNAF Combust. Meeting, Vol. 1 Oct. 1984 p 71-81 refs (For primary document see N85-22526 13-20)
(Contract F04611-83-C-0003)
Avail: NTIS HC A21/MF A01 CSCL 21/8

To carry out useful predictive analyses of solid propellant rocket or Ramjet combustion oscillation problems, it is necessary that all loss and gain mechanisms be accounted for. Flow of oscillatory energy from vortex shedding to the acoustic field of the chambe is one of these mechanisms. The coupling between the vortex instability which arises in regions of highly sheared flow and the chamber acoustic field represents a problem of great complexity. Several basic features of this coupling are addressed. Growth rate corrections for use in standard stability assessment codes are determined as well as the limit cycle processes of the vortical region of flow. The global limiting behavior of the coupled nonlinear acoustical/vortical flow is assessed. Perturbation expansion techniques are utilized to formulate the required theory; solutions are carried out to second-order in the composite wave amplitude of the system. The nonlinear solutions given demonstrate the transition to limit cycle oscillations in the shear layer as a consequence of the interactions between vortex elements and decay of the mean shear layer vorticity. Readily applied design rules for the avoidance of vortex driven pressure fluctuations in a combustion chamber are presented. A.R.H.

N85-22534# Air Force Rocket Propulsion Lab., Edwards AFB, Calif.
ACOUSTIC ENERGY EXCHANGE IN SHEARED MEAN FLOWS **c91**
J. D. Baum and J. N. Levine *In* APL 21st JANNAF Combust. Meeting, Vol. 1 Oct. 1984 p 83-90 refs (For primary document see N85-22526 13-20)
Avail: NTIS HC A21/MF A01 CSCL 20A

The interaction between the acoustic field in a chamber and a free shear layer (i.e., vortex shedding) and the so called flow turning effect is examined, and efforts to develop the computational capability to properly address such problems are detailed. Three finite difference solvers (two explicit and one implicit) were acquired and modified to solve a test case of acoustic wave propagation in the presence of sheared mean flow in a hard wall tube. A comparison between the explicit and implicit codes demonstrates the inability of one of the explicit codes to handle exponential distribution of mesh points in the radial direction with very fine grid distribution near the side walls. Results obtained demonstrate the ability of the implicit code to handle grid size ratios of 10000:1 and to obtain time accurate solutions. Assessment of available models of nonreflective boundary conditions shows that all of them reflect incident two dimensional waves. Therefore, the time evolution of acoustic refraction as the traveling wave traverses the length of the chamber was investigated. Initial results from the acoustic refraction study indicate the ability of the implicit code to calculate refraction. A.R.H.

N85-22535# Georgia Inst. of Tech., Atlanta. School of Aerospace Engineering.

INVESTIGATIONS OF REACTIVE AND NON REACTIVE ACOUSTIC BOUNDARY LAYERS IN POROUS WALLED DUCTS **c34**

U. G. Hegde, F. L. Chen, and B. T. Zinn *In* APL 21st JANNAF Combust. Meeting, Vol. 1 Oct. 1984 p 91-102 refs (For primary document see N85-22526 13-20)

Avail: NTIS HC A21/MF A01 CSCL 20/4

The acoustic boundary layer in porous walled ducts with side wall gas injection which is of interest in studies of propellant driving in unstable solid propellant rocket motors is considered. The characteristics of the acoustic boundary layer are investigated both in the presence and absence of a premixed, laminar flame located in the vicinity of the duct walls. The formulation, valid for low injection Mach numbers, is two dimensional and includes the effects of viscosity, thermal conductivity, steady state velocities and chemical reaction. It is shown that with increase of the steady wall injection velocity, the acoustic boundary layer thickness at a given frequency increases and its tendency to damp acoustic motions within the duct also increases. Whereas in the nonreactive case, the effect of the boundary layer is generally damping; in the reactive flow case substantial driving of acoustic motions can occur in the region of high heat release rate. The analysis also shows that the acoustic admittance at the boundary layer edge depends upon axial location varying most rapidly in regions adjacent to an acoustic pressure minimum. Results of experimental studies carried out for the nonreactive case are also reported and shown to be in good agreement with the theory. Author

N85-22536# United Technologies Corp., San Jose, Calif. Chemical Systems Div.

COUPLING BETWEEN VELOCITY OSCILLATIONS AND SOLID PROPELLANT COMBUSTION **c25**

R. S. Brown, A. M. Blackner, P. G. Willoughy, and R. Dunlap *In* APL 21st JANNAF Combust. Meeting, Vol. 1 Oct. 1984 p 103-112 refs (For primary document see N85-22526 13-20)

(Contract F49620-81-C-0027)

Avail: NTIS HC A21/MF A01 CSCL 21/2

Studies are being conducted to define and characterize the basic fluid mechanics and heat transfer mechanism controlling the coupling between acoustic velocities and solid propellant combustion. Oscillatory surface heat fluxes and radial profiles of the mean and oscillatory velocity are being measured at several axial stations in a cold flow rocket simulator. Recent studies have concentrated on measuring the structure of the acoustic waves and how this structure relates to the oscillatory heat flux data reported earlier. In particular, the radial profiles of the magnitude and phase (relative to the head end acoustic pressure) of the acoustic velocity have been measured at several axial stations. At low acoustic pressures (i.e., 0.05%) the acoustic waves extend across the entire cross section in the region upstream of the transition in the mean velocity profile. Nonplanar and nonlinear behavior is also observed in the near surface regions. Downstream of the velocity transition, the acoustic waves do not penetrate through the near wall turbulence. At higher acoustic pressures (i.e., 0.4%) the upstream nonlinearities increase in magnitude and extend across the entire port. Downstream of the velocity transition the core nonlinearities decay while the linear component penetrates through the turbulence to the wall. This paper, which is a progress report, presents a detailed discussion of these results. Author

N85-22537# Utah Univ., Salt Lake City. Dept. of Mechanical and Industrial Engineering.

ACOUSTIC ENERGY BALANCE METHOD **c71**

G. A. Flandro *In* APL 21st JANNAF Combust. Meeting, Vol. 1 Oct. 1984 p 113-128 refs (For primary document see N85-22526 13-20)

(Contract F04611-81-C-0007)

Avail: NTIS HC A21/MF A01 CSCL 20A

A useful analytical model for nonlinear rocket instability must adequately represent the following characteristics: (1) steep fronted waves, (2) limit cycle operation, and (3) triggering phenomena. To include all of these important attributes requires retention of terms to third order in the perturbation parameter representing the system amplitude. This leads to an extremely complicated analysis; means must be found to develop useful analytical models that retain some physical clarity. Application of energy methods often results in simplification of the formulation. The energy method is combined with a simplified representation of the wave structure to produce the approximate model for axial pressure fluctuations in a tubular port which demonstrates all of the nonlinear characteristics of importance. Effects of nonlinear combustion and losses in shock waves are included. Author

N85-22538# Alabama Univ., Huntsville. Dept. of Mechanical Engineering.

COUPLED ACOUSTIC AND HYDRODYNAMIC WAVE INSTABILITIES **c71**

T. J. Chung and J. L. Sohn *In* APL 21st JANNAF Combust. Meeting, Vol. 1 Oct. 1984 p 129-137 refs (For primary document see N85-22526 13-20)

(Grant AF-AFOSR-0084-83)

Avail: NTIS HC A21/MF A01 CSCL 20A

Unstable waves may occur as a result of acoustic and/or hydrodynamic oscillations. If these two different types of waves are coupled together, their physical interactions lead to extremely complicated phenomena. Theoretically, there exists an infinite number of frequencies for both acoustic and hydrodynamic oscillations. Realistically, however, only a limited number of combined frequencies are excited. The objective is to determine the combined action of acoustic and hydrodynamic frequencies at which instabilities may arise. A review of the works on this subject which were published earlier is presented. The mathematical formulations for the theory and some simple numerical examples are demonstrated. Author

N85-22539*# Jet Propulsion Lab., California Inst. of Tech., Pasadena.

CHARACTERIZATION OF HETEROGENEITY OF COMPOSITE PROPELLANTS AND ITS EFFECTS ON COMBUSTION BEHAVIOR **c28**

L. D. Strand and N. S. Cohen (Cohen (Norman S.) Professional Services, Inc.) *In* APL 21st JANNAF Combust. Meeting, Vol. 1 Oct. 1984 p 139-152 refs Sponsored in part by NASA (For primary document see N85-22526 13-20)

(Contracts AFOSR-ISSA-81-00019; AFOSR-ISSA-82-00030; AFOSR-ISSA-83-00052)

Avail: NTIS HC A21/MF A01 CSCL 21I

A series of experiments was carried out with three propellants to determine whether or not certain features of the microstructure could be measured and correlated with response function behavior. Frequency components in the microstructure were measured and correlated with particle size distribution. Frequency components were also measured in dynamic burning experiments carried out at constant pressure, but these were essentially independent of size distribution, and therefore not fully correlatable with size

distribution. Pressure coupled response function measurements completed the series and indicated that the inherent microstructure is not the source of heterogeneous effects. Author

N85-22540# Georgia Inst. of Tech., Atlanta. School of Aerospace Engineering.
INVESTIGATION OF THE CHARACTERISTICS OF THE VELOCITY-COUPLED RESPONSE FUNCTIONS OF SOLID PROPELLANTS **c28**
L. L. Narayanaswami, B. T. Zinn, and B. R. Daniel *In* APL 21st JANNAF Combust. Meeting, Vol. 1 Oct. 1984 p 153-163 refs (For primary document see N85-22526 13-20)
(Contract F49620-82-C-0013)
Avail: NTIS HC A21/MF A01 CSCL 21/9

The assumption that the propellant velocity coupled response function is a propellant property which is independent of location within the combustor was examined. The validity of this assumption was investigated in a modified impedance tube setup specifically developed for this study. It consisted of a driver propellant sample at the upstream end of the tube and test propellant samples on the side walls at a desired location downstream of the driver propellant. An acoustic driver located at the downstream end of the tube was used to simulate conditions in an unstable motor by exciting a standing acoustic wave of desired properties in the tube. During a test, the driver was turned on, all the propellant samples were ignited and a series of pressure transducers attached to the tube wall was used to measure the resulting standing wave structure. These data together with a specially developed data reduction program were used to determine the velocity coupled response functions of the test propellant samples. Tests were conducted with the test propellant samples at different locations along the impedance tube standing wave. The results of these tests clearly showed that the velocity coupled response function is strongly dependent upon the propellant sample location relative to the impedance tube standing wave. These results also indicate that predictions of existing solid propellant rocket motor stability programs are most likely invalid because they are based upon the erroneous assumption that the velocity coupled response functions of the solid propellants are constant throughout the combustor. Author

N85-22541# Naval Weapons Center, China Lake, Calif.
COMPARISONS OF SOLID PROPELLANT WITH INSTABILITY PREDICTIONS AND MOTOR FIRING EXPERIENCE **c25**
H. B. Mathes *In* APL 21st JANNAF Combust. Meeting, Vol. 1 Oct. 1984 p 165-175 refs (For primary document see N85-22526 13-20)
Avail: NTIS HC A21/MF A01 CSCL 21/2

Five rocket motors are described for which combustion stability predictions have been performed. Motor types range from a large booster motor which uses an aluminized propellant to a small tactical motor loaded with a reduced smoke propellant. Two types of stability analysis are discussed: a quasi-three dimensional code and a one dimensional code. Comparisons between predicted stability and observed motor behavior are made and conclusions regarding apparent mismatches between prediction and behavior are presented. Author

N85-22542# Brigham Young Univ., Provo, Utah.
MEASUREMENTS OF DISTRIBUTED COMBUSTION **c25**
P. C. Braithwaite, M. W. Beckstead, and R. L. Raun *In* APL 21st JANNAF Combust. Meeting, Vol. 1 Oct. 1984 p 177-186 refs (For primary document see N85-22526 13-20)
(Grant AF-AFOSR-0157-83)
Avail: NTIS HC A21/MF A01 CSCL 21/2

If a particle burns as it traverses a relatively large portion of the system, the interchange of energy between the burning particle and the acoustic environment can result in either a driving or damping contribution to the acoustics of the system. This mechanism is the subject considered. The current experimental technique does not involve solid propellant, instead it utilizes a gas fired Rijke burner with a paddle to control (stop and start) combustion oscillations. Advantages of this approach include allowing a separation of the three mechanisms mentioned above by testing an additive independent of the propellant burning surface, avoiding the use of solid propellants, and allowing for independent control of frequency, O/F ratio, temperature, and particle addition. Al and ZrC are commonly added to solid propellants and exhibit significantly different combustion characteristics, Al being very reactive and ZrC slightly reactive. Experimental results obtained using Al and ZrC in the Rijke burner indicate that both additives do cause an increase in the acoustic growth rate when compared to growth rates obtained without any particles in the system. The increase in the acoustic growth rate is the result of energy being added to the system by the distributed combustion of the particles. The increase in the acoustic growth rate due to distributed combustion was found to be directly related to the heat of reaction.G.L.C.

N85-22543# Brigham Young Univ., Provo, Utah.
DISTRIBUTED COMBUSTION: A MECHANISM OF ACOUSTIC SUPPRESSION **c25**
M. W. Beckstead *In* APL 21st JANNAF Combust. Meeting, Vol. 1 Oct. 1984 p 187-194 refs (For primary document see N85-22526 13-20)
(Grant AF-AFOSR-0157-83)
Avail: NTIS HC A21/MF A01 CSCL 21/2

Viscous dissipation of acoustic energy by drag forces on a suspended particle is the most commonly recognized mechanism, being a direct analogy to suspended moisture in fog. A second mechanism whereby an additive can effect acoustics occurs at the burning boundary of the system. Solid additives within the propellant can have a catalytic influence on the propellant combustion, modifying the combustion response. The best known example of this is probably Al_2O_3. Al_2O_3 is the particulate product of aluminum combustion which provides the viscous drag dissipation previously discussed. However, Al_2O_3 is also a weak combustion catalyst in composite propellants. An additive that influences the steady burning of a propellant can also be expected to influence the transient response of the propellant. The third mechanism considered is due to the effect of a particle burning as it traverses a relatively large portion of the system. As it does so, the interchange of energy between the burning particle and the acoustic environment can result in either a driving or damping contribution to the acoustics of the system. In the past, some experimental results from motors and/or T-burners have been difficult to interpret in terms of particule damping only or combustion response only. When considered in terms of distributed combustion, some results are more easily explained. Author

N85-22544# Scientific Research Associates, Inc., Glastonbury, Conn.
INTERNAL FLUID MECHANISM OF SOLID PROPELLANT ROCKET MOTORS **c34**
J. S. Sabnis, H. J. Gibeling, and H. McDonald *In* APL 21st JANNAF Combust. Meeting, Vol. 1 Oct. 1984 p 195-204 refs (For primary document see N85-22526 13-20)
(Contract F04611-83-C-0003)
Avail: NTIS HC A21/MF A01 CSCL 20/4

The steady state flow of a nonreacting ideal gas in a cylindrical port cold flow model is simulated by the numerical solution of the ensemble averaged Navier-Stokes equations in a nonorthogonal, body fitted, axisymmetric coordinate system. The numerical procedure utilizes a consistently split linearized block implicit scheme. The computed results are compared with the experimental data obtained in cylindrical port cold flow tests. Author

N85-22545# Hercules, Inc., Cumberland, Md.
WORKSHOP REPORT: CATALYSIS OF BURN RATE OF ENERGETIC BINDER PROPELLANTS **c25**
R. L. Foster *In* APL 21st JANNAF Combust. Meeting, Vol. 1 Oct. 1984 p 205-212 refs Also presented at 20th JANNAF Combus. Meeting, Monterey, Calif., Oct. 1983 (For primary document see N85-22526 13-20)
Avail: NTIS HC A21/MF A01 CSCL 21/2

The catalysis of burn rate of energetic binder propellants was discussed. The purpose was to provide a framework for techniques

for modifying the ballistic behavior of energetic binder propellants. Useful approaches for obtaining high rate, minimum smoke propellants remain elusive, and attempts to obtain high rate by modifying the nitramine have not been very successful. It was recommended that catalysis of the binder be re-examined as a possible approach for burning rate modification. Author

N85-22546# Georgia Inst. of Tech., Atlanta.
MECHANISM OF BURNING RATE ENHANCEMENT BY FERRIC OXIDE **c25**
E. W. Price and J. K. Sambamurthi *In* APL 21st JANNAF Combust. Meeting, Vol. 1 Oct. 1984 p 213-231 refs Sponsored in part by Air Force (For primary document see N85-22526 13-20)
(Contract N00014-79-C-0764; Grant AF-AFOSR-0356-83)
Avail: NTIS HC A21/MF A01 CSCL 21/2

The mechanism of burning rate enhancement of propellants by catalysts is examined by tests on ammonium perchlorate (AP) sandwiches and bimodal AP propellants. Burning rates were measured from motion pictures, and samples from quench tests were examined in the scanning electron microscope. The results indicated that effective catalysis depends on concentration of the catalyst on the binder surface so as to permit adequate contact of fuel vapors with the surface of the catalyst. This results in breakdown of fuel vapor molecules, permitting the oxidizer-fuel flame to stand closer to the surface. Author

N85-22547# Purdue Univ., Lafayette, Ind. School of Aeronautics and Astronautics.
EFFECT OF VARIABLE SOLID PHASE THERMAL PROPERTIES ON PROPELLANT COMBUSTION **c25**
Fred S. Blomshield and John R. Osborn *In* APL 21st JANNAF Combust. Meeting, Vol. 1 Oct. 1984 p 233-240 refs (For primary document see N85-22526 13-20)
Avail: NTIS HC A21/MF A01 CSCL 21/2

Mathematical models derived for describing the combustion of solid rocket propellants have in the past assumed that the thermal properties, specific heat, and thermal conductivity are constant throughout the solid phase portion of the combustion zone. The values for specific heat and thermal conductivity can vary as much as 50 to 100 percent for the temperatures in the solid phase combustion wave, values from about 250 to 1100 K. Thus, the variation in solid phase properties due to the temperature variation in the solid phase have significant effects on the buring rate, the temperature sensitivity and the pressure coupled response. The prediction of the effect of variable solid phase properties on the combustion properties is addressed. Parametric calculations were made to illustrate the effect of the magnitude of the variation of solid phase properties with temperature. The results indicate that significant differences exist between the values for the combustion parameters calculated using variable thermal properties as compared to those calculated using constant thermal properties. M.G.

N85-22548# Systems Research Labs., Inc., Dayton, Ohio.
APPLICATION OF FLUORESCENCE TO MEASUREMENT OF SURFACE TEMPERATURE IN SOLID PROPELLANTS **c28**
Larry F. Goss and Arthur A. Smith *In* APL 21st JANNAF Combust. Meeting, Vol. 1 Oct. 1984 p 241-249 refs (For primary document see N85-22526 13-20)
(Contract F49620-83-C-0138)
Avail: NTIS HC A21/MF A01 CSCL 21/9

Three rare-earth-ion crystals were shown to be good candidates for surface temperature measurements on energetic materials by laser induced fluorescence. Dy(+3):LaF3 displays a thermalization process with an energy gap of 1070/cm, resulting in a fluorescence intensity change of approx. 200 over a 700-K temperature range. Cr(+3):Al2O3 (ruby) displays an extreme temperature sensitivity to the lifetime of the R-fluorescence lines. The lifetimes are observed to change by a factor of approx. 230 over a 500-K temperature range. Er(+3):CaF2 shows a temperature sensitivity of 20 over a temperature range of 700 K, as measured by the lifetime of its E(4 S 3/2) fluorescence life. M.G.

N85-22549# Virginia Polytechnic Inst. and State Univ., Blacksburg.
MUTIPLE REFLECTION THEORY FOR MICROWAVE MEASUREMENT OF SOLID PROPELLANT BURNING RATES **c25**
W. F. OBrien, H. L. Wood, J. J. Kliger (Naval Ordnance Station, Indian Head, Md.), and C. B. Dale (Naval Ordnance Station, Md.) *In* APL 21st JANNAF Combust. Meeting, Vol. 1 Oct. 1984 p 251-259 refs (For primary document see N85-22526 13-20)
(Contract N00174-82-C-0039)
Avail: NTIS HC A21/MF A01 CSCL 21/2

Microwaves reflected from the regressing burning surface of solid propellants carry information which can be extracted to yield the local burning rate of the propellant. The signal is complex, with multiple reflections arising from each material interface in the path of the microwaves, including the propellant-combustion zone interface. It is shown that certain otherwise fixed microwave reflections within a slab propellant burner acquire a changing phase shift through interaction with the moving propellant combustion surface. The effect of this interaction on the burning rate measurement is studied through the use of computer simulation in several examples. Requirements are assessed for more complete models of microwave reflections for burning rate measurement in solid propellants. M.G.

N85-22550# Air Force Rocket Propulsion Lab., Edwards AFB, Calif.
IN-SITU BURNING RATE DETERMINATION USING FLASH RADIOGRAPHY **c25**
H. M. Pressley, Jr. and R. L. Glick (Purdue Univ., Lafayette, Ind.) *In* APL 21st JANNAF Combust. Meeting, Vol. 1 Oct. 1984 p 261-273 refs (For primary document see N85-22526 13-20)
Avail: NTIS HC A21/MF A01 CSCL 21/2

Direct in-situ methods for determining burning rates and corresponding environments in solid rocket motors have been based on radiography and interrupted burning. The former has relatively poor accuracy because measurements are subjective; the latter is relatively expensive - only one data set per motor firing is obtained. An approach based on a combination of indirect and radiographic methods is proposed and carried through to preliminary results. The method features direct measurement of port area (mass burning rate is measured directly), multiple radiographs per burn, estimates for instantaneous burning rates, and improved accuracy (achieved by eliminating subjective measurement and integrating film density data to attenuate random radiographic errors). Extraction of perimeter-mean burning rate is possible with nominally circular ports to improved accuracy and with non-circular ports to indirect-method accuracy. Examples of flash radiographs, transverse film density profiles, and propellant burning phenomena revealed by the radiographs are also presented. Author

N85-22551# Army Research and Development Command, Dover, N.J.
THE CRYSTAL AND MOLECULAR STRUCTURE OF A NEW PROPELLANT COMPOUND: TRIAMINOGUANIDIUM AZIDE NITRATE (TAZN) **c28**
A. J. Bracuti and Jan M. Troup (Molecular Structure Corp., College Station, Tex.) *In* APL 21st JANNAF Combust. Meeting, Vol. 1 Oct. 1984 p 293-299 refs (For primary document see N85-22526 13-20)
Avail: NTIS HC A21/MF A01 CSCL 21/9

A high nitrogen propellant compound, triaminoguanidinium azide nitrate (TAZN), was discovered. Single crystal X-ray diffraction data were obtained. The crystal and molecular structure of this orthorhombic (Pbca) compound was determined. Comparisons between the structures of TAGN and TAZN are discussed with emphasis upon possible hydrogen bonding. Author

N85-22552# Army Research and Development Command, Dover, N.J.
MOLECULAR DYNAMICS OF PROPELLANT GASES, PART 2 **c28**
T. Vladimiroff *In* APL 21st JANNAF Combust. Meeting, Vol. 1 Oct. 1984 p 301-306 refs (For primary document see N85-22526 13-20)

Avail: NTIS HC A21/MF A01 CSCL 21/9

The technique of molecular dynamics is used to calculate the pressure for nitrogen gas in the density range of 0.2 to 1.0 g/cu cm and in the temperature range of 500K to 3000K. The calculations assume that the motion of nitrogen gas molecules can be described using the laws of classical mechanics. Lennard-Jones and exponential-6 potentials are used to describe the molecular interactions. A system of 256 particles, in conjunction with a periodic boundary condition, is employed to simulate the bulk material. A predictor-corrector type of algorithm is used to integrate the equation of motion. The calculated pressures are compared with available equations of state and perturbation theory. It is found that the Lennard-Jones potential works well at 3000K and that the Hansen perturbation theory could become an effective method for calculating the pressure for real gases. M.G.

N85-22553# Colorado State Univ., Fort Collins.

AN INTEGRAL CLOSED LOOP COMBUSTION STABILITY MODEL-STATUS AND REVIEW c28

C. E. Mitchell *In* APL 21st JANNAF Combust. Meeting, Vol. 1 Oct. 1984 p 347-355 refs (For primary document see N85-22526 13-20)

Avail: NTIS HC A21/MF A01 CSCL 21/9

An integral closed loop stability model, for liquid propellant rocket engines is presented. The basics of the analytical approach, which leads to a set of integral equations to be solved successively, essentially following Picard's method, are discussed. The aspects of the stability problem which have been studied using the approach are reviewed. These include combustion distribution, acoustic absorber effects, nonlinear wave propagation effects, injector fact baffles, and velocity and pressure sensitive combustion responses. The types of stability predictions possible with the approach are discussed and some typical results of calculations exemplifying them are given. Author

N85-22554*# Rocketdyne, Canoga Park, Calif.

DEVELOPMENT OF A THREE-PHRASE COMBUSTION CODE FOR MODELING LIQUID ROCKET ENGINES c25

P. Y. Liang and Y. M. Chang *In* APL 21st JANNAF Combust. Meeting, Vol. 1 Oct. 1984 p 357-367 refs (For primary document see N85-22526 13-20)

(Contract NAS8-34928)

Avail: NTIS HC A21/MF A01 CSCL 21B

A two-dimensional/axisymmetric program for the simulation of three-phase reactive flows is presented. The three phases are: a multiple-species gaseous phase, a single-species liquid phase, and a particulate droplet phase. The liquid and gaseous phases are described with continuous Eulerian equations, while the droplets are described in a discrete Lagrangian fashion. The three phases are fully coupled together. An atomization model, a multireaction chemical kinetics model, and a subgrid scale turbulence model completes the description of a general liquid/gas bipropellant combustion process. The code development criteria and qualitative features are highlighted. M.G.

N85-22555*# Rocketdyne, Canoga Park, Calif.

ATOMIZATION DATA REQUIREMENTS FOR ROCKET COMBUSTOR MODELING

Allan J. Ferrenberg and Mahendra S. Varma *In* APL 21st JANNAF Combust. Meeting, Vol. 1 Oct. 1984 p 369-377 refs (For primary document see N85-22526 13-20)

(Contract NAS8-34504)

Avail: NTIS HC A21/MF A01 CSCL 21H

The complex computer codes, which model liquid rocket combustors, require information about the distribution and atomization of these liquid reactants. The available information is, in general, of questionable validity and applicability. Authors and users of combustion codes are often unaware of, or underestimate the importance of, these deficiencies in atomization data. These deficiencies and their importance are examined. Results of analyses performed with a state-of-the-art rocket combustion code are presented which demonstrate the important effects of such atomization information as initial droplet sizes and size distribution on vaporization rate and losses. Also, the questionable aspects and inapplicability of the available atomization data are discussed. One important and often neglected or misunderstood aspect of atomization data is the differences between spatial (concentration) and flux (often called temporal) droplet size distributions. These are described, and a computer model constructed to assess the difference between concentration and flux droplet size distributions is described and results presented. Experimental data are also given to demonstrate this difference. Finally, experimental results are presented that demonstrate the very great, and often neglected effect, of the local gas velocity field on atomization. Author

N85-22556# Pratt and Whitney Aircraft, West Palm Beach, Fla. Engineering Div.

HIGH-PRESSURE ROCKET ENGINE TURNAROUND DUCT COMPUTATIONAL FLUID DYNAMICS ANALYSIS c34

George B. Cox, Jr. *In* APL 21st JANNAF Combust. Meeting, Vol. 1 Oct. 1984 p 379-398 refs (For primary document see N85-22526 13-20)

Avail: NTIS HC A21/MF A01 CSCL 20D

Current and projected high-pressure, staged-combustion rocket engine designs, such as the XLR129 and space shuttle main engine (SSME), introduced a type of turnaround duct flowpath wherein the turnaround is accompanied by an increase in mean radius and a decrease in fluid velocity through a subsequent diffuser. This turnaround duct flowpath is needed in the rocket engine to conduct high-pressure turbopump turbine discharge gases toward the main injector while maintaining a compact turbomachinery and powerhead flowpath. Current experience in the SSME shows that this type of turnaround duct can experience flow separation with an attendant increase in flow turbulence levels. Advances in computational fluid dynamics techniques over the last decade produced a number of codes which are applicable to the analysis and prediction of flow field behavior within such ducts. A version of the TEACH code developed at Pratt & Whitney Engineering Division was used to analyze three representative turnaround duct configurations. The study included the effects of fluid properties, inlet velocity flowfields, solution grid mesh size, and numerical solution algorithm upon calculated flow. Results include flow streamline comparisons, velocity profiles, and calculated total pressure losses. The results showed that turnaround ducts of the type studied can exhibit separation but that appropriately designed turnaround ducts can be made to function without suffering from internal flow separation. R.J.F.

N85-22557# Rocketdyne, Canoga Park, Calif.

MINIMIZING PLUME CONTAMINATION PRODUCTION IN BIPROPELLANT THRUSTERS

E. A. DeGaetano and W. T. Webber *In* APL 21st JANNAF Combust. Meeting, Vol. 1 Oct. 1984 p 399-407 refs Sponsored in part by International Telecommunications Satellite Organization (For primary document see N85-22526 13-20)

Avail: NTIS HC A21/MF A01 CSCL 21/8

Under a 1-year program funded by the International Telecommunication Satellite Organization, the Rocketdyne Division of Rockwell International designed, fabricated, and tested a full-scale, advanced, storable, pressure-fed thruster for blowdown operation in the 1-lbf thrust range. The purpose of the program was a full-scale technology demonstration of an engine appropriate for use as a satellite station-keeping and attitude-control thruster. The primary features of the thruster are high performance, reduced plume contaminant production, and long life. Using nitrogen tetroxide and monomethylhydrazine, the thruster operates at 50 psia chamber pressure and produces a nominal vacuum specific impulse of 300 seconds with a 150:1 nozzle expansion ratio. The thruster chamber is made of beryllium and is radiation cooled. Reduction of the plume contaminant is accomplished by providing improved propellant evaporation for high combustion efficiency and by reduction of thruster propellant dribble volumes. Author

N85-22558# Colorado Univ., Boulder. Dept. of Mechanical Engineering.
CHEMICAL KINETICS OF GAS PHASE DECOMPOSITION PRODUCTS OF NITRAMINE PROPELLANTS
Melvyn C. Branch *In* APL 21st JANNAF Combust. Meeting, Vol. 1 Oct. 1984 p 409-415 refs (For primary document see N85-22526 13-20)
(Grant AF-AFOSR-0006-84)
Avail: NTIS HC A21/MF A01 CSCL 21/8

Nitramine based solid rocket propellants have the advantages of relatively low infrared and smoke emissions from their exhaust. Although a number of studies were directed toward chemical and physical processes in the condensed phase during heating or combustion, the understanding of gas phase chemical processes was not developed. The objective of the studies reported is to provide additional insight into the chemistry of reactions of gas phase species of importance in the combustion of nitramine propellants. Chemical kinetic modeling of the gas phase reactions is used to evaluate critical reaction paths and energetics and their possible influence on burn rate. Particular attention was given to the fizz reaction near the propellant surface and the preparation and flame zones standing off the surface. The chemical kinetic modeling shows a two zone behavior which is consistent with previous suggestions about the chemistry of the fizz and flame zones. The first zone is dominated by the rapid reaction between CH2O and NO2 while the second zone results from the slower exothermic reduction of NO. R.J.F.

N85-22559# Naval Research Lab., Washington, D. C. Chemistry Div.
KINETICS OF MECHANISM OF THE THERMAL DECOMPOSITION OF DIMETHYLNITRAMINE AND DIMETHYLNITROSAMINE **c28**
M. E. Umstead, S. A. Lloyd, D. S. Y. Hsu, and M. C. Lin *In* APL 21st JANNAF Combust. Meeting, Vol. 1 Oct. 1984 p 417-422 refs (For primary document see N85-22526 13-20)
Avail: NTIS HC A21/MF A01 CSCL 21/9

The kinetics and mechanism of the thermal decomposition of dimethylnitramine (DMNA) and dimethylnitrosamine (DMNSA) were studied at high temperatures in a shock tube with IR laser and UV diagnostics and at lower temperature in a static system. The understanding of the chemistry of these model compounds is an important step toward our ultimate elucidation of the complex mechanism of decomposition and burning characteristics of larger nitramines such as RDX and HMX. The unimolecular rate constant at the high-pressure limit for the thermal decomposition of DMNA was found to be k = 10(15.9 plus or minus 0.1) exp(-44,100 plus or minus 500/RT)s(-1). The reaction of (CH sub 3)sub 2 N with NO sub 2 (k=2x ten to the 10th power according the mechanism: (CH sub 3)sub 2 N + NO sub 2 yields 2CH sub 3 NO yields 2CH sub 3 + 2 NO is proposed to be an important initial chain-propagation step in the DMNA and the DMNSA + NO systems. Detailed kinetic modeling of these systems was carried out R.J.F.

N85-22560# Lockheed Missiles and Space Co., Palo Alto, Calif.
EFFECTS OF HMX ADDITION ON THE COMBUSTION OF ENERGETIC BINDERS **c28**
N. S. Cohen (Cohen (Norman S.) Professional Services, Inc.), J. C. Crowley, and G. A. Lo *In* APL 21st JANNAF Combust. Meeting, Vol. 1 Oct. 1984 p 423-432 refs (For primary document see N85-22526 13-20)
Avail: NTIS HC A21/MF A01 CSCL 21/9

A simplified model for the effects of HMX on the combustion of energetic binders is given. It was found that an exothermic condensed phase is an important feature of energetic binder combustion. The effects of HMX addition can be summarized by a reduction in the overall exothermicity of the condensed phase together with an increase in the heat feedback from the gas phase. Consequences include an increase in pressure exponent along with a reduction in temperature sensitivity. Effects on burn rate magnitude depend upon binder composition and pressure, but the energy tradeoffs keep the burning rates within a narrow range at a given pressure. HMX addition is also shown to thin the combustion zone, with possible implications for the effectiveness of ballistic modifiers. R.J.F.

N85-22561# Naval Research Lab., Washington, D. C. Chemistry Div.
THE CHEMISTRY OF RDX AND HMX CLUSTER IONS **c28**
Robert J. Doyle, Jr. and Joseph E. Campana *In* APL 21st JANNAF Combust. Meeting, Vol. 1 Oct. 1984 p 433-436 refs (For primary document see N85-22526 13-20)
Avail: NTIS HC A21/MF A01 CSCL 21/9

The heterocyclic nitramines, hexahydro-1,3,5-trinitro-1,3,5-triazine (RDX) and octahydro-1,3,5,7-tetranitro-1,3,5,7-tetrazocine (HMX), were found to form cluster ions of the general formula [(CH2NNO2)nH]+ where n=1,2,3,...,15 for RDX and n=1,2,3,...,56 for HMX. Two significant features of the resultant cluster ion distributions for RDX and HMX are the observation of magic numbers and their mutual uniqueness. These features are attributed to the molecular structure and to the intermolecular interactions inherent to the condensed phase of the precursors (RDX and HMX). The unicluster dissociation spectra of protonated RDX and HMX cluster ions reveal that these clusters may be the primary source of N2O in the vapor phase decomposition of RDX and HMX. R.J.F.

N85-22562# University of Southern California, Los Angeles. Dept. of Mechanical Engineering.
EFFECTS OF TEMPERATURE VARIATION AMONG DROPLETS IN AN EVAPORATING FUEL SPRAY **c28**
P. Roy Choudhury and Melvin Gerstein *In* APL 21st JANNAF Combust. Meeting, Vol. 1 Oct. 1984 p 455-463 refs (For primary document see N85-22526 13-20)
Avail: NTIS HC A21/MF A01 CSCL 21/4

It is well known that the boiling point of a typical fuel blend is different from those of the pure components. For an ideal mixture of liquids at a given state the new boiling point can be calculated either theoretically or can be obtained from experimental data (e.g., ASTM distillation curve). The ASTM distillation data for JP-4, for example, show that the boiling point can change by about 250 C depending upon the degree of evaporation. Droplets of different diameters in a spray undergo different degrees of evaporation and hence have different boiling temperatures. The purpose is to investigate the effect of temperature distribution in the spray on the local overall fuel-air ratio. Sprays of both JP-8 and JP-4 (ASTM distillation data) are used as examples in a flowing, one-dimensional stream at 20 atm and 680 K. The droplets undergo an initial phase of unsteady heating and finally steady evaporation follows when the wet-bulb temperature is reached. The results show that under most operating conditions the temperature distribution in a fuel spray can have a significant effect on the local fuel-air mixture and hence on the performance of an airbreathing propulsion system. The use of a constant mean boiling temperature rather than the variable boiling temperature will result in significant errors. R.J.F.

N85-22563# McDonnell-Douglas Research Labs., St. Louis, Mo.
THE ROLE OF CONVECTIVE PERTURBATIONS IN SUPERCRITICAL INLET OSCILLATIONS **c34**
T. J. Bogar and M. Sajben *In* APL JANNAF Combust. Meeting, Vol. 1 Oct. 1984 p 465-479 refs (For primary document see N85-22526 13-20)
Avail: NTIS HC A21/MF A01 CSCL 20/4

Available experimental evidence on supercritical diffuser flow oscillations is reviewed, focusing on features that conflict with quasi-one-dimensional, linear acoustic theory. A model is proposed in which convective, transverse perturbations initiated by the shock and carried by the boundary layers are the dominant downstream-moving disturbances. These disturbances in turn combine with upstream-moving acoustic waves to form the total oscillatory pattern. The boundary conditions at the two ends of the channel applicable to such flows are discussed. The reflection coefficients for pressure and velocity perturbations are related but not equal; some estimates of their values are given. The model offers a qualitative explanation for most non-acoustic features of the

oscillations and suggests a possible mechanism for inlet/combustor coupling. Author

N85-22564# Atlantic Research Corp., Gainesville, Va.
WORKSHOP REPORT: SWIRL ENHANCED COMBUSTION
c25
William Sargent *In* APL 21st JANNAF Combust. Meeting, Vol. 1 Oct. 1984 p 481-485 refs Also presented at 5th Swirl Workshop, Reno, Nev., Jan. 1984 (For primary document see N85-22526 13-20)
Avail: NTIS HC A21/MF A01 CSCL 21/2

A swirling flow workshop was held in conjunction with the 22nd AIAA Aerospace Sciences meeting in order to encourage participation by the academic community. Discussion indicated that stationary numerical procedures are now an effective design support tool although turbulence modeling and numerical procedures require enhancement. Laser velocimetry and spectroscopy are providing enhanced understanding of the turbulent and fluctuating properties of swirling flow. However, some disparity in results has been noted between new and older diagnostic techniques. The objective of the workshop was to review the theory and practice of swirling flows as they apply to the combustion of liquids, metals, and, carbonaceous fuels and the issues to be focused upon were: analytical methods, numerical methods, flow analog techniques, the effect of heat release, the effect of high confinement ratios, low intensity/high intensity swirl, combustion and swirl, and the effect of fuel injection. R.J.F.

N85-22565# European Space Agency, Paris (France).
PHOTOVOLTAIC GENERATORS IN SPACE
W. R. Burke, comp. Nov. 1984 461 p refs Partly in FRENCH and ENGLISH Proc. of 4th European Symp., Cannes, France, 18-20 Sep. 1984 by CNES, ESA and SNIAS
(ESA-SP-210; ISSN-0379-6566) Avail: NTIS HC A20/MF A01

Silicon and GaAs solar cells for spacecraft power supplies; space environment effects on solar cells; solar generator design, checkout, and calibration; electrical interfaces; solar blankets; and deployment and retraction mechanisms were discussed. For individual titles, see N85-22566 through N85-22626.

N85-22566# Institute of Space and Astronautical Science, Tokyo (Japan).
HISTORY AND FUTURE VIEWS ON SOLAR CELLS OF JAPANESE SCIENTIFIC SATELLITES
A. Ushirokawa, K. Takahashi, M. Kohbata, A. Suzuki (Sharp Corp., Shinjo-cho, Japan), T. Hirano (Sharp Corp., Shinjo-cho, Japan), T. Matsutani (Sharp Corp., Shinjo-cho, Japan), and T. Saga (Sharp Corp., Shinjo-cho, Japan) *In* ESA Photovoltaic Generators in Space Nov. 1984 p 3-9 (For primary document see N85-22565 13-20)
Avail: NTIS HC A20/MF A01

Solar cells and qualification tests of solar cells for MS-T5 and PLANET-A satellites which will explore Halley's comet in 1986 are described. For future satellites, requirements for power and weight of solar cells are expected to grow rapidly. Thin or ultrathin cells are intended to be the candidates for the satellites. The application of thin cells to satellites is compared with the former ones. Although thin cells have lower initial power output, they are more tolerant to space radiation. Author (ESA)

N85-22567# National Space Development Agency, Ibaraki (Japan).
THIN AND ULTRATHIN SILICON SOLAR CELLS FOR SPACE USE
S. Matsuda, T. Matsutani (Sharp Corp., Shinjo-cho, Japan), T. Saga (Sharp Corp., Shinjo-cho, Japan), T. Hirano (Sharp Corp., Shinjo-cho, Japan), and A. Suzuki (Sharp Corp., Shinjo-cho, Japan) *In* ESA Photovoltaic Generators in Space Nov. 1984 p 11-16 refs (For primary document see N85-22565 13-20)
Avail: NTIS HC A20/MF A01

In order to achieve longer life and reduced weight, ultrathin and thin solar cells, (thickness 55 and 100 or 200 microns) were developed. Five types of 280 micron cells are in use and 5 kinds of cells are ready for mass production. Besides back surface field (BSF) and back surface reflecton (BSR) the manufacturing process were improved to avoid the electrical output loss caused by thinning silicon substrates. The main improvements were phosphorus diffusion by PH3 (phosphine) gas source, double layer antireflective coating and fine grid lines. The 2 x 2 cm ultrathin BSFR cell has 73 mW electrical output, which is 2 mW larger than that of the 280 micron BSFR cell. This proves that the manufacturing process overcomes the disadvantage caused by the use of thin and ultrathin substrates. Author (ESA)

N85-22568# Applied Solar Energy Corp., City of Industry, Calif.
SPACE SOLAR CELLS: ADJUSTING TO NEW DEMANDS
P. A. Iles *In* ESA Photovoltaic Generators in Space Nov. 1984 p 17-23 refs (For primary document see N85-22565 13-20)
Avail: NTIS HC A20/MF A01

The use of established silicon solar cell technology to meet increased demands for spacecraft power supplies is described. Developments in gallium arsenide technology are summarized. Author (ESA)

N85-22569*# National Aeronautics and Space Administration. Lewis Research Center, Cleveland, Ohio.
THE HIGH VOLTAGE SILICON CELL: A COMPARATIVE ANALYSIS
V. G. Weizer, C. K. Swartz, R. E. Hart, and M. P. Godlewski *In* ESA Photovoltaic Generators in Space Nov. 1984 p 25-29 refs (For primary document see N85-22565 13-20)
Avail: NTIS HC A20/MF A01 CSCL 21H

An experimental technique capable of resolving the dark saturation current into its base and emitter components is used in an analysis in which the voltage limiting mechanisms for high voltage, low resistivity silicon solar cells were determined. Hi-low emitter cells, multistep diffused cells, ion-implanted emitter cell, MINMIS and MINP cells were studied. The results are at variance with prior expectations: the MINP and the MINMIS voltage improvements are due, to a considerable extent, to an optimization of the base component of the saturation current. This result is substantiated by an independent analysis of the material used to fabricate the devices. Author (ESA)

N85-22570# Telefunken Electronic G.m.b.H., Heilbronn (West Germany).
A 2 X 6 BACK SURFACE REFLECTION (BSR) SILICON SOLAR CELL
R. Schilling, K. Roy, and M. Krueger *In* ESA Photovoltaic Generators in Space Nov. 1984 p 31-36 refs (For primary document see N85-22565 13-20)
Avail: NTIS HC A20/MF A01

Production of the 3 in multi-element process for 10 ohm-cm, 180 micron thick, 1.81 cm x 6.19 cm back surface reflection silicon solar cells is described. Histograms of the electrical and thermo-optical characteristics as open circuit voltage, short circuit current, power output and reflectance at 1.5 microns, based on 10% sample base measurement for $>$ 100,000 cells are given. Electron irradiation experiments show a low power-degradation rate. The uniform blue response, periodically controlled, determines the uniform end of life behavior. The narrow distribution of the infrared reflection determines a uniform string characteristic at operating temperature. Dividing the circular wafer into several cells by laserscribing causes microfractures in the cell edges, but they do not penetrate deeper into the silicon after thermal cycling. Author (ESA)

N85-22571# Telefunken Electronic G.m.b.H., Heilbronn (West Germany).
EXPERIENCES WITH IMPLANTED BACK SURFACE FIELD (BSF) SOLAR CELLS
G. Strobl, K.-D. Rasch, W. Schmidt, and K.-H. Tentscher *In* ESA Photovoltaic Generators in Space Nov. 1984 p 37-40 refs (For primary document see N85-22565 13-20)
Avail: NTIS HC A20/MF A01

In order to identify back surface field (BSF) technology with

highest effectiveness under beginning and end of life (BOL, EOL) conditions solar cells (200 microns, 10 ohm-cm, crucible grown) were fabricated. For the formation of the BSF structure boron ion implantation, boron diffusion, evaporated aluminum alloying and screen-printed aluminum firing were used. Highest BOL and EOL power output is achieved with boron diffused and boron implanted BSF solar cells. The boron diffused BSF cells show a higher open-circuit voltage, yet a lower short circuit current compared with boron implanted cells. This tradeoff results in the same overall efficiency at BOL and EOL. These findings are confirmed under production conditions. Author (ESA)

N85-22572# Telefunken Electronic G.m.b.H., Heilbronn (West Germany).

A LOW COST APPROACH WITH LARGER DIAMETER SILICON WAFER

K.-D. Rasch and K. Roy *In* ESA Photovoltaic Generators in Space Nov. 1984 p 41-43 refs (For primary document see N85-22565 13-20)

(Contract ESTEC-5491/83/NL-PB(SC))

Avail: NTIS HC A20/MF A01

In solar cell production the 2.5 in silicon wafer was replaced by 3 and 4 in wafers. Analysis of the cell production costs shows that with increasing wafer diameter standard 2 x 4 cm cells can lead to a bad wafer utilization and therefore to an enhanced cost/cell area. From geometrical conditions, favorable cell sizes adapted to 3 and 4 in wafers can be defined. The potential cost reduction/cell area due to the optimized wafer utilization is 20% to 56% relative to the 2 x 4 cm cell dimension. Author (ESA)

N85-22573# Telefunken Electronic G.m.b.H., Heilbronn (West Germany).

BIFACIAL LIGHT SENSITIVE SPACE SOLAR CELL

K.-D. Rasch, G. Friedrich, G. Strobl, and K.-H. Tentscher *In* ESA Photovoltaic Generators in Space Nov. 1984 p 45-49 refs (For primary document see N85-22565 13-20)

Avail: NTIS HC A20/MF A01

A bifacial light sensitive solar cell for space solar generators is described. The bifacial cell converts direct Sun radiation and albedo radiation reflected by the Earth. Analysis shows superior overall characteristics of this structure compared to conventional cells. The efficiences of experimental cells (50 to 180 microns thick) are up to 30% higher. The benefit of the bifacial structure exists up to 1 x 10 to the 15th power MeV electrons/sq cm. The structure has a low solar absorptance (< 0.63) and is almost transparent for IR radiation. The estimated operating temperature is 10 to 20 C lower than for back surface reflection cells. Author (ESA)

N85-22574# Societe Nationale Industrielle Aerospatiale, Cannes (France).

GALLIUM ARSENIDE ARRAYS VERSUS SILICON ARRAYS FOR SPACE APPLICATION

L. Pelenc *In* ESA Photovoltaic Generators in Space Nov. 1984 p 53-56 refs (For primary document see N85-22565 13-20)

Avail: NTIS HC A20/MF A01

From the assumed performances (cost, efficiency, mass) of silicon solar cells and the solar arrays in the 1990's, the minimal requirements for gallium arsenide solar cells to be competitive when mounted on nonconcentrated or spinned solar arrays were determined. Results show that compared with a 10% EOL efficiency 100 micron thick silicon cell, a GaAs cell is competitive, if it is 13% to 14% EOL efficient, 200 to 250 microns thick, and 2 to 2.5 times silicon cost at bare cell level. Author (ESA)

N85-22575# National Space Development Agency, Ibaraki (Japan).

SPACE QUALIFIED AlGaAs/GaAs SOLAR CELLS

S. Matsuda, S. Yoshida (Mitsubishi Electric Corp., Hyogo, Japan), M. Otoda (Mitsubishi Electric Corp., Hyogo, Japan), K. Teramot (Mitsubishi Electric Corp., Hygogo, Japan), and A. Kawakami (Mitsubishi Electric Corp., Hygogo, Japan) *In* ESA Photovoltaic Generators in Space Nov. 1984 p 59-63 refs (For primary document see N85-22565 13-20)

Avail: NTIS HC A20/MF A01

High performance AlGaAs/GaAs solar cells with maximum air mass zero efficiency of 19.3% (typical 17.5%) were fabricated by liquid phase epitaxy using vertically separated three chambers to vertically load multiple GaAs substrates. The structure and fabrication technology of AlGaAs/GaAs solar cells are described and the results of qualification tests are presented. All qualification tests are successful and space applications are feasible. Author (ESA)

N85-22576# Mitsubishi Electric Corp., Hyogo (Japan).

AVAILABILITY OF AlGaAs/GaAs SOLAR CELLS IN SPACE

S. Yoshida, N. Imura, M. Goto, and S. Matsuda *In* ESA Photovoltaic Generators in Space Nov. 1984 p 65-68 refs (For primary document see N85-22565 13-20)

Avail: NTIS HC A20/MF A01

Performances of AlGaAs/GaAs solar cells are compared with those of Si solar cells. The power to weight and power to surface area for an AlGaAs/GaAs solar array and an Si solar array are calculated. Both arrays are designed to provide the same power at the end-of-life, defined as 7 yr in geosynchronous orbit. Results show that AlGaAs/GaAs cells have higher efficiency, temperature operation, radiation resistance, and specific power. Author (ESA)

N85-22577# Universidad Politecnica de Barcelona (Spain). Dept. de Electronica y Energia Solar.

COMPARATIVE STUDY OF GaAs SOLAR CELL POTENTIALITIES FOR SPACE APPLICATIONS

L. Castaner, L. Prat, J. Calderer, E. GarciaMoreno, C. Pol, F. Arrizabalaga, L. Closas, J. Garcia, and J. Cabestany *In* ESA Photovoltaic Generators in Space Nov. 1984 p 69-74 refs (For primary document see N85-22565 13-20)

(Contract ESTEC-5589/83/NL-PB(SC))

Avail: NTIS HC A20/MF A01

Scientific, technical, and engineering aspects of GaAs in space environment were studied. Analytical models for heterojunction and homojunction structures under electron and proton irradiation were developed, and electron bombardment and diffusion length measurements performed. A model concerning the mass, area, volume and power balance between silicon and GaAs systems is presented. Industrial costs to produce space qualified GaAs solar cells are discussed. Author (ESA)

N85-22578# Centre National d'Etudes Spatiales, Toulouse (France).

INVESTIGATION OF HIGH OUTPUT GALLIUM ARSENIDE SOLAR CELLS [ETUDES DE PHOTOPILES A L'ARSENIURE DE GALLIUM A HAUT RENDEMENT]

G. Keil-Simon and A. Cuquel *In* ESA Photovoltaic Generators in Space Nov. 1984 p 75-81 refs In FRENCH (For primary document see N85-22565 13-20)

Avail: NTIS HC A20/MF A01

The feasibility of manufacturing high energy conversion efficiency GaAs solar cells by liquid phase epitaxy of organometals is discussed. Homostructures with junctions close to the surface were developed, and their suitability for spaceborne utilization was tested. Results show that conversion efficiency of 20% is possible, and that GaAs cells are more resistant to the space radiation environment than silicon cells. Author (ESA)

N85-22579# Centro Informazioni Studi Esperienze, Milan (Italy).

DEVELOPMENT OF VERY THIN LARGE AREA GaAs SOLAR CELLS FOR SPACE APPLICATION

L. Bertotti and C. Flores *In* ESA Photovoltaic Generators in Space Nov. 1984 p 83-87 refs Sponsored in part by CNR (For primary document see N85-22565 13-20)

Avail: NTIS HC A20/MF A01

The fabrication and performances of thin and ultrathin GaAs solar cells obtained by chemical etching methods based on dissolution of the substrate, using NH4OH and H2O2, with recovery of the gallium from the etching solutions are described. The cells are bound to cover glass before substrate removal. In the etch-stop

technique a GaAlAs layer, grown between the substrate and the P-N junction, stops the chemical etching as the substrate is removed. Prototype 10 micron thick cells were produced with conversion efficiency of 14% and a power-to-mass ratio > 400 W/kg. A method based on accurate spray-etching of the substrate avoids the growth of the GaAlAs etch-stop layer. Cells 2 x 2 cm, 60 microns thick, with an efficiency of 16% were fabricated. Author (ESA)

N85-22580*# National Aeronautics and Space Administration. Lewis Research Center, Cleveland, Ohio.
GaAs AND 3-5 COMPOUND SOLAR CELLS STATUS AND PROSPECTS FOR USE IN SPACE
Dennis J. Flood and David J. Brinker *In* ESA Photovoltaic Generators in Space Nov. 1984 p 89-94 refs (For primary document see N85-22565 13-20)
Avail: NTIS HC A20/MF A01 CSCL 21H

The status and prospects of GaAs and 3-5 compound thin film and heterojunction solar cells for space missions are reviewed. Cell types considered include n+/p shallow homojunction thin film GaAs cells, 100x concentration ratio p/n and n/p GaAs small area concentrator cells; mechanically-stacked, two-junction tandem cells; and three-junction monolithic cascade cells. Author (ESA)

N85-22581# Centre National de la Recherche Scientifique, Toulouse (France). Lab. d'Automatique et d'Analyse des Systemes.
GaAlAs-GaAs SOLAR CELL DEVELOPMENT: PROSPECTIVE FOR SPACE APPLICATIONS UNDER CONCENTRATION
F. Therez, A. Chikouche, R. Alcubilla, D. Bielle-Daspet, M. Roux (ONERA, Toulouse), and R. Reulet (ONERA, Toulouse) *In* ESA Photovoltaic Generators in Space Nov. 1984 p 95-99 refs (For primary document see N85-22565 13-20)
(Contract CNRS-3870.01)
Avail: NTIS HC A20/MF A01

GaAlAs-GaAs solar cells were fabricated by liquid phase epitaxy in a process using supercooled melts. Epitaxial layers with smooth surfaces are produced. Layer uniformity improvements give reproducible results in the fabrication of GaAs devices. The cells utilize thin GaAlAs window layers. In order to better understand the electrical characteristics of the cells, the 2 kT direct current in GaAs diodes was analyzed, studying its dependence on surface area and perimeter value. The photovoltaic samples efficiency is 20.2% for low concentrated incident power density of 0.4 W/sq cm. Radiation damage on GaAs was studied. Author (ESA)

N85-22582# Societe Europeenne de Propulsion, Vernon (France).
DEVELOPMENT AND TESTING OF A SPACECRAFT SURFACE POTENTIAL MONITOR
D. Valentian, C. Roulle, L. Levy (ONERA, Toulouse), D. Sarrail (ONERA, Toulouse), and J. C. Larue (ESTEC, Noordwijk, Netherlands) *In* ESA Photovoltaic Generators in Space Nov. 1984 p 103-107 ref (For primary document see N85-22565 13-20)
Avail: NTIS HC A20/MF A01

A surface potential monitor was developed to measure the superficial electrostatic charging in solar cell covers and OSRs. The equipment correlates abrupt surface potential charges resulting from electrostatic discharges occuring during geomagnetic substorm events and spacecraft disturbances, and can also be used to drive an active spacecraft charging control system. The monitor must measure electrostatic fields up to 50 kW/mn and detect fields 100 times smaller. Temperature range is from minus 150 to + 80 C. It must sustain ionizing radiation and ultrahigh vacuum for 7 yr. Sensing area dimension is 20 x 20 mm. Height is 20 mm. Author (ESA)

N85-22583# Office National d'Etudes et de Recherches Aerospatiales, Toulouse (France). Dept. d'Etudes et de Recherches en Technologie.
PHENOMENOLOGY OF DISCHARGES IN SPACE: APPLICATION TO A SOLAR GENERATOR [PHENOMENOLOGIE DES DECHARGES DANS L'ESPACE: APPLICATION AU GENERATEUR SOLAIRE]
L. Levy and D. Sarrail *In* ESA Photovoltaic Generators in Space Nov. 1984 p 109-114 refs In FRENCH (For primary document see N85-22565 13-20)
Avail: NTIS HC A20/MF A01

A criterion of electric discharge between metal interconnections and protective filters was tested on a solar array model. The criterion states that there is a risk of discharge when the space environment induces a potential difference of 500 V between connection and filter, the connection being positive in relation to the filter. Tests show that the dielectric rigidity of the connector/filter coupling depends on the polarity of the potential difference. In the SPOT (French satellite) array discharges occur from 1000 V upwards. Author (ESA)

N85-22584# Giessen Univ. (West Germany). Inst. of Physics.
ELECTROSTATIC DISCHARGE TESTING ON A CARBON FIBER SOLAR PANEL STRUCTURE
N. K. Nikoiaizig, K. H. Groh, and H. W. Loeb *In* ESA Photovoltaic Generators in Space Nov. 1984 p 115-122 refs (For primary document see N85-22565 13-20)
(Contract ESTEC-5413/83/NL-PB)
Avail: NTIS HC A20/MF A01

Electrostatic charging of the ECS solar array structure was studied in a substorm test facility. Though the structure exhibits overall conductivity, irradiation tests show that the surface charges locally up to -1.4 kV. The surface potentials are not hazardous. Arc discharges are not observed. Conductivity of the material is reduced with decreasing sample temperature, resulting in a marked increase of the surface potential. Tests with a floating sample show that the solar array structure including Alcore charges up to high negative potentials corresponding to the energy of the impinging electron beam. Author (ESA)

N85-22585# Centre National de la Recherche Scientifique, Toulouse (France). Lab. d'Automatique et d'Analyse des Systemes.
TECHNOLOGICAL PROCESS EFFECT ON THE CARRIER LIFETIME DEGRADATION OF SILICON SOLAR CELL BASE LAYER IRRADIATED BY 1 MeV ELECTRONS (BORON DOPING CASE)
D. Bielle-Daspet, M. Lagouin, F. Therez, S. Rebiai, and A. Chikouche *In* ESA Photovoltaic Generators in Space Nov. 1984 p 123-130 refs (For primary document see N85-22565 13-20)
Avail: NTIS HC A20/MF A01

Value, degradation and thermal annealing recovery of carrier lifetime are compared in layer pieces, successively cut in the processed wafer, as well as in processed solar cell structures for floating zone and Czochralski grown silicon with 1 and 10 ohm/cm resistivity. Large changes in the lifetime and lifetime degradation values with technological process and process step were measured with the samples from the Czochralski material series. From comparison with DLTS results, [B1-O1] defects induced by the oxidation step of the solar cell process and further contribution of these defects to the formation of hole H2 traps, i.e., [V-O-B] defects, in the irradiated samples play a part in the changes measured. Author (ESA)

N85-22586# National Aeronautics and Space Administration. Lewis Research Center, Cleveland, Ohio.
THE EFFECTS OF LITHIUM COUNTERDOPING ON RADIATION DAMAGE AND ANNEALING IN N(+)P SILICON SOLAR CELLS
I. Weinberg, H. W. Brandhorst, Jr., S. Mehta, and C. K. Swartz *In* ESA Photovoltaic Generators in Space Nov. 1984 p 131-136 refs (For primary document see N85-22565 13-20)
Avail: NTIS HC A20/MF A01 CSCL 21H

Boron-doped silicon solar cells were counterdoped with lithium and the resultant n+p cells irradiated by 1 MeV electrons. Lithium counterdoped cells exhibit significantly increased radiation resistance with considerable annealing occurring at 100 C; DLTS studies indicate that the annealing behavior is controlled by a single defect at Ev + 0.43 eV. It is concluded that the increased radiation resistance of the counterdoped cells is due primarily to the interaction of lithium with oxygen, single vacancies and divacancies. It is speculated that the lithium-oxygen interaction is the most

effective in contributing to the increased radiation resistance.
Author (ESA)

N85-22587# Office National d'Etudes et de Recherches Aerospatiales, Toulouse (France). Centre d'Etudes et Recherches Techniques.
INVESTIGATION OF THE DEGRADATION OF GaAs PHOTOVOLTAIC CELLS BY PROTON AND ELECTRON IRRADIATION [ETUDE DE LA DEGRADATION DES PHOTOPILES AsGa SOUS IRRADIATIONS PAR PROTONS ET ELECTRONS].
J. Bernard, J. Bourrieau, R. Reulet, M. Roux, A. Suzuki (Sharp Corp., Shinjo-cho, Japan), and K. Sugawara (Sharp Corp., Shinjo-cho, Japan) *In* ESA Photovoltaic Generators in Space Nov. 1984 p 137-142 refs In FRENCH (For primary document see N85-22565 13-20)
Avail: NTIS HC A20/MF A01

Variations in short circuit and open circuit current, and in maximum power of GaAlAs and GaAs photovoltaic cells as a function of electron and proton irradiation energy were studied. Proton energies were 0.25, 0.4, 0.7, 1.5, and 10 MeV. Electron energies were 1 and 2 MeV. A numerical model of proton degradation which includes space environment constraints was developed and applied to proton flux received by a geostationary satellite. Results confirm the advantages of GaAs solar cells for space missions. Author (ESA)

N85-22588# Ceskoslovenska Akademie Ved, Prague. Inst. of Physics.
IN-ORBIT LASER REGENERATION OF THE RADIATION DAMAGED SOLAR ARRAYS
V. Poulek *In* ESA Photovoltaic Generators in Space Nov. 1984 p 143-148 refs (For primary document see N85-22565 13-20)
Avail: NTIS HC A20/MF A01

Experiments with scanning laser beam annealing of complete satellite solar panels were studied as a means of regenerating the solar cells of geostationary communication satellites. A spaceborne system is proposed. Ground simulations indicate no laser damage of individual cells or the panel; 25% power increase; 0.1% mass increase; and 0.5% cost increase. No changes in satellite construction or launcher are needed. Author (ESA)

N85-22589# AEG-Telefunken, Wedel (West Germany).
GIOTTO SOLAR ARRAY: DESIGN, MANUFACTURE AND TEST
K. Dettlaff, J. Koch, and B. Wodke *In* ESA Photovoltaic Generators in Space Nov. 1984 p 151-155 refs (For primary document see N85-22565 13-20)
Avail: NTIS HC A20/MF A01

The manufacturing and testing of Giotto satellite solar array panels and samples are described. On nearing Halley's comet the satellite passes into a high particle density area and may be destroyed, so to ensure data transmission for as long as possible the solar arrays charge internal batteries and act as a shield. Panel design was derived from tests on small samples to decide bonding and manufacturing sequences; large-sample tests with solar cells and interconnections; an engineering panel integrated into the spacecraft model; and a qualification panel which is also a spare flight panel. Author (ESA)

N85-22590# Messerschmitt-Boelkow-Blohm G.m.b.H., Ottobrunn (West Germany).
THE DFS-KOPERNIKUS SOLAR GENERATOR ELECTRICAL DESIGN
Ludwig Preuss *In* ESA Photovoltaic Generators in Space Nov. 1984 p 157-162 ref (For primary document see N85-22565 13-20)
Avail: NTIS HC A20/MF A01

The electrical layout of the DFS satellite solar generator; the techniques applied for technical verification; and experience using an existing solar generator with modifications (INTELSAT 5) are described. The DFS is three-axis stabilized, in geosynchronous orbit. Power is supplied by two identical solar generator wings. The power required at end of life equinox (after 10.3 yr in worst case conditions) is 1150W. Each wing consists of three rigid panels and a yoke which serves as a connection link to the satellite bearing and power transfer assembly. The solar cell arrays on the panels are identical, except that the array on the center panel of each wing is turned around by 180 deg to fit with the unsymmetric hold down points and to balance the magnetic moment of the wing. Reutilization of the INTELSAT concept required a complete redesign of electrical cabling. Author (ESA)

N85-22591# Deutsche Forschungs- und Versuchsanstalt fuer Luft- und Raumfahrt, Bonn (West Germany).
THE DFS-KOPERNIKUS SOLAR GENERATOR
Friedrich Diessner *In* ESA Photovoltaic Generators in Space Nov. 1984 p 163-167 refs (For primary document see N85-22565 13-20)
Avail: NTIS HC A20/MF A01

A short market survey is given on solar generators for communication satellites. This is done with respect to power, specific technology, mass and generator shape versus spacecraft mass, the historical evolution also being taken into consideration. The characteristics of the satellite will be described in general, and the solar generator in detail. The technology of the solar array is explained as well as the required modifications. An economic solution was found by the utilization of the already existing solar generator of INTELSAT 5. The design chosen will meet the user's requirements concerning power and low mass.
B.G.

N85-22592# Messerschmitt-Boelkow-Blohm G.m.b.H., Ottobrunn (West Germany).
ELECTRICAL DESIGN OF THE INTELSAT 6 SOLAR GENERATOR
Guenther LaRoche *In* ESA Photovoltaic Generators in Space Nov. 1984 p 169-176 refs (For primary document see N85-22565 13-20)
Avail: NTIS HC A20/MF A01

The INTELSAT 6 > 10 kW installed power solar array is described. A dual cylindrical solar panel concept is utilized. During launch, the outer cylindrical panel is placed over the inner solar panel and main body of the satellite. Once in orbit, the outer panel telescopes downward to expose the upper panel. Together the 2 panels generate a minimum of 2.1 kW electric power during a 10 yr mission in geostationary orbit. The design verification tests are summarized. Author (ESA)

N85-22593# Royal Netherlands Aircraft Factories Fokker, Schiphol-Oost. Space Div.
COMPUTER AIDED ENGINEERING APPLIED TO THE DESIGN AND VERIFICATION OF THE GENERIC ADVANCED RIGID ARRAY (ARA)
C. K. Wafelbakker *In* ESA Photovoltaic Generators in Space Nov. 1984 p 177-185 (For primary document see N85-22565 13-20)
Avail: NTIS HC A20/MF A01

Mechanical, thermal, electrical and geometrical programs for solar array design were created. Programs to calculate modes and frequency responses of panels and stowed wings with the panels modeled as beams; programs to deal with the lowest modes of the deployed wing; and programs to calculate solar cell operating temperature for open weave face skin panels were developed. The chain of analyses, from conceptual phase to solar array verification is automated. Author (ESA)

N85-22594# AEG-Telefunken, Wedel (West Germany).
DEVELOPMENT AND QUALIFICATION OF THE ELECTRICAL PART OF THE ADVANCED RIGID ARRAY (ARA)
D. Poeck and B. Goergens *In* ESA Photovoltaic Generators in Space Nov. 1984 p 187-190 (For primary document see N85-22565 13-20)
Avail: NTIS HC A20/MF A01

The impact of different solar cells on the power to mass ratio of the solar array was investigated. A 50 micron back surface field reflector (BSFR) cell with a 50 micron CMX coverglass has the highest possible power to mass ratio at end of life (EOL),

10 yr geostationary orbit. A 180 micron BSFR cell gives a higher EOL-power to mass ratio than all BSR cells, assuming array structure of 70 mg/sq cm or thicker ones. The hold down point sensitivity analysis shows that cell loss near hold down points can be minimized by using different cell dimensions. Due to the multielement laser scribing technique, every required special cell dimension can easily be manufactured. Two Advanced Rigid Array design verification test samples were manufactured. Both samples successfully sustained 2000 deep thermal cycles between +80 and minus 180 C. Author (ESA)

N85-22595# Societe Nationale Industrielle Aerospatiale, Cannes (France).
SPOT SOLAR ARRAY
Rodolphe Krawczyk and Lionel Decramer (CNES, Toulouse) *In* ESA Photovoltaic Generators in Space Nov. 1984 p 191-199 (For primary document see N85-22565 13-20)
Avail: NTIS HC A20/MF A01

The SPOT (French satellite) double deployment direction flexible foldout solar array is described. Its power can be adapted between 1 and 1.8 kW after 2 yr in low orbit. Mass = 154 kg. The spring loaded deployment system is illustrated. The pantographs, stowage box, and solar skins are shown. Possible performance improvements are indicated. Author (ESA)

N85-22596# Societe Nationale Industrielle Aerospatiale, Cannes (France).
RIGID SOLAR GENERATOR (GSR) SOLAR ARRAYS
G. A. Martin, R. Laget, G. Urbain, and J. L. Bastard *In* ESA Photovoltaic Generators in Space Nov. 1984 p 203-209 refs (For primary document see N85-22565 13-20)
Avail: NTIS HC A20/MF A01

The Telecom, TV-SAT, and Arabsat Solar arrays are described. The Telecom minimal power requirement of 110 W during the spinned transfer phase (solar array stowed on the spacecraft walls) and 1054 W summer solstice on orbit (3 axis stabilized), led to a 3 panels per wing solar array; panel dimensions: 1295.4 x 2047 mm. The TV-SAT and Arabsat arrays differ from Telecom by their partial deployment in transfer orbit. The arrays contain 14,256 solar cells for primary power and 1560 cells for battery charging. Cells are 180 micron thick back surface reflectors. Author (ESA)

N85-22597# Societe Nationale Industrielle Aerospatiale, Cannes (France). Div. Systemes Balistique et Spatiaux.
RETRACTABLE RIGID SOLAR GENERATOR (GSR)
Ph. Bobo *In* ESA Photovoltaic Generators in Space Nov. 1984 p 211-215 refs (For primary document see N85-22565 13-20)
Avail: NTIS HC A20/MF A01

A retractable rigid 6 kW solar array is described. The deployment-retraction system uses a pantograph, with retraction ensured by an electric motor pulling a cable fixed to the outermost panel. Panel structure is similar to TV-SAT, but with wrapped rather than woven carbon fibers. Extension to 10 kW appears feasible. Author (ESA)

N85-22598# European Space Agency. European Space Research and Technology Center, ESTEC, Noordwijk (Netherlands). Olympus Program Office.
DERIVATION OF THE OLYMPUS SOLAR ARRAY REQUIREMENTS
R. Steels and A. Dickinson *In* ESA Photovoltaic Generators in Space Nov. 1984 p 217-220 (For primary document see N85-22565 13-20)
Avail: NTIS HC A20/MF A01

Following a market survey, the potential for a large multipurpose platform to support satellite communications services was established. The process by which anticipated service requirements were translated into payload accommodation requirements and, through a series of system level tradeoffs, into requirements related to the solar array is described. Design requirements arising from transfer orbit stabilization options are outlined. Configurational tradeoffs, shuttle launch constraints, and system level requirements are reviewed. Author (ESA)

N85-22599# Spar Aerospace Ltd., Toronto (Ontario).
THE OLYMPUS SOLAR ARRAY DEVELOPMENT AND TEST PROGRAM
G. W. Marks, C. Anders, S. Draisey, and M. Elezki *In* ESA Photovoltaic Generators in Space Nov. 1984 p 221-235 (For primary document see N85-22565 13-20)
Avail: NTIS HC A20/MF A01

The test program for the Olympus satellite solar array was derived from a coordinated verification plan structured to verify all design variants of the array through the specified power generating range. Test and analysis programs are complementary such that where possible tests are carried out which verify worst cases for the generic design; otherwise, the test program provides inputs to analyses which extrapolate to the complete range. Electrical power output; release and deployment mechanisms; and stowed and deployment structural performance are tested. Author (ESA)

N85-22600# AEG-Telefunken, Wedel (West Germany).
DESIGN AND QUALIFICATION TESTING OF THE OLYMPUS SOLAR ARRAY BLANKET
L. Gerlach and G. Kuechler *In* ESA Photovoltaic Generators in Space Nov. 1984 p 237-241 refs (For primary document see N85-22565 13-20)
Avail: NTIS HC A20/MF A01

The design of the Olympus solar array blanket, based on the shadow protection shunt diode concept and the necessary protection against charging of the blanket during the satellite's geosynchronous mission is described. The electrical rearside connection; the locating cup design; test results from the development program; data from flight production; and optimization with respect to thermo-optical data of the anticharging layer and the solar cell shunt concept are summarized. Author (ESA)

N85-22601# British Aerospace Dynamics Group, Stevenage (England). Space and Communications Div.
THE PERFORMANCE OF THE OLYMPUS POWER SUBSYSTEM WITH ITS SOLAR ARRAY
R. B. A. Harris *In* ESA Photovoltaic Generators in Space Nov. 1984 p 243-246 refs (For primary document see N85-22565 13-20)
Avail: NTIS HC A20/MF A01

Performance predictions and power subsystem results of the Olympus satellite with its solar array are summarized. The power subsystem embodies the method of sequential shunt regulation of solar array power developed for the ECS/MARECS satellites to produce a single regulated 50 V power bus. The solar array, which may be matched to a spacecraft power requirement by the addition of solar array panels, is used by the power subsystem to give a satellite capability expandable from 2.8 to 7.8 kW. Despite switching delays due to shunt switching, the system meets specifications. Author (ESA)

N85-22602# European Space Agency. European Space Research and Technology Center, ESTEC, Noordwijk (Netherlands).
SURVIVAL TESTING OF SILICON SOLAR MODULES
J. C. Larue *In* ESA Photovoltaic Generators in Space Nov. 1984 p 249-256 refs (For primary document see N85-22565 13-20)
Avail: NTIS HC A20/MF A01

The survival testing and inspection of > 100 solar modules are discussed. Accelerated thermal cycling, thermal vacuum electrical continuity, dissection, flexing, and visual, infrared and X-ray inspection are described. The most critical survival parameter is extended thermal cycling. The most critical module component is the solar cell series interconnector; the silver coated molybdenum interconnector survives > 60,000 low Earth orbit or 1000 geostationary orbit eclipses (10 yr operational life). Further work is needed to reach this level of confidence with silver or aluminum interconnectors. Author (ESA)

N85-22603# Centre National d'Etudes Spatiales, Toulouse (France).
CALIBRATION OF SOLAR CELLS OUTSIDE THE ATMOSPHERE [CALIBRATION DE CELLULES SOLAIRES HORS ATMOSPHERE] c20
M. Roussel and A. Laporte *In* ESA Photovoltaic Generators in Space Nov. 1984 p 257-263 In FRENCH (For primary document see N85-22565 13-92)
Avail: NTIS HC A20/MF A01

A stratospheric balloon-based system for calibrating solar cells to be used as standards in laboratory tests is described. The system spends 8 hr in the stratosphere at an altitude where the solar spectrum is close to the air mass 0 value. Spectral response curves and a curve giving calibration value variation as a function of temperature are obtained. Accuracy is + or - 0.6%, with very good repeatability, especially for nonirradiated samples.
Author (ESA)

N85-22604# Centre National d'Etudes Spatiales, Toulouse (France).
INVERSE BEHAVIOR OF SILICON PHOTOVOLTAIC CELLS [COMPORTEMENT EN INVERSE DES CELLULES PHOTOVOLTAIQUES AU SILICIUM]
E. duTrieu, M. Roussel, A. Michel, J. Bernard (ONERA, Toulouse), and H. Benarfa (ONERA, Toulouse) *In* ESA Photovoltaic Generators in Space Nov. 1984 p 265-271 In FRENCH (For primary document see N85-22565 13-20)
Avail: NTIS HC A20/MF A01

A measuring device and a model for studying the effects on solar arrays of inverse voltage in constituent cells were developed. Tests on 1 and 10 ohm/cm cells are described. A large scatter of results is reported, but I(V) curves for 1 ohm/cm always evolve more rapidly than for 10 ohm/cm. Illuminated and shadowed cell behavior is markedly different. Although thermal dissipation and current leakage perturb measurements, it is possible to derive an expression for cell behavior. Author (ESA)

N85-22605# Physikalisch-Technische Bundesanstalt, Brunswick (West Germany).
NONLINEARITY AND SPECTRAL MISMATCH PROBLEMS OF SOLAR CELLS
J. Metzdorf and H. Kaase *In* ESA Photovoltaic Generators in Space Nov. 1984 p 273-277 refs (For primary document see N85-22565 13-20)
Avail: NTIS HC A20/MF A01

The influence of spectral mismatch and nonlinear photocurrent-irradiance characteristic on the indoor calibration of solar cells is discussed. While the direct method using a solar simulator with a matched reference cell is best suited to calibrate a large number of cells of similar spectral response, an indirect spectroradiometric procedure is recommended for the accurate calibration of reference cells. For range of application and time and effort involved, the differential spectral responsivity method is superior to a direct calibration of comparable high accuracy, since the latter requires the correction of the spectral mismatch. The need for and the utility of standardized AMn spectra is emphasized. Author (ESA)

N85-22606# Royal Aircraft Establishment, Farnborough (England).
ANALYSIS OF OPTIMUM FRONT COVER THICKNESS FOR LIGHTWEIGHT SOLAR ARRAYS
M. A. H. Davies, M. W. Walkden, and P. A. White *In* ESA Photovoltaic Generators in Space Nov. 1984 p 279-288 refs Sponsored by Intelsat (For primary document see N85-22565 13-20)
Avail: NTIS HC A20/MF A01

Solar cell coverslide thickness required to give the highest power to weight ratio for a solar array 10 yr geosynchronous mission was analyzed. It is found that the optimum thickness is less than is commercially available, and is 18 microns excluding adhesive. An experiment to corroborate the analysis was conducted, using the thinnest coverslides available, 50 and 80 microns. Covered cells were irradiated at the front and rear by 3 electron and 5 proton energies, the omnidirectional fluences of which represented a 10 yr geosynchronous environment. Agreement between theory and experiment is good. Author (ESA)

N85-22607# Centre National d'Etudes Spatiales, Toulouse (France).
PROBLEMS WITH ELECTRICAL INTERFERENCE BETWEEN SOLAR GENERATORS AND SHUNT TYPE REGULATORS [LES PROBLEMES D'INTERFACES ELECTRIQUES ENTRE LES GENERATEURS SOLAIRES ET LES REGULATEURS DE TYPE SHUNT]
R. Prido, C. Rouzies, and P. Tastet *In* ESA Photovoltaic Generators in Space Nov. 1984 p 291-297 In FRENCH (For primary document see N85-22565 13-20)
Avail: NTIS HC A20/MF A01

Shunt and series type voltage regulators for solar arrays were tested in solar simulators. Around 50V, series regulators greatly reduce the risk of hot-spot formation in the solar generators, but entail higher operating voltages (150V) in switches and higher amplitude current variations in electrical sections. Voltages in switches on leaving eclipse become very high, but use of diodes in parallel in the array avoids harmful effects. Author (ESA)

N85-22608# Institute of Space and Astronautical Science, Tokyo (Japan).
DEVELOPMENT OF HALLEY'S COMET EXPLORER PLANET-A SOLAR ARRAY
A. Ushirokawa, K. Takahashi, M. Kohbata, M. Kudoh (NEC Corp., Yokohama, Japan), and H. Arai (NEC Corp., Yokohama, Japan) *In* ESA Photovoltaic Generators in Space Nov. 1984 p 299-304 refs (For primary document see N85-22565 13-20)
Avail: NTIS HC A20/MF A01

A high efficiency body mount type solar array using lightweight materials and back surface reflector cells was developed for the Planet-A satellite Halley's comet mission. Output power to weight ratio is improved by 30% compared to that of existing body mount type scientific satellite solar arrays. The array is based on a one-piece cylindrical panel. The total array weighs 12.8 kg.
Author (ESA)

N85-22609# AEG-Telefunken, Wedel (West Germany).
CONCENTRATOR TECHNOLOGIES EVALUATION FOR LARGE SOLAR ARRAYS AND THEIR APPLICATION FOR SPACE STATIONS/PLATFORMS
W. Westphal and J. Rath *In* ESA Photovoltaic Generators in Space Nov. 1984 p 305-311 refs (For primary document see N85-22565 13-20)
Avail: NTIS HC A20/MF A01

Solar concentrator technologies were compared for use in a manned space station. A SOLA type array is recommended for development. Comparisons show that low concentration (LC) and Cassegrain devices are extremely sensitive contaminative environments. Cassegrain systems have complex structures with low manufacturing tolerances (especially as micro-versions). The LC-tetrahedral frustrum pointing accuracy required is 7 deg (at 90% output). Cassegrain pointing accuracy required is < 0.4 deg (at 90% output) which makes necessary extreme control systems (at required array size). Gallium arsenide cells do not show predicted or lab item properties and effectiveness as production line items. Author (ESA)

N85-22610*# National Aeronautics and Space Administration, Washington, D. C.
SPACE STATION SOLAR ARRAY
A. F. Forestieri *In* ESA Photovoltaic Generators in Space Nov. 1984 p 313-319 refs (For primary document see N85-22565 13-20)
Avail: NTIS HC A20/MF A01 CSCL 21H

Space station solar array configurations and power system technologies were compared. Planar silicon arrays offer low technology risk but high weight and drag area. Concentrator arrays of silicon or gallium arsenide (preferred) promise lower cost and drag area but increase technology risk. Planar and power tower require fewer control moment gyros (CMG's). Delta is more rigid

but requires more CMG's. Flexible body effects are not significant. All configurations can be assembled. Power tower is preferred for proximity operations. All configurations require 6 to 8 launches. Manned operations after two to three. All configurations can accommodate all candidate electrical power systems options.
Author (ESA)

N85-22611# Telespazio, S.p.A., Rome (Italy).
SOLAR ARRAY DYNAMICAL SIMULATION FOR ILLUMINATION AND TEMPERATURE VARIATION
M. Reticcioli and G. Mocci *In* ESA Photovoltaic Generators in Space Nov. 1984 p 321-331 refs (For primary document see N85-22565 13-20)
Avail: NTIS HC A20/MF A01

A lumped parameter electrical model of spacecraft solar arrays was developed. It takes dynamically into account array temperature and illumination variations, to simulate electrical performances during spacecraft sunlight transient events (eclipse emergence, panel reorientation). Computer simulations of solar array output characteristics in different spacecraft environmental conditions are presented.
Author (ESA)

N85-22612# AEG-Telefunken, Wedel (West Germany).
BLANKET INTEGRATED CUSHIONING OF FOLDABLE AND RETRACTABLE SOLAR ARRAYS
J. Koch *In* ESA Photovoltaic Generators in Space Nov. 1984 p 335-343 refs (For primary document see N85-22565 13-20)
Avail: NTIS HC A20/MF A01

Design and development of solar blanket integrating cushioning (BIC) options, and selection of concepts are described. Tests with components and modules to increase knowledge of material properties are summarized. Dynamic tests with a representative sample, consisting of several folds in stowed configuration and subjected to sinusoidal vibration under variation of boundary conditions, such as preload of the stack are outlined. For shuttle launch, a partial contact system is best, although a full contact (no BIC) design with throw away foil cushioning is feasible.
Author (ESA)

N85-22613# AEG-Telefunken, Wedel (West Germany).
CONCEPT FOR CONTROLLED FOLD BY FOLD DEPLOYMENT AND RETRACTION OF FLEXIBLE, FOLDABLE SOLAR GENERATORS
G. Behrens *In* ESA Photovoltaic Generators in Space Nov. 1984 p 345-348 (For primary document see N85-22565 13-20)
Avail: NTIS HC A20/MF A01

Control mechanisms for deploying and retracting spacecraft solar blankets were designed. A cog wheel mechanism which enables the blanket to be tensioned with its preload at an arbitrary position is incorporated to avoid out-of-plane oscillations during refolding or partial deployment.
Author (ESA)

N85-22614# AEG-Telefunken, Wedel (West Germany).
ASPECTS OF LOW COST MODULE TECHNOLOGY
H. Bebermeier *In* ESA Photovoltaic Generators in Space Nov. 1984 p 349-352 (For primary document see N85-22565 13-20)
Avail: NTIS HC A20/MF A01

Low cost and high performance technologies for a 30 kW low Earth orbit (LEO) solar array were analyzed to identify cost relations at module level. A test program was performed to identify lifetime and performance limitations for low cost and terrestrial components. Thick back surface field (BSF) cells are recommended for LEO applications, thin BSF or back surface reflector cells for geostationary applications. Ultrasonic welds of aluminum materials survived $>$ 10,000 LEO cycles with extrapolation to 50,000 feasible. For large, flexible arrays, a low cost technology (1 ohm/cm, 400 micron cell) and a high performance (bifacial cell module) are preferred.
Author (ESA)

N85-22615# European Space Agency, Paris (France).
EMISSIVITY ENHANCEMENT OF FUSED SILICA FOR SPACE APPLICATIONS
J. Rancourt, W. T. Beauchamp, J. Sanchez, and I. Sachs *In* ESA Photovoltaic Generators in Space Nov. 1984 p 353-356 refs (For primary document see N85-22565 13-20)
Avail: NTIS HC A20/MF A01

The emissivity of a fused silica solar cell cover at 300K was improved by suppressing the reststrahlen reflectance band in the 9 to 10 micrometer range. A thin film spacer layer transparent in the visible and the far infrared is coupled with a fused silica one to produce a 10 micrometer dark mirror for a fused silica substrate. In the visible spectrum the indices of the layers are matched with thin antireflection layers so that the average visible transmission can be made to exceed that of the bare substrate. The result is a cover which operates at a lower temperature than an uncoated one.
Author (ESA)

N85-22616# European Space Agency. European Space Research and Technology Center, ESTEC, Noordwijk (Netherlands).
DEPLOYMENT ANALYSIS OF THE OLYMPUS ASTROMAST ANT COMPARISON WITH TEST MEASUREMENTS
M. Eiden, O. Brunner, and C. Starvrinidis *In* ESA Photovoltaic Generators in Space Nov. 1984 p 357-363 refs (For primary document see N85-22565 13-20)
Avail: NTIS HC A20/MF A01

An analytical procedure to predict the deformations and member loads of a coilable deployable continuous longer on space mast (Astromast) in the transfer zone from stowed to deployed configuration is presented. The change from deployed mast state into the coiled configuration is computed with the large strain/displacement nonlinear finite element program LARSTRAN. Results are verified by test measurements on a demonstration model.
Author (ESA)

N85-22617*# National Aeronautics and Space Administration, Washington, D. C.
NASA PHOTOVOLTAIC RESEARCH AND TECHNOLOGY DEVELOPMENT PROGRAM FOR SPACE APPLICATIONS
Jerome P. Mullin, Dennis J. Flood (NASA. Lewis Research Center), and Henry W. Brandhorst, Jr. (NASA. Lewis Research Center) *In* ESA Photovoltaic Generators in Space Nov. 1984 p 367-371 (For primary document see N85-22565 13-20)
Avail: NTIS HC A20/MF A01 CSCL 21H

Photovoltaic cell and solar array NASA programs are reviewed, and the impact of missions such as the Columbus orbital space station on spaceborne energy technology is discussed. Estimates of power levels for the initial station range from 50 to 125 kW. A station requiring 125 kW requires an array output $>$ 300 kW, i.e., 2.5 times the total power generating capacity launched by NASA in the past 20 yr. Technologies considered include concentrator arrays, lithium counterdoped cells, GaAs cells, and three-junction monolithically grown cascade cells.
Author (ESA)

N85-22618# Societe Nationale Industrielle Aerospatiale, Cannes (France). Div. Systemes Balistique et Spatiaux.
STUDY OF CONCENTRATION FOR SPACE PHOTOVOLTAIC GENERATORS
Ph. Bobo *In* ESA Photovoltaic Generators in Space Nov. 1984 p 373-377 refs (For primary document see N85-22565 13-20)
Avail: NTIS HC A20/MF A01

Distributed concentration solar arrays consisting of several electrically interconnected small concentrators, and global concentration with one concentrator only per solar array wing were assessed for space missions. Distributed low concentration needs no specific mechanisms, has partial deployment capability, and a simple electrical network layout. However, it has large outline dimensions and low specific power. High concentration substantially reduces area, and can operate at very low illumination, but has low specific power, requires assembly of a large number of components, and has high misalignment sensitivity. Global concentration has high specific power, and small outline dimensions when stowed, but requires specific mechanisms, is problematic in partial deployment, and light flow on the electrical network is heterogeneous.
Author (ESA)

N85-22619# Alfateh Univ., Tripoli (Libya). Centre for Solar Energy Studies.
IMPROVED MODELING OF THE OPEN CIRCUIT VOLTAGE OF SOLAR CELLS
I. R. M. Mansour *In* ESA Photovoltaic Generators in Space Nov. 1984 p 381-387 refs Sponsored by National Academy for Scientific Research for Scientific Research (For primary document see N85-22565 13-20)
Avail: NTIS HC A20/MF A01

A model for the open-circuit voltage from a p-n junction solar cell is developed. The model incorporates recombination inside the quasi-neural regions and the front and back surfaces, and the effect of recombination inside the junction space-charge region due to monoenergetic traps. The open circuit voltage from a solar cell with recombination via an intermediate-trap energy level is obtained from the analytical solution of a general cubic equation. Major simplifications result for cases where recombination is via a deep-trap energy level and via a shallow-trap energy level. It is shown that under certain conditions, the open circuit voltage degradation is strongly influenced by the density and energy distribution of traps inside the space-charge region. Author (ESA)

N85-22620# European Space Agency. European Space Research and Technology Center, ESTEC, Noordwijk (Netherlands). Actuators and Mechanisms Section.
DEVELOPMENTS IN DEPLOYABLE MASTS TO SUPPORT FLEXIBLE SOLAR ARRAYS
M. Aguirre-Martinez *In* ESA Photovoltaic Generators in Space Nov. 1984 p 391-398 (For primary document see N85-22565 13-20)
Avail: NTIS HC A20/MF A01

The ERM nut and spindle driven telescopic solar array mast with circular shaped tube sections of thin walled filament wound carbon fiber reinforced epoxy; and the CTM mast based on a biconvex tube that can be flattened and rolled around a drum are presented. The ERM has minimum weight, minimum stowage diameter, the possibility to choose as stowage length the solar array width (or a half of it for double blanket wings), high stiffness and strength, and very high accuracy. The main disadvantage is its long stowage length. The CTM is a closed section giving very good torsional properties, and very high quality mast root stiffness and strength. The load deformation curve of the CTM is linear up to the failure point, there are no stiffness degradations for mederate to high loads. It offers considerable mass savings. Author (ESA)

N85-22621# Royal Netherlands Aircraft Factories Fokker, Schiphol-Oost. Space Div.
GENERIC DESIGN AND VERIFICATION OF AN ADVANCED RIGID ARRAY (ARA)
D. Mawira *In* ESA Photovoltaic Generators in Space Nov. 1984 p 399-406 refs (For primary document see N85-22565 13-20)
Avail: NTIS HC A20/MF A01

A 2 to 4 kW rigid solar array suitable for a variety of space applications was designed. Panel size, number of panels, yoke length, and number and location of hold down points are variable. The panel structure is a full depth honeycomb aluminum core with carbon fiber faces. Design verification philosophy is outlined. Author (ESA)

N85-22622# Departement d'Etudes et de Recherches en Technologie Spatiale, Toulouse (France).
ISOTROPIC PROTON IRRADIATION OF GaAs SOLAR CELLS
J. Bernard, R. Reulet, and R. L. Crabb (ESA/ESTEC, Noordwijk, Netherlands) *In* ESA Photovoltaic Generators in Space Nov. 1984 p 407-410 refs (For primary document see N85-22565 13-20)
Avail: NTIS HC A20/MF A01

In order to obtain radiation damage characteristics needed for solar array system studies, 18 state-of-the-art GaAlAs solar cells fitted with 150 micron thick cerium stabilized overslides were isotropically irradiated with protons. The cells were evaluated before and after bombardment by 5, 6, 7 and 8 MeV protons for fluences from 6E10 to 6E12 p/sqcm. The data facilitated the generation of proton/electron damage ratios and demonstrate a clear advantage of GaAs over Si cells in terms of intrinsic efficiency and radiation resistance, one 10 MeV proton being equivalent to 100, 1 MeV electrons. Author (ESA)

N85-22623# Royal Netherlands Aircraft Factories Fokker, Schiphol-Oost.
THE OLYMPUS SOLAR ARRAY STRUCTURE AND MECHANISMS
R. Zwanenburg *In* ESA Photovoltaic Generators in Space Nov. 1984 p 411-419 refs (For primary document see N85-22565 13-20)
Avail: NTIS HC A20/MF A01

The Olympus (L-SAT) 4 kW begining-of-life, foldout blanket type solar array is described. Design in modular and power levels from 3 to 7 kW are feasible. The main structural support element is a pallet consisting of a sandwich structure with CFRP face sheets and edgemembers. Deployment is assured by an Astromast, with specially designed tiedown and release systems for primary and secondary deployment. A transfer orbit tensioning mechanism and secondary deployment actuator were designed. Author (ESA)

N85-22624# European Space Agency. European Space Research and Technology Center, ESTEC, Noordwijk (Netherlands).
ANNEALING OF RADIATION DAMAGE IN BORON AND GALLIUM DOPED SILICON SOLAR CELLS
R. L. Crabb and A. A. Dollery (RAE, Farnborough, England) *In* ESA Photovoltaic Generators in Space Nov. 1984 p 421-424 (For primary document see N85-22565 13-20)
Avail: NTIS HC A20/MF A01

Electron irradiation experiments were undertaken to compare the radiation damage characteristics of gallium doped silicon solar cells with those of conventional boron doped cells. Unidirectional and omnidirectional 1 MeV electrons irradiated the cells with a range of fluences up to 10 to the 15th power/sqcm. Uncovered and covered cells were tested, the covered samples embodying CMX coverglass material. The irradiated cells were isochronally annealed at temperatures up to 500 C. The annealing signature for Ga doped cells is superior to that of the B doped cells up to 400 C, beyond which p-n junction damage is sustained, leading to a relapse with immediate performance degradation. Although the covered cells exhibit irreversible cover damage at a certain temperature, this is not the prime mover for shaping the annealing signatures, which retain the same character as for the uncovered cells. Author (ESA)

N85-22625# European Space Agency. European Space Research and Technology Center, ESTEC, Noordwijk (Netherlands).
GROWTH CAPABILITIES OF EUROPEAN RETRACTABLE SOLAR ARRAYS
R. L. Crabb *In* ESA Photovoltaic Generators in Space Nov. 1984 p 425-432 (For primary document see N85-22565 13-20)
Avail: NTIS HC A20/MF A01

A parametric design evaluation was undertaken to examine ways of stretching existing solar array designs to meet intermediate power levels from 6 to 18 kW. The study was confined to interfaces pertinent to the STS and a retrievable carrier design reference mission. All the solar arrays studied could be stretched with varying degrees of ease to meet the 18 kW target. Mass estimates range from 298 to 600 kg, the main design driver being the in-orbit dynamic loads specified. Author (ESA)

N85-22626# Centre National de la Recherche Scientifique, Valbonne (France).
HIGH OUTPUT PHOTOVOLTAIC CONVERSION: THE QUADRISPECTRAL PROJECT [CONVERSION PHOTOVOLTAIQUE A HAUT RENDEMENT: LE PROJET QUADRISPECTRAL]
B. Beaumont, J. P. Contour, P. Gibart, J. C. Guillaume, and C. Verie *In* ESA Photovoltaic Generators in Space Nov. 1984 p 433-440 refs In FRENCH (For primary document see N85-22565 13-20)
Avail: NTIS HC A20/MF A01

Silicon and gallium arsenide photovoltaic conversion ef-

ficiencies using one-cell technology are discussed. A design using four cells assembled in two monolithic tandems, separately epitaxied on GaAs and InP, coupled by dichroic optics, is presented. In each tandem the cells are linked in series by an epitaxied tunnel junction. Analytical models of a GaAs cell give an energy conversion efficiency of 18.4% (without concentration). Extended to the three other cells, an efficiency of 38.4% at 150x concentration is predicted. Author (ESA)

N85-22627# Army Missile Command, Redstone Arsenal, Ala. Propulsion Directorate.
CHARACTERIZATION STANDARDS FOR SOLID PROPELLANT ROCKET MOTORS
W. D. Stephens Oct. 1984 105 p
(AD-A150250; AD-E950655; AMSMI/RK-85-1-TR) Avail: NTIS HC A06/MF A01 CSCL 21/8

This document sets standards for the characterization of solid propellant rocket motor propulsion systems. The characteristics are presented as a check list for ten different component parts including the overall propulsion system, analysis, the rocket motor case, nozzle, propellant, liner, insulation, igniter, ingredients, and energy management. The characterization of a propulsion system is invariably limited by available time, manpower, funding, and other resources. However, the enclosed listing attempts to identify the characteristics, properties, required tests, and information which would make up the data base for a fully characterized solid rocket propulsion system. The list recognizes that different degrees of characterization would be required at different stages in the evolution of a propulsion system. The characterizations for an initial effort (as in the research or concept phase) might be distinctly different from the characterization done late in the evolution and just prior to production. Author (GRA)

N85-22628# Rockwell International Corp., Canoga Park, Calif. Rocketdyne Div.
LOW THRUST BIPROPELLANT ENGINE/REDUNDANT SEAT VALVE ASSEMBLY Final Report, Sep. 1982 - Aug. 1984
E. A. DeGaetano Edwards AFB, Calif. AFRPL Dec. 1984 110 p
(Contract F04611-82-C-0064)
(AD-A150293; RI/RD84-196; AFRPL-TR-84-066) Avail: NTIS HC A06/MF A01 CSCL 13/11

The Air Force Rocket Propulsion Laboratory awarded a contract in 1982 to Rocketdyne to demonstrate the performance of two low-thrust bipropellant engine/redundant seat value assemblies. The program focused on the integration and demonstration test of two independently developed redundant seat bipropellant valves and two low-thrust beryllium engines. The test program conducted on the redundant seat valve/engine assemblies included laboratory checkouts, random launch vibration simulation, calibration hot-fire, and durability hot-fire. This report contains a description of the test hardware and documents the results of the completed test program. GRA

N85-22426# Joint Publications Research Service, Arlington, Va.
ROCKET BODY CHARGE NEUTRALIZATION PROCESSES IN ARAKS EXPERIMENT (DATA FROM TWO LAUNCHES) Abstract Only
G. G. Managadze and S. B. Lyakhov *In its* USSR Rept.: Space (JPRS-USP-85-001) 4 Feb. 1985 p 45-46 Transl. into ENGLISH from Kosmicheskiye Issled. (USSR), v. 22, no. 1, Jan.-Feb. 1984 p 103-109 (For primary document see N85-22403 13-12)
Avail: NTIS HC A07

N85-22824# Joint Publications Research Service, Arlington, Va.
EFFECT OF COMPLIABILITY OF HOT WALLS IN LIQUID-PROPELLANT ENGINE ON LOW FREQUENCY INSTABILITY Abstract Only
A. I. Ganichev *In its* USSR Rept.: Eng. and Equipment (JPRS-UEQ-85-003) 12 Mar. 1985 p 81 Transl. into ENGLISH from Izv. Vyssh. Ucheb. Zaved.: Aviats. Tekhn. (Kazan, USSR), no. 1, Jan. - Mar. 1984 p 23-27 (For primary document see N85-22782 13-31)
Avail: NTIS HC A06

23 CHEMISTRY AND MATERIALS (GENERAL)

Includes biochemistry and organic chemistry.

N85-22629# Joint Publications Research Service, Arlington, Va.
USSR REPORT: CHEMISTRY
17 Jan. 1985 127 p ref Transl. into ENGLISH from various Russian articles
(JPRS-UCH-85-001) Avail: NTIS HC A06

Articles and abstracts are presented which address various topics in chemical engineering. Subject areas include aerosols, analytical, chemistry, catalysts, coal gasification, combustion, organophosphorus compounds, petroleum processing, polymers, and water treatment. For individual titles, see N85-22630 through N85-22637.

N85-22630# Joint Publications Research Service, Arlington, Va.
INFLUENCE OF EXTERNAL ELECTRIC FIELD ON STRUCTURAL-MECHANICAL PROPERTIES OF POWDERED MATERIALS Abstract Only **c27**
Ye. P. Toporov, G. I. Shcherbina, I. N. Aleynikova, N. B. Uryev, and V. Ye. Chernomaz *In its* USSR Rept.: Chem. (JPRS-UCH-85-001) 17 Jan. 1985 p 1 Transl. into ENGLISH from Kolloidnyy Zh. (Moscow), v. 46, no. 5, Sep. - Oct. 1984 p 1039-1041 (For primary document see N85-22629 13-23)
Avail: NTIS HC A06

Powdered polymers (10 micron diameter) and powdered metals (100 micron diameter), with and without a covering layer of powdered polymer, were measured for shear stress with a thixotrometer before and after application of a 4000 V/cm electric field. The field significantly changed the shear stress curve for the powdered polymer and the powdered metal with polymer, but not for the powdered metal alone. When tested in a dynamic vibratory condition, the powders showed a 10% increase in volume when the field was present. The decreased system viscosity may be due to polarization of charged particles by the field. Author

N85-22631# Joint Publications Research Service, Arlington, Va.
MULTIPLE ELEMENT NEUTRON-ACTIVATION ANALYSIS OF ATMOSPHERIC AEROSOLS WITH X-RAY AND GAMMA-SPECTROMETRIC RECORDING OF RADIONUCLIDES FORMED Abstract Only **c25**
S. G. Pushkin and E. N. Gilbert *In its* USSR Rept.: Chem. (JPRS-UCH-85-001) 17 Jan. 1985 p 1-2 Transl. into ENGLISH from Izv. Sibirskogo Otdeleniya Akad. Nauk SSSR: Ser. Khim. Nauk (Novosibirsk, USSR), no. 11, Jul. 1984 p 57-63 (For primary document see N85-22629 13-23)
Avail: NTIS HC A06

Neutron activation analysis yields the greatest quantity of information concerning the elemental composition of aerosols. Coaxial Ge(Li)- and planar Ge-detectors were used to compare limits of detection and selectivity of recording of 46 elements determined by the characteristic radiation of 54 radionuclides with half-life over 0.5 days. In the energy area < 160 keV the Ge(Li) detector recorded not over 9 peaks, whereas the planar Ge detector recorded over 60 peaks, indicating much greater selectivity of recording of characteristic radiation for this detector. The Ge detector can decrease the detection limit for many elements as well by 2 to 200 times in comparison to the Ge(Li) detector. Multiple element neutron activation analysis with one-time bombardment of aerosol samples by a flux of thermal neutrons of about 6 x 10 to the 13th power neutrons per square centimeter per second for 10 hours with 4 measurements of characteristic radiation of radionuclides with half-lives over 0.5 days has significantly increased the number of simultaneously determined elements, expanded the range of concentrations studied and reduced the total analysis time of many elements. Author

N85-22632# Joint Publications Research Service, Arlington, Va.
ONE MECHANISM OF FORMATION OF ORGANIC FRACTION IN ATMOSPHERIC AEROSOL Abstract Only c45
V. G. Morachevskiy, S. G. Zvenigorodskiy, and S. P. Smyshlyayev *In its* USSR Rept.: Chem. (JPRS-UCH-85-001) 17 Jan. 1985 p 2 Transl. into ENGLISH from Zh. Prikl. Khim. (Leningrad), v. 57, no. 9, Sep. 1984 p 1978-1982 (For primary document see N85-22629 13-23)
Avail: NTIS HC A06

A mechanism is suggested for development and growth of organic aerosol particles - heterogeneous reactions with organic matter in the gas phase. Reactions in the atmospheric methane cycle are suggested as a source of such surface-active organic formations. Processes determining the diurnal course of this component at the level of the earth's surface are analyzed. It is found that at night, methane-hydroperoxide is not formed, but as the sun rises the concentration of NO increases quite suddenly, while OH and HO2 increase more smoothly. On cloudy days the daily maximum of production of CH3OOH is less pronounced. During the hours after sunrise the concentration of OH and HO2 increases, increasing the production of CH3OOH, which reaches its maximum around noon. After 1 pm the concentration of OH decreases, while that of NO remains at its previous level, decreasing the rate of formation of CH3OOH. The total quantity of CH3OOH absorbed on the surface of aerosol particles as a result of heterogeneous interactions during one day is calculated.
Author

N85-22633# Joint Publications Research Service, Arlington, Va.
CURRENT PLANS FOR DEVELOPMENT OF CHEMICAL INDUSTRY c81
V. Listov *In its* USSR Rept.: Chem. (JPRS-UCH-85-001) 17 Jan. 1985 p 13-26 ref Transl. into ENGLISH from Planovoye Khoz. (Moscow), no. 9, Sep. 1984 p 15-26 (For primary document see N85-22629 13-23)
Avail: NTIS HC A06

The current state of the Soviety chemical industry is described and the importance of the industry's development in realizing social-economic goals is examined. Strategies for increasing general productivity and research are outlined which incorporate financing, incentives programs, and plant management. Issues associated with raw material resources, energy sources, and the labor force are discussed.
M.G.

N85-22634# Joint Publications Research Service, Arlington, Va.
CRITICAL EVENTS IN INELASTIC DEFORMATION OF GLASSY POLYMERS IN ADSORPTIVE MEDIUM Abstract Only c27
A. N. Shitov, G. M. Lukovkin, A. L. Volynskiy, and N. F. Bakeyev *In its* USSR Rept.: Chem. (JPRS-UCH-85-001) 17 Jan. 1985 p 78-79 Transl. into ENGLISH from Vysokomolekul. Soyedineniya (Moscow), v. 26, no. 9, Sep. 1984 p 1842-1847 (For primary document see N85-22629 13-23)
Avail: NTIS HC A06

The critical events of inelastic deformation in the glassy polymer PETP (sic) in response to stretching in n-butanol, n-heptanol, n-decanol, or ethylene glycol were analyzed. On stretching, the regions of low density gave rise to crazing. If there is sufficient time for crazing across the cross-section of the film, stress is eliminated before the flow limit is reached, and, if not, cracking takes place. The key factors affecting the transition of the glassy polymer into a highly dispersed state on stretching are the surface activity of the solvent, its viscosity, the geometric characteristics of the polymer, and the rate of induced deformation. These processes and the consequences of stretching can be defined in terms of Lazurkin's classical equation relating the rate of deformation to the energy activation.
Author

N85-22635# Joint Publications Research Service, Arlington, Va.
EFFECTS OF TRIAZINE COMPONENTS ON PHYSICOCHEMICAL PROPERTIES OF POLYBUTADIENE: URETHANE BLOCK COPOLYMERS Abstract Only c27
N. P. Bessonova, A. R. Korigodskiy, D. F. Kutepov, and Yu. K. Godovskiy *In its* USSR Rept.: Chem. (JPRS-UCH-85-001) 17 Jan. 1985 p 79 Transl. into ENGLISH from Vysokomolekul. Soyedineniya (Moscow), v. 26, no. 9, Sep. 1984 p 1877-1881 (For primary document see N85-22629 13-23)
Avail: NTIS HC A06

Calorimetric and physico-mechanical studies were conducted on the effects of triazine and oligobutadiene diols on the characteristics of polybutadiene: urethane block copolymers. The calorimetric studies pointed to the heterogeneity of the copolymers on the basis of glassy transition of the rigid and flexible blocks. These values agreed with the T sub g of the two constituent components, i.e., triazine-containing diols and 4,4'--diphenylmethane diisocyanate which constituted the rigid block, and oligobutadiene diols which represented the flexible block. This fact indicated complete phase separation of the two components, and the fact that the ratio of the elastic to the rigid blocks determined the overall properties of the entire copolymer. Copolymers with less than 50% w/w of the rigid blocks show typical thermoelastic characteristics. The rigidity attributable to the triazine diols was apparently due to formation of additional hydrogen bonds in which the polar heterocyclic triazines participated. Replacement of the aromatic diisocyanate by the aliphatic 1,6-hexamethylene diisocyanate resulted in increased flexibility.
Author

N85-22636# Joint Publications Research Service, Arlington, Va.
MECHANISM OF STRENGTHENING PLASTICS WITH RUBBERS Abstract Only c27
V. N. Kuleznev *In its* USSR Rept.: Chem. (JPRS-UCH-85-001) 17 Jan. 1985 p 85-86 Transl. into ENGLISH from Plast. Massy (Moscow), no. 10, Oct. 1984 p 21-22 (For primary document see N85-22629 13-23)
Avail: NTIS HC A06

Concepts on the mechanism of strengthening various plastics with rubber particles are reviewed. Plastics resistant to impact contain dispersed rubber particles in a matrix of brittle plastic mass. The reinforcing action of the rubber is explained by the fact that a filler particle represents a concentrator of stress leading to microcracks filled with oriented polymer of the matrix. The deformation of a sample on impact results in an appearance of overstress at the equatorial zone of a rubber particle. The rubber filler affects the brittle matrix of a plastic material by relieving plastic (forced elastic) deformation in presence of tensions concentrated around the particle.
Author

N85-22637# Joint Publications Research Service, Arlington, Va.
STUDY OF CHARACTER OF ADHESIVE INTERACTION AND BREAKING OF POLYIMID-ALUMINUM FOIL JUNCTION DURING PROCESS OF HARDENING Abstract Only c27
V. M. Startsev, N. F. Chugunova, A. Ye. Chalykh, L. P. Kazanskiy, and A. Ye. Rubtsov *In its* USSR Rept.: Chem. (JPRS-UCH-85-001) 17 Jan. 1985 p 88-89 Transl. into ENGLISH from Kolloidnyy Zh. (Moscow), v. 46, no. 5, Sep. - Oct. 1984 p 961-966 (For primary document see N85-22629 13-23)
Avail: NTIS HC A06

A 10% solution in dimethylformamide of a polyamido acid synthesized from the dianhydride of 3,3',4,4'-benzophenyltetracarboxylic acid and diaminodiphenyl ether was used to form a 50-micron coating on 100-micron aluminum foil. Resulting films were peeled off and the adhesive strength measured. Electron spectrometry of the separated surfaced showed the amount of aluminum remaining on the foil. Cross-sections of foil before and after adhesion were also studied with a scanning electron microscope. At room temperature, the adhesive strength of 680 g/cm was due almost entirely to the physical introduction of the polymer into surface defects of the foil. Breaking the adhesive bond required stretching the polymer from these defect areas and then breaking the rivet contacts that had been formed. At 20 to 80 C, partial destruction of the polyamido acid resulted in filling even smaller defects.
Author

24 COMPOSITE MATERIALS

Includes laminates.

N85-22638# Virginia Polytechnic Inst. and State Univ., Blacksburg. Dept. of Engineering Science and Mechanics.

DIRECTIONAL DEPENDENT ENGINEERING PROPERTIES OF ALUMINUM-ARAMID-EPOXY LAMINATES Final Report

Deidre A. Hirschfeld and Carl T. Herakovich Feb. 1985 97 p refs Prepared for Aluminum Co. of America, Alcoa Center, Pa. (CCMS-85-02; VPI-E-85-03) Avail: NTIS HC A05/MF A01 CSCL 11D

A theoretical analysis is made of hybrid laminates consisting of 7075-T6 Aluminum (Al) sheet and Aramid fibers in an epoxy matrix (AR). The laminates analyzed are: [Al/AR] sub T, [Al/AR/Al/AR/Al] sub T, [Al/AR/Al-Al] sub T, [Al/AR/-AR/Al sub 1/2] sub S, [Al/AR/-AR] sub S, and [AR/Al/-AR] sub S. Predictions of the inplane elastic and thermal properties as a function of fiber orientation are made. It is shown that properties vary by as much as an order magnitude with direction and that increasing the percentage of AR in the hybrid laminate increases the range of each property. Interlaminar forces and moments, which are related to interlaminar stresses, are also predicted as a function of fiber orientation. Finally, the maximum stress failure criterion is used to predict failure for off-axis tensile loading and for combined thermo-mechanical loading of one laminate. Author

N85-22639*# Clemson Univ., S.C. Dept. of Mechanical Engineering.

LONGITUDINAL SPLITTING IN UNIDIRECTIONAL COMPOSITES, ANALYSIS AND EXPERIMENTS Final Report

James G. Goree and Jeffrey M. Wolla Washington NASA Apr. 1985 112 p refs

(Grant NsG-1297)

(NASA-CR-3881; NAS 1.26:3881) Avail: NTIS HC A06/MF A01 CSCL 11D

An experimental study is conducted to determine the fracture behavior of center notched, unidirectional graphite/epoxy laminates when subjected to tensile loading. The actual behavior is compared to the behavior predicted by a mathematical model based on classical shear-lag assumptions. The model allows for damage to occur in the form of longitudinal matrix yielding and splitting with the matrix assumed to fail in pure shear. Results indicate that the model is capable of predicting split initiation stress levels accurately, but does not describe the subsequent split growth adequately. The model predicts rapid split growth following split initiation due to shear failure, while the actual behavior involves a slow split growth region prior to the rapid growth region. It is suggested that transverse matrix normal stresses are responsible for split initiation and the early, slow split growth. The model predicts the actual initiation stress levels reliably, and also appears to be able to predict the point at which the shear failure mode begins to dominate. The shear failure mode does eventually dominate, but at a slower rate than predicted. The nonuniform structure of the graphite/epoxy laminates is thought to be responsible for decreasing the split growth rate due to shear failure. R.J.F.

N85-22640# Georgia Inst. of Tech., Atlanta. School of Aerospace Engineering.

INTERLAMINAR FRACTURE TOUGHNESS IN RESIN MATRIX COMPOSITES Annual Scientific Report, 1 Jan. 1983 - 14 Feb. 1984

Lawrence W. Rehfield, Erian A. Armanios, and Ambur D. Reddy Apr. 1984 68 p

(Grant AF-AFOSR-0056-83; AF Proj. 2307)

(AD-A150565; AFOSR-85-0061TR) Avail: NTIS HC A04/MF A01 CSCL 11/4

This annual report summarizes the objectives, accomplishments and proposed new directions of research on mode II interlaminar fracture in resin matrix composites. A mode II interlaminar fracture specimen, test and analysis method for interpreting results have been successfully developed and demonstrated for the AS4/3502 material system. Experimental data have been obtained under both net tensile and compressive loading. Of considerable importance are the findings that (1) the AS4/3502 material system shows increasing resistance to crack growth in tension, (2) interlaminar fracture under compression is a totally unstable process, and (3) tension and compression behaviors are considerably different. The findings and the conclusions that are drawn from them point to new, promising directions for the work. Two new central directions that are suggested involve failure analysis using fractography, radiography and ultrasonic inspection and the quantitative evaluation of mode I suppression technology utilizing the new testing method. Papers, reports and presentations resulting from this research are listed. GRA

N85-22641# Oxford Univ. (England). Dept. of Engineering Science.

BEHAVIOR OF FIBER-REINFORCED COMPOSITES UNDER DYNAMIC TENSION Final Report, 30 Sep. 1982 - 14 Mar. 1984

K. Saka and J. Harding 21 Aug. 1984 52 p

(Grant AF-AFOSR-0346-82; AF Proj. 2307)

(AD-A150619; AFOSR-85-0063TR) Avail: NTIS HC A04/MF A01 CSCL 11/4

This British report describes a small gas gun, capable of accelerating a projectile 1m long by 25.4mm dia. to about 50m/s, and an extended split Hopkinson pressure bar apparatus which have been designed and constructed for the tensile impact testing of fiber-reinforced composite specimens at strain rates of the order of 1000/s. Commissioning tests have shown equilibrium in the specimen to be attained at an early stage in the test and the effects of stress wave reflections in the specimen grip regions on the calculated stress-strain response to be negligibly small. A technique has been developed for the preparation of low volume fraction model hybrid specimens, unidirectionally reinforced with a single layer of fiber tows, alternately of glass and of carbon fibers. Specimens have also been prepared from commercially supplied carbon/glass and carbon/kevlar epoxy plates with different stacking sequences for the carbon and glass or carbon and kevlar reinforcing mats to allow specimens with a range of hybrid fractions. In initial impact tests on the model specimens tensile failures were obtained but with a trend for fracture close to the specimen/loading bar interface rather than in the center of the parallel gauge section. Even so, a marked increase in fracture strength with strain rate was observed. Initial tests have also been performed on the woven reinforced carbon/glass hybrid specimens and the effect of hybrid fraction on the tensile modulus, fracture strength and fracture strain under impact loading has been determined. A preliminary study of the failure processes using optical and scanning electron microscopy has been undertaken. GRA

N85-22642# California Univ., Livermore. Lawrence Livermore Lab.

DEVELOPMENT OF EPOXY MATRICES FOR FILAMENT-WOUND GRAPHITE STRUCTURES

Roger J. Morgan, Connie M. Walkup, Fung Ming Kong, and Eleno T. Mones 27 Nov. 1984 13 p refs Presented at the 30th Natl. Meeting of the Soc. for the Advancement of Mater. and Process Eng., Anaheim, Calif., 19-21 Mar. 1985

(Contract W-7405-eng-48)

(DE85-003674; UCRL-90946; CONF-850323-1) Avail: NTIS HC A02/MF A01

A program to develop epoxy matrix systems for filament-wound graphite structures is discussed. The criteria for this matrix development program requires that the epoxide and amine components are processible and non-toxic; and the corresponding matrix itself is tough, possesses a Tg $>$ 120(0)C and does not lose its mechanical-thermal properties upon exposure to service environment conditions. Data is given on processible, hindered amine cured-epoxide matrices such as menthane or 2,5 dimethyl 2,5 hexane diamine cured bis-phenol-A-diglycidyl ether (DGEBA) epoxide systems in the presence of viscosity-lowering diluents. To produce tough, processible matrices that do not deteriorate upon exposure to service environment conditions requires a knowledge of the network structure formed and how such structure

may deteriorate under molecular flow. Permanent chemical changes that occur during this flow induced degradation process were monitored by stress-Fourier transform infrared spectroscopy. The ability to eliminate the aging of tough, cross-linked composite matrices upon molecular flow is discussed. DOE

N85-22643# Oak Ridge National Lab., Tenn.
PARTICULATE TOUGHENED SILICON CARBIDE
M. A. Janney Oct. 1984 9 p refs Presented at the Automotive Technol. Development Contractors Coordination Meeting, Dearborn, Mich., 29 Oct. 1984
(Contract DE-AC05-84OR-21400)
(DE85-004797; CONF-8410103-4) Avail: NTIS HC A02/MF A01

The addition of TiC to hot-pressed SiC increased both strength and fracture toughness and also improved high-temperature strength. Good oxidation resistance was retained with samples showing only limited attack of the TiC phase. A processing study showed that the average strength and the Weibull modulus of hot-pressed SiC and SiC-TiC composites were sensitive to carbon source and milling. DOE

N85-22698# Joint Publications Research Service, Arlington, Va.
USES OF COMPOSITE MATERIALS
V. Dovidenas *In its* USSR Rept.: Mater. Sci. and Met. (JPRS-UMS-85-002) 6 Feb. 1985 p 7-10 Transl. into ENGLISH from Komsomolskaya Pravda (USSR), no. 93, 12 May 1984 p 3 (For primary document see N85-22688 13-26)
Avail: NTIS HC A05/MF A01

N85-22699# Joint Publications Research Service, Arlington, Va.
INFLUENCE OF 3% NaCl SOLUTION ON RATE OF ACCUMULATION OF DAMAGE AND RESIDUAL STRENGTH OF ALUMINUM-BORON COMPOSITE Abstract Only
V. S. Utkin and I. A. Podolnyy *In its* USSR Rept.: Mater. Sci. and Met. (JPRS-UMS-85-002) 6 Feb. 1985 p 12 Transl. into ENGLISH from Fiz.-Khim. Mekh. Materialov (USSR), v. 20, no. 4, Jul.-Aug. 1984 p 52-55 Original language document announced as 84A-48637 (For primary document see N85-22688 13-26)
Avail: NTIS HC A05/MF A01

N85-22700# Joint Publications Research Service, Arlington, Va.
DEVELOPMENT AND STUDY OF TWO-MATRIX GLASS FIBER COMPOSITE WITH INCREASED TRANSVERSE DEFORMATION Abstract Only
V. V. Vasilyev and V. A. Salov *In its* USSR Rept.: Mater. Sci. and Met. (JPRS-UMS-85-002) 6 Feb. 1985 p 12-13 Transl. into ENGLISH from Mekh. Kompozitnykh Materialov (USSR), no. 4, Jul.-Aug. 1984 p 662-666 (For primary document see N85-22688 13-26)
Avail: NTIS HC A05/MF A01

N85-22701# Joint Publications Research Service, Arlington, Va.
TESTING OF WOUND MATERIALS FOR STRENGTH WITH LOADING IN THE REINFORCEMENT PLANE Abstract Only
V. Nikolayev and V. D. Popov *In its* USSR Rept.: Mater. Sci. and Met. (JPRS-UMS-85-002) 6 Feb. 1985 p 13 Transl. into ENGLISH from Mekh. Kompozitnykh Materialov (USSR), no. 4, Jul.-Aug. 1984 p 713-718 Original language document announces as 84A-47993 (For primary document see N85-22688 13-26)
Avail: NTIS HC A05/MF A01

N85-22702# Joint Publications Research Service, Arlington, Va.
EFFECT OF PHASE STATE OF TiC-NiTi POWDER COMPOSITE MATERIALS ON NATURE OF FAILURE AND MECHANICAL PROPERTIES Abstract Only
S. N. Kulkov, T. M. Poletika, A. Y. Chukhlomlin, and V. Y. Panin *In its* USSR Rept.: Mater. Sci. and Met. (JPRS-UMS-85-002) 6 Feb. 1985 p 13-14 Transl. into ENGLISH from Poroshkovaya Metallurgiya (USSR), no. 8, Aug. 1984 p 88-92 Original language document announced as 84A-48645 (For primary document see N85-22688 13-26)
Avail: NTIS HC A05/MF A01

N85-22703# Joint Publications Research Service, Arlington, Va.
DISSIPATION OF ENERGY IN COMPOSITE MATERIAL Abstract Only
I. K. Arkhipov, S. A. Golovin, and G. D. Petrushin *In its* USSR Rept.: Mater. Sci. and Met. (JPRS-UMS-85-002) 6 Feb. 1985 p 14 Transl. into ENGLISH from Problemy Prochnosti (USSR), no. 8, Aug. 1984 p 92-94 (For primary document see N85-22688 13-26)
Avail: NTIS HC A05/MF A01

N85-22704# Joint Publications Research Service, Arlington, Va.
DIVISION BOUNDARY IN Al-B COMPOSITE MATERIAL WITH BORON IN CONTACT WITH SOLID AND LIQUID ALUMINUM Abstract Only
B. A. Afefyev, A. Rebrov, and T. B. Zhurkova *In its* USSR Rept.: Mater. Sci. and Met. (JPRS-UMS-85-002) 6 Feb. 1985 p 15 Transl. into ENGLISH from Metallovedeniye i Termicheskaya Obrabotka Metallov (USSR), no. 8, Aug. 1984 p 15-17 (For primary document see N85-22688 13-26)
Avail: NTIS HC A05/MF A01

N85-22705# Joint Publications Research Service, Arlington, Va.
ESTIMATING DEGREE OF DEVELOPMENT OF PHYSICAL-CHEMICAL INTERACTION AMONG COMPONENTS IN Al-B FIBER COMPOSITE MATERIAL Abstract Only
M. K. Shorshorov, V. A. Kolesnichenko, and I. V. Kocheshkov *In its* USSR Rept.: Mater. Sci. and Met. (JPRS-UMS-85-002) 6 Feb. 1985 p 15 Transl. into ENGLISH from Metallovedeniye i Termicheskaya Obrabotka Metallov (USSR), no. 8, Aug. 1984 p 11-15 (For primary document see N85-22688 13-26)
Avail: NTIS HC A05/MF A01

N85-22706# Joint Publications Research Service, Arlington, Va.
SEGREGATION OF SILICON IN SILUMIN-CARBON FIBER COMPOSITES Abstract Only
T. A. Chernyshova, L. I. Kobeleva, M. I. Tylkina, and A. Rebrov *In its* USSR Rept.: Mater. Sci. and Met. (JPRS-UMS-85-002) 6 Feb. 1985 p 16 Transl. into ENGLISH from Metallovedeniye i Termicheskaya Obrabotka Metallov (USSR), no. 8, Aug. 1984 p 24-26 (For primary document see N85-22688 13-26)
Avail: NTIS HC A05/MF A01

N85-22707# Joint Publications Research Service, Arlington, Va.
POSSIBILITY OF PRODUCING MONOLITHIC COMPOSITE MATERIALS BASED ON NIOBIUM CARBIDE Abstract Only
V. V. Ploshkin, I. Y. Ulyanina, and V. P. Filonenko *In its* USSR Rept.: Mater. Sci. and Met. (JPRS-UMS-85-002) 6 Feb. 1985 p 16 Transl. into ENGLISH from Metallovedeniye i Termicheskaya Obrabotka Metallov (USSR), no. 8, Aug. 1984 p 26-27 (For primary document see N85-22688 13-26)
Avail: NTIS HC A05/MF A01

N85-22716# Joint Publications Research Service, Arlington, Va.
EFFECT OF OPERATING MEDIUM ON CYCLIC DURABILITY OF AD33-W COMPOSITE Abstract Only
V. S. Utkin, S. Y. Salibekov, and V. V. Sakharov *In its* USSR Rept.: Mater. Sci. and Met. (JPRS-UMS-85-002) 6 Feb. 1985 p 42 Transl. into ENGLISH from Poroshkovaya Metallurgiya (USSR), no. 8, Aug. 1984 p 77-80 Original language document announced as 84A-48644 (For primary document see N85-22688 13-26)
Avail: NTIS HC A05/MF A01

N85-22718# Joint Publications Research Service, Arlington, Va.
DEGASSIFICATION OF SILICON NITRIDE POWDERS OF VARIOUS ORIGINS Abstract Only
R. A. Andriyevskiy and M. A. Leontyev *In its* USSR Rept.: Mater. Sci. and Met. (JPRS-UMS-85-002) 6 Feb. 1985 p 43-44 Transl. into ENGLISH from Poroshkovaya Metallurgiya (USSR), no. 8, Aug. 1984 p 9-12 (For primary document see N85-22688 13-26)
Avail: NTIS HC A05/MF A01

N85-22751# Joint Publications Research Service, Arlington, Va.
EXPERIMENTAL STUDY OF ENTHALPY OF QUASIMONOCRYS-

TAL OF GRAPHITE AND CARBON GLASS IN TEMPERATURE RANGE OF 2890-3818 DEG K Abstract Only
L. M. Buchnev, A. I. Smylsov, I. A. Dmitriyev, A. F. Kuteynikov, and V. I. Kostikov *In its* USSR Rept.: Mater. Sci. and Met. (JPRS-UMS-85-002) 6 Feb. 1985 p 70-71 Transl. into ENGLISH from Dokl. Akad. Nauk SSSR (USSR), v. 278, no. 5, Oct. 1984 p 1109-1111 Original language document announced as 85A-15558 (For primary document see N85-22688 13-26)
Avail: NTIS HC A05/MF A01

25 INORGANIC AND PHYSICAL CHEMISTRY

Includes chemical analysis, e.g., chromatography; combustion theory; electrochemistry; and photochemistry.

For related information see also *77 Thermodynamics and Statistical Physics.*

N85-22644*# National Aeronautics and Space Administration. Lewis Research Center, Cleveland, Ohio.
FORMATION OF HIGH MOLECULAR WEIGHT PRODUCTS FROM BENZENE DURING BOUNDARY LUBRICATION
Wilfredo Morales Apr. 1985 18 p refs
(NASA-TM-86966; E-2433; NAS 1.15:86966) Avail: NTIS HC A02/MF A01 CSCL 07D

High molecular weight products were detected on the wear track of an iron disk at the end of a sliding friction and wear test using benzene as a lubricant. Size exclusion chromagography in conjunction with UV analysis gave evidence that the high molecular weight products are polyphenyl ether type substances. Organic electrochemistry was used to elucidate the possible surface reaction mechanisms. Author

N85-22645*# National Aeronautics and Space Administration, Washington, D. C.
RECENT TRENDS IN PARTICLE SIZE ANALYSIS TECHNIQUES
Suk-Ho Kang Nov. 1984 36 p refs Transl. into ENGLISH from Hwahak Konghak (S. Korea), v. 20, no. 1, Feb. 1982 p 1-13 Transl. by Kanner (Leo) Associates, Redwood City, Calif. Original doc. prep. by Korean Inst. of Chem. Engr.
(NASA-TM-77735; NAS 1.15:77735) Avail: NTIS HC A03/MF A01 CSCL 07D

Recent advances and developments in the particle-sizing technologies are briefly reviewed in accordance with three operating principles including particle size and shape descriptions. Significant trends of the particle size analysing equipment recently developed show that compact electronic circuitry and rapid data processing systems were mainly adopted in the instrument design. Some newly developed techniques characterizing the particulate system were also introduced. Author

N85-22646# Shell Research Ltd., Chester (England). Continuous Combustion Fuels Div.
THE INFLUENCE OF FUEL MOLECULAR COMPOSITION UPON FLAME-TUBE TEMPERATURE AND FLAME RADIATION IN A MODEL GAS-TURBINE PRIMARY ZONE
T. T. Bowden and J. H. Pearson Feb. 1984 44 p refs
(Contract MIN-DEF-A45A/578)
(K234; BR93796) Avail: NTIS HC A03/MF A01

Fuels containing known concentrations of well-defined hydrocarbon types were burned under conditions simulating those occurring in aviation gas turbine engines. The values of flame tube temperature and flame radiation were compared to predicted values. Results indicate that aromatic content is inappropriate as an inspection property for fuels containing fused bicyclic saturated hydrocarbons; that hydrogen content is a satisfactory inspection property for fuels containing simple aromatics and fused bicyclic saturated hydrocarbons; and that only smoke point is a satisfactory inspection property for fuels containing high concentrations of tetralins and naphthalenes. A kinetic explanation for the observed results is proposed. Author (ESA)

N85-22647# Smithsonian Astrophysical Observatory, Cambridge, Mass.
EXPERIMENTAL STUDIES OF LOW TEMPERATURE SURFACE INTERACTIONS OF ATOMIC HYDROGEN USING MASER TECHNIQUE Final Report, 30 Sep. 1977 - 30 Sep. 1984
R. F. C. Vessot and E. M. Mattison Jan. 1985 22 p
(Contract N00014-77-C-0777; RR0-1103)
(AD-A150216) Avail: NTIS HC A02/MF A01 CSCL 07/4

Measurements with an oscillating hydrogen maser of wall collision frequency shift of atomic hydrogen on surfaces of frozen CF4 at temperatures between 60 K and 30 K indicate the same wall interaction energy as for FEP-Teflon surfaces, but with 3 to 4 times less wallshift. This indicates that the surfaces of Teflon have 3 to 4 times the area of those of CF4. A substantial improvement in wall coating performance is shown to be possible with the coatings. GRA

N85-22648# Arizona State Univ., Tempe. Dept. of Mechanical and Aerospace Engineering.
SIZE AND VELOCITY DISTRIBUTIONS OF PARTICLES AND DROPLETS IN SPRAY COMBUSTION SYSTEMS Final Report, 1 Mar. 1980 - 15 Aug. 1984
E. D. Hirleman 1 Nov. 1984 153 p
(Contract N00014-79-C-0363)
(AD-A150355) Avail: NTIS HC A08/MF A01 CSCL 21/2

This research was concerned with laser/optical techniques for size and velocity measurements of particles and droplets in spray combustion systems. The initial efforts were directed toward a novel method for simultaneous size and velocity measurements of individual particles. A prototype instrument was designed, constructed, calibrated, and successfully applied. Our efforts to verify the performance and accuracy of this diagnostic led to a parallel research effort on the laser diffraction droplet sizing technique. Significant contributions to the calibration and scattering inversion aspects of this technique were made. Contributions to the problem of aerosol characterizations are discussed. Among the papers included in this final report are: Integral Transform for Particle sizing by Near-forward Light Scattering; Non-intrusive Laser-based Particle Diagnostics; Particle Sizing by Optical; Nonimaging techniques; Response Characteristics of Laser Diffraction Size Analyzers--Optical sample volume extent and lens effects; Single Beam Laser Velocimetry in Turbulent Flows; Response Characteristics of the Multiple-ratio, Single-particle Counter; and Developments in Non-Doppler Laser Velocimetry. GRA

N85-22649# United Technologies Research Center, East Hartford, Conn.
LASER DIAGNOSTIC ANALYSES OF SOOTING FLAMES Final Report, 1 Oct. 1980 - 30 Sep. 1984
G. M. Dobbs, A. C. Eckbreth, and L. R. Boedeker 29 Nov. 1984 50 p Prepared in cooperation with Princeton Univ., N.J.
(Contract N00014-81-C-0046)
(AD-A150478; UTRC/R84-955388-F) Avail: NTIS HC A03/MF A01 CSCL 21/2

Temperature distribution and soot particle size distributions have been measured in axisymmetric, laminar, diffusion flames in order to provide the basis for modelling the influence of fuel structure and temperature on soot formation. This document is the final report and management summary for the joint activities of UTRC and Princeton University. Coherent anti-Stokes Raman spectroscopy (CARS) was used for non-intrusive determination of temperature. Soot particle size and number densities were determined by Mie scattering. The experimental results were then applied to current models of soot formation in an effort to determine the physical and chemical basis for fuel structure and temperature effects on soot formation in diffusion flames. In the course of this first application of CARS and Mie diagnostics to diffusion flames, a large number of questions was raised in regard to the structure

of particulate-laden diffusion flames. Measured distributions were compared with a numerical flame-sheet model. GRA

N85-22650# Ohio State Univ., Columbus. Electroscience Lab.
AN ATLAS OF NITROGEN-BROADENED WATER VAPOR SPECTRA FROM 500 TO 5000 CM(-1), VOLUME 1
R. K. Long and E. K. Damon Sep. 1984 461 p
(Contract DAAG29-81-K-0084)
(AD-A150527; ESL-713774-4-Vol-1; ARO-17603.5-GS-Vol-1) Avail: NTIS HC A20/MF A01 CSCL 07/4

An Atlas of pressure broadened H20 spectra between 500 and 5000 per cm is presented. For each frequency, four spectra are presented, from top to bottom: 10.7 Torr pure H20; 10.7 Torr H20 plus 90 Torr N2; 10.7 Torr H20 plus 290 Torr N2; and 10.7 Torr H20 plus 730 Torr N2. All spectra are at 294 k and were taken with a path length of 821 meters. Tables of approximate line frequencies are also included. Volume 1 contains spectral plots and Volume 2 contains the line listings. GRA

N85-22651# Cornell Univ., Ithaca, N.Y. Lab. of Atomic and Solid State Physics.
RELATIONSHIP BETWEEN TOPOLOGICAL AND MAGNETIC ORDER IN SMALL METAL CLUSTERS Interim Report
B. K. Rao (Inst. of Physics, Bhubaneswar, India), P. Jena, and M. Manninen 11 Feb. 1985 16 p Prepared in cooperation with Virginia Commonwealth Univ., Richmond Sponsored in part by NSF, J.F. and K. M. Jeffries Trust, the Petroleum Research Fund and the Academy of Findland
(Contract N00014-82-K-0576)
(AD-A150547; Rept-11) Avail: NTIS HC A02/MF A01 CSCL 07/4

The equilibrium geometries and ionization potentials have been calculated self-consistently for lithium clusters consisting of up to five atoms. The exchange interaction is treated exactly while the correlation effects are included perturbatively. The correlation contribution is found to have important influence on the magnetism of the cluster and its relationship with the topology. GRA

N85-22652# IBM Research Lab., San Jose, Calif.
EXAFS OF MONOLAYERS ON SILVER ELECTRODES: SSRL PROPOSAL NUMBER 717M Progress Report, Jan. 1983 - Dec. 1984
D. E. Reisner, O. R. Melroy, J. G. Gordon, II , D. A. Buttry, G. L. Borges, and L. Blum (Puerto Rico Univ., Rio Piedras) 8 Jan. 1985 5 p
(Contract N00014-81-C-0776)
(AD-A150623; TR-16) Avail: NTIS HC A02/MF A01 CSCL 07/4

During our latest run, November '83, at the Stanford Synchrotron Radiation Laboratory, we were able to detect x-ray fluorescence from a monolayer of Pb on single crystal silver film. The jump at the Pb edge represented increase in count rate of 150 eps on a 1500 cps background. This signal is too small for useful EXAFS to be extracted with a reasonable data collection time, but planned improvements in the electronic instrumentation and the experimental setup will achieve an edge jump greater than 1000 cps on a comparable background. GRA

N85-22653# Ames Lab., Iowa. Dept. of Chemistry.
APPLICATION OF MODULATED HYDRODYNAMIC VOLTAMMETRY TO THE STUDY OF ANODIC ELECTROCATALYSIS Ph.D. Thesis
Deborah S. Austin Dec. 1984 204 p refs
(Contract W-7405-eng-82)
(DE85-004182; IS-T-1129) Avail: NTIS HC A10/MF A01

Square-wave hydrodynamically modulated voltammetry (QHMV) is used for the study of anodic reactions electrocatalyzed by surface oxides at noble metal electrodes. QHMV permits extraction of the convective-coupled faradaic component from the total electrode current. The positive potential limit for application of QHMV is observed to be 200 to 400 mV more positive than that for conventional cyclic voltammetry, depending on the electrode material. Small mass-transport coupled currents occurring simultaneously with oxide formation and O2 evolution can be characterized voltammetrically by application of QHMV. Results obtained by cyclic voltammetry and QHMV are described for several anoidic reactions at various noble metal electrodes. Major emphasis is placed on the anodic behavior of I(-) at a Pt electrode in acidic media. The convective components of the total electrode current include the mass-transport limited production of I2 (0.55 V); the mass-transport coupled oxidation of I(-) to IO3(-) (1.0 to 1.1 V), which is catalyzed by the anodic formation of PtOH; and the mass-transport limited formation of IO3(-) (1.5 V) which is electrocatalyzed by an OH intermediate product of O2 evolution. DOE

N85-22654# Argonne National Lab., Ill. Chemical Technology Div.
INVESTIGATION OF MANGANESE DIOXIDE AS AN IMPROVED SOLID DESICCANT
Anthony V. Fraioli 1984 23 p refs
(Contract W-31-109-eng-38)
(DE85-004034; DOE/NBM-5004/34) Avail: NTIS HC A02/MF A01

The preparation of a series of manganese oxides and the results of an analysis of their sorptive, structural, and surface characteristics with respect to water adsorption are described. A cusped Type III isotherm for the adsorption of water is reported for the first time. The data are interpreted as evidence of a first-order phase change from a two-dimensional gas to a liquid film in the first reversibly absorbed layer. It appears that the water adsorption characteristics of MnO2 compared to standard desiccants which exhibit Type II isotherms are due at least in part to differences in the physical topography and electronic properties of the desiccant substrates. MnO2 is a semiconductor with essentially-flat, monoenergetic surface structures, while standard desiccants like silica gel are electronic insulators with irregular, heteroenergetic surfaces. DOE

N85-22655# Los Alamos Scientific Lab., N. Mex.
USE OF MARKETS TO ELUCIDATE REACTING SPUTTERING PROCESSES
B. W. Springer, W. J. McCrearu, and R. C. Cordi 1984 19 p refs Presented at 31st Natl. Vacuum Symp., Reno, Nev., 3 Dec. 1984
(Contract W-7405-eng-36)
(DE85-005723; LA-UR-84-3805; CONF-841218-20) Avail: NTIS HC A02/MF A01

The reactive gases of nitrogen, ammonia, carbon monoxide and methane were introduced to a steady state deposition of aluminum using a planar magnetron operating at approx. 400 volts. The effect of the compound formed at the target was separated from the plasma/substrate effects. The resulting films were analyzed by auger depth profiling. The marker experiments show a decoupling of the target and plasma/substrate interaction within the sputter etch rate and doping time constraints. The data show evidence for the deposition of compound from the target which is thought to be due to the near surface modification from the cathode fall voltage. The energy partitioning of the carbon in either carbon monoxide or methane yields the expected results. The nitrogen and ammonia results were similar in nature due to the reduced voltage from the sputter power supply. The results are consistent with the target being doped, in that the nitrogen ranges in the target are essentially identical. It is indicated that a significant fraction is formed and sputtered from the target. The data are consistent with a model which indicates that the reactive species is implanted in the target, subsequently eroded away and contributes to the observed compound films. E.A.K.

N85-22656# Princeton Univ., N. J. School of Engineering and Applied Sciences.
COMPREHENSIVE MECHANISMS FOR COMBUSTION CHEMISTRY: AN EXPERIMENTAL AND NUMERICAL STUDY WITH EMPHASIS ON APPLIED SENSITIVITY ANALYSIS Progress Report, 16 Sep. 1983 - 10 Oct. 1984
F. L. Dryer 1984 25 p refs
(Contract DE-AC02-83ER-13045)

(DE85-000173; DOE/ER-13045/2) Avail: NTIS HC A02/MF A01

Accomplishments in combustion chemistry are reported. An extensive review of chemical kinetic modelling of hydrocarbon combustion chemistry and applications was published. Numerous uses of elementary sensitivity analysis in the development and study of elementary chemical kinetic mechanisms were demonstrated using the mechanisms for moist CO/H2/O2 chemistry at combustion temperatures. Kinetic modelling and sensitivity analysis codes were exercised at Brookhaven National Laboratories, and collatoration with local personnel (Drs. Bruce Klemm and J. Michaels) on the use of these aids in their elementary kinetics studies led to the evaluation of the sources and magnitudes of error in rate constants reported for the reactions, H2CO + OH H2O + HCO and H2CO + OH H2CO2 + H. Ethanol pyrolysis and oxidation experiments began and modelling work, particularly on acetaldehyde combustion chemistry, was re-initiated. Planning and desig of equipment and experimental program on the pyrolysis and oxidation of formaldehyde began. R.J.F.

N85-22528# Pennsylvania State Univ., University Park. Dept. of Mechanical Engineering.
STATUS OF BORON COMBUSTION RESEARCH
G. M. Faeth *In* APL 21st JANNAF Combust. Meeting, Vol. 1 Oct. 1984 p 15-29 refs (For primary document see N85-22526 13-20)
Avail: NTIS HC A21/MF A01 CSCL 21/2

N85-22530# Rensselaer Polytechnic Inst., Troy, N. Y. Dept. of Chemical Engineering and Environmental Engineering.
COMBUSTION KINETICS OF METAL ATOMS AND METALLIC RADICALS OVER WIDE TEMPERATURE RANGES
Arthur Fontijn *In* APL 21st JANNAF Combust. Meeting, Vol. 1 Oct. 1984 p 45-52 refs (For primary document see N85-22526 13-20)
(Grant AF-AFOSR-0073-82)
Avail: NTIS HC A21/MF A01 CSCL 21/2

N85-22531*# Colorado Univ., Boulder.
IGNITION PHENOMENA OF BULK ALUMINUM ALLOY AS A FUNCTION OF OXYGEN PRESSURE
Ke Nguyen, James W. Bransford (NBS, Washington, D.C.), and Melvyn C. Branch *In* APL 21st JANNAF Combust. Meeting, Vol. 1 Oct. 1984 p 53-61 refs Sponsored in cooperation with NASA. Marshall Space Flight Center and Air Force (For primary document see N85-22526 13-20)
Avail: NTIS HC A21/MF A01 CSCL 21B

N85-22532# Georgia Inst. of Tech., Atlanta. School of Aerospace Engineering.
COMBUSTION OF ZIRCONIUM CARBIDE
J. K. Sambamurthi, E. W. Price, R. K. Sigman, R. R. Panyam, and C. J. Park *In* APL 21st JANNAF Combust. Meeting, Vol. 1 Oct. 1984 p 63-70 refs (For primary document see N85-22526 13-20)
(Grant AF-AFOSR-0356-83)
Avail: NTIS HC A21/MF A01 CSCL 21/2

N85-22536# United Technologies Corp., San Jose, Calif. Chemical Systems Div.
COUPLING BETWEEN VELOCITY OSCILLATIONS AND SOLID PROPELLANT COMBUSTION
R. S. Brown, A. M. Blackner, P. G. Willoughy, and R. Dunlap *In* APL 21st JANNAF Combust. Meeting, Vol. 1 Oct. 1984 p 103-112 refs (For primary document see N85-22526 13-20)
(Contract F49620-81-C-0027)
Avail: NTIS HC A21/MF A01 CSCL 21/2

N85-22541# Naval Weapons Center, China Lake, Calif.
COMPARISONS OF SOLID PROPELLANT WITH INSTABILITY PREDICTIONS AND MOTOR FIRING EXPERIENCE
H. B. Mathes *In* APL 21st JANNAF Combust. Meeting, Vol. 1 Oct. 1984 p 165-175 refs (For primary document see N85-22526 13-20)
Avail: NTIS HC A21/MF A01 CSCL 21/2

N85-22542# Brigham Young Univ., Provo, Utah.
MEASUREMENTS OF DISTRIBUTED COMBUSTION
P. C. Braithwaite, M. W. Beckstead, and R. L. Raun *In* APL 21st JANNAF Combust. Meeting, Vol. 1 Oct. 1984 p 177-186 refs (For primary document see N85-22526 13-20)
(Grant AF-AFOSR-0157-83)
Avail: NTIS HC A21/MF A01 CSCL 21/2

N85-22543# Brigham Young Univ., Provo, Utah.
DISTRIBUTED COMBUSTION: A MECHANISM OF ACOUSTIC SUPPRESSION
M. W. Beckstead *In* APL 21st JANNAF Combust. Meeting, Vol. 1 Oct. 1984 p 187-194 refs (For primary document see N85-22526 13-20)
(Grant AF-AFOSR-0157-83)
Avail: NTIS HC A21/MF A01 CSCL 21/2

N85-22545# Hercules, Inc., Cumberland, Md.
WORKSHOP REPORT: CATALYSIS OF BURN RATE OF ENERGETIC BINDER PROPELLANTS
R. L. Foster *In* APL 21st JANNAF Combust. Meeting, Vol. 1 Oct. 1984 p 205-212 refs Also presented at 20th JANNAF Combus. Meeting, Monterey, Calif., Oct. 1983 (For primary document see N85-22526 13-20)
Avail: NTIS HC A21/MF A01 CSCL 21/2

N85-22546# Georgia Inst. of Tech., Atlanta.
MECHANISM OF BURNING RATE ENHANCEMENT BY FERRIC OXIDE
E. W. Price and J. K. Sambamurthi *In* APL 21st JANNAF Combust. Meeting, Vol. 1 Oct. 1984 p 213-231 refs Sponsored in part by Air Force (For primary document see N85-22526 13-20)
(Contract N00014-79-C-0764; Grant AF-AFOSR-0356-83)
Avail: NTIS HC A21/MF A01 CSCL 21/2

N85-22547# Purdue Univ., Lafayette, Ind. School of Aeronautics and Astronautics.
EFFECT OF VARIABLE SOLID PHASE THERMAL PROPERTIES ON PROPELLANT COMBUSTION
Fred S. Blomshield and John R. Osborn *In* APL 21st JANNAF Combust. Meeting, Vol. 1 Oct. 1984 p 233-240 refs (For primary document see N85-22526 13-20)
Avail: NTIS HC A21/MF A01 CSCL 21/2

N85-22549# Virginia Polytechnic Inst. and State Univ., Blacksburg.
MUTIPLE REFLECTION THEORY FOR MICROWAVE MEASUREMENT OF SOLID PROPELLANT BURNING RATES
W. F. OBrien, H. L. Wood, J. J. Kliger (Naval Ordnance Station, Indian Head, Md.), and C. B. Dale (Naval Ordnance Station, Md.) *In* APL 21st JANNAF Combust. Meeting, Vol. 1 Oct. 1984 p 251-259 refs (For primary document see N85-22526 13-20)
(Contract N00174-82-C-0039)
Avail: NTIS HC A21/MF A01 CSCL 21/2

N85-22550# Air Force Rocket Propulsion Lab., Edwards AFB, Calif.
IN-SITU BURNING RATE DETERMINATION USING FLASH RADIOGRAPHY
H. M. Pressley, Jr. and R. L. Glick (Purdue Univ., Lafayette, Ind.) *In* APL 21st JANNAF Combust. Meeting, Vol. 1 Oct. 1984 p 261-273 refs (For primary document see N85-22526 13-20)
Avail: NTIS HC A21/MF A01 CSCL 21/2

N85-22554*# Rocketdyne, Canoga Park, Calif.
DEVELOPMENT OF A THREE-PHRASE COMBUSTION CODE FOR MODELING LIQUID ROCKET ENGINES
P. Y. Liang and Y. M. Chang *In* APL 21st JANNAF Combust. Meeting, Vol. 1 Oct. 1984 p 357-367 refs (For primary document see N85-22526 13-20)

(Contract NAS8-34928)
Avail: NTIS HC A21/MF A01 CSCL 21B

N85-22564# Atlantic Research Corp., Gainesville, Va.
WORKSHOP REPORT: SWIRL ENHANCED COMBUSTION
William Sargent *In* APL 21st JANNAF Combust. Meeting, Vol. 1 Oct. 1984 p 481-485 refs Also presented at 5th Swirl Workshop, Reno, Nev., Jan. 1984 (For primary document see N85-22526 13-20)
Avail: NTIS HC A21/MF A01 CSCL 21/2

N85-22631# Joint Publications Research Service, Arlington, Va.
MULTIPLE ELEMENT NEUTRON-ACTIVATION ANALYSIS OF ATMOSPHERIC AEROSOLS WITH X-RAY AND GAMMA-SPECTROMETRIC RECORDING OF RADIONUCLIDES FORMED Abstract Only
S. G. Pushkin and E. N. Gilbert *In its* USSR Rept.: Chem. (JPRS-UCH-85-001) 17 Jan. 1985 p 1-2 Transl. into ENGLISH from Izv. Sibirskogo Otdeleniya Akad. Nauk SSSR: Ser. Khim. Nauk (Novosibirsk, USSR), no. 11, Jul. 1984 p 57-63 (For primary document see N85-22629 13-23)
Avail: NTIS HC A06

N85-22835# Joint Publications Research Service, Arlington, Va.
DEPENDENCE OF COMBUSTION OF HOMOGENEOUS KEROSENE-AIR MIXTURES ON HUMIDITY OF AIR Abstract Only
V. A. Sychenkov and V. M. Yankovskiy *In its* USSR Rept.: Eng. and Equipment (JPRS-UEQ-85-003) 12 Mar. 1985 p 87-88 Transl. into ENGLISH from Izv. Vyssh. Ucheb. Zaved.: Aviats. Tekhn. (Kazan, USSR), no. 1, Jan. - Mar. 1984 p 98-101 Original language document previously announced as A84-47577 (For primary document see N85-22782 13-31)
Avail: NTIS HC A06

N85-23551*# California Univ., Livermore. Lawrence Livermore Lab.
SHOCK COMPRESSION OF LIQUID HELIUM TO 56 GPa (560) KBAR Abstract Only
W. J. Nellis, N. C. Holmes, A. C. Mitchell, R. J. Trainor, G. K. Governo, M. Ross, and D. A. Young *In* NASA, Washington Repts. of Planetary Geol. and Geophys. program, 1984 Apr. 1985 p 217-219 refs Document previously announced as A84-48934 (For primary document see N85-23474 13-91)
Avail: NTIS HC A99/MF A01 CSCL 07D

N85-23553*# Massachusetts Inst. of Tech., Cambridge. Dept. of Earth, Atmospheric, and Planetary Sciences.
QUENCHING EFFECTS ON IRON SITE PARTITIONING IN THE APOLLO 17 ORANGE GLASS COMPOSITION Abstract Only
M. Darby Dyar *In* NASA, Washington Repts. of Planetary Geol. and Geophys. Program Apr. 1985 p 223-224 refs (For primary document see N85-23474 13-91)
Avail: NTIS HC A99/MF A01 CSCL 07D

N85-23554*# Massachusetts Inst. of Tech., Cambridge. Dept. of Earth, Atmospheric, and Planetary Science.
EXPERIMENTAL METHDS FOR QUENCHING STRUCTURES IN LUNAR-ANALOG SILICATE MELTS: VARIATIONS AS A FUNCTION OF QUENCH MEDIA AND COMPOSITION Abstract Only
M. Darby Dyar *In* NASA, Washington Repts. of Planetary Geol. and Geophys. Program Apr. 1985 p 225 Previously announced as A85-17669 (For primary document see N85-23474 13-91)
Avail: NTIS HC A99/MF A01 CSCL 07D

N85-23555*# Massachusetts Inst. of Tech., Cambridge. Dept. of Earth, Atmospheric, and Planetary Science.
HIBONITE: CRYSTAL CHEMISTRY AND ORIGIN OF BLUE COLORATION IN METEORITIC ASSEMBLAGES Abstract Only
Roger G. Burns and Virginia Mee Burns *In* NASA, Washington Repts. of Planetary Geol. and Geophys. Program Apr. 1985 p 226-228 refs (For primary document see N85-23474 13-91)
Avail: NTIS HC A99/MF A01 CSCL 07D

26 METALLIC MATERIALS

Includes physical, chemical, and mechanical properties of metals, e.g., corrosion; and metallurgy.

N85-22657# British Library Lending Div., Boston Spa (England).
FORMATION OF ALUMINA LAYERS ON IRON-BASE ALLOYS
J. Peters and H. J. Grabke [1984] 22 p refs Transl. into ENGLISH from Werkst. Korros. West Germany, v. 35, 1984 p 385-394
(BLL-T6418/BG/LRS/LRST737/84) Avail: British Library Lending Div., Boston Spa, England

The formation of Al2O3 layers was studied for ferritic alloys Fe-6Al-M and austenitic alloys Fe-27Ni-4Al-M where M - Ti,Zr, V,Nb. W, B. Si... (concentrations in wt%). One or more alloying elements M were added and in some cases carbon. The oxidation was performed at 1000 C in H2O-H2 mixtures at PO2 = 10 to the After 1/2 h oxidation, the oxide layers were investigated by X-ray structures analysis, scanning electron microscopy and Auger electron spectroscopy. The alloy Fe-6 Al and most doped alloys form badly adherent layers. However, on alloys with additions of 0.1 to 1% Ti. Zr. V or Y, the oxide layers are fine-grained and well-adherent. The Ti-doped ferritic alloys showed very protective layers, which is caused by the formation of a Ti(C. O)-layer beneath the alpha-Al2O3. The presence of the oxicarbide induces nucleation and improves the adherence of alpha Al2O3, according to epitaxial relations between ferrite and oxicarbide and between and between oxicarbide and alumina. The favourable influence of Ti and Zr on the Al2O3, formation is also effective on the austenitic alloys. R.J.F.

N85-22658# British Library Lending Div., Boston Spa (England).
DELAYED CRACKING STRENGTH OF EXPERIMENTAL GRADES OF 42 CD 4 STEEL IN AQUEOUS H2S SURROUNDINGS
J. C. Charbonnier, H. Margot-Marette, M. Aucouturier, and A. M. Brass [1985] 30 p refs Transl. into ENGLISH from Memoires et Etudes Sci. Revue de Metall., v. 81, no. 5, May 1984 p 225-228
(BLL-T6419/BG/LRS/LRST738/84) Avail: British Library Lending Div., Boston Spa, England

In order to improve the mechanical performance and corrosion strength under stress of low alloy steels, the behavior of laboratory castings of type 42 CD 4 of martensitic structure annealed at elevated temperature in aqeous H2S surroundings were studied. The chemical composition of the steels was modified by the edition of elements to slow down softening during the annealing and/or hardening of the matrix. Microstructural studies of the trapping, permeation, and desorption of hydrogen enabled hypotheses to be formulated in order to interpret the results. The vanadium-titanium or molybdenum-vanadium-titanium steels contain a family of dense, very fine precipitates which are uniformly distributed in the microstructure. These precipitates, identified as of the MC (V, Mo, Ti, Cr, Fe)C type are deep traps for hydrogen; by capturing hydrogen during mechanical stressing in aggressive surroundings, they slow down and possibly inhibit embrittlement. B.G.

N85-22659# Defence Research Information Centre, Orpington (England).
PREDICTION OF THE RESISTANCE OF STRUCTURAL MATERIALS TO CAVITATION EROSION
K. Steller and E. Partyka Dec. 1984 15 p refs Transl. into ENGLISH from Prace Inst. Maszyn Przeplywowych (Gdansk), nos. 83/84, 1983 p 179-187
(BLL-DRIC-Trans-7435-(3623.66)) Avail: British Library Lending Div., Boston Spa, Engl.

Different methods to evaluate the cavitation resistance of materials are reviewed and the different reactions to the changes of cavitation conditions are pointed out. It is noted that the results of the specimen tests are insufficient for the correct prediction of the resistance of materials to cavitation and it is necessary to know the results of loading caused by implosion of cavitation bubbles. Cavitation intensity measures are discussed and their

relation to the cavitation erosion is shown. Procedures used for the evaluation of the cavitation erosion hazard and prediction of material durability in field conditions are presented. E.A.K.

N85-22660*# National Aeronautics and Space Administration. Lewis Research Center, Cleveland, Ohio.
ORIENTATION AND TEMPERATURE DEPENDENCE OF SOME MECHANICAL PROPERTIES OF THE SINGLE-CRYSTAL NICKEL-BASE SUPERALLOY RENE N4. 3: TENSION-COMPRESSION ANISOTROPY
R. V. Miner, T. P. Gaab, J. Gayda, and K. J. Hemker (Cincinnati Univ.) 1985 21 p refs Presented at the 114th Ann. Meeting of the American Inst. of Mining, Metallurgical and Petroleum Engineers, New York, 24-28 Feb. 1985
(NASA-TM-86982; E-2525; NAS 1.15:86982) Avail: NTIS HC A02/MF A01 CSCL 11F

Single crystal superalloy specimens with various crystallographic directions along their axes were tested in compression at room temperature, 650, 760, 870, and 980 deg C. These results are compared with the tensile behavior studied previously. The alloy, Rene N4, was developed for gas turbine engine blades and has the nominal composition 3.7 Al, 4.2 Ti, 4 Ta, 0.5 Nb, 6 W, 1.5 Mo 9 Cr, 7.5 Co, balance Ni, in weight percent. Slip trace analysis showed that primary cube slip occurred even at room temperature for the [111] specimens. With increasing test temperature more orientations exhibited primary cube slip, until at 870 deg C only the [100] and [011] specimens exhibited normal octahedral slip. The yield strength for octahedral slip was numerically analysed using a model proposed by Lall, Chin, and Pope to explain deviations from Schmid's Law in the yielding behavior of a single phase Gamma prime alloy, Ni3(Al, Nb). The Schmid's Law deviations in Rene N4 were found to be largely due to a tension-compression anisotropy. A second effect, which increases trength for orientations away from [001], was found to be small in Rene N4. Analysis of recently published data on the single crystal superalloy PWA 1480 yielded the same result. R.J.F.

N85-22661*# Georgia Inst. of Tech., Atlanta. School of Physics.
STUDY OF THE EFFECTS OF IMPLANTATION ON THE HIGH Fe-Ni-Cr AND Ni-Cr-Al ALLOYS Final Report
M. W. Ribarsky 12 Apr. 1985 36 p refs
(Grant NAG3-255)
(NASA-CR-175625; NAS 1.26:175625) Avail: NTIS HC A03/MF A01 CSCL 11F

A theoretical study of the effects of implantation on the corrosion resistance of Fe-Ni-Cr and Ni-Cr-Al alloys was undertaken. The purpose was to elucidate the process by which corrosion scales form on alloy surfaces. The experiments dealt with Ni implanted with Al, exposed to S at high temperatures, and then analyzed using scanning electron microscopy, scanning Auger spectroscopy and X-ray fluorescence spectroscopy. Pair bonding and tight-binding models were developed to study the compositions of the alloys and as a result, a new surface ordering effect was found which may exist in certain real alloys. With these models, the behavior of alloy constituents in the presence of surface concentrations of O or S was also studied. Improvements of the models to take into account the important effects of long- and short-range ordering were considered. The diffusion kinetics of implant profiles at various temperatures were investigated, and it was found that significant non-equilibrium changes in the profiles can take place which may affect the implants' performance in the presence of surface contaminants. R.J.F.

N85-22662*# National Aeronautics and Space Administration. Marshall Space Flight Center, Huntsville, Ala.
AN ELECTROCHEMICAL STUDY OF THE CORROSION BEHAVIOR OF PRIMER COATED 2219-T87 ALUMINUM
Merlin D. Danford and Ralph H. Higgins Apr. 1985 27 p refs
(NASA-TP-2459; NAS 1.60:2459) Avail: NTIS HC A03/MF A01 CSCL 11F

The corrosion behavior for 2219-T87 aluminum coated with various primers, including those used for the external tank and solid rocket boosters of the Space Shuttle Transportation System, were investigated using electrochemical techniques. Corrosion potential time, polarization resistance time, electrical resistance time, and corrosion rate time measurements were all investigated. It was found that electrical resistance time and corrosion rate time measurement were most useful for studying the corrosion behavior of painted aluminum. Electrical resistance time determination give useful information concerning the porosity of paint films, while corrosion rate time curves give important information concerning overall corrosion rates and corrosion mechanisms. In general, the corrosion rate time curves all exhibited at least one peak during the 30 day test period, which was attributed, according to the proposed mechanisms, to the onset of the hydrogen evolution reaction and the beginning of destruction of the protective properties of the paint film. Author

N85-22663# Turku Univ. (Finland). Physical Lab.
MAGNETOVOLUME EFFECTS IN SOME Y-Ni INTERMETALLIC COMPOUNDS
M. Lehtinen, S. Parvianen, and H. Stenholm 1984 15 p refs
(ISSN-0066-2003; ISBN-951-41-0479-X) Avail: NTIS HC A02/MF A01

Thermal expansion of Y2Ni15, YNi7 were measured from 4.2 K to 200 K with a capacitive dilatometer. Contrary to the very weak itinerant ferromagnetic behavior of YNi3 the magnetic contribution to the expansion of Y2Ni7 is observed to be positive and related to the thermal variation of spontaneous magnetization. Magnetic effects in the expansion of Y2Ni15 are not pronounced. Author

N85-22664# Council for Scientific and Industrial Research, Pretoria (South Africa). Metals Div.
STRUCTURES OF ORDERED LINEAR DISLOCATION MULTIPOLES IN Cu-Al ALLOYS
N. R. Comins 1983 9 p refs Presented at the 1st CSIR(ROSA)-NSC(ROC) Metal Alloys and Ceram. Workshop, Hsinchu, Taiwan, 31 Aug. - 10 Sep. 1983
(ISSN-0379-6906) Avail: NTIS HC A02/MF A01

In Cu-Al alloys, during the early stages of deformation, the formation of linear dislocation multipole arrays is common. The weak-beam technique of electron microscopy was used to study the partial dislocation configurations in both vacancy and interstitial edge and near-edge multipoles. The structures are compared with calculated multipoles and the calculations were extended to include anisotropic elasticity effects. Realistic calculations of the stresses on secondary glide systems inside planar multipoles are discussed. The idea of superposition of internal stresses on plastic relaxation of multipoles is considered. R.J.F.

N85-22665# Defence Research Information Centre, Orpington (England).
METAL-SEMICONDUCTOR PHASE TRANSITION AND ITS APPLICATION
A. A. Bugaev, B. P. Zakharchenya, F. A. Chudnovsky, and Zh. I. Alferov, ed. Feb. 1984 307 p refs Transl. into ENGLISH of "USSR Academy of Sciences, A. F. Ioffe Order of Lenin Physical-Technical Institute" Leningrad, Nauka Publishers, 1979 Original language document was announced in IAA as A80-23076
(DRIC-T-7149; BR91266) Avail: NTIS HC A14/MF A01

Metal-semiconductor phase transition mechanisms; vanadium trioxide properties; metal-semiconductor phase transition in vanadium dioxide; magnell vanadium oxide series; phase transition in titanium, iron, nickel, and chromium compounds; and phenomenological features of metal-semiconductor phase transition are discussed. Optical properties of vanadium dioxide based media and devices; application of vanadium oxide based media for recording of holograms; operation of PTIRLR in coherent optical processing systems; and indicating and automatic monitoring devices based on vanadium oxides are considered. Author (ESA)

N85-22666# Salford Univ. (England). Dept. of Aeronautical and Mechanical Engineering.
CORROSION OF AIRCRAFT Al AND Al-Zn ION PLATED STEEL FASTENERS Final Report

O. A. Abu-Zeid 1984 73 p refs
Avail: NTIS HC A04/MF A01

The effect of coating material, coating thickness and coating conditions on the corrosion resistance of aluminum and aluminum-zinc coatings with different zinc contents was studied. Corrosion tests were performed on assemblies of Al and Al-Zn coated high strength steel bolts fastened into aluminum alloy blocks. It is found that the addition of Zn to Al coatings greatly improves their sacrificial corrosion protection with respect to steel and provides cathodic protection for the aluminum alloys. The galvanic currents and galvanic potentials of the coupled Al and Al-Zn ion plated fasteners to three aluminum alloys were measured. The average galvanic current densities were calculated and the minimum amount of Zn content in Al coatings to ensure anodic polarity of the coatings and consequently cathodic protection for the alloys is found. The addition of Zn reduces the average coefficient of friction and increases the wear life of aluminum coatings. Author (ESA)

N85-22667# Materials Quality Assurance Directorate, London (England).
THE CHARACTERISATION OF OXIDE FILMS ON TREATED ALUMINIUM ALLOYS
K. Cowey, P. McKee, and R. E. Piggott Mar. 1983 18 p refs
Sponsored by UK Procurement Executive Ministry of Defence
(MQAD-R-849; BR91695) Avail: NTIS HC A02/MF A01

The effects of hot and cold acid etching on the oxide films produced on aluminum alloys were studied using surface analytical techniques. The morphologies of the films were examined by scanning electron microscopy, the chemical features were studied using X-ray photo electron spectroscopy, and the oxide film compositions determined using Auger electron spectroscopy (AES). Determination of thickness of the oxide films and elemental depth analysis were performed by AES with argon ion beam etching. The hot and cold acid etching processes give differences in the oxide layer characteristics for the types of alloys examined.
Author (ESA)

N85-22668# Massachusetts Inst. of Tech., Cambridge. Dept. of Materials Science and Engineering.
RAPID SOLIDIFICATION PROCESSING OF MAGNESIUM ALLOYS Final Report, 1 Aug. 1982 - 31 Jul. 1983
M. C. Flemings and A. Mortensen Watertown, Mass. Army Materials and Mechanics Research Center Sep. 1984 52 p
(Contract DAAG46-82-K-0051)
(AD-A150270; AMMRC-TR-84-37) Avail: NTIS HC A04/MF A01 CSCL 13/8

This report comprises the second year of a two year program on a Rapid Solidification, extrusion processing and mechanical property measurement of Magnesium alloys. During the second year, samples were cast using a controlled atmosphere (He gas), and vertical wheel melt-spinning apparatus constructed at MIT. Casting conditions were thus perfected, to obtain larger quantities of ribbons of consistent quality. Extrusion procedures were investigated on rapidly solidified magnesium alloys. A gradual lowering of the extrusion temperature from 470 C to 210 C yielded improved mechanical properties on alloys ZK60, EZ33, and Mg-5.3%Zn. Optimal conditions were: a reduction in area ratio of about 1/30, and an extrusion temperature of about 200-250 C. Results on alloy ZK60, extruded under these conditions, displayed interesting mechanical properties, and made it comparable in specific properties to R.S.P. aluminum alloys. Tensile properties in the as extruded condition were: U.S. 53.0 ksi, and U.T.S. 56.3 ksi. The ductility in particular was significantly higher than that of wrought ZK60 alloy: 19.6% (typical mechanical properties of the conventional extruded material are: Y.S. 41 ksi, U.T.S. 51 ksi, elongation, 11%). GRA

N85-22669# Cornell Univ., Ithaca, N.Y.
EXPERIMENTAL AND NUMERICAL ANALYSIS OF ELECTRIC CURRENTS AND ELECTROMAGNETIC BLUNTING OF CRACKS IN THIN PLATES
G. R. Doelp, J. F. Abel, and F. C. Moon Dec. 1984 193 p
(Contract N00014-79-C-0224)
(AD-A150418; TR-84-12) Avail: NTIS HC A09/MF A01 CSCL 11/6

Electric currents in thin plates are analyzed numerically with emphasis on expanding the capabilities of existing finite element programs. Specifically, the ability to calculate transport currents is added to programs which originally computed only induced currents. The final programs are capable of handling transport currents alone or combined with induced currents generated by a transient external magnetic field. Experimental and analytical verification of the resulting program is presented. The second half of this study deals with the blunting of fatigue cracks by melting a hole at the crack tip by electromagnetic means. This technique is investigated experimentally for stainless steel 304 and titanium alloy Ti-6Al-4V. The blunting technique is described in detail, and the results from the testing program are presented. Analysis of the data emphasizes the hole sizes produced and their effect on the ultimate strength and fracture resistance of the test specimens. Electromagnetic blunting increases the ultimate static stress of stainless steel 304 plates by up to 19 percent and of Ti-6Al-4V by up to 78 percent. The effect of electromagnetic blunting on resistance to further fatigue remains to be investigated. GRA

N85-22670# Washington Univ., St. Louis, Mo. Semiconductor Research Lab.
CLUSTERING AND ORDERING IN 3-5 ALLOYS Annual Report, 1 Jun. 1983 - 31 May 1984
C. M. Wolfe, M. W. Muller, P. A. Fedders, S. Julie Hsieh, Elizabeth A. Patten, and K. A. Salzman 31 Jul. 1984 40 p
(Grant AF-AFOSR-0231-82; AF Proj. 2306)
(AD-A150604; WU/SRL-59583A-3; AFOSR-84-1276TR) Avail: NTIS HC A03/MF A01 CSCL 11/6

The 3-5 semiconducting alloys are typically grown by epitaxial techniques at temperatures where, in the absence of substrate effects, they are thermodynamically unstable. This can result in problems associated with clustering of like atoms or ordering of unlike atoms. Long-range ordering could yield interesting 3-5 ternary compounds. The mixing enthalpy of 3-5 semiconductor alloys is fairly well described by regular solution theory, with a thermodynamic interaction parameter that is sensitive to the lattice spacing of the binary constituents. An estimate of the interaction parameter is derived from a model which ascribes the mixing enthalpy to bond distortions associated with the alloy formation, and relates these to the macroscopic elastic properties of the crystal. Numerical estimates are given for the 18 alloys with cations Al, Ga, In and anions P, As, Sb, and these are compared with experimental values and alternative models. To within a single adjustable parameter, the predictions agree with experiment and are consistent with those of the delta lattice parameter (DLP) model. GRA

N85-22671# Massachusetts Inst. of Tech., Cambridge. Dept. of Mechanical Engineering.
MICROMECHANICAL MODELING OF MICROSTRUCTURAL DAMAGE IN CREEPING ALLOYS Final Report
A. S. Agon 15 Nov. 1984 86 p refs
(Contract DE-AC02-74ER-04461)
(DE85-003925; DOE/ER-04461/7) Avail: NTIS HC A05/MF A01

Fracture under service conditions at high temperatures in structures undergoing creep deformation is intergranular and cavities on grain boundaries are produced on interfaces of hard particles during transient sliding of grain boundaries. The growth of grain boundary cavities by a combination of continuum creep and diffusional flow is often constrained by the creep deformation of the surrounding grain matrix. The constrained growth and linking of grain boundary cavities produces isolated cracked grain boundary facets which continue to grow by continuum creep and in the process accelerate overall creep flow. Cracked grain boundary facets are the principal form of creep damage, and their density per unit volume can be taken as the parameter characterizing creep damage. This damage parameter can be incorporated into three-dimensional constitutive relations of creep deformation, and these relations can be used in large strain finite element programs to solve complex engineering problems of creeping structures. All the microstructural mechanics that enter into the above description

are verified in key experiments on cavitation and crack growth. DOE

N85-22672# Du Pont de Nemours (E. I.) and Co., Aiken, S.C.
HYDROGEN EFFECTS IN AUSTENITIC STAINLESS STEELS BASED ON THE Fe-Cr-Mn-N SYSTEM
G. R. Caskey, Jr. 26 Nov. 1984 21 p refs Presented at Symposium on the Scientific Basis for Nuclear Waste Management, Boston, 26-30 Nov. 1984
(Contract DE-AC09-76SR-00001)
(DE85-003617; DP-MS-84-74; CONF-841157-27) Avail: NTIS HC A02/MF A01

The effects of hydrogen on the mechanical properties of austenitic stainless steels were examined. One class of steels included in these studies based on the Fe-Cr-Mn-N system and also may contain up to 13% nickel. These steels are characterized by a ductile-to-brittle transition that disappears as the nickel content is raised and by a generally higher strength than the 300-series austenitic steels. The effects of hydrogen on these Fe-Cr-Mn-N (Ni) steels were reviewed and show that: small nickel additions greatly improve resistance to hydrogen damage; hydrogen solubility is greater than in Fe-Cr-Ni austenitic for the same conditions; hydrogen induced fracture mode changes are related to nickel content. These and other effects are discussed and compared to hydrogen effects in Fe-Cr-Ni alloys. DOE

N85-22673# Brookhaven National Lab., Upton, N. Y.
LOCAL ELECTROCHEMISTRY OF PITTING CORROSION IN STAINLESS STEELS
H. S. Isaacs and R. C. Newman 1984 23 p refs Presented at the Conf. on Corrosion Chem. within Pits, Crevices and Cracks, Teddington (England), 1 Oct. 1984
(Contract DE-AC02-76CH-00016)
(DE85-005207; BNL-35432; CONF-8410207-1) Avail: NTIS HC A02/MF A01

The following features of localised corrosion in stainless steels are described and illustrated: diffusion-controlled dissolution and salt films; active dissolution kinetics and the effects of allowing additions such as Mo; coupling of active dissolution and diffusion; the pitting potential; repassivation and the protection potential. In addition, the coupling of a pit anode and a passive surface is described with reference to neutral oxygenated chloride solutions. In the initiation stage of pitting, the pit draws current mostly from the capacitance of the passive film, not from the oxygen reduction reaction. Some implications of these aspects are discussed. DOE

N85-22674# Oak Ridge National Lab., Tenn. Metals and Ceramics Div.
THERMODYNAMICS OF COPPER-NICKEL ALLOYS CONTAINING ALUMINUM, SILICON, TITANIUM, AND CHROMIUM RELATIVE TO THEIR USE IN CERAMIC BRAZING
R. O. Williams Nov. 1984 26 p refs
(Contract DE-AC05-84OR-21400)
(DE85-004787; ORNL-6072) Avail: NTIS HC A03/MF A01

By varying the copper-to-nickel ratio the activity coefficients of Al, Si, Ti, and Cr can be varied over a wide range. Thus to a degree one can tailor the behavior of such alloys for usefulness in brazing ceramics. Futher, considerable amounts of these active elements can be present while the ability of carbon to reduce the surface oxide film in a high-vacuum system is retained. The critical aluminum concentrations required to prevent the formation of SiO_2, TiO, or Cr_2O_3 by reaction with Al_2O_3 are calculated. The simultaneous presence of the four active additions will presumably promote wetting without making the surface deoxidation more difficult. DOE

N85-22675# Brookhaven National Lab., Upton, N. Y.
APPLICATIONS OF THE VIBRATION PROBE TO LOCALIZED CURRENT MEASUREMENTS
Hugh S. Isaacs and Yuichi Ishikawa (Hitachi Ltd., Tsuchiura, Japan) 1985 10 p refs Presented at the Natl. Assoc. of Corrosion Engr. Ann. Meeting and Mater. Performance and Corrosion Show, Boston, 25 Mar. 1985
(Contract DE-AC02-76CH-00016)
(DE85-004702; BNL-35568; CONF-850311-6) Avail: NTIS HC A02/MF A01

The principles, advantages, and applications of a scanning vibrating electrode technique are presented. The technique was used to locate the position of localized corrosion and heterogeneities on surfaces and to determine their polarization characteristics. The technique was applied to the study of aluminum pitting, crevice corrosion of stainless steel and organic and metallic coatings on steels. DOE

N85-22676# Massachusetts Inst. of Tech., Cambridge.
CREEP CRACK GROWTH IN DUCTILE ALLOYS
A. S. Argon, C. W. Lau, B. Ozmat, and D. M. Parks 1984 20 p refs Presented at the IUTAM/ICF/ICM Eshelby Mem. Symp., Sheffield, England, 2-5 Apr. 1984 Submitted for publication
(Contract DE-AC02-77ER-04461)
(DE85-003937; CONF-8404219-1) Avail: NTIS HC A02/MF A01

Creep crack growth in ductile alloys involves considerable fragmentation of the crack tip region in its early phases of growth. This is a result of the defocusing action of crack tip blunting by both distortional and cavitational strains on the distribution of intergranular creep damage and is affected significantly by the initial sharpness of the crack. Specific models of intergranular damage combining nonsteady creep flow, evolution and growth of grain boundary facet cracks in the inelastic deformation field leading to final fracture were developed. When used in conjunction with finite element programs for crack tips, these damage models can explain such crack extension modes, the combination of mechanistic three dimensional damage models and large strain finite element codes, promise to be of wide-spread utility in predicting the development of creep damage under complex loading histories. M.G.

N85-22677# Rockwell International Corp., Golden, Colo. Space Operations Div.
MECHANICAL PROPERTIES OF ELECTRODEPOSITED NICKEL AND COPPER
J. L. Krankota, P. L. Thomas, ed., and I. C. Delaney, comp. 9 Nov. 1984 36 p refs
(Contract DE-AC04-76DP-03533)
(DE85-005321; RFP-3715) Avail: NTIS HC A03/MF A01

The strength and ductility of electrodeposited nickel and copper are similar to that of wrought and annealed sheet product. Percent elongation values for the thin (less than 50 mils, 1.25 mm) deposited sheet specimens strongly depend on the gage length. Reduction in thickness (related directly to reduction in area) is a better, more consistent indication of ductility at fracture. The effects of thickness and current density on strength and ductility are similar to those reported. However, little data are available for comparison of the biaxial properties. More data are needed on biaxial properties of Rocky Flats electrodeposits to delineate correlations with thickness and current density. Heat treatment of copper electrodeposits reduces the scatter in data, in addition to producing the expected increase in ductility and decrease in strength. The effect of heat treatment on nickel and copper deposit properties will be determined in future studies. The strength and ductility of electrodeposited nickel and copper are sufficient for Rocky Flats applications. DOE

N85-22678# Oak Ridge National Lab., Tenn.
TEM/FIM STUDY OF MODULATED MICROSTRUCTURES IN THE Fe-Be SYSTEM
M. K. Miller, M. G. Burke (Pittsburgh Univ., Pa), S. S. Brenner (Pittsburgh Univ., Pa.), and W. A. Soffa (Pittsburgh, Univ., Pa.) 1984 8 p refs Presented at the Microbeam Analysis Soc. Anal. Electron Microscopy Meeting, Bethlehem, Pa., 16 Jul. 1984
(Contract DE-AC05-84OR-21400; Grant NSF DMR-80-22225)
(DE85-005379; CONF-840767-11) Avail: NTIS HC A02/MF A01

Decomposition of Fe-rich Fe-Be alloys is studied by a variety of independent techniques. However, there remains some uncertainty concerning the coarsening behavior of the decomposed structure. A comparison of results of a combined transmission

electron microscopy (TEM)/atom probe field-ion microscopy (APFIM) study of the development of the modulated microstructure is presented. In addition to the metallurgical aspects of his investigation, an important feature of this research is the emphasis on the application of AEM and FIM as complementary research techniques. DOE

N85-22679# Pacific Northwest Lab., Richland, Wash.
ROLE OF SEGREGATED P AND S IN INTERGRANULAR STRESS CORROSION CRACKING OF NICKEL
R. H. Jones, M. J. Danielson, and D. R. Baer Oct. 1984 15 p refs Presented at the ASM Intern. Conf. on Corrosion of Nickel Base Alloys, Cincinnati, 23-25 Oct. 1984
(Contract DE-AC06-76RL-01830)
(DE85-004547; PNL-SA-12341; CONF-8410208-2) Avail: NTIS HC A02/MF A01

Effect of P and S on the intergranular corrosion and stress corrosion of Ni was evaluated with corrosion tests, crack tip corrosion modeling and stress corrosion tests and modeling. Corrosion tests were conducted on Ni + P and Ni + S alloys and Ni samples ion implanted with P and S. It is shown that both P and S reduce passivity in Ni and enhanced the corrosion rate but that P is oxidized and dissolves in the electrolyte while S remains on the surface. This difference in surface behavior of P and S was used to explain the difference in IGC and IGSCC behavior of Ni + P and Ni + S. It is suggested that active crevice and crack walls with Ni + S reduce the concentration gradient and hence the transport of Ni(+2) from tip to mouth which in turn reduces crack tip corrosion rate. The geometry, potential dependence and rates of IGC and IGSCC of Ni + P were compared and it is concluded that IGSCC is not controlled solely by anodic dissolution but that a mechanical contribution is involved. Strain assisted corrosion is ruled out while a corrosion assisted intergranular fracture process is shown to be feasible. E.A.K.

N85-22680# Wisconsin Univ., Madison.
REACTION OF AMORPHOUS NiNb FILMS WITH CRYSTALLINE METAL OVERLAYERS
E. A. Dobisz, B. L. Doyle, J. H. Perepezko, J. D. Wiley, and P. S. Peercy 1984 6 p refs Presented at the Symp. on the Scientific Basis for Nucl. Waste Management, Boston, 26 Nov. 1984 Prepared in cooperation with SNL, Albuquerque, N. Mex.
(Contract DE-AC04-76DP-00789; Grant DE-FG02-84ER-45096)
(DE85-005483; SAND-84-1292C; CONF-841157-53) Avail: NTIS HC A02/MF A01

In many cases the stability of amorphous films is influenced by interaction with metallic crystalline overlayers. Such interactions between Au, Ni, Nb and Ta overlayers and a-(Ni-Nb) films are reported. During interdiffusion Au overlayers acted with a-(Ni-Nb) to form two different adjacent crystalline layers. In order to study the influence of relaxation of the amorphous films on overlayer reaction several a-(Ni-Nb) samples were pre-annealed prior to Au deposition. High depth resolution Rutherford Backscattering Spectrometry (RBS) demonstrate that preannealing lowers the diffusion coefficient of Au in a-(Ni-Nb) at 450 C from 7.5x10(-22) m(2)/s to 8.7x10(-23) m(2)/s. During interdiffusion Ta was discovered to be substantially more inert than Au. For example, negligible interdiffusion between Ta and a-(Ni-Nb) at 505 C after 25 hours implies a diffusivity of less than 5x10(-24) m(2)/s. These observations allow assessment of some of the requirements for increasing the stability of crystalline-amorphous metal film layered structures. DOE

N85-22681# Oak Ridge National Lab., Tenn.
FIRST PRINCIPLES THEORY OF FERMI-SURFACE DRIVEN CONCENTRATION WAVES IN Cu/SUB C/Pd/SUB 1-c/ ALLOYS
G. M. Stocks, J. Wadsworth, and B. L. Gyorffy 1984 3 p refs Presented at the Symp. on the Scientific Basis for Nucl. Waste Management, Boston, 26 Nov. 1984 Prepared in cooperation with Bristol Univ., England
(Contract DE-AC05-84OR-21400)
(DE85-005367; CONF-841157-43) Avail: NTIS HC A02/MF A01

The first principles methods are based on the use of the Korringa-Kohn-Rostoker coherent-potential approximation (KKR-CPA). A mean-field theory of ordering in alloys was developed based on the KKR-CPA method for treating the underlying electronic structure. Contour maps are presented for the short-range order diffuse scattering from Cu(sub c)Pd(sub 1-c) alloys. The expression for (ALPHA)(K) is dominated by a contribution from the Fermi energy. The concentration waves are Fermi-surface driven. DOE

N85-22682# Brookhaven National Lab., Upton, N. Y.
MICROSCOPIC MAGNETIC STRUCTURE OF MULTIPLE BILAYERS OF THIN FILMS OF Fe AND Ge
C. F. Majkrzak, J. D. Axe, and P. Boeni Oct. 1984 18 p refs Presented at the 30th Ann. Conf. on Magnetism and Magnetic Mater., San Diego, Calif., 27 Nov. 1985
(Contract DE-AC02-76CH-00016; Grant NSF PCM-77-01133)
(DE85-004188; BNL-35481; CONF-841184-27) Avail: NTIS HC A02/MF A01

Multiple bilayers consisting of thin films of Fe and Ge with bilayer thicknesses down to 40 A were made by sputter deposition. It is found that the Ge layers are amorphous while the Fe layers are microcrystalline with > directions perpendicular to the plane of the substrate but with orthogonal directions in the plane randomly rotated about this axis. Neutron scattering measurements using a polarized beam were performed to study the Fe magnetism, particularly at the interface with the Ge. These data combined with X-ray diffraction data indicate a reduction in the moment of a fraction of the Fe atoms due primarily to interdiffusion at the interface. DOE

N85-22683# Los Alamos Scientific Lab., N. Mex. Materials Science and Technology Div.
AMERICIUM METAL PREPARATION ON THE MULTIGRAM SCALE
J. G. Reavis, S. A. Apgar, III, and L. J. Mullins 1984 14 p refs Presented at the Intern. Chem. Congr. of Pacific Basin Soc., Honolulu, 16 Dec. 1984
(Contract W-7405-eng-36)
(DE85-003735; LA-UR-84-3755; CONF-841210-6) Avail: NTIS HC A02/MF A01

Americium metal of approxiomately 99.5% purity can be produced on the 20 to 25-q scale by lanthanum reduction of the oxide in a very simple apparatus. As predicted from relative vapor pressures, volatile metal impurities such as calcium and magnesium accompany the americium during distillation. The major impurity detected was lanthanum at a concentrated predicted for the equilibrium vapor composition above lanthanum metal containing 1% americium. It is speculated that higher purity americium might be produced if distillation were to be discontinued earlier, with no attempt at quantitative recovery of the metal. DOE

N85-22684# Hanford Engineering Development Lab., Richland, Wash.
EFFECTS OF NEUTRON IRRADIATION AT 450(0)C AND 16 DPA ON THE PROPERTIES OF VARIOUS COMMERCIAL COPPER ALLOYS
H. R. Brager, H. L. Heinisch, and F. A. Garner Oct. 1984 11 p refs Presented at 1st Intern. Conf. on Fusion Reactor Mater., Tokyo, Japan, 3 Dec. 1984
(Contract DE-AC06-76FF-02170)
(DE85-005716; HEDL-SA-3174-FP; CONF-841246-18) Avail: NTIS HC A02/MF A01

High-purity copper and eight copper alloys were irradiated to approx. 16 dpa at approx. 450 C in the MOTA experiment in FFTF. These alloys were also examined after aging at 400 C for 1000 hours. The radiation-induced changes in the electrical condutivity, tensile properties and density were measured and compared to those of the aged materials. The changes in conductivity can be either positive or negative depending on the alloy. Changes in tensile properties of most, but not all, of the alloys seem to be primarily dependent on thermal effects rather than the effect of atomic displacements. Radiation at 450 C induced

changes in density varying from 0.66% densification to 16.6% swelling. The latter occurred in Cu-0.1% Ag and implies a swelling rate of at least approx. 1%/dpa. DOE

N85-22685# Bendix Corp., Kansas City, Mo.
DEVELOPMENT OF A SINTERED SHIM
R. Owens Jan. 1985 26 p ref
(Contract DE-AC04-76DP-00613)
(DE85-006183; BDX-613-3168) Avail: NTIS HC A03/MF A01

A shim used at Bendix Kansas City currently is machined from stainless steel wrought stock. This configuration also has been produced by the powder metallurgy (PM) process in net shape. The PM shape is slightly different because a 0.0762 mm (0.003 in.) step on a critical load-bearing surface was necessary for tool considerations. Speculation that this ridge would cut through the mating part was eliminated during physical testing. The tests simulated the loading of a set of wrought shims and a set of PM shims. During gross overloading of the assemblies, the PM assmbly failed at a higher load than the wrought parts. The mating parts showed no signs of the step cutting into the strap; failure in all cases occurred at a military specification hex head bolt which currently is used in production. DOE

N85-22686# Oak Ridge National Lab., Tenn.
MAGNETIC STUDIES OF Ni3Al(Fe) COMPOUNDS
S. T. Sekula, H. R. Kerchner, J. R. Thompson, and T. Leventouri Nov. 1984 9 p refs Presented at Mater. Res. Soc. Ann. Meeting, Boston, 26 Nov. 1984
(Contract DE-AC05-84OR-21400)
(DE85-005262; CONF-841157-58) Avail: NTIS HC A02/MF A01

Samples of the ordered intermetallic compound with the L12 structure and chemical composition Ni(sub 075-x)Al(sub 0.25-x)Fe (sub 2x) (doped with 0.2 at. % B) were studied over an Fe compositional range 0 less than or equal to 2x less than or equal to 0.20. For the greater Fe concentrations more conventional ferromagnetic systems are obtained. Well below the ferromagnetic Curie temperature T(sub c) the samples exhibit a spontaneous moment in small magnetic fields and at higher fields the isothermal magnetization data show a clear tendency toward saturation. The Curie temperature was found to increase from about 50 K for the Fe-free sample in the series to 410 K for the limiting concentration of 12 at. % Fe in the L12 structure. Samples with higher Fe content up to 20 at. % contain a second, disorder fcc phase with T(sub c) = or about 715 K. Peaks in the temperature dependence of the lattice parameter observed in x-ray studies yield T(sub c) values in reasonable agreement with the magnetic measurements. E.A.K.

N85-22687# Argonne National Lab., Ill.
GRAIN BOUNDARIES IN NiO
K. L. Merkle, J. F. Reddy, and C. L. Wiley 1984 8 p refs Presented at the Materials Res. Soc. Ann. Meeting, Boston, 26 Nov. 1984
(Contract W-31-109-eng-38)
(DE85-006129; CONF-841157-66) Avail: NTIS HC A02/MF A01

Defocus-imaging and high-resolution electron microscopy (HREM) are used to study tilt grain boundaries (GB) in NiO near the .001> axis over the whole range of possible misorientation. Faceting and structural periodicities within facets are observed in high- and low-angle GBs. A reduced atomic density at high-angle GBs is suggested by the defocus behavior. DOE

N85-22688# Joint Publications Research Service, Arlington, Va.
USSR REPORT: MATERIALS SCIENCE AND METALLURGY
6 Feb. 1985 81 p refs Transl. into ENGLISH from various Russian articles
(JPRS-UMS-85-002) Avail: NTIS HC A05/MF A01

News items, abstracts, and scientific reports on aspects of materials science and metallurgy including aluminum and its alloys, composite materials, energy effects; ferrous metallurgy; welding; titanium; superalloys; heat treatment; powder metallurgy; and steels are contained. For individual titles, see N85-22689 through N85-22751.

N85-22689# Joint Publications Research Service, Arlington, Va.
DEPENDENCE OF SUPERPLASTIC FLOW ON STATE OF GRAIN BOUNDARIES Abstract Only
O. A. Kaybyshev, R. Z. Valiyev, and N. K. Tsenev *In its* USSR Rept.: Mater. Sci. and Met. (JPRS-UMS-85-002) 6 Feb. 1985 p 1-2 Transl. into ENGLISH from Dokl. Akad. Nauk SSSR (USSR), v. 278, no. 1, Sep. 1984 p 93-97 (For primary document see N85-22688 13-26)
Avail: NTIS HC A05/MF A01

An experimental study of Al+ 2 atom.% Mg+ 0.10 atom.% Zr and Al+ 2 atom.% Cu+ 0.16 atom.% Zr was made for the purpose of determining the dependence of superplastic flow with attendant grain fragmentation on the state of grain boundaries. Specimens of these two alloys are producible with an equally ultrafine initial grain size but different initial states of the grain boundaries. An alloy with specially oriented grain boundaries will have worse superplastic characteristics than one with plain disoriented grain boundaries, because of weaker absorption of lattice dislocations and resulting slower slippage of grain boundaries. G.L.C.

N85-22690# Joint Publications Research Service, Arlington, Va.
FATIGUE AND CORROSION FATIGUE RESISTANCE OF ALUMINUM CASTING ALLOY VAL10 AND FORGING ALLOY AK6 Abstract Only
A. V. Karlashov, A. D. Gnatyuk, V. M. Polishchuk, and V. M. Beletskiy *In its* USSR Rept.: Mater. Sci. and Met. (JPRS-UMS-85-002) 6 Feb. 1985 p 2 Transl. into ENGLISH from Fiz.-Khim. Mekh. Materialov (USSR), v. 20, no. 4, Jul-Aug. 1984 p 47-49 (For primary document see N85-22688 13-26)
Avail: NTIS HC A05/MF A01

Results are presented from experimental studies of the influence of a 3% aqueous NaCl solution on the fatigue resistance to fracture upon cyclical loading of aluminum casting alloy VAL10 and forging alloy AK6, selected for comparison. The new alloy VAL10 is quite promising in terms of mechanical properties for casting important load bearing parts of products. The formable alloy AK6 is the closest in its static loading properties to VAL10. VAL10, having significantly less fatigue resistance in air than forging alloy AK6, does have satisfactory yield point in a corrosive medium with a long test base, 30% lower than AK6, and can therefore be used for the manufacture of lightly loaded parts. Author

N85-22691# Joint Publications Research Service, Arlington, Va.
STRUCTURAL STRENGHT OF STRIP D16T ALUMINUM ALLOY WITH LOW COPPER AND MAGNESIUM CONTENT Abstract Only
G. S. Neshpor, A. A. Armyagov, and G. I. Berezhnaya *In its* USSR Rept.: Mater. Sci. and Met. (JPRS-UMS-85-002) 6 Feb. 1985 p 2-3 Transl. into ENGLISH from Problemy Prochnosti (USSR), no. 9, Sep. 1984 p 54-58 (For primary document see N85-22688 13-26)
Avail: NTIS HC A05/MF A01

The static strength and fatigue limits of D16T aluminum alloy containing only 4.17 wt.% Cu and 1.20 wt.% Mg have been determined on the basis of 43 specimens of 1.85-mm-thick plated strip from the same ladle. Specimens of various widths and gauge lengths correspondingly equal to 5.65 /F (F- area of cross section) were tested mechanically for 0.2% yield strength, tensile strength, and percent elongation. The cracking rate under slow cycle (3 Hz) and fast cycle (40 Hz) loads was determined through statistical processing of corresponding data, the fatigue limit in each case being found from the dependence of crack length increment on the cumulative number of cycles with the crack length increasing steeply toward the end of life. Toughness and ductility of fracture were determined from histograms of net stress characterizing the residual strength. The results reveal a correlation between the given strength characteristics and indicate the ranges of their variation, typical of aluminum alloys in this group. Author

N85-22692# Joint Publications Research Service, Arlington, Va.
TEMPERATURE EFFECTS OF HETEROGENIZATED ANNEALING ON STRUCTURE AND PROPERTIES OF V95 ALUMINUM

ALLOY Abstract Only
V. V. Zakharov and Y. N. Kukushkin *In its* USSR Rept.: Mater. Sci. and Met. (JPRS-UMS-85-002) 6 Feb. 1985 p 3 Transl. into ENGLISH from Tsvetnyye Metally (USSR), no. 10, Oct. 1984 p 73-76 (For primary document see N85-22688 13-26)
Avail: NTIS HC A05/MF A01

Heterogenizated annealing of aluminum ingots after homogenization and before pressing is used to increase deformation, at an optimum temperature equal to that of minimal durability. Attempts to explain the deformation increases obtained by this method with solid solutions of Zn, Mg and Co in aluminum, by an electrical conductivity method, are discussed. Additional analysis relates to the morphology of excess phase particles emitted during annealing. Particles larger than 10 mkm did not increase resistance to deformation during pressing or reduce surface purity of semimanufactured products. Thermal and structural findings are summarized. Results showed that the pressure at initiation of pressing followed a curve with a pronounced minimum in a C form. A temperature of 325 C provided effective annealing. Longitudinal mechanical properties did not depend on the annealing temperature. Author

N85-22693# Joint Publications Research Service, Arlington, Va.
ANOMALIES OF ALUMINUM STRUCTURE AND PROPERTIES Abstract Only
G. G. Krushenko and S. I. Torshilova *In its* USSR Rept.: Mater. Sci. and Met. (JPRS-UMS-85-002) 6 Feb. 1985 p 3-4 Transl. into ENGLISH from Dokl. Akad. Nauk SSSR (USSR), v. 278, no. 1, Sep. 1984 p 97-100 Original language document announced as 85A-13456 (For primary document see N85-22688 13-26)
Avail: NTIS HC A05/MF A01

A study has been made of the effect of melt superheating (to 943, 1093, 1223, and 1353 K) on the grain size of A999 aluminum and without additions of other elements (Be, Mg, Si, Ti, Fe, Cu, Mn, and Zr). It is shown that an increase in the heating (and pouring) temperature to 1093 K produces an abrupt coarsening of the grain structure of aluminum in all the specimens studied, irrespective of the type and the amount of the additive. The anomalous grain coarsening is ascribed to the effect of the short range order of aluminum on the formation of the crystalline structure. G.L.C.

N85-22694# Joint Publications Research Service, Arlington, Va.
NEW DEFORMABLE SECONDARY ALUMINUM ALLOYS Abstract Only
G. Y. Goldbukht and S. N. Ananin *In its* USSR Rept.: Mater. Sci. and Met. (JPRS-UMS-85-002) 6 Feb. 1985 p 4-5 Transl. into ENGLISH from Tsvetnyye Metally (USSR), no. 9, Sep. 1984 p 74-76 (For primary document see N85-22688 13-26)
Avail: NTIS HC A05/MF A01

Two secondary aluminum alloys have been developed and tested. The V95-1 alloy belongs in the Al-Cu-Mg-Zn system with up to 1% Fe and 1.5% Si, in chemical composition being intermediate between the two commercial secondary alloys V95-2 and VDI. The AMM alloy belongs in the Al-Mg system and is available in two variants: AMM-1 with 1.4-4.2% Mg and 0.6-1.8% Cu is hardenable by quenching and aging, AMM-2 with 0.8-5.0% Mg and up to 0.5% Cu impurity is not hardenable by heat treatment. Both variants contain silicon (0.3-1.4% and 0.3-2.0% respectively) and zinc (up to 0.8% and 1.5% respectively), and can also contain iron (up to 0.9% and 1.5% respectively). Both variants of the AMM alloy and the V95-1 alloy have been thoroughly tested, after annealing and after hardening, for mechanical characteristics: tensile strength, 0.2% yield strength, percent elongation, resilience, toughness, and fatigue limits. The results have been evaluated statistically. The cost advantage of these secondary alloys over corresponding primary ones is substantial. Author

N85-22695# Joint Publications Research Service, Arlington, Va.
STUDY OF PROCESSES OF MODIFICATION OF Al-Si ALLOYS Abstract Only
G. M. Kimstach, Y. P. Mukhovetskiy, V. Borisov, and S. V. Lobanov *In its* USSR Rept.: Mater. Sci. and Met. (JPRS-UMS-85-002) 6 Feb. 1985 p 5 Transl. into ENGLISH from Metallovedeniye i Termicheskaya Obrabotka Metallov (USSR), no. 8, Aug. 1984 p 57-59 (For primary document see N85-22688 13-26)
Avail: NTIS HC A05/MF A01

The process of modification of hypereutectic Al-Si alloys with phosphorus was studied. It was found that in contrast to sodium, phosphorus does not increase the tendency of Al-Si melts toward gas saturation. Vacuum samples of the liquid metal before and after modification remain compact. Neither sodium nor phosphorus has a significant influence on the process of crystallization of aluminum. The change observed in the nature of crystallization of the Al-Si melt as a result of modification by various modifiers thus results not from an interaction of the atoms of aluminum, but rather primarily from changes in the nature of the Al-Si interaction in the modified alloy. Modification of Al-Si alloys with sodium leads to an increase in the Al-Si bond strength retaining the silicon atoms in the structure of the alloy, thus creating conditions for eutectic silicon particle size reduction. Modification with phosphorus probably causes weakening of the Al-Si chemical interaction, as a result of which the Al-Si bond forces become weaker and in the process of crystallization of the modified melt the silicon atoms are expelled from the bond with aluminum. This changes the conditions of birth of silicon crystallization centers and their growth. Author

N85-22696# Joint Publications Research Service, Arlington, Va.
USE OF ACOUSTICAL EMISSION METHOD TO STUDY SPECIFICS OF FRACTURE OF BORON REINFORCED PLASTIC STRUCTURAL ELEMENTS Abstract Only
V. A. Strizhalov, Y. V. Dobrovolskiy, M. P. Zemtsov, and S. I. Likhatskiy *In its* USSR Rept.: Mater. Sci. and Met. (JPRS-UMS-85-002) 6 Feb. 1985 p 5-6 Transl. into ENGLISH from Problemy Prochnosti (USSR), no. 8, Aug. 1984 p 26-32 Original language document announced as 84A-47443 (For primary document see N85-22688 13-26)
Avail: NTIS HC A05/MF A01

The short term strength of tubular metal specimens with a boron composite core has been determined experimentally using the acoustic emission method. An analysis of typical acoustic emission diagrams yields information on the contributions of the fracture of the individual structural components to the formation of the integral acoustic signal. It is shown that in both tension and compression, the fracture of the boron fibers is responsible for the largest contribution to the acoustic signal. It is noted that the acoustic emission method can be used for detecting the initial stages of microfracture in structures of this kind. V.L. (IAA)

N85-22697# Joint Publications Research Service, Arlington, Va.
ALUMINUM ALLOY ATs5K5 (5% Zn + 5% Ca) FOR SUPERPLASTIC FORMING Abstract Only
V. K. Portnoy, B. N. Stepanov, A. M. Liskin, and V. M. Ilyenko *In its* USSR Rept.: Mater. Sci. and Met. (JPRS-UMS-85-002) 6 Feb. 1985 p 6 Transl. into ENGLISH from Tsvetnyye Metally (USSR), no. 9, Sep. 1984 p 72-74 (For primary document see N85-22688 13-26)
Avail: NTIS HC A05/MF A01

A new aluminum alloy with 5% Zn and 5% Ca has been developed for superplastic forming which, unlike the special Supral alloy, can be produced with moderate cooling rates during crystallization in the semicontinuous casting process. Ingots of these alloys were produced by continuous casting at rates of 60-100 mm/min into a tilt crystallizer at 700-720 C. For microstructural analysis of the eutectic alloy, ingots were fragmented into strips by successively hot and cold rolling. This alloy was found to have high resistance to parting and general corrosion, low sensitivity to intergranular and pitting corrosion, and high resistance to corrosion cracking with attendant low residual stress and large residual sag. The hypereutectic alloy has the least percent elongation, evidently because of microvoids clustering around Al(3)ZnCa phasr grains, despite its high sensitivity of flow stress to strain rate. All three alloys are weldable, especially under pressure, and can be anodized or aluminum clad for surface coloration. G.L.C.

N85-22698# Joint Publications Research Service, Arlington, Va.
USES OF COMPOSITE MATERIALS **c24**
V. Dovidenas *In its* USSR Rept.: Mater. Sci. and Met. (JPRS-UMS-85-002) 6 Feb. 1985 p 7-10 Transl. into ENGLISH from Komsomolskaya Pravda (USSR), no. 93, 12 May 1984 p 3 (For primary document see N85-22688 13-26)
Avail: NTIS HC A05/MF A01

The use of composite materials in the design of automobiles, ships, aircraft, and spacecraft is described. Weight reduction and durability are two advantages of composite materials. Also discussed were the advantages of glass fiber reinforced plastics and carbon fiber reinforced plastics. B.G.

N85-22699# Joint Publications Research Service, Arlington, Va.
INFLUENCE OF 3% NaCl SOLUTION ON RATE OF ACCUMULATION OF DAMAGE AND RESIDUAL STRENGTH OF ALUMINUM-BORON COMPOSITE Abstract Only **c24**
V. S. Utkin and I. A. Podolnyy *In its* USSR Rept.: Mater. Sci. and Met. (JPRS-UMS-85-002) 6 Feb. 1985 p 12 Transl. into ENGLISH from Fiz.-Khim. Mekh. Materialov (USSR), v. 20, no. 4, Jul.-Aug. 1984 p 52-55 Original language document announced as 84A-48637 (For primary document see N85-22688 13-26)
Avail: NTIS HC A05/MF A01

Specimens of a unidirectional composite consisting of an AD33 aluminum alloy matrix reinforced with boron fibers were fatigued in pure symmetrical bending at 0.83 Hz in air and in a 3-percent NaCl solution. Experimental results were processed statistically with a confidence level of 90 percent. It is shown that the rate of damage accumulation increases with the initial amplitude and is significantly higher in the NaCl solution than in air. It is also shown that in aggressive media the rate of damage accumulation in the composite can be substantially reduced by using corrosion inhibitors, such as potassium chromate. V.L. (IAA)

N85-22700# Joint Publications Research Service, Arlington, Va.
DEVELOPMENT AND STUDY OF TWO-MATRIX GLASS FIBER COMPOSITE WITH INCREASED TRANSVERSE DEFORMATION Abstract Only **c24**
V. V. Vasilyev and V. A. Salov *In its* USSR Rept.: Mater. Sci. and Met. (JPRS-UMS-85-002) 6 Feb. 1985 p 12-13 Transl. into ENGLISH from Mekh. Kompozitnykh Materialov (USSR), no. 4, Jul.-Aug. 1984 p 662-666 (For primary document see N85-22688 13-26)
Avail: NTIS HC A05/MF A01

The increases of effectiveness and the expansion of the area of application of composite material requires the increase of limiting deformation of unidirectional materials in transverse extension. The natural means to transverse deformation is to increase the maximum deformation of the polymer binder. Increasing the deformation and decreasing Poisson's ratio of the binder allows production of a composite with the necessary transverse deformation. Separation of the function of one binder among two is suggested. In the first stage, glass fiber is saturated with a rigid binder and fully secured. In the second stage coils of these composite fibers are used to construct a material based on an elastic binder by the traditional method. In the three-component material thus produced the rigid binder supports joint work of monofilaments, the elastic binder provides the necessary transverse deformation of the unidirectional materials. E.A.K.

N85-22701# Joint Publications Research Service, Arlington, Va.
TESTING OF WOUND MATERIALS FOR STRENGTH WITH LOADING IN THE REINFORCEMENT PLANE Abstract Only **c24**
V. Nikolayev and V. D. Popov *In its* USSR Rept.: Mater. Sci. and Met. (JPRS-UMS-85-002) 6 Feb. 1985 p 13 Transl. into ENGLISH from Mekh. Kompozitnykh Materialov (USSR), no. 4, Jul.-Aug. 1984 p 713-718 Original language document announced as 84A-47993 (For primary document see N85-22688 13-26)
Avail: NTIS HC A05/MF A01

In order to prevent the buckling of relatively thin-walled filament-wound composite specimens during testing under external hydrostatic pressure, it is proposed that reinforcing elements be used on the outside of the test section. It is also recommended that the shear strength of tubular specimens in the layer plane be evaluated by using a special fixture whose parts can move relative to each other in the axial direction. Test results and the results of their statistical analysis are presented. V.L. (IAA)

N85-22702# Joint Publications Research Service, Arlington, Va.
EFFECT OF PHASE STATE OF TiC-NiTi POWDER COMPOSITE MATERIALS ON NATURE OF FAILURE AND MECHANICAL PROPERTIES Abstract Only **c24**
S. N. Kulkov, T. M. Poletika, A. Y. Chukhlomlin, and V. Y. Panin *In its* USSR Rept.: Mater. Sci. and Met. (JPRS-UMS-85-002) 6 Feb. 1985 p 13-14 Transl. into ENGLISH from Poroshkovaya Metallurgiya (USSR), no. 8, Aug. 1984 p 88-92 Original language document announced as 84A-48645 (For primary document see N85-22688 13-26)
Avail: NTIS HC A05/MF A01

A method is proposed for calculating stress intensity factors for TiC-NiTi composites. It is shown that the use of an alloy with martensitic transformations (NiTi) as the matrix makes it possible to substantially improve the ductile properties of the material. The principal mechanical characteristics of the composite (e.g., the ultimate strength in bending and compression, the plastic deformation limit, and hardness) are determined over a wide range of the hard fraction content. The effect of titanium additons on the phase composition and fracture mode of the composite is discussed. V.L. (IAA)

N85-22703# Joint Publications Research Service, Arlington, Va.
DISSIPATION OF ENERGY IN COMPOSITE MATERIAL Abstract Only **c24**
I. K. Arkhipov, S. A. Golovin, and G. D. Petrushin *In its* USSR Rept.: Mater. Sci. and Met. (JPRS-UMS-85-002) 6 Feb. 1985 p 14 Transl. into ENGLISH from Problemy Prochnosti (USSR), no. 8, Aug. 1984 p 92-94 (For primary document see N85-22688 13-26)
Avail: NTIS HC A05/MF A01

The relationship between stress and strain for uniaxial cyclical loading was studied by, assuming cyclical hardening of the matrix material. It is indicated that the theoretical model suggested for the behavior of composite materials satisfactorily describes the actual process of energy dissipation upon fluctuation of heterogeneous materials. The divergence between experimental and calculated internal scattering is explained by the influence of magnetoelastic effects appearing on cyclical deformation of ferromagnetic materials in the form of a maximum at high values of stress amplitudes. E.A.K.

N85-22704# Joint Publications Research Service, Arlington, Va.
DIVISION BOUNDARY IN Al-B COMPOSITE MATERIAL WITH BORON IN CONTACT WITH SOLID AND LIQUID ALUMINUM Abstract Only **c24**
B. A. Afefyev, A. Rebrov, and T. B. Zhurkova *In its* USSR Rept.: Mater. Sci. and Met. (JPRS-UMS-85-002) 6 Feb. 1985 p 15 Transl. into ENGLISH from Metallovedeniye i Termicheskaya Obrabotka Metallov (USSR), no. 8, Aug. 1984 p 15-17 (For primary document see N85-22688 13-26)
Avail: NTIS HC A05/MF A01

The influence of temperature and force factors on processes occurring at the fiber-matrix boundary in the production of an aluminum-boron composite material was determined. The division boundary in the composite, obtained by rolling of a batch of monolayers of matrix and reinforcing material and in specimens produced by soaking a bundle of fibers in liquid metal, was studied. During heat treatment, the phase AlB2 was found at the spinel-matrix boundary; upon liquid phase saturation, the phase AlB2 is formed in an actual composite material with an unalloyed matrix, decreasing fiber strength, while alloying of the matrix with magnesium decreases the quantity of interaction products and changes the phase composition of the transition zone. E.A.K.

N85-22705# Joint Publications Research Service, Arlington, Va.
ESTIMATING DEGREE OF DEVELOPMENT OF PHYSICAL-

CHEMICAL INTERACTION AMONG COMPONENTS IN Al-B FIBER COMPOSITE MATERIAL Abstract Only c24

M. K. Shorshorov, V. A. Kolesnichenko, and I. V. Kocheshkov *In its* USSR Rept.: Mater. Sci. and Met. (JPRS-UMS-85-002) 6 Feb. 1985 p 15 Transl. into ENGLISH from Metallovedeniye i Termicheskaya Obrabotka Metallov (USSR), no. 8, Aug. 1984 p 11-15 (For primary document see N85-22688 13-26)
Avail: NTIS HC A05/MF A01

The influence of degree of development of physical and chemical interactions at the fiber-matrix division boundary on the strength characteristics of A1-B composite materials was analyzed. The most promising method of estimating the degree of development of physical-chemical interaction between components of the composite based on results of shear strength testing of the material is discussed. The method of estimating the degree of physical-chemical interaction based on the relative bonding strength of the fibers with the matrix is simple and provides reliable results. The relative strength can be used to estimate the degree of physical-chemical interaction between fibers and matrix only if there are no intermetallide compounds in the area of interaction. E.A.K.

N85-22706# Joint Publications Research Service, Arlington, Va.
SEGREGATION OF SILICON IN SILUMIN-CARBON FIBER COMPOSITES Abstract Only c24

T. A. Chernyshova, L. I. Kobeleva, M. I. Tylkina, and A. Rebrov *In its* USSR Rept.: Mater. Sci. and Met. (JPRS-UMS-85-002) 6 Feb. 1985 p 16 Transl. into ENGLISH from Metallovedeniye i Termicheskaya Obrabotka Metallov (USSR), no. 8, Aug. 1984 p 24-26 (For primary document see N85-22688 13-26)
Avail: NTIS HC A05/MF A01

The reaction products at the interface boundary in composites of Al or the alloy Al2 containing about 12% Si and type LU carbon belt were studied. Specimens produced by vacuum compression saturation of the belt with the melt and model specimens using 40 micron diameter carbon monofibers were analyzed. Microstructure was studied on a microscope, distribution of elements in specimens with a microanalyzer, interaction products at the interphase boundary by electron microscope examination of extraction carbon replicas. Crystals of silicon carbide and primary crystals of silicon are observed on the surface of carbon fibers in the composites, which means the total content of aluminum carbide in the composite is decreased. E.A.K.

N85-22707# Joint Publications Research Service, Arlington, Va.
POSSIBILITY OF PRODUCING MONOLITHIC COMPOSITE MATERIALS BASED ON NIOBIUM CARBIDE Abstract Only c24

V. V. Ploshkin, I. Y. Ulyanina, and V. P. Filonenko *In its* USSR Rept.: Mater. Sci. and Met. (JPRS-UMS-85-002) 6 Feb. 1985 p 16 Transl. into ENGLISH from Metallovedeniye i Termicheskaya Obrabotka Metallov (USSR), no. 8, Aug. 1984 p 26-27 (For primary document see N85-22688 13-26)
Avail: NTIS HC A05/MF A01

A composite material based on niobium carbide with good heat resistance, erosion and chemical stability in special media, capable of withstanding great thermal shock was created. The initial material used was a powder of niobium carbide with particle size less than 10 micron; the binder consisted of particles of pure copper in the 10 to 12 micron fraction, which sublimates upon thermal shock and helps to decrease the temperature of parts. Copper also does not interact with niobium carbide under any conditions. The niobium carbide-copper composite was manufactured by the high-pressure method. Sintering under high pressure produced practically monolithic composites with minimal porosity. The major phases were uniformly distributed through the specimens and did not interact with each other. The composite material has good thermal shock resistance and is not subject to brittle fracture as are materials of this type produced by other methods. E.A.K.

N85-22708# Joint Publications Research Service, Arlington, Va.
ADEQUACY OF METAL ABLATION PROCESS WITH LASER RADIATION AND A SHOCK-COMPRESSED PLASMA Abstract Only

M. A. Sultanov *In its* USSR Rept.: Mater. Sci. and Met. (JPRS-UMS-85-002) 6 Feb. 1985 p 18 Transl. into ENGLISH from Fiz. i Khim. Obr. Mater. (USSR), no. 4, Jul.-Aug. 1984 p 35-38 (For primary document see N85-22688 13-26)
Avail: NTIS HC A05/MF A01

Mechanisms of interaction of a shock-compressed plasma and laser radiation with various metals are compared. It is noted that the origin of the radiation is not significant in the process of ablation of metals. When a supersonic plasma stream strikes a flat solid metal obstacle, a shock-compressed plasma is formed, in which radiation is greatly retarded due to the collisions among electrons and ions. In the quasisteady laser mode there are many peaks, the intensity and number of which decrease during the course of radiation. The unsteadiness of the process results from the nature of operation of the laser and heterogeneous distribution of light radiation intensity. When laser radiation and a moderate density plasma interact with metals the mechanism of destruction of the metals is somewhat similar. In both cases the process of interaction is accompanied by gas dynamic effects. The mechanism of ablation of metals under the influence of radiation is thermal in nature. E.A.K.

N85-22709# Joint Publications Research Service, Arlington, Va.
BREAKDOWN OF THIN PLATES BY RADIATION Abstract Only

V. P. Ageyev, M. V. Isakov, V. A. Martynov, V. V. Morozov, and V. V. Chernomordik *In its* USSR Rept.: Mater. Sci. and Met. (JPRS-UMS-85-002) 6 Feb. 1985 p 18-19 Transl. into ENGLISH from Fiz. i Khim. Obr. Mater. (USSR), no. 5, Sep.-Oct. 1984 p 9-11 (For primary document see N85-22688 13-26)
Avail: NTIS HC A05/MF A01

Heating of thermally thin plates by radiation till breakdown of the material during air blast or natural convection is analyzed phenomenologically. A thin plate has a temperature drop across the thickness much smaller than the mean temperature rise. The equation of heat balance is solved for two possible kinds of such plates. In the case of optically transparent materials heating is determined principally by absorption of radiation in the volume and intensity of incident radiation, R- reflection coefficients. The equation are solved for the threshold intensity of incident radiation which will break down the material at any temperature. With application of the mean-value theorem and linear approximation of the exponent in the relation for total incident radiation energy I sub (in) zeta, numerical calculations were made for polyethylene and polyethylene terephthalate (Mylar) films and for aluminum foils. E.A.K.

N85-22710# Joint Publications Research Service, Arlington, Va.
THEORY OF RELAXATION PROCESSES IN DECOMPOSING POLYMER MATERIALS DURING HIGH-INTENSITY CONVECTIVE HEATING Abstract Only c27

G. N. Isakov, V. V. Nesmelov, G. Y. Vishnevskiy, and Y. N. Zadorina *In its* USSR Rept.: Mater. Sci. and Met. (JPRS-UMS-85-002) 6 Feb. 1985 p 19 Transl. into ENGLISH from Dokl. Akad. Nauk SSSR (USSR), v. 278, no. 5, Oct. 1984 p 1112-1115 Original language document announced as 85A-15559 (For primary document see N85-22688 13-26)
Avail: NTIS HC A05/MF A01

The thermal breakdown of polymer materials is described mathematically with the breakdown process treated as a physio-chemical relaxation process associated with the mobility of the structural components of the molecular and hypermolecular subsystems. The mathematical problem of thermal breakdown during convective heating is reduced, assuming a constant transfer coefficient, to that of solving the equation of energy in solids of different symmetries and equations of chemical kinetics. The results obtained are found to be in good agreement with experimental data for polymethyl methacrylate and a polymer-based composite. V.L. (IAA)

N85-22711# Joint Publications Research Service, Arlington, Va.
EFFECT OF TRANSPARENT COATINGS ON GENERATION OF LASER-INDUCED SHOCK WAVES IN METALS Abstract Only

B. M. Zhiryakov and V. F. Obesnyuk *In its* USSR Rept.: Mater. Sci. and Met. (JPRS-UMS-85-002) 6 Feb. 1985 p 20-21 Transl. into ENGLISH from Fiz. i Khim. Obr. Mater. (USSR), no. 5, Sep. - Oct. 1984 p 29-33 (For primary document see N85-22688 13-26)
Avail: NTIS HC A05/MF A01

An experimental study with a Q-switched laser generating short pressure pulses for surface treatment of metals was made, of particular interest being measurement of pressure near the interaction epicenter with instruments more precise than a conventional piezoelectric quartz crystal. Foils and slabs of copper, brass, and aluminum were used as targets, their polished surfaces being covered with a dielectric liquid (distilled water or machine oil). A thin, strongly absorbing opaque layer formed at the metal-dielectric interface under impact of a giant radiation pulse and expanded rapidly during as well as after that pulse. One experiment measured the propagation of the shock wavefront. In another experiment a layer of liquid was placed on the metal surface covering an area much larger than just the light spot. Its thickness was varied, for measurement of the rate of its dispersal by laser-induced hock waves. The experimental data correlate well with theoretical calculations based on thermodynamics of shock waves and on heat balance. B.W.

N85-22712# Joint Publications Research Service, Arlington, Va.
DECOMPOSITION OF VTAN ALLOY SOLID SOLUTION UPON IRRADIATION AND THERMAL AGING Abstract Only
L. I. Ivanov, V. M. Lazorenko, Y. M. Platov, and S. V. Simakov *In its* USSR Rept.: Mater. Sci. and Met. (JPRS-UMS-85-002) 6 Feb. 1985 p 21 Transl. into ENGLISH from Fiz. i Khim. Obr. Mater. (USSR), no. 4, Jul.-Aug. 1984 p 27-30 (For primary document see N85-22688 13-26)
Avail: NTIS HC A05/MF A01

The alloy VTAN (VCTiNbN) is a dispersion hardened alloy which retains good mechanical properties up to 800 C. This article presents results of electron microscope studies of the structures of VTAN after various types of thermal and radiation aging. Specimens were preliminarily vacuum annealed and cooled at about 1 C/second. It is found that the good mechanical properties of this alloy are related not only to the presence of a TiN crystallization phase, but also the presence of a finely dispersed Ti(Nb, V)N phase formed during aging. Decomposition of the alloy upon bombardment is accompanied by the formation of a modulated structure not observed with thermal aging. B.W.

N85-22713# Joint Publications Research Service, Arlington, Va.
INFLUENCE OF LASER TREATMENT OF STRUCTURE AND MECHANICAL PROPERTIES IF MA21 ALLOY Abstract Only
R. K. Kalimullin, Y. Y. Kozhevnikov, I. Y. Fayzullin, and V. V. Valuyev *In its* USSR Rept.: Mater. Sci. and Met. (JPRS-UMS-85-002) 6 Feb. 1985 p 29 Transl. into ENGLISH from Metallovedeniye i Termicheskaya Obr. Metallov (USSR), no. 9, Sep. 1984 p 31-34 (For primary document see N85-22688 13-26)
Avail: NTIS HC A05/MF A01

An attempt was made to use very rapid heating and cooling obtained by laser surface heat treatment to increase the strength of cast magnesium alloy MA21 containing about 8% Li, 5% Al, 4% Cd, 1% Zn and 0.4% Mn. Test specimens were irradiated in the hot pressed state of a continuous CO2 laser and a pulsed laser. The microstructure of these alloys was studied on an optical microscope, fractographic analysis of specimens performed on an electron microscope by a two-step replica method. Mechanical testing, visual examination of specimens and measurement of microhardness indicated that the strength properties of the alloy were improved by laser treatment due to the formation of a hardened layer on the surface of the specimen. Ductility is reduced. The structure of the surface layer after laser treatment features fine grains and uniform distribution of phases through the volume. Author

N85-22714# Joint Publications Research Service, Arlington, Va.
SPECIFICS OF LASER HEAT TREATMENT OF HIGH STEEL TOOLS Abstract Only
V. S. Dyachenko, G. N. Terdokhlebov, and A. A. Korosteleva *In its* USSR Rept.: Mater. Sci. and Met. (JPRS-UMS-85-002) 6 Feb. 1985 p 29-30 Transl. into ENGLISH from Metallovedeniye i Termicheskaya Obr. Metallov (USSR), no. 9, Sep. 1984 p 25-28 (For primary document see N85-22688 13-26)
Avail: NTIS HC A05/MF A01

A study is made of the influence of laser radiation pulse power densities on the structure, hardness and wear resistance of high speed steel. Experiments were performed on plates of R9K5 steel following standard heat treatment, hardening and triple tempering at 550 C. The cutting tips of the specimens were irradiated on the back face by laser pulses of various strengths, each cutting tip irradiated with a single pulse. The structure and microhardness were studied in the immediate vicinity of the cutting edge. The results indicate that depending on power density W sub P, laser heat treatment may increase or decrease wear resistance. Positive results are achieved after treatment with a pulse with a power density which must be experimentally determined in each case. The optimal power must be selected from the structure of the steel, which should be a martensite-carbide mixture formed as a result of secondary hardening under the influence of the laser pulse. Author

N85-22715# Joint Publications Research Service, Arlington, Va.
HIGH TEMPERATURE ANTIFRICTION PROPERTIES OF TI SUB 1-SUB XNb SUB X C SUB 0.5N SUB 0.5 ALLOYS Abstract Only
Y. G. Tkachenko, S. S. Ordanyan, V. K. Yulyugin, D. Z. Yruchenko, I. B. Panteleyev, and L. G. Maskhuliya *In its* USSR Rept.: Mater. Sci. and Met. (JPRS-UMS-85-002) 6 Feb. 1985 p 42 Transl. into ENGLISH from Poroshkovaya Metallurgiya (USSR), no. 8, Aug. 1984 p 81-84 (For primary document see N85-22688 13-26)
Avail: NTIS HC A05/MF A01

The basic process controlling antifriction properties of contact materials at high temperatures in a vacuum is the degree of deformation and adhesion interaction. The present article reports on study of production, structure and properties of alloys with the composition Ti(1-x)Nb(x)C(0.5)N(0.5). Initial carbide and nitride powders with dispersion of less than 60 mkm were mixed and pulverized, then shaped and caked in an inert medium, resulting in porosity of less than 1%. X-ray analysis showed formation of complex carbonitrides with TiC or NbC lattice structures. Granules were 2-6 mkm in diameter. Friction and wear tests were conducted in a range of 20-1200 C. Results showed that the carbonitride with 0.77 ti had the optimum friction qualities, while titanium and niobium carbonitrides were the most brittle. The cobalt binder used contributed to ductile microdeformation. The powder composites tested are recommended for use in high-temperature friction assemblies. Author

N85-22716# Joint Publications Research Service, Arlington, Va.
EFFECT OF OPERATING MEDIUM ON CYCLIC DURABILITY OF AD33-W COMPOSITE Abstract Only c24
V. S. Utkin, S. Y. Salibekov, and V. V. Sakharov *In its* USSR Rept.: Mater. Sci. and Met. (JPRS-UMS-85-002) 6 Feb. 1985 p 42 Transl. into ENGLISH from Poroshkovaya Metallurgiya (USSR), no. 8, Aug. 1984 p 77-80 Original language document announced as 84A-48644 (For primary document see N85-22688 13-26)
Avail: NTIS HC A05/MF A01

Specimens of a composite consisting of and AD33 aluminum alloy matrix reinforced with boron fibers were tested in pure bending in a 3-percent NaCl solution, water, kerosene, and air. The ranges of loading parameters in which the media tested reduce the cyclic strength of the composite have been determined. For low volume fractions of accumulated damage (up to 8 percent), the effect of the corrosive media on the composite strength is hardly noticeable for a test base of 2 x 10 to the 5th cycles (not more than 150 hr). For cyclic stresses exceeding 0.6 of the tensile strength, the use of the composite in a 3-percent NaCl solution without corrosion protection is not recommended. V.L. (IAA)

N85-22717# Joint Publications Research Service, Arlington, Va.
STRUCTURAL DISTORTIONS OF ULTRA-DISPERSED TITAN-

IUM NITRIDE POWDERS Abstract Only
V. F. Petrunin, Y. G. Andreyev, T. N. Miller, Y. P. Grabis, A. G. Yermolayev, and F. M. Zelenyuk *In its* USSR Rept.: Mater. Sci. and Met. (JPRS-UMS-85-002) 6 Feb. 1985 p 43 Transl. into ENGLISH from Poroshkovaya Metallurgiya (USSR), no. 8, Aug. 1984 p 12-15 (For primary document see N85-22688 13-26)
Avail: NTIS HC A05/MF A01

Ultra-dispersed titanium nitride powders of more than 100 nm show comparatively high chemical activity, reduced caking temperatures and super-conductivity. Structural studies of such powders by neutron diffraction and X-ray methods are reported. Surface measurements ranged from 39,000 to 95,400 m2/kg. Large-grained TiN obtained by sintering was the control. Neutronograms showed the similarity of the various powders, as well as their similarity to NaCl cubic structure. Nitride composition was essentially stoichiometric, and there was a tendency toward atom shift as mean surface of the powders increased. Smaller particles had decreased lattice constants along with increased static components in atom shift mean square roots. Part of this phenomenon was attributed to deformational heterogeneity. Author

N85-22718# Joint Publications Research Service, Arlington, Va.
DEGASSIFICATION OF SILICON NITRIDE POWDERS OF VARIOUS ORIGINS Abstract Only c24
R. A. Andriyevskiy and M. A. Leontyev *In its* USSR Rept.: Mater. Sci. and Met. (JPRS-UMS-85-002) 6 Feb. 1985 p 43-44 Transl. into ENGLISH from Poroshkovaya Metallurgiya (USSR), no. 8, Aug. 1984 p 9-12 (For primary document see N85-22688 13-26)
Avail: NTIS HC A05/MF A01

Degassification in a temperature range of 25-1500 C from silicon nitrides obtained by high-temperature self-propagation, direct and plasma chemical synthesis processes is investigated. Powders were then placed in degassified molybdenum capsules for further treatment. Hydrogen emission was measured by automatic coulometer titration, oxygen and nitrogen by vacuum smelting. Results indicated that plasma chemical powder, the most dispersed, had heightened levels of oxygen and silicon. Active gas emission began at 300 C, then stabilized or decreased by about 1100 C. Lowest emission levels were observed with high-temperature self-propagation powders and the lowest with those produced chemically. Compared to other powders, the silicon nitride underwent degassification over a wider temperature range, but eventual quantities emitted were similar. The optimum temperature for degassification was judged to range up to 500 C. B.W.

N85-22719# Joint Publications Research Service, Arlington, Va.
COMPOSITION AND THICKNESS OF OXIDE COATINGS ON GRANULE SURFACES OF ALUMINUM ALLOYS Abstract Only
V. P. Antipin, V. A. Danilkin, V. A. Sidorov, S. Y. Kabanov, and N. V. Larin *In its* USSR Rept.: Mater. Sci. and Met. JPRS-UMS-85-002) 6 Feb. 1985 p 44 Transl. into ENGLISH from Poroshkovaya Metallurgiya (USSR), no. 8, Aug. 1984 p 4-9 (For primary document see N85-22688 13-26)
Avail: NTIS HC A05/MF A01

Properties of semimanufactured products of aluminum granules obtained by high-speed crystallization were studied by electron Auger-spectroscopy and secondary ion mass-spectrometry to determine thickness and composition of oxide coatings on A99 aluminum and an alloy containing 6% Mg, as well as other aluminum alloys, including ones with refractory components. Impurities stemming from the water used for crystallization were eliminated by using distilled water. Variations in the surface coatings were attributed in part to atomization procedures. The adjusted methods used provided acceptable coatings with no more than 10% variation in thickness. The vibration casting process provided oatings of 5-6 nm (or slightly more with A99). Similar results were obtained with centrifugal casting. Careful control of impurities was required, particularly in closed water cycle processes. Author

N85-22720# Joint Publications Research Service, Arlington, Va.
APPARATUS FOR PRODUCING AMORPHOUS AND MICROCRYSTALLINE METAL POWDERS Abstract Only
Y. M. Savitskiy, Y. V. Yefimov, V. N. Dmitriyev, O. P. Antipin, I. P. Kanavets, and T. M. Frolova *In its* USSR Rept.: Mater. Sci. and Met. (JPRS-UMS-85-002) 6 Feb. 1985 p 45 ref Transl. into ENGLISH from Fiz. i Khim. Obr. Metallov (USSR), no. 5, Sep.-Oct. 1984 p 122-124 (For primary document see N85-22688 13-26)
Avail: NTIS HC A05/MF A01

An apparatus was developed for quenching metal melts at superhigh rates in production of powder with specified grain dimensions. A hermetically closed vat contains a quartz or corundum crucible seated in a furnace (electric-arc, resistance, induction, electron-beam, or any other type) with superheated molten metal or alloy. The melt is discharged from the crucible through an orifice-gate at the tip of the spherical bottom, pouring vertically downward as a continuous thin jet on the teeth of a variable-high-speed motor-driven heavy quencher gear-drum. The teeth break the jet into identical fine batches of metal, the latter being cooled in the process by the cold polished drum surface. Solidified microparticles do not get welded to the drum surface but break away from it and fall into a receptacle. The drum is cooled from underneath with liquid-helium jets while it rotates and melt pours on it eccentrically from above, which ensures a uniform temperature around its surface and thus a uniform quenching rate. Author

N85-22721# Joint Publications Research Service, Arlington, Va.
SPECIFICS OF KINETICS OF POLYMORPHOUS CONVERSION UPON HEATING OF LOW CARBON STEELS Abstract Only
A. P. Surovtsev and V. V. Yarovoy *In its* USSR Rept.: Mater. Sci. and Met. (JPRS-UMS-85-002) 6 Feb. 1985 p 46 Transl. into ENGLISH from Metallovedeniye i Termicheskaya Obr. Metallov (USSR), no. 9, Sep. 1984 p 2-5 (For primary document see N85-22688 13-26)
Avail: NTIS HC A05/MF A01

Structural and phase transformations upon heating of low carbon unalloyed steel containing 0.025% to 0.33% C were studied. Specimens were heated at rates corresponding to furnace and induction heating, 7.5 to 200 C/min. Critical points were determined on a dilatometer and by measurement of residual resistivity in a double bridge circuit. It was found that the critical points as determined by diatometry and relative resistivity agreed rather well. Three major temperature intervals were found: transformation of pearlite to austenite, no transformation, and transformation of ferrite to austenite. The interval of no transformation between the two transformations is broader, the lower the content of carbon in the steel. With a carbon content of 0.25% or more the two transition temperatures are practically the same. Author

N85-22722# Joint Publications Research Service, Arlington, Va.
COMPARISON OF DYNAMIC-TENSION AND CONSTANT-LOAD STRENGTH CHARACTERISTICS OF HEAT-RESISTANT MATERIALS Abstract Only
V. V. Osasyuk, A. N. Olisov, and L. V. Shkabarov *In its* USSR Rept.: Mater. Sci. and Met. (JPRS-UMS-85-002) 6 Feb. 1985 p 46-47 Transl. into ENGLISH from Problemy Prochnosti (USSR), no. 9, Sep. 1984 p 31-33 (For primary document see N85-22688 13-26)
Avail: NTIS HC A05/MF A01

A relation between the strength characteristics of 12Kh1MF heat-resistant steel under dynamic tension and under constant load is established on an empirical basis. Some specimens of this material were tested at 575 C under dynamic tension with time limit in a 1231U-10 machine, one lot slower for an elongation rate of 11 mm/min; other specimens were tested at the same temperature under constant loads up to the level of tensile strength with short time-base (100 min) in an AIMA-5-1 machine. The data are represented graphically in the form of stress (strength)-time curves, whereupon the latter are analyzed by replacement of strength under short-duration dynamic loads with strength under equivalent long-duration alternating loads and calculation of stresses on this basis by the method of piecewise curve averaging. This procedure yields a close agreement between experimental data and hypotheses which allow summation of percent lifetimes. Author

N85-22723# Joint Publications Research Service, Arlington, Va.
LONG-TERM STRENGTH AND FRACTURE CRITERIA FOR EI698VD ALLOY UNDER COMPLEX STRESS CONDITIONS Abstract Only
Y. R. Golubovskiy *In its* USSR Rept.: Mater. Sci. and Met. (JPRS-UMS-85-002) 6 Feb. 1985 p 48 Transl. into ENGLISH from Problemy Prochnosti (USSR), no. 8, Aug. 1984 p 11-17 (For primary document see N85-22688 13-26)
Avail: NTIS HC A05/MF A01

Results are presented from a study of the long term strength of EI698VD nickel-based alloy under homogeneous planar stress conditions. The major normal stresses are used as the stress state characteristics. Long term strength equations and activation parameters of the fracture process under creep conditions in extension, extension with flexure and flexure with slight axial force are obtained. A long term strength criterion is suggested for a complex stress state. The specimens used in the test were made by stamping from a disk about 700 mm in diameter, then heat treated under normal conditions with aging. The material parameter is found to vary with the activation parameters of the fracture process, varying if the fracture process is controlled by different mechanisms. Author

N85-22724# Joint Publications Research Service, Arlington, Va.
SOME SPECIFICS OF DEVELOPMENT OF FATIGUE AND CREEP IN HEAT-RESISTANT ALLOYS WITH ASYMMETRICAL MULTICYCLE LOADING Abstract Only
V. P. Golub *In its* USSR Rept.: Mater. Sci. and Met. (JPRS-UMS-85-002) 6 Feb. 1985 p 48-49 Transl. into ENGLISH from Problemy Prochnosti (USSR), no. 8, Aug. 1984 p 17-22 (For primary document see N85-22688 13-26)
Avail: NTIS HC A05/MF A01

An attempt was made to demonstrate the leading role of fatigue or creep in the fracture of heat-resistant alloys on the basis of thermal activation analysis, particularly analysis of the regularities of change in activation energy of the fracture process. A cycle of experimental durability studies was performed over broad range of stresses and temperatures to determine the value of the thermal activation parameters. Heat-resisistant nickel-based alloys EI867, EP109, EVZhL12U and ZhS6U were used in the studies. The stress was changed at a rate of 35 Hz, and temperature interfal of the studies was 800 to 1100C. It was found that sudden changes in activation energy of fracture of heat-resistant nickel alloys indicates a change in the leading kinetic process controlling fracture from fatigue to creep at a critical value of amplitude. Author

N85-22725# Joint Publications Research Service, Arlington, Va.
CHANGE IN MICROSTRUCTURE OF HEAT-RESISTANT NICKEL ALLOYS UPON THERMAL CYCLING IN A CURRENT OF GAS Abstract Only
G. N. Tretyachenko, L. V. Kravchuk, R. I. Kuriat, G. R. Semenov, T. D. Kotikova, and S. G. Khaustova *In its* USSR Rept.: Mater. Sci. and Met. (JPRS-UMS-85-002) 6 Feb. 1985 p 49 Transl. into ENGLISH from Problemy Prochnosti (USSR), no. 8, Aug. 1984 p 37-40 Original language document announced as 84A-47445 (For primary document see N85-22688 13-26)
Avail: NTIS HC A05/MF A01

Wedge-shaped specimens of heat-resistant nickel-base alloys. EI826 and EP539, were subjected to thermal cycling in a gas flow, with the maximum temperature and thermal stress reaching 1035 C and 625 MPa, respectively. A metallographic examination of the specimens showed irreversible changes in the surface layer of the specimens. A correlation is established between the crack growth rate and fracture characteristics for different maximum temperatures and thermal stresses of the cycle. V.L. (IAA)

N85-22726# Joint Publications Research Service, Arlington, Va.
DEVELOPING PROCEDURES FOR THERMOMECHANICAL PROCESSING OF HIGH-DURABILITY VT22 TITANIUM ALLOY Abstract Only
A. A. Popov, L. I. Anisimova, and N. N. Bondaryuk *In its* USSR Rept.: Mater. Sci. and Met. (JPRS-UMS-85-002) 6 Feb. 1985 p 50 Transl. into ENGLISH from Tsvetnyye Metally (USSR), no. 10, Oct. 1984 p 84-87 (For primary document see N85-22688 13-26)
Avail: NTIS HC A05/MF A01

Previous studies had shown that increasing temperature from 625 C to 650 C brought spherization of particles; in the alpha-phase, recrystallization took place. Significant loss of durability and loss of plasticity were noted. Studies of VT22 titanium alloy rods, previously tempered at 800 and 900 C, and then subjected to cold deformation processing are presented. The resulting shaped rods were then aged at 450 to 700 C for 2 and 4 hours, and tested for blow resistance and breaking. The samples aged at 500 to 25 C emitted plate-like alpha-phase particles, but the coagulation found in hot-rolled products did not occur. This effect is attributed to reduction of resilient energy. Thus with other properties equal, cold-shaped alloys have higher plasticity and viscosity. Temperature and mechanical features of mixed alpha-beta alloys, where the fine platelet alpha-particles determine durability and larger particles determine plasticity, are discussed. Author

N85-22727# Joint Publications Research Service, Arlington, Va.
INFLUENCE OF ANNEALING ON CYCLIC AND SHORT-TERM STRENGTH OF THIN SHEETS OF VT1-0 TITANIUM AND OTR4 ALLOY Asbract Only
A. B. Kolomenskiy, I. I. Muravyev, B. A. Kolachev, and V. V. Shevchenko *In its* USSR Rept.: Mater. Sci. and Met. (JPRS-UMS-85-002) 6 Feb. 1985 p 50-51 Transl. into ENGLISH from Fiz.-Khim. Mekh. Mater. (USSR), v. 20, no. 4, Jul.-Aug. 1984 p 120-122 (For primary document see N85-22688 13-26)
Avail: NTIS HC A05/MF A01

The influence of the state of the surface and structural changes after annealing in air and in a vacuum on cyclical and short-term strength of thin sheets of TV1-0 titanium and OT4 titanium alloy are presented. Studies were performed on specimens 1.5 mm thick (VT1-0) and 1.2-2.0 mm thick (OT4) annealed at temperatures of 350 to 750 C for one and two hours in air muffle furnaces and in a vacuum furnace with residual pressure not over .00665 Pa, leakage not over 5.25 dm(3) Pa/s. The influence of surface oxidation and gas content on mechanical properties as studied on specimens which underwent preliminary vacuum annealing in packets at 660 C, two hours or 750 C, one hour for VT1-0 and 750 C, two hours for Ot4. The relief of characteristic surface hardening during annealing significantly decreased their cyclical and short term strength. The status of the surface after air and vacuum annealing influences short-cycle endurance at less than 75% of tensile strength for these alloys. An oxide film developed by annealing in air decreases repeated static loading endurance, cyclical loading strength and short-term tensile strength of both alloys. Author

N85-22728# Joint Publications Research Service, Arlington, Va.
RATIONAL USE OF TATANIUM IN NONFERROUS METALLURGY Abstract Only
Y. V. Dobrunov, V. A. Aleksandrov, and V. V. Volynskiy *In its* USSR Rept.: Mater. Sci. and Met. (JPRS-UMS-85-002) 6 Feb. 1985 p 51 Transl. into ENGLISH from Tsetvnyye Metally (USSR), no. 10, Oct. 1984 p 31-33 (For primary document see N85-22688 13-26)
Avail: NTIS HC A05/MF A01

Economics in using titanium in nonferrous metallurgy are crucial given limited supplies of the metal. Soviet use of titanium is outlined, and points out approaches to achieve more rational use. Soviet titanium use includes specialized titanium equipment, less standardized products, and repair and related uses. Wear patterns suggest that 20% reductions in thickness could be made in titanium-magnesium alloys used in various sterilized equipment, in rare-earth production equipment, in nickel and cobalt production, and in other specialized metal products and sulfuric acid products. The shortest service came from stamp-welded and cast titanium pumps, which broke down in 1 to 1.5 years due to abrasive and corrosive wear. In designing titanium components, aggressive agents and temperature must be taken into consideration. Sharp angles and other design features must be carefully controlled. The small linear expansion coefficient, cold durability and high

corrosion resistance to certain compounds make titanium alloys especially useful for tubes of 100 to 400-mm diameter with 2 to -5-mm walls, for chemically and thermally durable products.

N85-22729# Joint Publications Research Service, Arlington, Va.
STUDIES OF ELECTRICAL PROPERTIES OF SURFACE FILMS AND LOCALIZATION DURING ELECTROCHEMICAL DIMENSIONAL WORKING OF TITANIUM Abstract Only
Y. M. Rumyantsev, O. I. Nevskiy, V. I. Volkov, and Y. P. Grishina *In its* USSR Rept.: Mater. Sci. and Met. (JPRS-UMS-85-002) 6 Feb. 1985 p 52 Transl. into ENGLISH from Elektronnaya Obr. Mater. (USSR), no. 4, Jul.-Aug. 1984 p 14-17 (For primary document see N85-22688 13-26)
Avail: NTIS HC A05/MF A01

An estimate is presented of the localization of the process of dissolution of titanium alloy vT1-0 in electrolytes. The logarithmic scattering index is determined by a method which was recommended as a standard and is distinguished by the fact that the specific rate of metal removal is recorded for each value of interelectrode gap by a given period of time. It was found that addition of the bichromate ion results in an increase in Asubeff as a result of formation of a surface film of a new composition with different properties than in the initial NaCl solution. In systems where the anodic potential is a significant fraction of V subc, the secondary distribution of current significantly influences localization of electrochemical dimensional working. A necessary condition for a high degree of localization is presence on the surface being worked of a film whose electrical resistance undergoes significant changes over a narrow interval of interelectrode gap. Author

N85-22730# Joint Publications Research Service, Arlington, Va.
BASIS AND PYRAMIDAL SLIPPING IN SINGLE CRYSTALS OF ALPHA-ALLOY Ti-Al-Sn Abstract Only
N. V. Ageyev, Y. B. Rubina, and V. N. Kovaleva *In its* USSR Rept.: Mater. Sci. and Met. (JPRS-UMS-85-002) 6 Feb. 1985 p 52-53 Transl. into ENGLISH from Fiz. Metallov i Metallovedeniye (USSR), v. 58, no. 2, Aug. 1984 p 383-388 (For primary document see N85-22688 13-26)
Avail: NTIS HC A05/MF A01

Finely dispersed Ti-Al-Sn alloys were studied. A single crystal ingot 20 mm in diameter was grown by electron beam zone melting. Specimens were oriented so that the axis of compression was at about 14-18 deg or 45 deg [0001] axis. The side and end faces of the specimen were mechanically ground and electrically polished before deformation. The deformation mechanism was identified by means of tracks on the two surfaces observed with a GM double optical goniometer. Space slipping was observed at 293 and 77 K upon compression of the single-crystal specimens in the ,11<11(-2)2>22. direction. With an orientation of the compression axis of ,11<17(-2)(16)>26, active slipping occurs in /10(-1)1/ ,112<(-1)(-1)23> at 293 and 77K; at 4.2 K crystals of this orientation are deformed by twinning. Orientation boundaries of activity of various deformation systems in Ti-A1-Sn single crystals are calculated in compression and extension at 293 K. Author

N85-22731# Joint Publications Research Service, Arlington, Va.
SPECIFICS OF STRUCTURE AND MECHANICAL PROPERTIES OF METASTABLE BETA-TITANIUM ALLOYS AFTER DEFORMATION AND AGING Abstract Only
O. A. Yelkina, S. V. Sudareva, L. S. Meshchaninova, R. M. Lerinman, and O. D. Shashkov *In its* USSR Rept.: Mater. Sci. and Met. (JPRS-UMS-85-002) 6 Feb. 1985 p 53 Transl. into ENGLISH from Fiz. Metallov i Metallovedeniye (USSR), v. 58, no. 2, Aug. 1984 p 377-382 (For primary document see N85-22688 13-26)
Avail: NTIS HC A05/MF A01

Low-alloy beta-titanium alloys in the system Ti-Mo, Ti-Mo-Al, Ti-Mo-V, Ti-Mo-V-Al were studied. Compositions were selected to avoid the formation of athermic alpha prime prime-martensite upon hardening from the area. How discontinuous decomposition occurs in metastable beta-titanium alloys and by the ordinary process of recrystallization occurring in deformed alloys were determined. It is found that cold deformation of Ti-Mo, Ti-Mo-Al alloys results in a phenomenon similar to the trip effect in steels. A large number of alpha prime prime-martensite plates and twins with BCC lattice is formed. After deformation and subsequent aging of these alloys seeds of discontinuous decomposition arise at the points of intersection of deformation plates, where large stresses are concentrated. These areas apparently are responsible for the plasticity of the alloys. The deformation plates of alpha prime prime-martensite break down to form a finely dispersed periodic modulated structure of alpha and beta phases resistant to heat treatment. Sectors of the alloy which do not undergo transformation upon deformation and deformation plates with BCC structure break down to form finely dispersed mixtures of alpha and beta phases. This structure is responsible for the strength properties of the alloys. Author

N85-22732# Joint Publications Research Service, Arlington, Va.
PROBLEM OF PORE FORMATION MECHANISM IN WELDED JOINTS OF ALUMINUM ALLOYS IN THE SYSTEM ALUMINUM-MAGNESIUM-LITHIUM Abstract Only **c37**
V. I. Ryazantsev and V. A. Fedoseyev *In its* USSR Rept.: Mater. Sci. and Met. (JPRS-UMS-85-002) 6 Feb. 1985 p 56 Transl. into ENGLISH from Svarochnoye Proizvodstvo (USSR), no. 8, Aug. 1984 p 41-43 (For primary document see N85-22688 13-26)
Avail: NTIS HC A05/MF A01

The causes and mechanism of pore formation in alloys in the aluminum-magnesium-lithium system were studied. Specimens 1 to 10 mm thick and panels of both experimental and commercial alloys were used. Various methods of melting by fusion were used, including manual arc welding in argon, automatic AC welding in argon and DC welding in helium, welding with electromagnetic agitation and in chambers with a controlled atmosphere. Analysis of X-ray diagrams indicated that no matter what the welding method the nature of placement of pores was identical, a chain along the melting line. Porosity was found to be related to the presence of a 0.05 to 0.15 mm surface layer rich in compounds of lithium and oxide films with adsorbed moisture. The surface layer contains 10 to 30 times more hydrogen than when surfaces are treated by heat and vacuum, 60 times more in comparison to type 1201 alloys. When a thin surface layer is removed, porosity arises only after long-term storage as a result of the presence of oxide films with adsorbed moisture. Changing the hardening temperature from 450 to 400 C decreases the thickness of the surface layer which must be removed to obtain pore-free welded joints from 0.12 to 0.15 to 0.05 to 0.07 mm. Author

N85-22733# Joint Publications Research Service, Arlington, Va.
PROPERTIES OF WELDED JOINTS IN ARGON ARC WELDING OF TITANIUM ALLOY USING A PROTECTIVE COATING Abstract Only **c37**
B. Y. Mozeyko and V. V. Bazhenov *In its* USSR Rept.: Mater. Sci. and Met. (JPRS-UMS-85-002) 6 Feb. 1985 p 56 Transl. into ENGLISH from Svarochnoye Proizvodstvo (USSR), no. 8, Aug. 1984 p 28-29 (For primary document see N85-22688 13-26)
Avail: NTIS HC A05/MF A01

Arc welding of titanium alloys using coatings to protect the back side of the seam from gases uses various technological approaches depending on the type of joint to be made. Locations of coatings are illustrated for various types of butt, lap, and tee joints. Optimal conditions of automatic welding of longitudinal seams in flat specimens were found to be L sub w for 98A, V sub w = 8.5 m/hr, L sub d = 1.8 mm, Q sub Ar = 0.12 cu m/min for welding using the protective coating: I sub w = 105 A, V sub w = 8 m/hr, L sub d = 1.8 mm, Q sub Ar = 0.012 cu m/min for welding in argon. The ductility of welded joints produced using the protective coating was higher than joints made by welding in argon. The endurance was also higher. The tensile strength and impact toughness were approximately the same. Reliability in service was also approximately the same. Author

N85-22734# Joint Publications Research Service, Arlington, Va.
THERMAL HARDENING OF WELDED JOINTS IN TITANIUM ALLOYS WITH VARIOUS STRUCTURES Abstract Only **c37**
M. A. Khorev *In its* USSR Rept.: Mater. Sci. and Met. (JPRS-UMS-85-002) 6 Feb. 1985 p 57 Transl. into ENGLISH

from Svarochnoye Proizvodstvo (USSR), no. 8, Aug. 1984 p 26-27 (For primary document see N85-22688 13-26)
Avail: NTIS HC A05/MF A01

Pseudo-alpha alloys VT20, OT4; alpha and beta alloys VT6S, VT14, VT23; and beta alloys VT19 and tC6 were studied. Welded joints 3 mm thick made by automatic argon arc welding were annealed, hardened, and strengthened over a broad range of temperatures. The comparison was based on optimal conditions providing the maximum strength while retaining satisfactory ductility with angle of flexure 25 to 30 deg and impact toughness 0.25 to 0.3 mJ/sq m. It is found that the effectiveness of strengthening heat treatment is maximal for alloys containing beta stabilizing elements in a quantity equivalent to 8% molybdenum (the alloys tested contain 1.6 to 25%). It is shown that strengthening heat treatment can increase the strength of welded joints not only of alpha and beta but also of pseudo-alpha alloys. A specific approach is required to select methods and conditions of strengthening heat treatment for each type of alloy. Author

N85-22735# Joint Publications Research Service, Arlington, Va.
INFLUENCE OF WELDING DEFECTS AT MELTING BOUNDARY ON STATIC STRENGTH OF WELDED JOINT IN LARGE-DIAMETER PIPE Abstract Only **c37**
M. V. Shakhmatov, V. V. Yerofeyev, V. A. Lupin, and A. A. Ostsemin *In its* USSR Rept.: Mater. Sci. and Met. (JPRS-UMS-85-002) 6 Feb. 1985 p 57 Transl. into ENGLISH from Problemy Prochnosti (USSR), no. 8, Aug. 1984 p 111-116 (For primary document see N85-22688 13-26)
Avail: NTIS HC A05/MF A01

The influence of nonpenetrating defects, both internal and superficial, located at the boundary between the soft base metal and hard welded seam metal on the strength of the welded joint in large-diameter pipes was studied. The theoretical analysis is performed by the method of slip lines or static stress on welded joints assuming planar deformation, a valid assumption for large-diameter pipes. The influence of residual welding stresses is ignored. The soft metal is considered ideally rigid-plastic, the seam metal rigid. Calculation equations are suggested for estimation of the stress state and strength under these conditions. The results of an experimental study of the influence of defects of this type agree satisfactorily with the results of calculation. It is found that there is a range of permissible defect size which does not decrease strength of welded joints of this type. Author

N85-22736# Joint Publications Research Service, Arlington, Va.
MECHANICAL PROPERTIES AND BRITTLE FRACTURE RESISTANCE OF WELDED MULTILAYER ELEMENTS FOR HIGH PRESSURE VESSELS Abstract Only **c39**
V. M. Goritskiy, V. S. Kabanov, and S. A. Klimov *In its* USSR Rept.: Mater. Sci. and Met. (JPRS-UMS-85-002) 6 Feb. 1985 p 58 Transl. into ENGLISH from Avtomaticheskaya Svarka (USSR), no. 8, Aug. 1984 p 27-30 (For primary document see N85-22688 13-26)
Avail: NTIS HC A05/MF A01

The influence of diffusion welding conditions on the strength of bonding between layers and brittle fracture resistance of multilayer products of 16G2AF and St08kp steels was studied. The strength of the interlayer bonding of the plates was determined by tensile testing. Brittle fracture resistance was studied on a 17 layer specimen with a sharply notch across the plates. Impact toughness was determined in specimens with the notch plane oriented perpendicular to the joint plane of diffusion welding of layers. It was found that joints equal in strength to the base metal can be produced by welding under a pressure of at least 9.8 MPa, holding time 20 minutes, welding temperature 1173 to 1273 K, residual pressure 1.33 to 0.133 Pa. Impact toughness in specimens with a notch in the plane perpendicular to the plane diffusion welding yielded viscous fracture. When the notch was parallel to the plane of diffusion welding impact toughness dropped to 49 to 78 kJ/sq m. Changing the temperature of diffusion welding can regulate bonding between layers of a multilayer product and brittle fracture resistance. Author

N85-22737# Joint Publications Research Service, Arlington, Va.
ANALYSIS OF STRENGTH AND DUCTILITY OF WELDED JOINTS IN AMtsS AND AMg5 ALUMINUM ALLOYS Abstract Only **c39**
B. V. Grudzinskiy, A. T. Fomchenkov, N. G. Murkina, and A. N. Yeremeyev *In its* USSR Rept.: Mater. Sci. and Met. (JPRS-UMS-85-002) 6 Feb. 1985 p 58-59 Transl. into ENGLISH from Avtomaticheskaya Svarka (USSR), no. 8, Aug. 1984 p 71-72 (For primary document see N85-22688 13-26)
Avail: NTIS HC A05/MF A01

Results are presented from statistical analysis of strength and bending tests of welded production specimens over a period of five years. Analysis considered the type of alloy, state delivered, thickness of metal and welding methods. No significant variation in short-term tensile strength of welded joints was found as a function of method of welding (manual argon arc or mechanized plasma), thickness of metal or delivered conditions (hot rolled or annealed). All samples of AMtsS alloy met the requirements of the state standard. Welded joints in AMtsS alloy also have good ductility regardless of the variable factors. The strength of AMg5 welded joints varies broadly, primarily as a function of the status of the seam metal. Seventy percent of the specimens broke through the seam, apparently a result of burning of magnesium during welding. Ductility of welded joints in this alloy depends significantly on the thickness of the metal, less on the method of welding.
Author

N85-22738# Joint Publications Research Service, Arlington, Va.
EFFECT OF PROTECTIVE MEDIUM ON DURABILITY AND FRACTURE STRUCTURE ON SEAM ZONES OF THIN-WALLED TITANIUM ARTICLES PRODUCED BY DIFFUSION WELDING Abstract Only **c37**
S. I. Gusev, V. V. Peshkov, V. N. Milyutin, and M. K. Shorshorov *In its* USSR Rept.: Mater. Sci. and Met. (JPRS-UMS-85-002) 6 Feb. 1985 p 59 Transl. into ENGLISH from Svarochnoye Proizvodstvo (USSR), no. 10, Oct. 1984 p 21-22 (For primary document see N85-22688 13-26)
Avail: NTIS HC A05/MF A01

Currently machinebuilding makes wide use of thin-walled articles with high durability, rigidity, and small metal expenditure. Diffusion welding of seams in such articles using imitations consisting of cylinders of VT15 alloy with a beta-structure and a facing of OT4 alloy with fine-grained structure is discussed. Welding was done at 850 to 950 C at welding pressure of 0.4 MPa and time of 7.5 to 90 minutes, in a vacuum or argon medium. Structural strength was then assessed. Analysis of data showed that seam durability was dependent on welding temperature along with the protective medium used: a vacuum of 3.3-0.0010 Pa gave better durability then the argon or a 3.3 Pa vacuum. Where welding was done at 950 c, breaks came in the cylinder of VT15 alloy, while at lower welding temperatures the welded seam failed. When however, 0.002% O2 and 0.01 N2 were added to the argon medium, better joints were obtained than the 3.3 Pa vacuum.
Author

N85-22739# Joint Publications Research Service, Arlington, Va.
TECHNOLOGICAL PARAMETERS OF DIFFUSION WELDING PROCESSES IN HONEYCOMB TITANIUM ALLOY STRUCTURES Abstract Only **c37**
V. V. Peshkov and S. I. Gusev *In its* USSR Rept.: Mater. Sci. and Met. (JPRS-UMS-85-002) 6 Feb. 1985 p 59-60 Transl. into ENGLISH from Svarochnoye Proizvodstvo (USSR), no. 10, Oct. 1984 p 12-14 (For primary document see N85-22688 13-26)
Avail: NTIS HC A05/MF A01

Procedures for obtaining highly durable lining seams were studied based on the increasing use of titanium honeycomb designs in industry. Diffusion welding and the high-temperature creep of titanium alloys depends greatly on microstructure, and these factors were taken into consideration in designing the diffusion welding procedures. Metallographic analysis of the OT4 alloy leaf of 0.5 to 1.0 mm thickness showed its finely grained structure with no clearly delineated alpha-phase granules. Samples were then tested for thermal durability and for warping at 800 to 1000 C. The

importance of initial microstructure of the alloy and the nature of applied welding pressure were determined to be important factors in determining durability. Either pressure application after the procedure is under way or use of a filler with large-grained platelet structure was found to provide successful welds. Author

N85-22740# Joint Publications Research Service, Arlington, Va.
DURABILITY OF VT16 ALLOY COMPOUNDS OBTAINED BY DIFFUSION WELDING Abstract Only **c37**
N. F. Kazakov, N. A. Mashkova, V. Y. Varyanitsa, N. V. Yermakova, and O. V. Fedorova *In its* USSR Rept.: Mater. Sci. and Met. (JPRS-UMS-85-002) 6 Feb. 1985 p 60 Transl. into ENGLISH from Svarochnoye Proizvodstvo (USSR), no. 10, Oct. 1984 p 11-12 (For primary document see N85-22688 13-26)
Avail: NTIS HC A05/MF A01

Durability of diffusion welded samples was assessed to determine optimum conditions for producing welded joints. Joint durability and the nature of failures were the criteria for selecting welding parameters. Diffusion welding in a vacuum at high temperature and pressure were found to change properties of the materials welded, providing high durability while harmining use properties. Plastic properties were calculated in order to predict likely outcome of welding operations. Results showed that the best welding procedure, on the basic metal, provided high durability and high plasticity, and thereby sought-after wear resistance. Study of surface porosity in test samples furthered confirmed these conclusions. Welding temperature of 1170 C for 120 minutes at 8 MPa in a 0.1 vacuum were the recommended parameters. Author

N85-22741# Joint Publications Research Service, Arlington, Va.
RELIABILITY OF ROBOTIZED WELDING APPARATUS Abstract Only **c37**
V. A. Timchenko and A. S. Taratuta *In its* USSR Rept.: Mater. Sci. and Met. (JPRS-UMS-85-002) 6 Feb. 1985 p 60-61 Transl. into ENGLISH from Avtomaticheskaya Svarka (USSR), no. 9, Sep. 1984 p 61-65 (For primary document see N85-22688 13-26)
Avail: NTIS HC A05/MF A01

The operation of a robotized welding machine is broken down into two classes of functions, H-functions characterizing continuous use of equipment and II-functions characterizing periodically implementable procedures. Functions of both types are described in terms of time parameters and nonfailure probabilities, for the purpose of reliability and economic analysis. Reliability estimates are based on digital computer simulation of process and probability characteristics, rather than on generally inadequate analytical models, with the nonfailure probability stipulated as an exponentially decreasing function of time. In an overall reliability estimate for a typical robotized arc-welding machine are included 13 components of the robot-welder system. Calculations for the UD-223 robotized welding apparatus built at the Institute indicate that welding equipment and controls are the weakest links here, the probabilities of their failure-free operation over an 8-hour shift being only 0.95 and 0.975 respectively, while better robots now available can operate failure-free for 1000 h. Author

N85-22742# Joint Publications Research Service, Arlington, Va.
STRUCTURE AND MECHANICAL CHARACTERISTICS OF HETEROGENEOUS JOINTS PRODUCED BY LASER WELDING Abstract Only **c37**
A. N. Grezev, A. G. Grigoryant, A. G. Fedorov, and V. V. Ivanov *In its* USSR Rept.: Mater. Sci. and Met. (JPRS-UMS-85-002) 6 Feb. 1985 p 61 Transl. into ENGLISH from Avtomaticheskaya Svarka (USSR), no. 9, Sep. 1984 p 46-49 (For primary document see N85-22688 13-26)
Avail: NTIS HC A05/MF A01

Welding together different grades of steel is common practice in the manufacture of automobile transmissions, typically with parts made of St35 steel and 12Kh2N4A steel respectively being joined. A comparative evaluation of three welding methods for such joints was made on the basis of microstructural examination and mechanical tests, taking into consideration nonisothermal phase transformations at various cooling rates. Laser welding and electron beam welding were both found to produce seams with much narrower thermal influence zones and a finer grain structure in 12Kh2N4A steel than argon-arc welding, especially at high cooling rates, the highest toughness and resistance to cold cracking being found after laser welding. In St35 steel, with a higher carbon content and no other elements except impurities, laser welding was found to produce a high microhardness and low plasticity with resulting lower toughness and resistance to cold cracking than in the alloy steel. Author

N85-22743# Joint Publications Research Service, Arlington, Va.
METHOD OF CALCULATING STRENGTH OF JOINT PRODUCED BY COLD WELDING OF ALUMINUM UNDER DISCRETE LOADING Abstract Only **c39**
D. P. Kulagin *In its* USSR Rept.: Mater. Sci. and Met. (JPRS-UMS-85-002) 6 Feb. 1985 p 62 Transl. into ENGLISH from Avtomaticheskaya Svarka (USSR), no. 9, Sep. 1984 p 29-31 (For primary document see N85-22688 13-26)
Avail: NTIS HC A05/MF A01

Discrete increasing of the load with a movable vibratory tool during cold welding of aluminum was proposd, with a smaller force required than for increasing the load continuously. In order to evaluate the effectiveness of this method, it was necessary to determine the strength of a joint produced by it. This was done on the basis of a probabilistic model of randomly distributed contacts which mating metal surfaces make after cracking of the oxide films during plastic deformation. Data for this model were gathered in experiments with discrete loading (N = 2 to 16 operations), also with continuous loading (N = 1 operation) for reference. Discrete loading was effected in two ways, by decreasing the force to zero after each pulse with definite time intervals between successive pulses, or by increasing the force in steps and holding at constant levels for definite time invervals between steps. Theoretical relations were derived for the contact surface distribution and the effective breakdown force, as basis for calculating ultimate strains and stresses. Author

N85-22744# Joint Publications Research Service, Arlington, Va.
EFFECT OF MOISTURE IN INERT GASES ON DENSITY OF SEAM METAL AND ON MECHANICAL CHARACTERISTICS OF WELDED JOINTS OF ALUMINUM AND ALUMINUM ALLOYS Abstract Only **c37**
I. V. Dovbishchenko, V. S. Mashin, and D. M. Rabkin *In its* USSR Rept.: Mater. Sci. and Met. (JPRS-UMS-85-002) 6 Feb. 1985 p 62-63 Transl. into ENGLISH from Avtomaticheskaya Svarka (USSR), no. 9, Sep. 1984 p 17-19 (For primary document see N85-22688 13-26)
Avail: NTIS HC A05/MF A01

Mechanized bilateral welding of AD-0 commercial aluminim and of aluminum magnesium alloys (AMg3, AMg5) with a fusible electrode the inert gas shield on the porosity of the seam metal and on the mechanical characteristics of the joint. The joints were mechanically tested, after burning of the seam on both sides. The results reveal that adding 0.1-0.8 g/m3 of moisture to a pure argon shield increases the volume of pores in welded commercial aluminum up to eightfold, about twice as much as does adding moisture to a helium argon shield, while the porosity of seam is 50-60% lower after welding in a dry helium argon shield than after welding in a dry pure argon shield. The effect of moisture in the two gas shields is similar but less appreciable in the case of aluminum magnesium alloys. Accordingly, the mechanical characteristics of joints are less sensitive to and not as much degraded by moisture in the gas shield when aluminum magnesium alloys are welded than when commercial aluminum is welded. B.G.

N85-22745# Joint Publications Research Service, Arlington, Va.
CHARACTERISTICS OF SURFACE CRACK DEVELOPMENT IN ATtsS ALUMINUM ALLOY DURING SLOW-CYCLE LOADING Abstract Only
A. L. Kaplinskiy *In its* USSR Rept.: Mater. Sci. and Met. (JPRS-UMS-85-002) 6 Feb. 1985 p 67-68 Transl. into ENGLISH from Problemy Prochnosti (USSR), no. 9, Sep. 1984 p 28-31 (For primary document see N85-22688 13-26)

Avail: NTIS HC A05/MF A01

Surface cracking of the weldable high plasticity AMtsS aluminum manganese alloy under cyclic loads was studied experimentally on 10 mm thick rolled strip specimens. The mechanical characteristics of this material at room temperature (293 K) are: 0.2% yield strength 111.7 MPa, ultimate tensile strength 140 MPa, percent elongation 28.4, percent reduction 50.5, modulus of elasticity .000058 MPa. Tests were performed in a UE-50 machine with axial tension cycling at a frequency of 0.5 Hz, to a total of 120,000 cycles. Measurements and photographs taken throughout the process reveal, on correlation with the static fracture model, that cracking under a slowly cycling load proceeds in three stages: (1) linear elastic crack growth; (2) elastoplastic crack growth; and (3) quasi-static crack growth up to fatigue failure. Transition from elastoplastic to quasi-static cracking occurs as the nominal net stress has built up to the yield strength level. Cracking becomes unstable as the crack opening reaches its critical width under short duration static load. Author

N85-22746# Joint Publications Research Service, Arlington, Va.
AUTOMATIC MULTI-LAYER WELDING OF THICK CYLINDRICAL STRUCTURES UNDER FLUX Abstract Only **c37**
N. V. Pilipenko, Y. N. Rudenko, and A. N. Yastreb *In its* USSR Rept.: Mater. Sci. and Met. (JPRS-UMS-85-002) 6 Feb. 1985 p 67-68 Transl. into ENGLISH from Svarochnoye Proizvodstvo (USSR), no. 9, Sep. 1984 p 12-13 (For primary document see N85-22688 13-26)
Avail: NTIS HC A05/MF A01

A plant was set up to manufacture thick cylindrical structures such as hydraulic press cylinders and supporting rolls using automatic welding under flux. The system of equipment used allows assembly, preliminary heating and welding of cylindrical products. The system consists of a specialized assembly stand, a portal installation with welding equipment, an installation for conduction heating of blanks and cleaning of seams, and a vertical furnace for stress relief after welding. A photograph of the assembly and welding installation and a photograph of the automatic multilayer welding process are presented. The macrostructure of a cylindrical welded joint is illustrated. Products up to 500 mm thick can be automatically welded in a narrow slot. The mechanical properties of welded joints produced under AN-43 flux was found to satisfy the requirements of the technical conditions. The technology was used to produce a supporting roll shaft for a rolling mill and a hydraulic press cylinder with a wall thickness of 400 mm. Author

N85-22747# Joint Publications Research Service, Arlington, Va.
SOFTENING OF METAL NEAR SEAM DURING WELDING OF HEAT-RESISTANT NICKEL ALLOYS Abstract Only **c37**
B. F. Yakushin *In its* USSR Rept.: Mater. Sci. and Met. (JPRS-UMS-85-002) 6 Feb. 1985 p 68 Transl. into ENGLISH from Svarochnoye Proizvodstvo (USSR), no. 9, Sep. 1984 p 5-6 (For primary document see N85-22688 13-26)
Avail: NTIS HC A05/MF A01

The EP693 heat resistant alloy containing Ti and A1, as well as EP914, containing Nb and A1, were employed in a study of softening of the metal near the seam in welding of nickel alloys. Hardened sheet specimens 1.5 mm thick were treated by electric heating using a welding thermal cycle in order to determine the time required for dissolution or coagulation of the hardening phase. After imitation of the welding cycle the mechanical properties temperature interval. It was found that for EP693 holding at over 950 C for more than 1.8 seconds resulted in a great decrease in heat resistance, resulting from coagulation or partial dissolution of the hardening phases. For EP914, heat resistance decreases if the metal is held at over 950 C for more than 3.0 second, a result of the lower diffusion mobility of Nb in comparison to Ti. This indicates the advantage of electron beam welding methods over arc welding, since the time the metal spends at high temperature is significantly reduced. Author

N85-22748# Joint Publications Research Service, Arlington, Va.
CORROSION-RESISTANT AMORPHOUS ALLOYS Abstract Only
V. V. Shvets and Y. I. Babey *In its* USSR Rept.: Mater. Sci. and Met. (JPRS-UMS-85-002) 6 Feb. 1985 p 68-69 Transl. into ENGLISH from Fiz.-Khim. Mekh. Mater. (USSR), v. 20, no. 4, Jul.-Aug. 1984 p 3-10 (For primary document see N85-22688 13-26)
Avail: NTIS HC A05/MF A01

Corrosion resistant amorphous alloys of transition metals with metalloids such as P, B and C are obtained by rapid cooling from a melt. The structure of the alloys does not have the characteristic long range order of crystalline alloys. The anomalously high corrosion resistance of amorphous alloys and their capability for passivation in corrosive media are explained not only by the presence of specific alloying elements, but also by structural specifics such as the lack of grain boundaries, dislocations, and macro and micro segregations. The addition of molybdenum, tungsten, titanium and vanadium is very effective in increasing the corrosion resistance of iron and cobalt based amorphous alloys. The unique corrosion properties of amorphous alloys make them quite promising as corrosion resistant materials. Metallographic studies have shown that after laser treatment the roughness of the surface is reduced and is characteristically shiny and reflective. Ion implantation is an effective method of producing amorphous layers on the surface of metals and alloys. The corrosion resistance of iron plasma coatings on metal substrates is shown to be high. Author

N85-22749# Joint Publications Research Service, Arlington, Va.
STRUCTURE OF AMORPHOUS FILMS OF ALLOYS BASED ON Fe, CONDENSED FROM LASER EROSION PRODUCTS Abstract Only
Y. A. Skakov, V. S. Aleynikov, Y. F. Bondarenko, M. I. Voronova, N. V. Yedneral, Y. N. Ivanov, and N. V. Shevenkova *In its* USSR Rept.: Mater. Sci. and Met. (JPRS-UMS-85-002) 6 Feb. 1985 p 69 Transl. into ENGLISH from Dokl. Akad. Nauk SSSR (USSR), v. 278, no. 5, Oct. 1984 p 1120-1122 (For primary document see N85-22688 13-26)
Avail: NTIS HC A05/MF A01

Films from molecular clusters typically have a circular structure and a directional growth pattern that approximate the direction of the molecular flow. Atomization of a number of alloys by laser irradiation is reported. The alloys tested were Fe-10Cr-4Si-16B, Fe-10Cr-13P=7B and Fe-10Cr-10B-10C. Films were deposited on KCl crystals, then separated in distilled water and examined by an electron microscope. Results showed that relatively low energy uncharged particles were distributed in the direction of the laser impulse, yielding a thin amorphous film like a coating of Fe_3O_4. Only a small part of the ion vapor cloud resulting from the laser impulse left the zone of the laser's impact. Changes in structure were noted as the condensate began to form high density coatings in some locations that had a higher tendency toward oxidation. Such zones depended in size on the alloy and varied from 10 to 150 nm. It was shown that laser atomization is effective for obtaining amorphous films with homogeneous dense structure, but heating of the film during condensation must be taken into account. Author

N85-22750# Joint Publications Research Service, Arlington, Va.
ENERGY SPECTRUM OF PROCESSES OF STRUCTURAL RELAXATION OF AMORPHOUS ALLOY FeCo70Si15B10 Abstract Only
I. B. Kekalo, V. Y. Taranichev, and V. Y. Tsvetkov *In its* USSR Rept.: Mater. Sci. and Met. (JPRS-UMS-85-002) 6 Feb. 1985 p 70 Transl. into ENGLISH from Dokl. Akad. Nauk SSSR (USSR), v. 278, no. 5, Oct. 1984 p 1115-1120 (For primary document see N85-22688 13-26)
Avail: NTIS HC A05/MF A01

Amorphous alloys are known to lack metastable balance after tempering due to the freezing of various defects into their structure. Energy parameters of the process of single axis anisotrophy of relaxation of tension in an amorphous alloy with the composition Fe5Co70Si15B10 after tempering from a molten state are presented. Changes in physical structure during structural relaxation were related to rearrangement in the amorphous phase beginning

at temperatures below 250 C. A temperature range of 185 to 340 C was studied to determine kinetics of these changes. Data obtained were analyzed on the basis of a log normal distribution of relaxation times. Results showed that at temperatures below 230 C the elimination of excess free volume was weak and relaxation of tension took place in the amorphous matrix. The spectrum of activation energy was very narrow. Mathematical calculations of these processes are presented. Author

N85-22751# Joint Publications Research Service, Arlington, Va.
EXPERIMENTAL STUDY OF ENTHALPY OF QUASIMONOCRYSTAL OF GRAPHITE AND CARBON GLASS IN TEMPERATURE RANGE OF 2890-3818 DEG K Abstract Only c24
L. M. Buchnev, A. I. Smylsov, I. A. Dmitriyev, A. F. Kuteynikov, and V. I. Kostikov *In its* USSR Rept.: Mater. Sci. and Met. (JPRS-UMS-85-002) 6 Feb. 1985 p 70-71 Transl. into ENGLISH from Dokl. Akad. Nauk SSSR (USSR), v. 278, no. 5, Oct. 1984 p 1109-1111 Original language document announced as 85A-15558 (For primary document see N85-22688 13-26)
Avail: NTIS HC A05/MF A01

The enthalpies of UPV-1T quasi-monocrystalline graphite and glassy carbon (a hard nongraphitizable carbon material) have been determined experimentally with an accuracy to within one percent using the method of mixing. In the temperature range investigated, the experimental values of the enthalpies of quasi-monocrystalline graphite and glassy carbon are coincident within the experimental uncertainty. An X-ray analysis of the specimens shows that heating to 3818 K does not produce changes in the principal parameters of the crystal structure of these materials. V.L. (IAA)

27 NONMETALLIC MATERIALS

Includes physical, chemical, and mechanical properties of plastics, elastomers, lubricants, polymers, textiles, adhesives, and ceramic materials.

N85-22752 Polytechnic Inst. of New York, Brooklyn.
INFLUENCE OF HYDROGEN BONDING IN BLOCK COPOLYMERS AND THEIR BLENDS Ph.D. Thesis
Prosanto Kumar Mukerji 1984 162 p
Avail: Univ. Microfilms Order No. DA8420461

A series of block copolymers of the type AB and BAB were prepared from styrene and ethylene oxide under positive argon pressure. The molecular weights for poly(styrene-b-ethylene oxide) was 0.2234 with 0.5 mole fraction of ethylene oxide and those for poly(ethylene oxide-b-styrene-b-ethylene oxide) were between 50,000 to 55,000 with 0.3, 0.5, 0.6 mole fraction of ethylene oxide. All the block copolymers were modified up to 6 mole percent with 1-trifluoromethyl carbinol. The influence of hydrogen bonding on the bulk morphology of the block copolymers was studied by differential scanning calorimetry (DSC). The lowering of the melting temperature for the poly(ethylene oxide) segment was significant in the block copolymers of both types. This is explained on the basis of shorter lamellar thickness of the crystals and large number of imperfections in the crystals. Dissert. Abstr.

N85-22753# Defence Research Information Centre, Orpington (England).
ADSORPTION BEHAVIOUR OF NITROGEN COMPOUNDS ON TO POROUS POLYMER BEADS AND APPLICATIONS TO ATMOSPHERIC SAMPLING
R. J. Robinson Jan. 1985 16 p refs Transl. into ENGLISH from Taiki Osen Gakkaishi (Japan), v. 18, no. 5, 1983 p 425-431 (BLL-DRIC-Trans-7399-(3623.66)) Avail: British Library Lending Div., Boston Spa, Engl.

The adsorption of nitrogen compounds on to porous polymer beads was studied, and the possibilities of normal temperature collection of low concentrations of trimethyl amine, acetonitrile, and acrylonitrile for gas chromographic measurements were investigated. Using a dynamic adsorption method, the breakthrough curves for TENAX-GC, Poropak-I, Chromosorb 103, and alkaline Porosil A were measured, and the breakthrough volumes and their temperature characteristics were found for the various compounds. The saturation adsorption value were found from the adsorption volumes of trimethyl amine, acetonitrile, and acrylonitrile used to pack collection-tubes of TENAX-GC, Chromosorb 103, and alkalised Porasil A. With TENAX-GC and Chroomosorb 103 the air intake was small, but with Porasil A the take-up could be 30 litre. The adsorption isotherms at 25 C were produced, from the gas concentration dependence of the saturation volume and these were convex. E.A.K.

N85-22754*# Celanese Research Corp., Summit, N.J.
EXPLORATORY DEVELOPMENT OF FOAMS FROM LIQUID CRYSTAL POLYMERS Final Report
Tai-shung Chung Jan. 1985 58 p refs
(Contract NAS1-17290)
(NASA-CR-172510; NAS 1.26:172510) Avail: NTIS HC A04/MF A01 CSCL 11G

Two types of liquid crystal polymer (LCP) compositions were studied and evaluated as structural foam materials. One is a copolymer of 6-hydroxy-2-naphthoic acid, terephthalic acid, and p-acetoxyacetanilide (designed HNA/TA/AAA), and the other is a copolymer of p-hydroxybenzoic acid and 6-hydroxy-2-naphthoic acid (designated HBA/HNA). Experimental results showed that the extruded HNA/TA/AA foams have better mechanical quality and appearance than HBA/HNA foams. Heat treatment improved foam tensile strength and break elongation, but reduced their modulus. The injection molding results indicated that nitrogen foaming agents with a low-pressure process gave better void distribution in the injection molded LCP foams than those made by the conventional injection-molding machine and chemical blowing agents. However, in comparing LCP foams with other conventional plastic foams, HBA/HNA foams have better mechanical properties than foamed ABS and PS, but are comparable to PBT and inferior to polycarbonate foams, especially in heat-deflection temperature and impact resistance energy. These deficiencies are due to LCP molecules not having been fully oriented during the Union-Carbide low-pressure foaming process. Author

N85-22755*# National Aeronautics and Space Administration. Lewis Research Center, Cleveland, Ohio.
METALLIC AND METALLOCERAMIC COATING BY THERMAL DECOMPOSITION
R. C. Hendricks and G. McDonald 1985 7 p ref Presented at the 12th Intern. Conf. on Met. Coatings, Los Angeles, 15-19 Apr. 1985; sponsored by the American Vacuum Society
(NASA-TM-86992; E-2538; NAS 1.15:86992) Avail: NTIS HC A02/MF A01 CSCL 11G

Metallic and metalloceramic coatings were prepared by thermal decomposition of a number of inorganic and metallo-organic compounds. The compounds were applied by spraying and by immersion, especially on ceramic fibers and fiber forms, which are easily coated by this procedure. Penetration of low-density ceramics is examined, and procedures are described that were used for converting the deposited materials to metals, oxides, or metal oxide films. Multiple-component films were also prepared. Photomicrographs illustrate the structure of these films. R.J.F.

N85-22756*# National Aeronautics and Space Administration. Lewis Research Center, Cleveland, Ohio.
FILM AND INTERSTITIAL FORMATION OF METALS IN PLASMA-SPRAYED CERAMICS
R. C. Hendricks, G. McDonald, and R. L. Mullen (Case Western Reserve Univ., Cleveland) 1985 12 p refs Presented at the 12th Intern. Conf. on Metallurgical Coatings, Los Angeles, 15-19 Apr. 1985
(NASA-TM-86993; NAS 1.15:86993; E-2539) Avail: NTIS HC A02/MF A01 CSCL 11B

A method is described to electrodeposit noble metals such as platinum and ordinary metals such as copper on and within plasma-sprayed ceramic materials and ceramic fiber materials. Low-density ceramic fiber bodies were vacuum impregnated with plating solution and attached to an electrode. Light micrographs

illustrating the density and location of deposited materials are presented and discussed. Voids in the plasma-sprayed ceramic were filled with deposits that vary from spherical to lens-shaped circular and have particle size corresponding to the full range of void size. Multiple coatings of ceramic and metal can be sequenced. Author

N85-22757*# Southwest Research Inst., San Antonio, Tex.
SLIDING SEAL MATERIALS FOR ADIABATIC ENGINES Interim Report, Feb. 1984 - Feb. 1985
James Lankford Apr. 1985 70 p refs
(Contracts DEN3-352; DE-AI01-80CS-50194)
(NASA-CR-174893; NAS 1.26:174893; SRI-06-7963; DOE/NASA/0352-1) Avail: NTIS HC A04/MF A01 CSCL 11B

The sliding friction coefficients and wear rates of promising carbide, oxide, and nitride materials were measured under temperature, environmental, velocity, loading conditions that are representative of the adiabatic engine environment. In order to provide guidance needed to improve materials for this application, the program stressed fundamental understanding of the mechanisms involved in friction and wear. Microhardness tests were performed on the candidate materials at elevated temperatures, and in atmospheres relevant to the piston seal application, and optical and electron microscopy were used to elucidate the micromechanisms of wear following wear testing. X-ray spectroscopy was used to evaluate interface/environment interactions which seemed to be important in the friction and wear process. Electrical effects in the friction and wear processes were explored in order to evaluate the potential usefulness of such effects in modifying the friction and wear rates in service. However, this factor was found to be of negligible significance in controlling friction and wear. R.J.F.

N85-22758*# Oak Ridge National Lab., Tenn. Metal and Ceramics Div.
DISPERSED-METAL-TOUGHENED ALUMINA
T. N. Tiegs and A. J. Moorhead Feb. 1984 31 p refs
(NASA Order C-72801-D; Contract DE-AC05-84OR-21400)
(NASA-CR-174687; DOE/NASA/2801-1; NAS 1.26:174687; ORNL/TM-9518) Avail: NTIS HC A03/MF A01 CSCL 11B

Hot-pressed alumina with a fine dispersion of Cr metal particles showed good fracture toughness (K sub I sub c <MPa. m 1/2) and thermal shock resistance. However, the fracture strengths of these materials were relatively low (190 to 240 MPa vs 350 to 580 MPa for pure alumina). The good fracture toughness and thermal shock resistance were found to be related to the relatively large-grain duplex microstructure of the hot-pressed materials. The fracture toughness of alumina with dispersions of Ni and Pt was found to be inferior to that of the Al2O3-Cr materials. Hot-pressed solid solutions of Al2O3-Cr2O3 also showed good fracture toughness (K sub I sub c = 7.3 to 7.7 MPa.m 1/2), which was again due to the development of a relatively large-grain duplex microstructure. Author

N85-22759# Stanford Univ., Calif. Dept. of Chemical Engineering.
SYNTHESIS AND CHARACTERIZATION OF POLY(VINYLIDENE FLUORIDE) Final Report
C. W. Frank 18 Jan. 1985 4 p
(Contract N00014-81-K-0683)
(AD-A150291) Avail: NTIS HC A02/MF A01 CSCL 11/9

Poly(vinylidene fluoride) (PVF2) has been widely studied due to potential applications based on its ferroelectric nature, with both piezoelectric and pyroelectric devices possible. Structural analysis of PVF2, which involves characterization of both the polymorphism and the detailed molecular structure, has been a major area of research. One major thrust under this contract has been to examine the influence of head-to-head defects on the crystallization and melting behavior of PVF2. The first project of interest was to examine lamellar thickening during the alpha crystallization. In a second study, Hoffman-Weeks plots of melting temperature versus crystallization temperature were prepared in order to determine the equilibrium melting temperature. In the third study on crystallization and melting behavior, high temperature crystallization experiments were performed in order to determine the influence of the H/H content and the molecular weight on the solid state transformation from the alpha to the gamma phase. The second major thrust of our research has been an examination of the thermal degradation of PVF2 in solution. GRA

N85-22760# Colorado State Univ., Fort Collins. Dept. of Chemistry.
CHIRAL POLYMERS Final Report, 1 Sep. 1981 - 31 Aug. 1984
J. K. Stille and A. I. Meyers Oct. 1984 16 p
(Contract DAAG29-81-K-0170)
(AD-A150366; ARO-18630.2-CH) Avail: NTIS HC A02/MF A01 CSCL 07/3

Chiral vinyl monomers containing the oxazoline units, 2-vinyl-4-methoxy-methyl- and 4-hydroxymethyl-5-phenyloxazoline as well as a chiral oxazoline monomer bearing an acrylate polymerizable group were synthesized. In addition, an acrylamide monomer containing a chiral 1,3-dioxane unit as well as both racemic and (R)-alpha-methylene-gamma-methyl-gamma-butyrolactone were synthesized. The vinyloxazoline,, 2-vinyl-4-methoxymethyl-5-phenyloxazoline was copolymerized with styrene and divinylbenzene by suspension techniques to give polymer beads approx. 50 microns in diameter. The oxazoline monomer containing the polymerizable acrylate group and the acrylamide monomer containing the dioxolane unit also were copolymerized with styrene and divinyl benzene to give cross-linked polymer beads, approx. 50 microns in diameter. Racemic and chiral alpha-methylene-gamma-methyl-gamma-butyrolactone were homopolymerized by radical, anionic, and group transfer methods. Chiral lactone gave isotactic polymer, regardless of the method of polymerization. The styrene-bead copolymers were packed in HPLC columns, but none were especially effective in separating enantiomers in a racemic mixture. The chiral butyrolactone polymer was coated on silica, but this material did not effect resolution of racemic mixtures in an HPLC column. Originator furnished keywords are: Vinyl oxazolines, Alpha-methylene-gamma-methyl-gamma-butyrolactone, Chromatography, Copolymer beads, Chiral Monomers, HPLC, Chiral copolymers. GRA

N85-22761# California Inst. of Tech., Pasadena.
RESEARCH PROGRAM ON THE EFFECT OF PRESSURE ON THE MECHANICAL PROPERTIES OF POLYMERS, PART 2 Final Report
N. W. Tschoegl Oct. 1984 62 p refs
(Contract DE-AT03-76ER-75016)
(DE85-000995; DOE/ER-75016/T4) Avail: NTIS HC A03/MF A01

This research was directed toward the problem of bulk relaxation in polymers via measurements of the time dependent Poisson ratio. This report is concerned with the measurement of the time dependent Poissons ratio of viscoelastic materials in the transition region. DOE

N85-22762# Sandia Corp., Albuquerque, N. Mex.
EFFECT OF ALTERNATIVE AGING AND ACCIDENT SIMULATIONS ON POLYMER PROPERTIES
L. D. Bustard, J. Chenion (Commissariat a l'Energie Atomique, Gif-sur-Yvette, France), F. Carlin (Commissariar a l'Energie Atomique, Gif-sur-Yvette, France), C. Alba (Commissariat a l'Energie Atomique, Gif-sur-Yvette, France), G. Gaussens (Commissariat a l'Energie Atomique, Gif-sur-Yvette, France), and M. LeMeur (Commissariat a l'Energie Atomique, Fontenay-aux-Roses, France) 23 Oct. 1984 26 p refs Presented at 12th. Water Reactor Safety Res. Inform. Meeting, Gaithersburg, Md., 23 Oct., 1984
(Contract DE-AC04-76DP-00789)
(DE85-002642; SAND-84-1759C; CONF-8410142-35) Avail: NTIS HC A03/MF A01

The response of 18 US and French polymer materials to variations in aging and accident simulation techniques was determined by experimental program. A data base is provided by which to judge appropriate simulation practices. The overall research goal is to determine whether some aging and accident simulation

techniques are better suited for qualification activities than othe alternative simulation techniques. DOE

N85-22763# California Univ., Berkeley. Lawrence Berkeley Lab. Materials and Molecular Research Div.
DENSIFICATION AND DEFORMATION IN THE PRESENCE OF A LIQUID PHASE Ph.D. Thesis
John Edward Marion, II Jul. 1984 241 p refs
(Contract DE-AC03-76SF-00098)
(DE85-005101; LBL-18411) Avail: NTIS HC A11/MF A01

The mechanisms for creep and sintering of solid materials in the presence of a liquid phase are explored. The sintering behavior of a simple ceramic/glass system is studied. Densification involves concurrent viscous flow and solutin/reprecipitation processes for which equations are proposed. Comparison of these equations with microstructural observations suggests that thin equilibrium grain boundary films can support gradients in normal stresses required for diffusive matter transport through the liquid. Evidence is presented for the existence of significant structure within the thin grain boundary films. The final stage in the liquid-phase sintering process, the closure of pores, is modeled using an extreme value distribution to describe the sizes of the shrinking pores. The investigation focuses on high temperature deformation in the presence of a liquid phase. Electron microscopy results on creep damage in several liquid-phase sintered ceramic alloys exposed to creep strains at elevated temperatures are used to propose a sequence for the early stages of cavitation damage. Interface failure time models are generated for each step. DOE

N85-22764# Brookhaven National Lab., Upton, N. Y. Dept. of Applied Science.
HREELS AND AUGER STUDIES OF CONDUCTING POLYMERS
W. D. Jennings, G. S. Chottiner, C. Natarajan, A. V. Melo, R. W. Hoffman, W. E. OGrady, I. Lundstrom, and W. R. Salaneck Aug. 1984 30 p refs Presented at the 6th Symp. on Applied Surface Analysis, Dayton, Ohio, 6-8 Jun. 1984 Prepared in cooperation with Case Western Reserve Univ., Cleveland and Linkoeping Univ., (Sweden)
(Contract DE-AC02-76CH-00016)
(DE85-004541; BNL-35534; CONF-8406187-2) Avail: NTIS HC A03/MF A01

High Resolution Electron Energy Loss Spectroscopy (HREELS) and Auger Spectroscopy have been used to examine the surface of conducting polymer samples. The samples were 100 nm thick films of polypyrrole doped with either BF4 or ClO4 negative ions. The films were made in Sweden and shipped to the USA for study. HREELS spectra could be obtained without difficulty in the samples' as is condition. These spectra showed broad bands corresponding to known polypyrrole vibrational modes. Exposure of the polymer to oxygen had no effect, but water could be adsorbed on the samples at 130 K. In addition to vibrational excitations, broader electronic transitions were also identified. Auger studies were performed in an effort to characterize the surface. These studies indicate that considerable non-stoichiometry exists in the surface region. There were, as expected, problems due to questionable sample cleanliness, sample charging, and electron beam damage. DOE

N85-22765# Oak Ridge National Lab., Tenn. Solid State Div.
TIME-RESOLVED STUDIES OF RAPID SOLIDIFICATION IN HIGHLY UNDERCOOLED MOLTEN SILICON
D. H. Lowndes, G. E. Jellison, Jr., R. F. Wood, S. J. Pennycook, and R. W. Carpenter (Arizona State Univ., Tempe) Dec. 1984 7 p refs Presented at the Symp. on the Scientific Basis for Nucl. Waste Management, Boston, 27-30 Nov. 1984
(Contract DE-AC05-84OR-21400)
(DE85-004857; CONF-841157-47) Avail: NTIS HC A02/MF A01

A KrF (248 nm) pulsed laser was used to melt 90-, 190-, and 440-nm thick amorphous silicon layers produced by Si ion implantation into (100) crystalline Si substrates. Time-resolved reflectivity measurements at two different probe wavelengths (633 nm and 1.15 micron) and post-irradiation TEM measurements were used to study the formation of an undercooled liquid Si phase and the subsequent solidification processes. The time-resolved measurements provide new experimental information about the nucleation of fine-grained Si crystallites in undercooled liquid Si, at low laser energy densities (E/sub 1/), and about the growth of large-grained SI in the near-surface region at higher E/sub 1/. Measurements with the infrared probe beam reveal the presence of a buried, propagating liquid layer at low E/sub 1/. Model calculations indicate that this liquid layer is generated in part by the release of latent heat associated with the nucleation and growth process. DOE

N85-22766# Argonne National Lab., Ill. Materials Science and Technology Div.
NDE METHODS FOR GREEN CERAMICS
D. S. Kupperman, W. A. Ellingson, and H. Berger (Industrial Quality, Inc., Gaithersburg, Md.) Oct. 1984 32 p refs Presented at the Japan/US Seminar on Fundamentals of Structural Ceramics, Seattle, 1 Aug. 1984
(Contract W-31-109-eng-38)
(DE85-004019; CONF-8408133-2) Avail: NTIS HC A03/MF A01

A preliminary investigation of radiographic, ultrasonic, and nuclear magnetic resonance (NMR) imaging methods for the nondestructive evaluation of green (unfired) ceramics is described. Microradiography provides sharper images than ordinary radiographs, and very small defects are detected. The application of microradiography to ceramics is reviewed, and preliminary experiments with a commercial microradiography unit are described. Computerized axial tomographic (CAT) imaging with x-rays provides images of cross sections of an object and thus eliminates unwanted detail (noise). The CAT scanning provides for detection of flaws in the 10 to 100 (MU)m range. Initial CAT-scanning results for green-state ceramics are presented. However, ultrasonic velocity and attenuation data are presented which provide useful information related to density variations and the elastic anisotropy of the green state. The NMR study suggests that areas of high porosity may be detectable if the binder is burned out and replaced with a hydrogen-rich dopant such as water. DOE

N85-22767# California Univ., Livermore. Lawrence Livermore Lab.
IMPURITIES IN KEVLAR 49 FIBERS
C. O. Pruneda, R. J. Morgan, R. Lim, L. J. Gregory, and J. W. Fischer 11 Dec. 1984 11 p refs Presented at 30th Natl. Meeting of the Soc. for the Advan. of Mater. and Process Eng., Anaheim, Calif., 19 Mar. 1985
(Contract W-7405-eng-48)
(DE85-004996; UCRL-90947; CONF-850323-2) Avail: NTIS HC A02/MF A01

The impurities in Kevlar 49 fibers [poly(p-phenylene terephthalamide)PPTTA] are discussed in terms of the fiber fabrication processes. The impurities were monitored by inductivity coupled plasma emission and optical emission spectroscopy. The principal impurities Na2SO4 and total S were analyzed chemically. The chemical analyses together with C, N, H elemental analyses shows that there are 1.5 wt % impurities present in Kevlar 49 fibers of which approx. 50% are in the form of Na2SO4 and the remainder, probably in the form of benezene sulfonic -SO3H PPTA side groups. There are three of these acid groups per each PPTA macromolecule. Organic impurities, such as terephthalic acid are discussed in the light of degradation studies of PPTA-H2SO4 spinning dopes. Electroin microprobe x-ray spectroscopy and laser induced damage studies were utilized to investigate the distribution of impurities through the fiber cross-section. The distribution of impurities throughout the fiber are determined by the fiber fabrication processes and are discussed at the microscopic and molecular level. The defects caused by these impurities and their effect on the deformation and failure modes are considered. DOE

N85-22511*# Pennsylvania State Univ., University Park.
MASS SPECTRA OF NEUTRAL PARTICLES RELEASED DURING ELECTRICAL BREAKDOWN OF THIN POLYMER FILMS
B. R. F. Kendall *In* NASA. Lewis Research Center Spacecraft Environ. Interactions Technol., 1983 Mar. 1985 p 525-535 refs

(For primary document see N85-22470 13-18)
(Grant NsG-3301)
Avail: NTIS HC A99/MF E03 CSCL 11G

N85-22513*# Hughes Research Labs., Malibu, Calif.
KAPTON CHARGING CHARACTERISTICS: EFFECTS OF MATERIAL THICKNESS AND ELECTRON-ENERGY DISTRIBUTION
W. S. Williamson, C. R. Dulgeroff, J. Hymann, and R. Viswanathan (Hughes Space and Communications Group, Los Angeles) *In* NASA. Lewis Research Center Spacecraft Environ. Interactions Technol., 1983 Mar. 1985 p 547-558 refs (For primary document see N85-22470 13-18)
Avail: NTIS HC A99/MF E03 CSCL 11G

N85-22514*# SRI International Corp., Menlo Park, Calif.
ELECTRICAL CONDUCTION IN POLYMER DIELECTRICS
David B. Cotts *In* NASA. Lewis Research Center Spacecraft Environ. Interactions Technol., 1983 Mar. 1985 p 559-569 refs (For primary document see N85-22470 13-18)
(Contract F19628-81-C-0076)
Avail: NTIS HC A99/MF E03 CSCL 11G

N85-22630# Joint Publications Research Service, Arlington, Va.
INFLUENCE OF EXTERNAL ELECTRIC FIELD ON STRUCTURAL-MECHANICAL PROPERTIES OF POWDERED MATERIALS Abstract Only
Ye. P. Toporov, G. I. Shcherbina, I. N. Aleynikova, N. B. Uryev, and V. Ye. Chernomaz *In its* USSR Rept.: Chem. (JPRS-UCH-85-001) 17 Jan. 1985 p 1 Transl. into ENGLISH from Kolloidnyy Zh. (Moscow), v. 46, no. 5, Sep. - Oct. 1984 p 1039-1041 (For primary document see N85-22629 13-23)
Avail: NTIS HC A06

N85-22634# Joint Publications Research Service, Arlington, Va.
CRITICAL EVENTS IN INELASTIC DEFORMATION OF GLASSY POLYMERS IN ADSORPTIVE MEDIUM Abstract Only
A. N. Shitov, G. M. Lukovkin, A. L. Volynskiy, and N. F. Bakeyev *In its* USSR Rept.: Chem. (JPRS-UCH-85-001) 17 Jan. 1985 p 78-79 Transl. into ENGLISH from Vysokomolekul. Soyedineniya (Moscow), v. 26, no. 9, Sep. 1984 p 1842-1847 (For primary document see N85-22629 13-23)
Avail: NTIS HC A06

N85-22635# Joint Publications Research Service, Arlington, Va.
EFFECTS OF TRIAZINE COMPONENTS ON PHYSICOCHEMICAL PROPERTIES OF POLYBUTADIENE: URETHANE BLOCK COPOLYMERS Abstract Only
N. P. Bessonova, A. R. Korigodskiy, D. F. Kutepov, and Yu. K. Godovskiy *In its* USSR Rept.: Chem. (JPRS-UCH-85-001) 17 Jan. 1985 p 79 Transl. into ENGLISH from Vysokomolekul. Soyedineniya (Moscow), v. 26, no. 9, Sep. 1984 p 1877-1881 (For primary document see N85-22629 13-23)
Avail: NTIS HC A06

N85-22636# Joint Publications Research Service, Arlington, Va.
MECHANISM OF STRENGTHENING PLASTICS WITH RUBBERS Abstract Only
V. N. Kuleznev *In its* USSR Rept.: Chem. (JPRS-UCH-85-001) 17 Jan. 1985 p 85-86 Transl. into ENGLISH from Plast. Massy (Moscow), no. 10, Oct. 1984 p 21-22 (For primary document see N85-22629 13-23)
Avail: NTIS HC A06

N85-22637# Joint Publications Research Service, Arlington, Va.
STUDY OF CHARACTER OF ADHESIVE INTERACTION AND BREAKING OF POLYIMID-ALUMINUM FOIL JUNCTION DURING PROCESS OF HARDENING Abstract Only
V. M. Startsev, N. F. Chugunova, A. Ye. Chalykh, L. P. Kazanskiy, and A. Ye. Rubtsov *In its* USSR Rept.: Chem. (JPRS-UCH-85-001) 17 Jan. 1985 p 88-89 Transl. into ENGLISH from Kolloidnyy Zh. (Moscow), v. 46, no. 5, Sep. - Oct. 1984 p 961-966 (For primary document see N85-22629 13-23)
Avail: NTIS HC A06

N85-22710# Joint Publications Research Service, Arlington, Va.
THEORY OF RELAXATION PROCESSES IN DECOMPOSING POLYMER MATERIALS DURING HIGH-INTENSITY CONVECTIVE HEATING Abstract Only
G. N. Isakov, V. V. Nesmelov, G. Y. Vishnevskiy, and Y. N. Zadorina *In its* USSR Rept.: Mater. Sci. and Met. (JPRS-UMS-85-002) 6 Feb. 1985 p 19 Transl. into ENGLISH from Dokl. Akad. Nauk SSSR (USSR), v. 278, no. 5, Oct. 1984 p 1112-1115 Original language document announced as 85A-15559 (For primary document see N85-22688 13-26)
Avail: NTIS HC A05/MF A01

28 PROPELLANTS AND FUELS

Includes rocket propellants, igniters, and oxidizers; storage and handling; and aircraft fuels.

For related information see also *07 Aircraft Propulsion and Power, 20 Spacecraft Propulsion and Power,* and *44 Energy Production and Conversion.*

N85-22768# Ohio State Univ., Columbus. Dept. of Physics.
A STANDARD AIRCRAFT DIFFUSION FLAME: SPECTRAL CHARACTERISTICS AND A FEASIBILITY STUDY FOR DEVELOPING AN ALTERNATE CALIBRATION SOURCE FOR AIRCRAFT OPTICAL FIRE DETECTION SYSTEMS Final Report, 31 Mar. 1983 - 30 Sep. 1984
R. L. Hawkins and K. N. Rao Wright-Patterson AFB, Ohio Air Force Wright Aeronautical Labs. 30 Dec. 1984 29 p
(Contract F33615-83-K-2308)
(AD-A150231; AFWAL-TR-84-2080) Avail: NTIS HC A03/MF A01 CSCL 21/4

The standard aircraft diffusion flame source presents practical difficulties due to its lack of controllability and its production of large amounts of smoke and soot. A source which is more convenient to handle, but which emulates the spectral and power characteristics of the standard flame, might prove useful. The requirements of such a flame were evaluated by measuring the spectral and power characteristics of a standard aircraft diffusion flame over the spectral range 2.5 micrometers to 20 micrometers. The total power output in this range was on the order of 1000 watts. About one-fourth of this was from the 4.4 micrometers carbon dioxide emission and; a small amount was due to weaker emissions of water vapor and carbon dioxide; and the remainder was due to thermal emission from soot particles. GRA

N85-22769# Ballistic Research Labs., Aberdeen Proving Ground, Md.
A COMPREHENSIVE REVIEW OF BLACK POWDER Final Report
R. A. Sasse Jan. 1985 41 p
(AD-A150455; AD-F300568; BRL-TR-2630) Avail: NTIS HC A03/MF A01 CSCL 19/1

A diligent attempt has been made to scrutinize black powder and the charcoal it contains as fully as possible, utilizing modern testing techniques and various analytical chemical procedures. Although the tests performed are well established, their application to define a porous propellant represents a new point of view for investigating structure. From S.E.M. microphotographs and compaction studies, it is suggested that the pressing action used to make black powder results in plastic flow that produces a conglomerate and cohesive mass containing a matrix of inter-connecting passageways. The degree of openness of black powder grains and, in particular, internal surface area, pore volume, internal free volume, and density were all found to be related to burn rate. Thermodynamic calculations were cited that relate computed theoretical values to experimentally determined quantities. Closed bomb data embrace more than one combustion mode and as such do not directly relate to bulk values. From this interrogation, chemical and physical properties were related to combustion

phenomena. As work progressed it became evident that material produced by the Indiana Army Ammunition Plant will be, or has become, the most successfully characterized black powder produced in the United States. GRA

N85-22770# Massachusetts Inst. of Tech., Cambridge.
IHE MATERIAL QUALIFICATION TESTS DESCRIPTION AND CRITERIA
Robert J. Slape, comp. Jun. 1984 23 p refs
(Contract DE-AC04-76DP-00487)
(DE85-004649; MHSMP-84-22) Avail: NTIS HC A02/MF A01

The qualification tests presently being used at Pantex Plant, Lawrence Livermore National Laboratory, and Los Alamos National Laboratory that are required by the Department of Energy prior to the approval for an explosive as an Insensitive High Explosive (IHE) material are described. The acceptance criteria of each test for IHE qualification is also discussed. DOE

N85-22771# Delaware Univ., Newark. Dept. of Chemical Engineering.
TRIFUNCTIONAL CATALYSTS FOR CONVERSION OF SYNGAS TO ALCOHOLS Quarterly Report, 1 Sep. - 30 Nov. 1984
K. B. Bischoff, William Manogue, and G. Alex Mills 12 Dec. 1984 10 p
(Grant DE-FG22-84PC-70780)
(DE85-004577; DOE/PC-70780/1; QR-1) Avail: NTIS HC A02/MF A01

The following tasks are discussed briefly: (1) preparation of catalyst samples; (2) testing catalysts for syngas conversion; (3) measurement of surface composition and structure; (4) determination of nature of surface complexes; (5) reaction mechanism determination by isotopic tracers and kinetics; and (6) design, prepare and test optimized catalysts. Work has started on catalyst preparation and planning for near-term characterization. Considerable effort was expended in design of the system for testing syngas conversion, including the option of activation of a previously constructed system. A literature review is underway including current publications, to ensure advantage is being taken of the intensive research effort underway worldwide. DOE

N85-22772# Institute of Gas Technology, Chicago, Ill.
ANAEROBIC DIGESTION OF BIOMASS: STATUS SUMMARY AND RESEARCH DEVELOPMENT NEEDS, 1983 Topical Report, Jan. - Oct. 1983
D. P. Chynoweth, K. F. Fannin, D. E. Jerger, V. J. Srivastava, and R. Bijetina Jul. 1984 315 p refs Sponsored by Gas Research Inst.
(PB85-161925; GRI-84/0133.1) Avail: NTIS HC A14/MF A01 CSCL 21D

The statuse of anaerobic digestion is reviewed from the perspective of producing methane from biomass. Research needs are discussed and listed with priorization. Hydrolytic, intermediate, and methanogenic bacteria are discussed, as well as feed composition, pre-/posttreatment, nutrient requirements, and toxicity. Reactor designs, process start-up, operation, stability and control, kinetics and modeling, net energy, and process scale-up and commercialization are considered. Author

N85-22527# Naval Postgraduate School, Monterey, Calif.
SOLID PROPELLANT COMBUSTION DIAGNOSTICS AND AUTOMATED DATA RETRIEVAL FROM HOLOGRAMS
J. M. Glenn, K. J. Graham, R. K. Harris, Y. Lee, D. W. Netzer, and J. P. Powers *In* APL 21st JANNAF Combust. Meeting, Vol. 1 Oct. 1984 p 1-14 refs (For primary document see N85-22526 13-20)
(Contract F04611-84-X-0001)
Avail: NTIS HC A21/MF A01 CSCL 21/9

N85-22529# Pennsylvania State Univ., University Park.
GASIFICATION OF BORON OXIDE DROPS AND BORON SLURRY AGGLOMERATES IN COMBUSTION GASES
S. R. Turns, J. T. Holl, A. S. P. Solomon, and G. M. Faeth *In* APL 21st JANNAF Combust. Meeting, Vol. 1 Oct. 1984 p 31-44 refs (For primary document see N85-22526 13-20)
Avail: NTIS HC A21/MF A01 CSCL 21/2

N85-22539*# Jet Propulsion Lab., California Inst. of Tech., Pasadena.
CHARACTERIZATION OF HETEROGENEITY OF COMPOSITE PROPELLANTS AND ITS EFFECTS ON COMBUSTION BEHAVIOR
L. D. Strand and N. S. Cohen (Cohen (Norman S.) Professional Services, Inc.) *In* APL 21st JANNAF Combust. Meeting, Vol. 1 Oct. 1984 p 139-152 refs Sponsored in part by NASA (For primary document see N85-22526 13-20)
(Contracts AFOSR-ISSA-81-00019; AFOSR-ISSA-82-00030; AFOSR-ISSA-83-00052)
Avail: NTIS HC A21/MF A01 CSCL 21I

N85-22540# Georgia Inst. of Tech., Atlanta. School of Aerospace Engineering.
INVESTIGATION OF THE CHARACTERISTICS OF THE VELOCITY-COUPLED RESPONSE FUNCTIONS OF SOLID PROPELLANTS
L. L. Narayanaswami, B. T. Zinn, and B. R. Daniel *In* APL 21st JANNAF Combust. Meeting, Vol. 1 Oct. 1984 p 153-163 refs (For primary document see N85-22526 13-20)
(Contract F49620-82-C-0013)
Avail: NTIS HC A21/MF A01 CSCL 21/9

N85-22548# Systems Research Labs., Inc., Dayton, Ohio.
APPLICATION OF FLUORESCENCE TO MEASUREMENT OF SURFACE TEMPERATURE IN SOLID PROPELLANTS
Larry F. Goss and Arthur A. Smith *In* APL 21st JANNAF Combust. Meeting, Vol. 1 Oct. 1984 p 241-249 refs (For primary document see N85-22526 13-20)
(Contract F49620-83-C-0138)
Avail: NTIS HC A21/MF A01 CSCL 21/9

N85-22551# Army Research and Development Command, Dover, N.J.
THE CRYSTAL AND MOLECULAR STRUCTURE OF A NEW PROPELLANT COMPOUND: TRIAMINOGUANIDIUM AZIDE NITRATE (TAZN)
A. J. Bracuti and Jan M. Troup (Molecular Structure Corp., College Station, Tex.) *In* APL 21st JANNAF Combust. Meeting, Vol. 1 Oct. 1984 p 293-299 refs (For primary document see N85-22526 13-20)
Avail: NTIS HC A21/MF A01 CSCL 21/9

N85-22552# Army Research and Development Command, Dover, N.J.
MOLECULAR DYNAMICS OF PROPELLANT GASES, PART 2
T. Vladimiroff *In* APL 21st JANNAF Combust. Meeting, Vol. 1 Oct. 1984 p 301-306 refs (For primary document see N85-22526 13-20)
Avail: NTIS HC A21/MF A01 CSCL 21/9

N85-22553# Colorado State Univ., Fort Collins.
AN INTEGRAL CLOSED LOOP COMBUSTION STABILITY MODEL-STATUS AND REVIEW
C. E. Mitchell *In* APL 21st JANNAF Combust. Meeting, Vol. 1 Oct. 1984 p 347-355 refs (For primary document see N85-22526 13-20)
Avail: NTIS HC A21/MF A01 CSCL 21/9

N85-22559# Naval Research Lab., Washington, D. C. Chemistry Div.
KINETICS OF MECHANISM OF THE THERMAL DECOMPOSITION OF DIMETHYLNITRAMINE AND DIMETHYLNITROSAMINE
M. E. Umstead, S. A. Lloyd, D. S. Y. Hsu, and M. C. Lin *In* APL 21st JANNAF Combust. Meeting, Vol. 1 Oct. 1984 p 417-422 refs (For primary document see N85-22526 13-20)
Avail: NTIS HC A21/MF A01 CSCL 21/9

N85-22560# Lockheed Missiles and Space Co., Palo Alto, Calif.
EFFECTS OF HMX ADDITION ON THE COMBUSTION OF ENERGETIC BINDERS
N. S. Cohen (Cohen (Norman S.) Professional Services, Inc.), J. C. Crowley, and G. A. Lo *In* APL 21st JANNAF Combust. Meeting, Vol. 1 Oct. 1984 p 423-432 refs (For primary document see N85-22526 13-20)
Avail: NTIS HC A21/MF A01 CSCL 21/9

N85-22561# Naval Research Lab., Washington, D. C. Chemistry Div.
THE CHEMISTRY OF RDX AND HMX CLUSTER IONS
Robert J. Doyle, Jr. and Joseph E. Campana *In* APL 21st JANNAF Combust. Meeting, Vol. 1 Oct. 1984 p 433-436 refs (For primary document see N85-22526 13-20)
Avail: NTIS HC A21/MF A01 CSCL 21/9

N85-22562# University of Southern California, Los Angeles. Dept. of Mechanical Engineering.
EFFECTS OF TEMPERATURE VARIATION AMONG DROPLETS IN AN EVAPORATING FUEL SPRAY
P. Roy Choudhury and Melvin Gerstein *In* APL 21st JANNAF Combust. Meeting, Vol. 1 Oct. 1984 p 455-463 refs (For primary document see N85-22526 13-20)
Avail: NTIS HC A21/MF A01 CSCL 21/4

31 ENGINEERING (GENERAL)

Includes vacuum technology; control engineering; display engineering; and cryogenics.

N85-22773# Royal Naval Coll., Greenwich, London (England). Dept. of Nuclear Science and Technology.
FIELD-WORK REPORT: MEDWAY ESTUARY, 28 JUNE - 18 JULY 1983
D. J. McMillan and N. M. Lynn Dec. 1983 15 p
(RNC/NS/TR8; BR92219) Avail: NTIS HC A02/MF A01

Two tide gages were deployed in an estuary for testing against the standard tide gage. High-speed axial profiles were obtained. Monitoring of dye and fixed-point monitoring of water parameters, and monitoring of wind were carried out. The field-work was undertaken to test equipment and procedures in the field, to test the capabilities of an inflatable craft, to obtain information to improve the project's computer modelling technique, and to gain information for validation of a one dimensional transient estuary model. Author (ESA)

N85-22774# Naval Research Lab., Washington, D. C.
SURVEY OF THE STATE-OF-THE-ART OF MINIATURE CRYOCOOLERS FOR SUPERCONDUCTIVE DEVICES Final Report
J. L. Smith, Jr., G. Y. Robinson, Jr., and Y. Iwasa 31 Dec. 1984 63 p
(F62-582)
(AD-A150319; NRL-MR-5490) Avail: NTIS HC A04/MF A01 CSCL 20/13

This document presents the results of a survey of the state-of-the-art as applied to cryocoolers to cool small superconducting devices. The survey included visits to over 100 facilities involved in the production or development of small cryocoolers in the United States, Japan, Europe. Specifications of commercially available cryocoolers having capacities of one of five watts in the 80 to 4 K range are presented. The survey was sponsored by the Office of Naval Research. GRA

N85-22775# Naval Postgraduate School, Monterey, Calif.
DRAFTSMAN DISPLAYS: A GRAPHICAL TECHNIQUE FOR EXPLORATORY DATA ANALYSIS M.S. Thesis
M. D. Johnson, Jr. Jun. 1984 103 p
(AD-A150515) Avail: NTIS HC A06/MF A01 CSCL 12/1

This thesis develops and explores the graphical analysis of multivariate data sets through the use of a Draftsman technique of scatter plot displays. These plot displays are useful for determining associations and relationships between variables in order to promote an understanding of the characteristics of the data in exploratory and descriptive applications. General graphical enhancement techniques such as jittering and transformations are discussed and incorporated in the development of a computer program which produces Draftsman displays. A technical description of the Draftsman computer program is presented, and user implementation procedures discussed. An analysis is conducted on two varied sets of data to demonstrate the versatility and utility of the Draftsman display technique for exploring data structures. GRA

N85-22776# National Bureau of Standards, Washington, D.C. Center for Fire Research.
ENVIRONMENTAL CYCLING OF CELLULOSIC THERMAL INSULATION AND ITS INFLUENCE ON FIRE PERFORMANCE
J. Randall Lawson Aug. 1984 46 p refs
(Contract DE-AI05-78CR-06113)
(DE85-004295; NBSIR-84-2917) Avail: NTIS HC A03/MF A01

A study was conducted on climatological data for eleven cities located throughout the United States. Findings from this environmental study were used to develop conditioning cycles for a research project on the influence of environments on the fire performance of loose-fill cellulosic thermal insulation. Six cellulosic insulation materials with different compositions of fire retardant chemicals at an add-on level of 25% by weight were specially manufactured for this study. These materials were tested for fire performance using the smoldering combustion test and the attic flooring radiant panel test to establish a baseline. After the materials were exposed to the various environmental cycles, they were tested for fire performance. Results from these tests show that environmental exposure can have a significant effect on the fire performance of cellulosic insulation materials and indicates that long term fire protection provided by fire retardant compounds may be limited. DOE

N85-22777# Joint Publications Research Service, Arlington, Va.
CHINA REPORT: SCIENCE AND TECHNOLOGY
10 Oct. 1984 49 p refs Transl. into ENGLISH from various Chinese articles
(JPRS-CST-84-030) Avail: NTIS HC A03/MF A01

This China report on science and technology covers various research projects conducted in The Peoples Republic of China. Specific topics covered include: (1) applied sciences; (2) life sciences; and (3) astronautics. For individual titles, see N85-22778 through N85-22781.

N85-22778# Joint Publications Research Service, Arlington, Va. **c15**
NATION SAID TO RANK HIGH WITH 15 SATELLITES
In its China Rept: Sci. and Technol. (JPRS-CST-84-30) 10 Oct. 1984 p 27 refs Transl. into ENGLISH from Xinhua (Beijing, China), 5 Sep. 1984 (For primary document see N85-22777 13-31)
Avail: NTIS HC A03/MF A01

China's progress in carrier rocket and satellite technology is observed from a historical perspective. China started its astronautics industry in 1956 and launched its first carrier rocket in 1964. In May 1980, a carrier rocket was launched and recovered after splashdown in the destined areas. One year later, a single-launch vehicle sent three satellites into their respective orbits, and the following year China carried out a submarine-based carrier rocket launch. With the development of rocket technology, China set about a program for launching man-made Earth satellite from 1965. China's first satellite went into orbit in April 1970. It was followed by a scientific experiment satellite which sent back valuable data for 7 years circling the earth. A complete set of facilities have been built in the country for launching, monitoring and controlling rockets and satellites. China's space technology is making great contributions to the national economy. Data collected by satellites have been successfully applied in land and forestry resources surveys, mineral exploration, hydrogeological prospecting and environmental monitoring. B.W.

N85-22779# Joint Publications Research Service, Arlington, Va.
EXPERIMENTAL INVESTIGATION OF CRIPPLING STRENGTH OF CHINESE ALUMINUM ALLOY (LY12CZ) SECTIONS c39
Zhang Fubao *In its* China Rept: Sci. and Technol. (JPRS-CST-84-30) 10 Oct. 1984 p 32-37 refs Transl. into ENGLISH from Fudan Xuebao-Kexue Ban (Shanghai), no. 4, 1983 p 474-478 (For primary document see N85-22777 13-31)
Avail: NTIS HC A03/MF A01

The crippling strength under axial pressure of 7 types of LY12CZ aluminum alloy sections was tested using 48 samples with 3 different effective slenderness ratios. Three semi-experimental formulas were derived for calculating the crippling strength of domestically made aluminum alloy (LY12CZ) sections with an error range of + or - 10 percent. The formulas can be used in engineering design. B.W.

N85-22780# Joint Publications Research Service, Arlington, Va.
STUDY OF EFFECTIVE PHYSIOLOGICAL TEMPERATURE Abstract Only c54
Pang Cheng and Jiang Weiqing *In its* China Rept: Sci. and Technol. (JPRS-CST-84-030) 10 Oct. 1984 p 43 refs Transl. into ENGLISH from Yuhang Xuebao (Beijing, China), no. 2, 30 Apr. 1984 p 10-15 (For primary document see N85-22777 13-31)
Avail: NTIS HC A03/MF A01

The effect of temperature, humidity, and wind speed on the human body was studied under a variety of conditions. Experiments were conducted with 161 young men wearing 0.5C10 clothing in a high temperature cabin where microclimatic factors could be controlled in the following ranges: temperature 40-60 C, relative humidity 25-75 percent, wind speed 0.25-1.00 m/sec. The rates and magnitudes of changes in body temperature, heart beat rate, and perspiration were determined. It was discovered that each microclimatic factor does not affect the body independently. Instead, it is always related to other factors. The effect of wind speed is affected by temperature and humidity. When the temperature is higher than the body temperature, the wind speed has a heating effect due to convection. Otherwise, it has a cooling effect. When the ambient humidity is high, the heat dissipation effect is insignificant. In low humidity, the heat dissipation effect might cancel the convection heating effect at high temperatures. A mathematical expression was obtained based on the high temperature endurance data measured with 24 combinations of microclimatic factors. B.W.

N85-22781# Joint Publications Research Service, Arlington, Va.
SPACE INTERCEPTION GUIDANCE WITH UNCERTAIN FACTORS Abstract Only c13
Sun Shiqing *In its* China Rept: Sci. and Technol. (JPRS-CST-84-030) 10 Oct. 1984 p 44 refs Transl. into ENGLISH from Yuhang Xuebao (Beijing, China), no. 2, 30 Apr. 1984 p 32-42 Original language document previously announced as A84-43355 (For primary document see N85-22777 13-31)
Avail: NTIS HC A03/MF A01

Based on the interception manifold concept, a method is proposed for treating the interception guidance problem of a modern space vehicle with uncertain factors and any proper acceleration. The method in a sense is a generalization of the classical mode; it is simple and seems to satisfy various trajectory reuirements of the guidance process. C.D.(IAA)

N85-22782# Joint Publications Research Service, Arlington, Va.
USSR REPORT: ENGINEERING AND EQUIPMENT
12 Mar. 1985 106 p refs Transl. into ENGLISH from various Russian articles
(JPRS-UEQ-85-003) Avail: NTIS HC A06

News items, abstracts, and scientific reports on aspects of engineering and equipment including turbine and engine design; testing and materials; non-nuclear energy; navigation and guidance systems; nuclear energy; mechanics of solids; high energy devices, optics, and photography; industrial technology; aeronautics and space; and fluid mechanics. For individual titles, see N85-22783 through N85-22838.

N85-22783# Joint Publications Research Service, Arlington, Va.
PERIODIC MOVEMENTS OF AXISYMMETRICAL SATELLITE ABOUT CENTER OF MASS DUE TO GRAVITATIONAL MOMENT Abstract Only c13
V. V. Sazonov and M. Ye. Sidoryuk *In its* USSR Rept.: Eng. and Equipment (JPRS-UEQ-85-003) 12 Mar. 1985 p 1 Transl. into ENGLISH from Izv. Akad. Nauk SSSR: Mekhan. Tverdogo Tela (Moscow), no. 3, May - Jun. 1984 p 6-16 (For primary document see N85-22782 13-31)
Avail: NTIS HC A06

Periodic solutions of the system of ordinary differential equations describing the movement of the longitudinal axis of an axisymmetrical satellite in a Keplerian elliptical orbit caused by gravitational moment are investigated. Periodic solutions are of interest because the equilibrium positions can be employed as nominal unperturbed movements of an axisymmetrical satellite in the gravitational orientation mode. Investigation of these periodic solutions makes it possible to understand the characteristics of this orientation method more thoroughly. A class of symmetrical periodic solutions coinciding with periodic Lyapunov solutions and satisfying special boundary conditions in a circular orbit is indicated for weakly elliptical orbits. These solutions are extended numerically to the domain of large orbital eccentricity and amplitude values. The stability of the periodic solutions are investigated by examining variations of the characteristic equations in the corresponding systems of equations. Author

N85-22784# Joint Publications Research Service, Arlington, Va.
REDESIGN OF FUSELAGE COMPARTMENTS BY METHOD OF SPECIAL CONTOURS Abstract Only c05
F. K. Chistyakov, V. V. Naykhanov, and A. A. Dubanov *In its* USSR Rept.: Eng. and Equipment (JPRS-UEQ-85-003) 12 Mar. 1985 p 1-2 Transl. into ENGLISH from Izv. Vyssh. Ucheb. Zaved.: Aviats. Tekhn. (Kazan, USSR), no. 1, Jan. - Mar. 1984 p 106-108 (For primary document see N85-22782 13-31)
Avail: NTIS HC A06

The method of a special contour, useful in computer-aided aircraft design, is also applicable to iterative redesign of fuselage compartments with correction and adjustment of aerodynamic surfaces. On the basis of relevant geometrical relations, such a redesign of an already laid out fuselage compartment is shown to be possible by a purely mathematical procedure without introduction of any new method. This is demonstrated on a typical fuselage compartment which occupies the sector between ribs 3 and 7, thus spanning three intermediate ribs, bounded by the plane of maximum width and a meridional plane. Author

N85-22785# Joint Publications Research Service, Arlington, Va.
PROPAGATION OF THREE-DIMENSIONAL TURBULENT JET FROM LOBAR NOZZLE THROUGH SURROUNDING STREAM Abstract Only c34
V. I. Vasilyev, S. Yu. Krasheninnikov, and Yu. A. Rudi *In its* USSR Rept.: Eng. and Equipment (JPRS-UEQ-85-003) 12 Mar. 1985 p 3-4 Transl. into ENGLISH from Izv. Vyssh. Ucheb. Zaved.: Aviats. Tekhn. (Kazan, USSR), No. 1, Jan. - Mar. 1984 p 18-22 (For primary document see N85-22782 13-31)
Avail: NTIS HC A06

Propagation of the jet through the surrounding stream, after discharge from a lobar nozzle in a two-flow turbojet engine, is analyzed on the basis of an approximate mathematical model which describes mixing of two substances and facilities numerical calculations. The static pressure in the cylindrical mixing chamber is assumed to remain constant, with negligible molecular and thermal diffusion in the direction of flow so that the two equations of the boundary layer become parabolic. The one-parametric equation of turbulence is also parabolic. Mixing is assumed to occur at a low Mach number and the equation of state reduces to that for a perfect gas. The system is closed by an equation of continuity which, upon inclusion of the transverse velocity of secondary potential flow, becomes an elliptic Poisson equation. The initial conditions are characterized by the ratio of velocities and the ratio of densities at the nozzle throat as well as by the geometry of the boundary layer and the distribution of eddy

viscosity. The corresponding boundary value problem, formulated in dimensionless variables, is solved by numerical integration according to the method of false positions. Author

N85-22786# Joint Publications Research Service, Arlington, Va.
TIME-DEPENDENT FLOW OF STREAM SWIRLED IN VORTEX CHAMBER Abstract Only **c34**
Yu. A. Knysh and A. F. Uryvskiy *In its* USSR Rept.: Eng. and Equipment (JPRS-UEQ-85-003) 12 Mar. 1985 p 4 Transl. into ENGLISH from Izv. Vyssh. Ucheb. Zaved.: Aviats. Tekhn. (Kazan, USSR), no. 1, Jan. - Mar. 1984 p 27-31 (For primary document see N85-22782 13-31)
Avail: NTIS HC A06

Formation of the vortex core and closure of the vortex layer in a chamber with stream swirling before discharging as a free jet are analyzed, for the purpose of determining the boundaries between steady state and time dependent flow. As the mean free path of turbulent mixing increases going downstream, the vortex layer retains its annular form in short chambers and becames thicker toward the center in long chambers. Theoretical calculations by the method of integrals, assuming a nonzero Kolomogorov-Prandtl eddy viscosity in the mixing zone only, were verified experimentally by injection of CO2 into the second zone of reverse flow. While the swirling ratio was varied from 2.5 to 6 in two chambers, one short and one twice as long, 4.9 + or - 0.4% CO2 was injected into the former and 2.4 + or - 1.0% CO2 was injected into the latter. The results confirm that regular fluctuations in a swirled stream are caused by hydrodynamic restructurization without axial reverse flow within the vortex core, while no reverse flow and no regular fluctuations occur in the free jet when the swirling ratio is below critical. The critical swirling ratio is approximately 0.65, according to experimental data. Author

N85-22787# Joint Publications Research Service, Arlington, Va.
NATURAL CONVECTION DURING HEAT ACCUMULATION BY SUBSTANCES WITH CHANGE OF AGGREGATE STATE Abstract Only **c34**
A. G. Chukayev and A. M. Kuks *In its* USSR Rept.: Eng. and Equipment (JPRS-UEQ-85-003) 12 Mar. 1985 p 5 Transl. into ENGLISH from Izv. Vyssh. Ucheb. Zaved.: Aviats. Tekhn. (Kazan, USSR), no. 1, Jan. - Mar. 1984 p 55-59 Original language document previously announced as A84-47562 (For primary document see N85-22782 13-31)
Avail: NTIS HC A06

Heat transfer calculations are presented for a heat accumulator using the melting heat of a substance which changes its state of aggregation. It is shown that the approach adopted here makes it possible to evaluate the efficiency of using heat-storage materials in the pipe-tank system. The calculations, which allow for the effect of free convection in the liquid phase, have been made using the Boussinesq approximation. Results of a numerical experiment for NaNO3 salt show that the effect of natural convection on heat transfer is significant and that the heat flux to the material decreases as heat accumulates. V.L. (IAA)

N85-22788# Joint Publications Research Service, Arlington, Va.
SOME UNIQUE FEATURES OF ISENTROPHIC FLOW OF GAS UNDER HIGH PRESSURES Abstract Only **c34**
A. P. Bebyakov and V. Ya. Levin *In its* USSR Rept.: Eng. and Equipment (JPRS-UEQ-85-003) 12 Mar. 1985 p 5-6 Transl. into ENGLISH from Izv. Vyssh. Ucheb. Zaved.: Aviats. Tekhn. (Kazan, USSR), no. 1, Jan. - Mar. 1984 p 71-74 (For primary document see N85-22782 13-31)
Avail: NTIS HC A06

A mathematical model of thermodynamic expansion is constructed for a real gas flowing under high pressure. The corresponding system of three Cauchy equations in virial form di - vdp = 0 bar-V/v = const vdp + bar-Vdbar-V (i - enthalpy, v - volume, p - pressure, bar-V - velocity, F - area of nozzle cross section) is reformulated with the total differentials di and dp expressed as functions of partial derivatives so that the process is redescribed by an equation for dT/dv (temperature-volume characteristic) and an equation for d bar-V/dv (velocity-volume characteristic). These equations are supplemented with the equation of state pv = zRT for a real gas (z expressed as a polynomial with empirical coefficients) and an equation for the specific heat at constant pressure C sub p = C sub v - v(T,v,z) (C sub v - specific heat at constant volume). This system of equations was solved numerically for determining the effects of intermolecular interaction forces and of departure from an ideal gas taking into account the distinct discharge and thrust characteristics of high-pressure nozzles. Author

N85-22789# Joint Publications Research Service, Arlington, Va.
DETERMINATION OF BOUNDARY LINE BETWEEN REVERSE JET AND SURROUNDING STREAM Abstract Only **c34**
I. G. Gataullin and D. V. Maklakov *In its* USSR Rept.: Eng. and Equipment (JPRS-UEQ-85-003) 12 Mar. 1985 p 7 Transl. into ENGLISH from Izv. Vyssh. Ucheb. Zaved.: Aviats. Tekhn. (Kazan, USSR), no. 1, Jan. - Mar. 1984 p 79-81 Original language document previously announced as A84-47569 (For primary document see N85-22782 13-31)
Avail: NTIS HC A06

In the problem considered here, a jet issuing from a duct reverses its flow direction, turns around the edge of the duct outlet, and meets with an external flow at a critical point on the outer wall of the duct. The jet and the external flow then form a common line of flow, with flow velocity changing continuously on both sides of the line. The hydrodynamic and geometrical flow parameters are determined using the method of singular points. It is shown that as the velocity of the external flow increases, the point where the two flows meet shifts toward the edge of the duct outlet. V.L. (IAA)

N85-22790# Joint Publications Research Service, Arlington, Va.
METHOD FOR PROMPT MODELING OF QUASIPERIODIC MOVEMENT OF SOLID NEAR-AXISYMMETRICAL BODY IN ATMOSPHERE Abstract Only **c02**
V. M. Belokonov, I. V. Belokonov, and Yu. M. Zabolotnov *In its* USSR Rept.: Eng. and Equipment (JPRS-UEQ-85-003) 12 Mar. 1985 p 8 Transl. into ENGLISH from Izv. Akad. Nauk SSSR: Mekhan. Tverdogo Tela (Moscow), no. 2, Feb. 1984 p 43-50 (For primary document see N85-22782 13-31)
Avail: NTIS HC A06

A computer method for the rapid calculation of the motion in the atmosphere of a rigid axisymmetric body with slight asymmetry is based on the use of an implicit scheme of the averaging method. This method involves the exchange of the initial system of equations of rigid body dynamics relative to the center of mass for a transformed system. The rapid variables of the transformed system oscillate with a lesser frequency, and the form of this system is based on a description of rotational-oscillatory single-frequency motion. It is proven that, in the near-resonance regime, changes in the variables in the equation of the first approximation of the method of averaging are equal for both the initial and transformed systems. Advantages of the present approach, known as the method of artificial increase of oscillation periods, over explicit schemes of the method of averaging include universality of application and simplicity of computer implementation. The application of the method is similar for resonance and nonresonance regimes of body motion. A twenty-fold decrease in the amount of calculations was achieved. J.N. (IAA)

N85-22791# Joint Publications Research Service, Arlington, Va.
FLIGHT DYNAMICS OF AXISYMMETRICAL ROTATING BODIES IN AIR MEDIUM Abstract Only **c02**
I. T. Borisenok, B. Ya. Lokshin, and V. A. Privalov *In its* USSR Rept.: Eng. and Equipment (JPRS-UEQ-85-003) 12 Mar. 1985 p 8 Transl. into ENGLISH from Izv. Akad. Nauk SSSR: Mekhan. Tverdogo Tela (Moscow), no. 2, Feb. 1984 p 35-42 (For primary document see N85-22782 13-31)
Avail: NTIS HC A06

The free flight motion of a rigid axisymmetric body due to the action of its own weight, aerodynamic effects (autorotation), and possible reactive forces is examined. It is assumed that the central ellipsoid of inertia of the body is an ellipsoid of rotation about the

axis of symmetry, and that the center of gravity is at the geometric center of the body. The region of stability of vertical descent is approximated by dividing a system of characteristic equations into fast and slow parts. It is shown that, for given gyroscopic forces, the presence of the nonconservative Magnus moment may lead to a loss of stability of this type of motion. The stability of the case of planar motion, where the Magnus force and weight form an equilibrium force system, and of the case of spiral motion is considered. Stability is also studied for the case of the center of mass at an arbitrary point on the axis of symmetry, and for the case of an axisymmetric body not having an equatorial plane of symmetry. Conditions for the equilibrium and procession of a rotating parachute in a wind tunnel are identified. J.N.

N85-22792# Joint Publications Research Service, Arlington, Va.
HYPERSONIC FLOW ABOUT TRIANGULAR AIRFOIL AT LARGE ANGLES OF ATTACK Abstract Only **c02**
V. N. Golubkin *In its* USSR Rept.: Eng. and Equipment (JPRS-UEQ-85-003) 12 Mar. 1985 p 9 Transl. into ENGLISH from Prikl. Mat. i Mekhan. (Moscow), v. 48, no. 3, May - Jun. 1984 p 376-382 (For primary document see N85-22782 13-31)
Avail: NTIS HC A06

The thin shock layer method is employed to investigate a previously unknown flow mode about a triangular airfoil with angles of attack close to eta/2. A formulation is given for the flow problem, and analytical expressions are derived for the gas dynamic functions, as well as equations which connect the shape of the wing surface and the shock wave. The method is presented for solving inverse problems of flow about solid airfoils with attached shock. A flow mode about a triangular wing is demonstrated in which the shock wave is attached to the apex of the wing, but which can be either attached or detached from the leading edge. Author

N85-22793# Joint Publications Research Service, Arlington, Va.
ABSOLUTE STABILITY OF UNSTEADY MOVEMENT OF AXISYMMETRICAL ROTATING FLIGHT VEHICLE Abstract Only **c02**
V. I. Skorodinskiy *In its* USSR Rept.: Eng. and Equipment (JPRS-UEQ-85-003) 12 Mar. 1985 p 9 Transl. into ENGLISH from Izv. Akad. Nauk SSSR: Mekhan. Tverdogo Tela (Moscow), no. 3, May - Jun. 1984 p 17-21 (For primary document see N85-22782 13-31)
Avail: NTIS HC A06

Linear-rectilinear horizontal flight movement of an axisymmetrical rotating finned flight vehicle in air is examined. Unsteady flow about the vehicle is taken into account, as well as Magnus-type effects due to the fins and the rotation about the axis of symmetry. The problem is solved by methods from the theory of absolute stability. A necessary and sufficient condition for the absolute stability of unsteady movements is identified. The complete region of absolute stability obtained is larger than the region found with the help of the Yakubovich criterion. The assumption of an unsteady flow is found to have no effect on the stability of the class of constrained movements of an axisymmetrical rotating flight vehicle examined, indicating that it is necessary and sufficient to examine only steady-state movements within that class in order to investigate the symptotic stability of the entire class of unsteady movements. Author

N85-22794# Joint Publications Research Service, Arlington, Va.
REFLEX ATTACHMENT FOR LINE ALIGNMENT IN SPECTRAL DIFFRACTION DEVICES Abstract Only **c74**
V. M. Kelman and I. V. Rodnikova *In its* USSR Rept.: Eng. and Equipment (JPRS-UEQ-85-003) 12 Mar. 1985 p 10-13 refs Transl. into ENGLISH from Izv. Akad. Nauk Kazakhskoy SSR: Ser. Fiz.-Mat. (Alma-Ata, USSR), no. 6, Jun. 1983 p 76-79 (For primary document see N85-22782 13-31)
Avail: NTIS HC A06

Spectrometers with diffraction gratings, just as prism devices, are characterized by distortions of spectral lines connected with the inclined course of beams from the sections of the slit source lying higher and lower than the optical axis of the system. This distortion can be substantially reduced by introducing into the optical circuit of the spectral device an attachment to the grating which is a telescopic system of two cylindrical mirrors. The basic optical circuit of a monochromator with a plane grating and one of the possible variants of this attachment are illustrated. H is clear from the results of the calculations that the reflex attachment with a turning mechanism ensuring coordinated turning of the grating and the attachment, reduces the bending diflection by two orders in the entire wave-length range of the monochromator, i.e., almost completely aligns its spectral lines. A similar reflex attachment calculated in an appropriate way conserve also for compensating line distortions in prism spectrometers. B.G.

N85-22795# Joint Publications Research Service, Arlington, Va.
RUBY WAVEFRONT-CONJUGATION LASER FOR OBTAINING HIGH TEMPERATURE PLASMA Abstract Only **c75**
V. A. Boyko, G. A. Koldashov, A. Ya. Fayenov, A. I. Fedosimov, and I. N. Tsigler *In its* USSR Rept.: Eng. and Equipment (JPRS-UEQ-85-003) 12 Mar. 1985 p 14-15 Transl. into ENGLISH from Pribory i Tekhn. Eksperim. (Moscow), no. 3, May - Jun. 1984 p 188-190 (For primary document see N85-22782 13-31)
Avail: NTIS HC A06

A ruby laser for heating a high temperature plasma is described in which the amplifier section is divided into two parts and performs sequential wavefront conjugation in order to improve the brightness characteristics of the radiation, to limit the noise of the amplifier stages and to make the leading edge of the pulse as short as possible. Repeated inversion of the wavefront results in the radiation pulse consisting of a train of two or three pulses spaced 37 nsec apart and having duration of 3 to 5 nsec; the leading edge of the pulses is more than an order of magnitude shorter than the pulse produced by ruby lasers with analogous power but not employing conjugation. The laser is employed for high temperature beryllium plasma heating. The device is simple and compact, and can be used for systematic investigations of the characteristics of heating high temperature plasma by radiation. Author

N85-22796# Joint Publications Research Service, Arlington, Va.
NEODYMIUM YAG LASER PUMPED WITH RADIATION FROM HIGH FREQUENCY ELECTRODELESS DISCHARGE Abstract Only **c36**
S. N. Golikova, P. S. Fusev, V. P. Fuskov, V. A. Zhukov, S. M. Pechenegov, V. D. Sazhayev, A. B. Sinitsyn, N. V. Teterev, and B. F. Trinchuk *In its* USSR Rept.: Eng. and Equipment (JPRS-UEQ-85-003) 12 Mar. 1985 p 15 Transl. into ENGLISH from Pribory i Tekhn. Eksperim. (Moscow), no. 3, May - Jun. 1984 p 190-193 (For primary document see N85-22782 13-31)
Avail: NTIS HC A06

A system for pumping a solid state laser employing electrodeless discharge is described in which the annular cavity of the lamp consists of three ballast cavities: the main (discharge) cavity and two additional cavities placed coaxially on both sides of the main cavity. The system provides enhanced longevity (approximately 1000 hours) and superior stability. Continuous lasing power exceeding 25 watts is provided in all modes. The system has withstood 75,000 cycles with no significant degradation in output parameters. It is suggested that progress in the development of efficient power sources operating at 27.12 MHz will improve the efficiency of the laser significantly and make them competitive with traditional lasers. Author

N85-22797# Joint Publications Research Service, Arlington, Va.
VARIABLE FLEXING DEVICE FOR TARGETS IN INTERNAL BEAMS OF CHARGED PARTICLE ACCELERATORS Abstract Only **c72**
Ye. I. Rozum *In its* USSR Rept.: Eng. and Equipment (JPRS-UEQ-85-003) 12 Mar. 1985 p 16 Transl. into ENGLISH from Pribory i Tekhn. Eksperim. (Moscow), no. 2, Mar. - Apr. 1984 p 18-19 (For primary document see N85-22782 13-31)
Avail: NTIS HC A06

A device is described which makes it possible to flex single crystal targets and to orient targets at any angle within a beam of

charged particles. The flexing moment is applied through two pairs of metal cylinders placed parallel to one another and to the faces of a single crystal plate. The cylinders in each pair are placed 1 mm apart on opposite sides of the rectangular plate; the points to which the flexing moments are applied are 18 mm apart. Single crystals ranging from 0.1 to 1 mm thick with radii of up to 200 mm can be flexed within approximately 15%; the crystallographic directions of the flexed target can be oriented to within 30 minutes through a range of angles of -40 to + 180 deg with respect to the charged particle beam, assuming that the neutral position corresponds to the case in which the normal to the surface of the target coincides with the axis of the particle beam. Author

N85-22798# Joint Publications Research Service, Arlington, Va.
SYSTEM FOR FORMING AND FOCUSING HIGH CURRENT BEAM OF DEUTERIUM IONS Abstract Only **c72**
A. S. Belov *In its* USSR Rept.: Eng. and Equipment (JPRS-UEQ-85-003) 12 Mar. 1985 p 16 Transl. into ENGLISH from Pribory i Tekhn. Eksperim. (Moscow), no. 2, Mar. - Apr. 1984 p 20-22 (For primary document see N85-22782 13-31)
Avail: NTIS HC A06

A three-electrode beam formation system is described which is more resistant to heat load than a grid system and which focuses the ion beam by virtue of the electrode shape. A multi-aperture system is employed in the source to extract the ions from the plasma. The electrodes employed are spherical and incorporate circular emission openings. Additional focusing is obtained by virtue of the fact that the streams of ions from the emission openings of the first electrode, which are accelerated in the space between the electrodes, are offset with respect to the centers of the openings in the secondary electrode. The beam current at 12 keV is 1.5 A, with 1000 mA/sq. cm. current density 17 cm from the source. The deuterium ion source is a part of a polarized-proton source under development. Author

N85-22799# Joint Publications Research Service, Arlington, Va.
DIELECTRIC DETECTOR DEVICE FOR REGISTERING HEAVY COSMIC RADIATION PARTICLES Abstract Only **c93**
Ye. V. Gorchakov, N. L. Grigorov, V. A. Iozenas, R. A. Nymik, Yu. V. Trigubov, and G. G. Zenchev *In its* USSR Rept.: Eng. and Equipment (JPRS-UEQ-85-003) 12 Mar. 1985 p 17 Transl. into ENGLISH from Pribory i Tekhn. Eksperim. (Moscow), no. 2, Mar. - Apr. 1984 p 35 (For primary document see N85-22782 13-31)
Avail: NTIS HC A06

A device for recording charged cosmic radiation particles aboard a satellite is described in which two detectors - one movable and the other stationary - are employed to determine the registration time. The position of the detectors for which a particle is registered is determined by comparing the sections of the track caused by the same particle in both detectors, thus making it possible to determine the recording time and place. The recording time is determined precisely during experiments extending over several days by moving the movable detector reciprocally in sinc with the period of rotation of the satellite about the Earth. Author

N85-22800# Joint Publications Research Service, Arlington, Va.
NEW TECHNIQUE FOR FLUID FEED IN SIMULTANEOUS MULTISURFACE GRINDING Abstract Only **c37**
Ye. S. Kiselev, A. N. Unyanin, and Yu. N. Moiseyev *In its* USSR Rept.: Eng. and Equipment (JPRS-UEQ-85-003) 12 Mar. 1985 p 20 Transl. into ENGLISH from Vestn. Mashinostr. (Moscow), no. 6, Jun. 1984 p 56-57 (For primary document see N85-22782 13-31)
Avail: NTIS HC A06

When several surfaces are simultaneously ground with the same machine tool, even gravity feed of lubricating fluid may not adequately cover all contact zones. Particularly vulnerable are areas on flat end faces of a part and transitions from flat to cylindrical surface segments. The ultrasonic method of lubrication, by feeding the fluid from an acoustically vibrating, partially enclosed nozzle, reduces heating and stressing in the critical areas. The cuneiform acoustic radiator now used for this purpose is, however, not the optimum one. Various nozzle configurations for grinding were studied with the latest model of a ZB161 machine tool was made at the Ulyanovsk Polytechnic Institute. Author

N85-22801# Joint Publications Research Service, Arlington, Va.
EFFECT OF ZERO-WEAR IN FRICTION PAIRS OPERATING IN ABRASIVE MEDIA Abstract Only **c37**
M. V. Golub, V. I. Kharlamenko, and V. N. Malyshev *In its* USSR Rept.: Eng. and Equipment (JPRS-UEQ-85-003) 12 Mar. 1985 p 21 Transl. into ENGLISH from Vestn. Mashinostr. (Moscow), no. 5, May 1984 p 29-31 (For primary document see N85-22782 13-31)
Avail: NTIS HC A06

Ensuring high wear-resistance in friction pairs requires proper heat treatment and thermomechanical or other treatment of the surfaces, and optimum selection of materials. New composite materials, cermets, with hard grains dispersed in a plastic matrix selectively soluble in the ambient medium at contact temperature - especially when the ambient medium is a poor lubricant are presented. The simplest and preferable combination is a zero-wear composite paired with a material such as steel which satisfies all other performance requirements. This principle was applied to a thrust bearing with bilateral wear-resistant surfaces at both ends. They are made of TM-1 material, containing fine-disperse powder of tundsten carbide with cobalt and granular cast tungsten carbide in a 1:3 ratio, with heat-resistant sealant and cupronickel impregnant. They were produced by molding, sintering, and bonding to a steel substrate, followed by cooling and finishing treatment. Their wear and friction characteristics, dependence of relative wear resistance on mean grain diameter, dependence of total volume worn on abrasive content in lubricating water, and dependence of friction coefficient on contract pressure are found to be 0.5-20% better than those characteristics of silicided graphite bearings. E.A.K.

N85-22802# Joint Publications Research Service, Arlington, Va.
USE OF FERROFLUIDS IN MACHINING OF METALS
V. V. Podgorkov *In its* USSR Rept.: Eng. and Equipment (JPRS-UEQ-85-003) 12 Mar. 1985 p 21-22 Transl. into ENGLISH from Vestn. Mashinostr. (Moscow), no. 6, Jun. 1984 p 54-55 (For primary document see N85-22782 13-31)
Avail: NTIS HC A06

Ferrofluids controlled by an external magnetic field are suitable as lubricants for moving metal machining parts. Empirical relations of the form M sub c = kDt sub bs sup av sup c were established for the unit cutting torque M sub c as function of the drill diameter, the depth of hole t, the feed rate s, and the cutting rate v when holes in Al3V aluminum alloy, TsAM10-5 zinc alloy, VT1 titanium alloy, or 12Cr18Ni10Ti stainless are cut with a drill of R6M5 high-speed steel using a fixture made of nonmagnetic stainless and a ferrofluid based on MVP mineral tool oil as lubricant. Values of the coefficient and the exponents were determined by the Student significance test and Fisher adequacy test. It is found that ferrofluid as lubricant is more effective in machining of nonmagnetic materials. E.A.K.

N85-22803# Joint Publications Research Service, Arlington, Va.
CYCLIC INDUSTRIAL ROBOTS WITH MECHANICAL ENERGY STORING DEVICES: MULTIPOSITIONAL SYSTEM WITH ONE OR SEVERAL DEGREES OF FREEDOM Abstract Only **c37**
A. I. Korendyasev, B. L. Salamandra, and L. I. Tyves *In its* USSR Rept.: Eng. and Equipment (JPRS-UEQ-85-003) 12 Mar. 1985 p 24 Transl. into ENGLISH from Stanki i Instrument (Moscow), no. 6, Jun. 1984 p 4-8 (For primary document see N85-22782 13-31)
Avail: NTIS HC A06

Multipositional cyclic robots with mechanical energy storing devices are considered, and the problem optimization of speed of action is solved by shrinking the constant-velocity paths to near-zero so that the entire travel consists of an acceleration path and a deceleration path. A system with one degree of freedom is used as a model. The corresponding system of two coupled linear differential equations of motion is solved for the quasistatic mode and for the normal modes, after it has been reduced to

two independent equations with the two energy storing devices dynamically decoupled. One energy storing device for each degree of freedom ensures transferability to any of 2N positions within the field of the industrial robot. The theoretical results of engineering analysis and design are confirmed by prototypes of cyclic industral robots. Displacement and velocity diagrams confirm the absence of dynamic coupling and the predicted high speed and stability of operation with an insensitivity to static imbalance within 10%. E.A.K.

N85-22804# Joint Publications Research Service, Arlington, Va.
DESIGN OF TIGHTENING DEVICE AND CALCULATION OF FORCES IN MANIPULATOR TRANSMISSIONS WITH BASE-DRIVE MOUNTED Abstract Only c37
A. G. Ovakimov, I. V. Kalabin, and I. A. Timofeyev *In its* USSR Rept.: Eng. and Equipment (JPRS-UEQ-85-003) 12 Mar. 1985 p 25 Transl. into ENGLISH from Stanki i Instrument (Moscow), no. 6, Jun. 1984 p 8-11 (For primary document see N85-22782 13-31)
Avail: NTIS HC A06

An automatic manipulator with n-degrees of freedom is considered. Its differential motor-drive is mounted on the base and consisting of n-transmission channels in an arrangement that ensures decoupling of movements. Selective closing of backlash is effected by a built-in tightening device, an elastic torsion bar connecting the output shafts of two auxiliary channels from the manipulator and the drive. Analysis and synthesis of the drive for given manipulator kinematics are based on the equations of balance in matrix form and the principle of virtual displacements. The tightening torque is calculated and possible manipulator positions are considered. E.A.K.

N85-22805# Joint Publications Research Service, Arlington, Va.
OPTOELECTRONIC SAFETY SYSTEM FOR ROBOTIZED TECHNOLOGICAL COMPLEX Abstract Only c37
S. G. Batrakov, Ye. M. Kanayev, and B. M. Chertkov *In its* USSR Rept.: Eng. and Equipment (JPRS-UEQ-85-003) 12 Mar. 1985 p 25-26 Transl. into ENGLISH from Stanki i Instrument (Moscow), no. 5, May 1984 p 8-10 (For primary document see N85-22782 13-31)
Avail: NTIS HC A06

An optoelectronic protective system was developed. The system operates within the infrared with centralized control requiring a minimum of connecting cables. It is based on the light barrier principle with a small threshold distance and its structure is modular. The advantages of the system are small size, low power requirement, and large distance from transmitter to receiver. The transmitter contains an AI107 GaAs light-emitting diode (940-960 nm wavelength) activated by a sequence of 0.8 A current pulses of 44.4 micros duration with a repetition rate of 0.9 kHz coming from a multivibrator through a pulse shaper. The transmitter optics are a filter and a short-focus lens with an alignment tube. The receiver optics are a diaphragm for blocking out background light and a coverging lens. The photodiode is followed by electronics consisting of an amplifier and a limiter, a filter for noise suppression, and an integrator-converter. The latter drives an optotransistor switch for commutation of external current signals of up to 200 mA with the necessary decoupling. A light-emitting diode in the receiver serves as monitor of incoming radiation. The light barrier is 15 m wide. E.A.K.

N85-22806# Joint Publications Research Service, Arlington, Va.
HYDRAULIC BRAKES FOR INDUSTRIAL ROBOTS Abstract Only c37
P. I. Knysh *In its* USSR Rept.: Eng. and Equipment (JPRS-UEQ-85-003) 12 Mar. 1985 p 26-27 Transl. into ENGLISH from Stanki i Instrument (Moscow), no. 5, May 1984 p 10-12 (For primary document see N85-22782 13-31)
Avail: NTIS HC A06

Hydraulic brakes greatly enhance the performance of the passive control system of an industrial robot. They can be installed directly in the hinges of the automatic manipulator. A hydraulic brake was designed for equal volumes of fluid entering one cavity and leaving the others. The performance of a brake is analyzed and calculated for the corresponding hydrodynamic relations. The family of Q(x) curves are presented that represent the flow rate as function of the clearance opening rather than of the pressure head and are classified into four regions: (1) no flow with valve fully closed; (2) laminar flow with valve opening comparable with width of annular clearance; (3) turbulent flow with wide opening; (4) valve fully open and further travel of the slide not adding to the flow rate. The interdependence of flow rate, flow coefficient, and Reynolds number is included in the mathematical model of the flow characteristic. E.A.K.

N85-22807# Joint Publications Research Service, Arlington, Va.
CYCLIC INDUSTRIAL ROBOTS WITH MECHANICAL ENERGY STORING DEVICES: PRINCIPLES OF DRIVE DESIGN Abstract Only c37
L. M. Bolotin, A. I. Korendyasev, B. L. Salamandra, and L. I. Tyves *In its* USSR Rept.: Eng. and Equipment (JPRS-UEQ-85-003) 12 Mar. 1985 p 27 Transl. into ENGLISH from Stanki i Instrument (Moscow), no. 4, Apr. 1984 p 7-10 (For primary document see N85-22782 13-31)
Avail: NTIS HC A06

A novel approach for industrial robots which is based on the principle of an oscillatory system, conversion of kinetic energy to potential energy rather than heat is presented. The system requires energy-storage devices and minimum damping. Both design principles are evaluated and compared with the corresponding equation of motion for a structure with one degree of freedom. Springs and stops are designed to match the mass and friction losses are considered. This principle was applied for the construction of a high-speed industrial robot for a punch press which can produce small stampings in 60 to 80 double-stroke cycles per minute. The use of energy-storing devices has increased the productivity to 25 cycles/min requiring a drive motor with a power rating of 6 W only. E.A.K.

N85-22808# Joint Publications Research Service, Arlington, Va.
ASSEMBLY ROBOT CONTROL ALGORITHMS Abstract Only c37
P. D. Krutko, N. A. Lakota, and V. I. Solntsev *In its* USSR Rept.: Eng. and Equipment (JPRS-UEQ-85-003) 12 Mar. 1985 p 28 Transl. into ENGLISH from Izv. Vyssh. Ucheb. Zaved.: Mashinostr. (Moscow), no. 1, Jan. 1984 p 39-43 (For primary document see N85-22782 13-31)
Avail: NTIS HC A06

The synthesis of control algorithms for an assembly robot is examined and it is assumed that the positioning arm has force and torque sensing means. The synthesis is based on the concepts of inverse dynamic problems and employs essentially nonlinear equations to produce mathematical models describing the kinematics of the positioning the kinematics of the positioning arm and the dynamics of the drives. Structural diagrams of the mathematical model and the control algorithm are presented. Microprocessors can be employed for the transcendal calculations required for determining the inputs, and analog computer components can be employed to realize the control principles. E.A.K.

N85-22809# Joint Publications Research Service, Arlington, Va.
TIME DEPENDENT INTERACTION OF INTERNAL PRESSURE WAVE WITH SYSTEM OF TWO SPHERICAL SHELLS Abstract Only c39
Yu. V. Saprykin *In its* USSR Rept.: Eng. and Equipment (JPRS-UEQ-85-003) 12 Mar. 1985 p 37 Transl. into ENGLISH from Prikl. Mekhan. (Kiev), no. 6, Jun. 1984 p 40-46 (For primary document see N85-22782 13-31)
Avail: NTIS HC A06

Time-dependent deformation of a system of spherical shells acted upon by an external arbitrary located point wave source was examined. A system consisting of two thin elastic concentrically arranged spherical shells surrounded by and filled with acoustic media was analyzed. Boundary conditions on the surfaces of the shells are defined. The problem is solved by representing the sought quantities in the form of a Legendre polynomial series and

applying Laplace transformation to find the formulas relating the components of the displacement vector and potentials of each of the media. A system of two thin steel elastic spherical shells filled with and surrounded by water is analyzed. It is found that the hydroelastic behavior of the shells depends upon the profile of the incident wave and the ratio of the shell radi. The presence of an outer shell reduces the amount of displacement of the embedded shell. E.A.K.

N85-22810# Joint Publications Research Service, Arlington, Va.
INTERACTION OF CYLINDRICAL SHELL WITH CONCENTRATED MASS MOVING ALONG ITS INNER SURFACE Abstract Only **c39**
N. S. Kondrashov *In its* USSR Rept.: Eng. and Equipment (JPRS-UEQ-85-003) 12 Mar. 1985 p 37-38 Transl. into ENGLISH from Prikl. Mekhan. (Kiev), no. 6, Jun. 1984 p 47-52 (For primary document see N85-22782 13-31)
Avail: NTIS HC A06

The problem of steady-state oscillations of a cylindrical shell caused by a concentrated mass moving over its inner surface was examined. The problem is related to the interaction of turbine housings with the takeoff blades. It is found that the critical velocity of a shell and concentrated mass is lower than the corresponding eigenfrequency. The reduction for a small mass, which has no effect on the frequency of the combined oscillations, is proportional to the mode number of the surrounding form, and increases with an increase in the concentrated mass. No critical velocity exists when the flexure is axisymmetrical. The results of calculations for a pair of steel shells are presented. E.A.K.

N85-22811# Joint Publications Research Service, Arlington, Va.
STEADY-STATE REACTION OF THREE-LAYERED CYLINDRICAL SHELL TO EFFECT OF MOVING LOAD Abstract Only **c39**
V. I. Pozhuyev *In its* USSR Rept.: Eng. and Equipment (JPRS-UEQ-85-003) 12 Mar. 1985 p 38 Transl. into ENGLISH from Prikl. Mekhan. (Kiev), no. 6, Jun. 1984 p 52-59 (For primary document see N85-22782 13-31)
Avail: NTIS HC A06

The effect of moving torsional loads on an infinitely long three-layered cylindrical shell with asymmetrical structure was investigated. The movement of the bearing layers is described by Timoshenko equations augmented with terms to allow for the reaction from the direction of the filler in examining axisymmetrical twisting of the shell by surface loads. Calculations using the derived formulas are performed as an example for two identical bearing layers. The findings are used to investigate the reaction of a three-layered cylindrical shell to the movement of an axisymmetrical load forming any angle with the tangent to the shell by analyzing the forces in terms of normal and tangential components. E.A.K.

N85-22812# Joint Publications Research Service, Arlington, Va.
DETERMINATION OF STRESSES AND DEFORMATIONS IN LINEARLY ELASTIC CONICAL SHELL SUBJECTED TO AERODYNAMIC LOADING AND HEATING Abstract Only **c39**
I. G. Muravskiy *In its* USSR Rept.: Eng. and Equipment (JPRS-UEQ-85-003) 12 Mar. 1985 p 39 Transl. into ENGLISH from Prikl. Mekhan. (Kiev), no. 6, Jun. 1984 p 64-70 (For primary document see N85-22782 13-31)
Avail: NTIS HC A06

The stress-strain state in nonuniformly heated shells is investigated within the framework of a nonlinear theory. The relationship between the stress intensity and deformation intensity is represented by a uniform nonlinear deformation law. A machine experiment is described in which the necessary and sufficient number of expansion terms in the loading function temperature Z2(0) and T2(0) are found. It is found that increasing the number of parts into which the shell is separated beyond 12 has no influence on the end result. The section of the shell in which plastic deformations occur is identified. The maximum deformations computed with allowance for physical nonlinearity are 30% greater than the linear deformations. E.A.K.

N85-22813# Joint Publications Research Service, Arlington, Va.
STABILITY OF THREE-LAYER GLASS-REINFORCED PLASTIC SHELLS OF ROTATION Abstract Only **c39**
O. N. Ivanov, L. S. Orlovskiy, and D. A. Mysyk *In its* USSR Rept.: Eng. and Equipment (JPRS-UEQ-85-003) 12 Mar. 1985 p 40 Transl. into ENGLISH from Prikl. Mekhan. (Kiev), no. 6, Jun. 1984 p 107-109 (For primary document see N85-22782 13-31)
Avail: NTIS HC A06

The stability of three-layer glass-reinforced plastic shells of rotation subjected to radial external pressure was investigated. The bearing layers are formed by spiral-winding and orthotropic glass-reinforced plastic strips on a form. An intermediate layer of low-modulus rubber is employed which secures the bearing layers of the shell after heat treatment. It is assumed that the main directions of elasticity of the bearing layers differ from the lines of main curvature of the coordinate surface of the shell. The intermediate layer is viewed as a three-dimensional low-modulus body. Four differential equations are derived which define the stability of a three-dimensional shell with spiral-wound bearing layers. The averaged results of stability testing of three-layer threads with intermediate layers of different thickness are tabulated. E.A.K.

N85-22814# Joint Publications Research Service, Arlington, Va.
AXISYMMETRICAL OSCILLATIONS OF SHELL SYSTEMS SUBJECTED TO IMPULSE LOADS Abstract Only **c39**
P. Z. Logovoy and V. N. Chaban *In its* USSR Rept.: Eng. and Equipment (JPRS-UEQ-85-003) 12 Mar. 1985 p 41 Transl. into ENGLISH from Prikl. Mekhan. (Kiev), no. 6, Jun. 1984 p 110-113 (For primary document see N85-22782 13-31)
Avail: NTIS HC A06

The dynamics of a composite shell of rotation subjected to transverse impulse loading applied to the free end of the shell and distributed uniformly along the directrix is examined axisymmetrically. The load is present long enough for the perturbations to propagate along the entire shell; the triangular pulse is applied to orthotropic shell material. The cylindrical and conical parts of the shell are of different thicknesses. Equations describing the movement of the shell are derived. A FORTRAN program is developed for solving the finite-difference equations by computer. The oscillations of the composite shell are characterized by the acceleration as a function of time. It is found that the maximum amplitude of the tangential accelerations are more than 5% of the amplitudes of normal accelerations at the same points; more accelerations in the first cylindrical part of the shell attenuate quite rapidly over time. E.A.K.

N85-22815# Joint Publications Research Service, Arlington, Va.
SPECTRAL FREQUENCY OF EIGENVALUES IN OPTIMAL PROBLEMS OF STABILITY OF CYLINDRICAL SHELLS OF VARIABLE THICKNESS Abstract Only **c39**
N. G. Medvedev and N. P. Totskiy *In its* USSR Rept.: Eng. and Equipment (JPRS-UEQ-85-003) 12 Mar. 1985 p 41 Transl. into ENGLISH from Prikl. Mekhan. (Kiev), no. 6, Jun. 1984 p 113-116 (For primary document see N85-22782 13-31)
Avail: NTIS HC A06

The optimum thickness of the shell which is a member of a class of piecewise-linear continuous functions which are symmetrical with respect to the center of the shell and depend upon the axial coordinate was studied. It is shown that when the thickness is varied optimally the frequency of the least positive eigenvalue defining the critical load is equal to 12, i.e., an optimal shell has 12 forms of loss of stability - one general and 11 local. The critical loading for an optimal shell is approximately twice as great as that for a shell with constant thickness which weighs the same. E.A.K.

N85-22816# Joint Publications Research Service, Arlington, Va.
ELASTICITY FORMULAS FOR THIN-WALLED SHELLS WITH PIEZOCERAMIC LAYERS Abstract Only **c39**
V. I. Gololobov *In its* USSR Rept.: Eng. and Equipment (JPRS-UEQ-85-003) 12 Mar. 1985 p 42 Transl. into ENGLISH

from Prikl. Mekhan. (Kiev), no. 6, Jun. 1984 p 117-120 (For primary document see N85-22782 13-31)
Avail: NTIS HC A06

A technical theory of electroelasticity for homogeneous single-layer piezoceramic shells is extended to multilayered shells made of a nonhomogeneous material. A laminated shell consisting of layers with constant thickness in which the electrical potential values are assigned on the surfaces of the piezoceramic layers is examined. Elasticity formulas are derived which are independent of the unknown characteristics of the electric field and which, in conjunction with the motion equations and geometric equations of the theory of thin shells, describe the problem of electroelasticity of the oscillations of nonhomogeneous laminated shells and, in conjunction with the heat conductivity equation, the problem of piezoceramic shell heating. E.A.K.

N85-22817# Joint Publications Research Service, Arlington, Va.
NORMAL MODE CALCULATIONS FOR FUSELAGE TYPE INTRICATE STRUCTURES BY REGARDING THEM AS SYSTEMS WITH SUPERPOSED CONSTRAINTS Abstract Only c05
V. Borisov *In its* USSR Rept.: Eng. and Equipment (JPRS-UEQ-85-003) 12 Mar. 1985 p 43 Transl. into ENGLISH from Izv. Vyssh. Ucheb. Zaved.: Aviats. Tekhn. (Kazan, USSR), no. 1, Jan. - Mar. 1984 p 102-105 (For primary document see N85-22782 13-31)
Avail: NTIS HC A06

Calculations of the normal modes of intricate structures in the fuselage class are considered, these structures are systems with superposed constraints. Two groups of constraints are imposed, one limiting vibrations in all solid body modes and one limiting vibrations in k fundamental elastic modes. The corresponding two independent systems of equations are solved by iteration of matrices or by iteration of the subspace, the algorithm of the first method looping once for each matrix and the algorithm of the second method having a single loop. The latter is superior because it includes simultaneous refinement of the fundamental modes and frequencies, but it effectiveness is limited by capabilities of the computer and standard programs. A preferable hybrid two-loop algorithm is proposed, the first loop dealing with all solid body modes and the second loop dealing with only the k fundamental elastic modes. E.A.K.

N85-22818# Joint Publications Research Service, Arlington, Va.
CONTROLLED MOVEMENT OF ELASTIC MANIPULATOR WITH DISTRIBUTED PARAMETERS Abstract Only c37
V. Ye. Berbyuk and M. V. Demidyuk *In its* USSR Rept.: Eng. and Equipment (JPRS-UEQ-85-003) 12 Mar. 1985 p 43-44 Transl. into ENGLISH from Izv. Akad. Nauk SSSR: Mekhan. Tverdogo Tela (Moscow), no. 2, Feb. 1984 p 59-67 (For primary document see N85-22782 13-31)
Avail: NTIS HC A06

A system of integral differential equations in partial derivatives and boundary conditions is derived for a manipulator which performs both rotary and reciprocating movement. The control problem of moving the manipulator from its neutral state to a given position and damping elastic oscillations is investigated. An algorithm is proposed which makes it possible to reduce the problem of mathematical physics and a torque problem. Numerical analyses are described which confirm the effectiveness of the algorithm. E.A.K.

N85-22819# Joint Publications Research Service, Arlington, Va.
INVESTIGATION OF DYNAMICS OF MANIPULATOR WITH ELASTIC SECTIONS Abstract Only c37
S. A. Mikhaylov and F. L. Shernousko *In its* USSR Rept.: Eng. and Equipment (JPRS-UEQ-85-003) 12 Mar. 1985 p 44 Transl. into ENGLISH from Izv. Akad. Nauk SSSR: Mekhan. tverdogo Tela (Moscow), no. 2, Feb. 1984 p 51-58 (For primary document see N85-22782 13-31)
Avail: NTIS HC A06

Spatially controlled movements of an anthropomorphic manipulator with elastic sectopms are investigated by an asymptotic method developed for the general case of a multiple section manipulator, and by numerical modeling. The proposed method can be used to analyze and calculate the elastic oscillations of a manipulator as it moves and to determine the forces operating in the manipulator construction and the torque developed by the motors. E.A.K.

N85-22820# Joint Publications Research Service, Arlington, Va.
STABILITY OF CYLINDRICAL SHELLS WITH ONE-WAY CONSTRAINTS Abstract Only c39
A. N. Yeremichev *In its* USSR Rept.: Eng. and Equipment (JPRS-UEQ-85-003) 12 Mar. 1985 p 49 Transl. into ENGLISH from Izv. Vyssh. Ucheb. Zaved.: Mashinostr. (Moscow), no. 1, Jan. 1984 p 20-24 (For primary document see N85-22782 13-31)
Avail: NTIS HC A06

The stability is investigated of cylindrical shells with flexure restricted from the inside only or from the outside only (one-way constraints) subjected to axial compression. Turned bronze, steel and polymer shells with a nominal inside diameter of 40 mm and thickness ranging from 0.21 to 1.16 mm are investigated. Two types of loss of stability are noted during compression of a clamped cylindrical shell: axial, due to axial stresses, and radial due to radial compression. The type of loss is determined by the relative thickness, the Poisson coefficient of the shell material and the initial errors. Author

N85-22821# Joint Publications Research Service, Arlington, Va.
NONLINEAR BEHAVIOR AND STABILITY OF THIN SPHERICAL SHELLS SUBJECTED TO NON-AXISYMMETRICAL LOADING Abstract Only c39
L. A. Shapovalov, V. N. Semenov, and Yu. I. Klyuyev *In its* USSR Rept.: Eng. and Equipment (JPRS-UEQ-85-003) 12 Mar. 1985 p 49-50 Transl. into ENGLISH from Izv. Vyssh. Ucheb. Zaved.: Mashinostr. (Moscow), no. 1, Jan. 1984 p 16-19 (For primary document see N85-22782 13-31)
Avail: NTIS HC A06

Two identical spherical segments secured to a ring without eccentricity are examined. An algorithm is developed for investigating the nonlinear behavior and stability of the structure upon the application of non-axisymmetrical radial loading. Fourier analysis and finite-element approximation are employed in conjunction with the Bubnov-Galerkin method, as well as parameter stepping with solution found in each step through a modified Newton-Raffson method. The numerical results are compared with the solutions of test problems for the case of local loading of the ring by two concentrated forces. It is found that increasing the number of terms in the Fourier series beyond 5-7 has little influence on the results, but increase the dimensionality of the problem and the computation time. The findings agree qualitatively with results obtained through a finite-difference approach involving integration of linearized equilibrium equations. Author

N85-22822# Joint Publications Research Service, Arlington, Va.
ANALYSIS OF INTERACTION OF DYNAMICALLY ADJUSTABLE GYROSCOPES ON ELASTIC PLATFORM BY FINITE-ELEMENT METHOD Abstract Only c35
A. V. Zbrutskiy and S. A. Sarapulov *In its* USSR Rept.: Eng. and Equipment (JPRS-UEQ-85-003) 12 Mar. 1985 p 51 Transl. into ENGLISH from Prikl. Mekhan. (Kiev), no. 6, Jun. 1984 p 120-124 (For primary document see N85-22782 13-31)
Avail: NTIS HC A06

The drift of a dynamically tunable gyroscope in the general case of spatial movement of the pedestal and its mutual influence with known analytical expressions for the eigenfunctions of the elastic platform is investigated. Gyroscope errors due to interaction in a dynamic system consisting of two different dynamically tunable gyroscopes and a platform are analyzed by using a finite-element approximation of the elastic platform as a shell. The finite-element method makes it possible to investigate the mutual influence of dynamically tunable gyroscopes installed on an elastic platform of an arbitrary shell type. The system reduction algorithm derived makes it possible to select the parameters of platform and to make a final analytical estimates of the interaction. Author

N85-22823# Joint Publications Research Service, Arlington, Va.
EFFICIENCY OF ALGORITHMS FOR GAS-AIR CHANNEL DIAGNOSTICS IN GAS TURBINE ENGINES BASED ON GAS THERMODYNAMIC PARAMETERS Abstract Only **c07**
A. M. Akhmedzyanov and K. F. Galiullin *In its* USSR Rept.: Eng. and Equipment (JPRS-UEQ-85-003) 12 Mar. 1985 p 80 Transl. into ENGLISH from Izv. Vyssh. Ucheb. Zaved.: Aviats. Tekhn. (Kazan, USSR), no. 1, Jan. - Mar. 1984 p 7-13 (For primary document see N85-22782 13-31)
Avail: NTIS HC A06

Five algorithms of diagnosing the flow of gas and air through the main channel of a gas turbine engine are evaluated comparatively for efficiency: (1) identification of mathematical model by the method of least squares, (2) sifting various combinations of square series-parallel matrices based on adequate linear models; (3) nonlinear optimization by the method of steepest descent; (4) nonlinear optimization with first three terms of the Taylor series by the method of conjugate gradients; (5) solving an indeterminate system of linear algebraic equations. One of the efficiency criteria is the difference between real and diagnosed values of a defective state parameter, the other one is the difference between the value of a defective state parameter and the value of a nearly state parameter. Analytical calculations and computer experiments based on mathematical models of various engine configurations have revealed that the algorithm of matrix sifting is most efficient for diagnosis, but the algorithm of least squares becomes most efficient at higher levels of noise resulting from inaccuracy of state parameter determination and from inadequacy of the mathematical model. Author

N85-22824# Joint Publications Research Service, Arlington, Va.
EFFECT OF COMPLIABILITY OF HOT WALLS IN LIQUID-PROPELLANT ENGINE ON LOW FREQUENCY INSTABILITY Abstract Only **c20**
A. I. Ganichev *In its* USSR Rept.: Eng. and Equipment (JPRS-UEQ-85-003) 12 Mar. 1985 p 81 Transl. into ENGLISH from Izv. Vyssh. Ucheb. Zaved.: Aviats. Tekhn. (Kazan, USSR), no. 1, Jan. - Mar. 1984 p 23-27 (For primary document see N85-22782 13-31)
Avail: NTIS HC A06

The problem of low-frequency instability in a liquid-propellant engine is analyzed, taking into account compliability of the hot walls in the feed channel with displacer and compressibility of the liquid. The corresponding system of two linearized partial differential equations of flow with perturbations yields the pressure and the velocity as functions of a dimensionless chamber and the pipeline are found with the aid of the Laplace transformation. The stability limits are then determined after D-partitioning with subsequent separation of real and imaginary parts. The results reveal that as the compliance of walls toward the other end of the chamber increases, the boundaries of low-frequency instability deform, and the maximum value of the parameter M psi sub phi increase (M = V sub n/alpha, V sub n - nominal velocity of liquid, alpha - acoustic velocity in channel, psi sub phi - hydraulic loss factor), corresponding the sharpness of spikes along those boundaries. Author

N85-22825# Joint Publications Research Service, Arlington, Va.
EXERGETICAL ANALYSIS OF TURBOJET ENGINE CYCLE Abstract Only **c07**
K. A. Malinovskiy *In its* USSR Rept.: Eng. and Equipment (JPRS-UEQ-85-003) 12 Mar. 1985 p 81-82 Transl. into ENGLISH from Izv. Vyssh. Ucheb. Zaved.: Aviats. Tekhn. (Kazan, USSR), no. 1, Jan. - Mar. 1984 p 32-37 (For primary document see N85-22782 13-31)
Avail: NTIS HC A06

The turbojet engine cycle is analyzed in terms of exergy rather than energy, the former being defined as the maximum useful external work done by a body during transition from a given state to the state of equilibrium with the ambient medium. The exergy function e = i - i aub 0 - T sub 0 (s-s sub 0) (i - enthalpies, s-entropies, T sub 0 - ambient temperature) is evaluated directly for an air-turbojet engine burning kerosene, without special graphs and tables (which are not available). The exergy balance behind injector, behind compressor, behind combustion chamber, behind turbine, and in nozzle throat is calculated accordingly. On the basis of these, cycle balances and other relevant thermodynamic relations are then determined for the specific thrust and the energy efficiency of such an altitude H = O. Author

N85-22826# Joint Publications Research Service, Arlington, Va.
ENERGY LOSSES AT LEADING EDGE OF TURBINE BLADE DURING MULTIROW JET COOLING Abstract Only **c07**
V. V. Rumyantsev and I. P. Makov *In its* USSR Rept.: Eng. and Equipment (JPRS-UEQ-85-003) 12 Mar. 1985 p 82 Transl. into ENGLISH from Izv. Vyssh. Ucheb. Zaved.: Aviats. Tekhn. (Kazan, USSR), no. 1, Jan. - Mar. 1984 p 37-40 (For primary document see N85-22782 13-31)
Avail: NTIS HC A06

Multirow jet cooling of turbine blades is evaluated relative to single-row jet cooling. The hydraulic drag coefficient and the discharge coefficient at the leading edge were measured, to indicate the energy losses at that edge, with the Reynolds number referred to the jet diameter d varied over the (1-8), 10 to the 4th power range and the distance H from deflector spout to inner housing wall varied over the H/d = 0.5-2 range. In the case of two symmetric rows of cooling jets both coefficients were found to increase linearly with the Reynolds number and to remain independent of the H/d ratio, both being somewhat larger than in the case of single-row jet cooling. In the case of three symmetric rows of cooling jets both coefficients were found first to increase sublinearly with increasing H/d ratio and then, after becoming independent of the latter in the H/d > 1.5 range, to increase almost linearly with the Reynolds number. In this case the conditions are similar to those at a plane shield struck by a circular jet and, with increasing of the H/d ratio, become more favorable for eddying. Author

N85-22827# Joint Publications Research Service, Arlington, Va.
EXPERIMENTAL DETERMINATION OF OPTIMUM RATIO OF RUNNER BLADE HEIGHT AT EXIT TO RUNNER BLADE HEIGHT AT ENTRANCE OF RADIAL INWARD-FLOW MICROTURBINES Abstract Only **c07**
N. T. Tikhonov, A. N. Tikhonov, and V. N. Matveyev *In its* USSR Rept.: Eng. and Equipment (JPRS-UEQ-85-003) 12 Mar. 1985 p 83 Transl. into ENGLISH from Izv. Vyssh. Ucheb. Zaved.: Aviats. Tekhn. (Kazan, USSR), no. 1, Jan. - Mar. 1984 p 40-44 Original language document previously announced as A84-47559 (For primary document see N85-22782 13-31)
Avail: NTIS HC A06

Optimum outlet-inlet rotor blade height ratios are determined experimentally for rotors with h2/h1 ratios of 1.54, 1.90, 2.44, 2.91, 3.43, 3.77, and 4.50. Expressions are obtained which relate the blade height ratio to the partial admission, the expansion ratio, and the velocity ratio. For turbines with variable partial admission, it is recommended that the blade height ratio be selected for the maximum value of partial admission. V.L. (IAA)

N85-22828# Joint Publications Research Service, Arlington, Va.
SOME UNIQUE FEATURES IN OPERATION OF TWO-STAGE TURBOJET ENGINE WITH AFTERBURNER Abstract Only **c07**
B. D. Fishbeyn *In its* USSR Rept.: Eng. and Equipment (JPRS-UEQ-85-003) 12 Mar. 1985 p 83-84 Transl. into ENGLISH from Izv. Vyssh. Ucheb. Zaved.: Aviats. Tekhn. (Kazan, USSR), no. 1, Jan. - Mar. 1984 p 45-49 (For primary document see N85-22782 13-31)
Avail: NTIS HC A06

The performance of a two-stage turbojet engine during cut-in of the afterburner pump with attendant increase of power drain from the turbocompressor is evaluated, for the purpose of programming the turbocompressor and engine regulation. On the basis of power and fule-air thermodynamics, the increment of power drain during climb and during flight at speed M = 2.8 is calculated as a linear function of the two-staging factor over its m = 0.4 range. Calculations for 1.0 excess air and for 2.5 excess

air, with the ratio of pressure rise in the afterburner pump to effective drop of specific enthalpy varied from 5 to 60, yield the corresponding displacements of compressor and afterburner operating lines as well as of their intersection points representing concurrent operation of compressor and afterburner. These results indicate how the regulation of engine and compressor must be programmed for optimum performance during and following cut-in of the afterburner pump. Author

N85-22829# Joint Publications Research Service, Arlington, Va.
HYDRODYNAMIC SIMULATION OF TRANSIENT PROCESSES IN INJECTION SYSTEM OF AIRCRAFT ENGINES DURING PUMP UNSWIRLING Abstract Only **c07**
V. V. Chervakov, N. S. Yershov, and B. V. Ovsyannikov *In its* USSR Rept.: Eng. and Equipment (JPRS-UEQ-85-003) 12 Mar. 1985 p 84 Transl. into ENGLISH from Izv. Vyssh. Ucheb. Zaved.: Aviats. Tekhn. (Kazan, USSR), no. 1, Jan. - Mar. 1984 p 49-54 Original language document previously announced as A84-47561 (For primary document see N85-22782 13-31)
Avail: NTIS HC A06

The operation of the pump of an aircraft engine during startup is studied, and a mathematical model describing the feed system of the engine is developed. Sets of criteria and boundary conditions are obtained for the hydrodynamic modeling of transient processes that occur in the feed system of the engine as the pump accelerates to its normal speed. V.L. (IAA)

N85-22830# Joint Publications Research Service, Arlington, Va.
EFFECT OF WATER INJECTION INTO AIR FOR TURBINE COOLING ON ECONOMY OF OPERATION OF GAS TURBINE ENGINE WITH AFTERBURNING Abstract Only **c07**
G. M. Gorelov, V. P. Danilchenko, and V. Ye. Reznik *In its* USSR Rept.: Eng. and Equipment (JPRS-UEQ-85-003) 12 Mar. 1985 p 85 Transl. into ENGLISH from Izv. Vyssh. Ucheb. Zaved.: Aviats. Tekhn. (Kazan, USSR), no. 1, Jan. - Mar. 1984 p 81-83 (For primary document see N85-22782 13-31)
Avail: NTIS HC A06

Formulas are presented for calculating fuel savings resulting from the injection of water into the air that cools turbine blades and nozzle guide vanes. It is shown that the fuel economy achieved depends to a large degree on the maximum gas temperature at the turbine inlet. It is calculated that the fuel saved during one hour of operation with the afterburner on can be sufficient for a 1.5 to 2-hr flight at an altitude of 11 km and Mach 0.8. V.L. (IAA)

N85-22831# Joint Publications Research Service, Arlington, Va.
PRESSURE DROP AND COEFFICIENTS OF INTERNAL HEAT TRANSFER NECESSARY FOR TRANSPIRATION COOLING Abstract Only **c34**
S. G. Dezideryev, A. G. Karimova, and P. P. Makarov *In its* USSR Rept.: Eng. and Equipment (JPRS-UEQ-85-003) 12 Mar. 1985 p 85 Transl. into ENGLISH from Izv. Vyssh. Ucheb. Zaved.: Aviats. Tekhn. (Kazan, USSR), no. 1, Jan. - Mar. 1984 p 83-85 (For primary document see N85-22782 13-31)
Avail: NTIS HC A06

The pressure drop and the coefficients of internal heat transfer necessary for transpiration cooling of high-temperature turbine nozzles and blades with the use of porous materials are calculated semi-empirically. Equating the empirical hydraulic drag coefficient in pores zeta = 420/Re sub d (Re sub d - Reynolds number for air in pores) to the theoretical hydraulic drag coefficient in pores zeta - d delta P/1/2 rho bar (V sup 2) delta yields the pressure drop delta P=1/2 rho bar (V sup 2) delta zeta/d = 210 G mu delta/rho (d sup 2)2 (rho, mu-density and dynamic viscosity of air at mean temperature and mean pressure, bar V - velocity of air in pores, delta - thickness of porous layer, d - diameter of pores, G - flow rate of air per unit surface area, 2 - porosity factor). B.W.

N85-22832# Joint Publications Research Service, Arlington, Va.
ANNULAR GROOVE IN COMPRESSOR CASING AS DEVICE FOR CONTROL OF AIR STREAM Abstract Only **c07**
V. N. Yershov, A. P. Yefimenko, and V. Yu. Nezym *In its* USSR Rept.: Eng. and Equipment (JPRS-UEQ-85-003) 12 Mar. 1985 p 86 Transl. into ENGLISH from Izv. Vyssh. Ucheb. Zaved.: Aviats. Tekhn. (Kazan, USSR), no. 1, Jan. - Mar. 1984 p 85-86 (For primary document see N85-22782 13-31)
Avail: NTIS HC A06

As a result of extensive experimental and theoretical studies at the Kharkov Institute of Aviation concerning the incipience of rotatory separation low in axial compressors, there has been developed a device for controlling the air stream so as to extend the range of nonseparation flow. It is an annular groove cut in the compressor casing around the runner. Two basic configurations have been evaluated comparatively and relative to a uniform radial gap between smooth casing and straight smooth runner blade edge: (1) axially tapered radial gap between slanted groove bottom in the casing and straight smooth runner blade edge; (2) uniform radial gap between slanted groove bottom in the casing and parallel axially slanted runner blade edge dovetailing into the groove. Both width and height of the dovetailing blade edge segment were varied, and tests performed with an S-17 compressor stage (outside diameter 0.46 m, relative hub diameter 0.84) at average referred circumferential velocities of 83-193 m/s have yielded satisfactory results. Author

N85-22833# Joint Publications Research Service, Arlington, Va.
EXPERIMENTALLY DETERMINED CHARACTERISTICS OF VORTEX HEATERS Abstract Only **c07**
Sh. A. Piralishvili and N. N. Novikov *In its* USSR Rept.: Eng. and Equipment (JPRS-UEQ-85-003) 12 Mar. 1985 p 86-87 Transl. into ENGLISH from Izv. Ucheb. Zaved.: Aviats. Tekhn. (Kazan, USSR), no. 1, Jan. - Mar. 1984 p 93-95 (For primary document see N85-22782 13-31)
Avail: NTIS HC A06

An experimental study of vortex gas heaters was made for the purpose of establishing their performance capabilities, most important being the temperature rise in regions farthest from the discharge nozzle in the case of a 1:1 ratio of cooled gas mass to compressed gas mass flowing simultaneously through the turbulizing nozzle. Data were obtained specifically on the performance of a vortex tube operating as heater without discharge of preheated gas mass. The separating chamber was 0.025 m in diameter with an L/D = 9 length-to-diameter ratio, with a variable radius hole in the diaphragm, an with tight asbestos insultation ensuring adeabaticity. The cylindrical turbulizing chamber with perforated lateral surface was 0.01875 m in diameter. Measurements included dependence of temperature rise on inlet pressure, radial profile of temperature rise, dependence of temperature rise on inlet temperature, and isotherms corresponding to various hole sizes in the diaphragm of the discharge nozzle and various sizes of the throat cross section in the turbulizing nozzle. B.W.

N85-22834# Joint Publications Research Service, Arlington, Va.
MATHEMATICAL MODELING OF TRANSIENT PERFORMANCE OF GAS TURBINE ENGINE Abstract Only **c07**
Yu. A. Skortsov *In its* USSR Rept.: Eng. and Equipment (JPRS-UEQ-85-003) 12 Mar. 1985 p 87 Transl. into ENGLISH from Izv. Vyssh. Ucheb. Zaved.: Aviats. Tekhn. (Kazan, USSR), no. 1, Jan. - Mar. 1984 p 96-98 (For primary document see N85-22782 13-31)
Avail: NTIS HC A06

Two systems of differential equations describing the transient performance of a gas turbine engine are compared, one representing a piecewise-constant approximation and one representing a piecewise linear approximation. The laws of energy, mass, and momentum conservation are formulated in both cases for flow in a stream tube idealing the flow of gas. Equations of the piecewise-constant approximation must be normalized to the Cauchy form, which complicates the algorithm of calculations. Piecewise-linear approximation requires a form of expressing the mean velocity u sub m = (p(sub m), rho(sub m), V(sub m)) through the velocities u sub i and u sub +1 in two consecutive fixed sections (p = pressure, rho - density, v - specific volume). Piecewise-constant approximation does not simplify the problem when the mean velocity is a function of both local ones um = f (u(sub 1), u sub i +1) while assuming that u sub m = u sub i or

u sub m = u (sub i +1) +1 simplifies the calculations with a sacrifice in accuracy. Piecewise-constant approximation can become more accurate than piecewise-linear approximation under less stringent constraints on the gas flow parameters. Author

N85-22835# Joint Publications Research Service, Arlington, Va.
DEPENDENCE OF COMBUSTION OF HOMOGENEOUS KEROSENE-AIR MIXTURES ON HUMIDITY OF AIR Abstract Only **c25**
V. A. Sychenkov and V. M. Yankovskiy *In its* USSR Rept.: Eng. and Equipment (JPRS-UEQ-85-003) 12 Mar. 1985 p 87-88 Transl. into ENGLISH from Izv. Vyssh. Ucheb. Zaved.: Aviats. Tekhn. (Kazan, USSR), no. 1, Jan. - Mar. 1984 p 98-101 Original language document previously announced as A84-47577 (For primary document see N85-22782 13-31)
Avail: NTIS HC A06

An experimental study has been carried out to investigate the effect of the addition of steam into the air on the combustion characteristics of homogeneous kerosene-air mixtures. It is found that as the humidity of the air increases, the combustion process becomes less intense. This result is ascribed to the fact that part of the heat produced during combustion is used to heat inert water vapors. V.L. (IAA)

N85-22836# Joint Publications Research Service, Arlington, Va.
EFFECT OF GAS STREAM SWEEPING PAST THE EFFLUENT OF A PERFORATED PLATE ON HEAT TRANSFER INSIDE THE PERFORATIONS Abstract Only **c34**
V. A. Trushin, K. M. Iskakov, and Z. S. Iskhakov *In its* USSR Rept.: Eng. and Equipment (JPRS-UEQ-85-003) 12 Mar. 1985 p 88 Transl. into ENGLISH from Izv. Vyssh. Ucheb. Zaved.: Aviats. Tekhn. (Kazan, USSR), no. 1, Jan. - Mar. 1984 p 101-103 Original language document previously announced as A84-47578 (For primary document see N85-22782 13-31)
Avail: NTIS HC A06

An analysis of heat transfer inside the perforations of air-cooled turbine blades suggests that transverse gas flow at the outlet of the perforations may be one of he factors affecting the heat transfer process. To investigate the effect of transverse flow, experiments have been carried out on perforated plates 1, 2, 3, and 4 mm thick with 0.6-1.4-mm-diameter perforations. It is found that in the Reynolds number range 2,000-50,000, transverse gas flow at the outlet of the perforations (injection ratio, 0.6-2.8) has no effect on heat transfer iside the perforations. V.L. (IAA)

N85-22837# Joint Publications Research Service, Arlington, Va.
SELECTION OF AIR INTAKE PARAMETERS FOR SUPERSONIC-FLOW OPERATION Abstract Only **c34**
V. I. Bazhanov and A. A. Stepchkov *In its* USSR Rept.: Eng. and Equipment (JPRS-UEQ-85-003) 12 Mar. 1985 p 89-90 Transl. into ENGLISH from Izv. Vyssh. Ucheb. Zaved.: Aviats. Tekhn. (Kazan, USSR), no. 1, Jan. - Mar. 1984 p 69-71 Original language document previously announced as A84-47565 (For primary document see N85-22782 13-31)
Avail: NTIS HC A06

An optimum system of skewed shock waves is selected for supersonic flight velocities (Mach 4-6) under the condition that the total stream rotation angle behind the skewed shock waves do not exceed a certain critical value corresponding to the onset of sonic flow. The approach proposed here is illustrated by an example in which systems of skewed shock waves are calculated for Mach 6. V.L. (IAA)

N85-22838# Joint Publications Research Service, Arlington, Va.
ESTIMATION OF GAS TURBINE ENGINE BOOST PROVIDED BY INJECTING WATER BEHIND COMPRESSOR Abstract Only **c07**
A. N. Prokofyev *In its* USSR Rept.: Eng. and Equipment (JPRS-UEQ-85-003) 12 Mar. 1985 p 90 Transl. into ENGLISH from Izv. Vyssh. Ucheb. Zaved.: Mashinostr. (Moscow), no. 4, Apr. 1984 p 80-82 (For primary document see N85-22782 13-31)
Avail: NTIS HC A06

The injection of water into the duct of gas turbine engines in order to boost output is examined. The maximum amount of water injected is determined as a function of the required increase in compression pressure, the compressor efficiency, the water temperature and the temperature and moisture content of the atmospheric air. The influence of the parameters of the compressor and the initial content of the air on the maximum amount of water injected is investigated. The use of the method for making a thermodynamic analysis of the heat-regenerating gas turbine engine employed for transportation is presented. It is found that injecting the maximum amount of water behind the compressor increases the nominal engine power by 27% while reducing relative fuel consumption by 7%. Author

N85-22839# Joint Publications Research Service, Arlington, Va.
USSR REPORT: MACHINE TOOLS AND METALWORKING EQUIPMENT
11 Mar. 1985 52 p Transl. ito ENGLISH from various Russian articles
(JPRS-UMM-85-005) Avail: NTIS HC A04

Progress on machine tools and metal-working equipment is reported. Topics discussed incude: advances in cutting tool technology, developments in forge press automation, hydraulic forge presses, implementation of plasma cutting technology, automated lines and aggregated machining. For individual titles, see N85-22840 through N85-22842.

N85-22840# Joint Publications Research Service, Arlington, Va.
ADVANCES IN CUTTING TOOL TECHNOLOGY SURVEYED
V. P. Zhod *In its* USSR Rept.: Machine Tools and Metalworking Equipment (JPRS-UMM-85-005) 11 Mar. 1985 p 1-7 refs Transl. into ENGLISH from Mashinostritel (Moscow), no. 8, Aug. 1984 p 9-11 (For primary document see N85-22839 13-31)
Avail: NTIS HC A04/MF A01

Progress in machinebuilding which has increased the level of automation and the intensification of the production processes due to the wide use of automatic metalcutting equipment, and the increase in the share of materials difficult to machine that have special mechanical properties are discussed. The metal-cutting tool that organizes the production of products is examined. The creation of a highly productive cutting tool, which increased the technical standards which allow intensification of machining modes and utilization of the possibilities of automatic equipment are considered. This is achieved by saving tool materials by a material that is capable of preserving, and increasing the productivity of machining. A progressive cutting tool and the development of a tool with a mechanical attachment of multifaceted plates, are outlined. E.A.K.

N85-22841# Joint Publications Research Service, Arlington, Va.
DIAMOND CUTTERS' GRINDERS
B. F. Romanov *In its* USSR Rept.: Machine Tools and Metalworking Equipment (JPRS-UMM-85-005) 11 Mar. 1985 p 8-12 Transl. into ENGLISH from Mashinostroitel (Moscow), no. 8, Aug. 1984 p 10-11 (For primary document see N85-22839 13-31)
Avail: NTIS HC A04/MF A01

The development of diamond tool designs is determined by the development of the technology for the synthesis of artificial diamonds. The technology of synthesizing artificial diamonds involves the production of mono and polycrystalline diamonds and composition diamond-containing materials. High strength and thermally stable monocrystalline diamonds brands AS30 to AS80 in a size of up to 800 micrometers, and polycrystalline diamonds: black diamonds, ballas (Synthetic Fiber) in a size up to 10mm, are manufactured. Production of single-layer and double-layer diamond plates used in cutting tools is organized. The raw materials base with the constant decrease in the use of natural diamonds is the basis for the development of the manufacture of a wide array of diamond tools. New areas of applications for tools using natural diamonds, such as diamond cutters for turning high-precision parts, straightening tools, hardness gages are outlined. Diamond cutters with natural diamonds are used to grind surfaces which have exceptionally high requirements with respect to the reflecting capacity and roughness. E.A.K.

N85-22842# Joint Publications Research Service, Arlington, Va.
NEW TOOLING FOR PLASMA CUTTING TECHNOLOGY
M. T. Korotkikh, M. A. Shaterin, and V. B. Shterin *In its* USSR Rept.: Machine Tools and Metalworking Equipment (JPRS-UMM-85-005) 11 Mar. 1985 p 28-30 refs Transl. into ENGLISH from Mashinostroitel (Moscow), Aug. 1984 p 15-16 (For primary document see N85-22839 13-31)
Avail: NTIS HC A04/MF A01

When milling the edges of sheet intermediate products made of high strength manganese and other special steels and alloys with plasma preheating, milling cutters equipped with plates of metal-ceramic hard alloys are used. With plasma heating, it is most advisable to use cylindrical milling tools. The tooth of the milling tool cuts into the soft metal which reduces the unit loads on the cutting wedge of the tool. It becomes possible to use plates with the slope angle of the cutting edge equal or near zero, which considerably simplifies the making of the tool. The milling tool design makes it technologically efficient to produce basing surfaces for setting the cutting components. The through wedge grooves of the rings may be ground which produces very flat supporting surfaces and, therefore, high rigidity of the interface between the plate and the support. The use of tetrahedral plates with a flat forward surface with a 90 deg tip angle utilizes all eight cutting edges of the plate. The use of such milling tools with plasma preheating of the intermediate product insures high machining productivity even if the tool is equipped with hard alloy plates without tungsten. E.A.K.

N85-22843# Joint Publications Research Service, Arlington, Va.
CHINA REPORT: SCIENCE AND TECHNOLOGY
20 Feb. 1985 205 p refs Transl. into ENGLISH from various Chinese articles
(JPRS-CST-85-005) Avail: NTIS HC A10/MF A01

Reports of scientific research projects in China are given. Lithography, laser applications, remote sensing, satellite tracking and celestial mechanics are among the topics discussed. For individual titles, see N85-22844 through N85-22849.

N85-22844# Joint Publications Research Service, Arlington, Va.
LASER APPLICATIONS IN LAST 10 YEARS REVIEWED c36
Lu Zhiguo *In its* Chinese Rept.: Sci. and Technol. (JPRS-CST-85-005) 20 Feb. 1985 p 24-36 refs Transl. into ENGLISH from Zhongguo Jiguang (Shanghai), no. 10, 20 Oct. 1984 p 577-583 (For primary document see N85-22843 13-31)
Avail: NTIS HC A10/MF A01

A survey of the progress of laser applications in China in the past 10 years (1974-1984) in industry, holography information processing, instrumentation and other scientific research is given. Laser welding, laser drilling, and signal processing applications are discussed. R.J.F.

N85-22845# Joint Publications Research Service, Arlington, Va.
ANALYSIS OF FIBER-GYROSCOPES DISCUSSED c35
Sun Li and Deng Feifan *In its* Chinese Rept.: Sci. and Technol. (JPRS-CST-85-005) 20 Feb. 1985 p 37-43 refs Transl. into ENGLISH from Zhongguo Jiguang (Shanghai), no. 10, 20 Oct. 1984 p 598-601 (For primary document see N85-22843 13-31)
Avail: NTIS HC A10/MF A01

An analytical formula for calculating the optimum length of resonator type fiber-gyroscopes was deduced. Taking into account stimulated Brillouin scattering, the sensitivity limit of fiber-gyroscopes, the determination of the coupling coefficient, and the requirements of splice loss are discussed. Author

N85-22846# Joint Publications Research Service, Arlington, Va.
X-RAY LITHOGRAPHY AND VLSI CIRCUITS c33
Gu Bichun *In its* Chinese Rept.: Sci. and Technol. (JPRS-CST-85-005) 20 Feb. 1985 p 44-55 refs Transl. ino ENGLISH from Wuli (Beijing, China), v. 13, no. 1, Jan. 1984 p 15-20 (For primary document see N85-22843 13-31)
Avail: NTIS HC A10/MF A01

The use of X-ray lithography techniques in the production of very large scale integration integrated circuits is discussed. Requirements, high accuracy registration techniques, production costs, and electron beam printing processes are covered. R.J.F.

N85-22847# Joint Publications Research Service, Arlington, Va.
DEVELOPMENT, PROSPECT OF SATELLITE DYNAMICS DISCUSSED c13
Huang Kuyi *In its* Chinese Rept.: Sci. and Technol. (JPRS-CST-85-005) 20 Feb. 1985 p 84-95 refs Transl. into ENGLISH from Ziran Zazhi (Shanghai), no. 9, 1984 p 663-667 (For primary document see N85-22843 13-31)
Avail: NTIS HC A10/MF A01

Problems of celestial mechanics as they apply to artificial satellites are discussed. Satellite perturbation, laser ranging, satellite-borne photography, and geodynamics are among the topics discussed. R.J.F.

N85-22848# Joint Publications Research Service, Arlington, Va.
GEOLOGICAL REMOTE SENSING DEVELOPS RAPIDLY, FINDS BROAD APPLICATIONS c43
Yang Guangqing *In its* Chinese Rept.: Sci. and Technol. (JPRS-CST-85-005) 20 Feb. 1985 p 96-102 refs Transl. into ENGLISH from Zhongguo Dizhi (Beijing, China), no. 10, 13 Oct. 1984 p 23-26 (For primary document see N85-22843 13-31)
Avail: NTIS HC A10/MF A01

The development of geological remote sensing in China is discussed. Specific applications covered include mapping, geological surveys, locating mineral deposits, site selection for large construction projects, water resources surveys, and seismological investigations. R.J.F.

N85-22849# Joint Publications Research Service, Arlington, Va.
CARD'S LOW-SPEED WIND TUNNEL DESCRIBED c09
Wang Maoxun and Pan Ruikang *In its* Chinese Rept: Sci. and Technol. (JPRS-CST-85-005) 20 Feb. 1985 p 160-166 refs Transl. into ENGLISH from Guoji Hangkong (Beijing, China), no. 10, 5 Oct. 1984 p 2-4 (For primary document see N85-22843 13-31)
Avail: NTIS HC A10/MF A01

A low speed wind tunnel is described. The 8 m x 6 m wind tunnel is a large-scale, low-speed open-type wind tunnel with dual in-line closed test sections. Overall length is 237 m, maximum width is 40 m, maximum height is 20.5 m, and it is made up of the intake apparatus, stabilizing section, first construction section, first test section, second construction section, second test section, first diffusion section, fan section, second diffusion section, and air exit. The ceiling of each test section has movable gates, in the center of the floor there is a turntable that can rotate 360 deg, and in the sidewalls and ceiling there are many observation windows. The important performance parameters of the two test sections are given. The first test section is primarily for low-speed tests of helicopters and V/STOL aircraft, and research on testing industrial aerodynamic surfaces. For this reason, when the wind tunnel was designed, the demands for quality of flow field were low, they just had to be able to satisfy test demands. The second test section is the main work section of this wind tunnel; the quality of its flow field achieved design norms and the unified stipulated norms for low-speed wind tunnels nationwide. R.J.F.

32 COMMUNICATIONS

Includes land and global communications; communications theory; and optical communications.

For related information see also *04 Aircraft Communications and Navigation* and *17 Spacecraft Communications, Command and Tracking.*

N85-22850 Communications Research Centre, Ottawa (Ontario). Information Technology and Systems Branch.
EXPERIMENTAL RESULTS ON THE APPLICATION OF CONVOLUTIONAL CODING AND VITERBI DECODING AS A FREQUENCY DIVERSITY TECHNIQUE IN HF DATA TRANSMISSION

B. D. McLarnon Feb. 1985 21 p refs
(CRC-1377) Avail: Issuing Activity

A method of using coding and soft-decision decoding techniques to replace a conventional diversity combiner is examined. It uses a rate-1/2 convolutional code and Viterbi decoding in a dual diversity configuration at 75 bps, and is easily implemented with an eight-bit microprocessor. The results of comparisons between the coding technique and standard diversity combining on several short-and medium-range HF links are given, and its advantages and limitations in HF data systems applications are discussed. Author

N85-22851 Clemson Univ., S.C.
DATA COMPRESSION FOR NOISELESS CHANNELS Ph.D. Thesis
Silvia Gilbert Cathey 1984 137 p
Avail: Univ. Microfilms Order No. DA-8426762

A data compression method to compress strings of digital data and to encode the compressed data for transmission over a noiseless channel is presented. Several aspects of information theory and lattice theory are combined to produce a method by which an optimum way of reorganizing and combining source words can be found. The source considered here has identification bits and data bits intermingled. Source words that are related in some fashion, either sequentially or by position in a group of words, are stacked and new subsources formed by taking source words vertically rather than horizontally. A partition lattice is then formed with the partition being over source combination. A minimal length chain can be found which connects the minimum-entropy partition for each level. By using the truncated lattice method, this chain may be calculated directly with a significant reduction in work to find the optimum partition for the given constraints on a system. Several examples are given and a practical application to the on-board F-15 radar system is discussed. Dissert. Abstr.

N85-22852 Colorado Univ., Boulder.
TRANSIENT ANALYSIS OF LOADED THIN-WIRE ANTENNAS AND TRANSMISSION LINES Ph.D. Thesis
Ahmad Hoorfar 1984 348 p
Avail: Univ. Microfilms Order No. DA8428657

Analytical time-domain solutions for thin-wire cylindrical antennas and transmission lines based upon the singularity expansion method (SEM) are obtained, and the effects of impedance loading on the transient behavior of these structures are investigated. An SEM analysis of a terminated transmission line as well as a transmission line with an arbitrarily located load is presented. Equipped with an approximate frequency-domain expression for the current, a theory for determining analytical time-domain SEM solutions for an unloaded as well as a loaded thin-wire cylindrical antenna is presented. Excellent agreement between the results from this approximate analytical theory and the numerical works is obtained for an antenna with the antenna parameter omega = to or > 9. Dissert. Abstr.

N85-22853 National Inst. for Aeronautics and Systems Technology, Pretoria (South Africa).
BEAMWIDTH CONTROL IN PYRAMIDAL HORNS
C. A. vanderNeut 1983 8 p refs
(R-NIAS-27; Y-1) Copyright. Avail: Issuing Activity

Four methods are discussed to control or modify a horn's beamwidth. The methods are: (1) introduction of an exponential ridge; (2) pinwall sidewalls; (3) introducing a dielectric slab in the aperture; and (4) omitting the sidewalls altogether. Measured curves are shown for all cases, giving beamwidth variation with frequency. E.A.K.

N85-22854*# Research Triangle Inst., Research Triangle Park, N.C.
FIREFIGHTERS' COMMUNICATION TRANSCEIVER TEST PLAN Final Report
Robert J. Wallace 24 May 1984 64 p refs
(Contract NAS8-35816)
(NASA-CR-171419; NAS 1.26:171419) Avail: NTIS HC A04/MF A01 CSCL 17B

The requirements for the operational testing of the firefighters communication transceiver were identified. The major concerns centered around the integrity and reliability of the firefighter/microphone interface. The major concern about the radio hardware was that it be intrinsically safe in hazardous atmospheres and that the system not interfere with the fit or facial seal of self-contained breathing apparatus (SCBA). The greatest concern for operational testing purposes as the reliability and clarity of the line of communication between the firefighter and those on the fireground with whom he must maintain contact. A desire to test any units developed in both training exercises and in real responses to hazardous material incidents was expressed. It is felt that a VOX-microphone built into the SCBA facemask gives the best performance. A voice-pickup product device which combines a bone conduction microphone and a speaker into a single ear mounted unit is examined. Author

N85-22855*# Jet Propulsion Lab., California Inst. of Tech., Pasadena.
A COMPARISON OF METROPOLITAN AND NON-METROPOLITAN EMPLOYMENT CHARACTERISTICS: INDICATIONS OF THE SIZE OF NON-METROPOLITAN MOBILE COMMUNICATION SERVICES USER CLASSES
R. E. Wilcox 15 Feb. 1985 104 p refs
(Contract NAS7-918)
(NASA-CR-175648; JPL-Pub-85-9; NAS 1.26:175648) Avail: NTIS HC A06/MF A01 CSCL 17B

The similarities and differences between areas inside and outside U.S. metropolitan areas were evaluated in terms of their commercial/industrial and government employment characteristics. The comparison focuses on the levels, shares, and composition of employment in the commercial/industrial and government sectors that represent potential classes of land mobile communications users. The major findings of the analysis are as follows: (1) non-metropolitan commercial/industrial user classes of land mobile communication services exist in significant numbers; (2) the compositions of non-metropolitan and metropolitan commercial/industrial user classes of land mobile communication services closely resemble each other; (3) non-metropolitan areas have significant levels of the government user classes that represent potential markets for land mobile communication services; and (4) non-metropolitan local governments have a significantly larger proportion of their employment in the primary user classes of private land mobile radio service than do metropolitan local governments. M.G.

N85-22856 British Broadcasting Corp., Kingswood (England). Engineering Div.
ELECTRONIC GENERATION OF TEXT FOR TELEVISION
N. E. Tanton Nov. 1984 25 p refs
(BBC-RD-1984/14) Avail: BBC, Kingswood Warren, Tadworth, Surrey, England

The image quality of present-day television character generators is compared with the quality of text images derived by scanning real artwork. To illustrate and identify the causes of image distortion (aliasing) prevalent in these and other synthetic television images, the spectral consequences of scanning a scene and of representing any image with a two-level (1-bit) signal are discussed. A method of electronically generating and displaying filtered text images for television is described together with a comparison of various filtering methods. The resulting images are largely free from aliasing and have a quality equal to or better than that of scanned artwork. Author

N85-22857 British Broadcasting Corp., Kingswood (England). Engineering Div.
DIGITAL STANDARDS CONVERSION: INTERPOLATION THEORY AND APERTURE SYNTHESIS
C. K. P. Clarke and N. E. Tanton Dec. 1984 52 p refs
(BBC-RD-1984/20) Avail: BBC, Kingswood Warren, Tadworth, Surrey, England

A frequency domain approach is used to investigate digital

interpolation for standards conversion. To illustrate the background theory, one-dimensional sampling and interpolation is described in general terms, including methods for synthesising interpolation apertures and the effects of aperture quantisation. With the two-dimensional vertical-temporal sampling of television scanning, interpolation can be carried out as two one-dimensional processes or, with improved performance but somewhat greater complexity, as a single two-dimensional processes or, with improved performance but somewhat greater complexity, as a single two-dimensional process. Standards conversion impairments are shown to arise from the interpolation frequency characteristic departing from the ideal low-pass form in particular regions of the television signal spectrum. Also identified are the positions in the vertical-temporal spectrum of cross-luminance, cross-color and other residual impairments left by PAL or NTSC decoding. Using an experimental converter, apertures of duration two, three and four field periods were developed. For two-field apertures the performance is a compromise between movement judder, line flicker and vertical resolution; four-field apertures give stationary pictures of good resolution, free from flicker and other aliasing effects and reduce impairments left by color decoding. Movement impairments, remain because of the overlap of spectral components which results with normal television scanning. M.G.

N85-22858# Royal Signals and Radar Establishment, Malvern (England).
THE CHINESE REMAINDER THEOREM AND MULTI-PRF RADARS
J. Clarke Feb. 1984 12 p ref
(AD-A141375; RSRE-MEMO-3650; BR91491) Avail: NTIS HC A02/MF A01

The Chinese remainder theorem is quoted and a proof from first principles is given such that no prior knowledge of number theory is required. The application of the method of the Chinese remainder theorem is explained. An example on the processing of radar detections in a multi-PRF radar is presented. Author (ESA)

N85-22859# Royal Signals and Radar Establishment, Malvern (England).
A FULLY DISTRIBUTED APPROACH TO THE DESIGN OF A 16 K BIT/SEC VHF PACKET RADIO NETWORK
M. S. Hazell and B. H. Davies Feb. 1984 39 p refs
(AD-A141282; RSRE-84003; BR91513) Avail: NTIS HC A03/MF A01

System design considerations for a packet radio network operating in the mobile tactical environment are outlined. Survivability is of primary importance and a fully distributed approach in which all nodes are functionally equivalent and the network self-configuring is favored. Channel access (CA), routing and congestion control algorithms are presented. The CA algorithm, an adaptive CSMA scheme, maintains good throughput-delay performance irrespective of the number of active users and offered loading. It compensates for hidden terminal effects in multiple hop networks. The routing strategy exploits the inherent path redundancy of the semibroadcast environment to offset the high packet loss rate due to collisions, interference and fading. Aspects which ensure effective routing in the face of rapid topological change and consequent out-moded routing data are outlined. A prototype which allows a conventional tactical VHF transceiver to be adapted for use as a packet radio unit is described.
Author (ESA)

N85-22860# Admiralty Underwater Weapons Establishment, Portland (England).
THE IMAGING OF INTERNAL WAVES BY THE SEASAT-A SYNTHETIC APERTURE RADAR
M. T. Bagg and K. I. Johnson (Newcastle-upon-Tyne Polytechnic, England) Aug. 1984 28 p refs
(ARE(PORTLAND)TN-720/84; BR93397) Avail: NTIS HC A03/MF A01

Results from 5 million sq km of optical survey processed SEASAT-SAR imagery of the Northeast Atlantic are presented. Markings attributed to internal wave activity were collated on maps with the bathymetry and surface meteorology. Two thirds of the imagery shows evidence of such activity. The markings occur extensively at locations from Iceland to the Azores. Simple analysis techniques were applied systematically to compare the very large data sets involved. The characteristics of the internal wave features are discussed. Imagery of the region between Scotland and Iceland is studied. Author (ESA)

N85-22861# Royal Signals and Radar Establishment, Malvern (England).
COMPARING DIFFERENT THEORETICAL DESIGNS OF SIX-PORT REFLECTOMETER JUNCTIONS
E. J. Griffin and T. E. Hodgetts Apr. 1984 19 p refs
(AD-A149419; RSRE-MEMO-3684; BR93573) Avail: NTIS HC A02/MF A01

A derivation of numerical procedures for comparing theoretical designs of six-port junctions for use in measuring the voltage reflection coefficient of passive loads is presented. It is shown that the maximum uncertainty in measuring any passive load can be minimized by a suitable choice of components, in each of four different designs. The relative merits of these designs in terms of selecting a best compromise for use in a dual six-port network analyzer are discussed. Author (ESA)

N85-22862# Royal Signals and Radar Establishment, Malvern (England).
EDGE DETECTION IN SAR IMAGERY USING GRADIENT OPERATORS
S. C. Giess 1984 15 p refs
(AD-A149411; RSRE-MEMO-3743; BR93642) Avail: NTIS HC A02/MF A01

Problems in the detection of edge features on high resolution synthetic aperture radar (SAR) images using gradient operators were studied. An algorithm, proposed as a model of the human visual system, which embodied these techniques was investigated and is found to give poor performance on SAR images. This poor performance suggests that edge detection by gradient operators alone is not appropriate for SAR images. Author (ESA)

N85-22863# Royal Signals and Radar Establishment, Malvern (England).
SYSTEM DYNAMICS AND NETWORK CONTROL
T. E. G. King Jul. 1984 30 p refs
(AD-A149420; RSRE-MEMO-3755; BR93577) Avail: NTIS HC A03/MF A01

The evaluation of the performance of adaptive controls in communications networks is discussed. Analytical tools are assessed and the system dynamics technique is described. The application of system dynamics to the investigation of network controls is considered and results for nodal congestion control, sliding window flow controls, and adaptive routing are given. The relevance of system dynamics to the simulation of large realistic networks is examined. Author (ESA)

N85-22864# General Research Corp., Santa Barbara, Calif.
RESEARCH EFFORTS IN SUPPORT OF RESONANCE EXTRACTION STUDIES. VOLUME 1: IMPROVEMENT AND VALIDATION OF TWFD (THIN-WIRE FREQUENCY-DOMAIN): A THIN-WIRE FREQUENCY-DOMAIN SCATTERING CODE Final Report, 10 Jan. 1982 - 30 Sep. 1983
J. R. Auton, T. L. Larry, and M. L. VanBlaricum Nov. 1984 50 p
(Contract N00014-80-C-0299)
(AD-A150296; AD-F300559; GRC-CR-84-1309) Avail: NTIS HC A03/MF A01 CSCL 20/14

The development of a thin-wire frequency-domain (TWFD) method of moments code was discussed in a previous report 1. Since that time this code has undergone further development and numerical testing. The purpose of the code is to provide a theoretical and numerical basis to aid in understanding the resonance region electromagnetic scattering from thin-wire stick models. This frequency domain code augments a time-domain code (TWTD) which calculates the scattered transient response for an impulsive incident field. The outputs from both of these

codes have provided numerical predictions which have been indispensible in assessing our ability to extract resonance information from actual scattering range data. GRA

N85-22865# Michigan Univ., Ann Arbor. Solid-State Electronics Lab.
MAGNETOSTATIC-WAVE PROPAGATION IN A FINITE YIG-LOADED RECTANGULAR WAVEGUIDE Interim Report, 1 Oct. 1981 - 30 Jun. 1984
M. Radmanesh Wright-Patterson AFB, Ohio Air Force Wright Aeronautical Labs. Nov. 1984 161 p
(Contract F33615-81-K-1429)
(AD-A150332; TR-170; AFWAL-TR-84-1174) Avail: NTIS HC A08/MF A01 CSCL 20/14

The objective of this investigation is to study magnetostatic-wave propagation in a rectangular waveguide loaded with a finite YIG slab, to understand the effect of physical parameters on the dispersion and group time-delay characteristics, and to obtain better design criteria for magnetostatic-wave devices. An analysis was carried out for two basic geometrical configurations: (1) a YIG slab of arbitrary thickness placed inside a waveguide in contact with each sidewall, and (2) a thin YIG slab of finite width placed symmetrically inside a waveguide such that there is an equal air gap between the slab and each sidewall. For each of these basic geometries, the magnetic bias field was assumed to be either parallel or normal to the slab in the transverse plane of the waveguide. For Case 1, the mode analysis technique was used to obtain the dispersion relations while in Case 2 the integral equation method was used to derive the approximate dispersion relations. Numerical simulations were carried out for various geometrical configurations. Sample numerical calculations of the propagation constant and delay characteristics are presented in the frequency range of 4 to 10 GHz. These numerical results were obtained from the numerical simulation will be important in the design of magnetostatic-wave devices. GRA

N85-22866# Southeastern Center for Electrical Engineering Education, Inc., St. Cloud, Fla.
BASIC EMC (ELECTROMAGNETIC INTERFERENCE) TECHNOLOGY ADVANCEMENT FOR c3 SYSTEMS. VOLUME 3A: PROBABILISTIC ANALYSIS OF COMBINATIONAL CIRCUITS WITH RANDOM DELAYS Final Report, Sep. 1982 - Dec. 1983
A. Ephrath and D. D. Weiner Griffiss AFB, N.Y. RADC Aug. 1984 207 p
(Contract F30602-81-C-0062)
(AD-A150349; RADC-TR-82-286-Vol-3A) Avail: NTIS HC A10/MF A01 CSCL 09/5

Random propagation delays are encountered in digital integrated circuits due to fluctuations in the fabrication process. These delays can be further increased due to the presence of electromagnetic interference. System performance can be evaluated from the expected values of the output signals. Analytical methods for determining the output expected values of combinational circuits with random delays are developed in this dissertation. Given the input expectations, the network logic functions, and p.d.f.'s of the delays associated with the gates of the network, it is shown how to obtain the output expected values. Two types of delay elements are considered: (1) the pure delay elements, whose output is a delayed, but undistorted, replica of the input, and (2) the discriminating delay element, where input rise and fall transitions experience different delays. Two degrees of network complexity are dealt with: (1) tree-like networks, in which there is only one path from every network input to any network, and (2) networks with reconvergent fanouts, where more than one path exists from some inputs to some outputs. To simplify analysis of very large circuits, an approximate model is proposed where the circuits are subdivided into large logic blocks. The analytical techniques previously derived for individual gates are then applicable. Various strategies for characterizing the delays of the large logic blocks are considered and examined by means of computer simulations. GRA

N85-22867# Colorado School of Mines, Golden. Center for Wave Phenomena.
TWO-AND-ONE-HALF DIMENSIONAL IN-PLANE WAVE PROPAGATION
N. Bleistein 16 Dec. 1984 48 p
(Contract N00014-84-K-0049)
(AD-A150467; CWP-014) Avail: NTIS HC A03/MF A01 CSCL 20/14

The purpose of this paper is to collect certain wave propagation results in two-and-one-half dimensions - defined as three dimensional propagation in a medium that has variations in two dimensions only. The results of interest are for sources and receivers in the plane determined by the two directions of parameter variation. The objective of this work is to reduce the analysis of the in-plane propagation to two dimensional analysis while retaining - at least asymptotically - the proper three dimensional geometrical spreading. We do this for the free space Green's function and for the Kirchhoff approximate upward scattered field from a single reflector. In both cases, we carry out a derivation under the assumption of a background velocity with two dimensional - c(x,z) - variation; we specialize the results to a constant background velocity and a depth dependent background velocity. For the convenience of the user we have included a glossary and two tables of equation numbers to help in finding specific results. Keywords include: Ray method; Geometrical optics; Wave propagation; Green's function; Jacobian; Travel time; and WKB. GRA

N85-22868# Bolt, Beranek, and Newman, Inc., Cambridge, Mass.
RESEARCH IN CONTINUOUS SPEECH RECOGNITION Final Report, 1 Oct. 1981 - 15 Nov. 1984
R. Schwartz, Y. L. Chow, O. Kimball, M. Krasner, and J. Makhoul Dec. 1984 34 p
(Contract N00014-81-C-0738; ARPA Order 4311)
(AD-A150474; BBN-5799) Avail: NTIS HC A03/MF A01 CSCL 17/2

This final report describes the results of a three-year project in an ongoing basic research effort to develop techniques for the automatic recognition of speech sounds (phonemes) in unrestricted continuous speech. A basic working phonetic recognition system has been designed, implemented on a VAX 11/780, and tested. At over 75% phonetic accuracy, the results have already exceeded previously-published phonetic recognition results on continuous speech for a single speaker. Our future goal will be to increase the recognition accuracy to over 80% for many speakers. GRA

N85-22869# Naval Postgraduate School, Monterey, Calif.
COMPUTER AIDED ANTENNA DESIGN AND FREQUENCY SELECTION FOR HF COMMUNICATIONS M.S. Thesis
W. P. Averill Jun. 1984 174 p
(AD-A150485) Avail: NTIS HC A08/MF A01 CSCL 17/2

Efficient and reliable high frequency skywave communication can be obtained only if wave propagation paths are carefully analyzed and if an antenna which transmits and receives signals along the desired paths can be selected and designed. A micro-computer based program was developed to accomplish this task. GRA

N85-22870# Michigan Univ., Ann Arbor. Coll. of Engineering.
THE POTENTIAL FOR ADVANCED COMPUTERIZED AIDS FOR COMPREHENSIBLE WRITING OF TECHNICAL DOCUMENTS
D. E. Kieras 14 Jan. 1985 35 p
(Contract N00014-81-C-0699)
(AD-A150501; TR-85/ONR-17) Avail: NTIS HC A03/MF A01 CSCL 05/6

It is widely agreed that technical documents for equipment are poorly written and hard to comprehend. This has been a long-standing problem because the information-processing demands of editing and revision are so high that many comprehensibility problems go undetected. However, many of these problems can be detected by computerized systems that scan a document and point out where the writing can be improved. Existing systems of this type are based on conventional writing customs, rather than on the research literature on comprehension, and give poor

advice or miss important problems. They also do not process the input document to any depth. An approach to advanced writing aids is described; such a system would base its criticisms on what is known about the cognition psychology of comprehension, and would make use of techniques from artificial intelligence for processing the language. Some examples of the relevant research results are presented, and a demonstration system of this type is briefly described. GRA

N85-22871# Naval Research Lab., Washington, D. C.
LOW-BIT RATE SPEECH ENCODERS BASED ON LINE-SPECTRUM FREQUENCIES (LSF) Interim Report
G. S. Kang and L. J. Fransen 24 Jan. 1985 62 p
(AD-A150518; NRL-8857) Avail: NTIS HC A04/MF A01 CSCL 17/2

After nearly a dozen years of research and development, the narrowband linear predictive coder (LPC) operating at 2400 bits per second (b/s) has become a practical means to transmit speech at less than 5% of the bit rate of the original digitized speech. The 2400-b/s LPC is expected to be deployed extensively on various military platforms. Recently, however, there has been a growing interest in very-low-data-rate (VLDR) (800 b/s or less) voice communication for certain specialized military communications. Likewise, there is a demand for a voice processor operating at 4800 b/s that outperforms significantly the current 2400-b/s LPC is for operation in less than favorable environments. We present in this report a means for implementing 800- and 4800-b/s voice processors. Both processors use a similar speech synthesis filter in which control parameters are line-spectrum frequencies (LSFs). The LSFs are frequency-domain parameters transformed directly from the prediction coefficients used in the conventional-narrowband LPC. The use of frequency-domain parameters is highly significant because they allow filter coefficient quantization in accordance with properties of auditory perception (i.e., coarser representation of higher frequency components of the speech spectrum). The excitation signal at the 800-b/s rate is similar to that used in the conventional-narrowband LPC. On the other hand, the excitation signal at 4800 b/s is the baseband residual signal. At 800 b/s, speech intelligibility as measured by the diagnostic rhyme test (DRT) is 87 for three male speakers; this is about 1.4 points lower than that of the 2400-b/s LPC. GRA

N85-22872# Naval Research Lab., Washington, D. C. Transmission Technology Branch.
THE USE OF A HIGH-SPEED 12-BIT A/D CONVERTER FOR DIGITAL SAMPLING OF COMMUNICATION SIGNAL CARRIERS Final Report, Oct. 1983 - Aug. 1984
E. L. Althouse, S. Mesias, and D. M. Kopp 31 Dec. 1984 36 p
(AD-A150578; NRL-MR-5518) Avail: NTIS HC A03/MF A01 CSCL 17/2

The use of an A/D converter is considered for digital sampling of modulated waveforms obtained from an antenna. Demodulation is assumed to occur following the digital sampling process, either by using a high speed digital processor or by using a more conventional receiver following reconstruction of the analog waveform by a D/A converter. Since many communication carriers are not conditioned for jam-resistance by coding and spectrum-spreading techniques, a large instantaneous linear dynamic range is necessary to permit the detection and modulation of a small desired signal in the presence of a strong inband interfering signal. Consequently, our interest lies in A/D converters having a large number of quantization bits - a condition that is necessary for large linear dynamic range. The effects of A/D device parameters such as quantization resolution (number of bits), sampling rate, and aperture uncertainty are discussed. A 12-bit A/D converter having an aperture uncertainty of 25 psec and a maximum sampling rate of 5 MHz was used to experimentally determine the magnitude of the spurious-free dynamic range that could be obtained with present off-the-shelf technology. A larger number of quantization bits would have resulted in unacceptably slow speed and an unacceptably low maximum frequency limitation. A smaller number of bits would have yielded a smaller spurious-free dynamic range. Since we did not have a digital processing facility to analyze the A/D directly, a D/A converter, deglitcher (sample-and-hold), and a high quality spectrum analyzer were used to evaluate the A/D performance. Consequently, the results reported are characteristic of the composite A/D-D/A-deglitcher system rather than the A/D alone. GRA

N85-22873# Columbia Univ., New York.
INTEGRATED DIGITAL NETWORKS Final Report, 1 Sep. 1982 - 30 Sep. 1984
Mischa Schwartz, Thomas Stern, and Aurel Lazar 30 Sep. 1984 14 p
(Contract N00014-82-K-0508)
(AD-A150605) Avail: NTIS HC A02/MF A01 CSCL 17/2

The basic problem described in this document is that of transmitting mixtures of traffic of disparate types over a variety of communication networks. Typical examples include the transmission of interactive data, long streams of data (e.g., file transfers), voice, video, and facsimile in an integrated fashion. Network types include local area networks, metropolitan area networks, large geographically-dispersed terrestrial networks, and satellite networks. Ongoing standards work in the C CITT, supported by telephone administrations worldwide, has focused on the concept of Integrated Services Digital Networks (ISDN) toward which worldwide telecommunications will be moving. Computer manufacturers with a great deal of interest in communications (IBM is a prominent example) have begun to devote considerable effort as well to the concept of traffic integration over networks. GRA

N85-22874# California Univ., Livermore. Lawrence Livermore Lab.
NUMERICAL/ELECTROMAGNETICS CODE (NEC)
J. K. Breakall, G. J. Burke, and B. K. Miller 28 Nov. 1984 10 p refs Presented at the Electromagnetics Code Symp., Zurich, 5-7 Mar. 1985
(Contract W-7405-eng-48)
(DE85-004999; UCRL-90560; CONF-850392-1) Avail: NTIS HC A02/MF A01

A hybrid numerical electrodynamics code (NEC) code which uses an Electric Field Integral Equation (EFIE) to model wire-like objects and a Magnet Field Integral Equation (EFIE) to model wire-like objects and a Magnetic Field Integral Equation (MFIE) to model surface-like objects with time harmonic excitation is discussed. A three-term sinusoidal spline basis is employed for the wire current while a pulse basis is used for the surface current, with delta-function weights employed everywhere. Provision is made for connection of wires to surfaces via an attachment, or interpolation, basis. NEC includes a number of features for efficient modeling of antennas and scatterers in their environments. The most recent addition, in the version NEC-3, was the capability of modeling wires that are buried or penetrate the ground-air interface. The current status of NEC-3 and plans for Future NEC are discussed. Some typical results are included. DOE

N85-22875# California Univ., Livermore. Lawrence Livermore Lab.
SURFACE WAVE EXCITATION STUDY
G. J. Burke, R. J. King, and E. K. Miller Sep. 1984 34 p refs
(Contract W-7405-eng-48)
(DE85-005301; UCID-20214) Avail: NTIS HC A03/MF A01

Relative communication efficiency (RCE) as defined by Fenwick and Weeks compares the field of a test antenna to that of a reference antenna at the same location for equal input power to each antenna. Thus, RCE is similar to power gain but is definable in the presence of ground. The effectiveness of antennas in launching TM surface waves was compared. Antennas considered included the vertical dipole, monople on a ground stake, monopole on a radial-wire ground screen, Beverage antenna and vertical half rhombic. Since the performance of these antennas is strongly dependent on parameters such as the number wires in a ground screen or the length of a Beverage antenna, results are presented with parameters varying over a reasonable range. Thus, antenna performance can be weighed against the effort and limitations of construction. DOE

N85-22876# Sandia Labs., Albuquerque, N. Mex. Antenna Development Div.
VARIATIONAL AND MOMENT METHOD SOLUTIONS OF THE FIELDS IN A PARALLEL-PLATE WAVEGUIDE-APERTURE SYSTEM
John M. Jarem Dec. 1984 44 p refs
(DE85-006288; SAND-84-1642) Avail: NTIS HC A03/MF A01
The aperture fields which are excited in a slot aperture in a ground plane when excited by a TEM wave in a parallel-plate waveguide are found by a moment method technique. A variational formulation of the problem is also presented, and its solution is shown to be identical to the moment method solution. A numerical example corresponding to a slot width of a = .375 lambda is solved. The coefficients and aperture admittance of this example are given. Plots of the electric field and evanescent electric field of the system are also given. Author

N85-22505*# TRW Space Technology Labs., Redondo Beach, Calif.
CHARACTERISTICS OF EMI GENERATED BY NEGATIVE METAL-POSITIVE DIELECTRIC VOLTAGE STRESSES DUE TO SPACECRAFT CHARGING
R. C. Chaky and G. T. Inouye *In* NASA. Lewis Research Center Spacecraft Environ. Interactions Technol., 1983 Mar. 1985 p 437-452 refs (For primary document see N85-22470 13-18)
Avail: NTIS HC A99/MF E03 CSCL 20N

N85-22509*# Rome Air Development Center, Hanscom AFB, Mass.
DISCHARGE PULSE PHENOMENOLOGY
Arthur R. Frederickson *In* NASA. Lewis Research Center Spacecraft Environ. Interactions Technol., 1983 Mar. 1985 p 483-509 refs (For primary document see N85-22470 13-18)
Avail: NTIS HC A99/MF E03 CSCL 20N

N85-22908# Joint Publications Research Service, Arlington, Va.
ASSESSMENT OF EFFECTIVENESS OF SIGNAL-CODE CONSTRUCTIONS IN TIME DIVISION-MULTI-ACCESS SATELLITE SYSTEMS Abstract Only
S. L. Portnoy and D. R. Ankudinov *In its* USSR Rept.: Electron. and Elec. Eng. (JPRS-UEE-85-002) 23 Jan. 1985 p 1 Transl. into ENGLISH from Elektrosvyaz (Moscow), no. 5, May 1984 p 11-14 (For primary document see N85-22907 13-33)
Avail: NTIS HC A05/MF A01

N85-22909# Joint Publications Research Service, Arlington, Va.
SATELLITE CHANNELS IN PACKET-SWITCHING NETWORKS Abstract Only
V. A. Gorskiy and M. A. Grigor'eva *In its* USSR Rept.: Electron. and Elec. Eng. (JPRS-UEE-85-002) 23 Jan. 1985 p 2 Transl. into ENGLISH from Elektrosvyaz (Moscow), no. 5, May 1984 p 9-11 (For primary document see N85-22907 13-33)
Avail: NTIS HC A05/MF A01

N85-22910# Joint Publications Research Service, Arlington, Va.
SATELLITE BRIDGES IN COMMUNICATIONS NETWORKS Abstract Only
G. B. Askinazi *In its* USSR Rept.: Electron. and Elec. Eng. (JPRS-UEE-85-002) 23 Jan. 1985 p 2 Transl. into ENGLISH from Elektrosvyaz (Moscow), no. 5, May 1984 p 5-8 (For primary document see N85-22907 13-33)
Avail: NTIS HC A05/MF A01

N85-22911# Joint Publications Research Service, Arlington, Va.
KINETIC RAYLEIGH-TAYLOR INSTABILITY THEORY IN THE IONOSPHERE NEAR EQUATOR Abstract Only
B. N. Gershman and A. N. Shevchenko *In its* USSR Rept.: Electron. and Elec. Eng. (JPRS-UEE-85-002) 23 Jan. 1985 p 3 Transl. into ENGLISH from Izv. Uchebn. Zavedeniy: Radiofiz. (Gorkiy), v. 27, no. 6, Jun. 1984 p 679-684 Original language document was announced in IAA as A84-49001 (For primary document see N85-22907 13-33)
Avail: NTIS HC A05/MF A01

N85-22912# Joint Publications Research Service, Arlington, Va.
EXITATION OF LOW-FREQUENCY RESONANCE WAVES BY MOVING CONDUCTOR IN SPACE PLASMA Abstract Only
B. S. Abramovich and B. Ye. Nemtsov *In its* USSR Rept.: Electron. and Elec. Eng. (JPRS-UEE-85-002) 23 Jan. 1985 p 3 Transl. into ENGLISH from Izv. Vysshikh Uchebn. Zavedeniy: Radiofiz. (Gorkiy), v. 27, no. 6, Jun. 1984 p 685-689 (For primary document see N85-22907 13-33)
Avail: NTIS HC A05/MF A01

N85-22913# Joint Publications Research Service, Arlington, Va.
SCATTERING OF ELECTROMAGNETIC WAVES BY CHARGED PARTICLES Abstract Only
A. A. Lushnikov, V. V. Maksimenko, A. Ya. Simonov, and A. G. Sutugin *In its* USSR Rept.: Electron. and Elec. Eng. (JPRS-UEE-85-002) 23 Jan. 1985 p 6 Transl. into ENGLISH from Izv. Vysshikh Uchebn. Zavedeniy: Radiofiz. (Gorkiy), v. 27, no. 6, Jun. 1984 p 726-733 Original language document was announced in IAA as A84-49006 (For primary document see N85-22907 13-33)
Avail: NTIS HC A05/MF A01

N85-22914# Joint Publications Research Service, Arlington, Va.
DIFFRACTION OF PLANE TM-WAVE ON CONTINUOUSLY IRREGULAR ELLIPTICAL PLASMA Abstract Only
A. V. Moroz *In its* USSR Rept.: Electron. and Elec. Eng. (JPRS-UEE-85-002) 23 Jan. 1985 p 6 Transl. into ENGLISH from Izv. Vysshikh Uchebn. Zavedeniy: Radiofiz. (Gorkiy), v. 27, no. 6, Jun. 1984 p 770-774 Original language document was announced in IAA as A84-49010 (For primary document see N85-22907 13-33)
Avail: NTIS HC A05/MF A01

N85-22915# Joint Publications Research Service, Arlington, Va.
MOVING TARGET DETECTION Abstract Only
V. M Frolushkin and L. Ya. Novoseltsev *In its* USSR Rept.: Electron. and Elec. Eng. (JPRS-UEE-85-002) 23 Jan. 1985 p 5 Transl. into ENGLISH from Izv. Vysshikh Uchebn. Zavedeniy: Radiofiz. (Kiev), v. 27, no. 7, Jul. 1984 p 11-15 Original language document was announced in IAA as A84-44443 (For primary document see N85-22907 (13-33)
Avail: NTIS HC A05/MF A01

N85-22917# Joint Publications Research Service, Arlington, Va.
PROCESSING OF SIGNALS IN EXPERIMENTS WITH SCATTERING OF SHORT RADIO PULSES BY CONDUCTING SPHERE Abstract Only
A. A. Kostylev *In its* USSR Rept.: Electron. and Elec. Eng. (JPRS-UEE-85-002) 23 Jan. 1985 p 6 Transl. into ENGLISH from Radiotekhn. (Moscow), no. 8, Aug. 1984 p 64-66 (For primary document see N85-22907 13-33)
Avail: NTIS HC A05/MF A01

N85-22919# Joint Publications Research Service, Arlington, Va.
COORDINATE DETERMINATION ERRORS IN MEASURING CHARACTERISTICS OF RADIATION FIELD OF AIRBORNE ANTENNAS Abstract Only
E. D. Gazazyan and V. G. Panchenko *In its* USSR Rept.: Electron. and Elec. Eng. (JPRS-UEE-85-002) 23 Jan. 1985 p 7 Transl. into ENGLISH from Izmeritel. Tekhn. (Moscow), no. 9, Sep. 1984 p 54-56 (For primary document see N85-22907 13-33)
Avail: NTIS HC A05/MF A01

N85-22921# Joint Publications Research Service, Arlington, Va.
STEREO DECODER WITHOUT SUBCARRIER RESTORATION Abstract Only
A. Porokhnyuk *In its* USSR Rept.: Electron. and Elec. Eng. (JPRS-UEE-85-002) 23 Jan. 1985 p 12 Transl. into ENGLISH from Radiotekhn. (Moscow), no. 7, Jul. 1984 p 22-24 (For primary document see N85-22907 13-33)
Avail: NTIS HC A05/MF A01

N85-22922# Joint Publications Research Service, Arlington, Va.
ERROR PROBABILITY DURING OPTIMAL NONCOHERENT

RECEPTION OF BINARY SIGNALS IN MULTIBEAM CHANNEL Abstract Only
A. I. Fomin, P. N. Serdyukov, and V. V. Mezhevich *In its* USSR Rept.: Electron. and Elec. Eng. (JPRS-UEE-85-002) 23 Jan. 1985 p 13 Transl. into ENGLISH from Radiotekhn. (Moscow), no. 8, Aug. 1984 p 48-50 (For primary document see N85-22907 13-33)
Avail: NTIS HC A05/MF A01

N85-22923# Joint Publications Research Service, Arlington, Va.
REGULAR SYNTHESIS OF PAIRS OF PHASE-KEYED BINARY MINIMAX SIGNALS Abstract Only
Kh. I. Luchanskaya and V. Ya. Khevrolin *In its* USSR Rept.: Electron. and Elec. Eng. (JPRS-UEE-85-002) 23 Jan. 1985 p 14 Transl. into ENGLISH from Radiotekhn. (Moscow), no. 8, Aug. 1984 p 50-53 (For primary document see N85-22907 13-33)
Avail: NTIS HC A05/MF A01

N85-22924# Joint Publications Research Service, Arlington, Va.
INTERFERENCE IMMUNITY OF FIBER-OPTIC COMMUNICATION LINES WITH SPECTRAL MULTIPLEXING OF CHANNELS Abstract Only
A. Kh. Petrosyan and M. A. Nshanyan *In its* USSR Rept.: Electron. and Elec. Eng. (JPRS-UEE-85-002) 23 Jan. 1985 p 14 Transl. into ENGLISH from Radiotekhn. (Moscow), no. 8, Aug. 1984 p 71-74 (For primary document see N85-22907 13-33)
Avail: NTIS HC A05/MF A01

N85-22926# Joint Publications Research Service, Arlington, Va.
HORIZONTAL DEFLECTION TS-257 Abstract Only
N. Katsnelson and Ye. Shpilman *In its* USSR Rept.: Electron. and Elec. Eng. (JPRS-UEE-85-002) 23 Jan. 1985 p 17 Transl. into ENGLISH from Radiotekhn. (Moscow), no. 9, Sep. 1984 p 24-28 (For primary document see N85-22907 13-33)
Avail: NTIS HC A05/MF A01

N85-22927# Joint Publications Research Service, Arlington, Va.
THEORY OF OPTIMUM M-FILTRATION OF SIGNALS AGAINST BACKGROUND OF CORRELATED INTERFERENCE Abstract Only
V. S. Golikov and N. I. Kravchenko *In its* USSR Rept.: Electron. and Elec. Eng. (JPRS-UEE-85-002) 23 Jan. 1985 p 19 Transl. into ENGLISH from Izv. Vysshikh Uchebn. Zavedeniy: Radioelektron. (Kiev), v. 27, no. 7, Jul. 1984 p 15-19 Original language document was announced in IAA as A84-44444 (For primary document see N85-22907 13-33)
Avail: NTIS HC A05/MF A01

N85-22928# Joint Publications Research Service, Arlington, Va.
DISPERSION OF PHASE-SHIFT KEYED SYSTEMS WITH FIXED NUMBER OF BLOCKS Abstract Only
E. Ye. Mitselmager and R. D. Mukhamedyarov *In its* USSR Rept.: Electron. and Elec. Eng. (JPRS-UEE-85-002) 23 Jan. 1985 p 19 Transl. into ENGLISH from Izv. Vysshikh Uchebn. Zavedeniy: Radioelektron. (Kiev), v. 27, no. 7, Jul. 1984 p 32-36 (For primary document see N85-22907 13-33)
Avail: NTIS HC A05/MF A01

N85-22929# Joint Publications Research Service, Arlington, Va.
NOISE TOLERANCE OF DIGITAL DEMODULATOR FOR COMPLEX SIGNAL SYSTEM EMPLOYING BINARY QUANTIZATION Abstract Only
A. V. Bessalov *In its* USSR Rept.: Electron. and Elec. Eng. (JPRS-UEE-85-002) 23 Jan. 1985 p 20 Transl. into ENGLISH from Izv. Vysshikh Uchebn. Zavedeniy: Radioelektron. (Kiev), v. 27, no. 7, Jul. 1984 p 46-49 (For primary document see N85-22907 13-33)
Avail: NTIS HC A05/MF A01

N85-22930# Joint Publications Research Service, Arlington, Va.
ANALYSIS OF CHARACTERISTICS OF DIGITAL DISCRIMINATORS FOR PHASE-SHIFT KEYED SIGNALS Abstract Only
In its USSR Rept.: Electron. and Elec. Eng. (JPRS-UEE-85-002) 23 Jan. 1985 p 20 Transl. into ENGLISH from Izv. Vysshikh Uchebn. Zavedeniy: Radioelektron. (Kiev), v. 27, no. 7, Jul. 1984 p 49-54 (For primary document see N85-22907 13-33)
Avail: NTIS HC A05/MF A01

N85-22931# Joint Publications Research Service, Arlington, Va.
COMBINED PROCESSING METHOD AND MATCHED FILTER FOR DISCRETE COMPOSITE FREQUENCY PHASE-SHIFT KEYED SIGNAL Abstract Only
V. S. Belyayev *In its* USSR Rept.: Electron. and Elec. Eng. (JPRS-UEE-85-002) 23 Jan. 1985 p 21 Transl. into ENGLISH from Izv. Vysshikh Uchebn. Zavedeniy: Radioelektron. (Kiev), v. 27, no. 7, Jul. 1984 p 61-63 (For primary document see N85-22907 13-33)
Avail: NTIS HC A05/MF A01

N85-22940# Joint Publications Research Service, Arlington, Va.
DYNAMICS OF ADAPTIVE SIGNAL CORRECTOR Abstract Only
A. M. Lazarev and Yu. V. Shevchenko *In its* USSR Rept.: Electron. and Elec. Eng. (JPRS-UEE-85-002) 23 Jan. 1985 p 27 Transl. into ENGLISH from Radiotekhn. (Moscow), no. 8, Aug. 1984 p 40-43 (For primary document see N85-22907 13-33)
Avail: NTIS HC A05/MF A01

N85-22941# Joint Publications Research Service, Arlington, Va.
PERFORMANCE OF TIME-POSITION DISCRIMINATOR OF COMPOSITE SIGNAL Abstract Only
O. F. Bokk, A. M. Savvinov, and G. D. Kolesnichenko *In its* USSR Rept.: Electron. and Elec. Eng. (JPRS-UEE-85-002) 23 Jan. 1985 p 28 Transl. into ENGLISH from Radiotekhn. (Moscow), no. 8, Aug. 1984 p 29-33 (For primary document see N85-22907 13-33)
Avail: NTIS HC A05/MF A01

N85-22942# Joint Publications Research Service, Arlington, Va.
EFFICIENCY OF DIGITAL COMPENSATOR OF STRONG NON-GAUSSIAN INTERFERENCE Abstract Only
V. V. Audeyev, Yu. N. Parshin, and I. A. Minayeva *In its* USSR Rept.: Electron. and Elec. Eng. (JPRS-UEE-85-002) 23 Jan. 1985 p 28 Transl. into ENGLISH from Radiotekhn. (Moscow), no. 8, Aug. 1984 p 33-35 (For primary document see N85-22907 13-33)
Avail: NTIS HC A05/MF A01

N85-22943# Joint Publications Research Service, Arlington, Va.
MATHEMATICAL MODEL OF DISCRIMINATOR FOR SIGNALS WITH FLUCTUATIONS AND THERMAL NOISE Abstract Only
V. B. Binshtok *In its* USSR Rept.: Electron. and Elec. Eng. (JPRS-UEE-85-002) 23 Jan. 1985 p 29 Transl. into ENGLISH from Radiotekhn. (Moscow), no. 8, Aug. 1984 p 13-17 (For primary document see N85-22907 13-33)
Avail: NTIS HC A05/MF A01

N85-22944# Joint Publications Research Service, Arlington, Va.
INTERFERENCE IMMUNITY OF BINARY SYSTEMS WITH SECOND-ORDER PHASE-DIFFERENCE MODULATION IN VARIOUS RECEPTION MODES Abstract Only
Yu. B. Okunev and L. M. Fink *In its* USSR Rept.: Electron. and Elec. Eng. (JPRS-UEE-85-002) 23 Jan. 1985 p 30 Transl. into ENGLISH from Radiotekhn. (Moscow), no. 8, Aug. 1984 p 3-8 (For primary document see N85-22907 13-33)
Avail: NTIS HC A05/MF A01

N85-22945# Joint Publications Research Service, Arlington, Va.
IONOSPHERIC DISTORTIONS OF DIGITAL SIGNALS WITH WIDEBAND MODULATION Abstract Only
I. M. Teplyakov *In its* USSR Rept.: Electron. and Elec. Eng. (JPRS-UEE-85-002) 23 Jan. 1985 p 31 Transl. into ENGLISH from Radiotekhn. (Moscow), no. 8, Aug. 1984 p 8-13 (For primary document see N85-22907 13-33)
Avail: NTIS HC A05/MF A01

N85-22946# Joint Publications Research Service, Arlington, Va.
COMPARATIVE ANALYSIS OF NOISE TOLERANCE OF QUASI-

COHERENT PHASE SHIFT KEYING SIGNAL DEMODULATORS Abstract Only
V. Ye. Martirosov and N. N. Belousov *In its* USSR Rept.: Electron. and Elec. Eng. (JPRS-UEE-85-002) 23 Jan. 1985 p 32 Transl. into ENGLISH from Elektrosvyaz (Moscow), no. 5, May 1984 p 48-50 (For primary document see N85-22907 13-33)
Avail: NTIS HC A05/MF A01

N85-22947# Joint Publications Research Service, Arlington, Va.
OPTIMUM PATH SELECTION IN AUTOMATED RADIO RELAY LINK DESIGN Abstract Only
O. S. Danilovich and V. N. Kichigin *In its* USSR Rept.: Electron. and Elec. Eng. (JPRS-UEE-85-002) 23 Jan. 1985 p 32 Transl. into ENGLISH from Elektrosvyaz (Moscow), no. 5, May 1984 p 15-19 (For primary document see N85-22907 13-33)
Avail: NTIS HC A05/MF A01

N85-22948# Joint Publications Research Service, Arlington, Va.
CALCULATION OF AMPLITUDE-PHASE CHARACTERISTICS OF SIGNAL SCATTERED OBLIQUELY ON METEOR TRAIL Abstract Only
R. G. Khuzyashev *In its* USSR Rept.: Electron. and Elec. Eng. (JPRS-UEE-85-002) 23 Jan. 1985 p 34 Transl. into ENGLISH from Izv. Vysshikh Uchebn. Zavedeniy: Radiofiz. (Gorkiy), v. 27, no. 9, Sep. 1984 p 1110-1115 (For primary document see N85-22907 13-33)
Avail: NTIS HC A05/MF A01

N85-22949# Joint Publications Research Service, Arlington, Va.
DOMAIN OF APPLICABILITY OF ASYMPTOTIC DESCRIPTION OF RADIO PULSE FIELDS NEAR CRITICAL FREQUENCY Abstract Only
Yu. I. Orlov and N. N. Fedorov *In its* USSR Rept.: Electron. and Elec. Eng. (JPRS-UEE-85-002) 23 Jan. 1985 p 34 Transl. into ENGLISH from Izv. Vysshikh Uchebn. Zavedeniy: Radiofiz. (Gorkiy), v. 27, no. 9, Sep. 1984 p 1130-1135 (For primary document see N85-22907 13-33)
Avail: NTIS HC A05/MF A01

N85-22950# Joint Publications Research Service, Arlington, Va.
SPECTRA OF INCIDENTAL INTERFERENCE RESULTING FROM NONLINEAR CONVERSION OF SIGNALS FROM TRANSMITTERS Abstract Only
B. G. Telezhnyy *In its* USSR Rept.: Electron. and Elec. Eng. (JPRS-UEE-85-002) 23 Jan. 1985 p 35 Transl. into ENGLISH from Radiotekhn. (Moscow), no. 8, Aug. 1984 p 46-47 (For primary document see N85-22907 13-33)
Avail: NTIS HC A05/MF A01

N85-22968# Joint Publications Research Service, Arlington, Va.
ABSORPTION OF RADIATION BY WATER VAPOR IN WINDOWS OF RELATIVE TRANSPARENCY OF 95-145 MICROMETER RANGE Abstract Only
B. A. Sverdlov and N. I. Furashov *In its* USSR Rept.: Electron. and Elec. Eng. (JPRS-UEE-85-002) 23 Jan. 1985 p 57-58 Transl. into ENGLISH from Izv. Vysshikh Uchebn. Zavedeniy: Radiofiz. (Gorkiy), v. 27, no. 9, Sep. 1984 p 1087-1095 Original language document was announced in IAA as A85-15026 (For primary document see N85-22907 13-33)
Avail: NTIS HC A05/MF A01

N85-22972# Joint Publications Research Service, Arlington, Va.
THREE-MIRROR OPEN RESONATOR FOR MILLIMETER WAVE BAND Abstract Only
A. A. Vertiy, N. A. Popenko, Yu. P. Popkov, and S. I. Tarapov *In its* USSR Rept.: Electron. and Elec. Eng. (JPRS-UEE-85-002) 23 Jan. 1985 p 61 Transl. into ENGLISH from Izv. Vysshikh Uchebn. Zavedeniy: Rasiofiz. (Gorkiy), v. 27, no. 6, Jun. 1984 p 775-781 (For primary document see N85-22907 13-33)
Avail: NTIS HC A05/MF A01

N85-22977# Joint Publications Research Service, Arlington, Va.
INTERFERENCE FLUX DURING REFLECTION OF HETEROGENEOUS WAVES Abstract Only
K. N. Bakinovskiy, A. I. Kirilenko, and A. D. Titov *In its* USSR Rept.: Electron. and Elect. Eng. (JPRS-UEE-85-001) 9 Jan. 1985 p 1 Transl. into ENGLISH from Izv. Vysshikh Uch. Zaved.: Radiofiz. (USSR), v. 27, no. 7, Jul. 1984 p 948 (For primary document see N85-22976 13-33)
Avail: NTIS HC A05/MF A01

N85-22979# Joint Publications Research Service, Arlington, Va.
AXIAL FOCUSING OF SIGNAL FROM DISTANT POINT RADIATOR REFLECTED TWICE IN DEEP PARABOLOID Abstract Only
M. I. Fayngaold *In its* USSR Rept.: Electron. and Elect. Eng. (JPRS-UEE-85-001) 9 Jan. 1985 p 2 Transl. into ENGLISH from Izv. Vysshikh Uch. Zaved.: Radiofiz. (USSR), v. 27, no. 7, Jul. 1984 p 944-947 (For primary document see N85-22976 13-33)
Avail: NTIS HC A05/MF A01

N85-22980# Joint Publications Research Service, Arlington, Va.
INVESTIGATION OF GENERATION OF OSCILLATIONS USING ANOMALOUS DOPPLER EFFECT Abstract Only
D. V. Gorozhanin, B. I. Ivanov, and M. I. Kapchinskiy *In its* USSR Rept.: Electron. and Elect. Eng. (JPRS-UEE-85-001) 9 Jan. 1985 p 3 Transl. into ENGLISH from Izv. Vysshikh Uch. Zaved.: Radiofiz. (USSR), v. 27, no. 7, Jul. 1984 p 880-891 Original language document announced as A84-48155 (For primary document see N85-22976 13-33)
Avail: NTIS HC A05/MF A01

N85-22983# Joint Publications Research Service, Arlington, Va.
MODELS OF DISCONTINOUS RANDOM FIELDS Abstract Only
V. Y. Kontrovich *In its* USSR Rept.: Electron. and Elect. Eng. (JPRS-UEE-85-001) 9 Jan. 1985 p 4-5 Transl. into ENGLISH from Radiotekh. i Elektron. (USSR), v. 29, no. 8, Aug. 1984 p 1551-1554 (For primary document see N85-22976 13-33)
Avail: NTIS HC A05/MF A01

N85-22984# Joint Publications Research Service, Arlington, Va.
EXPERIMENTAL VERIFICATION OF BEAM DEFLECTION FROM HYBRID REFLECTOR ANTENNA WITHIN WIDE-ANGLE SECTOR Abstract Only
B. Y. Kinber, V. I. Klassen, A. K. Tobolev, and A. V. Shishlov *In its* USSR Rept.: Electron. and Elect. Eng. (JPRS-UEE-85-001) 9 Jan. 1985 p 5 Transl. into ENGLISH from Radiotekh. i Elektron. (USSR), v. 29, no. 8, Aug. 1984 p 1462-1471 (For primary document see N85-22976 13-33)
Avail: NTIS HC A05/MF A01

N85-22985# Joint Publications Research Service, Arlington, Va.
PROBLEM OF DIFFRACTION BY WAVY SURFACE: COMPARISON OF NUMERICAL METHODS OF SOLUTION Abstract Only
L. A. Vaynshteyn and A. I. Sukov *In its* USSR Rept.: Electron. and Elect. Eng. (JPRS-UEE-85-001) 9 Jan. 1985 p 6 Transl. into ENGLISH from Radiotekh. i Elektron. (USSR), v. 29, no. 8, Aug. 1984 p 1472-1478 (For primary document see N85-22976 13-33)
Avail: NTIS HC A05/MF A01

N85-22987# Joint Publications Research Service, Arlington, Va.
SCATTERING OF WAVES BY AXISYMMETRICAL EDGE Abstract Only
V. A. Kaloshin and A. P. Popov *In its* USSR Rept.: Electron. and Elect. Eng. (JPRS-UEE-85-001) 9 Jan. 1985 p 7 Transl. into ENGLISH from Radiotekh. i Elektron. (USSR), v. 29, no. 8, Aug. 1984 p 1502-1509 Original language document announced as 84A-48606 (For primary document see N85-22976 13-33)
Avail: NTIS HC A05/MF A01

N85-22988# Joint Publications Research Service, Arlington, Va.
ERROR IN COMPENSATING PHASE FLUCTUATIONS OF WAVE FIELD BY MEANS OF ADAPTIVE REFLECTORS WITH CONTINUOUS OR COMPOUND SURFACE Abstract Only

V. G. Taranenko *In its* USSR Rept.: Electron. and Elect. Eng. (JPRS-UEE-85-001) 9 Jan. 1985 p 8 Transl. into ENGLISH from Radiotekh. i Elektron. (USSR), v. 29, no. 8, Aug. 1984 p 1510-1515 (For primary document see N85-22976 13-33)
Avail: NTIS HC A05/MF A01

N85-22989# Joint Publications Research Service, Arlington, Va.
ADAPTIVE CONTROL OF AIRBORNE RADAR ANTENNAS Abstract Only
G. S. Zelenkov, A. G. Mikerov, N. D. Polyakhov, V. V. Putov, and A. V. yakovlev *In its* USSR Rept.: Electron. and Elect. Eng. (JPRS-UEE-85-001) 9 Jan. 1985 p 8-9 Transl. into ENGLISH from Izv. Vysshikh Uch. Zaved.: Proborostroyeniye (USSR), v. 27, no. 9, Sep. 1984 p 83-90 Original language document announced as 85A-13784 (For primary document see N85-22976 13-33)
Avail: NTIS HC A05/MF A01

N85-22990# Joint Publications Research Service, Arlington, Va.
SYNTHESIS OF OPTIMUM SINGLE-CHANNEL DISCRETE SIGNALS AND FILTERS Abstract Only
V. M. Koshevoy and A. A. Kononov *In its* USSR Rept.: Electron. and Elect. Eng. (JPRS-UEE-85-001) 9 Jan. 1985 p 9 Transl. into ENGLISH from Izv. Vysshikh Uch. Zaved.: Radioelektron. (USSR), v. 27, no. 8, Aug. 1984 p 62-65 (For primary document see N85-22976 13-33)
Avail: NTIS HC A05/MF A01

N85-22991# Joint Publications Research Service, Arlington, Va.
EFFICIENCY OF MULTITARGET SIGNAL DETECTION BY DIGITAL RADAR DATA PROCESSING DEVICES Abstract Only
V. Y. Plekin and M. M. Lednev *In its* USSR Rept.: Electron. and Elect. Eng. (JPRS-UEE-85-001) 9 Jan. 1985 p 10 Transl. into ENGLISH from Izv. Vysshikh Uch. Zaved.: Radioelektron. (USSR), v. 27, no. 8, Aug. 1984 p 75-78 (For primary document see N85-22976 13-33)
Avail: NTIS HC A05/MF A01

N85-22992# Joint Publications Research Service, Arlington, Va.
SYNTHESIS OF OPTIMUM ALGORITHMS FOR SECONDARY PROCESSING Abstract Only
A. M. Shloma and V. P. Volonkov *In its* USSR Rept.: Electron. and Elect. Eng. (JPRS-UEE-85-001) 9 Jan. 1985 p 10-11 Transl. into ENGLISH from Izv. Vysshikh Uch. Zaved.: Radioelektron. (USSR), v. 27, no. 8, Aug. 1984 p 22-28 Original language document announced as A84-46212 (For primary document see N85-22976 13-33)
Avail: NTIS HC A05/MF A01

N85-22995# Joint Publications Research Service, Arlington, Va.
CORRECTNESS OF REFLECTION CHARACTERISTICS OF RADIO ABSORBENT MATERIALS Abstract Only
M. A. Monin *In its* USSR Rept.: Electron. and Elect. Eng. (JPRS-UEE-85-001) 9 Jan. 1985 p 12 Transl. into ENGLISH from Radiotekh. (USSR), no. 9, Sep. 1984 p 83-84 (For primary document see N85-22976 13-33)
Avail: NTIS HC A05/MF A01

N85-22996# Joint Publications Research Service, Arlington, Va.
SHORT-RANGE RADIOTECHNICAL POINT SENSOR Abstract Only
O. I. Shelukhin, Y. P. Kernov, and V. I. Shelukhin *In its* USSR Rept.: Electron. and Elect. Eng. (JPRS-UEE-85-001) 9 Jan. 1985 p 12 Transl. into ENGLISH from Radiotekh. (USSR), no. 9, Sep. 1984 p 45-47 (For primary document see N85-22976 13-33)
Avail: NTIS HC A05/MF A01

N85-22997# Joint Publications Research Service, Arlington, Va.
FACTORIZED ALGORITHMS FOR COMBINED SPATIAL AND TEMPORAL PROCESSING OF RADAR SIGNALS Abstract Only
V. I. Chaykovskiy *In its* USSR Rept.: Electron. and Elect. Eng. (JPRS-UEE-85-001) 9 Jan. 1985 p 13 Transl. into ENGLISH from Radiotekh. (USSR), no. 9, Sep. 1984 p 40-42 (For primary document see N85-22976 13-33)
Avail: NTIS HC A05/MF A01

N85-22998# Joint Publications Research Service, Arlington, Va.
EXACT DESIGN FORMULAS FOR FIELD INTENSITY OF DIPOLE DEPLOYED ABOVE FLAT HOMOGENEOUS EARTH WITH FINITE CONDUCTIVITY Abstract Only
L. S. Tartakovskiy *In its* USSR Rept.: Electron. and Elect. Eng. (JPRS-UEE-85-001) 9 Jan. 1985 p 13 Transl. into ENGLISH from Radiotekh. (USSR), no. 9, Sep. 1984 p 29-34 (For primary document see N85-22976 13-33)
Avail: NTIS HC A05/MF A01

N85-23005# Joint Publications Research Service, Arlington, Va.
METHODS OF DIGITAL CORRECTION FOR CHANNELS OF MULTICHANNEL RADAR RECEIVERS Abstract Only
Y. I. Abramovich, V. G. Kachur, and V. F. Struchev *In its* USSR Rept.: Electron. and Elect. Eng. (JPRS-UEE-85-001) 9 Jan. 1985 p 25 Transl. into ENGLISH from Radiotekh. i Elektron. (USSR), v. 29, no. 8, Aug. 1984 p 1544-1550 (For primary document see N85-22976 13-33)
Avail: NTIS HC A05/MF A01

N85-23012# Joint Publications Research Service, Arlington, Va.
ASYMPTOTICALLY OPTIMUM MULTIALTERNATIVE SEQUENTIAL PROCEDURES FOR DISCERNMENT OF PROCESSES MINIMIZING AVERAGE LENGTH OF OBSERVATIONS Abstract Only
M. M. Fishman *In its* USSR Rept.: Electron. and Elect. Eng. (JPRS-UEE-85-001) 9 Jan. 1985 p 30 Transl. into ENGLISH from Radiotekh. i Elektron. (USSR), v. 29, no. 8, Aug. 1984 p 1516-1524 (For primary document see N85-22976 13-33)
Avail: NTIS HC A05/MF A01

N85-23013# Joint Publications Research Service, Arlington, Va.
EXTRACTION OF SIGNALS FROM BACKGROUND INTERFERENCE WITH UNKNOWN PARAMETERS IN QUANTIZED SAMPLE Abstract Only
A. N. Dmitriyenko *In its* USSR Rept.: Electron. and Elect. Eng. (JPRS-UEE-85-001) 9 Jan. 1985 p 31 Transl. into ENGLISH from Radiotekh. i Elektron. (USSR), v. 29, no. 8, Aug. 1984 p 1525-1530 (For primary document see N85-22976 13-33)
Avail: NTIS HC A05/MF A01

N85-23014# Joint Publications Research Service, Arlington, Va.
APPLICABILITY OF LOG-NORMAL MODEL TO PROBABILITISTIC DESCRIPTION OF QUASI-PULSE INTERFERENCE Abstract Only
V. D. Rubtsov and A. N. Zaytsev *In its* USSR Rept.: Electron. and Elect. Eng. (JPRS-UEE-85-001) 9 Jan. 1985 p 31-32 Transl. into ENGLISH from Elektron. (USSR), v. 29, no. 8, Aug. 1984 p 1531-1535 (For primary document see N85-22976 13-33)
Avail: NTIS HC A05/MF A01

N85-23015# Joint Publications Research Service, Arlington, Va.
ACCURACY OF APPROXIMATION OF BAYES ESTIMATES IN PRESENCE OF NONINFORMATIVE PARAMETERS Abstract Only
A. P. Trifonov and Y. P. Yenina *In its* USSR Rept.: Electron. and Elect. Eng. (JPRS-UEE-85-001) 9 Jan. 1985 p 32 Transl. into ENGLISH from Radiotekh. i Elektron. (USSR), v. 29, no. 8, Aug. 1984 p 1536-1543 (For primary document see N85-22976 13-33)
Avail: NTIS HC A05/MF A01

N85-23016# Joint Publications Research Service, Arlington, Va.
RECEPTION OF SIGNAL WITH UNKNOWN AMPLITUDE AND DURATION SUBMERGED IN WHITE NOISE Abstract Only
A. P. Trifonov and V. K. Buteyko *In its* USSR Rept.: Electron. and Elect. Eng. (JPRS-UEE-85-001) 9 Jan. 1985 p 35 Transl. into ENGLISH from Izv. Vysshikh Uch. Zaved.: Radioelektron. (USSR), v. 27, no. 8, Aug. 1984 p 28-34 Original language document announced as A84-46213 (For primary document see N85-22976 13-33)
Avail: NTIS HC A05/MF A01

N85-23017# Joint Publications Research Service, Arlington, Va.
USE OF BIGAUSSIAN APPROXIMATION TO DESCRIBE FADING IN SCATTERING COMMUNICATIONS CHANNEL Abstract Only
L. T. Sushkova, Y. Y. Marchenko, and V. V. Bryksin *In its* USSR Rept.: Electron. and Elect. Eng. (JPRS-UEE-85-001) 9 Jan. 1985 p 36 Transl. into ENGLISH from Radiotekh. (USSR), no. 9, Sep. 1984 p 87-88 (For primary document see N85-22976 13-33)
Avail: NTIS HC A05/MF A01

N85-23019# Joint Publications Research Service, Arlington, Va.
COMPUTING CONVOLUTION OF MULTIFREQUENCY SIGNAL EMPLOYING TRUNCATED FAST FOURIER TRANSFORM ALGORITHMS Abstract Only
V. U. Sysoyev *In its* USSR Rept.: Electron. and Elect. Eng. (JPRS-UEE-85-001) 9 Jan. 1985 p 37 Transl. into ENGLISH from Radiotekh. (USSR), no. 9, Sep. 1984 p 53-56 (For primary document see N85-22976 13-33)
Avail: NTIS HC A05/MF A01

N85-23020# Joint Publications Research Service, Arlington, Va.
SYNTHESIS OF QUASI-OPTIMUM ALGORIGTHMS FOR SIGNAL RECOGNITION AGAINST BACKGROUND OF CORRELATED NOISE EMPLOYING DISCRETE SPECTRAL TRANSFORMATIONS Abstract Only
A. I. Rog, A. A. Sirota, E. N. Khkhlov, and V. V. Tukhvatulin *In its* USSR Rept.: Electron. and Elect. Eng. (JPRS-UEE-85-001) 9 Jan. 1985 p 37 Transl. into ENGLISH from Radiotekh. (USSR), no. 9, Sep. 1984 p 58-61 Original language document announced as A85-15756 (For primary document see N85-22976 13-33)
Avail: NTIS HC A05/MF A01

N85-23021# Joint Publications Research Service, Arlington, Va.
PROBABILITY OF DETECTION OF PULSED SIGNALS EMPLOYING ZERO-GATING INTERFERENCE SUPPRESSION Abstract Only
Y. D. Ivanov *In its* USSR Rept.: Electron. and Elect. Eng. (JPRS-UEE-85-001) 9 Jan. 1985 p 38 Transl. into ENGLISH from Radiotekh. (USSR), no. 9, Sep. 1984 p 61-63 (For primary document see N85-22976 13-33)
Avail: NTIS HC A05/MF A01

N85-23023# Joint Publications Research Service, Arlington, Va.
RECEPTION NOISE IMMUNITY OF MULTIPOSITION SIGNALS Abstract Only
V. S. Girshov *In its* USSR Rept.: Electron. and Elect. Eng. (JPRS-UEE-85-001) 9 Jan. 1985 p 39 Transl. into ENGLISH from Radiotekh. (USSR), no. 9, Sep. 1984 p 68-69 (For primary document see N85-22976 13-33)
Avail: NTIS HC A05/MF A01

N85-23024# Joint Publications Research Service, Arlington, Va.
NOISE TOLERANCE OF DIVERSITY RECEPTION IN FREQUENCY-ADAPTIVE DIGITAL TRANSMISSION SYSTEMS Abstract Only
M. Y. Lesman and G. S. Tukh *In its* USSR Rept.: Electron. and Elect. Eng. (JPRS-UEE-85-001) 9 Jan. 1985 p 39-40 Transl. into ENGLISH from Radiotekh. (USSR), no. 9, Sep. 1984 p 35-37 (For primary document see N85-22976 13-33)
Avail: NTIS HC A05/MF A01

N85-23025# Joint Publications Research Service, Arlington, Va.
ANALYSIS OF INTERFERENCE CAUSED BY INTERFERING RADIO SIGNALS IN COMMUNICATIONS SYSTEMS WITH FREQUENCY SEPARATION OF TELEPHONE CHANNELS AND FREQUENCY MODULATION Abstract Only
N. I. Kalashnikov and A. P. Stepanov *In its* USSR Rept.: Electron. and Elect. Eng. (JPRS-UEE-85-001) 9 Jan. 1985 p 40 Transl. into ENGLISH from Izv. Vysshikh Uch. Zaved.: Radioelektron. (USSR), v. 27, no. 9, Sep. 1984 p 61-62 (For primary document see N85-22976 13-33)
Avail: NTIS HC A05/MF A01

N85-23026# Joint Publications Research Service, Arlington, Va.
INVESTIGATION OF INFLUENCE OF COMMUNICATIONS LINK AND SYNCHRONIZATION ERROR ON NOISE TOLERENCE OF GROUP TRANSMISSION OF BINARY INFORMATION BASED ON ORTHOGONAL WALSH FUNCTION Abstract Only
V. A. Vershinin and V. S. Lando *In its* USSR Rept.: Electron. and Elect. Eng. (JPRS-UEE-85-001) 9 Jan. 1985 p 40 Transl. into ENGLISH from Izv. Vysshikh Uch. Zaved.: Radioelektron. (USSR), v. 27, no. 9, Sep. 1984 p 28-32 (For primary document see N85-22976 13-33)
Avail: NTIS HC A05/MF A01

N85-23027# Joint Publications Research Service, Arlington, Va.
APPROXIMATE RULES FOR SIGNAL DETECTION AGAINST BACKGROUND OF GAUSSIAN CORRELATED INTERFERENCE Abstract Only
V. M. Frolushkin *In its* USSR Rept.: Electron. and Elect. Eng. (JPRS-UEE-85-001) 9 Jan. 1985 p 41 Transl. into ENGLISH from Izv. Vysshikh Uch. Zaved.: Radioelektron. (USSR), v. 27, no. 9, Sep. 1984 p 14-19 (For primary document see N85-22976 13-33)
Avail: NTIS HC A05/MF A01

N85-23028# Joint Publications Research Service, Arlington, Va.
USE OF IMPORTANCE SAMPLING TO INVESTIGATE SIGNAL DETECTION SYSTEMS BY SIMULATED METHOD Abstract Only
S. Z. Kuzmin and S. S. Kostina *In its* USSR Rept.: Electron. and Elect. Eng. (JPRS-UEE-85-001) 9 Jan. 1985 p 41-42 Transl. into ENGLISH from Izv. Vysshikh Uch. Zaved.: Radioelektron. (USSR), v 27, no. 9, Sep. 1984 p 8-14 (For primary document see N85-22976 13-33)
Avail: NTIS HC A05/MF A01

N85-23029# Joint Publications Research Service, Arlington, Va.
NOISE IMMUNITY OF INFORMATION TRANSMISSION SYSTEM WITH PSEUDORANDOM FREQUENCY SWITCHING UNDER WORST-CASE INTERFERENCE CONDITIONS Abstract Only
A. M. Chudnov *In its* USSR Rept.: Electron. and Elect. Eng. (JPRS-UEE-85-001) 9 Jan. 1985 p 42 Transl. into ENGLISH from Izv. Vysshikh Uch. Zaved.: Radioelektron. (USSR), v. 27, no. 9, Sep. 1984 p 3-8 (For primary document see N85-22976 13-33)
Avail: NTIS HC A05/MF A01

N85-23130# Joint Publications Research Service, Arlington, Va.
REGIONS OF PROPAGATION OF SHORT-WAVE PERTURBATIONS IN SPHERICAL LAYER OF ROTATING FLUID Abstract Only
G. A. Kivman and N. B. Maslova *In its* USSR Rept.: Earth Sci. (JPRS-UES-85-002) 1 Feb. 1985 p 25-26 Transl. into ENGLISH from Okeanol. (Moscow), v. 24, no. 3, May - Jun. 1984 p 392-397 (For primary document see N85-23116 13-42)
Avail: NTIS HC A07/MF A01

N85-23639*# New Mexico Univ., Albuquerque. Dept. of Geology.
INTRA-ERUPTION GEOLOGIC MAP FROM AN X-BAND RADAR IMAGE DURING THE MAY 18, 1980 ERUPTION OF MOUNT ST. HELENS, WASHINGTON Abstract Only
C. W. Criswell and W. B. Elston *In* NASA, Washington Repts. of Planetary Geol. and Geophys. Program, 1984 Apr. 1985 p 466-469 refs (For primary document see N85-23474 13-91)
Avail: NTIS HC A99/MF A01 CSCL 17I

N85-23640*# Arizona State Univ., Tempe. Dept. of Geology.
RADAR OBSERVATIONS OF FISSURE-FED BASALTIC LAVA FLOWS, CRATERS OF THE MOON, IDAHO Abstract Only
L. Martel and R. Greeley *In* NASA, Washington Repts. of Planetary Geol. and Geophys. Program, 1984 Apr. 1985 p 470 (For primary document see N85-23474 13-91)
Avail: NTIS HC A99/MF A01 CSCL 17I

N85-23642*# Arizona State Univ., Tempe. Dept. of Geology.
ANALYSES OF RADAR IMAGES OF SMALL CRATERS Abstract

Only
R. Greeley, P. R. Christensen, and J. F. McHone *In* NASA, Washington Repts. of Planetary Geol. and Geophys. Program, 1984 Apr. 1985 p 474-475 refs (For primary document see N85-23474 13-91)
Avail: NTIS HC A99/MF A01 CSCL 17I

33 ELECTRONICS AND ELECTRICAL ENGINEERING

Includes test equipment and maintainability; components, e.g., tunnel diodes and transistors; microminiaturization; and integrated circuitry.

For related information see also *60 Computer Operations and Hardware* and *76 Solid-State Physics.*

N85-22877* National Aeronautics and Space Administration. Marshall Space Flight Center, Huntsville, Ala.
POWER CONTROL FOR ac MOTOR Patent
Richard W. Dabney, inventor (to NASA) Issued 18 Dec. 1984 8 p Filed 14 Jun. 1983 Supersedes N83-28329 (21 - 17, p 2743)
(NASA-Case-MFS-25861-1; NAS 1.71:MFS-25861-1; US-Patent-4,489,264; US-Patent-Appl-SN-504345; US-Patent-Class-318-729; US-Patent-Class-318-812) Avail: US Patent and Trademark Office CSCL 09A

A motor controller employing a triac through which power is supplied to a motor is described. The open circuit voltage appearing across the triac controls the operation of a timing circuit. This timing circuit triggers on the triac at a time following turn off which varies inversely as a function of the amplitude of the open circuit voltage of the triac.

Official Gazette of the U.S. Patent and Trademark Office

N85-22878 Princeton Univ., N. J.
APPROACHES AND ALGORITHMS FOR ROBUST SIGNAL PROCESSING Ph.D. Thesis
Charles George Boncelet, Jr. 1984 167 p
Avail: Univ. Microfilms Order No. DA-8428320

The development of approaches and algorithms for robust signal processing are discussed. Robust signal processing, refers to the problem of smoothing, filtering or estimating noisy and unknown signals. The linear estimation problem in the formalism of linear regression is considered. The specific problem of filtering or smoothing a discrete time sequence is considered and a new method is proposed. This method is compared to more traditional methods in a Monte Carlo study. A new algorithm is presented which called the ABC algorithm, to compute a variant of the Huber regression estimate. An extensive Monte Carlo study of the corresponding location estimate is presented. The ABC algorithm is a partitioning algorithm and allows for exact computations. Its important theoretical consequences for linear programming are discussed. The problem of calculating the densities of order statistics and statistics derived from them is considered. A new algorithm is presented which allows the random variables to be nonidentically distributed. Dissert. Abstr.

N85-22879 Florida Univ., Gainesville.
DRIFT FIELDS AND BOUNDARY CONDITIONS AT GRAIN BOUNDARIES IN BIPOLAR P/N JUNCTION SILICON DEVICES Ph.D. Thesis
Yueh-Hsin Chen 1984 106 p
Avail: Univ. Microfilms Order No. DA-8429195

An analytical treatment is presented of drift-field solar cells and more generally of bipolar p/n junction devicies containing a built-in drift field. Design implications are discussed quantitatively for a thin drift-field Si p/n(x) junction solar cell. Experimental data on the performance of non-optimal drift-field solar cells and discussions on determination of critical parameters such as minority-carrier lifetime by several different methods are also included. Efforts are made toward solving the current-voltage characteristics of a semiconductor filament in the steady state excited by a time-independent and space-inite surface recombination velocity (zero excess carrier density) on the lateral surfaces is developed. It is demonstrated that the exact solution for total current crossing the injecting face diverges. Author

N85-22880 Florida Univ., Gainesville.
OPTIMUM DESIGN OF ELECTRICAL MOTORS FOR MULTILINK MANIPULATORS AND AUTOMATED MANUFACTURING SYSTEMS Ph.D. Thesis
Taein Choi 1984 220 p
Avail: Univ. Microfilms Order No. DA8429196

The problem of finding the optimum design of electric motors used as actuators in robotic manipulators and in manufacturing machines is addressed. The optimization may provide a minimum time of operation and/or minimum losses of energy for the actuator. The development of design technologies is reviewed, yielding a recommendation for a hierarchical procedure for motor design using small computers. Information from the catalogues of 1800 motors was organized into a computer database, MOTOR-USA. Analysis of the database shows that the DC PM motor has the best performance characteristics among all types of motors. The design of a generalized electric motor is formulated using a doubly excited magnetic field system. The generalized examples of transformer and synchronous motor designs lead to an important result: there exists an optimum machine configuration which remains unchanged when the power of the motor is changed over a broad range.

Dissert. Abstr.

N85-22881 Texas Technological Univ., Lubbock.
REPETITIVE ENERGY TRANSFERS FROM AN INDUCTIVE ENERGY STORE Ph.D. Thesis
Emanuel Marvin Honig 1984 177 p
Avail: Univ. Microfilms Order No. DA8427984

By producing a pulse train with a peak power of 75 MW at a pulse repetition rate of 5 kpps in a one-ohm load system, the fully-controlled, high-power, high-repetition-rate operation of an inductive energy storage and transfer system with survivable switches was demonstrated. Triggered vacuum gap switches were used as repetitive, current-zero opening switches and several repetitive transfer circuits using the counterpulse technique were developed. The switching and transfer process is analyzed and the dependency of the output pulse risetime on specific load conditions is determined. Repetitive railgun operation was enabled (in theory) by developing transfer circuits capable of recovering the energy remaining in the load inductance after each output pulse. Dissert. Abstr.

N85-22882 California Univ., Los Angeles.
A GENERALIZED SOLUTION TO A CLASS OF PRINTED CIRCUIT ANTENNAS Ph.D. Thesis
Pisti B. Katehi-Tseregounis 1984 132 p
Avail: Univ. Microfilms Order No. DA8428527

The theory and design of antennas excited by a microstrip transmission line or by a gap generator are examined. The antennas and the strip transmission line may be embedded inside or printed on the substrate. A theortical approach is implemented which accounts accurately for the physical effects involved including surface waves. The Green's function was obtained by synthesizing the fields of Hertzian dipoles which are oriented in arbitrary directions and which are printed on or embedded in the substrate. The method of solution is based on solving the Pocklington integral equation by employing the method of moments with proper choice of expansion and testing functions. The excitation mechanism is taken into account effectively by considering it as part of the antenna. The current distribution is obtained both on the transmission line and the printed antennas by matrix inversion. The method accounts for conductor thickness and for arbitrary substrate parameters. As an example, printed strip dipoles excited by a transmission line embedded in the substrate or by a voltage gap generator are considered. Dissert. Abstr.

N85-22883 California Univ., Berkeley.
ADVANCED MIXED-MODE SIMULATION TECHNIQUES Ph.D. Thesis
James Ellis Kleckner 1984 195 p
Avail: Univ. Microfilms Order No. DA-8427016

The increasing complexity of integrated circuits has resulted in higher costs for the simulation of those circuits. As a result, designers resort to abstract models to describe the circuit behavior that are less expensive to evaluate than detailed models. This leads to the problem of verifying that the abstract models are coinsistent with the detailed models by replace. Mixed-mode simulators were developed which allow the use of abstract and detailed models in the same simulation program, providing faster simulation speeds and the ability to verify the consistency of the abstract and detailed models. Advanced algorithms and techniques for mixed-mode simulations are presented. Mixed-mode simulation was extended to allow simultaneous simulation of models at the detailed electrical, logic, and register-transfer levels i.e., those levels that can be represented by schematic diagrams. Mixed-mode simulation of widely differing models can be performed using a program architecture that facilitates the addition of new simulation levels without sacrificing either simulation speed or accuracy.
Dissert. Abstr.

N85-22884 California Univ., Los Angeles.
INVESTIGATIONS OF THE HIGH FREQUENCY PERFORMANCE OF IMPACT AVALANCHE TRANSIT-TIME DIODES Ph.D. Thesis
Nelson Shen-Tsai Lee 1984 172 p
Avail: Univ. Microfilms Order No. DA8428538

The high frequency performance of impact avalanche transit time (IMPATT) diodes is investigated. Theoretical studies of the IMPATT performance were made by simulating the operation of the device numerically. Simulations were made of the IMPATTs operating at 100 to 400 GHz. GaAs abrupt structure diodes were found to operate up to 400 GHz, which extends the upper frequency limit of 200 GHz for GaAs devices established previously. Above 200 GHz, the efficiencies of the IMPATTs fall below one percent. Diffusion and distributed generation effects degrade the efficiency of the diodes as the frequency of operation is increased. The generation of carriers becomes less localized in millimeter frequency diodes as the ionization coefficient becomes saturated. Read-type structure IMPATTs are not able to operate above 200 GHz because the generation region in those devices is too narrow for adequate avalanching current. Diffusion effects cause the carrier pulse to spread as it drifts across the device. Diffusion current at the boundary of the active region of the IMPATT causes the carriers to diffuse in and out of the active layer. Heterostructure IMPATTs were shown to have higher efficiencies than comparable conventional structures. Dissert. Abstr.

N85-22885*# National Aeronautics and Space Administration. Langley Research Center, Hampton, Va.
ELECTROSTATIC FORMING AND TESTING OF POLYMER FILMS ON A 16-FOOT DIAMETER TEST FIXTURE
John W. Goslee, William F. Hinson, and William T. Davis Feb. 1985 34 p refs
(NASA-TM-86328; NAS 1.15:86328) Avail: NTIS HC A03/MF A01 CSCL 09A

The large space systems technology program investigated different forms of large, lightweight, deployable structures which could be carried on the Space Shuttle. Different forms and concepts of antennas as a type of large space system were investigated. The electrostatically controlled membrane reflector made of metallized material concept was chosen. The concept is a good candidate for creating an antenna with high surface quality and has the ability to be packaged and deployed from the Shuttle with a significant reduction in weight compared to other antenna types. E.A.K.

N85-22886*# Jet Propulsion Lab., California Inst. of Tech., Pasadena.
PERIODIC BINARY SEQUENCE GENERATORS: VLSI CIRCUITS CONSIDERATIONS
M. Perlman Dec. 1984 200 p refs
(Contract NAS7-918)
(NASA-CR-175649; JPL-Pub-85-7; NAS 1.26:175649) Avail: NTIS HC A09/MF A01 CSCL 09C

Feedback shift registers are efficient periodic binary sequence generators. Polynomials of degree r over a Galois field characteristic 2(GF(2)) characterize the behavior of shift registers with linear logic feedback. The algorithmic determination of the trinomial of lowest degree, when it exists, that contains a given irreducible polynomial over GF(2) as a factor is presented. This corresponds to embedding the behavior of an r-stage shift register with linear logic feedback into that of an n-stage shift register with a single two-input modulo 2 summer (i.e., Exclusive-OR gate) in its feedback. This leads to Very Large Scale Integrated (VLSI) circuit architecture of maximal regularity (i.e., identical cells) with intercell communications serialized to a maximal degree. Author

N85-22887# California Univ., Livermore. Lawrence Livermore Lab. Electronics Engineering Dept.
ELECTRONICS ENGINEERING DEPARTMENT EE TECHNICAL REVIEW
Apr. 1984 33 p refs
(Contract W-7405-eng-48)
(UCRL-50025-84-1) Avail: NTIS HC A03/MF A01

Progress in electronic engineering is reported. Topics discussed include: motion control system for the large optics diamond turning machine, a rotating turbine camera controller that extends capability and improves reliability, the ring seating system, and the LGF data acquisition system. E.A.K.

N85-22888# University Coll., Cork (Ireland). Microelectronics Research Center.
LOW CAPACITANCE E-BEAM FABRICATED BEAM-LEAD SCHOTTKY BARRIER DIODES
U. S. Lidholm and G. T. Wrixon Nov. 1984 39 p
(Contract DAJA37-81-C-0261)
(AD-A150238; TR-3) Avail: NTIS HC A03/MF A01 CSCL 09/3

A unique method has been proposed in earlier reports for fabricating low capacitance beam-lead diodes for use in millimeter and sub-millimeter integrated circuits. This consists in millimeter integrated circuits. This consists in removing all the GaAs material except from a small region (20 micrometers in diameter) in the immediate location of the actual Schottky contact. This will have the effect of drastically reducing the beam overlay capacitance leading to a device whose capacitance is dominated by the junction capacitance. This will therefore not suffer the conversion loss degradation observed in conventional beam-lead devices at frequencies greater than about 100GHz. In this report the major processing steps necessary to fabricate the diode are described in detail. There were developed on bulk GaAs. GRA

N85-22889# Army Missile Command, Redstone Arsenal, Ala. Research Directorate.
ACOUSTO-OPTICALLY ADDRESSED FOURIER TRANSFORM MATCHED FILTERS
D. A. Gregory and L. L. Huckabee Aug. 1984 24 p
(AD-A150298; AD-E950657; AMSMI/RR-84-8-TR) Avail: NTIS HC A02/MF A01 CSCL 09/1

Matched filters made using the Vander Lugt technique are addressed using an acousto-optic beam deflector with good correlation signals resulting. This method may be used to address arrays of matched filters at high scan rates thus providing the large optical memory necessary for absolute object recognition and discrimination in a variety of applications. Author (GRA)

N85-22890# Random Applications, Inc., Montrose, Colo.
ON FILTER BINARY PROCESSES
R. F. Pawula and S. O. Rice Nov. 1984 40 p
(Contract F49620-83-C-0085)
(AD-A150328; AFOSR-85-0055TR) Avail: NTIS HC A03/MF A01 CSCL 20/3

The problem of calculating the probability density function of

the output of an RC filter driven by a binary random process with intervals generated by an equilibrium renewal process is studied. New integral equations, closely related to McFadden's original integral equations, are derived, and solved by a matrix approximation method and by iteration. Transformations of the integral equations into differential equations are being investigated. Some numerical results which compare the matrix and iteration solutions with both exact solutions and approximate solutions based upon the Fokker-Planck equation are presented. GRA

N85-22891# Martin Marietta Aerospace, Denver, Colo.
EOS (ELECTRICAL OVERSTRESS) PROTECTION FOR VLSI (VERY LARGE SCALE INTEGRATION) DEVICES Final Report, Jun. 1982 - Mar. 1984
D. D. Wilson, W. E. Echols, and M. G. Rossi Griffiss AFB, N.Y. RADC Sep. 1984 284 p
(Contract F30602-82-C-0111)
(AD-A150333; MCR-84-506; RADC-TR-84-183) Avail: NTIS HC A13/MF A01 CSCL 09/1

Many of the major semiconductor manufacturers have published the results of their own in-house design evaluations of new electrostatic discharge (ESD) protection networks. Several major users have published test and evaluation results on the ESD protection networks used on a wide cross-section of popular device types available today. The present work was undertaken to expand that data base and to compare the failure mechanisms which occur in devices subjected to both the human body and the charged device ESD simulation tests. The conclusions of this report are similar to those other workers. Failure mechanisms induced with the human body model are primarily electrothermal junction shorting, often associated with aluminum/silicon contacts near the bonding pads (an interlevel polysilicon layer placed between the aluminum and silicon in such contacts significantly raises the failure threshold). Layout mistakes such as closer spacing of protective network components to other junctions can cause significantly lowered failure thresholds for a pin. Interlayer oxide shorts were found to occur in some networks. The charged device test induced failures at much lower voltages but the failure mechanisms were similar in the best protective networks. In almost every case there were easily recognized reasons for increased sensitivity on one or more pins which could be fixed by minor layout changes. GRA

N85-22892# BDM Corp., Albuquerque, N. Mex.
ELECTRICAL OVERSTRESS PROTECTION OF SUBMICRON DEVICES Final Report, Sep. 1982 - Feb. 1984
R. J. Antinone and P. A. Young Griffiss AFB, N.Y. RADC Sep. 1984 139 p
(Contract F30602-82-C-0110)
(AD-A150334; BDM/A-84-114-TR-R1; RADC-TR-84-179) Avail: NTIS HC A07/MF A01 CSCL 09/1

The objective of this program was to further define the electrical overstress (EOS) sensitivity characterization procedures for microelectric devices and to investigate the EOS sensitivity of micron and submicron linewidth circuit structures. Another objective was to investigate improved EOS protection schemes and evaluate their benefits versus performance and cost penalties. The approach chosen to achieve these objectives was to attempt to design input protection networks which would protect an MOS device fabricated from a submicron process from an electrostatic discharge (ESD) threat. The program included the definition of ESD threats, examination of the characteristics of existing input protection networks, a study of the factors which limit the effectiveness of protection networks, and consideration of alternate approaches to achieve ESD hardness. The limiting factors which are expected to determine the electrical overstress sensitivity of micron and submicron design rule microcircuit technologies were investigated using computer-aided modeling techiques. Network analysis codes were used to exercise lumped circuit analogs of the electrical and thermal properties of the devices under study when subjected to ESD stress. Simple time domain network analysis codes suitable for microcomputers were used and are discussed in the report. The minimum cross-sectional areas of aluminum and polysilicon interconnects and semiconductor devices which are capable of withstanding an ESD event were established. Two candidate submicron technologies were considered in this study, CMOS and NMOS. GRA

N85-22893# Tracor, Inc., Austin, Tex.
EXTERNALLY COMPENSATED CRYSTAL OSCILLATOR (ECXO) STUDY Final Report, Jun. 1981 - Dec. 1983
O. J. Baltzer and C. S. Stone Griffiss AFB, N.Y. RADC Jul. 1984 69 p
(Contract F19628-81-C-0087)
(AD-A150335; TRACOR-T84-AE-9124U; RADC-TR-84-166) Avail: NTIS HC A04/MF A01 CSCL 09/5

The primary objective of this contract was an investigation and exploratory development of an externally compensated crystal oscillator (EXCO) in which frequency-temperature compensation of the C-mode frequency of an SC-cut quartz crystal is achieved by utilizing the concurrent B-mode frequency as a highly sensitive digital temperature sensor. The digitized B-mode output, used in conjunction with a microcomputer and a stored frequency/temperature look-up table or a suitable compensation algorithm, is able to provide precise and accurate clock corrections over a much wider range than that possible with a conventional TCXO oscillator (a temperature compensated oscillator which employs a voltage-variable capacitor for direct oscillator frequency control). GRA

N85-22894# Air Force Weapons Lab., Kirtland AFB, N. Mex.
SEM (SCANNING ELECTRON MICROSCOPE) INVESTIGATION OF SILICON DIODES USING THE ELECTRON BEAM INDUCED CURRENT METHOD Final Report
M. E. Snyder Dec. 1984 97 p
(AF Proj. ILI-R)
(AD-A150356; AFWL-TR-84-13) Avail: NTIS HC A05/MF A01 CSCL 09/1

Semiconductor device failure due to an electrical overstress is a primary concern in the nuclear hardening of strategic weapon systems. To acquire the postmortem knowledge necessary to determine the device failure mode, a reliable diagnostic basis in semiconductor physics is necessary. Efforts to achieve a comprehensive understanding of device failure have been hampered by a lack of adequate diagnostic tools and methods of study. This project's primary goal is to develop an experimental tool to study device failure, incorporating the scanning electron microscope (SEM) operated in the electron beam induced current(EBIC) mode. This technique, in conjunction with secondary electron imaging, will provide researchers with a diagnostic tool to qualitatively study the type of failure that occurs in semiconductor devices. Although SEM operation in the EBIC mode has been recognized as an excellent diagnostic tool for device investigators, the Air Force Weapons Laboratory (AFWL) does not possess this basic expertise. The addition of this tool will augment many aspects of ongoing research at the AFWL. To demonstrate the utility of EBIC, this effort will use EBIC and simple auxiliary measurements to determine the failure states of a twin set of specially designed semiconductor diodes. GRA

N85-22895# California Univ., Santa Barbara. Dept. of Electrical and Computer Engineering.
DEVELOPMENT OF A PLANAR HETEROJUNCTION BIPOLAR TRANSISTOR FOR VERY HIGH SPEED LOGIC Annual Technical Report, 1 Oct. 1983 - 30 Sep. 1984
S. I. Long 21 Nov. 1984 51 p
(Grant AF-AFOSR-0344-82)
(AD-A150374; AFOSR-84-1236TR; ATR-2) Avail: NTIS HC A04/MF A01 CSCL 09/1

The objective of this research project is to develop heterostructure bipolar transistors for very-high-speed logic. During the second year of effort, significant progress was made on (Al,Ga)As/GaAs HBTs of both emitter-down and emitter-up configurations, with current gains of 10 or greater being observed in both cases for base dopings which exceed emitter dopings. Structural modifications were evaluated which led to increased injection and reduced

recombination currents. Annealing systems were constructed and characterized for activation of Be ion-implantations. Promising initial studies of (In,Ga)P/GaAs HBTs has led to their inclusion in this research project for the third year of effort. GRA

N85-22896# Cornell Univ., Ithaca, N.Y.
PRE- AND POST-PROCESSING FOR STREAM-FUNCTION EDDY CURRENT CALCULATIONS
J. F. Abel, F. C. Moon, and T. J. McCoy Dec. 1984 11 p
(Contract N00014-79-C-0224)
(AD-A150417; TR-84-13) Avail: NTIS HC A02/MF A01 CSCL 20/3

A stream function or vector potential for the current density vector has been used to develop a finite element code called EDDY2 for calculating induced currents in thin conducting plates for steady-state harmonic external fields. While two-dimensional, the code includes self-field effects for harmonic fields for skin depths on the order of the plate thickness and larger. The input to this FORTRAN program includes the geometry and properties of the plate, the boundary conditions, and a description of the external magnetic field; this information must all be expressed in terms of the nodes and elements of the computational mesh devised by the analyst. The program produces values of the stream function of the nodes and, at sampling points interior to each element, values of the eddy current, the temperature induced in a half cycle of the current, and the time-averaged magnetic pressure. Although this program has proven to be computationally effective, as with all finite element programs, a significant amount of effort is consumed by the preparation of error-free input data and the reduction and presentation of the analysis results. To expedite the consideration of a large number of configurations in research or design, interactive graphics techniques can be used. Two programs are explained and demonstrated through an example problem which is part of a study of power dissipation in plates as a function of plate geometry. The particular configuration chosen for this example is a rectangular plate with opposite semicircular notches at the center of the long sides. GRA

N85-22897# Clarkson Coll. of Technology, Potsdam, N.Y. Dept. of Electrical and Computer Engineering.
CONTROL OF CASCADED INDUCTION GENERATOR SYSTEMS Final Technical Report, 1 Sep. 1983 - 30 Aug. 1984
T. H. Ortmeyer 13 Dec. 1984 63 p
(Grant AF-AFOSR-0268-83)
(AD-A150429; AFOSR-84-1259TR) Avail: NTIS HC A04/MF A01 CSCL 10/2

This report documents an investigation of the stability and control of cascaded doubly fed machines (CDFM). These machines are brushless variable speed constant frequency electric power generators with potential for application in aircraft. A previous analytical study indicated the CDFM system would be controllable in the subsynchronous operating mode with a passive RL load. The present study contains two steps. First is an investigation of the machine operation in the supersynchronous mode. The second step is an investigation of machine operation with output capacitors providing excitation VARs for the machine and load. Step 1 results show that the machines exhibit stability characteristics in the supersynchronous mode similar to those observed in the subsynchronous mode. Step 2 results show that output capacitors degrade the system performance, particularly at light loads. The results show that output current feedback can be employed to improve the system performance. GRA

N85-22898# North Carolina Univ., Chapel Hill. Operations Research and Systems Analysis.
A MONTE CARLO SAMPLING PLAN FOR ESTIMATING NETWORK RELIABILITY
G. S. Fishman Oct. 1984 49 p
(Grant AF-AFOSR-0140-84)
(AD-A150511; UNC/ORSA/TR-84/8; AFOSR-85-0046TR) Avail: NTIS HC A03/MF A01 CSCL 09/3

This paper presents a relatively complete and comprehensive description of a general class of Monte Carlo sampling plans for estimating g = g(s,T), the probability that s is connected to all nodes in T. The paper also provides procedures for implementing these plans. Each plan uses known lower and upper bounds B,A on g to produce an estimator of g that has a smaller variance (A-g)(g-B)/K than one obtains for crude Monte Carlo sampling (B=0, A=1) on K independent replications. The paper describes worst case bounds on sample sizes K, in terms of B and A, for meeting absolute and relative error criteria. It also gives the worst case bound on the amount of variance reduction that can be expected when compared with crude Monte Carlo sampling. An example illustrates the variance reductions achievable with these plans. The paper next shows how to assess the credibility that a specified error criterion for g is met as the Monte Carlo experiment progresses and then shows how confidence intervals can be computed for g. GRA

N85-22899# Georgia Inst. of Tech., Atlanta. School of Electrical Engineering.
TWO-DIMENSIONAL SIGNAL PROCESSING AND STORAGE AND THEORY AND APPLICATIONS OF ELECTROMAGNETIC MEASUREMENTS Annual Report, 1 Apr. - 31 Dec. 1984
R. W. Schafer and D. T. Paris 1 Jan. 1985 26 p
(Contract DAAG29-84-K-0024)
(AD-A150590) Avail: NTIS HC A03/MF A01 CSCL 09/3

This is an annual report on research conducted under the auspices of the Joint Services Electronics Program. Specific topics covered are: digital signal processing, parallel processing architectures, two-dimensional optical storage and processing, hybrid optical/digital signal processing, electromagnetic measurements in the time domain, and automatic radiation measurements for near-field and far-field transformations. GRA

N85-22900# Westinghouse Electric Corp., Pittsburgh, Pa. Research and Development Center.
RELUCTANCE AND DOUBLY-EXCITED RELUCTANCE MOTORS
C. J. Heyne and A. M. El-Antably Nov. 1984 153 p refs
(Contract DE-AC05-84OR-21400)
(DE85-003585; ORNL/Sub-81-95013/1) Avail: NTIS HC A08/MF A01

Since the energy crisis in 1974, there was increasing awareness of conserving energy. Industrial ac motors from 1 to 125 hp are estimated to consume 60% of the total electricity produced in the United States. Significant energy conservation could be achieved if the efficiency of these motors is improved. The work described was sponsored by the Division of Electric Energy Systems (EES) of the United States Department of Energy (DOE) through a subcontract with the Power Systems Technology Program at the Oak Ridge National Laboratory (Oak Ridge, Tennessee, USA). The design, analysis, and test of two types of motors designed to have a high efficiency and power factor are described. The first type, reluctance motors (RMs), are similar to synchronous motors but without dc excitation. A novel 3-phase RM was designed and tested, and it was found to have superior efficiency when compared with a similar induction motor. DOE

N85-22901# Los Alamos Scientific Lab., N. Mex.
PORTABLE ELECTROCHEMICAL CELL INTERROGATOR
James D. Doss and Charles W. McCabe Nov. 1984 8 p refs
(Contract W-7405-eng-36)
(DE85-005186; LA-10274-MS) Avail: NTIS HC A02/MF A01

A portable electronic instrument for interrogating electrochemical cells is described. The instrument is powered by a 9-V battery and has an LCD digital readout. It can read out any instrument that has electrochemical cells that increase in impedance upon deplating. DOE

N85-22902# Sandia Labs., Albuquerque, N. Mex.
HIGH SHEET RESISTANCE, ARSENIC IMPLANTED POLYCRYSTALLINE SILICON FOR INTEGRATED CIRCUIT RESISTORS
W. K. Schubert Nov. 1984 35 p refs
(Contract DE-AC04-76DP-00789)

(DE85-004355; SAND-84-2022) Avail: NTIS HC A03/MF A01

The electrical properties of high sheet resistance polycrystalline silicon were investigated to facilitate its use in fabricating integrated circuit resistors. The effects of ion implantation dose, energy and annealing procedures were studied. Sheet resistances ranging from 10(2) to 10(9) omega/square were produced. A double depletion layer, thermionic emission model for electrical transport across grain boundaries accounts for many of the electrical properties, including the correlation of high activation energies with high sheet resistances. A reverse annealing peak in the sheet resistance is found for annealing temperatures between 900 and 1100 C. This irreversible effect is stronger in more lightly doped samples. The final sheet resistance value is primarily determined by the implantation dose and the highest processing temperature used. DOE

N85-22903# General Electric Co., Schenectady, N. Y.
THE FERRITE PERMANENT MAGNET AC MOTOR: A TECHNICAL AND ECONOMICAL ASSESSMENT
E. Richter, T. J. E. Miller, T. W. Newmann, and T. L. Hudson (ORNL) 1984 7 p refs Presented at conf.
(Contract DE-AC05-84OR-21400)
(DE85-002480; CONF-8409108-6) Avail: NTIS HC A02/MF A01

The design and analysis study for the conceptual design of an economical high efficiency ac motor based on permanent magnets is summarized. Material considerations, design trade-off options and transient and steady state performance under normal and abnormal conditions were considered. The baseline comparison is the high efficiency induction motor. The permanent magnet (PM) motor must fit into the same frame size and surpass the induction motor on a life cost basis that includes 2.5 years of operation at a 50% duty cycle. It is indicated that a motor with ferrite magnets meets the objectives of the program in ratings of up to 25 hp. A 7.5 hp motor design is carried through the conceptual design stage. E.A.K.

N85-22904# Varian Associates, Palo Alto, Calif.
DESIGN CONSIDERATIONS FOR A 100 Kw CW, 140 GHz GYROTRON OSCILLATOR
K. Felch, R. Bier, L. Fox, H. Huey, L. Ives, H. Jory, and S. Spang 1984 5 p refs Presented at conf.
(Contract DE-AC05-84OR-21400)
(DE85-005282; CONF-841234-6) Avail: NTIS HC A02/MF A01

A gyrotron oscillator capable of generating 100 kW of CW power is currently under development. The tube is being designed for operation in the TE sub O31 cavity mode with the electron beam located at the second radial electric field maximum in the cavity. The electron beam will be produced by a magnetron injection gun and the 56 kG magnetic field required for 140 GHz operation will be provided by a superconducting magnet. Initial design calculations for the important elements of the tube are reported and the various technology issues of the tube design are discussed. Author

N85-22905# Varian Associates, Palo Alto, Calif.
A 60 GHz 200 kW CW GYROTRON WITH HIGH OUTPUT MODE PURITY
H. Jory, K. Felch, R. Bier, L. Fox, H. Huey, L. Ives, N. Lopez, J. Manca, J. Shively, and S. Spang 1984 4 p refs Presented at conf.
(Contract DE-AC05-84OR-21400)
(DE85-005283; CONF-841234-4) Avail: NTIS HC A04/MF A01

For the first-time, a Varian 60 GHz gyrotron, designed specifically to generate microwaves in a single output mode, was operated at power levels up to 200 kW CW. High output mode purity is required for the efficicent utilization of gyrotrons as high power microwave sources for electron cyclotron resonance heating (ECRH) in magnetic fusion plasmas. Using mode-specific directional couplers, measurements of the output made content indicated that greater than 95% of the microwave output was in the desired TE sub O2 mode, with only small percentages in the neighboring TE sub O1 and TE sub O3 circular electric fields. The pure mode CW design uses a 2.5-inch diameter collector. The collector has a magnetic field arrangement which capably avoids excessive heating by distributing the 640 KW CW beam over a sufficient collector area. With pure mode operation, window temperatures are 10 c to 15 c higher than with mixed mode operation. Author

N85-22906# National Bureau of Standards, Boulder, Colo.
CRITICAL CURRENT MEASUREMENTS ON AN NbTi SUPERCONDUCTING WIRE STANDARD REFERENCE MATERIAL Final Report
L. F. Goodrich, D. A. Vecchia, E. S. Pittman, J. W. Ekin, and A. F. Clark Sep. 1984 70 p
(PB85-118594; NBS/SP-260/91; LC-84-601108) Avail: NTIS HC A04/MF A01; also available SOD HC as SN003-003-02614-0 CSCL 09A

Procedures for preparing and measuring five candidate conductors are described. Evaluation criteria are discussed by which one of the five conductors was selected for the critical current SRM. The designated superconducting wire, SRM 1457, was subdivided and wound onto 500 spools for distribution. Certified critical current measurements were made on a sample of these spools. Material variability, or inhomogeneity, along the whole wire is included in a statistical model based on the dependence of critical current on temperature and electric field. Critical currents for SRM 1457 are certified at magnetic fields of 2, 4, 6, and 8 T for temperatures from 3.90 to 4.24 K and electric field criteria from 0.05 to 0.2 microV/cm. Statistical tolerance limits and estimated systematic errors are combined to give an overall uncertainty in the certified values. The total uncertainty is no greater than 2.57 percent of the reported critical current at any of the four magnetic fields. GRA

N85-22907# Joint Publications Research Service, Arlington, Va.
USSR REPORT: ELECTRONICS AND ELECTRICAL ENGINEERING Abstracts Only
23 Jan. 1985 80 p Transl. into ENGLISH from various Russian articles
(JPRS-UEE-85-002) Avail: NTIS HC A05/MF A01

Research in electronics and electrical engineering is addressed in this U.S.S.R. report. Topics covered include: (1) aerospace and electronic systems; (2) antennas and propagation; (3) broadcasting and consumer electronics; (4) circuits and systems; (5) communications; (6) components, hybrids and manufacturing technology; (7) computers; (8) electrical insulation; (9) electron devices; (10) industrial electronics and control instrumentation; (11) magnetics; (12) microwave theory and techniques; (13) power engineering and quantum electronics/electro-optics. For individual titles, see N85-22908 through N85-22975.

N85-22908# Joint Publications Research Service, Arlington, Va.
ASSESSMENT OF EFFECTIVENESS OF SIGNAL-CODE CONSTRUCTIONS IN TIME DIVISION-MULTI-ACCESS SATELLITE SYSTEMS Abstract Only **c32**
S. L. Portnoy and D. R. Ankudinov *In its* USSR Rept.: Electron. and Elec. Eng. (JPRS-UEE-85-002) 23 Jan. 1985 p 1 Transl. into ENGLISH from Elektrosvyaz (Moscow), no. 5, May 1984 p 11-14 (For primary document see N85-22907 13-33)
Avail: NTIS HC A05/MF A01

Energy losses in TDMA satellite circuits are investigated on the basis of the model of a Gaussian memoryless channel incorporating a signal code construction. The signal code construction is a consolidated two stage construction with a modulation system as the inner stage and correcting codes as the outer stage. Signal code constructions employing Gray codes, cascade codes and M-ary block codes are considered. Real TDMA systems are analyzed on the assumptions that the calculations are made using an audio frequency equivalent of the circuit, the relay carries a single trunk, the timing and carrier frequency synchronization is ideal, the signal is transmitted in the continuous stream, and there is no noise at the input of the receiving filter. The effectiveness of a signal code construction employing cascade codes on a real satellite link incorporating MDVU-40 equipment is modeled. The method can be used to select the signal code construction in a communications channel for the required data rate, and to maximize

the energy gain and attainable transmission rate over the relay trunk. B.W.

N85-22909# Joint Publications Research Service, Arlington, Va.
SATELLITE CHANNELS IN PACKET-SWITCHING NETWORKS Abstract Only **c32**
V. A. Gorskiy and M. A. Grigoryeva *In its* USSR Rept.: Electron. and Elec. Eng. (JPRS-UEE-85-002) 23 Jan. 1985 p 2 Transl. into ENGLISH from Elektrosvyaz (Moscow), no. 5, May 1984 p 9-11 (For primary document see N85-22907 13-33)
Avail: NTIS HC A05/MF A01

The separate and combined use of terrestrial and satellite channels in computer communications networks is examined for varying traffic loads and for different communications system parameters. The division of traffic between the terrestrial and satellite legs used to minimize the average packet delivery time through the network is analyzed. The terrestrial leg consists of several repeater sections connected by multichannel transmission circuits. It is found that inclusion of a satellite channel in a system improves system characteristics upon reaching a certain network load threshold, which depends upon the throughput capacity of the terrestrial leg, the number of channels on that leg and the number of legs in the network. When the throughput capacities are the same, the combined use of terrestrial and satellite channels is feasible only for a network load of rho = 0.4-0.5 for single channel sections and rho = 0.1-0.2 for multichannel sections. B.W.

N85-22910# Joint Publications Research Service, Arlington, Va.
SATELLITE BRIDGES IN COMMUNICATIONS NETWORKS Abstract Only **c32**
G. B. Askinazi *In its* USSR Rept.: Electron. and Elec. Eng. (JPRS-UEE-85-002) 23 Jan. 1985 p 2 Transl. into ENGLISH from Elektrosvyaz (Moscow), no. 5, May 1984 p 5-8 (For primary document see N85-22907 13-33)
Avail: NTIS HC A05/MF A01

The use of satellite bridges satellite communication channels set up in a parallel to terrestrial communication links to connect distant nodes directly is described. The use of local bridges between two nodes, between which traffic to concentrated, is discussed. In a radial network, bridges are set up between the center and network nodes which are less heavily loaded than others. These are called distribution bridges. Bypass bridges are set up in networks in which the load is uniformly distributed among nodes connected by the each-to-each principle. By augmenting the parallel terrestrial channels, satellite bridges improve the economic effectiveness of communication networks. Author

N85-22911# Joint Publications Research Service, Arlington, Va.
KINETIC RAYLEIGH-TAYLOR INSTABILITY THEORY IN THE IONOSPHERE NEAR EQUATOR Abstract Only **c32**
B. N. Gershman and A. N. Shevchenko *In its* USSR Rept.: Electron. and Elec. Eng. (JPRS-UEE-85-002) 23 Jan. 1985 p 3 Transl. into ENGLISH from Izv. Uchebn. Zavedeniy: Radiofiz. (Gorkiy), v. 27, no. 6, Jun. 1984 p 679-684 Original language document was announced in IAA as A84-49001 (For primary document see N85-22907 13-33)
Avail: NTIS HC A05/MF A01

A linear theory of Rayleigh-Taylor instability, based on a kinetic description with the collision integral in the BGK form, is developed for application to irregularities connected with the spread F phenomenon. Electrostatic disturbances are examined for the near equatorial F region, and formulas are derived for the growth rates in the collisional and collisionless regimes. A comparison is made with results obtained on the basis of the quasi-hydrodynamic description. B.J. (IAA)

N85-22912# Joint Publications Research Service, Arlington, Va.
EXITATION OF LOW-FREQUENCY RESONANCE WAVES BY MOVING CONDUCTOR IN SPACE PLASMA Abstract Only **c32**
B. S. Abramovich and B. Ye. Nemtsov *In its* USSR Rept.: Electron. and Elec. Eng. (JPRS-UEE-85-002) 23 Jan. 1985 p 3 Transl. into ENGLISH from Izv. Vysshikh Uchebn. Zavedeniy: Radiofiz. (Gorkiy), v. 27, no. 6, Jun. 1984 p 685-689 (For primary document see N85-22907 13-33)
Avail: NTIS HC A05/MF A01

The excitation of low frequency resonance waves as a conductor is moved along a magnetic field is investigated. A thin ideal cylindrical conductor moving in a plasma along a constant magnetic field is examined. It is demonstrated that plasma oscillations can be generated effectively at the lower resonance frequency, causing absolute instability of the oscillations of the current on the conducting body. The threshold of occurrence and the increments of this electron ion instability are computed, the instability is found to be periodic with large increments. The possibility of low frequency resonance instability occurring as man made satellites travel through the upper ionosphere is assessed. Author

N85-22913# Joint Publications Research Service, Arlington, Va.
SCATTERING OF ELECTROMAGNETIC WAVES BY CHARGED PARTICLES Abstract Only **c32**
A. A. Lushnikov, V. V. Maksimenko, A. Ya. Simonov, and A. G. Sutugin *In its* USSR Rept.: Electron. and Elec. Eng. (JPRS-UEE-85-002) 23 Jan. 1985 p 6 Transl. into ENGLISH from Izv. Vysshikh Uchebn. Zavedeniy: Radiofiz. (Gorkiy), v. 27, no. 6, Jun. 1984 p 726-733 Original language document was announced in IAA as A84-49006 (For primary document see N85-22907 13-33)
Avail: NTIS HC A05/MF A01

The behavior of charged dielectric spherical (aerosol) particles in an external electromagnetic field is analyzed. The position of the dipole plasma resonance on the particle is determined, assuming that electrons, interacting via Coulomb potential, move freely on the particle surface. The vertex equation is solved in the chaotic phase approximation. A calculation is made of surface plasmon damping due to the thermal decay of plasma oscillations into single particle excitations. Since the plasmon damping is small, the elastic scattering cross section can increase by many order of magnitude near resonance. The possibility of the experimental detection of this resonance is discussed. B.J. (IAA)

N85-22914# Joint Publications Research Service, Arlington, Va.
DIFFRACTION OF PLANE TM-WAVE ON CONTINUOUSLY IRREGULAR ELLIPTICAL PLASMA Abstract Only **c32**
A. V. Moroz *In its* USSR Rept.: Electron. and Elec. Eng. (JPRS-UEE-85-002) 23 Jan. 1985 p 6 Transl. into ENGLISH from Izv. Vysshikh Uchebn. Zavedeniy: Radiofiz. (Gorkiy), v. 27, no. 6, Jun. 1984 p 770-774 Original language document was announced in IAA as A84-49010 (For primary document see N85-22907 13-33)
Avail: NTIS HC A05/MF A01

The modified Born approximation is used to solve the two dimensional problem of the diffraction of a plane TM wave by a smoothly elliptical plasma cylinder with a special permittivity profile. Results of numerical calculations are presented which illustrate the effect of the asymmetry of the elliptical cylinder on the scattering pattern. B.J. (IAA)

N85-22915# Joint Publications Research Service, Arlington, Va.
MOVING TARGET DETECTION Abstract Only **c32**
V. M Frolushkin and L. Ya. Novoseltsev *In its* USSR Rept.: Electron. and Elec. Eng. (JPRS-UEE-85-002) 23 Jan. 1985 p 5 Transl. into ENGLISH from Izv. Vysshikh Uchebn. Zavedeniy: Radiofiz. (Kiev), v. 27, no. 7, Jul. 1984 p 11-15 Original language document was announced in IAA as A84-44443 (For primary document see N85-22907 13-33)
Avail: NTIS HC A05/MF A01

Algorithms are synthesized for the operation of moving target indicators in the case of the detection of signals with unknown amplitude, initial phase, and Doppler frequency on a background of Gaussian interference with an unknown covariance matrix (this matrix taking into account the cross correlation of processes in the quadrature channels). It is shown that such detectors have a multichannel structure with respect to Doppler frequency and carry

out the detection with an indication of the frequency band.
B.J. (IAA)

N85-22916# Joint Publications Research Service, Arlington, Va.
KAM-250 ANTENNA SWITCH Abstract Only
V. M. Lozinskiy and N. M. Obikhvost *In its* USSR Rept.: Electron. and Elec. Eng. (JPRS-UEE-85-002) 23 Jan. 1985 p 5 Transl. into ENGLISH from Elektrosvyaz (Moscow), no. 5, May 1984 p 57 (For primary document see N85-22907 13-33)
Avail: NTIS HC A05/MF A01

This article describes the KAM-250 antenna switch, which is designed for switching antennas and short wave transmitters with a power of less than 250 kW working into 300 ohm balanced feeders. The frequency range of the switch is 3 to 27 MHz. Automatic grounding of nonworking leads is provided. There are four versions of this device which differ in the number of lead-ins and the type of control. The switch is built as a 750 x 1980 x 1320 mm finished rack; the racks can be employed as stand alone switches, or can be ganged to produce switches with different capacities. Author

N85-22917# Joint Publications Research Service, Arlington, Va.
PROCESSING OF SIGNALS IN EXPERIMENTS WITH SCATTERING OF SHORT RADIO PULSES BY CONDUCTING SPHERE Abstract Only **c32**
A. A. Kostylev *In its* USSR Rept.: Electron. and Elec. Eng. (JPRS-UEE-85-002) 23 Jan. 1985 p 6 Transl. into ENGLISH from Radiotekhn. (Moscow), no. 8, Aug. 1984 p 64-66 (For primary document see N85-22907 13-33)
Avail: NTIS HC A05/MF A01

Two algorithms of signal processing in radar experiments with radio pulse scattering are constructed, one for obtaining the pulse response characteristic and one for obtaining the frequency characteristic by means of transient probing signals, with a conducting sphere used as a scatterer so as to eliminate the dependence of both backscattering characteristics on the aspect ratio. Each algorithm evaluates the discrete analog of the respective characteristic. The corresponding equation for the pulse response characteristic, specifically considered here, contains an ill conditioned matrix and must be regularized with some positive definite matrix before it can be solved as a variational problem for the prior estimate with error minimization. Replacing the linear convolution with a cyclic one results in a faster algorithm, especially with the use of fast Fourier transforms. A ridge estimate can be similarly obtained for the frequency characteristic. Author

N85-22918# Joint Publications Research Service, Arlington, Va.
MULTIFUNCTIONAL ELEMENTS FOR INTEGRATED OPTICS Abstract Only **c74**
V. I. Volman and N. D. Kozyrev *In its* USSR Rept.: Electron. and Elec. Eng. (JPRS-UEE-85-002) 23 Jan. 1985 p 6-7 Transl. into ENGLISH from Radiotekhn. (Moscow), no. 8, Aug. 1984 p 37-40 (For primary document see N85-22907 13-33)
Avail: NTIS HC A05/MF A01

The feasibility of producing universal elements and thus minimizing the number of standard components for integrated optics is theoretically examined. A typical such element would be a wafer of an optically transparent material with an externally voltage-controllable refractive index. Parallel conducting strips are deposited on both surfaces of the wafer so as to form two orthogonal arrays of electrode pairs. Application of appropriate voltages will produce any desired distribution of the refractive index, a generally three-dimensional one and in this particular configuration a two-dimensional one, characterized by the amplitude distribution u(x,y) and the phase distribution v(x,y) in the plane of the wafer. Considering that the refractive index of an only weakly nonhomogeneous medium is a purely real quantity, the first-order partial differential equation constraining the distribution of the refractive index yields the phase distribution v(x,y) when the amplitude distribution u(x,y) is known. The corresponding boundary-value problem is solved here for two practical cases which admit a solution in closed form, namely where mu = F (mu) with argument mu = phi (x) psi (y) and mu = phi (x)+ psi (y), respectively.
Author

N85-22919# Joint Publications Research Service, Arlington, Va.
COORDINATE DETERMINATION ERRORS IN MEASURING CHARACTERISTICS OF RADIATION FIELD OF AIRBORNE ANTENNAS Abstract Only **c32**
E. D. Gazazyan and V. G. Panchenko *In its* USSR Rept.: Electron. and Elec. Eng. (JPRS-UEE-85-002) 23 Jan. 1985 p 7 Transl. into ENGLISH from Izmeritel. Tekhn. (Moscow), no. 9, Sep. 1984 p 54-56 (For primary document see N85-22907 13-33)
Avail: NTIS HC A05/MF A01

Expressions are derived for estimating the coordinate errors in measuring the characteristics of the radiation field of airborne antennas. Errors in six coordinates must be taken into account at any given moment: the azimuth, elevation, slant range, heading, pitch and roll of the aircraft. It is recommended that straight-line flights be employed. Maneuvers should be used only in extreme cases, such as for measurements in the upper hemisphere. Conditions are specified under which it is possible to measure the characteristics of airborne antennas not equipped with maneuvering sensors, recording means or telemetry. Author

N85-22920# Joint Publications Research Service, Arlington, Va.
REDUCTION OF AMPLITUDE-PHASE DISTORTIONS OF MOVABLE MICROWAVE COUPLING CIRCUIT FOR ANTENNA FIELD MEASUREMENTS Abstract Only
L. A. Letnov and V. G. Skorov *In its* USSR Rept.: Electron. and Elec. Eng. (JPRS-UEE-85-002) 23 Jan. 1985 p 7 Transl. into ENGLISH from Izmeritel. Tekhn. (Moscow), no. 9, Sep. 1984 p 56-57 (For primary document see N85-22907 13-33)
Avail: NTIS HC A05/MF A01

A radio holography system for measuring the amplitude-phase distribution of antenna fields in the aperture is described. The system incorporates a movable microwave coupling circuit between the amplitude-phase meter and the scanning probe which is designed to prevent the amplitude-phase distortions of the microwave circuit from influencing the measurement results. This is achieved by determining the instabiliy of the electrical length of the circuit at every moment and accordingly correcting the measurement results by computer. The block diagram of the system is presented, and the transformation of the signal as it passes through the system is analyzed. In order to reduce errors caused by signals reflected from the metal surfaces of the microwave devices, all metal members of the scanner are coated with an absorbing material. By doing this, the total error resulting from the added microwave devices does not exceed a few tenths of a degree in phase, and approximately 0.1 dB in amplitude. Author

N85-22921# Joint Publications Research Service, Arlington, Va.
STEREO DECODER WITHOUT SUBCARRIER RESTORATION Abstract Only **c32**
A. Porokhnyuk *In its* USSR Rept.: Electron. and Elec. Eng. (JPRS-UEE-85-002) 23 Jan. 1985 p 12 Transl. into ENGLISH from Radiotekhn. (Moscow), no. 7, Jul. 1984 p 22-24 (For primary document see N85-22907 13-33)
Avail: NTIS HC A05/MF A01

A stereo decoder is described which includes automatic phase-lock frequency control in the shaper of switching pulses and does not require restoring the spectrum of polarity-modulated oscillations. This eliminates the need for restoring the subcarrier-frequency signal to detection level and the need for compensating amplitude and phase distorations of the ultrasonic component in the spectrum of the complex stereo signal. The gist of this innovation is that the complex stereo signal proceeds from the FM detector to a proportionally differentiating filter and, after conversion in the latter, is demodulated by two synchronous detectors. The switching pulses necessary for synchronous detection are produced by a pulse shaper consisting of an oscillator with automatic phase-lock frequency control and a band-pass filter for the synchronizing voltage. Automatic control is provided by a paraphrase amplifier-limiter with one transistor and diode-diode logic shaping the signal which triggers a push-pull phase detector.

The output signal from this detector proceeds through a low-pass filter to a voltage-controlled multivibrator oscillator built with diode-diode logic. B.W.

N85-22922# Joint Publications Research Service, Arlington, Va.
ERROR PROBABILITY DURING OPTIMAL NONCOHERENT RECEPTION OF BINARY SIGNALS IN MULTIBEAM CHANNEL Abstract Only **c32**
A. I. Fomin, P. N. Serdyukov, and V. V. Mezhevich *In its* USSR Rept.: Electron. and Elec. Eng. (JPRS-UEE-85-002) 23 Jan. 1985 p 13 Transl. into ENGLISH from Radiotekhn. (Moscow), no. 8, Aug. 1984 p 48-50 (For primary document see N85-22907 13-33)
Avail: NTIS HC A05/MF A01

A general expression is derived for the error probability during noncoherent reception of discrete signals in channels with both fast and slow fading. The fast fading is approximated with an m-distribution (m sub 1 corresponds to a Rayleigh distribution) and the slow fading is assumed to have a log normal distribution, the latter also readily approximated with an m-distribution. The error probability is also a function of the approximation error. E.A.K.

N85-22923# Joint Publications Research Service, Arlington, Va.
REGULAR SYNTHESIS OF PAIRS OF PHASE-KEYED BINARY MINIMAX SIGNALS Abstract Only **c32**
Kh. I. Luchanskaya and V. Ya. Khevrolin *In its* USSR Rept.: Electron. and Elec. Eng. (JPRS-UEE-85-002) 23 Jan. 1985 p 14 Transl. into ENGLISH from Radiotekhn. (Moscow), no. 8, Aug. 1984 p 50-53 (For primary document see N85-22907 13-33)
Avail: NTIS HC A05/MF A01

A regular method is proposed for synthesizing pairs of phase-keyed binary signals with minimum values of maximum autocorrelation and crosscorrelation peaks. The method is based on the mutual energy spectrum of two code sequences and representation of the corresponding polynomial as the product of two. It involves selection of + and - signs in one sequence to minimize the maximum of the crosscorrelation function and to derive the second sequence from the first one to minimize the side peaks of the autocorrelation function. The method is demonstrated on pairs of Barker sequences, of M-sequences, and of sequences which with any given autocorrelation function have the minimax of the crosscorrelation functions. The method yields a smaller minimax than the Gold method, only very long sequences obtained by both methods have similar characteristics. E.A.K.

N85-22924# Joint Publications Research Service, Arlington, Va.
INTERFERENCE IMMUNITY OF FIBER-OPTIC COMMUNICATION LINES WITH SPECTRAL MULTIPLEXING OF CHANNELS Abstract Only **c32**
A. Kh. Petrosyan and M. A. Nshanyan *In its* USSR Rept.: Electron. and Elec. Eng. (JPRS-UEE-85-002) 23 Jan. 1985 p 14 Transl. into ENGLISH from Radiotekhn. (Moscow), no. 8, Aug. 1984 p 71-74 (For primary document see N85-22907 13-33)
Avail: NTIS HC A05/MF A01

The performance of fiber-optic communication lines with spectral multiplexing of channels is analyzed for interference immunity and its improvement. The major sources of interference and insertion losses are crossovers, which generate crosstalk, and demultiplexers in the receiver. The signal intensity at the output of the j-th demultiplexer for the i-th spectral channel is calculated first, assuming independent signal sources. The the ratio of peak signal power to average interference power is calculated, considering quantum noise, thermal and shot noise, mode beats, and background illumination. A demultiplexer is designed on this basis, but optimization of the channels is an indeterminate problem of which the solution depends on the optimality criterion and on the given values of the other interference indicators not selected as optimality criterion. The interference immunity of such communication lines can be improved by post-detector compensation of crosstalk, which requires only a multipole network with appropriate j-th input to i-th output transmission coefficients, and by considering that the interference immunity will decrease as the useful signal bandwidth increases. E.A.K.

N85-22925# Joint Publications Research Service, Arlington, Va.
AL-124 LIGHT-EMITTING DIODE IN 30 MBIT/S FIBER-OPTIC COMMUNICATION LINE Abstract Only
A. A. Vilisov, N. A. Gorbatov, S. N. Marchenko, and V. A. Chaplygin *In its* USSR Rept.: Electron. and Elec. Eng. (JPRS-UEE-85-002) 23 Jan. 1985 p 15 Transl. into ENGLISH from Radiotekhn. (Moscow), no. 8, Aug. 1984 p 77-79 (For primary document see N85-22907 13-33)
Avail: NTIS HC A05/MF A01

An AL-124 light-emitting diode as a transmitter for a high-speed fiber-optic communication line was studied. A quartz-polymer fiber with a core diameter of 200 micron, a numerical aperture slightly larger than 0.2, and an attenuation coefficient of 40 dB/km was used as a multimode light guide. The electric power supply in the transmitter stage consisted of a TTL gate built with series 530LA-16/17 microcircuits on the diode - side and a capacitance-resistance-capacitance pi-network on the diode + side. Light pulses with rise time and fall time not exceeding 20 ns are generated by an AL-124 diode upon excitation produce the necessary voltage drop across. This excitation was provided by an electric pulse signal through the TTL gate. It is indicated that the performance of an AL-124 light-emitting diode is adequate for data transmission by a binary pulse-position code at at rate of 30 Mbit/s over fiber-optic lines. E.A.K.

N85-22926# Joint Publications Research Service, Arlington, Va.
HORIZONTAL DEFLECTION TS-257 Abstract Only **c32**
N. Katsnelson and Ye. Shpilman *In its* USSR Rept.: Electron. and Elec. Eng. (JPRS-UEE-85-002) 23 Jan. 1985 p 17 Transl. into ENGLISH from Radiotekhn. (Moscow), no. 9, Sep. 1984 p 24-28 (For primary document see N85-22907 13-33)
Avail: NTIS HC A05/MF A01

The MRK-1 radio-frequency television channel includes controls for line and frame sweeps and metricwaveband (I to II to III) and decimetric-waveband (IV to V) selectors. The metricwave band selector consists of separate r-f amplifiers and heterodynes for each of the three frequency bands, in addition to a high-pass ladder filter, a mixer, an intermediate-frequency stage, and an automatic gain control common for all. The decimetric-waveband selector (470-790 MHz) is coupled on its output side through a matching resistor and a switching diode to the mixer of the metric-waveband selector. Its input stage is a fixed high-pass filter and has a capacitor which partially compensates the input inductance of the r-f amplifier transistors. An i-f image filter on surface acoustic waves with an interdigital transducer and a K174UR5 microcircuit, a two-stage transistor amplifier which compensates the attenuation of i-f signals in the filter, automatic frequency trim for the heterodynes, synchronous detectors for video signals, an amplifier-limiter and a phase detector for audio signals from the SAW filter in the sound track are included. E.A.K.

N85-22927# Joint Publications Research Service, Arlington, Va.
THEORY OF OPTIMUM M-FILTRATION OF SIGNALS AGAINST BACKGROUND OF CORRELATED INTERFERENCE Abstract Only **c32**
V. S. Golikov and N. I. Kravchenko *In its* USSR Rept.: Electron. and Elec. Eng. (JPRS-UEE-85-002) 23 Jan. 1985 p 19 Transl. into ENGLISH from Izv. Vysshikh Uchebn. Zavedeniy: Radioelektron. (Kiev), v. 27, no. 7, Jul. 1984 p 15-19 Original language document was announced in IAA as A84-44444 (For primary document see N85-22907 13-33)
Avail: NTIS HC A05/MF A01

Consideration is given to the identification of signals according to the Neumann-Pearson criterion on a background of additive normal noise by means of linear discrete M-ary filters. It is shown that the impulse response of the optimal filter depends on the form of the signal and the M-ary correlation function of the noise. The noise immunity of conventional and M-ary optimal linear filters is examined for the case of additive normal correlated noise. B.J. (IAA)

N85-22928# Joint Publications Research Service, Arlington, Va.
DISPERSION OF PHASE-SHIFT KEYED SYSTEMS WITH FIXED NUMBER OF BLOCKS Abstract Only **c32**
E. Ye. Mitselmager and R. D. Mukhamedyarov *In its* USSR Rept.: Electron. and Elec. Eng. (JPRS-UEE-85-002) 23 Jan. 1985 p 19 Transl. into ENGLISH from Izv. Vysshikh Uchebn. Zavedeniy: Radioelektron. (Kiev), v. 27, no. 7, Jul. 1984 p 32-36 (For primary document see N85-22907 13-33)
Avail: NTIS HC A05/MF A01

An exact formula is derived for the dispersion of signal systems with a fixed number of blocks; it is proven that signal systems with M* blocks have the least dispersion. It is also proven that the dispersion of signal systems with least number of blocks becomes smaller as the quantity [M-M sub 0] decreases; where M sub zero = (N+1)/2 and N = number of elements in signal. The results of calculating the dispersions for several signals systems are presented. It is concluded that the dispersion of signal systems increases near-expotentially as the figure [M-M sub 0] increases. E.A.K.

N85-22929# Joint Publications Research Service, Arlington, Va.
NOISE TOLERANCE OF DIGITAL DEMODULATOR FOR COMPLEX SIGNAL SYSTEM EMPLOYING BINARY QUANTIZATION Abstract Only **c32**
A. V. Bessalov *In its* USSR Rept.: Electron. and Elec. Eng. (JPRS-UEE-85-002) 23 Jan. 1985 p 20 Transl. into ENGLISH from Izv. Vysshikh Uchebn. Zavedeniy: Radioelektron. (Kiev), v. 27, no. 7, Jul. 1984 p 46-49 (For primary document see N85-22907 13-33)
Avail: NTIS HC A05/MF A01

An approximate expression is derived for the error probability during digital correlation processing of a system of m orthogonal (or quasiorthogonal) systems. In order to simplify the structure of the digital demodulator, binary quantization is considered. The noise tolerance of nonlinear digital and linear analog demodulators is compared for Gaussian and incoherent harmonic interference. Experimental error probabilities which agree well with the theory are obtained by computer modeling of the demodulator. It is found that a nonlinear demodulator employing binary quantization can be improved by adding variable quantizer thresholds. E.A.K.

N85-22930# Joint Publications Research Service, Arlington, Va.
ANALYSIS OF CHARACTERISTICS OF DIGITAL DISCRIMINATORS FOR PHASE-SHIFT KEYED SIGNALS Abstract Only **c32**
In its USSR Rept.: Electron. and Elec. Eng. (JPRS-UEE-85-002) 23 Jan. 1985 p 20 Transl. into ENGLISH from Izv. Vysshikh Uchebn. Zavedeniy: Radioelektron. (Kiev), v. 27, no. 7, Jul. 1984 p 49-54 (For primary document see N85-22907 13-33)
Avail: NTIS HC A05/MF A01

The discrimination and fluctuation characteristics of digital discriminators employed in circuits which track the time position of phase-shift keyed signals were analyzed. The nature of the error signal probability distribution at the discriminator output is examined. Expressions are derived for the discrimination and fluctuation characteristics of a digital time discriminator with the assumption that the random quantitites at the inputs to the subtractor are independent of one another. The mean square equivalent fluctuations, referred to the discriminator input, are plotted for convenience in comparing different types of discriminators. E.A.K.

N85-22931# Joint Publications Research Service, Arlington, Va.
COMBINED PROCESSING METHOD AND MATCHED FILTER FOR DISCRETE COMPOSITE FREQUENCY PHASE-SHIFT KEYED SIGNAL Abstract Only **c32**
V. S. Belyayev *In its* USSR Rept.: Electron. and Elec. Eng. (JPRS-UEE-85-002) 23 Jan. 1985 p 21 Transl. into ENGLISH from Izv. Vysshikh Uchebn. Zavedeniy: Radioelektron. (Kiev), v. 27, no. 7, Jul. 1984 p 61-63 (For primary document see N85-22907 13-33)
Avail: NTIS HC A05/MF A01

A combined method is proposed for processing complex signals with large bases. An expression is derived for the complex frequency response of the matched filter for a discrete composite frequency phase-shift keyed signal. A matched filter is designed which consists of N-frequency channels with different signal delays in each channel and a block in each channel, or a common block, for optimum processing of the phase-shift keyed signal. In the combined processing method, a signal is first processed by a radio-frequency matched filter, after which RF filters filter off the component frequencies of the signal for the individual channels and combine them temporally by a multitap ultrasonic quartz delay line. The phase-shift keyed signal is then translated to the video region by synchronous detection and mixing. The pseudorandom coding combination which is extracted is processed in video-frequency matched filters. Tests on an experimental filter show that the theoretical conclusions are valid, and confirm the possibility of using complex signals and combined filters for processing them in communications and other radio systems. E.A.K.

N85-22932# Joint Publications Research Service, Arlington, Va.
PIEZOELECTRIC FILTER WITH LOW-Q INDUCTANCES Abstract Only
G. N. Yergiyev and A. M. Ivanitskiy *In its* USSR Rept.: Electron. and Elec. Eng. (JPRS-UEE-85-002) 23 Jan. 1985 p 21 Transl. into ENGLISH from Izv. Vysshikh Uchebn. Zavedeniy: Radioelektron. (Kiev), v. 27, no. 7, Jul. 1984 p 73-75 (For primary document see N85-22907 13-33)
Avail: NTIS HC A05/MF A01

A passive bridge circuit for a narrow band filter was investigated in which the Q-factor of the inductance coils depends upon the requirements for the amplitude-frequency characteristic within the effective delay band. Each arm of the bridge circuit contains a quartz resonator in series with an inductance. Formulas are derived for the increase in attenuation of a filter with inductances in comparison with that of a filter without inductances at the same frequency. The use of the formula is demonstrated by designing a filter section with inductances. The experimental and measured amplitude frequency characteristics agree well. E.A.K.

N85-22933# Joint Publications Research Service, Arlington, Va.
OPTIMAL SYNTHESIS OF SURFACE ACOUSTIC WAVE FILTERS Abstract Only
V. M. Dashenkov and A. S. Rukhlenko *In its* USSR Rept.: Electron. and Elec. Eng. (JPRS-UEE-85-002) 23 Jan. 1985 p 22 Transl. into ENGLISH from Izv. Vysshikh Uchebn. Zavedeniy: Radioelektron. (Kiev), v. 27, no. 7, Jul. 1984 p 76-78 (For primary document see N85-22907 13-33)
Avail: NTIS HC A05/MF A01

An optimum method is proposed for synthesizing surface acoustic-wave filters employing nonrecursive digital filter design methods. The method provides an optimum solution for the entire period of the frequency response. The method is tested with filters with different bandwidths and with complex frequency responses, such as television filters. The proposed method can be employed for other multiplicative Chebyshev approximation problems in which the solution is represented as the product of fixed and optimized parts. The proposed algorithm makes an allowance for the general case of an alternating fixed function, which expands its area of application. E.A.K.

N85-22934# Joint Publications Research Service, Arlington, Va.
ANALYSIS AND OPTIMIZATION OF PARAMETERS OF FANNED SURFACE ACOUSTIC WAVE TRANSDUCERS Abstract Only
Yu. F. Zinkovskiy and Ye. A. Nelin *In its* USSR Rept.: Electron. and Elec. Eng. (JPRS-UEE-85-002) 23 Jan. 1985 p 22 Transl. into ENGLISH from Izv. Vysshikh Uchebn. Zavedeniy: Radioelektron. (Kiev), v. 27, no. 7, Jul. 1984 p 79-81 (For primary document see N85-22907 13-33)
Avail: NTIS HC A05/MF A01

The radiation conductance of interdigital surface acoustic-wave (SAW) transducers employing fan-shaped finger placement is examined. An expression is derived for the active component of the radiation conductance using the approximation of the normal components of the electrical field. The expression derived agrees

with the existing formula for the active component of the radiation conductance of a nonapodized SAW filter with an aperture equal to half the width of the acoustic beam emitted by the transducer. Conversion losses are analyzed as a function of the parameters of fanned interdigital transducers. Expressions are derived for the optimum aperture for which center-frequency losses are minimal. The use of fanned SAW filters to realize a given phase-frequency characteristic is promising. E.A.K.

N85-22935# Joint Publications Research Service, Arlington, Va.
CODE LOCK WITH MICROCIRCUIT Abstract Only
A. Korobka and I. May *In its* USSR Rept.: Electron. and Elec. Eng. (JPRS-UEE-85-002) 23 Jan. 1985 p 24 Transl. into ENGLISH from Radiotekhn. (Moscow), no. 9, Sep. 1984 p 37 (For primary document see N85-22907 13-33)
Avail: NTIS HC A05/MF A01

A code lock with a microcircuit was invented which contains only a very few components. Two DD-triggers control the state of two identical transistors. When both transistors are turned on simultaneously the transistor VS1 is turned on so that the electromagnet YA1 pulls in the bolt and the door opens. This will happen only when a logic 1 appears at the inverted output of the first trigger and at the straight output of the second one. After the door is opened, a button on it resets the contactors to return both triggers to their original state. The electromagnetic is designed to produce the necessary pull force and sufficient power when under rectified 127 V line voltage, with the neutral wire of the lock circuit always connected to the - terminal of the power supply. E.A.K.

N85-22936# Joint Publications Research Service, Arlington, Va.
RECOMMENDATION ON USE OF SERIES K157UL1 MICROCIRCUITS Abstract Only
K. Petrov *In its* USSR Rept.: Electron. and Elec. Eng. (JPRS-UEE-85-002) 23 Jan. 1985 p 25 Transl. into ENGLISH from Radiotekhn. (Moscow), no. 7, Jul. 1984 p 43-44 (For primary document see N85-22907 13-33)
Avail: NTIS HC A05/MF A01

The series of K157UL1A/B microcircuits are low-noise two-channel playback preamplifiers for stereo tape recorders. The characteristics of the K157UL1A microcircuit are noise voltage V sub n, in = 0.46 uV and noise current I sub n, in = 120 nA referred to the input, in the 20-20,000 Hz frequency range, based on measurements and calculations with the aid of spectral density curves. The characteristics of the K157UL1B microcircuit are somewhat worse. The K157UL1A microcircuit can be used in the playback channel only when its transmission coefficient is at least 50, otherwise the preamplifier becomes unstable. Its resistors and capacitors must be selected and matched for necessary gain and time constants at the various tape speeds. This microcircuit can be considered for use in the recording preamplifier and final amplifier stages. E.A.K.

N85-22937# Joint Publications Research Service, Arlington, Va.
SPACE-TIME RESPONSE CHARACTERISTICS OF ACOUSTOOPTIC FILTER FOR COMPRESSION OF LINEARLY FREQUENCY-MODULATED SIGNAL Abstract Only
Yu. G. Vasilyev *In its* USSR Rept.: Electron. and Elec. Eng. (JPRS-UEE-85-002) 23 Jan. 1985 p 25-26 Transl. into ENGLISH from Radiotekhn. (Moscow), no. 8, Aug. 1984 p 74-76 (For primary document see N85-22907 13-33)
Avail: NTIS HC A05/MF A01

The performance of an acoustooptic compression filter operating with interaction of a laser beam and a linearly frequency-modulated acoustic wave is evaluated in terms of the space-time response, namely dependence of that response on the deviation of laser beam incidence from the Bragg angle. The field of the light wave in the first diffraction order in the exit plane of such a light modulator is calculated for an incident modulating acoustic signal. The resulting space-time response in the focusing plane reveals that deviation from the Bragg angle lowers the amplitude and causes an additional transverse shift in the focusing plane. Accordingly, this deviation determines the wave parameter and the thickness of the modulator necessary for optimal processing of linearly frequency-modulated radio signals. Author

N85-22938# Joint Publications Research Service, Arlington, Va.
SYNTHESIS OF LOW-PASS FILTERS USING COUPLED LINES WITH UNMATCHED LOADS Abstract Only
V. P. Meshchanov, V. M. Loginov, and L. V. Shikova *In its* USSR Rept.: Electron. and Elec. Eng. (JPRS-UEE-85-002) 23 Jan. 1985 p 26 Transl. into ENGLISH from Radiotekhn. (Moscow), no. 8, Aug. 1984 p 67-69 (For primary document see N85-22907 13-33)
Avail: NTIS HC A05/MF A01

Use of coupled nonhomogeneous lines with directionality of the second kind and unmatched loads is proposed for synthesis of microwave low-pass filters, which must have nonperiodic amplitude-frequency characteristics and be electromagnetically compatible with other radioelectronic devices. Two completely symmetric segments of such lines are connected into a chain network with two of the four output arms either open or shorted. The attenuation characteristic of the resulting octupole depends entirely on the scattering coefficients of its component quadruples. The wave transmission matrix of this notching line is evaluated on the basis of known relations between coefficients of the scattering matrix and of the transmission matrix, the T sub 11 element of the latter matrix being calculated according to Kammler's recurrence relations (IEEE Trans. MTT-17, No. 8, 1969). The problem of synthesis for given pass and suppression bands is solved as a problem in nonlinear programming. Numerical results are given for a typical such filter the optimum amplitude-frequency characteristic. R.J.F.

N85-22939# Joint Publications Research Service, Arlington, Va.
PREFILTRATION IN KALMAN FILTER WITH A PRIORI INDETERMINACY Abstract Only
O. I. Shelukhin and S. P. Alyabyev *In its* USSR Rept.: Electron. and Elec. Eng. (JPRS-UEE-85-002) 23 Jan. 1985 p 27 Transl. into ENGLISH from Radiotekhn. (Moscow), no. 8, Aug. 1984 p 53-57 (For primary document see N85-22907 13-33)
Avail: NTIS HC A05/MF A01

A stable nonlinear discrete Kalman filter is synthesized for measurement objects with a priori indeterminate, and variable, signal and noise distribution. A robust algorithm of prefiltration is used for obtaining stable maximum-likelihood estimates of the state of a dynamic system in the case of non-Gaussian noise. The estimation problem is expressed in the form of a recurrence relation containing a positive-definite symmetric matrix, whereupon the synthesis problem is formulated in terms of a system of corresponding difference equations in which the measurement errors have been converted to Gaussian ones. Author

N85-22940# Joint Publications Research Service, Arlington, Va.
DYNAMICS OF ADAPTIVE SIGNAL CORRECTOR Abstract Only c32
A. M. Lazarev and Yu. V. Shevchenko *In its* USSR Rept.: Electron. and Elec. Eng. (JPRS-UEE-85-002) 23 Jan. 1985 p 27 Transl. into ENGLISH from Radiotekhn. (Moscow), no. 8, Aug. 1984 p 40-43 (For primary document see N85-22907 13-33)
Avail: NTIS HC A05/MF A01

An adaptive signal corrector in the form of transversal filter used as a delay line with adjustable weight factors at the taps is considered for use in transmission of digital data over frequency-limited channels. A data signal proceeds from such a channel through a synchronous detector and a readout switch to the corrector. The stability of this device and the convergence rate, in the mean-square sense, of its algorithm of pseudosteepest descent are evaluated on the basis of a general analysis applicable to any kind of modulation. The calculations yield the mean-square error at the corrector output and its convergence to a fixed value for a constant adaptation factor within the $0<Mu<1$ range as well as the steady-state error as a function of the number of taps. The results reveal that the convergence rate is not always a monotonically increasing function of the adaptation factor and, when the number of taps is large, reaches its maximum at the optimum

value of the adaptation factor. There is also an upper bound for the adaptation factor which corresponds to the stability limit.
Author

N85-22941# Joint Publications Research Service, Arlington, Va.
PERFORMANCE OF TIME-POSITION DISCRIMINATOR OF COMPOSITE SIGNAL Abstract Only **c32**
O.F. Bokk, A. M. Savvinov, and G. D. Kolesnichenko *In its* USSR Rept.: Electron. and Elec. Eng. (JPRS-UEE-85-002) 23 Jan. 1985 p 28 Transl. into ENGLISH from Radiotekhn. (Moscow), no. 8, Aug. 1984 p 29-33 (For primary document see N85-22907 13-33)
Avail: NTIS HC A05/MF A01

Optimal time-position discrimination involving multiplication of the signal+noise mixture by the time derivative of its video copies with maximum slope in the range of small deviations, is compared with time-position discrimination involving multiplication of the signal+noise mixture by the difference of its video copies shifted in time symmetrically forward and backward from the instant of readout. In terms of the output signal-to-noise ratio, the advantage multiplying by the derivative of video copies at time Tau = 0 is equal to the advantage of multiplying by the difference of video copies at times Tau = plus or minus Tau sub kappa. As the time shift decreases toward zero, both methods of discrimination become equally efficient but the magnitude of the transmission coefficient decreases sharply. This is demonstrated on a signal with a uniform finite spectrum. Author

N85-22942# Joint Publications Research Service, Arlington, Va.
EFFICIENCY OF DIGITAL COMPENSATOR OF STRONG NON-GAUSSIAN INTERFERENCE Abstract Only **c32**
V. V. Avdeyev, Yu. N. Parshin, and I. A. Minayeva *In its* USSR Rept.: Electron. and Elec. Eng. (JPRS-UEE-85-002) 23 Jan. 1985 p 28 Transl. into ENGLISH from Radiotekhn. (Moscow), no. 8, Aug. 1984 p 33-35 (For primary document see N85-22907 13-33)
Avail: NTIS HC A05/MF A01

A digital compensator of strong non-Gaussian wideband interference is considered which contains a band limiter, a subtractor, first and second multipliers, and a low-pass filter with a transfer function K = 1/pT as a bridge between the two multipliers. The interference suppression factor of such a compensator is calculated, considering that the phase distribution in the high-frequency region will be the same at all points along the compensator structure only when there is no parasitic phase shift of the voltage in the band limiter and in the second multiplier. The interference suppression factor is, accordingly, inversely proportional to the sine of the phase shift squared. A digital compensator thus ensures a higher stability of phase characteristics than does an analog one. Conversion from analog to digital compensation involves quantization of the orthogonal input signal components as well as of the limiter output signal and time discretization with numerical solution of the resulting difference equation which describes the compensation process. The efficiency of such a compensator was evaluated by the method of statistical simulation, with either a harmonic oscillation with known phase or an oscillation with phase-keyed pseudorandom M-sequence as a model signal. R.J.F.

N85-22943# Joint Publications Research Service, Arlington, Va.
MATHEMATICAL MODEL OF DISCRIMINATOR FOR SIGNALS WITH FLUCTUATIONS AND THERMAL NOISE Abstract Only **c32**
V. B. Binshtok *In its* USSR Rept.: Electron. and Elec. Eng. (JPRS-UEE-85-002) 23 Jan. 1985 p 29 Transl. into ENGLISH from Radiotekhn. (Moscow), no. 8, Aug. 1984 p 13-17 (For primary document see N85-22907 13-33)
Avail: NTIS HC A05/MF A01

A statistical model is constructed for describing an angle discriminator in a radar station with a conical scan and with a digital computer as a data processing base. The model consists of four modules. The first one pertains to the antenna radiation pattern and scanning mode. The second one pertains to the amplitude fluctuations and thermal noise, with a generator of random normal numbers as well as with appropriate multiplications and additions. The third one pertains to passage of signal and interference through a receiver with amplitude detection and automatic gain control. The fourth one pertains to signal filtration and estimation, with a band-pass filter, phase detector, low-pass filter, and strobing device. The amplitude distribution of incoming reflected signals is assumed to be a Rayleigh or quasi-Rayleigh random one, the thermal noise in the receiver is assumed to be a white one with zero mean and unity standard devivation, and the center frequency of the band-pass filter is assumed to be equal to the scan frequency. R.J.F.

N85-22944# Joint Publications Research Service, Arlington, Va.
INTERFERENCE IMMUNITY OF BINARY SYSTEMS WITH SECOND-ORDER PHASE-DIFFERENCE MODULATION IN VARIOUS RECEPTION MODES Abstract Only **c32**
Yu. B. Okunev and L. M. Fink *In its* USSR Rept.: Electron. and Elec. Eng. (JPRS-UEE-85-002) 23 Jan. 1985 p 30 Transl. into ENGLISH from Radiotekhn. (Moscow), no. 8, Aug. 1984 p 3-8 (For primary document see N85-22907 13-33)
Avail: NTIS HC A05/MF A01

Reception of signals with binary second-order phase-difference modulation is analyzed for interference immunity in various channels with Gaussian noise and, on this basis, second-order phase-difference modulation is compared with first-order phase-difference modulation from the demodulator standpoint. In the case of a channel with deterministic or slowly fluctuating parameters and of correspondingly optimum coherent or quasi-coherent reception, the attainable interference immunity is the same for second-order phase-difference modulated signals as for first-order phase-difference modulated ones, even though errors are not bunched in pairs here but distributed over one element. Two simple demodulators of signals with single second-order phase-difference modulation are proposed for a channel with a widely fluctuating and non a priori estimable random frequency, and an absolutely invariant one with an interference limiting band-pass filter at the input and a relatively invariant one consisting of several parallel autocorrelation demodulators of first-order phase-difference modulated signals. R.J.F.

N85-22945# Joint Publications Research Service, Arlington, Va.
IONOSPHERIC DISTORTIONS OF DIGITAL SIGNALS WITH WIDEBAND MODULATION Abstract Only **c32**
I. M. Teplyakov *In its* USSR Rept.: Electron. and Elec. Eng. (JPRS-UEE-85-002) 23 Jan. 1985 p 31 Transl. into ENGLISH from Radiotekhn. (Moscow), no. 8, Aug. 1984 p 8-13 (For primary document see N85-22907 13-33)
Avail: NTIS HC A05/MF A01

Wideband digital signals for satellite communication systems, either pseudonoise signals with phase keying or coherent signals with frequency-time keying, are analyzed for distortions occurring during their propagation through the ionospheric waveguide and appearing in a coherently scanning receiver. Calculation of phase shifts and energy losses along the signal trajectory, taking into account the phase-frequency characteristic of an ionospheric layer with a frequency-dependent refractive index, reveals that phase distortions of such signals are caused by dispersiveness of the medium and fluctuation of the electron concentration along the path with resulting fluctuation of the signal arrival time. No distortion results, however, from the extra time delay associated with the linear component of the phase-frequency characteristic. As a specific example, an ionospheric layer with a statistically uniform and isotropic refractive index is considered, and a receiver with correlator or matched filter, in which case fluctuation of the signal arrival time can become predominant at low carrier frequencies corresponding to decimetric and metric waves. Author

N85-22946# Joint Publications Research Service, Arlington, Va.
COMPARATIVE ANALYSIS OF NOISE TOLERANCE OF QUASI-COHERENT PHASE SHIFT KEYING SIGNAL DEMODULATORS Abstract Only **c32**
V. Ye. Martirosov and N. N. Belousov *In its* USSR Rept.: Electron.

and Elec. Eng. (JPRS-UEE-85-002) 23 Jan. 1985 p 32 Transl. into ENGLISH from Elektrosvyaz (Moscow), no. 5, May 1984 p 48-50 (For primary document see N85-22907 13-33)
Avail: NTIS HC A05/MF A01

The noise tolerance of quasi-coherent PSK signal demodulators employing phase-locked loops to filter the reference oscillation is analyzed comparatively for the Siforof scheme, the Costas scheme, the reversible Karshin demodulator, the remodulator-comparator scheme and the adaptive demodulator scheme. The phase of reference oscillation in these quasi-coherent demodulators represents a random process, so that the phase error between the received and references signals is also random. It is found that increasing the initial frequency detuning reduces the noise tolerance of quasi-coherent PSK reception. The reversible and remodulation-comparator schemes have the poorest noise tolerance because of their steady-state phase error, which is twice that of the other schemes. When the frequency instability and amplitude of the received signal are high, it is best to use the adaptive demodulated structure. The formulas derived can be used to select the structure for a quasi-coherent PSK signal demodulator according to the required systemwide indicators of the digital transmission system, and to assess its noise tolerance during the design phase. Author

N85-22947# Joint Publications Research Service, Arlington, Va.
OPTIMUM PATH SELECTION IN AUTOMATED RADIO RELAY LINK DESIGN Abstract Only **c32**
O. S. Danilovich and V. N. Kichigin *In its* USSR Rept.: Electron. and Elec. Eng. (JPRS-UEE-85-002) 23 Jan. 1985 p 32 Transl. into ENGLISH from Elektrosvyaz (Moscow), no. 5, May 1984 p 15-19 (For primary document see N85-22907 13-33)
Avail: NTIS HC A05/MF A01

This study investigates the selection of the locations of radio relay stations so that the stability of the radio relay link satisfies the corresponding CCIR recommendations, so that the effective station construction and operation costs are minimized. A mathematical model for selecting the optimum radio relay link route is described. The construction of a hypothetical radio relay link 1400 km long with an average repeater section link of 50 km is analyzed as an example. The algorithm is shown to be especially effective for rough terrain where it is often impossible to place the stations close to roads. Author

N85-22948# Joint Publications Research Service, Arlington, Va.
CALCULATION OF AMPLITUDE-PHASE CHARACTERISTICS OF SIGNAL SCATTERED OBLIQUELY ON METEOR TRAIL Abstract Only **c32**
R. G. Khuzyashev *In its* USSR Rept.: Electron. and Elec. Eng. (JPRS-UEE-85-002) 23 Jan. 1985 p 34 Transl. into ENGLISH from Izv. Vysshikh Uchebn. Zavedeniy: Radiofiz. (Gorkiy), v. 27, no. 9, Sep. 1984 p 1110-1115 (For primary document see N85-22907 13-33)
Avail: NTIS HC A05/MF A01

Diffraction processes occurring during oblique incidence of a plane radio wave on a cylinder with an irregular radius are investigated for the case of the decaying of a meteor trail. The boundary problem for the differential equation of the functions of the radial coordinate is found and solved by reduction to a Cauchy problem. Expressions are derived for the amplitudes and phases of the reflection H- and E-waves in a cylindrical coordinate system. The behavior of the amplitude and phase of the reflected waves with both polarizations are investigated as a function of the angles theta, phi and the normalized radius. It is found that a rigorous solution of the wave equations for oblique incidence makes it possible to calculate the characteristics of the reflected signal more accurately than by the approximate method. Author

N85-22949# Joint Publications Research Service, Arlington, Va.
DOMAIN OF APPLICABILITY OF ASYMPTOTIC DESCRIPTION OF RADIO PULSE FIELDS NEAR CRITICAL FREQUENCY Abstract Only **c32**
Yu. I. Orlov and N. N. Fedorov *In its* USSR Rept.: Electron. and Elec. Eng. (JPRS-UEE-85-002) 23 Jan. 1985 p 34 Transl. into ENGLISH from Izv. Vysshikh Uchebn. Zavedeniy: Radiofiz. (Gorkiy), v. 27, no. 9, Sep. 1984 p 1130-1135 (For primary document see N85-22907 13-33)
Avail: NTIS HC A05/MF A01

Practical bounds for the applicability of asymptotic methods for investigating unsteady fields in the vicinity of the critical frequency are found. Numerical examples are presented to illustrate the validity of estimates for homogeneous and heterogeneous plasmas. The approximations of the space-time geometric theory of diffraction, and far-zone approximations, are examined for a homogeneous plasma, and then extended to a heterogeneous ionospheric layer. It is found that the applicability of asymptotic descriptions of the pulse envelopes agrees well with the estimates. This method for determining the conditions for the applicability of an asymptotic description of unsteady fields near the critical frequency can extended to signals with arbitrary amplitude-phase modulation. Author

N85-22950# Joint Publications Research Service, Arlington, Va.
SPECTRA OF INCIDENTAL INTERFERENCE RESULTING FROM NONLINEAR CONVERSION OF SIGNALS FROM TRANSMITTERS Abstract Only **c32**
B. G. Telezhnyy *In its* USSR Rept.: Electron. and Elec. Eng. (JPRS-UEE-85-002) 23 Jan. 1985 p 35 Transl. into ENGLISH from Radiotekhn. (Moscow), no. 8, Aug. 1984 p 46-47 (For primary document see N85-22907 13-33)
Avail: NTIS HC A05/MF A01

The interference spectrum resulting from nonlinear conversion of signals from n transmitters with single-band modulation, the most common kind of modulation, is evaluated on the basis of a quantitative correlation analysis. The characteristic of the nonlinear converter is approximated with a finite power series. It is shown that the width of the spectrum of incidental interference is readily calculated for each signal harmonic and any number of signals (transmitters) producing intermodulation interference. Author

N85-22951# Joint Publications Research Service, Arlington, Va.
METHOD OF SEPARATELY DETERMINING ELECTROPHYSICAL PROPERTIES OF BULKY CONDUCTOR Abstract Only
Yu. I. Steblev *In its* USSR Rept.: Electron. and Elec. Eng. (JPRS-UEE-85-002) 23 Jan. 1985 p 36 Transl. into ENGLISH from Elektrichestvo (Moscow), no. 8, Aug. 1984 p 41-45 (For primary document see N85-22907 13-33)
Avail: NTIS HC A05/MF A01

A method of determining the electrical conductivity and the magnetic permeability of bulky conductors such as plates or cylinders from field intensity measurements is described, the gist being to explicate each of these two parameters from the readings of electric field intensity and magnetic field intensity at the conductor surface or in a plane of symmetry. The method is based theoretically on Fourier-Bessel integral transformation of the differential field equations for the corresponding conductor medium. The integral relations are then mapped so as to yield the necessary relations between two field functionals and the space distributions of the electromagnetic field components. Further explication and numerical integration yield the ratio of calculated to measured conductivity and permeability. The procedure is demonstrated on a numerical example of a plane-parellel field above a heavy plate. Author

N85-22952# Joint Publications Research Service, Arlington, Va.
NOISE CHARACTERISTICS OF SULFUR-DOPED SILICON DIODES Abstract Only **c76**
Z. O. Mkhitaryan, R. S. Barsegyan, and V. M. Arutyunyan *In its* USSR Rept.: Electron. and Elec. Eng. (JPRS-UEE-85-002) 23 Jan. 1985 p 40 Transl. into ENGLISH from Izv. Vysshikh Uchebn. Zavedeniy: Radiofiz. (Gorkiy), no. 9, Sep. 1984 p 1218-1220 (For primary document see N85-22907 13-33)
Avail: NTIS HC A05/MF A01

The findings from an experimental investigation of the noise properties of sulfur-doped silicon p(+) - n - n(+) structures are presented. The frequency and current characteristics of the noise at 20 Hz to 20 KHz and temperatures of 77 and 300 K were

measured. The noise was amplified by a preamplifier and a narrowband selective amplifier, and were measured using an S4-48 spectrum analyzer. The silicon was doped with sulfur by diffusion. The noise characteristics were investigated at room temperature in the linear and initial quadratic sections of the voltage-current characteristic. Two plateaus were identified in the noise spectrum at room temperature. It is concluded from the form of the relationship between the spectral density of the current noise frequency and current passing through the diode that the noise occurring in sulfur-doped silicon structures is generation-recombination noise. Author

N85-22953# Joint Publications Research Service, Arlington, Va.
MEASUREMENT OF INTERNAL THERMAL RESISTANCE FOR QUALITY CONTROL OF SEMICONDUCTOR DEVICES Abstract Only **c76**
S. K. Zakharenko and Yu. G. Semenov *In its* USSR Rept.: Electron. and Elec. Eng. (JPRS-UEE-85-002) 23 Jan. 1985 p 41-42 Transl. into ENGLISH from Radiotekhn. (Moscow), no. 8, Aug. 1984 p 89-90 (For primary document see N85-22907 13-33)
Avail: NTIS HC A05/MF A01

A method of measuring the internal thermal resistance of semiconductor devices is proposed for purposes of quality control in mass production. This method eliminates the temperature chamber with or without a calibration curve and the measurement of the temperature dependence of heat-sensitive parameters in the existing methods. It involves comparative testing with an etalon device selected from a lot of 20 to 30 production samples and requires calculation of the mathematical expectation and the standard deviation of thermal resistance for the lot from the readings of thermal resistance between junction and case in each sample of the lot. The test circuit contains an 0-type galvanometer with an accept-reject scale, a thermocouple, three voltmeters, two ammeters, one microammeter, one single-pole two-position switch, one double-pole two-position switch, and nine resistors two of which are used for power equalizing. Measurements are made in the steady state, after a warm-up period (up to 15 min for power transistors). This method requires only half as many operations as the existing ones and a transistor is tested up to three times faster without sacrifice in precision. Author

N85-22954# Joint Publications Research Service, Arlington, Va.
MATHEMATICAL MODEL OF ELECTROMAGNETIC SUSPENSION DEVICE WITH TWO CONTROL WINDINGS Abstract Only
Yu. D. Vyshkov and B. A. Zhumagazin *In its* USSR Rept.: Electron. and Elec. Eng. (JPRS-UEE-85-002) 23 Jan. 1985 p 44 Transl. into ENGLISH from Elektrichestvo (Moscow), no. 8, Aug. 1984 p 73-74 (For primary document see N85-22907 13-33)
Avail: NTIS HC A05/MF A01

A mathematical model is constructed for description of an electromagnetic suspension device with two variable air gaps (II-core and keeper pivoted at center) with two control windings. The corresponding system of four differential equations, namely two equations of motion and two equations of Kirchhoff's second law for the two-loop electric circuit, are linearized in partial derivatives. Energy state functions analogous to thermodynamic state functions are introduced for relating forces and moments to gap widths and currents. The magnetic energy and the flux linkages are calculated on this basis, for subsequent evaluation of the resultant electromagnetic force as a function of the two currents and the space rates of change of self- and mutual inductances. M.G.

N85-22955# Joint Publications Research Service, Arlington, Va.
STATUS OF AND OUTLOOK FOR PRODUCING MEANS OF TRANSMITTING UNITS OF PLANE ANGLE, ANGULAR VELOCITY AND ACCELERATION WITH RING LASERS Abstract Only **c36**
B. E. Blanter, Ye. P. Krivtsov, D. P. Lukyanov, A. Ye. Sinelnikov, Yu. V. Filatov, and Yu. N. Shestopalov *In its* USSR Rept.: Electron. and Elec. Eng. (JPRS-UEE-85-002) 23 Jan. 1985 p 45-46 Transl. into ENGLISH from Izmeritel. Tekhn. (Moscow), no. 7, Jul. 1984 p 27-29 (For primary document see N85-22907 13-33)
Avail: NTIS HC A05/MF A01

The ring laser method of goniometry combines the universality and efficiency of the constant angular velocity method, while it eliminates the intracycle flutter in this otherwise very simple and stable method based on the direct proportionality of the angular displacement to the period of revolution and requiring only measurement of the time interval between two successive pulses. The transducer with a ring laser converts most accurately direct angle readings into electric signals, with attendant summation of beat signals produced by oppositely traveling waves during that interval between successive pulses. The performance of such a transducer is enhanced by addition of feedback for stabilization and of auxiliary other transducers for compensation of inevitable slow drift of the average angular velocity. The applications for such discrete laser goniometers extend now from gyro platform and turntables to production and calibration of instrument scales in manufacturing plants, typically of scales imprinted on metallic films and checked by direct recording of the interference patterns which waves of the ring laser produce. It can also be used for checking the position and the rotation of an object not kinematically coupled to the goniometer, with the aid of multifacet scanning prisms on a rotating platform. Author

N85-22956# Joint Publications Research Service, Arlington, Va.
OUTLOOK FOR REALIZATION OF PROXIMITY EFFECT AND JOSEPHSON DIRECT CURRENT IN HELIUM-2 Abstract Only **c76**
L. V. Kiknadze, Yu. G. Mamaladze, and O. D. Cheyshvili *In its* USSR Rept.: Electron. and Elec. Eng. (JPRS-UEE-85-002) 23 Jan. 1985 p 46 Transl. into ENGLISH from Izmeritel. Tekhn. (Moscow), no. 7, Jul. 1984 p 29-30 (For primary document see N85-22907 13-33)
Avail: NTIS HC A05/MF A01

Basic concepts and physical mechanisms are developed for predicting the possibility of a proximity effect and a Josephson direct current in liquid helium under conditions of superfluidity in the normal-state region. The proximity effect, a consequence of a continuous wave function, has real meaning only when the coherence radius is much larger than interatomic distances. In liquid helium the conditions are unfavorable for this, inasmuch as there is no other characteristic distance here besides the interatomic one, except when the density of the superfluid component decreases while the coherence radius increases. Such a stimulation of quantum-mechanical coherence by suppression of superfluidity is examined closer, particularly its temperature dependence and pressure dependence. The optimum conditions are established for direct-current superconduction through narrow channels or across microporous barriers, such a flow contributing to suppression of superfluidity. The critical or maximum possible Josephson current is calculated on the basis of these concepts. The underlying Ginzburg-Pitayevskiy theory is applied to two cases important from the standpoint of development of squids. The corresponding second-order cubic differential equation of equilibrium is formulated and solved numerically first for liquid helium in a gravitational field and then for the Josephson effect in a porous barrier between two free volumes of helium-2. M.G.

N85-22957# Joint Publications Research Service, Arlington, Va.
COMPARISON REFERENCE ETALON OF UNIT LASER RADIATION POWER Abstract Only **c36**
I. N. Govor, A. V. Kubarev, and V. V. Ozolin *In its* USSR Rept.: Electron. and Elec. Eng. (JPRS-UEE-85-002) 23 Jan. 1985 p 47 Transl. into ENGLISH from Izmeritel. Tekhn. (Moscow), no. 7, Jul. 1984 p 34-35 (For primary document see N85-22907 13-33)
Avail: NTIS HC A05/MF A01

An etalon was developed for comparing national secondary and governmental primary standards of laser radiation power. It contains, in addition to two reference instrument transducers operating by different principles and having different spectral characteristics, a laser source emitting at the 0.63 micron wavelength with high power stability, a recording instrument, a calibrating instrument, and signal shaping-checking circuits. The

first reference transducer is a nonselective calorimetric one, a model of a black body consisting of two parallel conical copper shells with a 15 deg taper inserted one inside the other with two thin-film equivalent resistors between them. The second reference transducer is a precise photothermoelectric one for comparison of standard with similar spectral and space distributions of the radiation power, also for checking the performance of the calorimetric reference transducer. It consists of a photoelectric cell and a thermoelectric cell in thermal contact with one another through an integrating sphere on which they are placed not far apart. An auxiliary photodiode is provided for checking the radiation power level after it has stabilized. The instability of this etalon does not exceed 0.5 x 10 to the -4th power during 1 hour. Author

N85-22958# Joint Publications Research Service, Arlington, Va.
MEASURING INTENSITY OF ELECTRIC FIELD PRODUCED BY ELECTROMAGNETIC PULSE WITH AID OF ACTIVE PROBES Abstract Only
Yu. I. Buyanov, E. A. Gostishchev, V. B. Ponomarev, A. V. Samoylik, and N. I. Yagushkin *In its* USSR Rept.: Electron. and Elec. Eng. (JPRS-UEE-85-002) 23 Jan. 1985 p 47-48 Transl. into ENGLISH from Izmeritel. Tekhn. (Moscow), no. 7, Jul. 1984 p 50-51 (For primary document see N85-22907 13-33)
Avail: NTIS HC A05/MF A01

The performance of wideband active probes for measuring the electric field of a weak electromagnetic pulse within the Fraunhofer region of a strong radiation source is evaluated in terms of the proportionality factor between the electric field intensity and the voltage across the probe load, this factor also being the equivalent gauge length of such a probe. Such a probe is usually made of a thin wire segment, placed above a metal surface perpendicular to it, and connected at the lower end through a cable to an impedance load. The current distribution along such a probe is calculated by the method of superposition of traveling waves, whereupon the equivalent gauge length is determined in terms of actual geometrical dimensions and electrical circuit parameters. For a capacitive load with a very large time constant this gauge length does not depend on the frequency of incoming signals. Moreover, in the usual cases of a load capacitance much larger than the stray probe to earth capacitance, the load voltage is directly proportional to the quantity (h + 1/2 l)l (h- length of connecting cable in the field of the electromagnetic pulse, l- actual length of probe) and the probe behaves like a miniature antenna with top feed. Author

N85-22959# Joint Publications Research Service, Arlington, Va.
SQUARE-PULSE GENERATOR Abstract Only
L. Teslenko *In its* USSR Rept.: Electron. and Elec. Eng. (JPRS-UEE-85-002) 23 Jan. 1985 p 49-50 Transl. into ENGLISH from Radio (Moscow), no. 7, Jul. 1984 p 28-30 (For primary document see N85-22907 13-33)
Avail: NTIS HC A05/MF A01

A square pulse generator is described which consists of a master oscillator and a kipp oscillator, the former controlling the pulse repetition period over the 2 x 10 to the -7th power/10 sec range and the latter controlling the pulse duration period over the 5 x 10 to the -8th power/5 sec range. This eliminates the problem of separately varying both, which is not possible in conventional square pulse generators. Addition of a polarity and amplitude regulation from zero to maximum, not limited by the low input impedance of TTL circuits and the consequently low resistance of the time delaying variable resistor. Using a transistor switch in the master oscillator minimizes the effect of temperature and supply voltage fluctuations on the pulse characteristics. Such a generator can be used for tuning digital and other pulse devices with positive, negative, or bipolar supply voltage. Its characteristics are maximum pulse rise time 40 ns across a 100 pF load capacitor at the TTL output and 100 ns at the universal output; maximum pulse fall time 30 ns across a 100 pF load capacitor at the TTL output and 300 ns across the universal output; minimum load resistance across the TTL output for a 2.4 V pulse amplitude 240 ohm; maximum pulse amplitude across a 10 kohm load resistance at the universal output +/- 14 V. M.G.

N85-22960# Joint Publications Research Service, Arlington, Va.
SIMPLE SWEEP FREQUENCY GENERATOR Abstract Only
I. Yegorov *In its* USSR Rept.: Electron. and Elec. Eng. (JPRS-UEE-85-002) 23 Jan. 1985 p 50-51 Transl. into ENGLISH from Radio (Moscow), no. 7, Jul 1984 p 31-32 (For primary document see N85-22907 13-33)
Avail: NTIS HC A05/MF A01

A sweep frequency generator is described whose center frequency can be varied from 10 kHz to 50 MHz, with seven 1 to 3 and 3 to 10 scales covering the 10 kHz to 30 MHz range and one 3 to 5 scale for the 30 to 50 MHz range. It consists of a tunable pulse generator with output voltage attenuator, a diode mixer for calibration, and a sawtooth voltage generator as a source of frequency deviation. The pulse generator is a multivibrator with two emitter coupled transistors and two diodes in the collector circuit of one. The first diode extends the tuning range and increases the frequency deviation, the second diode provides the necessary base bias to the other transistor. The pulse repetition rate is modulated either directly by the sweep voltage of the calibrating oscilloscope, this voltage being applied to the base of the transistor with the two diodes in its collector circuit through an additional attenuator or a special emitter follower, or by the separate sawtooth voltage generator. The latter is a conventional two transistor multivibrator and produces signals at any constant frequency within the 40 to 60 Hz range. The mixer receives unmodulated signals from a reference frequency source and produces different frequency signals which are sent through an RCR-filter to a calibrating oscilloscope. Author

N85-22961# Joint Publications Research Service, Arlington, Va.
OPTICAL REFLECTOMETER FOR MULTIMODE FIBER LIGHTPIPES Abstract Only **c74**
Yu. V. Vvedenskiy, Yu. M. Gryaznov, A. B. Zuyev, and Yu. Ye. Spirichev *In its* USSR Rept.: Electron. and Elec. Eng. (JPRS-UEE-85-002) 23 Jan. 1985 p 52 Transl. into ENGLISH from Izmeritel. Tekhn. (Moscow), no. 9, Sep. 1984 p 30-32 (For primary document see N85-22907 13-33)
Avail: NTIS HC A05/MF A01

A simple optical reflectometer is described for localizing damage in lightpipes and measuring losses by the backscattering method. The structural diagram of the reflectometer, which utilizes no scarce optical components, is presented. The light pulse from a radiation source is fed through a directional coupler into the fiber being investigated. The reflected signals are extracted by the coupling devices and input to a photodetector, after which they are displayed on a screen consisting of an R5-11 line irregularity meter. The optical source employed is a 32 DL-101 laser diode. A photomultiplier tube is employed as the photodetector. The optical system of the device is easy to fabricate and align, and employs no fiber optic coupler. The possibility of working with any type of multimode fiber makes the device convenient for various research operations in fiber optics. Author

N85-22962# Joint Publications Research Service, Arlington, Va.
LIQUID MASS FLOW RATE COMPUTER Abstract Only **c35**
N. N. Antov, V. A. Troynikov, and V. C. Sotnikov *In its* USSR Rept.: Electron. and Elec. Eng. (JPRS-UEE-85-002) 23 Jan. 1985 p 53 Transl. into ENGLISH from Izmeritel. Tekhn. (Moscow), no. 9, Sep. 1984 p 35-36 (For primary document see N85-22907 13-33)
Avail: NTIS HC A05/MF A01

A flow rate computer is proposed which implements an algorithm for dividing the volumetric flow rate, measured by a turbine flow meter, into the signal from the liquid flow velocity head meter signal (the device actually measures the axial force acting upon the turbine, rather than the velocity Head). The block diagram of the device is presented and traced. The accuracy with which the numerator, denominator and their ratio are calculated and multiplied by the constant is limited by the corresponding digitization errors, which can be reduced to the required level by selecting the measurement interval. The choice of measurement interval is not affected by dispersion of the parameters of the transducers, which makes it possible to use the same inverval for

different transducers. The device permanently scores all transducer parameters in memory, which permits them to be corrected in accordance with test results. Author

N85-22963# Joint Publications Research Service, Arlington, Va.
METROLOGICAL SUPPORT FOR REMOTE TRANSPORT VEHICLE SPEEDOMETERS Abstract Only **c35**
A. Ye. Ksenzenko and V. I. Matveyev *In its* USSR Rept.: Electron. and Elec. Eng. (JPRS-UEE-85-002) 23 Jan. 1985 p 53 Transl. into ENGLISH from Izmeritel. Tekhn. (Moscow), no. 9, Sep. 1984 p 38-39 (For primary document see N85-22907 13-33)
Avail: NTIS HC A05/MF A01

The S-2M bench used to calibrate the Bar'yer-2 and Bar'yer remote speedometers, which operate in the 3 centimeter waveband, is described. The device can simulate the simultaneous movement of several vehicles and allows their speeds and distances to be programmed independently and accurately. This makes it possible to set up complicated calibration conditions, including the simulated passing of one vehicle by another. The range of simulated speeds is wider than that in similar devices, and a wide class of interfering factors can be simulated. High calibration accuracy is ensured by employing embedded self calibration means which are controlled centrally with minimum operator intervention. The block diagram of the device is presented and analyzed; operating procedures are explained. The S-2M bench has been certified and recommended for commercial production. Author

N85-22964# Joint Publications Research Service, Arlington, Va.
USE OF ELECTRONIC CODING-FREQUENCY METERS TO MEASURE PARAMETERS OF PULSED RADIO SIGNALS Abstract Only **c35**
A. P. Pokhilyuk *In its* USSR Rept.: Electron. and Elec. Eng. (JPRS-UEE-85-002) 23 Jan. 1985 p 55 Transl. into ENGLISH from Izmeritel. Tekhn. (Moscow), no. 9, Sep. 1984 p 53-54 (For primary document see N85-22907 13-33)
Avail: NTIS HC A05/MF A01

An expression is derived for calculating the combined additional error in measuring the frequency, period and frequency ratio of pulsed signals. The types of modifications which must be made to the structural diagram of the electronic counting frequency meter in order to facilitate measurement of the phase shift between radio pulses, the relative pulse duration and the carrier frequency of the modulating oscillation are described. It is found that the addition of a phase shift carrier frequency converter to the electronic counting frequency meter makes it possible to measure the phase offset between two signals. This converter incorporates two amplifier limiters and an exclusive OR gate, or a flip-flop converter. The use of a gating and envelope extraction device makes it possible to measure the parameters of the modulating pulse train: pulse and pause duration, period, carrier frequency, relative duration, etc. By updating commercially produced frequency meters it becomes possible, at low expense, to use them to measure the parameters of the carrier of pulsed radio signals with little additional error. Author

N85-22965# Joint Publications Research Service, Arlington, Va.
EFFECT OF VARIANCE OF PHOTORECEIVER FREQUENCY CHARACTERISTICS ON CHARACTERISTICS OF MEASURING INSTRUMENTS Abstract Only **c35**
R. B. Shemshedinov and V. F. Kaleganov *In its* USSR Rept.: Electron. and Elec. Eng. (JPRS-UEE-85-002) 23 Jan. 1985 p 56 Transl. into ENGLISH from Radiotekhn. (Moscow), no. 8, Aug. 1984 p 79-81 (For primary document see N85-22907 13-33)
Avail: NTIS HC A05/MF A01

Because variance of the amplitude frequency characteristic of photoreceivers in optoelectronic measuring in instruments is a major factor which destabilizes the performance of such instruments, the effect of this variance on signal detectability and resolution is evaluated for design purposes. The signal to noise ratio at the photoreceiver output is calculated for a photoreceiver which consists of a pulse signal amplifier and a detector, assuming that under certain conditions such as a changing ambient temperature its transfer function differs from the optimum one by a certain scale factor. The results for a Gaussian input signal indicate that the amplifier stage and the variance of its amplitude frequency characteristic play the dominant role in degrading the instrument performance, the maximum signal to noise ratio being decreased and the signal waveform being changed in terms of shifting peaks and zero crossovers. Consequently, the point by which the signal arrival time is recorded also shifts and the signal time resolution becomes worse. Adaptive measures are recommended for compensating these effects of variance, such as temperature sensitive automatic bandwidth regulation in the photoreceiver and automatic threshold regulation in the amplitude discriminator. Author

N85-22966# Joint Publications Research Service, Arlington, Va.
PARAMETERS OF AMPLITUDE-MODULATED SIGNAL UPON REFLECTIONS Abstract Only **c74**
G. V. Merkishin *In its* USSR Rept.: Electron. and Elec. Eng. (JPRS-UEE-85-002) 23 Jan. 1985 p 56-57 Transl. into ENGLISH from Radiotekhn. (Moscow), no. 8, Aug. 1984 p 21-23 (For primary document see N85-22907 13-33)
Avail: NTIS HC A05/MF A01

Reflection of a coherent optical signal with amplitude modulation by two specularly reflecting surfaces is analyzed, such signals being used for measurement of distances between objects by interference methods. The parameters of the signal recorded by a square law photodetector in the Fraunhofer region are calculated, assuming that the radiant flux intensity varies harmonically in time and that the reflection coefficient at the farther surface is equal to or smaller than the reflection coefficient at the nearer one. Both amplitude and phase of the fundamental modulation frequency component of the photodetector current are found to depend on the location of the photodetector in the plane of interference and on the distance between objects. Both this distance and the photodetector aperture are assumed to be much smaller than the distance from the photodetector to the nearer object. Consequently, the maximum and minimum amplitudes and corresponding phases of the photodetector current carry information about the distance between two objects. In practice it is more expedient to measure the space time parameters of the interference pattern with a linear array of low sensitivity photodetectors rather than with a single one. Author

N85-22967# Joint Publications Research Service, Arlington, Va.
COUPLED-CAVITY GYROTRONS WITH MODE CONVERSION Abstract Only
V. Ye. Zapevalov, S. A. Malygin, V. G. Pavelyev, and Sh. E. Tsimring *In its* USSR Rept.: Electron. and Elec. Eng. (JPRS-UEE-85-002) 23 Jan. 1985 p 57 Transl. into ENGLISH from Izv. Vysshikh Uchebn. Zavedeniy: Radiofiz. (Gorkiy), v. 27, no. 9, Sep. 1984 p 1194-1201 (For primary document see N85-22907 13-33)
Avail: NTIS HC A05/MF A01

The start up characteristics and steady state characteristics of gyrotrons incorporating coupled cavities and mode conversion are analyzed for the approximation of a fixed high frequency field structure. The results are presented of experiments with gyrotrons at the second harmonic of the cyclotron frequency employing coupled cavities with modes H4,1,1-H4,2,1. Experiments with two types of coupled cavity gyrotrons are described. The findings indicate that highly efficient gyrotrons employing coupled cavities and mode conversion can be implemented. The good agreement between the calculated and experimental characteristics indicate that the methods used to design the electrodynamic system are sufficiently accurate, and that the output parameters can be estimated with the approximation of a fixed high frequency field structure. Author

N85-22968# Joint Publications Research Service, Arlington, Va.
ABSORPTION OF RADIATION BY WATER VAPOR IN WINDOWS OF RELATIVE TRANSPARENCY OF 95-145 MICROMETER RANGE Abstract Only **c32**
B. A. Sverdlov and N. I. Furashov *In its* USSR Rept.: Electron. and Elec. Eng. (JPRS-UEE-85-002) 23 Jan. 1985 p 57-58 Transl. into ENGLISH from Izv. Vysshikh Uchebn. Zavedeniy: Radiofiz. (Gorkiy), v. 27, no. 9, Sep. 1984 p 1087-1095 Original language

document was announced in IAA as A85-15026 (For primary document see N85-22907 13-33)
Avail: NTIS HC A05/MF A01

The results of spectrometric measurements and theoretical calculations of the absorption coefficients for pure and atmospheric water vapor in six submillimeter windows of relative transparency are compared. It is found that in all the windows the measured absorption exceeded the theoretically calculated values by about 1.14. For pure water vapor the divergence was even larger. The divergence is compared with data from a number of other studies and is found to be in agreement. Some recommendations are offered for reducing the discrepancy in order to obtain more accurate data. I.H. (IAA)

N85-22969# Joint Publications Research Service, Arlington, Va.
MAGNETIC NOISE IN SINGLE-MACHINE ROTATING FREQUENCY CONVERTERS Abstract Only
V. I. Popov *In its* USSR Rept.: Electron. and Elec. Eng. (JPRS-UEE-85-002) 23 Jan. 1985 p 59 Transl. into ENGLISH from Elektrichestvo (Moscow), no. 9, Sep. 1984 p 38-43 (For primary document see N85-22907 13-33)
Avail: NTIS HC A05/MF A01

The magnetic noise in rotating frequency converters with two magnetic fields in a common structure of an induction machine, each field having a different number of pole pairs corresponding to the frequency conversion ratio, is evaluated on the basis of harmonic analysis of the resultant magnetic induction in the air gap and the radial forces it generates. The rotor in small and medium-size machines is regarded as a solid cylinder so that the hollow stator cylinder remains the principal source of noise. Constraints on the numbers of stator slots and rotors slots are established so as to ensure minimum higher-frequency tooth noise and vibration, while structural requirements are stipulated for minimizing lower-frequency noise and vibration and avoiding resonances at any frequency. Typical design calculations for a three-phase motor-generator machine operating at 1:3 frequency converter are shown, including the amplitudes of design-controlled vibrations of magnetic origin. Author

N85-22970# Joint Publications Research Service, Arlington, Va.
PLAYBACK AMPLIFIER WITH HIGH INTERFERENCE IMMUNITY Abstract Only
V. Dudik *In its* USSR Rept.: Electron. and Elec. Eng. (JPRS-UEE-85-002) 23 Jan. 1985 p 59-60 Transl. into ENGLISH from Radiotekhn. (Moscow), no. 7, Jul. 1984 p 46 (For primary document see N85-22907 13-33)
Avail: NTIS HC A05/MF A01

A method of improving the interference immunity of a playback amplifier is proposed which has already been successfully applied to the Mayaka-202 portable tape recorder. The input stage of the amplifier, consisting of a linear one-transistor circuit and an operational amplifier with frequency-dependent negative feedback, is placed separately from the next stages in the immediate vicinity of the playback head. It may even not be necessary to shield the printed-circuit board which carries the amplifier input stage alone, shielding being necessary when all amplifier stages are mounted on one printed-circuit board. The interstage connecting cable is now 300 mm long but carries a 15 to 25 mV signal rather than a 0.3 to 0.5 mV one so that the relative pickup level is reduced by a factor equal to the transistor gain, while the cable to the playback head is now only 30 to 40 mm long so that the interference level drops by as much as 14 dB. The method is equally applicable to tape recorders with feedthrough channel and to plain tape phonographs. Author

N85-22971# Joint Publications Research Service, Arlington, Va.
SIMPLE DETONATION METER Abstract Only **c35**
N. Sukhov *In its* USSR Rept.: Electron. and Elec. Eng. (JPRS-UEE-85-002) 23 Jan. 1985 p 60 Transl. into ENGLISH from Radiotekhn. (Moscow), no. 7, Jul. 1984 p 40-42 (For primary document see N85-22907 13-33)
Avail: NTIS HC A05/MF A01

A new instrument for measuring the detonation factor (sound distortion caused by parasitic frequency modulation within the 0.2 to 200 Hz range) has been built with only three transistors and two microcircuit chips, but it performs as well as the existing commercial 41 instrument. This instrument can operate from any unipolar 14 + or - 1 V d.c. source with a voltage ripple not exceeding 0.5 mV, drawing a maximum current of 25 mA. Its alignment and calibration require only a d.c. voltmeter with 10 kohm/V input resistance and a 3150 Hz sine-wave or square-wave generator. It can then be used for checking tape recorders with the use of test tapes already carrying phonograms of 3150 Hz signals. Three readings must be taken, at the beginning and at the end of a cassette or spool as well as somewhere in the middle, the highest reading being the conclusive one. The detonation factor in the test tape must be smaller than one third of the measured one. The instrument can also be used without test tapes, but the procedure is then more laborious. G.L.C.

N85-22972# Joint Publications Research Service, Arlington, Va.
THREE-MIRROR OPEN RESONATOR FOR MILLIMETER WAVE BAND Abstract Only **c32**
A. A. Vertiy, N. A. Popenko, Yu. P. Popkov, and S. I. Tarapov *In its* USSR Rept.: Electron. and Elec. Eng. (JPRS-UEE-85-002) 23 Jan. 1985 p 61 Transl. into ENGLISH from Izv. Vysshikh Uchebn. Zavedeniy: Rasiofiz. (Gorkiy), v. 27, no. 6, Jun. 1984 p 775-781 (For primary document see N85-22907 13-33)
Avail: NTIS HC A05/MF A01

The fixed characteristics of an open resonator having a prism with total internal reflection with dielectric specimens located nearby are investigated experimentally and theoretically (in a plane wave approximation). It is found that the determination of the special characteristics of a three-mirror open resonator in plane-wave approximation can be extended to the case of open resonators with spherical mirrors. The experimental and theoretical results agree to within 7% for an open resonator with a dielectric half-plane. It is found that the measurement sensitivity increases as the sighting parameter becomes smaller, but that the Q-factor of the oscillation drops off sharply when the dielectric half-plane is less than 0.3 mm from the facet of the prism. Author

N85-22973# Joint Publications Research Service, Arlington, Va.
APPLICATION OF K176-SERIES MICROCIRCUITS Abstract Only
S. Alekseyev *In its* USSR Rept.: Electron. and Elec. Eng. (JPRS-UEE-85-002) 23 Jan. 1985 p 61 Transl. into ENGLISH from Radiotekhn. (Moscow), no. 6, Jun. 1984 p 32-35 (For primary document see N85-22907 13-33)
Avail: NTIS HC A05/MF A01

The characteristics of the K176IYe18 microcircuit are analyzed by an example of an alarm clock in which the alarm is driven by a special audio signal generator provided by the microcircuit. The schematic diagram of the clock is presented and traced. The K176IY317 microcircuit is also described: this device serves as a calendar which counts the days of the week and month. A schematic diagram showing the connection of the day-date microcircuit to the clock is presented. The adjustment and setting of the clock and calendar are explained. Author

N85-22974# Joint Publications Research Service, Arlington, Va.
EXTRACTION OF SURFACE-WAVE ENERGY FROM PLASMA WAVEGUIDE Abstract Only **c75**
G. I. Zaginaylov, A. N. Kondratenko, and V. M. Kuklin *In its* USSR Rept.: Electron. and Elec. Eng. (JPRS-UEE-85-002) 23 Jan. 1985 p 62 Transl. into ENGLISH from Izv. Vysshikh Uchebn. Zavedeniy: Radiofiz. (Gorkiy), v. 27, no. 9, Sep. 1984 p 1178-1184 (For primary document see N85-22907 13-33)
Avail: NTIS HC A05/MF A01

The possibility of extracting surface-wave energy from a plasma waveguide as the result of scattering on an abrupt irregularity in the permittivity is examined. The scattered field is expressed in the general case through an infinite number of constants which satisfy two infinite systems of algebraic equations. Several important special cases capable of approximate solution are analyzed. It is found that the radiated power increases with

an increase in the phase velocity of the incident wave in all cases considered; the maximum of the directivity pattern shifts to the region of small angles of inclination with respect to the axis of the waveguide. It is determined analytically that the power and directivity of the radiation for a thin layer can vary widely as a function of the frequency of the incident wave, the density of the plasma and the thickness of the layer. The findings may be helpful in radio electronics, plasma diagnosis and the development of surface-wave antennas based on plasma waveguides. Author

N85-22975# Joint Publications Research Service, Arlington, Va.
INTENSITY FLUCTUATIONS OF FOCUSED LASER BEAM DURING REFLECTION IN TURBULENT ATMOSPHERE Abstract Only c36
V. V. Boronoyev, V. D. Dashinimayev, G. I. Zandanova, V. N. Poplaukhin, and E. A. Trubacheyev *In its* USSR Rept.: Electron. and Elec. Eng. (JPRS-UEE-85-002) 23 Jan. 1985 p 65 Transl. into ENGLISH from Izv. Vysshikh Uchebn. Zavedeniy: Radiofiz. (Gorkiy), v. 27, no. 6, Jun. 1984 p 810-812 (For primary document see N85-22907 13-33)
Avail: NTIS HC A05/MF A01

The relative dispersion of intensity fluctuations in a reflected focused laser beam are investigated experimentally as a function of the diffraction parameter of a transmitter, the type of reflector and the intensity of the turbulence along the propagation path. The measurements were made on a uniform horizontal path 300 m long with simultaneous optical measurements of the structural characteristic of the fluctuations in the index of refraction of the air. It is found that the dispersion of the intensity fluctuations in a narrow beam exceeds the corresponding quantity in a wider beam, as is the case for a collimated beam. The saturation level of the relative dispersion of the intensity fluctuations of the reflected focused beam is closed to the saturation level of relative dispersion in a spherical wave. This is apparently because a spherical wave reaches the receiver after the focused beam is reflected. The direct and reflected waves cover the entire distance from the transmitter to the receiver without passing through correlated atmospheric irregularities. The relative dispersion of the intensity fluctuations of a reflected focused laser beam is found to depend upon the diffraction parameter of the radiating aperture, as well as the type of reflector, as in the case for a collimate beam.
Author

N85-22976# Joint Publications Research Service, Arlington, Va.
USSR REPORT: ELECTRONICS AND ELECTRICAL ENGINEERING
9 Jan. 1985 100 p refs Transl. into ENGLISH from various Russian articles
(JPRS-UEE-85-001) Avail: NTIS HC A05/MF A01

Abstracts of articles addressing various topics in electronics and electrical engineering are presented. Subject areas include: antennas and propagation, communications, circuits and systems, commuters, electron devices, microwave techniques, magnetics, industrial electronics and control instrumentation, quantum electronics/electro-optics, and energy and transportation engineering. For individual titles, see N85-22977 through N85-23053.

N85-22977# Joint Publications Research Service, Arlington, Va.
INTERFERENCE FLUX DURING REFLECTION OF HETEROGENEOUS WAVES Abstract Only c32
K. N. Bakinovskiy, A. I. Kirilenko, and A. D. Titov *In its* USSR Rept.: Electron. and Elect. Eng. (JPRS-UEE-85-001) 9 Jan. 1985 p 1 Transl. into ENGLISH from Izv. Vysshikh Uch. Zaved.: Radiofiz. (USSR), v. 27, no. 7, Jul. 1984 p 948 (For primary document see N85-22976 13-33)
Avail: NTIS HC A05/MF A01

The incidence of an electrically polarized wave on the interface boundary between two absorbing media is examined for the case in which reflection and transmission are accompanied by conversion of the polarization (wave types); the coupling of the wave amplitudes at the boundary is described by 2 x 2 reflection and transmission matrices. The incident wave is assigned on a polarization basis which makes it fairly simple to determine the properties of non-coplanar reflection of heterogeneous waves when the phase normal vector, the amplitude normal vector and normal to the interface boundary is examined. The occurrence of two kinds of interference fluxes is noted. The first is generally associated with the interference between incident and reflected waves of the same types (polarization), while the second is caused by the superimposition of different types of waves. Author

N85-22978# Joint Publications Research Service, Arlington, Va.
ABSOLUTE MEASUREMENTS OF RADIATION INTENSITY FROM CASSIOEIE-A, CYGNUS-A AND CRAB NEBULA IN 60-100 cm BAND Abstract Only c89
M. Y. Miller *In its* USSR Rept.: Electron. and Elect. Eng. (JPRS-UEE-85-001) 9 Jan. 1985 p 1-2 Transl. into ENGLISH from Izv. Vysshikh Uch. Zaved.: Radiofiz. (USSR), v. 27, no. 7, Jul. 1984 p 934-938 (For primary document see N85-22976 13-33)
Avail: NTIS HC A05/MF A01

The title measurements made during August to October 1982 at the Staraya Pustyn polygon of NIRFI (Scientific-Research Radio Physics Institute) are described. The measurements were made with a 5 meter black disk in the Fresnel zone of a 12 meter radiotelescope. The disk, which filled a solid angle of 60 deg 7 min and stood at an angle of 20 deg to the horizon, was placed on a 25 meter tower 42 meters from the aperture plane of the radiotelescope. The radiation from the source was received with the radio focused at infinity. The following experimental parameters are tabulated: source flux, wavelength, diffraction correction, diffraction correction error, error in increment of calibration standard temperature, error determined by random sensitivity threshold, and a combined mean square measurement error. Spectra are plotted for Cassiopeia-A, Cygnus-A and the Crab Nebula. Author

N85-22979# Joint Publications Research Service, Arlington, Va.
AXIAL FOCUSING OF SIGNAL FROM DISTANT POINT RADIATOR REFLECTED TWICE IN DEEP PARABOLOID Abstract Only c32
M. I. Fayngaold *In its* USSR Rept.: Electron. and Elect. Eng. (JPRS-UEE-85-001) 9 Jan. 1985 p 2 Transl. into ENGLISH from Izv. Vysshikh Uch. Zaved.: Radiofiz. (USSR), v. 27, no. 7, Jul. 1984 p 944-947 (For primary document see N85-22976 13-33)
Avail: NTIS HC A05/MF A01

Double reflection of a signal in a deep paraboloid is investigated for the general case in which the incident signal source is on the optical axis of the reflector at a finite distance so that the incident wave is spherical. It is found that even slight divergence of the incident radiation disturbs the structure of the exiting beam significantly; however, the axial focusing is retained and may even increase causing, inter alia, the occurrence of a second volumetric focus outside the paraboloid. The possibility of exploiting the corresponding effects is discussed. The problem is investigated in beam approximation; the diffraction effect is taken into account along the axis, where the beam approximation does not apply.
Author

N85-22980# Joint Publications Research Service, Arlington, Va.
INVESTIGATION OF GENERATION OF OSCILLATIONS USING ANOMALOUS DOPPLER EFFECT Abstract Only c32
D. V. Gorozhanin, B. I. Ivanov, and M. I. Kapchinskiy *In its* USSR Rept.: Electron. and Elect. Eng. (JPRS-UEE-85-001) 9 Jan. 1985 p 3 Transl. into ENGLISH from Izv. Vysshikh Uch. Zaved.: Radiofiz. (USSR), v. 27, no. 7, Jul. 1984 p 880-891 Original language document announced as A84-48155 (For primary document see N85-22976 13-33)
Avail: NTIS HC A05/MF A01

A nonrelativistic beam device was used to generate slow cyclotron waves via the anomalous Doppler effect. The generation is shown to be accompanied by an increase in the energy of the transverse motion of the electron beam. Particular consideration is given to an investigation of the relationship between the total energy of the cyclotron wave and the kinetic energy of the transverse motion. A simple form of this relationship is established theoretically and experimentally; irrespective of the beam configuration and the type of excited cyclotron mode, it is equal to the

ratio of the wave frequency to the electron cyclotron frequency.
L.M. (IAA)

N85-22981# Joint Publications Research Service, Arlington, Va.
TIME SPECTRA OF INTENSITY FLUCTUATIONS ALONG REFLECTING PATH Abstract Only **c74**
Y. A. Monastyrnyy, G. Y. Patrushev, A. I. Petrov, and V. V. Pokasov *In its* USSR Rept.: Electron. and Elect. Eng. (JPRS-UEE-85-001) 9 Jan. 1985 p 3-4 Transl. into ENGLISH from Izv. Vysshikh Uch. Zaved.: Radiofiz. (USSR), v. 27, no. 7, Jul. 1984 p 907-912 Original language document announced as A84-48158 (For primary document see N85-22976 13-33)
Avail: NTIS HC A05/MF A01

Results are presented of synchronous measurements of time spectra of intensity fluctuations of light beams with different diffraction dimensions along straight and lidar-sounding paths with reflection from a mirror disk and a corner cube reflector. The differences are found to be especially significant for a spherical wave reflected from a flat mirror (owing to the fluctuation amplification effect) and for a narrow collimated beam during reflection from the corner. As compared with calculation results, the experimental spectra are found to be wider and their peaks are smaller under constant-wind conditions, which is explained by magnitude of intensity fluctuations and the velocity of the wind transport of optical irregularities. L.M. (IAA)

N85-22982# Joint Publications Research Service, Arlington, Va.
TEMPERATURE DEPENDENCE OF PROPAGATION OF HIGH-CURRENT ELECTRON BEAM THROUGH DRIFT SPACE Abstract Only **c72**
M. A. Vlasov, I. P. Denisova, and S. V. Nikonov *In its* USSR Rept.: Electron. and Elect. Eng. (JPRS-UEE-85-001) 9 Jan. 1985 p 4 Transl. into ENGLISH from Radiotekh. i Elektron. (USSR), v. 29, no. 8, Aug. 1984 p 1595-1599 (For primary document see N85-22976 13-33)
Avail: NTIS HC A05/MF A01

Propagation of a cold high-current electron beam with cylindrically symmetric neutralization through the drift space is analyzed, taking into account nonisochronous betratron oscillations and resulting collisionless relaxation during intermixing of particle trajectories. The dependence of that relaxation and of the equilibrium state on the initial temperature is determined, assuming an isotropic initial temperature distribution. The distribution of transverse velocity components is assumed to become anisotropic, as a result of radial motion of electrons and attendant fluctuations of the beam radius about some average. The corresponding second-order differential equation is a cylindrical system of coordinates is solved numerically by the method of coaxial current tubes with appropriate boundary conditions. The results agree closely with theoretical analysis of the transient process. Author

N85-22983# Joint Publications Research Service, Arlington, Va.
MODELS OF DISCONTINOUS RANDOM FIELDS Abstract Only **c32**
V. Y. Kontrovich *In its* USSR Rept.: Electron. and Elect. Eng. (JPRS-UEE-85-001) 9 Jan. 1985 p 4-5 Transl. into ENGLISH from Radiotekh. i Elektron. (USSR), v. 29, no. 8, Aug. 1984 p 1551-1554 (For primary document see N85-22976 13-33)
Avail: NTIS HC A05/MF A01

When the theory of state variables is applied to optimal synthesis of signal processing devices in space-time channels, it becomes necessary to simulate signals and interference with stochastic partial differential equations. Models of interference are discontinuous random fields, typically with a Poisson distribution. Stochastic partial differential equations generating such fields as their solution include a linear equation, wave equations such as those describing propagation through randomly nonhomogeneous media, and Kollmogorov-Feller equations corresponding to point or multipoint probability distributions. The statistical characteristics of stationary uniform fields satisfying these equations are analyzed, assuming that such discontinuous random fields exist. Author

N85-22984# Joint Publications Research Service, Arlington, Va.
EXPERIMENTAL VERIFICATION OF BEAM DEFLECTION FROM HYBRID REFLECTOR ANTENNA WITHIN WIDE-ANGLE SECTOR Abstract Only **c32**
B. Y. Kinber, V. I. Klassen, A. K. Tobolev, and A. V. Shishlov *In its* USSR Rept.: Electron. and Elect. Eng. (JPRS-UEE-85-001) 9 Jan. 1985 p 5 Transl. into ENGLISH from Radiotekh. i Elektron. (USSR), v. 29, no. 8, Aug. 1984 p 1462-1471 (For primary document see N85-22976 13-33)
Avail: NTIS HC A05/MF A01

An experiment with a hybrid reflector antenna was performed for the purpose of correlating actual beam deflections through a wide range of angles with theoretical calculations on the basis of the geometrical optics approximation. A special antenna was built for this experiment, allowing up to 30 deg deflections of a 1 deg wide beam. It consisted of a radiator in the form of an accurate E-plane waveguide array and an asymmetric reflector in the shape of a parabolic cylinder. Excitation amplitudes and phases were regulated by means of dielectric and dissipative matching inserts in the waveguides. The near-field region was probed by the compensation method in an anechoic chamber, diffraction components and edge waves as well as interference of the latter with the geometrical optics field causing oscillations of the readings and attendant deviations from theory. The error of the geometrical optics approximation is found not to exceed the error of measurements and not to depend on the deflection angle. At small deflection angles the geometrical optics approximation characterizes a spherical wave, indicating the size and the position of the radiator as the deflection angle approaches zero. At large deflection angles the approximation yields more asymmetric side lobes. Author

N85-22985# Joint Publications Research Service, Arlington, Va.
PROBLEM OF DIFFRACTION BY WAVY SURFACE: COMPARISON OF NUMERICAL METHODS OF SOLUTION Abstract Only **c32**
L. A. Vaynshteyn and A. I. Sukov *In its* USSR Rept.: Electron. and Elect. Eng. (JPRS-UEE-85-001) 9 Jan. 1985 p 6 Transl. into ENGLISH from Radiotekh. i Elektron. (USSR), v. 29, no. 8, Aug. 1984 p 1472-1478 (For primary document see N85-22976 13-33)
Avail: NTIS HC A05/MF A01

The problem of diffraction of a wave whose field satisfies the equation (D squared phi/D x squared) + (D squared phi/D y squared) + K squared by a periodically wavy surface is solved by reduction to an integral equation of the first kind for the simplest (Dirichlet) boundary condition squared = 0. The numerical integration is performed independently by three methods. The integral-equation method is based on series expansion of the two functions in the integral equation. In the Rayleigh method the reflected field is resolved into diffraction waves all the way to the surface, where the boundary condition is an equally-reflected field and incident field. In the Masel-Merril-Miller method the Rayleigh hypothesis and the Dirichlet condition are extended by analytic continuation. Numerical solutions obtained for a sinusoidally wavy surface on an M-10 calculator, with the aid of fast Fourier transformation, indicate that high-capacity high-speed computers should make it feasible to advance from approximate methods such as perturbations and physical optics to more rigorous exact mathematical ones. Author

N85-22986# Joint Publications Research Service, Arlington, Va.
SYNTHESIS OF MULTISTEP DIRECTIONAL COUPLERS WITH NONMINIMUM-PHASE CHARACTERISTICS Abstract Only
A. P. Gorbachev and S. G. Neverov *In its* USSR Rept.: Electron. and Elect. Eng. (JPRS-UEE-85-001) 9 Jan. 1985 p 6-7 Transl. into ENGLISH from Radiotekh. i Elektron. (USSR), v. 29, no. 8, Aug. 1984 p 1479-1486 Original language document announced as A84-48605 (For primary document see N85-22976 13-33)
Avail: NTIS HC A05/MF A01

Multistep directional couplers with nonminimal phase properties are studied which make it possible to design a number of devices with different signal phase differences given the same frequency

characteristic of their moduli. Features of the synthesis of such couplers are elucidated, and an algorithm is proposed for analyzing their phase characteristics. It is shown that couplers of this type can be realized in a printed-circuit design, and that they can find application as independent elements of microwave systems and as components of multibeam pattern-forming devices with stabilization of beam positions of the antenna array. L.M. (IAA)

N85-22987# Joint Publications Research Service, Arlington, Va.
SCATTERING OF WAVES BY AXISYMMETRICAL EDGE Abstract Only **c32**
V. A. Kaloshin and A. P. Popov *In its* USSR Rept.: Electron. and Elect. Eng. (JPRS-UEE-85-001) 9 Jan. 1985 p 7 Transl. into ENGLISH from Radiotekh. i Elektron. (USSR), v. 29, no. 8, Aug. 1984 p 1502-1509 Original language document announced as 84A-48606 (For primary document see N85-22976 13-33)
Avail: NTIS HC A05/MF A01

A method of physical theory of diffraction (PTD) in an axisymmetric problem is used to obtain the first two terms of the uniform asymptotics of the radiation pattern of an edge wave with respect to inverse semiinteger powers of the wavenumber expressed through a two-term uniform asymptotics of the corresponding two-dimensional problem. As examples, calculations are made of: (1) the uniform asymptotics of the correction refining the Kirchhoff approximation for the radiation pattern of an axisymmetric reflector antenna; and (2) the asymptotics of the radiation pattern of symmetric modes from the open end of a circular flanged waveguide. An improvement of the PTD method is proposed for calculating the second term of the uniform asymptotics of an edge wave with respect to inverse powers of the wavenumber; the example of the diffraction of a toroidal wave by a bicone is considered. L.M. (IAA)

N85-22988# Joint Publications Research Service, Arlington, Va.
ERROR IN COMPENSATING PHASE FLUCTUATIONS OF WAVE FIELD BY MEANS OF ADAPTIVE REFLECTORS WITH CONTINUOUS OR COMPOUND SURFACE Abstract Only **c32**
V. G. Taranenko *In its* USSR Rept.: Electron. and Elect. Eng. (JPRS-UEE-85-001) 9 Jan. 1985 p 8 Transl. into ENGLISH from Radiotekh. i Elektron. (USSR), v. 29, no. 8, Aug. 1984 p 1510-1515 (For primary document see N85-22976 13-33)
Avail: NTIS HC A05/MF A01

Adaptive reflectors are considered for compensation of phase fluctuations of a wave field in optical or radio telescopes, the mechanism being based on the relation between the space characteristics of phase fluctuations and the dimensions of the controllable reflector surface segment. Three methods of such a compensation were developed: (1) progressive shifting of movable reflector segments; (2) progressive shifting as well as tilting of movable reflector segments; and (3) bending of continuous fixed reflector surface. The dispersion of phase fluctuations in the reflected wave field is calculated for each case as a function of the statistical characteristics of phase fluctuations in the incident field and as a function of the characteristic dimension of the controllable reflector surface. This dispersion characterizes the compensation error and depends on the ratio of that characteristic reflector dimension to the coherence radius of turbulence in the atmosphere. In turn, the ratio of this error to the dispersion of phase fluctuations in a turbulent atmosphere depends on the ratio of characteristic reflector dimensions to telescope aperture diameter. R.J.F.

N85-22989# Joint Publications Research Service, Arlington, Va.
ADAPTIVE CONTROL OF AIRBORNE RADAR ANTENNAS Abstract Only **c32**
G. S. Zelenkov, A. G. Mikerov, N. D. Polyakhov, V. V. Putov, and A. V. yakovlev *In its* USSR Rept.: Electron. and Elect. Eng. (JPRS-UEE-85-001) 9 Jan. 1985 p 8-9 Transl. into ENGLISH from Izv. Vysshikh Uch. Zaved.: Proborostroyeniye (USSR), v. 27, no. 9, Sep. 1984 p 83-90 Original language document announced as 85A-13784 (For primary document see N85-22976 13-33)
Avail: NTIS HC A05/MF A01

Various types of adaptive control systems for airborne radar antennas are examined, including systems with a reference model and signal autotuning, systems with a tunable identifier, systems with play, and systems with play and elastic couplings. The advantages of adaptive systems are outlined, with particular attention given to the reduction of system weight and cost and to the improvement of system precision. L.M. (IAA)

N85-22990# Joint Publications Research Service, Arlington, Va.
SYNTHESIS OF OPTIMUM SINGLE-CHANNEL DISCRETE SIGNALS AND FILTERS Abstract Only **c32**
V. M. Koshevoy and A. A. Kononov *In its* USSR Rept.: Electron. and Elect. Eng. (JPRS-UEE-85-001) 9 Jan. 1985 p 9 Transl. into ENGLISH from Izv. Vysshikh Uch. Zaved.: Radioelektron. (USSR), v. 27, no. 8, Aug. 1984 p 62-65 (For primary document see N85-22976 13-33)
Avail: NTIS HC A05/MF A01

Synthesis of optimum discrete signals and filters for single-channel processing, specifically signals with linear frequency-modulation of the phase, is considered on the basis of the quadratic optimality criterion. In the case of signals with a reciprocal indeterminacy function, the problem reduces to finding the complex signal and filter envelopes which will maximize the crest-to-valley ratio in the time-frequency plane. The most typical five variants of the problem are: (1) with the signal vector given, find the filter vector which maximizes that ratio; (2) find both signal and filter vectors which will maximize that ratio; (3) with absolute values of the signal given, find both signal and filter vectors which will maximize that ratio; (4) with the filter matched to the signal, find the signal vector which maximizes that ratio; and (5) with the filter matched to the signal and absolute values of the signal given, find the signal vector which will maximize that ratio. A suboptimum procedure is proposed for solving these problems, a procedure less unwieldy than optimal solution and based on minimization of the proximity criterion. As such a criterion is regarded the distance between the law of signal phase modulation and the sought signal in the L(2) space. Author

N85-22991# Joint Publications Research Service, Arlington, Va.
EFFICIENCY OF MULTITARGET SIGNAL DETECTION BY DIGITAL RADAR DATA PROCESSING DEVICES Abstract Only **c32**
V. Y. Plekin and M. M. Lednev *In its* USSR Rept.: Electron. and Elect. Eng. (JPRS-UEE-85-001) 9 Jan. 1985 p 10 Transl. into ENGLISH from Izv. Vysshikh Uch. Zaved.: Radioelektron. (USSR), v. 27, no. 8, Aug. 1984 p 75-78 (For primary document see N85-22976 13-33)
Avail: NTIS HC A05/MF A01

The efficiency of multitarget signal detection by a multichannel digital radar data processing device which uses the algorithm of discrete Fourier transformation for spectral analysis is estimated, considering that each frequency channel contains a phase detector, and analog-to-digital converter, a memory, a Fourier transformation stage, a sampler of maximum amplitudes, a threshold device, and an output commutator switch. The problem is formulated for M channels processing m statistically independent signals which cannot jump from one channel to another during detection. Into consideration is taken the possibility of a high false-alarm probability at a low signal-to-noise ratio, because of the detection threshold then being exceeded in $n > m$ channels. The correct-detection probability D m/M is calculated on this basis. The theoretical results were verified on a computer by statistical simulation of algorithms of the Monte Carlo method, a generator of random numbers and with a noise generator shaping a normal white noise accompanied by a consonantly fluctuating phase packet with unknown initial phase. Author

N85-22992# Joint Publications Research Service, Arlington, Va.
SYNTHESIS OF OPTIMUM ALGORITHMS FOR SECONDARY PROCESSING Abstract Only **c32**
A. M. Shloma and V. P. Volonkov *In its* USSR Rept.: Electron. and Elect. Eng. (JPRS-UEE-85-001) 9 Jan. 1985 p 10-11 Transl. into ENGLISH from Izv. Vysshikh Uch. Zaved.: Radioelektron. (USSR), v. 27, no. 8, Aug. 1984 p 22-28 Original language

document announced as A84-46212 (For primary document see N85-22976 13-33)
Avail: NTIS HC A05/MF A01

The method of fiducial statistical inferences is used to synthesize an optimal secondary-processing algorithm in conditions of a priori indeterminacy. A recursive adaptive algorithm of trajectory filtering is presented which is based on randomized estimates.
B.J. (IAA)

N85-22993# Joint Publications Research Service, Arlington, Va.
OPTIMIZATION OF NUMBER OF PULSES IN DETECTION OF FLUCTUATING OPTICAL SIGNALS Abstract Only c74
F. I. Khaytun and R. B. Shemshedinov *In its* USSR Rept.: Electron. and Elect. Eng. (JPRS-UEE-85-001) 9 Jan. 1985 p 11 Transl. into ENGLISH from Radiotekh. (USSR), no. 9, Sep. 1984 p 88-91 (For primary document see N85-22976 13-33)
Avail: NTIS HC A05/MF A01

Optimization of the number of pulses in the observation interval in detecting amplitude fluctuating optical signals is examined for the cases of detectors not employing interpulse processing and detectors employing discrete signal accumulation (binary integration). Optimization of the number of pulses consists of finding the minimum value of the discrete function defining the amount of energy consumed in emitting N pulses. Said discrete function is computed for normal, uniform and exponential signal amplitude distributions. Author

N85-22994# Joint Publications Research Service, Arlington, Va.
DIFFRACTION OF PERIODIC GROUNDING SYSTEM OF FINITE LENGTH Abstract Only
G. I. Veselov, Y. N. Alekhin, and V. V. Litvinovich *In its* USSR Rept.: Electron. and Elect. Eng. (JPRS-UEE-85-001) 9 Jan. 1985 p 11-12 Transl. into ENGLISH from Radiotekh. (USSR), no. 9, Sep. 1984 p 80-83 Original language document announced as A85-15761 (For primary document see N85-22976 13-33)
Avail: NTIS HC A05/MF A01

The method of partial regions is used to analyze wave diffraction by the junction of a regular waveguide and a periodic slow wave structure (SWS) of finite length, with allowance for the full discrete spectrum of the natural modes (including the complex ones) of the system. The proposed algorithm reduces the diffraction problem to the solution of an infinite system of linear algebraic equations, having a high rate of convergence and solution stability during reduction. The convergence is investigated, and numerical results are analyzed. L.M. (IAA)

N85-22995# Joint Publications Research Service, Arlington, Va.
CORRECTNESS OF REFLECTION CHARACTERISTICS OF RADIO ABSORBENT MATERIALS Abstract Only c32
M. A. Monin *In its* USSR Rept.: Electron. and Elect. Eng. (JPRS-UEE-85-001) 9 Jan. 1985 p 12 Transl. into ENGLISH from Radiotekh. (USSR), no. 9, Sep. 1984 p 83-84 (For primary document see N85-22976 13-33)
Avail: NTIS HC A05/MF A01

The coefficient of reflection, defined as r(2) = P/P sub O where R(2) is the power coefficient reflection and P, P sub O the power of plane wave reflected from an incident upon specimen, is shown to be incorrect for the case of diffuse scattering radio absorbent materials. It is found that the effective scattering area of diffuse scattering radio absorbent material must be measured as a function of the angle of irradiation. Examples of the effective scattering area indicatrax are shown for mirror and diffuse scattering radio absorbent material. Radio absorbent materials can exhibit mirror reflection, as well as simultaneous diffusing and diffraction reflection; the corresponding coefficients are found from the effective scattering area of the specimens. Author

N85-22996# Joint Publications Research Service, Arlington, Va.
SHORT-RANGE RADIOTECHNICAL POINT SENSOR Abstract Only c32
O. I. Shelukhin, Y. P. Kernov, and V. I. Shelukhin *In its* USSR Rept.: Electron. and Elect. Eng. (JPRS-UEE-85-001) 9 Jan. 1985 p 12 Transl. into ENGLISH from Radiotekh. (USSR), no. 9, Sep. 1984 p 45-47 (For primary document see N85-22976 13-33)
Avail: NTIS HC A05/MF A01

Microwave radiotechnical point sensors employed for position finding of objects in a monitored region are described. The short range radiotechnical point sensor includes a direct signal channel consisting of a transmitting device and a direct channel receiver, and a reflected signal channel formed by the same transmitter and a reflected signal receiver. The operation of the device is described, and formulas are derived for estimating the potential correct detection and false alarm probabilities of devices operating at short ranges. Author

N85-22997# Joint Publications Research Service, Arlington, Va.
FACTORIZED ALGORITHMS FOR COMBINED SPATIAL AND TEMPORAL PROCESSING OF RADAR SIGNALS Abstract Only c32
V. I. Chaykovskiy *In its* USSR Rept.: Electron. and Elect. Eng. (JPRS-UEE-85-001) 9 Jan. 1985 p 13 Transl. into ENGLISH from Radiotekh. (USSR), no. 9, Sep. 1984 p 40-42 (For primary document see N85-22976 13-33)
Avail: NTIS HC A05/MF A01

Digital spatial and temporal maximum likelihood processing algorithms for dealing with complex envelopes of band signals from two dimensional antenna arrays are synthesized. Factoring the canonical combined processing algorithm, or its representation as a sequence of several procedures, reduces the amount of computation significantly and makes the computation easier to organize. The possibility of factoring is determined by the features of the structure of the signal matrix and the properties of its elements. The factored algorithm implements three functionally identical multiplications of a three dimensional data matrix and some two dimensional matrix operator. Each such procedure is broken down into simpler multiplications of different vector sections of the data matrix by the matrix operator. The group nature of the procedures makes it possible to parallel the computation and the three stage structure of the algorithm facilitates pipelining. Factoral maximum likelihood space and temporal processing algorithms are found to be a successful alternative for existing canonical and traditional algorithms for processing band signals in digital systems employing discrete arrays. Author

N85-22998# Joint Publications Research Service, Arlington, Va.
EXACT DESIGN FORMULAS FOR FIELD INTENSITY OF DIPOLE DEPLOYED ABOVE FLAT HOMOGENEOUS EARTH WITH FINITE CONDUCTIVITY Abstract Only c32
L. S. Tartakovskiy *In its* USSR Rept.: Electron. and Elect. Eng. (JPRS-UEE-85-001) 9 Jan. 1985 p 13 Transl. into ENGLISH from Radiotekh. (USSR), no. 9, Sep. 1984 p 29-34 (For primary document see N85-22976 13-33)
Avail: NTIS HC A05/MF A01

Formulas are derived and plotted which can be used for practical calculation of the field intensity of a balanced or unbalanced vertical or horizontal dipole deployed over a flat homogeneous ground with finite conductivity regardless of the angle of inclination of the beam connecting the transmitting and receiving points. Beam and wave expressions for the field are considered and conditions are derived for the applicability of geometric optics. The approximate region of wavelengths within which the dipole field formulas are applicable is analyzed. Author

N85-22999# Joint Publications Research Service, Arlington, Va.
CHANGE OF ELECTRICAL CHARACTERISTICS OF RADIO-FREQUENCY CABLES UNDER THERMAL EFFECT Abstract Only
A. V. Lobanov, P. P. Pavlov, and N. N. Khrenkov *In its* USSR Rept.: Electron. and Elect. Eng. (JPRS-UEE-85-001) 9 Jan. 1985 p 14 Transl. into ENGLISH from Elektron. (USSR), no. 9, Sep. 1984 p 45-46 (For primary document see N85-22976 13-33)
Avail: NTIS HC A05/MF A01

Four basic temperature dependent electrical parameters of r-f cables are described by expressions which facilitate an analysis of their sensitivity to temperature effects, these parameters being capacitance, wave impedance, attenuation factor and phase shift

factor. Calculations for coaxial cables are based on an equivalent dielectric permittivity of the insulation system, including air gap between dielectric and outer conductor produced in the manufacturing process as well as the air gap between dielectric and inner conductor produced by variation of the radius of the latter. Mechanical strains affecting the system geometry are found from the solution to Lame's problem for thin walled cylinders and Hooke's law extended to a three dimensional state of stress. For illustration, numerical results are given for RK-3-28-Pr high precision cables with monolithic Teflon-4D insulation (dielectric constant epsilon = 2.03 at 20 C). Author

N85-23000# Joint Publications Research Service, Arlington, Va.
SPECTRAL EVALUATION OF IRREGULARITY OF SUPERCONDUCTING COAXIAL CABLES Abstract Only
D. Y. Galperovich, A. A. Laptev, and A. Y. Podshivalov *In its* USSR Rept.: Electron. and Elect. Eng. (JPRS-UEE-85-001) 9 Jan. 1985 p 14-15 Transl. into ENGLISH from Elektron. (USSR), no. 9, Sep. 1984 p 46-48 (For primary document see N85-22976 13-33)
Avail: NTIS HC A05/MF A01

Conventional superconducting coaxial cables are considered, with Teflon-4D insulation between the inner conductor made of niobium wire and the outer conductor made of monolithic lead tubing. Irregularity of such cables is not structural but produced in the manufacturing process. It has been found to consist of a random component and quasi-periodic strongly correlated deviations of geometric dimensions, particularly the diameter, over the cable length. This compound irregularity has been evaluated on two specimens of such a cable, by spectral analysis of the wave impedance as function of the cable length. Profilograms of the diameter variation over the cable length were supplemented with space frequency spectra, following a Fourier transformation of the wave impedance, namely the frequency spectrum of the transform modulus squared (phase relations not being relevant here) and of the reflection coefficient. Reflectometer readings and echograms were processed by the method of the instantaneous mean. An inverse transformation has yielded the profile of wave impedance over the cable length. Author

N85-23001# Joint Publications Research Service, Arlington, Va.
SURGE STRENGTH OF SYMMETRIC CABLE WITH MONOLITHIC POLYETHYLENE INSULATION OF QUADS Abstract Only
V. K. Miroshnichenko *In its* USSR Rept.: Electron. and Elect. Eng. (JPRS-UEE-85-001) 9 Jan. 1985 p 15 Transl. into ENGLISH from Elektron. (USSR), no. 9, Sep. 1984 p 48-50 (For primary document see N85-22976 13-33)
Avail: NTIS HC A05/MF A01

The lightning resistance of MKP sub m AS h sub p-4x4x1.05 + 2x0.7 symmetric railroad communication cables operating along the Baykal-Amur line was evaluated in terms of the dielectric strength of their insulation system, in failure-free operation. The insulation system in these cables consists of monolithic polyethylene around each quad core and polyethylene sleeving around each aluminum sheath. Experimental data for this evaluation had been obtained by measurement of the voltage between conductor bundle and sheath, this voltage being the highest during a lightning stroke, not only along cable segments between repeater points but also in splices and in potheads. A comparison with similar data in MKSA sub p SH sub p 4x4x1.2 cables indicates that the tested MKP sub m AS h sub p cables have a much higher surge strength. Author

N85-23002# Joint Publications Research Service, Arlington, Va.
THEORY OF DIAPHRAGM LIGHT MODULATORS WITH ELECTRICAL INPUT SIGNAL Abstract Only **c74**
Y. P. Gushcho and A. S. Sigov *In its* USSR Rept.: Electron. and Elect. Eng. (JPRS-UEE-85-001) 9 Jan. 1985 p 16 Transl. into ENGLISH from Zh. Nauchnoy i Prikl. Fotografii i Kinematografii (USSR), v. 29, no. 5, Sep.-Oct. 1984 p 324-328 (For primary document see N85-22976 13-33)
Avail: NTIS HC A05/MF A01

A theory of diaphragm light modulators employing potential and charge relief control is presented which allows for irregularity of the electrical field, finite diaphragm thickness and finite mechanical constants. The deforming electrical forces and mechanics of deformation of a diaphragm of finite thickness are analyzed. It is recommended that the thickness of the membrane should be made as little as possible in order to improve modular sensitivity; only after this has been done should the modulo of elasticity of the material be reduced. The findings may be extended to diaphragm light modulators with optical input signals. Author

N85-23003# Joint Publications Research Service, Arlington, Va.
A POSTERIORI INCREASE OF RESOLVING POWER OF OPTICAL SYSTEM FORMING AVERAGED MONOCHROMATIC IMAGES Abstract Only **c74**
P. A. Bakut, A. I. Deryugina, and V. I. Mandrosov *In its* USSR Rept.: Electron. and Elect. Eng. (JPRS-UEE-85-001) 9 Jan. 1985 p 16 Transl. into ENGLISH from Radiotekh. i Elektron. (USSR), v. 29, no. 8, Aug. 1984 p 1589-1594 (For primary document see N85-22976 13-33)
Avail: NTIS HC A05/MF A01

An optical imager is considered which, with a diffraction-limited lens system, forms monochromatic images of objects with random surface roughness by transforming the light intensity distribution in the plane of the object into an averaged light intensity distribution in the plane of the image. The coherent pulse response of such a device with a Gaussian aperture function is calculated from the approximate solution to the corresponding Fredholm integral equation of the second kind with the field-point scattering function. On this basis the feasibility is of superresolution through increase of the resolving power by a posteriori signal processing. For illustration, this method is applied to a two-point object not resolvable according to the Rayleigh criterion. Author

N85-23004# Joint Publications Research Service, Arlington, Va.
DISPERSION CHARACTERISTICS OF SMALL-MODE GRADIENT OPTICAL FIBERS Abstract Only **c74**
L. A. Frenkel *In its* USSR Rept.: Electron. and Elect. Eng. (JPRS-UEE-85-001) 9 Jan. 1985 p 17 Transl. into ENGLISH from Radiotekh. i Elektron. (USSR), v. 29, no. 8, Aug. 1984 p 1451-1456 (For primary document see N85-22976 13-33)
Avail: NTIS HC A05/MF A01

The performance of fiber-optic waveguides axially regular but with a radially variable or only piecewise-uniform refractive index is analyzed, of particular interest being the variation of group velocity and the dispersion characteristics that determine it. The fiber core of a loss-less waveguide is assumed to have the same magnetic permeability as the ambient medium, and the latter to have a uniform dielectric constant. The dispersion equation is derived and the wave number as a function of the frequency is calculated for the HE sub 11 mode, considering that the two tangential field components must be continuous at the waveguide-sheath interface. The corresponding boundary-value problem for the Maxwell field equations is formulated in a cylindrical coordinate system. It is solved by eliminating the radial field components from these equations, defining the initial conditions, and subsequently applying the Runge-Kutta method of the appropriate order of precision. The process involves minimizing two functions, namely the jumps of the two tangential field components at the interface as functions of the wave number and of a coefficient which characterize the ratio of the two longitudinal waveguide-mode field components. Author

N85-23005# Joint Publications Research Service, Arlington, Va.
METHODS OF DIGITAL CORRECTION FOR CHANNELS OF MULTICHANNEL RADAR RECEIVERS Abstract Only **c32**
Y. I. Abramovich, V. G. Kachur, and V. F. Struchev *In its* USSR Rept.: Electron. and Elect. Eng. (JPRS-UEE-85-001) 9 Jan. 1985 p 25 Transl. into ENGLISH from Radiotekh. i Elektron. (USSR), v. 29, no. 8, Aug. 1984 p 1544-1550 (For primary document see N85-22976 13-33)
Avail: NTIS HC A05/MF A01

The efficiency of adaptively tunable digital corrective filters in

channels of radar receivers with space processing of signals is evaluated from the standpoint of optimization by cyclic convolution. Calculations for two signals at the output, one from each of any two channels, and a signal with a white noise at the input indicate that a matrix-circulant minimizing the dispersion of error and representable in the form D = U* lambda U (U*- Hermitian conjugate, lambda - diagonal matrix of circulant eigenvalues, U-matrix of discrete Fourier transformation) will yield filters at least as efficient as transversal filters with an equivalent memory.
Author

N85-23006# Joint Publications Research Service, Arlington, Va.
ALGORITHM IN WALSH FUNCTION BASIS FOR ANALYSIS OF INTEGRATED MICROCIRCUITS ON MOS-STRUCTURES Abstract Only
L. N. Pavlov and Y. M. Kalnibolotskiy *In its* USSR Rept.: Electron. and Elect. Eng. (JPRS-UEE-85-001) 9 Jan. 1985 p 25-26 Transl. into ENGLISH from Izv. Vysshikh Uch. Zaved.: Radioelektron. (USSR), v. 27, no. 8, Aug. 1984 p 39-44 (For primary document see N85-22976 13-33)
Avail: NTIS HC A05/MF A01

Use of a Walsh function basis facilitates computer-aided design and performance analysis of integrated microcircuits, especially of those built on MOS structures for discrete processing of analog signals. As the integration scale increases here, so does the variance of correspondingly smaller geometrical dimensions and so does the deviation of electrophysical parameters. An analysis with direct application of the Walsh function basis then becomes difficult and unwieldy so that a faster convergence is needed for coverage of a wide range of simultaneously varying circuit parameters and external conditions, while taking into account all possible nonlinearities in the output characteristics. An algorithm is proposed to meet this need for any number of variable parameters, an algorithm which optimizes the convergence by minimizing the norm of differences between output (solution) vectors obtained in successive iterations. This is achieved by conversion of the deviations matrix into the Gray code, that can be regarded as a diadic vector. The procedure is demonstrated for the case where deviations of circuit components, signal sources, and power supplies are describable by Rademacher functions.
Author

N85-23007# Joint Publications Research Service, Arlington, Va.
INVESTIGATION OF BIMODAL PARAMAGNETIC FILTER Abstract Only
V. G. Zaytsev *In its* USSR Rept.: Electron. and Elect. Eng. (JPRS-UEE-85-001) 9 Jan. 1985 p 27 Transl. into ENGLISH from Radiotekh. (USSR), no. 9, Sep. 1984 p 85-87 (For primary document see N85-22976 13-33)
Avail: NTIS HC A05/MF A01

Analytical expressions are proposed for the working attenuation and phase response of a bimodal microwave paramagnetic filter. The bandwidth of the filter is found to increase as the amount of paramagnetic material until the bandwidth of the cavity is reached, which is determined by its Q-factor. This relationship makes it possible to select the optimum amount of material as a function of the requirements for the filter, whether the narrowest possible bandwidth, or minimum losses. A number of paramagnetic bimodal filters are investigated with center frequencies between 5 and 10 GHz. Comparison between the calculated and experimental curves within the passband of the filter indicates that the expressions for the working attenuation and phase response agree closely.
Author

N85-23008# Joint Publications Research Service, Arlington, Va.
PROGRAMMABLE FILTER WITH FANNED INTERDIGITAL SURFACE ACOUSTIC WAVE TRANSDUCER Abstract Only
S. A. Dobershteyn and A. N. Rozhdestvenskiy *In its* USSR Rept.: Electron. and Elect. Eng. (JPRS-UEE-85-001) 9 Jan. 1985 p 27 Transl. into ENGLISH from Izv. Vysshikh Uch. Zaved.: Radioelektron. (USSR), v. 27, no. 9, Sep. 1984 p 69-71 (For primary document see N85-22976 13-33)
Avail: NTIS HC A05/MF A01

A programmable filter with a fanned interdigital transducer and array of small-aperture receiving transducers is investigated. The amplitude-frequency characteristics of the filter are formed by combining elements of the array in a common receiving system by means of electronic switches and a summing amplifier. The form of the amplitude-frequency characteristic is improved by using weighted processing of the electrodes of the fanned interdigital transducer by capacitive weighting. The array elements consist of small-aperture fanned transducers. A formula is derived for the frequency response of the filter. The frequency responses of a programmable filter with Hamming-function weighting of the electrodes are calculated. A programmable surface acoustic wave filter is fabricated on a Y-cut 128 deg lithium niobate piezosubstrate. It is found that such programmable filters make it possible to synthesize a wide set of frequency responses, and can be used for frequency selection in radio communication systems.
Author

N85-23009# Joint Publications Research Service, Arlington, Va.
GYRATOR FREQUENCY SELECTORS WITH BANDWIDTH INDEPENDENT OF INPUT SIGNAL LEVEL Abstract Only
V. A. Sikyak and Y. M. Verkhovskiy *In its* USSR Rept.: Electron. and Elect. Eng. (JPRS-UEE-85-001) 9 Jan. 1985 p 28 Transl. into ENGLISH from Izv. Vysshikh Uch. Zaved.: Radioelektron. (USSR), v. 27, no. 9, Sep. 1984 p 76-77 (For primary document see N85-22976 13-33)
Avail: NTIS HC A05/MF A01

A frequency selector is described in which the bandwidth is independent of the level of the input signal. The selector employs two channels in which the amplitude-frequency characteristics are formed by combining the signals from the outputs of the gyrators, which are part of the resonators, with the help of summing amplifiers. A working model is described. The use of resonators connected in parallel and antiphase followed by detection of the output voltage of the summing amplifiers and comparison by a dc comparator is recommended for gyrator frequency selectors. The dynamic range of the filter can be increased, and the operating band stability improved, by using detectors with low threshold voltage.
E.A.K.

N85-23010# Joint Publications Research Service, Arlington, Va.
SYNTHESIS OF QUASI-OPTIMUM TWO-LEVEL SIGNAL DISCRIMINATOR WITH LEVEL CHANGING AT UNKNOWN POINT Abstract Only
A. Y. Kraskovskiy *In its* USSR Rept.: Electron. and Elect. Eng. (JPRS-UEE-85-001) 9 Jan. 1985 p 28 Transl. into ENGLISH from Izv. Vysshikh Uch. Zaved.: Radioelektron. (USSR), v. 27, no. 9, Sep. 1984 p 46-50 (For primary document see N85-22976 13-33)
Avail: NTIS HC A05/MF A01

Optimum estimates were derived for the moments at which the level of a two-level signal changes. It is assumed that digitizing of an additive mixture of a binary signal and normal random noise results in a sequence of random quantities with irregularity manifested by a change in the mathematical expectation at an unknown point. A circuit is derived for a quasioptimum two-level signal discriminator. The noise tolerance of the proposed discrimination method is estimated; graphs are plotted to illustrate the behavior of the logarithm, and the error probabilities which occur in testing the hypothesis of level has change by using the likelihood ratio. The receiving synthesizer is most effective under conditions of a priori indeterminacy with regard to the moment of delay of the signal.
E.A.K.

N85-23011# Joint Publications Research Service, Arlington, Va.
USE OF WALSH FUNCTIONS FOR CALCULATING CHARACTERISTICS OF DIGITAL FITLERS WITH IMPULSE RESPONSE OF FINITE DURATION Abstract Only
A. V. Titov *In its* USSR Rept.: Electron. and Elect. Eng. (JPRS-UEE-85-001) 9 Jan. 1985 p 29 Transl. into ENGLISH from Izv. Vysshikh Uch. Zaved.: Radioelektron. (USSR), v. 27, no. 9, Sep. 1984 p 50-53 Original language document announced as A85-11791 (For primary document see N85-22976 13-33)
Avail: NTIS HC A05/MF A01

The paper examines a method for the calculation of digital FIR (finite impulse response) filters using the spectral characteristics of Walsh functions in the frequency domain. This method, which makes it possible to represent any FIR filter as a parallel connection of Walsh filters, is distinguished by a relative simplicity of theoretical relationships and by the clarity of the physical interpretation of the results obtained. L.M. (IAA)

N85-23012# Joint Publications Research Service, Arlington, Va.
ASYMPTOTICALLY OPTIMUM MULTIALTERNATIVE SEQUENTIAL PROCEDURES FOR DISCERNMENT OF PROCESSES MINIMIZING AVERAGE LENGTH OF OBSERVATIONS Abstract Only c32
M. M. Fishman *In its* USSR Rept.: Electron. and Elect. Eng. (JPRS-UEE-85-001) 9 Jan. 1985 p 30 Transl. into ENGLISH from Radiotekh. i Elektron. (USSR), v. 29, no. 8, Aug. 1984 p 1516-1524 (For primary document see N85-22976 13-33)
Avail: NTIS HC A05/MF A01

The problem of multialternative sequential discernment of processes is formulated in terms of conditionally optimum procedures minimizing the average length of observations, without any probabilistic assumptions about any one occurring process, rather than in terms of Bayes procedures minimizing the average risk. The problem is to find the procedure that will transform inequalities into equalities. The problem is formulated for various models of signal observation and data processing: (1) discernment of signals from background interference by a multichannel system; (2) discernment of pulse sequences with unknown time delay; (3) discernment of harmonic signals with unknown frequency. An asymptotically optimum sequential procedure is constructed which compares the statistics of the likelihood ratio with the mean-weighted likelihood ratio and estimates the upper bound for conditional average lengths of observations. This procedure is shown to remain valid as the upper bound for the probability of erroneous partial solutions decreases approaching zero and the number of hypotheses increases approaching infinity. It also remains valid under certain special constraints on the probability such as a threshold. A comparison with a fixed-length procedure reveals that this sequential procedure decreases the length of observations to one quarter, on the average, when the probability of erroneous partial solutions is low. E.A.K.

N85-23013# Joint Publications Research Service, Arlington, Va.
EXTRACTION OF SIGNALS FROM BACKGROUND INTERFERENCE WITH UNKNOWN PARAMETERS IN QUANTIZED SAMPLE Abstract Only c32
A. N. Dmitriyenko *In its* USSR Rept.: Electron. and Elect. Eng. (JPRS-UEE-85-001) 9 Jan. 1985 p 31 Transl. into ENGLISH from Radiotekh. i Elektron. (USSR), v. 29, no. 8, Aug. 1984 p 1525-1530 (For primary document see N85-22976 13-33)
Avail: NTIS HC A05/MF A01

Decision rules were constructed for detection of signals appearing with background interference in amplitude-quantized samples. The rules are to ensure that the false-alarm probability will not depend on the interference parameters and, therefore, the latter need not be a priori known. Samples with a finite number of realizations L = (M + 1) sub V are considered, including nonrandomized and randomized decision rules for acceptance of the signal present hypothesis through group and its subgroups identification on the basis of their sufficient statistics. The correct-detection probability is calculated for each case. Simple examples demonstrate that ignorance of the interference parameters is much less costly in the case of quantized samples than in the case of nonquantized ones. E.A.K.

N85-23014# Joint Publications Research Service, Arlington, Va.
APPLICABILITY OF LOG-NORMAL MODEL TO PROBABILITISTIC DESCRIPTION OF QUASI-PULSE INTERFERENCE Abstract Only c32
V. D. Rubtsov and A. N. Zaytsev *In its* USSR Rept.: Electron. and Elect. Eng. (JPRS-UEE-85-001) 9 Jan. 1985 p 31-32 Transl. into ENGLISH from Elektron. (USSR), v. 29, no. 8, Aug. 1984 p 1531-1535 (For primary document see N85-22976 13-33)
Avail: NTIS HC A05/MF A01

The log-normal probablistic description of a quasipulse interference such as atmospheric noise, based on the physically verifiable exponential dependence of pulse amplitude on attenuation along the propagation path, is validated in accordance with the central-limit theorem in Lyapunov's theory of probability. Conditions are established for extending the description of the interference envelope with the two-dimensional log-normal model. The additional necessary and sufficient condition in the case of atmospheric noise is constancy of its two-dimensional distribution along the propagation path and thus that the fluctuations of radio wave attenuation have two-dimensional correlation function and energy spectrum. Accordingly, the log-normal model does not apply as well to polar regions during auroral perturbations in the ionosphere as it does to atmospheric noise in the temperate zones. Theoretical and experimental curves indicate that the log-normal model may also approximate industrial interference. E.A.K.

N85-23015# Joint Publications Research Service, Arlington, Va.
ACCURACY OF APPROXIMATION OF BAYES ESTIMATES IN PRESENCE OF NONINFORMATIVE PARAMETERS Abstract Only c32
A. P. Trifonov and Y. P. Yenina *In its* USSR Rept.: Electron. and Elect. Eng. (JPRS-UEE-85-001) 9 Jan. 1985 p 32 Transl. into ENGLISH from Radiotekh. i Elektron. (USSR), v. 29, no. 8, Aug. 1984 p 1536-1543 (For primary document see N85-22976 13-33)
Avail: NTIS HC A05/MF A01

The asymptotic behavior of multidimensional a posterior distributions as the signal-to-noise ratio increases is used for construction of quasioptimum estimates. It is found that a maximum-likelihood estimate approximates a Bayes estimates with asymptotically decreasing mean square error. The procedure is applicable to a signal with a multidimensional Gaussian distribution of unknown parameters, calculation of the approximation error becoming quite simple when all unknown parameters are not energy related. A pulse signal with linear frequency modulation mixed with a white noise at the receiver input illustrates how the presence of a noninformative parameter, in this case the Gaussian random frequency, decreases the accuracy of this approximation for estimating the Gaussian random position of the signal in time. E.A.K.

N85-23016# Joint Publications Research Service, Arlington, Va.
RECEPTION OF SIGNAL WITH UNKNOWN AMPLITUDE AND DURATION SUBMERGED IN WHITE NOISE Abstract Only c32
A. P. Trifonov and V. K. Buteyko *In its* USSR Rept.: Electron. and Elect. Eng. (JPRS-UEE-85-001) 9 Jan. 1985 p 35 Transl. into ENGLISH from Izv. Vysshikh Uch. Zaved.: Radioelektron. (USSR), v. 27, no. 8, Aug. 1984 p 28-34 Original language document announced as A84-46213 (For primary document see N85-22976 13-33)
Avail: NTIS HC A05/MF A01

Error probabilities were obtained for the detection of a rectangular pulse of unknown amplitude and duration. Expressions are derived for the distribution and scatter of joint estimates of the maximum likelihood of signal amplitude and duration. Results of mathematical modeling are presented. B.J. (IAA)

N85-23017# Joint Publications Research Service, Arlington, Va.
USE OF BIGAUSSIAN APPROXIMATION TO DESCRIBE FADING IN SCATTERING COMMUNICATIONS CHANNEL Abstract Only c32
L. T. Sushkova, Y. Y. Marchenko, and V. V. Bryksin *In its* USSR Rept.: Electron. and Elect. Eng. (JPRS-UEE-85-001) 9 Jan. 1985 p 36 Transl. into ENGLISH from Radiotekh. (USSR), no. 9, Sep. 1984 p 87-88 (For primary document see N85-22976 13-33)
Avail: NTIS HC A05/MF A01

An algorithm is presented for the analytical description of the statistical properties of fading in a scattering radio channel. Two Gaussian random processes W1 (x) and W2 (x) with parameters a1, delta 1, a2, delta 2, respectively where a1; delta 1- mathematical

expectation, as the expression approximating the arbitrary probability density W*(x) of the composition are considered. A graph analytical method is proposed for estimating the parameters a sub 1, a sub 2, delta and lambda from the known estimates of the moments of the empirical distribution described. The proposed method is used to describe the real statistics of signal level variation in a troposcatter radio channel as an example. E.A.K.

N85-23018# Joint Publications Research Service, Arlington, Va.
MACHINE ANALYSIS OF RESONANCE CHARACTERISTICS OF PLATE-TYPE RADIO ELECTRONIC EQUIPMENT CONSTRUCTIONS Abstract Only
A. M. Tartakovskiy *In its* USSR Rept.: Electron. and Elect. Eng. (JPRS-UEE-85-001) 9 Jan. 1985 p 36 Transl. into ENGLISH from Radiotekh. (USSR), no. 9, Sep. 1984 p 94-95 (For primary document see N85-22976 13-33)
Avail: NTIS HC A05/MF A01

The numerical solution of the problem of finding the lower natural frequencies and forms of flexural oscillations of plate-type constructions for any manner of securing and with allowance for irregular distribution of components and parts with respect to mass over the plate was examined. The problem is solved by the finite-difference method, in which difference analogs of the equation of the technical theory of plate flexure and boundary conditions are constructed for a certain grid region. An iterative process is derived for calculating the actual form and frequency. A program for automatic preparation of source data, and another for calculating the natural frequencies and forms, were developed in accordance with the algorithm. An example of calculating the first two intrinsic forms and natural frequencies of boards containing components fastened at four and five points is presented. E.A.K.

N85-23019# Joint Publications Research Service, Arlington, Va.
COMPUTING CONVOLUTION OF MULTIFREQUENCY SIGNAL EMPLOYING TRUNCATED FAST FOURIER TRANSFORM ALGORITHMS Abstract Only **c32**
V. U. Sysoyev *In its* USSR Rept.: Electron. and Elect. Eng. (JPRS-UEE-85-001) 9 Jan. 1985 p 37 Transl. into ENGLISH from Radiotekh. (USSR), no. 9, Sep. 1984 p 53-56 (For primary document see N85-22976 13-33)
Avail: NTIS HC A05/MF A01

The use of fast Fourier transform (FFT) alsorithms to compute the discrete Fourier transform and its inverse for multifrequency signals was analyzed. The use of truncated FFT algorithms to eliminate redundant computations associated with finding unneeded spectral samples is explained. The number of multiplications is found as a function of the number of non zero samples of the discrete spectrum of a signal for N = 256 and N = 300 assuming that non zero samples follow one another in the spectrum. It is found that there is a significant range of numbers of non zero samples for the truncated version for which truncated algorithms provide a significant reduction in the number of operations. It is noted that for certain relative positioning of non zero samples in the spectrum the benefit is increased significantly. E.A.K.

N85-23020# Joint Publications Research Service, Arlington, Va.
SYNTHESIS OF QUASI-OPTIMUM ALGORITHMS FOR SIGNAL RECOGNITION AGAINST BACKGROUND OF CORRELATED NOISE EMPLOYING DISCRETE SPECTRAL TRANSFORMATIONS Abstract Only **c32**
A. I. Rog, A. A. Sirota, E. N. Khkhlov, and V. V. Tukhvatulin *In its* USSR Rept.: Electron. and Elect. Eng. (JPRS-UEE-85-001) 9 Jan. 1985 p 37 Transl. into ENGLISH from Radiotekh. (USSR), no. 9, Sep. 1984 p 58-61 Original language document announced as A85-15756 (For primary document see N85-22976 13-33)
Avail: NTIS HC A05/MF A01

A method is proposed for comparative estimation of the information capabilities of various discrete spectral transformations for recognizing signals in the presence of correlated noise. The approach can be used to construct a probability-recognition time relationship in which the individual points correspond to decision-making algorithms with the same operating structure, different only in the use in type of discrete transformation performed in advance. This relationship can be used to determine the need for using a transformation and to select said transformation to satisfy the restrictions regarding the complexity and speed of the recognition algorithms. Fourier and Walsh, as well as other computationally economical transformations, can be used. Author

N85-23021# Joint Publications Research Service, Arlington, Va.
PROBABILITY OF DETECTION OF PULSED SIGNALS EMPLOYING ZERO-GATING INTERFERENCE SUPPRESSION Abstract Only **c32**
Y. D. Ivanov *In its* USSR Rept.: Electron. and Elect. Eng. (JPRS-UEE-85-001) 9 Jan. 1985 p 38 Transl. into ENGLISH from Radiotekh. (USSR), no. 9, Sep. 1984 p 61-63 (For primary document see N85-22976 13-33)
Avail: NTIS HC A05/MF A01

A compensation method is presented which can be used to extract a pulse signal from a mixture of signal and continuous interference which combines a compensator and zero-gating interference suppression device. The noise suppression device consists of a zero counter and an analog switch with voltage applied to its input. The switch opens only when the interference is zero. The blanking pulse is so short that the interference voltage during the pulse can be disregarded. The probability of pulse signals coinciding with interference nulls is investigated, assuming that the interference levels in the primary and auxiliary channels are different, but that the nulls coincide. The false alarm probability is investigated, and a formula is derived for the maximum correct detection probability which can be realized. Author

N85-23022# Joint Publications Research Service, Arlington, Va.
NEW CONVOLUTION AND DISCRETE FOURIER TRANSFORMATION ALGORITHMS BASED ON RECTANGULAR TRANSFORMATIONS OVER FIELD OF ROOTS OF UNITY Abstract Only **c64**
A. T. Baykova *In its* USSR Rept.: Electron. and Elect. Eng. (JPRS-UEE-85-001) 9 Jan. 1985 p 38 Transl. into ENGLISH from Radiotekh. (USSR), no. 9, Sep. 1984 p 66-68 (For primary document see N85-22976 13-33)
Avail: NTIS HC A05/MF A01

Effective methods are examined for computing the cyclic convolution and discrete Fourier transform of long and multidimensional sequences employing cyclic convolution of short sequences as base operations. The algorithms for the latter operations are orthogonal rectilinear transformations obtained by computing the residue of the product of the corresponding polynomials of degree (N - 1) and the absolute value of the polynomial Z(N) - 1, where N is the convolution length. The case of expansion of the field of rational numbers to the field of the roots of the Nth power of unity for simple N is examined. The number of actual operations required for complex multiplication over the field in question is tabulated for N = 3, 5, 7; the maximum number of sequences which can be processed simultaneously is N - 1. It is found that the effectiveness of the new algorithms increases as the dimensionality and length of the transformed sequence. Author

N85-23023# Joint Publications Research Service, Arlington, Va.
RECEPTION NOISE IMMUNITY OF MULTIPOSITION SIGNALS Abstract Only **c32**
V. S. Girshov *In its* USSR Rept.: Electron. and Elect. Eng. (JPRS-UEE-85-001) 9 Jan. 1985 p 39 Transl. into ENGLISH from Radiotekh. (USSR), no. 9, Sep. 1984 p 68-69 (For primary document see N85-22976 13-33)
Avail: NTIS HC A05/MF A01

The noise immunity of coherent reception of signals employing multiple phase modulation, and of optimum noncoherent reception of signals employing multiple phase-difference modulation, is analyzed for channels with fixed parameters and white noise for a Gray keying code. Formulas are derived for the error probability in k-tuple phase modulation and for k-tuple phase-difference modulation. The findings are particularly valuable when the signal energy to spectral noise power density ratio is relatively small, in which case the existing approximate relationships are too rough. Author

N85-23024# Joint Publications Research Service, Arlington, Va.
NOISE TOLERANCE OF DIVERSITY RECEPTION IN FREQUENCY-ADAPTIVE DIGITAL TRANSMISSION SYSTEMS Abstract Only **c32**
M. Y. Lesman and G. S. Tukh *In its* USSR Rept.: Electron. and Elect. Eng. (JPRS-UEE-85-001) 9 Jan. 1985 p 39-40 Transl. into ENGLISH from Radiotekh. (USSR), no. 9, Sep. 1984 p 35-37 (For primary document see N85-22976 13-33)
Avail: NTIS HC A05/MF A01

This study investigates the influence of inaccurate estimation of the signal-to-noise ratio on the mean error probability in a frequency-adaptive digital transmission system employing space-diversity reception. The system operates by combining M spatially-separated signals and analyzing the equivalent signal-to-noise ratio for each of the N frequencies allocated for communications. The best frequency (in terms of the maximum signal-to-noise ratio at the output of the combining device) is sent back to the transmitter over the feedback channel, so that the signal can be emitted at the optimum frequency. The analysis assumes that signal feeding in the diversity branches is statistically homogeneous and mutually independent; additive interferences are approximated by normal white noise. It is found that the mean error probability is a strong function of the accuracy with which the signal-to-noise ratio is estimated (sample size n); for n = (5 - 6)N this probability is the same as that of a hypothetical system in which the average signal-to-noise ratio in any of M statistically homogeneous diversity branches is assumed to be known. B.W.

N85-23025# Joint Publications Research Service, Arlington, Va.
ANALYSIS OF INTERFERENCE CAUSED BY INTERFERING RADIO SIGNALS IN COMMUNICATIONS SYSTEMS WITH FREQUENCY SEPARATION OF TELEPHONE CHANNELS AND FREQUENCY MODULATION Abstract Only **c32**
N. I. Kalashnikov and A. P. Stepanov *In its* USSR Rept.: Electron. and Elect. Eng. (JPRS-UEE-85-001) 9 Jan. 1985 p 40 Transl. into ENGLISH from Izv. Vysshikh Uch. Zaved.: Radioelektron. (USSR), v. 27, no. 9, Sep. 1984 p 61-62 (For primary document see N85-22976 13-33)
Avail: NTIS HC A05/MF A01

Analytical formulas are derived which can be used directly to find the interference level caused by an interfering radio signal in a telephone channel at the upper portion of the group spectrum, as well as the highest interference value in any telephone channel. Formulas are derived for the signal voltages at the input to the receiver, the interference power at the output of the frequency detector and the spectral power densities of the valid and interfering radio signals. The concept of an interference attenuation factor is introduced: this factor relates the ratio of the power of the measurement signal in the circuit of the valid signal and the interference at the output of the telephone channel with the ratio of the power of the valid and interfering signals at the receiver input. Author

N85-23026# Joint Publications Research Service, Arlington, Va.
INVESTIGATION OF INFLUENCE OF COMMUNICATIONS LINK AND SYNCHRONIZATION ERROR ON NOISE TOLERENCE OF GROUP TRANSMISSION OF BINARY INFORMATION BASED ON ORTHOGONAL WALSH FUNCTION Abstract Only **c32**
V. A. Vershinin and V. S. Lando *In its* USSR Rept.: Electron. and Elect. Eng. (JPRS-UEE-85-001) 9 Jan. 1985 p 40 Transl. into ENGLISH from Izv. Vysshikh Uch. Zaved.: Radioelektron. (USSR), v. 27, no. 9, Sep. 1984 p 28-32 (For primary document see N85-22976 13-33)
Avail: NTIS HC A05/MF A01

The influence of the communications link and the synchronization error on the noise tolerance of a modem for group transmission of binary information based on orthogonal Walsh functions (by finding the probability of incorrect reception of a message binary code element) is investigated. The influence of the link and synchronization error are analyzed on the basis of the transient response of the communications link. An example is presented in which the number of interfering pulses over the processing interval is described by a Poisson distribution. It is found that group transmission is more noise tolerant than serial transmission when pulse interference is present. The lower the level of interference consisting of normal noise, the greater the gain in noise tolerance. The influence of the communications link and synchronization error becomes more significant as the number of binary code elements increases because of reduced influence of pulse. Author

N85-23027# Joint Publications Research Service, Arlington, Va.
APPROXIMATE RULES FOR SIGNAL DETECTION AGAINST BACKGROUND OF GAUSSIAN CORRELATED INTERFERENCE Abstract Only **c32**
V. M. Frolushkin *In its* USSR Rept.: Electron. and Elect. Eng. (JPRS-UEE-85-001) 9 Jan. 1985 p 41 Transl. into ENGLISH from Izv. Vysshikh Uch. Zaved.: Radioelektron. (USSR), v. 27, no. 9, Sep. 1984 p 14-19 (For primary document see N85-22976 13-33)
Avail: NTIS HC A05/MF A01

Two approximate signal detection rules for the case of a correlated Gaussian interference background with unknown signal and interference parameters are proposed. The first is for the case in which the occurrence of a signal causes the mathematical expectation of the input to be non-zero; the other is for the case in which the signal changes the variance of the input. The proposed rules represent optimum procedures for detecting signals in white Gaussian noise, modified for detection in the presence of correlated interference. The proposed rules depend upon only one additional unknown parameter - the effective number of degrees of freedom. Signal detectors employing these principles are clearly simpler than detectors which estimate each unknown element of the correlation matrix. An analogous approach is likely to achieve positive results for non-Gaussian distributions as well. Author

N85-23028# Joint Publications Research Service, Arlington, Va.
USE OF IMPORTANCE SAMPLING TO INVESTIGATE SIGNAL DETECTION SYSTEMS BY SIMULATED METHOD Abstract Only **c32**
S. Z. Kuzmin and S. S. Kostina *In its* USSR Rept.: Electron. and Elect. Eng. (JPRS-UEE-85-001) 9 Jan. 1985 p 41-42 Transl. into ENGLISH from Izv. Vysshikh Uch. Zaved.: Radioelektron. (USSR), v 27, no. 9, Sep. 1984 p 8-14 (For primary document see N85-22976 13-33)
Avail: NTIS HC A05/MF A01

The use of importance sampling for investigating signal detection systems by simulation employing only a posteriori information about the response of the system to a given input is examined. In the importance sampling method, the initial input is replaced in the simulation by a modified input, after which the system response is corrected by the appropriate weight coefficient. The input is modified such that the detection probability for a given accuracy is estimated according to the smallest possible number of experiments. The case is considered in which the set of modified inputs includes the probability density of which differs from that of the original input only in the values of the parameters f sub mod (x alpha) = f(x alpha sub mod). The number of experiments required to achieve the required accuracy in estimating the probability in direct modeling and in modeling employing modified inputs is calculated. It is found that the importance sampling method makes it possible to estimate small false alarm probabilities with an acceptable number of trials. B.W.

N85-23029# Joint Publications Research Service, Arlington, Va.
NOISE IMMUNITY OF INFORMATION TRANSMISSION SYSTEM WITH PSEUDORANDOM FREQUENCY SWITCHING UNDER WORST-CASE INTERFERENCE CONDITIONS Abstract Only **c32**
A. M. Chudnov *In its* USSR Rept.: Electron. and Elect. Eng. (JPRS-UEE-85-001) 9 Jan. 1985 p 42 Transl. into ENGLISH from Izv. Vysshikh Uch. Zaved.: Radioelektron. (USSR), v. 27, no. 9, Sep. 1984 p 3-8 (For primary document see N85-22976 13-33)
Avail: NTIS HC A05/MF A01

A method is proposed for analyzing the noise immunity of data transmission systems employing pseudorandom frequency

switching for worst-case distribution of intereference by frequencies. The problem is formulated as a minimax game problem of synthesizing counteracting dynamic systems. The effectiveness of the transmission system is defined by its noise immunity, represented by the average error probability. The optimum interference strategy is assigned by finding the distribution function of the interference by frequencies. The noise immunity of a pseudorandom frequency-switching transmission system in which information is transmitted at each frequency by phase-shift keyed pseudorandom (wideband) signals, employing coherent processing in the receiver, is estimated as an example. Author

N85-23030# Joint Publications Research Service, Arlington, Va.
STABILITY OF HIGHLY NONLINEAR OXIDE-ZINC RESISTORS UNDER CONTINUOUS VOLTAGE OF INDUSTRIAL FREQUENCY Abstract Only
K. B. Demyanenko and A. S. Sergeyev *In its* USSR Rept.: Electron. and Elect. Eng. (JPRS-UEE-85-001) 9 Jan. 1985 p 43 Transl. into ENGLISH from ElektroTekh. (USSR), no. 9, Sep. 1984 p 25-28 (For primary document see N85-22976 13-33)
Avail: NTIS HC A05/MF A01

An experimental study of ZnO resistors for high-voltage overvoltage limiters without spark gaps was made, the purpose being to determine the dependence of their aging rate on the applied voltage and on the ambient temperature as well as on their initial current-voltage characteristic. Tests were performed on 150 strings of 10-15 resistors 28 mm in diameter each, connected in series and inserted in a thermosetting polyethylene tube. These strings were tested for a cumulative time of 115, 000 hours with the ambient temperature varied from 0 C to 75 C and with the amplitude of the continuous voltage at 50 Hz frequency varied from 58% to 76% of the residual voltage. Accordingly, the aging process was found to have three stages: (1) initial transient buildup of aging rate; (2) power rising as linear function of time; and (3) power rising faster than resistor temperature, following loss of thermal balance and stability. An empirical relation for the aging rate is derived on this basis, including a voltage parameter which characterizes both current-voltage and power-voltage relations in the resistors. B.W.

N85-23031# Joint Publications Research Service, Arlington, Va.
ELECTRODYNAMIC STABILITY OF COMPOSITE LIQUID-METAL CONTACTS Abstract Only
Osip Borisovich Bron and Vladimir Lvovich Belyayev *In its* USSR Rept.: Electron. and Elect. Eng. (JPRS-UEE-85-001) 9 Jan. 1985 p 44 Transl. into ENGLISH from Izv. Vysshikh Uch. Zaved.: ElektroMekh. (USSR), no. 8, Aug. 1984 p 76-81 (For primary document see N85-22976 13-33)
Avail: NTIS HC A05/MF A01

Composite liquid-metal contacts which included microstructural analysis of the material and electrodynamic tests were studied. The contacts consisted either of cloth or fine-grain filler impregnated with liquid Ga-In-Sn alloy between two hard-metal electrodes. Microstructural analysis was performed with a universal photomicrograph under x50 to 100 magnification. The results reveal wetting patterns in air and between electrodes, immediately after impregnation and over subsequent periods of time ranging from a few days to several months. Seven different electrode pairs were used, made respectively of copper with rough finish, copper with fine finish, tinned copper, brass with rough finish, brass with fine finish, brass mesh, and glass cloth for comparison. The results indicate that, regardless of material and surface finish, complete wetting does not occur immediately but gradually, with attendant increasing of the true contact area and correspondingly decreasing contact resistance. Electrodynamic stability was established on the basis of measurement of bounce forces during closure and under heavy short circuit. Author

N85-23032# Joint Publications Research Service, Arlington, Va.
PLANAR FERROELECTRIC MICROCAPACITORS FOR MICROWAVE DEVICES Abstract Only
M. I. Gubler, V. N. Keys, M. N. Malyshev, and L. T. TerMartirosyan *In its* USSR Rept.: Electron. and Elect. Eng. (JPRS-UEE-85-001) 9 Jan. 1985 p 44-45 Transl. into ENGLISH from Izv. Vysshikh Uch. Zaved.: Radioelektron. (USSR), v. 27, no. 9, Sep. 1984 p 83-84 Original language document announced as A85-11795 (For primary document see N85-22976 13-33)
Avail: NTIS HC A05/MF A01

The properties of heteroepitaxial ferroelectric block structures based on (Ba/0.6/, Sr/0.4/)TiO3 solid solution are investigated experimentally. The characteristic temperature dependences of the capacitance and tangent of the dielectric-loss angle of these microcapacitors were determined in the temperature range of -100 to +100 C. The measurements indicate that these structures may be used as microcapacitors in microwave devices. Their performance can be improved by improving film structure, reducing the defect concentration, and decreasing the thickness of the transition layer. L.M. (IAA)

N85-23033# Joint Publications Research Service, Arlington, Va.
OPTIMIZATION OF OVERALL DIMENSIONS OF ENCLOSURES FOR LOW-VOLTAGE DEVICES AND EQUIPMENT Abstract Only
Davyd Markovich Zektser and Boris Vladimirovich Klimenko *In its* USSR Rept.: Electron. and Elect. Eng. (JPRS-UEE-85-001) 9 Jan. 1985 p 50 Transl. into ENGLISH from Izv. Vysshikh Uch. Zaved.: Elektromekh. (USSR), no. 8, Aug. 1984 p 95-101 (For primary document see N85-22976 13-33)
Avail: NTIS HC A05/MF A01

The problem of optimizing the overall three dimensions of enclosures for low voltage equipment from the standpoint of wall (insulation) material economy is regarded as one of minimizing the volume or the mass of enclosure material rather than of the surface area. This treatment applies where mechanical and thermal stresses determine the minimum wall thickness. In the ideal case where all three dimensions of the parallelepiped are free to be varied, a cubical enclosure with all walls of the same thickness will require the least material. In practical design situations, however, some dimensions are fixed. In one typical case one dimension is fixed by the modulus of elasticity or shear. Here, for a given volume of equipment and thus a given capacity of the enclosure, the latter with the two other dimensions equal and thus having a pair of square parallel walls, will require the least material. In another typical case one dimension is fixed by constraints on the equipment configuration. Here, with the other two dimensions free to be varied, none of them depends on the wall thickness. B.G.

N85-23034# Joint Publications Research Service, Arlington, Va.
DIELECTRIC MEASUREMENTS IN INFRALOW-FREQUENCY BAND Abstract Only
A. A. Belov, V. V. Potemkin, and M. V. Shchetinin *In its* USSR Rept.: Electron. and Elect. Eng. (JPRS-UEE-85-001) 9 Jan. 1985 p 51 Transl. into ENGLISH from Izv. Vysshikh Uch. Zaved.: Radioelektron. (USSR), v. 27, no. 9, Sep. 1984 p 94-96 Original language document announced as A84-11797 (For primary document see N85-22976 13-33)
Avail: NTIS HC A05/MF A01

A high sensitivity instrument has been developed on the basis of a bridge circuit capacitive sensor technique for measuring the reliable measurement of quasi-static variations of permittivity on the level of Delta epsilon prime = Delta epsilon double prime = 0.000001 in a narrow infralow frequency band over a period of 3 to 4 days. A circuit diagram of the device is presented, and measurement results are examined. L.M. (IAA)

N85-23035# Joint Publications Research Service, Arlington, Va.
WINDING INSULATION IN ELECTROMAGNETIC SYSTEMS FOR TOKAMAK REACTOR PLANTS Abstract Only
V. V. Maslov and S. G. Trubachev *In its* USSR Rept.: Electron. and Elect. Eng. (JPRS-UEE-85-001) 9 Jan. 1985 p 51-52 Transl. into ENGLISH from Elektrotekh. (USSR), no. 8, Aug. 1984 p 35-38 (For primary document see N85-22976 13-33)
Avail: NTIS HC A05/MF A01

Magnetic containment of the plasma in nuclear fusion reactors of the Tokamak type requires electromagnets with insulation which

must withstand high temperatures and thermal shocks as well as ionizing radiation in various forms and electric fields, and mechanical loads. Insulation materials to ensure adequate thermophysical and mechanical properties are evaluated, followed by design of insulation systems with satisfactory performance characteristics. Data on neutron fluence energy characteristics and radiation absorption doses during neutron interactions are essential for such an evaluation. Materials considered for insulation in electromagnets with superconductor and cryoresistance windings are glass mica tape with epoxy compound impregnation, glass cloth with epoxy compound impregnation (STE), polyimide glass cloth with adhesive coating (LSNL), glass Textolite with epoxy phenolic binder (STEN), epoxy resin paste with mineral fillers (PE), and polyurethane compound modified by epoxy resin with mineral filler (KPU). Author

N85-23036# Joint Publications Research Service, Arlington, Va.
THERMALLY STIMULATED CONDUCTIVITY IN SEMI-INSULATING GALLIUM ARSENIDE Abstract Only
V. S. Rinkyavichyus and G. S. Kavalyauskene *In its* USSR Rept.: Electron. and Elect. Eng. (JPRS-UEE-85-001) 9 Jan. 1985 p 53 Transl. into ENGLISH from Litovskiy Fiz. Sb. (USSR), v. 24, no. 2, Feb. 1984 p 90-94 (For primary document see N85-22976 13-33)
Avail: NTIS HC A05/MF A01

Single crystals of semi-insulating chromium compensated n-type GaAs with specific resistance on the order of 10 to the 8th power to 10 to the 9th power ohms cm grown by the Chokhral'sk method are investigated. The specimens measured 1.2 by 0.35 by 0.1 cu cm. Thermally stimulated thermal emf and thermally stimulated conductivity were investigated by repeated heating; thermally stimulated conductivity was investigated by the t sub m to t sub stop method, in which the thermally stimulated conductivity is measured after heating the excited specimen to a temperature of t sub stop As t sub stop is gradually increased by 2 to 5 K, a series of conductivity curves is measured, making it possible to establish the presence of several overlapping maxima. The activation energy of the adhesion levels of the holes and the capture cross section of the charge carriers are determined. Four conductivity maxima are observed between 100 and 300 K which correspond to activation energies ranging from 0.14 to 0.29 eV and a capture cross section of the order of 10 to the minus 22nd power sq cm. The overlapping third and fourth maxima correspond to a 0.29 eV hole adhesion level with capture cross sections differing by an order of magnitude. Author

N85-23037# Joint Publications Research Service, Arlington, Va.
NON-SELF-MAINTAINED HIGH-VOLTAGE LOW-PRESSURE DISCHARGE Abstract Only
V. S. Boldasov, A. I. Kuzmichev, and D. S. Fillipychev *In its* USSR Rept.: Electron. and Elect. Eng. (JPRS-UEE-85-001) 9 Jan. 1985 p 54 Transl. into ENGLISH from Izv. Vysshikh Uch. Zaved.: Radiofiz. (USSR), v. 27, no. 7, Jul. 1984 p 925-933 (For primary document see N85-22976 13-33)
Avail: NTIS HC A05/MF A01

The characteristics of, and the physical processes underlying, a nonself maintained high voltage discharge occurring during the emission of electrons into a low pressure space between flat metal electrodes are investigated. The discharge is studied in kinetic approximation for pressures equal to or greater than the critical pressure, with allowance for the movement of charged particles in the self consistent field and the ionization of gas by cathode and secondary electrons, ions and fast neutrals which are formed when the ions are recharged. The role of these processes is assessed, and the transmission of current through the gas discharge space is analyzed. The mechanisms underlying the development of breakdown in thyratrons is clarified. The use of the discharge of a cathode with defined electron emission current makes it possible to analyze processes occurring at pressures greater than and less than the critical pressure, to determine the perveance of the high voltage interval for subcritical pressures, and the current of the transition to the plasma form for supercritical pressures. Author

N85-23038# Joint Publications Research Service, Arlington, Va.
ANALYSIS AND DESIGN OF LINEAR MICROWAVE TRANSISTOR AMPLIFIERS Abstract Only
G. V. Petrov *In its* USSR Rept.: Electron. and Elect. Eng. (JPRS-UEE-85-001) 9 Jan. 1985 p 54-55 Transl. into ENGLISH from Radiotekh. i Elektron. (USSR), v. 29, no. 8, Aug. 1984 p 1555-1560 (For primary document see N85-22976 13-33)
Avail: NTIS HC A05/MF A01

The characteristics of linear microwave amplifiers can be analyzed on the basis of S- or T-parameters of a four pole network, with the noise factor calculated in terms of equivalent Tau or t-parameters. Here the corresponding system of two algebraic equations are formulated in parameters of the transmission (T and t) matrices. Their solution for gain and stability factor reveals that an absolutely stable or potentially unstable amplifier is possible, with passive matching circuits used in most cases. Three procedures for design of a transistor amplifier with thermal noise under a resistive load are shown: (1) amplifier with given noise factor and unity voltage standing wave ratio at the output; (2) amplifier with given noise factor and minimum VSWR at both output and input; and (3) amplifier with given gain and minimum VSWR at both output and input. All three design variants are illustrated with numerical data. Author

N85-23039# Joint Publications Research Service, Arlington, Va.
NUMERICAL SIMULATION OF INVERTERS WITH I2L ELEMENTS INCLUDING EFFECTS OF HIGH DOPING LEVEL Abstract Only
I. I. Abramov *In its* USSR Rept.: Electron. and Elect. Eng. (JPRS-UEE-85-001) 9 Jan. 1985 p 55 Transl. into ENGLISH from Izv. Vysshikh Uch. Zaved.: Radioelektron. (USSR), v. 27, no. 8, Aug. 1984 p 16-22 (For primary document see N85-22976 13-33)
Avail: NTIS HC A05/MF A01

Numerical simulation of semiconductor structures, specifically I(2)L inverters, is considered with the effects of high doping levels taken into account. The corresponding system of fundamental equations is solved for three models of bandgap narrowing: (1) Vol'fson-Subashiyev model for n-type doping and for p-type doping; (2) Lanyon-Taft model for n-type doping or p-type doping; and (3) Slotboom-DeGraaff model for bipolar transistor. All these continuous models include degeneracy, impurity deionization, doping level dependence of charge carrier lifetime and Auger recombination coefficients, temperature changes, mobility and concentration changes in the base region. Simulation can accordingly be based on Boltzmann statistics with the aid of experimental data and disregarding the asymmetry of bandgap narrowing (A = 0.5), except in the Vol'fson-Subashiyev model, while Fermi statistics will contain the error of twice accounting for degeneracy. Calculations for multidimensional simulation of a unicollector I(2)L inverter with the doping level /N sub g - N sub a/ reaching 10 to the 20th power/cu cm under the collector center and 10 to the 18th power/cu cm under the injector were made by the fast converging method of two step vector relaxation written in FORTRAN-4 for a YeS computer. Author

N85-23040# Joint Publications Research Service, Arlington, Va.
ELECTROTHERMAL TRANSDUCER WITH SHORT TIME CONSTANT Abstract Only
S. G. Bogdanov and L. K. Bogdanova *In its* USSR Rept.: Electron. and Elect. Eng. (JPRS-UEE-85-001) 9 Jan. 1985 p 56 Transl. into ENGLISH from Izv. Vysshikh Uch. Zaved.: Radioelektron. (USSR), v. 27, no. 9, Sep. 1984 p 41-46 (For primary document see N85-22976 13-33)
Avail: NTIS HC A05/MF A01

The possibility is investigated of obtaining electrothermal transducers (devices which employ conversion of an input electrical signal in a resistive heat source to a heat flux, of the heat flux to the temperature of a working body, and conversion of the latter in a heat sensing element to an output signal) with minimal thermal inertia. The factors limiting the speed of electrothermal transducers are analyzed. A condition is derived for achieving the minimum thermal time constant which holds for any amount of heat release.

It is shown experimentally that electrothermal transducers can have thermal time constants on the order of a few microseconds. Through theoretical analysis and experimental measurements of static resistance to heat release, the condition for achieving the maximum thermal time constant is satisfied up to frequencies on the order of 1/MHz given the current level of technology, making it possible to expect the construction of transducers with time constants of 10 to the minus 7th power seconds. Author

N85-23041# Joint Publications Research Service, Arlington, Va.
SYNTHESIS OF OPTIMUM SMOOTH TRANSITION IN MICROSTRIP THROUGH LINE ON MICROWAVE INTEGRATED CIRCUIT Abstract Only
A. A. Yashin and Y. M. Choban *In its* USSR Rept.: Electron. and Elect. Eng. (JPRS-UEE-85-001) 9 Jan. 1985 p 65 Transl. into ENGLISH from Radiotekh. i Elektron. (USSR), v. 29, no. 8, Aug. 1984 p 1617-1619 (For primary document see N85-22976 13-33)
Avail: NTIS HC A05/MF A01

A problem in designing microstrip trough lines as transmission lines for microwave hybrid-film integrated circuits is the synthesis of the optimum smooth widening of the center conductor on the dielectric substrate. Such a transition is described by the relation c(z)= Phi [b(z)] sub Z (sub0)(z) = const or , more explicitly c(z)= Phi [b(z)] sub C (sub1)(z) = const (z- longitudinal coordinate, 1- length, 2b- width of center conductor, 2c- clearance between outer conductors, Z sub O- wave impedance, C sub 1 - capacitance per unit length). It can be accurately synthesized according to the single-model T-approximation of the electrodynamic process, on the basis of quasi-steady solutions to the corresponding singular integral equations and with conformal mapping. This is demonstrated by calculations made for a typical trough line as well as for a coplanar one. Author

N85-23042# Joint Publications Research Service, Arlington, Va.
MILLIMETER-WAVE RANGE MASERS: A REVIEW Abstract Only c36
N. T. Cherpak *In its* USSR Rept.: Electron. and Elect. Eng. (JPRS-UEE-85-001) 9 Jan. 1985 p 67 Transl. into ENGLISH from Izv. Vysshikh Uch. Zaved.: Radiofiz. (USSR), v. 27, no. 7, Jul. 1984 p 815-851 Original language document announced as A84-48152 (For primary document see N85-22976 13-33)
Avail: NTIS HC A05/MF A01

The paper surveys work done on millimeter-wave traveling-wave masers in the USSR, USA, and Sweden, mainly in the 1970's. Particular consideration is given to: the physical principles and characteristics of traveling-wave masers; the search for and investigation of active media; the design of electrodynamic systems for the interaction of the active medium with microwave fields; the establishment of conditions of stable amplification; and the development of such elements as nonreciprocal components, pumping sources, and transmission lines. The current status and future prospects of the physics and technology of masers are briefly examined. L.M. (IAA)

N85-23043# Joint Publications Research Service, Arlington, Va.
EFFECT OF SPACE-CHARGE FIELD ON OUTPUT CHARACTERISTICS OF O-TYPE OSCILLATORS WITH DISTRIBUTED INTERACTION Abstract Only
D. M. Vavriv, O. A. Tretyakov, and A. A. Shmatko *In its* USSR Rept.: Electron. and Elect. Eng. (JPRS-UEE-85-001) 9 Jan. 1985 p 67-68 Transl. into ENGLISH from Radiotekh. i Elektron. (USSR), v. 29, no. 8, Aug. 1984 p 1571-1579 Original language document announced as A84-48610 (For primary document see N85-22976 13-33)
Avail: NTIS HC A05/MF A01

A theoretical study is made of the effect of the space-charge field of a two-dimensional electron beam on the physical features of the operation of a prolonged-interaction resonance oscillator. It is shown that the space-charge field can produce a significant increase in the output power and efficiency, and the regimes of stationary and nonstationary oscillation are analyzed. An examination of the energy conservation law shows that, although the energy component required to overcome the Coulomb repulsion forces is small in itself, it facilitates the establishment of conditions for the effective conversion of electron kinetic energy into the oscillation energy of the resonator. L.M. (IAA)

N85-23044# Joint Publications Research Service, Arlington, Va.
INTEGRATED OPTICAL COMPONENTS UTILIZING ACOUSTOOPTIC AND ELECTROOPTIC DIFFRACTION IN MICRO-WAVEGUIDES Abstract Only
V. A. Voznesenskiy, L. G. Gassanov, and G. S. Felinskiy *In its* USSR Rept.: Electron. and Elect. Eng. (JPRS-UEE-85-001) 9 Jan. 1985 p 68 Transl. into ENGLISH from Izv. Vysshikh Uch. Zaved.: Radioelektron. (USSR), v. 27, no. 8, Aug. 1984 p 9-16 (For primary document see N85-22976 13-33)
Avail: NTIS HC A05/MF A01

The diffraction efficiency of integrated optics using microwaveguides with electrooptic and acoustooptic effects is calculated from truncated equations for coupled modes describing steady-state interaction of an incident wave and the wave diffracted by a surface acoustic wave, considering, specifically, Bragg diffraction of light. The resulting wave equation is solved either in the Wentzel-Kramers-Brillouin approximation or by piecewise-linear approximation. The result yields the dependence of diffraction efficiency on the voltage applied to the electrooptic phase grating. Theoretical data are correlated with experimental data on waveguides in Y-cut LiNbO3 crystals with 35 nm to 50 nm thick titanium films. Phase gratings were formed by interdigital capacitor arrays, for operation as modulator. Measurements were made in the Raman-Nath diffraction mode as well as in the Bragg diffraction mode. A.R.H.

N85-23045# Joint Publications Research Service, Arlington, Va.
MATHEMATICAL MODELING OF TWO-FREQUENCY LASER SOUNDING OF SCATTERING MEDIA Abstract Only c36
A. V. Belinskiy *In its* USSR Rept.: Electron. and Elect. Eng. (JPRS-UEE-85-001) 9 Jan. 1985 p 75 Transl. into ENGLISH from Zh. Nauchnoy i Prikl. Fotografii i Kinematografii (USSR), v. 29, no. 5, Sep.-Oct. 1984 p 343-348 (For primary document see N85-22976 13-33)
Avail: NTIS HC A05/MF A01

A mathematical model of two-frequency pulsed laser sounding of optically transparent scattering media is developed. Allowance is made for nonlinear interaction of the radiation at two frequencies separated by an amount close to the Raman resonance frequency of the medium. A system of differential equations is cited that describes the interaction between pulses at the two different frequencies. The energy characteristics of the radiation resulting from elastic scattering of the Stokes radiation pulse are analyzed for the approximation of single scattering. Relationships are derived which connect the optical characteristics of the medium with the radiation flux at the entrance pupil of the receiving system and which can be used in developing methods for sounding scattering media. Author

N85-23046# Joint Publications Research Service, Arlington, Va.
GEOPHYSICAL LASER INTERFEROMETER WITH 12.5 METER BASE Abstract Only c36
A. S. Gorshkov and M. N. Dubrov *In its* USSR Rept.: Electron. and Elect. Eng. (JPRS-UEE-85-001) 9 Jan. 1985 p 75-76 Transl. into ENGLISH from Radiotekh. i Elektron. (USSR), v. 29, no. 9, Aug. 1984 p 1638-1641 (For primary document see N85-22976 13-33)
Avail: NTIS HC A05/MF A01

The long-base laser interferometer installed in Garm (TaSSR) for geophysical observations during seismic activity includes a Lamb-stabilized LG-32 laser (wavelength 0.63 micrometer), a matching telescope, a light beam splitter with a pair of plane 45 deg mirrors behind, a protective straight light guide, and a reversing plane 90 deg mirror at the other end. The base length, namely the distance between light splitter and reversing mirror, is 12.5 m and the path difference in this asymmetric Michelson interferometer is 25 m. The interference-type phase meter contains an acoustooptic modulator. This instrument recorded strains within the 0 to 1 Hz frequency range, as well as a local earthquake

during December 1978. A high-frequency stability for high accuracy of strain measurements requires decoupling the laser, increasing the diameter of the light guide, and decreasing the diameter of the light beam. Author

N85-23047# Joint Publications Research Service, Arlington, Va.
INVESTIGATION OF DYNAMICS OF RADIATION SPECTRUM OF INJECTION LASERS BY INFRARED IMPULSE FOURIER SPECTROSCOPY Abstract Only **c36**
A. A. Akimov, A. S. Logginov, and K. Y. Senatorov *In its* USSR Rept.: Electron. and Elect. Eng. (JPRS-UEE-85-001) 9 Jan. 1985 p 76 Transl. into ENGLISH from Izv. Vysshikh Uch. Zaved.: Radioelektron. (USSR), v. 27, no. 9, Sep. 1984 p 90-92 (For primary document see N85-22976 13-33)
Avail: NTIS HC A05/MF A01

An infrared pulsed Fourier spectroscopy method is developed for investigating non-steady state processes in radiation which occur during pulsed pumping of injection lasers. The method can be employed for wavelengths exceeding 1.3 micrometers, where electrooptical chronography is impossible because of the uavailability of photocathodes with the appropriate red boundary. Spectral dynamics are investigated experimentally by obtaining the autocorrelation function of the field using a Michaelson interferometer, employing a high speed photodiode with high sensitivity at the emitted wavelengths, and employing a strobing device to investigate the temporal behavior of the process occurring in the spectrum. A diagram of the experimental set up is presented. The proposed method is more sensitive than the standard approach employing a monochromator and strobed photodetector. Author

N85-23048# Joint Publications Research Service, Arlington, Va.
INVARIANCE OF PROBABILITY CHARACTERISTICS OF DETECTOR TO SHAPE OF OPTICAL PULSE SIGNALS Abstract Only **c36**
K. Y. Rumyantsev and V. S. Firsov *In its* USSR Rept.: Electron. and Elect. Eng. (JPRS-UEE-85-001) 9 Jan. 1985 p 77 Transl. into ENGLISH from Izv. Vysshikh Uch. aved.: Radioelektron. (USSR), v. 27, no. 9, Sep. 1984 p 62-64 (For primary document see N85-22976 13-33)
Avail: NTIS HC A05/MF A01

Four approximations of the description of the shape of optical signals at the receiving end of a laser system are analyzed: rectangular, sinusoidal, Rayleigh and normal. The parameters for the Rayleigh and normal approximations are based on 99.7% of the energy being concentrated in the interval [O, T(1)]. A detector is analyzed in which the maximum value of the random process is extracted at the output of the photodetector in the observation interval and compared with a threshold. It is found that the probability characteristics of a detector for pulsed light signals depend upon the ratio of the signal and background radiation power, as well as their absolute values. The probability characteristics of the detector are determined by the useful optical radiant energy, and are independent of the form of the signal when the bandwidth of the receiving/amplifying channel is optimum. The bandwidth, depends upon the ratio of the power of the signal and background radiation. Author

N85-23049# Joint Publications Research Service, Arlington, Va.
GENERATION OF LONGITUDINAL ACOUSTIC WAVES BY MODULATED HELICON WAVES Abstract Only **c71**
N. Y. Vigdorchik *In its* USSR Rept.: Electron. and Elect. Eng. (JPRS-UEE-85-001) 9 Jan. 1985 p 78 Transl. into ENGLISH from Izv. Vysshikh Uch. Zaved.: Radiofiz. (USSR), v. 27, no. 7, Jul. 1984 p 897-902 (For primary document see N85-22976 13-33)
Avail: NTIS HC A05/MF A01

Modulation processes occurring in metals and semiconductors in a strong magnetic field are investigated. It is shown that the modulation of an initial helicon wave of finite amplitude propagating in metals causes a change in the spectrum of the longitudinal acoustic wave. The propagation of nonlinear steady-state waves in metals is investigated; the possibility of solitary waves (envelope solitons) existing in them is proved. Author

N85-23050# Joint Publications Research Service, Arlington, Va.
ACOUSTOOPTIC DEMODULATION OF FREQUENCY-MODULATED SIGNALS Abstract Only **c71**
M. P. Vasilyev *In its* USSR Rept.: Electron. and Elect. Eng. (JPRS-UEE-85-001) 9 Jan. 1985 p 78-79 Transl. into ENGLISH from Radiotekh. i Elektron. (USSR), v. 29, no. 8, Aug. 1984 p 1605-1609 (For primary document see N85-22976 13-33)
Avail: NTIS HC A05/MF A01

A waveguide receives light from a monochromatic source through a collimator and sound through a piezoceramic converter array, with a sound absorber at the back end. The waveguide transmits modulated light through a cylindrical integrating lens to a multichannel photodetector array with a light spot from each channel projected on an opaque screen behind. The space-time distribution of a linearly frequency modulated signal, calculated for Raman-Nath diffraction by a sound wave in the optical aperture, corresponds to the electromagnetic field of the light wave in the focal plane of the integrating lens. Almost the total light energy remains within the first + or - pair of diffraction peaks. The demodulator sensitivity to changes in the demodulator sensitivity to changes in the luminous flux and thus to changes in the frequency during deflection of the light spots will be higher when the aperture in each channel is of a different size. A.R.H.

N85-23051# Joint Publications Research Service, Arlington, Va.
ACOUSTOOPTIC CELL AS SPACE-FREQUENCY FILTER Abstract Only **c71**
V. I. Balakshiy *In its* USSR Rept.: Electron. and Elect. Eng. (JPRS-UEE-85-001) 9 Jan. 1985 p 79 Transl. into ENGLISH from Radiotekh. i Elektron. (USSR), v. 29, no. 8, Aug. 1984 p 1610-1616 (For primary document see N85-22976 13-33)
Avail: NTIS HC A05/MF A01

With an acoustooptic cell regarded as a linear space-frequency filter, the feasibility of space filtration of optical signals by such a cell is examined from the standpoint of selective diffraction characteristics of the interaction medium. Diffraction characteristics of the interaction medium. Diffraction of a space-modulated light wave by an elastic ultrasound wave with arbitrary spectral composition is considered, assuming a low diffraction efficiency. The optical radiation pattern of a cell with a birefringent medium is calculated in a general form applicable to monochromatic and polychromatic elastic sound waves, to isotropic and anisotropic interaction modes, and to Bragg as well as Raman-Nath diffraction modes. In the case of high diffraction efficiency such an acoustooptic cell is a linear filter only when harmonic ultrasound waves interact with light waves. The transfer function of a Bragg filter and the dependence of its bandwidth on the acoustic power indicate that such a filter becomes even more selective. Author

N85-23052# Joint Publications Research Service, Arlington, Va.
ACCURACY OF RANDOM SIGNAL SPECTRAL PARAMETER ESTIMATION AGAINST INTERFERENCE BACKGROUND IN ACOUSTOOPTICAL SPECTRUM ANALYZERS Abstract Only **c71**
G. S. Nakhmanson *In its* USSR Rept.: Electron. and Elect. Eng. (JPRS-UEE-85-001) 9 Jan. 1985 p 80 Transl. into ENGLISH from Radiotekh. (USSR), no. 9, Sep. 1984 p 49-52 (For primary document see N85-22976 13-33)
Avail: NTIS HC A05/MF A01

The use of photodetectors based on charge coupled devices as optoelectronic transducers in acoustooptical spectrum analyzers is investigated. The structural diagram of an acoustooptical spectrum analyzer for parallel spectral analysis over a wide range of frequencies is presented. A formula is derived for the intensity distribution of the light field in the output focal plane of the lens of an ultrasonic light modulator operating in the Bragg diffraction mode. It is found that such devices can be used to estimate the spectral parameters of random signals with the required accuracy. Author

N85-23053# Joint Publications Research Service, Arlington, Va.
EXPERIMENTAL STUDY OF HIGH-STABILITY OSCILLATOR WITH SURFACE-ACOUSTIC-WAVE RESONATOR IN FEEDBACK

LOOP Abstract Only c71
Y. V. Gulyayev, V. I. Grigoryevskiy, A. M. Kmita, A. P. Kundin, and O. A. maltsev *In its* USSR Rept.: Electron. and Elect. Eng. (JPRS-UEE-85-001) 9 Jan. 1985 p 80 Transl. into ENGLISH from Radiotekh. i Elektron. (USSR), v. 29, no. 8, Aug. 1984 p 1641-1642 (For primary document see N85-22976 13-33)
Avail: NTIS HC A05/MF A01

An oscillator with feedback through a surface acoustic wave resonator was built and tested for frequency stability. The resonator with two inputs contained an interdigital transducer array bare on one side and metallized on the other, inside the cavity between two reflecting structures separated by a distance of 201 acoustic half wavelength on an ST-cut quartz substrate. The resonator has been designed for an operating frequency of 126 MHz and its performance, in terms of amplitude frequency and phase frequency characteristics is analogous to that of a volume acoustic wave quartz resonator. The short time frequency stability of the oscillator, measured with a Ch3-34A instrument, was found to be within 5.10-9 averaged over 1 s. Author

N85-22515*# Communications Satellite Corp., Clarksburg, Md. COMSAT Lab.
INVESTIGATIONS OF RADIATION-INDUCED AND CARRIER-ENHANCED CONDUCTIVITY
A. Meulenberg, Jr., L. W. Parker (Parker (Lee W.), Inc., Concord, Mass.), E. J. Yadlowski (H-Y Tek Corp., Radford, Va.), and R. C. Hazelton (H-Y Tek Corp., Radford, Va.) *In* NASA. Lewis Research Center Spacecraft Environ. Interactions Technol., 1983 Mar. 1985 p 571-590 refs (For primary document see N85-22470 13-18)
Avail: NTIS HC A99/MF E03 CSCL 09C

N85-22846# Joint Publications Research Service, Arlington, Va.
X-RAY LITHOGRAPHY AND VLSI CIRCUITS
Gu Bichun *In its* Chinese Rept.: Sci. and Technol. (JPRS-CST-85-005) 20 Feb. 1985 p 44-55 refs Transl. ino ENGLISH from Wuli (Beijing, China), v. 13, no. 1, Jan. 1984 p 15-20 (For primary document see N85-22843 13-31)
Avail: NTIS HC A10/MF A01

N85-23172# Joint Publications Research Service, Arlington, Va.
STUDY OF PHASE RADIOGEODETIC SYSTEMS WITH PHASE-LOCKED LOOPS Abstract Only
V. P. Glumov, O. S. Golod, V. V. Sizov, and E. I. Ter-Saakov *In its* USSR Rept.: Earth Sci. (JPRS-UES-85-002) 1 Feb. 1985 p 99 Transl. into ENGLISH from Izv. Vyssh. Ucheb. Zaved., Geod. i Aerofotosyemka (Moscow), no. 3, May - Jun. 1984 p 14-20 (For primary document see N85-23116 13-42)
Avail: NTIS HC A07/MF A01

34 FLUID MECHANICS AND HEAT TRANSFER

Includes boundary layers; hydrodynamics; fluidics; mass transfer; and ablation cooling.

For related information see also *02 Aerodynamics* and *77 Thermodynamics and Statistical Physics.*

N85-23054# British Library Lending Div., Boston Spa (England).
EXAMINATION OF THE CONTACT WETTING ANGLE IN THE VICINITY OF CRITICAL TEMPERATURE
V. P. Zheleznyi 8 Feb. 1985 6 p refs Transl. into ENGLISH from Issled. Protsessov Teplo i Massoperenosa, Kiev, 1979 p 127-130
(BLL-T6416/BG/CRS/LR-ST735/84) Avail: British Library Lending Div., Boston Spa, England

The data on the contact angle of wetting theta of the solid body by a liquid are required for solving various problems in science and technology and, in particular, for the experimental determination of the thermophysical properties, such as density and surface tension. This aspect is of great importance because recently published studies show that the contact wetting angle rapidly increases at temperature t = (T sub cr-T)/T sub cr t< 0.2 so that it is necessary to question the reliability of the data on the surface tension coefficient of liquids determined by means of the capillary method. Comparison of the data on the surface tension of SF sub 6 obtained by the capillary lift method and by the method of light diffusion on capillary waves was used as a basis for concluding that satisfactory wetting in the vicinity of the critical point is retained in the Freon - IZBI glass system in the range 0.02 <t<. R.J.F.

N85-23055 Rensselaer Polytechnic Inst., Troy, N. Y.
TURBULENCE MEASUREMENTS IN SHOCK INDUCED FLOWS Ph.D. Thesis
James William Trolier 1984 157 p
Avail: Univ. Microfilms Order No. DA8428361

Turbulence levels were made in the incident and reflected flows of a shock tube. Measurements were made with a double wire hot wire anemometer. Small disturbance approximations were used to relate voltage fluctuations to mass flux and total temperature fluctuations. Computed velocity and density fluctuations, using a zero pressure fluctuation level assumption, followed mass flux and total temperature fluctuations, respectively. An apparent strong influence of driver diaphragm opening characteristics on turbulence level was noted. At fixed Mach number and flow temperature, turbulence intensities are a function of Reynolds number, pressure difference across the diaphragm, and diaphragm material. Measurements of turbulence amplification across the reflected shock were made. Velocity turbulence amplification levels decreased with Reynolds number. Density and total temperature amplification levels are typically 60 to 80% lower than velocity amplification. Standard hot wire techniques can successfully be applied to measure turbulence levels in shock induced flows. Dissert. Abstr.

N85-23056*# United Technologies of New Mexico, Inc., East Hartford, Conn.
INVESTIGATION OF PARABOLIC COMPUTATIONAL TECHNIQUES FOR INTERNAL HIGH-SPEED VISCOUS FLOWS Final Report
O. L. Anderson and G. D. Power Apr. 1985 40 p refs
(Contract NAS1-17561)
(NASA-CR-172555; NAS 1.26:172555; R84-956611) Avail: NTIS HC A03/MF A01 CSCL 20D

A feasibility study was conducted to assess the applicability of an existing parabolic analysis (ADD-Axisymmetric Diffuser Duct), developed previously for subsonic viscous internal flows, to mixed supersonic/subsonic flows with heat addition simulating a SCRAM-JET combustor. A study was conducted with the ADD code modified to include additional convection effects in the normal momentum equation when supersonic expansion and compression waves were present. It is concluded from the present study that for the class of problems where strong viscous/inviscid interactions are present a global iteration procedure is required. G.L.C.

N85-23057*# Lockheed Missiles and Space Co., Huntsville, Ala. Computational Mechanics Group.
HPFTP FLOW DIVERTER ANALYSIS Monthly Progress Report
L. W. Spadley 1 Feb. 1985 2 p
(Contract NAS8-35984)
(NASA-CR-171424; NAS 1.26:171424; LMSC-HREC-PR-F042316) Avail: NTIS HC A02/MF A01 CSCL 20D

A computational fluid flow analysis on the flow diverter system under consideration for the Space Shuttle main engine high pressure fuel turbopump (SSME HPFTP) is proposed. A three dimensional viscous flow environment is computed to optimize the geometric configuration and location of the flow diverter system. The analysis consists of a fully turbulent cold flow calculation by Navier-Stokes equations and a Baldwin-Lomax turbulence model. The equations are numerically by a finite difference/element procedure. The results will provide the steady and unsteady pressure field and thermal environment required to assess the usefulness of the flow diverter system in deflecting the cold flow away from the hot turbine components. A geometry optimization

study determines the best diverter shape and location to avoid larger thermal gradients on the rotor/stator components. E.A.K.

N85-23058# Defence Research Information Centre, Orpington (England).
TURBULENT FLOWS OF SURFACANT SOLUTIONS
P. B. Aslanov, S. N. Maksyutenko, I. L. Povkh, A. P. Simonenko, and A. B. Stupin Nov. 1984 26 p refs Transl. into ENGLISH from Mekhan. Zhidkosti i Gaza, (USSR), no. 1, 1983 p 37
(AD-B089137L; DRIC-T-7376; BR93714) Avail: NTIS HC A03/MF A01

Velocity profiles and turbulence intensity in surfactant solutions were measured. Occurrence of turbulent energy and dissipation of averaged motion energy were calculated. The influence of electrolytes and temperature on reduction in hydrodynamic resistance was investigated. Results show that micelle-forming surfactants can be used to control liquid turbulent transfer processes. Author (ESA)

N85-23059# Pennsylvania State Univ., University Park. Applied Research Lab.
GRID GENERATION FOR A PUMP COLLECTOR
G. H. Hoffman 4 Oct. 1984 33 p
(Contract N00024-79-C-6043)
(AD-A150217; ARL/PSU/TM-85-12) Avail: NTIS HC A03/MF A01 CSCL 20/4

A simple scheme is presented which generates a surface-fitted grid for a pump collector with application to numerical solution of frozen vorticity flow inside the collector (the application to be covered in a later report). The scheme is two-dimensional in nature, but by a simplification of the collector geometry generates a three-dimensional grid. The procedure is very fast, requiring between two and three seconds of CPU time on an IBM 370/3033. Example grids are presented for several collector geometries. To develop a capability for computing such a grid would require considerable time and effort. The development time can be reduced drastically by making two simplifying assumptions about the collector geometry. Thus, a two-dimensional grid can be fitted to the cross sections of the simplified geometry and then rotated about the O axis to produce a three-dimensional grid. GRA

N85-23060# Ballistic Research Labs., Aberdeen Proving Ground, Md.
LIQUID MOMENT ON A FILLED CONING CYLINDER DURING SPIN-UP: AD HOC MODEL Final Technical Report
N. Gerber Dec. 1984 51 p
(AD-A150280; AD-F300562; BRL-TR-2628) Avail: NTIS HC A04/MF A01 CSCL 19/1

A liquid-filled right circular cylinder, coning at constant frequency and small amplitude, impulsively begins spinning with a fixed angular velocity. The ensuing history of the moment, i.e., pressure plus viscous shear, exerted by the liquid on the container is investigated here by computation of the quasi-steady state response of the fluid to the motion of the shell. The partial differential equations of flow are linearized, and a modal analysis (separated variable solution) is applied. The difficulty with endwall boundary conditions which arises from stipulating a modal analysis is avoided by specifying a heuristic boundary condition and then satisfying it aproximately. The current procedure for approximating the boundary condition is an improvement over the one employed in previous work (ARBRL-TR-02563) to obtain the pressure moment. Calculations indicate that peaks of overturning moment occur at or near those times when the coning frequency is equal to one of the frequencies of inertial oscillations of the liquid. This phenomenon of resonance extends the results of Stewartson obtained for inviscid perturbations in solid body rotation. Included here also are a discussion of the accuracy of a part of the method and comparisons with output of the inviscid perturbation method and the above-mentioned previous method. GRA

N85-23061# Hebrew Univ., Jerusalem (Israel). Dept. of Atmospheric Sciences.
THE ORIENTATION DISTRIBUTION OF NONSPHERICAL AEROSOL PARTICLES WITHIN A CLOUD Interim Report, Dec. 1983 - Mar. 1984
Isaiah Gallily Nov. 1984 21 p
(Contract DAJA45-83-C-0004; DA Proj. 1L1-62662-A-552)
(AD-A150600; CRDC-CR-84118) Avail: NTIS HC A02/MF A01 CSCL 20/4

The orientation distribution function of fibrous and platelet-like aerosol particles was calculated for a general laminar flow by solving the Fokker-Plank equation. It has been found that this function shows maxima and minima, which indicates a preferred orientation. The cases of point source and a laminar jet are brought out as an example. GRA

N85-23062# California Univ., Berkeley. Lawrence Berkeley Lab. Earth Science Div.
EFFECTS OF FRACTURE ROUGHNESS ON FLUID FLOW THROUGH A SINGLE DEFORMABLE FRACTURE
Y. W. Tsang and P. A. Witherspoon Oct. 1984 16 p refs Presented at the Intern. Congr. on Hydrology of Rocks of Low Permeability, Tucson, Ariz., 7-12 Jan. 1985
(Contract DE-AC03-76SF-00098)
(DE85-004593; LBL-17514; CONF-850101-4) Avail: NTIS HC A02/MF A01

The cubic law for fluid flow through a single fracture commonly employed in simulations of fluid flow through a fractured medium assumes the smooth parallel-plate idealization of each fracture. Results of theoretical investigations on the effects of fracture surface roughness on fluid flow through a single deformable fracture are summarized. A theory to relate the geometrical characteristics of the fracture to its mechanical properties is constructed so that an aperture density distribution for the fracture may be derived from fracture stress-strain measurements. A review of available fracture roughness profiles showed that the aperture density distributions of real fractures may take on various shapes: sharply peaked, broad and flat, skewed and peaked toward the large apertures or toward the small apertures. The different shapes give rise qualitatively different variations of flow rate with normal stress applied to the fracture. Calculations were first carried out for flow with no tortuosity; then the effect of path tortuosity and connectivity on fluid flow rate were investigated. DOE

N85-23063# Sandia Labs., Albuquerque, N. Mex. Aerodynamics Dept.
SIGNIFICANCE OF THE THIN-LAYER NAVIER-STOKES APPROXIMATION
F. G. Blottner 20 Jan. 1985 10 p refs Presented at 3rd Symp. on Numerical and Phys. Aspects of Aerodyn. Flows, Long Beach, Calif., 20 Jan. 1985
(Contract DE-AC04-76DP-00789)
(DE85-002630; SAND-84-2345C; CONF-850139-1) Avail: NTIS HC A02/MF A01

The terms neglected in the thin-layer approximation are evaluated by transforming the equations into curvilinear surface coordinates and comparing these equations with the second order Navier-Stokes equations. In this formulation of the thin-layer equations, it is determined that the longitudinal curvature terms of second-order boundary layer theory are missing. The complete Navier-Stokes equations are required before the surface coordinate transformation in order to retain the curvature terms in the resulting governing equations. In addition, it is shown that the thin-layer equations with the Cartesian velocity components as dependent varables are not readily reduced to he boundary layer equations. DOE

N85-23064# Idaho National Engineering Lab., Idaho Falls.
MAGNETIC REFRIGERATION AND HEAT PUMPING DESIGN OPTIONS
Lance D. Kirol 1984 21 p refs Presented at the Magnetic Refrigeration Workshop, Los Alamos, N.Mex., 20 Sep. 1984
(Contract DE-AC07-76ID-01570)
(DE85-003405; EGG-M-21984; CONF-8409186-1) Avail: NTIS HC A02/MF A01

Magnetic cycles have potential for refrigeration and heat

pumping from temperatures of 4 K or below to over 500 K. Theoretical studies have repeatedly indicated that demagnetization refrigeration has significant potential advantage over gas expansion or vaporization refrigeration. Tests of physical models have shown that there are many design problems to be overcome. However, these tests have not exposed any fundamental reasons why high efficiency and capacity predicted by analysis cannot be realized. Adequate solutions to all design problems have not been found, and practical machines have not been demonstrated. Continued study, testing, and exchange of ideas is necessary for rapid development of this technology. Most studies conducted to date have focused on a single magnetic refrigerator design concept and on problems associated with that configuration. Performance considerations and design options are discussed. Concepts discussed should be applicable to the entire range of possible cycle temperatures, although most results and conclusions are derived from high-temperature magnetic heat pump studies at the Idaho National Engineering Laboratory. DOE

N85-23065# Tennessee Univ., Knoxville. Dept. of Mechanical and Aerospace Engineering.
COOLING PERFORMANCE IMPROVEMENT OF A HORIZONTAL GROUND COUPLED HEAT PUMP
Bernie A. McGraw, Robert N. Baugh, William S. Johnson, and William Griffith 1984 13 p refs Presented at the 7th Heat Pump Technol. Conf., Tulsa, Okla., 15-16 Oct. 1984
(Contract DE-AC05-84OR-21400)
(DE85-002470; CONF-8410153-5) Avail: NTIS HC A02/MF A01

Performance of the horizontal-coil ground-coupled heat pump system for the summers of 1983 and 1984 is described. The overall coefficients of performance (COP) were 1.80 (1983) and 2.41 (1984) while the overall cooling seasonal performance factor (SPF) was 1.11 (1983) and 1.43 (1984) with the system located within the conditioned space. If the system was outside the conditioned space, an SPF of 1.31 (1983) and 1.76 (1984) should be realized. In both years, the systems were identical with the exception that prior to the 1984 cooling season, the ground coil was excavated and a new one of identical length was installed using sand as a backfill material. Although the 1984 SPF was 29% higher than that measured in 1983, the improvement cannot be totally attributed to the backfill material. During the summer of 1983, 30% more cooling degree days were in current than in 1984. A decrease in runtime (as a result of lower ambient temperatures) would also increase the performance factor. Author

N85-23066# California Univ., Davis. Dept. of Mathematics.
DIFFUSION DEPOSITION IN FIBROUS FILTERS FOR PARALLEL AND TRANSVERSE FLOW MODELS
D. O. Banks, G. J. Kurowski, and R. A. Boyles 18 Sep. 1984 20 p refs
(Contract W-7405-eng-48)
(DE85-006149; UCRL-15637) Avail: NTIS HC A02/MF A01

Diffusional deposition for air flow parallel to a cylindrical collector is examined and an expression for this deposition rate is obtained. This expression indicates that the deposition rate for parallel flow is of the same order of magnitude as that for transverse flow and, hence, is significant. DOE

N85-22535# Georgia Inst. of Tech., Atlanta. School of Aerospace Engineering.
INVESTIGATIONS OF REACTIVE AND NON REACTIVE ACOUSTIC BOUNDARY LAYERS IN POROUS WALLED DUCTS
U. G. Hegde, F. L. Chen, and B. T. Zinn *In* APL 21st JANNAF Combust. Meeting, Vol. 1 Oct. 1984 p 91-102 refs (For primary document see N85-22526 13-20)
Avail: NTIS HC A21/MF A01 CSCL 20/4

N85-22544# Scientific Research Associates, Inc., Glastonbury, Conn.
INTERNAL FLUID MECHANISM OF SOLID PROPELLANT ROCKET MOTORS
J. S. Sabnis, H. J. Gibeling, and H. McDonald *In* APL 21st JANNAF Combust. Meeting, Vol. 1 Oct. 1984 p 195-204 refs (For primary document see N85-22526 13-20)
(Contract F04611-83-C-0003)
Avail: NTIS HC A21/MF A01 CSCL 20/4

N85-22556# Pratt and Whitney Aircraft, West Palm Beach, Fla. Engineering Div.
HIGH-PRESSURE ROCKET ENGINE TURNAROUND DUCT COMPUTATIONAL FLUID DYNAMICS ANALYSIS
George B. Cox, Jr. *In* APL 21st JANNAF Combust. Meeting, Vol. 1 Oct. 1984 p 379-398 refs (For primary document see N85-22526 13-20)
Avail: NTIS HC A21/MF A01 CSCL 20D

N85-22563# McDonnell-Douglas Research Labs., St. Louis, Mo.
THE ROLE OF CONVECTIVE PERTURBATIONS IN SUPERCRITICAL INLET OSCILLATIONS
T. J. Bogar and M. Sajben *In* APL JANNAF Combust. Meeting, Vol. 1 Oct. 1984 p 465-479 refs (For primary document see N85-22526 13-20)
Avail: NTIS HC A21/MF A01 CSCL 20/4

N85-22785# Joint Publications Research Service, Arlington, Va.
PROPAGATION OF THREE-DIMENSIONAL TURBULENT JET FROM LOBAR NOZZLE THROUGH SURROUNDING STREAM Abstract Only
V. I. Vasilyev, S. Yu. Krasheninnikov, and Yu. A. Rudi *In its* USSR Rept.: Eng. and Equipment (JPRS-UEQ-85-003) 12 Mar. 1985 p 3-4 Transl. into ENGLISH from Izv. Vyssh. Ucheb. Zaved.: Aviats. Tekhn. (Kazan, USSR), No. 1, Jan. - Mar. 1984 p 18-22 (For primary document see N85-22782 13-31)
Avail: NTIS HC A06

N85-22786# Joint Publications Research Service, Arlington, Va.
TIME-DEPENDENT FLOW OF STREAM SWIRLED IN VORTEX CHAMBER Abstract Only
Yu. A. Knysh and A. F. Uryvskiy *In its* USSR Rept.: Eng. and Equipment (JPRS-UEQ-85-003) 12 Mar. 1985 p 4 Transl. into ENGLISH from Izv. Vyssh. Ucheb. Zaved.: Aviats. Tekhn. (Kazan, USSR), no. 1, Jan. - Mar. 1984 p 27-31 (For primary document see N85-22782 13-31)
Avail: NTIS HC A06

N85-22787# Joint Publications Research Service, Arlington, Va.
NATURAL CONVECTION DURING HEAT ACCUMULATION BY SUBSTANCES WITH CHANGE OF AGGREGATE STATE Abstract Only
A. G. Chukayev and A. M. Kuks *In its* USSR Rept.: Eng. and Equipment (JPRS-UEQ-85-003) 12 Mar. 1985 p 5 Transl. into ENGLISH from Izv. Vyssh. Ucheb. Zaved.: Aviats. Tekhn. (Kazan, USSR), no. 1, Jan. - Mar. 1984 p 55-59 Original language document previously announced as A84-47562 (For primary document see N85-22782 13-31)
Avail: NTIS HC A06

N85-22788# Joint Publications Research Service, Arlington, Va.
SOME UNIQUE FEATURES OF ISENTROPHIC FLOW OF GAS UNDER HIGH PRESSURES Abstract Only
A. P. Bebyakov and V. Ya. Levin *In its* USSR Rept.: Eng. and Equipment (JPRS-UEQ-85-003) 12 Mar. 1985 p 5-6 Transl. into ENGLISH from Izv. Vyssh. Ucheb. Zaved.: Aviats. Tekhn. (Kazan, USSR), no. 1, Jan. - Mar. 1984 p 71-74 (For primary document see N85-22782 13-31)
Avail: NTIS HC A06

N85-22789# Joint Publications Research Service, Arlington, Va.
DETERMINATION OF BOUNDARY LINE BETWEEN REVERSE JET AND SURROUNDING STREAM Abstract Only
I. G. Gataullin and D. V. Maklakov *In its* USSR Rept.: Eng. and Equipment (JPRS-UEQ-85-003) 12 Mar. 1985 p 7 Transl. into ENGLISH from Izv. Vyssh. Ucheb. Zaved.: Aviats. Tekhn. (Kazan, USSR), no. 1, Jan. - Mar. 1984 p 79-81 Original language document previously announced as A84-47569 (For primary

document see N85-22782 13-31)
Avail: NTIS HC A06

N85-22831# Joint Publications Research Service, Arlington, Va.
PRESSURE DROP AND COEFFICIENTS OF INTERNAL HEAT TRANSFER NECESSARY FOR TRANSPIRATION COOLING Abstract Only
S. G. Dezideryev, A. G. Karimova, and P. P. Makarov *In its* USSR Rept.: Eng. and Equipment (JPRS-UEQ-85-003) 12 Mar. 1985 p 85 Transl. into ENGLISH from Izv. Vyssh. Ucheb. Zaved.: Aviats. Tekhn. (Kazan, USSR), no. 1, Jan. - Mar. 1984 p 83-85 (For primary document see N85-22782 13-31)
Avail: NTIS HC A06

N85-22836# Joint Publications Research Service, Arlington, Va.
EFFECT OF GAS STREAM SWEEPING PAST THE EFFLUENT OF A PERFORATED PLATE ON HEAT TRANSFER INSIDE THE PERFORATIONS Abstract Only
V. A. Trushin, K. M. Iskakov, and Z. S. Iskhakov *In its* USSR Rept.: Eng. and Equipment (JPRS-UEQ-85-003) 12 Mar. 1985 p 88 Transl. into ENGLISH from Izv. Vyssh. Ucheb. Zaved.: Aviats. Tekhn. (Kazan, USSR), no. 1, Jan. - Mar. 1984 p 101-103 Original language document previously announced as A84-47578 (For primary document see N85-22782 13-31)
Avail: NTIS HC A06

N85-22837# Joint Publications Research Service, Arlington, Va.
SELECTION OF AIR INTAKE PARAMETERS FOR SUPERSONIC-FLOW OPERATION Abstract Only
V. I. Bazhanov and A. A. Stepchkov *In its* USSR Rept.: Eng. and Equipment (JPRS-UEQ-85-003) 12 Mar. 1985 p 89-90 Transl. into ENGLISH from Izv. Vyssh. Ucheb. Zaved.: Aviats. Tekhn. (Kazan, USSR), no. 1, Jan. - Mar. 1984 p 69-71 Original language document previously announced as A84-47565 (For primary document see N85-22782 13-31)
Avail: NTIS HC A06

35 INSTRUMENTATION AND PHOTOGRAPHY

Includes remote sensors; measuring instruments and gages; detectors; cameras and photographic supplies; and holography.

For aerial photography see *43 Earth Resources.* For related information see also *06 Aircraft Instrumentation,* and *19 Spacecraft Instrumentation.*

N85-23067*# National Aeronautics and Space Administration. Langley Research Center, Hampton, Va.
ELECTROACOUSTICAL IMAGING TECHNIQUE FOR ENCODING INCOHERENT RADIANCE FIELDS AS GABOR ELEMENTARY SIGNALS
C. L. Fales and F. O. Huck Mar. 1985 16 p refs
(NASA-TM-86372; NAS 1.15:86372) Avail: NTIS HC A02/MF A01 CSCL 14B

A technique is presented for directly encoding incoherent radiance fields as Gabor elementary signals. This technique uses an electro-acoustic sensor to modulate the electronic charges induced by the incident radiance field with the electric fields generated by Gaussian modulated sinusoidal acoustic waves. The resultant signa' carries the amplitude and phase information required for localizing spatial frequencies of the radiance field. These localized spatial frequency representations provide a link between the either geometric or Fourier transform representations currently used in computer vision and pattern recognition. Author

N85-23068*# Jet Propulsion Lab., California Inst. of Tech., Pasadena.
MICROWAVE BLACKBODIES FOR SPACEBORNE RECEIVERS
J. M. Stacey 1 Mar. 1985 50 p ref
(Contract NAS7-918)
(NASA-CR-175647; JPL-Pub-85-10; NAS 1.26:175647) Avail: NTIS HC A03/MF A01 CSCL 14B

The properties of microwave blackbody targets are explained as they apply to the calibration of spaceborne receivers. Also described are several practicable, blackbody targets used to test and calibrate receivers in the laboratory and in the thermal vacuum chamber. Problems with the precision and the accuracy of blackbody targets, and blackbody target design concepts that overcome some of the accuracy limitations present in existing target designs, are presented. The principle of the Brewster angle blackbody target is described where the blackbody is applied as a fixed-temperature test target in the laboratory and as a variable-temperature target in the thermal vacuum chamber. The reflectivity of a Brewster angle target is measured in the laboratory. From this measurement, the emissivity of the target is calculated. Radiatively cooled thermal suspensions are discussed as the coolants of blackbody targets and waveguide terminations that function as calibration devices in spaceborne receivers. Examples are given for the design of radiatively cooled thermal suspensions. Corrugated-horn antennas used to observe the cosmic background and to provide a cold-calibration source for spaceborne receivers are described. M.G.

N85-23069*# New Technology, Inc., Huntsville, Ala.
NEW ATMOSPHERIC SENSOR ANALYSIS STUDY Progress Report for period ending 28 Feb. 1985
K. G. Parker 8 Mar. 1985 4 p
(Contract NAS8-36179)
(NASA-CR-171426; NAS 1.26:171426; PR1359) Avail: NTIS HC A02/MF A01 CSCL 14B

A progress report of the activities pertaining to the Atmospheric Sensor Analysis Study is given. The current revision of the Perkin-Elmer Operating System OS/32 MT 7.2.1 was installed on the Atmospheric Modeling and Simulation System (AMASS). This software appears to offer a means of distributing disc storage among the user community in a more optimal manner than previously available using the file manager. Next Generation Weather Radar (NEXRAD) software has been received from the National Severe Storms Laboratory (NSSL) and has been loaded onto the Perkin-Elmer. Extensive modifications will be required to permit the software to be compatible with the operating system. B.W.

N85-23070# Sandia Labs., Albuquerque, N. Mex. Digital Systems Development Div.
TECHNICAL MANUAL: DESCRIPTION AND OPERATION SLAVED TRACKING SYSTEM
Kenneth C. Bauhs Aug. 1984 64 p
(Contract DE-AC04-76DP-00789)
(DE85-004807; SAND-80-2050) Avail: NTIS HC A04/MF A01

Physical and functional descriptions, operating procedures, and safety precautions for the Slaved Tracking System (STS) are presented. The STS is a mobile unit designed to provide close-up, high-quality motion pictures and video tapes of laydown bombs and rockets during the final phase of their trajectory to impact point. Radiometer devices mounted with the optics can also be used to track rocket exhaust emissions. The STS receives binary range and encoder information from Sandia's Laser Tracker System (LTS) to provide the STS with steering signals to track vehicle. These signals are transmitted by microwave or hard-wire communications lines. The communications link is shown. The STS yields optimum photographic coverage with a field-of-view of +-5 ft on targets traveling up to 2000 f/s at a cross range of 1500 ft. The boresight of the fixed optics points directly at a 12-in. gimballed tracking mirror that provides satisfactory photographic lighting under most conditions. DOE

N85-23071# Rockwell International Corp., Golden, Colo. Space Operations Div.
LOW TEMPERATURE CALIBRATION FIXTURE
Robert L. Thompson, Robert S. Stant, and Richard Sackuvich 4 Nov. 1984 10 p refs
(Contract DE-AC04-76DP-03533)
(DE85-003969; RFP-3607; DOE/TIC-4500-Rev-73) Avail: NTIS

HC A02/MF A01

A very inexpensive, easy-to-use calibration fixture was developed and tested. The fixture allows calibrations from -195 to -20 C with a worst case transfer uncertainty of less than + or - 0.1 C. Construction and testing details are provided. DOE

N85-23072# Los Alamos Scientific Lab., N. Mex.
HIGH-RESOLUTION SIT TV TUBE FOR SUBNANOSECOND IMAGE SHUTTERING
G. J. Yates, B. H. Vine, I. Aeby, D. L. Dunbar, N. S. P. King, S. A. Jaramillo, N. N. Thayer, and B. W. Noel Sep. 1984 77 p refs (Contract W-7405-eng-36)
(DE85-005189; LA-9771-MS) Avail: NTIS HC A04/MF A01

A new ultrafast high-resolution image shutter tube with reasonable gain and shuttering efficiency has been designed and tested. The design uses a grid-gated silicon-intensified-target (SIT) image section and a high-speed focus projection and scan (FPS) vidicon read-out section in one envelope to eliminate resolution losses from external coupling. The design features low-gate-interface capacity, a high-conductivity shutter grid, and a segmented low-resistivity photocathode for optimum gating speed. Optical gate widths as short as 400 ps + or - 100 ps for full shuttering of the 25-mm-diam input window with spatial resolution as high as 15 1p/mm have been measured. Some design criteria, most of the electrical and optical performance data for several variations in the basic design, and a comparison (of several key response functions) with similarly tested 18- and 25-mm-diam proximity-focused microchannel-plate (MCP) image intensifier tubes (MCPTs) are included. DOE

N85-22442# Joint Publications Research Service, Arlington, Va.
EVALUATING ACCURACY IN ORIENTATION OF TOPOGRAPHIC PHOTOGRAPH AND SATELLITE-CENTERED DIRECTION FROM STAR PHOTOGRAPH Abstract Only
M. I. Shcherbakov *In its* USSR Rept.: Space (JPRS-USP-85-001) 4 Feb. 1985 p 74 Transl. into ENGLISH from Izv. Vysshikh Uch. Zaved.: Geod. i Aerofotosyemka (USSR), no. 1, Jan.-Feb. 1984 p 49-55 Original language document announced as A84-34490 (For primary document see N85-22403 13-12)
Avail: NTIS HC A07

N85-22443# Joint Publications Research Service, Arlington, Va.
METHOD FOR APPROXIMATING AUTOCORRELATION FUNCTIONS FOR DESCRIBING AREAL PHOTOIMAGE FEATURES Abstract Only
V. V. Gavrilov *In its* USSR Rept.: Space (JPRS-USP-85-001) 4 Feb. 1985 p 74-75 Transl. into ENGLISH from Izv. Vysshikh Uch. Zaved.: Geod. i Aerofotosyemka (USSR), no. 2, Mar.-Apr. 1984 p 68-72 (For primary document see N85-22403 13-12)
Avail: NTIS HC A07

N85-22444# Joint Publications Research Service, Arlington, Va.
EXPERIENCE IN AUTOMATED INTERPRETATION OF AEROSPACE PHOTOGRAPHS Abstract Only
I. K. Lurye *In its* USSR Rept.: Space (JPRS-USP-85-001) 4 Feb. 1985 p 75-76 Transl. into ENGLISH from Vestnik Moskovskogo Univ., Ser. 5: Geografiya (USSR), no. 4, Jul.-Aug. 1984 p 63-69 (For primary document see N85-22403 13-12)
Avail: NTIS HC A07

N85-22445# Joint Publications Research Service, Arlington, Va.
GEOINDICATION METHOD FOR INTERPRETING AERIAL AND SPACE PHOTOGRAPHS: STATUS AND PROSPECTS Abstract Only
B. N. Mozhayev and A. G. Zhuchenko *In its* USSR Rept.: Space (JPRS-USP-85-001) 4 Feb. 1985 p 76 Transl. into ENGLISH from Sov. Geologiya (USSR), no. 8, Aug. 1984 p 60-65 (For primary document see N85-22403 13-12)
Avail: NTIS HC A07

N85-22822# Joint Publications Research Service, Arlington, Va.
ANALYSIS OF INTERACTION OF DYNAMICALLY ADJUSTABLE GYROSCOPES ON ELASTIC PLATFORM BY FINITE-ELEMENT METHOD Abstract Only
A. V. Zbrutskiy and S. A. Sarapulov *In its* USSR Rept.: Eng. and Equipment (JPRS-UEQ-85-003) 12 Mar. 1985 p 51 Transl. into ENGLISH from Prikl. Mekhan. (Kiev), no. 6, Jun. 1984 p 120-124 (For primary document see N85-22782 13-31)
Avail: NTIS HC A06

N85-22845# Joint Publications Research Service, Arlington, Va.
ANALYSIS OF FIBER-GYROSCOPES DISCUSSED
Sun Li and Deng Feifan *In its* Chinese Rept.: Sci. and Technol. (JPRS-CST-85-005) 20 Feb. 1985 p 37-43 refs Transl. into ENGLISH from Zhongguo Jiguang (Shanghai), no. 10, 20 Oct. 1984 p 598-601 (For primary document see N85-22843 13-31)
Avail: NTIS HC A10/MF A01

N85-22962# Joint Publications Research Service, Arlington, Va.
LIQUID MASS FLOW RATE COMPUTER Abstract Only
N. N. Antov, V. A. Troynikov, and V. C. Sotnikov *In its* USSR Rept.: Electron. and Elec. Eng. (JPRS-UEE-85-002) 23 Jan. 1985 p 53 Transl. into ENGLISH from Izmeritel. Tekhn. (Moscow), no. 9, Sep. 1984 p 35-36 (For primary document see N85-22907 13-33)
Avail: NTIS HC A05/MF A01

N85-22963# Joint Publications Research Service, Arlington, Va.
METROLOGICAL SUPPORT FOR REMOTE TRANSPORT VEHICLE SPEEDOMETERS Abstract Only
A. Ye. Ksenzenko and V. I. Matveyev *In its* USSR Rept.: Electron. and Elec. Eng. (JPRS-UEE-85-002) 23 Jan. 1985 p 53 Transl. into ENGLISH from Izmeritel. Tekhn. (Moscow), no. 9, Sep. 1984 p 38-39 (For primary document see N85-22907 13-33)
Avail: NTIS HC A05/MF A01

N85-22964# Joint Publications Research Service, Arlington, Va.
USE OF ELECTRONIC CODING-FREQUENCY METERS TO MEASURE PARAMETERS OF PULSED RADIO SIGNALS Abstract Only
A. P. Pokhilyuk *In its* USSR Rept.: Electron. and Elec. Eng. (JPRS-UEE-85-002) 23 Jan. 1985 p 55 Transl. into ENGLISH from Izmeritel. Tekhn. (Moscow), no. 9, Sep. 1984 p 53-54 (For primary document see N85-22907 13-33)
Avail: NTIS HC A05/MF A01

N85-22965# Joint Publications Research Service, Arlington, Va.
EFFECT OF VARIANCE OF PHOTORECEIVER FREQUENCY CHARACTERISTICS ON CHARACTERISTICS OF MEASURING INSTRUMENTS Abstract Only
R. B. Shemshedinov and V. F. Kaleganov *In its* USSR Rept.: Electron. and Elec. Eng. (JPRS-UEE-85-002) 23 Jan. 1985 p 56 Transl. into ENGLISH from Radiotekhn. (Moscow), no. 8, Aug. 1984 p 79-81 (For primary document see N85-22907 13-33)
Avail: NTIS HC A05/MF A01

N85-22971# Joint Publications Research Service, Arlington, Va.
SIMPLE DETONATION METER Abstract Only
N. Sukhov *In its* USSR Rept.: Electron. and Elec. Eng. (JPRS-UEE-85-002) 23 Jan. 1985 p 60 Transl. into ENGLISH from Radiotekhn. (Moscow), no. 7, Jul. 1984 p 40-42 (For primary document see N85-22907 13-33)
Avail: NTIS HC A05/MF A01

36 LASERS AND MASERS

Includes parametric amplifiers.

N85-23073 California Univ., Berkeley.
MODE CONTROL AND WAVELENGTH TUNING IN OPEN ENDED MICHELSON INTERFEROMETRIC SEMICONDUCTOR LASER Ph.D. Thesis
Ismail Hassan Abdel Fattah 1984 215 p
Avail: Univ. Microfilms Order No. DA8426957

The use of interferometric techniques to stablize and control

the longitudinal mode behavior of the semiconductor laser was studied. A new type of laser cavity was introduced, the open ended Michelson interferometer cavity (OEMI). Wave propagation in the OEM cavity was studied and the resonant condition of the cavity was derived by scattering matrix method. The optimum dimension of the laser cavity was studied. A rate equation model was developed, and used to study the lasting properties of the OEMI laser and to compare the OEMI laser characteristics with those of conventional Fabry-Perot lasers. AlGaAs lasers with the OEMI cavity structure were fabricated by conventional liquid phase epitaxy techniques. Two methods of light confinement in the junction plane were used in fabricating the laser, gain guiding and inverted ridge waveguide. Two tuning modes were observed, small continuous tuning where the lasing wavelength changed by 2.5A without mode switching, and wavelength switching where the operating wavelength jumped in steps of 10 to 15A. It is found that the rate equation model is in good agreement with the experimental results. Dissert. Abstr.

N85-23074# Technology Applications, Inc., Falls Church, Va.
DIGITAL LASER PLATEMAKER MODIFICATIONS Final Technical Report, Oct. 1983 - Sep. 1984
Fort Belvoir, Va. Army Engineer Topographic Labs. Dec. 1984 49 p
(Contract DAAK70-83-C-0165)
(AD-A150190; ETL-0379) Avail: NTIS HC A03/MF A01 CSCL 14/5

The Digital Laser Platemaker (LPM) is a high resolution, high accuracy system developed as a prototype to expose large format pressplate or film that is compatible with the Defense Mapping Agency lithographic production process. The LPM reads compressed digital data in raster format from magnetic tape. Through an electro-mechanical system, laser generated light is aimed and modulated to expose images on photosensitive media. A series of investigations were conducted on the Army's digital laser platemaker to identify and correct deficiencies and increase system overall operability. A new footbar was designed and installed which reduced media loading errors. Accuracy testing indicates that inter-image error is less than 0.002 inch, while intra-image error is not within tolerance. Testing results are encouraging that intra-image errors can be further reduced, but additional work is needed in the areas of accuracy testing and alignment of some of the optical components. While the existing machine is functional, there are several areas where components should be redesigned for a production model. GRA

N85-23075# Army Missile Command, Redstone Arsenal, Ala. Directed Energy Directorate.
NEAR FIELD/FAR FIELD (NF/FF) ENERGY LOSS IN ELECTRIC DISCHARGE LASERS (EDL's): A MODE-MEDIUM INTERACTION
J. H. Bentley Aug. 1984 10 p
(AD-A150299; AD-E950650; AMSMI/RH-84-5-TR) Avail: NTIS HC A02/MF A01 CSCL 20/5

High energy CO2 EDL's (Electric Discharge Lasers) with unstable resonators exhibit a mode-medium interaction which spreads the focussed beam and causes loss in the far-field. Mirror edge Fresnelling may result in amplified feedback which causes a parallel-piped structure to be burned into the lasing medium. Possible confirming experiments are described. Author (GRA)

N85-23076# Colorado Univ., Boulder. Dept. of Chemistry.
CHEMICAL STABILIZATION OF LASER DYES Final Report, 1 Jul. 1981 - 1 Oct. 1984
T. H. Koch Nov. 1984 7 p
(Contract DAAG29-81-K-0146)
(AD-A150451; ARO-18135.4-CH) Avail: NTIS HC A02/MF A01 CSCL 07/5

Coumarin laser dyes upon excitation degrade to produce products which absorb at the lasing wavelength. This results in attenuation of dye laser output. Modes of degradation of coumarin dye lasers under both anaerobic and aerobic conditions were determined and methods of stabilization of dye lasers were established. GRA

N85-23077# Illinois Univ., Urbana. Dept. of Electrical and Computer Engineering.
NON-LINEAR OPTICAL TECHNIQUES FOR VISIBLE AND UV LASERS AND THIN FILM DEPOSITION Annual Report, 1 Oct. 1983 - 30 Sep. 1984
J. G. Eden Nov. 1984 15 p
(Contract F49620-83-C-0003)
(AD-A150489; AFOSR-84-1263TR) Avail: NTIS HC A02/MF A01 CSCL 07/5

Experiments are described in which lasers are used to generate specific Column IIIA metal ions. The first studies involved ion pair production in the metal-halide molecules (such as thallium iodide) by illuminating the vapor with 193 nm radiation. More recent experiments have succeeded in producing Al(+) ions by the multiphoton ionization (MPI) of metal alkyls (such as trimethylaluminum) in the visible. Another aspect of the current work is focusing on the use of ultraviolet radiation to enhance the growth rate of semiconductor films grown near pyrolytic threshold. The use of gaseous sensitizers (such as ammonia) to improve film growth rates and quality is also being explored. Finally, a simple photochemical means for improving the efficiency of a commercial XeCl laser by more than 50% has also been discovered. GRA

N85-23078# Sandia Corp., Albuquerque, N. Mex.
THERMODYNAMIC AND KINETIC STUDIES OF PULSED LASER ANNEALING FROM TRANSIENT CONDUCTIVITY MEASUREMENTS
P. S. Peercy and M. O. Thompson 26 Nov. 1985 25 p refs Presented at Symp. on the Sci. Basis for Nucl. Waste Management, Boston, 26 Nov. 1984
(Contract DE-AC04-76DP-00789)
(DE85-003677; SAND-84-1230C; CONF-841157-23) Avail: NTIS HC A02/MF A01

Simultaneous measurements of the transient conductance and time-dependent surface reflectance of the melt and solidification dynamics produced by pulsed laser irradiation of Si are reviewed. These measurements demonstrate that the melting temperature of amorphous Si is reduced 200 + or = 50 K from that of crystalline Si and that explosive crystallization in amorphous Si is mediated by thin (less than or equal to 20 nm) molten layer that propagates at approx. 15 m/sec. Studies with 3.5 nsec pulses permit an estimate of the dependence of the solidification velocity on undercooling. Measurements of the effect of As impurities on the solidification velocity demonstrate that high As concentrations decrease the melting temperature of Si (approx. 150 K for 7 at. %), which can result in surface nucleation to produce buried melts. Finally, the silicon-germanium alloy system is shown to be ideal model system for the study of superheating and undercooling. The Si50Ge50 alloy closely models amorphous Si, and measurements of layered Si-Ge alloy structures indicate superheating up to 120 K without nucleation of internal melts. DOE

N85-23079# Oak Ridge National Lab., Tenn. Solid State Div.
TIME-RESOLVED ELLIPSOMETRY AND REFLECTIVITY MEASUREMENTS OF THE OPTICAL PROPERTIES OF SILICON DURING PULSED EXCIMER LASER IRRADIATION
G. E. Jellison, Jr. and D. H. Lowndes Dec. 1984 7 p refs Presented at the Mater. Res. Soc. Meeting on Energy Beam-Solid Interactions and Transient Thermal Process., Boston, 26 Nov. 1984
(Contract DE-AC05-84OR-21400)
(DE85-005091; CONF-841157-45) Avail: NTIS HC A02/MF A01

Several advances in time-resolved optical measurement techniques have been made, which allow a more detailed determination of the optical properties of silicon immediately before, during, and after pulsed laser irradiation. It is now possible to follow in detail the time-resolved reflectivity signal near the melting threshold; measurements indicate that melting occurs in a spatially inhomogeneous way. Time-resolved ellipsometry was used to

accurately measure the optical properties of the high reflectivity (molten) phase, and of the hot, solid silicon before and after the laser pulse. Before and after the high reflectivity phase, the time-resolved ellipsometry measurements are entirely consistent with the known optical properties of crystalline silicon at temperatures up to its melting point. DOE

N85-23080# Monsanto Research Corp., Dayton, Ohio.
LOW JITTER TRIGGER FOR AN EXCIMER LASER
Carl J. Kershner, Edward T. Burgess, and Dean Faklis 11 Dec. 1984 6 p refs
(Contract DE-AC04-76DP-00053)
(DE85-005732; MLM-3213) Avail: NTIS HC A02/MF A01

The use of a highly focused beam from a small Q-switched Nd-YAG laser to trigger the high-voltage spark gap switch of a rare gas excimer laser is described. The design results in an order of magnitude improvement in jitter, and also leads to greatly improved trigger reliability and less electromagnetic interference to electronic equipment in the vicinity of the operating excimer laser. DOE

N85-23081# Oak Ridge National Lab., Tenn. Fusion Energy Div.
FEASIBILITY OF ALPHA PARTICLE MEASUREMENT BY CO2 LASER THOMSON SCATTERING
D. P. Hutchinson, K. L. VanderSluis, J. Sheffield, and D. J. Sigmar Dec. 1984 19 p refs
(Contract DE-AC05-84OR-21400)
(DE85-004938; ORNL/TM-9090) Avail: NTIS HC A02/MF A01

The feasibility of O2 laser Thomson scattering from a multicomponent burning plasma was evaluated for the measurement of the velocity distribution of D-T produced alpha particles. The density and velocity distribution of the alpha particles from their initial energy of 3.5 MeV down to near-thermal energies may be measured by small angle (<1 (0)) Thomson scattering. A computer simulation of the experiment indicates that a 100 MW pulsed laser combined with a bank of heterodyne receivers will be able to measure a scattered signal from the alpha particles with a post-detection signal-to-noise ratio of 75 for an assumed alpha density of 7.5 x 10(11) cm(-3). DOE

N85-23082# Sandia Labs., Albuquerque, N. Mex.
ACTIVATION OF Si-N MODES IN SILICON BY PULSED LASER ANNEALING
H. J. Stein, P. S. Peercy, and C. R. Hills 1984 7 p refs Presented at the Symp. on the Scientific Basis for Nucl. Waste Management, Boston, 26 Nov. 1984
(Contract DE-AC04-76DP-00789)
(DE85-002988; SAND-84-1254C; CONF-841157-36) Avail: NTIS HC A02/MF A01

Retention and bonding of nitrogen implanted into crystalline Si were examined by infrared absorption (IR) and transmission electron microscopy (TEM) after furnace and pulsed laser annealing. Localized Si-N vibrational modes for N-N pairs are observed, and the associated ir band intensities increase upon pulsed annealing. Furace annealing above 600(0)C decreases the ir intensity for N-N pairs and fine structure defects appear in TEM. Subsequent laser annealing removes most of the fine structure and reactivates the pair spectrum which were interpreted as dissolution of N precipitates and pair formation upon quenching from the melt. Any realistic model for N in Si must include the formation and consequences of N-N pairs. DOE

N85-23083# Oak Ridge National Lab., Tenn.
TIME RESOLVED X-RAY STUDIES DURING PULSED LASER IRRADIATION OF Ge
J. Z. Tischler, B. C. Larson, and D. M. Mills 1984 8 p refs Presented at Mater. Res. Soc. Ann. Meeting, Boston, Mass., 26 Nov. 1984 Prepared in cooperation with Cornell Univ., Ithaca, N.Y.
(Contract DE-AC05-84OR-21400)
(DE85-005263; CONF-841157-51) Avail: NTIS HC A02/MF A01

Synchrotron X-ray pulses from the Cornell high energy synchrotron source (CHESS) were used to carry out nanosecond resolution measurements of the temperature distributions in Ge during UV pulsed-laser irradiation. The KrF laser pulses of 25 ns FWHM with an energy density of 0.6 J/sq cm were used. The temperatures were determined from X-ray Bragg profile measurements of thermal expansion induced strain on [111] oriented Ge. The data indicate the presence of a liquid-solid interface near the melting point, and large temperature gradients in the solid; these Ge results are analogous to previous ones for Si. The measured temperature distributions are compared with those obtained from heat flow calculations, and the overheating and undercooling of the interface relative to the equilibrium melting point are discussed. DOE

N85-23084# Los Alamos Scientific Lab., N. Mex.
LOS ALAMOS FREE ELECTRON LASER: ACCELERATOR PERFORMANCE
R. W. Warren, W. E. Stein, M. T. Lynch, R. L. Sheffield, and J. S. Fraser 1984 30 p refs Presented at Free Electron Laser Conf., Castelgandolfo, Italy, 3 Sep. 1984
(Contract W-7405-eng-36)
(DE85-005722; LA-UR-84-3793; CONF-8409144-3) Avail: NTIS HC A /MF A01

The free electron (FEL) laser oscillator has operated over a wavelength range from 9 to 11 (MU)m with a peak output power of 5 MW and an average output power of 6 kW over a 70-(MU)s pulse length. The FEL is driven by a conventional RF linear accelerator operating at 1.3 GHz with a nominal energy of 20 MeV. Particularly important parts of the beamline are the electron gun, the subharmonic and fundamental-bunching systems, the accelerator, the feedback controllers, the steering and focusing systems, the cherenkov radiators used as beam-position monitors, and the slow and fast deflectors used with the diagnostic spectrometer at the exit of the beamline. Problems are discussed and the performance of these components is presented. DOE

N85-22796# Joint Publications Research Service, Arlington, Va.
NEODYMIUM YAG LASER PUMPED WITH RADIATION FROM HIGH FREQUENCY ELECTRODELESS DISCHARGE Abstract Only
S. N. Golikova, P. S. Fusev, V. P. Fuskov, V. A. Zhukov, S. M. Pechenegov, V. D. Sazhayev, A. B. Sinitsyn, N. V. Teterev, and B. F. Trinchuk *In its* USSR Rept.: Eng. and Equipment (JPRS-UEQ-85-003) 12 Mar. 1985 p 15 Transl. into ENGLISH from Pribory i Tekhn. Eksperim. (Moscow), no. 3, May - Jun. 1984 p 190-193 (For primary document see N85-22782 13-31)
Avail: NTIS HC A06

N85-22844# Joint Publications Research Service, Arlington, Va.
LASER APPLICATIONS IN LAST 10 YEARS REVIEWED
Lu Zhiguo *In its* Chinese Rept.: Sci. and Technol. (JPRS-CST-85-005) 20 Feb. 1985 p 24-36 refs Transl. into ENGLISH from Zhongguo Jiguang (Shanghai), no. 10, 20 Oct. 1984 p 577-583 (For primary document see N85-22843 13-31)
Avail: NTIS HC A10/MF A01

N85-22955# Joint Publications Research Service, Arlington, Va.
STATUS OF AND OUTLOOK FOR PRODUCING MEANS OF TRANSMITTING UNITS OF PLANE ANGLE, ANGULAR VELOCITY AND ACCELERATION WITH RING LASERS Abstract Only
B. E. Blanter, Ye. P. Krivtsov, D. P. Lukyanov, A. Ye. Sinelnikov, Yu. V. Filatov, and Yu. N. Shestopalov *In its* USSR Rept.: Electron. and Elec. Eng. (JPRS-UEE-85-002) 23 Jan. 1985 p 45-46 Transl. into ENGLISH from Izmeritel. Tekhn. (Moscow), no. 7, Jul. 1984 p 27-29 (For primary document see N85-22907 13-33)
Avail: NTIS HC A05/MF A01

N85-22957# Joint Publications Research Service, Arlington, Va.
COMPARISON REFERENCE ETALON OF UNIT LASER RADIATION POWER Abstract Only
I. N. Govor, A. V. Kubarev, and V. V. Ozolin *In its* USSR Rept.: Electron. and Elec. Eng. (JPRS-UEE-85-002) 23 Jan. 1985 p

47 Transl. into ENGLISH from Izmeritel. Tekhn. (Moscow), no. 7, Jul. 1984 p 34-35 (For primary document see N85-22907 13-33)
Avail: NTIS HC A05/MF A01

N85-22975# Joint Publications Research Service, Arlington, Va.
INTENSITY FLUCTUATIONS OF FOCUSED LASER BEAM DURING REFLECTION IN TURBULENT ATMOSPHERE Abstract Only
V. V. Boronoyev, V. D. Dashinimayev, G. I. Zandanova, V. N. Poplaukhin, and E. A. Trubacheyev *In its* USSR Rept.: Electron. and Elec. Eng. (JPRS-UEE-85-002) 23 Jan. 1985 p 65 Transl. into ENGLISH from Izv. Vysshikh Uchebn. Zavedeniy: Radiofiz. (Gorkiy), v. 27, no. 6, Jun. 1984 p 810-812 (For primary document see N85-22907 13-33)
Avail: NTIS HC A05/MF A01

N85-23042# Joint Publications Research Service, Arlington, Va.
MILLIMETER-WAVE RANGE MASERS: A REVIEW Abstract Only
N. T. Cherpak *In its* USSR Rept.: Electron. and Elect. Eng. (JPRS-UEE-85-001) 9 Jan. 1985 p 67 Transl. into ENGLISH from Izv. Vysshikh Uch. Zaved.: Radiofiz. (USSR), v. 27, no. 7, Jul. 1984 p 815-851 Original language document announced as A84-48152 (For primary document see N85-22976 13-33)
Avail: NTIS HC A05/MF A01

N85-23045# Joint Publications Research Service, Arlington, Va.
MATHEMATICAL MODELING OF TWO-FREQUENCY LASER SOUNDING OF SCATTERING MEDIA Abstract Only
A. V. Belinskiy *In its* USSR Rept.: Electron. and Elect. Eng. (JPRS-UEE-85-001) 9 Jan. 1985 p 75 Transl. into ENGLISH from Zh. Nauchnoy i Prikl. Fotografii i Kinematografii (USSR), v. 29, no. 5, Sep.-Oct. 1984 p 343-348 (For primary document see N85-22976 13-33)
Avail: NTIS HC A05/MF A01

N85-23046# Joint Publications Research Service, Arlington, Va.
GEOPHYSICAL LASER INTERFEROMETER WITH 12.5 METER BASE Abstract Only
A. S. Gorshkov and M. N. Dubrov *In its* USSR Rept.: Electron. and Elect. Eng. (JPRS-UEE-85-001) 9 Jan. 1985 p 75-76 Transl. into ENGLISH from Radiotekh. i Elektron. (USSR), v. 29, no. 9, Aug. 1984 p 1638-1641 (For primary document see N85-22976 13-33)
Avail: NTIS HC A05/MF A01

N85-23047# Joint Publications Research Service, Arlington, Va.
INVESTIGATION OF DYNAMICS OF RADIATION SPECTRUM OF INJECTION LASERS BY INFRARED IMPULSE FOURIER SPECTROSCOPY Abstract Only
A. A. Akimov, A. S. Logginov, and K. Y. Senatorov *In its* USSR Rept.: Electron. and Elect. Eng. (JPRS-UEE-85-001) 9 Jan. 1985 p 76 Transl. into ENGLISH from Izv. Vysshikh Uch. Zaved.: Radioelektron. (USSR), v. 27, no. 9, Sep. 1984 p 90-92 (For primary document see N85-22976 13-33)
Avail: NTIS HC A05/MF A01

N85-23048# Joint Publications Research Service, Arlington, Va.
INVARIANCE OF PROBABILITY CHARACTERISTICS OF DETECTOR TO SHAPE OF OPTICAL PULSE SIGNALS Abstract Only
K. Y. Rumyantsev and V. S. Firsov *In its* USSR Rept.: Electron. and Elect. Eng. (JPRS-UEE-85-001) 9 Jan. 1985 p 77 Transl. into ENGLISH from Izv. Vysshikh Uch. aved.: Radioelektron. (USSR), v. 27, no. 9, Sep. 1984 p 62-64 (For primary document see N85-22976 13-33)
Avail: NTIS HC A05/MF A01

N85-23439# Joint Publications Research Service, Arlington, Va.
RESEARCH, DEVELOPMENT OF LASER GLASSES IN CHINA
Gan Fuxi *In its* China Rept.: Sci. and Technol. (JPRS-CST-85-003) 28 Jan. 1985 p 94-114 refs Transl. into ENGLISH from Zhongguo Jiguang (Shanghai), v. 11, no. 8, 20 Aug. 1984 p 449-459 (For primary document see N85-23433 13-81)
Avail: NTIS HC A11/MF A01

N85-23440# Joint Publications Research Service, Arlington, Va.
RESEARCH PROGRESS ON LASER CRYSTALS IN CHINA
Zhang Yingxia *In its* China Rept.: Sci. and Technol. (JPRS-CST-85-003) 28 Jan. 1985 p 115-121 Transl. into ENGLISH from Zhongguo Jiguang (Shanghai), v. 11, no. 8, 20 Aug. 1984 p 460-463 (For primary document see N85-23433 13-81)
Avail: NTIS HC A11/MF A01

37 MECHANICAL ENGINEERING

Includes auxiliary systems (non-power); machine elements and processes; and mechanical equipment.

N85-23085*# National Aeronautics and Space Administration. Lewis Research Center, Cleveland, Ohio.
FRICTIONAL AND STRUCTURAL CHARACTERIZATION OF ION-NITRIDED LOW AND HIGH CHROMIUM STEELS
Talivaldis Spalvins 1985 17 p refs Presented at the 12th Intern. Conf. on Metallurgical Coatings, Los Angeles, 15-19 Apr. 1985
(NASA-TM-86991; E-2487; NAS 1.15:86991) Avail: NTIS HC A02/MF A01 CSCL 13I

Low Cr steels AISI 41410, AISI 4340, and high Cr austenitic stainless steels AISI 304, AISI 316 were ion nitrided in a dc glow discharge plasma consisting of a 75 percent H2 - 25 percent N2 mixture. Surface compound layer phases were identified, and compound layer microhardness and diffusion zone microhardness profiles were established. Distinct differences in surface compound layer hardness and diffusion zone profiles were determined between the low and high Cr alloy steels. The high Cr stainless steels after ion nitriding displayed a hard compound layer and an abrupt diffusion zone. The compound layers of the high Cr stainless steels had a columnar structure which accounts for brittleness when layers are exposed to contact stresses. The ion nitrided surfaces of high and low Cr steels displayed a low coefficient of friction with respect to the untreated surfaces when examined in a pin and disk tribotester. Author

N85-23086# Royal Aircraft Establishment, Farnborough (England).
LIFE TESTING OF RUBBER SEALS
A. J. Kearse Aug. 1983 17 p refs
(AD-A143193; RAE-TR-83069; RAE-FS(F)-207; BR90541) Avail: NTIS HC A02/MF A01

Dynamic rod seals for aircraft actuators were life tested. Pressure distribution under a rubber seal was measured, and the relationship of this to seal performance is considered. Lubrication properties of different combinations of seals and fluids are discussed. Seal condition at failure is described. Seal life decreases as temperature increases. Friction shows little or no variation with temperature for a rectangular seal, but increases with temperature of a tee seal, particularly when using OM15 fluid. Friction also varies with the seal/fluid combination. Seal failures are due to a combination of mechanical damage to the seal rubber elements or backing rings or both, and material changes in the rubber element. Author (ESA)

N85-23087# Army Test and Evaluation Command, Aberdeen Proving Ground, Md.
LABORATORY TESTS OF RECIPROCATING INTERNAL COMBUSTION ENGINES Final Report
24 Jan. 1985 25 p Supersedes MTP-2-2-700 dated 2 Nov. 1966, AD-718 009
(AD-A150143; TOP-2-2-700; MTP-2-2-700) Avail: NTIS HC A02/MF A01 CSCL 21/7

This report provides procedures for evaluating performance and endurance of reciprocating internal combustion engines under laboratory conditions. Power train components such as transmissions and transmission steering devices are not covered in this TOP (Test Operations Procedure). GRA

N85-23088# Rensselaer Polytechnic Inst., Troy, N. Y.
OPTIMUM DESIGN AND AUTOMATED DYNAMIC ANALYSIS OF FLEXIBLE MECHANISMS Final Report, 22 Sep. 1980 - 30 Sep. 1984
I. G. Tadjbakhsh 10 Dec. 1984 4 p
(Contract DAAG29-80-K-0096)
(AD-A150152; ARO-17575.6-EG) Avail: NTIS HC A02/MF A01 CSCL 13/5

Flexible Mechanisms such as slider crank and four-bar mechanisms are modeled and their dynamic instability and optimum design analyzed. The primary aim of the project was a thorough understanding and analysis of conditions of dynamic instability in flexible components of mechanisms and robots. Dynamic instability characterizes the behavior when amplitude of vibrations have a tendency to become unbounded with the passage of time. Other aims of the study included the optimal design of mechanisms on the basis of flexibility and control of stresses and deflections.GRA

N85-23089# General Electric Co., Lynn, Mass. Aircraft Engine Business Group.
T700 CUTTER LIFE IMPROVEMENT PROGRAM Final Report, Sep. 1981 - Mar. 1984
D. M. Dombrowski Mar. 1984 124 p
(Contract DAAK50-81-C-0029)
(AD-A150450; R84AEB010) Avail: NTIS HC A06/MF A01 CSCL 13/9

The purpose of the T700 Cutter Life Improvement Program was to reduce the number of cutters used for the blisk and impeller airfoil milling operations from 134 to less than 90 cutters per engine set, thereby reducing T700 engine cost. The objective was achieved by stiffening toolholders, improving cutter designs, and changing cutter material. Other parameters investigated include cutting speeds, cutting fluids, surface coating, and surface treatment of the cutters. Phase 1 of the program was mainly analytical, phase 2 involved more extensive laboratory testing of cutter designs, materials, cutting fluids machining parameters, and production verification of the laboratory results. A computer simulation program was used to study effect of spindle and tool compliance and eccentricity, cutter geometry, and cutting parameters on cutting forces and tool deflections. This is the first computer simulation program to accurately predict milling forces and tool breakage when tool deflection is significant. Cutter failure investigation was conducted to understand modes/causes of tool failure. As a result, adjustments to NC program were made, deficiencies in the cutter geometry were corrected to improve cutter life. GRA

N85-22732# Joint Publications Research Service, Arlington, Va.
PROBLEM OF PORE FORMATION MECHANISM IN WELDED JOINTS OF ALUMINUM ALLOYS IN THE SYSTEM ALUMINUM-MAGNESIUM-LITHIUM Abstract Only
V. I. Ryazantsev and V. A. Fedoseyev *In its* USSR Rept.: Mater. Sci. and Met. (JPRS-UMS-85-002) 6 Feb. 1985 p 56 Transl. into ENGLISH from Svarochnoye Proizvodstvo (USSR), no. 8, Aug. 1984 p 41-43 (For primary document see N85-22688 13-26)
Avail: NTIS HC A05/MF A01

N85-22733# Joint Publications Research Service, Arlington, Va.
PROPERTIES OF WELDED JOINTS IN ARGON ARC WELDING OF TITANIUM ALLOY USING A PROTECTIVE COATING Abstract Only
B. Y. Mozeyko and V. V. Bazhenov *In its* USSR Rept.: Mater. Sci. and Met. (JPRS-UMS-85-002) 6 Feb. 1985 p 56 Transl. into ENGLISH from Svarochnoye Proizvodstvo (USSR), no. 8, Aug. 1984 p 28-29 (For primary document see N85-22688 13-26)
Avail: NTIS HC A05/MF A01

N85-22734# Joint Publications Research Service, Arlington, Va.
THERMAL HARDENING OF WELDED JOINTS IN TITANIUM ALLOYS WITH VARIOUS STRUCTURES Abstract Only
M. A. Khorev *In its* USSR Rept.: Mater. Sci. and Met. (JPRS-UMS-85-002) 6 Feb. 1985 p 57 Transl. into ENGLISH from Svarochnoye Proizvodstvo (USSR), no. 8, Aug. 1984 p 26-27 (For primary document see N85-22688 13-26)
Avail: NTIS HC A05/MF A01

N85-22735# Joint Publications Research Service, Arlington, Va.
INFLUENCE OF WELDING DEFECTS AT MELTING BOUNDARY ON STATIC STRENGTH OF WELDED JOINT IN LARGE-DIAMETER PIPE Abstract Only
M. V. Shakhmatov, V. V. Yerofeyev, V. A. Lupin, and A. A. Ostsemin *In its* USSR Rept.: Mater. Sci. and Met. (JPRS-UMS-85-002) 6 Feb. 1985 p 57 Transl. into ENGLISH from Problemy Prochnosti (USSR), no. 8, Aug. 1984 p 111-116 (For primary document see N85-22688 13-26)
Avail: NTIS HC A05/MF A01

N85-22738# Joint Publications Research Service, Arlington, Va.
EFFECT OF PROTECTIVE MEDIUM ON DURABILITY AND FRACTURE STRUCTURE ON SEAM ZONES OF THIN-WALLED TITANIUM ARTICLES PRODUCED BY DIFFUSION WELDING Abstract Only
S. I. Gusev, V. V. Peshkov, V. N. Milyutin, and M. K. Shorshorov *In its* USSR Rept.: Mater. Sci. and Met. (JPRS-UMS-85-002) 6 Feb. 1985 p 59 Transl. into ENGLISH from Svarochnoye Proizvodstvo (USSR), no. 10, Oct. 1984 p 21-22 (For primary document see N85-22688 13-26)
Avail: NTIS HC A05/MF A01

N85-22739# Joint Publications Research Service, Arlington, Va.
TECHNOLOGICAL PARAMETERS OF DIFFUSION WELDING PROCESSES IN HONEYCOMB TITANIUM ALLOY STRUCTURES Abstract Only
V. V. Peshkov and S. I. Gusev *In its* USSR Rept.: Mater. Sci. and Met. (JPRS-UMS-85-002) 6 Feb. 1985 p 59-60 Transl. into ENGLISH from Svarochnoye Proizvodstvo (USSR), no. 10, Oct. 1984 p 12-14 (For primary document see N85-22688 13-26)
Avail: NTIS HC A05/MF A01

N85-22740# Joint Publications Research Service, Arlington, Va.
DURABILITY OF VT16 ALLOY COMPOUNDS OBTAINED BY DIFFUSION WELDING Abstract Only
N. F. Kazakov, N. A. Mashkova, V. Y. Varyanitsa, N. V. Yermakova, and O. V. Fedorova *In its* USSR Rept.: Mater. Sci. and Met. (JPRS-UMS-85-002) 6 Feb. 1985 p 60 Transl. into ENGLISH from Svarochnoye Proizvodstvo (USSR), no. 10, Oct. 1984 p 11-12 (For primary document see N85-22688 13-26)
Avail: NTIS HC A05/MF A01

N85-22741# Joint Publications Research Service, Arlington, Va.
RELIABILITY OF ROBOTIZED WELDING APPARATUS Abstract Only
V. A. Timchenko and A. S. Taratuta *In its* USSR Rept.: Mater. Sci. and Met. (JPRS-UMS-85-002) 6 Feb. 1985 p 60-61 Transl. into ENGLISH from Avtomaticheskaya Svarka (USSR), no. 9, Sep. 1984 p 61-65 (For primary document see N85-22688 13-26)
Avail: NTIS HC A05/MF A01

N85-22742# Joint Publications Research Service, Arlington, Va.
STRUCTURE AND MECHANICAL CHARACTERISTICS OF HETEROGENEOUS JOINTS PRODUCED BY LASER WELDING Abstract Only
A. N. Grezev, A. G. Grigoryant, A. G. Fedorov, and V. V. Ivanov *In its* USSR Rept.: Mater. Sci. and Met. (JPRS-UMS-85-002) 6 Feb. 1985 p 61 Transl. into ENGLISH from Avtomaticheskaya Svarka (USSR), no. 9, Sep. 1984 p 46-49 (For primary document see N85-22688 13-26)
Avail: NTIS HC A05/MF A01

N85-22744# Joint Publications Research Service, Arlington, Va.
EFFECT OF MOISTURE IN INERT GASES ON DENSITY OF SEAM METAL AND ON MECHANICAL CHARACTERISTICS OF WELDED JOINTS OF ALUMINUM AND ALUMINUM ALLOYS Abstract Only
I. V. Dovbishchenko, V. S. Mashin, and D. M. Rabkin *In its* USSR Rept.: Mater. Sci. and Met. (JPRS-UMS-85-002) 6 Feb. 1985 p 62-63 Transl. into ENGLISH from Avtomaticheskaya Svarka

(USSR), no. 9, Sep. 1984 p 17-19 (For primary document see N85-22688 13-26)
Avail: NTIS HC A05/MF A01

N85-22746# Joint Publications Research Service, Arlington, Va.
AUTOMATIC MULTI-LAYER WELDING OF THICK CYLINDRICAL STRUCTURES UNDER FLUX Abstract Only
N. V. Pilipenko, Y. N. Rudenko, and A. N. Yastreb *In its* USSR Rept.: Mater. Sci. and Met. (JPRS-UMS-85-002) 6 Feb. 1985 p 67-68 Transl. into ENGLISH from Svarochnoye Proizvodstvo (USSR), no. 9, Sep. 1984 p 12-13 (For primary document see N85-22688 13-26)
Avail: NTIS HC A05/MF A01

N85-22747# Joint Publications Research Service Arlington, Va.
SOFTENING OF METAL NEAR SEAM DURING WELDING OF HEAT-RESISTANT NICKEL ALLOYS Abstract Only
B. F. Yakushin *In its* USSR Rept.: Mater. Sci. and Met. (JPRS-UMS-85-002) 6 Feb. 1985 p 68 Transl. into ENGLISH from Svarochnoye Proizvodstvo (USSR), no. 9, Sep. 1984 p 5-6 (For primary document see N85-22688 13-26)
Avail: NTIS HC A05/MF A01

N85-22800# Joint Publications Research Service, Arlington, Va.
NEW TECHNIQUE FOR FLUID FEED IN SIMULTANEOUS MULTISURFACE GRINDING Abstract Only
Ye. S. Kiselev, A. N. Unyanin, and Yu. N. Moiseyev *In its* USSR Rept.: Eng. and Equipment (JPRS-UEQ-85-003) 12 Mar. 1985 p 20 Transl. into ENGLISH from Vestn. Mashinostr. (Moscow), no. 6, Jun. 1984 p 56-57 (For primary document see N85-22782 13-31)
Avail: NTIS HC A06

N85-22801# Joint Publications Research Service, Arlington, Va.
EFFECT OF ZERO-WEAR IN FRICTION PAIRS OPERATING IN ABRASIVE MEDIA Abstract Only
M. V. Golub, V. I. Kharlamenko, and V. N. Malyshev *In its* USSR Rept.: Eng. and Equipment (JPRS-UEQ-85-003) 12 Mar. 1985 p 21 Transl. into ENGLISH from Vestn. Mashinostr. (Moscow), no. 5, May 1984 p 29-31 (For primary document see N85-22782 13-31)
Avail: NTIS HC A06

N85-22803# Joint Publications Research Service, Arlington, Va.
CYCLIC INDUSTRIAL ROBOTS WITH MECHANICAL ENERGY STORING DEVICES: MULTIPOSITIONAL SYSTEM WITH ONE OR SEVERAL DEGREES OF FREEDOM Abstract Only
A. I. Korendyasev, B. L. Salamandra, and L. I. Tyves *In its* USSR Rept.: Eng. and Equipment (JPRS-UEQ-85-003) 12 Mar. 1985 p 24 Transl. into ENGLISH from Stanki i Instrument (Moscow), no. 6, Jun. 1984 p 4-8 (For primary document see N85-22782 13-31)
Avail: NTIS HC A06

N85-22804# Joint Publications Research Service, Arlington, Va.
DESIGN OF TIGHTENING DEVICE AND CALCULATION OF FORCES IN MANIPULATOR TRANSMISSIONS WITH BASE-DRIVE MOUNTED Abstract Only
A. G. Ovakimov, I. V. Kalabin, and I. A. Timofeyev *In its* USSR Rept.: Eng. and Equipment (JPRS-UEQ-85-003) 12 Mar. 1985 p 25 Transl. into ENGLISH from Stanki i Instrument (Moscow), no. 6, Jun. 1984 p 8-11 (For primary document see N85-22782 13-31)
Avail: NTIS HC A06

N85-22805# Joint Publications Research Service, Arlington, Va.
OPTOELECTRONIC SAFETY SYSTEM FOR ROBOTIZED TECHNOLOGICAL COMPLEX Abstract Only
S. G. Batrakov, Ye. M. Kanayev, and B. M. Chertkov *In its* USSR Rept.: Eng. and Equipment (JPRS-UEQ-85-003) 12 Mar. 1985 p 25-26 Transl. into ENGLISH from Stanki i Instrument (Moscow), no. 5, May 1984 p 8-10 (For primary document see N85-22782 13-31)
Avail: NTIS HC A06

N85-22806# Joint Publications Research Service, Arlington, Va.
HYDRAULIC BRAKES FOR INDUSTRIAL ROBOTS Abstract Only
P. I. Knysh *In its* USSR Rept.: Eng. and Equipment (JPRS-UEQ-85-003) 12 Mar. 1985 p 26-27 Transl. into ENGLISH from Stanki i Instrument (Moscow), no. 5, May 1984 p 10-12 (For primary document see N85-22782 13-31)
Avail: NTIS HC A06

N85-22807# Joint Publications Research Service, Arlington, Va.
CYCLIC INDUSTRIAL ROBOTS WITH MECHANICAL ENERGY STORING DEVICES: PRINCIPLES OF DRIVE DESIGN Abstract Only
L. M. Bolotin, A. I. Korendyasev, B. L. Salamandra, and L. I. Tyves *In its* USSR Rept.: Eng. and Equipment (JPRS-UEQ-85-003) 12 Mar. 1985 p 27 Transl. into ENGLISH from Stanki i Instrument (Moscow), no. 4, Apr. 1984 p 7-10 (For primary document see N85-22782 13-31)
Avail: NTIS HC A06

N85-22808# Joint Publications Research Service, Arlington, Va.
ASSEMBLY ROBOT CONTROL ALGORITHMS Abstract Only
P. D. Krutko, N. A. Lakota, and V. I. Solntsev *In its* USSR Rept.: Eng. and Equipment (JPRS-UEQ-85-003) 12 Mar. 1985 p 28 Transl. into ENGLISH from Izv. Vyssh. Ucheb. Zaved.: Mashinostr. (Moscow), no. 1, Jan. 1984 p 39-43 (For primary document see N85-22782 13-31)
Avail: NTIS HC A06

N85-22818# Joint Publications Research Service, Arlington, Va.
CONTROLLED MOVEMENT OF ELASTIC MANIPULATOR WITH DISTRIBUTED PARAMETERS Abstract Only
V. Ye. Berbyuk and M. V. Demidyuk *In its* USSR Rept.: Eng. and Equipment (JPRS-UEQ-85-003) 12 Mar. 1985 p 43-44 Transl. into ENGLISH from Izv. Akad. Nauk SSSR: Mekhan. Tverdogo Tela (Moscow), no. 2, Feb. 1984 p 59-67 (For primary document see N85-22782 13-31)
Avail: NTIS HC A06

N85-22819# Joint Publications Research Service, Arlington, Va.
INVESTIGATION OF DYNAMICS OF MANIPULATOR WITH ELASTIC SECTIONS Abstract Only
S. A. Mikhaylov and F. L. Shernousko *In its* USSR Rept.: Eng. and Equipment (JPRS-UEQ-85-003) 12 Mar. 1985 p 44 Transl. into ENGLISH from Izv. Akad. Nauk SSSR: Mekhan. tverdogo Tela (Moscow), no. 2, Feb. 1984 p 51-58 (For primary document see N85-22782 13-31)
Avail: NTIS HC A06

38 QUALITY ASSURANCE AND RELIABILITY

Includes product sampling procedures and techniques; and quality control.

N85-23090*# National Aeronautics and Space Administration. Langley Research Center, Hampton, Va.
RELIABILITY BOUNDS FOR FAULT-TOLERANT SYSTEMS WITH COMPETING RESPONSES TO COMPONENT FAILURES
Larry D. Lee Apr. 1985 16 p refs
(NASA-TP-2409; L-15853; NAS 1.60:2409) Avail: NTIS HC A02/MF A01 CSCL 14D

Bounds are established on the probability of system failure for fault-tolerant systems of the type used, for example, in aviation control. Event series leading to system failure are assumed to follow a semi-Markov model in which the potential sojourn times associated with component failures have exponential distributions and those associated with system responses have distributions with unspecified form. A product form of the bounds is derived by using a model that provides for multiple competing system responses to component failures. Author

N85-23091# University Coll., London (England). Dept. of Electronic and Electrical Engineering.
INVESTIGATION OF STEEL STRUCTURES USING ULTRASONIC WAVES Progress Report, 1 Apr. 1983 - 29 Feb. 1984
M. Punjani and L. J. Bond Jun. 1984 42 p refs Revised
(Contracts MOD-2047/090-AMTE-13; MOD-2047/091-AMTE-13) (BR93258) Avail: NTIS HC A03/MF A01

A theory for wave propagation in stressed polycrystalline media is presented. The second and third order elastic constants were calculated using acoustoelastic coefficients obtained from experiment. Experimental results of the magnitude of the longitudinal strains in five statically stressed steel specimens are presented. Results suggest that the characterization of longitudinal strain is feasible from one free surface. Author (ESA)

N85-23092# Ohio State Univ., Columbus. Dept. of Preventive Medicine.
EFFECTS OF ASSUMING INDEPENDENT COMPONENT FAILURE TIMES, IF THEY ARE ACTUALLY DEPENDENT, IN A SERIES SYSTEM Annual Report, 1 Sep. 1983 - 30 Sep. 1984
Melvin L. Moeschberger and John P. Klein 26 Oct. 1984 92 p (Grant AF-AFOSR-0307-82; AF Proj. 2304)
(AD-A150582; AFOSR-85-0001TR; RF-763265/714837) Avail: NTIS HC A05/MF A01 CSCL 12/1

The overall objective of this proposal is to investigate the robustness to departures from independence of methods currently in use in reliability studies when competing failure modes or competing causes of failure associated with a single mode are present in a series system. The first specific aim is to examine the error one makes in modeling a series system by a model which assumes statistically independent component lifetimes when in fact the component lifetimes follow some multivariate distribution. The second specific aim is to assess the effects of the independence assumption error in estimating component parameters from life tests on series systems. In both cases, estimates of such errors will be determined via mathematical analysis and computer simulations for several prominent multivariate distributions. A graphical display of the errors for representative distributions will be made available to researchers who wish to assess the possible erroneous assumption of independent competing risks. A third aim is to tighten the bounds on estimates of component reliability when the risks belong to a general dependence class of distributions (for example, positive quadrant dependence, positive regression dependence, etc.). Major decisions involving reliability studies, based on competing risk methodology, have been made in the past and will continue to be made in the future. This study will provide the user of such techniques with a clearer understanding of the robustness of the analyses to departures from independent risks, an assumption commonly made by the methods currently in use. GRA

39 STRUCTURAL MECHANICS

Includes structural element design and weight analysis; fatigue; and thermal stress.

For applications see *05 Aircraft Design, Testing and Performance* and *18 Spacecraft Design, Testing and Performance.*

N85-23093 Houston Univ., Tex.
SHAPE OPTIMIZATION FOR MINIMAL STRESS CONCENTRATION Ph.D. Thesis
Bahir Helmy Eldiwany 1984 88 p
Avail: Univ. Microfilms Order No. DA8428113

Two general inverse problems are solved in order to find the configuration of an inhomogeneity that minimizes the stress concentration in an elastic solid. For an antiplane shear deformation of an elastic half space with a groove cut in the boundary, conformal mapping methods are used to find the shape of the groove bottom such that the euclidean stress norm is rendered constant on the boundary. For three-dimensional problems concerning an infinite elastic matrix with an inhomogeneity, the Newtonian potential is utilized to find the shape of the inhomogeneity such that certain stress components are uniform on the surface of the inhomogeneity. Several limiting cases are considered and certain results in the literature are verified. Further, the solution of the optimization problem for minimizing the stress concentration in an infinite elastic matrix with a rigid inclusion is obtained by reducing the problem to an inverse problem of the type mentioned and some numerical examples are presented. Dissert. Abstr.

N85-23094 Iowa Univ., Iowa City.
FATIGUE LIFE, CRACK INITIATION, AND PROPAGATION OF 304 STAINLESS STEEL WITH NON-PROPORTIONAL AXIAL-TORSIONAL STRAIN-PATHS Ph.D. Thesis
Chwen-Chin Yang 1984 185 p
Avail: Univ. Microfilms Order No. DA8428307

The concepts of energy probability, damage accumulation and path dependence are used to formulate a criterion for multiaxial fracture under the condition of low cycle fatigue. A time like parameter termed fatigue intrinsic time is introduced to measure damage accumulation in fatigue. This concept is an extension of the endochronic theory of viscoelasticity, which is based on the postulate that the history of deformation of a microelement is described with respect to its own intrinsic time scale, defined as the length of the plastic strain path. A set of strain controlled experiments was performed with strain paths especially designed to highlight the characteristics of path dependence in the multiaxial fatigue tests. Crack initiation and propagation were also studied based on the same set of multiaxial tests. Path dependence does show significant influences on these effects. A fracture mechanics model for the extension of a straight crack under nonsymmetric plane loading condition was also applied to describe the observed direction of fatigue crack propagation under biaxial straining. Dissert. Abstr.

N85-23095 California Univ., Berkeley.
ELASTIC WAVE SCATTERING FROM AN INTERFACE CRACK IN A LAYERED HALF SPACE Ph.D. Thesis
Huey-Ju Pearl Yang 1984 71 p
Avail: Univ. Microfilms Order No. DA8427137

The plane strain, time-harmonic problem of a single elastic layer of one material on a half space of a different material with a single crack at the interface was investigated. The required Green's functions are derived for dilational and rotational point sources in the uncracked layered half space. These functions are then used to derive the scattered field potentials for arbitrary incident fields in the cracked layered half space. The potentials are used to reduce the problem to a system of singular integral equations for determining the gradients of the crack opening displacements in the scattered field. The integral equations are analyzed to determine the crack tip singularity. The integral equations are solved numerically to determine the Mode 1 and Mode 2 stress intensity factors as a function of a dimensionless wave number for various ratios of crack length to layer depth. Dissert. Abstr.

N85-23096*# Massachusetts Inst. of Tech., Cambridge.
ON HYBRID AND MIXED FINITE ELEMENT METHODS
Th. H. H. Pian [1981] 19 p refs
(Grant NAG3-33)
(NASA-CR-175551; NAS 1.26:175551) Avail: NTIS HC A02/MF A01 CSCL 20K

Three versions of the assumed stress hybrid model in finite element methods and the corresponding variational principles for the formulation are presented. Examples of rank deficiency for stiffness matrices by the hybrid stress model are given and their corresponding kinematic deformation modes are identified. A discussion of the derivation of general semi-Loof elements for plates and shells by the hybrid stress method is given. It is shown that the equilibrium model by Fraeijs de Veubeke can be derived by the approach of the hybrid stress model as a special case of semi-Loof elements. Author

N85-23097*# Lehigh Univ., Bethlehem, Pa.
ELASTICITY SOLUTION OF AN ADHESIVELY BONDED JOINT
G. N. Aksel and F. Erdogan Jan. 1985 110 p refs
(Grant NGR-39-007-011)
(NASA-CR-175591; NAS 1.26:175591) Avail: NTIS HC A06/MF A01 CSCL 20K

The plane strain of adhesively bonded structures consisting of two different isotropic adherends is considered. By expressing the x-y components of the displacements in terms of Fourier integrals and using the corresponding boundary and continuity conditions, the integral equations for the general problem are obtained and solved numerically by applying Gauss-Chebyshev integration scheme. The shear and the normal stresses in the adhesive are calculated for various geometries and material properties for a stiffened plate under uniaxial tension. Numerical results involving the stress intensity factors and the strain energy release rate are presented. The closed-form expressions for the Fredholm kernels are provided to obtain the solution for an arbitrary geometry and material properties. For the general geometry, the contribution of the normal stress is quite significant, while for symmetric geometries, the shear stress is dominant, the normal stress vanishes if the adherends are of the same material and the same thickness. A.R.H.

N85-23098*# Lehigh Univ., Bethlehem, Pa. Dept. of Mechanical Engineering and Mechanics.
A CLAMPED RECTANGULAR PLATE CONTAINING A CRACK
Renji Tang (Lanzhou Univ., China) and F. Erdogan Mar. 1985 27 p refs
(Grants NGR-39-007-011; NSF MEA-84-14477)
(NASA-CR-175590; NAS 1.26:175590) Avail: NTIS HC A03/MF A01 CSCL 20K

The general problem of a rectangular plate clamped along two parallel sides and containing a crack parallel to the clamps is considered. The problem is formulated in terms of a system of singular integral equations and the asymptotic behavior of the stress state near the corners is investigated. Numerical examples are considered for a clamped plate without a crack and with a centrally located crack, and the stress intensity factors and the stresses along the clamps are calculated. Author

N85-23099*# Lehigh Univ., Bethlehem, Pa.
STRESS INTENSITY FACTOR IN A TAPERED SPECIMEN
Liu Xue-Hui (Northwestern Polytechnical Univ., Xian, China) and F. Erdogan Apr. 1985 27 p refs
(Grants NGR-39-007-011; NSF MEA-84-14477)
(NASA-CR-175589; NAS 1.26:175589) Avail: NTIS HC A03/MF A01 CSCL 20K

The general problem of a tapered specimen containing an edge crack is formulated in terms of a system of singular integral equations. The equations are solved and the stress intensity factor is calculated for a compact and for a slender tapered specimen, the latter simulating the double cantilever beam. The results are obtained primarily for a pair of concentrated forces and for crack surface wedge forces. The stress intensity factors are also obtained for a long strip under uniform tension which contains inclined edge cracks. Author

N85-23100*# National Aeronautics and Space Administration. Langley Research Center, Hampton, Va.
SPLINE-BASED RAYLEIGH-RITZ METHODS FOR THE APPROXIMATION OF THE NATURAL MODES OF VIBRATION FOR FLEXIBLE BEAMS WITH TIP BODIES Final Report
I. Gary Rosen Mar. 1985 33 p refs Submitted for publication
(Contract NAS1-17070; Grant AF-AFOSR-0393-84)
(NASA-CR-172566; ICASE-85-22; NAS 1.26:172566) Avail: NTIS HC A03/MF A01 CSCL 20K

Rayleigh-Ritz methods for the approximation of the natural modes for a class of vibration problems involving flexible beams with tip bodies using subspaces of piecewise polynomial spline functions are developed. An abstract operator theoretic formulation of the eigenvalue problem is derived and spectral properties investigated. The existing theory for spline-based Rayleigh-Ritz methods applied to elliptic differential operators and the approximation properties of interpolatory splines are useed to argue convergence and establish rates of convergence. An example and numerical results are discussed. Author

N85-23101*# Jet Propulsion Lab., California Inst. of Tech., Pasadena.
FRACTURE MECHANICS EVALUATION OF GaAs
C. P. Chen 15 Oct. 1984 74 p refs
(Contract NAS7-918)
(NASA-CR-175657; JPL-84-81; NAS 1.26:175657) Avail: NTIS HC A04/MF A01 CSCL 20K

A data base of mechanical and fracture properties for GaAs was generated. The data for single crystal GaAs will be used to design reusable GaAs solar modules. Database information includes; (1) physical property characterizations; (2) fracture behavior evaluations; and (3) strength of cells determined as a function of cell processing and material parameters. G.L.C.

N85-23102# Shock and Vibration Information Center (Defense), Washington, D. C.
THE SHOCK AND VIBRATION DIGEST, VOLUME 16, NO. 12
Judith Nagle-Eshleman, ed. Dec. 1984 158 p refs
(AD-A150594) Avail: SVIC, Code 5804, Naval Research Lab., Washington, D.C. 20375 CSCL 20/11

The feature article concerns itself with the use of the Laplace equation to solve wave propagation problems and those involving membrane and plate vibrations. A review of machine tool vibrations is also presented. Other subject areas presented are: mechanical systems, structural systems, vehicle systems, biological systems, mechanical and structural components, and analysis and design in vibration. For individual titles, see N85-23103 through N85-23104.

N85-23103# Shock and Vibration Information Center (Defense), Washington, D. C.
APPLICATIONS OF THE CONFORMAL MAPPING METHOD TO THE SOLUTION OF MECHANICAL VIBRATIONS PROBLEMS
P. A. A. Laura (Inst. of Applied Mech., Puerto Belgrano Naval Base, Argentina) *In its* The Shock and Vibration Digest, Volume 16, No. 12 Dec. 1984 p 3-7 refs (For primary document see N85-23102 13-39)
Avail.: SVIC, Code 5804, Naval Research Lab., Washington, D.C. 20375 CSCL 20/11

Traditional applications of the method of conformal mapping are governed by the Laplace equation. The equation has also been used to solve wave propagation problems and those involving membrane and plate vibrations. In many instances it has been possible to obtain elegant approximate analytical solutions and algorithmic procedures; they have been implemented on desk computers and programmable pocket calculators. Author

N85-23104# Shock and Vibration Information Center (Defense), Washington, D. C.
MACHINE TOOL VIBRATIONS: A REVIEW
V. Ramamurti (Indian Inst. of Technol., Madras) and D. Ganapathi Rao (Indian Inst. of Technol., Madras) *In its* The Shock and Vibration Digest, Volume 16, No. 12 Dec. 1984 p 9-13 refs (For primary document see N85-23102 13-39)
Avail.: SVIC, Code 5804, Naval Research Lab., Washington, D.C. 20375 CSCL 20/11

The general concept of machine tool chatter was discussed, as have methods adopted for reducing it. A unified systems approach for chatter analysis was presented. A theoretical approach for predicting chatter was verified experimentally by turning a slender bar on a turret lathe. The conclusion after an experimental study of carbide face milling cutters was that increased tool wear due to vibration is governed mainly by the stiffness of certain elements in the cutting mechanism. Self-excited oscillations of machine tools was studied. Dynamic analysis and optimal selection of parameters of a lathe spindle under random cutting loads was undertaken. Free vibration behavior of lathe spindles was studied. Methods were developed to study static

and dynamic behaviors of machine tools. A test procedure for vibration analysis was developed to check a machining setup. Static stiffness of machine tool spindles was also a subject of discussion. E.R.

N85-23105# Office National d'Etudes et de Recherches Aerospatiales, Paris (France).
THE LOW FREQUENCY BEHAVIOR OF AN IMMERSED STRUCTURE AT A STANDSTILL IN A HIGH DENSITY FLUID WITH FREE SURFACE
A. Laurent 1983 18 p refs In FRENCH; ENGLISH summary Presented at Session ATMA 1983, Paris, 18-22 Apr. 1983
(TP-1983-31) Avail: NTIS HC A02/MF A01

The mechanical behavior of stable immersed axisymmetric shell at low frequency, in a high density fluid with free surface, was studied. The fluid structure interaction and the air fluid interface were examined. The modal method which defines an eigenvector base is described. The Neumann problem yields resonances of the mechanical system to which a shell's deformation a damping ratio and a directional radiation correspond. The free surface effects the pressure levels and the shape of the directional pressure radiation. The correlation of the displacements of the shell with the corresponding directional pressure radiation is recommended for identification of a submerged structure. The method was applied to an axisymmetric ring stiffened structure with nonaxisymmetric mass and stiffness perturbations. E.A.K.

N85-23106# National Inst. for Aeronautics and Systems Technology, Pretoria (South Africa). Aeroelasticity Div.
FIBRE COMPOSITE LAMINATED PLATE ANALYSIS USING A CARD PROGRAMMABLE CALCULATOR (HP41C/CV)
A. P. N. Sutherland Oct. 1983 155 p refs
(NIAST-83/88; ISBN-0-7988-3020-4) Avail: NTIS HC A08/MF A01

The HP 41C/CV programs which perform the stiffness and strength calculations for composite laminates are presented. Two sets of programs are given, each to be used interactively: (1) symmetric laminates or sandwich beams comprising one type of ply material only; and (2) general laminates comprising up to three different ply materials. The programs include nonmechanical effects. The strength ratios (reserve factors) calculated are for first ply failure (FPF) and are based on mechanical strain. Behavior beyond FPF is not included. Classical lamination theory (CLT) is used. E.A.K.

N85-23107# Admiralty Marine Technology Establishment, Teddington (England).
INTENSITY VECTORS OF SOUND SCATTERING BY A SPHERICAL SHELL
J. H. James Jul. 1984 21 p refs
(AD-A147847; AMTE(N)-TM-84080; BR93176) Avail: NTIS HC A02/MF A01

Mathematical formulas from which target strength spectra and acoustic intensity vectors are calculated are given. The excitation is a time-harmonic plane wave. Intensity vector plots show the considerable distortion of the incident sound field that may be present when an elastic scatterer is excited at a resonant frequency. Author (ESA)

N85-23108# Lockheed-Georgia Co., Marietta.
ADVANCED LIFE ANALYSIS METHODS. VOLUME 1: CRACKING DATA SURVEY AND NDI (NONDESTRUCTIVE INSPECTION) ASSESSMENT FOR ATTACHMENT LUGS Final Report, 3 Sep. 1980 - 30 Sep. 1984
T. R. Brussat, K. Kathiresan, and T. M. Hsu Wright-Patterson AFB, Ohio Air Force Wright Aeronautical Labs. Sep. 1984 64 p
(Contract F33615-80-C-3211)
(AD-A150419; LG82ER0117-1; AFWAL-TR-84-3080-Vol-1) Avail: NTIS HC A04/MF A01 CSCL 13/5

Results of a survey of cracking data and an evaluation of NDI capability for aircraft attachment lugs are presented. This survey and evaluation are part of an overall effort involving fatigue testing and analyses to develop the design criteria and analytical methods necessary to ensure the damage tolerance of pin-loaded lugs. Cracking data from coupon and full scale fatigue tests and from service failures are summarized in terms of causes of initial cracking and final failure; initial crack type, shape, location and multiplicity; and final critical crack size. Existing NDI capability is reviewed, and an inspectable initial flaw size criterion for lugs is proposed, subject to experimental verification. GRA

N85-23109# Lockheed-Georgia Co., Marietta.
ADVANCED LIFE ANALYSIS METHODS. VOLUME 2: CRACK GROWTH ANALYSIS METHODS FOR ATTACHMENT LUGS Final Report, 3 Sep. 1980 - 30 Sep. 1984
K. Kathiresan, T. M. Hsu, and T. R. Brussat Wright-Patterson AFB, Ohio Air Force Wright Aeronautical Labs. Sep. 1984 186 p
(Contract F33615-80-C-3211)
(AD-A150420; LG82ER0117-2; AFWAL-TR-84-3080-Vol-2) Avail: NTIS HC A09/MF A01 CSCL 13/5

Analysis procedures for the assessment of the damage tolerance of aircraft attachment lugs are developed and presented. Stress and fracture analyses are conducted for simple male straight shank lugs subjected to symmetric loading and tapered lugs subjected to symmetric and off-axis lodings. Solutions of stress distributions and stress intensity factors are obtained for various parameters. The parametric variations include lug outer-to-inner radius ratios corner and through-the-thickness cracks, crack lengths and aspect ratios, with and without interference-fit bushing and loads above and below yield of the lugs. Methods of varying degree of sophistication are considered in the development of stress intensity factor solutions for cracks in attachment lugs. For through-the-thickness crack problems, simple compounding method, two-dimensional cracked finite element method, and the weight function method are used. In the case of corner cracks, solutions are obtained using simple compounding method, weight function method and rigorous three-dimensional hybrid displacement cracked finite element method. The stress distributions and the stress intensity factors are consolidated into a crack growth analysis procedure including several crack growth models and spectrum retardation models to predict the fracture and crack growth behaviors in attachment lugs. GRA

N85-23110# Argonne National Lab., Ill. Components Technology Div.
FLOW-INDUCED VIBRATIONS OF A CIRCULAR CYLINDER DUE TO TURBULENT INTERNAL FLOWS
H. Chung 1985 16 p refs Presented at the Offshore Mech. and Arctic Eng. Symp., Dallas, Tex., 17 Feb. 1985
(Contract W-31-109-eng-38)
(DE85-002766; CONF-850219-2) Avail: NTIS HC A02/MF A01

Flow-induced vibration characteristics were experimentally investigated for a circular cyclinder subjected to a turbulent internal flow. The free libration characteristics of the cylinder in air and in fluid were analyzed. The obtained free vibration characteristics were used to aid interpretation of the flow-induced vibration test results. It is shown that the cylinder was excited by the turbulent axial flow and experienced a narrow-band random vibration consisting of many localized shell-modes. The RMS vibration amplitude was small. However, it monotonically increased with the flow rate. DOE

N85-23111# Los Alamos Scientific Lab., N. Mex.
STEEL CONTAINMENT BUCKLING
J. G. Bennett, G. W. Fly, and N. E. Baker 1984 13 p refs Presented at 12th Water Reactor Safety Res. Inform. Meeting, Gaithersburg, Md., 23 Oct. 1984
(Contract W-7405-eng-36)
(DE85-003744; LA-UR-84-3483; CONF-8410142-67) Avail: NTIS HC A02/MF A01

The steel containment buckling program is in its fourth phase which is directed at the evaluation of the effects of the structural failure mode of steel containments when the membrane stresses are compressive. The structural failure mode for this state of stress in instability or buckling is discussed. The program investigated:

(1) the effect on overall buckling capacity of the ASME area replacement method for reinforcing around circular penetrations; (2) a set of benchmark experiments on ring-stiffened shells having reinforced and framed penetrations; (3) large and small scale experiments on knuckle region buckling from internal pressure and post buckling behavior to failure for vessel heads having torispherical geometries; and (4) buckling under time-dependent loadings (dynamic buckling). DOE

N85-22736# Joint Publications Research Service, Arlington, Va.
MECHANICAL PROPERTIES AND BRITTLE FRACTURE RESISTANCE OF WELDED MULTILAYER ELEMENTS FOR HIGH PRESSURE VESSELS Abstract Only
V. M. Goritskiy, V. S. Kabanov, and S. A. Klimov *In its* USSR Rept.: Mater. Sci. and Met. (JPRS-UMS-85-002) 6 Feb. 1985 p 58 Transl. into ENGLISH from Avtomaticheskaya Svarka (USSR), no. 8, Aug. 1984 p 27-30 (For primary document see N85-22688 13-26)
Avail: NTIS HC A05/MF A01

N85-22737# Joint Publications Research Service, Arlington, Va.
ANALYSIS OF STRENGTH AND DUCTILITY OF WELDED JOINTS IN AMtsS AND AMg5 ALUMINUM ALLOYS Abstract Only
B. V. Grudzinskiy, A. T. Fomchenkov, N. G. Murkina, and A. N. Yeremeyev *In its* USSR Rept.: Mater. Sci. and Met. (JPRS-UMS-85-002) 6 Feb. 1985 p 58-59 Transl. into ENGLISH from Avtomaticheskaya Svarka (USSR), no. 8, Aug. 1984 p 71-72 (For primary document see N85-22688 13-26)
Avail: NTIS HC A05/MF A01

N85-22743# Joint Publications Research Service, Arlington, Va.
METHOD OF CALCULATING STRENGTH OF JOINT PRODUCED BY COLD WELDING OF ALUMINUM UNDER DISCRETE LOADING Abstract Only
D. P. Kulagin *In its* USSR Rept.: Mater. Sci. and Met. (JPRS-UMS-85-002) 6 Feb. 1985 p 62 Transl. into ENGLISH from Avtomaticheskaya Svarka (USSR), no. 9, Sep. 1984 p 29-31 (For primary document see N85-22688 13-26)
Avail: NTIS HC A05/MF A01

N85-22779# Joint Publications Research Service, Arlington, Va.
EXPERIMENTAL INVESTIGATION OF CRIPPLING STRENGTH OF CHINESE ALUMINUM ALLOY (LY12CZ) SECTIONS
Zhang Fubao *In its* China Rept: Sci. and Technol. (JPRS-CST-84-30) 10 Oct. 1984 p 32-37 refs Transl. into ENGLISH from Fudan Xuebao-Kexue Ban (Shanghai), no. 4, 1983 p 474-478 (For primary document see N85-22777 13-31)
Avail: NTIS HC A03/MF A01

N85-22809# Joint Publications Research Service, Arlington, Va.
TIME DEPENDENT INTERACTION OF INTERNAL PRESSURE WAVE WITH SYSTEM OF TWO SPHERICAL SHELLS Abstract Only
Yu. V. Saprykin *In its* USSR Rept.: Eng. and Equipment (JPRS-UEQ-85-003) 12 Mar. 1985 p 37 Transl. into ENGLISH from Prikl. Mekhan. (Kiev), no. 6, Jun. 1984 p 40-46 (For primary document see N85-22782 13-31)
Avail: NTIS HC A06

N85-22810# Joint Publications Research Service, Arlington, Va.
INTERACTION OF CYLINDRICAL SHELL WITH CONCENTRATED MASS MOVING ALONG ITS INNER SURFACE Abstract Only
N. S. Kondrashov *In its* USSR Rept.: Eng. and Equipment (JPRS-UEQ-85-003) 12 Mar. 1985 p 37-38 Transl. into ENGLISH from Prikl. Mekhan. (Kiev), no. 6, Jun. 1984 p 47-52 (For primary document see N85-22782 13-31)
Avail: NTIS HC A06

N85-22811# Joint Publications Research Service, Arlington, Va.
STEADY-STATE REACTION OF THREE-LAYERED CYLINDRICAL SHELL TO EFFECT OF MOVING LOAD Abstract Only
V. I. Pozhuyev *In its* USSR Rept.: Eng. and Equipment (JPRS-UEQ-85-003) 12 Mar. 1985 p 38 Transl. into ENGLISH from Prikl. Mekhan. (Kiev), no. 6, Jun. 1984 p 52-59 (For primary document see N85-22782 13-31)
Avail: NTIS HC A06

N85-22812# Joint Publications Research Service, Arlington, Va.
DETERMINATION OF STRESSES AND DEFORMATIONS IN LINEARLY ELASTIC CONICAL SHELL SUBJECTED TO AERODYNAMIC LOADING AND HEATING Abstract Only
I. G. Muravskiy *In its* USSR Rept.: Eng. and Equipment (JPRS-UEQ-85-003) 12 Mar. 1985 p 39 Transl. into ENGLISH from Prikl. Mekhan. (Kiev), no. 6, Jun. 1984 p 64-70 (For primary document see N85-22782 13-31)
Avail: NTIS HC A06

N85-22813# Joint Publications Research Service, Arlington, Va.
STABILITY OF THREE-LAYER GLASS-REINFORCED PLASTIC SHELLS OF ROTATION Abstract Only
O. N. Ivanov, L. S. Orlovskiy, and D. A. Mysyk *In its* USSR Rept.: Eng. and Equipment (JPRS-UEQ-85-003) 12 Mar. 1985 p 40 Transl. into ENGLISH from Prikl. Mekhan. (Kiev), no. 6, Jun. 1984 p 107-109 (For primary document see N85-22782 13-31)
Avail: NTIS HC A06

N85-22814# Joint Publications Research Service, Arlington, Va.
AXISYMMETRICAL OSCILLATIONS OF SHELL SYSTEMS SUBJECTED TO IMPULSE LOADS Abstract Only
P. Z. Logovoy and V. N. Chaban *In its* USSR Rept.: Eng. and Equipment (JPRS-UEQ-85-003) 12 Mar. 1985 p 41 Transl. into ENGLISH from Prikl. Mekhan. (Kiev), no. 6, Jun. 1984 p 110-113 (For primary document see N85-22782 13-31)
Avail: NTIS HC A06

N85-22815# Joint Publications Research Service, Arlington, Va.
SPECTRAL FREQUENCY OF EIGENVALUES IN OPTIMAL PROBLEMS OF STABILITY OF CYLINDRICAL SHELLS OF VARIABLE THICKNESS Abstract Only
N. G. Medvedev and N. P. Totskiy *In its* USSR Rept.: Eng. and Equipment (JPRS-UEQ-85-003) 12 Mar. 1985 p 41 Transl. into ENGLISH from Prikl. Mekhan. (Kiev), no. 6, Jun. 1984 p 113-116 (For primary document see N85-22782 13-31)
Avail: NTIS HC A06

N85-22816# Joint Publications Research Service, Arlington, Va.
ELASTICITY FORMULAS FOR THIN-WALLED SHELLS WITH PIEZOCERAMIC LAYERS Abstract Only
V. I. Gololobov *In its* USSR Rept.: Eng. and Equipment (JPRS-UEQ-85-003) 12 Mar. 1985 p 42 Transl. into ENGLISH from Prikl. Mekhan. (Kiev), no. 6, Jun. 1984 p 117-120 (For primary document see N85-22782 13-31)
Avail: NTIS HC A06

N85-22820# Joint Publications Research Service, Arlington, Va.
STABILITY OF CYLINDRICAL SHELLS WITH ONE-WAY CONSTRAINTS Abstract Only
A. N. Yeremichev *In its* USSR Rept.: Eng. and Equipment (JPRS-UEQ-85-003) 12 Mar. 1985 p 49 Transl. into ENGLISH from Izv. Vyssh. Ucheb. Zaved.: Mashinostr. (Moscow), no. 1, Jan. 1984 p 20-24 (For primary document see N85-22782 13-31)
Avail: NTIS HC A06

N85-22821# Joint Publications Research Service, Arlington, Va.
NONLINEAR BEHAVIOR AND STABILITY OF THIN SPHERICAL SHELLS SUBJECTED TO NON-AXISYMMETRICAL LOADING Abstract Only
L. A. Shapovalov, V. N. Semenov, and Yu. I. Klyuyev *In its* USSR Rept.: Eng. and Equipment (JPRS-UEQ-85-003) 12 Mar. 1985 p 49-50 Transl. into ENGLISH from Izv. Vyssh. Ucheb. Zaved.: Mashinostr. (Moscow), no. 1, Jan. 1984 p 16-19 (For primary document see N85-22782 13-31)
Avail: NTIS HC A06

42 GEOSCIENCES (GENERAL)

N85-23112*# National Aeronautics and Space Administration. Goddard Space Flight Center, Greenbelt, Md.
OZONE CORRELATIVE MEASUREMENTS WORKSHOP
Ernest Hilsenrath, ed. Washington Mar. 1985 75 p refs Workshop held in Greenbelt, Md., 16-18 Nov. 1983
(NASA-CP-2362; Rept-85B0183; NAS 1.55:2362) Avail: NTIS HC A04/MF A01 CSCL 04A

A study was conducted to determine the necessary parameters for the correlation of data on Earth ozone. Topics considered were: (1) measurement accuracy; (2) equipment considerations (SBUV); and (3) ground based measurements to support satellite data. For individual titles, see N85-23113 through N85-23115.

N85-23113*# National Aeronautics and Space Administration. Goddard Space Flight Center, Greenbelt, Md.
SCIENTIFIC REQUIREMENTS FOR OZONE MEASUREMENTS c46
In its Ozone Correlative Meas. Workshop Mar. 1985 35 p refs (For primary document see N85-23112 13-42)
Avail: NTIS HC A04/MF A01 CSCL 04A

A study was conducted to determine the necessary parameters for the correlation of data on Earth ozone. First, requirements for the needed measurement accuracy for the change in ozone (yearly percent decrease) over a ten year period were determined. Secondly, the capabilities of the solar backscatter ultraviolet spectrometer instrumentation (SBUV) were examined. These included satellite coverage, radiometric calibration accuracy, instrument degradation, and algorithm accuracy. Third, and finally, ground based total and vertical zone distribution measurements, which could be used to support satellite observations, were considered. G.L.C.

N85-23114*# National Aeronautics and Space Administration. Goddard Space Flight Center, Greenbelt, Md.
METHOD FOR DETERMINING THE NUMBER OF CORRELATIVE MEASUREMENTS REQUIRED TO VALIDATE THE SBUV/2 OZONE RETRIEVALS c46
John E. Frederick *In its* Ozone Correlative Meas. Workshop Mar. 1985 4 p (For primary document see N85-23112 13-42)
Avail: NTIS HC A04/MF A01 CSCL 04A

A method for determining the number of correlative measurements required to validate solar backscatter ultraviolet spectrometer /2 (SBUV/2) ozone retrieval was considered. Calculations for 1%, 2%, and 5% precisions were made. G.L.C.

N85-23115*# National Aeronautics and Space Administration. Goddard Space Flight Center, Greenbelt, Md.
MEASUREMENT REQUIREMENTS FOR THE DETECTION OF OZONE TRENDS c46
John E. Frederick *In its* Ozone Correlative Meas. Workshop Mar. 1985 19 p (For primary document see N85-23112 13-42)
Avail: NTIS HC A04/MF A01 CSCL 04A

The number of measurements and period of collection in order to detect a trend in the vertical distribution of ozone was studied. Specific issues considered include the impact of: (1) short term ozone variability over the measurement site, and (2) the precision of the measuring instrument on the ability to detect trends to a given confidence limit. G.L.C.

N85-23116# Joint Publications Research Service, Arlington, Va.
USSR REPORT: EARTH SCIENCES Abstracts Only
1 Feb. 1985 143 p Transl. into ENGLISH from various Russian articles
(JPRS-UES-85-002) Avail: NTIS HC A07/MF A01

News items, abstracts, and scientific reports on aspects of Earth sciences including arctic and antarctic research, meteorology, oceanography, and terrestrial geophysics are contained. For individual titles, see N85-23117 through N85-23185.

N85-23117# Joint Publications Research Service, Arlington, Va.
ARCTIC-NORTH ATLANTIC RIFT MEGASYSTEM Abstract Only c46
V. S. Surkov, O. G. Zhero, and L. V. Smirnov *In its* USSR Rept.: Earth Sci. (JPRS-UES-85-002) 1 Feb. 1985 p 1 Transl. into ENGLISH from Geol. i Geofiz. (Novosibirsk), no. 8, Aug. 1984 p 3-11 (For primary document see N85-23116 13-42)
Avail: NTIS HC A07/MF A01

Late in the Paleozoic on the Eurasian and American continents a new continental crust was formed which over several stages of development became highly anisotropic, rigid and quite thick. The new stage of thermal and magnetic effects of the mantle which began at the end of the Paleozoic in the northern segment of the Earth caused destruction of the crust on a large scale, manifested as the formation during the Mesozoic and Cenozoic of a number of rift systems, as well as the North Atlantic and Arctic mid-oceanic ridges. These come together to form a single Arctic-North Atlantic rift megasystem. The component systems are described briefly. The late Paleozoic-Cenozoic stage must be considered a period of appearance of destructive processes involving splitting of the lithosphere into plates and their separation. Subsidence of tremendous areas of the Earth and the formation of large megabasins with very thick Mesozoic-Cenozoic deposits and reserves of hydrocarbons are genetically related to this mega-system. B.G.

N85-23118# Joint Publications Research Service, Arlington, Va.
ANTARCTIC GLACIATION, OR WHAT ARE CATASTROPHES IN EARTH'S HISTORY Abstract Only c43
D. Kvasov *In its* USSR Rept.: Earth Sci. (JPRS-UES-85-002) 1 Feb. 1985 p 4 Transl. into ENGLISH from Znaniye-Sila (Moscow), no. 8, Aug. 1984 p 28-30 (For primary document see N85-23116 13-42)
Avail: NTIS HC A07/MF A01

Several theories are discussed to explain the glaciation of the Antartic. The only one which seems to fit other observations from around the world at the same time is that 30 to 35 million years ago Australia moved away from the Antarctic and a cold southern current around Australia and the Antarctic developed, causing eastern Antarctica to be covered by glaciers. Today, South America and Australia have moved away from the Antarctic completely allowing the current generated by the westerly winds in the Southern Hemisphere to circulate around Antarctica, separating this current from the Pacific current. The cold water now does not flow northward into the tropics as strongly as previously when Antarctica and Australia were connected, and warm currents no longer flow from the tropics around Antarctica. This has warm currents no longer flowing from the tropics around Antarctica. This has resulted in the cooling and glaciation of Antarctica as a whole, and significant warming of the tropics. Author

N85-23119# Joint Publications Research Service, Arlington, Va.
MOISTURE VARIATION IN NORTHERN HEMISPHERE TEMPERATE LATITUDES Abstract Only c47
G. I. Mosolova and N. P. Mukhina *In its* USSR Rept.: Earth Sci. (JPRS-UES-85-002) 1 Feb. 1985 p 6 Transl. into ENGLISH from Vestn. Leningr. Univ.: Geol., Geografiya (Leningrad), no. 6, issue 1, Mar. 1984 p 48-56 (For primary document see N85-23116 13-42)
Avail: NTIS HC A07/MF A01

Multiyear (1981 to 1959) investigations were made of variations in the precipitation anomalies in the temperate latitudes of the Northern Hemisphere in the range 70 to 40 deg N and 125 deg W to 90 deg E. Data on precipitation anomalies were used for each 5 deg in latitude and longitude. The period examined was mainly May to June because the yield of agricultural crops is determined by the precipitation occurring in those months. Long term variations were determined and periods of accumulation of anomalies of the same sign were ascertained. The integral difference curves method was used for this purpose. Normalized integral difference curves were constructed for each of the mentioned regions. Their analysis made it possible to discriminate periods of different duration in these regions with high and low moisture levels. The in- and

out-of phase variations of precipitation anomalies are given for these regions for five-year intervals, since for agriculture it is important to evaluate precipitation anomalies and the coincidence or noncoincidence of their sign in different regions for each year.
B.G.

N85-23120# Joint Publications Research Service, Arlington, Va.
RELATIONSHIP OF INDIAN MONSOON INTENSITY TO TIME OF ONSET Abstract Only **c47**
M. G. Filippova *In its* USSR Rept.: Earth Sci. (JPRS-UES-85-002) 1 Feb. 1985 p 6-7 Transl. into ENGLISH from Vestn. Mosk. Univ., Ser. 5: Geografiya (Moscow), no. 5, Sep. - Oct. 1984 p 65-69 (For primary document see N85-23116 13-42)
Avail: NTIS HC A07/MF A01

Climatic variability of the dates of onset of the Indian monsoon and total annual precipitation were studied. The total precipitation for the year indicates the intensity of summer monsoon circulation, since 75 to 90% of the total annual precipitation in India occurs during the summer monsoon rains. Initial data consisted of long term series of observations of the total annual precipitation and time of onset of the monsoon at Bombay. In most cases when the monsoon begins early precipitation is less than normal, when late, greater than normal. If the monsoon begins very early or late, it will not do the same the next year. Both monsoon onset date and total precipitation exhibit synchronous oscillations with a period of two to three years. Fluctuations of monsoon onset date with a period of 4 and 7 years and total precipitation with periods of 4 to 6 and 11 to 13 years occur independently of one another.
Author

N85-23121# Joint Publications Research Service, Arlington, Va.
EL NINO, THE CAPRICIOUS CHILD Abstract Only **c48**
K. N. Fedorov *In its* USSR Rept.: Earth Sci. (JPRS-UES-85-002) 1 Feb. 1985 p 7 Transl. into ENGLISH from Priroda (Moscow), no. 8, Aug. 1984 p 65-74 (For primary document see N85-23116 13-42)
Avail: NTIS HC A07/MF A01

A popularized description of El Nino, the large-scale climatic event in the Pacific Ocean responsible for severe weather anomalies along the west coasts of North and South America in 1982, is presented. Color diagrams illustrate the relationship between ocean currents and prevailing winds producing the anomaly. It is noted that the experts still do not know whether the warming of the ocean water during El Nino causes the fading of the trade winds to be replaced by predominantly western winds, or vice versa. El Nino of 1982 to 1983 was thoroughly observed and documented, and scientists are now studying the interrelationships, causes and effects of the various phenomena involved.
Author

N85-23122# Joint Publications Research Service, Arlington, Va.
MODELING OF MECHANISM OF POSITIVE FEEDBACK BETWEEN MEAN EARTH SURFACE TEMPERATURE AND ATMOSPHERIC CARBON DIOXIDE IN GEOLOGIC TIME SCALE Abstract Only **c47**
V. I. Melnichuk *In its* USSR Rept.: Earth Sci. (JPRS-UES-85-002) 1 Feb. 1985 p 7-8 Transl. into ENGLISH from Dokl. Akad. Nauk SSSR (Moscow), v. 277, no. 4, Aug. 1984 p 836-839 (For primary document see N85-23116 13-42)
Avail: NTIS HC A07/MF A01

Effects are studied which are not directly related to the emission of industrial carbon dioxide gas into the atmosphere but do influence the distribution of CO2 between the ocean and the atmosphere. An increase in temperature caused by any factor which is constantly active over hundreds of years and a resulting decrease in the solubility of CO2 in sea water can lead to a transition of excess CO2 from the ocean into the atmosphere and a resultant increase in the greenhouse effect. If in the preindustrial period there was equilibrium between CO2 in the ocean and in the atmosphere, anthropogenic factors should disrupt this equilibrium. This may have a strong influence on the climate of the earth over a period of several hundre years. After a thousand years, the process of increasing the partial pressure of CO2 in the atmosphre should stop, hence the solubility of carbonates will increase and the bonding of CO2 in rift zones of the mid-oceanic ridges may increase. The carbonate system of the ocean thus provides feedback comparable in effectiveness to atmospheric mechanisms which should be considered in modeling the climate of future centuries.
Author

N85-23123# Joint Publications Research Service, Arlington, Va.
NUMERICAL EXPERIMENTS WITH SIMPLE MODEL OF OCEAN CLIMATE Abstract Only **c48**
M. Ya. Verbitskiy *In its* USSR Rept.: Earth Sci. (JPRS-UES-85-002) 1 Feb. 1985 p 9 Transl. into ENGLISH from Okeanol. (Moscow), v. 24, no. 3, May - Jun. 1984 p 385-391 (For primary document see N85-23116 13-42)
Avail: NTIS HC A07/MF A01

A simplified model of the ocean as part of a three component ocean-atmosphere-glaciers climatic system is formulated. The idealized ocean has the width Lambda + Lambda prime and the depth H = const., where Lambda is the width of the ocean, Lambda prime << Lambda is the width of the western boundary layer in which the transfer of heat and mass occurs in the direction from the equator to the poles. Vertically the ocean is divided into two regions (layer of seasonal and main thermocline with the depth h = const. and abyssal depths). The western boundary layer is discriminated only in the upper part of the ocean. The equations of hydrothermodynamics are written for the ocean outside the equatorial region, for the Ekman and coastal boundary layers in geostrophic, quasistatic and Boussinesq approximations on the assumption that sea water density is dependent only on temperature. The model is used in computing the present day temperature regime of the ocean.
B.G.

N85-23124# Joint Publications Research Service, Arlington, Va.
NUMERICAL INVESTIGATION OF EVOLUTION OF ENERGY SPECTRUM OF SLIGHTLY NONLINEAR ROSSBY WAVES Abstract Only **c46**
G. M. Reznik and T. E. Soomere *In its* USSR Rept.: Earth Sci. (JPRS-UES-85-002) 1 Feb. 1985 p 10 Transl. into ENGLISH from Okeanol. (Moscow), v. 24, no. 3, May - Jun. 1984 p 373-384 (For primary document see N85-23116 13-42)
Avail: NTIS HC A07/MF A01

Nonlinear effects and the Beta-effect play an extremely important role in the dynamics of oceanic and atmospheric movements. The joint influence of these two factors is exceedingly difficult to study because the solution of the problem requires use of simple model physical systems. Accordingly, a very simple system was employed which takes into account nonlinearity, the Beta-effect and a large number of wave harmonics: a system of weakly interacting Rossby waves with random amplitudes on the Beta-plane in a barotropic ocean of constant depth. The behavior of such a system is described by a kinetic equation for the spectral density of energy F = F (Chi, tau). With this as a point of departure, it was found that: nonlinear interactions lead to an intensification of the zonal component of a current and to an isotropic distribution of energy for wave vectors adequately distant from a meridional direction; initially the asymmetric spectrum tends with time to become symmetric due to interaction with the almost zonal component of the current. The rates of energy transfer in absolute value and for different azimuths of the wave vectors are compared.
B.G.

N85-23125# Joint Publications Research Service, Arlington, Va.
SPECIAL FEATURES OF COMPUTATIONS OF VERTICAL DISTRIBUTION OF CONCENTRATION OF SUSPENDED SEDIMENTS UNDER MARINE CONDITIONS Abstract Only **c48**
R. D. Kosyan *In its* USSR Rept.: Earth Sci. (JPRS-UES-85-002) 1 Feb. 1985 p 15-16 Transl. into ENGLISH from Okeanol. (Moscow), v. 24, no. 3, May - Jun. 1984 p 498-504 (For primary document see N85-23116 13-42)
Avail: NTIS HC A07/MF A01

When computing the discharge of sediments in the coastal zone of the sea it is essential that the distribution of the concentration of suspended sediment be calculated correctly for

a definite class of waves. A semiempirical model was given for the vertical distribution of the relative concentration of suspended sediments, which describes better than any other the concentration profile. However, the model was checked only on the basis of laboratory results. Accordingly, on the basis of in situ observations made at different times, an effort was made to find the conditions under which this dependence can be used for computations in the shore zone of the sea and restrictions on its use were determined. The equation for the profile of the concentrations of sediments derived is subjected to a number of tests for a variety of variables. The equation can be used in practical computations in the zone of transformation and insignificant dissipation of wave energy in the entire thickness of the flow, except for the thin bottom layer. In computing the profile the best results can be attrained by substituting into the formula the values of wave characteristics corresponding to the maximum spectral density.
B.G.

N85-23126# Joint Publications Research Service, Arlington, Va.
ABSOLUTE MOVEMENT OF PACIFIC OCEAN PLATE DURING LAST 120 MILLION YEARS Abstract Only **c46**
M. V. Kononov *In its* USSR Rept.: Earth Sci. (JPRS-UES-85-002) 1 Feb. 1985 p 16 Transl. into ENGLISH from Okeanol. (Moscow), v. 24, no. 3, May - Jun. 1984 p 484-492 (For primary document see N85-23116 13-42)
Avail: NTIS HC A07/MF A01

Three paleomagnetic poles of the Pacific Ocean plate were determined as well as the trajectory of apparent migration of the Pacific Ocean plate pole. A map of the Pacific Ocean paleoequators was compiled on the basis of data on the time of passage of abyssal drilling borehole points through the equatorial region. Latitudinal drift according to paleomagnetic data is 42 deg for 120 million years and 24 deg for 80 million years with a mean rate of 3.3 to 3.9 cm/year, and according to paleoclimatic data 36 deg for 100 million years with a rate of 3.6 cm/year. In the interval 120 to 80 million years there was a jump in the rate from 3.6 to 5 cm/year. The trajectories of hot points reveal two stages in restructuring of translational motion of the plate between the intervals 125 to 70 and 70 to 43 million years from WNW to northerly movement and between the intervals 70 to 43 and 43 to 0 million years from northerly to northwesterly movement. Data obtained from independent sources indicate that during the last 125 million years the Pacific Ocean plate has moved about 9,000 km in a northwesterly direction. A.R.H.

N85-23127# Joint Publications Research Service, Arlington, Va.
DETERMINING DEGREE OF PARTIAL MELTING OF ASTHENOSPHERE FROM SEISMIC DATA Abstract Only **c46**
Ye. I. Pristavakina *In its* USSR Rept.: Earth Sci. (JPRS-UES-85-002) 1 Feb. 1985 p 17 Transl. into ENGLISH from Okeanol. (Moscow), v. 24, no. 3, May - Jun. 1984 p 477-483 (For primary document see N85-23116 13-42)
Avail: NTIS HC A07/MF A01

An effort is made to ascertain the percentage volume of the molten phase in the total volume of asthenospheric matter. The problem is examined using a model formulated on the assumption that the oceanic lithosphere is formed due to the crystallization of molten upper mantle matter and movement of lithospheric plates from the rift zones to the oceanic basins. At depths of 70 km to 90 km there is a considerable change in the Poisson coefficient, this corresponding to the lithosphere-asthenosphere boundary. The considerable change in this parameter may be evidence of presence of melt in the asthenosphere. The ratio of V(p) and V(s) changes at these depths, increasing by a factor of 1.030, which would indicate presence of about 3% melt beneath the considered parts of the lithosphere. Data on the distribution of conductivity in the mantle are an independent source of information on presence of melt and at temperature 1100 C to 1300 C the conductivity would be such as to explain partial melting. All of the mentioned data are consistent with partial melting. A.R.H.

N85-23128# Joint Publications Research Service, Arlington, Va.
DETERMINING ADSORPTION OF SURFACE-ACTIVE SUBSTANCES BY SEA BOTTOM DEPOSITS Abstract Only **c48**
M. P. Nesterova, O. S. Mochalova, and N. M. Antonova *In its* USSR Rept.: Earth Sci. (JPRS-UES-85-002) 1 Feb. 1985 p 18 Transl. into ENGLISH from Okeanol. (Moscow), v. 24, no. 3, May - Jun. 1984 p 464-469 (For primary document see N85-23116 13-42)
Avail: NTIS HC A07/MF A01

The adsorption of surface-active substances produced in the United States and in the Soviet Union by bottom deposits of different fractional composition in sea water with different salinities was investigated. Spectrophotometry analyses revealed a number of regularities in the adsorption of dispersing agents by bottom deposits. The combination of such factors as the salinity of sea water and the granulometric composition of the sediment changes the relative degree of adsorption of dispersing agents in a wide range from several percent to an almost complete elimination of surface-active substances from solution. With transition from fresh to saline water, there can be a marked change in the content of dissolved surface-active agents in water due to adsorption processes. This must be considered when studying the pollution of water bodies by these substances at the boundary of hydrochemical barriers (when sea and river waters mix). A.R.H.

N85-23129# Joint Publications Research Service, Arlington, Va.
POSSIBLE ROLE OF OCEAN BIOTA IN GLOBAL CARBON BALANCE Abstract Only **c47**
V. G. Gorshkov *In its* USSR Rept.: Earth Sci. (JPRS-UES-85-002) 1 Feb. 1985 p 20 Transl. into ENGLISH from Okeanol. (Moscow), v. 24, no. 3, May - Jun. 1984 p 453-459 (For primary document see N85-23116 13-42)
Avail: NTIS HC A07/MF A01

The quantity of phytoplankton production in the ocean outside the zone of its synthesis was estimated. When life is present in the ocean, dissolved organic substances can perform the function of an organic buffer evening-out CO2 fluctuations in the atmosphere. In this case the oxidation of dissolved organic matter and the emission of CO2 into the atmosphere should occur considerably more slowly than the synthesis of dissolved organic matter and CO2 absorption from the atmosphere. Available data on oceanic dissolved organic matter are consistent with a possible increase in the quantity of dissolved organic matter by 10% during the last 20 years, but the same quantity of carbon could be released into the atmosphere during this same time due to a reduction in forest cover. Accordingly, the total global balance of carbon remains unchanged. A.R.H.

N85-23130# Joint Publications Research Service, Arlington, Va.
REGIONS OF PROPAGATION OF SHORT-WAVE PERTURBATIONS IN SPHERICAL LAYER OF ROTATING FLUID Abstract Only **c32**
G. A. Kivman and N. B. Maslova *In its* USSR Rept.: Earth Sci. (JPRS-UES-85-002) 1 Feb. 1985 p 25-26 Transl. into ENGLISH from Okeanol. (Moscow), v. 24, no. 3, May - Jun. 1984 p 392-397 (For primary document see N85-23116 13-42)
Avail: NTIS HC A07/MF A01

Small free oscillations of a rotating stratified fluid were investigated. It is demonstrated that the spectrum of free oscillations contains a segment [-alpha, alpha] and is contained in the segment [-beta, beta]. This assertion represents a refinement and generalization of the greenspan hypothesis. The regions of propagation of short waves in a thin spherical layer are described and the accuracy of their description in the traditional approximation is evaluated. At low frequencies the short waves are localized. The structure of the regions of their propagation is essentially dependent on stratification. In the case of a poorly stratified fluid the traditional approximation filters waves in the equatorial region.
A.R.H.

N85-23131# Joint Publications Research Service, Arlington, Va.
USE OF THREE OMEGA RADIONAVIGATION SYSTEM POSITION LINES FOR SOLVING PROBLEMS IN MARINE GEODESY Abstract Only **c04**
V. A. Monakhov and I. A. Iordanskiy *In its* USSR Rept.: Earth

Sci. (JPRS-UES-85-002) 1 Feb. 1985 p 28 Transl. into ENGLISH from Izv. Vyssh. Ucheb. Zaved.: Geod. i Aerofotosyemka (Moscow), no. 2, Mar. - Apr. 1984 p 26-30 (For primary document see N85-23116 13-42)
Avail: NTIS HC A07/MF A01

A method is described for using three position lines which gives a considerable increase in the accuracy of ship position determinations. A program, formulated for use with the Omega radionavigation system, requires use of an Elektronika D3-28 minicomputer can be used for other radiogeodetic and radionavigation systems capable of forming three position lines. The basis for the presented method is the iteration method with the use of approximate ship's coordinates. The results of implementation of the program (ship's coordinates and mean square position error) are fed out to a computer display. In the computations the mean square error in determining the ship's coordinates from the three position lines for the Omega is 0.9 km (with use of two position lines--1.6 km); the accuracy in computing the ship's coordinates does not exceed 2', corresponding to an accuracy in determining the ship's position of less than 75 m. Computations under the program require 10 seconds. A.R.H.

N85-23132# Joint Publications Research Service, Arlington, Va.
DRIFTING ICE AS MECHANICAL FACTOR IN PURIFYING AND POLLUTING HYDROSPHERE Abstract Only **c45**
V. V. Izmaylov *In its* USSR Rept.: Earth Sci. (JPRS-UES-85-002) 1 Feb. 1985 p 28-29 Transl. into ENGLISH from Izv. Vsesoyuznogo Geogr. Obshch. (Leningrad), v. 116, no. 3, May - Jun. 1984 p 221-237 (For primary document see N85-23116 13-42)
Avail: NTIS HC A07/MF A01

The SP-22 drifting station was used to ascertain the migration of petroleum products artifically introduced into young, one-year and perennial ice and icebergs. In ice of different structure and texture during the spring-summer season the rate of migration of petroleum hydrocarbons in an upward direction varied from 2 to 49 cm/day. The temperature gradient in the atmosphere - petroleum product - ice (snow) - sea water system plays the dominant role in movement of a petroleum product toward the ice surface. The petroleum products sooner or later appear on the surface of the ice cover as a result of operation of the vertical migration mechanism. At the surface the petroleum hydrocarbons are transformed under the influence of evaporation, photooxidation and biological utilization. A knowledge of ice drift in the regions of its melting makes it possible to determine regions of probable purification of waters from petroleum products by ice and to indicate the places of dumping of pollutants at the centers of melting of the ice cover. A.R.H.

N85-23133# Joint Publications Research Service, Arlington, Va.
WORLD OCEAN LEVEL OSCILLATIONS AND THEIR RELATIONSHIP TO CHANGE IN INFLOW OF CONTINENTAL WATERS Abstract Only **c48**
K. P. Voskresenskiy, V. I. Babkin, T. Ye. Grigorkina, and V. Yu. Barkhatova *In its* USSR Rept.: Earth Sci. (JPRS-UES-85-002) 1 Feb. 1985 p 29-30 Transl. into ENGLISH from Izv. Vsesoyuznogo Geogr. Obshch. (Leningrad), v. 116, no. 3, May - Jun. 1984 p 224-231 (For primary document see N85-23116 13-42)
Avail: NTIS HC A07/MF A01

Matrices of the probabilities of transition of ocean levels, inflow of continental waters, and Wolf numbers from one class to others reveal some regularities in variations in ocean levels during the observation period 1918 to 1964. In the world ocean as a whole, there is a low probability of transition of relatively low levels into medium and high levels. For the world ocean, years with a low level with a high probability will be followed by years with a low level, and years with a high level will be followed by years with a high level. The statistical analysis suggests an influence of years of high and low solar activity on the processes responsible for ocean level. A similar analysis is presented for the influence of the inflow of continental waters on ocean level. A.R.H.

N85-23134# Joint Publications Research Service, Arlington, Va.
CONTRIBUTION TO THEORY OF OCEAN-ATMOSPHERE GAS EXCHANGE Abstract Only **c45**
V. S. Savenko and V. L. Lebedev *In its* USSR Rept.: Earth Sci. (JPRS-UES-85-002) 1 Feb. 1985 p 30-31 Transl. into ENGLISH from Dokl. Akad. Nauk SSSR (Moscow), v. 275, no. 5, Apr. 1984 p 1185-1189 (For primary document see N85-23116 13-42)
Avail: NTIS HC A07/MF A01

An expression was derived for the intensity of a gas flow applicable to a gas exchange model when there is molecular-diffusional absorption (release) of gas from one half-space (air) to the other (water) during a time equal to the mean period of presence of water particles at the surface to the time of their sinking with maintenance of a constant gas concentration at the interface. The work of other authors is reviewed with emphasis on behavior of the cold film (convection time scale). A series of equations is derived for computing the effective lifetime of the cold film, the principal parameter of the convective-diffusional theory of gas exchange. It is shown that there is a jumplike change in exchange processes with transition from free to forced convection. A.R.H.

N85-23135# Joint Publications Research Service, Arlington, Va.
USE OF PALEOMAGNETIC DATA IN TECTONIC ANALYSIS OF OCEANIC STRUCTURES Abstract Only **c46**
V. Kh. Gevorkyan, V. S. Markovskiy, and I. E. Lomakin *In its* USSR Rept.: Earth Sci. (JPRS-UES-85-002) 1 Feb. 1985 p 34 Transl. into ENGLISH from Geol. Zh. (Kiev), v. 44, no. 5, Sep. - Oct. 1984 p 85-87 (For primary document see N85-23116 13-42)
Avail: NTIS HC A07/MF A01

Laboratory work was carried out for thermal demagnetization of the remanent magnetization of an oceanic tholeutes and the determination of its resistance to destruction by a variable magnetic field in order to evaluate the reliability of use of paleomagnetic information for tectonic constructions. The vector of remanent magnetization, whose mean direction is characterized by a declination of 297 deg and an inclination of +57 deg, represents the direction of the geomagnetic field during the cooling of basaltic magma. It is shown that paleomagnetic data, together with the results of a geological and geomorphological survey, make it possible to determine the principal features of one sector of the Arabian Sea-Indian Ocean Ridge. The vector of remanent magnetization of rocks should be studied for interpretation of the tectonic nature of lithospheric blocks. A.R.H.

N85-23136# Joint Publications Research Service, Arlington, Va.
CALCULATION OF LEVEL SURFACE IN PROBLEMS OF LARGE-SCALE OCEAN CIRCULATION Abstract Only **c48**
A. L. Berestov and S. A. Yefremov *In its* USSR Rept.: Earth Sci. (JPRS-UES-85-002) 1 Feb. 1985 p 35-36 Transl. into ENGLISH from Dokl. Akad. Nauk SSSR (Moscow), v. 277, no. 4, Aug. 1984 p 961-964 (For primary document see N85-23116 13-42)
Avail: NTIS HC A07/MF A01

The possibility of a direct method of calculating the sea level surface in models of large-scale ocean circulation was demonstrated. In order for a finite difference system to be adequate to a physical process, the integral laws of conservation must be fulfilled, conserving masses with no sources or sinks, and conserving energy and momentum with no dissipative or external forces. Equations are derived to model the general circulation of the atmosphere. The difficulty of applying these equations to describe the large-scale circulation of the ocean results from the fact that in modeling ocean dynamics two problems arise which do not exist in computation of the general circulation of the atmosphere. These include the need to consider bottom relief and the problem of assigning boundary conditions in multiply connected areas. The method here suggested allows calculation of the sea level of the surface of the ocean directly using the initial equations of hydrodynamics. This approach allows significantly simpler and more accurate solution of the problem of hydrodynamics of the ocean and construction of a model considering satellite observation data. Author

N85-23137# Joint Publications Research Service, Arlington, Va.
DOUBLE AND INVERSE TAYLOR-HOGG VORTICES IN A STRATIFIED OCEAN Abstract Only **c48**

V. N. Zyryanov *In its* USSR Rept.: Earth Sci. (JPRS-UES-85-002) 1 Feb. 1985 p 36 Transl. into ENGLISH from Dokl. Akad. Nauk SSSR (Moscow), v. 277, no. 4, Aug. 1984 p 967-971 (For primary document see N85-23116 13-42)
Avail: NTIS HC A07/MF A01

The formation of a column of rotating fluids over a dome-shaped bottom relief feature when a current occurs in a homogeneous fluid is analyzed. It is shown that consideration of the beta effect leads to new phenomena in a stratified ocean: formation above the underwater feature of double and inverse Taylor-Hogg vortices and closing of the Taylor-Hogg satellite vortex near the bottom. When a baroclinic mode of flow vortexing arises above an underwater mountain in a constant current, it changes its direction in the surface layers because the cyclonic satellite vortex arising downstream from the mountain in the bottom layers close the deep Taylor-Hogg cone with its upper portion. In the surface layers downstream from the mountain a new anticone vortex satellite arisese with its points directed downward. With a current flow past a crater a double vortex cyclone-anticyclone cone arises near the bottom, above which in the surface layers an inverted conical vortex is formed. These are called double and inverted vortex Taylor-Hogg cones. Author

N85-23138# Joint Publications Research Service, Arlington, Va.
MATHEMATICAL-CARTOGRAPHIC MODEL FOR STUDY OF DISTRIBUTION OF HYDROCHEMICAL ELEMENTS IN SEA WATER (USING DISSOLVED OXYGEN IN THE PACIFIC OCEAN AS AN EXAMPLE) Abstract Only c48
A. A. Zolotiv and S. N. Servenyuk *In its* USSR Rept.: Earth Sci. (JPRS-UES-85-002) 1 Feb. 1985 p 37 Transl. into ENGLISH from Vestn. Mosk. Univ., Ser. 5: Geogr. (Moscow), no. 4, Jul. - Aug. 1984 p 51-55 (For primary document see N85-23116 13-42)
Avail: NTIS HC A07/MF A01

There has been interest lately in studies of the structure of distribution of hydrochemical elements in ocean waters by various modeling methods. The essence of modeling of this type is discussed using the example of studying the structure of distribution of oxygen in the Pacific Ocean. Initial information is a series of 7 maps of dissolved oxygen at various depths from the surface to 2000 meters. The problem was, using fixed values of the index at the discrete monitor points and continuous functions and maps to describe the structure of the spatial distribution with the necessary accuracy. This was done using a method of three-dimensional polynomial regression for which the independent variables are the spatial coordinates; the dependent variable is the quantitative characteristic being studied. The criterion used to evaluate the quality of analytic description is defined in advance. Equations are obtained to describe the distribution of dissolved oxygen at the depth studied. Author

N85-23139# Joint Publications Research Service, Arlington, Va.
HORIZONTAL COHERENCE OF TEMPERATURE MICROSTRUCTURE IN UPPER OCEAN LAYER Abstract Only c48
N. D. Berezhnaya, A. A. Lubitskiy, and A. D. Rozenberg *In its* USSR Rept.: Earth ci. (JPRS-UES-85-002) 1 Feb. 1985 p 40 Transl. into ENGLISH from Izv. Akad. Nauk SSSR: Fiz. Atmosfery i Okeana (Moscow), v. 20, no. 8, Aug. 1984 p 741-748 (For primary document see N85-23116 13-42)
Avail: NTIS HC A07/MF A01

Results are presented from field studies of horizontal coherence of temperature microstructure in a small sea. The purpose was to produce quantitative characteristics of the spatial variability of microstructural elements in variously stratified layers of the sea. Measurements were performed in the summer of 1977 in the Caspian Sea from a nonmoving station on a piling. The depth of the sea at the point was 40 m. The temperature structure was studied by soundings through the depth of the water by two horizontally separated sensors. The microstructure of the temperature field apparently results from rather intensive small-scale turbulence generated by surface waves and differences in current velocities. The spectral density of temperature fluctuations in the thermocline is several orders of magnitude greater than the level of hardware noise, indicating that the observed effect is genuine. The relatively ordered microscopic jump in temperature extending horizontally or a small-scale internal wave propagating at an angle to the horizontal leads to an increase in coherence. Author

N85-23140# Joint Publications Research Service, Arlington, Va.
FINE STRUCTURE OF VERTICAL DISTRIBUTION OF LIGHT ATTENUATION INDEX OF SEA WATER Abstract Only c74
V. I. Burenkov, A. P. Vasilkov, and L. A. Stefantsev *In its* USSR Rept.: Earth Sci. (JPRS-UES-85-002) 1 Feb. 1985 p 43 Transl. into ENGLISH from Izv. Akad. Nauk SSSR: Fiz. Atmosfery i Okeana (Moscow), v. 20, no. 8, Aug. 1984 p 773-776 (For primary document see N85-23116 13-42)
Avail: NTIS HC A07/MF A01

A study is made of some of the results of investigation of the fine structure of the attenuation index, epsilon performed at various times at the Oceanology Institute imeni P. P. Shirshov, USSR Academy of Sciences. Measurements were made by means of a submerged transparency meter with built-in temperature and pressure sensors, allowing simultaneous recording of changes in attenuation and temperature with depth. Two types of heterogeneities are observed in the fine structure of vertical epsilon distributions: narrow local layers of reduced transparency, not over 2-3 m thick with transparency change usually not over 0.1 to 0.02 1/m; and quasistep structures, alternation of layers with high and low epsilon gradients, sometimes up to tens of meters thick and persisting over longer times. Sample vertical distributions are diagrammed. It is concluded that quasistep structures are rather common in the vertical profiles of the attenuation index. The depth of layers with a higher gradient of the attenuation index and temperature usually coincides. This indicates that fine structure heterogeneities in epsilon profiles result from preprocesses responsible for the existence of quasistep structures in the temperature profile as well. Author

N85-23141# Joint Publications Research Service, Arlington, Va.
EVOLUTION OF SET OF ROSSBY WAVES TOWARD ANISOTROPIC EQUILIBRIUM STATE Abstract Only c48
G. M. Reznik and T. E. Soomere *In its* USSR Rept.: Earth Sci. (JPRS-UES-85-002) 1 Feb. 1985 p 45 Transl. into ENGLISH from Okeanol. (Moscow), v. 24, no. 4, Jul. - Aug. 1984 p 558-565 (For primary document see N85-23116 13-42)
Avail: NTIS HC A07/MF A01

Results of numerical studies of a kinetic equation for weakly linear Rossby waves are presented. The results of numerical calculations indicate with some certainty that when there are no energy sources or sinks the spectrum approaches an equilibrium spectrum described by an equation presented in this article, the sum of the spectrum of zonal flow and equilibrium spectrum of two-dimensional turbulence, regardless of the initial form of the spectrum. The relative fraction of energy of the zonal flow depends on the initial conditions; dissipation increases energy transfer to the zonal flow. Author

N85-23142# Joint Publications Research Service, Arlington, Va.
STABILITY OF ROSSBY WAVES WITHIN FRAMEWORK OF THREE-COMPONENT ANALYSIS Abstract Only c48
A. P. Mirabel *In its* USSR Rept.: Earth Sci. (JPRS-UES-85-002) 1 Feb. 1985 p 45 Transl. into ENGLISH from Okeanol. (Moscow), v. 24, no. 4, Jul. - Aug. 1984 p 566-573 (For primary document see N85-23116 13-42)
Avail: NTIS HC A07/MF A01

The behavior of small but finite disturbances was studied in the problem of stability of a Rossby wave. The spatial structure of the disturbances can be represented in a form suggested by Gill. A criterion for instability of two-dimensional Rossby waves with respect to disturbances consisting of two waves of the same type was formulated. The initial nonlinear stage of development of the instability was studied in a simple model of the process of a three-wave interaction. It is shown that the instability grows most effectively when the wave vectors of the largest disturbance at the point of resonance of the three waves vary by more than 15 deg from a straight north-south direction. Supercritical states of the three-wave interaction are investigated. Author

N85-23143# Joint Publications Research Service, Arlington, Va.
MORE PRECISE CURVE OF DEPENDENCE BETWEEN DENSITY AND VELOCITY OF LONGITUDINAL WAVES IN CONSOLIDATED CRUST AND TOP OF MANTLE IN OCEANIC STRUCTURES Abstract Only **c48**
O. M. Rusakov *In its* USSR Rept.: Earth Sci. (JPRS-UES-85-002) 1 Feb. 1985 p 51-52 Transl. into ENGLISH from Dokl. Akad. Nauk Ukr. SSR, Ser. B: Geol., Khim i Biol Nauki (Kiev), no. 5, May 1984 p 21-24 (For primary document see N85-23116 13-42)
Avail: NTIS HC A07/MF A01

The correlation dependence RHO=f(V sub p) is universally used in determining the density of the consolidated oceanic crust on the basis of the velocity of propagation of seismic waves. However, the procedure for deriving the correlation between RHO and V sub p cannot be considered correct. First, the range of rocks used in deriving the dependence did not include all the types of rocks which according to present-day data make up the bottom of the crust and the top of the mantle. Second, for half the samples the values of the parameters were grouped in a narrow range. Third, the least squares method used in the analysis gives fictitious results. As a result of the incorrect procedure for deriving the formula the latter gives adequate RHO values only in a limited region. For this reason it is necessary to construct a curve which correctly reflects the correlation between velocity and density for the entire consolidated crust and upper mantle. The author used 735 determinations of Rho and V sub p in constructing this curve. In contrast to the earlier work, the samples constituted a full range of rock types for the consolidated crust and top of the mantle. Author

N85-23144# Joint Publications Research Service, Arlington, Va.
CRUSTAL AND UPPER MANTLE DENSITY MODEL OF OWEN FAULT ZONE Abstract Only **c46**
In its USSR Rept.: Earth Sci. (JPRS-UES-85-002) 1 Feb. 1985 p 53 Transl. into ENGLISH from Geofiz. Zh. (Kiev), v. 6, no. 3, May - Jun. 1984 p 51-57 (For primary document see N85-23116 13-42)
Avail: NTIS HC A07/MF A01

The Owen fault zone extends parallel to the Arabian and African coast for 3,000 km. Its strike is 50 to 55 deg. The zone consists of four main parts: active, Chain, Owen and Murray ridges. Almost along the entire extent of the fault there is an asymmetry of bottom relief (one of the slopes of the ridges adjacent to the depression is always steeper). New data have been obtained making possible a more detailed description of the density structure of the fault zone. A systematic geophysical survey was made which took in virtually the entire Owen zone. The gravity field was interpreted along 16 profiles. G.L.C.

N85-23145# Joint Publications Research Service, Arlington, Va.
RADIOSODAR SYSTEM FOR REMOTE SYNCHRONOUS MEASUREMENTS OF WIND SPEED, TEMPERATURE AND ITS FLUCTUATIONS Abstract Only **c47**
I. V. Petenko and Ye. A. Shurygin *In its* USSR Rept.: Earth Sci. (JPRS-UES-85-002) 1 Feb. 1985 p 55 Transl. into ENGLISH from Izv. Akad. Nauk SSSR: Fiz. Atmosfery i Okeana (Moscow), v. 20, no. 8 p 77-772 (For primary document see N85-23116 13-42)
Avail: NTIS HC A07/MF A01

A radar-sodar measurement system for atmospheric studies developed by the Soviet Academy of Sciences is described. The system combines a number of separate sounding instruments to provide simultaneous measurements of wind velocity, temperature, and their fluctuations in the atmospheric boundary layer. Among the instruments combined in the system are: a Doppler radar; an amplification component to compensate for spherical divergence and the narrow bandwidth of signals; SNR analyzers; a dual-component horizontal sodar; a vertical 12 ft sodar; and a microprocessor for processing data. The system was tested and provided atmospheric measurements which were comparable to conventional separate sodar and radar sounding measurements. I.H. (IAA)

N85-23146# Joint Publications Research Service, Arlington, Va.
POSSIBILITY OF DETERMINING ATMOSPHERIC WEATHER PARAMETERS BY RADIO AND RADIOOPTICAL MEASUREMENTS OF REFRACTION OF COSMIC SOURCES Abstract Only **c47**
K. P. Gaykovich *In its* USSR Rept.: Earth Sci. (JPRS-UES-85-002) 1 Feb. 1985 p 56 Transl. into ENGLISH from Izv. Akad. Nauk SSSR: Fiz. Atmosfery i Okeana (Moscow), v. 20, no. 8, Aug. 1984 p 675-682 (For primary document see N85-23116 13-42)
Avail: NTIS HC A07/MF A01

Joint measurements of optical and radio refraction within the atmosphere can be used to provide data on density and moisture content profiles of the atmosphere through which the rising and setting of celestial bodies is observed. Numerical experiments were performed to determine model profiles for use in such experiments. Calculations were performed in a closed system in which refraction calculated for model profiles was used to retrieve the E, T and P profiles, which corresponded quite accurately to the initial model profiles. Errors were assigned using a random number generator and the corresponding errors in meteorological parameters were calculated. It was found that errors in computing the index of refraction are proportional to the relative error in measurement of refraction. Studies were performed both for measurement of refraction from an elevation of 500 m and measurement of refraction from space. The presence of vertical autocorrelations among meteorological parameters can in principle be used to increase the accuracy of results still further. Author

N85-23147# Joint Publications Research Service, Arlington, Va.
INFRARED AEROSOL ABSORPTION INDEX Abstract Only **c46**
L. B. Gabelko and Yu. S. Lyubovtseva *In its* USSR Rept.: Earth Sci. (JPRS-UES-85-002) 1 Feb. 1985 p 56-57 Transl. into ENGLISH from Izv. Akad. Nauk SSSR: Fiz. Atmosfery i Okeana (Moscow), v. 20, no. 8, Aug. 1984 p 715-724 Original language document was announced in IAA as A84-48648 (For primary document see N85-23116 13-42)
Avail: NTIS HC A07/MF A01

The imagery part of the complex index for the absorption of atmospheric aerosol in the 2.5 to 14 micron wavelength interval is calculated. The calculations are performed on the basis of simultaneous optical (IR), chemical, and mass-spectrometric analyses of aerosol samples in urban and background conditions. It is shown that the most important factor affecting IR light absorption is the finely dispersed fraction of the aerosol. An index is also calculated for the absorption of organic constituents in the aerosol. It is found that the organic constituents contribute the largest fraction of IR light absorption in the finely dispersed aerosol, together with ammonium sulfate and soot (crystallized carbon). Author

N85-23148# Joint Publications Research Service, Arlington, Va.
STUDY OF STRATIGRAPHY OF THE PRECAMBRIAN SOVIET BALTIC SHIELD Abstract Only **c46**
K. O. Krats, V. A. Negrutsa, Yu. B. Bogdanov, V. G. Gaskelberg, V. G. Zagorodnyy, T. F. Negrutsa, M. A. Semikhatov, and K. A. Shurkin *In its* USSR Rept.: Earth Sci. (JPRS-UES-85-002) 1 Feb. 1985 p 58 Transl. into ENGLISH from Sov. Geol. (Moscow), no. 7, Jul. 1984 p 105-118 (For primary document see N85-23116 13-42)
Avail: NTIS HC A07/MF A01

Studies of the stratigraphy of the Precambrian Soviet Baltic shield were undertaken by a consortium of the institutes and organizations represented by the authors. All the work proceeded in accordance with the stratigraphic codex of the USSR considering past experience and methodological requirements on the development of stratigraphy. A summary simplified model of regional stratigraphic systems of Precambrian deposits in the Soviet Baltic shield is presented in tabular form and the subdivisions used are explained. Definitions are given for each of the major strata distinguished in the plan. Suggestions are made for future improvements in the stratigraphic plan. R.J.F.

N85-23149# Joint Publications Research Service, Arlington, Va.
OBSERVATION OF LONG-PERIOD OSCILLATIONS OF EARTH Abstract Only **c46**
N. G. Savina, S. Ya. Tipisev, Ye. M. Linkov, and I. B. Yanovskaya *In its* USSR Rept.: Earth Sci. (JPRS-UES-85-002) 1 Feb. 1985 p 60 Transl. into ENGLISH from Izv. Akad. Nauk SSSR: Fiz. Zemli (Moscow), no. 8, Aug. 1984 p 3-12 (For primary document see N85-23116 13-42)
Avail: NTIS HC A07/MF A01

Results are presented from analysis of steady observations performed on the Leningrad State University long-period seismometric channel covering periods of 4 to 300 minutes. In addition to studying the spectral composition of long-period oscillations, the relationship of these oscillations with earthquakes was investigated. A strong earthquake occurred on 25 May 1981 during the time when the long-period channel was continuously recording. Comparison of the results of statistical analysis of long-period oscillation spectra recorded by the modified long-period channel and the low frequency spectrum following the earthquake of 25 May 1981 with the results of previous investigations shows that the spectral composition of the seismic oscillations with periods of 58 to 100 minutes is stable. The amplitude of superlong-period oscillations is comparable to the amplitude of the basic spheroidal tones of the natural oscillations of the Earth. Based on analysis of records before and after the earthquake of 25 May 1981 it is shown that superlong-period oscillations can be excited by strong earthquakes. R.J.F.

N85-23150# Joint Publications Research Service, Arlington, Va.
NUMERICAL MODELING OF PLANE STICK-SLIP FAULT Abstract Only **c46**
S. S. Arefyev and V. M. Grayzer *In its* USSR Rept.: Earth Sci. (JPRS-UES-85-002) 1 Feb. 1985 p 60 Transl. into ENGLISH from Izv. Akad. Nauk SSSR: Fiz. Zemli (Moscow), no. 8, Aug. 1984 p 13-21 (For primary document see N85-23116 13-42)
Avail: NTIS HC A07/MF A01

A numerical study is presented of differences in movements from complex and simple faults. Based on a dislocation model of a focus, the displacements near a complex fault consisting of several smooth sections are calculated. The kinematic approach used allows calculation of the radiation from a complex fault without studying the causes of delays and interruptions in the process of movement of the fault. The possibility is shown of modeling a fault of the stick-slip type, assumed to consist of several straight dislocations. Displacements from smooth and complex faults are compared, varying the pairing rate and displacement step at the fault for constant seismic moment. It is shown that the amplitude of displacements from a source of the second type is greater than from one of the first. The reasons for this increase include the discreteness of the fault and the variation in displacement in its sectors. It is shown tht the displacement sepctra from smooth faults and stick-slip faults are different. Model calculations are compared with seismic observations and laboratory experiments. Author

N85-23151# Joint Publications Research Service, Arlington, Va.
SCATTERING OF ELASTIC WAVES ON FRACTURES RANDOMLY DISTRIBUTED IN A THREE-DIMENSIONAL MEDIUM Abstract Only **c46**
S. A. Strizhkov and V. I. Ponyatovskaya *In its* USSR Rept.: Earth Sci. (JPRS-UES-85-002) 1 Feb. 1985 p 62 Transl. into ENGLISH from Izv. Akad. Nauk SSSR: Fiz. Zemli (Moscow), no. 8, Aug. 1984 p 72-77 (For primary document see N85-23116 13-42)
Avail: NTIS HC A07/MF A01

The purpose of this work is to determine the variation in basic characteristics of the wave field formed in a jointed medium, such as the intensity of fluctuations of amplitude, correlation radius, scattering coefficient and frequency composition of waves, as functions of jointing parameters. Fractures are simulated by flat plates randomly distributed and chaotically oriented in a three-dimensional medium. Experiments were performed using an alabaster model, a rectangular block measuring 50 x 50 x 120 mm. The plates were introduced into liquid alabaster which was then agitated. Models made in this way contain randomly distributed and chaotically oriented fractures. The influence of these fractures appears as fluctuations in the wave field formed in the medium. The data obtained in experimental studies showed that the dimensions of heterogeneities determined by waves in the jointed medium and the dimensions of the fractures themselves coincide only if the distance between fractures is rather great. If the distance between fractures is less than the wavelength, the dimensions of the heterogeneities located by the wave depend on wavelength. R.J.F.

N85-23152# Joint Publications Research Service, Arlington, Va.
NATURAL ELECTROMAGNETIC RADIATION IN SEISMICALLY ACTIVE REGIONS Abstract Only **c46**
N. I. Migunov, G. A. Sobolev, and A. A. Khromov *In its* USSR Rept.: Earth Sci. (JPRS-UES-85-002) 1 Feb. 1985 p 63-64 Transl. into ENGLISH from Izv. Akad. Nauk SSSR: Fiz. Zemli (Moscow), no. 7, Jul. 1984 p 55-63 (For primary document see N85-23116 13-42)
Avail: NTIS HC A07/MF A01

A study is made of results of investigations performed using direction-finding apparatus determining the direction of arrival of electromagnetic signals with an accuracy to three degrees. The arrival time of signals is recorded with an accuracy to 1 ms. Analysis of the signal shape allows computation of the distance to the signal source. The results of observations do not prove the existence of changes in electromagnetic radiation during earthquakes, but do make this assumption seem likely. A promising trend for further research is a changeover to active methods for studying mechanicoelectrical phenomena and conditions for propagation of radio waves in seismic regions. Combined studies including seismoelectric soundings of the crust and radio transillumination of the atmosphere are worth pursuing. The lack of a reliable method for short-term prediction of earthquakes makes a study of electromagnetic precursors interesting. Author

N85-23153# Joint Publications Research Service, Arlington, Va.
DETERMINATION OF DENSITY OF THE CRUST AND UPPER MANTLE FROM DEEP SEISMIC SOUNDING AND GRAVIMETRY, 2 Abstract Only **c46**
T. V. Romanyuk and V. N. Strakhov *In its* USSR Rept.: Earth Sci. (JPRS-UES-85-002) 1 Feb. 1985 p 64 Transl. into ENGLISH from Izv. Akad. Nauk SSSR: Fiz. Zemli (Moscow), no. 7, Jul. 1984 p 64-80 (For primary document see N85-23116 13-42)
Avail: NTIS HC A07/MF A01

A number of purely methodological problems related to deep seismic sounding data and gravimetry are discussed. Computer programs for simple situations in which density does not fluctuate within individual blocks and results of model calculations are given. The purpose of the calculations was to provide a quantitative estimate of the difficulty in retrieval of cross-section density when background components are present in the delta g field and there are rather intense medium-frequency noises simulating the influence of unknown large density heterogeneities in the upper portion of the cross-section. The most important conclusion is that the use of the rho = f(v) equation cannot support selection of a field with the required accuracy. Consequently, the concept of the presence of fluctuations in density through the cross section must be accepted and gravitational modeling of errors in seismic constructions with simple layers must be undertaken. R.J.F.

N85-23154# Joint Publications Research Service, Arlington, Va.
INDUCTION EXCITATION OF DEEP CONDUCTING ZONES Abstract Only **c46**
M. N. Berdichevskiy, A. I. Bilinskiy, V. M. Kobzova, and I. P. Moroz *In its* USSR Rept.: Earth Sci. (JPRS-UES-85-002) 1 Feb. 1985 p 65 Transl. into ENGLISH from Izv. Akad. Nauk SSSR: Fiz. Zemli (Moscow), no. 7, Jul. 1984 p 85-89 (For primary document see N85-23116 13-42)
Avail: NTIS HC A07/MF A01

New data are given on induction excitation of deep conducting zones. Data were obtained at the Applied Problems of Mathematics

and Mechanics Institute on a physical modeling installation using an electrolytic bath in combination with metal shields. Physical modeling shows that the induction mechanism of excitation of deep conducting zones can make a more or less significant contriution to magnetotelluric sounding curves. A zone measuring 2 and 5 times its depth in the vertical and horizontal directions can be taken as the threshold zone. If a conducting zone 30 km thick lies at a depth of 10 km and extends for hundreds of kilometers, the MT curve may be deflected from the normal by tens of percent. The conducting asthenospheric zone should appear in MT curves if its thickness reaches 150-200 km and it extends for 1,000 or more kilometers. The major difficulty is that induction excitation of isolated conducting zones does not fall within the framework of the Tikhonov-Cagniard model, and interpretation of MT curves must be accomplished in a class of three-dimensional models. Author

N85-23155# Joint Publications Research Service, Arlington, Va.
STUDY OF RESOLUTION OF DEEP MT SOUNDINGS BY MEANS OF PHYSICAL MODEL Abstract Only **c46**
M. N. Berdichevskiy, A. I. Bilinskiy, V. M. Kobzova, and I. P. Moroz *In its* USSR Rept.: Earth Sci. (JPRS-UES-85-002) 1 Feb. 1985 p 65-66 Transl. into ENGLISH from Izv. Akad. Nauk. SSSR: Fiz. Zemli (Moscow), no. 7, Jul. 1984 p 85-89 (For primary document see N85-23116 13-42)
Avail: NTIS HC A07/MF A01

Two problems are studied: the influence of deep fractures through which conductive redistribution of current occurs; and the excitation of deep conducting zones by an anomalous magnetic field of near surface origin. Both problems are studied by means of a physical installation consisting of an electrolytic bath, a system of metal shields, and a frame antenna forming a quasihomogeneous field. A simple three-dimensional model is studied yielding a qualitative concept of the influence of fractures. Model MT curves are presented obtained over the center of a metal disk which lies at the bottom surface of a conducting layer (the electrolyte) which is over a poorly conducting layer and another conducting layer. The model merely indicates that fractures, even if rather small, cause deep conducting zones to be accessible for MT soundings. Formal, one-dimensional interpretation of MT curves may thus lead to serious errors, but allow at least qualitative detection of deep conducting zones. Reliable quantitative interpretation requires analysis of two-dimensional and three-dimensional models. The theory of deep MT soundings should be oriented primarily on a study of the mechanism of galvanic excitaion of crust and mantle conducting zones. R.J.F.

N85-23156# Joint Publications Research Service, Arlington, Va.
NATURE OF SEISMIC IMAGES WITH AMPLITUDE AND TIME FLUCTUATIONS OF RECORDED OSCILLATIONS Abstract Only **c46**
Yu. K. Tyapkin *In its* USSR Rept.: Earth Sci. (JPRS-UES-85-002) 1 Feb. 1985 p 66 Transl. into ENGLISH from Izv. Akad. Nauk SSSR: Fiz. Zemli (Moscow), no. 7, Jul. 1984 p 90-97 (For primary document see N85-23116 13-42)
Avail: NTIS HC A07/MF A01

The following problem is solved: a wave f sub o (xo, yo, t) e reflected from a flat horizontal boundary is recorded at the flat horizontal surface of the z = 0. The boundary is assumed absolutely reflecting and constant in its physical properties. The process of formation of the seismic image at depth z in a homogeneous isotropic absolutely elastic space based on the wave field fixed at the surface is described by a focusing integral transform. The situation is complicated by amplitude distortions and time shifts of the recorded wave. The influence of these types of noise on the nature and quality of images produced is described. The admissible value of dispersion A(x sub 0, 40) and delta (x0, y0) is estimated which will still allow correlation of horizons or isolation of anomalies in dynamic parameters on the images. It is concluded that as seismic holographic images are formed, the presence of amplitude and time fluctuations in the recorded field resulting from variability in conditions of wave reception leads to amplitude-phase fluctuations of images. B.W.

N85-23157# Joint Publications Research Service, Arlington, Va.
SPACE AND TIME DISTRIBTUION OF AFTERSHOCKS Abstract Only **c46**
N. D. Zhalkovskiy and V. I. Muchnaya *In its* USSR Rept.: Earth Sci. (JPRS-UES-85-002) 1 Feb. 1985 p 67 Transl. into ENGLISH from Geol. y Geofiz. (Novosibirsk), no. 8, Aug. 1984 p 108-117 (For primary document see N85-23116 13-42)
Avail: NTIS HC A07/MF A01

The equations used to determine the distribution of aftershocks in space and time are refined to determine whether the growth of the number of aftershocks with an increase in earthquake magnitude is related to an increase in the volume of the area occupied by the hypocenter or whether the degree of activation of the area also depends on the earthquake magnitude. The results show that an increase in the number of aftershocks with increasing seismic moments of an earthquake is fully defined by the increase in volume of the area over which they extend. The degree of activation of the area of an aftershock is not dependent on the magnitude of the earthquake itslf. The earthquake magnitude also does not influence attenuation of the frequency of development of aftershocks over time. B.W.

N85-23158# Joint Publications Research Service, Arlington, Va.
DETERMINING VECTOR OF RADIOINTERFEROMETER BASE FROM OBSERVATIONS OF NATURAL RADIO EMISSION WITH NARROW SPECTRUM Abstract Only **c46**
G. A. Shanurov *In its* USSR Rept.: Earth Sci. (JPRS-UES-85-002) 1 Feb. 1985 p 67-68 Transl. into ENGLISH from Izv. Vyssh. Uchеb Zaved.: Geod. i Aerofotosyemka (Moscow), no. 2, Mar. - Apr. 1984 p 9-13 (For primary document see N85-23116 13-42)
Avail: NTIS HC A07/MF A01

Radio-interferometry with a very long base makes it possible to determine the vector of a base with a length of several thousand kilometers with an error not exceeding 10 cm. Regional geodetic networks, such as for measuring crustal deformations, can be constructed using 4- and 9-m mobile antennas operating together with a 60-m antenna. The measured parameters are the time lag in arrival of the wave front at one station relative to another and the interference frequency f, related to the lag tau by the expression f = upsilon delta tau/delta tau (t is time, upsilon is radio frequency). Highly precise tau measurement is possible only with a width of the reception and signal registry band of hundreds of MHz. The results of f measurement contain no information on the polar component delta Z of the base vector and the equatorial components delta X and delta Y are determined with a far lesser accuracy than from f tau measurements. A method is described for determining all three components of the base vector from measurements of the interference frequency f and the phase difference of a narrow-band signal received at both radio interferometer stations. B.W.

N85-23159# Joint Publications Research Service, Arlington, Va.
STRUCTURE OF ICELAND AND OCEAN FLOOR SPREADING Abstract Only **c46**
V. V. Ez *In its* USSR Rept.: Earth Sci. (JPRS-UES-85-002) 1 Feb. 1985 p 73-74 Transl. into ENGLISH from Geotektonika (Moscow), no. 3, May - Jun. 1984 p 100-111 (For primary document see N85-23116 13-42)
Avail: NTIS HC A07/MF A01

The conclusion that the Earth's crust of Iceland was formed as a result of spreading is consistent with a number of facts: (1) the western zone of most recent volcanism in Iceland is precisely on the strike of the submarine Reykjanes Ridge, regarded as the axial rift of the Mid-Atlantic Ridge and accordingly as the spreading axis; (2) the age of Icelandic rocks emerging at the surface increases from its central part to its western and eastern margins; and the radiological age of the rocks emerging at the surface on the continuation of one of the clearly expressed linear magnetic anomalies in the ocean coincides closely with other earlier estimates on the age of this anomaly. On the basis of an analysis of the structural data summarized in this article the conclusion is drawn that the plicated structure began to form at the time of accumulation of the plateau basalt stratum as a result of nonuni-

formly distributed vertical movements. It is demonstrated that the development of neovolcanic zones (regarded as rifts) is attributable to the association of recent volcanism with a system of rejuvenating faults constituting part of an earlier forming unified network of dislocations occupying the entire island. B.W.

N85-23160# Joint Publications Research Service, Arlington, Va.
REVIEW OF PROBLEMS IN LITHOLOGY Abstract Only c43
P. P. Timofeyev *In its* USSR Rept.: Earth Sci. (JPRS-UES-85-002) 1 Feb. 1985 p 75 Transl. into ENGLISH from Vestn. Akad. Nauk SSSR (Moscow), no. 9, Sep. 1984 p 69-77 (For primary document see N85-23116 13-42)
Avail: NTIS HC A07/MF A01

The fundamental problems in modern lithology and its role in the development of geological science are reviewed; the further development of the mineral raw material base of the country dictates that significant work be done for advancing this field. The different aspects of lithology are examined, with discussion of the contributions made to the development of lithology by different researchers and the work which has been and is being done along these lines by different research and field organizations. It is emphasized that even the geological community has underappreciated the importance of work in the field of lithology. Much attention is given to the relationship between lithology and the formation and patterns of distribution of mineral deposits. It is essential that lithologists contribute more fully to solution of problems related to the localization of ore bodies and the process of formation of sedimentary layers and their changes in the course of geological history with the formation of mineral deposits. The further development of lithology cannot be restricted to the isolated study of individual objects, regions, continental blocks or sediments of the oceans and seas. B.W.

N85-23161# Joint Publications Research Service, Arlington, Va.
MAGMATISM IN CONTINENT-OCEAN TRANSITION ZONE (DEVELOPMENT OF IDEAS OF A. N. ZAVARITSKIY) Abstract Only c46
O. A. Bogatikov, V. I. Kovalenko, I. D. Ryabchikov, and A. A. Tsvetkov *In its* USSR Rept.: Earth Sci. (JPRS-UES-85-002) 1 Feb. 1985 p 76 Transl. into ENGLISH from Izv. Akad. Nauk SSSR: Ser. Geol. (Moscow), no. 6, Jun. 1984 p 8-27 (For primary document see N85-23116 13-42)
Avail: NTIS HC A07/MF A01

An article in which A.N. Zavaritskiy first demonstrated the presence of seismic focal zones in nature and predicted their possible tectonic role was published in 1946. Zavaritskiy correctly postulated that recent tectonic movements must be studied in zones of concentration of volcanoes and deep-focus earthquakes. He related the grandiose tectogi and magmatic phenomena along the periphery of the Pacific Ocean to movement in a seismic focal zone. The general characteristics of Zavaritskiy-Benioff zones are described from the point of view of magmatic petrology and evolution of island arc magmatism. The problem of genesis of andesites typomorphic for the magmatism of island arcs is discussed and the related problems of growth of the continents are defined. The fundamental ideas of A.N. Zavaritskiy later led to the discovery of zones of magma formation in the world system of mid-oceanic ridges and at hot points and the magmatism of the destructive boundaries of lithospheric plates, which later became the cornerstone of plate tectonics. B.W.

N85-23162# Joint Publications Research Service, Arlington, Va.
POSSIBILITY OF MAPPING ACTIVE TECTONIC STRUCTURES FROM MERCURY GAS AUREOLES OVER SEA SURFACE Abstract Only c43
A. A. Ganeyev, N. R. Mashyanov, G. B. Sveshnikov, and S. Ye. Sholupov *In its* USSR Rept.: Earth Sci. (JPRS-UES-85-002) 1 Feb. 1985 p 77-78 Transl. into ENGLISH from Dokl. Akad. Nauk SSSR (Moscow), v. 275, no. 5, Apr. 1984 p 1162-1164 (For primary document see N85-23116 13-42)
Avail: NTIS HC A07/MF A01

Direct measurements of Hg content in the atmosphere were made in the Bering Sea area and the northwestern Pacific Ocean along the shores of Chukotka and Kamchatka. The shipboard observations were made with a Zeemen selective atomic absorption spectrometer. This instrument registered the concentration of atmospheric Hg in the air layer between the radiation source and receiver on a path 1 m long. The profile intersected the shelf, continental slope, regions of abyssal depressions, rises and ridges in the northern part of the Kuril-Kamchatka island arc. In a number of regions there were increased concentrations of Hg vapor over the sea surface exceeding the atmosheric clarke of concentrated by a factor of 2 to 3. The greatest number of anomalous zones was in regions of shallow depths 200-1,000 m; a few such cases were observed over abyssal parts of the Pacific Ocean where the depths were greater than 4,000 m. The strongest Hg anomalies over the sea surface were situated on the contnental shelf in regions of active tectonic zones associated with deep faults extending into the continental parts of Chukotak and Kamchatka. B.W.

N85-23163# Joint Publications Research Service, Arlington, Va.
NORMAL AND ANOMALOUS GEOTHERMAL FIELDS AND THEIR RELATIONSHIP TO HIERARCHY OF GEOLOGICAL BODIES Abstract Only c46
S. S. Sardarov, Jr., A. V. Savin, and M. G. Pashuk *In its* USSR Rept.: Earth Sci. (JPRS-UES-85-002) 1 Feb. 1985 p 78-79 Transl. into ENGLISH from Dokl. Akad. Nauk SSSR (Moscow), v. 275, no. 5, Apr. 1984 p 1084-1087 (For primary document see N85-23116 13-42)
Avail: NTIS HC A07/MF A01

The principle of a hierarchy of geological bodies and specifically the rank approach is used in clarifying the problem of the geothermal background (or normal geothermal field). it is proposed that the concept of a local background be introduced as the heat flow characterizing the geothermal regime of an object of a higher order (rank, class, scale) than the studied object. For example, for an arch the local geothermal background is the heat flow determining the regime of a syneclise, for a syneclise -- the flow determining a platform regime. The problem of finding the local background involves the breakdown of the really determined distribution of heat flow values into elementary distributions; the distribution with the maximum weight must be assumed normal. The background heat flow is the mathematical expectation of an 'elementary' normal distribution with a maximum weight. Specific cases are examined in which all the elementary distribution are assumed to be normal. All the distribution parameters were computed by the least squares method. B.W.

N85-23164# Joint Publications Research Service, Arlington, Va.
VARIATIONS IN RESISTIVITY OF UPPER CRUSTAL LAYER Abstract Only c46
A. Ya. Sidorin *In its* USSR Rept.: Earth Sci. (JPRS-UES-85-002) 1 Feb. 1985 p 80 Transl. into ENGLISH from Dokl. Akad. Nauk SSSR (Moscow), v. 278, no. 2, Sep. 1984 p 330-334 (For primary document see N85-23116 13-42)
Avail: NTIS HC A07/MF A01

A stationary system of year-round observations of changes in resistivity of the upper layer of the Earth's crust was organized in the Garm Test Area. Year-round observations of variation in temperature at various depths were also made, allowing in situ determination of the temperature conductivity coefficient under the specific conditions of the test range. Equations are presented which can be used to estimate the changes in apparent resistivity. The equations indicate that the thicknesses of the diurnal and annual temperature change skin layers are 0.1 and 2.1 m. Variations in resistivity and temperature at a depth of 3.1 m are diagrammed. The results showed that the estimates of annual changes in apparent resistivity based on temperature changes alone are insufficient. Reliable estimates require a cycle of observations of surface layer resistivity at various points. Author

N85-23165# Joint Publications Research Service, Arlington, Va.
BOUNDARY VELOCITIES OF LONGITUDINAL SEISMIC WAVES AND LATERAL INHOMOGENEITIES OF UPPER OCEAN MANTLE Abstract Only c46

N. Ya. Kunin, N. V. Goncharova, G. I. Semenova, S. V. Usenko, E. R. Sheykhzade, and Yu. G. Zorina *In its* USSR Rept.: Earth Sci. (JPRS-UES-85-002) 1 Feb. 1985 p 82-83 Transl. into ENGLISH from Dokl. Akad. Nauk SSSR (Moscow), v. 278, no. 1, Sep. 1984 p 76-81 (For primary document see N85-23116 13-42)
Avail: NTIS HC A07/MF A01

Data on boundary velocities of longitudinal refracted waves along the surface of the upper ocean mantle (the Mohorovicic discontinuity), expressed by the notation v sub g m are presented. Studies were made in the Pacific, Atlantic and Indian Oceans over widely diverse regions. Typical studies of this sort have used travel-time curves of 40-50 km in length; first arrivals approximating a straight line exceed 5-10 km on such travel-time curves. Soundings and profile observations indicated that relatively small vertical velocity gradients were found for as much as 100-300 km. Results show that much of the North Atlantic and most of the Indian Ocean, as well as the Mediterranean Sea and European parts of the Atlantic to the latitude of Gorky-Odessa in the USSR, Arabia, Greenland and much of Africa share an enormous homogeneous region with only normal and suppressed V sub g m readings. High values for V sub gm prevail in the Pacific, southern Indian and Atlantic Ocean zones. Oceanic and continental regions showed great similarities. B.W.

N85-23166# Joint Publications Research Service, Arlington, Va.
DISCRIMINATION OF NORMAL AND ANOMALOUS MAGNETIC AND ELECTRIC FIELDS IN GEOELECTROMAGNETIC VARIATIONS Abstract Only **c46**
V. v. Aksenov *In its* USSR Rept.: Earth Sci. (JPRS-UES-85-002) 1 Feb. 1985 p 83 Transl. into ENGLISH from Geol. i Geofiz. (Novosibirsk), no. 7, Jul. 1984 p 121-126 (For primary document see N85-23116 13-42)
Avail: NTIS HC A07/MF A01

Algorithms are presented which discriminate between magnetic and electric fields observed in the world network and which are spherically divided by algorithms into normal an anomalous parts. The algorithms can break the field down into electric and magnetic fields, distinguishing external and internal origin fields in both types, retrieving all six electromagnetic components of the field based on measured magnetic components. Unambiguous discrimination of normal and abnomalous fields, separation of the fields of deep anomalies from fields of surface anomalies in magnetic and electric fields, requires measurement of three magnetic components of the variation field and assignment of two conductivities. E.A.K.

N85-23167# Joint Publications Research Service, Arlington, Va.
REFLECTED WAVE TRAVEL-TIME CURVES IN STRATIFIED MEDIA WITH VERTICALLY HETEROGENEOUS LAYERS AND SLIGHTLY SLOPING CURVED BOUNDARIES Abstract Only **c46**
E. A. Blyas *In its* USSR Rept.: Earth Sci. (JPRS-UES-85-002) 1 Feb. 1985 p 84 Transl. into ENGLISH from Geol. i Geofiz. (Novosibirsk), no. 7, Jul. 1984 p 107-114 (For primary document see N85-23116 13-42)
Avail: NTIS HC A07/MF A01

Numerical methods to determine travel time curves do not allow sufficient study of the influence of various heterogeneities on kinematic parameters of reflected waves. The problem of transfer of slight deviations in boundaries from the horizontal to changes in time fields was studied. Approximate equations for the coefficients of an expansion for a medium with near horizontal boundaries and vertically heterogeneous strata are presented. The influence of curving of boundaries on the coefficients of the expansion and therefore on the limiting parameters of the reflected wave travel time curve is analyzed. The method, reacts strongly to the presence of curved refracting boundaries in the upper portion of the cross section. E.A.K.

N85-23168# Joint Publications Research Service, Arlington, Va.
STUDY OF GEOLOGICAL MEDIA BASED ON SCATTERED EARTHQUAKE WAVES Abstract Only **c46**
V. G. Bovenko and B. Ye. Shcherbakova *In its* USSR Rept.: Earth Sci. (JPRS-UES-85-002) 1 Feb. 1985 p 86 Transl. into ENGLISH from Dokl. Akad. Nauk SSSR (Moscow), v. 278, no. 3, Sep. 1984 p 575-580 (For primary document see N85-23116 13-42)
Avail: NTIS HC A07/MF A01

Specifics of the wave field in the exchange wave method were analyzed. A model of the geological medium as random and ordered heterogeneous provided solutions. The localization of scattering heterogeneities is performed by dynamic cross sections method. The physical basis of the method of investigation of geological media based on longitudinal and scattered exchange waves from earthquakes was derived by physical and mathematical modeling. The process of scattering of ultrasonic pulse waves in a medium dimension a local heterogeneity of circular shape with a transverse dimension of approximately 15 times the longitudinal wavelength, located at a depth of about five longitudinal wavelengths were studied. The source of oscillations was located beneath the center of the heterogeneity by about an additional five wavelengths. The detection among the scattered exchange waves of PS and SP waves with an intensity of the same order of magnitude as that of the transmitted P and S waves is shown. This result is confirmed by mathematical modeling of the scattering of harmonic oscillations. Subvertical zones of heterogeneities identified with fault are localized determination of their position, slope angle and possible penetration depth. E.A.K.

N85-23169# Joint Publications Research Service, Arlington, Va.
CONSIDERATION OF HETEROGENEITY OF GRAVITY FIELDS IN LOCAL HIGH PRECISION GEODETIC CONSTRUCTIONS Abstract Only **c46**
A. A. Konopikhin, L. V. Ogorodova, and A. P. Yuzefovich *In its* USSR Rept.: Earth Sci. (JPRS-UES-85-002) 1 Feb. 1985 p 97 Transl. into ENGLISH from Izv. Vyssh. Ucheb. Zaved., Geod. i Aerofotosyemka (Moscow), no. 3, May - Jun. 1983 p 66-72 (For primary document see N85-23116 13-42)
Avail: NTIS HC A07/MF A01

The influence of heterogeneity of the gravity field on measurement of elements of local geodetic constructions and methods for their examination was estimated. Local values of elements of the gravitational field, i.e., those caused by gravity anomalies in the immediate vicinity of the geodetic station are determined. It is also possible to obtain information on changes in these elements over comparatively short distances, characteristic for local high precision geodetic constructions. In the plains region with a quiet gravitational field, corrections for heterogeneities over distances of 5 to 100 m are comparable with the accuracy of the geodetic measurement. Computation of the precise values of the corrections at each station in the network requires calculation of the radius of the area of anomalies considered, calculation of the necessary density of survey in the immediate neighborhood of stations, and execution of a gravimetric survey. Variometric observations are used for consideration of heterogeneities in the gravity field.E.A.K.

N85-23170# Joint Publications Research Service, Arlington, Va.
MATHEMATICAL MODELING OF RESULTS OF GEOMETRIC LEVELING IN VARIABLE GRAVITY FIELD Abstract Only **c46**
I. G. Vovk *In its* USSR Rept.: Earth Sci. (JPRS-UES-85-002) 1 Feb. 1985 p 97-98 Transl. into ENGLISH from Izv. Vyssh. Ucheb. Zaved., Geod. i Aerofotosyemka (Moscow), no. 3, May - Jun. 1984 p 72-75 (For primary document see N85-23116 13-42)
Avail: NTIS HC A07/MF A01

Changes in elevation recorded during geometric leveling may be the result of vertical movement of level surfaces due to change in gravitational potential. The influence of variations in the gravity field on the results of geometric leveling when changes in the field occur during field observations were determined. Mathematical modeling methods are used to solve the problem which allows preestimation of possible changes in normal elevations along a level line and determination of the need for gravimetric work. If changes in the gravity field can be reliably estimated by using a model, mathematical modeling methods based on experimental data on factors influencing changes in the field allow estimation of changes in normal elevations without making gravity determinations. E.A.K.

N85-23171# Joint Publications Research Service, Arlington, Va.
RELATIONSHIP BETWEEN BRIGHTNESS SPECTRUM OF PHOTOGRAPHIC IMAGE AND SPECTRUM OF RISES ON A WATER SURFACE WITH WAVES Abstract Only **c74**
I. I. Strizhkin *In its* USSR Rept.: Earth Sci. (JPRS-UES-85-002) 1 Feb. 1985 p 98 Transl. into ENGLISH from Izv. Vyssh. Ucheb. Zaved., Geod. i Aerofotosyemka (Moscow), no. 3, May - Jun. 1984 p 90-95 (For primary document see N85-23116 13-42)
Avail: NTIS HC A07/MF A01

A method was developed to determine the wave spectrum of a water surface by spectral analysis of sea surface photographs and utilize the transfer function between the spectrum of slopes and the spectrum of rises. Various methods are possible for determining the slopes of spectra from photographs: determination of height of surface profiles using stereoscopic pairs and statistical processing of data or microphotometry of an individual photograph. The interrelationship between the slope spectrum and the spectrum of rises is analyzed. Factors influencing the formation of the photographic image of a wave and the slope spectrum are studied. The influence of the survey scale on the slope spectrum is analyzed. The influence of illumination conditions on the slope spectrum is discussed. The influence of illumination conditions is considered in determining the requirements for photographic surveying of waves to decrease distortions. E.A.K.

N85-23172# Joint Publications Research Service, Arlington, Va.
STUDY OF PHASE RADIOGEODETIC SYSTEMS WITH PHASE-LOCKED LOOPS Abstract Only **c33**
V. P. Glumov, O. S. Golod, V. V. Sizov, and E. I. Ter-Saakov *In its* USSR Rept.: Earth Sci. (JPRS-UES-85-002) 1 Feb. 1985 p 99 Transl. into ENGLISH from Izv. Vyssh. Ucheb. Zaved., Geod. i Aerofotosyemka (Moscow), no. 3, May - Jun. 1984 p 14-20 (For primary document see N85-23116 13-42)
Avail: NTIS HC A07/MF A01

Phase type difference systems with a two channel compensation station are widely used in the creation of geodetic bases at sea. To increase the operating range of such systems and the accuracy of these measurements balance and single side band modulation is used in the reference channel. Synchronous detectors with phase locked loop are used for the same purpose. One effective method of expanding the interception band of phase locked loops is discrete phasing of the tuned oscillator by the input signal. The discriminating characteristics of an open phase locked loop with periodic phasing of the tuned oscillator by the input signal and a sawtooth phase detector characteristic is described. A basis for selection of operating conditions of a phase locked loop in a system which can help to optimize operating conditions of radiogeodetic systems is presented. E.A.K.

N85-23173# Joint Publications Research Service, Arlington, Va.
THERMOHYDRODYNAMIC MODEL: HYDROTHERMAL SYSTEM, SHALLOWLY SEATED MAGMA CHAMBER Abstract Only **c46**
A. V. Kiryukhin *In its* USSR Rept.: Earth Sci. (JPRS-UES-85-002) 1 Feb. 1985 p 101 Transl. into ENGLISH from Vulkanol. i Seysmologiya (Moscow), no. 3, May - Jun. 1984 p 25-34 (For primary document see N85-23116 13-42)
Avail: NTIS HC A07/MF A01

The results of numerical modeling of heat exchange in the Hawaiian geothermal reservoir demonstrate the possibility of appearance of a hydrothermal system over a magma chamber. This matter was investigated in hydrothermal system. The equations for the conservation of mass and energy are discussed. Two possible variants of interaction between the magma chamber and the hydrothermal system were computated stationary dry magma chamber and dry magma chamber changing volume in dependence on the discharge of magma and taking into account heat exchange with the surrounding rocks. It is shown that the thermal supplying of the hydrothermal system can be ensured by the extraction of heat from a magma chamber which lies at a depth of 3 km and is melted out due to receipt of 40 cubic km of basalt melt with a temperature of 1,300 C. The initial data correspond with computations made with the model to the temperature values in the geothermal reservoir and a natural heat transfer comparable with the actually observed values. E.A.K.

N85-23174# Joint Publications Research Service, Arlington, Va.
POLYNOMIAL PARAMETERIZATION IN INVERSE GRAVIMETRIC PROBLEM Abstract Only **c46**
G. G. Rempel and G. I. Tatkov *In its* USSR Rept.: Earth Sci. (JPRS-UES-85-002) 1 Feb. 1985 p 107 Transl. into ENGLISH from Geol. i Geofiz. (Novosibirsk), no. 4, Apr. 1984 p 99-105 (For primary document see N85-23116 13-42)
Avail: NTIS HC A07/MF A01

An algorithm for solution of the inverse gravimetric problem was formulated. A polynomial parameterization makes it easy to formulize and consider a priori data on the configuration and position of an anomaly forming object. The plane inverse gravimetric problem is formulated. The form and position of its upper and lower surface are determined. In such a formulation the problem has a unique solution and can be used in ore geophysics. The algorithm was tested in test models and an interpretation of the gravity field along one of the profiles indicated that the algorithm rather rapidly converges to a precise solution. The algorithm has a high noise immunity. In an interpretation in three dimensional space the polynomials P sub m(x), O sub n(x) must be replaced by their spatial analogues. E.A.K.

N85-23175# Joint Publications Research Service, Arlington, Va.
PRIMARY PROCESSING OF EXPERIMENTAL MAGNETOVARIATION SOUNDING DATA USING SPLINE FUNCTIONS Abstract Only **c46**
O. N. Balykina *In its* USSR Rept.: Earth Sci. (JPRS-UES-85-001) 1 Feb. 1985 p 108 Transl. into ENGLISH from Geol. i Geofiz. (Novosibirsk), no. 4, Apr. 1984 p 120-124 (For primary document see N85-23116 13-42)
Avail: NTIS HC A07/MF A01

Problems in the processing of various kinds of observational data are discussed. A continuous smooth curve is best plotted in a cloud of experimental points on a plane. The problems related to approximation of a cloud of impedance values in the example of data from deep magnetovariation sounding was examined. An algorithm is developed for the continuous approximation of the cloud of points on a plane in the form of a cubic spline. E.A.K.

N85-23176# Joint Publications Research Service, Arlington, Va.
APPLICATION OF FIELD X-RAY: RADIOMETRIC ANALYSIS IN EXPLORATORY GEOLOGY AND MEANS FOR ITS IMPROVEMENT Abstract Only **c46**
D. B. Barkhatov and N. I. Butomo *In its* USSR Rept.: Earth Sci. (JPRS-UES-85-002) 1 Feb. 1985 p 109 Transl. into ENGLISH from Vestn. Leningr. Univ.: Geol., Geogr. (Leningrad), no. 6, issue 1, Mar. 1984 p 96-100 (For primary document see N85-23116 13-42)
Avail: NTIS HC A07/MF A01

Developments in field X-ray - radiometric analysis in application to the field of geology have become possible due to continued improvement in microcomputers. The speedy collection and on the spot processing of geological and geophysical data has become possible in such regions as the Arctic. Such work was recently carried out in the Arctic in a region of complexly folded Proterozoic strata in a zone with a length of 250 to 300 km and a width of 20 to 30 km. Metallogenetically promising complexes and formations and shows of mineral raw materials were studied. Experimental work with RRK-103 apparatus was carried out during 1980 to 1982. It was possible to detect concentrations of copper, zinc, lead, rubidium and zirconium; and 400 samples were obtained. Geochemical maps of the region and correlation graphs of the content of a number of elements in the sections were established. B.G.

N85-23177# Joint Publications Research Service, Arlington, Va.
POSSIBILITIES OF AERIAL ELECTRIC PROSPECTING BY LONG CABLE METHOD FOR DETECTING POORLY CONDUCTING STRATA Abstract Only **c43**
A. V. Veshev, S. S. Gudovskikh, and Ye. F. Lyubtseva *In its*

USSR Rept.: Earth Sci. (JPRS-UES-85-002) 1 Feb. 1985 p 111 Transl. into ENGLISH from Vestn. Leningr. Univ.: Geol., Geogr. (Leningrad), no. 6, issue 1, Mar. 1984 p 19-28 (For primary document see N85-23116 13-42)
Avail: NTIS HC A07/MF A01

The long-cable method is being used successfully in solving structural mapping problems in various ore regions in the USSR. The nature of the anomalous field of an alternating current flowing in a cable of finite length for aerial electric prospecting over thick well- and poorly conducting strata at different distances from the cable were previously studied. On the basis of the results, the possibilities of discriminating poorly conducting strata by this method for solving problems in geological mapping were clarified. Expressions are derived for the dependence of the anomalous field of a cable of finite length on observation altitude, depth of the upper surface of the stratum and its thickness. The anomalous field over two poorly conducting strata with different distances between them was also studied. The modeling was done with an apparatus described earlier (the principal parameters of the modeling apparatus are given; modeling scales of 1:10,000 and 1:15,000 were used). The results indicate that the method can be employed in identifying bodies with both high and low conductivity. The effectiveness can be considerably improved when measurements are made of the horizontal component of the electric field parallel with the horizontal component of the magnetic field. B.G.

N85-23178# Joint Publications Research Service, Arlington, Va.
GEOMAGNETIC PRECURSORS OF INTENSIVE EARTHQUAKES IN THE 1-0.-2 Hz FREQUENCY RANGE OF GEOMAGNETIC PULSATIONS Abstract Only **c46**
Ya. M. Gogatishvili *In its* USSR Rept.: Earth Sci. (JPRS-UES-85-002) 1 Feb. 1985 p 112 Transl. ito ENGLISH from Geomagnetizm i Aeronomiya (Moscow), v. 24, Jul. - Aug. 1984 p 697-700 (For primary document see N85-23116 13-42)
Avail: NTIS HC A07/MF A01

During intensive geotectonic processes such as earthquakes, pulsations are observed in the geomagnetic field at a frequency of 0.02 to 1 Hz with anomalously high amplitudes. These pulsations usually apppear as beat phenomena lasting from several minutes to several hours. It has been found that the pulsations are excited only in magnetic compontents of the terrestrial electromagnetic field. The periods and amplitudes of the pulsations are nonlinearly related to the intensity of the earthquakes. Pulsations of this type are not observed when earthquakes do not occur. Additional analysis shows that frequently the pulsations precede intensive earthquakes by 10 to 200 minutes, then drop for about 1 hour, then appear once again during the actual earthquake. Oscillograms of such pulsations are presented. The periods and amplitudes of the geomagnetic pulsations preceding earthquakes are found to be linearly related to the magnitude of the earthquakes. A regression equation relating earthquake magnitude to pulsation characteristics is presented. Author

N85-23179# Joint Publications Research Service, Arlington, Va.
SOLUTION OF DIRECT MAGNETOMETRIC PROBLEM ON SPHERICAL EARTH Abstract Only **c46**
A. G. Manukyan and V. I. Starostenko *In its* USSR Rept.: Earth Sci. (JPRS-UES-85-002) 1 Feb. 1985 p 113 Transl. into ENGLISH from Dokl. Akad. Nauk Ukr. SSR, Ser. B: Geol., Khim. i Biol. Nauki (Kiev), no. 5, May 1984 p 11-14 (For primary document see N85-23116 13-42)
Avail: NTIS HC A07/MF A01

The origin of the spherical coordinate system is at the center of a spherical Earth. The inhomogeneous body examined is a spherical rectangular parallelpiped, a body bounded by stipulated coordinate surfaces. First formulas for the magnetic potential are derived, followed by derivation of expressions for magnetic field strength components. In essence, the determinations of gravitational and magnetic effects from a three-dimensional spherical body are reduced to numerical computation of triple integrals, accomplished using Gauss-Legendre quadrature formulas. Different variants of the vector field are considered. The algorithm is intended for formulating magnetic modells of large geological structures with the Earth's sphericity taken into account. A.R.H.

N85-23180# Joint Publications Research Service, Arlington, Va.
DETERMINING DEEP HEAT FLOW AND RATE OF HORIZONTAL PERCOLATION FROM TEMPERATURE MEASUREMENTS IN AQUIFER Abstract Only **c43**
M. M. Mitnik *In its* USSR Rept.: Earth Sci. (JPRS-UES-85-002) 1 Feb. 1985 p 113-114 Transl. into ENGLISH from Dokl. Akad. Nauk Ukr. SSR, Ser. B: Geol., Khim. i Biol. Nauki (Kiev), no. 5, May 1984 p 14-17 (For primary document see N85-23116 13-42)
Avail: NTIS HC A07/MF A01

A method is presented for determining the deep heat flow on the basis of aquifer temperature which is undistorted by the movement of ground water. Formulas are derived, the parameters used are: the equilibrium temperature which is established at the depth corresponding to the middle of the stratum; the thermal conductivity coefficient for the covering rocks; the heat flow through the bottom of the stratum in the absence of the influence of water movement; temperature of the neutral layer; density; heat capacity; rate of percolation; and thickness of the aquifer. The problem is solved by the least squares method. Test computations of the method were made and used in studying a hydrothermal deposit in southern Kamchatka. The proposed method makes it possible, using geothermal measurements in an aquifer, to find the deep heat flow undistorted by convection and to determine the rate of percolation in this stratum. A.R.H.

N85-23181# Joint Publications Research Service, Arlington, Va.
SEISMIC WAVES AND DISPERSION RELATIONS Abstract Only **c46**
V. P. Rudnitskiy *In its* USSR Rept.: Earth Sci. (JPRS-UES-85-002) 1 Feb. 1985 p 114 Transl. into ENGLISH from Dokl. Akad. Nauk Ukr. SSR, Ser. B: Geol., Khim. i Biol. Nauki (Kiev), no. 5, May 1984 p 17-20 (For primary document see N85-23116 13-42)
Avail: NTIS HC A07/MF A01

The propagation of plane waves in a homogeneous medium with a finite relaxation kernel is described by the Volterra integro-differential equation. However, it is shown that the case most common in seismology cannot be described using the Volterra equation due to the inadequately general formulation of the initial problem. A full description of attenuating waves is possible by examining complex oscillations in a homogeneous medium with an imaginary relaxation kernel which in a special case can degenerate into the Dirac Delta Function. Proceeding of this basis, the required solution is found in Fourier transform space. A numerical estimate of C sub true can be obtained on the basis of stipulated x, n(omega) and v(omega) using a discrete Fourier transform. G.L.C.

N85-23182# Joint Publications Research Service, Arlington, Va.
GEOMAGNETIC FIELD DYNAMICS Abstract Only **c46**
L. I. Vigilyanskaya *In its* USSR Rept.: Earth Sci. (JPRS-UES-85-002) 1 Feb. 1985 p 121 Transl. into ENGLISH from Geofiz. Zh. (Kiev), v. 6, no. 3, May - Jun. 1984 p 69-73 (For primary document see N85-23116 13-42)
Avail: NTIS HC A07/MF A01

In the laboratory one of the processes of formation of low-temperature chemical remanent magnetization of sedimentary formations was investigated. It was found that the magnetization acquired by iron minerals during their low-temperature synthesis from ion solutions precisely indicates the direction of the magnetic field operative at the time of transpiring of the chemical reactions. There is a close linear correlation between this magnetization and field strength. Many experiments were carried out for studying the nature of natural remanent magnetiztion of sedimentary rocks in the Ukraine and Moldavia. The nature of the natural remanent magnetization of the weathered crust of crystalline rocks, fossil soils, loesses, clays, siltstones and reddish sandstones was determined. Study of the vector of natural remanent magnetization of sedimentary rocks is valuable in solving some problems related to the regime of geomagnetic field generation. G.L.C.

N85-23183# Joint Publications Research Service, Arlington, Va.
INTERRELATIONSHIP OF EARTHQUAKE MAGNITUDE AND LITHOSPHERIC-ASTHENOSPHERIC THERMODYNAMIC PARAMETERS IN SEISMICALLY ACTIVE ZONES Abstract Only **c46**
L. I. Tuliani *In its* USSR Rept.: Earth Sci. (JPRS-UES-85-002) 1 Feb. 1985 p 122 Transl. into ENGLISH from Geofiz. Zh. (Kiev), v. 6, no. 3, May - Jun. 1984 p 73-76 (For primary document see N85-23116 13-42)
Avail: NTIS HC A07/MF A01

An analysis of extensive data on earthquakes in such seismically active zones as the Caucasus, Tien Shan and Japanese islands made it possible to develop an energy scale applicable to any seismically active zone. Earthquakes in seismically active orogenic regions with magnitudes $M > 5$ characterize the lithosphere; those with magnitudes $M < 5$ characterize the asthenosphere, magma ducts and chambers. This conclusion was applied earlier in determining the thickness of the lithosphere and explaining inhomogeneities in structure of the crust and upper mantle in the Caucasus, Northern Tien Shan and Japan. Determinations of the bottom of the lithosphere correlated well with other geological and geophysical data. G.L.C.

N85-23184# Joint Publications Research Service, Arlington, Va.
CORRECTING DEPTH LINE ON NONLONGITUDINAL SEISMIC PROFILE Abstract Only **c46**
D. V. Lysynchuk *In its* USSR Rept.: Earth Sci. (JPRS-UES-85-002) 1 Feb. 1985 p 123-124 Transl. into ENGLISH from Geofiz. Zh. (Kiev), v. 6, no. 3, May - Jun. 1984 p 83-85 (For primary document see N85-23116 13-42)
Avail: NTIS HC A07/MF A01

Longitudinal-nonlongitudinal profiling is universally used in seismic work by the common depth point method in the Dnieper-Donets Depression. The depth section along a nonlongitudinal profile is related to the midline between profiles. There is frequently a considerable time nonclosure of reflections in a closed system of profiles. The computation scheme is simple. The problem of finding the displacements delta L of the depth line of a nonlongitudinal profile relative to the midline for a single reflection in a homogeneous isotropic medium is examined. It is shown that by knowing the echo depth of the reflecting surface on a longitudinal profile and the slope of this surface across the profiles, as well as the distance between the longitudinal and nonlongitudinal profiles, it is always possible to determine the displacement of the depth line relative to the midline. In making practical computations it is convenient to use grid overlays with isolines. G.L.C.

N85-23185# Joint Publications Research Service, Arlington, Va.
METHOD FOR PROCESSING BROAD-PROFILE DATA Abstract Only **c46**
Yu. A. Vasilyev and N. Z. Prokhur *In its* USSR Rept.: Earth Sci. (JPRS-UES-85-002) 1 Feb. 1985 p 124 Transl. into ENGLISH from Geofiz. Zh. (Kiev), v. 6, no. 3, May - Jun. 1984 p 85-88 (For primary document see N85-23116 13-42)
Avail: NTIS HC A07/MF A01

Data from areal observation systems afford a possibility for determining the velocity and geometrical parameters of a medium with known differential characteristics of the time fields (for example, surface gradients of the time field of their components). In the special example of an areal observation system, a so-called broad profile system. This possibility is illustrated for a variant of localized, widely separated excitation and ception bases moving autonomously along the broad profile. The distance between the centers of the bases can be varied in dependence of deep and surface conditions, the anticipated depth of the discontinuity to be studied, resolution of the processing system and other factors, which lessens the requirements on the regularity and geometrical trueness of the observation system. The case examined is a field set-up of three sources and nine detectors with 27 different seismic traces being used in giving the required sections of the time fields. The seismic information from the broad profile is accumulated, yielding adequate statistical material and ensuring a local nature of the investigation. G.L.C.

43 EARTH RESOURCES

Includes remote sensing of earth resources by aircraft and spacecraft; photogrammetry; and aerial photography.

For instrumentation see *35 Instrumentation and Photography.*

N85-23186*# National Aeronautics and Space Administration. Goddard Space Flight Center, Greenbelt, Md.
LANDSAT-4 SCIENCE CHARACTERIZATION EARLY RESULTS. VOLUME 4: APPLICATIONS
John L. Barker, ed. Washington Jan. 1985 442 p refs Symp. held in Greenbelt, Md., 22-24 Feb. 1983 Original contains imagery. Original photography may be purchased from the EROS Data Center, Sioux Falls., S. D. 57198 ERTS 4 Vol.
(E85-10070; NASA-CP-2355-Vol-4; Rept-85B0115-Vol-4; NAS 1.55:2355-Vol-4) Avail: NTIS HC A19/MF A01 CSCL 08B

The excellent quality of TM data allows researchers to proceed directly with applications analyses, without spending a significant amount of time applying various corrections to the data. The early results derived of TM data are discussed for the following applications: agriculture, land cover/land use, soils, geology, hydrology, wetlands biomass, water quality, and snow. For individual titles, see N85-23187 through N85-23212.

N85-23187*# National Aeronautics and Space Administration. Goddard Space Flight Center, Greenbelt, Md.
OVERVIEW OF TM APPLICATIONS RESEARCH REPORTS
Darrel L. Williams *In its* LANDSAT-4 Sci. Characterization Early Results, Vol. 4 Jan. 1985 p 1-6 ERTS (For primary document see N85-23186 13-43)
Avail: NTIS HC A19/MF A01 CSCL 05B

Applications-oriented users of TM data have every reason to be excited about the possibility of opening up other horizons using TM data. The data appear to be of excellent quality, and the investigations conducted to date, although preliminary, substantiate the findings of earlier research conducted with simulated TM data. Techniques used for sensor/data quality evaluation; data processing, analysis, and display; and comparisons of TM versus MSS data are summarized. A.R.H.

N85-23188*# National Aeronautics and Space Administration. Goddard Space Flight Center, Greenbelt, Md.
IMPACT OF THEMATIC MAPPER SENSOR CHARACTERISTICS ON CLASSIFICATION ACCURACY
Darrel L. Williams, James R. Irons, Brian L. Markham, Ross F. Nelson, David L. Toll, Richard S. Latty (Maryland Univ., College Park), and Mark L. Stauffer (Computer Science Corp.) *In its* LANDSAT-4 Sci. Characterization Early Results, Vol. 4 Jan. 1985 p 7-24 refs Original contains imagery. Original photography may be purchased from the EROS Data Center, Sioux Falls, S.D. 57198 ERTS (For primary document see N85-23186 13-43)
Avail: NTIS HC A19/MF A01 CSCL 14B

A fixed effect, three factor (two levels per factor) analysis of variance was used to quantitatively assess the significance of the improved spectral, spatial and radiometric resolution capabilities of the LANDSAT-4 thematic mapper sensor relative to the familiar MSS sensor. TM data acquired over the Washington, D.C. area were progressively degraded in spectral, spatial and radiometric characteristics to simulate the MSS, and classification accuracies were derived in a consistent manner for all eight treatments in the ANOVA design. Statistical testing of the significance of differences in classification accuracies between treatments indicated that the increased number of spectral bands and the improved quantization capabilities afforded by the TM sensor design would lead to significant improvements in classification accuracies attainable relative to MSS. In contrast, however, the improved spatial resolution provided by the TM sensor did not enhance classification accuracy. This latter result was felt to be more a function of the type of classification algorithms available. A.R.H.

N85-23189*# International Business Machines Corp., Palo Alto, Calif. Scientific Center.

ANALYSIS AND EVALUATION OF THE LANDSAT-4 MSS AND TM SENSORS AND GROUND DATA PROCESSING SYSTEMS: EARLY RESULTS

Ralph Bernstein and Jeffrey B. Lotspiech *In* NASA. Goddard Space Flight Center LANDSAT-4 Sci. Characterization Early Results, Vol. 4 Jan. 1985 p 25-90 refs Original contains imagery. Original photography may be purchased from the EROS Data Center, Sioux Falls, S.D. 57198 ERTS (For primary document see N85-23186 13-43)

(Contract NAS5-27355)

Avail: NTIS HC A19/MF A01 CSCL 14B

The MSS and TM sensor performances were evaluated by studying both the sensors and the characteristics of the data. Information content analysis, image statistics, band-to-band registration, the presence of failed or failing detectors, and sensor resolution are discussed. The TM data were explored from the point of view of adequacy of the ground processing and improvements that could be made to compensate for sensor problems and deficiencies. Radiometric correction processing, compensation for a failed detector, and geometric correction processing are also considered. A.R.H.

N85-23190*# California Univ., Berkeley. Remote Sensing Research Programs.

CHARACTERIZATION OF LANDSAT-4 TM AND MSS IMAGE QUALITY FOR THE INTERPRETATION OF CALIFORNIA'S AGRICULTURAL RESOURCES

Stephen D. DeGloria and Robert N. Colwell *In* NASA. Goddard Space Flight Center LANDSAT-4 Sci. Characterization Early Results, Vol. 4 Jan. 1985 p 91-118 refs Original contains imagery. Original photography may be purchased from the EROS Data Center, Sioux Falls, S.D. 57198 ERTS (For primary document see N85-23186 13-43)

(Contract NAS5-27377)

Avail: NTIS HC A19/MF A01 CSCL 02C

The quality of LANDSAT-4 MSS and TM data was determined by analyzing TM spectral and spatial performance in terms of spectral variability of natural targets and the TM-ground instantaneous field-of-view (IFOV) variability in level and mountainous terrain; and by assessing the suitability of TM and MSS image products for characterizing renewable resourse features. The TM data should be extremelly valuable for crop type and area proportion estimation; undating agricultural land use survey maps at 1:24,000 scale and smaller, field boundary definition; and determining the size and location of individual farmsteads. Ongoing research activities are focused on making spectral and spatial analyses of both MSS and TM analytical film products. The improved spectral, spatial, and radiometric quality of the TM data, should promote a renewed emphasis and interest in direct visual interpretation of these image products, both for updating and improving land stratification in support of resource inventory and for enhancing the image analyst's contribution to computer-assisted analysis procedures. A.R.H.

N85-23191*# Earth Satellite Corp., Chevy Chase, Md.

EVALUATION OF THEMATIC MAPPER PERFORMANCE AS APPLIED TO HYDROCARBON EXPLORATION

John R. Everett, Charles Sheffield, and Jon Dykstra *In* NASA. Goddard Space Flight Center LANDSAT-4 Sci. Characterization Early Results, Vol. 4 Jan. 1985 p 119-126 ERTS (For primary document see N85-23186 13-43)

Avail: NTIS HC A19/MF A01 CSCL 08G

The role data from the first three LANDSAT satellites have in geologic exploration and their current level of acceptance is reviewed and the advantages of LANDSAT 4 TM data over MSS data are discussed. Specially enhanced Thematic Mapper imager can make a very significant contribution to the oil and gas and mineral exploration industries. The TM's increased spatial resolution enables the production of larger scale imagery, which greatly increases the amount of geomorphic and structural information interpretable. TM's greater spectral resolution, combined with the smaller, more homogeneous pixels, should enable a far greater confidence in mapping lithologies and detecting geobotanical anomalies from space. The results from its applications to hydrocarbon and mineral exploration promise to bring the majority of the geologic exploration community into that final stage of acceptance and routine application of the satellite data. A.R.H.

N85-23192*# Jet Propulsion Lab., California Inst. of Tech., Pasadena.

GEOLOGIC UTILITY OF LANSDAT-4 TM DATA

Michael Abrams, Anne B. Kahle, Alan Gillespie, James Conel, and Harold Lang *In* NASA. Goddard Space Flight Center LANDSAT-4 Sci. Characterization Early Results, Vol. 4 Jan. 1985 p 127-130 refs ERTS (For primary document see N85-23186 13-43)

Avail: NTIS HC A19/MF A01 CSCL 08G

The performance of the TM vis-a-vis various geological applications was quantified by analyzing: (1) the geological utility of the data with respect to the increased spatial resolution and number of bands (compared to the MSS); (2) the geometric accuracy; (3) the radiometric performance of the TM scanner. Preliminary analyses were performed on TM scenes: over Death Valley, California, and over southern Arizona. Both scenes were acquired in CCT-PT format, where the data were geometrically and radiometrically corrected. Overall, the TM data appears to contain a marked increase in geologically useful information; however, a number of instrumental or processing artifacts may well limit the ability of the geologist to fully extract this information. A.R.H.

N85-23193*# National Aeronautics and Space Administration. Earth Resources Labs., Bay St. Louis, Miss.

AN INITIAL ANALYSIS OF LANDSAT-4 THEMATIC MAPPER DATA FOR THE DISCRIMINATION OF AGRICULTURAL, FORESTED WETLANDS, AND URBAN LAND COVER

Dale A. Quattrochi *In* NASA. Goddard Space Flight Center LANDSAT-4 Sci. Characterization Early Results, Vol. 4 Jan. 1985 p 131-152 refs Original contains imagery. Original photography may be purchased from the EROS Data Center, Sioux Falls, S.D. 57198 ERTS (For primary document see N85-23186 13-43)

Avail: NTIS HC A19/MF A01 CSCL 08B

The capabilities of TM data for discriminating land covers within three particular cultural and ecological realms was assessed. The agricultural investigation in Poinsett County, Arkansas illustrates that TM data can successfully be used to discriminate a variety of crop cover types within the study area. The single-date TM classification produced results that were significantly better than those developed from multitemporal MSS data. For the Reelfoot Lake area of Tennessee TM data, processed using unsupervised signature development techniques, produced a detailed classification of forested wetlands with excellent accuracy. Even in a small city of approximately 15,000 people (Union City, Tennessee). TM data can successfully be used to spectrally distinguish specific urban classes. Furthermore, the principal components analysis evaluation of the data shows that through photointerpretation, it is possible to distinguish individual buildings and roof responses with the TM. A.R.H.

N85-23194*# National Aeronautics and Space Administration. Lyndon B. Johnson Space Center, Houston, Tex.

PRELIMINARY EVALUATION OF THEMATIC MAPPER IMAGE DATA QUALITY

R. B. MacDonald, F. G. Hall, D. E. Pitts, R. M. Bizzell, S. Yao, C. Sorensen, E. Reyna, and J. Carnes *In* NASA. Goddard Space Flight Center LANDSAT-4 Sci. Characterization Early Results, Vol. 4 Jan. 1985 p 153-162 ref Prepared in cooperation with Lockheed Engineering and Management Services Co., Inc., Houston, Tex. Original contains imagery. Original photography may be purchased from the EROS Data Center, Sioux Falls, S. D. 57198 ERTS (For primary document see N85-23186 13-43)

Avail: NTIS HC A19/MF A01 CSCL 05B

Improvements in the ability to monitor renewable resources/ vegegation due to improvements in the spatial, spectral and radiometric resolution of TM data were evaluated. Results presented from the first 4 months of analysis presented include:

(1) geometric performance; (2) band-to-band registration; (3) modulation transfer function; and (4) crop separabililty performance. Crop separability in Webster County, Iowa and in Mississippi County, Arkansas as determined by cluster and principal components analyses is assessed. A.R.H.

N85-23195*# National Aeronautics and Space Administration. Goddard Space Flight Center, Greenbelt, Md.
ASSESSMENT OF COMPUTER BASED GEOLOGIC MAPPING OF ROCK UNITS IN THE LANDSAT-4 SCENE OF NORTHERN DEATH VALLEY, CALIFORNIA
Nicholas M. Short *In its* LANDSAT-4 Sci. Characterization Early Results, Vol. 4 Jan. 1985 p 163-216 refs Original contains imagery. Original photography may be purchased from the EROS Data Center, Sioux Falls, S.D. 57198 ERTS (For primary document see N85-23186 13-43)
Avail: NTIS HC A19/MF A01 CSCL 08G

Geologists obtain low accuracy levels when maps derived from LANDSAT MSS data are compared with those made by conventional methods. Procedures developed for the IDIMS computer system and used to classify a subset of a TM image of the Death Valley, California - Nevada border are described. Despite the superior resolution, broader spectral coverage, and greater sensitivity inherent to the TM, the actual recorded measured accuracy was in the same narrow range (30 to 60%) recorded for MSS data from earlier LANDSATs. The supervised classification approach appears to be superior to the unsupervised approach when applied to vegetation-sparse surfaces composed of spectrally contrasting rock/soil units distributed in relatively flat to low relief terrain. As spatial resolution improves and optimal spectral bands for identifying rock materials are specified, use of classified multispectral remote sensing data from air and space when coupled with supporting field calibration and checks should become the dominant way in which geologic mapping is carried out in future decades. A.R.H.

N85-23196*# Technische Univ., Munich (West Germany).
A CONCEPT FOR THE PROCESSING AND DISPLAY OF THEMATIC MAPPER DATA
Rupert Haydn *In* NASA. Goddard Space Flight Center LANDSAT-4 Sci. Characterization Early Results, Vol. 4 Jan. 1985 p 217-236 refs ERTS (For primary document see N85-23186 13-43)
Avail: NTIS HC A19/MF A01 CSCL 05B

The thematic mapper system provides spectral information in seven carefully selected spectral bands. The challenge is to devise the best approach for presenting this complex spectral information in a pictorial format which can be understood and accepted as a standard by the growing user community. For photointerpretation purposes, the overall approach in the processing of multispectral, and especially of Thematic Mapper data is based on the independent definition and optimization of individual panchromatic and spectral (interpretive) components and the combined display of these individual interpretive components in a perceivable manner. Processing of the Thematic Mapper data within the framework of interpretive components requires the application of special intensity, hue, saturation (IHS) and synthetic stereo (SST) display techniques. The results to date using these techniques demonstrate improved visual separability of spectral surface categories relative to standard multispectral color composites as well as a greater potential for conducting meaningful spectral-diagnostic analysis. A.R.H.

N85-23197*# National Aeronautics and Space Administration. Goddard Space Flight Center, Greenbelt, Md.
QUICK LOOK ANALYSIS OF TM DATA OF THE WASHINGTON, DISTRICT OF COLUMBIA, AREA
Darrel L. Williams, James R. Irons, Brian L. Markham, Ross F. Nelson, David L. Toll, Richard S. Latty (Maryland Univ., College Park), and Mark L. Stauffer (Computer Sciences Corp., Silver Spring, Md.) *In its* LANDSAT-4 Sci. Characterization Early Results, Vol. 4 Jan. 1985 p 237-250 refs Original contains imagery. Original photography may be purchased from the EROS Data Center, Sioux Falls, S.D. 57198 ERTS (For primary document see N85-23186 13-43)
Avail: NTIS HC A19/MF A01 CSCL 08B

Classification capabilities with TM data result from the interactive effects of all of the sensor's attributes which complicates a more quantitative evaluation of the effects of individual sensor improvements. An experiment conducted to quantify the effect of individual sensor parameters (e.g., spectral, spatial, and radiometric resolution) on classification accuracy is described on classification accuracy. Preliminary results obtained using TM data acquired over the Washington, D.C., area indicate that the additional number of spectral bands and quantization levels of the TM relative to the MSS increase capabilities for the recognition and discrimination of land cover/use categories by per-pixel maximum likelihood classification. The refinement of spatial resolution, however, seems to hinder classification. A.R.H.

N85-23198*# Delaware Univ., Newark. Coll. of Marine Studies.
REMOTE SENSING OF COASTAL WETLANDS BIOMASS USING THEMATIC MAPPER WAVEBANDS
Michael A. Hardisky and Vytautas Klemas *In* NASA. Goddard Space Flight Center LANDSAT-4 Sci. Characterization Early Results, Vol. 4 Jan. 1985 p 151-270 refs ERTS (For primary document see N85-23186 13-43)
(Contract NAS5-27580; Grant NSF DAR-80-17836)
Avail: NTIS HC A19/MF A01 CSCL 08B

Spectral data, simulating thematic mapper bands 3, 4 and 5 were gathered in salt and brackish marshes using a hand-held radiometer. Simple regression models were developed equating spectral radiance indicies with total live biomass for S. alterniflora in a salt marsh and for a variety of plant species in a brackish marsh. Models were then tested and compared to harvest estimates of biomass. In the salt marsh, biomass estimates from spectral data were similar to harvest biomass estimates during most of the growing season. Estimates of annual net aerial primary productivity calculated from spectral data were within 21% of production estimated from harvest data. During August, biomass estimates from spectral data in the brackish marsh were similar to biomass estimated by harvesting techniques but not always comparable at other times in the growing season. A.R.H.

N85-23199*# Agricultural Research Service, Beltsville, Md. Hydrology Lab.
A PRELIMINARY COMPARISON OF THE INFORMATION CONTENT OF DATA FROM THE LANDSAT 4 THEMATIC MAPPER AND MULTISPECTRAL SCANNER
John C. Price *In* NASA. Goddard Space Flight Center LANDSAT-4 Sci. Characterization Early Results, Vol. 4 Jan. 1985 p 271-280 refs ERTS (For primary document see N85-23186 13-43)
Avail: NTIS HC A19/MF A01 CSCL 05B

The thematic mapper (TM) on LANDSAT 4, acquires 6 spectral channels at 30 meter resolution as well as a thermal IR channel at 120 meter resolution. Because both MSS and TM can acquire data simultaneously, the advantages and disadvantages of the two instruments can be directly compared. The information content of the two instruments is compared for areas in a representative agricultural region. Although the parameter information does not equate in an obvious way to the value or utility of the data, it provides a basis for physical interpretation. By focusing on the redundancy of the digital data, the estimation of information content suggests possibilities for algorithms dealing with subsets of the image data, as well as transformations which reduce the total volume of data to be analyzed. To the degree that a satisfactory description by a reduced data set is possible, there exist implications both for design of future satellite instruments and for analysis procedures. A.R.H.

N85-23200*# Technicolor Government Services, Inc., Sioux Falls, S. Dak.
EARLY RESULTS OF INVESTIGATIONS OF LANDSAT 4 THEMATIC MAPPER AND MULTISPECTRAL SCANNER APPLICATIONS
F. G. Sadowski, J. A. Sturdevant, W. H. Anderson, P. M. Seevers, J. W. Feuquay, L. K. Balick, F. A. Waltz, and D. T. Lauer (EROS

Data Center) *In* NASA. Goddard Space Flight Center LANDSAT-4 Sci. Characterization Early Results, Vol. 4 Jan. 1985 p 281-298 refs Original contains imagery. Original photography may be purchased from the EROS Data Center, Sioux Falls, S. D. 57198 ERTS (For primary document see N85-23186 13-43)
Avail: NTIS HC A19/MF A01 CSCL 08B

The TM digital data were evaluated for their potential to provide improved land cover information. The analyses included: (1) testing for information that may be offered by the new TM spectral bands, and (2) comparing data characteristics for equivalent spectral bands of the TM and MSS sensors. The analyses were conducted on several large samples of pixels corresponding to five broad land cover classes. Some TM spectral data are presented and evaluated as single-band, black-and-white images, and in several three-band color-composite images. Some data transformations which can be used to present TM data in a manner that is potentially more useful for analysis or display are demonstrated. These transformations enable generating hue, intensity, and saturation data space from red, green, and blue color space, as well as perspective view images. A.R.H.

N85-23201*# National Aeronautics and Space Administration. Lyndon B. Johnson Space Center, Houston, Tex.
THEMATIC MAPPER DATA QUALITY AND PERFORMANCE ASSESSMENT IN RENEWABLE RESOURCES/AGRICULTURE/ REMOTE SENSING
R. M. Bizzell and H. L. Prior *In* NASA. Goddard Space Flight Center LANDSAT-4 Sci. Characterization Early Results, Vol. 4 Jan. 1985 p 299-312 refs Original contains imagery. Original photography may be purchased from the EROS Data Center, Sioux Falls, S.D. 57198 ERTS (For primary document see N85-23186 13-43)
(Proj. AgRISTARS)
Avail: NTIS HC A19/MF A01 CSCL 05B

Analysis of the early thematic mapper (TM) data indicate the TM sensor and associated ground processing are performing equal to the high expectations and within advertised specifications. The overall TM system with improved resolution, together with additional and more optimumly placed spectral bands shows much promise for benefits in future analysis activities. By selecting man-made features of known dimensions (e.g., highways, airfields, buildings, and isolated water bodies), an assessment was made of the TM performance relative to the specified 30-meter (98-foot) resolution. The increase of spatial resolution of TM (30 m) over MSS (80 M) appears to be significant not only in resolving spectrally distinct classes that were previously undefinable but also in distinguishing within-field variability. An Important result of the early TM evaluation and pre-TM analyses was the development of an integrated system to receive LANDSAT-4 TM (as well as MSS) data and analyze the data via various approaches. B.G.

N85-23202*# National Aeronautics and Space Administration. Goddard Space Flight Center, Greenbelt, Md.
PRELIMINARY COMPARISONS OF THE INFORMATION CONTENT AND UTILITY OF TM VERSUS MSS DATA
Brian L. Markham *In its* LANDSAT-4 Sci. Characterization Early Results, Vol. 4 Jan. 1985 p 313-324 refs Original contains imagery. Original photography may be purchased from the EROS Data Center, Sioux Falls, S.D. 57198 ERTS (For primary document see N85-23186 13-43)
Avail: NTIS HC A19/MF A01 CSCL 05B

Some preliminary indications were provided as to the relative merits of actual TM data versus MSS data for land cover mapping related applications. Three analyses were designed which had sensitivity to the differences in spectral, spatial and radiometric parameters between the TM and MSS. In the water body analysis, a primarily spatially related test, the detectability of small uniform targets was examined. The principal components analysis, an examination of the inherent dimensionality of the data, was more spectrally and radiometrically related. The spectral clustering analysis, also heavily spectrally and radiometrically influenced, provided information on the types of targets separable on TM versus MSS data. These analyses were to be conducted with simultaneously collected LANDSAT-4 complete TM (7 band) and MSS (4 band) data. In actuality, 4-band TM data, and archived LANDSAT-2 MSS data of the same area were used. B.G.

N85-23203*# Delaware Univ., Newark. Coll. of Marine Studies.
ASSESSING LANDSAT TM AND MSS DATA FOR DETECTING SUBMERGED PLANT COMMUNITIES
Steven G. Ackleson and Vytautas Klemas *In* NASA. Goddard Space Flight Center LANDSAT-4 Sci. Characterization Early Results, Vol. 4 Jan. 1985 p 325-336 refs ERTS (For primary document see N85-23186 13-43)
Avail: NTIS HC A19/MF A01 CSCL 08B

The spectra, spacial, and radiometric characteristics of LANDSAT TM and MSS data for detecting and monitoring submerged plant communities were assessed. The following preliminary results focus upon the spectral aspects of the problem in which a submerged plant canopy is to be distinguished from a surrounding bottom of sand or mud. The effectiveness of an orbiting sensor in discriminating between submerged features and how strongly the bottom signal is attenuated by the water column. In optically shallow water the inherent contrast is the controlling factor. Thus, the optimum sensor band is that which correlates with the greatest inherent contrast between the submerged features. In optically deeper water, the optimum sensor band is that in which the bottom signal is attenuated the least. Author

N85-23204*# Agricultural Research Service, Durant, Okla.
A FIRST EVALUATION OF LANDSAT TM DATA TO MONITOR SUSPENDED SEDIMENTS IN LAKES
F. R. Schiebe, J. C. Ritchie, and G. O. Boatwright *In* NASA. Goddard Space Flight Center LANDSAT-4 Sci. Characterization Early Results, Vol. 4 Jan. 1985 p 337-348 refs Prepared in cooperation with Agricultural Research Service, Beltsville, Md. and Agricultural Research Service, Houston, Tex. Original contains imagery. Original photography may be purchased from the EROS Data Center, Sioux Falls, S.D. 57198 ERTS (For primary document see N85-23186 13-43)
Avail: NTIS HC A19/MF A01 CSCL 08H

The use of LANDSAT to monitor and track changes in the water quality of Lake Chicot, Arizona was assessed using MSS and TM digital data from nine water sites. Results show that: (1) TM Bands 1, 2, 3, and 4 appear to be providing information on concentrations of particulate matter suspended in surface waters. These bands are also highly interrelated for water samples; (2) preliminary evaluation indicates that TM Band 3 showed the best relationship to surface suspended solids; (3) TM Bands 5 and 7 are useful for separating water from nonwater areas; (4) the MSS Bands 2 and 3 can be related to suspended solids in surface water, as has already been shown from previous LANDSAT research; and (5) analysis of TM Band 6 indicates that while synoptic temperature patterns may be discerned, the digital sensitivity to a two degree temperature difference is low. A.R.H.

N85-23205*# California Univ., Santa Barbara.
SNOW REFLECTANCE FROM THEMATIC MAPPER
Jeff Dozier *In* NASA. Goddard Space Flight Center LANDSAT-4 Sci. Characterization Early Results, Vol. 4 Jan. 1985 p 349-358 refs Previously announced as N83-32144 Original contains imagery. Original photography may be purchased from the EROS Data Center, Sioux Falls, S.D. 57198 ERTS (For primary document see N85-23186 13-43)
Avail: NTIS HC A19/MF A01

Calculations of snow reflectance in all 6 TM reflective bands (i.e., 1,2,3,4,5, and 7) using a delta Eddington model show that snow reflectance in bands 4,5, and 7 is sensitive to grain size. Efforts to interpret the surface optical grain size for the spectral extension of albedo are described. Results show the TM data include spectral channels suitable for snow/cloud discrimination and for snow albedo measurements that can be extended throughout the solar spectrum. Except for band 1, the dynamic range is large enough that saturation occurs only occasionally. The finer resolution gives much better detail on the snowcovered area and might make it possible to use textural information instead

of the snowline as an index to the amount of snow melt runoff.
A.R.H.

N85-23206*# National Aeronautics and Space Administration. Lyndon B. Johnson Space Center, Houston, Tex.
PRELIMINARY EVALUATION OF TM FOR SOILS INFORMATION
David R. Thompson, Keith E. Henderson, A. Glen Houston, and David E. Pitts *In* NASA. Goddard Space Flight Center LANDSAT-4 Sci. Characterization Early Results, Vol. 4 Jan. 1985 p 359-368 refs Original contains imagery. Original photography may be purchased from the EROS Data Center, Sioux Falls, S.D. 57198 ERTS (For primary document see N85-23186 13-43)
Avail: NTIS HC A19/MF A01 CSCL 08M

The capability of the LANDSAT TM for providing information for soil association maps and for detecting soil properties (variability within vegetated fields) was assessed using TM imagery of fields in Mississippi County, Arkansas that were planted with rice, cotton, and soybeans. Results indicate that the TM bands are providing information that is related to the soil properties within the field. Over large areas, these bands also appear to provide information that is related to the soil properties that are important to plant condition. While these results are only an indication of the information that TM can provide, they do indicate the TM data--especially, the mid-TR and thermal bands--show the capability for separating vegetated soil landscapes on a broad basis. The analysis at the field level with a growing crop also indicates that TM, with its additional and narrower bands and improved spatial and radiometric resolution is influenced by within field variability due to soils that has to be accounted for in the analysis of TM data.
A.R.H.

N85-23207*# Natural Environment Research Council, London (England).
THE USE OF THEMATIC MAPPER DATA FOR LAND COVER DISCRIMINATION: PRELIMINARY RESULTS FROM THE UK SATMAP PROGRAMME
M. J. Jackson, J. R. Baker, J. R. G. Townshend (Reading Univ., England), J. E. Gayler (Reading Univ., England), and J. R. Hardy (Reading Univ., England) *In* NASA. Goddard Space Flight Center LANDSAT-4 Sci. Characterization Early Results, Vol. 4 Jan. 1985 p 369-386 refs Previously announced as N84-13631 Original contains imagery. Original photography may be purchased from the EROS Data Center, Sioux Falls, S.D. 57198 ERTS (For primary document see N85-23186 13-43)
Avail: NTIS HC A19/MF A01

The principal objectives of the UK SATMaP program are to determine thematic mapper (TM) performance with particular reference to spatial resolution properties and geometric characteristics of the data. So far, analysis is restricted to images from the U.S. and concentrates on spectra and radiometric properties. The results indicate that the data are inherently three dimensional compared with the two dimensional character of MSS data. Preliminary classification results indicate the importance of the near infrared band (TM 4), at least one middle infrared band (TM 5 or TM 6) and at least one of the visible bands (preferably either TM 3 or TM 1). The thermal infrared also appears to have discriminatory ability despite its coarser spatial resolution. For band 4 the forward and reverse scans show somewhat different spectral responses in one scene but this effect is absent in the other analyzed. From examination of the histograms it would appear that the full 8 bit quantization is not being effectively utilized for all the bands.
M.G.

N85-23208*# National Aeronautics and Space Administration. Goddard Space Flight Center, Greenbelt, Md.
PRELIMINARY STUDY OF INFORMATION EXTRACTION OF LANDSAT TM DATA FOR A SUBURBAN/REGIONAL TEST SITE
David L. Toll *In its* LANDSAT-4 Sci. Characterization Early Results, Vol. 4 Jan. 1985 p 387-402 refs Original contains imagery. Original photography may be purchased from the EROS Data Center, Sioux Falls, S.D. 57198 ERTS (For primary document see N85-23186 13-43)
Avail: NTIS HC A19/MF A01 CSCL 05B

A substantial amount of spectral information is available from TM (as compared to MSS) data for a 14.25 square km area between Beltsville and Laurel, Maryland. Large buildings and street patterns were resolved in the TM imagery. While there was added information content in TM data for discriminating surburban/regional land cover, characteristics of MSS can improve land cover discrimination over TM when conventional classification procedures are used on digital data. The improved qualitization of TM is likely valuable in situations where there are spectral similarities between classes. The spatial resolution in TM decreased land cover discrimination as a result of increased within class variability. For many general digital evaluations, inclusion of four bands representing the four spectral regions can provide much useful land cover discrimination. Inclusion of TM 6 indicates an improvement in spectral class discrimination. Of primary spectral importance is the discrimination between water, vegetative surfaces, and impervious surfaces due to differences in thermal properties. Results from the principle component transformed data clearly indicates additional information content in TM over MSS.
A.R.H.

N85-23209*# National Aeronautics and Space Administration. Goddard Space Flight Center, Greenbelt, Md.
COMPARATIVE TECHNIQUES USED TO EVALUATE THEMATIC MAPPER DATA FOR LAND COVER CLASSIFICATION IN LOGAN COUNTY, WEST VIRGINIA
J. O. Brumfield (Marshall Univ., Huntington, W. Va.), R. G. Witt, H. W. Blodget, and R. F. Marcell (Computer Sciences Corp., Silver Spring, Md.) *In its* LANDSAT-4 Sci. Characterization Early Results, Vol. 4 Jan. 1985 p 403-414 refs ERTS (For primary document see N85-23186 13-43)
Avail: NTIS HC A19/MF A01 CSCL 08B

Several digital data processing techniques were evaluated in an effort to identify and map active/abandoned, partially reclaimed, and fully revegetated surface mine areas in the central portion of Logan County. The TM data were first subjected to various enhancement procedures, including a linear contrast stretch, principal components and canonical analysis transformations. At the same time, four general procedures were followed to produce six classifications as a means of comparing the techniques involved. Preliminary results show that various feature extraction/data reduction techniques provide classification results equal or superior to the more straightforward unsupervised clustering technique. Analyst interaction time for labelling clusters is reduced using the canonical analysis and principal components procedures, though the canonical technique has clearly produced better results to date.
A.R.H.

N85-23210*# National Aeronautics and Space Administration. Goddard Space Flight Center, Greenbelt, Md.
COMPARISON OF MSS AND TM DATA FOR LANDCOVER CLASSIFICATION IN THE CHESAPEAKE BAY AREA: A PRELIMINARY REPORT
P. J. Mulligan, J. C. Gervin, and Y. C. Lu (Computer Sciences Corp., Greenbelt, Md.) *In its* LANDSAT-4 Sci. Characterization Early Results, Vol. 4 Jan. 1985 p 415-420 refs ERTS (For primary document see N85-23186 13-43)
Avail: NTIS HC A19/MF A01 CSCL 05B

An area bordering the Eastern Shore of the Chesapeake Bay was selected for study and classified using unsupervised techniques applied to LANDSAT-2 MSS data and several band combinations of LANDSAT-4 TM data. The accuracies of these Level I land cover classifications were verified using the Taylor's Island USGS 7.5 minute topographic map which was photointerpreted, digitized and rasterized. The the Taylor's Island map, comparing the MSS and TM three band (2 3 4) classifications, the increased resolution of TM produced a small improvement in overall accuracy of 1% correct due primarily to a small improvement, and 1% and 3%, in areas such as water and woodland. This was expected as the MSS data typically produce high accuracies for categories which cover large contiguous areas. However, in the categories covering smaller areas within the map there was generally an improve-

ment of at least 10%. Classification of the important residential category improved 12%, and wetlands were mapped with 11% greater accuracy. A.R.H.

N85-23211*# National Aeronautics and Space Administration. Goddard Space Flight Center, Greenbelt, Md.
COMPARISON OF LAND COVER INFORMATION FROM LANDSAT MULTISPECTRAL SCANNER (MSS) AND AIRBORNE THEMATIC MAPPER SIMULATOR (TMS) DATA FOR HYDROLOGIC APPLICATIONS
J. C. Gervin, Y. C. Lu (Computer Sciences Corp., Greenbelt, Md.), and R. F. Marcell (Computer Sciences Corp., Greenbelt, Md.) *In* NASA. Goddard Space Flight Center LANDSAT-4 Sci. Characterization Early Results, Vol. 4 Jan. 1985 p 421-430 refs ERTS (For primary document see N85-23186 13-43)
Avail: NTIS HC A19/MF A01 CSCL 05B

Thematic mapper simulator (TMS) data produced a more accurate and spatially contiguous classification than MSS for the Clinton River Basin in Michigan. While the accuracy of the 4-band TMS data set was as good as the 7-band, the 3-band TMS data sets were also better than the MSS. The combination of bands selected based on the transformed divergence technique provided one band in each of the major regions of the spectrum: visible (band 3), near IR (band 4), middle IR (band 5) and thermal IR (band 7). These results should be viewed with some caution, since the data are from a TMS rather than the actual TM and the MSS data were obtained in early summer while the TMS was flown in late summer. The higher accuracies for the developed categories (residential and commercial) should improve the predictions of runoff in flood forecasting models and of flood damage for damage calculation models appreciably. A.R.H.

N85-23212*# National Aeronautics and Space Administration. Goddard Space Flight Center, Greenbelt, Md.
RELATIVE ACCURACY ASSESSMENT OF LANDSAT-4 MSS AND TM DATA FOR LEVEL 1 LAND COVER INVENTORY
E. M. Middleton, Y. C. Lu (Computer Sciences Corp., Silver Spring, Md.), R. G. Witt, and R. S. Sekhon (Computer Sciences Corp., Silver Spring, Md.) *In its* LANDSAT-4 Sci. Characterization Early Results, Vol. 4 Jan. 1985 p 431-446 refs ERTS (For primary document see N85-23186 13-43)
Avail: NTIS HC A19/MF A01 CSCL 05B

Digital data for the Washington, DC scene simultaneously acquired by the LANDSAT-4 Multispectral Scanner (MSS) and the LANDSAT-4 thematic mapper (TM) was compared. Classification success for the TM and MSS data sets was determined by a per pixel comparison with digitized ground verification data (GVD). These GVD were comprised of Level 7 land cover (developed, agriculture, forest, water, wetlands, and barren) for four USGS 7.5 minute topographic quadrangle maps. The relative improvement in classification success for TM was between 11% and 14%, or about a factor of 1.3, for these data. This represents a meaningful improvement in accuracy for Level 7 land cover categorization for TM relative to MSS, particularly when errors of omission and commission were considered. A.R.H.

N85-23213*# Kansas Univ. Center for Research, Inc., Lawrence. Remote Sensing Lab.
THE MICROWAVE PROPAGATION AND BACKSCATTERING CHARACTERISTICS OF VEGETATION Final Report
F. T. Ulaby, Principal Investigator and E. A. Wilson Dec. 1984 231 p refs ERTS
(Grant NAG5-272)
(E85-10088; NASA-CR-175523; NAS 1.26:175523) Avail: NTIS HC A11/MF A01 CSCL 20N

A semi-empirical model for microwave backscatter from vegetation was developed and a complete set of canope attenuation measurements as a function of frequency, incidence angle and polarization was acquired. The semi-empirical model was tested on corn and sorghum data over the 8 to 35 GHz range. The model generally provided an excellent fit to the data as measured by the correlation and rms error between observed and predicted data. The model also predicted reasonable values of canopy attenuation. The attenuation data was acquired over the 1.6 to 10.2 GHz range for the linear polarizations at approximately 20 deg and 50 deg incidence angles for wheat and soybeans. An attenuation model is proposed which provides reasonable agreement with the measured data. Author

N85-23214*# Arizona Univ., Tucson.
AN INVESTIGATION OF SEVERAL ASPECTS OF LANDSAT-5 DATA QUALITY Quarterly Progress Report
Robert C. Wrigley, Principal Investigator 20 Dec. 1984 17 p Sponsored by NASA ERTS
(E85-10096; NASA-CR-175531; NAS 1.26:175531) Avail: NTIS HC A02/MF A01 CSCL 05B

Band-to-band registration, geodetic registration, interdector noise, and the modulation transfer function (MTE) are discussed for the Palmer County; TX scene. Band combinations for several LANDSAT 4 and LANDSAT 5 scenes; the geodetic registration test for the Sacramento, CA area; periodic noise components in TM band 5; and grey level measurements by detector for Great Salt Lake (UT) dark water forescans and backscans are considered. Results of MTF analyses of the San Mateo Bridge and of TM high resolution and aerial Daedalus scanner imagery are consistent and appear to be repeatable. An oil-on-sand target was constructed on the White Sands Missile Range in New Mexico. The two-image analysis procedure used is summarized. A.R.H.

N85-23215*# MacQuarie Univ., North Ryde (Australia).
[MAGSAT ANOMALY FIELD DATA OF THE CRUSTAL PROPERTIES OF AUSTRALIA]
[1983] 88 p refs Original contains color imagery. Original photography may be purchased from the EROS Data Center, Sioux Falls, S.D. 57198 ERTS
(E85-10100; NASA-CR-175615; NAS 1.26:175615) Avail: NTIS HC A05/MF A01 CSCL 05B

Progress is reported in producing maps of Australia showing; crustal magnetic anomalies at constant elevation; bulk surface magnetization; and the geomagnetic field intensity, inclination and declination for the Australian region from global models of the geomagnetic field derived from MAGSAT data. The development of a data base management system is also considered. For individual titles, see N85-23216 through N85-23220.

N85-23216*# MacQuarie Univ., North Ryde (Australia). Centre fot Geophysical Exploration Research.
AN INVESTIGATION OF THE CRUSTAL PROPERTIES OF AUSTRALIA AND SURROUNDING REGIONS DERIVED FROM INTERPRETATION OF MAGSAT ANOMALY FIELD DATA Final Report
B. David Johnson, C. N. G. Dampney, and B. J. J. Embleton (CSIRO, North Ryde, Australia) *In its* MAGSAT Anomaly Field Data of the Crustal Propeties of Australia [1983] 40 p refs Original contains color imagery. Original photography may be purchased from the EROS Data Center, Sioux Falls., S.D. 57198 ERTS (For primary document see N85-23215 13-43)
Avail: NTIS HC A05/MF A01 CSCL 08G

The 2 deg averaged data set was analyzed and filtered to produce a magnetic anomaly map of the Australian continental region. The map was overlain on a tectonic map of Australia and correlations were made. A data set was selected that is dominated by relatively low elevation profiles with small changes of elevation within the Australian area in an effort to maximize the crustal anomaly field signal and reduce the eifect of variation in satellite elevation. Support systems, both hardware and software are described and best-worst case errors encountered during processing of MAGSAT investigator tapes are summarized. The Broken Ridge anomaly was studied for model development purposes. A.R.H.

N85-23217*# MacQuarie Univ., North Ryde (Australia). School of Mathematics and Physics.
GADB: A DATABASE FACILITY FOR MODELLING NATURALLY OCCURRING GEOPHYSICAL FIELDS
C. N. G. Dampney *In its* MAGSAT Anomaly Field Data of the

Crustal Properties of Australia [1983] 12 p refs ERTS (For primary document see N85-23215 13-43)
Avail: NTIS HC A05/MF A01 CSCL 05B

In certain kinds of geophysical surveys, the fields are continua, but measured at discrete points referenced by their position or time of measurement. Systems of this kind are better modelled by databases built from basic data structures attuned to representing traverses across continua that are not of pre-defined fixed length. The general Array DataBase is built on arrays (ordered sequencies of data) with each array holding data elements of one type. The arrays each occupy their own physical data set, in turn inter-related by a hierarchy to other arrays over the same space/time reference points. The GADB illustrates the principle that a data facility should reflect the fundamental properties of its data, and support retrieval based on the application's view. The GADB is being tested by its use in NASA's project MAGSAT.
A.R.H.

N85-23218*# MacQuarie Univ., North Ryde (Australia). Centre for Geophysical Exploration Research.
DATA SELECTION TECHNIQUES IN THE INTERPRETATION OF MAGSAT DATA OVER AUSTRALIA
B. David Johnson and C. N. G. Dampney *In its* MAGSAT Anomaly Field Data of the Crustal Properties of Australia [1983] 6 p Presented at the 52nd Ann. Meeting of the Soc. of Exploration Geophys., Dallas, 17-21 Oct. 1982 Original contains color imagery. Original photography may be purchased from the EROS Data Center, Sioux Falls., S.D. 57198 ERTS (For primary document see N85-23215 13-43)
Avail: NTIS HC A05/MF A01 CSCL 05B

The MAGSAT data require critical selection in order to produce a self-consistent data set suitable for map construction and subsequent interpretation. Interactive data selection techniques are described which involve the use of a special-purpose profile-oriented data base and a colour graphics display. The careful application of these data selection techniques permits validation every data value and ensures that the best possible self-consistent data set is being used to construct the maps of the magnetic field measured at satellite altitudes over Australia. A.R.H.

N85-23219*# National Aeronautics and Space Administration. Goddard Space Flight Center, Greenbelt, Md.
REMANENT MAGNETIZATION MODEL FOR THE BROKEN RIDGE SATELLITE MAGNETIC ANOMALY
B. David Johnson (Macquarie Univ., North Ryde, Australia) *In* Macquarie Univ. MAGSAT Anomaly Field Data of the Crustal Properties of Australia [1983] 22 p refs ERTS (For primary document see N85-23215 13-43)
Avail: NTIS HC A05/MF A01 CSCL 08G

A crustal model for the interpretation of the Broken Ridge satellite magnetic anomaly was constructed from bathymetric data assuming an Airy-type isostatic compensation. An average crustal magnetization of 6 A.m is required to account for the observed anomaly amplitudes provided that the whole crust is homogeneously magnetized. In contrast, a model representing only the topographic expression of the Broken Ridge, above the surrounding sea floor, requires a magnetization of the order of 40 A.m-1. Since this latter figure is much higher than is to be expected from studies of magnetic properties of oceanic rocks, it is concluded that the majority of the crustal volume of Broken Ridge is magnetized relatively uniformly. The direction of the source magnetization is consistent with an inclination shallower than the present geomagnetic field and close to that of an axial dipole. Since a more northerly source location for Broken Ridge is contrary to the paleolatitude data it is though that the magnetization represents a magnetization obtained by averaging the geomagnetic field direction over a sufficient time to remove secular variation effects. This pattern is indicative of viscous magnetization. A.R.H.

N85-23220*# MacQuarie Univ., North Ryde (Australia). School of Mathematics and Physics.
PRECEDENCY CONTROL AND OTHER SEMANTIC INTEGRITY ISSUES IN A WORKBENCH DATABASE
C. N. G. Dampney *In its* MAGSAT Anomaly Field Data of the Crustal Properties of Australia [1983] 8 p refs (For primary document see N85-23215 13-43)
Avail: NTIS HC A05/MF A01 CSCL 05B

Most database systems model the current state of a system of real world discrete and simple entities together with their relationships. By examining instead a database system that is a workbench and models more complicated entities, a fresh perspective is gained. Specifically, semantic integrity is analysed. Four aspects distinct from physical integrity are identified, namely - access, failure, concurrency and precedency. Access control is shown to be the consequence of semantic interdependency between data and its matching semantic routines. Failure, concurrency precedency controls are concerned with preventing processes interfering with each other. Precedency is a new concept in the database context. It expresses a constraint between processes that act on the database. As processes create, update and delete entities they in general obey a partial ordering imposed by the semantics of their actions. Precedency control ensures that data remains consistent with respect to this partial order.
Author

N85-23221*# National Aeronautics and Space Administration. Goddard Space Flight Center, Greenbelt, Md.
CALCULATIONS OF MICROWAVE BRIGHTNESS TEMPERATURE OF ROUGH SOIL SURFACES: BARE FIELD
Tsan Mo (Computer Sciences Corp., Beltsville, Md.), Thomas J. Schmugge, and James R. Wang Mar. 1985 88 p refs
(NASA-TM-86200; NAS 1.15:86200) Avail: NTIS HC A05/MF A01 CSCL 08M

A model for simulating the brightness temperatures of soils with rough surfaces is developed. The surface emissivity of the soil media is obtained by the integration of the bistatic scattering coefficients for rough surfaces. The roughness of a soil surface is characterized by two parameters, the surface height standard deviation sigma and its horizontal correlation length l. The model calculations are compared to the measured angular variations of the polarized brightness temperatures at both 1.4 GHz and 5 GHz frequences. A nonlinear least-squares fitting method is used to obtain the values of delta and l that best characterize the surface roughness. The effect of shadowing is incorporated by introducing a function S(theta), which represents the probability that a point on a rough surface is not shadowed by other parts of the surface. The model results for the horizontal polarization are in excellent agreement with the data. However, for the vertical polarization, some discrepancies exist between the calculations and data, particularly at the 1.4 GHz frequency. Possible causes of the discrepancy are discussed. B.W.

N85-23222*# Jet Propulsion Lab., California Inst. of Tech., Pasadena.
SCIENCE OPPORTUNITIES USING THE NASA SCATTEROMETER ON N-ROSS
M. H. Freilich 1 Feb. 1985 44 p refs
(Contract NAS7-918)
(NASA-CR-175639; JPL-Pub-84-57; NAS 1.26:175639) Avail: NTIS HC A03/MF A01 CSCL 14B

The National Aeronautics and Space Administration scatterometer (NSCAT) is to be flown as part of the Navy Remote Ocean Sensing System (N-ROSS) scheduled for launch in 1989. The NSCAT will provide frequent accurate and high-resolution measurements of vector winds over the global oceans. NSCAT data will be applicable to a wide range of studies in oceanography, meteorology, and instrument science. The N-ROSS mission, is outlined, are described. The capabilities of the NSCAT flight instrument and an associated NASA research ground data-processing and distribution system, and representative oceanographic meteorological, and instrument science studies that may benefit from NSCAT data are surveyed. Author

N85-23223*# National Aeronautics and Space Administration. Goddard Space Flight Center, Greenbelt, Md.
REMOTE SENSING OF SNOW AND EVAPOTRANSPIRATION

Thomas Schmugge, ed. Washington Feb. 1985 176 p refs Proc. of 2nd workshop held in Honolulu, Hawaii, 15-19 Nov. 1983 Original contains color illustrations
(NASA-CP-2363; Rept-84B0036; NAS 1.55:2363) Avail: NTIS HC A09/MF A01 CSCL 08L

The use of snowmelt runoff models from both the U.S. and Japan for simulating discharge on basins in both countries is discussed as well as research in snowpack properties and evapotranspiration using remotely sensed data. For individual titles, see N85-23224 through N85-23236.

N85-23224*# National Aeronautics and Space Administration, Washington, D. C.
NASA'S LAND REMOTE SENSING PLANS FOR THE 1980'S
Howard C. Higg, Kristine M. Butera, and Mark Settle *In* NASA Goddard Space Flight Center Remote Sensing of Snow and Evapotranspiration Feb. 1985 p 1-5 (For primary document see N85-23223 13-43)
Avail: NTIS HC A09/MF A01 CSCL 05A

Research since the launch of LANDSAT-1 has been primarily directed to the development of analysis techniques and to the conduct of applications studies designed to address resource information needs in the United States and in many other countries. The current measurement capabilities represented by MSS, TM, and SIR-A and B, coupled with the present level of remote sensing understanding and the state of knowledge in the discipline earth sciences, form the foundation for NASA's Land Processes Program. Science issues to be systematically addressed include: energy balance, hydrologic cycle, biogeochemical cycles, biological productivity, rock cycle, landscape development, geological and botanical associations, and land surface inventory, monitoring, and modeling. A global perspective is required for using remote sensing technology for problem solving or applications context. A successful model for this kind of activity involves joint research with a user entity where the user provides a test site and ground truth and NASA provides the remote sensing techniques to be tested.
A.R.H.

N85-23225*# Science and Technology Agency, Tokyo (Japan). National Inst. of Resources.
GENERAL REPORT OF THE RESEARCHES OF SNOWPACK PROPERTIES, SNOWMELT RUNOFF AND EVAPOTRANSPIRATION IN JAPAN
Kaname Takeda *In* NASA Goddard Space Flight Center Remote Sensing of Snow and Evapotranspiration Feb. 1985 p 7-8 (For primary document see N85-23223 13-43)
Avail: NTIS HC A09/MF A01 CSCL 08L

A method was developed for estimating the distribution of snow and the snow water equivalent in Japan by combining LANDSAT data with the degree day method. A snow runoff model was improved and applied to the Okutadami River basin. The Martinec Rango model from the U.S. was applied to Japanese river basins to verify its applicability. This model was then compared with the Japanese model. Analysis of microwave measurements obtained by a radiometer on a tower over dry snow in Hokkaido indicate a certain correlation between brightness temperature and snowpack properties. A correlation between brightness temperature and depth of dry snow in an inland plain area was revealed in NIMBUS SMMR data obtained from the U.S. Calculation of evaporation using airborne remote sensing data and a Priestley-Taylor type of equation shows that the differentiation of evaporation with vegetation type is not remarkable because of little evapotransportation in winter.
A.R.H.

N85-23226*# Agricultural Research Service, Beltsville, Md. Hydrology Lab.
SNOWMELT-RUNOFF MODEL UTILIZING REMOTELY-SENSED DATA
A. Rango *In* NASA Goddard Space Flight Center Remote Sensing of Snow and Evapotranspiration Feb. 1985 p 9-27 ref (For primary document see N85-23223 13-43)
Avail: NTIS HC A09/MF A01 CSCL 08L

Remotely sensed snow cover information is the critical data input for the Snowmelt-Runoff Model (SRM), which was developed to simulatke discharge from mountain basins where snowmelt is an important component of runoff. Of simple structure, the model requires only input of temperature, precipitation, and snow covered area. SRM was run successfully on two widely separated basins. The simulations on the Kings River basin are significant because of the large basin area (4000 sq km) and the adequate performance in the most extreme drought year of record (1976). The performance of SRM on the Okutadami River basin was important because it was accomplished with minimum snow cover data available. Tables show: optimum and minimum conditions for model application; basin sizes and elevations where SRM was applied; and SRM strengths and weaknesses. Graphs show results of discharge simulation.
A.R.H.

N85-23227*# Science and Technology Agency, Tokyo (Japan). Environmental Research and Technology Inst.
SNOWMELT RUNOFF MODEL IN JAPAN
Kenji Ishihara, Yoshiaki Nishimura, and Kaname Takeda *In* NASA Goddard Space Flight Center Remote Sensing of Snow and Evapotranspiration Feb. 1985 p 29-52 refs (For primary document see N85-23223 13-43)
Avail: NTIS HC A09/MF A01 CSCL 08L

The preliminary Japanese snowmelt runoff model was modified so that all the input variables arc of the antecedent days and the inflow of the previous day is taken into account. A few LANDSAT images obtained in the past were effectively used to verify and modify the depletion curve induced from the snow water equivalent distribution at maximum stage and the accumulated degree days at one representative point selected in the basin. Together with the depletion curve, the relationship between the basin ide daily snowmelt amount and the air temperature at the point above are exhibited homograph form for the convenience of the model user. The runoff forecasting procedure is summarized.
A.R.H.

N85-23228*# Science and Technology Agency, Tokyo (Japan). Environmental Research and Technology Inst.
APPLICATION OF MARTINEC-RANGO MODEL TO RIVER BASIN IN JAPAN
Kenji Tshihara, Masayuki Inoue, and Kaname Takeda *In* NASA Goddard Space Flight Center Remote Sensing of Snow and Evapotranspiration Feb. 1985 p 53-59 refs (For primary document see N85-23223 13-43)
Avail: NTIS HC A09/MF A01 CSCL 08H

Variables and parameters used in applying the Martinec-Rango model to Japan's Okutadami River basin are given. The calculated inflow for three snowmelt seasons is shown in relation to the observed inflow. When the peak inflow occurs, two values of the calculated and the observed do not coincide with each other. A one day lag can be seen between them. Most periods in the season (except peak stage) exhibited a good agreement.
A.R.H.

N85-23229*# Science and Technology Agency, Tokyo (Japan).
DISTRIBUTION OF SNOW AND MAXIMUM SNOW WATER EQUIVALENT OBTAINED BY LANDSAT DATA AND DEGREE DAY METHOD
Kaname Takeda, Hiroaki Ochiai, and Shoji Takeuchi *In* NASA Goddard Space Flight Center Remote Sensing of Snow and Evapotranspiration Feb. 1985 p 60-64 (For primary document see N85-23223 13-43)
Avail: NTIS HC A09/MF A01 CSCL 08H

Maximum snow water equivalence and snowcover distribution are estimated using several LANDSAT data taken in snowmelting season over a four year period. The test site is Okutadami-gawa Basin located in the central position of Tohoku-Kanto-Chubu District. The year to year normalization for snowmelt volume computation on the snow line is conducted by year to year correction of degree days using the snowcover percentage within the test basin obtained from LANDSAT data. The maximum snow water equivalent map in the test basin is generated based on the normalized snowmelt volume on the snow line extracted from four LANDSAT data taken in a different year. The snowcover distribution on an arbitrary day in snowmelting of 1982 is estimated from the

maximum snow water equivalent map. The estimated snowcover is compared with the snowcover area extracted from NOAA-AVHRR data taken on the same day. The applicability of the snow estimation using LANDSAT data is discussed. Author

N85-23230*# National Aeronautics and Space Administration. Goddard Space Flight Center, Greenbelt, Md.
MICROWAVE RADIOMETER OBSERVATIONS OF SNOWPACK PROPERTIES AND COMPARISON OF U.S. JAPANESE RESULTS
A. T. C. Chang *In its* Remote Sensing of Snow and Evapotranspiration Feb. 1985 p 65-74 (For primary document see N85-23223 13-43)
Avail: NTIS HC A09/MF A01 CSCL 08L

Microwave data collected by field experiments over Vermont and Hokkaido and Nimbus-7 SMMR over North Dakota and Hokkaido were studied. The measured 37 GHz brightness temperatures show considerable effect of volume scattering by snow grains. The 37 GHz brightness for a new snowpack with average grain radius of 0.25 mm is generally about 40 K higher than the naturally compacted pack with average grain radius of 0.4 mm. The scattering effect is much less distinct for the 6.6 GHz. However, the layering effect is much stronger at the longer wavelength. For 10.7 and 18 GHz, the effect of layering and scattering vary due to different combinations of internal snow grain distribution and layering structures. Over the Hokkaido test site, the SMMR data are too coarse for the snow field. A better spatial resolution is required to study these snow fields. A.R.H.

N85-23231*# Chiba Univ. (Japan). Inst. of Color and Image Technology.
STUDIES ON PHYSICAL PROPERTIES OF SNOW BASED ON MULTI CHANNEL MICROWAVE RADIOMETER
Kiyoshi Tsuchiya and Kaname Takeda *In* NASA Goddard Space Flight Center Remote Sensing of Snow and Evapotranspiration Feb. 1985 p 75-87 refs (For primary document see N85-23223 13-43)
Avail: NTIS HC A09/MF A01 CSCL 08L

The analysis of the data observed over a snow field with a breadboard model of MSR (microwave scanning radiometer) to be installed in MOS-1 (Marine Observation Satellite-1) indicates that: (1) the influence of incident angle on brightness temperature is larger in horizontal polarization component than in vertical polarization component. The effect of incident angle depends upon the property of snow with larger value for dry snow; (2) the difference of snow surface configuration consisting of artifically made parallel ditches of 5 cm depth and 5 cm width with spacing of 10 and 30 cm respectively which are oriented normal to electrical axis do not affect brightness temperature significantly; and (3) there is high negative correlation between brightness temperature and snow depth up to the depth of 70 cm which suggests that the snow depth can be measured with a two channel microwave radiometer up to this depth. Author

N85-23232*# Chiba Univ. (Japan). Inst. of Color and Image Technology.
ANALYSIS OF NIMBUS-7 SMMR DATA
Kiyoshi Tsuchiya, Kaname Takeda (Science and Technology Agency, Tokyo), and Katsutoshi Kozai (Science and Technology Agency, Tokyo) *In* NASA Goddard Space Flight Center Remote Sensing of Snow and Evapotranspiration Feb. 1985 p 89-97 refs (For primary document see N85-23223 13-43)
Avail: NTIS HC A09/MF A01 CSCL 08L

Measurements obtained with the SMMR OF NIMBUS-7 over Hokkaido snow field show that the relationship between snow depth and brightness temperature changes when snow depth becomes deeper than 50 cm. Average brightness temperature of the daytime indicates negative correlations with snow depth except for 6.6 GHz channel data which indicates weak positive correlation. Author

N85-23233*# Tsukuba Univ. (Japan). Environmental Research Center.
ESTIMATION OF REGIONAL EVAPOTRANSPIRATION USING REMOTELY SENSED LAND SURFACE TEMPERATURE. PART 1: MEASUREMENT OF EVAPOTRANSPIRATION AT THE ENVIRONMENTAL RESEARCH CENTER AND DETERMINATION OF PRIESTLEY-TAYLOR PARAMETER
K. Kotada, S. Nakagawa, K. Kai, M M. Yoshino, K. Takeda (Science and Technology Agency, Tokyo), and K. Seki (Science and Technology Agency, Tokyo) *In* NASA Goddard Space Flight Center Remote Sensing of Snow and Evapotranspiration Feb. 1985 p 99-114 refs (For primary document see N85-23223 13-43)
Avail: NTIS HC A09/MF A01 CSCL 08H

In order to study the distribution of evapotranspiration in the humid region using remote sensing technology, the parameter (alpha) in the Priestley-Taylor model was determined. The daily means of the parameter alpha = 1.14 can be available from summer to autumn and alpha = to approximately 2.0 in winter. The results of the satellite and the airborne sensing done on 21st and 22nd January, 1983, are described. Using the vegetation distribution in the Tsukuba Academic New Town, as well as the radiation temperature obtained by remote sensing and the radiation data observed at the ground surface, the evapotranspiration was calculated for each vegetation type by the Priestley-Taylor method. The daily mean evapotranspiration on 22nd January, 1983, was approximately 0.4 mm/day. The differences in evapotranspiration between the vegetation types were not detectable, because the magnitude of evapotranspiration is very little in winter. Author

N85-23234*# Tsukuba Univ. (Japan). Environmental Research Center.
ESTIMATION OF REGIONAL EVAPOTRANSPIRATION USING REMOTELY SENSED LAND SURFACE TEMPERATURE. PART 2: APPLICATION OF EQUILIBRIUM EVAPORATION MODEL TO ESTIMATE EVAPOTRANSPIRATION BY REMOTE SENSING TECHNIQUE
K. Kotoda, S. Nakagawa, K. Kai, M. M. Yoshino, K. Takeda (Science and Technology Agency, Tokyo), and K. Seki (Science and Technology Agency, Tokyo) *In* NASA Goddard Space Flight Center Remote Sensing of Snow and Evapotranspiration Feb. 1985 p 115-127 refs Original contains color illustrations (For primary document see N85-23223 13-43)
Avail: NTIS HC A09/MF A01 CSCL 08H

In a humid region like Japan, it seems that the radiation term in the energy balance equation plays a more important role for evapotranspiration then does the vapor pressure difference between the surface and lower atmospheric boundary layer. A Priestley-Taylor type equation (equilibrium evaporation model) is used to estimate evapotranspiration. Net radiation, soil heat flux, and surface temperature data are obtained. Only temperature data obtained by remotely sensed techniques are used. A.R.H.

N85-23235*# National Aeronautics and Space Administration. Goddard Space Flight Center, Greenbelt, Md.
MICROWAVE REMOTE SENSING OF SOIL MOISTURE
Thomas J. Schmugge *In its* Remote Sensing of Snow and Evapotranspiration Feb. 1985 p 129-148 refs (For primary document see N85-23223 13-43)
Avail: NTIS HC A09/MF A01 CSCL 08M

Because of the large contrast between the dielectric constant of liquid water and that of dry soil at microwave wavelength, there is a strong dependence of the thermal emission and radar backscatter from the soil on its moisture content. This dependence provides a means for the remote sensing of the moisture content in a surface layer approximately 5 cm thick. The feasibility of these techniques is demonstrated from field, aircraft and spacecraft platforms. The soil texture, surface roughness, and vegetative cover affect the sensitivity of the microwave response to moisture variations with vegetation being the most important. It serves as an attenuating layer which can totally obscure the surface. Research indicates that it is possible to obtain five or more levels of moisture discrimination and that a mature corn crop is the limiting vegetation situation. Author

N85-23236*# Maryland Univ., College Park. Dept. of Civil Engineering.
TESTING AN ENERGY BALANCE MODEL FOR ESTIMATING ACTUAL EVAPOTRANSPIRATION USING REMOTELY SENSED DATA
R. J. Gurney and P. J. Camillo (SAR, Riverdale, Md.) *In* NASA Goddard Space Flight Center Remote Sensing of Snow and Evapotranspiration Feb. 1985 p 149-167 refs (For primary document see N85-23223 13-43)
Avail: NTIS HC A09/MF A01 CSCL 08H

An energy-balance model is used to estimate daily evapotranspiration for 3 days for a barley field and a wheat field near Hannover, Federal Republic of Germany. The model was calibrated using once-daily estimates of surface temperatures, which may be remotely sensed. The evaporation estimates were within the 95% error bounds of independent eddy correlation estimates for the daytime periods for all three days for both sites, but the energy-balance estimates are generally higher; it is unclear which estimate is biassed. Soil moisture in the top 2 cm of soil, which may be remotely sensed, may be used to improve these evaporation estimates under partial ground cover. Sensitivity studies indicate the amount of ground data required is not excessive.
Author

N85-23237*# National Aeronautics and Space Administration. Langley Research Center, Hampton, Va.
CHARACTERISTIC VECTOR ANALYSIS OF INFLECTION RATIO SPECTRA: NEW TECHNIQUE FOR ANALYSIS OF OCEAN COLOR DATA
Gary W. Grew Apr. 1985 26 p refs
(NASA-TP-2428; NAS 1.60:2428; L-15885) Avail: NTIS HC A03/MF A01 CSCL 05B

Characteristic vector analysis applied to inflection ratio spectra is a new approach to analyzing spectral data. The technique applied to remote data collected with the multichannel ocean color sensor (MOCS), a passive sensor, simultaneously maps the distribution of two different phytopigments, chlorophyll alpha and phycoerythrin, the ocean. The data set presented is from a series of warm core ring missions conducted during 1982. The data compare favorably with a theoretical model and with data collected on the same mission by an active sensor, the airborne oceanographic lidar (AOL). E.A.K.

N85-23238*# Pennsylvania State Univ., University Park. Dept. of Meteorology.
[A METHOD FOR ESTIMATING SOIL MOISTURE AVAILABILITY] Semiannual Report
Toby N. Carlson 22 Mar. 1985 15 p refs
(Grant NAG5-184)
(NASA-CR-175606; NAS 1.26:175606) Avail: NTIS HC A02/MF A01 CSCL 08M

A method for estimating values of soil moisture based on measurements of infrared surface temperature is discussed. A central element in the method is a boundary layer model. Although it has been shown that soil moistures determined by this method using satellite measurements do correspond in a coarse fashion to the antecedent precipitation, the accuracy and exact physical interpretation (with respect to ground water amounts) are not well known. This area of ignorance, which currently impedes the practical application of the method to problems in hydrology, meteorology and agriculture, is largely due to the absence of corresponding surface measurements. Preliminary field measurements made over France have led to the development of a promising vegetation formulation (Taconet et al., 1985), which has been incorporated in the model. It is necessary, however, to test the vegetation component, and the entire method, over a wide variety of surface conditions and crop canopies. Author

N85-23239# Analytic Sciences Corp., Reading, Mass.
FEATURE EXTRACTION ASSESSMENT STUDY Final Report, Apr. 1982 - Aug. 1984
M. J. Carlotto, V. T. Tom, and G. K. Wallace Fort Belvoir, Va. Army Engineer Topographic Labs. Nov. 1984 298 p
(Contract DACA76-82-C-0004)
(AD-A150189; ETL-0377) Avail: NTIS HC A13/MF A01 CSCL 08/2

The purpose of the feature extraction assessment study (FEAS) is to assess the degree to which the DMA feature extraction process can be automated by 1985. The major conclusion of the study is that given the state-of-the-art in image understanding and pattern recognition, a fully automated system for extracting DMA features cannot be built by 1985 using either conventional black and white or multi-spectral/multi-source imagery. Based on an assessment of feature extraction processes operating solely on black and white imagery, a concept of operation for a semi-automated system is formulated, however, which involves the use of machine vision techniques to support the image analyst in a synergistic fashion. An assessment of multi-spectral and multi-source (MS/MS) imagery is also performed to determine if its use would benefit the feature extraction process. GRA

N85-23240# Edgerton, Germeshausen and Grier, Inc., Las Vegas, Nev. Aerial Measurements Operations Office.
COMPREHENSIVE, INTEGRATED, REMOTE SENSING AT DOE SITES
Jerry G. Lackey and Zolin G. Burson 1984 10 p Presented at the 5th DOE Environmental Protection Information Meeting, Albuquerque, N. Mex., 6 Nov. 1984
(Contract DE-AC08-83NV-10282)
(DE85-004867; EGG-10282-1070; CONF-841187-27) Avail: NTIS HC A02/MF A01

The Department of Energy's comprehensive, integrated remote sensing (CIRS) program aims to provide a state-of-the-art data base of remotely sensed data or all users of such information at large DOE sites. The primary types of remote sensing provided consist of: (1) large format aerial photography; (2) video from aerial platforms; (3) multispectral scanning; and (4) airborne nuclear radiometric surveys. Implementation of the CIRS Program began with field operations at the Savannah River Plant in 1982 and is continuing at the DOE site at a level of effort of about $1.5 m per year. Integrated remote sensing studies were subsequently extended to the West Valley Demonstration Project in the summer and fall of 1984. The Program's eventual extension to cover all large DOE sites on a continuing basis is expected. DOE

N85-23241# Office of Technology Assessment, Washington, D.C.
TECHNOLOGIES TO SUSTAIN TROPICAL FOREST RESOURCES
1984 346 p refs
(TI85-901085; OTA-F-214; LC-84-601018) Avail: NTIS HC A15/MF A01; also available SOD

Various technologies to develop tropical forest resources are discussed. Techniques to manage forest, undisturbed and disturbed, and technologies to use forests to protect related resources such as agriculture and water are outlined. Techniques to prepare people for the various tasks involved in developing and implementing technologies to sustain the resources are also treated. E.A.K.

N85-22440# Joint Publications Research Service, Arlington, Va.
REMOTE SENSING USED FOR STUDY OF FOREST RESOURCES
A. Metalnikov, V. Yezhkov, and P. Moroz *In its* USSR Rept.: Space (JPRS-USP-85-001) 4 Feb. 1985 p 67-72 Transl. into ENGLISH from Ekonomicheskaya Gaz. (USSR), no. 34, Aug. 1984 p 16 (For primary document see N85-22403 13-12)
Avail: NTIS HC A07

N85-22441# Joint Publications Research Service, Arlington, Va.
EVALUATING ACCURACY IN DETERMINING POSITION OF EARTH'S CENTER OF MASS AND ELEMENTS OF ORIENTATION OF GEODETIC COORDINATE SYSTEM Abstract Only
M. M. Mashimov and K. V. Malets *In its* USSR Rept.: Space (JPRS-USP-85-001) 4 Feb. 1985 p 73 Transl. into ENGLISH from Izv. Vysshikh Uch. Zaved.: Geod. i Aerofotosyemka (USSR), no. 1, Jan.-Feb. 1984 p 45-49 (For primary document see

N85-22403 13-12)
Avail: NTIS HC A07

N85-22446# Joint Publications Research Service, Arlington, Va.
NEW METHOD OF RECONSTRUCTING CONDITIONS OF RECENT DIFFERENTIATION OF OIL AND GAS IN THE AMUDARYA BASIN (BASED ON RESULTS OF INTERPRETATION OF SPACE PHOTOGRAPHS) Abstract Only
G. I. Amurskiy, N. N. Solovyev, and V. A. Kuzminov *In its* USSR Rept.: Space (JPRS-USP-85-001) 4 Feb. 1985 p 77 Transl. into ENGLISH from Izv. Akad. Nauk SSSR: Ser. Geologicheskaya (USSR), no. 6, Aug. 1984 p 112-122 (For primary document see N85-22403 13-12)
Avail: NTIS HC A07

N85-22449# Joint Publications Research Service, Arlington, Va.
EXPERIENCE IN COMBINED SPECIAL MAPPING USING SPACE INFORMATION Abstract Only
V. A. Astakhova, V. V. Kozlov, and V. I. Ryabchikova *In its* USSR Rept.: Space (JPRS-USP-85-001) 4 Feb. 1985 p 79-80 Transl. into ENGLISH from Geod. i Kartografiya (USSR), no. 7, Jul. 1984 p 40-44 (For primary document see N85-22403 13-12)
Avail: NTIS HC A07

N85-22450# Joint Publications Research Service, Arlington, Va.
COMBINED ANALYSIS OF THE DYNAMICS OF COMPLEX ECOSYSTEMS BASED ON REPEATED REMOTE MEASUREMENTS Abstract Only
B. V. Vinogradov, U. A. Shvede, and A. N. Kaptsov *In its* USSR Rept.: Space (JPRS-USP-85-001) 4 Feb. 1985 p 80 Transl. into ENGLISH from Dokl. Akad. Nauk SSSR (USSR), v. 277, no. 6, Aug. 1984 p 1505-1509 Original language document announced as A85-11587 (For primary document see N85-22403 13-12)
Avail: NTIS HC A07

N85-22848# Joint Publications Research Service, Arlington, Va.
GEOLOGICAL REMOTE SENSING DEVELOPS RAPIDLY, FINDS BROAD APPLICATIONS
Yang Guangqing *In its* Chinese Rept.: Sci. and Technol. (JPRS-CST-85-005) 20 Feb. 1985 p 96-102 refs Transl. into ENGLISH from Zhongguo Dizhi (Beijing, China), no. 10, 13 Oct. 1984 p 23-26 (For primary document see N85-22843 13-31)
Avail: NTIS HC A10/MF A01

N85-23118# Joint Publications Research Service, Arlington, Va.
ANTARCTIC GLACIATION, OR WHAT ARE CATASTROPHES IN EARTH'S HISTORY Abstract Only
D. Kvasov *In its* USSR Rept.: Earth Sci. (JPRS-UES-85-002) 1 Feb. 1985 p 4 Transl. into ENGLISH from Znaniye-Sila (Moscow), no. 8, Aug. 1984 p 28-30 (For primary document see N85-23116 13-42)
Avail: NTIS HC A07/MF A01

N85-23160# Joint Publications Research Service, Arlington, Va.
REVIEW OF PROBLEMS IN LITHOLOGY Abstract Only
P. P. Timofeyev *In its* USSR Rept.: Earth Sci. (JPRS-UES-85-002) 1 Feb. 1985 p 75 Transl. into ENGLISH from Vestn. Akad. Nauk SSSR (Moscow), no. 9, Sep. 1984 p 69-77 (For primary document see N85-23116 13-42)
Avail: NTIS HC A07/MF A01

N85-23162# Joint Publications Research Service, Arlington, Va.
POSSIBILITY OF MAPPING ACTIVE TECTONIC STRUCTURES FROM MERCURY GAS AUREOLES OVER SEA SURFACE Abstract Only
A. A. Ganeyev, N. R. Mashyanov, G. B. Sveshnikov, and S. Ye. Sholupov *In its* USSR Rept.: Earth Sci. (JPRS-UES-85-002) 1 Feb. 1985 p 77-78 Transl. into ENGLISH from Dokl. Akad. Nauk SSSR (Moscow), v. 275, no. 5, Apr. 1984 p 1162-1164 (For primary document see N85-23116 13-42)
Avail: NTIS HC A07/MF A01

N85-23177# Joint Publications Research Service, Arlington, Va.
POSSIBILITIES OF AERIAL ELECTRIC PROSPECTING BY LONG CABLE METHOD FOR DETECTING POORLY CONDUCTING STRATA Abstract Only
A. V. Veshev, S. S. Gudovskikh, and Ye. F. Lyubtseva *In its* USSR Rept.: Earth Sci. (JPRS-UES-85-002) 1 Feb. 1985 p 111 Transl. into ENGLISH from Vestn. Leningr. Univ.: Geol., Geogr. (Leningrad), no. 6, issue 1, Mar. 1984 p 19-28 (For primary document see N85-23116 13-42)
Avail: NTIS HC A07/MF A01

N85-23180# Joint Publications Research Service, Arlington, Va.
DETERMINING DEEP HEAT FLOW AND RATE OF HORIZONTAL PERCOLATION FROM TEMPERATURE MEASUREMENTS IN AQUIFER Abstract Only
M. M. Mitnik *In its* USSR Rept.: Earth Sci. (JPRS-UES-85-002) 1 Feb. 1985 p 113-114 Transl. into ENGLISH from Dokl. Akad. Nauk Ukr. SSR, Ser. B: Geol., Khim. i Biol. Nauki (Kiev), no. 5, May 1984 p 14-17 (For primary document see N85-23116 13-42)
Avail: NTIS HC A07/MF A01

N85-23434# Joint Publications Research Service, Arlington, Va.
DEVELOPMENT, ACHIEVEMENTS IN CHINA'S CARTOGRAPHY WORK
In its China Rept.: Sci. and Technol. (JPRS-CST-85-003) 28 Jan. 1985 p 44-53 Transl. into ENGLISH from Cehui Tongbao (Beijing), no. 4, 25 Aug. 1984 p 1-6 (For primary document see N85-23433 13-81)
Avail: NTIS HC A11/MF A01

N85-23435# Joint Publications Research Service, Arlington, Va.
ACCOMPLISHMENTS OF INSTITUTE OF CARTOGRAPHY SUMMARIZED
Luo Shiming *In its* China Rept.: Sci. and Technol. (JPRS-CST-85-003) 28 Jan. 1985 p 54-60 Transl. into ENGLISH from Cehui Tongbao (Beijing), no. 4, 25 Aug. 1984 p 6-10 (For primary document see N85-23433 13-81)
Avail: NTIS HC A11/MF A01

N85-23587*# Whittier Coll., Calif. Dept. of Geology.
CATASTROPHIC-FLOOD FEATURES IN SWEDISH LAPLAND AS A TERRESTRIAL ANALOG FOR MARTIAN CHANNEL FLOWS Abstract Only
Lisa A. Rossbacher and Dallas D. Rhodes *In* NASA, Washington Repts. of Planetary Geol. and Geophys. Program Apr. 1985 p 319-321 refs (For primary document see N85-23474 13-91)
Avail: NTIS HC A99/MF A01 CSCL 08H

N85-23622*# Washington Univ., Seattle. Dept. of Geological Sciences.
DETERMINING MINERAL TYPES AND ABUNDANCES FROM REFLECTANCE MEASUREMENTS Abstract Only.
Milton O. Smith and John B. Adams *In* NASA, Washington Repts. of Planetary Geol. and Geophys. Program, 1984 Apr. 1985 p 415-417 refs (For primary document see N85-23474 13-91)
Avail: NTIS HC A99/MF A01 CSCL 08G

N85-23623*# Geological Survey, Denver, Colo.
DETERMINATION OF MINERAL TYPE, ABUNDANCE, AND GRAIN SIZE WITH REMOTELY OBTAINED REFLECTANCE SPECTRA Abstract Only
Roger N. Clark *In* NASA, Washington Repts. of Planetary Geol. and Geophys. Program, 1984 Apr. 1985 p 418-420 refs (For primary document see N85-23474 13-91)
Avail: NTIS HC A99/MF A01 CSCL 08G

N85-23624*# Massachusetts Univ., Amherst. Dept. of Geology-Geography.
AUTOMATED EXTRACTION OF ABSORPTION BANDS FROM REFLECTANCE SPECIAL Abstract Only
R. L. Huguenin, L. Vale, D. McIntire, and J. Jones *In* NASA, Washington Repts. of Planetary Geol. and Geophys. Program, 1984 Apr. 1985 p 421-428 (For primary document see N85-23474 13-91)
Avail: NTIS HC A99/MF A01 CSCL 20F

N85-23641*# Geological Survey, Flagstaff, Ariz.
LATE TERTIARY AND QUATERNARY RIVER SYSTEMS OF THE EASTERN SAHARA AS MAPPED ON SHUTTLE RADAR AND LANDSAT IMAGES Abstract Only
John F. McCauley, Carol S. Breed, and Gerald G. Schaber *In* NASA, Washington Repts. of Planetary Geol. and Geophys. Program, 1984 Apr. 1985 p 471-473 (For primary document see N85-23474 13-91)
Avail: NTIS HC A99/MF A01 CSCL 08H

N85-23655*# California Univ., Livermore. Lawrence Livermore Lab.
CREEP OF ICE: FURTHER STUDIES Abstract Only
H. C. Heard, W. B. Durham, and S. H. Kirby *In* NASA, Washington Repts. of Planetary Geol. and Geophys. Program, 1984 Apr. 1985 p 513-515 refs (For primary document see N85-23474 13-91)
Avail: NTIS HC A99/MF A01 CSCL 08L

44 ENERGY PRODUCTION AND CONVERSION

Includes specific energy conversion systems, e.g., fuel cells and batteries; global sources of energy; fossil fuels; geophysical conversion; hydroelectric power; and wind power.

For related information see also *07 Aircraft Propulsion and Power, 20 Spacecraft Propulsion and Power, 28 Propellants and Fuels,* and *85 Urban Technology and Transportation.*

N85-23242*# National Aeronautics and Space Administration. Lewis Research Center, Cleveland, Ohio.
DEVELOPMENT OF LARGE, HORIZONTAL-AXIS WIND TURBINES Final Report
Darrell H. Baldwin and Jerry Kennard (Sverdrup Technology, Inc., Middleburg Heights, Ohio) Mar. 1985 15 p refs
(Contract DE-AI01-76ET-20320)
(NASA-TM-86950; E-2471; DOE/NASA/20320-62; NAS 1.15:86950) Avail: NTIS HC A02/MF A01 CSCL 10B

A program to develop large, horizontal-axis wind turbines is discussed. The program is directed toward developing the technology for safe, reliable, environmentally acceptable large wind turbines that can generate a significant amount of electricity at costs competitive with those of conventional electricity-generating systems. In addition, these large wind turbines must be fully compatible with electric utility operations and interface requirements. Several ongoing projects in large-wind-turbine development are directed toward meeting the technology requirements for utility applications. The machines based on first-generation technology (Mod-OA and Mod-1) successfully completed their planned periods of experimental operation in June, 1982. The second-generation machines (Mod-2) are in operation at selected utility sites. A third-generation machine (Mod-5) is under contract. Erection and initial operation of the Mod-5 in Hawaii should take place in 1986. Each successive generation of technology increased reliability and energy capture while reducing the cost of electricity. These advances are being made by gaining a better understanding of the system-design drivers, improving the analytical design tools, verifying design methods with operating field data, and incorporating new technology and innovative designs. Information is given on the results from the first- and second-generation machines (Mod-OA, - 1, and -2), the status of the Department of Interior, and the status of the third-generation wind turbine (Mod-5). R.J.F.

N85-23243*# National Aeronautics and Space Administration. Lewis Research Center, Cleveland, Ohio.
OPERATIONAL PERFORMANCE OF THE PHOTOVOLTAIC-POWERED GRAIN MILL AND WATER PUMP AT TANGAYE, BURKINA FASO (FORMERLY UPPER VOLTA) Final Report
James E. Martz and Allen F. Roberts (Michigan Univ., Ann Arbor) Mar. 1985 28 p refs
(NASA Order DSB-5710-2-79)
(NASA-TM-86970; E-2496; NAS 1.15:86970) Avail: NTIS HC A03/MF A01 CSCL 10B

A photovoltaic (PV) system powering a grain mill and water pump was installed in the remote African village of Tangaye, Burkina Faso (formerly Upper Volta) under the sponsorship of the U.S. Agency for International Development (AID) and by the National Aeronautics and Space Administration (NASA) Lewis Research Center (LeRC) in early 1979. The presence reports covers the second two years of operation from April 1981 through June 1983. During this time, the grain mill and water pump were operational 96 and 88 percent of the time respectively, and the PV system generated sufficient electricity to enable the grinding of about 111 metric tons of finely ground flow and the pumping of over 5000 cm sq of water from the 10 m deep well. The report includes a description of the current configuration of the system, a review of system performance, a discussion of the socioeconomic impact of the system on the villagers and a summary of results and conclusions covering the entire four-year period. Author

N85-23244*# Jet Propulsion Lab., California Inst. of Tech., Pasadena.
NEW HIGH-EFFICIENCY SILICON SOLAR CELLS Final Report, 11 Aug. 1983 - 28 Feb. 1985
Taher Daud and Gerald T. Crotty 1 Mar. 1985 42 p refs Sponsored in part by Solar Energy Research Inst.
(Contract NAS7-918)
(NASA-CR-175643; JPL-Pub-85-6; NAS 1.26:175643) Avail: NTIS HC A03/MF A01 CSCL 10A

A design for silicon solar cells was investigated as an approach to increasing the cell open-circuit voltage and efficiency for flat-plate terrestrial photovoltaic applications. This deviates from past designs, where either the entire front surface of the cell is covered by a planar junction or the surface is textured before junction formation, which results in an even greater (up to 70%) junction area. The heavily doped front region and the junction space charge region are potential areas of high recombination for generated and injected minority carriers. The design presented reduces junction area by spreading equidiameter dot junctions across the surface of the cell, spaced about a diffusion length or less from each other. Various dot diameters and spacings allowed variations in total junction area. A simplified analysis was done to obtain a first-order design optimization. Efficiencies of up to 19% can be obtained. Cell fabrication involved extra masking steps for selective junction diffusion, and made surface passivation a key element in obtaining good collection. It also involved photolithography, with line widths down to microns. A method is demonstrated for achieving potentially high open-circuit voltages and solar-cell efficiencies. Author

N85-23245# Midwest Research Inst., Golden, Colo. Solar Energy Research Inst.
A THEORETICAL ANALYSIS OF SOLAR-DRIVEN NATURAL CONVECTION ENERGY CONVERSION SYSTEMS
Eric W. Jacobs and David D. Laiser Jan. 1984 38 p refs
(Contract DE-AC02-83CH-10093)
(DE84-004431; SERI/TR-211-1950) Avail: NTIS HC A03/MF A01

Using the phenomenon of natural convection, or buoyancy, was proposed as a way to utilize solar energy. Theoretical analyses of the ideal thermodynamic cycle efficiencies potentially attainable by natural convection energy conversion systems are summarized. Computer simulations of these models were used to facilitate calculation procedures. Conclusions for a cost analysis to determine the economic potential of natural convection towers are presented. B.G.

N85-23246# Midwest Research Inst., Golden, Colo. Solar Energy Research Inst.
ABSTRACTS OF 6TH ANNUAL REVIEW MEETING ON PHOTOVOLTAIC ADVANCED RESEARCH AND DEVELOPMENT
1984 88 p refs Meeting held in Golden, Colo., 29-31 Oct. 1984
(Contract DE-AC02-83CH-10093)

(DE84-013047; SERI/CP-211-2507; CONF-841021-Absts) Avail: NTIS HC A05/MF A01

Brief summaries are given for 55 presentations given at this meeting. Areas covered include: amorphous silicon, polycrystalline thin-film materials and devices, characterization and measurements research, high efficiency silicon and other high efficiency concepts. DOE

N85-23247# Sandia Labs., Albuquerque, N. Mex. Wind Energy Research Div.

STRUCTURAL DESIGN OF THE SANDIA 34-M VERTICAL AXIS WIND TURBINE

Dale E. Berg 1985 12 p refs Presented at the 4th ASME Wind Energy Symp., Dallas, 17-20 Feb. 1985

(Contract DE-AC04-76DP-00789)

(DE85-002631; SAND-84-1287C; CONF-850218-1) Avail: NTIS HC A02/MF A01

Sandia National Laboratories, as the lead DOE laboratory for Vertical Axis Wind Turbine (VAWT) development, is currently designing a 34-meter diameter Darrieus-type VAWT. This turbine will be a research test bed which provides a focus for advancing technology and validating design and fabrication techniques in a size range suitable for utility use. Structural data from this machine will allow structural modeling to be refined and verified for a turbine on which the gravity effects and stochastic wind loading are significant. Performance data from it will allow aerodynamic modeling to be refined and verified. The design effort incorporates Sandia's state-of-the-art analysis tools in the design of a complete machine. The analytic tools used in this design are discussed and the conceptual design procedure is described. DOE

N85-23248# Oak Ridge National Lab., Tenn. Engineering Technology Div.

LATENT HEAT STORAGE IN COOLING SYSTEMS

J. J. Tomlinson 1984 8 p refs

(Contract DE-AC05-84OR-21400)

(DE85-005355; DOE/OR-21400/T82) Avail: NTIS HC A02/MF A01

In building space conditioning applications where cooling is a major component, thermal energy storage can be used to shift the electrical cooling load imposed on a utility during peak cooling loads and small buildings located in summer peaking utility service areas are particularly attractive for application of this technology. Ice is the latent heat storage material most commonly used as the thermal storage medium for building cooling; however, new materials including clathrates, salt hydrates, and liquid-liquid systems are being explored. Cool storage applications are explored and provides an overview of research underway to develop these new latent heat materials is provided. DOE

N85-23249# Oak Ridge National Lab., Tenn. Engineering Technology Div.

OVERVIEW OF LATENT STORAGE FOR PASSIVE SOLAR APPLICATIONS

J. J. Tomlinson 1984 12 p refs

(Contract DE-AC05-84OR-21400)

(DE85-005354; DOE/OR-21400/T81) Avail: NTIS HC A02/MF A01

The state of the art passive solar systems satisfies a portion of the space heating needs in many locations in the US; however, analyses of typical building heating requirements and available solar radiation indicate that the solar flux on a horizontal or south facing vertical surface is sufficient to meet the entire building heating load during the winter. Since buildings consume approximately one third of the primary energy budget, and space heating for these buildings is a major component, significant reductions in purchased energy requirements for buildings are possible through development and implementation of new, advanced, cost effective passive solar technologies. Passive solar storage techniques, available products and selected current research activities are reviewed. DOE

N85-23250# Argonne National Lab., Ill.

USING FUEL CELLS OR ANODE DEPOLARIZATION TO REDUCE ELECTROWINNING ENERGY CONSUMPTION

G. M. Cook 1985 13 p refs Presented at 114th AIME Ann. Meeting (includes Soc. of Mining Engr.), New York, N.Y., 24 Feb. 1985

(Contract W-31-109-eng-38)

(DE85-006187; CONF-850211-3) Avail: NTIS HC A02/MF A01

Some existing and proposed metal electrowinning plant sites have hydrogen available to reduce the need for purchased energy. Hydrogen can reduce the energy consumption of electrowinning processes by depolarizing the anode; alternatively, it can be used in a fuel cell to generate dc electricity and heat at high efficiency. The use of H2 to depolarize an anode in zinc electrowinning has been shown to reduce overall cell voltage. This paper examines the increased complexity that the depolarized anode and molten carbonate fuel cell technologies impose upon the electrowinning process, assesses the extent of energy savings that are available, and provides insight into the impact on capital and operating costs. DOE

N85-23251# Texas Technological Univ., Lubbock. Dept. of Mathematics.

ROSA: A COMPUTER MODEL FOR OPTICAL POWER RATIO CALCULATIONS

R. M. Anderson and W. T. Ford 15 Jul. 1984 131 p refs

(Contract DE-AC04-83AL-21557)

(DE85-005174; DOE/AL-21557/T1) Avail: NTIS HC A07/MF A01

The Ratio of Solid Angles (ROSA) computer code was developed as part of the crosbyton solar power project (CSPP) for calculation of optical power concentrations due to reflection from a spherical segment mirror. The CSPP is concerned with the development of a technology for producing electric power from steam generated by reflection of the Sun's rays from a fixed-mirror solar bowl onto a tracking receiver. The ROSA code gives optical power concentration ratio profiles at points along the receiver surface. The ROSA code is written for a spherical segment mirror and the rim angle of the mirror is an input variable. Orientation of the axis of symmetry of the bowl is specified in terms of a vertical-east-north coordinate system. Location of the Sun relative to this coordinate system is also an input variable. The code permits any convex surface of revolution as a receiver. This report consists of two parts, a technical reference manual and a user's guide. The reference manual provides the background material and derivations necessary for the implementation of the code. Computer listings for ROSA are also included in the reference manual. The user's guide contains an explanation of the input data for the program, special user supplied subroutine requirements, a discussion of the output data, sample output and graphs of sample concentration profiles. DOE

N85-23252# Physical Sciences, Inc., Andover, Mass.

MOLTEN CARBONATE FUEL CELL PERFORMANCE MODEL UPDATE, DRAFT Quarterly Report, Apr. - Jun. 1984

G. Wilemski, A. Gelb, and N. H. Kemp Aug. 1984 17 p refs

(Contract DE-AC21-81FE-15078)

(DE85-005423; DOE/MC-15078/7-3; PSI-TR-455) Avail: NTIS HC A02/MF A01

This report contains a description of recent improvements on the heterogeneous film model of porous electrodes is given. This model is intended to be a reasonable depiction of ERC's ceramic coated Ni anodes and to serve as a first approximation to GE's and ANL's Ni/Cr anodes. The connectivity of the porous coated, metal network was treated by imaging the idealized cylindrical model elements to be packed into a simple cubic structure. Treating the connectivity adds a degree of realism to the model and, by properly accounting for volume excluded at cube corners, forces the lateral dimensions of the cylindrical elements to more nearly conform with dimensions apparent in SEM's of actual electrodes. Work on the computer codes needed to calculate vertical concentration gradients in the gas flow channels has also progressed.

The cathode code is running and capable of rapidly producing fully converged numerical results. DOE

N85-23253# Carrier Corp., Syracuse, N.Y.
DEVELOPMENT OF A SINGLE-FAMILY ABSORPTION CHILLER FOR USE IN A SOLAR HEATING AND COOLING SYSTEM, PHASE 3, VOLUME 2 Final Report
R. C. Reimann and W. J. Biermann Oct. 1984 132 p refs
(Contract DE-AC03-77CS-31587)
(DE85-003218; DOE/CS-31587/T3-Vol-2) Avail: NTIS HC A10/MF A01

Supporting information is presented on: properties of a chemical system for solar fired, air-cooled absorption equipment, air-side performance of a one-inch tube, absorber plate-fin coil, listings of the programs used for simulation and data reduction, and evaluation of the Carrier three-tone chiller in an integrated heating and cooling system. DOE

N85-23254# Argonne National Lab., Ill.
CATHODE MATERIALS FOR MOLTEN CARBONATE FUEL CELLS
J. L. Smith, G. H. Kucera, N. Q. Minh, R. D. Pierce, and J. P. Ackerman 1985 10 p refs Presented at Natl. Assoc. of Corrosion Engr. Ann. Meeting and Materials Performance and Corrosion Show, Boston, 25 Mar. 1985
(Contract W-31-109-eng-38)
(DE85-004078; CONF-850311-4) Avail: NTIS HC A02/MF A01

Cathodes in carbonate fuel cells are limited in longevity by dissolution of NiO from the cathode and precipitation as Ni in the electrolyte. Alternative cathode materials are sought through a process of identifying the stable forms of candidate ceramics in the cathode environment, evaluating their properties, and modifying the conductivity, if necessary, through the use of dopants. DOE

N85-22499*# National Aeronautics and Space Administration. Lewis Research Center, Cleveland, Ohio.
DISCHARGES ON A NEGATIVELY BIASED SOLAR CELL ARRAY IN A CHARGED-PARTICLE ENVIRONMENT
David B. Snyder *In its* Spacecraft Environ. Interactions Technol. Mar. 1985 p 379-388 refs Previously announced as N84-23690 (For primary document see N85-22470 13-18)
Avail: NTIS HC A99/MF E03 CSCL 10A

N85-22519*# National Aeronautics and Space Administration. Marshall Space Flight Center, Huntsville, Ala.
SPACE TEST PROGRAM OF HIGH-VOLTAGE SOLAR ARRAY-SPACE PLASMA INTERACTIONS
M. R. Carruth, Jr. (NASA. Marshall Space Flight Center, Huntsville, Ala.) and Carolyn K. Purvis *In its* Spacecraft Environ. Interactions Technol., 1983 Mar. 1985 p 619-635 refs (For primary document see N85-22470 13-18)
Avail: NTIS HC A99/MF E03 CSCL 10A

45 ENVIRONMENT POLLUTION

Includes air, noise, thermal and water pollution; environment monitoring; and contamination control.

N85-23255 Utah State Univ., Logan.
STAGNATION ZONE IMPACTION ON A SIMPLE TERRAIN FEATURE IN STABLE FLOW Ph.D. Thesis
Timothy C. Spangler 1984 159 p
Avail: Univ. Microfilms Order No. DA8428053

Prediction of the dispersion and surface impact of aerosol plumes in complex terrain is a complicated and important question. Seven cases are analyzed from the Environmental Protection Agency Small Hill Impaction Study that represent plumes on a stagnating streamline upwind of a simple terrain feature. The nearly identical cases, meteorologically, are divided into two groups because of the two very different levels of surface impact. The two different levels were clearly correlated to Richardson number and turbulent eddy velocities. The surface concentrations are compared to standard Gaussian dispersion models and a modified Gaussian model is developed that utilizes a variable sector average for horizontal dispersion and a turbulence determined mixing of the plume over the last few meters to the terrain. It is concluded that two similarity criteria are needed to adequately predict stable plume impact in complex terrain. Dissert. Abstr.

N85-23256# Battelle Columbus Labs., Ohio.
COMPOSITION AND PHOTOCHEMICAL REACTIVITY OF TURBINE ENGINE EXHAUST Final Report, Jan. 1982 - Mar. 1984
C. W. Spicer, M. W. Holdren, T. F. Lyon, and R. M. Riggin Tyndall AFB, Fla. AFESC Sep. 1984 196 p
(Contract F08635-82-C-0131)
(AD-A150559; AFESC/ESL-TR-84-28) Avail: NTIS HC A09/MF A01 CSCL 07/3

The environmental impact of organic compounds emitted from jet aircraft turbine engines has not been firmly established due to the lack of data regarding the emission rates and identities of the compounds. The objectives of this project were to identify and quantify the organic compounds present in gaseous emissions from jet engines and to study a photochemical reactivity of these compounds. These objectives were met through a five-task approach. Tasks 1 and 2 involved sampling and analysis methods development and validation. This report reviews the Task 1 and 2 studies, and describes Tasks 3-5 in detail. Task 3 involved detailed exhaust organic composition studies with two full-scale turbine engines utilizing three fuels. Task 4 investigated the photochemical reactivity of the exhausts, and Task 5 involved analysis and interpretation of results. GRA

N85-23257# Oak Ridge National Lab., Tenn.
AREAS WITH FOREST SOILS SENSITIVE TO ACIDIC DEPOSITION UNDER ALTERNATIVE DAMAGE HYPOTHESES
R. S. Turner 1984 9 p refs Presented at Natl. Acid Precipitation Assessment Program Meeting, Asheville, N.C., 13 Nov. 1984
(Contract DE-AC05-84OR-21400)
(DE85-005257; CONF-8411137-1) Avail: NTIS HC A02/MF A01

The potential for acidic deposition to induce changes in forest soils is reviewed. The hypothesized roles of these soil changes in decreased tree growth and forest dieback are examined. Several damage mechanisms are examined, and maps are made for each set of hypotheses showing the areal distribution of those soils that could change to a chemical state injurious or less conductive to three growth. The hypotheses concerning acid deposition effects on soil processes are reviewed. The hypotheses fall into two categories: (1) changes in soil-plant nutrient relationships; and (2) changes in the availability of toxic elements to plants. The development of criteria for spatially estimating soil and forest effects for each hypothesis selected, and environmental factors are considered. The factors examined depend on the specific hypothesis, however soil chemical properties, vegetation cover and type, and the properties and amount of deposition are emphasized. Mapping potentially sensitive ecosystems, using computer manipulation of the environmental data are presented. Selected areas shown on the maps as being sensitive to change or damage by acid deposition are checked assess the validity of the maps. Site assessments includes general observations of condition and dynamics of the ecosystems, tree growth-increment cores, and soil and vegetation sampling for laboratory analyses. DOE

N85-22632# Joint Publications Research Service, Arlington, Va.
ONE MECHANISM OF FORMATION OF ORGANIC FRACTION IN ATMOSPHERIC AEROSOL Abstract Only
V. G. Morachevskiy, S. G. Zvenigorodskiy, and S. P. Smyshlyayev *In its* USSR Rept.: Chem. (JPRS-UCH-85-001) 17 Jan. 1985 p 2 Transl. into ENGLISH from Zh. Prikl. Khim. (Leningrad), v. 57, no. 9, Sep. 1984 p 1978-1982 (For primary document see N85-22629 13-23)
Avail: NTIS HC A06

N85-23132# Joint Publications Research Service, Arlington, Va.
DRIFTING ICE AS MECHANICAL FACTOR IN PURIFYING AND POLLUTING HYDROSPHERE Abstract Only

V. V. Izmaylov *In its* USSR Rept.: Earth Sci. (JPRS-UES-85-002) 1 Feb. 1985 p 28-29 Transl. into ENGLISH from Izv. Vsesoyuznogo Geogr. Obshch. (Leningrad), v. 116, no. 3, May - Jun. 1984 p 221-237 (For primary document see N85-23116 13-42)
Avail: NTIS HC A07/MF A01

N85-23134# Joint Publications Research Service, Arlington, Va.
CONTRIBUTION TO THEORY OF OCEAN-ATMOSPHERE GAS EXCHANGE Abstract Only
V. S. Savenko and V. L. Lebedev *In its* USSR Rept.: Earth Sci. (JPRS-UES-85-002) 1 Feb. 1985 p 30-31 Transl. into ENGLISH from Dokl. Akad. Nauk SSSR (Moscow), v. 275, no. 5, Apr. 1984 p 1185-1189 (For primary document see N85-23116 13-42)
Avail: NTIS HC A07/MF A01

46 GEOPHYSICS

Includes aeronomy; upper and lower atmosphere studies; ionospheric and magnetospheric physics; and geomagnetism.

For space radiation see *93 Space Radiation.*

N85-23258* National Aeronautics and Space Administration. Goddard Space Flight Center, Greenbelt, Md.
CRUSTAL DYNAMICS PROJECT: CATALOGUE OF SITE INFORMATION
Carey E. Noll, Beth A. Creamer, Henry G. Linder, Richard J. Allenby, and Gilbert D. Mead Mar. 1985 309 p refs
(NASA-TM-87452; NAS 1.15:87452; X-601-85-6) Avail: Issuing Activity CSCL 08G

A catalogue of site information for the crustal dynamics project is presented. It contains information and descriptions of those sites used by the project as observing stations for making the precise geodetic measurements useful for studies of the earth's crustal movements and deformation. E.A.K.

N85-23259 Texas A&M Univ., College Station.
NORMAL-FAULT AND FOLD DEVELOPMENT IN SEDIMENTARY ROCKS ABOVE A PRE-EXISTING BASEMENT NORMAL FAULT Ph.D. Thesis
Thomas Lewis Patton, III 1984 224 p
Avail: Univ. Microfilms Order No. DA8428803

Comparisons of field, experimental, and theoretical data on the deformation in a sedimentary layer due to movement on an underlying, pre-existing basement fault, provide the basis for a conceptual normal-fault model in such a layer. Initial displacement along a 70 deg basement normal fault generates arcuate maximum-compressive-stress and shear-fracture trajectories immediately above the basement-fault tip. Their concave surface face the downthrown (hanging-wall) side of the layer. Both a region of low mean stress (compression positive) and high differential stress also overlie the basement-fault tip, providing optimal conditions for failure. Failure occurs by stress release along shear-fracture trajectories, resulting in short, upward-steepening normal faults which may obtain a reverse sense of separation before dieing out toward the downthrown side of the layer. Dissert. Abstr.

N85-23260 Colorado Univ., Boulder.
MAGNETIC LOCATION OF EARTH'S CORE-MANTLE BOUNDARY AND ESTIMATES OF THE ADJACENT FLUID MOTION Ph.D. Thesis
Coerte Van Voorhies 1984 367 p
Avail: Univ. Microfilms Order No. DA-8428692

An electromagnetic theory is combined with reduced geomagnetic data which advances understanding of the fluid dynamics of earth's outer core. The simple earth model adopted consists of an impenetrable, electrically insulating mantle surrounding a spherical, inviscid, and perfectly conducting liquid outer core. Steady, purely toroidal flows do not fit the secular variation models at S sub cmb nearly so well as do steady, combined toroidal-poloidal flows. This is also true when the steady motion hypothesis is relaxed. These and other results constitute direct evidence for weak vertical motions near the top of the core. The derived flows possess a bulk westward drift of about 0.107 deg/yr, but are complicated by the superposition of jets, verticies, and upwelling. It is found that on decade time intervals and megameter length scales, the reduced geomagnetic data are adequately described by the quasisteady, large scale, combined toroidal-poloidal circulation of a frozen-flux core beneath an insulating mantle. Dissert. Abstr.

N85-23261 Utah State Univ., Logan.
TWO-DIMENSIONAL NUMERICAL MODEL OF SENSIBLE AND LATENT HEAT TRANSPORT IN AN IRRIGATED FIELD UNDER ADVECTIVE CONDITIONS Ph.D. Thesis
Melissa E. Agulto 1984 163 p
Avail: Univ. Microfilms Order No. DA8428002

The modification of the temperature and humidity profiles over a well-watered alfalfa field under advective conditions was studied. Vertical profiles of potential tempeature and specific humidity were taken sequentially at the upwind, center field, and downwind side of the experimental plot in Avra Valley, near Tucson, Arizona, to a height of about 70 m. The observed profiles of specific humidity indicate a lapse condition growing stronger and deeper with downwind distance from the leading edge. The potential temperature profiles showed a change from thermal instability at the upwind side to increased thermal stability with downwind fetch to a height of about 16 m under light wind conditions, and about 30 m under stronger winds. These results suggest the depth in the atmosphere to which sensible heat is extracted to enhance evapotranspiration. Results of the profile measurements of humidity and temperature were used as a data-base to derive the two-dimensional fields of specific humidity and potential temperature using two-dimensional, steady state diffusion models for sensible and latent heat transport. Dissert. Abstr.

N85-23262 Colorado State Univ., Fort Collins.
SLOW MOTIONS IN THE TROPICAL TROPOSPHERE Ph.D. Thesis
John Roberts Anderson 1984 149 p
Avail: Univ. Microfilms Order No. DA8427845

Quasi periodic variations with periods of 40 to 50 days have been observed in several tropical meteorological parameters. Possible mechanisms for the oscillation time scale are examined. An observational study of the seasonal variation of the observed oscillation period is presented which indicates that it is unlikely that a Doppler shifted traveling wave mechanism is responsible for the 40 to 50 day period. A new possible mechanism is proposed where the time scale results from the advection of perturbation quantities by a Hadley cell basic state circulation. The results of a forced calculation with this basic state indicate the possibility that the slow motions couple to the cumulus convection through a modulation of the basic state static stability. A non-zonally symmetric forced calculation produces wind fields in good agreement with observations. Dissert. Abstr.

N85-23263 Colorado State Univ., Fort Collins.
THE RELATIONSHIP BETWEEN MARINE AEROSOL PARTICLES AND SATELLITE-DETECTED RADIANCE Ph.D. Thesis
Philip Andrew Durkee 1984 141 p
Avail: Univ. Microfilms Order No. DA-8427854

Brightness variations in satellite images of cloud-free, ocean regions have been hypothesized to be caused by marine aerosol particle variations. The relationship between marine aerosol particles and satellite-detected radiance is examined. The causes of particle variations which lead to upwelling radiance variation, particularly relative humidity effects, are investigated. First, a two-stream radiative transfer model is used to calculate upwelling radiance variations caused by calculated aerosol particle variations. Second, an experiment designed to relate near-simultaneous satellite images to marine boundary layer characteristics was conducted off short of southern California from 20 September to 7 October, 1982. Satellite images were analyzed in real-time and used to direct an aircraft regions of brightness variations detected in the images. Dissert. Abstr.

N85-23264 Colorado State Univ., Fort Collins.
A THEORETICAL STUDY OF THE OZONE QUASI-BIENNIAL OSCILLATION IN THE TROPICAL STRATOSPHERE Ph.D. Thesis
Xuide Ling 1984 180 p
Avail: Univ. Microfilms Order No. DA8428665

A two-dimensional coupled system of dynamics, radiation and photochemistry is developed based on parameterizations in radiation and photochemistry and other important assumptions. The quasibiennial oscillation (QBO) of stratospheric ozone between 18 and 36 km in the tropical region is simulated by using the zonal wind QBO specified from observations as a known function in the 2-dimensional system. The results show that the ozone QBO is determined by different mechanisms in different regions. Above 30 km, photochemistry controls the ozone QBO and the ozone QBO is out of phase with the temperature QBO. Below 28 km, both photochemistry and dynamical transport contribute to the ozone QBO. As a result of that, the ozone QBO shows a relative in-phase relation with the temperature QBO. In the transition region between 28 and 30 km, the ozone QBO undergoes a drastic phase adjustment and reaches the minimum amplitude.
Dissert. Abstr.

N85-23265*# State Univ. of New York, Binghamton. Dept. of Geological Sciences.
CRUSTAL DYNAMICS STUDIES IN CHINA Final Report
Francis T. Wu 31 Mar. 1985 62 p
(Contract NAG5-240)
(NASA-CR-175617; NAS 1.26:175617) Avail: NTIS HC A04/MF A01 CSCL 08G

Geodynamics of Mainland China and Taiwan are discussed. The following research was performed: (1) the tectonics along the Tanlu fault in eastern China; (2) tectonics in the Taiwan Strait behind the collision zone in Taiwan; and (3) analysis of faulting in the vicinity of the Altyn Tagn fault. It is found that the existence of the fault is traced back to at least Jurassic with the deposition of conglomerate sandstones in the troungh along the present Tanlu fault branches in the Shantung Province. Taiwan is the product of collision between the Phillipine plate and the Asian plate and Taiwan came into being because of a former island arc. E.A.K.

N85-23266# Aeronautical Research Labs., Melbourne (Australia). Chemistry and Physics Lab.
BELOW-ROOM-TEMPERATURE WATER-VAPOR CONTINUUM ABSORPTION WITHIN THE 8- TO 10 MICRON ATMOSPHERIC TRANSMISSION WINDOW
G. L. Loper, M. A. ONeill, and J. A. Gelbwachs 11 May 1984 102 p refs
(Contract F04701-83-C-0084)
(TR-0084(4945-09)-1; SD-TR-84-14) Avail: NTIS HC A06/MF A01

Results of the weak water-continuum absorption within the 8 to 12 micron atmospheric transmission window are described. A highly sensitive photoacoustic detection technique was used in conjunction with a line-tunable CO2 laser 10.4 micron band. These measurements were performed over a range of atmospheric temperatures and water pressure important to the attenuation of radiation for long-slant atmospheric transmission paths. Water continuum CO2 laser absorption spectra are reported for temperatures between 27 and -10 C. The water continuum are best modeled by assuming simultaneous contributions of water dimer and collisional broadening mechanisms to the continuum. At room temperature and below, the water dimer mechanism becomes more important than the collisional broadening mechanism. B.G.

N85-23267# Saint Louis Univ., Mo. Dept. of Earth and Atmospheric Sciences.
ATTENUATION OF SEISMIC WAVES AT REGIONAL DISTANCES Final Technical Report, 1 Oct. 1982 - 30 Sep. 1984
O. W. Nuttli and B. J. Mitchell 27 Nov. 1984 132 p
(Contract F49620-83-C-0015; ARPA Order 4397)
(AD-A150198; AFOSR-84-1272TR) Avail: NTIS HC A07/MF A01 CSCL 08/11

The coda-Q method was applied to determine the anelastic attenuation of 1-sec period Lg waves at NTS(Nevada Test Site), East Kazakh, the Indian subcontinent, and the South American continent. Mb(Lg) m sub b (Lg) versus explosion yield calibration curves are given for NTS explosions in hard rock and in alluvium. The NTS hard-rock calibration curve, when applied to explosions in other regions of the United States and in the French Sahara, gives realistic yield estimates. The technique also is applied to selected Soviet explosions in East Kazakh. M sub b (Lg) and M sub b (P) values were used to estimate the M sub b (P) bias between NTS and eastern North America. Assuming that explosions and earthquakes of the same M sub b (P) value excite Lg waves of equal amplitude, the P-wave magnitude bias between NTS and eastern North America. Assuming that explosions and earthquakes of the same M sub b (P) value excite Lg waves of equal amplitude, the P-wave magnitude bias between NTS and eastern North America is 0.31 magnitude units. A tentative value for the bias between NTS and Shagan River is 0.41 magnitude units, but this value may be changed. Frequency-dependence of crustal Q seems significant in regions of high Q, but are small or non-existent in regions of low Q values. GRA

N85-23268# Argonne National Lab., Ill. Energy and Environmental System Div.
PROCEEDINGS OF THE GEOSCIENCE INSTRUMENTATION WORKSHOP
Daniel M. Rote Oct. 1984 48 p refs Workshop held at Argonne, Ill., 19-20 Apr. 1984 Sponsored in part by Chicago Univ.
(Contract W-31-109-eng-38)
(DE85-004359; ANL/EES-TM-266; CONF-8404216) Avail: NTIS HC A03/MF A01

A workshop was held to explore the question as to how collaborations between various universities, national laboratories, and companies might help alleviate some of the problems facing the geoscience community by assessing the nature and extent of the so-called instrumentation crisis. Issues of general interest to the geoscience community, issues of special interest to the academic community, and issues of interest to the national laboratories were addressed. The discussions of the several issues are summarized, and recommendations are made concerning many if not all of the issues, particularly concerning field and laboratory instrumentation. Issues include funding, access to facilities, off-the-shelf technology, and lack of well-trained staff. DOE

N85-23269*# National Aeronautics and Space Administration. Langley Research Center, Hampton, Va.
CUMULUS CLOUD VENTING OF MIXED LAYER OZONE
J. K. S. Ching (EPA, Research Triangle Park, N.C.), S. T. Shipley, E. V. Browell, and D. A. Brewer (Systems and Applied Sciences Corp.) Jan. 1985 9 p refs
(NASA-TM-87429; NAS 1.15:87429; PB85-144137;
EPA-600/D-84-299) Avail: NTIS HC A02/MF A01 CSCL 04A

Observations are presented which substantiate the hypothesis that significant vertical exchange of ozone and aerosols occurs between the mixed layer and the free troposphere during cumulus cloud convective activity. The experiments utilized the airborne Ultra-Violet Differential Absorption Lidar (UV-DIAL) system. This system provides simultaneous range resolved ozone concentration and aerosol backscatter profiles with high spatial resolution. Evening transects were obtained in the downwind area where the air mass had been advected. Space-height analyses for the evening flight show the cloud debris as patterns of ozone typically in excess of the ambient free tropospheric background. This ozone excess was approximately the value of the concentration difference between the mixed layer and free troposphere determined from independent vertical soundings made by another aircraft in the afternoon. GRA

N85-22423# Joint Publications Research Service, Arlington, Va.
PROTONS WITH ENERGIES ABOVE 30 KeV IN EARTH'S RADIATION BELT AT LOW ALTITUDES DURING MAGNETICALLY QUIET TIME CLOSE TO GEOMAGNETIC EQUATOR Abstract Only

N. A. Vlasova, B. N. Knyazev, A. S. Kovtyukh, A. G. Kozlov, M. I. Panasyuk, S. Y. Reyzman, and E. N. Sosnovets *In its* USSR Rept.: Space (JPRS-USP-85-001) 4 Feb. 1985 p 43 Transl. into ENGLISH from Kosmicheskiye Issled. (USSR), v. 22, no. 1, Jan.-Feb. 1984 p 53-66 (For primary document see N85-22403 13-12)
Avail: NTIS HC A07

N85-22424# Joint Publications Research Service, Arlington, Va.
ONE-DIMENSIONAL MODEL OF AURORAL MAGNETIC FORCE WITH LONGITUDINAL CURRENT AND CYCLOTRON HEATING OF IONS Abstract Only
M. A. Volkov, A. V. Volosevich, and Y. I. Galperin *In its* USSR Rept.: Space (JPRS-USP-85-001) 4 Feb. 1985 p 44 Transl. into ENGLISH from Kosmicheskiye Issled. (USSR), v. 22, no. 1, Jan.-Feb. 1984 p 67-86 Original language document announced as A84-26982 (For primary document see N85-22403 13-12)
Avail: NTIS HC A07

N85-22431# Joint Publications Research Service, Arlington, Va.
INCREASE IN HYDROGEN EMISSION OF UPPER ATMOSPHERE FOLLOWING LAUNCHES OF SPACE VEHICLES Abstract Only
N. M. Martsvaladze and L. M. Fishkova *In its* USSR Rept.: Space (JPRS-USP-85-001) 4 Feb. 1985 p 48 Transl. into ENGLISH from Kosmicheskiye Issled. (USSR), v. 22, no. 1, Jan.-Feb. 1984 p 136-137 Original language document announced as A84-26992 (For primary document see N85-22403 13-12)
Avail: NTIS HC A07

N85-22447# Joint Publications Research Service, Arlington, Va.
USE OF MOBILE SURFACE STATION FOR SYNCHRONOUS SATELLITE MEASUREMENTS IN SEISMOLOGICAL RESEARCH Abstract Only
G. K. Mardirosyn and D. N. Mishev *In its* USSR Rept.: Space (JPRS-USP-85-001) 4 Feb. 1985 p 77-78 Transl. into ENGLISH from Izv. Akad. Nauk Armyanskoy SSR: Nauki o Zemle (USSR), v. 37, no. 3, May-Jun. 1984 p 47-56 (For primary document see N85-22403 13-12)
Avail: NTIS HC A07

N85-22448# Joint Publications Research Service, Arlington, Va.
APPROXIMATE PERTURBING PART OF GEOPOTENTIAL BY POLYNOMIALS OF STIPULATED FORM Abstract Only
Y. V. Plakhov and A. V. Paramzin *In its* USSR Rept.: Space (JPRS-USP-85-001) 4 Feb. 1985 p 78-79 Transl. into ENGLISH from Izv. Vysshikh Uch. Zaved.: Geod. i Aerofotosyemka (USSR), no. 3, May-Jun. 1984 p 61-66 (For primary document see N85-22403 13-12)
Avail: NTIS HC A07

N85-22523*# Rice Univ., Houston, Tex.
ARGON ION POLLUTION OF THE MAGNETOSPHERE
Ramon E. Lopez *In* NASA. Lewis Research Center Spacecraft Environ. Interactions Technol., 1983 Mar. 1985 p 675-692 refs (For primary document see N85-22470 13-18)
Avail: NTIS HC A99/MF E03 CSCL 04A

N85-23113*# National Aeronautics and Space Administration. Goddard Space Flight Center, Greenbelt, Md.
SCIENTIFIC REQUIREMENTS FOR OZONE MEASUREMENTS
In its Ozone Correlative Meas. Workshop Mar. 1985 35 p refs (For primary document see N85-23112 13-42)
Avail: NTIS HC A04/MF A01 CSCL 04A

N85-23114*# National Aeronautics and Space Administration. Goddard Space Flight Center, Greenbelt, Md.
METHOD FOR DETERMINING THE NUMBER OF CORRELATIVE MEASUREMENTS REQUIRED TO VALIDATE THE SBUV/2 OZONE RETRIEVALS
John E. Frederick *In its* Ozone Correlative Meas. Workshop Mar. 1985 4 p (For primary document see N85-23112 13-42)
Avail: NTIS HC A04/MF A01 CSCL 04A

N85-23115*# National Aeronautics and Space Administration. Goddard Space Flight Center, Greenbelt, Md.
MEASUREMENT REQUIREMENTS FOR THE DETECTION OF OZONE TRENDS
John E. Frederick *In its* Ozone Correlative Meas. Workshop Mar. 1985 19 p (For primary document see N85-23112 13-42)
Avail: NTIS HC A04/MF A01 CSCL 04A

N85-23117# Joint Publications Research Service, Arlington, Va.
ARCTIC-NORTH ATLANTIC RIFT MEGASYSTEM Abstract Only
V. S. Surkov, O. G. Zhero, and L. V. Smirnov *In its* USSR Rept.: Earth Sci. (JPRS-UES-85-002) 1 Feb. 1985 p 1 Transl. into ENGLISH from Geol. i Geofiz. (Novosibirsk), no. 8, Aug. 1984 p 3-11 (For primary document see N85-23116 13-42)
Avail: NTIS HC A07/MF A01

N85-23124# Joint Publications Research Service, Arlington, Va.
NUMERICAL INVESTIGATION OF EVOLUTION OF ENERGY SPECTRUM OF SLIGHTLY NONLINEAR ROSSBY WAVES Abstract Only
G. M. Reznik and T. E. Soomere *In its* USSR Rept.: Earth Sci. (JPRS-UES-85-002) 1 Feb. 1985 p 10 Transl. into ENGLISH from Okeanol. (Moscow), v. 24, no. 3, May - Jun. 1984 p 373-384 (For primary document see N85-23116 13-42)
Avail: NTIS HC A07/MF A01

N85-23126# Joint Publications Research Service, Arlington, Va.
ABSOLUTE MOVEMENT OF PACIFIC OCEAN PLATE DURING LAST 120 MILLION YEARS Abstract Only
M. V. Kononov *In its* USSR Rept.: Earth Sci. (JPRS-UES-85-002) 1 Feb. 1985 p 16 Transl. into ENGLISH from Okeanol. (Moscow), v. 24, no. 3, May - Jun. 1984 p 484-492 (For primary document see N85-23116 13-42)
Avail: NTIS HC A07/MF A01

N85-23127# Joint Publications Research Service, Arlington, Va.
DETERMINING DEGREE OF PARTIAL MELTING OF ASTHENOSPHERE FROM SEISMIC DATA Abstract Only
Ye. I. Pristavakina *In its* USSR Rept.: Earth Sci. (JPRS-UES-85-002) 1 Feb. 1985 p 17 Transl. into ENGLISH from Okeanol. (Moscow), v. 24, no. 3, May - Jun. 1984 p 477-483 (For primary document see N85-23116 13-42)
Avail: NTIS HC A07/MF A01

N85-23135# Joint Publications Research Service, Arlington, Va.
USE OF PALEOMAGNETIC DATA IN TECTONIC ANALYSIS OF OCEANIC STRUCTURES Abstract Only
V. Kh. Gevorkyan, V. S. Markovskiy, and I. E. Lomakin *In its* USSR Rept.: Earth Sci. (JPRS-UES-85-002) 1 Feb. 1985 p 34 Transl. into ENGLISH from Geol. Zh. (Kiev), v. 44, no. 5, Sep. - Oct. 1984 p 85-87 (For primary document see N85-23116 13-42)
Avail: NTIS HC A07/MF A01

N85-23144# Joint Publications Research Service, Arlington, Va.
CRUSTAL AND UPPER MANTLE DENSITY MODEL OF OWEN FAULT ZONE Abstract Only
In its USSR Rept.: Earth Sci. (JPRS-UES-85-002) 1 Feb. 1985 p 53 Transl. into ENGLISH from Geofiz. Zh. (Kiev), v. 6, no. 3, Ma - Jun. 1984 p 51-57 (For primary document see N85-23116 13-42)
Avail: NTIS HC A07/MF A01

N85-23147# Joint Publications Research Service, Arlington, Va.
INFRARED AEROSOL ABSORPTION INDEX Abstract Only
L. B. Gabelko and Yu. S. Lyubovtseva *In its* USSR Rept.: Earth Sci. (JPRS-UES-85-002) 1 Feb. 1985 p 56-57 Transl. into ENGLISH from Izv. Akad. Nauk SSSR: Fiz. Atmosfery i Okeana (Moscow), v. 20, no. 8, Aug. 1984 p 715-724 Original language document was announced in IAA as A84-48648 (For primary document see N85-23116 13-42)
Avail: NTIS HC A07/MF A01

N85-23148# Joint Publications Research Service, Arlington, Va.
STUDY OF STRATIGRAPHY OF THE PRECAMBRIAN SOVIET BALTIC SHIELD Abstract Only
K. O. Krats, V. A. Negrutsa, Yu. B. Bogdanov, V. G. Gaskelberg, V. G. Zagorodnyy, T. F. Negrutsa, M. A. Semikhatov, and K. A. Shurkin *In its* USSR Rept.: Earth Sci. (JPRS-UES-85-002) 1 Feb. 1985 p 58 Transl. into ENGLISH from Sov. Geol. (Moscow), no. 7, Jul. 1984 p 105-118 (For primary document see N85-23116 13-42)
Avail: NTIS HC A07/MF A01

N85-23149# Joint Publications Research Service, Arlington, Va.
OBSERVATION OF LONG-PERIOD OSCILLATIONS OF EARTH Abstract Only
N. G. Savina, S. Ya. Tipisev, Ye. M. Linkov, and T. B. Yanovskaya *In its* USSR Rept.: Earth Sci. (JPRS-UES-85-002) 1 Feb. 1985 p 60 Transl. into ENGLISH from Izv. Akad. Nauk SSSR: Fiz. Zemli (Moscow), no. 8, Aug. 1984 p 3-12 (For primary document see N85-23116 13-42)
Avail: NTIS HC A07/MF A01

N85-23150# Joint Publications Research Service, Arlington, Va.
NUMERICAL MODELING OF PLANE STICK-SLIP FAULT Abstract Only
S. S. Arefyev and V. M. Grayzer *In its* USSR Rept.: Earth Sci. (JPRS-UES-85-002) 1 Feb. 1985 p 60 Transl. into ENGLISH from Izv. Akad. Nauk SSSR: Fiz. Zemli (Moscow). no. 8, Aug. 1984 p 13-21 (For primary document see N85-23116 13-42)
Avail: NTIS HC A07/MF A01

N85-23151# Joint Publications Research Service, Arlington, Va.
SCATTERING OF ELASTIC WAVES ON FRACTURES RANDOMLY DISTRIBUTED IN A THREE-DIMENSIONAL MEDIUM Abstract Only
S. A. Strizhkov and V. I. Ponyatovskaya *In its* USSR Rept.: Earth Sci. (JPRS-UES-85-002) 1 Feb. 1985 p 62 Transl. into ENGLISH from Izv. Akad. Nauk SSSR: Fiz. Zemli (Moscow), no. 8, Aug. 1984 p 72-77 (For primary document see N85-23116 13-42)
Avail: NTIS HC A07/MF A01

N85-23152# Joint Publications Research Service, Arlington, Va.
NATURAL ELECTROMAGNETIC RADIATION IN SEISMICALLY ACTIVE REGIONS Abstract Only
N. I. Migunov, G. A. Sobolev, and A. A. Khromov *In its* USSR Rept.: Earth Sci. (JPRS-UES-85-002) 1 Feb. 1985 p 63-64 Transl. into ENGLISH from Izv. Akad. Nauk SSSR: Fiz. Zemli (Moscow), no. 7, Jul. 1984 p 55-63 (For primary document see N85-23116 13-42)
Avail: NTIS HC A07/MF A01

N85-23153# Joint Publications Research Service, Arlington, Va.
DETERMINATION OF DENSITY OF THE CRUST AND UPPER MANTLE FROM DEEP SEISMIC SOUNDING AND GRAVIMETRY, 2 Abstract Only
T. V. Romanyuk and V. N. Strakhov *In its* USSR Rept.: Earth Sci. (JPRS-UES-85-002) 1 Feb. 1985 p 64 Transl. into ENGLISH from Izv. Akad. Nauk SSSR: Fiz. Zemli (Moscow), no. 7, Jul. 1984 p 64-80 (For primary document see N85-23116 13-42)
Avail: NTIS HC A07/MF A01

N85-23154# Joint Publications Research Service, Arlington, Va.
INDUCTION EXCITATION OF DEEP CONDUCTING ZONES Abstract Only
M. N. Berdichevskiy, A. I. Bilinskiy, V. M. Kobzova, and I. P. Moroz *In its* USSR Rept.: Earth Sci. (JPRS-UES-85-002) 1 Feb. 1985 p 65 Transl. into ENGLISH from Izv. Akad. Nauk SSSR: Fiz. Zemli (Moscow), no. 7, Jul. 1984 p 85-89 (For primary document see N85-23116 13-42)
Avail: NTIS HC A07/MF A01

N85-23155# Joint Publications Research Service, Arlington, Va.
STUDY OF RESOLUTION OF DEEP MT SOUNDINGS BY MEANS OF PHYSICAL MODEL Abstract Only
M. N. Berdichevskiy, A. I. Bilinskiy, V. M. Kobzova, and I. P. Moroz *In its* USSR Rept.: Earth Sci. (JPRS-UES-85-002) 1 Feb. 1985 p 65-66 Transl. into ENGLISH from Izv. Akad. Nauk. SSSR: Fiz. Zemli (Moscow), no. 7, Jul. 1984 p 85-89 (For primary document see N85-23116 13-42)
Avail: NTIS HC A07/MF A01

N85-23156# Joint Publications Research Service, Arlington, Va.
NATURE OF SEISMIC IMAGES WITH AMPLITUDE AND TIME FLUCTUATIONS OF RECORDED OSCILLATIONS Abstract Only
Yu. K. Tyapkin *In its* USSR Rept.: Earth Sci. (JPRS-UES-85-002) 1 Feb. 1985 p 66 Transl. into ENGLISH from Izv. Akad. Nauk SSSR: Fiz. Zemli (Moscow), no. 7, Jul. 1984 p 90-97 (For primary document see N85-23116 13-42)
Avail: NTIS HC A07/MF A01

N85-23157# Joint Publications Research Service, Arlington, Va.
SPACE AND TIME DISTRIBTUION OF AFTERSHOCKS Abstract Only
N. D. Zhalkovskiy and V. I. Muchnaya *In its* USSR Rept.: Earth Sci. (JPRS-UES-85-002) 1 Feb. 1985 p 67 Transl. into ENGLISH from Geol. y Geofiz. (Novosibirsk), no. 8, Aug. 1984 p 108-117 (For primary document see N85-23116 13-42)
Avail: NTIS HC A07/MF A01

N85-23158# Joint Publications Research Service, Arlington, Va.
DETERMINING VECTOR OF RADIOINTERFEROMETER BASE FROM OBSERVATIONS OF NATURAL RADIO EMISSION WITH NARROW SPECTRUM Abstract Only
G. A. Shanurov *In its* USSR Rept.: Earth Sci. (JPRS-UES-85-002) 1 Feb. 1985 p 67-68 Transl. into ENGLISH from Izv. Vyssh. Ucheb Zaved.: Geod. i Aerofotosyemka (Moscow), no. 2, Mar. - Apr. 1984 p 9-13 (For primary document see N85-23116 13-42)
Avail: NTIS HC A07/MF A01

N85-23159# Joint Publications Research Service, Arlington, Va.
STRUCTURE OF ICELAND AND OCEAN FLOOR SPREADING Abstract Only
V. V. Ez *In its* USSR Rept.: Earth Sci. (JPRS-UES-85-002) 1 Feb. 1985 p 73-74 Transl. into ENGLISH from Geotektonika (Moscow), no. 3, May - Jun. 1984 p 100-111 (For primary document see N85-23116 13-42)
Avail: NTIS HC A07/MF A01

N85-23161# Joint Publications Research Service, Arlington, Va.
MAGMATISM IN CONTINENT-OCEAN TRANSITION ZONE (DEVELOPMENT OF IDEAS OF A. N. ZAVARITSKIY) Abstract Only
O. A. Bogatikov, V. I. Kovalenko, I. D. Ryabchikov, and A. A. Tsvetkov *In its* USSR Rept.: Earth Sci. (JPRS-UES-85-002) 1 Feb. 1985 p 76 Transl. into ENGLISH from Izv. Akad. Nauk SSSR: Ser. Geol. (Moscow), no. 6, Jun. 1984 p 8-27 (For primary document see N85-23116 13-42)
Avail: NTIS HC A07/MF A01

N85-23163# Joint Publications Research Service, Arlington, Va.
NORMAL AND ANOMALOUS GEOTHERMAL FIELDS AND THEIR RELATIONSHIP TO HIERARCHY OF GEOLOGICAL BODIES Abstract Only
S. S. Sardarov, Jr., A. V. Savin, and M. G. Pashuk *In its* USSR Rept.: Earth Sci. (JPRS-UES-85-002) 1 Feb. 1985 p 78-79 Transl. into ENGLISH from Dokl. Akad. Nauk SSSR (Moscow), v. 275, no. 5, Apr. 1984 p 1084-1087 (For primary document see N85-23116 13-42)
Avail: NTIS HC A07/MF A01

N85-23164# Joint Publications Research Service, Arlington, Va.
VARIATIONS IN RESISTIVITY OF UPPER CRUSTAL LAYER Abstract Only
A. Ya. Sidorin *In its* USSR Rept.: Earth Sci. (JPRS-UES-85-002) 1 Feb. 1985 p 80 Transl. into ENGLISH from Dokl. Akad. Nauk SSSR (Moscow), v. 278, no. 2, Sep. 1984 p 330-334 (For primary document see N85-23116 13-42)
Avail: NTIS HC A07/MF A01

N85-23165# Joint Publications Research Service, Arlington, Va.
BOUNDARY VELOCITIES OF LONGITUDINAL SEISMIC WAVES AND LATERAL INHOMOGENEITIES OF UPPER OCEAN MANTLE Abstract Only
N. Ya. Kunin, N. V. Goncharova, G. I. Semenova, S. V. Usenko, E. R. Sheykhzade, and Yu. G. Zorina *In its* USSR Rept.: Earth Sci. (JPRS-UES-85-002) 1 Feb. 1985 p 82-83 Transl. into ENGLISH from Dokl. Akad. Nauk SSSR (Moscow), v. 278, no. 1, Sep. 1984 p 76-81 (For primary document see N85-23116 13-42)
Avail: NTIS HC A07/MF A01

N85-23166# Joint Publications Research Service, Arlington, Va.
DISCRIMINATION OF NORMAL AND ANOMALOUS MAGNETIC AND ELECTRIC FIELDS IN GEOELECTROMAGNETIC VARIATIONS Abstract Only
V. v. Aksenov *In its* USSR Rept.: Earth Sci. (JPRS-UES-85-002) 1 Feb. 1985 p 83 Transl. into ENGLISH from Geol. i Geofiz. (Novosibirsk), no. 7, Jul. 1984 p 121-126 (For primary document see N85-23116 13-42)
Avail: NTIS HC A07/MF A01

N85-23167# Joint Publications Research Service, Arlington, Va.
REFLECTED WAVE TRAVEL-TIME CURVES IN STRATIFIED MEDIA WITH VERTICALLY HETEROGENEOUS LAYERS AND SLIGHTLY SLOPING CURVED BOUNDARIES Abstract Only
E. A. Blyas *In its* USSR Rept.: Earth Sci. (JPRS-UES-85-002) 1 Feb. 1985 p 84 Transl. into ENGLISH from Geol. i Geofiz. (Novosibirsk), no. 7, Jul. 1984 p 107-114 (For primary document see N85-23116 13-42)
Avail: NTIS HC A07/MF A01

N85-23168# Joint Publications Research Service, Arlington, Va.
STUDY OF GEOLOGICAL MEDIA BASED ON SCATTERED EARTHQUAKE WAVES Abstract Only
V. G. Bovenko and B. Ye. Shcherbakova *In its* USSR Rept.: Earth Sci. (JPRS-UES-85-002) 1 Feb. 1985 p 86 Transl. into ENGLISH from Dokl. Akad. Nauk SSSR (Moscow), v. 278, no. 3, Sep. 1984 p 575-580 (For primary document see N85-23116 13-42)
Avail: NTIS HC A07/MF A01

N85-23169# Joint Publications Research Service, Arlington, Va.
CONSIDERATION OF HETEROGENEITY OF GRAVITY FIELDS IN LOCAL HIGH PRECISION GEODETIC CONSTRUCTIONS Abstract Only
A. A. Konopikhin, L. V. Ogorodova, and A. P. Yuzefovich *In its* USSR Rept.: Earth Sci. (JPRS-UES-85-002) 1 Feb. 1985 p 97 Transl. into ENGLISH from Izv. Vyssh. Ucheb. Zaved., Geod. i Aerofotosyemka (Moscow), no. 3, May - Jun. 1983 p 66-72 (For primary document see N85-23116 13-42)
Avail: NTIS HC A07/MF A01

N85-23170# Joint Publications Research Service, Arlington, Va.
MATHEMATICAL MODELING OF RESULTS OF GEOMETRIC LEVELING IN VARIABLE GRAVITY FIELD Abstract Only
I. G. Vovk *In its* USSR Rept.: Earth Sci. (JPRS-UES-85-002) 1 Feb. 1985 p 97-98 Transl. into ENGLISH from Izv. Vyssh. Ucheb. Zaved., Geod. i Aerofotosyemka (Moscow), no. 3, May - Jun. 1984 p 72-75 (For primary document see N85-23116 13-42)
Avail: NTIS HC A07/MF A01

N85-23173# Joint Publications Research Service, Arlington, Va.
THERMOHYDRODYNAMIC MODEL: HYDROTHERMAL SYSTEM, SHALLOWLY SEATED MAGMA CHAMBER Abstract Only
A. V. Kiryukhin *In its* USSR Rept.: Earth Sci. (JPRS-UES-85-002) 1 Feb. 1985 p 101 Transl. into ENGLISH from Vulkanol. i Seysmologiya (Moscow), no. 3, May - Jun. 1984 p 25-34 (For primary document see N85-23116 13-42)
Avail: NTIS HC A07/MF A01

N85-23174# Joint Publications Research Service, Arlington, Va.
POLYNOMIAL PARAMETERIZATION IN INVERSE GRAVIMETRIC PROBLEM Abstract Only
G. G. Rempel and G. I. Tatkov *In its* USSR Rept.: Earth Sci. (JPRS-UES-85-002) 1 Feb. 1985 p 107 Transl. into ENGLISH from Geol. i Geofiz. (Novosibirsk), no. 4, Apr. 1984 p 99-105 (For primary document see N85-23116 13-42)
Avail: NTIS HC A07/MF A01

N85-23175# Joint Publications Research Service, Arlington, Va.
PRIMARY PROCESSING OF EXPERIMENTAL MAGNETOVARIATION SOUNDING DATA USING SPLINE FUNCTIONS Abstract Only
O. N. Balykina *In its* USSR Rept.: Earth Sci. (JPRS-UES-85-001) 1 Feb. 1985 p 108 Transl. into ENGLISH from Geol. i Geofiz. (Novosibirsk), no. 4, Apr. 1984 p 120-124 (For primary document see N85-23116 13-42)
Avail: NTIS HC A07/MF A01

N85-23176# Joint Publications Research Service, Arlington, Va.
APPLICATION OF FIELD X-RAY: RADIOMETRIC ANALYSIS IN EXPLORATORY GEOLOGY AND MEANS FOR ITS IMPROVEMENT Abstract Only
D. B. Barkhatov and N. I. Butomo *In its* USSR Rept.: Earth Sci. (JPRS-UES-85-002) 1 Feb. 1985 p 109 Transl. into ENGLISH from Vestn. Leningr. Univ.: Geol., Geogr. (Leningrad), no. 6, issue 1, Mar. 1984 p 96-100 (For primary document see N85-23116 13-42)
Avail: NTIS HC A07/MF A01

N85-23178# Joint Publications Research Service, Arlington, Va.
GEOMAGNETIC PRECURSORS OF INTENSIVE EARTHQUAKES IN THE 1-0,-2 Hz FREQUENCY RANGE OF GEOMAGNETIC PULSATIONS Abstract Only
Ya. M. Gogatishvili *In its* USSR Rept.: Earth Sci. (JPRS-UES-85-002) 1 Feb. 1985 p 112 Transl. ito ENGLISH from Geomagnetizm i Aeronomiya (Moscow), v. 24, Jul. - Aug. 1984 p 697-700 (For primary document see N85-23116 13-42)
Avail: NTIS HC A07/MF A01

N85-23179# Joint Publications Research Service, Arlington, Va.
SOLUTION OF DIRECT MAGNETOMETRIC PROBLEM ON SPHERICAL EARTH Abstract Only
A. G. Manukyan and V. I. Starostenko *In its* USSR Rept.: Earth Sci. (JPRS-UES-85-002) 1 Feb. 1985 p 113 Transl. into ENGLISH from Dokl. Akad. Nauk Ukr. SSR, Ser. B: Geol., Khim. i Biol. Nauki (Kiev), no. 5, May 1984 p 11-14 (For primary document see N85-23116 13-42)
Avail: NTIS HC A07/MF A01

N85-23181# Joint Publications Research Service, Arlington, Va.
SEISMIC WAVES AND DISPERSION RELATIONS Abstract Only
V. P. Rudnitskiy *In its* USSR Rept.: Earth Sci. (JPRS-UES-85-002) 1 Feb. 1985 p 114 Transl into ENGLISH from Dokl. Akad. Nauk Ukr. SSR, Ser. B: Geol., Khim. i Biol. Nauki (Kiev), no. 5, May 1984 p 17-20 (For primary document see N85-23116 13-42)
Avail: NTIS HC A07/MF A01

N85-23182# Joint Publications Research Service, Arlington, Va.
GEOMAGNETIC FIELD DYNAMICS Abstract Only
L. I. Vigilyanskaya *In its* USSR Rept.: Earth Sci. (JPRS-UES-85-002) 1 Feb. 1985 p 121 Transl. into ENGLISH from Geofiz. Zh. (Kiev), v. 6, no. 3, May - Jun. 1984 p 69-73 (For primary document see N85-23116 13-42)
Avail: NTIS HC A07/MF A01

N85-23183# Joint Publications Research Service, Arlington, Va.
INTERRELATIONSHIP OF EARTHQUAKE MAGNITUDE AND LITHOSPHERIC-ASTHENOSPHERIC THERMODYNAMIC PARAMETERS IN SEISMICALLY ACTIVE ZONES Abstract Only
L. I. Tuliani *In its* USSR Rept.: Earth Sci. (JPRS-UES-85-002) 1 Feb. 1985 p 122 Transl. into ENGLISH from Geofiz. Zh. (Kiev), v. 6, no. 3, May - Jun. 1984 p 73-76 (For primary document see

N85-23116 13-42)
Avail: NTIS HC A07/MF A01

N85-23184# Joint Publications Research Service, Arlington, Va.
CORRECTING DEPTH LINE ON NONLONGITUDINAL SEISMIC PROFILE Abstract Only
D. V. Lysynchuk *In its* USSR Rept.: Earth Sci. (JPRS-UES-85-002) 1 Feb. 1985 p 123-124 Transl. into ENGLISH from Geofiz. Zh. (Kiev), v. 6, no. 3, May - Jun. 1984 p 83-85 (For primary document see N85-23116 13-42)
Avail: NTIS HC A07/MF A01

N85-23185# Joint Publications Research Service, Arlington, Va.
METHOD FOR PROCESSING BROAD-PROFILE DATA Abstract Only
Yu. A. Vasilyev and N. Z. Prokhur *In its* USSR Rept.: Earth Sci. (JPRS-UES-85-002) 1 Feb. 1985 p 124 Transl. into ENGLISH from Geofiz. Zh. (Kiev), v. 6, no. 3, May - Jun. 1984 p 85-88 (For primary document see N85-23116 13-42)
Avail: NTIS HC A07/MF A01

N85-23437# Joint Publications Research Service, Arlington, Va.
RAPID ADVANCES IN GEOLOGICAL WORK
Sun Daguang *In its* China Rept.: Sci. and Technol. (JPRS-CST-85-003) 28 Jan. 1985 p 70-72 Transl. into ENGLISH from Guangming Ribao (Beijing), 22 Aug. 1984 p 2 (For primary document see N85-23433 13-81)
Avail: NTIS HC A11/MF A01

N85-23438# Joint Publications Research Service, Arlington, Va.
CHARACTERISTICS OF ALUMYTE DEPOSITS DISCUSSED
Xiao Zengqi, Cao Xianming, and Luo Shengqi *In its* China Rept.: Sci. and Technol. (JPRS-CST-85-003) 28 Jan. 1985 p 74-82 Transl. into ENGLISH from Zhongguo Dizhi (Beijing), no. 7, 1984 p 12-16 (For primary document see N85-23433 13-81)
Avail: NTIS HC A11/MF A01

N85-23564*# Jet Propulsion Lab., California Inst. of Tech., Pasadena.
THERMAL INFRARED OBSERVATIONS OF LAVA FLOWS DURING THE 1984 MAUNA LOA ERUPTION Abstract Only
David C. Pieri, R. Gillespie, Ann B. Kahle, James Kahle (California Div. of Mines and Geology), and Stephen M. Baloga *In* NASA, Washington Repts. of Planetary Geol. and Geophys. Program Apr. 1985 p 251-255 refs (For primary document see N85-23474 13-91)
Avail: NTIS HC A99/MF A01 CSCL 08K

N85-23565*# Arizona State Univ., Tempe. Dept. of Geology.
FIELD MEASUREMENTS OF THE 1983 ROYAL GARDENS LAVA FLOWS, KILAUEA VOLCANO, AND 1984 MAUNA LOA LAVA FLOWS, HAWAII Abstract Only
Jonathan Fink and Jim Zimbelman *In* NASA, Washington Repts. of Planetary Geol. and Geophys. Program Apr. 1985 p 256-258 refs (For primary document see N85-23474 13-91)
Avail: NTIS HC A99/MF A01 CSCL 08K

N85-23566*# Hawaii Univ., Honolulu. Inst. of Geophysics.
SURFACE STRUCTURES OF HAWAIIAN LAVAS Abstract Only
Scott K. Rowland and George P. L. Walker *In* NASA, Washington Repts. of Planetary Geol. and Geophys. Program Apr. 1985 p 259-260 refs (For primary document see N85-23474 13-91)
Avail: NTIS HC A99/MF A01 CSCL 08L

N85-23567*# Arizona State Univ., Tempe. Dept. of Geology.
BASALTIC PRESSURE RIDGES: FORMATION AND RELATIONSHIP TO FLOW EMPLACEMENT Abstract Only
E. Theilig *In* NASA, Washington Repts. of Planetary Geol. and Geophys. Program Apr. 1985 p 261-262 (For primary document see N85-23474 13-91)
Avail: NTIS HC A99/MF A01 CSCL 08G

N85-23568*# Oregon State Univ., Corvallis. Dept. of Geography.
MORPHOLOGIC EVOLUTION OF THE MOUNT ST. HELENS CRATER AREA, WASHINGTON Abstract Only
Gary L. Beach *In* NASA, Washington Repts. of Planetary Geol. and Geophys. Program Apr. 1985 p 263-265 refs (For primary document see N85-23474 13-91)
Avail: NTIS HC A99/MF A01 CSCL 08K

N85-23569*# New Mexico Univ., Albuquerque. Dept. of Geology.
VOLCANISM OF THE COLORADO PLATEAU (BASIN AND RANGE TRANSITION): IMPLICATIONS FOR CRUSTAL PROCESSES Abstract Only
Christopher D. Condit and Wolfgang E. Elston *In* NASA, Washington Repts. of Planetary Geol. and Geophys. Program Apr. 1985 p 266-268 refs (For primary document see N85-23474 13-91)
Avail: NTIS HC A99/MF A01 CSCL 08K

N85-23570*# State Univ. of New York, Buffalo. Dept. of Geological Sciences.
THE GEOLOGY OF EAST BUTTE, A RHYOLITIC VOLCANIC DOME ON THE EASTERN SNAKE RIVER PLAIN, IDAHO Abstract Only
John E. Bretches and John S. King *In* NASA, Washington Repts. of Planetary Geol. and Geophys. Program Apr. 1985 p 269-271 refs (For primary document see N85-23474 13-91)
Avail: NTIS HC A99/MF A01 CSCL 08G

N85-23571*# State Univ. of New York, Buffalo. Dept. of Geological Sciences.
THE GEOLOGY OF MT. HOPE, A SILICIC VOLCANIC CENTER IN WEST CENTRAL ARIZONA Abstract Only
Ardyth M. Simmons and John S. King *In* NASA, Washington Repts. of Planetary Geol. and Geophys. Program Apr. 1985 p 272-274 refs (For primary document see N85-23474 13-91)
Avail: NTIS HC A99/MF A01 CSCL 08G

N85-23572*# Arizona State Univ., Tempe. Dept. of Geology.
A SILICIC SHIELD VOLCANO IN BOLIVIA Abstract Only
P. R. Christensen and R. Greeley *In* NASA, Washington Repts. of Planetary Geol. and Geophys. Program Apr. 1985 p 275-276 refs (For primary document see N85-23474 13-91)
Avail: NTIS HC A99/MF A01 CSCL 08L

N85-23573*# Hawaii Univ., Honolulu. Inst. of Geophysics.
SUBMARINE VOLCANIC ERUPTIONS AND POTENTIAL ANALOGS FOR VENUS Abstract Only
L. Wilson, P. J. MouginisMark, P. Fryer, and L. R. Gaddis *In* NASA, Washington Repts. of Planetary Geol. and Geophys. Program Apr. 1985 p 277-279 refs (For primary document see N85-23474 13-91)
Avail: NTIS HC A99/MF A01 CSCL 08K

N85-23574*# Arizona State Univ., Tempe. Dept. of Geology.
HYDROVOLCANISM Abstract Only
Michael F. Sheridan and Kenneth H. Wohletz (LASL) *In* NASA, Washington Repts. of Planetary Geol. and Geophys. Program Apr. 1985 p 280-282 refs (For primary document see N85-23474 13-91)
Avail: NTIS HC A99/MF A01 CSCL 08K

N85-23582*# Arizona State Univ., Tempe. Dept. of Geology.
A COMPARISON OF TERRESTRIAL SALTATION FLUX IN THE LABORATORY AND THE FIELD Abstract Only
S. H. Williams and R. Greeley *In* NASA, Washington Repts. of Planetary Geol. and Geophys. Program Apr. 1985 p 305-306 refs (For primary document see N85-23474 13-91)
Avail: NTIS HC A99/MF A01 CSCL 08G

N85-23588*# Oregon State Univ., Corvallis. College of Oceanography.
EXPERIMENTS AND ANALYSES OF THE FORMATION OF

EROSIONAL SCOUR MARKS WITH IMPLICATIONS TO THE ORIGIN OF THE MARTIAN OUTFLOW CHANNELS Abstract Only
Paul D. Komar *In* NASA, Washington Repts. of Planetary Geol. and Geophys. Program Apr. 1985 p 322-324 refs (For primary document see N85-23474 13-91)
Avail: NTIS HC A99/MF A01 CSCL 08G

N85-23590*# California State Polytechnic Univ., Pomona. Dept. of Earth Science.
TERRESTRIAL ANALOG STUDIES FOR MARTIAN PATTERNED GROUND Abstract Only
Lisa A. Rossbacher *In* NASA, Washington Repts. of Planetary Geol. and Geophys. Program Apr. 1985 p 329-331 refs Sponsored in part by Uppsala Univ., Sweden (For primary document see N85-23474 13-91)
(Grant NAGw-517)
Avail: NTIS HC A99/MF A01 CSCL 08G

N85-23604*# Arizona State Univ., Tempe. Dept. of Geology.
PLANETARY ANALOGS IN ANTARCTICA: MARS Abstract Only
Michael C. Malin *In* NASA, Washington Repts. of Planetary Geol. and Geophys. Program, 1984 Apr. 1985 p 371-373 refs (For primary document see N85-23474 13-91)
Avail: NTIS HC A99/MF A01 CSCL 08G

N85-23605*# Arizona State Univ., Tempe.
PLANETARY ANALOGS IN ANTARCTICA: ICY SATELLITES Abstract Only
Michael C. Malin *In* NASA, Washington Repts. of Planetary Geol. and Geophys. Program, 1984 Apr. 1985 p 374-375 refs (For primary document see N85-23474 13-91)
Avail: NTIS HC A99/MF A01 CSCL 08L

N85-23626*# Sul Ross State Univ., Alpine, Tex. Dept. of Geology.
ANALYSIS OF SMIRR DATA FOR VOLCANIC AND SEDIMENTARY TERRAINS OF THE TRANS-PECOS REGION, TEXAS Abstract Only
H. Grady Blount and James L. WhitfordStark *In* NASA, Washington Repts. of Planetary Geol. and Geophys. Program, 1984 Apr. 1985 p 432-433 refs (For primary document see N85-23474 13-91)
Avail: NTIS HC A99/MF A01 CSCL 08G

N85-23628*# National Aeronautics and Space Administration. Lyndon B. Johnson Space Center, Houston, Tex.
CHEMICAL WEATHERING OF SOILS FROM THE DRY VALLEYS OF ANTARCTICA: A TERRESTRIAL ANALOG OF MARTIAN WEATHERING PROCESSES Abstract Only
Everett K. Gibson, Jr. *In* NASA, Washington Repts. of Planetary Geol. and Geophys. Program, 1984 Apr. 1985 p 437-439 refs (For primary document see N85-23474 13-91)
Avail: NTIS HC A99/MF A01 CSCL 08G

N85-23629*# Jet Propulsion Lab., California Inst. of Tech., Pasadena.
PROPERTIES OF FILAMENTARY SUBLIMATION RESIDUES FROM DISPERSIONS OF CLAY IN ICE Abstract Only
James B. Stephens, Timothy J. Parker, R. Stephen Saunders, Eric G. Laue, and Fraser P. Fanale (Hawaii Univ., Honolulu) *In* NASA, Washington Repts. of Planetary Geol. and Geophys. Program, 1984 Apr. 1985 p 440-442 refs (For primary document see N85-23474 13-91)
Avail: NTIS HC A99/MF A01 CSCL 08L

N85-23644*# Jet Propulsion Lab., California Inst. of Tech., Pasadena.
TERRESTRIAL ANALOGS FOR PLANETARY WRINKLE RIDGES Abstract Only
J. B. Plescia (Geological Survey, Flagstaff, Ariz.) and M. Golombek *In* NASA, Washington Repts. of Planetary Geol. and Geophys. Program, 1984 Apr. 1985 p 482-484 refs (For primary document see N85-23474 13-91)
Avail: NTIS HC A99/MF A01 CSCL 08G

N85-23648*# McDonnell Automation Co., St. Louis, Mo. Dept. of Earth and Planetary Sciences.
BOUGUER IMAGES OF THE NORTH AMERICAN CRATON Abstract Only
R. E. Arvidson, D. I. Bindschadler, S. Bowring, M. Eddy, E. Guinness, and C. Leff *In* NASA, Washington Repts. of Planetary Geo. and Geophys. Program, 1984 Apr. 1985 p 494-496 refs (For primary document see N85-23474 13-91)
Avail: NTIS HC A99/MF A01 CSCL 08G

47 METEOROLOGY AND CLIMATOLOGY

Includes weather forecasting and modification.

N85-23270 California Univ., Los Angeles.
CUMULUS EFFECTS ON THE LARGE-SCALE VORTICITY AND MOMENTUM FIELDS IN THE TROPICAL ATMOSPHERE Ph.D. Thesis
Chung-Hsiung Sui 1984 170 p
Avail: Univ. Microfilms Order No. DA8428579

The relationship between the residual of large-scale vorticity budget and cumulus convection in the tropical eastern Atlantic is studied using the data taken during the Phase 3 of GARP (Global Atmospheric Research Program) Atlantic Tropical Experiment (GATE). The appearance of large vorticity budget residual in the upper and middle troposphere is clearly associated with intense deep cumulus convection. The association becomes less clear in the lower troposphere particularly when there is strong vertical wind shear. An effort is made to recover the cumulus-induced time rate of change of the rotational part of wind from the vorticity budget residual. It is found that cumulus convection strongly decelerates large-scale flow especially in the upper troposphere. Parameterized expressions for the cumulus-induced time rate of change of momentum and for the vorticity budget residual, Z, are derived in a mutually consistent manner. The parameterizations are expressed in terms of cumulus mass flux, detrainment, momentum as well as large-scale momentum and vorticity.
Dissert. Abstr.

N85-23271*# Pennsylvania State Univ., University Park. Dept. of Meteorology.
ANALYSIS OF THE INFLOW LAYER AND AIR-SEA INTERACTIONS IN HURRICANE FREDERIC (1979) Annual Progress Report
William M. Frank Apr. 1985 8 p refs
(Grant NAG5-398)
(NASA-CR-175616; NAS 1.26:175616) Avail: NTIS HC A02/MF A01 CSCL 04B

The current study is attempting to overcome the problem of uncertain heights of the satellite winds. The effective heights of the satellite wind vectors were determined. Satellite, aircraft, rawinsonde and surface wind measurements were integrated into a three dimensional analysis of the storm in flow layer over water. Similar analyses of the thermodynamic field in the inflow layer were conducted. Diagnostic budget analyses of moisture, sensible heat kinetic energy and momentum in the inflow layer were conducted. Air-sea interactions were also examined. B.W.

N85-23272*# Colorado Univ., Boulder. Cooperative Inst. for Research in Environmental Sciences.
EMPIRICAL AND MODELED SYNOPTIC CLOUD CLIMATOLOGY OF THE ARCTIC OCEAN Annual Progress Report, Apr. 1984 - Mar. 1985
roger G. Barry and Robert G. Crane 1985 10 p
(Grant NAG5-417)
(NASA-CR-175628; NAS 1.26:175628) Avail: NTIS HC A02/MF A01 CSCL 04B

A daily climatology of the atmospheric circulation of the Arctic and the associated cloud conditions were determined. These are used for comparisons with the variability of general circulation model, generated circulation, and cloud cover for the same region. E.A.K.

N85-23273*# National Aeronautics and Space Administration. Marshall Space Flight Center, Huntsville, Ala.
PRELIMINARY STUDY OF INPHASE GUSTS AND MOMENT FORCE WIND LOADS OVER THE FIRST 150 METERS AT KSC, FLORIDA
John W. Kaufman May 1985 22 p refs
(NASA-TM-86501; NAS 1.15:86501) Avail: NTIS HC A02/MF A01 CSCL 04B

A mathematical/statistical analysis of inphase gusts and wind velocity moment forces over the first 150 m at the Kennedy Space Center (KSC) is presented. The wind velocity profile data were acquired at the KSC 150 m ground wind tower. The results show that planetary boundary layer (PBL) winds can sustain near peak speeds for periods up to 60 sec and longer. This is proven from calculating the autocorrelation functions of moment forces for several 10 min cases of wind profile data. The results show that lower atmospheric planetary boundary layer winds have periodic variations for long periods of time. This flow characteristic is valuable as aerospace vehicle engineering and design criteria where wind loading must be determined. E.A.K.

N85-23274# Naval Postgraduate School, Monterey, Calif.
MEAN FLOW AND TURBULENCE IN COMPLEX TERRAIN NPS (NAVAL POSTGRADUATE SCHOOL)/VANDENBERG MEASUREMENT SYSTEM Report, for Aug. 1983 - Mar. 1984
G. E. Schacher and T. P. Stanton Mar. 1984 132 p
(AD-A150184; NPS-61-84-005) Avail: NTIS HC A07/MF A01 CSCL 04/2

A data acquisition system has been installed at Vandenberg Air Force Base to obtain meteorological data from 12 of the existing 23 towers. Data processing and storage includes means and standard deviations for time periods of 15 sec, 5 min, 15 min, and 1 hr. The 15 sec data contains those quantities needed to form averages, with standard deviations, over any longer time period. All data contains turbulence frequency components to 1 Hz. The purpose of the project is to characterize turbulence in complex terrain for use in diffusion modeling. GRA

N85-23275# Air Force Wright Aeronautical Labs., Wright-Patterson AFB, Ohio.
1981 wC-130 AIRBORNE LIGHTNING CHARACTERIZATION PROGRAM DATA REVIEW Interim Report, Jul. 1981 - Dec. 1983
B. P. Kuhlman, M. J. Reazer, and P. L. Rustan Aug. 1984 77 p
(AD-A150230; AFWAL-TR-84-3024) Avail: NTIS HC A05/MF A01 CSCL 04/1

This report presents a review of airborne lightning data collected in late August 1981 by a wC-130 aircraft flying at 1500 to 18000 feet in the vicinity of thunderstorms over the Florida peninsula. Eleven electric and magnetic field sensors mounted on the aircraft provided outputs which were recorded both as continuous analog data with 2 megahertz bandwidth and as digital records of 164 microsecond windows with 20 megahertz bandwidth. Large amounts of data were collected for many parts of cloud-to-ground and intracloud lightning processes, including first and subsequent return strokes, stepped and dart-stepped leaders, preliminary breakdown pulses and intracloud pulses. Risetimes and field rates-of-change have been calculated and compared with ground-based measurements. The data analyzed include 1034 lightning flashes from the analog record and 518 digital recordings, the latter including 347 return strokes, 68 events occurring ahead of the return stroke and 97 events from intracloud discharges. Submicrosecond risetimes were found in all the discharge phases analyzed and field rates-of-change for some intracloud processes approached rates-of-change for return strokes. GRA

N85-23276# Naval Oceanography Command Detachment, Asheville, N.C.
SUMMARY OF METEOROLOGICAL OBSERVATIONS, SURFACE (SMOS), FALLON, NEVADA Reference Report, 1973 - 1982
Aug. 1984 355 p
(AD-A150481) Avail: NTIS HC A16/MF A01 CSCL 04/2

This data report consists of a six part statistical summary of surface weather observations. The six parts are: (Part 1) Weather Conditions/Atmospheric Phenomena, (Part 2) Precipitation/Snowfall/Snow Depth, (Part 3) Surface Winds, (Part 4) Ceiling versus Visibility/Sky Cover, (Part 5) Psychrometric Summaries, and (Part 6) Station Pressure/Sea Level Pressure. GRA

N85-23277# Naval Oceanography Command Detachment, Asheville, N.C.
SUMMARY OF METEOROLOGICAL OBSERVATIONS, SURFACE (SMOS) CAMP PENDLETON, CALIFORNIA Reference Report, 1973 - 1982
Sep. 1984 361 p
(AD-A150482) Avail: NTIS HC A16/MF A01 CSCL 04/2

This data report consists of a six part statistical summary of surface weather observations. The six parts are: (Part 1) Weather Conditions/Atmospheric Phenomena, (Part 2) Precipitation/Snowfall/Snow Depth, (Part 3) Surface Winds, (Part 4) Ceiling versus Visibility/Sky Cover, (Part 5) Psychrometric Summaries, and (Part 6) Station Pressure/Sea Level Pressure. GRA

N85-23278# Naval Oceanography Command Detachment, Asheville, N.C.
SUMMARY OF METEOROLOGICAL OBSERVATIONS, SURFACE (SMOS), BERMUDA Reference Report, 1973 - 1982
Sep. 1984 362 p
(AD-A150537) Avail: NTIS HC A16/MF A01 CSCL 04/2

This data report consists of a six part statistical summary of surface weather observations. The six parts are: (Part 1) Weather Conditions/Atmospheric Phenomena, (Part 2) Precipitation/Snowfall/Snow Depth, (Part 3) - Surface Winds, (Part 4) Ceiling versus Visibility/Sky Cover, (Part 5) Psychrometric Summaries, and (Part 6) Station Pressure/Sea Level Pressure. Author (GRA)

N85-23279# Naval Oceanography Command Detachment, Asheville, N.C.
SUMMARY OF METEOROLOGICAL OBSERVATIONS, SURFACE (SMOS), BEAUFORT, SOUTH CAROLINA Reference Report, 1973 - 1982
Aug. 1984 365 p
(AD-A150538) Avail: NTIS HC A16/MF A01 CSCL 04/2

This data report consists of a six part statistical summary of surface weather observations. The six parts are: (Part 1) Weather Conditions/Atmospheric Phenomena, (Part 2) Precipitation/Snowfall/Snow Depth, (Part 3) Surface Winds, (Part 4) Ceiling versus Visibility/Sky Cover, (Part 5) Psychrometric Summaries, and (Part 6) Station Pressure/Sea Level Pressure. Author (GRA)

N85-23280# Naval Oceanography Command Detachment, Asheville, N.C.
SUMMARY OF METEOROLOGICAL OBSERVATIONS SURFACE (SMOS), SIGONELLA, SICILY/NAVY Progress Report, 1973 - 1982
Nov. 1984 360 p
(AD-A150539) Avail: NTIS HC A16/MF A01 CSCL 04/2

This data report consists of a six part statistical summary of surface weather observations. The six parts are: (Part 1) Weather Conditions/Atmospheric Phenomena, (Part 2) Precipitation/Snowfall/Snow Depth, (Part 3) Surface Winds, (Part 4) Ceiling versus Visibility/Sky Cover, (Part 5) Psychrometric Summaries, and (Part 6) Station Pressure/Sea Level Pressure. Author (GRA)

N85-23281# Naval Oceanography Command Detachment, Asheville, N.C.
SUMMARY OF METEOROLOGICAL OBSERVATIONS, SURFACE (SMOS), ALAMEDA, CALIFORNIA Progress Report, 1973 - 1982
Nov. 1984 374 p
(AD-A150609) Avail: NTIS HC A16/MF A01 CSCL 04/2

This data report consists of a six part statistical summary of surface weather observations. The six parts are: (Part 1) Weather Conditions/Atmospheric Phenomena, (Part 2) Precipitation/Snowfall/Snow Depth, (Part 3) Surface Winds, (Part 4) Ceiling

versus Visibility/Sky Cover, (Part 5) Psychrometric Summaries, and (Part 6) Station Pressure/Sea Level Pressure. GRA

N85-23282# National Oceanic and Atmospheric Administration, Oak Ridge, Tenn. Atmospheric Turbulence and Diffusion Lab.
PORTABLE AUTOMATED MESONET (PAM) DATA FROM THE 1980 EXPERIMENT IN ANDERSON CREEK VALLEY
Carmen J. Nappo and Lynne C. Satterfield Aug. 1984 935 p ref
(Contract W-7405-eng-48)
(DE85-004361; UCID-20227; ASCOT-84-4) Avail: NTIS HC A99/MF E03

During the 1980 ASCOT field study in Anderson Creek Valley, Ca., the National Center for Atmospheric Research operated its Portable Automated Mesonet (PAM) system from 9 to 25 September. These data provide continuous measurements of surface-layer winds, temperature, atmospheric pressures, and relative humidities at 27 stations. Wind speed and direction were measured at 4 m (AGL), and temperature, pressure and relative humidity were measured at 2 m (AGL). Observation sampling rate was 1 Hz, and these values were processed into one-minute averages which are stored on magnetic tape. The one-minute average wind direction was calculated as the prevailing wind direction, i.e., the direction of the one-minute averaged wind vector. The data are organized by day and station. In order to simplify examination, the observation periods are divided into daytime (0600 to 2100 LST) and nighttime (1800 to 0900 LST) segments. The data have been edited to remove obvious outliers. The plots are constructed from the one-minute observations. DOE

N85-23283# National Oceanic and Atmospheric Administration, Oak Ridge, Tenn. Atmospheric Turbulence and Diffusion Lab.
THE ASCOT DATA ANALYSIS WORKSHOP
C. J. Nappo, S. Barr, W. E. Clements, T. Yamada, W. Neff (NOAA, Boulder, Colo.), and W. Porch Nov. 1984 43 p refs Workshop held in Livermore, Calif., 7 Nov. 1984 Prepared in cooperation with LASL, Los Alamos N. Mex. and LLNL, Calif.
(Contract W-7405-eng-48)
(DE85-004407; ASCOT-84-7; CONF-8311213-Summ) Avail: NTIS HC A03/MF A01

This Atmospheric Studies in Complex Terraion (ASCOT) workshop was convened to identify and formulate critical questions and hypotheses concerning the physics and modeling of transport and diffusion in drainage flows, and to ascertain the degree to which existing data can provide insight into these questions and hypotheses. The intent was not to seek immediate solutions, but to discuss the problems, consider unanswered questions, and determine whether the existing data are sufficient to provide the answers. Specific areas considered were: evaluation of the spatial and temporal variability of drainage flow along slopes and within basins; evaluation of pooling region phenomena; evaluation of current theories of drainage flow on simple slopes; and flow characteristics of Brush Creek, Colorado with application to future field experiments. DOE

N85-23284# Sandia Labs., Albuquerque, N. Mex. Applied Mechanics Div.
MARKOV METHOD FOR SIMULATING NON-GAUSSIAN WIND SPEED TIME SERIES
Paul S. Veers and Gerald M. McNerney 1985 16 p refs Presented at the ASME Wind Energy Symp., Dallas, 17-22 Feb. 1985
(Contract DE-AC04-76DP-00789)
(DE85-003450; SAND-84-1227C; CONF-850218-2) Avail: NTIS HC A02/MF A01

A method which can be used to construct a wind simulator capable of generating wind time series with any distribution of hourly averages, exponentially decaying autocorrelation function, and a Gaussian realization of the turbulence is discussed. The method is based on a Markov random walk for hourly averages and an inverse hourly transform of the power spectrum to produce short-term turbulence. A description of the applications for which the model was developed is given. DOE

N85-23285# Lamont-Doherty Geological Observatory, Palisades, N. Y.
VARIATION OF ARCTIC CLOUD COVER IN SUMMER
George J. Kukla Dec. 1984 10 p refs
(Contract DE-AC02-81EV-10665)
(DE85-004507; DOE/EV-10665/5) Avail: NTIS HC A02/MF A01

The variation of Arctic cloud cover in time and space during the summers of 1979, and part of 1978 was charted from satellite imagery in 3 to 7 day intervals. Three classes of cloud thickness were separately mapped. Confirming the finding of the earlier report dealing with the 1979 data, the optically thick clouds were found to be considerably less common than expected from earlier analyses of drifting station reports. The proportion of thick cloud increased in connection with low pressure systems advecting continental air masses over the Arctic Basin. The data available to date indicate that the thickest cloud cover over the central Arctic was observed in August. Throughout spring and summer of the analysed years, clear sky episodes all over the Arctic Basin lasted long enough to significantly affect the surface radiation balance and the dissipation of snow and ice cover. Results indicate that general circulation models require realistic representation of poleward advection of continental air masses and of the conditions accompanying snow and ice melt. DOE

N85-23119# Joint Publications Research Service, Arlington, Va.
MOISTURE VARIATION IN NORTHERN HEMISPHERE TEMPERATE LATITUDES Abstract Only
G. I. Mosolova and N. P. Mukhina *In its* USSR Rept.: Earth Sci. (JPRS-UES-85-002) 1 Feb. 1985 p 6 Transl. into ENGLISH from Vestn. Leningr. Univ.: Geol., Geografiya (Leningrad), no. 6, issue 1, Mar. 1984 p 48-56 (For primary document see N85-23116 13-42)
Avail: NTIS HC A07/MF A01

N85-23120# Joint Publications Research Service, Arlington, Va.
RELATIONSHIP OF INDIAN MONSOON INTENSITY TO TIME OF ONSET Abstract Only
M. G. Filippova *In its* USSR Rept.: Earth Sci. (JPRS-UES-85-002) 1 Feb. 1985 p 6-7 Transl. into ENGLISH from Vestn. Mosk. Univ., Ser. 5: Geografiya (Moscow), no. 5, Sep. - Oct. 1984 p 65-69 (For primary document see N85-23116 13-42)
Avail: NTIS HC A07/MF A01

N85-23122# Joint Publications Research Service, Arlington, Va.
MODELING OF MECHANISM OF POSITIVE FEEDBACK BETWEEN MEAN EARTH SURFACE TEMPERATURE AND ATMOSPHERIC CARBON DIOXIDE IN GEOLOGIC TIME SCALE Abstract Only
V. I. Melnichuk *In its* USSR Rept.: Earth Sci. (JPRS-UES-85-002) 1 Feb. 1985 p 7-8 Transl. into ENGLISH from Dokl. Akad. Nauk SSSR (Moscow), v. 277, no. 4, Aug. 1984 p 836-839 (For primary document see N85-23116 13-42)
Avail: NTIS HC A07/MF A01

N85-23129# Joint Publications Research Service, Arlington, Va.
POSSIBLE ROLE OF OCEAN BIOTA IN GLOBAL CARBON BALANCE Abstract Only
V. G. Gorshkov *In its* USSR Rept.: Earth Sci. (JPRS-UES-85-002) 1 Feb. 1985 p 20 Transl. into ENGLISH from Okeanol. (Moscow), v. 24, no. 3, May - Jun. 1984 p 453-459 (For primary document see N85-23116 13-42)
Avail: NTIS HC A07/MF A01

N85-23145# Joint Publications Research Service, Arlington, Va.
RADIOSODAR SYSTEM FOR REMOTE SYNCHRONOUS MEASUREMENTS OF WIND SPEED, TEMPERATURE AND ITS FLUCTUATIONS Abstract Only
I. V. Petenko and Ye. A. Shurygin *In its* USSR Rept.: Earth Sci. (JPRS-UES-85-002) 1 Feb. 1985 p 55 Transl. into ENGLISH from Izv. Akad. Nauk SSSR: Fiz. Atmosfery i Okeana (Moscow), v. 20, no. 8 p 77-772 (For primary document see N85-23116 13-42)
Avail: NTIS HC A07/MF A01

N85-23146# Joint Publications Research Service, Arlington, Va.
POSSIBILITY OF DETERMINING ATMOSPHERIC WEATHER PARAMETERS BY RADIO AND RADIOOPTICAL MEASUREMENTS OF REFRACTION OF COSMIC SOURCES Abstract Only
K. P. Gaykovich *In its* USSR Rept.: Earth Sci. (JPRS-UES-85-002) 1 Feb. 1985 p 56 Transl. into ENGLISH from Izv. Akad. Nauk SSSR: Fiz. Atmosfery i Okeana (Moscow), v. 20, no. 8, Aug. 1984 p 675-682 (For primary document see N85-23116 13-42)
Avail: NTIS HC A07/MF A01

48 OCEANOGRAPHY

Includes biological, dynamic and physical oceanography; and marine resources.

N85-23286 Texas A&M Univ., College Station.
A TECTONIC MODEL OF AN INCIPIENT SPREADING CENTER AND ITS MARGINS: THE NORTHERN RED SEA AND THE DEAD SEA RIFT Ph.D. Thesis
Joseph Mart 1984 180 p
Avail: Univ. Microfilms Order No. DA-8428785

The northern Red Sea and the Dead Sea rift represent the incipient stage of accreting plate boundary, occurring partly at sea and partly on land. The evolution of the Red Sea as a deviatoric boundary between the Arabian and the Nubian plates started in the Late Oligocene-Early Miocene and has been active since. Oceanic crust is found in the axial trough of the central Red Sea but its northern province is still underlain by thinned and extended continental crust. The crystalline basement of the northern Red Sea is covered by a sequence of Late Miocene evaporites, unconformably overlain by unconsolidated sediments of Plio-Pleistocene age. The general trend of the northern Red Sea is NW-SE, but the presented data show there series of rifts and diapirs trending approximately N-S. Elongated rifts and diapirs were encountered also in the Fulf of Elat, oriented to the NNE-SSW. The terrain adjacent to the northern Redf Sea and the Dead Sea rift is strongly uplifted, indicating that the region was affected by vertical as well as horizontal tectonic activity. Dissert. Abstr.

N85-23287*# North Carolina State Univ., Raleigh.
GEOGRAPHIC VARIATION IN THE RELATIONSHIPS OF TEMPERATURE, SALINITY OR SIGMA SUB t VERSUS PLANT NUTRIENT CONCENTRATIONS IN THE WORLD OCEAN Final Technical Report, 1 Sep. 1982 - 31 Apr. 1985
Daniel Kamykowski and Sara-Joan Zentara 1985 73 p refs
(Grant NAGw-367)
(NASA-CR-175621; NAS 1.26:175621) Avail: NTIS HC A04/MF A01 CSCL 08A

A NODC data set representing all regions of the world ocean was analyzed for temperature and sigma-t relationships with nitrate, phosphate or silicic acid. Six cubic regressions were for each ten degree square of latitude and longitude containing adequate data. World maps display the locations that allow the prediction of plant nutrient concentrations from temperature or sigma-t. Geographic coverage improves along the sequence: nitrate, phosphate, and silicic acid and is better for sigma-t than for temperature. Contour maps of the approximate temperature of sigma-t at which these nitrients are no longer measurable in a parcel of water are generated, based on a percentile analysis of the temperature or sigma-t at which less than a selected amount of plant nutrient occurs. Results are stored on magnetic tape in tabular form. The global potential to predict plant nutrient concentrations from remotely sensed temperature of sigma-t and to emphasize the latitudinally and longitudinally changing phytoplankton growth environment in present and past oceans is demonstrated. A.R.H.

N85-23288# Defence Research Information Centre, Orpington (England).
LUMINESCENCE IN THE OCEAN
G. S. Karabashev Nov. 1984 18 p refs Transl. into ENGLISH from Opt. Morya (USSR), 1983 p 5-17
(AD-B089136L; DRIC-T-7375; BR93715) Avail: NTIS HC A02/MF A01

The luminosity of ocean water and fluorescence of organic matter present in the oceans are discussed. Studies of chlorophyll, anthropogenic pollution and ocean water dynamics are summarized. A noncontact fluorescent sounding method is described.
Author (ESA)

N85-23289# Science Applications, Inc., McLean, Va.
ICE STATISTICS AND ACOUSTIC SCATTERING IN THE ARCTIC BASIN
R. R. Greene 1 Oct. 1984 41 p
(Contract N00014-84-C-0180)
(AD-A150141; SAIC-84/1132) Avail: NTIS HC A03/MF A01 CSCL 20/1

Acoustic propagation in the Arctic is intimately related to the structure of surface pack ice. In this paper, reflection loss and transmission loss are calculated based upon statistical models of ice roughness. Statistical models of ice ridges are introduced and techniques for estimating the roughness spectrum of ridged surfaces are developed. Next, a model for estimating the mean reflection loss is introduced. The reflection loss formulas are based on the statistical models for roughness. Transmission loss calculations using High-Angle parabolic equation (ARCHAPE) in a simulated Arctic environment are compared with data. The results demonstrate that rough surface scattering from random-depth ice keel structures can account for the observed rate of transmission loss in the Arctic. GRA

N85-23290# Georgia Univ., Athens. Inst. of Ecology.
PRODUCTION AND TURNOVER OF SUSPENDED ORGANIC DETRITUS IN THE COASTAL WATER OF THE SOUTHEASTERN CONTINENTAL SHELF Progress Report
L. R. Pomeroy 1 Dec. 1984 122 p refs
(Contract DE-AS09-76EV-00639)
(DE85-003977; DOE/EV-00639/26) Avail: NTIS HC A03/MF A01

Progress in three studies on the production and fate of suspended organic matter in the southeast coastal waters is reported and plans for future activities are outlined. The study topics include: the role of bacteria in the production and utilization of particulate organic materialls and macroflocs; the suspension of particulates of benthic orgin; particulate transport; and microbial food web modeling. M.G.

N85-23121# Joint Publications Research Service, Arlington, Va.
EL NINO, THE CAPRICIOUS CHILD Abstract Only
K. N. Fedorov *In its* USSR Rept.: Earth Sci. (JPRS-UES-85-002) 1 Feb. 1985 p 7 Transl. into ENGLISH from Priroda (Moscow), no. 8, Aug. 1984 p 65-74 (For primary document see N85-23116 13-42)
Avail: NTIS HC A07/MF A01

N85-23123# Joint Publications Research Service, Arlington, Va.
NUMERICAL EXPERIMENTS WITH SIMPLE MODEL OF OCEAN CLIMATE Abstract Only
M. Ya. Verbitskiy *In its* USSR Rept.: Earth Sci. (JPRS-UES-85-002) 1 Feb. 1985 p 9 Transl. into ENGLISH from Okeanol. (Moscow), v. 24, no. 3, May - Jun. 1984 p 385-391 (For primary document see N85-23116 13-42)
Avail: NTIS HC A07/MF A01

N85-23125# Joint Publications Research Service, Arlington, Va.
SPECIAL FEATURES OF COMPUTATIONS OF VERTICAL DISTRIBUTION OF CONCENTRATION OF SUSPENDED SEDIMENTS UNDER MARINE CONDITIONS Abstract Only
R. D. Kosyan *In its* USSR Rept.: Earth Sci. (JPRS-UES-85-002) 1 Feb. 1985 p 15-16 Transl. into ENGLISH from Okeanol. (Moscow), v. 24, no. 3, May - Jun. 1984 p 498-504 (For primary document see N85-23116 13-42)
Avail: NTIS HC A07/MF A01

N85-23128# Joint Publications Research Service, Arlington, Va.
DETERMINING ADSORPTION OF SURFACE-ACTIVE SUBSTANCES BY SEA BOTTOM DEPOSITS Abstract Only
M. P. Nesterova, O. S. Mochalova, and N. M. Antonova *In its* USSR Rept.: Earth Sci. (JPRS-UES-85-002) 1 Feb. 1985 p 18 Transl. into ENGLISH from Okeanol. (Moscow), v. 24, no. 3, May - Jun. 1984 p 464-469 (For primary document see N85-23116 13-42)
Avail: NTIS HC A07/MF A01

N85-23133# Joint Publications Research Service, Arlington, Va.
WORLD OCEAN LEVEL OSCILLATIONS AND THEIR RELATIONSHIP TO CHANGE IN INFLOW OF CONTINENTAL WATERS Abstract Only
K. P. Voskresenskiy, V. I. Babkin, T. Ye. Grigorkina, and V. Yu. Barkhatova *In its* USSR Rept.: Earth Sci. (JPRS-UES-85-002) 1 Feb. 1985 p 29-30 Transl. into ENGLISH from Izv. Vsesoyuznogo Geogr. Obshch. (Leningrad), v. 116, no. 3, May - Jun. 1984 p 224-231 (For primary document see N85-23116 13-42)
Avail: NTIS HC A07/MF A01

N85-23136# Joint Publications Research Service, Arlington, Va.
CALCULATION OF LEVEL SURFACE IN PROBLEMS OF LARGE-SCALE OCEAN CIRCULATION Abstract Only
A. L. Berestov and S. A. Yefremov *In its* USSR Rept.: Earth Sci. (JPRS-UES-85-002) 1 Feb. 1985 p 35-36 Transl. into ENGLISH from Dokl. Akad. Nauk SSSR (Moscow), v. 277, no. 4, Aug. 1984 p 961-964 (For primary document see N85-23116 13-42)
Avail: NTIS HC A07/MF A01

N85-23137# Joint Publications Research Service, Arlington, Va.
DOUBLE AND INVERSE TAYLOR-HOGG VORTICES IN A STRATIFIED OCEAN Abstract Only
V. N. Zyryanov *In its* USSR Rept.: Earth Sci. (JPRS-UES-85-002) 1 Feb. 1985 p 36 Transl. into ENGLISH from Dokl. Akad. Nauk SSSR (Moscow), v. 277, no. 4, Aug. 1984 p 967-971 (For primary document see N85-23116 13-42)
Avail: NTIS HC A07/MF A01

N85-23138# Joint Publications Research Service, Arlington, Va.
MATHEMATICAL-CARTOGRAPHIC MODEL FOR STUDY OF DISTRIBUTION OF HYDROCHEMICAL ELEMENTS IN SEA WATER (USING DISSOLVED OXYGEN IN THE PACIFIC OCEAN AS AN EXAMPLE) Abstract Only
A. A. Zolotiv and S. N. Servenyuk *In its* USSR Rept.: Earth Sci. (JPRS-UES-85-002) 1 Feb. 1985 p 37 Transl. into ENGLISH from Vestn. Mosk. Univ., Ser. 5: Geogr. (Moscow), no. 4, Jul. - Aug. 1984 p 51-55 (For primary document see N85-23116 13-42)
Avail: NTIS HC A07/MF A01

N85-23139# Joint Publications Research Service, Arlington, Va.
HORIZONTAL COHERENCE OF TEMPERATURE MICROSTRUCTURE IN UPPER OCEAN LAYER Abstract Only
N. D. Berezhnaya, A. A. Lubitskiy, and A. D. Rozenberg *In its* USSR Rept.: Earth ci. (JPRS-UES-85-002) 1 Feb. 1985 p 40 Transl. into ENGLISH from Izv. Akad. Nauk SSSR: Fiz. Atmosfery i Okeana (Moscow), v. 20, no. 8, Aug. 1984 p 741-748 (For primary document see N85-23116 13-42)
Avail: NTIS HC A07/MF A01

N85-23141# Joint Publications Research Service, Arlington, Va.
EVOLUTION OF SET OF ROSSBY WAVES TOWARD ANISOTROPIC EQUILIBRIUM STATE Abstract Only
G. M. Reznik and T. E. Soomere *In its* USSR Rept.: Earth Sci. (JPRS-UES-85-002) 1 Feb. 1985 p 45 Transl. into ENGLISH from Okeanol. (Moscow), v. 24, no. 4, Jul. - Aug. 1984 p 558-565 (For primary document see N85-23116 13-42)
Avail: NTIS HC A07/MF A01

N85-23142# Joint Publications Research Service, Arlington, Va.
STABILITY OF ROSSBY WAVES WITHIN FRAMEWORK OF THREE-COMPONENT ANALYSIS Abstract Only
A. P. Mirabel *In its* USSR Rept.: Earth Sci. (JPRS-UES-85-002) 1 Feb. 1985 p 45 Transl. into ENGLISH from Okeanol. (Moscow), v. 24, no. 4, Jul. - Aug. 1984 p 566-573 (For primary document see N85-23116 13-42)
Avail: NTIS HC A07/MF A01

N85-23143# Joint Publications Research Service, Arlington, Va.
MORE PRECISE CURVE OF DEPENDENCE BETWEEN DENSITY AND VELOCITY OF LONGITUDINAL WAVES IN CONSOLIDATED CRUST AND TOP OF MANTLE IN OCEANIC STRUCTURES Abstract Only
O. M. Rusakov *In its* USSR Rept.: Earth Sci. (JPRS-UES-85-002) 1 Feb. 1985 p 51-52 Transl. into ENGLISH from Dokl. Akad. Nauk Ukr. SSR, Ser. B: Geol., Khim i Biol Nauki (Kiev), no. 5, May 1984 p 21-24 (For primary document see N85-23116 13-42)
Avail: NTIS HC A07/MF A01

51 LIFE SCIENCES (GENERAL)

Includes genetics.

N85-23291# Jet Propulsion Lab., California Inst. of Tech., Pasadena.
ANALYSIS OF BIOLOGICAL PARTICLES BY MASS SPECTROMETRY Final Technical Report, Jun. 1981 - Jun. 1984
M. P. Sinha 23 Oct. 1984 145 p
(Contracts MIPR-50-81; MIPR-119-84)
(AD-A149952; ARO-18137.5-CH) Avail: NTIS HC A07/MF A01 CSCL 06/13

A new method has been developed for the rapid characterization of aerosol particles of biological nature using the technique of Particle Analysis by Mass Spectrometry (PAMS). PAMS is a combination of particle beam generation with mass spectrometry. Mass spectral measurements were made on individual biological aerosol particles using this method. The generation of mass spectra directly from aerosols on a single particle basis makes PAMS a unique method for the detection and identification of biological particles in air on a instantaneous basis. Aerosols of various organic compounds, and microorganisms were produced by nebulizing their suspensions, and were introduced into the ion source of a quadrupole mass spectrometer in the form of a beam. It is found that the particle beam method provides a well-controlled means for introducing one particle at a time into the ion source. Two methods for the volatilization and ionization of particles were studied: thermal volatilization followed by electron impact ionization, and laser-induced volatilization and ionization. GRA

N85-23292# Brookhaven National Lab., Upton, N. Y. Biology Dept.
MODULATION OF LIGHT ENERGY TRANSDUCTION IN PHOTOSYNTHESIS
John Bennett Jul. 1984 9 p refs Presented at the 9th Intern. Congr. on Photobiology, Philadelphia, 3 Jul. 1984
(Contract DE-AC02-76CH-00016)
(DE85-004711; BNL-35577; CONF-840783-4) Avail: NTIS HC A02/MF A01

Modulation of light energy transduction in photosynthesis is discussed. Specific topics discussed include: (1) longer term modulation of light energy transduction; (2) the photoinhibition of photosystem-2 activity in plants exposed to high light intensities; (3) the molecular basis of chilling sensitivity in plants; and (4) the adaptation of cyanobacteria to changes in light quality. DOE

N85-23293# California Univ., Berkeley. Lawrence Berkeley Lab.
INTERACTION OF METALS AND METALLOIDS WITH BIOMEMBRANES
R. J. Mehlhorn Sep. 1984 20 p refs Presented at Dahlem Workshop on the Importance of Chem. Speciation in Environ. Processes, Berlin, West Germany, 2 Sep. 1984
(Contract DE-AC03-76SF-00098)
(DE85-004902; LBL-17925; CONF-8409199-1) Avail: NTIS HC A02/MF A01

The interaction of metal (loid)s with membranes can have a significant role in their biological effects. To the extent that

membranes prevent the entry of these species into cells, they will inhibit damaging effects. However, many interactions with membranes can result in direct damage, or, more seriously, can lead to an amplification of toxicity. Direct damage can include structural alteration such as a disruption of vital lipid-protein associations on introduction of new surface changes. More substantial damage can occur when metals or metalloids act catalytically to impair membrane function, e.g., by providing ion conductance pathways or by promoting free radical reactions which may cause massive oxidation of membrane lipids. Factors involved in the interaction of compounds with membranes are studied. DOE

52 AEROSPACE MEDICINE

Includes physiological factors; biological effects of radiation; and weightlessness.

N85-23294# Defence Research Information Centre, Orpington (England).
THE AUDIOMAT: AN AUTOMATIC AUDIOMETER FOR USE IN OCCUPATIONAL AUDIOMETRY
G. F. Smoorenburg, J. L. vanRaaij, and A. M. Mimpen Mar. 1984 50 p refs Transl. into English of rept. IZF-1983-17 Inst. voor Zintuigfys. TNO (Netherlands), Oct. 1983
(DRIC-T-7138; BR91771) Avail: NTIS HC A03/MF A01

The Audiomat, an audiometer for use in occupational hygiene which automatically runs an audiometric program using a microprocessor is described. The audiometric programs can be tailored to customer demands. It can be used as an independent unit or it can be linked to an ITT 2020 microcomputer. When the Audiomat is used as an independent unit, data can be read from a liquid crystal display or printed using a simple printing device. When it is linked to the microcomputer data can be stored on a diskette. Using the microcomputer, four audiomats can be controlled simultaneously and asynchronously. The four measurements can be followed simultaneously on a video display. Author (ESA)

N85-23295# Indiana Univ., Bloomington. School of Medicine.
SLEEP DEPRIVATION AND EXERCISE TOLERANCE Annual Summary Report, 1 Feb. 1982 - 31 Jan. 1983
B. J. Martin Jan. 1983 7 p
(Contract DAMD17-81-C-1023; DA Proj. 3E1-62777-A-879)
(AD-A150180; ASR-2) Avail: NTIS HC A02/MF A01 CSCL 06/19

Fifty hours of sleep loss failed to alter physiological responses to prolonged heavy exercise. At the same time it decreased significantly the ability to tolerate such exercise. These results suggest that psychological effects of sleeplessness may ultimately be most significant for subjects in exercise. GRA

N85-23296# Indiana Univ., Bloomington. School of Medicine.
SLEEP DEPRIVATION AND EXERCISE TOLERANCE Annual Report, 1 Feb. 1983 - 31 Jan. 1984
Bruce J. Martin Jan. 1984 7 p
(Contract DAMD17-81-C-1023; DA Proj. 3E1-62777-A-879)
(AD-A150566; AR-3) Avail: NTIS HC A02/MF A01 CSCL 06/19

Fifty hours of sleep loss failed to alter thermoregulation in severe cold stress: subjects chose identical work rates to minimize fatigue and cold sensation. Two nights of fragmented sleep worsened mood during exercise but produced no measured change in physiological responses to work or in stress hormone levels. The results suggest that sleep loss is not a true physiological stress but instead manifests itself primarily as a psychological stress. GRA

N85-23297# Indiana Univ., Bloomington. School of Medicine.
SLEEP DEPRIVATION AND EXERCISE TOLERANCE Annual Summary Report, 1 Feb. 1984 - 31 Jan. 1985
Bruce J. Martin Jan. 1985 9 p
(Contract DAMD17-81-C-1023; DA Proj. 3E1-62777-A-879)
(AD-A150626; ASR-4) Avail: NTIS HC A02/MF A01 CSCL 06/19

The purpose of this study is to identify the effects of sleep deprivation on the physiological and psychological responses to exercise. Standard techniques in human exercise physiology are utilized. During this year, we found that fragmenting two nights of sleep prior to heavy exercise had no effect on physiological response to that exercise. Heart rate, metabolic rate, and body temperature were identical to control, in contrast to sleepiness and mood disturbance, both of which were significantly elevated. In past work, such psychological effects were correlated with decreased exercise tolerance. Also, we found that a 36 hour sleepless period prior to prolonged mild exercise has no influence on physiological responses to that exercise, though it as well significantly elevated mood disturbance. Because neither form of sleep loss changed stress hormonal levels in subsequent exercise, we conclude that sleep loss of this form is primarily a psychological and not a physiological stress. GRA

N85-23298# Argonne National Lab., Ill. Biological and Medical Research Div.
DISTRIBUTION OF RADIUM AND PLUTONIUM IN HUMAN BONE
Robert A. Schlenker 1984 21 p refs Presented at the 18th European Symp. on Calcified Tissue, Angers (France), 11 Oct. 1984
(Contract W-31-109-eng-38)
(DE85-005025; CONF-8410161-3) Avail: NTIS HC A02/MF A01

This covers aspects of current and recent work on the distribution of radium and plutonium near the surfaces of human bone are presented as well as applications of the data. Methods, surface deposit thickness, radium distribution near the endosteal surface, the use of alpha spectrometry in conjunction with autoradiography, radium distribution in the mastoid, and factors affecting plutonium specific activity are considered. Emphasis is placed on the alpha pectrometry technique because of its usefulness and its recent application to problems of local dosimetry. DOE

N85-22522*# Air Force Geophysics Lab., Hanscom AFB, Mass.
ASTRONAUT HAZARD DURING FREE-FLIGHT POLAR EVA
William N. Hall *In* NASA. Lewis Research Center Spacecraft Environ. Interactions Technol., 1983 Mar. 1985 p 663-674 refs (For primary document see N85-22470 13-18)
Avail: NTIS HC A99/MF E03 CSCL 06R

N85-23441# Joint Publications Research Service, Arlington, Va.
ARMED FORCES SPECIAL SYMPOSIUM ON MEDICINE OF ALTITUDES
Kuang Yung *In its* China Rept.: Sci. and Technol. (JPRS-CST-85-003) 28 Jan. 1985 p 123-130 Transl. into ENGLISH from Jiefangjun Zazhi (Beijing), no. 4, 20 Aug. 1984 p 311-312 (For primary document see N85-23433 13-81)
Avail: NTIS HC A11/MF A01

53 BEHAVIORAL SCIENCES

Includes psychological factors; individual and group behavior; crew training and evaluation; and psychiatric research.

N85-23299*# Federation of American Societies for Experimental Biology, Bethesda, Md. Life Sciences Research Office.
RESEARCH OPPORTUNITIES IN HUMAN BEHAVIOR AND PERFORMANCES
Julien M. Christensen and John M. Talbot Washington NASA Apr. 1985 79 p refs
(Contract NASw-3924)
(NASA-CR-3886; NAS 1.26:3886) Avail: NTIS HC A05/MF A01 CSCL 05I

The NASA research program in the biological and medical aspects of space flight includes investigations of human behavior and performance. The research focuses on psychological and

psychophysiological responses to operational and environmental stresses and demands of spaceflight, and encompasses problems in perception, cognition, motivation, psychological stability, small group dynamics, and performance. The primary objective is to acquire the knowledge and methodology to aid in achieving high productivity and essential psychological support of space and ground crews in the Space Shuttle and space station programs. The Life Sciences Research Office (LSRO) of the Federation of American Societies for Experimental Biology reviewed its program in psychology and identified its research for future program planning to be in line with NASA's goals. B.G.

N85-23300# Council for Scientific and Industrial Research, Pretoria (South Africa). Human Development Div.
HUMAN COGNITION AND INTELLIGENCE: TOWARDS AN INTEGRATED THEORETICAL PERSPECTIVE
J. M. Verster Mar. 1983 120 p refs
(CSIR-SR-PERS-350; ISBN-0-7988-2339-9) Avail: NTIS HC A06/MF A01

A selective review of theoretical and empirical research bearing on the nature of human cognition and intelligence is given. Developments over more than a century are traced, but disproportionate emphasis is given to the rapid advances of the past decade. A critical re-evaluation is given of early conceptions of intelligence, the first attempts at intelligence testing, and classic factor-analytic work on intellectual structure. The search for an appropriate taxonomic system of cognitive performance is examined, followed by critical commentary on comparative studies of cognitive structure and function over the life-span, across cultures, and between the sexes. Theoretical issues concerning the neurological basis of cognitive function are briefly reviewed and empirical data on the electrophysiological correlates of cognitive performance are considered. R.J.F.

N85-23301# Delaware Univ., Newark.
BRAIN MECHANISMS UNDERLYING INDIVIDUAL DIFFERENCES IN REACTION TO STRESS: AN ANIMAL MODEL Final Report, 23 Jun. 1980 - 22 Sep. 1984
J. Siegel and P. M. Saxton 6 Dec. 1984 14 p
(Contract DAAG29-80-K-0015)
(AD-A150195; ARO-17085.3-LS) Avail: NTIS HC A02/MF A01 CSCL 06/16

The cat and rat were investigated as animal models for the correlation of individual behavior with a readily obtainable electrophysiological measure, viz. augmenting/reducing of the visual evoked potential (VEP). The VEP in cats was found to be an identifiable individual signature, stable over periods of more than one year. The VEP in response to an intensity series of light flashes at a medium range of intensities was reliable over time and showed significant individual differences in response to the more intense stimuli. Some cats showed increasing VEP amplitudes to intense simulation (augmenters), while others showed cortical inhibition, reducing the amplitude of the VEP to more intense stimuli (reducers). Augmenter cats were more exploratory and active in a behavioral chamber, and when confronted with a variety of novel and/or aversive stimuli were more reactive and responsive. This behavioral difference predicted task performance in an operant conditioning chamber. The augmenter cats were more reactive and were not as effective in exerting inhibitory control on behavior as were the reducers. Reducer cats learned a bar press inhibitory task more quickly, were less distracted by loud noise bursts and were able to tolerate more difficult tasks than the augmenter cats. GRA

N85-23302# Yale Univ., New Haven, Conn. School of Organization and Management.
ASSESSING THE BEHAVIOR AND PERFORMANCE OF TEAMS IN ORGANIZATIONS: THE CASE OF AIR TRANSPORT CREWS Interim Report
J. R. Hackman and R. L. Helmreich 15 Dec. 1984 47 p
(Contract N00014-80-C-0555)
(AD-A150359; SOM-WP-62; TR-5) Avail: NTIS HC A03/MF A01 CSCL 05/9

This report examines methodological and conceptual issues in assessing the behavior and performance effectiveness of work teams in organizations. The intent is to identify issues of general applicability by focussing in detail on problems in assessing crews that fly jet transports for scheduled airlines. Special attention is given to the historical, political, and organizational context within which assessment takes place, and to special challenges that arise when teams (rather than individuals) are assessed. GRA

54 MAN/SYSTEM TECHNOLOGY AND LIFE SUPPORT

Includes human engineering; biotechnology; and space suits and protective clothing.

N85-23303# Naval Air Development Center, Warminster, Pa. Aircraft and Crew Systems Technology Directorate.
TIGHT RIBBON ARM PROTECTION (TRAP) FOR AIRCREWMAN EJECTION
D. Lorch and M. Schultz Jul. 1984 27 p
(W05-84)
(AD-A150464; NADC-84115-60) Avail: NTIS HC A03/MF A01 CSCL 01/3

When an aircrewman ejects as high speed from a damaged aircraft the windblast (high Q force) can cause arm fractures and dislocations. These injuries may be so severe that he is unable to help himself survive after the parachute descent. The TRAP (TIGHT RIBBON ARM PROTECTION) was designed to provide ejection seat arm restraint; it consists of two nylon ribbons sewn onto either side of the crewman's parachute harness (either seat-mounted or torso harness mounted). Each of these pulls down off the crewman's shoulder and automatically tightens over his arm as the ejection seat moves up into the air stream. The crewman hooks up the TRAP to snubber lines as he connects into the aircraft restraint. Initial tests indicate that the TRAP system may be able to solve the arm restraint problem. GRA

N85-23304# Royal Aircraft Establishment, Farnborough (England). Protective Equipment Section.
THE APPLICATION OF ANTHROPOMETRIC SURVEY DATA TO AIRCREW CLOTHING SIZING
Judy E. Aplin May 1984 29 p
(AD-A150545; RAE-TR-84050; DRIC-BR-93752) Avail: NTIS HC A03/MF A01 CSCL 06/14

Since completion of the 1970/71 anthropometric survey of 2000 Royal Air Force aircrew, the Protective Equipment Section of Flight Systems (Farnborough) Department has made full use of the acquired data to support its advisory role on aircrew protective clothing sizing. Computer analysis of the data has been undertaken to provide sizing information relevant to a variety of garment types and numerically different size-rools. This Report outlines the general approach adopted for the sizing of body-cover garments and headgear. The influences of the choice of control dimensions and subsidiary measurement range limitation upon the size-rolls for aircrew one-piece coverall type garments are discussed. GRA

N85-22404# Joint Publications Research Service, Arlington, Va.
TASS UPDATE ON UNMANNED FLIGHT OF SALYUT-7
In its USSR Rept.: Space (JPRS-USP-85-001) 4 Feb. 1985 p 3-10 Transl. into ENGLISH from Izvestiya (USSR), 20 Dec. 1984 p 1 (For primary document see N85-22403 13-12)
Avail: NTIS HC A07

N85-22780# Joint Publications Research Service, Arlington, Va.
STUDY OF EFFECTIVE PHYSIOLOGICAL TEMPERATURE Abstract Only
Pang Cheng and Jiang Weiqing *In its* China Rept: Sci. and Technol. (JPRS-CST-84-030) 10 Oct. 1984 p 43 refs Transl. into ENGLISH from Yuhang Xuebao (Beijing, China), no. 2, 30 Apr. 1984 p 10-15 (For primary document see N85-22777 13-31)
Avail: NTIS HC A03/MF A01

55 PLANETARY BIOLOGY

Includes exobiology; and extraterrestrial life.

No abstracts in this category.

59 MATHEMATICAL AND COMPUTER SCIENCES (GENERAL)

N85-23305*# National Aeronautics and Space Administration. Marshall Space Flight Center, Huntsville, Ala.
AN INTEGRAL REPRESENTATION OF THE GENERALIZED EULER-MASCHERONI CONSTANTS
O. R. Ainsworth (Alabama Univ., Tuscaloosa) and L. W. Howell Apr. 1985 14 p refs
(NASA-TP-2456; NAS 1.60:2456) Avail: NTIS HC A02/MF A01 CSCL 12A

The limit series for the Euler-Mascheroni constants is represented as an integral. Using this new representation, the first 200 values are computed along with assorted others up to 2000. The first 13 roots of gamma sub n, where n is a positive continuous variable, are also given. M.G.

60 COMPUTER OPERATIONS AND HARDWARE

Includes computer graphics and data processing.
For components see *33 Electronics and Electrical Engineering.*

N85-23306# British Library Lending Div., Boston Spa (England).
MICROCOMPUTER: CONTROLLED STATISTICS ANALYZER
W. Schoenberger, K. Urbanski, and J. Wahrburg 6 Feb. 1985 11 p refs Transl. into ENGLISH from Messen + Pruefen/ Automatik (West Germany), May 1979 p 373-376
(BLL-CE-Trans-7971-(9022.09)) Avail: British Library Lending Div., Boston Spa, Engl.

The statistical analysis of randomly fluctuating analog measured values is gaining increasing significance in the most varied areas of technical data processing. In most cases, one or more signals such as current, voltage, temperature, flow rate or magnitudes equivalent to power are continuously detected and recorded in a system. These test records can be used to read mean values and trends but it is difficult to use then for calculating statistical parameters and laws such as variance, frequency distribution or correlation with other measured values. A universal microcomputer is described which has been developed especially for the statistical analysis of random signals. The dynamic range of the analog signals is in each case divided into 64 classes. All calculating and control operations are executed by an inbuilt microcomputer 8080 which makes it possible to classify and calculate mean value, variance, the 99% class and the cumulative frequency function of each input signal in on-line operation. B.W.

N85-23307# British Library Lending Div., Boston Spa (England).
REQUIREMENTS PLACED ON INFORMATION PROCESSING EQUIPMENT
B. Zube [1976] 7 p refs Transl. into ENGLISH from Elektrotech. Z., A., v. 97, no. 1, 1976 p 18-19
(BLL-CE-TRANS-7983-(9022.09)) Avail: NTIS HC A02/MF A01

Transient overvoltages from high-voltage system and from plant circuits can ave detrimental effects on information processing equipment in installations of the electricity supply undertaking, i.e., on circuit protection, telecontrol and data processing devices and can cause malfunctions and damage in components. The conventional overvoltage protection devices which are successful in these cases in telephone engineering cannot be easily used here because they can cause signal distortion and thus more malfunctions. In this report the various programmes are considered and reference is made to the fact that adequate protection both of conventional and of modern static equipment, and thus also the reliable operation of transmission systems and equipment is possible with strict applications of the measures recommended.
Author

N85-23308# Royal Aircraft Establishment, Farnborough (England).
OPERATIONAL LOADS MEASUREMENT: A PHILOSOPHY AND ITS IMPLEMENTATION
Dorothy M. Holford and J. R. Sturgeon Mar. 1984 37 p refs
(AD-A149445; RAE-TR-84031; RAE-Mater/Struct-76; BR93043) Avail: NTIS HC A03/MF A01

A philosophy of operational data acquisition, for structural objectives for in-flight load measurement is reviewed, highlighting the constraints such activities place on the data acquisition system. A system which can be tailored to perform tasks ranging from the collection of time histories of flight parameters or strain gages to complex fatigue load analyses throughout the airframe is described. The system comprises a digital cassette recorder and a data acquisition unit within which a microprocessor is used for control of data acquisition and in-flight data analysis. System requirements in terms of accuracy, bandwidth and sampling rates are discussed for a range of aircraft types and operating conditions. Operation modes are illustrated, showing the value of studying operational data in terms of fatigue life management, fatigue life monitoring, operational practices and design procedures.
Author (ESA)

N85-23309# Illinois Univ., Chicago. Dept. of Mathematics.
OPTIMAL ALLOCATION OF COMPONENTS IN PARALLEL-SERIES AND SERIES-PARALLEL SYSTEMS
E. El-Neweihi, F. Proschan, and J. Sethuraman (Florida State Univ., Tallahassee) Nov. 1984 32 p
(Contracts DAAG29-82-K-0168; AFOSR-82-K-0007; Grant AF-AFOSR-0170-80)
(AD-A150169; FSU-TR-M690; TR-D-73-ARO; ARO-19367.22-MA; AFOSR-84-173TR) Avail: NTIS HC A03/MF A01 CSCL 09/2

This paper considers the problem of optimal allocation of components to parallel-series and series-parallel systems to maximize the reliability of the system or the expected number of working subsystems. For parallel-series systems the optimal allocation is completely described and it depends only on the ordering of component reliabilities. For series-parallel systems, we describe a partial ordering among allocations that can lead to the optimal allocation. The powerful techniques of Schur functions are used to obtain these results. Finally, we describe how these problems can be cast as integer linear programming problems and therefore can also be attacked by other methods. GRA

N85-23310# McDonnell-Douglas Corp., St. Louis, Mo.
PARALLEL TEST METHOD FOR LSI (LARGE SCALE INTEGRATION) MICROPROCESSORS Final Technical Report, Oct. 1981 - Apr. 1983
R. M. Koenig, Jr. Griffiss AFB, N.Y. RADC Feb. 1984 135 p
(Contract F30602-81-C-0269)
(AD-A150237; RADC-TR-84-32) Avail: NTIS HC A07/MF A01 CSCL 09/2

The parallel testing concept consists of connecting together the corresponding inputs and outputs of devices-under-test to perform monitored testing. Failures are detected by changes in supply current to the paralleled set and isolated by differences in individual device currents. The parallel testing concept was first presented by R. Alan Blore of the Rome Air Development Center (RADC) at the International Symposium for Testing and Failure Analysis in 1980. GRA

N85-23311# Massachusetts Inst. of Tech., Cambridge. Artificial Intelligence Lab.

PRESENTATION BASED USER INTERFACES
E. C. IV Cicarelli Aug. 1984 198 p
(Contract N00014-75-C-0522)
(AD-A150311; AI-TR-794) Avail: NTIS HC A09/MF A01 CSCL 09/2

A prototype presentation system base is described. It offers mechanisms, tools, and ready-made parts for building user interfaces. A general user interface model underlies the base, organized around the concept of a presentation: a visible text or graphic form conveying information. The base and model emphasize domain independence and style independence, to apply to the widest possible range of interfaces. The primitive presentation system model treats the interface as a system of processes maintaining a semantic relation between an application data base and a presentation data base, the symbolic screen description containing presentations. A presenter continually updates the presentation data base from the application data base. The user manipulates presentations with a presentation editor. A recognizer translates the user's presentation manipulation into application data base commands. The primitive presentation system can be extended to model more complex systems by attaching additional presentation systems. In order to illustrate the model's generality and descriptive capabilities, extended model structures for several existing user interfaces are discussed. The base provides support for building the application and presentation data bases, linked together into a single, uniform network, graphics to continuously display it, and editing functions. A variety of tools and mechanisms help create and control presenters and recognizers. To demonstrate the base's utility, three interfaces to an operating system were constructed, embodying different styles: icon, menu, and graphical annotation. GRA

N85-23312# Naval Postgraduate School, Monterey, Calif. Dept. of Computer Science.
A DESIGN ANALYSIS AND IMPLEMENTATION OF A USER-FRIENDLY INTERFACE FOR THE UNIX OPERATING SYSTEM M.S. Thesis
Frederick Earl Groenert, Jr. Jun. 1984 159 p
(AD-A150558) Avail: NTIS HC A08/MF A01 CSCL 09/2

The user interface is a crucial, but often overlooked, part of the computer and software package. It is often the last thing designed. Short term memory aids and session pacing are two of the most important areas in which the machine can assist the user. Inclusion of a screen pointing device brings the computer closer to communicating on human terms. Basing the interface on a common metaphor, e.g., a desk top, can make it easy to learn and use. In this thesis three facets of the interface are examined. Communication from the machine, to the machine, and the dialog between user and machine. The Amiable interface designed for the UNIX operating system is described. Amiable is implemented on a SUN model 150 Workstation in the Naval Postgraduate School Computer Science Laboratory. Interface design is a hard problem, much remains to be done. GRA

N85-23313# California Univ., Livermore. Lawrence Livermore Lab.
EXPLOITING MULTIPROCESSORS: ISSUES AND OPTIONS
James R. McGraw and Timothy S. Axelrod 31 Oct. 1984 24 p refs Presented at the Code Developers Conf., San Diego, Calif., 6-8 Nov. 1984
(Contract W-7405-eng-48)
(DE85-003144; UCRL-91734; CONF-8411126-1) Avail: NTIS HC A02/MF A01

Problems involved in moving applications programs to multiprocessors and strategies currently being considered to resolve these problems are discussed. We first identify problems encountered in programming the HEP and Cray X-MP multiprocessors and explain why these problems are likely to exist on any of the multiprocessors available for use at the national laboratories. We then survey a spectrum of possible approaches and identify the costs and remaining research issues associated with each. The bottom line is that we do not currently have any easy solutions; significant planning must begin now if we are to effectively use these new systems. DOE

N85-23314# Brookhaven National Lab., Upton, N. Y.
ROLE OF OPTICAL DISK AT COMPUTING CENTERS
Arnold M. Peskin 1984 7 p refs Presented at the Intern. Soc. for Optical Eng. Meeting, Los Angeles, 21 Jan. 1985
(Contract DE-AC02-76CH-00016)
(DE85-005124; BNL-35551; CONF-850137-1) Avail: NTIS HC A02/MF A01

Mass storage plays an increasingly important part in the changing role of the traditional open-shop computing center precipitation by the trend toward decentralization. A large number of mass storage applications are of the write-once type, for which the emerging optical disk technology is well suited. Some of the broad application areas are experiment data capture, shared reference data bases, program and documentation libraries, and medical studies requiring individual patient data. The utility of currently available optical disk products is being investigated for these applications for a variety of computing environments including those of IBM, DEC-VAX, and UNIX products. DOE

N85-23315# Los Alamos Scientific Lab., N. Mex.
BOTTLENECKOLOGY: EVALUATING SUPERCOMPUTERS
J. Worlton 1985 3 p refs Presented at the IEEE Spring COMP/CON Meeting, San Francisco, 25 Feb. 1985
(Contract W-7405-eng-36)
(DE85-005574; LA-UR-84-3942; CONF-850255-1) Avail: NTIS HC A02/MF A01

Evaluating supercomputer performance is more difficult than evaluating performance for other types of computers because of the wide range of performances encounted. Depending on the purpose of the evaluation, methods of evaluation can be used that trade off level of effort and accuracy, including rules of thumb, analytical models, testing, and simulation. DOE

N85-23316# Federal Compiler Testing Center, Falls Church, Va. Federal Software Testing Center.
VALIDATION SUMMARY REPORT, BURROUGHS CORPORATION, 820 FORTRAN RELEASE 4.0
9 Mar. 1984 15 p
(PB84-227792; VSR-OIT/FSTC-84/139) Avail: NTIS HC A02/MF A01 CSCL 09B

A Validation Summary Report (VSR) for the Burroughs Corporation, B20 FORTRAN Release 4.0 running under the BTOS Release 4.0 provides a consolidated summary of the results obtained from the validation of the subject compiler against the 1978 FORTRAN Standard (X3.9-1978/FIPS PUB 69). The compiler was validated against the Subset Level FORTRAN level of FIPS PUB 69. The VSR is made up of several sections showing all the discrepancies found - if any. These include an overview of the validation which lists all categories of discrepancies within X3.9-1978, and a detailed listing of discrepancies together with the tests which failed. Author

61 COMPUTER PROGRAMMING AND SOFTWARE

Includes computer programs, routines, and algorithms.

N85-23317*# National Aeronautics and Space Administration. Langley Research Center, Hampton, Va.
A THEORETICAL BASIS FOR THE ANALYSIS OF REDUNDANT SOFTWARE SUBJECT TO COINCIDENT ERRORS
Dave E. Eckhardt, Jr. and Larry D. Lee Jan. 1985 40 p refs
(NASA-TM-86369; NAS 1.15:86369) Avail: NTIS HC A03/MF A01 CSCL 09B

Fundamental to the development of redundant software techniques fault-tolerant software, is an understanding of the impact of multiple-joint occurrences of coincident errors. A theoretical basis for the study of redundant software is developed which provides a probabilistic framework for empirically evaluating the effectiveness

of the general (N-Version) strategy when component versions are subject to coincident errors, and permits an analytical study of the effects of these errors. The basic assumptions of the model are: (1) independently designed software components are chosen in a random sample; and (2) in the user environment, the system is required to execute on a stationary input series. The intensity of coincident errors, has a central role in the model. This function describes the propensity to introduce design faults in such a way that software components fail together when executing in the user environment. The model is used to give conditions under which an N-Version system is a better strategy for reducing system failure probability than relying on a single version of software. A condition which limits the effectiveness of a fault-tolerant strategy is studied, and it is posted whether system failure probability varies monotonically with increasing N or whether an optimal choice of N exists. E.A.K.

N85-23318*# National Aeronautics and Space Administration. Langley Research Center, Hampton, Va.
EXPLOITING PARALLEL COMPUTING WITH LIMITED PROGRAM CHANGES USING A NETWORK OF MICROCOMPUTERS
J. L. Rogers, Jr. and J. Sobieszczanski-Sobieski Feb. 1985 16 p refs
(NASA-TM-86387; NAS 1.15:86387) Avail: NTIS HC A02/MF A01 CSCL 09B

Network computing and multiprocessor computers are two discernible trends in parallel processing. The computational behavior of an iterative distributed process in which some subtasks are completed later than others because of an imbalance in computational requirements is of significant interest. The effects of asynchronus processing was studied. A small existing program was converted to perform finite element analysis by distributing substructure analysis over a network of four Apple IIe microcomputers connected to a shared disk, simulating a parallel computer. The substructure analysis uses an iterative, fully stressed, structural resizing procedure. A framework of beams divided into three substructures is used as the finite element model. The effects of asynchronous processing on the convergence of the design variables are determined by not resizing particular substructures on various iterations. E.A.K.

N85-23319*# Atsuko Computing International, Huntsville, Ala.
DIGITAL PROCESSING OF MESOSCALE ANALYSIS AND SPACE SENSOR DATA Final Report
John S. Hickey and Shogo Karitani 11 Feb. 1985 17 p refs
(Contract NAS8-35917)
(NASA-CR-171429; NAS 1.26:171429; ACI-021185-FR) Avail: NTIS HC A02/MF A01 CSCL 05B

The mesoscale analysis and space sensor (MASS) data management and analysis system on the research computer system is presented. The MASS data base management and analysis system was implemented on the research computer system which provides a wide range of capabilities for processing and displaying large volumes of conventional and satellite derived meteorological data. The research computer system consists of three primary computers (HP-1000F, Harris/6, and Perkin-Elmer 3250), each of which performs a specific function according to its unique capabilities. The overall tasks performed concerning the software, data base management and display capabilities of the research computer system in terms of providing a very effective interactive research tool for the digital processing of mesoscale analysis and space sensor data is described. E.A.K.

N85-23320*# National Aeronautics and Space Administration. Langley Research Center, Hampton, Va.
M68000 RNF TEXT FORMATTER USER'S MANUAL
Ralph W. Will and Carolyn Grantham Mar. 1985 107 p
(NASA-TM-86327; NAS 1.15:86327) Avail: NTIS HC A06/MF A01 CSCL 09B

A powerful, flexible text formatting program, RNF, is described. It is designed to automate many of the tedious elements of typing, including breaking a document into pages with titles and page numbers, formatting chapter and section headings, keeping track of page numbers for use in a table of contents, justifying lines by inserting blanks to give an even right margin, and inserting figures and footnotes at appropriate places on the page. The RNF program greatly facilitates both preparing and modifying a document because it allows you to concentrate your efforts on the content of the document instead of its appearance and because it removes the necessity of retyping text that has not changed. M.G.

N85-23321*# National Aeronautics and Space Administration. Langley Research Center, Hampton, Va.
CONSTRUCTION OF A MENU-BASED SYSTEM Final Report
Robert E. Noonan and W. Robert Collins Feb. 1985 13 p refs Submitted for publication
(Contracts NAS1-17070; NAG1-534)
(NASA-CR-172560; ICASE-85-16; NAS 1.26:172560) Avail: NTIS HC A02/MF A01 CSCL 09B

The development of the user interface to a software code management system is discussed. The user interface was specified using a grammar and implemented using a LR parser generator. This was found to be an effective method for the rapid prototyping of a menu based system. M.G.

N85-23322# Massachusetts Inst. of Tech., Cambridge. Lab. for Information and Decision.
A PERSPECTIVE ON MULTIACCESS CHANNELS
R. G. Gallager Jan. 1985 80 p
(Contract N00014-84-K-0357; DARPA Order 3045)
(AD-A150183; LIDS-P-1428) Avail: NTIS HC A05/MF A01 CSCL 09/4

The Information Theoretic Approach and the Collision Resolution Approach to Multiaccess Channels are reviewed in terms of the Underlying Communication Problems that both are modelling. We give some perspective on the strengths and weakness of these approaches and argue for the need of a more combined approach focused on coding and decoding techniques. For the last ten years there have been at least three bodies of research on multiaccess channels, each proceeding in virtual isolation from the others and each using totally different models. The objective here is to contrast these bodies of work and to give some perspective on what is needed to provide some unification between the areas. We shall refer to the three areas as collision resolution, multiaccess information theory, and spread spectrum. GRA

N85-23323# Air Force Human Resources Lab., Williams AFB, Ariz.
LOW ALTITUDE TEXTURE COMPARISON DATA BASE AND SMOOTH SHADED TEXTURE Final Technical Paper Oct. 1982 - Jul. 1983
M. Phelps Dec. 1984 15 p
(AF Proj. 112-3)
(AD-A150342; AFHRL-TP-84-33) Avail: NTIS HC A02/MF A01 CSCL 09/2

Various methods have been used to apply texture to computer-image ground terrain. This texture most often resembles a checkerboard or plaid pattern of multicolored squares which spread along the path of flight. With such texturing, low-level flight becomes much easier. Though checkerboard texture patterns make it possible to fly close to the ground, they add nothing to the realism of the scene and become monotonous after such a short time. The F-111 digital image generator (DIG) visual system has a smooth shading algorithm which can be used to create terrain texture of a different sort. Smooth shading varies the intensity of the colors on the ground in a random fashion to produce texture that is more pleasing to the eye and more natural in appearance than regular predictable checkered patterns. It has not yet been determined whether this new texturing scheme is more effective in furnishing the needed visual cues for low-altitude flight. The aim of this paper is to document the techniques used to create smooth shaded texture on the DIG and to describe the layout of a data base constructed for the purpose of comparing its effectiveness to that of a plaid checkerboard type of texture known as gingham texture. GRA

N85-23324# Naval Postgraduate School, Monterey, Calif.
PRINCIPLES OF SOFTWARE ENGINEERING ENVIRONMENT DESIGN M.S. Thesis
J. R. Frost Jun. 1984 108 p
(AD-A150352) Avail: NTIS HC A06/MF A01 CSCL 09/2

The history of programming languages, operating systems and computer hardware is briefly reviewed. Then the general methodology of established engineering disciplines is examined. Software engineering is then examined in light of its history and by analogy with the general engineering methodology. Here, a critical difference between software engineering methods and those of other disciplines is revealed. Software design is not separated from its implementation nor is there an effective means to communicate a software design from a designer to an implementor. It is shown that without an analog to the engineering blueprint, software engineering is not, and cannot become, a true engineering discipline. In following the engineering analogy, 21 principles of software engineering environment design are put forth. These touch on technical, management and ergonomic issues. Finally, it is concluded that work on software engineering environments holds much more promise for improved productivity than the traditional approach of programming language design. GRA

N85-23325# Naval Postgraduate School, Monterey, Calif.
MICROCOMPUTERS AND THE ELECTRICAL ENGINEER M.S. Thesis
J. R. Hague Jul. 1984 101 p
(AD-A150499) Avail: NTIS HC A06/MF A01 CSCL 09/2

This thesis describes the legal aspects of software usage in the educational environment and some of the engineering applications of the microcomputer and its associated software. The usage of wordprocessing and spreadsheet applications in electrical engineering are discussed with specific applications demonstrated. GRA

N85-23326# Kestrel Inst., Palo Alto, Calif.
SYNTHESIS OF TREE-STRUCTURED COMPUTING SYSTEMS THROUGH USE OF CLOSURES Final Technical Report, 1 Oct. 1983 - 30 Aug. 1984
R. King 29 Nov. 1984 45 p
(Contract F49620-82-C-0007)
(AD-A150502; KES-U-84-6; AFOSR-85-0065TR) Avail: NTIS HC A03/MF A01 CSCL 09/2

During this past year we have concerned ourselves with the synthesis of tree structures. These structures offer, in our opinion, the best hope of achieving subpolynomial running times for typical problems without a degree of interconnection that makes physical implementation difficult. One would like to be able to synthesize trees using divide & conquer. Divide & conquer is an appealing technique for tree synthesis because of the isomorphism between the shape of the desired synthesized system and the recursive descent implicit in divide & conquer. Additionally, the technique makes good use of theorem proving techniques which are rapidly being developed for other purposes. Certain problems arise, however, when one tries to use divide & conquer to synthesize a tree-structured computing system. The basic difficulty is that nodes that are high in the tree are required to either compute or communicate large amounts of data. Our primary solution to this problem is to replace the original specification, which in general declares the existence of an output array that depends on various elements of the input array, into an equivalent specification; which declares the existence of a certain closure, or specialized functional object, together with a declaration that it be applied. GRA

N85-23327# KMS Fusion, Inc., Ann Arbor, Mich.
PARALLEL PROCESSING FOR COMPUTATIONAL CONTINUUM DYNAMICS
J. F. McGrath, D. L. Hicks, and L. M. Liebrock Jan. 1985 23 p
(Contract F49620-84-C-0111)
(AD-A150513; KMSF-U1539; AFOSR-85-0045TR) Avail: NTIS HC A02/MF A01 CSCL 20/10

The numerical solution of many problems in continuum dynamics is seriously limited by the computation rates attainable on computers with serial architecture. Parallel processing machines can achieve much higher rates. However, applying additional processors to a calculation is only part of the solution. In this report, parallel algorithms are developed for explicit and implicit, Lagrangian and Eulerian finite difference schemes for computational continuum dynamics in one spatial dimension. First, the explicit conservation equations in the Lagrangian reference frame are readily reformulated for concurrent processing. Second, and implicit solution is derived for these equations. This is important because it yields unconditional stability. The parallelism is achieved via a block implicit numerical scheme. Third, a rezoning algorithm is employed with each Lagrangian integration step to transform the mesh back to the Eulerian reference frame. Along the algorithmic development path, a zone-by-zone parallelization gives way to a block-by-block technique both of which are self-scheduling. Then the latter is compared to an approach that keeps the parallel processes alive for many time steps. At each step of this research exploiting the architectural advantages of the HEP H1000 (Heterogeneous Element Processor) computer.
Author (GRA)

N85-23328# Massachusetts Inst. of Tech., Cambridge. Center for Information Systems Research.
PERFORMANCE EVALUATION OF DISTRIBUTED SYSTEMS WITH UNBALANCED FLOWS: AN ANALYSIS OF THE INFOPLEX DATA STORAGE HIERARCHY Ph.D. Thesis
Y. Y. R. Wang and S. E. Madnick Jul. 1984 272 p
(Contract N00039-83-C-0463)
(AD-A150528; CISR-TR-15) Avail: NTIS HC A12/MF A01 CSCL 09/2

A software engineering methodology to evaluate systems performance early in the design process is presented. Specifically, a technique is presented to compute performance measures for distributed systems with unbalanced flows due to asynchronously spawned parallel tasks - a common phenomenon in modern information systems which results in a primary effect on performance. With this technique, a cost effective tool can be developed to analyze an architectural design and produce measures such as throughput, utilization, and response time so that potential performance problems can be identified and erroneous design decisions reduced. An algorithm based on Buzen's convolution has been developed to test the necessary and sufficient conditions for system stability as well as to compute the closed system throughput. An average of less than four iterations has been reported for the efficient algorithm. A comparative study of the INFOPLEX data storage hierarchy using TAD, a cost effective tool based this iterative algorithm versus detailed simulations has been conducted and highly consistent results have been observed. Author (GRA)

N85-23329# Naval Postgraduate School, Monterey, Calif.
LEXICON: A STRUCTURED MODELING SYSTEM FOR OPTIMIZATION M.S. Thesis
R. D. Clemence, Jr. Jun. 1984 98 p
(AD-A150536) Avail: NTIS HC A05/MF A01 CSCL 09/2

Linear Programming (LP) is used infrequently for routine decision-making. Even in situations where LP is an extremely attractive tool, there is too much cost, frustration, delay and risk incurred in conversion of a mathematical hypothesis into a valid LP solution. This thesis outlines an entirely new approach to specifying and generating LP's which departs fundamentally from classical methods in an ambitious attempt to mitigate their most onerous disadvantages. These ideas are implemented and tested in a new modeling language and software system called LEXICON. Using LEXICON, a model is conceived, formulated, specified, expressed, internally documented, verified and directly executed in a single form. The LEXICON language is derived from a modeling form proposed by Geoffrion. The software engineering of the LEXICON system admits expansion of the language, portability, and linkage with contemporary real-time LP solvers. GRA

N85-23330# RAND Corp., Santa Monica, Calif.
ROSS: AN OBJECT-ORIENTED LANGUAGE FOR CON-

STRUCTING SIMULATIONS Interim Report
Davis McArthur, Philip Klahr, and Sanjai Narain Dec. 1984 25 p
(Contract F49620-82-C-0018)
(AD-A150556; RAND/R-3160-AF; LC-84-22879;
ISBN-0-8330-0608-8) Avail: NTIS HC A02/MF A01 CSCL 09/2

This report provides an overview of ROSS, an object-oriented language currently being developed at Rand. The goal of ROSS is to provide a programming environment in which users can conveniently design, test, and modify large knowledge-based simulations of complex mechanisms. Object-oriented programming languages, and ROSS in particular, enforce a message-passing style of programming in which the system to be modeled is represented as a set of objects and their behaviors (rules for object interaction). This style is especially suited to simulation, since the mechanism or process to be simulated may have a decomposition that maps naturally onto objects, and the real-world interactions between the objects may be easily modeled by object behaviors and object message transmissions. In addition to describing some of the basic ROSS commands and features, the report discusses some software that interfaces directly with ROSS, including a sophisticated screen-oriented editor and a color graphics package. Facilities for browsing among objects and their behaviors are also described, and examples of browsing and editing are presented using SWIRL, a military combat simulation written in ROSS. GRA

N85-23331# Massachusetts Inst. of Tech., Cambridge. Lab. for Computer Science.
ORPHAN DETECTION IN THE ARGUS SYSTEM M.S. Thesis
Edward Franklin Walker Jun. 1984 125 p
(Contract N00014-83-K-0125)
(AD-A150562; MIT/LCS/TR-326) Avail: NTIS HC A06/MF A01 CSCL 09/2

In a distributed system, an activity running at one node can request another node to perform some service. This request results in an activity being created at the latter node to perform the requested service. The former node may then crash, destroying the activity that requested the service, but leaving behind the activity performing the service. Such surviving activities are known as orphans. Orphans are undesirable since they waste resources and can view inconsistant data. This thesis presents an algorithm that detects and exterminates orphans before they can view inconsistant data. The algorithm has the desirable property that no non-orphans are mistakenly identified as orphans and exterminated. An underlying premise of the algorithm is that orphan detection and extermination should delay normal computation as little as possible. The algorithm works by piggybacking information concerning orphans on various messages that flow about the system. The algorithm piggybacks an impractical amount of data on messages. The main contribution of this thesis is the development of a method called deadlining. This method works in conjunction with the algorithm to detect orphans before they view inconsistant data, while substantially reducing the amount of data piggybacked on messages. An analytic model is used to predict the actual performance of the deadlining. GRA

N85-23332# California Univ., Livermore. Lawrence Livermore Lab.
FORTRAN IN THE 90'S
Jeanne Martin 9 Oct. 1984 4 p Presented at the 14th Cray User Group Meeting, San Francisco, 1-5 Oct. 1984
(Contract W-7405-eng-48)
(DE85-006154; UCRL-91634; CONF-8410219-1) Avail: NTIS HC A02/MF A01

There are many who expect the use of FORTRAN to die away by the end of the century, if not sooner. There are others, who perhaps are responsible for hundreds of thousands of lines of FORTRAN in heavily used production codes, who want it to exist unchanged forever. The FORTRAN standards committee, ANSI/X3J3, has plans based on neither of these scenarios. Instead they envision an orderly evolution of the language to meet the needs of scientific programmers in the computing world of the future. DOE

N85-23333# Argonne National Lab., Ill. Mathematics and Computer Science Div.
SECOND THOUGHTS ON THE MATHEMATICAL SOFTWARE EFFORT: A PERSPECTIVE
W. J. Cody Oct. 1984 20 p refs
(Contract W-31-109-eng-38)
(DE85-004831; ANL-84-83) Avail: NTIS HC A02/MF A01

The mathematical software effort bridges the gap between the discovery of numerical algorithms and the consumption of numerical software. The spectrum of activities is surprisingly wide, including tasks often associated with numerical analysis, program design and testing, programming practices, language standards, documentation standards, software organization, distribution methods, and even the specification of arithmetic engines. The most important accomplishments in the field over the last twenty years are highlighted. Current problems and future challenges posed by the rapid advance of technology are also discussed. DOE

N85-23334# Argonne National Lab., Ill. Mathematics and Computer Science Div.
IMPLEMENTATION OF SOME CONCURRENT ALGORITHMS
J. J. Dongarra, A. H. Sameh (Illinois Univ., Urbana), and D. C. Sorensen Oct. 1984 20 p refs
(Contract W-31-109-eng-33)
(DE85-004687; ANL/MCS-TM-25) Avail: NTIS HC A02/MF A01

Three parallel algorithms for computing the QR-factorization of a matrix are presented. The discussion is primarily concerned with implementation of these algorithms on a computer that supports tightly coupled parallel processes sharing a large common memory. The three algorithms are a Householder method based upon high-level modules, a Windowed Householder method that avoids fork-join synchronization, and a Pipelined Givens method that is a variant of the data-flow type algorithms offering large enough granularity to mask synchronization costs. Numerical experiments were conducted on the Denelcor HEP computer. The computational results indicate that the Pipelined Givens method is preferred and that this is primarily due to the number of array references required by the various algorithms. Author

N85-23335# California Univ., Berkeley. Lawrence Berkeley Lab.
INTRODUCTION TO CHART: A GRAPHIC ANALYSIS AND DISPLAY SYSTEM, REVISION
J. Herbig and V. Sventek Aug. 1984 159 p
(Contract DE-AC03-76SF-00098)
(DE85-004612; LBL-PUB-3034-Rev) Avail: NTIS HC A08/MF A01

Chart, an interactive graphics program is described that can be used to create tables of data and to display data as a graph. Several different graphic forms are available, including bar charts, line graphs, and pie charts. Chart is interactive: this means that commands are typed by the user at a terminal and their effects are seen in a few seconds. It is easy to experiment with different display formats and then choose the one that displays your data most effectively. Chart also makes it easy to start with a simple table and then gradually add additional features such as titles, footnotes, and complex column headings in gradual steps. Each step gives the user a clearer idea of what the final published table or graph should look like in order to best communicate the meaning of the data. DOE

N85-23336# California Univ., Livermore. Lawrence Livermore Lab.
SIGPI: A USER'S MANUAL FOR THE FAST COMPUTATION OF THE PROBABILISTIC PERFORMANCE OF A COMPLEX SYSTEM
C. J. Patenaude 21 Dec. 1984 31 p refs
(Contract W-7405-eng-48)
(DE85-005447; UCID-20279) Avail: NTIS HC A /MF A01

The SIGPI program is described which used two fast complementary methods of computing the probabilistic performance of complex systems: the PI method and the Sigma method. The former exploits the fact that, when system variables are carefully

defined, these variables are often statistically independent conditional to the environment in which they are embedded, a very convenient fact from a computational point of view. The latter computes the probability of combinations of events produced by the PI method by disjointing the events, thereby allowing the exact computation of performance. The computational complexity of the overall process is a polynomial function of the number of components. When statistical independence is not possible, dependent data can be used in the calculation, although both speed and accuracy may suffer. For super-large problems, where costs of precise answers may be prohibitive, a desired accuracy can be specified, and the SIGPI algorithms will halt when that accuracy has been reached. DOE

62 COMPUTER SYSTEMS

Includes computer networks.

N85-23337*# National Aeronautics and Space Administration. Langley Research Center, Hampton, Va.
MEASUREMENT OF SIFT OPERATING SYSTEM OVERHEAD
Daniel L. Palumbo and Ricky W. Butler Apr. 1985 27 p refs
(NASA-TM-86322; L-15855; NAS 1.15:86322) Avail: NTIS HC A03/MF A01 CSCL 09B

The overhead of the software implemented fault tolerance (SIFT) operating system was measured. Several versions of the operating system evolved. Each version represents different strategies employed to improve the measured performance. Three of these versions are analyzed. The internal data structures of the operating systems are discussed. The overhead of the SIFT operating system was found to be of two types: vote overhead and executive task overhead. Both types of overhead were found to be significant in all versions of the system. Improvements substantially reduced this overhead; even with these improvements, the operating system consumed well over 50% of the available processing time. E.A.K.

N85-23338# Royal Signals and Radar Establishment, Malvern (England).
RESEARCH USING A DISCUS BASED NETWORK EMULATOR
T. G. Connelly and M. P. Griffiths Mar. 1984 26 p refs
(AD-A141294; RSRE-MEMO-3539; BR91414) Avail: NTIS HC A03/MF A01

The development of an emulated network based on an array of DISCUS processors is proposed. With this system, the investigation of complex networks is possible at greatly reduced effort and cost compared with the use of a real network. This may be particularly significant in the area of network recovery and error path retracing procedures. Network centralization means that the problems of results monitoring and alteration of network parameters and configuration are greatly simplified. Real and emulated networks can be connected, to provide a more realistic environment for the emulated nodes. Author (ESA)

63 CYBERNETICS

Includes feedback and control theory.

For related information see also *54 Man/System Technology and Life Support.*

N85-23339# Naval Ocean Systems Center, San Diego, Calif.
ARTIFICIAL INTELLIGENCE AND BIONICS WORKSHOP HELD AT STOWE, VERMONT ON 11-15 JUNE 1984
J. E. Haun and P. E. Nachtigall Nov. 1984 91 p Workshop held in Stowe, Vt., 11-15 Jun. 1984
(AD-A150463; NOSC/TR-1003) Avail: NTIS HC A05/MF A01 CSCL 06/4

This report summarizes the results of the Artificial Intelligence and Bionics Workshop, hosted by Naval Ocean Systems Center, and sponsored by the Office of Naval Research. The goal of the workshop as stated in the overview that was sent to the participants is summarized as follows: This workshop will investigate possible applications of current knowledge of animal sensory, cognitive and motor abilities to discover new directions or issues in the continuing effort to build intelligent systems. It has been organized to foster a productive dialogue between scholars in artificial intelligence and biological intelligence, including such areas as neurophysiology, sensory processes, information capture and transfer, cognitive processing and biomechanical implementation. Our effort will be to explore useful biological models in the further development of artificial intelligence. GRA

N85-23340# Edgerton, Germeshausen and Grier, Inc., Idaho Falls, Idaho.
CONTRIBUTION OF INSTRUMENTATION AND CONTROL SOFTWARE TO SYSTEM RELIABILITY
Michael O. Fryer 1984 7 p refs Presented at the Symp. on New Technol. in Nucl. Power Plant Instrumentation and Control, Washington, 28 Nov. 1984
(Contract DE-AC07-76ID-01570)
(DE85-004693; EGG-M-25484; CONF-841122-3) Avail: NTIS HC A02/MF A01

A new method of reliability assessment of combined software/hardware systems is presented. The method is based on a procedure called fault tree analysis which determines how component failures can contribute to system failure. Fault tree analysis is a well developed method for reliability assessment of hardware systems and produces quantitative estimates of failure probability based on component failure rates. It is shown how software control logic can be mapped into a fault tree that depicts both software and hardware contributions to system failure. DOE

64 NUMERICAL ANALYSIS

Includes iteration, difference equations, and numerical approximation.

N85-23341# National Research Inst. for Mathematical Sciences, Pretoria (South Africa).
AN ANALYSIS OF A DYNAMIC PROJECT COST PROBLEM
Abraham Mehrez and Moshe Sniedovich Nov. 1983 30 p refs Submitted for publication
(CSIR-TWISK-338) Avail: NTIS HC A03/MF A01

A stochastic allocation model for a sequential financial problem involving the allocation of funds to uncertain future payments is presented. It is shown that under certain conditions the optimal allocation policies are piecewise linear with the budget available and that there exists an intimate relationship between these policies and the myopic policies obtained from the solution of a sequence of single-payment problems. Certain technical and methodological issues associated with a chance constrained version of the problem are also discussed. B.W.

N85-23342# National Research Inst. for Mathematical Sciences, Pretoria (South Africa).
ON AN ITERATIVE SCHEME FOR THE SOLUTION OF CONSTRAINED VARIATIONAL EQUATIONS
M. C. Cambiaggio and H. G. Miller Dec. 1983 12 p refs Submitted for publication
(CSIR-TWISK-341) Avail: NTIS HC A02/MF A01

An iterative method for the solution of constrained variational equations proposed by Mang et al, has been investigated. Serious difficulties are found in the iterative scheme for satisfying the equation of constraint. A simple calculation in an exactly soluble model has been performed to illustrate the lack of convergence of the method. Author

N85-23343# Stanford Univ., Calif. Dept. of Operations Research.
CONFIDENCE INTERVALS USING THE REGENERATIVE METHOD FOR SIMULATION OUTPUT ANALYSIS
P. W. Glynn and D. L. Iglehart Sep. 1984 8 p

(Contract DAAG29-84-K-0030; Grant NSF MCS-82-03483)
(AD-A150147; TR-3; ARO-20927.3-MA) Avail: NTIS HC A02/MF A01 CSCL 12/1

The regenerative method is a mathematically rigorous method for obtaining confidence intervals for steady state parameters. In this paper the qualitative structure of asymptotic confidence intervals is discussed in general. This structure is then specialized to confidence intervals for steady state parameters produced by the regenerative method. GRA

N85-23344# University of Southern California, Los Angeles.
NUMERICAL ALGORITHMS AND SOFTWARE FOR MATRIX RICCATI EQUATIONS Final Report, 1 Jul. 1981 - 30 Jun. 1984
A. J. Laub 25 Oct. 1984 7 p
(Contract DAAG29-81-K-0131)
(AD-A150148; ARO-18289.15-MA) Avail: NTIS HC A02/MF A01 CSCL 12/1

Numerical issues related to the computational solution of the algebraic matrix Riccati equation were studied. The approach used the generalized eigenproblem formulation for the solution of general forms of algebraic Riccati equations arising in both continuous- and discrete-time applications. These general forms result from control and filtering problems for systems in generalized state space form. A Newton-type iterative refinement procedure for the generalized Riccati solution was derived. Balancing to improve numerical condition was studied. A FORTRAN package called RICPACK was developed. Numerical experiments with RICPACK were performed to investigate a number of proposed condition numbers. Experience with RICPACK to date indicates that it is the most powerful software yet developed to solve general classes of Riccati equations reliably for a few hundred or less problems. The special structure of models of physical systems given in linear second-order form was also examined. Exploiting that structure in solving associated Riccati equations was studied. Tests for controllability and observability were derived in terms of the original second-order-model matrices. GRA

N85-23345# Massachusetts Inst. of Tech., Cambridge. Artificial Intelligence Lab.
ZERO-CROSSINGS ON LINES OF CURVATURE
A. Yuille Dec. 1984 24 p
(Contract N00014-80-C-0505)
(AD-A150171; AI-M-718) Avail: NTIS HC A02/MF A01 CSCL 12/1

We investigate the relations between the structure of the image and events in the geometry of the underlying surface. We introduce some elementary differential geometry and use it to define a coordinate system on the object based on the lines of curvature. Using this coordinate system we can prove results connecting the extrema, ridges and zero-crossings in the image to geometrical features of the object. We show that extrema of the image typically correspond to points on the surface with zero Gaussian curvature and that parabolic lines often give rise to ridges, or valleys, in the image intensity. We show that directional zero-crossings of the image along the lines of curvature generally correspond to extrema of curvature along such lines. GRA

N85-23346# Florida State Univ., Tallahassee.
SCHUR-OSTROWSKI THEOREMS FOR FUNCTIONALS ON L1(0,1)
W. Chan, F. Proschan, and J. Sethuraman Aug. 1984 29 p
(Contracts F49620-82-K-0007; DAAG29-82-K-0168)
(AD-A150193; FSU-STATISTICS-M684; TR-D-69-ARO; AFOSR-84-1245TR; ARO-19367.21-MA) Avail: NTIS HC A03/MF A01 CSCL 12/1

Hardy, Littlewood and Polya (1934) introduced the partial ordering of majorization among n-dimensional real vectors. Many well known inequalities can be recast as the statement that certain functions are increasing with respect to this ordering. Such functions are said to be Schur-convex. An important result in the theory of majorization is the Shur-Ostrowski Theorem, which characterizes Schur-convex functions. The concept of majorization has been extended to elements of L sub 1(0,1) by Ryff (1963). A functional on L sub 1(0,1) that is increasing with respect to the ordering of majorization is said to be Schur-convex. In this paper, the authors prove an analog of the Schur-Ostrowski condition which characterizes Schur-convex functionals in terms of their Gateaux differentials. They also introduce another partial ordering in L sub 1(0,1) called unrestricted majorization. This partial ordering is similar to majorization but does not involve the use of decreasing rearrangements. The authors establish a characterization of non-decreasing functionals on L1(0,1) with respect to the partial ordering of unrestricted majorization through another analog of the Schur-Ostrowski condition. GRA

N85-23347# RGB Associates, Inc., Wayland, Mass.
ALGORITHMS FOR RECONSTRUCTION OF PARTIALLY KNOWN, BAND LIMITED FOURIER TRANSFORM PAIRS FROM NOISY DATA Final Technical Report, Aug. 1982 - Apr. 1983
R. Barakat Griffiss AFB, N.Y. RADC Apr. 1984 224 p
(Contract F30602-82-C-0146; ARPA Order 3655; AF Proj. C65-5)
(AD-A150194; RADC-TR-84-72) Avail: NTIS HC A10/MF A01 CSCL 12/1

This paper is a summary of more detailed mathematical work by the author on recovery of partially know Fourier transforms. These problems of inversion of the finite Fourier transform and of phase retrieval are known to be ill-posed. We draw a distinction in the resultant ill-conditioning of the problems between global ill-conditioning (due to existence of multiple exact solutions) and local ill-conditioning (due to existence of large neighborhoods of the true solution, all of whose members are indistinguishable from the true solution if the data is noisy). We then develop extensions of known algorithms that attempt to reduce at least the effects of local ill-conditioning on numerical solutions by using the idea of filtered singular value decomposition, and present some numerical examples of the use of those algorithms. GRA

N85-23348# Air Force Armament Lab., Eglin AFB, Fla.
ON A MATHEMATICAL STRUCTURE FOR AN IMAGE ALGEBRA Report, for Jan. - Mar. 1984
L. A. Ankeney and H. N. Urquhart 25 Apr. 1984 10 p
(AD-A150228; AFATL-TR-85-04) Avail: NTIS HC A02/MF A01 CSCL 12/1

The processing of images based on well-defined mathematical techniques has remained a subject of great interest for many years. In particular, mathematical theories associated with the processing, enhancement, analysis, and recognition of sensed imagery have received significant amount of attention and effort as witnessed by the number of publications, organizations, and conferences devoted to this subject. The interest in this field of research is due to several factors, including: (1) the wide-ranging fields of application (e.g., from biomedical and industrial uses to military applications), (2) the widespread availability of processing hardware (with increasing speeds and reliability, accompanied by decreasing costs), (3) the challenge of developing software that accomplishes tasks heretofore only accomplished by humans, and (4) the tantalizing applicability of rigorous, analytical methodologies which form the existing mathematical basis of present embryotic image processing theory (e.g., the formulation and development of image transforms, operators, and their mathematical properties). Consequently, the broad field of image processing theory and its application has rapidly evolved into one of today's most active and exciting areas of research. GRA

N85-23349# Stanford Univ., Calif. Lab. for Computational Statistics.
CONSISTENCY OF SMOOTHING WITH RUNNING LINEAR FITS
A. B. Owen and J. C. Marhoul Nov. 1984 17 p
(Contract N00014-83-K-0472)
(AD-A150232; LCS-TR-8) Avail: NTIS HC A02/MF A01 CSCL 12/1

We establish the mean square consistency of running (ordinary) least squares linear regression smoothers, under realistic conditions on the joint distribution of the abscissa and ordinate (X

and Y below) variables. The windows used in the running least squares fits need not be centered on the points for which they are used. In fact, we show that taking a window of points entirely to one side of a data point, fitting a line to that window and using the value of that line at the target point is consistent. It follows that the Supersmoother of Friedman and Stuetzle (1982) and the Split Linear Smoother of McDonald and Owen (1984) are both consistent. GRA

N85-23350# Stanford Univ., Calif. Dept. of Statistics.
A MODEL FOR LARGE SPARSE CONTINGENCY TABLES
J. C. Marhoul Dec. 1984 78 p
(Contracts N00014-83-K-0472; N00014-83-G-0121; DAAG29-82-K-0056)
(AD-A150320; LCS-TR-13) Avail: NTIS HC A05/MF A01 CSCL 12/1

The intent is to indicate that non-linear regression with categorical predictors yields a reasonable methodology for analyzing large sparse tables. GRA

N85-23351# California Univ., Los Angeles.
APPROXIMATION IN OPTIMAL CONTROL AND IDENTIFICATION OF LARGE SPACE STRUCTURES Final Scientific Report, 15 Aug. 1983 - 14 Aug. 1984
J. S. Gibson Jan. 1985 18 p
(Grant AF-AFOSR-0317-83)
(AD-A150323; AFOSR-85-0049TR) Avail: NTIS HC A02/MF A01 CSCL 12/1

This project dealt with the application of distributed system theory to control and identification of large flexible space structures. The main analytical tools were control theory for infinite dimensional systems and approximation theory for distributed systems. Both theoretical results and practical numerical approximation schemes were developed. The research dealt with both continuous-time and discrete-time control and identification. In each case, an ideal infinite dimensional compensator was used to guide the design of implementable finite dimensional compensators. Most of the research dealt with optimal linear-quadratic control theory, but significant preliminary results were obtained on infinite dimensional autoregressive-moving-average models of distributed systems. These models will be used in adaptive control and identification of flexible space structures. GRA

N85-23352# Pittsburgh Univ., Pa. Center for Multivariate Analysis.
MULTIVARIATE ANALYSIS AND ITS APPLICATIONS Final Report, 15 Dec. 1981 - 30 Sep. 1984
P. R. Krishnaiah and C. R. Rao Nov. 1984 34 p
(Contract F49620-82-K-0001)
(AD-A150324; AFOSR-85-0009TR) Avail: NTIS HC A03/MF A01 CSCL 12/1

A summary of the work done under the contract is reported here. The work involved a broad spectrum of topics in the area of multivariate analysis. These topics include contingency tables, distribution theory, selection of variables, classification and pattern recognition and statistical inference. GRA

N85-23353# Pittsburgh Univ., Pa. Center for Multivariate Analysis.
A NOTE ABOUT THE STRONG CONVERGENCE OF THE NONPARAMETRIC ESTIMATION OF A REGRESSION FUNCTION
Z. Fang Sep. 1984 10 p
(Contract F49620-82-K-0001)
(AD-A150325; TR-84-45; AFOSR-85-0005TR) Avail: NTIS HC A02/MF A01 CSCL 12/1

Consider the regression model that are unordered design variables, g unknown function defined with mean 0 and finite moment of order p 1. The asymptotic behavior of estimator g sub n are studied. GRA

N85-23354# Duke Univ., Durham, N. C. Dept. of Computer Science.
THE DESIGN OF A UNIFIED PACKAGE FOR THE SOLUTION OF STOCHASTIC PETRI NET MODELS
K. S. Trivedi, G. Ciardo, A. Bobbio, and J. B. Dugan 1984 24 p
(Grant AF-AFOSR-0132-84)
(AD-A150326; AFOSR-85-0013TR) Avail: NTIS HC A02/MF A01 CSCL 12/1

This paper describes the philosophical differences between three current Stochastic Petri Net models in an attempt to merge the most important (and non-contradictory) aspects into one. It previews the design of a package for the solution of this unified model. GRA

N85-23355# Stanford Univ., Calif. Dept. of Statistics.
REGENERATIVE STOCHASTIC PETRI NETS
P. J. Haas and G. S. Shedler Oct. 1984 39 p
(Contract DAAG29-84-K-0030; Grant NSF MCS-82-03483)
(AD-A150343; TR-4; ARO-20927.4-MA) Avail: NTIS HC A03/MF A01 CSCL 12/1

The stochastic Petri net (SPN) framework permits formal specification of many discrete-event simulations. We define an SPN as a stochastic process and, using structural properties of the SPN and recurrence theory for generalized semi-Markov processes, establish conditions which ensure that an SPN is a regenerative process and that the expected time between regeneration points is finite. Steady-state estimation procedures for ring network simulations follow from these results. GRA

N85-23356# Maryland Univ., College Park. Center for Automation Research.
AXIAL REPRESENTATIONS OF SHAPE
A. Rosenfeld Dec. 1984 47 p
(Contract F49620-83-C-0082)
(AD-A150387; CAR-TR-102; CS-TR-1462; AFOSR-85-0047TR)
Avail: NTIS HC A03/MF A01 CSCL 12/1

Classes of ribbonlike planar shapes can be defined by specifying an arc, called the spine or axis, and a geometric figure such as a disk or line segment, called the generator, that sweeps out the shape by moving along the spine, changing size as it moves. Shape descriptions of this type have been considered by Blum, Brooks, Brady, and others. This paper considers such descriptions from the standpoints of both generation and recovery (i.e., given a shape generated in this way, to determine the axis and generation rule that gave rise to it), and discusses their relative advantages. GRA

N85-23357# Maryland Univ., College Park. Center for Automation Research.
PARALLEL UPDATE OF MINIMUM SPANNING TREES IN LOGARITHMIC TIME
I. V. Ramakrishnan and S. Pawagi Nov. 1984 19 p
(Contracts F49620-83-C-0082; N00014-84-K-0530)
(AD-A150497; CAR-TR-97; CS-TR-1452; AFOSR-85-0069TR)
Avail: NTIS HC A02/MF A01 CSCL 12/1

Parallel algorithms are presented for updating a minimum spanning tree when the cost of an edge changes or when a new node is inserted in the underlying graph. The machine model used is a parallel random access machine which allows simultaneous reads but prohibits simultaneous writes into the same memory location. The algorithms described in this paper for updating a minimum spanning tree require O(log n) time and O(n square) processors. These algorithms are efficient when compared to previously known algorithms for initial construction of a minimum spanning tree that require O(log n to the base 2) time and use O(n square) processors. GRA

N85-23358# Pittsburgh Univ., Pa. Center for Multivariate Analysis.
ON LIMIT OF THE LARGEST EIGENVALUE OF THE LARGE DIMENSIONAL SAMPLE COVARIANCE MATRIX
Y. Q. Yin (China Univ. of Science and Technology), Z. D. Bai (China Univ. of Science and Technology), and P. R. Krishnaiah Oct. 1984 20 p
(Contract F49620-82-K-0001; AF Proj. 2304)

(AD-A150589; TR-84-44; AFOSR-85-0006TR) Avail: NTIS HC A02/MF A01 CSCL 12/1

The authors showed that the largest eigenvalue of the sample covariance matrix tends to a limit under certain conditions when both the number of variables and the sample size tend to infinity. The above result is proved under the mild restriction that the fourth moment of the elements of the sample sums of squares and cross products (SP) matrix exist. GRA

N85-23359# Naval Postgraduate School, Monterey, Calif. Dept. of Electrical Engineering.

IMAGE DATA COMPRESSION USING UNEVEN KNOTS SELECTION M.S. Thesis

Cesar Tadeu deMiranda Jun. 1984 254 p

(AD-A150602) Avail: NTIS HC A12/MF A01 CSCL 12/1

Application of B-spline functions over uneven knots in image processing is studied here. The subject is on compression of image signals. The algorithm for selecting uneven knots from the contours of the image is pursued here. A specific closeness error constraint appropriate for 3-D data is used here. The image reconstruction problem is tackled in two distinct ways, namely triangulation method and thin plates spline method. Some procedures to evaluate the fidelity of the image reconstruction schemes are provided too. A set of experiments in a broad variety of aerophotograph images is performed in order to test and validate the overall algorithm. GRA

N85-23360# Illinois Univ., Chicago. Dept. of Mathematics, Statistics and Computer Science.

OPTIMAL DESIGNS FOR COMPARISONS BETWEEN TWO SETS OF TREATMENTS

Dibyen Majumdar Oct. 1984 27 p

(Grant AF-AFOSR-0170-80; AF Proj. 2304)

(AD-A150621; TR-84-7; AFOSR-85-0008TR) Avail: NTIS HC A03/MF A01 CSCL 12/1

Suppose v treatments are to be compared in b blocks of size k each. Also suppose that the treatments are divided into 2 sets of u and w = v - u treatments. A-optimal designs are obtained for estimating all the differences of two treatments, one from each set. Optimal row-column designs are also obtained. Some new optimal designs for comparing several treatments with a single control are obtained as special cases. Author (GRA)

N85-23361# Los Alamos Scientific Lab., N. Mex.

ALGORITHM FOR SINGULAR DECOMPOSITION

D. C. Ross 19 Aug. 1984 9 p refs Presented at SPIE Annual Technical Syposium, San Diego, Ca., 19 Aug. 1984

(Contract W-7405-eng-36)

(DE85-016488; LA-UR-84-2336-Rev; CONF-840872-14-Rev) Avail: NTIS HC A02/MF A01

An iterative algorithm for the singular value decomposition (SVD) of a non-zero m x n matrix M is described and illustrated numerically. Derivations of the algorithm and sufficient conditions for convergence are outlined. DOE

N85-23362# Oak Ridge National Lab., Tenn. Mathematics and Statistics Research Section.

SPARSE MATRIX COMPUTATIONS

Michael T. Heath 1984 5 p refs Presented at the 23rd IEEE Conf. on Decision and Control, Las Vegas, Nev., 12 Dec. 1984

(Contract DE-AC05-84OR-21400)

(DE85-004780; CONF-841255-1) Avail: NTIS HC A02/MF A01

Numerical linear algebra plays a vital role in all parts of computational mathematics, such as differential equations and optimization, and in many application areas, such as control theory. Large systems in these areas generally lead to linear algebra problems involving large sparse matrices (i.e., matrices of large dimension, but whose entries are mostly zeros). Efficient use of computer resources in solving such sparse matrix problems requires special techniques which have a distinct flavor compared to those used for dense matrices. The current state of the art in sparse matrix computations is surveyed including the solution of systems of linear algebraic equations, linear least squares problems, and eigenvalue problems. Emphasis is placed on direct methods, but iterative methods are also considered. The concrete and useful expression of algorithms in the form of computer software is also addressed. DOE

N85-23363# Sandia Labs., Albuquerque, N. Mex. Numerical Mathematics Div.

RUNGE-KUTTA FORMULA WITH CHEAP ERROR ESTIMATE

L. F. Shampine and L. S. Baca Dec. 1984 18 p refs

(Contract DE-AC04-76DP-00789)

(DE85-005674; SAND-84-2190) Avail: NTIS HC A02/MF A01

A Runge-Kutta formula with a local error estimate derived from Simpson's rule enjoyed some popularity in continuous simulation because the error estimate is free and because Hermite interpolation provides and approximate solution between steps. The procedure is analyzed here and compared to an alternative due to England. Interpolation can be justified for both procedures. The Simpson error estimate turns out to be badly flawed, but even if it were not, England's scheme would be substantially more efficient. DOE

N85-23364# Oak Ridge National Lab., Tenn.

INTRODUCTION TO COMBINATORIAL GEOMETRY

T. A. Gabriel and M. B. Emmett 1985 19 p refs Presented at LEP Experimenters' Workshop on Shower Simulation, Geneva, 29 Jan. 1985

(Contract DE-AC05-84OR-21400)

(DE85-003266; CONF-850140-1) Avail: NTIS HC A02/MF A01

The combinatorial geometry package as used in many three-dimensional multimedia Monte Carlo radiation transport codes, such as HETC, MORSE, and EGS, is becoming the preferred way to describe simple and complicated systems. Just about any system can be modeled using the package with relatively few input statements. This can be contrasted against the older style geometry packages in which the required input statements could be large even for relatively simple systems. The geometric bodies which are generally included in most combinatorial geometry packages are: (1) box, (2) right parallel piped, (3) sphere, (4) right circular cylinder, (5) right elliptic cylinder, (6) ellipsoid, (7) truncated right cone, (8) right angle wedge, and (9) arbitrary polyhedron. The data necessary to describe each of these bodies are given. As can be easily noted, there are some subsets included for simplicity. DOE

N85-23365# Colorado Univ., Boulder. Dept. of Electrical Engineering.

USER'S AND PROGRAMMER'S GUIDE TO THE MECHANICS OF MOVING FINITE ELEMENT CODE

R. F. Sincovec and S. Aslam 1984 71 p

(Contract W-7405-eng-48)

(DE85-006165; UCRL-15645) Avail: NTIS HC A04/MF A01

This document presents the details of the mathematics of the Moving Finite Element (MFE) method. The code is a direct implementation of the mathematical mechanics. The intent is to give the prospective user insight into how the code works, and we present sufficient material so that the user can modify the code if desired. This document also serves as a programmer's guide. This document is in no way a complete treatise on the MFE method; the user is referred to references which appear at the end of this document. DOE

N85-23022# Joint Publications Research Service, Arlington, Va.

NEW CONVOLUTION AND DISCRETE FOURIER TRANSFORMATION ALGORITHMS BASED ON RECTANGULAR TRANSFORMATIONS OVER FIELD OF ROOTS OF UNITY Abstract Only

A. T. Baykova *In its* USSR Rept.: Electron. and Elect. Eng. (JPRS-UEE-85-001) 9 Jan. 1985 p 38 Transl. into ENGLISH from Radiotekh. (USSR), no. 9, Sep. 1984 p 66-68 (For primary document see N85-22976 13-33)

Avail: NTIS HC A05/MF A01

65 STATISTICS AND PROBABILITY

Includes data sampling and smoothing; Monte Carlo method; and stochastic processes.

N85-23366# Mitre Corp., McLean, Va.
SURFACE SCATTERING
K. M. Case Jan. 1985 63 p
(Contract F19628-84-C-0001)
(AD-A150252; JSR-83-211) Avail: NTIS HC A04/MF A01 CSCL 12/1

For many practical purposes we are interested in the scattering of sound produced by an irregular interface separating two homogenous media. Here we present a method of treating the problem when the interface is a smooth one which has been slightly perturbed. This is, of course, a problem which has attracted much attention in the literature. In this note a form of perturbation theory is developed which shows how a straightforward, if tedious, calculation of higher order terms can be made. This report makes an initial effort in trying to solve the problem of predicting scattering from an irregular interface between two homogeneous but different media (e.g. air-water, water-ocean bottom). This work is limited to a single frequency and uses a form of Green's Theorem. GRA

N85-23667# Stanford Univ., Calif. Dept. of Operations Research.
REGENERATIVE SIMULATION OF NON-MARKOVIAN STOCHASTIC SYSTEMS
D. L. Iglehart and G. S. Shedler Sep. 1984 30 p Presented at the ARO Workshop on Logistics, Washington, D.C., May 1984
(Contract DAAG29-84-K-0030; Grant NSF MCS-82-03483)
(AD-A150344; TR-2; ARO-20927.2-MA) Avail: NTIS HC A03/MF A01 CSCL 12/1

Discrete-event simulations are often non-Markovian in the sense that the underlying stochastic process of the simulation cannot be modeled as a Markov chain with countable state space. We discuss regenerative simulation methods for non-Markovian systems whose underlying stochastic process can be represented as a generalized semi-Markov process. Applications to modeling and simulation of ring and bus networks are given. GRA

N85-23368# Stanford Univ., Calif. Dept. of Statistics.
WHY DO NONINVERTIBLE ESTIMATED MOVING AVERAGES OCCUR?
T. W. Anderson and A. Takemura Nov. 1984 57 p
(Contract DAAG29-82-K-0156)
(AD-A150388; TR-13; ARO-19065.13-MA) Avail: NTIS HC A04/MF A01 CSCL 12/1

The positive probability that an estimated moving average process is noninvertible is studied for maximum likelihood estimation of a univariate process. Upper and lower bounds for the probability in the first-order case are obtained as well as limits when the sample size tends to infinity. Higher order moving average models and autoregressive moving average models are also treated. GRA

N85-23369# Duke Univ., Durham, N. C. Dept. of Computer Science.
AUTOMATIC SYMBOLIC SOLUTION OF MARKOV CHAINS
R. Marie, A. Reibman, and K. S. Trivedi 1984 22 p
(Grant AF-AFOSR-0132-84)
(AD-A150476; CS-1984-23; AFOSR-85-0012TR) Avail: NTIS HC A02/MF A01 CSCL 12/1

Continuous time Markov chains are commonly used in system performance modeling. Increasing system complexity and non-Markovian behavior can drastically increase the size of a Markov model's state space. Accordingly, approximation techniques have been introduced to reduce the resources needed to solve Markov chain models. In this paper the authors discuss a method for automatically deriving symbolic solutions of Markov chains. Symbolic solutions should provide insight when attempting to evaluate the validity of both Markov models and approximation techniques for their solution. (Author). GRA

N85-23370# Pittsburgh Univ., Pa. Center for Multivariate Analysis.
BOOTSTRAPPING THE KALMAN FILTER
D. S. Stoffer Dec. 1984 27 p
(Contract F49620-82-K-0001)
(AD-A150509; TR-84-51; AFOSR-85-0014TR) Avail: NTIS HC A03/MF A01 CSCL 12/1

The bootstrap is proposed as a method for estimating the precision of forecasts and estimates of parameters of the Kalman filter model. It is shown that when the system and the filter is in steady state the bootstrap applied to the Gaussian innovations yields asymptotically consistent standard errors. That the bootstrap works well with moderate sample sizes and supplies robustness against departures from normality is substantiated by empirical evidence. GRA

N85-23371# Pittsburgh Univ., Pa. Center for Multivariate Analysis.
INFORMATIVE GEOMETRY OF PROBABILITY SPACES
J. Burbea Dec. 1984 59 p
(Contract F49620-85-C-0008)
(AD-A150510; TR-84-52; AFOSR-85-0015TR) Avail: NTIS HC A04/MF A01 CSCL 12/1

This paper is concerned with the geometrical properties that are induced by the local information contents and structures of the parameter space of probability distributions. Of particular interest in this investigation is the Rao distance which is the geodesic distance induced by the differential metric associated with the Fisher information matrix of the parameter space. Moreover, following Efron, Dawid and Amari, some affine connections are introduced into the informative geometry of parameter space and thereby elucidating the role of the curvature in statistical studies. In addition, closed form expressions of the Rao distances for certain families of probability distributions are given and discussed. GRA

N85-23372# North Carolina Univ., Chapel Hill. Center for Stochastic Processes.
SKEWED STABLE VARIABLES AND PROCESSES
Clyde D. Hardin, Jr. (Wisconsin Univ., Milwaukee) Sep. 1984 28 p
(Contract F49620-82-C-0009; AF Proj. 2304)
(AD-A150549; TR-79; AFOSR-84-1273TR) Avail: NTIS HC A03/MF A01 CSCL 12/1

We consider here general (i.e., possibly skewed or asymmetric) stable distribution and processes. A decomposition result and a moment equality are given for these distributions. More importantly, we determine the form of all stable independent increments processes, construct a Wiener-type stochastic integral with respect to these processes, and prove a representation theorem for general stable processes analogous to (and in some sense including) the spectral representation theorem for symmetric stable processes. Author (GRA)

66 SYSTEMS ANALYSIS

Includes mathematical modeling; network analysis; and operations research.

N85-22386# Joint Publications Research Service, Arlington, Va.
OPTIMAL DESIGN EFFORTS IN SHANGHAI DESCRIBED
In its China Rept: Sci. and Technol. (JPRS-CST-84-008) 26 Mar. 1984 p 9-18 refs Transl. into ENGLISH from Yunchouxue Zazhi (Shanghai), no. 1, Oct. 1982 p 54-58 (For primary document see N85-22384 13-05)
Avail: NTIS HC A03/MF A01

67 THEORETICAL MATHEMATICS

Includes topology and number theory.

No abstracts in this category.

70 PHYSICS (GENERAL)

For geophysics see *46 Geophysics*. For astrophysics see *90 Astrophysics*. For solar physics see *92 Solar physics*.

N85-23373# Colorado State Univ., Fort Collins. Dept. of Electrical Engineering.
MAGNETIC FIELD INTERACTIONS WITH MATERIAL DISCONTINUITIES Final Report, 15 Jun. 1981 - 14 Sep. 1984
W. Lord Oct. 1984 36 p
(Contract DAAG29-81-K-0115)
(AD-A150197; ARO-17923.1-MS) Avail: NTIS HC A03/MF A01 CSCL 20/3

All methods of nondestructive testing (NDT) rely for their operation on the interaction of an energy source with defects in the material under test. Such interactions are extremely difficult to model analytically because of the awkward boundaries associated with realistic defect shapes and the inherent nonlinear behavior of many material properties. The major contribution of this project work has been to show that finite element analysis techniques can be used to model electromagnetic energy/defect interactions associated with the active leakage field, residual leakage field, eddy current and pulsed eddy current NDT methods. Developed code has been used to study probe design, to simulate testing geometries too difficult to replicate in a laboratory environment and to aid in the development of defect characterization algorithms. GRA

71 ACOUSTICS

Includes sound generation, transmission and attenuation. For noise pollution see *45 Environment Pollution*.

N85-23374*# National Aeronautics and Space Administration. Langley Research Center, Hampton, Va.
A COMMUNITY SURVEY OF HELICOPTER NOISE ANNOYANCE CONDUCTED UNDER CONTROLLED NOISE EXPOSURE CONDITIONS
James M. Fields (Bionetics Corp., Hampton, Va.) and Clemans A. Powell Mar. 1985 188 p refs
(Contract NAS1-16978)
(NASA-TM-86400; NAS 1.15:86400) Avail: NTIS HC A09/MF A01 CSCL 20A

Reactions to low numbers of helicopter noise events (less than 50 per day) were studied in a community setting. Community residents were repeatedly interviewed about daily noise annoyance reactions on days when helicopter noise exposures were, without the residents' knowledge, controlled. The effects of maximum noise level and number of noise events on helicopter noise annoyance are consistent with the principles contained in LEQ-based noise indices. The effect of the duration of noise events is also consistent with LEQ-based indices. After removing the effect of differences in noise levels (LEQ) there is not an important difference between reactions to impulsive and nonimpulsive types of helicopters. EPNL, where corrected for number of overflights, and LEQ are approximately equally successful in representing the characteristics of noise which are related to human response. The new type of design provided estimates of the parameters in a noise reaction model which would not obtained with a similar degree of precision from conventional study designs. Author

N85-23375*# Bionetics Corp., Hampton, Va.
RESEARCH ON THE EFFECT OF NOISE AT DIFFERENT TIMES OF DAY: MODELS, METHODS AND FINDINGS
James M. Fields Apr. 1985 83 p refs
(Contract NAS1-16978)
(NASA-CR-3888; NAS 1.26:3888) Avail: NTIS HC A05/MF A01 CSCL 20A

Social surveys of residents' responses to noise at different times of day are reviewed. Some of the discrepancies in published reports about the importance of noise at different times of day are reduced when the research findings are classified according to the type of time of day reaction model, the type of time of day weight calculated and the method which is used to estimate the weight. When the estimates of nighttime weights from 12 studies are normalized, it is found that they still disagree, but do not support stronger nighttime weights than those used in existing noise indices. Challenges to common assumptions in nighttime response models are evaluated. Two of these challenges receive enough support to warrant further investigation: the impact of changes in numbers of noise events may be less at night than in the day and nighttime annoyance may be affected by noise levels in other periods. All existing social survey results in which averages of nighttime responses were plotted by nighttime noise levels are reproduced. Author

N85-23376*# Bolt, Beranek, and Newman, Inc., Cambridge, Mass.
AN EXPERIMENTAL INVESTIGATION OF THE CHOPPING OF HELICOPTER MAIN ROTOR TIP VORTICES BY THE TAIL ROTOR
Ali R. Ahmadi Sep. 1984 111 p refs
(Contract NAS2-11313)
(NASA-CR-177338; NAS 1.26:177338; BBN-5756) Avail: NTIS HC A06/MF A01 CSCL 20A

The chopping of helicopter main rotor tip vortices by the tail rotor was experimentally investigated. This is a problem of blade vortex interaction (BVI) at normal incidence where the vortex is generally parallel to the rotor axis. The experiment used a model rotor and an isolated vortex and was designed to isolate BVI noise from other types of rotor noise. Tip Mach number, radical BVI station, and free stream velocity were varied. Fluctuating blade pressures, farfield sound pressure level and directivity, velocity field of the incident vortex, and blade vortex interaction angles were measured. Blade vortex interaction was found to produce impulsive noise which radiates primarily ahead of the blade. For interaction away from the blade tip, the results demonstrate the dipole character of BVI radiation. For BVI close to the tip, three dimensional relief effect reduces the intensity of the interaction, despite larger BVI angle and higher local Mach number. Furthermore, in this case, the radiation patern is more complex due to diffraction at and pressure communication around the tip. Author

N85-23377*# Bolt, Beranek, and Newman, Inc., Canoga Park, Calif.
WIND TUNNEL ACOUSTIC STUDY OF A PROPELLER INSTALLED BEHIND AN AIRPLANE EMPENNAGE: DATA REPORT
J. F. Wilby and E. G. Wilby Jan. 1985 267 p refs
(Contract NAS2-11085)
(NASA-CR-177335; NAS 1.26:177335; BBN-5658) Avail: NTIS HC A12/MF A01 CSCL 20A

The open test section of the NASA-Ames 7- by 10- ft wind tunnel was used for an acoustic test of a propeller mounted behind an airplane empennage. The empennage was attached to a model fuselage and the propeller with its electric motor drive was mounted separately so that the relative positions of empennage and propeller could be varied. A single vertical fin, and a V-tail with, and without, a dorsal fin configurations were used the model propeller had four blades (SR-1). Data were recorded at several locations for two tunnel flow speeds (45.7) and 62.5 m/s) and propeller speeds in the range 4000 to 8200 rpm. Data reduction was performed in narrowband and one-third octave band spectra, with emphasis on harmonics of the passage frequency blade. The influence of flow speed, propeller rpm, empennage configuration, axial and vertical

separation between propeller axis and empennage centerline, and empennage angle of incidence on propeller harmonic levels and acoustic field directivity are studied. A.R.H.

N85-23378# Admiralty Marine Technology Establishment, Teddington (England).
NUMERICAL RESULTS OF ACOUSTIC RADIATION, TRANSMISSION AND REFLECTION OF STEEL PLATE IN WATER
E. J. Clement Feb. 1984 28 p refs
(AMTE(N)-TM-84037; BR91161) Avail: NTIS HC A03/MF A01

Plots of acoustic power versus frequency, and acoustic pressure directivity at selected frequencies, are given for thin, thick and exact plate theories in which the excitation is a vertical time-harmonic point force; they illustrate the range of applicability of the approximate theories. Plots of acoustic power and pressure directivity are given for exact plate theory in which the excitation is a longitudinal force. Plots of pressure transmission and reflection coefficients are given for exact plate theory. Contour and perspective plots of pressure-frequency-angle data, obtained from exact theory, illustrate the acoustic properties of the plate. Author (ESA)

N85-23379# Texas Univ., Austin. Applied Research Lab.
THE EFFECTS OF INTERNAL WAVES ON ACOUSTIC NORMAL MODES
M. C. Penland Dec. 1984 151 p
(Contract N00014-80-C-0490)
(AD-A150235; ARL-TR-84-14) Avail: NTIS HC A08/MF A01 CSCL 20/1

In describing the effects of internal waves on acoustic normal modes excited by a time-harmonic point source, all previous descriptions have neglected the existence of azimuthal fluctuations in the acoustic field. This study compares this azimuthally symmetric case with the case where azimuthal fluctuations in the acoustic field are taken into account. Although azimuthal variations enhance the randomization of interference effects so that different depth modes decorrelate more quickly in range, this enhancement is generally small. This mean energy flux vector (j) becomes radial at long ranges; the vertical components of (j) decay somewhat more quickly with range when azimuthal fluctuations are considered than when they are neglected. Author (GRA)

N85-23380# Mitre Corp., McLean, Va.
VERTICAL DISCRIMINATION IN THE SOUND CHANNEL
S. M. Flatte Jan. 1985 75 p
(Contract F19628-84-C-0001)
(AD-A150254; JSR-83-216) Avail: NTIS HC A04/MF A01 CSCL 20/1

This report describes the theory underlying vertical discrimination for vertical arrays on the sound-channel axis. It presents full wave-propagation calculations, including diffractive effects in the parabolic approximation, that quantiatively predict the behavior of finite arrays, even near caustics. These results confirm experimental observations and provide a single, approximate rule for the length of a vertical array necessary to distinguish between two acoustic sources. The formula is independent of range. GRA

N85-23381# Puerto Rico Univ., Mayaguez. Dept. of Physics.
ELASTIC WAVE SCATTERING FROM CAVITIES AND SOUND INCLUSIONS ANALYZED BY THE RESONANCE METHOD Final Report, 30 Sep. 1981 - 29 Sep. 1984
P. P. Delsanto, J. D. Alemar, and E. Rosario 17 Oct. 1984 6 p
(Grant DAAG29-81-G-0016)
(AD-A150315; ARO-18757.8-MA-H) Avail: NTIS HC A02/MF A01 CSCL 20/1

The specific details of the results of this contract have been previously reported. This investigation of acoustic and ultrasonic scattering has examined both direct scattering and much more difficult inverse scattering problems. GRA

N85-23382# Yale Univ., New Haven, Conn. Dept. of Mechanical Engineering.
PROPERTIES OF MATERIALS USING ACOUSTIC WAVES Annual Report, 1 Nov. 1983 - 31 Oct. 1984
R. E. Apfel Oct. 1984 86 p
(Contract N00014-76-C-0527; RR0-1108)
(AD-A150465) Avail: NTIS HC A05/MF A01 CSCL 20/1

Our goal of characterizing materials using acoustic waves was forwarded through a number of projects: (1) We have refined our modulated radiation pressure technique for characterizing the interfaces between liquids so that we can automatically track changes in interfacial tension over time due to contaminants, surfactants, etc. (2) We have improved and simplified our acoustic scattering apparatus for measuring distributions of the properties of microparticle samples, which will allow us to distinguish particulates in liquids by size, compressibility, and density. (3) We are continuing work on theoretical approaches to nonlinear acoustics which should permit us to cast problems with geometric and other complexities into a manageable form. (4) Our studies of cavitation have enabled us to derive an analytic expression which predicts the acoustic pressure threshold for cavitation at the micrometer scale - where surface tension effects are important. This work has relevance to the consideration of possible bioeffects from diagnostic ultrasound. (5) Other projects include the calibration of hydrophones using acoustically levitated samples, and the investigation of solitary waves of the sort discovered by Wu, Keolian and Rudnick. GRA

N85-23383# Washington Univ., Seattle. Lab. for Applied Physics.
HIGH-FREQUENCY ACOUSTIC VARIABILITY IN THE ARCTIC
M. Schulkin, G. R. Garrison, and T. Wen May 1984 79 p
(Contracts N00014-77-C-0309; N00024-81-C-6042)
(AD-A150550; APL-UW-8312) Avail: NTIS HC A05/MF A01 CSCL 20/1

Fluctuations in acoustic intensity have been studied for two locations in the Arctic - the Chukchi Sea (1974) and the Kane Basin (1979) - using the same measurement and analysis techniques. A five-frequency transducer covering the range 10-75 kHz was moved continuously in the vertical direction from 10 to 70 m. The results were used to determine the vertical correlation length and the coefficient of variation (rms variance) for the intensity at the five frequencies simultaneously. Conductivity and temperature vs depth were measured continuously before and after each set of acoustic runs. These profiles were used to construct sound ray diagrams and to compute the refractive index variance. For direct-path propagation in both locations, it was found that when the acoustic intensity variance at low spatial wavenumbers is filtered out the remaining variance depends on the first power of the frequency and approximately the square of the range. This internal-wave-like behavior is supported by additional evidence. The vertical correlation lengths observed for the direction-path intensity indicate that the scattering features have lifetimes longer than a few seconds and les than a few minutes. The study suggests that the scattering structures are related to anisotropic eddies that tend toward isotropy as they cascade to smaller size. Plots of a strength parameter vs a diffraction parameter show that after deterministic variations are removed from the measurements the remaining variations lie in the unsaturated direct-path region. GRA

N85-23384# Ohio State Univ., Columbus. Dept. of Welding Engineering.
INVESTIGATIONS OF ULTRASONIC WAVE INTERACTIONS AT BOUNDARIES SEPARATING ANISOTROPIC MATERIALS Summary Report
Laszio Adler Nov. 1984 74 p refs
(Contract DE-FG02-84ER-45057)
(DE85-003506; DOE/ER-45057/T1) Avail: NTIS HC A04/MF A01

Interaction of ultrasonic waves at boundaries separating anisotropic materials was studied. The five chapters are titled: theoretical studies of elastic wave interaction with anisotropic boundaries, materials preparation, experimental study of wave propagation in anisotropic materials and scattering, Rayleigh angle backscattering, and beam displacement due to anisotropy. DOE

N85-22537# Utah Univ., Salt Lake City. Dept. of Mechanical and Industrial Engineering.
ACOUSTIC ENERGY BALANCE METHOD
G. A. Flandro *In* APL 21st JANNAF Combust. Meeting, Vol. 1 Oct. 1984 p 113-128 refs (For primary document see N85-22526 13-20)
(Contract F04611-81-C-0007)
Avail: NTIS HC A21/MF A01 CSCL 20A

N85-22538# Alabama Univ., Huntsville. Dept. of Mechanical Engineering.
COUPLED ACOUSTIC AND HYDRODYNAMIC WAVE INSTABILITIES
T. J. Chung and J. L. Sohn *In* APL 21st JANNAF Combust. Meeting, Vol. 1 Oct. 1984 p 129-137 refs (For primary document see N85-22526 13-20)
(Grant AF-AFOSR-0084-83)
Avail: NTIS HC A21/MF A01 CSCL 20A

N85-23049# Joint Publications Research Service, Arlington, Va.
GENERATION OF LONGITUDINAL ACOUSTIC WAVES BY MODULATED HELICON WAVES Abstract Only
N. Y. Vigdorchik *In its* USSR Rept.: Electron. and Elect. Eng. (JPRS-UEE-85-001) 9 Jan. 1985 p 78 Transl. into ENGLISH from Izv. Vysshikh Uch. Zaved.: Radiofiz. (USSR), v. 27, no. 7, Jul. 1984 p 897-902 (For primary document see N85-22976 13-33)
Avail: NTIS HC A05/MF A01

N85-23050# Joint Publications Research Service, Arlington, Va.
ACOUSTOOPTIC DEMODULATION OF FREQUENCY-MODULATED SIGNALS Abstract Only
M. P. Vasilyev *In its* USSR Rept.: Electron. and Elect. Eng. (JPRS-UEE-85-001) 9 Jan. 1985 p 78-79 Transl. into ENGLISH from Radiotekh. i Elektron. (USSR), v. 29, no. 8, Aug. 1984 p 1605-1609 (For primary document see N85-22976 13-33)
Avail: NTIS HC A05/MF A01

N85-23051# Joint Publications Research Service, Arlington, Va.
ACOUSTOOPTIC CELL AS SPACE-FREQUENCY FILTER Abstract Only
V. I. Balakshiy *In its* USSR Rept.: Electron. and Elect. Eng. (JPRS-UEE-85-001) 9 Jan. 1985 p 79 Transl. into ENGLISH from Radiotekh. i Elektron. (USSR), v. 29, no. 8, Aug. 1984 p 1610-1616 (For primary document see N85-22976 13-33)
Avail: NTIS HC A05/MF A01

N85-23052# Joint Publications Research Service, Arlington, Va.
ACCURACY OF RANDOM SIGNAL SPECTRAL PARAMETER ESTIMATION AGAINST INTERFERENCE BACKGROUND IN ACOUSTOOPTICAL SPECTRUM ANALYZERS Abstract Only
G. S. Nakhmanson *In its* USSR Rept.: Electron. and Elect. Eng. (JPRS-UEE-85-001) 9 Jan. 1985 p 80 Transl. into ENGLISH from Radiotekh. (USSR), no. 9, Sep. 1984 p 49-52 (For primary document see N85-22976 13-33)
Avail: NTIS HC A05/MF A01

N85-23053# Joint Publications Research Service, Arlington, Va.
EXPERIMENTAL STUDY OF HIGH-STABILITY OSCILLATOR WITH SURFACE-ACOUSTIC-WAVE RESONATOR IN FEEDBACK LOOP Abstract Only
Y. V. Gulyayev, V. I. Grigoryevskiy, A. M. Kmita, A. P. Kundin, and O. A. maltsev *In its* USSR Rept.: Electron. and Elect. Eng. (JPRS-UEE-85-001) 9 Jan. 1985 p 80 Transl. into ENGLISH from Radiotekh. i Elektron. (USSR), v. 29, no. 8, Aug. 1984 p 1641-1642 (For primary document see N85-22976 13-33)
Avail: NTIS HC A05/MF A01

72 ATOMIC AND MOLECULAR PHYSICS

Includes atomic structure and molecular spectra.

N85-23385# Washington State Univ., Pullman. Dept. of Chemistry.
OBSERVATION OF A NOVEL LOW-LYING EXCITED STATE IN ZINC COMPLEXES Interim Report
K. A. Truesdell and G. A. Crosby 22 Jan. 1985 7 p
(Contract N00014-83-K-0609)
(AD-A150188; TR-2-ONR) Avail: NTIS HC A02/MF A01 CSCL 20/8

A novel low-lying excited state(s) has been observed from emission studies of complexes of the type M(BS)2(S-phen) (M = Zn(II), Cd(II); BS = benzene thiol; s-phen = substituted 1,10-phenanthroline) at 77 K. The state is tentatively assigned to a charge-transfer configuration in which the thiol donates charge through the closed d-shell to the N-heterocyclic state geometry with respect to the ground state. The state decays on the order of microseconds, but its spin signature has not yet been determined. GRA

N85-23386# Massachusetts Inst. of Tech., Cambridge. Dept. of Chemistry.
SEQUENTIAL EXCITATION PREPARATION OF MOLECULAR ENERGY LEVELS WITH SPECIAL STRUCTURAL AND CHEMICAL PROPERTIES Final Report, 1 Oct. 1982 - 30 Sep. 1984
R. W. Field and J. L. Kinsey 26 Nov. 1984 12 p
(Contract F49620-83-C-0010)
(AD-A150301; AFOSR-84-1231TR) Avail: NTIS HC A02/MF A01 CSCL 20/8

This report pertains to: (1) Stimulated Emission Pumping Studies of Formaldehyde. The Stimulated Emission Pumping (SEP) technique was applied for the first time to a polyatomic molecule, H2CO. SEP spectroscopy has provided an unprecedentedly complete picture of the structure of H2CO at high levels of excitation; (2) The H2CO S sub O yields H2+CO Barrier. Stark Quantum Beat and Anticrossing Spectroscopy were used to measure the homogeneous width of two S sub 0 rotation-vibration levels near the top of the S sub 0 barrier; (3) Collisional Studies of H2CO A 1A sub 1 Level. Two pulsed-cw variants of SEP, Transient Gain and Transient Gain and Transient Polarization Spectroscopy enable measurement of single-J level collisional depopulation and depolarization rates and state-of-state transfer rates free of the multiple-collision effects and limited resolution of resolved fluorescence studies; (4) Spectroscopic Studies of Na2. Two new techniques were demonstrated. Modulated gain spectroscopy has allowed observation of the levels of Na2 states near the Na (2S level)+Na(2P level) dissociation limit. Perturbation facilitated Optical-Optical Double Resonance has made the Na2 triplet valence and Rydberg states accessible to sub-Doppler spectroscopy. GRA

N85-23387# Cornell Univ., Ithaca, N.Y. Lab. of Atomic and Solid State Physics.
HARTREE-FOCK INTERACTION BETWEEN A HELIUM ATOM AND LITHIUM-METAL: A TEST FOR THE EFFECTIVE MEDIUM THEORY Interim Report
B. K. Rao, P. Jena, D. Schillady, A. Hintermann, and M. Manninen 11 Feb. 1985 14 p
(Contract N00014-82-K-0576)
(AD-A150468; Rept-10) Avail: NTIS HC A02/MF A01 CSCL 12/1

The interaction of a helium atom with 6 and 10 atom clusters of lithium has been calculated using the unrestricted Hartree-Fock method, Hartree-Fock method with correlation corrections, and the effective medium theory. Inside the cluster the helium embedding energy is found to be proportional to the electron density of the cluster. The proportionality constant obtained by the Hartree-Fock method is in fair agreement with that calculated in the homogeneous electron gas using the local density approximation. Outside the cluster, in the region compatible with the helium diffraction experiments, the self-consistent calculations give much larger repulsion than the effective medium theory. GRA

N85-23388# Cornell Univ., Ithaca, N.Y. Lab. of Atomic and Solid State Physics.
ADSORPTION SITE, ADSORPTION ENERGY AND NORMAL VIBRATION FREQUENCY OF H/Ni(100) VIA TOTAL ENERGY CALCULATIONS Interim Report
Cyrus Umrigar and John W. Wilkins 7 Feb. 1985 12 p
(Contract N00014-82-K-0576)
(AD-A150555; Rept-8) Avail: NTIS HC A02/MF A01 CSCL 07/4

Density-functional total energy calculations of H/Ni(100) show that the equilibrium H position is in the center site, 0.6 a sub o above the plane of the surface Ni atoms (with a Ni-H bond length of 1.8 A). The bridge-site minimum lies only 0.1 eV higher than the center site minimum, whereas the top site minimum lies about 0.3 eV higher. This is consistent with a high hydrogen surface mobility. GRA

N85-23389# Oregon Univ., Eugene. Dept. of Physics.
THRESHOLD DOUBLE PHOTOIONIZATION OF ARGON WITH SYNCHROTRON RADIATION
G. Bradley Armen, Teijo Aberg, Kh Rezaul Karim, Jon C. Levin, Bernd Crasemann, George Brown (Stanford Univ.), Mau Hsiung Chen (LLNL), and Gene E. Ice (ORNL) Oct. 1984 14 p Sponsored in part by DOE
(Contract F49620-84-C-0039; ARPA Order 4087; AF Proj. 2301)
(AD-A150615; AFOSR-85-0059TR) Avail: NTIS HC A02/MF A01 CSCL 20/8

Auger satellite have been measured to determine the probability of M-shell excitation accompanying K-shell photoionization of Ar, as function of photon energy. The theoretically predicted difference between the dependence of shakeup and shakeoff probabilities on the photon energy near threshold is demonstrated. Results are critically compared with calculations. Author (GRA)

N85-23390# Naval Postgraduate School, Monterey, Calif.
A SPATIALLY INCOHERENT AND TEMPORALLY COHERENT SOURCE M.S. Thesis
J. S. Peterson Jun. 1984 92 p
(AD-A151281) Avail: NTIS HC A05/MF A01 CSCL 20/8

The ability to create is spatially incoherent and temporally coherent sources is a major military concern when considering atmospheric turbulence effects on laser beam propagation. Young's double slit experiment is used to measure the degree of spatial coherence of the source when various diffusive materials are placed between the laser and double slit. A photo-multiplier tube is used for detection of an argon-ion laser signal. Experimental results show that the spatial coherence of the source is affected signigicantly by the location of the diffusive materials and the size of the laser beam. For this particular experimental geometry, opal glass placed 17 cm from the double slit degrades the spatial coherence of the source by 99.5%. By expanding the beam diameter 2.5 times the original size, the spatial coherence of a diffused beam is decreased by an average of 95% over a 10 cm region. In addition to experimental observations, the applicable sections of partial coherence theory are discussed. GRA

N85-23391# Los Alamos Scientific Lab., N. Mex.
HIGH-FIELD DIPOLES FOR FUTURE ACCELERATORS
Stefan Wipf, L. Sep. 1984 47 p refs
(Contract W-7405-eng-36)
(DE85-002315; LA-10219-MS) Avail: NTIS HC A03/MF A01

The concept for building superconducting accelerator dipoles with record high fields is presented. The highest possible current density in the winding are favored. It is indicated that there is an optimal range of pinning strength for a superconducting material and that it is not likely for multifilamentary conductors to ever equal the potential performance of tape conductors. A dipole design with a tape-wound, inner high-field winding is suggested. Methods are detailed to avoid degradation caused by flux jumps and to overcome problems with the dipole ends. Concerns for force support structure and field precision are also addressed. An R and D program leading to a prototype 11-T dipole is outlined. Past and future importance of superconductivity to high-energy physics is evident from a short historical survey. Successful dipoles in the 10-T to 20-T range will allow options for upgrading present largest accelerators. DOE

N85-23392# Rensselaer Polytechnic Inst., Troy, N. Y. Dept. of Physics.
THEORETICAL ASPECTS OF ELECTROWEAK AND OTHER INTERACTIONS IN MEDIUM-ENERGY NUCLEAR PHYSICS Annual Report
N. C. Mukhopadhyay Nov. 1984 35 p refs
(Contract DE-AC02-83ER-40114)
(DE85-003821; DOE/ER-40114/3) Avail: NTIS HC A03/MF A01

The project had three distinct parts: (1) searches for new particles in nuclear physics; (2) theory of nuclear electroweak processes; and (3) atomic physics involving hyperfine interaction of muons with polarized and oriented nuclei. The progress made in all these areas is discussed. Electroweak and other interactions in medium energy nuclear physics were investigated. DOE

N85-23393# Cornell Univ., Ithaca, N.Y.
COLLECTIVE ACCELERATION OF IONS USING HIGH CURRENT RELATIVISTIC ELECTRON BEAMS
1985 13 p
(Contract DE-AC02-80ER-10569)
(DE85-004889; DOE/ER-10569/T3) Avail: NTIS HC A02/MF A01

Ion acceleration was obtained experimentally in the beat wave configuration, wave acceleration demonstrated in the converging guide geometry, and strong electric fields were obtained and measured in the waves. The simulation effort in the Cornell theory program has proceeded to the point where satisfactory wave propagation was throughout the converging guide, non-linear wave propagation effects have been detected and studied, and a design of a converging guide assembly completed with acceleration of test ions. Numerical values of the wave phase velocities obtained match, or are lower than those found experimentally under comparable conditions. The simulation electric fields agree to within a factor of two with those measured experimentally. A variety of new problems were identified which require further study. These include the observation of fast waves in the beam and also, in the long pulse (approx. 0.5 (MU)sec) system, the onset of backward wave oscillations. The reflection of waves from the end of the wave growth structure has been observed recently by the MRC group who are working on design approaches to minimizing this effect. The different aspects of the Cornell theory and experiment program are reviewed. DOE

N85-23394# Rockefeller Univ., New York.
EXPERIMENTAL STUDIES OF ELEMENTARY PARTICLE INTERACTIONS AT HIGH ENERGIES Technical Progress Report
R. L. Cool 12 Nov. 1984 22 p refs
(Contract DE-AC02-81ER-40033)
(DE85-004795; DOE/ER-40033/70) Avail: NTIS HC A02/MF A01

The research progress at CERN is briefly dscribed (experiments R-110 and UA-6). Research at FNAL is discussed involving the analysis of the inclusive photon dissociation experiment, E-612, and the design of a luminosity monitor and a recoil spectrometer to be installed inside the vacuum pipe of the collider. Also, research on the Livermore Laboratory program (electron neutrino mass experiment) is discussed. Reports published are listed. DOE

N85-23395# Pacific Northwest Lab., Richland, Wash.
MEAN DELTA-RAY ENERGIES IN ION MOLECULE COLLISIONS
W. E. Wilson Jun. 1983 13 p refs
(Contract DE-AC06-76RL-01830)
(DE85-005524; PNL-SA-11484) Avail: NTIS HC A02/MF A01

A simple analytic expression is presented for obtaining the mean energy of energetic delta-rays arising when positive ions pass through tissue like matter; calculated values are compared with experiment. Author

N85-22477*# National Aeronautics and Space Administration. Lewis Research Center, Cleveland, Ohio.
LABORATORY STUDIES OF KAPTON DEGRADATION IN AN OXYGEN ION BEAM
Dale C. Ferguson *In its* Spacecraft Environ. Interactions Technol., 1983 Mar. 1985 p 81-90 refs (For primary document see N85-22470 13-18)
Avail: NTIS HC A99/MF E03 CSCL 18H

N85-22510*# JAYCOR, San Diego, Calif.
DISCHARGE CHARACTERISTICS OF DIELECTRIC MATERIALS EXAMINED IN MONO-, DUAL-, AND SPECTRAL ENERGY ELECTRON CHARGING ENVIRONMENTS
P. Coakley, M. Treadway, N. Wild, and B. Kitterer *In* NASA. Lewis Research Center Spacecraft Environ. Interactions Technol., 1983 Mar. 1985 p 511-524 refs (For primary document see N85-22470 13-18)
(Contract F29601-82-C-0015)
Avail: NTIS HC A99/MF E03 CSCL 18H

N85-22516*# Beers Associates, Inc., Reston, Va.
A SIMPLE MODEL OF ELECTRON BEAM INITIATED DIELECTRIC BREAKDOWN
B. L. Beers, R. E. Daniell, and T. N. Delmer *In* NASA. Lewis Research Center Spacecraft Environ. Interactions Technol., 1983 Mar. 1985 p 591-598 refs (For primary document see N85-22470 13-18)
(Contract F19601-82-C-0023)
Avail: NTIS HC A99/MF E03 CSCL 20H

N85-22797# Joint Publications Research Service, Arlington, Va.
VARIABLE FLEXING DEVICE FOR TARGETS IN INTERNAL BEAMS OF CHARGED PARTICLE ACCELERATORS Abstract Only
Ye. I. Rozum *In its* USSR Rept.: Eng. and Equipment (JPRS-UEQ-85-003) 12 Mar. 1985 p 16 Transl. into ENGLISH from Pribory i Tekhn. Eksperim. (Moscow), no. 2, Mar. - Apr. 1984 p 18-19 (For primary document see N85-22782 13-31)
Avail: NTIS HC A06

N85-22798# Joint Publications Research Service, Arlington, Va.
SYSTEM FOR FORMING AND FOCUSING HIGH CURRENT BEAM OF DEUTERIUM IONS Abstract Only
A. S. Belov *In its* USSR Rept.: Eng. and Equipment (JPRS-UEQ-85-003) 12 Mar. 1985 p 16 Transl. into ENGLISH from Pribory i Tekhn. Eksperim. (Moscow), no. 2, Mar. - Apr. 1984 p 20-22 (For primary document see N85-22782 13-31)
Avail: NTIS HC A06

N85-22982# Joint Publications Research Service, Arlington, Va.
TEMPERATURE DEPENDENCE OF PROPAGATION OF HIGH-CURRENT ELECTRON BEAM THROUGH DRIFT SPACE Abstract Only
M. A. Vlasov, I. P. Denisova, and S. V. Nikonov *In its* USSR Rept.: Electron. and Elect. Eng. (JPRS-UEE-85-001) 9 Jan. 1985 p 4 Transl. into ENGLISH from Radiotekh. i Elektron. (USSR), v. 29, no. 8, Aug. 1984 p 1595-1599 (For primary document see N85-22976 13-33)
Avail: NTIS HC A05/MF A01

73 NUCLEAR AND HIGH-ENERGY PHYSICS

Includes elementary and nuclear particles; and reactor theory.

For space radiation see *93 Space Radiation.*

No abstracts in this category.

74 OPTICS

Includes light phenomena.

N85-23396* National Aeronautics and Space Administration. Pasadena Office, Calif.
OPTICAL SYSTEM Patent
James B. Breckinridge (JPL, California Inst. of Tech., Pasadena), Norman A. Page (JPL, California Inst. of Tech., Pasadena), Roland V. Shack (JPL, California Inst. of Tech., Pasadena), and Robert R. Shannon, inventors (to NASA) (JPL, California Inst. of Tech., Pasadena) Issued 5 Feb. 1985 14 p Filed 23 Mar. 1983 Supersedes N83-25541 (21 - 14, p 2320) Sponsored by NASA (NASA-Case-NPO-15801-1; NAS 1.71:NPO-15801-1; US-Patent-4,497,540; US-Patent-Appl-SN-478130; US-Patent-Class-350-168; US-Patent-Class-350-505; US-Patent-Class-350-619; US-Patent-Class-356-323; US-Patent-Class-356-330; US-Patent-Class-356-331) Avail: US Patent and Trademark Office CSCL 20F

Disclosed is an otpical system used in a spacecraft to observe a remote surface and provide a spatial and spectral image of this surface. The optical system includes aspheric and spherical mirrors aligned to focus at a first focal plane an image of the surface, and a mirror at this first focal plane which reflects light back on to the spherical mirror. This spherical mirror collimates the light and directs it through a prism which disperses it. The dispersed light is then focused on an array of light responsive elements disposed at a second focal plane. The prism is designed such that it disperses light into components of different wavelengths, with the components of shorter wavelengths being dispersed more than the components of longer wavelengths to present at the second focal plane a distribution pattern in which preselected groupings of the components are dispersed over essentially equal spacing intervals. Author

N85-23397 California Univ., San Diego.
OPTICAL MEMORY RESEARCH AND ITS APPLICATION TO DIGITAL OPTICAL PROCESSING Ph.D. Thesis
Howard Stephen Barr 1984 365 p
Avail: Univ. Microfilms Order No. DA8423912

For many years optical processing was known for its inherent parallelism, yielding high throughput operations. Combined with the higher accuracy (and usual flexibility) present in digital systems, the potential for performing high accuracy-high throughput image processing operations can be realized by a digital optical processor. The concept of digital optical processing can be compared to many electronic processor architectures. Various architectures from the distributed to pipelined to associative systems all display an increasing parallelism for compromised processing element complexity. A PLZT-CdS device is proposed which can perform the required logic and memory operations. This device is examined for its theoretical operation describing the transient behavior of its thin film structure. A double pulse electrical operation is described which can properly shape the device response, allowing image (information) storage. Dissert. Abstr.

N85-23398 Royal Signals and Radar Establishment, Malvern (England).
PERFORMANCE ESTIMATE OF A REFLECTING LIGHT PIPE FOR INFRARED DETECTORS
J. Warner Feb. 1984 23 p refs
(AD-A141269; RSRE-MEMO-3661; BR91490) Copyright. Avail: NTIS HC A02/MF A01

Scanner optics ray tracing programs were used to calculate the transmittance of a truncated pyramid reflector that increase the apparent size of an infrared detector of placed immediately over it. The dependence of flux concentration with pyramid geometry and ray angles is presented. It is shown that concentration factors > five can be achieved. Author (ESA)

N85-23399# Dayton Univ., Ohio.
SAMPLE INTRODUCTION METHODS FOR IMPROVING THE PARTICLE DETECTION CAPABILITY OF THE SPECTROMETRIC

OIL ANALYSIS PROGRAM Final Technical Report, 25 Apr. 1983 - 25 Apr. 1984
W. E. Rhine and R. E. Kauffman 4 Jan. 1985 185 p
(Contract N68335-83-C-0625)
(AD-A150139; UDR-TR-84-37; NAEC-92-185) Avail: NTIS HC A09/MF A01 CSCL 20/6

A program is being conducted to improve the particle detention capability of the rotating disk electrode arc/spark source atomic emission spectrometer, i.e., the A/E35U-3. This spectrometer is the primary spectrometer used by over 200 of the tri-service Joint Oil Analysis Program (JOAP) laboratories. The initial investigation determined the factors which limit the particle detention capability of the A/E35U-3 spectrometers. This report discusses the next effort which was conducted to improve the particle detention capability of the A/E35U-3 spectrometer. Acid dissolution, spark-to-residue and spark-in-vapor methods were investigated. The resultant data indicated that these methods can improve the particle detention capability of the spark source emission spectrometers. GRA

N85-23400# Florida Univ., Gainesville. Space Astronomy Lab.
A SYSTEMATIC STUDY OF LIGHT SCATTERING BY IRREGULARLY SHAPED PARTICLES Final Report, 29 May 1981 - 28 Aug. 1984
R. T. Wang 26 Nov. 1984 16 p
(Contract DAAG29-81-K-0104)
(AD-A150192; ARO-18100.6-GS) Avail: NTIS HC A02/MF A01 CSCL 20/6

This final report summarizes the research activities under the Systematic Study of Light Scattering by Irregularly Shaped Particles. The beginning one and one-half years were devoted to the analysis of existing experimental data and the related theoretical light-scattering studies, in parallel with the reconstruction, renovation and calibration of the microwave analog scattering facility then relocated from the Albany, N.Y. area. The following one and one-half year period was devoted to actual measurement tasks and analysis of data in our original proposal; e.g., the investigations of scattering by interacting spheres and by particles with rough surfaces. Simultaneous with these measurements a number of 2:1 finite cylinders were also measured on their extinction properties when they were either preferentially or randomly oriented in space. GRA

N85-23401# Arizona Univ., Tucson. Optical Sciences Center.
RESEARCH IN THE OPTICAL SCIENCES Final Report, 1 Oct. 1979 - 30 Sep. 1984
R. R. Shannon Oct. 1984 87 p
(Contracts F49620-80-C-0022; MIPR-ARO-103-83)
(AD-A150196; ARO-15412.20-PH; AFOSR-85-0132TR) Avail: NTIS HC A05/MF A01 CSCL 20/6

Research during the fifth year of contract F49620-80-C-0022 is described. Discussed are: optical bistability in thin evaporated films; long-range surface-plasmon polaritons; nonlinear guided wave interactions; theory of two-photon Doppler-free spectroscopy; X-ray image intensifiers with electronic readout; optical bistability; optical bistability experiments to improve solid-state devices and basic understanding; modulated emittance spectroscopy; high-resolution wavefront sensing through the atmosphere; aberrated Gaussian beams; ion beam processing of optical coatings on plastics; optical coatings for the X-ray to ultraviolet wavelength range. The degrees awarded to students receiving JSOP support are listed. Also included are the papers published under JSOP support from 1979 to 1983. GRA

N85-23402# Arizona Univ., Tucson.
OPTICAL PROCESSING IN RADON SPACE Final Report, Jul. 1983 - Jul. 1984
H. H. Barrett 15 Nov. 1984 22 p
(Grant AF-AFOSR-0249-82)
(AD-A150289; AFOSR-84-1267TR) Avail: NTIS HC A02/MF A01 CSCL 20/6

Signals of M dimensions (M>1) can be reduced to one-dimensional data by integration over M-1 dimensions. This operation is known as the Radon transform. Many useful two-dimensional signal processing operations can be performed rapidly by first producing the one-dimensional projection data and operating on the projections with efficient one-dimensional processors, such as surface acoustic wave devices. Such operations as spectrum analysis, complex Fourier transformation, production of the Wigner distribution function, and convolution can be performed in this manner, and may be done more rapidly or more accurately than by more conventional methods. GRA

N85-23403# Naval Postgraduate School, Monterey, Calif.
TIME-RESOLVED REFLECTIVITY MEASUREMENT OF EXTRINSIC SILICON DURING PULSED LASER IRRADIATION M.S. Thesis
G. D. Johnson and E. L. Chenoweth Jun. 1984 100 p
(AD-A150350) Avail: NTIS HC A05/MF A01 CSCL 20/6

Time-resolved reflectivity (TRR) of crystalline silicon has been measured with nanosecond resolution during and immediately after pulsed neodymium glass laser irradiation (1.06 micrometers, full width at half maximum pulse duration of 20 ns) over a range of pulsed laser energy densities. The TRR information was used to determine energy density thresholds for melting and damaging the polished surface of extrinsic silicon wafers. Reflectivity initially increased under laser irradiation and then returned to its original value for energy densities between 0.46 J/sq cm and 1.05 sq cm. For energy densities greater than 1.05 J/sq cm, the final value of reflectivity was less than the original value due to permanent target damage. The damage threshold was substantiated with optical photomicrographs. A qualitative examination was undertaken to determine the change in specular and diffuse reflection from the target surface as a function of the degree of laser-induced damage. GRA

N85-23404# Naval Research Lab., Washington, D. C.
THE EFFECT OF THE CHOICE OR RESPONSE MATRIX ON UNFOLDED BONNER SPHERE SPECTRA
K. A. Lowry and T. L. Johnson 31 Dec. 1984 49 p
(S15-80)
(AD-A150462; NRL-MR-5493) Avail: NTIS HC A03/MF A01 CSCL 20/6

The effect of the choice of response matrix on neutron spectra unfolded from Bonner sphere data was studied. In particular, the variation of integral parameters calculated from the unfolded spectra was determined for six matrices. It was determined that, depending on the choice of matrix, the calculated neutron fluence varies by approximately + or - 15%, the average neutron energy by + or - 40%, the dose by + or 30%, the dose equivalent by up to a factor of 4, and the quality factor by + or - 35%. For personnel monitoring devices, the calculated response varied by up to a factor of 4 for the Navy albedo badge, a factor of 7 for a cadmium-covered albedo badge, a factor of 6 for a CR-39 dosimeter, and more than two orders of magnitude for NTA type emulsion film. Two of the response matrices gave results in good agreement with other calculated and experimental data. GRA

N85-23405# New Mexico Univ., Albuquerque. Dept. of Mathematics.
NONRELATIVISTIC KAPITZA-DIRAC SCATTERING
E. A. Coutsias and J. K. McIver 1984 56 p
(Grant AF-AFOSR-0277-82)
(AD-A150622; AFOSR-85-0068TR) Avail: NTIS HC A04/MF A01 CSCL 20/14

We use techniques of Singular Perturbation theory to investigate the scattering of nonrelativistic charged particles by a standing light wave (Kapitza-Dirac scattering). Unlike previous treatments, we give explicit results for the effects of the time dependent part of the field. For low field intensity/low particle energy we show that the leading order effects can be found from an averaged equation and we compute corrections. For the strong fields that can be produced by modern lasers and/or high particle energies we show that the time dependence of the potential leads to focusing. Our methods can be applied to other problems with time-periodic potentials. GRA

N85-23406# Los Alamos Scientific Lab., N. Mex.
EFFECTS OF FOCUSING ON HRS FOCAL-PLANE POLARIMETER MEASUREMENTS
R. W. Fergerson Sep. 1984 26 p refs
(Contract W-7405-eng-36)
(DE85-004627; LA-10153-MS) Avail: NTIS HC A03/MF A01

The focusing properties of the high resolution proton spectrometer cause mixing inside the spectrometer among scattered particle polarization components in all three directions. This implies the need for a correction to the relations between focal plane polarizations and polarization transfer (PT) observables. One method for dealing with this problem is developed. The correction to the PT observables for angular regions at the edge of the spectrometer can be as large as 0.1 at an incident proton energy of 800 MeV. For data that are summed to produce one data point per spectrometer setting, this correction tends to be insignificant. At angles larger than 5 deg, it is sufficient to deal with corrections resulting from scattering off the spectrometer central momentum ray in the vertical and horizontal directions sequentially. This approximation greatly simplifies the implementation of this correction. DOE

N85-23407# National Bureau of Standards, Gaithersburg, Md. Electromagnetic Technology Div.
TECHNICAL DIGEST: SYMPOSIUM ON OPTICAL FIBER MEASUREMENTS, 1984
Oct. 1984 150 p refs Symp. held at Boulder, Colo., 2-3 Oct. 1984 Prepared in cooperation with Optical Society of America and IEEE
(PB85-114700; NBS/SP-683; LC-84-601092) Avail: NTIS HC A07/MF A01; also available SOD as SN003-003-02604-2 CSCL 20F

This volume contains summaries of 31 papers presented at the Symposium on Optical Fiber Measurements held October 2-3, 1984, at the National Bureau of Standards, Boulder, Colorado. Subjects include measurements on single-mode fiber, multimode fiber, fiber designed for sensing applications, instrumentation, field measurements, and standards. GRA

N85-22794# Joint Publications Research Service, Arlington, Va.
REFLEX ATTACHMENT FOR LINE ALIGNMENT IN SPECTRAL DIFFRACTION DEVICES Abstract Only
V. M. Kelman and I. V. Rodnikova *In its* USSR Rept.: Eng. and Equipment (JPRS-UEQ-85-003) 12 Mar. 1985 p 10-13 refs Transl. into ENGLISH from Izv. Akad. Nauk Kazakhskoy SSR: Ser. Fiz.-Mat. (Alma-Ata, USSR), no. 6, Jun. 1983 p 76-79 (For primary document see N85-22782 13-31)
Avail: NTIS HC A06

N85-22918# Joint Publications Research Service, Arlington, Va.
MULTIFUNCTIONAL ELEMENTS FOR INTEGRATED OPTICS Abstract Only
V. I. Volman and N. D. Kozyrev *In its* USSR Rept.: Electron. and Elec. Eng. (JPRS-UEE-85-002) 23 Jan. 1985 p 6-7 Transl. into ENGLISH from Radiotekhn. (Moscow), no. 8, Aug. 1984 p 37-40 (For primary document see N85-22907 13-33)
Avail: NTIS HC A05/MF A01

N85-22961# Joint Publications Research Service, Arlington, Va.
OPTICAL REFLECTOMETER FOR MULTIMODE FIBER LIGHTPIPES Abstract Only
Yu. V. Vvedenskiy, Yu. M. Gryaznov, A. B. Zuyev, and Yu. Ye. Spirichev *In its* USSR Rept.: Electron. and Elec. Eng. (JPRS-UEE-85-002) 23 Jan. 1985 p 52 Transl. into ENGLISH from Izmeritel. Tekhn. (Moscow), no. 9, Sep. 1984 p 30-32 (For primary document see N85-22907 13-33)
Avail: NTIS HC A05/MF A01

N85-22966# Joint Publications Research Service, Arlington, Va.
PARAMETERS OF AMPLITUDE-MODULATED SIGNAL UPON REFLECTIONS Abstract Only
G. V. Merkishin *In its* USSR Rept.: Electron. and Elec. Eng. (JPRS-UEE-85-002) 23 Jan. 1985 p 56-57 Transl. into ENGLISH from Radiotekhn. (Moscow), no. 8, Aug. 1984 p 21-23 (For primary document see N85-22907 13-33)
Avail: NTIS HC A05/MF A01

N85-22981# Joint Publications Research Service, Arlington, Va.
TIME SPECTRA OF INTENSITY FLUCTUATIONS ALONG REFLECTING PATH Abstract Only
Y. A. Monastyrnyy, G. Y. Patrushev, A. I. Petrov, and V. V. Pokasov *In its* USSR Rept.: Electron. and Elect. Eng. (JPRS-UEE-85-001) 9 Jan. 1985 p 3-4 Transl. into ENGLISH from Izv. Vysshikh Uch. Zaved.: Radiofiz. (USSR), v. 27, no. 7, Jul. 1984 p 907-912 Original language document announced as A84-48158 (For primary document see N85-22976 13-33)
Avail: NTIS HC A05/MF A01

N85-22993# Joint Publications Research Service, Arlington, Va.
OPTIMIZATION OF NUMBER OF PULSES IN DETECTION OF FLUCTUATING OPTICAL SIGNALS Abstract Only
F. I. Khaytun and R. B. Shemshedinov *In its* USSR Rept.: Electron. and Elect. Eng. (JPRS-UEE-85-001) 9 Jan. 1985 p 11 Transl. into ENGLISH from Radiotekh. (USSR), no. 9, Sep. 1984 p 88-91 (For primary document see N85-22976 13-33)
Avail: NTIS HC A05/MF A01

N85-23002# Joint Publications Research Service, Arlington, Va.
THEORY OF DIAPHRAGM LIGHT MODULATORS WITH ELECTRICAL INPUT SIGNAL Abstract Only
Y. P. Gushcho and A. S. Sigov *In its* USSR Rept.: Electron. and Elect. Eng. (JPRS-UEE-85-001) 9 Jan. 1985 p 16 Transl. into ENGLISH from Zh. Nauchnoy i Prikl. Fotografii i Kinematografii (USSR), v. 29, no. 5, Sep.-Oct. 1984 p 324-328 (For primary document see N85-22976 13-33)
Avail: NTIS HC A05/MF A01

N85-23003# Joint Publications Research Service, Arlington, Va.
A POSTERIORI INCREASE OF RESOLVING POWER OF OPTICAL SYSTEM FORMING AVERAGED MONOCHROMATIC IMAGES Abstract Only
P. A. Bakut, A. I. Deryugina, and V. I. Mandrosov *In its* USSR Rept.: Electron. and Elect. Eng. (JPRS-UEE-85-001) 9 Jan. 1985 p 16 Transl. into ENGLISH from Radiotekh. i Elektron. (USSR), v. 29, no. 8, Aug. 1984 p 1589-1594 (For primary document see N85-22976 13-33)
Avail: NTIS HC A05/MF A01

N85-23004# Joint Publications Research Service, Arlington, Va.
DISPERSION CHARACTERISTICS OF SMALL-MODE GRADIENT OPTICAL FIBERS Abstract Only
L. A. Frenkel *In its* USSR Rept.: Electron. and Elect. Eng. (JPRS-UEE-85-001) 9 Jan. 1985 p 17 Transl. into ENGLISH from Radiotekh. i Elektron. (USSR), v. 29, no. 8, Aug. 1984 p 1451-1456 (For primary document see N85-22976 13-33)
Avail: NTIS HC A05/MF A01

N85-23140# Joint Publications Research Service, Arlington, Va.
FINE STRUCTURE OF VERTICAL DISTRIBUTION OF LIGHT ATTENUATION INDEX OF SEA WATER Abstract Only
V. I. Burenkov, A. P. Vasilkov, and L. A. Stefantsev *In its* USSR Rept.: Earth Sci. (JPRS-UES-85-002) 1 Feb. 1985 p 43 Transl. into ENGLISH from Izv. Akad. Nauk SSSR: Fiz. Atmosfery i Okeana (Moscow), v. 20, no. 8, Aug. 1984 p 773-776 (For primary document see N85-23116 13-42)
Avail: NTIS HC A07/MF A01

N85-23171# Joint Publications Research Service, Arlington, Va.
RELATIONSHIP BETWEEN BRIGHTNESS SPECTRUM OF PHOTOGRAPHIC IMAGE AND SPECTRUM OF RISES ON A WATER SURFACE WITH WAVES Abstract Only
I. I. Strizhkin *In its* USSR Rept.: Earth Sci. (JPRS-UES-85-002) 1 Feb. 1985 p 98 Transl. into ENGLISH from Izv. Vyssh. Ucheb. Zaved., Geod. i Aerofotosyemka (Moscow), no. 3, May - Jun. 1984 p 90-95 (For primary document see N85-23116 13-42)
Avail: NTIS HC A07/MF A01

75 PLASMA PHYSICS

Includes magnetohydrodynamics and plasma fusion.
For ionospheric plasmas see *46 Geophysics.* For space plasmas see *90 Astrophysics.*

N85-23408 Wisconsin Univ., Madison.
CONFINEMENT PROPERTIES OF HIGH ENERGY DENSITY PLASMAS IN THE WISCONSIN LEVITATED OCTUPOLE Ph.D. Thesis
Jonathan Chadsey Twichell 1984 250 p
Avail: Univ. Microfilms Order No. DA8422714

The confinement of particles and energy is critically dependent on the plasma-wall interaction. Results detailing this interaction are presented. High power ICRF heated and gun afterglow plasmas were studied to detail the mechanisms determining particle and energy confinement. An extensive zero-D simulation code is used to assist in interpreting the experimental data. Physically reasonable models for plasma surface interactions, time dependent coronal treatment of impurities and multiple region treatment of neutrals are used in modeling the plasma. Extensive diagnostic data are used to verify the model. Non-heated plasmas decay from 28 to 3eV allowing clear identification of wall impact energy thresholds for desorption and particle reflection. The charge state distribution of impurities verifies the reflux to plasma diffusion rate ratio. Close agreement between the simulation and experimental data is found. Dissert. Abstr.

N85-23409*# Iowa Univ., Iowa City. Dept. of Physics and Astronomy.
PERIODIC SUBSTORM ACTIVITY IN THE GEOMAGNETIC TAIL
C. Y. Huang, T. E. Eastman, L. A. Frank, and D. J. Williams (Johns Hopkins Univ., Laurel, Md.) Jan. 1983 35 p refs Submitted for publication
(NASA-CR-175629; NAS 1.26:175629; U-of-IOWA-83-6) Avail: NTIS HC A03/MF A01 CSCL 20I

On 19 May 1978 an anusual series of events is observed with the Quadrispherical LEPEDEA on board the ISEE-1 satellite in the Earth's geomagnetic tail. For 13 hours periodic bursts of both ions and electrons are seen in all the particle detectors on the spacecraft. On this day periodic activity is also seen on the ground, where multiple intensifications of the electrojets are observed. At the same time the latitudinal component of the interplanetary magnetic field shows a number of strong southward deflections. It is concluded that an extended period of substorm activity is occurring, which causes repeated thinnings and recoveries of the plasma sheet. These are detected by ISEE, which is situated in the plasma sheet boundary layer, as periodic dropouts and reappearances of the plasma. Comparisons of the observations at ISEE with those at IMP-8, which for a time is engulfed by the plasma sheet, indicate that the activity is relatively localized in spatial extent. For this series of events it is clear that a global approach to magnetospheric dynamics, e.g., reconnection, is inappropriate. Author

N85-23410# Colorado Univ., Boulder. Boulder.
ION TRANSPORT IN BEAM-PLASMA INTERACTIONS Annual Report, 30 Sep. 1983 - 30 Sep. 1984
R. A. Stern 30 Sep. 1984 8 p
(Grant AF-AFOSR-0325-83)
(AD-A150145; Rept-153-3223; AFOSR-84-1257TR) Avail: NTIS HC A02/MF A01 CSCL 20/9

This interim report covers work performed on the topic of laser-fluorescence measurements of ion beam scattering and transport of background ions during beam-plasma interactions. Achievements to date include (1) construction and operation of the plasma device, (2) assembly of a diagnostic pulsed laser, and (3) assembly and emplacement of the detection system. Future work plans, personnel changes and general scientific activities are described. GRA

N85-23411# Naval Research Lab., Washington, D. C.
INCREASED HOT-ELECTRON PRODUCTION AT QUARTER-CRITICAL DENSITY IN LONG-SCALELENGTH, LASER-PLASMA INTERACTIONS Memorandum Report, Sep. - Oct. 1984
F. C. Young, M. J. Herbst, C. K. Manka, S. P. Obenschain, and J. H. Gardner 11 Feb. 1985 14 p
(AD-A150519; NRL-MR-5484) Avail: NTIS HC A02/MF A01 CSCL 20/5

Hot-electron fractions measured in Nd-laser-plasma interactions at 1014W/cm2 increase from <0.02% to 0.3% as the plasma scalelength at quarter-critical density (nc/4)is systematically increased from 140 microns to 320 microns. Correlated X-ray and 3w/2 emissions indicate that the hot electrons are produced by a nc/4 instability. GRA

N85-23412# Massachusetts Inst. of Tech., Cambridge. Plasma Fusion Center.
LOWER HYBRID HEATING AND CURRENT DRIVE, AND ION CYCLOTRON HEATING EXPERIMENTS ON THE ALCATOR C AND THE VERSATOR II TOKAMAKS
M. Porkolab, B. Blackwell, P. Bonoli, D. Griffin, S. Knowlton, B. Lloyd, J. Moody, J. J. Schuss, Y. Takase, S. Texter et al Aug. 1984 15 p refs Presented at the 10th Intern. Conf. on Plasma Phys. and Controlled Nucl. Fusion Res., London, 12-19 Sep. 1984
(DE85-004918; DOE/ET-51013/131; PFC/CP-84-14; CONF-840910-20) Avail: NTIS HC A02/MF A01

Lower hybrid electron Landau heating experiments were carried out on the Alcator C Tokamak at densities 0.8 x 10(14) less than or equal to anti n(cm(-3)) less than or equal to 1.7 x 10(14), and at B = 7 T - 11 T. Using SiC coated graphite limiters, upon injection of 850 kW of power at a density of anti n/sub e/ approx. = 1.3 x 10(14)cm(-3) in deuterium typical temperature increases of (DELTA)Ti approx. = 0.7 keV, (DELTA)T/sub e/ approx. = 1.0 keV were observed. Initial results from the Alcator C 180 MHz ICRF heating program are reported. Significant heating results were obtained in the hydrogen minority regime; upon injection of 400 kW of RF power the ion temperature rose by as much as 600 eV at a density of anti n/sub e/ less than or equal to 1.9 x 10(14) cm9-3). In Versator II, during lower hybrid current drive experiments the global particle confinement increased by approximately a factor of two above the ohmic discharge value when the Parail-Poqutse electron tail instability was stabilized. DOE

N85-23413# Oak Ridge National Lab., Tenn.
ULTRAHIGH-SENSITIVITY THRESHOLD NEUTRON DETECTOR FOR PLASMA DIAGNOSITCS
K. H. Valentine, M. K. Kopp, G. Allin, W. T. Clay, and V. C. Miller 1984 6 p refs Presented at Nucl. Sci. Symp., Orlando, Fla., 31 Oct. 1984
(Contract DE-AC05-84OR-21400)
(DE85-005270; CONF-841007-52) Avail: NTIS HC A02/MF A01

An ultrahigh-sensitivity fast fission counter was developed to selectively detect high-energy neutrons (E sub n > 1 MeV) produced by D-D and D-T fusion reactions in thermonuclear plasmas. Discrimination against slow and epithermal neutrons produced by scattering or electrodissociation of deuterium was achieved by sensitizing the detector with 100 g of highly depleted (238)UO2, which has a fission threshold for neutron energies E sub n > 1 MeV. The capacitive signal loading effects of the detector's large electrode area (5 m(2)) were mitigated by using a transmission-line electrode configuration. Wideband, low-noise preamplifiers were developed to match the 25- (UC OMEGA) characteristic impedance of the transmission line. The neutron sensitivity of the detector was shown to be 0.07 counts.s(-1). (neutron (cm(2).s))(-1) for E sub n > 2 MeV in initial laboratory testing. DOE

N85-22414# Joint Publications Research Service, Arlington, Va.
HYDROMAGNETIC PRECURSORS OF INTERPLANETARY PLASMA BURST Abstract Only
A. V. Gulyelmi and K. G. Ivanov *In its* USSR Rept.: Space (JPRS-USP-85-001) 4 Feb. 1985 p 36 Transl. into ENGLISH from Geomagnetizm i Aeronomiya (USSR), v. 24, no. 3, May-Jun.

1984 p 489-491 Original language document announced as A84-40100 (For primary document see N85-22403 13-12)
Avail: NTIS HC A07

N85-22472*# National Aeronautics and Space Administration, Washington, D. C.
SUPRATHERMAL PLASMA OBSERVED ON STS-3 MISSION BY PLASMA DIAGNOSTICS PACKAGE
W. Paterson, L. A. Frank, H. Owens, J. S. Pickett, G. B. Murphy, and S. D. Shawhan *In* NASA. Lewis Research Center Spacecraft Environ. Interactions Technol., 1983 Mar. 1985 p 13-17 refs Prepared in cooperation with Iowa Univ., Iowa City (For primary document see N85-22470 13-18)
(Grant NAG3-449)
Avail: NTIS HC A99/MF E03 CSCL 20I

N85-22483*# Southwest Research Inst., San Antonio, Tex.
POLAR PLASMAS AS OBSERVED BY DYNAMICS EXPLORERS 1 AND 2
J. Barfield, J. Burch, C. Gurgiolo, C. Lin, D. Winningham, and N. A. Saflekos *In* NASA. Lewis Research Center Spacecraft Environ. Interactions Technol., 1983 Mar. 1985 p 155-176 refs (For primary document see N85-22470 13-18)
(Contracts NAS5-26363; NAS5-25693; F19628-82K-0024; FY7121-83-N-001)
Avail: NTIS HC A99/MF E03 CSCL 20I

N85-22492*# Kansas Univ., Lawrence.
SELF-CONSISTENT SIMULATION OF PLASMA INTERACTIONS WITH SECONDARY-EMITTING INSULATORS
S. T. Brandon, R. L. Rusk, T. P. Armstrong, and J. Enoch *In* NASA. Lewis Research Center Spacecraft Environ. Interactions Technol., 1983 Mar. 1985 p 287-303 refs (For primary document see N85-22470 13-18)
Avail: NTIS HC A99/MF E03 CSCL 20I

N85-22494*# National Aeronautics and Space Administration. Lewis Research Center, Cleveland, Ohio.
THE PIX-2 EXPERIMENT: AN OVERVIEW
Carolyn K. Purvis *In its* Spacecraft Environ. Interactions Technol. Mar. 1985 p 321-332 refs (For primary document see N85-22470 13-18)
Avail: NTIS HC A99/MF E03 CSCL 20I

N85-22495*# National Aeronautics and Space Administration. Lewis Research Center, Cleveland, Ohio.
PLASMA INTERACTION EXPERIMENT 2 (PIX 2): LABORATORY AND FLIGHT RESULTS
Norman T. Grier *In its* Spacecraft Environ. Interactions Technol. Mar. 1985 p 333-347 (For primary document see N85-22470 13-18)
Avail: NTIS HC A99/MF E03 CSCL 20I

N85-22496*# National Aeronautics and Space Administration. Lewis Research Center, Cleveland, Ohio.
RAM-WAKE EFFECTS ON PLASMA CURRENT COLLECTION OF THE PIX 2 LANGMUIR PROBE
Dale C. Ferguson *In its* Spacecraft Environ. Interactions Technol. Mar. 1985 p 349-357 refs (For primary document see N85-22470 13-18)
Avail: NTIS HC A99/MF E03 CSCL 20I

N85-22497*# National Aeronautics and Space Administration. Lewis Research Center, Cleveland, Ohio.
NASCAP SIMULATION OF PIX 2 EXPERIMENTS
James C. Roche and Myron J. Mandell (Systems, Science and Software, San Diego) *In its* Spacecraft Environ. Interactions Technol. Mar. 1985 p 359-366 (For primary document see N85-22470 13-18)
Avail: NTIS HC A99/MF E03 CSCL 20I

N85-22498*# National Aeronautics and Space Administration. Lewis Research Center, Cleveland, Ohio.
AN INVESTIGATION OF ARC DISCHARGING ON NEGATIVELY BIASED DIELECTRIC CONDUCTOR SAMPLES IN A PLASMA
William L. Miller *In its* Spacecraft Environ. Interactions Technol. Mar. 1985 p 367-377 refs (For primary document see N85-22470 13-18)
Avail: NTIS HC A99/MF E03 CSCL 20I

N85-22795# Joint Publications Research Service, Arlington, Va.
RUBY WAVEFRONT-CONJUGATION LASER FOR OBTAINING HIGH TEMPERATURE PLASMA Abstract Only
V. A. Boyko, G. A. Koldashov, A. Ya. Fayenov, A. I. Fedosimov, and I. N. Tsigler *In its* USSR Rept.: Eng. and Equipment (JPRS-UEQ-85-003) 12 Mar. 1985 p 14-15 Transl. into ENGLISH from Pribory i Tekhn. Eksperim. (Moscow), no. 3, May - Jun. 1984 p 188-190 (For primary document see N85-22782 13-31)
Avail: NTIS HC A06

N85-22974# Joint Publications Research Service, Arlington, Va.
EXTRACTION OF SURFACE-WAVE ENERGY FROM PLASMA WAVEGUIDE Abstract Only
G. I. Zaginaylov, A. N. Kondratenko, and V. M. Kuklin *In its* USSR Rept.: Electron. and Elec. Eng. (JPRS-UEE-85-002) 23 Jan. 1985 p 62 Transl. into ENGLISH from Izv. Vysshikh Uchebn. Zavedeniy: Radiofiz. (Gorkiy), v. 27, no. 9, Sep. 1984 p 1178-1184 (For primary document see N85-22907 13-33)
Avail: NTIS HC A05/MF A01

76 SOLID-STATE PHYSICS

Includes superconductivity.

For related information, see also *33 Electronics and Electrical Engineering* and *36 Lasers and Masers.*

N85-23414*# Michigan Technological Univ., Houghton. Dept. of Chemistry and Chemical Engineering.
RAMAN STRUCTURAL STUDIES OF THE NICKEL ELECTRODE Progress Report, 20 Feb. - 20 Mar. 1984
B. C. Cornilsen 1985 39 p refs
(Grant NAG3-519)
(NASA-CR-175619; NAS 1.26:175619) Avail: NTIS HC A03/MF A01 CSCL 20L

Raman spectroscopy is sensitive to empirically controlled nickel electrode structural variations, and has unique potential for structural characterization of these materials. How the structure relates to electrochemical properties is examined so that the latter can be more completely understood, controlled, and optimized. Electrodes were impregnated and cycled, and cyclic voltammetry is being used for electrochemical characterization. Structural variation was observed which has escaped detection using other methods. Structural changes are induced by: (1) cobalt doping, (2) the state of change or discharge, (3) the preparation conditions and type of buffer used, and (4) the formation process. Charged active mass has an NiOOH-type structure, agreeing with X-ray diffraction results. Discharged active mass, however, is not isostructural with beta-Ni(OH)2. Chemically prepared alpha phases are not isostructural either. A disordered structural model, containing point defects, is proposed for the cycled materials. This model explains K(+) incorporation. Band assignments were made and spectra interpreted for beta-Ni(OH)2, electrochemical NiOOH and chemically precipitated NiOOH. Author

N85-23415# Royal Signals and Radar Establishment, Malvern (England).
INVESTIGATION OF THE EFFECT OF ANNEALING ON THE DISLOCATION AND SUB-GRAIN BOUNDARY CONTENT OF SOLVENT-EVAPORATION-GROWN CdTe
Nicholas Troughton Mar. 1984 15 p refs
(AD-A144087; RSRE-MEMO-3680; BR92218) Avail: NTIS HC A02/MF A01 CSCL 20/2

Solvent-evaporation grown CdTe wafers were examined using optical microscopy and etching techniques to determine the subgrain boundary structure and density. Results indicate that the material contains subgrains of the order of 100 to 300 micron

diameter, the boundaries of which are formed by polygonized dislocations in densities exceeding 100,000/cm. Annealing for periods > 24—hr at temperatures above 800C reduces sub-grain boundary dislocation density and, in the best case, completely removes boundaries. Author (ESA)

N85-23416# California Univ., Livermore. Lawrence Livermore Lab.
MOLECULAR DYNAMICS STUDIES OF ENERGY TRANSFER PROCESSES IN CRYSTAL SYSTEMS Annual Summary Report, 1 Oct. 1983 - 30 Sep. 1984
A. M. Karo and F. E. Walker 30 Nov. 1984 9 p
(Contract N00014-84-F-0094)
(AD-A150161) Avail: NTIS HC A02/MF A01 CSCL 20/2

Computer molecular dynamics studies have been carried out on the problem of attaining a fundamental understanding of shock-induced initiation of energetic materials. The studies focus on an important specific facet of this problem, namely, the energy transfer processes in crystal systems, particularly in molecular lattices. Code development for the CRAY computer during the preceding year is reviewed and the shock studies that were carried out are listed. Plans for additional studies of the underlying mechanisms of intermolecular-intramolecular energy transfer and the dynamics of intramolecular energy exchange in shock-loaded systems are presented. GRA

N85-23417# Battelle Pacific Northwest Labs., Richland, Wash.
ELECTRICAL AND THERMAL TRANSPORT PROPERTY STUDIES OF HIGH-TEMPERATURE THERMOELECTRIC MATERIALS Interim Report, 15 Aug. 1983 - 15 May 1984
J. L. Bates, J. E. Garnier, L. C. Olsen, and C. W. Griffin Jul. 1984 105 p
(Contract F49620-83-C-0109)
(AD-A150167; AFOSR-84-1210TR) Avail: NTIS HC A06/MF A01 CSCL 11/2

The first year of this research emphasized the study of electronically conducting oxides with varied transport characteristics, an evaluation of theoretical models, and the determination of a high-temperature transport property data base. Oxide systems based on SnO2-In2O3, (La, Y) (Mg,Ca,Sr) CrO3, HfO2-RxOy-In3O3 and La(Sr)MnO3 were selected for initial studies and represent different crystallographic/defect structures and transport characteristics. The electrical conductivity, Seeback coefficient and thermal conductivity for these oxides are being measured and have provided a preliminary data base for evaluating transport properties and the figure of merit. The purpose of this report is to describe the technical results obtained during the first year's study of high-temperature thermoelectric materials. The scope of the research is (1) to develop theoretical models for electrical, thermal, and thermoelectric behavior of refractory oxide materials, (2) to determine electrical transport properties necessary to develop and test these models, (3) to determine methods for increasing the figure of merit in refractory oxide systems by varying composition, defect structure. microstructure, etc., and (4) to use these models to establish theoretical and empirical limits of the figure of merit for these oxides and other refractory materials. GRA

N85-23418# Arizona State Univ., Tempe. Center for Solid State Science.
TRANSPORT PROPERTIES OF SILICA THERMALLY GROWN ON SILICON Final Report, 1 Feb. 1982 - 31 Aug. 1984
J. B. Wagner, Jr. 20 Nov. 1984 71 p
(Contract DAAG29-82-K-0052)
(AD-A150304; ARO-17888.3-MS) Avail: NTIS HC A04/MF A01 CSCL 20/3

The total, ionic and electronic conductivity of silica thermally grown on silicon have been determined between 25 960 C. Therefrom the ionic transport numbers have been calculated. Utilizing an open circuit emf method, the average ionic transport numbers for silica thermally grown on silicon, for vitreous silica and for single crystalline quartz have been determined between 550 and 950 C. In general, all the silicas studied exhibit mixed conduction, i.e., conduction via ions and electrons. The ionic contribution increases with temperature and attains a maximum at 800 to 900 C. The open circuit emf studies show smaller values of the average ionic transference numbers than those values obtained via conductivity measurements. This apparent discrepancy is attributed to migration of oxygen through pores in the SiO2 grown on Si in the case of the open circuit emf measurement. High resolution transmission electron microscopic studies confirmed the presence of small pores (5 to 8 A in diameter) in the Si02 grown silicon under both wet and dry conditions. A preliminary study of the reaction between molybdenum and SiO2 grown thermally on silicon wafers has been carried out. The Mo appears to diffuse into the SiO2 at 1000 and 1100 C as determined by Rutherford Back Scattering techniques. GRA

N85-23419# Cornell Univ., Ithaca, N.Y. Lab. of Atomic and Solid State Physics.
OBSERVATION OF SURFACE VIBRATIONAL RESONANCES ON (110) SURFACES OF FCC METALS Interim Report
J. A. Stroscio, M. Persson, S. R. Bare, and W. Ho 8 Feb. 1985 14 p
(Contracts N00014-82-K-0576; N00014-81-K-0505)
(AD-A150469; Rept-6) Avail: NTIS HC A02/MF A01 CSCL 20/2

Inelastic dipole scattering of electrons from surface vibrational resonances of celan Cu(110) and Ni(110) surfaces has been observed. The resonances are shown by surface lattice dynamics calculations to be a characteristic signature of the (110) surface of fcc metals. The calculated spectral energies and shapes are in excellent agreement with experiments and shows that there are no significant changes in the surface force constants from the bulk values. GRA

N85-23420# Cornell Univ., Ithaca, N.Y. Lab. of Atomic and Solid State Physics.
DIPOLE ACTIVE SURFACE VIBRATIONAL RESONANCES ON CLEAN AND HYDROGEN COVERED Ni(110) Interim Report
Joseph A. Stroscio, M. Persson, Simon R. Bare, and W. Ho 11 Feb. 1985 18 p Sponsored in part by the Swedish Natural Science Research Council
(Contracts N00014-82-K-0576; N00014-81-K-0505; Grant NSF DMR-82-17227)
(AD-A150546; Rept-9) Avail: NTIS HC A02/MF A01 CSCL 07/4

A vibrational resonance of the surface metal atoms on the clean Ni(110) surface is observed by electron energy loss spectroscopy. The dipole coupling arises from the incomplete screening of the moving ion cores by the conduction electrons in the surface region. Surface lattice dynamical calculations are in excellent agreement with the measured spectra for the clean surface and show that there are no significant deviations in the surface force constant from the bulk value. This resonance results from a pseudo band gap in the longitudinal bulk phonon dispersion relation along the (110) direction. On the (1x2) reconstructed surface induced by hydrogen chemisorption, a dramatic decrease in intensity of the resonance is observed. GRA

N85-23421*# Superwave Technology, Inc., Santa Clara, Calif.
DEMONSTRATION OF FEASIBILITY OF DEPOSITING SEMICONDUCTOR LAYERS USING MICROWAVE ENHANCED PLASMA TECHNIQUES Quarterly Technical Report, 1 Jun. - 1 Sep. 1984
1984 13 p refs
(Contract NAS7-100)
(NASA-CR-174392; DOE/JPL-956828/2; NAS 1.26:174392; DE85-000625) Avail: NTIS HC A02/MF A01 CSCL 20L

The feasibility of low temperature deposition of dielectric films was demonstrated. The highlights of the activity revolved around the deposition system integration, system test and some modifications. A thin film of Si3N4 is deposited through the plasma reaction of nitrogen gas and SiH4 at room temperature. Fine tuning of the system parameters such as gas flow control, partial pressure control, gas distribution in the reaction chamber and deposition rate is investigated. DOE

N85-23422# Massachusetts Inst. of Tech., Cambridge. National Magnet Lab.
IMPROVEMENT IN MAGNETIC FIELD PROPERTIES OF VANADIUM-GALLIUM SUPERCONDUCTORS BY ENHANCEMENT OF SPIN-ORBIT SCATTERING Final Report
P. M. Tedrow and R. Meservy 31 Aug. 1984 3 p
(Contract DE-AC02-83ER-45026)
(DE85-002893; DOE/ER-45026/2) Avail: NTIS HC A02/MF A01

The high-magnetic field characteristics of the practical superconductor vanadium-gallium were improved by enhancing the spin-orbit scattering rate in this material. To this end, thin films of V-Ga of various compositions were made by electron-beam codeposition. Third elements with high atomic number Z were added to these films during deposition. High-Z impurities are expected to be most effective in increasing the spin-orbit scattering rate. The elements added were Nb, Ta, Sn, Pt and Pb. These impurities were added at a level of about one percent. DOE

N85-23423# California Univ., Berkeley. Lawrence Berkeley Lab. Materials and Molecular Research Div.
MICROSTRUCTURAL STUDY ON THE PROCESSING AND PROPERTIES OF HIGH-FIELD A15 SUPERCONDUCTING MATERIALS Ph.D. Thesis
I. Wei Daniel Wu Aug. 1984 320 p refs
(Contract DE-AC03-76SF-00098)
(DE85-004652; LBL-16999) Avail: NTIS HC A14/MF A01

Superconducting properties of high-field A15 materials were studied in terms of the physical and chemical states of the A15 phases. Higher critical current is achieved through microstructural control. The A15 materials investigated include the V3Ga and Nb3A1 phases formed by a direct-precipitation process, the multifilamentary Nb3Sn formed by the bronze-process, and the bronze-processed Nb3Sn with a Mg addition. The direct-precipitation process was found to have an intrinsically inferior critical current and lower stability, due to the large effective grain size, of stoichiometric composition, and the high stability of bcc films between A15 grains. For the bronze-processed Nb2Sn multifilamentary wire, microscopic examination reveals that the reacted layer consists of a three-shell composite structure. A mechanism to account for the formation of this structure is proposed. The critical current density is apparently determined by the areal fraction, grain size and composition of the central, fine-grained layer. DOE

N85-23424# California Univ., Berkeley. Lawrence Berkeley Lab. Materials and Molecular Research Div.
MACROSCOPIC QUANTUM TUNNELLING IN A CURRENT BIASED JOSEPHSON JUNCTION
J. M. Martinis, M. H. Devoret, J. Clarke, and C. Urbina Nov. 1984 6 p refs Presented at the 4th Simposio Chileno de Fisica, Santiago, 26-28 Dec. 1984
(Contract DE-AC03-76SF-00098)
(DE85-004603; LBL-18681; CONF-841247-3) Avail: NTIS HC A02/MF A01

An attempt is discussed to answer experimentally the question: do macroscopic variables obey quantum mechanics. More precisely, this experiment deals with the question of quantum-mechanical tunnelling of a macroscopic variable, a subject related to the famous Schrodinger's cat problem in the theory of measurement. DOE

N85-23425# Ames Lab., Iowa.
ANOMALOUS MAGNETISM OF CeRh3B2 UNDER PRESSURE
S. A. Shaheen (Bochum Univ., West Germany), J. S. Schilling (Bochum Univ., West Germany), P. Klavins, C. B. Vining, and R. N. Shelton (Geneva Univ., Switzerland) 1984 13 p refs Presented at the Intern. Conf. on Valence Fluctuations, Koln (West Germany), 27-30 Aug. 1984
(Contract W-7405-eng-82)
(DE85-003069; IS-M-522; CONF-840876-4) Avail: NTIS HC A02/MF A01

Whereas CeRh3B2 possesses the highest magnetic ordering temperature (T sub c approx. = 115K) of any Ce-compound with nonmagnetic constituents, LaRh3B2 becomes superconducting below 2.5K. Recent magnetization measurements under pressure as well as lattice parameter and specific heat studies shed light on the nature of the anomalous magnetic state in CeRh3B2. DOE

N85-23426# Tulane Univ., New Orleans, La.
ELECTRONIC TRANSPORT IN HYDROGENATED AMORPHOUS SILICON FILMS
Rolf Koenenkamp Oct. 1984 125 p refs
(Contract DE-AC02-83CH-10093)
(DE85-002901; SERI/STR-211-2469) Avail: NTIS HC A06/MF A01

In this study the parameters characterizing the electronic transport in glow discharge deposited amorphous (a) Si:H, a-Si:C:H and a-Si:Sn:H films are investigated. For the investigation five experimental techniques are employed. These are the photocurrent reversal, time of flight, charge collection, junction recovery and surface photovoltage experiments. In the photocurrent reversal experiment the on going dispute concerning the magnitude of the drift mobilities in a-Si:H is addressed. It is established that the current transients observed in this type of experiment are due to the drift of photogenerated excess carriers. The details of the results are in excellent agreement with the low mobility picture which has been gained by means of transient photoconductivity experiments. In the time of flight and charge collection measurements, the drift mobilities, carrier ranges, capture cross sections for shallow and deep trapping, and the distribution of bandtail state, are determined. B.W.

N85-23427# Oak Ridge National Lab., Tenn.
STRUCTURAL CHARACTERIZATION BY INTENSITY MEASUREMENTS OF ELECTRON DIFFRACTION PATTERNS
J. Bentley, G. L. Lehman, and A. T. Fisher 1984 11 p refs Presented at Microbeam Analysis Soc. Anal. Electron Microscopy Meeting, Bethlehem, Pa., 16 Jul. 1984 Prepared in cooperation with Oak Ridge Associated Universities, Inc., Tenn.
(Contract DE-AC05-84OR-21400)
(DE85-004803; CONF-840767-12) Avail: NTIS HC A02/MF A01

The preliminary measurement of intensity distribution in selected area (SAD) and convergent beam electron diffraction (CBED) patterns from specimens that contain ordered or modulated structures is discussed. The aim is that such information may be used to quantify lattice strain, composition modulations and chemical order in such materials. The interpretation of the intensity data is expected to be complex because of dynamical multiple scattering effects. Characterization of the materials used in this work by other techniques such as X-ray diffraction, will be used in an evaluation of the usefulness and reliability of the electron diffraction data. DOE

N85-23428# Oak Ridge National Lab., Tenn.
INFLUENCE OF SUBSTRATE HEATING AND THERMAL ANNEALING ON THE SURFACE CRYSTALLINITY IN SINGLE Si CRYSTALS IMPLANTED WITH HIGH DOSES OF (16)O
T. P. Sjoreen, O. W. Holland, D. Fathy, K. More, and R. F. Davis Nov. 1984 16 p refs Presented at 8th Conf. on the Appl. of Accelerators in Res. and Ind., Denton, Tex., 12 Nov. 1984 Prepared in cooperation with Microelectronics Center of North Carolina, Research Triangle Park, North Carolina State Univ., Raleigh
(Contract DE-AC05-84OR-21400)
(DE85-005264; CONF-841117-36) Avail: NTIS HC A02/MF A01

The dependence of near-surface crystallinity on substrate heating during high dose O(+) implantation into Si and post implantation annealing was studied. It is shown that the damage morphology in the crystalline region above the SiO2 layer is very sensitive to substrate temperature and that, under optimum implant conditions which minimize damage conditions in the near surface, annealing does not improve the near surface crystallinity. Rutherford backscattering/channeling spectroscopy and cross-sectional transmission electron microscopy were used to analyze the microstructure of the samples. DOE

N85-22952# Joint Publications Research Service, Arlington, Va.
NOISE CHARACTERISTICS OF SULFUR-DOPED SILICON DIODES Abstract Only
Z. O. Mkhitaryan, R. S. Barsegyan, and V. M. Arutyunyan *In its* USSR Rept.: Electron. and Elec. Eng. (JPRS-UEE-85-002) 23 Jan. 1985 p 40 Transl. into ENGLISH from Izv. Vysshikh Uchebn. Zavedeniy: Radiofiz. (Gorkiy), no. 9, Sep. 1984 p 1218-1220 (For primary document see N85-22907 13-33)
Avail: NTIS HC A05/MF A01

N85-22953# Joint Publications Research Service, Arlington, Va.
MEASUREMENT OF INTERNAL THERMAL RESISTANCE FOR QUALITY CONTROL OF SEMICONDUCTOR DEVICES Abstract Only
S. K. Zakharenko and Yu. G. Semenov *In its* USSR Rept.: Electron. and Elec. Eng. (JPRS-UEE-85-002) 23 Jan. 1985 p 41-42 Transl. into ENGLISH from Radiotekhn. (Moscow), no. 8, Aug. 1984 p 89-90 (For primary document see N85-22907 13-33)
Avail: NTIS HC A05/MF A01

N85-22956# Joint Publications Research Service, Arlington, Va.
OUTLOOK FOR REALIZATION OF PROXIMITY EFFECT AND JOSEPHSON DIRECT CURRENT IN HELIUM-2 Abstract Only
L. V. Kiknadze, Yu. G. Mamaladze, and O. D. Cheyshvili *In its* USSR Rept.: Electron. and Elec. Eng. (JPRS-UEE-85-002) 23 Jan. 1985 p 46 Transl. into ENGLISH from Izmeritel. Tekhn. (Moscow), no. 7, Jul. 1984 p 29-30 (For primary document see N85-22907 13-33)
Avail: NTIS HC A05/MF A01

N85-23552*# Arizona Univ., Tucson. Lunar and Planetary Lab.
MODELLING EQUILIBRIUM AND FRACTIONAL CRYSTALLIZATION IN THE SYSTEM MgO-FeO-CaO-Al2O3-SiO2 Abstract Only
Floyd Herbert *In* NASA, Washington Repts. of Planetary Geol. and Geophys. Program, 1984 Apr. 1985 p 220-222 refs (For primary document see N85-23474 13-91)
Avail: NTIS HC A99/MF A01 CSCL 02L

N85-23556*# Massachusetts Inst. of Tech., Cambridge. Dept. of Earth, Atmospheric, and Planetary Science.
CRYSTAL CHEMISTRY OF METEORITIC HIBONITES Abstract Only
Roger G. Burns and Virginia Mee Burns *In* NASA, Washington Repts. of Planetary Geol. and Geophys. Program Apr. 1985 p 228 Previously announced as A85-17675 (For primary document see N85-23474 13-91)
Avail: NTIS HC A99/MF A01 CSCL 20L

77 THERMODYNAMICS AND STATISTICAL PHYSICS

Includes quantum mechanics; and Bose and Fermi statistics.

For related information see also *25 Inorganic and Physical Chemistry* and *34 Fluid Mechanics and Heat Transfer.*

N85-23429# North Carolina State Univ., Raleigh. Precision Engineering Lab.
THERMAL AND THERMOELASTIC EFFECTS IN ROLLING/SLIDING CONTACTS Final Report, 1 Jun. 1982 - 30 Sep. 1984
T. A. Dow, D. K. Lawson, and F. Sadeghi 30 Sep. 1984 76 p
(Contract N00014-82-K-0551)
(AD-A150435; PEL-005) Avail: NTIS HC A05/MF A01 CSCL 20/13

This report describes a theoretical and experimental study of thermal and thermomechanical effects on frictionally and electrically heated rolling/sliding surfaces. A 2-D thermal analysis is used to predict the temperature distribution through the thickness of the lubricant film in an elastohydrodynamic (EHD) contact. The relative magnitude of shear and compressive heating as well as the losses due to conduction and convection are compared for pure rolling and slip conditions. GRA

N85-23430# California Univ., Livermore. Lawrence Livermore Lab. Materials Physics Div.
H-DIVISION MATERIALS PHYSICS PROGRESS Quarterly Report, Apr. - Jun. 1984
John A. Moriarty, ed. 7 Dec. 1984 66 p refs
(Contract W-7405-eng-48)
(DE85-004990; UCID-18574-84-2) Avail: NTIS HC A04/MF A01

The following topics are reported; railgun development; ultrahigh-pressure underground nuclear driven equation-of-state experiment; possible missing structure in the rare-earth series; promotion energies and cohesion: a simple, accurate scheme for solids; a general correlation of thermal conductivity with equation of state; interdiffusion in a dense, binary ionic mixture; oscillator strengths calculated from effective potentials; compliant material response characterizational numerical coupling of an unstable boundary layer flow and a compliant surface; and three-particle heat flow in one dimension via the Boltzmann equations. DOE

N85-23550*# Arizona Univ., Tucson. Lunar and Planetary Lab.
THEORETICAL THERMODYNAMICS OF MIXTURES AT HIGH PRESSURES Abstract Only
W. B. Hubbard *In* NASA, Washington Repts. of Planetary Geol. and Geophys. Program, 1984 Apr. 1985 p 214-216 refs (For primary document see N85-23474 13-91)
(Grant NAGw-192)
Avail: NTIS HC A99/MF A01 CSCL 20M

80 SOCIAL SCIENCES (GENERAL)

Includes educational matters.

No abstracts in this category.

81 ADMINISTRATION AND MANAGEMENT

Includes management planning and research.

N85-23431*# National Aeronautics and Space Administration, Washington, D. C.
SMALL BUSINESS INNOVATION RESEARCH: ABSTRACTS OF 1984. PHASE 1 AWARDS
Jan. 1985 76 p
(NASA-TM-87427; NAS 1.15:87427) Avail: NTIS HC A05/MF A01 CSCL 05A

On September 27, 1984, the National Aeronautics and Space Administration announced the selection of Phase I projects for the Small Business Innovation Research Program. These awards resulted from the evaluation of proposals submitted in response to the 1984 Program Solicitation, SBIR 84-1. In order to make available information on the technical content of the Phase I projects supported by the NASA SBIR Program, the abstracts of those proposals which resulted in awards of contracts are given. In addition, the name and address of the firm performing the work are given for those who may desired additional information about the project. Propulsion, aerodynamics, computer techniques, exobiology and composite materials are among the areas covered. R.J.F.

N85-23432# Massachusetts Inst. of Tech., Cambridge.
MOTION PLANNING WITH SIX DEGREES OF FREEDOM
B. R. Donald May 1984 265 p
(Contracts N00014-81-K-0494; N00014-80-C-0505; N00014-82-K-0334)

(AD-A150312; AI-TR-791) Avail: NTIS HC A12/MF A01 CSCL 06/4

The motion planning problem is of central importance to the fields of robotics, spatial planning, and automated design. In robotics we are interested in the automatic synthesis of robot motions, given high-level specifications of tasks and geometric models of the robot and obstacles. The Mover's problem is to find a continuous, collision-free path for a moving object through an environment containing obstacles. This thesis describes the first known implementation of a complete algorithm (at a given resolution) for the full six degree of freedom Movers' problem. The algorithm transforms the six degree of freedom planning problem into a point navigation problem in a six-dimensional configuration space (called C-Space). The C-Space obstacles, which characterize the physically unachievable configurations, are directly represented by six-dimensional manifolds whose boundaries are five dimensional C-surfaces. Implementing the point navigation operators requires solving fundamental representational and algorithmic questions: we will derive new structural properties of the C-Space constraints and show how to construct and represent C-surfaces and their intersection manifolds. GRA

N85-23433# Joint Publications Research Service, Arlington, Va.
CHINA REPORT: SCIENCE AND TECHNOLOGY
28 Jan. 1985 246 p refs Transl. into ENGLISH from various Chinese articles
(JPRS-CST-85-003) Avail: NTIS HC A11/MF A01

The January 1985 China Report on science and technology contains information pertaining to the following: (1) national development; (2) applied sciences; (3) life sciences; (4) enviornmental quality; and abstracts of the following types of research projects: (a) computer development applications; (b) electronics; (c) engineering; (d) metallurgy; (e) mining; and (f) physics. For individual titles, see N85-23434 through N85-23441.

N85-23434# Joint Publications Research Service, Arlington, Va.
DEVELOPMENT, ACHIEVEMENTS IN CHINA'S CARTOGRAPHY WORK **c43**
In its China Rept.: Sci. and Technol. (JPRS-CST-85-003) 28 Jan. 1985 p 44-53 Transl. into ENGLISH from Cehui Tongbao (Beijing), no. 4, 25 Aug. 1984 p 1-6 (For primary document see N85-23433 13-81)
Avail: NTIS HC A11/MF A01

An overview of cartographic science in post revolutionary China is presented. Among the topics discussed are: (1) training and establishment of training facilities; (2) establishment of a national cartographic bureau; (3) geodetic survey work; (4) benchmark establishment; (5) drafing basic national topographic maps; and (6) map compilation and publishing work. G.L.C.

N85-23435# Joint Publications Research Service, Arlington, Va.
ACCOMPLISHMENTS OF INSTITUTE OF CARTOGRAPHY SUMMARIZED **c43**
Luo Shiming *In its* China Rept.: Sci. and Technol. (JPRS-CST-85-003) 28 Jan. 1985 p 54-60 Transl. into ENGLISH from Cehui Tongbao (Beijing), no. 4, 25 Aug. 1984 p 6-10 (For primary document see N85-23433 13-81)
Avail: NTIS HC A11/MF A01

An overview of China's Cartographic Sciences Research Institute, its various divisions and their assigned functions is presented. The Institute's specialized organizations include: a Geodetic Survey Research Office; an Aerial Photography Survey Research Office; a Drafting Office; a Place Names Research Office; an Instrument Research Laboratory; an Information Research Office; and a Trial Manufacturing Workshop. Following new developments in the technical sphere, the State Remote Sensing Central Information Department was established in 1981, and the Aerial Photography Survey Research Office was changed to the Aerial Photography Survey and Remote Sensing Research Office. Construction of the Satellite Geodetic Survey Experiment Station may begin before the end of this year. G.L.C.

N85-23436# Joint Publications Research Service, Arlington, Va.
PHYSICISTS' ROLE IN NEW TECHNOLOGICAL DEVELOPMENT DISCUSSED
Song Fijun *In its* China Rept.: Sci. and Technol. (JPRS-CST-85-003) 28 Jan. 1985 p 64-69 Transl. into ENGLISH from Wuli (Beijing), no. 8, 1984 p 466-468, 462 (For primary document see N85-23433 13-81)
Avail: NTIS HC A11/MF A01

The position of the physicist in the realm of applied product research and development was reviewed. G.L.C.

N85-23437# Joint Publications Research Service, Arlington, Va.
RAPID ADVANCES IN GEOLOGICAL WORK **c46**
Sun Daguang *In its* China Rept.: Sci. and Technol. (JPRS-CST-85-003) 28 Jan. 1985 p 70-72 Transl. into ENGLISH from Guangming Ribao (Beijing), 22 Aug. 1984 p 2 (For primary document see N85-23433 13-81)
Avail: NTIS HC A11/MF A01

A summary of developments in China's mineral survey and mining program is given. China has now discovered 150 minerals, 135 of them in proven reserve; 20 are in the first rank worldwide. G.L.C.

N85-23438# Joint Publications Research Service, Arlington, Va.
CHARACTERISTICS OF ALUMYTE DEPOSITS DISCUSSED **c46**
Xiao Zengqi, Cao Xianming, and Luo Shengqi *In its* China Rept.: Sci. and Technol. (JPRS-CST-85-003) 28 Jan. 1985 p 74-82 Transl. into ENGLISH from Zhongguo Dizhi (Beijing), no. 7, 1984 p 12-16 (For primary document see N85-23433 13-81)
Avail: NTIS HC A11/MF A01

China has good geological conditions for alumyte mineralization. It is abundant in alumyte resources and occupies an important place in the world. A preliminary investigation into the geological characteristics of alumyte deposits in China was compiled. G.L.C.

N85-23439# Joint Publications Research Service, Arlington, Va.
RESEARCH, DEVELOPMENT OF LASER GLASSES IN CHINA **c36**
Gan Fuxi *In its* China Rept.: Sci. and Technol. (JPRS-CST-85-003) 28 Jan. 1985 p 94-114 refs Transl. into ENGLISH from Zhongguo Jiguang (Shanghai), v. 11, no. 8, 20 Aug. 1984 p 449-459 (For primary document see N85-23433 13-81)
Avail: NTIS HC A11/MF A01

The development and characteristics of neodum doped glass for laser applications is reviewed. Included were (1) improvements in the manufacturing quality; and (4) a basic investigation of laser glasses. G.L.C.

N85-23440# Joint Publications Research Service, Arlington, Va.
RESEARCH PROGRESS ON LASER CRYSTALS IN CHINA **c36**
Zhang Yingxia *In its* China Rept.: Sci. and Technol. (JPRS-CST-85-003) 28 Jan. 1985 p 115-121 Transl. into ENGLISH from Zhongguo Jiguang (Shanghai), v. 11, no. 8, 20 Aug. 1984 p 460-463 (For primary document see N85-23433 13-81)
Avail: NTIS HC A11/MF A01

Current Chinese research on laser crystals is now quite extensive and involves more than 30 research teams with nearly 1,000 technicians and workers actively engaged in the study of more than 20 types of laser cyrstals. Neodymium-doped yttrium aluminum garnet (Nd:YAG) and ruby (Cr:Al2O3) lasers have been manufactured and are widely employed. There are several new and promising crystals now under study which will find applications, and both basic and exploratory research have given rise to new developments. G.L.C.

N85-23441# Joint Publications Research Service, Arlington, Va.
ARMED FORCES SPECIAL SYMPOSIUM ON MEDICINE OF ALTITUDES **c52**
Kuang Yung *In its* China Rept.: Sci. and Technol. (JPRS-CST-85-003) 28 Jan. 1985 p 123-130 Transl. into ENGLISH from Jiefangjun Zazhi (Beijing), no. 4, 20 Aug. 1984 p 311-312 (For

primary document see N85-23433 13-81)
Avail: NTIS HC A11/MF A01

Summaries from the symposium on the medicine of altitude and the symposium on monoclonal antibodies are presented.

G.L.C.

N85-23442# Joint Publications Research Service, Arlington, Va.
USSR REPORT: SCIENCE AND TECHNOLOGY POLICY
27 Feb. 1985 102 p refs Transl. into ENGLISH from various Russian articles
(JPRS-UST-85-002) Avail: NTIS HC A06

Scientific and technological policies are presented and discussed. Some areas covered are: (1) Economic mechanism of integration of science and production; (2) Scientific and technical progress and factors of intensification of the economy; (3) Contributions of technical community to scientific and technical progress; (4) Coordination of regional management of scientific and technical activity; and (5) dissemination of information on advanced know how. For individual titles, see N85-23443 through N85-23444.

N85-23443# Joint Publications Research Service, Arlington, Va.
ECONOMIC MECHANISM OF INTEGRATION OF SCIENCE, PRODUCTION
Yu. V. Lebedev *In its* USSR Rept.: Sci. and Technol. Policy (JPRS-UST-85-002) 27 Feb. 1985 p 1-13 refs Transl. into ENGLISH from Izv. Akad. Nauk SSSR: Ser. Ekon. (Moscow), no. 5, Sep. - Oct. 1984 p 37-48 (For primary document see N85-23442 13-81)
Avail: NTIS HC A06

The important problem of the acceleration of scientific and technical progress and the improvement of the economic and organizational forms of the integration of science and production is examined. The basic principles of this integration at the level of the economic activity of the industrial enterprise are specified. The possibilities of the use of the standardized method for the implementation of the new forms of the organization of scientific activity and the individualized approach to the evaluation of the results of scientific organizations and industrial enterprises in scientific and technical progress are established. Author

N85-23444# Joint Publications Research Service, Arlington, Va.
SCIENTIFIC, TECHNICAL PROGRESS AS FACTOR OF INTENSIFICATION OF ECONOMY
V. P. Loginov *In its* USSR Rept.: Sci. and Technol. Policy (JPRS-UST-85-002) 27 Feb. 1985 p 14-26 refs Transl. into ENGLISH from Ekon. i Mat. Metody (Moscow), v. 20, no. 4, Jul. - Aug. 1984 p 581-590 (For primary document see N85-23442 13-81)
Avail: NTIS HC A06

The second half of the 20th century was marked by repeated revolutions in the broad spheres of science and technology. Fundamentally new discoveries in physics, chemistry, biology, medicine, space research and other fields of knowledge are transforming the nature of physical production and are leading to substantial changes in social life, as well as in the daily life of people. Scientific and technical progress is becoming a more and more powerful factor of the economic and social development of all countries, while the competition of the two socioeconomic systems--the world of socialism and the world of capitalism--depends to a greater and greater extent on the implementation of the achievements of science and technology. The interconnection of scientific and technical progress and the intensive type of expanded reproduction, as well as questions of scientific, technical and structural policy are discussed. Author

N85-22633# Joint Publications Research Service, Arlington, Va.
CURRENT PLANS FOR DEVELOPMENT OF CHEMICAL INDUSTRY
V. Listov *In its* USSR Rept.: Chem. (JPRS-UCH-85-001) 17 Jan. 1985 p 13-26 ref Transl. into ENGLISH from Planovoye Khoz. (Moscow), no. 9, Sep. 1984 p 15-26 (For primary document see N85-22629 13-23)
Avail: NTIS HC A06

82 DOCUMENTATION AND INFORMATION SCIENCE

Includes information storage and retrieval technology; micrography; and library science.

For computer documentation see *61 Computer Programming and Software.*

N85-23445* National Aeronautics and Space Administration, Washington, D. C.
NASA PATENT ABSTRACTS BIBLIOGRAPHY. A CONTINUING BIBLIOGRAPHY. SECTION 2: INDEXES
Jan. 1985 469 p
(NASA-SP-7039(26); NAS 1.21:7039(26)) Avail: NTIS HC A20/MF A01 CSCL 05B

A subject index is provided for over 4300 patents and patent applications for the period May 1969 through December 1984. Additional indexes list personal authors, corporate authors, contract numbers, NASA case numbers, U.S. patent class numbers, U.S. patent numbers, and NASA accession numbers. Author

N85-23446 Colorado Univ., Boulder.
PERSONAL DECISION MAKING: THE INFLUENCE OF PERCEIVED LOCUS OF CONTROL AND DEGREEE OF RATIONALITY ON INFORMATION SEEKING STRATEGIES Ph.D. Thesis
Nancy S. F. Jackson 1984 184 p
Avail: Univ. Microfilms Order No. DA8428659

Information seeking strategies that are used by persons making decisions were identified. A decision is defined as a choice among alternatives. Using Janis' conflict model and the concept of reactance, five information seeking strategies are described. The strategies derive from the individual's perceived locus of control, degree of rationally and are titled vigilance avoidance, reactance, hypervigilance, and unconflicted. Strategies are related to information seeking in such a way that subjective uncertainty ratio will vary in predictable patterns as a function of the information seeking strategy used. The results show that only the strategy avoidance is significantly different from the others in terms of its overall variability. Three major areas of value found in clarifying decision making issues are: the expansion of the decision making model for future research; exploration of the interaction of task and individual difference variables in decision making; and the use of subjective predictability of information use as a criteria for decision evaluation. Author

N85-23447*# Jet Propulsion Lab., California Inst. of Tech., Pasadena.
ACTIVITIES OF THE JET PROPULSION LABORATORY, 1 JANUARY - 31 DECEMBER 1983 Annual Report, 1 Jan. - 31 Dec. 1983
[1984] 66 p refs Original contains color illustrations
(NASA-CR-175555; NAS 1.26:175555) Avail: NTIS HC A04/MF A01 CSCL 05B

There are many facets to the Jet Propulsion Laboratory, for JPL is an organization of multiple responsibilities and broad scope, of diverse talents and great enterprise. The Laboratory's philosophy, mission, and goals have been shaped by its ties to the California Institute of Technology (JPL's parent organization) and the National Aeronautics and Space Administration (JPL's principal sponsor). JPL's activities for NASA in planetary, Earth, and space sciences currently account for almost 75 percent of the Laboratory's overall effort. JPL Research activities in the following areas are discussed: (1) deep space exploration; (2) telecommunications systems; (3) Earth observations; (4) advanced technology; (5) defense programs; and (6) energy and technology applications. B.W.

N85-23448# Interactive Systems Corp., Littleton, Colo.
HEXAGONAL DATA BASE STUDY Final Report, Oct. 1983 - Oct. 1984 on Phase 2
L. Gibson, W. Gomer, and D. Lucas Fort Belvoir, Va. Army Engineer Topographic Labs. Oct. 1984 74 p Original contains color illustrations
(Contract DAAK70-82-C-0133)
(AD-A150176; ETL-0360) Avail: NTIS HC A04/MF A01 CSCL 09/2

This is a final report for a study in the application of hexagonal data structures to handling geographic information. This report presents the results of an experimental software implementation utilizing hexagonal data structures applied to test data base. This report covers work performed during the second year of a study of data representation and processing. It is based on a coordinate system called GBT which addresses hexagonal regions in a plane. During the first year of the study, ISC software which uses the hexagonal scheme was tested on polygonal map data such as land use areas and flood plains. Results of the project are described in Hexagonal Data Base Study (September 1983). Portions of the theoretical discussion given in that report are included Chapter 2 of the current report. In the second year's work on this project we have incorporated raster imagery into the system. Line and point data were integrated with the polygon information. An extended query capability was added to handle these new data forms. The resulting enhanced system was tested on a small data set supplied by the U.S. Army Engineer Topographic Laboratories (ETL). GRA

N85-23449# Naval Postgraduate School, Monterey, Calif. Dept. of Computer Science.
GENERAL DESIGN CONSIDERATIONS OF AN AIR FORCE INFORMATION SYSTEM M.S. Thesis
Engin Aytacer, Jr. Jun. 1984 118 p
(AD-A150611) Avail: NTIS HC A06/MF A01 CSCL 09/4

General design issues of an Air Force information system are considered in this thesis. The current structure of the system is presented with its requirements. Information storing, retrieving and updating procedures are described. An example of a logical database is designed. Networking issues are expressed in an undetailed way. Finally, a set of high-end minicomputers are evaluated to present the approximate cost of this system. And a general methodology for minicomputer selection process is presented. GRA

N85-23450# Massachusetts Inst. of Tech., Cambridge. Center for Information Systems Research.
THE HIERARCHICAL DATABASE DECOMPOSITION APPROACH TO DATABASE CONCURRENCY CONTROL Ph.D. Thesis
Meichun Hsu Dec. 1984 290 p
(Contract N00039-83-C-0463)
(AD-A150612; CISR-TR-16; M010-8312-16) Avail: NTIS HC A13/MF A01 CSCL 09/2

A generally accepted criterion for correctness of database concurrency control is the criterion of serializability of transactions. The classical approaches to enforcing serializability are the two-phase locking and the timestamping methods. Either approach requires that a read operation from a transaction be registered in the form of a read timestamp or a read lock so that a write operation from a concurrent transaction will not interfere improperly with the read operation. However, setting a lock or leaving a timestamp with a data element is an expensive operation. The purpose of the current research is to seek ways to reduce the overhead of synchronization of certain types of read accesses, and at the same time achieving the goal of serializability. GRA

N85-23451# Los Alamos Scientific Lab., N. Mex.
INTEL IDIS EVALUATION
Jesse M. Cheadle and Marcus E. Glassmire 1984 7 p Presented at the Assoc. of System 2000 Users for Technol. Exchange (ASTUTE) Conf., Hilton Head, S.C., 11-15 Nov. 1984
(Contract W-7405-eng-36)
(DE85-003748; LA-UR-84-3537; CONF-8411114-2) Avail: NTIS HC A02/MF A01

An evaluation of a computer system called the Intel Database Information System (IDIS), which was recently performed at the Los Alamos National Laboratory is discussed. The evaluation consisted of the development of a possible application for the Compensation and Benefits Section of the Personnel Administration Division at Los Alamos. DOE

83 ECONOMICS AND COST ANALYSIS

Includes cost effectiveness studies.

No abstracts in this category.

84 LAW AND POLITICAL SCIENCE

Includes space law; international law; international cooperation; and patent policy.

N85-23452# Committee on Science and Technology (U. S. House).
AUTHORIZING APPROPRIATIONS TO THE NATIONAL AERONAUTICS AND SPACE ADMINISTRATION FOR FISCAL YEAR 1986
Washington GPO 1985 223 p Presented to accompany H.R. 1714 to the Comm. of the Whole House on the State of the Union, 99th Congr., 1st Sess., 28 Mar. 1985
(H-Rept-99-32; GPO-44-360) Avail: US Capitol, House Document Room

The authorization of appropriations for aerospace research and development were discussed. The appropriation concerned: space flights, research and program management, control and data communications, and construction of facilities. E.A.K.

N85-23453# Naval Postgraduate School, Monterey, Calif.
COPYRIGHT LAW, COMPUTER SOFTWARE, AND GOVERNMENT ACQUISITION M.S. Thesis
P. R. Dauphinias Sep. 1984 81 p
(AD-A150347) Avail: NTIS HC A05/MF A01 CSCL 09/2

This thesis examines copyright law as it relates to computer software and how this law affects the Government acquisition of computer software. Following a differentation of copyright law, patent law, and trade secrets, a brief history of the evolution of copyright law is presented. Current Government software acquisition practices are examined with respect to copyright statutes. The 1984 Betamax case is examined and related to software issues which concern the Government as an entity. Finally, considerations which influence software procurement and copyrights are examined. GRA

85 URBAN TECHNOLOGY AND TRANSPORTATION

Includes applications of space technology to urban problems; technology transfer; technology assessment; and surface and mass transportation.

For related information see *03 Air Transportation and Safety, 16 Space Transportation,* and *44 Energy Production and Conversion.*

N85-23454*# Technology and Economics, Inc., Cambridge, Mass.
TECHNOLOGY AND ECONOMICS, INC. TECHNOLOGY APPLICATION TEAM Annual Report
Timothy Ballard and David J. MacFadyen Feb. 1981 43 p
(Contract NASw-3336)
(NASA-CR-175630; NAS 1.26:175630) Avail: NTIS

HC A03/MF A01 CSCL 13B

Technology + Economics, Inc. (T+E), under contract to the NASA Headquarters Technology Transfer Division, operates a Technology Applications Team (TATeam) to assist in the transfer of NASA-developed aerospace technology. T+E's specific areas of interest are selected urban needs at the local, county, and state levels. T+E contacts users and user agencies at the local, state, and county levels to assist in identifying significant urban needs amenable to potential applications of aerospace technology. Once viable urban needs have been identified in this manner, or through independent research, T+E searches the NASA technology database for technology and/or expertise applicable to the problem. Activities currently under way concerning potential aerospace applications are discussed. B.W.

N85-23455# Air Force Logistics Command, Wright-Patterson AFB, Ohio.

ELECTRIC AND HYBRID VEHICLE DEMONSTRATION PROJECT Final Report

1984 8 p

(Contract DE-AI08-80CS-50208)

(DE85-003939; DOE/CS-50208/1) Avail: NTIS HC A02/MF A01

Some 15 electric vehicles at three AFLC bases were used to demonstrate their functional capabilities within the federal fleet by performing functions usually accomplished by internal combustion vehicles (ICV). The nine pickups and six vans were conventional internal combustion powered vehicles with the 90 horsepower engine and gasoline tank replaced by a 30 horsepower electric motor and lead acid propulsion batteries. Charging stations were constructed on the using installations to allow the vehicles to charge overnight. Deep cycling was required to develop memory of batteries. The batteries required a regular maintenance program including equalizing charges, terminal inspection and cleaning to avoid corrosion damage to battery terminals, connectors and wires. Weak batteries in the pack formed hazardous hydrogen gas during charge causing two explosions at one of the using bases. This ultimately resulted in termination of the program. Other problems encountered during the program are listed. DOE

N85-23456# Idaho National Engineering Lab., Idaho Falls.

ELECTRIC VEHICLE TEST PROGRAM: INEL TRANSITION QUALIFICATION TEST PLAN

H. W. Heiselmann and H. E. Knauts Nov. 1984 49 p

(Contract DE-AC07-76ID-01570)

(DE85-005171; EGG-SE-6746) Avail: NTIS HC A03/MF A01

This test plan sets forth the requirements necessary to qualify the test facility and equipment installation at the Idaho National Engineering Laboratory in order to continue DOE programmatic testing of electric vehicles. Briefly, dynamometer tests will be performed on the Electric Test Vehicle 1-2 (ETV1-2) at constant speeds of 35, 45, and 55 mph and for the schedule D driving cycle. DOE

88 SPACE SCIENCES (GENERAL)

N85-23457*# Cornell Univ., Ithaca, N.Y.

PLANETARY GEOLOGY IN THE 1980S

Joseph Veverka 1984 199 p refs

(Grant NsG-7156)

(NASA-SP-467; NAS 1.21:467) Avail: NTIS HC A09/MF A01; also available from NASA Information Center, Washington, D.C. 20546 $19.00 CSCL 03C

The geologic aspects of solar system studies are defined and the goals of planetary geology are discussed. Planetary geology is the study of the origin, evolution, and distribution of matter condensed in the form of planets, satellites, asteroids, and comets. It is a multidisciplinary effort involving investigators with backgrounds in geology, chemistry, physics, astronomy, geodesy, cartography, and other disciplines concerned with the solid planets. The report is primarily restricted to the kinds of experiments and observations made through unmanned missions. B.W.

89 ASTRONOMY

Includes radio and gamma-ray astronomy; celestial mechanics; and astrometry.

N85-23458 California Univ., Los Angeles.

A SURVEY FOR GALACTIC PLANE ULTRAVIOLET-EXCESS OBJECTS: SPACE DENSITIES FOR WHITE DWARFS, SUB-DWARFS, AND CATACLYSMIC VARIABLES Ph.D. Thesis

Ronald Alan Downes 1984 163 p

Avail: Univ. Microfilms Order No. DA8428506

A survey for galactic plane ultraviolet-excess (UV-excess) objects covering about 1000 square degrees of sky was undertaken. Photographic plates were obtained, with both UV and blue filters, to select the UV-excess candidates, which were then observed spectroscopically to determine their classification. Most of the objects selected wre nearby early-type stars with low interstellar reddening; however, a collection of hot white dwarfs, subdwarf O(sdO) stars, subdwarf B(sdB) stars, and cataclysmic variables was also found. Photoelectric photometry was obtained for these stars, and a statistical analysis was performed to determine the space densities and scale heights for the four classes of objects. Dissert. Abstr.

N85-23459 Brigham Young Univ., Provo, Utah.

THE COLOR EXCESSES OF CLASSICAL CEPHEIDS AND THE STRUCTURE OF OUR GALAXY Ph.D. Thesis

Chulhee Kim 1984 114 p

Avail: Univ. Microfilms Order No. DA8427784

Color excesses of 446 classical cepheids were taken from literature and transformed to a single homogeneous system. On the basis of these color excess data, fundamental data for 401 classical cepheids were compiled and a discussion of Galactic structure based on their space distribution is given. Major spiral arms were traced from the distribution of long-period cepheids on the projected Galactic plane and the position of these spiral features were compared with those from other optical tracers such as HII regions and OB star groups. The z-coordinate distribution of cepheids confirms the finding that the cepheid layer is inclined toward a formal Galactic plane and the Sun is located above the cepheid plane. It was found that the z-distribution fits better to the parabolic form than a barometric form and a scale height of 54 pc was found. The correlation between the distribution of cepheids and the dust complexes within 2 kpc from the Sun is investigated. Dissert. Abstr.

N85-23460*# Hawaii Univ., Honolulu. Inst. for Astronomy.

RESEARCH IN PLANETARY STUDIES AND OPERATION OF MAUNA KEA OBSERVATORY Semiannual Progress Report, Jan. - Dec. 1984

Donald N. B. Hall Apr. 1985 61 p refs

(Grant NGL-12-001-057)

(NASA-CR-175618; NAS 1.26:175618; SAR-28; SAR-29) Avail: NTIS HC A04/MF A01 CSCL 03A

Astronomical observations of the major planets, satellites, asteroids and comets are presented for January to December of 1984. Other related research activities are presented. G.L.C.

N85-23461*# Smithsonian Astrophysical Observatory, Cambridge, Mass.

A NORMAL INCIDENCE, HIGH RESOLUTION X-RAY TELESCOPE FOR SOLAR CORONAL OBSERVATIONS Semiannual Progress Report, 1 Nov. 1984 - 30 Apr. 1985

Leon Golub Apr. 1985 56 p

(Grant NAGw-397)

(NASA-CR-175622; NAS 1.26:175622; SAPR-5) Avail: NTIS HC A04/MF A01 CSCL 03A

The following major activities were advanced or completed: complete design of the entire telescope assembly and fabrication

of all front-end components; specification of all rocket skin sections including bulkheads, feedthroughs and access door; fabrication, curing, and delivery of the large graphite-epoxy telescope tube; engineering analysis of the primary mirror vibration test was completed and a decision made to redesign the mirror attachment to a kinematic three-point mount; detail design of the camera control, payload and housekeeping electronics; and multilayer mirror flats with 2d spacings of 50 A and 60 A. B.G.

N85-23462*# Arizona Univ., Tucson.
INNOVATIVE RESEARCH IN THE DESIGN AND OPERATION OF LARGE TELESCOPES FOR SPACE: ASPECTS OF GIANT TELESCOPES IN SPACE Semiannual Status Reports, 14 Nov. 1983 - 14 Nov. 1984
J. R. P. Angel 9 Apr. 1985 15 p
(Grant NAGw-221)
(NASA-CR-175626; NAS 1.26:175626) Avail: NTIS HC A02/MF A01 CSCL 03A

The capability and understanding of how to finish the reflector surfaces needed for large space telescopes is discussed. The technology for making very light glass substrates for mirrors is described. Other areas of development are in wide field imaging design for very fast primaries, in data analysis and retrieval methods for astronomical images, and in methods for making large area closely packed mosaics of solid state array detectors. Author

N85-23463*# National Aeronautics and Space Administration. Marshall Space Flight Center, Huntsville, Ala.
BIG MAC: A BOLOMETER ARRAY FOR MID-INFRARED ASTRONOMY, CENTER DIRECTOR'S DISCRETIONARY FUND Final Report
C. M. Telesco, R. Decher, and C. Baugher Feb. 1985 29 p refs
(NASA-TM-86502; NAS 1.15:86502) Avail: NTIS HC A03/MF A01 CSCL 03A

The infrared array referred to as Big Mac (for Marshall Array Camera), was designed for ground based astronomical observations in the wavelength range 5 to 35 microns. It contains 20 discrete gallium-doped germanium bolometer detectors at a temperature of 1.4K. Each bolometer is irradiated by a square field mirror constituting a single pixel of the array. The mirrors are arranged contiguously in four columns and five rows, thus defining the array configuration. Big Mac utilized cold reimaging optics and an up looking dewar. The total Big Mac system also contains a telescope interface tube for mounting the dewar and a computer for data acquisition and processing. Initial astronomical observations at a major infrared observatory indicate that Big Mac performance is excellent, having achieved the design specifications and making this instrument an outstanding tool for astrophysics.
Author

N85-23464# Cambridge Univ. (England). Inst. of Astronomy.
UNIVERSITY OF CAMBRIDGE INSTITUTE OF ASTRONOMY REPORT OF ACTIVITIES Annual Report, 1983 - 1984
[1984] 44 p refs
Avail: NTIS HC A03/MF A01

Activities are reported in the study of: galaxy formation, clustering, and cosmology; quasars; gravitational lenses; active galaxies; stars and star clusters; relativity; black holes; plasma physics; and astronomical telescopes and other instruments.
A.R.H.

N85-22978# Joint Publications Research Service, Arlington, Va.
ABSOLUTE MEASUREMENTS OF RADIATION INTENSITY FROM CASSIOEIE-A, CYGNUS-A AND CRAB NEBULA IN 60-100 cm BAND Abstract Only
M. Y. Miller *In its* USSR Rept.: Electron. and Elect. Eng. (JPRS-UEE-85-001) 9 Jan. 1985 p 1-2 Transl. into ENGLISH from Izv. Vysshikh Uch. Zaved.: Radiofiz. (USSR), v. 27, no. 7, Jul. 1984 p 934-938 (For primary document see N85-22976 13-33)
Avail: NTIS HC A05/MF A01

N85-22408# Joint Publications Research Service, Arlington, Va.
ALL-UNION CONFERENCE OF RADIO ASTRONOMERS
V. M. Kontorovich *In its* USSR Rept.: Space (JPRS-USP-85-001) 4 Feb. 1985 p 28-31 Transl. into ENGLISH from Zemlya i Vselennaya (USSR), no. 3, May-Jun. 1984 p 61-64 (For primary document see N85-22403 13-12)
Avail: NTIS HC A07

N85-22409# Joint Publications Research Service, Arlington, Va.
MODERN PROBLEMS IN POLARIMETRY OF SOLID SURFACES OF COSMIC BODIES Abstract Only
Y. G. Shkuratov, L. A. Arkimov, and V. P. Tishkovets *In its* USSR Rept.: Space (JPRS-USP-85-001) 4 Feb. 1985 p 32 Transl. into ENGLISH from Astronomicheskiy Vestnik (USSR), v. 18, no. 3, Jul.-Sep. 1984 p 163-178 (For primary document see N85-22403 13-12)
Avail: NTIS HC A07

N85-22432# Joint Publications Research Service, Arlington, Va.
DETERMINATION OF ANGULAR RESOLUTION OF CODED APERTURE GAMMA-RAY TELESCOPE Abstract Only
Y. D. Kotov, S. A. Lazarev, B. I. Luchkov, Y. V. Smirnov, and V. N. Yurov *In its* USSR Rept.: Space (JPRS-USP-85-001) 4 Feb. 1985 p 49 Transl. into ENGLISH from Kosmicheskiye Issled. (USSR), v. 22, no. 1, Jan.-Feb. 1984 p 141-143 (For primary document see N85-22403 13-12)
Avail: NTIS HC A07

90 ASTROPHYSICS

Includes cosmology; and interstellar and interplanetary gases and dust.

N85-23465 Florida Univ., Gainesville.
GAS DYNAMICS OF THE BARRED SPIRAL GALAXY NGC 3359 Ph.D. Thesis
John Roger Ball 1984 299 p
Avail: Univ. Microfilms Order No. DA8429182

The dynamics of the neutral hydrogen gas in the bright northern barred spiral galaxy NGC 3359 were studied. Observations of the 21 cm line at the Very Large Array were reduced to give single-channel maps with spatial resolution of 18', and a velocity resolution of 25 km/s. The acquisition, calibration, and reduction of the data are discussed in some detail. Maps of the integrated column density and mean velocity of the atomic hydrogen, derived from the channel maps, provide the principal data for an investigation of the dynamics associated with the spiral structure of the galaxy. The observed velocity field of NGC 3359 shows large kinematical deviations from simple rotation. The locations of the disturbances are closely correlated with the optical and 21 cm spiral structure, and indicate that significant spiral streaming motions are present in the arms. Numerical modeling of the galaxy, using the well-known beam scheme hydrodynamical code, to attempt to reproduce the observed kinematics is discussed.
Dissert. Abstr.

N85-23466 California Univ., Berkeley.
STUDIES OF GALACTIC HI IN 21-CENTIMETER ABSORPTION Ph.D. Thesis
Shrinivas Ramchandra Kulkarni 1984 232 p
Avail: Univ. Microfilms Order No. DA8427022

Various galactic phenomena were studied using the 21-cm HI line in absorption as a probe. An observing technique developed and used at the Very Large Array and a spectral line interferometer built at Arecibo is described. With these instruments a low-latitude HI-absorption survey was conducted which obtained very sensitive absorption spectra towards 3C123 and 3C147 and the reliability of single dish absorption-spectra towards weak sources at high latitudes was evaluated. Preliminary analysis of the low latitude survey indicates that the mid-plane density of HI in the inner galaxy is 0.5/cu.cm. after accounting for optical depth effects. A model independent proof that the fraction of Not-Strongly Absorbing HI increases with the absolute value of Z is found. For the first time, the spin temperature of intercloud HI is between 1000 K and

2000 K. Using the existing absorption data, a new model was proposed for the HI vertical structure which accounts for the existence of high-z HI and the thermal electron layer in a self-consistent fashion. Dissert. Abstr.

N85-23467 Dartmouth Coll., Hanover, N.H.
A MODEL FOR ECLIPSING CATACLYSMIC VARIABLES Ph.D. Thesis
Jon Allan Hagnuson 1984 133 p
Avail: Univ. Microfilms Order No. DA8426776

A new and improved model was developed to derive the elements of eclipsing cataclysmic variables (CVs). Roche geometry was used to simulate the eclipse of a flat accretion disk which was divided into multiple equipotential rings of black body spectral contribution. The temperature of each ring was adjusted, using a chi square fitting routine, until the data and the simulations achieved a best fit value. Only the rising side of the eclipse light curve was used, in order to avoid asymmetries in the disk produced by the shock bulge and hot spot. A variation of this model was used to establish the radial dependence of the emission line source intensity. The line profile was fit through eclipse by simulating emission sources around multiple equipotential rings. The Balmer line source intensity is found to decrease by a power of -2.09 with radius in LX Ser and by -2.65 in DQ Her. The He I 5876 A line vanishes near the white dwarf in both stars indicating an ionization cavity. Dissert. Abstr.

N85-23468 Harvard Univ., Cambridge, Mass.
THEORETICAL AND OBSERVATIONAL STUDIES OF STELLAR ACTIVITY Ph.D. Thesis
Jurgen Harry Max Michael Schmitt 1984 211 p
Avail: Univ. Microfilms Order No. DA8419457

Doubly-diffusive MHD instabilities are studied as a means of breaking up a diffuse magnetic field at the bottom of the solar convection zone. The analysis is linear and local, and assumes short meridional wavelengths; the effects of rotation and diffusion of vorticity, magnetic fields and heat are included. Results show that the instability depends sensitivity on the temperature stratification, but rather insensitivity on the assumed magnetic field configuration; instability time scales considerably less than the solar cycle period can be easily obtained. A new model for the region of the convective overshoot underneath the solar convection zone is developed. It assumes highly asymmetric up and down-flows, and utilizes semiempirical models, developed for the description of plume motions in the Earth's atmosphere. Using these plume equations together with the stellar structure equations, a set of differential equations suitable for the study of convective overshoot phenomena in astrophysical contexts are derived. Dissert. Abstr.

N85-23469 Indiana Univ., Bloomington.
DYNAMICS OF GAS DISKS IN TRIAXIAL GALAXIES Ph.D. Thesis
Thomas Yoshiahu Steiman-Cameron 1984 285 p
Avail: Univ. Microfilms Order No. DA8426685

Increasing evidence has accumulated since the mid 1970's arguing that many, if not all, undisturbed galaxies may have triaxial mass distributions. The steady state configurations (preferred planes) of gas disks in triaxial galaxies with static and rotating surface figures is determined. In addition, the evolution of a gas disk as it settles into the steady state is followed for both axisymmetric and triaxial galaxies. Observational tests are provided for triaxial galactic geometry and give more accurate measures of settling times than those previously published. The preferred planes for gas disks in static and tumbling triaxial galaxies are determined using an analytic method derived from celestial mechanics. The evolution of gas disks which are not in the steady state is followed using numerical methods. Dissert. Abstr.

N85-23470 Utah State Univ., Logan.
EXCITATION OF LOW-FREQUENCY PLASMA WAVES BY A CONDUCTING, TETHERED SATELLITE Ph.D. Thesis
Craig E. Rasmussen 1984 169 p
Avail: Univ. Microfilms Order No. DA8428046

Because Alfven waves play an important role in natural space phenomena, there has developed in recent years an interest in exciting these low frequency waves in situ in the magnetosphere. Previous investigators have treated the excitation of Alfven waves from a magnetohydrodynamic viewpoint which reduces the problem to solving a one-dimensional wave equation. This approach is applicable only for very low frequencies. Two questions that previous research has left unanswered are at what point the magnetohydrodynamic theory breaks down and how the amplitude of the waves changes as the frequency is increased above the magnetohydrodynamic threshold. Answers are sought to these questions by solving the nonhomogenous wave equation in a cold uniform plasma-nonhomogenous in the sense that a known current source is included in the formulation. The method of solution employs a phase integral method to solve the inverse-Fourier transform of the wave equation which leads to a solution asymptotically valid in the far field of the source. Dissert. Abstr.

N85-23471*# Smithsonian Astrophysical Observatory, Cambridge, Mass.
VIKING RADIO SCIENCE DATA ANALYSIS AND SYNTHESIS Final Report, 30 Dec. 1982 - 31 Mar. 1985
Irwin I. Shapiro Apr. 1985 15 p refs
(Grant NAGw-411)
(NASA-CR-175631; NAS 1.26:175631) Avail: NTIS HC A02/MF A01 CSCL 03B

Viking radio data analysis and synthesis was used for the following: (1) Solar System Model and Data Set; (2) Rotation of Mars; and (3) Solar System Constants and Tests of Relativity. G.L.C.

N85-23472# California Univ., Berkeley. Lawrence Berkeley Lab. Nuclear Science Div.
COOLING OF NEUTRON STARS WITH HYPERONS
O. V. Maxwell (Florida International Univ., Miami) Nov. 1984 9 p refs
(Contract DE-AC03-76SF-00098)
(DE85-004641; LBL-18703) Avail: NTIS HC A02/MF A01

Measurements associated with the pulsed emission from pulsars and X-ray binaries are sensitive to details of emission and accretion mechanisms and consequently, depend more upon the surface properties of neutron stars than their interior properties. Even where a dependence upon interior conditions can be established, this dependence is often masked by other considerations and typically involves just the overall M vs. R relation, which is not particularly sensitive to the detailed composition of the star. The possibility of detecting unpulsed blackbody X-rays from neutron star surfaces provides a more direct and fairly sensitive probe of interior conditions. Detecting such radiation allows a surface temperature to be established for the star (assuming a particular value for the radius) which, through solutions of the general relativistic heat transport equations in the crust, provides an estimate of the interior temperature. Because young neutron stars cool primarily by means of neutrino emission from the interior, the latter quantity is rather sensitive to the interior equation of state. DOE

N85-22416# Joint Publications Research Service, Arlington, Va.
LAGRANGIAN SOLUTIONS IN PHOTOGRAVITATIONAL RESTRICTED CIRCULAR THREE-BODY PROBLEM Abstract Only
L. G. Lukyanov *In its* USSR Rept.: Space (JPRS-USP-85-001) 4 Feb. 1985 p 38 Transl. into ENGLISH from Astronomicheskiy Zh. (USSR), v. 61, no. 3, May-Jun. 1984 p 564-570 (For primary document see N85-22403 13-12)
Avail: NTIS HC A07

N85-22418# Joint Publications Research Service, Arlington, Va.
COMPUTATION OF ELLIPTICAL FUNCTIONS IN PROBLEMS OF CELESTIAL MECHANICS Abstract Only
I. A. Gerasimov *In its* USSR Rept.: Space (JPRS-USP-85-001) 4 Feb. 1985 p 39-40 Transl. into ENGLISH from Astronomicheskiy Zh. (USSR), v. 61, no. 3, May-Jun. 1984 p 609-610 (For primary

document see N85-22403 13-12)
Avail: NTIS HC A07

N85-22425# Joint Publications Research Service, Arlington, Va.
HELIUM ATOMS IN INTERSTELLAR AND INTERPLANETARY SPACE. II: DETERMINATION OF DIRECTION OF INTERSTELLAR GAS MOTION RELATIVE TO SUN Abstract Only
V. G. Kurt, Y. N. Mironova, Z. L. Berto, and F. Dalodye *In its* USSR Rept.: Space (JPRS-USP-85-001) 4 Feb. 1985 p 45 Transl. into ENGLISH from Kosmicheskiye Issled. (USSR), v. 22, no. 1, Jan.-Feb. 1984 p 97-102 (For primary document see N85-22403 13-12)
Avail: NTIS HC A07

N85-22434# Joint Publications Research Service, Arlington, Va.
INTERPLANETARY SHOCK WAVES DURING APRIL AND MAY OF 1981 Abstract Only
G. N. Zastenker and N. L. Borodkova *In its* USSR Rept.: Space (JPRS-USP-85-001) 4 Feb. 1985 p 58-59 Transl. into ENGLISH from Kosmicheskiye Issled. (USSR), v. 22, no. 1, Jan.-Feb. 1984 p 87-96 Original language document announced as A84-26983 (For primary document see N85-22403 13-12)
Avail: NTIS HC A07

91 LUNAR AND PLANETARY EXPLORATION

Includes planetology; and manned and unmanned flights. For spacecraft design see *18 Spacecraft Design Testing, and Performance*. For space stations see *15 Launch Vehicles and Space Vehicles*.

N85-23473 Colorado Univ., Boulder.
ANALYSIS AND INTERPRETATION OF OBSERVATIONS OF AIRGLOW AT 297 NM IN THE VENUS THERMOSPHERE Ph.D. Thesis
Malcolm Aaron LeCompte 1984 241 p
Avail: Univ. Microfilms Order No. DA8428664

Limb profiles taken by the Pioneer Venus orbiter ultraviolet spectrometer at 297 nm were analyzed. The emission, associated with the O(1S) yields O(3P) transition of atomic oxygen, is shown to be due primarily to photodissociative excitation of CO2 below 175 km. Dissociative recombination of O2 is an important secondary source. The slant intensity profile near 115 km exhibits structure because of the strong temperature dependence of O(1S) quenching by CO2. The structure is due to the presence of gravity waves in this region. A temperature profile deduced from the data is consistent with reported measurements. Slant intensities observed above 175 km were brighter than pre-flight expectations. Photoelectron impact excitation of carbon, C(3P) yields C(5S) gives rise to emissions which appear in the instrumental bandpass. Other sources are photoelectron impact on O and CO2. Dissert. Abstr.

N85-23474*# National Aeronautics and Space Administration, Washington, D. C.
REPORTS OF THE PLANETARY GEOLOGY AND GEOPHYSICS PROGRAM, 1984
Henry E. Holt, comp. and T. R. Watters, comp. Apr. 1985 615 p refs
(NASA-TM-87563; NAS 1.15:87563) Avail: NTIS HC A99/MF A01 CSCL 03B

Topics include outer planets and satellites; asteroids and comets; Venus; lunar origin and solar dynamics; cratering process; planetary interiors, petrology, and geochemistry; volcanic processes; aeolian processes and landforms; fluvial processes; geomorphology; periglacial and permafrost processes; remote sensing and regolith studies; structure, tectonics, and stratigraphy; geological mapping, cartography, and geodesy; and radar applications. For individual titles, see N85-23475 through N85-23672.

N85-23475*# Jet Propulsion Lab., California Inst. of Tech., Pasadena.
HOT SPOTS ON Io: CORRELATION OF INFRARED EMISSION AND VISIBLE REFLECTANCE Abstract Only
A. S. McEwen (Geological Survey, Flagstaff, Ariz.), L. A. Soderblom (Geological Survey, Flagstaff, Ariz.), D. L. Matson, and T. V. Johnson *In* NASA, Washington Repts. of Planetary Geol. and Geophys. Program, 1984 Apr. 1985 p 3-5 refs (For primary document see N85-23474 13-91)
Avail: NTIS HC A99/MF A01 CSCL 03B

The Voyager 1 infrared spectrometer (IRIS) data and two recently compiled data sets (Voyager imaging mosaics and measurements of Io's thermal emission from the NASA Infrared Telescope Facility) are correlated. These data were used to refine the correlation between dark spot optical properties (albedo and color) and thermal emission, to examine this correspondence on a satellite-wide scale, and to identify additional hot spots not included in the IRIS inventory. The results suggest the hot spots are liquid sulfur lava lakes, for the following reasons: (1) the melting point of sulfur is 390 K, and the model hot spot temperatures range from approximately 200 to 450 K; (2) the albedos and color of the dark spots, measured from the global mosaics, are consistent with laboratory measurements for liquid sulfur; (3) high resolution images of the dark features show morphologies suggestive of lava lakes; and (4) this hypothesis provides a simple and direct explanation for why dark spots are hot on Io. B.G.

N85-23476*# Geological Survey, Menlo Park, Calif.
Io: GENERATION OF SILICATE MAGMA BY SHEAR MELTING AT THE BASE OF A BASALTIC LITHOSPHERE Abstract Only
Michael H. Carr *In* NASA, Washington Repts. of Planetary Geol. and Geophys. Program, 1984 Apr. 1985 p 6-8 refs (For primary document see N85-23474 13-91)
Avail: NTIS HC A99/MF A01 CSCL 03B

Tidal theory and observational evidence indicates that about 1 w/sq. m. of energy is released at the surface of Io. In order to place limits on how much tidal energy can be dissipated within a rigid lithosphere, depth-temperature profiles were calculated for different lithosphere thickness assuming that the tidal energy was dissipated uniformly throughout the lithosphere. Thus a thick lithosphere implies that a significant fraction of the tidal energy is dissipated below the depth where solidus temperatures are reached. One possibility is that Io has a crust consisting of a low melting temperature fraction such as basalt, overlying a mantle of a high melting temperature fraction such as peridotite. Thus, if the lithosphere of Io is thicker than 30 km, as appears probable, then high rates of silicate volcanism are implied and a significant fraction of the tidal energy must be dissipated by viscous deformation rather than rigid flexure. B.G.

N85-23477*# Planetary Science Inst., Tucson, Ariz.
STABILITY OF THE GALILEAN SATELLITES IN DEEP ORBITAL RESONANCE Abstract Only
Richard Greenberg *In* NASA, Washington Repts. of Planetary Geol. and Geophys. Program, 1984 Apr. 1985 p 9-11 refs (For primary document see N85-23474 13-91)
Avail: NTIS HC A99/MF A01 CSCL 03B

The Galilean satellites are locked in the Laplace resonance, which is responsible for forcing their significant orbital eccentricites. The eccentricites in turn result in tidal energy dissipation within the satellites that is responsible for the great thermal activity on Io, including both volcanism observed by Voyager and heat flux measured from Earth. The resonance results from the nearly 2:1 commensurability of orbital periods (or equivalently of mean motions) taken by pairs. These geometrical relations enhance the mutual gravitational effects. Yoder pointed out that tides raised on Io tend to drive the system out of resonance (toward greater nu and correspondingly smaller eccentricities) while tides raised on Jupiter tend to drive the system towards deeper resonance (smaller nu and larger forced eccentricities). The possible behavior of the system in deep resonance is investigated. B.G.

N85-23478*# Arizona State Univ., Tempe. Dept. of Geology.
TOPOGRAPHIC EVIDENCE FOR SHIELD VOLCANISM ON Io Abstract Only
E. F. Albin, J. M. Moore, and R. Greeley *In* NASA, Washington Repts. of Planetary Geol. and Geophys. Program, 1984 Apr. 1985 p 12 refs (For primary document see N85-23474 13-91)
Avail: NTIS HC A99/MF A01 CSCL 03B

A volcano was identified whose morphology, especially topography, supports and extends current evidence that shield volcanoes occur on Io. The feature is centered at 30 deg. S, 246 deg w and lies in a region near the terminator. The presence of shield volcanism on Io was inferred from the planimetric configuration of flaws on such features as Ra Patera. A central edifice roughly 40 to 50 km in diameter is situated on intervent plains material, and a broad, slightly elliptical base 75 to 90 km across. The size of this feature is comparable to large shield volcanoes found on Earth. In addition, the topography is similar to some terrestrial shield volcanoes that exhibit a change in slope; the steepening may be explained by shorter and/or thicker flows emplaced during late stage eruptions. B.G.

N85-23479*# Arizona State Univ., Tempe. Dept. of Geology.
SULFUR VOLCANOES ON Io? Abstract Only
R. Greeley and J. Fink *In* NASA, Washington Repts. of Planetary Geol. and Geophys. Program, 1984 Apr. 1985 p 14 (For primary document see N85-23474 13-91)
Avail: NTIS HC A99/MF A01 CSCL 03B

The unusual rheological properties of molten sulfur, in which viscosity decreases approximately four orders of magnitude as it cools from 170 to 120 C, may result in distinctive volcanic flow morphologies that allow sulfur flows and volcanoes to be identified on Io. Search of high resolution Voyager images reveals three features--Atar Patera, Daedalus Patera, and Kibero Patera--considered to be possible sulfur volcanoes based on their morphology. All three average 250 km in diameter and are distinguished by circular-to-oval central masses surrounded by irregular, widespread flows. Geometric relations indicate that the flows were emplaced after the central zone and appear to have emanated from their margins. The central zones are interpreted to be domes representing the high temperature stage of sulfur formed initially upon eruption. Rapid quenching formed a crust which preserved this phase of the emplacement. Upon cooling to 170 C, the sulfur reached a low viscosity runny stage and was released as the thin, widespread flows. Author

N85-23480*# Jet Propulsion Lab., California Inst. of Tech., Pasadena.
GEOMORPHIC CLASSIFICATION OF LAVA FLOWS ON Io Abstract Only
David C. Pieri *In* NASA, Washington Repts. of Planetary Geol. and Geophys. Program, 1984 Apr. 1985 p 15-19 refs (For primary document see N85-23474 13-91)
Avail: NTIS HC A99/MF A01 CSCL 03B

The lava flows on Io are classified into the following categories: broad, filamental, digitate, intercalated, sheet, and contained. Each classification is described according to flow distribution, geomorphology, color, thickness, and source. B.G.

N85-23481*# Jet Propulsion Lab., California Inst. of Tech., Pasadena.
SULFUR OXYGEN PROCESSES ON Io Abstract Only
Robert M. Nelson and William D. Smythe *In* NASA, Washington Repts. of Planetary Geol. and Geophys. Program, 1984 Apr. 1985 p 20-22 refs (For primary document see N85-23474 13-91)
Avail: NTIS HC A99/MF A01 CSCL 03B

The presence of allotropic sulfur as a possible major constituent of Io's surface and the properties of sulfur in combination with various sulfur-oxygen compounds believed to be present on Io's surface and in its atmosphere are studied by a series of laboratory experiments. B.G.

N85-23482*# Pittsburgh Univ., Pa. Dept. of Geology and Planetary Sciences.
THE VIOLET ABSORBER ON Io: DISULFUR MONOXIDE DERIVATIVES Abstract Only
Bruce Hapke *In* NASA, Washington Repts. of Planetary Geol. and Geophys. Program, 1984 Apr. 1985 p 23 (For primary document see N85-23474 13-91)
Avail: NTIS HC A99/MF A01 CSCL 03B

Following the Voyager flybys of Jupiter it was generally accepted that the surface of Io is covered with SO2 frost and elemental sulfur. However, several difficulties have recently become apparent with this hypothesis. The S2O, which is readily formed under a variety of conditions from the dissociation of SO2, may be an important compound on Io, but at that time no reflectance data on the frost was available. The reflectance spectra of S2O/SO2 mixtures as low temperature frosts and their derivatives, polysulfur oxides, were measured at a variety of temperatures. Specific features possessed by these frosts and identified on Io are bands at 340 nm and 440 nm and a maximum at 800 nm, with decreasing IR reflectance. Thus, this material can account for many of the features in the spectrum of Io. So S2O rather than elemental S is probably the reddening agent on Io, and there is presently no good evidence for S on the surface. Author

N85-23483*# Brown Univ., Providence, R. I. Dept. of Geological Sciences.
PATTERNS OF FRACTURE AND TIDAL STRESSES DUE TO NONSYNCHRONOUS ROTATION: IMPLICATIONS FOR FRACTURING ON EUROPA Abstract Only
E. M. Parmentier and P. Helfenstein *In* NASA, Washington Repts. of Planetary Geol. and Geophys. Program, 1984 Apr. 1985 p 24-26 refs (For primary document see N85-23474 13-91)
Avail: NTIS HC A99/MF A01 CSCL 03B

Global lineaments on Europa were interpreted as fractures in an icy crust. A variety of lineament types were identified, which appear to form a systematic pattern on the surface. For a synchronously rotating body, the patterns of fractures observed could be produced by a combination of stresses due to orbital recession, orbital eccentricity, and internal contraction. However, it was recently suggested that the forced eccentricity of Europa's orbit may result in nonsynchronous rotation. The hypothesis that fractures in a thin icy crust may have formed in response to stresses resulting from nonsynchronous rotation is studied. B.G.

N85-23484*# Washington Univ., St. Louis, Mo. Center for the Space Sciences.
DARK HALO CRATERS AND THE THICKNESS OF GROOVED TERRAIN ON GANYMEDE Abstract Only
Paul M. Schenk and William B. McKinnon *In* NASA, Washington Repts. of Planetary Geol. and Geophys. Program, 1984 Apr. 1985 p 27-29 refs (For primary document see N85-23474 13-91)
(Grant NAGw-432)
Avail: NTIS HC A99/MF A01 CSCL 03B

Dark halo craters on grooved terrain on Ganymede represent potential probes of the subsurface geology. These craters are surrounded by a broad, diffuse low albedo annulus, or halo and have apparently lost the bright rim and ray deposits associated with very young craters. The recognition of dark halo craters, almost all greater than 12 km in diameter, indicates that material darker and redder than grooved terrain material forms a stratigraphy horizon at about 1 km depth the present surface of grooved terrain in Uruk Sulcus. This material is most likely downdropped cratered terrain material, which only larger craters have excavated into. This is most consistent with extensional tectonic models for grooved terrain formation whereby the lithosphere is stretched and blocks of ancient cratered terrain are downdropped along bounding faults, and subsequently resurfaced by a shallow layer of relatively clean icy material. Evidence for the preservation of cratered terrain material at shallow depth beneath grooved terrain material poses great difficulties for alternative grooved and smoothed terrain formation mechanisms. B.G.

N85-23485*# Brown Univ., Providence, R. I. Dept. of Geological Sciences.
FORMATION OF BRIGHT TERRAIN BANDS ON GANYMEDE

BY UNSTABLE LITHOSPHERE EXTENSION Abstract Only
M. T. Zuber and E. M. Parmentier *In* NASA, Washington Repts. of Planetary Geol. and Geophys. Program, 1984 Apr. 1985 p 30-32 refs (For primary document see N85-23474 13-91)
Avail: NTIS HC A99/MF A01 CSCL 03B

The surface of Ganymede, as seen in Voyager images, was greatly modified by tectonic activity. Geologic evidence is consistent with the formation of younger bright terrain by the emplacement of icy material into rift zones formed in the older dark terrain. To better understand the formation of both terrestrial rift zones and bright terrain bands on Ganymede, the mechanics of rift initiation by the growth of necking instabilities in an extending lithosphere are studied. In particular, how an initial, small perturbation in lithosphere thickness at the lithosphere/asthenosphere boundary is amplified by uniform horizontal extension is studied. The lithosphere is treated as a layer of power-law viscous fluid of thickness H overlying a weaker, viscous mantle substrate. In order to assess the relative importance of buoyant upwelling and mechanical instability in rift formation, both density and strength stratification were incorporated into the model. Author

N85-23486*# Hawaii Univ., Hilo. Inst. for Astronomy.
POLAR CAP FORMATION ON GANYMEDE Abstract Only
Carl B. Pilcher and Edward J. Shaya *In* NASA, Washington Repts. of Planetary Geol. and Geophys. Program, 1984 Apr. 1985 p 33-34 (For primary document see N85-23474 13-91)
Avail: NTIS HC A99/MF A01 CSCL 03B

Since thermal migration is not an effective mechanism for water transport in the polar regions at the Galilean satellites, some other process must be responsible for the formation of Ganymede's polar caps. It is proposed that Ganymede's polar caps are the optical manifestation of a process that began with the distribution of an ice sheet over the surface of Ganymede. The combined processes of impact gardening and thermal migration led, in regions at latitudes less than 40 to 45 deg., to the burial of some fraction of this ice, the migration of some to the polar caps margins, and a depletion of free ice in the optical surface. At higher latitudes, no process was effective in removing ice from the optical surface, so the remanants of the sheet are visible today. B.G.

N85-23487*# Cornell Univ., Ithaca, N.Y.
INVESTIGATIONS OF PLANETARY RING PHENOMENA Abstract Only
Joseph A. Burns and Mark R. Showalter *In* NASA, Washington Repts. of Planetary Geol. and Geophys. Program, 1984 Apr. 1985 p 35-37 refs (For primary document see N85-23474 13-91)
Avail: NTIS HC A99/MF A01 CSCL 03B

The structure of Jupiter's rings was studied in an effort to understand the processes that generate the rings. The faint material in the Saturn system was investigated leading to the discovery of a new ring and a way to interpret the wavy features surrounding Encke's division in terms of perturbing moonlets. The interaction of faint rings and magnetospheres helped identify some of the charged particle absorbers seen by Pioneer 11 in the neighborhood of the F ring. Angular momentum drain might account for the slow rotations of intermediate sized asteroids. Much of the Jovian ring structure can be understood in terms of debris loss from satellites, rapid orbital evolution, resonance, and charged dust dynamics. B.G.

N85-23488*# National Aeronautics and Space Administration. Ames Research Center, Moffett Field, Calif.
STUDIES OF PLANETARY RINGS Abstract Only
Jeff Cuzzi *In* NASA, Washington Repts. of Planetary Geol. and Geophys. Program, 1984 Apr. 1985 p 38-43 refs (For primary document see N85-23474 13-91)
Avail: NTIS HC A99/MF A01 CSCL 03B

Dynamic processes in ring structures (spiral density waves; shepherding processes; and erosional transport and global redistribution of ring materials) and planetary ring observations (Jupiter's ring; the nature of the F ring; and the irregular structure of Saturn's B ring) were examined. B.G.

N85-23489*# Cornell Univ., Ithaca, N.Y. Dept. of Astronomy.
DYNAMICAL STUDIES OF SATURN'S RINGS Abstract Only
Philip D. Nicholson and Carolyn C. Porco (Arizona Univ., Tucson) *In* NASA, Washington Repts. of Planetary Geol. and Geophys. Program, 1984 Apr. 1985 p 44-45 refs (For primary document see N85-23474 13-91)
Avail: NTIS HC A99/MF A01 CSCL 03B

The data returned by the Voyager on the Saturnian system has revealed the structure of Saturn's ring system to be dominated by many abrupt transitions in optical depth, narrow well-defined ringlets and gaps, and spiral density and bending waves. A handful of these features were attributed with reasonable certainty to the resonant influence of external satellites, but the vast majority of the structure remains unexplained. The entire C ring was studied with particular emphasis on the search for unrecognized eccentric or inclined features, and the role, if any, played by satellite resonances in controlling C ring structure. B.G.

N85-23490*# Herzberg Inst. of Astrophysics, Ottawa (Ontario).
METEOROIDAL IMPACTS, PLASMA, FINE STRUCTURE OF RINGLETS AND SPOKES ON SATURN'S RING B Abstract Only
A. F. Cook, G. E. Hunt (Imperial Coll., London), and Robert Barrey (Imperial Coll., London) *In* NASA, Washington Repts. of Planetary Geol. and Geophys. Program, 1984 Apr. 1985 p 47 (For primary document see N85-23474 13-91)
Avail: NTIS HC A99/MF A01 CSCL 03B

The role of bombardment of the rings by the dominant size of meteoroids is examined. Also considered are the circumstances which explain the observed presence of spokes on both the illuminated and unilluminated faces of the ring; leading-trailing asymmetry in the behavior of the spokes, and the forward tilt in the spokes. B.G.

N85-23491*# Virginia Univ., Charlottesville.
INTERACTION OF THE MAGNETOSPHERIC IONS WITH THE SURFACES OF THE ICY SATELLITES OF SATURN Abstract Only
R. E. Johnson *In* NASA, Washington Repts. of Planetary Geol. and Geophys. Program, 1984 Apr. 1985 p 48-49 (For primary document see N85-23474 13-91)
Avail: NTIS HC A99/MF A01 CSCL 03B

The extraordinary connection between the compositions of the surfaces of the satellites and ring particles and the composition of the magnetospheric plasmas in which they are embedded is examined. What may be even more exciting is this connection is being developed and understood via a combination of laboratory and satellite measurements. This interaction has stimulated new research on radiation effects in materials which will be technologically useful. Laboratory measurements have begun to characterize the changes induced in ice by ion and electron bombardment. Most attention was paid to measurements of the atoms and molecules ejected via ion bombardment, but work was initiated on changes in the spectral character of the ice. Recent results on CH4 and mixtures of HZO and CH4 indicate that a considerable amount of chemistry is induced in such ices via bombardment. B.G.

N85-23492*# California Inst. of Tech., Pasadena. Div. of Physics, Mathematics, and Astronomy.
PLASMA PRODUCTION BY METEOROID IMPACT Abstract Only
P. K. Haff and A. Eviatar (California Univ., Los Angeles) *In* NASA, Washington Repts. of Planetary Geol. and Geophys. Program, 1984 Apr. 1985 p 50-51 refs (For primary document see N85-23474 13-91)
Avail: NTIS HC A99/MF A01 CSCL 03B

Material ejected from the surfaces of satellites in the outer solar system plays an important role in the magnetospheres of the outer planets, and may dominate the mass loading, as in the vicinity of the Jovian satellite Io. At least four potential ejection mechanisms can be identified - intrinsic geologic activity, thermal sublimation, sputtering, and micrometeoroid impact vaporization.

On all the icy satellites, except possibly Enceladus, sputtering and impact vaporization are the only two potentially important sources of magnetospheric plasma. Sputtering was shown to be an important mass source at both Jupiter and Saturn. The impact mechanism as a plasma source is assessed. B.G.

N85-23493*# National Aeronautics and Space Administration. Ames Research Center, Moffett Field, Calif.
ORIGIN AND EVOLUTION OF THE SATURN SYSTEM Abstract Only
James B. Pollack *In* NASA, Washington Repts. of Planetary Geol. and Geophys. Program, 1984 Apr. 1985 p 53-54 (For primary document see N85-23474 13-91)
Avail: NTIS HC A99/MF A01 CSCL 03B

As was the case for Jupiter, Saturn formed either as a result of a gas instability within the solar nebula or the accretion of a solid core that induced an instability within the surrounding solar nebula. In either case, the protoplanet's history can be divided into three major stages: early, quasi-hydrostatic evolution (stage 1); very rapid contraction (stage 2); and late, quasi-hydrostatic contraction (stage 3). During the early history of the Saturn system, giant impact events may have catastrophically disrupted most of the original satellites of Saturn. Such disruption, followed by reaccretion, may be responsible, in part, for the occurrence of Trojans and coorbital moons in the Saturn system, the apparent presence of a stochastic component in the trend of satellite density with radial distance, and the present population of ring particles. Saturn's excess luminosity and viscous dissipation are also discussed in relation to the satellite formation. B.G.

N85-23494*# California Inst. of Tech., Pasadena.
GIANT PLANETS AND THEIR SATELLITES: COSMOCHEMISTRY, EVOLUTION AND STRUCTURE Abstract Only
D. J. Stevenson *In* NASA, Washington Repts. of Planetary Geol. and Geophys. Program, 1984 Apr. 1985 p 55-57 refs (For primary document see N85-23474 13-91)
Avail: NTIS HC A99/MF A01 CSCL 03B

The following topics were discussed: surface state of Titan; statistical mechanical treatment of clathrate hydrates; planetary dynamos; formation of the giant planets; the e-ring; Uranian satellites and atmosphere; 10 sulfur lakes; episodic tidal evolution; resurfacing of Ganymede; and the origin of the Moon. B.G.

N85-23495*# National Aeronautics and Space Administration. Ames Research Center, Moffett Field, Calif.
THE STRUCTURE AND COMPOSITION OF URANUS AND NEPTUNE Abstract Only
R. T. Reynolds and M. Podolak (Tel-Aviv Univ.) *In* NASA, Washington Repts. of Planetary Geol. and Geophys. Program, 1984 Apr. 1985 p 58-60 refs (For primary document see N85-23474 13-91)
Avail: NTIS HC A99/MF A01 CSCL 03B

Uranus and Neptune form a special class of planetary objects; intermediate in mass and composition between the giant Hydrogen-rich planets, Jupiter and Saturn, and the small, rocky terrestrial planets. Their structure and composition are not only of intrinsic importance, but also should provide information as to the nature of the protoplanetary nebula and the processes of planetary formation. A detailed set of theoretical models of these planets within the framework of two and three shell models was constructed. The ratio of ice to rock (1/r) is varied. The three shell model fits the data on the two planets best. B.G.

N85-23496*# National Aeronautics and Space Administration. Ames Research Center, Moffett Field, Calif.
STUDIES OF ICY BODIES: URANIAN SATELLITES AND COMETARY NUCLEI Abstract Only
S. W. Squyres and R. T. Reynolds *In* NASA, Washington Repts. of Planetary Geol. and Geophys. Program, 1984 Apr. 1985 p 61-63 refs (For primary document see N85-23474 13-91)
Avail: NTIS HC A99/MF A01 CSCL 03B

The evolution and structure of icy bodies of the solar system are summarized. The effect of tidal evolution, eccentricities, and decay time on Titania, Oberon, Miranda, Umbriel and Ariel is discussed. Observational measurements of the masses and radii of these satellites have recently become sufficiently reliable to use in investigation. Also considered is the problem of the sub-surface temperature distribution and heat transfer of icy comet nuclei. B.G.

N85-23497*# Washington Univ., St. Louis, Mo. Center for the Space Sciences.
ON THE ORIGIN OF TRITON AND PLUTO Abstract Only
W. B. McKinnon *In* NASA, Washington Repts. of Planetary Geol. and Geophys. Program, 1984 Apr. 1985 p 64-66 (For primary document see N85-23474 13-91)
(Grant NAGw-432)
Avail: NTIS HC A99/MF A01 CSCL 03B

Lyttleton's (1936) hypothesis that Triton and Pluto originated as adjacent prograde satellites of Neptune is evaluated, and it is shown that with the presently accepted masses of Triton and Pluto-Charon, the momentum and energy exchange required to sell Triton on a retrograde orbit is impossible. The Pluto-Charon system could not have acquired its present angular momentum state during an ejection event unless a physical collision was involved, which is quite unlikely. The simplest hypothesis is that Triton and Pluto are independent representatives of large outer solar system planetesimals. Triton is simply captured, with spectacular consequences that include runaway melting of interior ices and release to the surface of clathrated CH4, CO, and N2. Condensed remnants of this protoatmosphere could account for features in Triton's unique spectrum. C.D.

N85-23498*# Jet Propulsion Lab., California Inst. of Tech., Pasadena.
STUDY AND ESTIMATION OF PLANET-CROSSING ASTEROID POPULATIONS: DISCOVERIES AND ANALYSIS Abstract Only
Eleanor F. Helin and R. Scott Dunbar *In* NASA, Washington Repts. of Planetary Geol. and Geophys. Program, 1984 Apr. 1985 p 69-71 refs (For primary document see N85-23474 13-91)
Avail: NTIS HC A99/MF A01 CSCL 03B

The populations of the various classes of planet-crossing asteroids, based on the results of the systematic Planet-Crossing Asteroid Survey (PCAS) search program are evaluated. Knowledge of the populations is crucial to the stimation of lunar and terrestrial planet cratering rates from asteroidal and cometary sources needed to establish the chronology of other surface features on those bodies. A secondary objective is to identify the sources of these crater-forming objects and their relative importance in producing the observed planet-crossing asteroid population. Some key PCAS asteroid discoveries relevant to the population problem and the progress in using the available search data to update and refine earlier estimates of the planet-crossing asteroid population are described. Author

N85-23499*# Jet Propulsion Lab., California Inst. of Tech., Pasadena.
SMALL SOLAR SYSTEM BODIES Abstract Only
J. G. Williams and J. Gibson *In* NASA, Washington Repts. of Planetary Geol. and Geophys. Program, 1984 Apr. 1985 p 72-73 (For primary document see N85-23474 13-91)
Avail: NTIS HC A99/MF A01 CSCL 03B

The feasibility of using ranging data to a spacecraft lander on a synchronously rotating satellite to determine the satellite's orbit, the planet's orbit, the lander coordinates, and the principal term of forced physical librations was studied. Classifications of asteroids into their proper elements and families are also presented. Measurements and reduction of positions on comets and the minor planets with less common orbits was the focus for the astrometry program. B.G.

N85-23500*# Hawaii Inst. of Geophysics, Honolulu. Planetary Geosciences Div.
THE OLIVINE ASTEROIDS: DISCOVERY, MINERALOGY, AND RELATIONSHIP TO PALASITES Abstract Only

J. F. Bell, B. R. Hawke, and M. J. Gaffey *In* NASA, Washington Repts. of Planetary Geol. and Geophys. Program, 1984 Apr. 1985 p 74-76 refs (For primary document see N85-23474 13-91)
Avail: NTIS HC A99/MF A01 CSCL 03B

Telescopic observations have recently revealed the existence of a new class of asteroids whose surfaces show the spectral signature of abundant olivine. The mineralogy of a well-observed example (446 Aeternitas) is discussed and the implications for the origins of the olivine-rich meteorites and the thermal evolution of asteroids outlined. Author

N85-23501*# Planetary Science Inst., Tucson, Ariz.
ASTEROID COLLISIONAL EVOLUTION STUDIES Abstract Only
Donald R. Davis, Clark R. Chapman, Stuart J. Weidenschilling, and Richard Greenberg *In* NASA, Washington Repts. of Planetary Geol. and Geophys. Program, 1984 Apr. 1985 p 77-79 refs (For primary document see N85-23474 13-91)
Avail: NTIS HC A99/MF A01 CSCL 03B

Understanding asteroid collisional evolution is important for characterizing the physical state of asteroids today and for learning about the processes that acted in this region of the solar system early in its history. The collisional outcome algorithm in the numerical simulation of asteroid evolution was revised to reflect pressure-strengthening. Asteroid collisions are now treated as a distribution of oblique impacts rather than as only head-on collisions. The initial and evolved size distribution of a plausible asteroid population is compared with the observed size distribution. Asteroid accretion times and reconstruction of the primordial solar nebula suggest that there was significantly more mass in this part of the solar system when the asteroids were accreting. B.G.

N85-23502*# Cornell Univ., Ithaca, N.Y. Dept. of Astronomy.
CONVEX-PROFILE INVERSION OF ASTEROID LIGHTCURVES Abstract Only
Steven J. Ostro and Robert Connelly *In* NASA, Washington Repts. of Planetary Geol. and Geophys. Program, 1984 Apr. 1985 p 80-82 refs Previously announced in IAA as A84-33717 (For primary document see N85-23474 13-91)
Avail: NTIS HC A99/MF A01 CSCL 03B

A lightcurve inversion method that yields a two-dimensional convex profile is introduced. The number of parameters that characterize the profile is limited only by the number of Fourier harmonics used to represent the parent lightcurve. The implementation of the method is outlined by a recursive quadratic programming algorithm, and its application to photoelectric lightcurves and radar measurements is discussed. Special properties of the lightcurves of geometrically scattering ellipsoids are pointed out, and those properties are used to test the inversion method and obtained a criterion for judging whether any lightcurve could actually be due to such an object. Convex profiles for several asteroids are shown, and the method's validity is discussed from a physical as well as purely statistical point of view. C.D. (IAA)

N85-23503*# Arizona State Univ., Tempe. Dept. of Geology.
SURFACES OF ASTEROIDS AND COMETARY NUCLEI Abstract Only
Michael C. Malin *In* NASA, Washington Repts. of Planetary Geol. and Geophys. Program, 1984 Apr. 1985 p 83-85 refs (For primary document see N85-23474 13-91)
Avail: NTIS HC A99/MF A01 CSCL 03B

The types of landforms and processes that may exist on cometary nuclei and asteroidal surfaces are investigated. Acknowledging that some asteroids may be cometary nuclei in disguise, asteroids are treated in this report as a simpler case than comets, owing to their more limited response to the state environment. Larger bodies ($D > 100$ km) will not be discussed, even though they are recognized to be extremely important. This limitation permits only processes depending on exogenic phenomena to be considered (excluding processes such as volcanism on Vesta, for example), thus focusing discussion on the more unique aspects of these bodies, namely, their size and number. B.W.

N85-23504*# Hawaii Inst. of Geophysics, Honolulu. Planetary Geosciences Div.
AN IDEALIZED SHORT PERIOD COMET MODEL: SURFACE INSOLATION, H2O FLUX, DUST FLUX AND MANTLE EVOLUTION Abstract Only
Fraser P. Fanale and James R. Salvail *In* NASA, Washington Repts. of Planetary Geol. and Geophys. Program, 1984 Apr. 1985 p 86-87 Previously announced in IAA as A85-20381 (For primary document see N85-23474 13-91)
Avail: NTIS HC A99/MF A01 CSCL 03B

The present cometary activity model integrates feedback processes that involve the transport of heat, gas, and dust, as well as dust mantle development, and includes the effects of latitude, rotation, and spin orientation. Attention is given to the development, structural change, and distribution of dust mantles and their mutual interaction with ice surface temperature and gas and dust production. The results obtained suggest that an initially homogeneous, short period comet with a cosmic dust to water ice ratio, as well as typical orbit, rotation rate, and grain size distribution, would develop only a thin, less than 1 mm cyclic mantle at all points on the nucleus. Most H2O dust histories deduced from brightness data are noted to be in reasonable agreement with the model, allowing for uncertainty in radius and albedo. The exceptional case of Comet Encke is discussed. O.C. (IAA)

N85-23505*# Jet Propulsion Lab., California Inst. of Tech., Pasadena.
COMET THERMAL MODELING Abstract Only
Paul R. Weissman and Hugh H. Kieffer *In* NASA, Washington Repts. of Planetary Geol. and Geophys. Program, 1984 Apr. 1985 p 88 (For primary document see N85-23474 13-91)
Avail: NTIS HC A99/MF A01 CSCL 03B

Past thermal models of cometary nuclei have tended to be restricted to hemispherical averages and have ignored many important effects such as surface heat flow, rotation period, or coma opacity. A computer based model called KRC/COM was developed which includes these and many other important effects to give a more accurate physical model of sublimation from icy cometary nuclei. Halley's Comet was used as a test case because of the high interest in the 1986 perihelion passage of that comet. B.W.

N85-23506*# Jet Propulsion Lab., California Inst. of Tech., Pasadena.
DYNAMICS OF LONG-PERIOD COMETS Abstract Only
Paul R. Weissman *In* NASA, Washington Repts. of Planetary Geol. and Geophys. Program, 1984 Apr. 1985 p 89-91 (For primary document see N85-23474 13-91)
Avail: NTIS HC A99/MF A01 CSCL 03B

Dynamical studies of the origin and evolution of long period comets in the Oort cloud during the past year have concentrated on four areas: (1) interpretation of IRAS observations of dust shells around Vega and some 40 other main sequence stars as evidence for cometary clouds around each of these stars; (2) the dynamical plausibility of an unseen solar companion star orbiting in the Oort cloud and causing periodic cometary showers which result in biological extinction events on the earth; (3) a review of the current hypotheses for cometary formation with particular attention to how each mechanism supplies the required mass of comets to the Oort cloud; and (4) development of new dynamics software to simulate the passage of individual stars directly through the Oort cloud. Each of these efforts is described in detail. B.W.

N85-23507*# National Astronomy and Ionosphere Center, Arecibo, Puerto Rico.
VOLCANISM AND RIFT FORMATION IN BETA REGIO, VENUS: NEW RADAR RESULTS Abstract Only
D. B. Campbell, J. W. Head (Brown Univ.), J. K. Harmon, and A. A. Hine *In* NASA, Washington Repts. of Planetary Geol. and Geophys. Program, 1984 Apr. 1985 p 95-96 refs Previously announced as N84-21450 (For primary document see N85-23474 13-91)

Avail: NTIS HC A99/MF A01 CSCL 03B

A high resolution (approximately 2 km) image of Beta Regio, Venus, obtained with the Arecibo radar system, reveals additional details of structure which seem to confirm past suggestions that this region consists of a rift system and associated volcanism. Numerous long linear features approximately parallel to the north-south trending trough discovered by the Pioneer-Venus Orbiter are interpreted as being indicative of extensive faulting and the detail for the radar reflectivity anomaly coincident with Theia Mons suggests that it is a major volcano situated on what would be the western bounding fault of the rift system.

A.R.H. (IAA)

N85-23508*# Brown Univ., Providence, R. I. Dept. of Geological Sciences.

CHARACTERISTICS OF BASALTIC LAVA FLOWS ON VENUS Abstract Only

Lionel Wilson, James B. Garvin, and James W. Head *In* NASA, Washington Repts. of Planetary Geol. and Geophys. Program, 1984 Apr. 1985 p 97-98 refs (For primary document see N85-23474 13-91)

Avail: NTIS HC A99/MF A01 CSCL 03B

Some ideas relating to the formation of lava flows on Venus are reviewed. The surface morphological features seen in the panoramic images made by the Venera 13 and 14 landers are examined in detail. The major element compositions measured by the Soviet probes indicate that the surface rocks at the Venera 13 site resemble a terrestrial tholeite composite whereas the Venera 14 rocks are similar to terrestrial alkali basalts. Few data exist on the rheological properties of such magma types on Earth; these properties are a strong function of magma volatile content, and there are important gaps in our knowledge of the typical volatiles to be associated with the magmas on Venus. However, the suggestion that Venusian magmas may be water poor together with consideration of the fact that the high Venusian surface temperatures may cause magmas to experience up to 50 K less cooling during their rise to the surface than corresponding terrestrial counterparts, leads to the finding that Venusian magmas may typically have plastic viscosities, E, up to a factor of three greater than terrestrial counterparts on eruption. A similar analysis of yield strength variations with temperature, magma composition and volatile content suggests that temperature will exert the main control and that Venusian magma yield strengths, Y, may be a factor of several times smaller than those of terrestrial equivalents.

B.W.

N85-23509*# Massachusetts Inst. of Tech., Cambridge. Center for Space Research.

VENUS SURFACE COMPOSITION FROM RADIO/RADAR MEASUREMENTS Abstract Only

Gordon H. Pettengill, Peter G. Ford, and Bruce M. Chapman *In* NASA, Washington Repts. of Planetary Geol. and Geophys. Program, 1984 Apr. 1985 p 99-100 refs (For primary document see N85-23474 13-91)

Avail: NTIS HC A99/MF A01 CSCL 03B

Three different radio techniques were used to study the electrical properties of the surface of Venus. The reflectivity of the surface at near normal incidence was studied using radar from the Pioneer Venus Orbiter (PVO) spacecraft. These measurements have inferred the corresponding dielectric constants. Surface emissivities were calculated using measurements of thermal emission brightness temperature obtained both from spacecraft and from the ground. These measurements also have inferred dielectric constant. The degree of linear polarization associated with thermal energy emitted from the surface at various angles was examined. The dielectric constant was calculated. The radar data have provided the highest surface resolution of the three techniques, and were the first to show the unusually high values of Fresnel reflection coefficient (approaching 0.40 in extreme cases) that are associated with many of the elevated regions of Venus. The distribution of small scale surface roughness was estimated.

B.W.

N85-23510*# Brown Univ., Providence, R. I. Dept. of Geological Sciences.

SURFACE UNITS ON VENUS DERIVED FROM PIONEER-VENUS ALTIMETRY, ROUGHNESS, AND REFLECTIVITY MEASUREMENTS Abstract Only

A. R. Peterfreund, J. W. Head, J. B. Garvin, and S. A. Zisk (Haystack Observatory, Westford, Mass.) *In* NASA, Washington Repts. of Planetary Geol. and Geophys. Program, 1984 Apr. 1985 p 101-102 refs (For primary document see N85-23474 13-91)

Avail: NTIS HC A99/MF A01 CSCL 03B

The nature of the Venusian surface was revealed by Pioneer-Venus (PV) observations to be diverse at scales from tens to hundreds of kilometers. Spatial correlations of elevation, surface roughness, and radar reflectivity were investigated as a means of assessing the degree of homogeneity of surface radar properties within topographic provinces and develop a map of possible geologic boundaries. Correlations were performed in a supervised fashion whereby unit boundaries were selected on the basis of statistical and empirical studies of the individual data sets. Interpretations of these units in terms of geologic characteristics are based on the determination of physical units which are model dependent.

B.W.

N85-23511*# Brown Univ., Providence, R. I. Dept. of Geological Sciences.

CLASSIFICATION OF CIRCULAR FEATURES ON VENUS Abstract Only

E. R. Stofan, J. W. Head, and R. Grieve *In* NASA, Washington Repts. of Planetary Geol. and Geophys. Program, 1984 Apr. 1985 p 103-104 refs (For primary document see N85-23474 13-91)

Avail: NTIS HC A99/MF A01 CSCL 03B

Among the unanswered questions concerning Venus are the age of its surface and the mechanisms of lithospheric heat transfer (conduction, plate recycling, and hot spot volcanism). If there is a large population of impact craters, then the surface is ancient and Venus is characterized by conduction like the Moon, and Mercury, rather than plate recycling and hot spot volcanism. Alternatively, if there is a large population of volcanic craters, then the surface is younger and other mechanisms of heat transfer likely dominate. Previous studies have emphasized various aspects of the observational, theoretical, experimental, and comparative planetological studies of cratering on Venus, and several have reached divergent opinions concerning the age of the Venus surface. A major source of uncertainty in previous studies is the possible inclusion of circular features of nonimpact (volcanic or tectonic) origin in the so called impact crater population. A classification scheme of circular features on Venus is developed in order to further distinguish their origin and distribution.

B.W.

N85-23512*# Jet Propulsion Lab., California Inst. of Tech., Pasadena.

VENUS GRAVITY: GLOBAL FIELD RESULTS Abstract Only

N. A. Mottinger, W. L. Sjogren, and B. G. Bills (Lunar Planetary Inst.) *In* NASA, Washington Repts. of Planetary Geol. and Geophys. Program, 1984 Apr. 1985 p 105-107 refs (For primary document see N85-23474 13-91)

Avail: NTIS HC A99/MF A01 CSCL 03B

The Pioneer Venus Orbiter has provided a vast amount of gravity data, since March 1979. High resolution results have revealed the high correlation between topography and gravity. These data were acquired at relatively low spacecraft altitudes (150 km) where atmospheric effects and high frequency variations were significant and modelling with global spherical harmonics was difficult. During 1982 data were acquired over a complete Venus rotation where the lowest altitudes were 1000 km or more, thus removing atmospherics and high frequency gravity effects. These data that have been reduced to produce a tenth degree and order spherical harmonic model of the global gravity field of Venus. The reduction technique used a least squares where 78 independent arcs of data were combined in a simultaneous inversion. The tenth degree and order gravity field solution has 117 parameters describing the spherical harmonic coefficients.

This provides approximately 1800 km feature resolution. These coefficients are presented as a geoid map. B.W.

N85-23513*# Smithsonian Astrophysical Observatory, Cambridge, Mass.

GEOPHYSICAL INTERPRETATION OF VENUS GRAVITY DATA Abstract Only

R. D. Reasenberg *In* NASA, Washington D.C. Repts. of Planetary Geol. and Geophys. Program, 1984 Apr. 1985 p 108-110 refs (For primary document see N85-23474 13-91)

Avail: NTIS HC A99/MF A01 CSCL 03B

The subsurface distribution of Venus was investigated through the analysis of the data from Pioneer Venus Orbiter (PVO). In particular, the Doppler tracking data were used to map the gravitational potential. These were compared to the topographic data from the PVO radar (ORAD). In order to obtain an unbiased comparison, the topography data obtained from the PVO-ORAD were filtered to introduce distortions which are the same as those of the gravity models. Both the gravity and filtered topography maps are derived by two stage processes with a common second stage. In the first stage, the topography was used to calculate a corresponding spacecraft acceleration under the assumptions that the topography has a uniform given density and no compensation. In the second stage, the acceleration measures found in the first stage were passed through a linear inverter to yield maps of gravity and topography. Because these maps are the result of the same inversion process, they contain the same distortion; a comparison between them is unbiased to first order. B.W.

N85-23514*# Woods Hole Oceanographic Institution, Mass.

GRAVITY FIELD OF VENUS AND COMPARISON WITH EARTH Abstract Only

Carl Bowin *In* NASA, Washington Repts. of Planetary Geol. and Geophys. Program, 1984 Apr. 1985 p 111-113 refs (For primary document see N85-23474 13-91)

Avail: NTIS HC A99/MF A01 CSCL 03B

The acceleration (gravity) anomaly estimates by spacecraft tracking, determined from Doppler residuals, are components of the gravity field directed along the spacecraft Earth line of sight (LOS). These data constitute a set of vector components of a planet's gravity field, the specific component depending upon where the Earth happened to be at the time of each measurement, and they are at varying altitudes above the planet surface. From this data set the gravity field vector components were derived using the method of harmonic splines which imposes a smoothness criterion to select a gravity model compatible with the LOS data. Given the piecewise model it is now possible to upward and downward continue the field quantities desired with a few parameters unlike some other methods which must return to the full dataset for each desired calculation. B.W.

N85-23515*# Jet Propulsion Lab., California Inst. of Tech., Pasadena.

THE SUPPORT OF LONG WAVELENGTH LOADS ON VENUS Abstract Only

W. Bruce Benerdt and R. Stephen Saunders *In* NASA, Washington Repts. of Planetary Geol. and Geophys. Program, 1984 Apr. 1985 p 114-116 refs (For primary document see N85-23474 13-91)

Avail: NTIS HC A99/MF A01 CSCL 03B

One of the great surprises of the Pioneer Venus mission was the high degree of correlation between topography and gravity found at all wavelengths. This implies a close relationship between topography and lateral subsurface density anomalies, such as those due to passive or dynamic compensation. Sleep-Phillips type compensation model with a variable crustal thickness and a variable upper mantle density was developed. The thin shell theory was used to investigate three end member cases: (1) loading by topographic construction, resulting in a downward deflection of the surface (no mantle support); (2) completely compensated support of a constructional load (no surface deflection); and (3) topography due entirely to upward deflection of the surface supported by a low density upper mantle (no surface load). In general, the models imply relatively thick crust and dense upper mantle for Ishtar Terra and Ovda Regio (western Aphrodite), thinned crust and buoyant upper mantle for Tethus Regio and regions near Sappho and Alpha Regio, and a nearly uniform crust with a buoyant upper mantle for Beta Regio and Atla Regio (eastern Aphrodite). B.W.

N85-23516*# Massachusetts Inst. of Tech., Cambridge. Atmospheric and Planetary Sciences.

VENUS CHASMATA: A LITHOSPHERE STRETCHING MODEL Abstract Only

Sean C. Solomon and James W. Head (Brown Univ.) *In* NASA, Washington Repts. of Planetary Geol. and Geophys. Program, 1984 Apr. 1985 p 117-118 refs (For primary document see N85-23474 13-91)

Avail: NTIS HC A99/MF A01 CSCL 03B

An outstanding problem for Venus is the characterization of its style of global tectonics, an issue intimately related to the dominant mechanism of lithospheric heat loss. Among the most spectacular and extensive of the major tectonic features on Venus are the chasmata, deep linear valleys generally interpreted to be the products of lithospheric extension and rifting. Systems of chasmata and related features can be traced along several tectonic zones up to 20,000 km in linear extent. A lithospheric stretching model was developed to explain the topographic characteristics of Venus chasmata and to constrain the physical properties of the Venus crust and lithosphere. B.W.

N85-23517*# Brown Univ., Providence, R. I. Dept. of Geological Sciences.

A STATISTICAL TREATMENT OF THE REGIONAL SLOPE CHARACTERISTICS OF VENUS AND EARTH Abstract Only

V. I. Shapiro and J. W. Head *In* NASA, Washington Repts. of Planetary Geol. and Geophys. Program, 1984 Apr. 1985 p 119-120 refs (For primary document see N85-23474 13-91)

Avail: NTIS HC A99/MF A01 CSCL 03B

Regional slope is a scale dependent parameter that describes the planar gradient over some (relative broad) area of topography. As such, it has a fundamental relevance to the geological evolution of a planetary surface. It is controlled by the interaction of those processes which tend to increase or reduce surface relief (e.g., tectonism, volcanism, impact cratering, weathering, viscous relaxation) and in turn, exerts control on the erosion, transportation and deposition of surface materials. The regional slope values, measured over 3 by 3 regions for Venus and Earth are calculated. The regional slope frequency distribution information was analyzed for Venus and Earth. The effects on terrestrial regional slope resulting from the removal of the ocean load from sea floor topography were examined. B.W.

N85-23518*# National Aeronautics and Space Administration. Ames Research Center, Moffett Field, Calif.

RESPONSE OF EARTH'S ATMOSPHERE TO INCREASES IN SOLAR FLUX AND IMPLICATIONS FOR LOSS OF WATER FROM VENUS Abstract Only

James F. Kasting, James G. Pollock, and thomas P. Ackerman *In* NASA, Washington Repts. of Planetary Geol. and Geophys. Program, 1984 Apr. 1985 p 121 refs Document previously announced as A84-33710 (For primary document see N85-23474 13-91)

Avail: NTIS HC A99/MF A01 CSCL 03B

A one dimensional radiative convective model is used to compute temperature and water vapor profiles as functions of solar flux for earthlike atmosphere. The troposphere is assumed to be fully saturated with a moist adiabatic lapse rate, and changes in cloudiness are neglected. Predicted surface temperatures increase monotonically from -1 to 111 C as the solar flux is increased from 0.81 to 1.45 times its present value. The results imply that the surface temperature of a primitive water rich Venus should have been at least 80-100 C and may have been much higher, water vapor should have been a major atmospheric constituent at all altitudes, leading to the rapid hydrodynamic escape of hydrogen. The oxygen left behind by this process was

presumably consumed by reactions with reduced minerals in the crust. C.D. (IAA)

N85-23519*# Planetary Science Inst., Tucson, Ariz.
LUNAR ORIGIN: ROLE OF GIANT IMPACTS Abstract Only
William K. Hartmann *In* NASA, Washington Repts. of Planetary Geol. and Geophys. Program, 1984 Apr. 1985 p 125-126 refs Original language document previously announced as N85-13749 (For primary document see N85-23474 13-91)
Avail: NTIS HC A99/MF A01 CSCL 03B

The explanation that lunar origin involved giant impacts remains attractive. Large planetesimals are consistent with current accretion models, and may have been widely scattered in the early solar systems; their existence is a reasonably, assumption in Moon origin models. Isotopic data require the Moon's formation primarily from local material resembling Earth's upper mantle, not material from elsewhere in the solar system. Giant impacts are stochastic, class predictable events that would provide the required type of ejected Earth mantle material without requiring large moons to form near other planets (a problem with less stochastic processes). Such material may have mixed with incoming meteorites during lunar formation, affecting lunar chemistry. Author (IAA)

N85-23520*# Planetary Science Inst., Tucson, Ariz.
A CIRCUM-TERRESTRIAL COMPOSITIONAL FILTER Abstract Only
Clark R. Chapman and Richard Greenberg *In* NASA, Washington Repts. of Planetary Geol. and Geophys. Program, 1984 Apr. 1985 p 127-128 refs (For primary document see N85-23474 13-91)
Avail: NTIS HC A99/MF A01 CSCL 03B

A major question about the moon is its under abundance of iron. It is the purpose of this research to understand whether a metal-silicate fractionation of heliocentrically orbiting bodies can be achieved through collisional interactions with a circum-terrestrial swarm. Rates of diffusion are investigated and the mutual collisional destruction within the population is examined. The interactions of these differentiated planetesimals and their collisional products (both silicate mantle fragments and iron cores) with a swarm of Earth orbiting lunesimals (perhaps ejecta from the Earth) of km scale, totaling a mass of order 0.1 lunar mass, extending out 10 or 20 Earth radii are considered. It is found that such a small near Earth population of lunesimals can filter out silicate rich material, while passing iron cores, and form a moon composed partly of terrestrial material, but more substantially of the captured silicate rich portions of the planetesimals. B.W.

N85-23521*# Planetary Science Inst., Tucson, Ariz.
MODELS OF ANGULAR MOMENTUM INPUT TO A CIRCUM-TERRESTRIAL SWARM FROM ENCOUNTERS WITH HELIOCENTRIC PLANETESIMALS Abstract Only
Donald R. Davis, Richard Greenberg, and Floyd Hebert (Arizona Univ., Tucson) *In* NASA, Washington Repts. of Planetary Geol. and Geophys. Program, 1984 Apr. 1985 p 129-131 refs (For primary document see N85-23474 13-91)
Avail: NTIS HC A99/MF A01 CSCL 03B

Models of lunar origin in which the Moon accretes in orbit about the Earth from material approaching the Earth from heliocentric orbits must overcome a fundamental problem: the approach orbits of such material would be, in the simplest approximation, equally likely to be prograde or retrograde about the Earth, with the result that accretion of such material adds mass but not angular momentum to circumterrestrial satellites. Satellite orbits would then decay due to the resulting drag, ultimately impacting onto the Earth. One possibility for adding both material and angular momentum to Earth orbit is investigated: imbalance in the delivered angular momentum between pro and retrograde Earth passing orbits which arises from the three body dynamics of planetesimals approaching the Earth from heliocentric space. In order to study angular momentum delivery to circumterrestrial satellites, the near Earth velocities were numerically computed as a function of distance from the Earth for a large array of orbits systematically spanning heliocentric phase space. B.W.

N85-23522*# Planetary Science Inst., Tucson, Ariz.
CAPTURE OF PLANETESIMALS INTO A CIRCUMTERRESTRIAL SWARM Abstract Only
Stuart J. Weidenschilling *In* NASA, Washington Repts. of Planetary Geol. and Geophys. Program, 1984 Apr. 1985 p 132-133 refs (For primary document see N85-23474 13-91)
Avail: NTIS HC A99/MF A01 CSCL 03B

The lunar origin model considered in this report involves processing of protolunar material through a circumterrestrial swarm of particles. Once such a swarm has formed, it can gain mass by capturing infalling planetesimals and ejecta from giant impacts on the Earth, although the angular momentum supply from these sources remains a problem. The first stage of formation of a geocentric swarm by capture of planetesimals from initially heliocentric orbits is examined. The only plausible capture mechanism that is not dependent on very low approach velocities is the mutual collision of planetesimals passing within Earth's sphere of influence. The dissipation of energy in inelastic collisions or accretion events changes the value of the Jacobi parameter, allowing capture into bound geocentric orbits. This capture scenario was tested directly by many body numerical integration of planetesimal orbits in near Earth space. B.W.

N85-23523*# Planetary Science Inst., Tucson, Ariz.
ORBITAL RESONANCES AND PLANETARY ACCRETION IN THE SOLAR NEBULA Abstract Only
S. J. Weidenschilling and D. R. Davis *In* NASA, Washington Repts. of Planetary Geol. and Geophys. Program, 1984 Apr. 1985 p 134-136 refs (For primary document see N85-23474 13-91)
Avail: NTIS HC A99/MF A01 CSCL 03B

Planetesimal orbital evolution in a resisting medium near an accreting protoplanet was studied to explore mechanisms for capture into Trojan and satellite orbits. Various mechanisms for capture into libration were proposed, e.g., increase in Jupiter/Sun mass ratio, change in Jovian orbital radius, and collisions of asteroids with interplanetary dust. Studies include effects of solar nebula gas drag on orbital evolution. In general, the gas deviates from Keplerian motion, causing secular decay of planetesimal orbits, as well as damping eccentricity. The motion of bodies near Jupiter under the effect of a resisting medium was numerically explored. The equations of motion were integrated using the formalism of the planar restricted three body problem, modified to include effects by gas drag and a growing Jupiter. B.W.

N85-23524*# Carnegie Institution of Washington, D. C.
ACCUMULATION OF THE TERRESTRIAL PLANETS Abstract Only
G. W. Wetherill *In* NASA, Washington Repts. of Planetary Geol. and Geophys. Program, 1984 Apr. 1985 p 137-139 refs (For primary document see N85-23474 13-91)
Avail: NTIS HC A99/MF A01 CSCL 03B

The validity of the two body approximation in calculations of planetary growth is examined. Use of this approximation is essential to practical 3 dimensional simulations of planetary growth. With regard to gravitational perturbations, the changes in semimajor axis, eccentricity, and inclination resulting from close planetesimal encounters (near 1 A.U.) out to 10 Tisserand sphere of influence radii were calculated by two and three dimensional numerical integration. These were compared with the results of treating the encounter as a two body problem, as is customary in Monte Carlo calculations of orbital evolution and in numerical and analytical studies of planetary accumulation. It is found that for values of (V/V sub e) approx. < 0.35 (V = relative velocity, V = escape velocity of largest body), the two body approximation fails to describe the outcome of individual encounters. In this low velocity region, the two body gravitational focusing cross section is no longer valid. B.W.

N85-23525*# Planetary Science Inst., Tucson, Ariz.
EVOLUTION OF GRAINS IN A TURBULENT SOLAR NEBULA Abstract Only
S. J. Weidenschilling *In* NASA, Washington Repts. of Planetary Geol. and Geophys. Program, 1984 Apr. 1985 p 140-142 refs

(For primary document see N85-23474 13-91)
Avail: NTIS HC A99/MF A01 CSCL 03B

Planetesimal formation by gravitational instability of a dust layer requires a nonturbulent solar nebula. The assumption that the solar nebula is a turbulent, convective accretion disk is explored. Self consistent models of a convective disk depend on high opacity of the disk material, which must be provided by grains. Grain coagulation is implied by the requirement of forming planetesimals, as the turbulent velocities (approx. 1/3 sound speed) in the accretion disk would disrupt any dust layer. Collisional coagulation could form large planetesimals, simultaneously leaving a sufficient fraction of matter in small grains to maintain the nebula's opacity. Or, coagulation of grains into small (approx. cm) aggregates could lower the opacity enough for turbulence to decay. The evolution of a population of grains in a turbulent solar nebula is calculated numerically. B.W.

N85-23526*# National Aeronautics and Space Administration. Ames Research Center, Moffett Field, Calif.
THE FORMATION OF PREPLANETARY DISKS FROM THE COLLAPSE OF ROTATING MOLECULAR CLOUD CORES Abstract Only
Patrick Cassen, Frank H. Shu (California Univ., Berkeley), and Susan Tereby (California Univ., Berkeley) *In* NASA, Washington Repts. of Planetary Geol. and Geophys. Program, 1984 Apr. 1985 p 143-145 refs (For primary document see N85-23474 13-91)
Avail: NTIS HC A99/MF A01 CSCL 03B

Solutions that describe the collapse of a molecular cloud core that is initially in unstable equilibrium, embedded within an envelope of uniform density, and rotating at the same rate as the envelope are given. Hydrodynamic equations, including self gravity, are deduced to a set of ordinary differential equations, which are solved by the method of matched asymptotic expansions. Results of these calculations are: (1) the range of stellar masses derived seems to correspond to realistic ranges of observed stellar masses and interstellar cloud parameters, (2) the proper measure of dissipation rate is the ratio of accretion time to viscous diffusion time, and (3) the pressure distribution on the surface of an accreting protostar is nonuniform in a way that favors the channeling of a stellar wind into a bipolar flow directed along the rotation axis. E.R.

N85-23527*# Harvard-Smithsonian Center for Astrophysics, Cambridge, Mass.
RESEARCH ON THE EARLY HISTORY OF THE SOLAR SYSTEM Abstract Only
A. G. W. Cameron *In* NASA, Washington Rept. of Planetary Geol. and Geophys. Program, 1984 Apr. 1985 p 146-148 refs (For primary document see N85-23474 13-91)
Avail: NTIS HC A99/MF A01 CSCL 03B

The evolution of a dissipating turbulently viscous disk of gas and dust formed during the collapse of an interstellar cloud fragment and how it relates to the early history of the solar system is discussed. Results from calculations on modelling the inner parts of the primitive solar nebula subject to the assumption of a steady inward flow are given. Other calculations are reviewed which simulate the accretion of a star from an accretion disk. Scenarios for the evolution of the primitive solar nebula and the formation of the Moon as a result of a major collision with the protoearth are described. E.R.

N85-23528*# Smithsonian Astrophysical Observatory, Cambridge, Mass.
VIKING RADIO SCIENCE DATA ANALYSIS AND SYNTHESIS Abstract Only
I. I. Shapiro and R. D. Reasenberg *In* NASA, Washington Repts. of Planetary Geol. and Geophys. Program, 1984 Apr. 1985 p 149-151 refs Prepared in cooperation with Harvard-Smithsonian Center for Astrophysics (For primary document see N85-23474 13-91)
Avail: NTIS HC A99/MF A01 CSCL 03B

The objectives of the analysis of the Viking radio tracking data are: (1) the study of Mars, its rotation, topography, and internal structure; (2) the development of a general dynamical model of the solar system; and (3) tests of the fundamental laws of gravitation. The central element in the data analysis is the Planetary Ephemeris Program (PEP) which embodies the mathematical models of the solar system. The asteroid model in PEP is changed to better estimate the mass of a fictitious uniform ring and the masses of eight separate asteroids. A model of the rotation of Mars include a secular rate of change of the period and both annual and semiannual variations in the phase of rotation. Other modifications to this model are discussed. E.R.

N85-23529*# Jet Propulsion Lab., California Inst. of Tech., Pasadena.
GRAVITY FIELD OF THE JOVIAN SYSTEM FROM PIONEER AND VOYAGER TRACKING DATA Abstract Only
J. K. Campbell and S. P. Synnott *In* NASA, Washington Repts. of Planetary Geol. and Geophys. Program, 1984 Apr. 1985 p 152-154 refs Document previously announced as A85-22797 (For primary document see N85-23474 13-91)
Avail: NTIS HC A99/MF A01 CSCL 03B

Data sets from the Voyager and Pioneer flybys of Jupiter and the Galilean satellites are employed to characterize the Jovian magnetic field and the effects of the Io torus on transmissions. Both optical and Doppler radio data are considered, except for periods when the Jovian radiation environment disturbed the oscillator stability of the radio transmitters. Account is taken of small accelerations of the spacecraft by tidal forces of a single rising satellite, density differences in the Great Red Spot producing a columnar gravitational change, and three unknown objects in the inner Jovian system. Correction parameters are developed for the effects on the S-band data induced by the Jovian plasmasphere inwards from the Io torus. Calculations are then made of the planet and satellite masses, gravity harmonic coefficients, and orientation of the rotational pole. Large reductions in the uncertainties in previous mass esimates are obtained. M.S.K. (IAA)

N85-23530*# California Inst. of Tech., Pasadena. Seismological Lab.
IMPACT AND COLLISIONAL PROCESSES IN THE SOLAR SYSTEM Abstract Only
Thomas J. Ahrens *In* NASA, Washington Repts. of Planetary Geol. and Geophys. Program, 1984 Apr. 1985 p 157-159 refs Original document previously announced as N85-17914 (For primary document see N85-23474 13-91)
Avail: NTIS HC A99/MF A01

The mechanical and thermodynamic aspects of shock impact cratering and accretionary processes on solid planets and satellites are being investigated experimentally. The recently proposed model of Melosh, describing the physics controlling the size and velocity of only lightly shocked spalled ejecta surrounding the crushed rock region of an impact crater, was studied at the Ames gun facility. Spall velocity measurements using lead and aluminum bullets were conducted. In addition, shock temperatures of silicates and volatile bearing minerals were measured using radiative techniques. Finally impact devolatilization of minerals and accretion of planetary atmospheres were examined. Measurements of the release isentropes of $CaCO_3$ were carried out. The effect on the water budgets of planets of reactions which occur when metallic iron (which would be present in chondritic material) is introduced into a simple accretion model is under investigation. R.S.F. (IAA)

N85-23531*# California Inst. of Tech., Pasadena.
IMPACT CRATERING CALCULATION Abstract Only
Thomas J. Ahrens and John L. OKeefe *In* NASA, Washington Repts. of Planetary Geol. and Geophys. Program, 1984 Apr. 1985 p 160-163 refs (For primary document see N85-23474 13-91)
Avail: NTIS HC A99/MF A01 CSCL 03B

Impact cratering, both normal and oblique, on planetary surfaces is discussed and energy partitioning, ejecta distribution, (both with regard to size, velocity, energy content, and size sorting), the condensation physics of impact induced vapor, and the loss of planetary atmospheres during accretion of terrestrial and icy planets are considered. The possible origin of SNC meteorites, impact into porous regolith, equation of state of water and ice,

and a possible model for the accretion of the Jovian and Saturnian satellites are examined. A.R.H.

N85-23532*# Washington Univ., Seattle.
IMPACT CRATER SCALING LAWS Abstract Only Progress Report
K. A. Holsapple *In* NASA, Washington Repts. of Planetary Geol. and Geophys. Program, 1984 Apr. 1985 p 164-166 refs (For primary document see N85-23474 13-91)
Avail: NTIS HC A99/MF A01 CSCL 03B

The effects of the impactor size and velocity, of the material properties of the impactor and impacted body, and of the gravitational field strength were examined. The dependence of the coupling parameter on the Gruniesen parameter and the us/up slope values that characterize a Tillotson material model were tested. Whether a code calculation can recover the scaling exponents that can be derived theoretically for an idealized perfectly-porous material that crushes at zero strength and subsequently is incompressible was investigated. A model that was close to the idealized case was generated in a form suitable for code calculations and utilized for a series of one dimensional calculations. The code calculation demonstrated the theoretical coupling parameter. Calculations of impacts using a physically real porous material model seem to indicate a coupling parameter of the same form applicable to a nonporous material, distinctly different from that expected from other theoretical and experimental results for porous materials. The one dimensional calculations are being extended to two dimensional impacts. A.R.H.

N85-23533*# Boeing Aerospace Co., Seattle, Wash.
CENTRIFUGE IMPACT CRATERING EXPERIMENTS Abstract Only
Robert M. Schmidt, Kevin R. Housen, and Michael D. Bjorkman *In* NASA, Washington Repts. of Planetary Geol. and Geophys. Program, 1984 Apr. 1985 p 167-169 refs (For primary document see N85-23474 13-91)
Avail: NTIS HC A99/MF A01 CSCL 03B

The kinematics of crater growth, impact induced target flow fields and the generation of impact melt were determined. The feasibility of using scaling relationships for impact melt and crater dimensions to determine impactor size and velocity was studied. It is concluded that a coupling parameter determines both the quantity of melt and the crater dimensions for impact velocities greater than 10km/s. As a result impactor radius, a, or velocity, U cannot be determined individually, but only as a product in the form of a coupling parameter, delta U micron. The melt volume and crater volume scaling relations were applied to Brent crater. The transport of melt and the validity of the melt volume scaling relations are examined. E.A.K.

N85-23534*# Planetary Science Inst., Tucson, Ariz.
PROGRESS ON EXPERIMENTAL IMPACT STUDIES Abstract Only
W. K. Hartmann, D. R. Davis, and S. J. Weidenschilling *In* NASA, Washington Repts. of Planetary Geol. and Geophys. Program, 1984 Apr. 1985 p 170 refs (For primary document see N85-23474 13-91)
Avail: NTIS HC A99/MF A01 CSCL 03B

Experimental impact studies were undertaken. Ejecta velocity distributions and related results from regolith targets were studied. The velocity distributions, energy partitioning, and related properties from 14 impacts at speeds 5 to 2321 m/s in vacuo into regolith-like fine powders were derived. Data are analyzed on: velocity and mass distributions as a function of azimuth around the crater during oblique impacts catastrophic disruption of spherical targets of variable strength, and catastrophic disruption of irregular-shaped natural rock targets and artificial granular aggregate targets. E.A.K.

N85-23535*# Planetary Science Inst., Tucson, Ariz.
PROGRESS ON STUDIES OF EARLY INTENSE CRATERING Abstract Only
William K. Hartmann *In* NASA, Washington Repts. of Planetary Geol. and Geophys. Program, 1984 Apr. 1985 p 171-173 refs (For primary document see N85-23474 13-91)
Avail: NTIS HC A99/MF A01 CSCL 03B

The existence and effects of saturation cratering throughout the solar system was studied. It is found that saturation equilibrium cratering exists nowhere in the solar system, and that diameter distributions in even the most heavily cratered provinces reveal initial production functions related to impacting bodies. Different populations of impactors in different epochs and regions of the solar system are identified. The hypotheses are crucial for interpretation of planetary history. The crater counts on frontside lunar uplands, used as a basic reference curve identified with one of their populations of early impactors, are confirmed. This crater population is deficient in 1 to 16 km craters, which may be obliterated by the lavas. It is concluded that this curve is not representative of heavily cratered highlands, and is of questionable value as a standard comparison curve. The role of giant impacts during the intense early bombardment period was studied. Giant impact(s) on the primeval Earth may have initiated lunar formation. E.A.K.

N85-23536*# Geological Survey, Menlo Park, Calif.
WHY NOT A CONSTANT EARLY LUNAR IMPACT RATE? Abstract Only
Don E. Wilhelms *In* NASA, Washington Repts. of Planetary Geol. and Geophys. program, 1984 Apr. 1985 p 174-176 refs (For primary document see N85-23474 13-91)
Avail: NTIS HC A99/MF A01 CSCL 03B

Two distinct episodes of impacting are recorded on the Moon's surface. An early episode marked by an intense barrage that included basin-forming projectiles ended about 3.8 aeons ago when the Orientale basin was created. The second episode, after 3.2 or 3.3 aeons ago, was marked by a much lower impact rate. These very different rates are separated by a short transition period during the Late Imbrian Epoch. It is found that a constant preimbrian impact rate is consistent with all the relevant observations and with the following lunar historical scenario: (1) crustal solidification between about 4.3 and 4.25 aeons ago; (2) formation of Procellarum, South Pole-Aitken, about 22 now-obliterated basins, and about 2,850 now-obliterated 30 to 300 km craters between 4.25 and 4.1 aeons ago; and (3) formation of 39 still-preserved basins, 1,200 still-perserved craters, and 2,200 now-obliterated craters between 4.1 and 3.85 aeons ago. At the constant rate, the amount of mass that impacted the Moon since crustal solidification would not greatly exceed the amount that has left a permanent visible record. E.A.K.

N85-23537*# Arizona Univ., Tucson. Lunar and Planetary Lab.
MARTIAN TERRAIN AGES Abstract Only
Robert G. Strom and Nadine G. Barlow *In* NASA, Washington Repts. of Planetary Geol. and Geophys. Program, 1984 Apr. 1985 p 177-179 refs (For primary document see N85-23474 13-91)
Avail: NTIS HC A99/MF A01 CSCL 03B

The cratering record in the inner Solar System shows two crater populations based on their size/frequency distributions. The heavily cratered surfaces of the Moon, Mercury and Mars all show a similar multisloped crater size distribution which represents the period of heavy bombardment. On the younger plains units of the Moon and Mars the crater size/frequency distribution has about a -3 slope over the same diameter range. The different crater population represents the accumulation of craters since the end of heavy bombardment. The high flux of the early impacting objects dominated the cratering record prior to 3.8 BY. If heavy bombardment was primarily the result of comets (1) or a disrupted planetesimal (2), then heavy bombardment ended simultaneously on all of the inner planets. If, on the other, heavy bombardment was caused by accretional remnants, then it may have extended as much as 1 BY later on Mars than on the Moon and other terrestrial planets (3). Martian surfaces can be dated relative to the end of heavy bombardment by the type of crater population superposed on them. The relative ages of surfaces within these two time divisions can be determined by crater densities. E.A.K.

N85-23538*# Washington Univ., St. Louis, Mo. Center for the Space Sciences.
IMPACTS IN ICE: COMMISSIONS OF SOLAR SYSTEM CRATER POPULATION Abstract Only
W. B. McKinnon *In* NASA, Washington Repts. of Planetary Geol. and Geophys. Program, 1984 Apr. 1985 p 180-182 refs (For primary document see N85-23474 13-91)
Avail: NTIS HC A99/MF A01 CSCL 03B

The classical phases of cratering are compression, excavation, and modification. Recent theory, however, supports and alternative sequence of physical events: (1) coupling - energy and momentum are transferred, and the cratering flow field is set up; (2) power-law-growth the flow field expands, with transient cavity dimensions expressible as a simple power law function of time; and (3) late phase - some combination of gravity, strength, and viscosity limits cavity growth, initially causing a deviation from power-law behavior and eventually determining the size and shape of the final (transient) crater. The dominant mechanism that limits cavity growth defines a cratering regime and a single variable, the coupling parameter, determines the scaling laws in the various regimes. The coupling parameter is intermediate in dimensionality between energy and momentum and its exact form is determined. For simple materials with rate and scale independent strength, the transition crater diameter between the strength and gravity regimes is, within reasonable bounds, independent of velocity. Even the smallest craters observed by Voyager appear to be gravity dominated. E.A.K.

N85-23539*# Houston Univ., Tex.
PROBLEMS IN RECOVERING CRATER PRODUCTION FUNCTIONS Abstract Only
Alex Woronow *In* NASA, Washington Repts. of Planetary Geol. and Geophys. Program, 1984 Apr. 1985 p 183-185 refs (For primary document see N85-23474 13-91)
Avail: NTIS HC A99/MF A01 CSCL 03B

Two techniques proposed for the recovery of the crater production functions on densely cratered surfaces were appraised. The first technique classifies craters according to their degree of rim preservation, then interprets the statistics of the freshest craters as closely mimicing the full population's production function. This method is misleading for densely cratered surfaces. The second technique measures and weighs each crater diameter by the fraction of the crater that remains unoverlapped by subsequent impacts. The method is theoretically sound even at saturation crater densities, though it too fails at high densities. Author

N85-23540*# Houston Univ., Tex. Dept. of Geoscience.
A PARMETRIC STUDY OF CRATER-SATURATION SIMULATION Abstract Only
Alex Woronow *In* NASA, Washington Repts. of Planetary Geol. and Geophys. Program, 1984 Apr. 1985 p 186-188 refs (For primary document see N85-23474 13-91)
Avail: NTIS HC A99/MF A01 CSCL 03B

Computer models of cratered surfaces often use inputs of uncertain nature and importance. This work evaluates the sensitivity of the resulting crater-saturation estimates to the input parameters, principally applicable to the study of craters upward from 8km diameter. In order of decreasing importance, crater saturation simulations are found to be sensitive to: (1) the dynamic range of crater diameters used; (2) the effectiveness of ejecta-blanket obliteration assumed; and (3) the number of points taken to describe the crater rim. The size of the largest crater in proportion to the size of the simulated surface has no effect on the results when the edges of the simulated surface are correctly treated and craters are counted by the fraction of the crater within the simulated area. A similar procedure is recommended when gathering crater size-density data from images. E.A.K.

N85-23541*# Geological Survey, Menlo Park, Calif.
AVERAGE SPACING FOR RINGS OF INDIVIDUAL MULTI-RING BASINS IS 2.0(0.5)D Abstract Only
R. J. Pike, P. D. Spudis, and G. D. Clow (Geological Survey, Flagstaff, Ariz.) *In* NASA, Washington Repts. of Planetary Geol. and Geophys. Program, 1984 Apr. 1985 p 189-191 refs (For primary document see N85-23474 13-91)
Avail: NTIS HC A99/MF A01 CSCL 03B

The mathematically regular spacing of the concentric rings of planetary impact basins are examined. It is shown that a constant radial increment of x (sub 0.5) D, where x is about 2.0 and D is ring diameter, separates adjacent statistical groups of rings and arcs of multiring basins on Mars, Mercury, and the Moon. Statistics of spacing for adjacent rings of individual basins on the three planets are presented, and single basins from ring measurements of newly-recognized basins on Mercury and Mars are revised. Analysis of ring rank: ring diameter for adjacent rings of individual basins also yields an average spacing of about 2.0 (sup 0.5) D, specifically (2.01 + or - 0.26) (sup 0.5) D. E.A.K.

N85-23542*# Geological Survey, Menlo Park, Calif.
RING-DIAMETER RATIOS FOR MULTI-RING BASINS AVERAGE 2.0(0.5)D Abstract Only
R. J. Pike and P. D. Spudis (Geological Survey, Flagstaff, Ariz.) *In* NASA, Washington Repts. of Planetary Geol. and Geophys. Program, 1984 Apr. 1985 p 192-194 refs (For primary document see N85-23474 13-91)
Avail: NTIS HC A99/MF A01 CSCL 03B

The spacing of the concentric rings of planetary impact basins was studied. It is shown that a radial increment of x (sup 0.5) D, where x is about 2.0 and D = ring diameter, separates both (1) adjacent least-squares groups of rings and arcs of multi-ring basins on Mars, Mercury, and the Moon; and (2) adjacent rings of individual basins on the three planets. Statistics for ratios of ring diameters are presented, the first and most-applied parameter of ring spacing. It is found that ratios excluding rings flanking the main ring also have a mean spacing increment of about 2.0. Ratios including such rings, as for the least-squares groups, and (1) above, have a larger increment, averaging 2.1. The F-test indicates, that these spacings of basin ring locations, and mode of ring formation are controlled by the mechanics of the impact event itself, rather than by crustal properties. E.A.K.

N85-23543*# Arizona Univ., Tucson. Lunar and Planetary Lab.
MORPHOLOGY AND MECHANICS OF TERRACES IN LUNAR CRATERS Abstract Only
Steven K. Croft *In* NASA, Washington Repts. of Planetary Geol. and Geophys. Program, 1984 Apr. 1985 p 195-199 refs (For primary document see N85-23474 13-91)
Avail: NTIS HC A99/MF A01 CSCL 03B

The morphology and morphometry of terrace provide information on the mechanical conditions of failure and enlargement of impact craters. A simple, perfect plasticity model for terrace formation was proposed, but the preliminary terrace width measurements used to support the model were insufficient to provide a rigorous test. Lunar crater terraces were studied morphometrically. Roughly 1,000 terraces in 53 fresh lunar craters were measured using Apollo and Lunar Orbiter vertical stereo photography. Terrace widths and their order inward from the rim were measured along eight equally spaced radials in each crater. A list of the craters including rim diameters and geologic data is presented. E.A.K.

N85-23544*# Massachusetts Univ., Amherst. Dept. of Geology and Geography.
NEWLY DISCOVERED MARTIAN IMPACT BASINS Abstract Only
Marianne Stam *In* NASA, Washington Repts. of Planetary Geol. and Geophys. Program, 1984 Apr. 1985 p 200-201 refs (For primary document see N85-23474 13-91)
Avail: NTIS HC A99/MF A01 CSCL 03B

Three previously unrecognized Martian impact basins were discovered through detailed mapping of landforms, structures and terrains near Cassini and Al Qahira basins. Al Qahira A lies on the Martian dichotomy boundary and intersects the older basin, Al Qahira. It has four rings that are expressed by a variety of landforms. Southwestward Al Qahira A is out by a younger Basin, Al Qahira B. Al Qahira B is a highly degraded basin with one identifiable ring. Its ring is expressed by a few massifs, knobs and

inward-facing scarps, but is recognized by the distributions of wrinkle ridges and plains units. Cassini A lies southward of the younger Cassini Basin and is intersected by it. It probably has four rings. The importance of detailed mapping of various types of landforms and terrains to the discovery of basins on Mars are demonstrated. E.A.K.

N85-23545*# Arizona State Univ., Tempe. Dept. of Geology.
THE NATURE OF MARTIAN FLOW EJECTA CRATERS Abstract Only
v. M. Horner and R. Greeley *In* NASA, Washington Repts. of Planetary Geol. and Geophys. Program, 1984 Apr. 1985 p 202-203 refs (For primary document see N85-23474 13-91)
Avail: NTIS HC A99/MF A01 CSCL 03B

Ejecta with flow features and discrete termini surround many fresh Martian craters. Several morphologies of the flow-like ejecta are observed; they are found globally and in nearly all terrains. It is suggested that the morphology of flow ejecta craters is related to the amount of subsurface volatiles and/or to atmospheric drag effects. It was attempted to constrain factors which could contribute to the ejecta morphology such as latitude, elevation, and terrain unit, however, they involved only one or two constrained variables or used global data sets based on Mariner 9 information. Viking-based data sets are becoming available and may provide a better base from which an understanding of the factors which governs ejecta morphology may be obtained. Block sizes of Martian flow ejecta may provide clues to the ejecta emplacement process. Author

N85-23546*# Jet Propulsion Lab., California Inst. of Tech., Pasadena.
INTERACTION OF MARTIAN FLOW EJECTA BLANKETS WITH PRE-EXISTING IMPACT CRATERS: MORPHOLOGICAL OBSERVATIONS Abstract Only
David C. Pieri, Michael Hurick, and Stephen M. Baloga *In* NASA, Washington Repts. of Planetary Geol. and Geophys. Program 1984 Apr. 1985 p 204-205 refs (For primary document see N85-23474 13-91)
Avail: NTIS HC A99/MF A01 CSCL 03B

The evidence of interaction between impact flow ejecta blankets and pre-existing landforms such as craters, scarps, and wrinkle ridges may yield important clues as to the nature of the ejecta emplacement process. The morphology of flow ejecta blankets and the interactions of these blankets with pre-emplacement impact craters were characterized. About 80 small satellite craters on or in 3 well-expressed low ejecta parent impact craters were recognized. Interaction of the blanket with pre-existing structures was studied, and several types were described. These are: (1) infilling; (2) encroachment; (3) overflow; and (4) breaching. Examination of the overall morphology of three ejecta blankets reveals a range of thickness, from depths sufficient to completely bury craters in the 5 km diameter range in distal areas of the blankets, to very thin blankets which allow subtle pre-existing topography to be visible within a half the diameter of the parent crater. Radial and azimuthal symmetries appear to exist within the blankets over a range of morphologies. It also appears that there is a weak linear correlation between the diameter of craters with nearly 100% infilling and distance from the center of the parent crater. E.A.K.

N85-23547*# Arizona Univ., Tucson. Lunar and Planetary Lab.
RIPPLE RING BASINS ON GANYMEDE AND CALLISTO
Steeven K. Croft *In* NASA, Washington Repts. of Planetary Geol. and Geophys. Program, 1984 Apr. 1985 p 206-208 refs (For primary document see N85-23474 13-91)
Avail: NTIS HC A99/MF A01 CSCL 03B

The unusual morphology of the Valhalla multiple or ripple-ring basin in Callisto was totally unexpected in light of the morphologies of large impact structures on the terrestrial planets. Two other ripple-ring basins (RRB's), Asgard and a smaller structure near the crater Adlinda are also described. Several additional RRB's were found on Callisto, an example of which is shown. A previously unrecognized RRB on Ganymede was also found. An image and geologic sketch map of this RRB are shown. Morphometric and positional data for all known RRB's are given. R.K.S.

N85-23548*# Cornell Univ., Ithaca, N.Y. Dept. of Geological Sciences.
IMPLICATIONS OF CONVECTION IN THE MOON AND THE TERRESTRIAL PLANETS Abstract Only
Donald L. Turcotte *In* NASA, Washington Repts. of Planetary Geol. and Geophys. Program, 1984 Apr. 1985 p 211 refs (For primary document see N85-23474 13-91)
Avail: NTIS HC A99/MF A01 CSCL 03B

The early evolution of the Moon and its implications for the early evolution of the Earth was studied. The study is divided into two parts: (1) studies of core formation. Cosmochemical studies strongly favor a near-homogeneous accretion of the Earth. It is shown that core segregation probably occurred within the first 10,000 years of Earth history. It is found that dissipative heating may be a viable mechanism for core segregation if sufficiently large bodies of liquid iron can form; (2) early thermal evolution of the Earth and Moon. The energy associated with the accretion of the Earth and the segregation of the core is more than sufficient to melt the entire Earth. The increase in the mantle liquidus with depth (pressure) is the dominant effect influencing heat transfer through the magma ocean. It is found that a magma ocean with a depth of 100 km would have existed as the Earth accreted. It is concluded that this magma ocean zone refined the earth resulting in the simultaneous formation of the core and the atmosphere during accretion. The resulting mantle was a well-mixed solid with a near pyrolite composition. E.A.K.

N85-23549*# California Univ., Los Angeles. Dept. of Chemistry and Biochemistry.
HIGH PRESSURE COSMOCHEMISTRY OF MAJOR PLANETARY INTERIORS: LABORATORY STUDIES OF THE WATER-RICH REGION OF THE SYSTEM AMMONIA-WATER Abstract Only
Malcolm Nicol, Mary Johnson, and Andrea S. Koumvakalis *In* NASA, Washington Repts. of Planetary Geol. and Geophys. Program, 1984 Apr. 1985 p 212-213 refs (For primary document see N85-23474 13-91)
Avail: NTIS HC A99/MF A01 CSCL 03B

The behavior of gas-ice mixtures in major planets at very high pressures was studied. Some relevant pressure-temperature-composition (P-T-X) regions of the hydrogen (H_2)-helium (He)-water (H_2O-ammonia (NH_3)-methane (CH_4) phase diagram were determined. The studies, and theoretical model, of the relevant phases, are needed to interpret the compositions of ice-gas systems at conditions of planetary interest. The compositions and structures of a multiphase, multicomponent system at very high pressures care characterized, and the goal is to characterize this system over a wide range of low and high temperatures. The NH_3-H_2O compositions that are relevant to planetary problems yet are easy to prepare were applied. The P-T surface of water was examined and the corresponding surface for NH_3 was determined. The T-X diagram of ammonia-water at atmospheric pressure was studied and two water-rich phases were found, NH_3-$2H_2O$ (ammonia dihydrate), which melts incongruently, and $NH_3.H_2O$ (ammonia monohydrate), which is nonstoichiometric and melts at a higher temperature than the dihydrate. It is suggested that a P-T surface at approximately the monohydrate composition and the P-X surface at room temperature is determined. Author

N85-23550*# Arizona Univ., Tucson. Lunar and Planetary Lab.
THEORETICAL THERMODYNAMICS OF MIXTURES AT HIGH PRESSURES Abstract Only c77
W. B. Hubbard *In* NASA, Washington Repts. of Planetary Geol. and Geophys. Program, 1984 Apr. 1985 p 214-216 refs (For primary document see N85-23474 13-91)
(Grant NAGw-192)
Avail: NTIS HC A99/MF A01 CSCL 20M

The development of an understanding of the chemistry of mixtures of metallic hydrogen and abundant, higher-z material such as oxygen, carbon, etc., is important for understanding of fundamental processes of energy release, differentiation, and develop-

ment of atmospheric abundances in the Jovian planets. It provides a significant theoretical base for the interpretation of atmospheric elemental abundances to be provided by atmospheric entry probes in coming years. Significant differences are found when non-perturbative approaches such as Thomas-Fermi-Dirac (TFD) theory are used. Mapping of the phase diagrams of such binary mixtures in the pressure range from approx. 10 Mbar to approx. 1000 Mbar, using results from three-dimensional TFD calculations is undertaken. Derivation of a general and flexible thermodynamic model for such binary mixtures in the relevant pressure range was facilitated by the following breakthrough: there exists an accurate nd fairly simple thermodynamic representation of a liquid two-component plasma (TCP) in which the Helmholtz free energy is represented as a suitable linear combination of terms dependent only on density and terms which depend only on the ion coupling parameter. It is found that the crystal energies of mixtures of H-He, H-C, and H-O can be satisfactorily reproduced by the same type of model, except that an effective, density-dependent ionic charge must be used in place of the actual total ionic charge.
E.A.K.

N85-23551*# California Univ., Livermore. Lawrence Livermore Lab.
SHOCK COMPRESSION OF LIQUID HELIUM TO 56 GPa (560) KBAR Abstract Only **c25**
W. J. Nellis, N. C. Holmes, A. C. Mitchell, R. J. Trainor, G. K. Governo, M. Ross, and D. A. Young *In* NASA, Washington Repts. of Planetary Geol. and Geophys. program, 1984 Apr. 1985 p 217-219 refs Document previously announced as A84-48934 (For primary document see N85-23474 13-91)
Avail: NTIS HC A99/MF A01 CSCL 07D

Shock-wave data are presented for liquid helium which has been compressed to densities up to five times greater than the normal liquid. The helium was heated to temperatures up to 21,000 K, while the maximum pressure attained was 56 GPa. The properties of helium and hydrogen are important for modeling the giant planets Saturn and Jupiter where these elements are the major constituents. Conditions on Saturn are of particular interest because studies have suggested that this planet has an internal energy source which is associated with unmixing and gravitational separation the hydrogen-helium fluid at pressures below 1 TPa. The existence of this phase transition depends very sensitively on the hydrogen and helium equation of state. In the experiments, strong shock waves were generated by the impact of planar projectiles into cryogenic specimen holders. G.R. (IAA)

N85-23552*# Arizona Univ., Tucson. Lunar and Planetary Lab.
MODELLING EQUILIBRIUM AND FRACTIONAL CRYSTALLIZATION IN THE SYSTEM MgO-FeO-CaO-Al2O3-SiO2 Abstract Only **c76**
Floyd Herbert *In* NASA, Washington Repts. of Planetary Geol. and Geophys. Program, 1984 Apr. 1985 p 220-222 refs (For primary document see N85-23474 13-91)
Avail: NTIS HC A99/MF A01 CSCL 02L

A mathematical modelling technique for use in petrogenesis calculations in the system MgO-FeO-CaO-Al2O3-SiO2 is reported. Semiempirical phase boundary and elemental distribution information was combined with mass balance to compute approximate equilibrium crystallization paths for arbitrary system compositions. The calculation is applicable to a range of system compositions and fractionation calculations are possible. The goal of the calculation is the computation of the composition and quantity of each phase present as a function of the degree of solidification. The degree of solidification is parameterized by the heat released by the solidifying phases. The mathematical requirement for the solution of this problem is: (1) An equation constraining the composition of the magma for each solid phase in equilibrium with the liquidus phase, and (2) an equation for each solid phase and each component giving the distribution of that element between that phase and the magma. E.A.K.

N85-23553*# Massachusetts Inst. of Tech., Cambridge. Dept. of Earth, Atmospheric, and Planetary Sciences.
QUENCHING EFFECTS ON IRON SITE PARTITIONING IN THE APOLLO 17 ORANGE GLASS COMPOSITION Abstract Only **c25**
M. Darby Dyar *In* NASA, Washington Repts. of Planetary Geol. and Geophys. Program Apr. 1985 p 223-224 refs (For primary document see N85-23474 13-91)
Avail: NTIS HC A99/MF A01 CSCL 07D

Mare petrogenesis and the structure of the lunar interior were studied. Analyses of the spectral signatures of glasses was useful to remote sensing applications in areas of the moon where glass is in significant proportions in the lunar soil. The studies provided information on Fe site occupancies in glasses, which are used to construe oxygen fugacities at the lunar surface. Data were obtained through work on synthetic analogues of lunar glasses. However, recent Mossbauer studies of an Apollo 15 green glass composition have shown that synthetic glasses are extremely sensitive to variations in quenching media. Glass structure and Fe(3+)/Fe(2+) ratios are strongly controlled by quenching conditions, which may mask the effects of the original glass' formation temperature or oxygen partial pressure. Synthetic glasses were often run at low fugacities on Pt wires. The effects of quench media on the Apollo 17 orange glass composition are considered.
Author

N85-23554*# Massachusetts Inst. of Tech., Cambridge. Dept. of Earth, Atmospheric, and Planetary Science.
EXPERIMENTAL METHODS FOR QUENCHING STRUCTURES IN LUNAR-ANALOG SILICATE MELTS: VARIATIONS AS A FUNCTION OF QUENCH MEDIA AND COMPOSITION Abstract Only **c25**
M. Darby Dyar *In* NASA, Washington Repts. of Planetary Geol. and Geophys. Program Apr. 1985 p 225 Previously announced as A85-17669 (For primary document see N85-23474 13-91)
Avail: NTIS HC A99/MF A01 CSCL 07D

Compositions analogous to lunar green, organge, and brown glasses were synthesized under consistent conditions, then quenched into a variety of different media when the samples were removed from the furnace. Iron valence and coordination are a direct function of quench media used, spanning the range from brine/ice (most effective quench), water, butyl phthalate, silicone oil, liquid nitrogen, highly reducing CO-CO2 gas, to air (least efficient quench). In the green and brown glasses, Fe(3+) in four-fold and six-fold coordination is observed in the slowest-quenched samples; Fe(2+) coordination varies directly with quench efficiency. Less pronounced changes were observed in the Ti-rich orange glass. Therefore the remote-sensed spectrum of a glass-bearing regolith on the Moon may be influenced by the process by which the glass cooled, and extreme caution must be used when comparing spectra of synthetic glass analogs with real lunar glasses.
Author (IAA)

N85-23555*# Massachusetts Inst. of Tech., Cambridge. Dept. of Earth, Atmospheric, and Planetary Science.
HIBONITE: CRYSTAL CHEMISTRY AND ORIGIN OF BLUE COLORATION IN METEORITIC ASSEMBLAGES Abstract Only **c25**
Roger G. Burns and Virginia Mee Burns *In* NASA, Washington Repts. of Planetary Geol. and Geophys. Program Apr. 1985 p 226-228 refs (For primary document see N85-23474 13-91)
Avail: NTIS HC A99/MF A01 CSCL 07D

The blue color and optical spectra of hibonite, a common constituent of refractory inclusions in carbonaceous chondrites, are discussed. Because they may be manifestations of exotic cation species stabilized in unusual coordination sites in the hibonite crystalstructure. Hibonite, ideally CaAl12O19, is conducive to atomic substitution of host Ca2+ and Al3+ ions by a variety of lanthanide and first series transition elements. The latter cations are responsible for the colors of many rock-forming minerals as a result of intraelectronic or intervalence transitions. The visible-region spectra of most oxide and silicate minerals are generally well understood. Assignments of absorption bands in meteoritic hibonite optical spectra due to uncertainties of cation valencies and complexities in the crystal structure are examined. The crystal

chemistry of hibonite is reviewed, Mossbauer spectral measurements of iron-bearing hibonite and electronic transitions that may be responsible for the blue coloration of meteoritic hibonites are discussed. Author

N85-23556*# Massachusetts Inst. of Tech., Cambridge. Dept. of Earth, Atmospheric, and Planetary Science.
CRYSTAL CHEMISTRY OF METEORITIC HIBONITES Abstract Only **c76**
Roger G. Burns and Virginia Mee Burns *In* NASA, Washington Repts. of Planetary Geol. and Geophys. Program Apr. 1985 p 228 Previously announced as A85-17675 (For primary document see N85-23474 13-91)
Avail: NTIS HC A99/MF A01 CSCL 20L

The characteristics of cation vacancies and site occupancies of natural hibonites in meteors are discussed. Note is taken of the effect of the specific locations of the hibonites in the matrices on the crystal chemistry, electronic stabilities, and spectral features of the metal ions which replace the Al(3+). Hibonites form beta-alumina hexagonal cells with 26 cation sites. Fe cations are found in octahedral, tetrahedral, and five-fold coordinates. Fe(2+) is found in face-shared Al(3) octahedra, a siting explained in terms of ionic radius and crystal field stabilization energy criteria. Spectral colors are attributed to V(3+) and Ti(3+) field transitions at 400 and 700 nm, respectively, although the 700 nm line may arise from transitions of Ti(3+) to Ti(4+) or Fe(2+) to Fe(3+) during heating. Excesses of Mg-26 can be traced to decay of nebular Al-26. M.S.K. (IAA)

N85-23557*# Arizona State Univ., Tempe. Dept. of Chemistry and Geology.
MAGMAS AS SELECTIVE FILTERS OF VOLATILES BETWEEN PLANETARY MANTLES AND SURFACES Abstract Only
John R. Holloway and Sigurdur Jakobsson *In* NASA, Washington Repts. of Planetary Geol. and Geophys. Program Apr. 1985 p 229-231 refs (For primary document see N85-23474 13-91)
Avail: NTIS HC A99/MF A01 CSCL 03B

The composition of early planetary atmospheres and biospheres which is a knowledge of the relationship between mantle volatiles and volcanic gases was analyzed. In the case of Earth it appears that volcanic rocks and gases are relatively oxidized compared to the upper mantle. In the case of the C-O-H volatiles, (H2O, CO2, CO, CH4, H2) the volcanic gases are enriched in H2O and CO2 while the volatiles in the mantle may be dominated by H2O, H2 and possibly CH4. An experimental technique was perfected for phase equilibrium studies in the 5-30 kbar range which allows accurate control of volatile species activities in the fluid phase. The system was used to measure the relative solubilities of H2O, CO2, CO, CH4 and H2 in magmas at 10 kbar pressure. It is found that mantle magmas will selectively screen volatiles from planetary surfaces, forcing volcanic gases towards the neutral QFM oxidation state where H2O is the dominant species. E.A.K.

N85-23558*# Washington Univ., St. Louis, Mo. Center for the Space Sciences.
THE EVOLUTION OF CO2 ON MARS Abstract Only
Ralph Kahn *In* NASA, Washington Repts. of Planetary Geol. and Geophys. Program Apr. 1985 p 232-234 (For primary document see N85-23474 13-91)
Avail: NTIS HC A99/MF A01 CSCL 03B

The consequences of the hypothesis that the evolution of CO2 is directly linked to the occurrence of at least transitory pockets of moisture were exposed. The current conditions preclude the existence of open bodies of liquid water and the formation of moisture in disequilibrium is not excluded by any known constraints. The water evaporation rate is inversely proportional to PCO2, and the existence of a limiting value (P*) for which liquid water can form in the Mars environment is postulated. The evolution of PCO2 is controlled largely by relatively rapid aqueous chemistry forming carbon-containing sedimentary rocks, perhaps during early history in open water, but more recently in transitory pockets of moisture in the soil. Once the total atmospheric pressure is reduced to near P*, the occurrence of transitory moisture is inhibited, and atmospheric CO2 is no longer depleted by an efficient mechanism. The role of the carbonate reservoir in the current overall carbon budget on Mars, according to this scheme, is illustrated. E.A.K.

N85-23559*# Northeast Louisiana State Coll., Monroe. Dept. of Geosciences.
RIDGED PLAINS OF LUNAE PLANUM: THICKNESS DISTRIBUTION REVISED Abstract Only
R. A. DeHon *In* NASA, Washington Repts. of Planetary Geol. and Geophys. Program Apr. 1985 p 237-238 refs (For primary document see N85-23474 13-91)
Avail: NTIS HC A99/MF A01 CSCL 03B

New data are used to revise the isopach of plains-forming material in the Lunae Planum region. The distribution of data points in the region has not increased; consequently, the new map is still valid for generalized thickness trends only. The isopach map is based on a total of 65 points; 32 points represent thickness estimates at partially buried craters. The remaining 33 points define the limits of plains-forming materials (zero thickness). Suitable buried craters are randomly distributed and sparse near the western edge and northern portion of the area. The overall thickness trend is similar to the previously mapped distribution, but there is a significant reduction in thickness values. E.A.K.

N85-23560*# Iowa Univ., Iowa City. Dept. of Geology.
VOLCANIC DEBRIS FLOWS IN THE ELYSIUM REGION OF MARS Abstract Only
Eric H. Christiansen and Michael P. Ryan *In* NASA, Washington Repts. of Planetary Geol. and Geophys. Program Apr. 1985 p 239-241 refs (For primary document see N85-23474 13-91)
Avail: NTIS HC A99/MF A01 CSCL 03B

Photogeologic studies of the Elysium volcanic province appear to provide a specific example of the importance of volcanic-ice interaction to produce the channels of Hrad and Granicus Valles. In addition, these studies shows that the channels lie on the surface of a large sedimentary deposit which is interpreted as an accumulation of volcanic debris flows or lahars. In spite of some similarities with Martian outflow channels, this latter difference may distinguish the Elysium channels from other types of Martian channels. Geologic relations are described which demonstrate that the debris flows formed amidst other volcanic activity in the Elysium region thereby suggesting that the magmatism was important to the generation of the mobilizing liquid. The lahars resulted from the melting of ground ice and liquefaction of subsurface materials. The intersection of this fluid reservoir with the regional fracture system lead to the rapid expulsion of a muddy slurry down the steep western slope of the province. A.R.H.

N85-23561*# Northeast Louisiana State Coll., Monroe. Dept. of Geosciences.
THICKNESS OF RIDGED PLAINS MATERIALS IN HESPERIA PLANUM, MARS Abstract Only
R. A. DeHon *In* NASA, Washington Repts. of Planetary Geol. and Geophys. Program Apr. 1985 p 242-244 refs (For primary document see N85-23474 13-91)
Avail: NTIS HC A99/MF A01 CSCL 03B

The thickness distribution of plains-forming materials in Hesperia Planum is determined by the diameter of partially buried craters. As with all Martian thickness studies, the distribution of measured thicknesses is sparse due to a low number of suitable partially buried craters. The resulting isopach of plains materials has a low level of confidence but is sufficient for generalized thickness trends. The mean of the thickness estimates is 360 + or - 120 m. The isopach of plains-forming materials exhibits an uneven thickness distribution. Average thickness, determined by grid sampling over the region, is 216 + or - 153 m. Local lenses exceed 500 m. A fifth order trend surface provides a partial match (coefficient of correlation = 0.657) to the isopach. A.R.H.

N85-23562*# Jet Propulsion Lab., California Inst. of Tech., Pasadena.
ESTIMATES OF LAVA ERUPTION RATES AT ALBA PATERA,

MARS Abstract Only
Stephen M. Baloga and David C. Pieri *In* NASA, Washington Repts. of Planetary Geol. and Geophys. Program Apr. 1985 p 245-247 refs (For primary document see N85-23474 13-91)
Avail: NTIS HC A99/MF A01 CSCL 03B

The Martian volcanic complex Alba Patera exhibits a suite of well-defined, long and relatively narrow lava flows qualitatively resembling those found in Hawaii. Even without any information on the duration of the Martian flows, eruption rates (total volume discharge/duration of the extrusion) estimates are implied by the physical dimensions of the flows and the likely conjecture that Stephan-Boltzmann radiation is the dominating thermal loss mechanism. The ten flows in this analysis emanate radially from the central vent and were recently measured in length, plan areas, and average thicknesses by shadow measurement techniques. The dimensions of interest are shown. Although perhaps morphologically congruent to certain Hawaiian flows, the dramatically expanded physical dimensions of the Martian flows argues for some markedly distinct differences in lava flow composition for eruption characteristics. R.J.F.

N85-23563*# Hawaii Univ., Honolulu. Inst. of Geophysics.
EMPLACEMENT OF LONG LAVA FLOWS ON MAUNA LOA (HAWAII) AND ALBA (MARS) Abstract Only
P. J. MouginisMark, G. P. L. Walker, L. R. Gaddis, S. Rowland, and L. Wilson (Lancaster Univ., England) *In* NASA, Washington Repts. of Planetary Geol. and Geophys. Program Apr. 1985 p 248-250 refs (For primary document see N85-23474 13-91)
Avail: NTIS HC A99/MF A01 CSCL 03B

Spacecraft images revealed that extremely long lava flows (more than 200 km long) exist on the surface of Mars and Io. Compared to terrestial volcanic eruptions, the occurrence of these long flows is very unusual, and may hint at a different style of either magma production or eruption. Attempts to model the emplacement of the long flows on other planets, using a Bingham rheological model, were only partially successful. The objective is to conduct field measurements on long lava flows in Hawaii (where individual flows such as those of 1859 and 1881 exceed 40 km in length) in order to document and interpret their flow characteristics. In this way, a better understanding of the formation of long lava flows is sought as well as a determination of whether the Mauna Loa flows are terrestrial analogs to the long flows seen on Mars and Io. R.J.F.

N85-23564*# Jet Propulsion Lab., California Inst. of Tech., Pasadena.
THERMAL INFRARED OBSERVATIONS OF LAVA FLOWS DURING THE 1984 MAUNA LOA ERUPTION Abstract Only **c46**
David C. Pieri, R. Gillespie, Ann B. Kahle, James Kahle (California Div. of Mines and Geology), and Stephen M. Baloga *In* NASA, Washington Repts. of Planetary Geol. and Geophys. Program Apr. 1985 p 251-255 refs (For primary document see N85-23474 13-91)
Avail: NTIS HC A99/MF A01 CSCL 08K

Thermal infrared videotape images of the flowing lava streams and the vent areas at 10.6 microns were made, as well as some broadband images in the 8 to 12 micron range (for gas plume detection). These data were calibrated with on-site hand-held radiometer measurements, in-flow thermocouple measurements, and with later laboratory kiln measurements. Infrared video data are useful in quantitatively assessing the pattern and mode of flow thermal losses, particularly with regard to radiative losses from established/incipient floating crust. The general cooling of the flows downstream was readily apparent. Upper reaches of the active flow exhibited nearly crust-free main channels, radiating at about 700 to 800 degrees C. Below about the 7500 foot level (about 8 km from the vent) the flows formed nearly continuous crust and tended to spread, become less well-defined and founder due to a reduction in slope. Nevertheless, in thermal IR observations, the surface trace of the active subsurface channel was visible, radiating at about 500 to 700 degrees C. At the active flow front, most solid crust radiated at temperatures less than 500 to 600 degrees C, however bright high temperature interiors (approximately 900 to 1000 degrees C) were clearly visible though evolving fissures. R.J.F.

N85-23565*# Arizona State Univ., Tempe. Dept. of Geology.
FIELD MEASUREMENTS OF THE 1983 ROYAL GARDENS LAVA FLOWS, KILAUEA VOLCANO, AND 1984 MAUNA LOA LAVA FLOWS, HAWAII Abstract Only **c46**
Jonathan Fink and Jim Zimbelman *In* NASA, Washington Repts. of Planetary Geol. and Geophys. Program Apr. 1985 p 256-258 refs (For primary document see N85-23474 13-91)
Avail: NTIS HC A99/MF A01 CSCL 08K

Theoretical models used in the remote determination of lava flow rheology and compositions rely on estimates of such geometric and flow parameters as volume flow rates, levee heights, and channel dimensions, as well as morphologic and structural patterns on the flow surfaces. Quantitative measures of these variables are difficult to obtain, even under optimum conditions. Detailed topographic profiles across several Hawaiian lava flows that were carefully monitored by the U.S. Geological Survey during their emplacement in 1983 were surveyed in order to test various flow emplacement models. Twenty two accurate channel cross sections were constructed by combining these profiles with digitized pre-flow topographic measurements. Levee heights, shear zone widths, and flow depths could then be read directly from the cross sections and input into the models. The profiles were also compared with ones constructed for some Martian lava flows. R.J.F.

N85-23566*# Hawaii Univ., Honolulu. Inst. of Geophysics.
SURFACE STRUCTURES OF HAWAIIAN LAVAS Abstract Only **c46**
Scott K. Rowland and George P. L. Walker *In* NASA, Washington Repts. of Planetary Geol. and Geophys. Program Apr. 1985 p 259-260 refs (For primary document see N85-23474 13-91)
Avail: NTIS HC A99/MF A01 CSCL 08L

Surface and internal lava structures can be valid indicators of lava viscosity and rheology, provided that care is taken to identify and eliminate structures which are strain-rate-dependent. Here, a spectrum of types among Hawaiian basaltic flows is found ranging from pahoehoe to a'a, that are interpreted as marking a progression in lava viscosity and a change in rheology. The most fluid type in this spectrum is normal pahoehoe that has a smooth but commonly wrinkled or folded (ropy) surface. The next type, distinctly more viscous and probably non-Newtonian in rheology, is spiny pahoehoe which is characterized by a spinose surface and an absence of ropy structures. Preliminary studies on the long lavas of Mauna Loa indicated, perhaps surprisingly, that there is no clear-cut correlation of lava length with type in this spectrum of lavas, indicating that viscosity/yield strength of the basaltic lavas per se are not the primary controls determining flow length. Flowage of the lava through lava tubes, while it may help to account for the long flow distance of some lavas, is not a generally applicable explanation for long flow length. R.J.F.

N85-23567*# Arizona State Univ., Tempe. Dept. of Geology.
BASALTIC PRESSURE RIDGES: FORMATION AND RELATIONSHIP TO FLOW EMPLACEMENT Abstract Only **c46**
E. Theilig *In* NASA, Washington Repts. of Planetary Geol. and Geophys. Program Apr. 1985 p 261-262 (For primary document see N85-23474 13-91)
Avail: NTIS HC A99/MF A01 CSCL 08G

Pressure ridges and pressure plateau are common but not ubiquitous surface features on terrestrial basaltic lava flows and may reflect a specific flow emplacement mechanism. Many of the ridges are large enough to be detected on high-resolution orbital images; therefore, understanding these features could provide a means for interpreting volcanic flows on the mechanism of pressure ridge formation and how their formation relates to flow emplacement. Results from detailed field studies indicate that pressure ridges and plateaus: (1) are emplaced as individual flow lobes, (2) can be composed of primary or secondary material, (3) are dependent on duration and volume of activity within the flow unit, (4) are penecontemporaneous in formation, and (5) are indicative

of slowly advancing flows with numerous flow lobes continuously forming and overriding each other. R.J.F.

N85-23568*# Oregon State Univ., Corvallis. Dept. of Geography.
MORPHOLOGIC EVOLUTION OF THE MOUNT ST. HELENS CRATER AREA, WASHINGTON Abstract Only c46
Gary L. Beach *In* NASA, Washington Repts. of Planetary Geol. and Geophys. Program Apr. 1985 p 263-265 refs (For primary document see N85-23474 13-91)
Avail: NTIS HC A99/MF A01 CSCL 08K

The large rockslide-avalanche that preceded the eruption of Mount St. Helens on 18 May 1980 removed approximately 2.8 cubic km of material from the summit and north flank of the volcano, forming a horseshoe-shaped crater 2.0 km wide and 3.9 km long. A variety of erosional and depositional processes, notably mass wasting and gully development, acted to modify the topographic configuration of the crater area. To document this morphologic evolution, a series of annual large-scale topographic maps is being produced as a base for comparitive geomorphic analysis. Four topographic maps of the Mount St. Helens crater area at a scale of 1:4000 were produced by the National Mapping Division of the U. S. Geological Survey. Stereo aerial photography for the maps was obtained on 23 October 1980, 10 September 1981, 1 September 1982, and 17 August 1983. To quantify topographic changes in the study area, each topographic map is being digitized and corresponding X, Y, and Z values from successive maps are being computer-compared. R.J.F.

N85-23569*# New Mexico Univ., Albuquerque. Dept. of Geology.
VOLCANISM OF THE COLORADO PLATEAU (BASIN AND RANGE TRANSITION): IMPLICATIONS FOR CRUSTAL PROCESSES Abstract Only c46
Christopher D. Condit and Wolfgang E. Elston *In* NASA, Washington Repts. of Planetary Geol. and Geophys. Program Apr. 1985 p 266-268 refs (For primary document see N85-23474 13-91)
Avail: NTIS HC A99/MF A01 CSCL 08K

On the Colorado Plateau-Basin and Range transition in Arizona and New Mexico, basaltic volcanism takes two physiographic forms: (1) Major central composite volcanoes (e.g., San Francisco Peaks) in which basaltic magma differentiates at shallow crustal levels to siliceous and members and (2) large numbers of small cinder cones and a few domes that result from numerous discrete magma batches which apparently had little opportunity for differentiation. This study represents the first look at the petrogenesis of Plateau-bounding volcanic fields, based on rigorous stratigraphic controls, in combination with major and trace-element constraints. The emerging pattern of large volcanic constructs associated with shallow fractional crystallization, and numerous cinder cones associated with limited or no shallow differentiation may provide an analogue for interpreting petrogenetic patterns and/or tectonic settings on Mars. R.J.F.

N85-23570*# State Univ. of New York, Buffalo. Dept. of Geological Sciences.
THE GEOLOGY OF EAST BUTTE, A RHYOLITIC VOLCANIC DOME ON THE EASTERN SNAKE RIVER PLAIN, IDAHO Abstract Only c46
John E. Bretches and John S. King *In* NASA, Washington Repts. of Planetary Geol. and Geophys. Program Apr. 1985 p 269-271 refs (For primary document see N85-23474 13-91)
Avail: NTIS HC A99/MF A01 CSCL 08G

East Butte is a prominent volcanic dome located on the eastern Snake River Plain. It is situated 51 km west of Idaho Falls in the southeast corner of the Idaho National Engineering facility. East Butte rises 350 meters above the Quaternary basalt flows which encircle its 2.4 kilometer diameter base. Its maximum elevation is 2003 meters above sea level. East Butte is composed dominantly of rhyolite. Armstrong and others (1975) determined a K-Ar age of 0.6 +/- m.y. for a rhyolite sample from East Butte. Detailed geologic mapping revealed East Butte to be a single, large cumulo-dome composed dominantly of rhyolite. Major element geochemical analyses indicate that the rhyolite of East Butte is mildly peralkaline (molecular excess of Na2O and K2O over Al2O3 and compositionally homogeneous. Color variations in the East Butte rhyolite result from varying amounts of chemical and physical weathering and to the degree of devitrification that the glass in the groundmass of the rhyolite underwent. R.J.F.

N85-23571*# State Univ. of New York, Buffalo. Dept. of Geological Sciences.
THE GEOLOGY OF MT. HOPE, A SILICIC VOLCANIC CENTER IN WEST CENTRAL ARIZONA Abstract Only c46
Ardyth M. Simmons and John S. King *In* NASA, Washington Repts. of Planetary Geol. and Geophys. Program Apr. 1985 p 272-274 refs (For primary document see N85-23474 13-91)
Avail: NTIS HC A99/MF A01 CSCL 08G

The purpose was to establish a detailed history of the sequence of geologic events which occurred at Mt. Hope and an area 6.8 miles in diameter surrounding it. The final result will be comprised of information collected during field mapping, with data from petrographic studies and wet chemical analyses. From this it should be possible to suggest relationships to other volcanic regions, particularly bimodal suites in the transition zone, and gain a clearer picture of the petrologic nature of this area. Field work conducted this past summer confirmed the bimodal nature of volcanism at Mt. Hope. The symmetrical, radial cone is comprised of several rhyolites with numerous intrusions of intermediate-composition dikes and two breccia pipes near the summit. R.J.F.

N85-23572*# Arizona State Univ., Tempe. Dept. of Geology.
A SILICIC SHIELD VOLCANO IN BOLIVIA Abstract Only c46
P. R. Christensen and R. Greeley *In* NASA, Washington Repts. of Planetary Geol. and Geophys. Program Apr. 1985 p 275-276 refs (For primary document see N85-23474 13-91)
Avail: NTIS HC A99/MF A01 CSCL 08L

Volcan Quemado and its environs provides an excellent site to study the radar signature of a silicic volcanic construct. This feature differs from basaltic terrains primarily by the evidence of explosive eruptions associated with silica-rich magmas. These explosions produced a complex of distinctive craters that are visible on radar because of their steep inner walls and exposed bedrock units. Explosive events also generated surface deposits of fine (1 mm to 10 cm) material that mantles the region around the volcano to a distance of 20 to 30 km from its center. These features are very different from those observed on basaltic flows, which typically lack violet, explosive events. In these terrains, the surface is dominated by radar-rough flows with steep, lobate flow fronts. Craters are less common, although maars are found in some regions. These comparisons suggest that spaceborne radar may be able to distinguish surface characteristics that can be used to identify volcanic eruptive styles on Venus, Mars, and other solar-system bodies. R.J.F.

N85-23573*# Hawaii Univ., Honolulu. Inst. of Geophysics.
SUBMARINE VOLCANIC ERUPTIONS AND POTENTIAL ANALOGS FOR VENUS Abstract Only c46
L. Wilson, P. J. MouginisMark, P. Fryer, and L. R. Gaddis *In* NASA, Washington Repts. of Planetary Geol. and Geophys. Program Apr. 1985 p 277-279 refs (For primary document see N85-23474 13-91)
Avail: NTIS HC A99/MF A01 CSCL 08K

As part of an analysis program to better understand the diversity of volcanic processes on the terrestrial planets, an investigation of the volcanic landforms which exist on the Earth's ocean floor was initiated. In part, this analysis is focused toward gaining a better understanding of submarine volcanic landforms in their own right, but also it is hoped that these features may show similarities to volcanic landforms on Venus, due to the high ambient water (Earth) and atmospheric (Venus) pressures. A series of numerical modelling experiments was performed to investigate the relative importance of such attributes as water pressure and temperature on the eruption process, and to determine the rate of cooling and emplacement of lava flows in the submarine environment. Investigations to date show that the confining water pressure and the

buoyancy effects of the surrounding water significantly affect the styles of volcanism on the ocean floor. In the case of Venusian volcanism, confining pressures will not be as great as that found at the ocean's abyssal plains, but nevertheless the general trend toward reducing magma vesiculation will hold true for Venus as well as the ocean floor. Furthermore, other analogs may also be found between submarine volcanism and Venusian activity. R.J.F.

N85-23574*# Arizona State Univ., Tempe. Dept. of Geology.
HYDROVOLCANISM Abstract Only **c46**
Michael F. Sheridan and Kenneth H. Wohletz (LASL) *In* NASA, Washington Repts. of Planetary Geol. and Geophys. Program Apr. 1985 p 280-282 refs (For primary document see N85-23474 13-91)
Avail: NTIS HC A99/MF A01 CSCL 08K

Hydrovolcanism is a common phenomena produced by the interaction of magma or magmatic heat with an external source of water, such as a surface body, an aquifer, or a glacier. The effects include hydrofracture of existing rock units in the subsurface and the formation of hyaloclastites in a subaqueous environment. Hydroexplosions originate within a few kilometers of the surface. They may be relatively small, phreatic events or devastating complex blasts. Large-scale experiments determined that the optimal mixing ratio of water to basaltic melt (thermite plus silicates) for efficient conversion of thermal energy into mechanical energy is in the range of 0.1 to 0.3. Based on experimental results, eruptions can be classified as dominantly magmatic if the ratio of external water to magma is less than 0.2. Eruptions with water/melt ratios in the range of 0.2 to 1.0 are highly explosive and carry tephra in a hot vapor that contains dominantly superheated (dry) steam. R.J.F.

N85-23575*# Geological Survey, Menlo Park, Calif.
OBSERVED CHANGES AT VIKING LANDER 1 Abstract Only
Henry J. Moore *In* NASA, Washington Repts. of Planetary Geol. and Geophys. Program Apr. 1985 p 285-289 refs (For primary document see N85-23474 13-91)
Avail: NTIS HC A99/MF A01 CSCL 03B

A local dust storm raged in Chryse Planitia, Mars, in June 1981. The changes wrought in the vicinity of the lander (Mutch Memorial Station) by this storm sometime near Sol 1742 were partly described previously. Here, changes related to the storm are itemized, evidence for wind directions during the peak of the storm are cited, and two observations unrelated to the storm are noted. The observations suggest that the eroding winds of the Sol 1742 storm were more easterly (N. 35 deg to 90 deg E.) than those (N. 5 deg to 11 deg E.) that formed the large wind tails; and fragments in erosional residues are 0.7 cm and larger, but smaller ones may be present. Some fragments 0.4 to 0.5 cm and smaller were somehow removed, at least locally; wind speeds of the 1742 local storm were probably greater than those of a previous local dust storm (25 to 30 m/s) that occurred during the same season on Sol 423 because the earlier storm did not alter the surface; the major, if not entire, amount of erosion by the storm occurred between Sols 1728 and 1757; and erosion chiefly occurred where the surface configuration and material properties were altered by the lander and its sampler. R.J.F.

N85-23576*# Cornell Univ., Ithaca, N.Y. Lab. for Planetary Studies.
SEASONAL AND SECULAR VARIATION OF THE SOLIS LACUS ALBEDO FEATURE: RELATION TO THE MARTIAN DUST-TRANSPORT CYCLE Abstract Only
Steven W. Lee *In* NASA, Washington Repts. of Planetary Geol. and Geophys. Program Apr. 1985 p 290-292 refs (For primary document see N85-23474 13-91)
Avail: NTIS HC A99/MF A01 CSCL 03B

As documented over the course of thirty-six Martian years, dramatic seasonal and secular variations occur in albedo features in the Solis Planum region of Mars. The most striking of these is the classical dark albedo features, Solis Lacus. Solis Lacus is generally most distinct during southern spring and summer. Mariner 9 and Viking Orbiter images reveal that Solis Lacus contains and is surrounded by a conspicuous pattern of bright and dark wind streaks. A seasonal dust-transport cycle is proposed to explain these observations. During later southern spring or early summer, dust is eroded from the surface and transported from the region by local dust storms which may become a global dust storm. Removal of dust over a wide area results in the dark Solis Lacus feature. During the cessation stage of global dust-storm activity (typically mid- to late-southern summer), enhanced deposition in the lee of obstacles forms the prominent patterns of bright streaks observed within and around Solis Lacus. As the year progresses (southern fall and winter), sedimentation from the atmospheric dust load occurs over the entire region, decreasing the contrast of the albedo features to their surroundings. Dust-storm activity the following year renews the cycle by again removing dust from the region. R.J.F.

N85-23577*# Cornell Univ., Ithaca, N.Y. Lab. for Planetary Studies.
EOLIAN EROSION ON MARS: THREE SCALES Abstract Only
P. G. Thomas *In* NASA, Washington Repts. of Planetary Geol. and Geophys. Program Apr. 1985 p 293-294 refs (For primary document see N85-23474 13-91)
Avail: NTIS HC A99/MF A01 CSCL 03B

Formation and erosion of deposits on Mars with vertical scales of 100 to 1,000 meters and horizontal scales of >100 km may have occurred at rates very different from present ones. Evidence for the rates on small scales comes from observations of dust storms and photometry of wind streaks. These observations cover scales less than 1 cm vertically and time scales less than 10 years. Intermediate scale features such as yardangs and sand dunes are more difficult to evaluate, but for dunes, plausible rates of transport may be calculated. Net eolian action in some areas may be so low that in order to study the large features one needs to select those likely to have been modified more rapidly and that exhibit distinctive contrasts with surrounding areas. Best suited for such study are relatively soft deposits overlying more resistant substrates. Viking Orbiter images of four of the largest such areas were examined to test how the erosional features correlate with patterns attributable to winds, properties of deposits, or non-eolian erosion, and for constraints on erosion and transport rates. R.J.F.

N85-23578*# Arizona State Univ., Tempe. Dept. of Geology.
THE ORIGIN OF REGIONAL DUST DEPOSITS ON MARS Abstract Only
P. R. Christensen *In* NASA Washington Repts. of Planetary Geol. and Geophys. Program Apr. 1985 p 295-296 refs (For primary document see N85-23474 13-91)
Avail: NTIS HC A99/MF A01 CSCL 03B

Recently, additional evidence was derived from the Viking Infrared Thermal Mapper observations that allows a more complete model for the formation of Low Thermal inertia-high Albedo regions to be proposed. The first observation is that dust appears to be currently accumulating in the low thermal inertia regions. Following each global dust storm a thin layer of dust is deposited globally, as evidenced by an increase in surface albedo seen from orbit and from the Viking Lander sites. During the period following the storm, the bright dust fallout is subsequently removed from low albedo regions, as indicated by the post-storm darkening of these surfaces and by an increase in the atmospheric dust content over dark regions relative to the bright, low thermal inertia regions. Thus, the fine dust storm material is removed from dark regions but not from the bright regions, resulting in a net accumulation within the bright, low thermal inertia regions. Once deposition has begun, the covering of exposed rocks and sand and the accumulation of fine material on the surface make removal of material increasingly difficult, thereby enhancing the likelihood that material will accumulate within the low thermal inertia regions. R.J.F.

N85-23579*# Washington Univ., St. Louis, Mo. Center for the Space Sciences.
ON THE LATITUDINAL DISTRIBUTION OF DEBRIS IN THE NORTHERN HEMISPHERE OF MARS Abstract Only
E. A. Guinness, C. E. Leff, and R. E. Arvidson *In* NASA, Washington

Repts. of Planetary Geol. and Geophys. Program Apr. 1985 p 297-299 refs (For primary document see N85-23474 13-91)
Avail: NTIS HC A99/MF A01 CSCL 03B

Examination of Mariner 9 images showed evidence of debris mantling on Mars. The evidence included craters that appeared to be filled with debris and an apparent lack of small craters. Based on such data, it was suggested that a circumpolar debris mantle exists poleward of about 30N and 30S latitudes. The presence of a debris layer has important implications for the modulation over time of atmospheric pressure by the cap-regolith-atmosphere system. Preliminary efforts in providing constraints on the thickness and distribution of debris are discussed. The initial approach is to examine crater size-frequency data for selected regions on Mars, later expanding the study to include an inventory of aeolian features and other direct indicators of debris deposition. The crater size-frequency distributions for ten regions between latitudes 20N and 80N and covering a range of longitudes were discovered. Crater data were derived from Viking Orbiter images with resolutions of between 26 and 75 meters/pixel. R.J.F.

N85-23580*# Jet Propulsion Lab., California Inst. of Tech., Pasadena.
TRANSFORMATION OF POLAR ICE SUBLIMATE RESIDUE INTO MARTIAN CIRCUMPOLAR SAND Abstract Only
R. Stephen Saunders, Timothy J. Parker, James B. Stephens, Eric G. Laue, and Fraser P. Fanale (Hawaii Univ.) *In* NASA, Washington Repts. of Planetary Geol. and Geophys. Program Apr. 1985 p 300-302 refs (For primary document see N85-23474 13-91)
Avail: NTIS HC A99/MF A01 CSCL 03B

The experimental demonstration that a credible Martian sand may be formed from dust-bearing ice provides a new set of possible explanations for some of the observed Martian aeolian landforms. It is hypothesized that a light-weight fluffy rind is formed on the polar caps. This could provide material easily entrainable by Martian winds, which generally blow equatorward from the poles. These winds would peel the fluffy rind from the surface of the subliming summer polar caps and from the equatorward slopes of the polar troughs. These pieces of material would then be rolled into lumps (of high sailarea/mass ratio) by the wind. They would become pigmented as they saltate across the surface, perhaps gathering carbonaceous meteoritic dust or other impurities on their surfaces, or through chemical reactions with the ice-free environment away from their point of origin. Once they became trapped in topographic wind shadows, they would form dune structures because they are hydraulically equivalent to sand particles. R.J.F.

N85-23581*# Arizona State Univ., Tempe. Dept. of Geology.
THE EFFECT OF PARTICLE DENSITY ON AEOLIAN TRANSPORT Abstract Only
S. H. Williams and R. Greeley *In* NASA, Washington Repts. of Planetary Geol. and Geophys. Program Apr. 1985 p 303-304 refs (For primary document see N85-23474 13-91)
Avail: NTIS HC A99/MF A01 CSCL 03B

A set of experiments using a wide range of particle densities was performed in an open-circuit, terrestrial-atmospheric-pressure wind tunnel at Arizona State University. The results show that saltation flux equations derived for typical geologic material overpredict the flux of low-density particles. Walnut shells (approximately 1.1 g/cc) were used in the experiment and correspond to volcanic ash or ice. Less mass is transported by the wind in the case of low particle density because the style of transport is different. There is a direct, counter-intuitive relationship between particle density and transport height. Measurements of the vertical distribution of material show that the low-density walnut shells travel in a zone within 10 cm of the surface while high-density (approximately 4.5 g/cc) chromite particles travel as 50 cm. Furthermore, the overall saltation rate of the chromite is approximately four times greater than the walnut shells at the same freestream wind speed, even though the wind is much further above threshold for the walnut shells. R.J.F.

N85-23582*# Arizona State Univ., Tempe. Dept. of Geology.
A COMPARISON OF TERRESTRIAL SALTATION FLUX IN THE LABORATORY AND THE FIELD Abstract Only **c46**
S. H. Williams and R. Greeley *In* NASA, Washington Repts. of Planetary Geol. and Geophys. Program Apr. 1985 p 305-306 refs (For primary document see N85-23474 13-91)
Avail: NTIS HC A99/MF A01 CSCL 08G

Aeolian transport of surficial material is an important part of the terrestrial geologic cycle. In many areas of geological interest, sand is not transported by the wind at the rate predicted by studies made in idealized conditions. Furthermore, calculated surface-abrasion rates based on laboratory saltation fluxes are often unrealistically high. This work is an attempt to quantify and discuss discrepancies between saltation rates under ideal conditions and in the field under natural conditions. The saltation-flux data persented by Sharp (1) will be used as the field data. Sharp measured saltation flux during four periods in the early 1950's in the Whitewater River drainage. Meteorological conditions at the experiment site were extrapolated from the airport records and from wind speeds measured simultaneously by Hunter. Wind speeds above threshold were sorted into 4-MPH bins and the frequency of observation over each experimental period was calculated. A saltation flux for each bin was calculated and summed to yield a predicted saltation rate for that period. When the predicted fluxes were compared with those measured by Sharp, large discrepancies were found. R.J.F.

N85-23583*# Arizona State Univ., Tempe. Dept. of Geology.
POTENTIAL BEDFORMS ON VENUS: WIND TUNNEL SIMULATIONS Abstract Only
S. J. Bougan, J. R. Marshall, and R. Greeley *In* NASA, Washington Repts. of Planetary Geol. and Geophys. Program Apr. 1985 p 307-308 refs (For primary document see N85-23474 13-91)
Avail: NTIS HC A99/MF A01 CSCL 03B

Wind tunnel studies involving mixtures of particle sizes (bimodal and multimodal distributions) indicate the microdunes and related ridge- and wave-like structures can occur over a wider range of conditions. The results indicate that the bedforms develop as a consequence of the effective sorting capability of the high-density Venusian atmosphere. Four mixtures of different particle-size distributions were investigated. The results of these experiments suggest that: (1) small-scale bedforms on Venus may be more common than previously anticipated from simulations involving only unimodal sands; (2) small particles are rapidly sorted on Venus if winds slightly above threshold are available; (3) coarse particles are transported in traction within the bedforms as well as rolled by saltating fines, suggesting that the capacity of wind on Venus to transport material is greater than anticipated from previous flux studies and (4) microdunes and related ridges and waves with coarse and fine layers can be produced during sorting. R.J.F.

N85-23584*# Arizona State Univ., Tempe. Dept. of Geology.
MICRODUNES AND OTHER AEOLIAN BEDFORMS ON VENUS: WIND TUNNEL SIMULATIONS Abstract Only
R. Greeley, J. R. Marshall, and R. N. Leach (Santa Clara Univ., Calif.) *In* NASA, Washington Repts. of Planetary Geol. and Geophys. Program Apr. 1985 p 309 Previously announced as A85-12739 (For primary document see N85-23474 13-91)
Avail: NTIS HC A99/MF A01

The development of aeolian bedforms in the simulated Venusian environment has been experimentally studied in the Venus Wind tunnel. It is found that the development of specific bedforms, including ripples, dunes, and waves, as well as their geometry, are controlled by a combination of factors including particle size, wind speed, and atmospheric density. Microdunes are formed which are analogous to full-size terrestrial dunes and are characterized by the development of slip faces, internal cross-bedding, a low ratio of saltation path length to dune length, and a lack of particle-size sorting. They begin to develop at wind speeds just above saltation threshold and evolve into waves at higher velocities. At wind speeds of about 1.5 m/sec and higher, the bed is flat and featureless. This evolution is explained by a model based on

the interaction of alternating zones of erosion and deposition and particle saltation distances. C.B. (IAA)

N85-23585*# Arizona Univ., Tucson. Dept. of Geoscience.
PALEOHYDROLOGIC IMPLICATIONS OF VALLEY NETWORKS OF MARS Abstract Only
Victor R. Baker *In* NASA, Washington Repts. of Planetary Geol. and Geophys. Program Apr. 1985 p 313-315 refs (For primary document see N85-23474 13-91)
Avail: NTIS HC A99/MF A01 CSCL 03B

Valley networks in the heavily cratered terrains of Mars represent an ancient epoch of hydrologic conditions greatly different from those of today. Available crater counts on the valley networks indicate formation during the high flux of impacting bodies charaterizing the early heavy bombardment phase of Martian history. Two populations of valleys are recognized in the equatorial regions of Mars: pristine and degraded. The latter probably formed at the very end of the heavy bombardment phase, extending into the post-heavy bombardment by formation in the intercrater plains. Pristine valleys generally form segments of larger networks with degraded components. This suggests that valley formation was a prolonged process coeval with the heavy bombardment period and extending just beyond that period in martian history. The pristine networks and pristine portions of compound networks on Mars show morphological attributes consistent with an origin by headward growth through spring sapping. On Earth spring sapping occurs where groundwater out-streamflow can be generated by insolation changes associated with orbital parameters or with geothermal effects, such as might be associated with impact or with the volcanic emplacement of the intercrater plains. Thus, it is appropriate to specify the most conservation deviation from modern hydrologic conditions on Mars that could account for the ancient epoch of valley formation. R.J.F.

N85-23586*# Rhode Island Univ., Kingston. Dept. of Geology.
FLUVIAL DRAINAGE BASINS AND VALLEY NETWORKS: EASTERN MARGARITIFER SINUS, MARS Abstract Only
Jon C. Boothroyd and John A. Grant *In* NASA, Washington Repts. of Planetary Geol. and Geophys. Program Apr. 1985 p 316-318 refs (For primary document see N85-23474 13-91)
Avail: NTIS HC A99/MF A01 CSCL 03B

The fluvial drainage of the eastern Margaritifer Sinus (MC-19NE, SE) and northeastern Argyre (MC-26NE) Quadrangles is dominated by two major longitudinal valley networks, the Parana/Loire system on the east, and the Samara Himera system to the west. It is believed that both of these drainages are through-going to the northwest and debouch into Margaritifer Chaos (general location: 12S, 22.5W). The Parana/Loire drainage is bounded on the east in part by an ancient multi-ringed impact basin. The Parana multi-digitate network drains northwest into a depositional basin, and impact basin floor, characterized by positive relief chaos. It is believed that Loire Vallis heads in the basin; thus Parana and Loire Valles may be treated as one system. Samara Valles heads in the northeastern Argyre Quadrangle and extends as a major truck valley to the northwest. Samara Valles cuts through the hills forming one of the concentric rings of the Ladon impact basin and joins the Himera drainage to trend in a more northerly direction to Margaritifer Chaos. The downstream portion of Himera is considered to be part of the Samara R.J.F.

N85-23587*# Whittier Coll., Calif. Dept. of Geology.
CATASTROPHIC-FLOOD FEATURES IN SWEDISH LAPLAND AS A TERRESTRIAL ANALOG FOR MARTIAN CHANNEL FLOWS Abstract Only c43
Lisa A. Rossbacher and Dallas D. Rhodes *In* NASA, Washington Repts. of Planetary Geol. and Geophys. Program Apr. 1985 p 319-321 refs (For primary document see N85-23474 13-91)
Avail: NTIS HC A99/MF A01 CSCL 08H

Catastrophic flooding associated with deglaciation created unusual landscapes in several areas of northern Sweden. These areas in Swedish Lapland are distinguished by the large grain-size material that forms them. The presence of boulders at both Viking landing sites suggests the relevance of this analog. The Baldakatj area of Swedish Lapland offers terrestrial analogs for erosional remnants on Mars. Although the Baldakatj features are an order of magnitude or more smaller than the Martian forms, they created in boulder-rich till that may be a good approximation of the near-surface material on Mars. The Baldakatj area also includes other landforms that could reasonably be expected to occur with the Martian outflow channels, including boulder deltas, large transported blocks, and large-scale bedforms. R.J.F.

N85-23588*# Oregon State Univ., Corvallis. College of Oceanography.
EXPERIMENTS AND ANALYSES OF THE FORMATION OF EROSIONAL SCOUR MARKS WITH IMPLICATIONS TO THE ORIGIN OF THE MARTIAN OUTFLOW CHANNELS Abstract Only c46
Paul D. Komar *In* NASA, Washington Repts. of Planetary Geol. and Geophys. Program Apr. 1985 p 322-324 refs (For primary document see N85-23474 13-91)
Avail: NTIS HC A99/MF A01 CSCL 08G

The objectives of the present study of erosional scour marks on Mars involve flume experiments to examine the details of scour patterns around a variety of obstacle shapes, and to review the engineering literature on the scour around bridge piers to determine whether those results might provide a quantitative evaluation of the flows which formed the scour marks in the outflow channels. The flume experiments completed to date examined the scour which develops around a circular island and around a streamlined island (having a lemniscate shape with length/width = 3.0). The islands themselves are non-erodable solids, but are surrounded by a fine-grained sediment bed. The scour patterns which occur around the circular island agree with those produced by prototype bridge piers and by scale-model piers employed in the engineering studies. The scour patterns around the model streamlined islands correspond extremely well with those seen adjacent to the streamlined islands on Mars, providing still more confirmation for a water-flow origin. R.J.F.

N85-23589*# Arizona State Univ., Tempe. Dept. of Geology.
RELATIVE TIME-SCALE FOR CHANNELING EVENTS WITHIN CHAOTIC TERRAINS, MARGARITIFER SINUS, MARS Abstract Only
David Janke *In* NASA, Washington Repts. of Planetary Geol. and Geophys. Program Apr. 1985 p 325 (For primary document see N85-23474 13-91)
Avail: NTIS HC A99/MF A01 CSCL 03B

A relative time scale for ordering channel and chaos forming events was constructed for areas within the Margaritifer Sinus region of Mars. Transection and superposition relationships of channels, chaotic terrain, and the surfaces surrounding them were used to create the relative time scale; crater density studies were not used. Channels and chaos in contact with one another were treated as systems. These systems were in turn treated both separately (in order to understand internal relationships) and as members of the suite of Martian erosional forms (in order to produce a combined, master time scale). Channeling events associated with chaotic terrain development occurred over an extended geomorphic period. The channels can be divided into three convenient groups: those that pre-date intercrater plains development post-plains, pre-chasma systems; and those associated with the development of the Vallis Marineris chasmata. No correlations with cyclic climatic changes, major geologic events in other regions on Mars, or triggering phenomena (for example, specific impact events) were found. B.G.

N85-23590*# California State Polytechnic Univ., Pomona. Dept. of Earth Science.
TERRESTRIAL ANALOG STUDIES FOR MARTIAN PATTERNED GROUND Abstract Only c46
Lisa A. Rossbacher *In* NASA, Washington Repts. of Planetary Geol. and Geophys. Program Apr. 1985 p 329-331 refs Sponsored in part by Uppsala Univ., Sweden (For primary document see N85-23474 13-91)
(Grant NAGw-517)

Avail: NTIS HC A99/MF A01 CSCL 08G

A recurring problem in understanding Martian patterned ground is explaining its large size. Terrestrial patterned ground in Swedish Lapland offers an analog that may help explain this. In cold, arid regions with strong winds, polygonal features are accentuated paralled to the dominant wind direction. Preliminary results of a comparison between Martian polygonal troughs and dominant wind directions suggests a good correlation. This evolutionary model involving aeolian modification of Martian polygonal ground helps explain the large size features without requiring multiple, deep freeze-thaw cycles. A well-established geographical technique, nearest neighbor analysis, can be modified and applied to the distribution of patterned ground on Earth and Mars. The procedure determines the R-statistic, which reflects the degree to which on observation departs from an expected random pattern. The R-statistic is independent of scale, and therefore it can be applied to any size of type of pattern. Preliminary results indicate that there may be a correlation between the R-statistic and the process that create the polygons. B.G.

N85-23591*# Massachusetts Univ., Amherst. Dept. of Geology and Geography.

ORIGIN OF MARTIAN POLYGONAL TERRAIN: PRELIMINARY RESULTS Abstract Only

George E. McGill *In* NASA, Washington Repts. of Planetary Geol. and Geophys. Program Apr. 1985 p 332-334 refs (For primary document see N85-23474 13-91)

Avail: NTIS HC A99/MF A01 CSCL 03B

The morphological characteristics of Martian polygonal terrain, and of the fractures defining the polygons were reviewed. The age relationships between the fractures defining the polygons and the material making up the polygonal terrain of Adamas Labyrinthus will be determined. This involves detailed mapping, with the relative ages of Key map units and the fractures determined by superposition and crater counts. The common occurrence of circular fracture patterns within the polygonal terrain is consistent with differential compaction over crater rims, and is easily accounted for by the tensile stresses that would be reasonably expected to occur in such places. B.G.

N85-23592*# Geological Survey, Menlo Park, Calif.

RADIATION-DOMINATED SNOWMELT ON MARS Abstract Only

Gary D. Clow *In* NASA, Washington Repts. of Planetary Geol. and Geophys. Program Apr. 1985 p 335-336 refs (For primary document see N85-23474 13-91)

Avail: NTIS HC A99/MF A01 CSCL 03B

A set of microclimatic conditions conducive to the generation of liquid water is being sought to see whether their requirements are any less stringent than those suggested by the global-climatic models. In particular, the melting of snow and ice in the equatorial zone (where the valley networks are preferentially situated) is investigated with a model that includes detailed infrared radiation transfer between the atmosphere and the snow, penetration of sunlight into the snow, sensible heat transfer to the atmosphere, and water vapor diffusion within the surface boundary layer. IR fluxes are calculated by using pressure and temperature dependent forms for the band absorptances of CO2 and H2O in the spectral range 50 to 2000/cm. B.G.

N85-23593*# Hawaii Univ., Honolulu. Planetary Geosciences Div.

MARS: LONG TERM CHANGES IN THE STATE AND DISTRIBUTION OF H2O Abstract Only

Fraser P. Fanale, James R. Salvail, Aaron P. Zent, and Susan E. Postawko *In* NASA, Washington Repts. of Planetary Geol. and Geophys. Program, 1984 Apr. 1985 p 337 (For primary document see N85-23474 13-91)

Avail: NTIS HC A99/MF A01 CSCL 03B

A model for H2O distribution and migration on Mars was formulated which takes into account: (1) thermal variations at all depths in the regolith due to variations in obliquity, eccentricity and the solar constant; (2) variations in atmospheric PH2O caused by corresponding changes in polar surface insolation; and (3) the finite kinetics of H2O migration in both the regolith and atmosphere. Results suggest that regolith H2O transport rates are more strongly influenced by polar-controlled atmospheric PH2O variations than variations in pore gas PH2 brought about by thermal variations at the buried ice interface. The configuration of the ice interface as a function of assumed soil parameter and time is derived. Withdrawal of ice proceeds to various depths at latitudes <50 deg and is accompanied by filling of regolith pores at latitudes >50 deg and transfer of H2O to the polar cap. The transfer has a somewhat oscillatory character, but only $<$ 1g/sq cm is shifted into and out the regolith during each obliquity cycle. It is concluded that this process combined with periodic thermal cycles played a major role in development of the fretted terrain, deflationary features in general, patterned ground, the north polar cap and the layered terrain. M.G.

N85-23594*# Texas A&M Univ., College Station. Dept. of Geology.

PERMAFROST AND SUBSURFACE ICE IN THE SOLAR SYSTEM Abstract Only

Duwayne M. Anderson *In* NASA, Washington Repts. of Planetary Geol. and Geophys. Program, 1984 Apr. 1985 p 338-343 refs (For primary document see N85-23474 13-91)

Avail: NTIS HC A99/MF A01 CSCL 03B

The properties and behavior of planetary permafrost are discussed with reference to the ability of such surfaces to sustain loads characteristics of spacecraft landing and planetary bases. In most occurrences, water ice is in close proximity to, or in contact with, finely divided silicate mineral matter. When ice contacts silicate mineral surfaces, a liquid-like, transition zone is created. Its thickness ranges from several hundred Angstron units at temperatures near 0 degrees C to about three Angstrom units at -150 degrees C. When soluble substances are present, the resulting brine enlarges the interfacial zone. When clays are involved, although the interfacial zone may be small, its extent is large. The unfrozen, interfacial water may amount to 100% or more weight at a temperature of -5 degrees C. The presence of this interfacial unfrozen water acts to confer plasticity to permafrost, enabling it to exhibit creep at all imposed levels of stress. Nucleation processes and load-bearing capacity are examined. M.G.

N85-23595*# National Aeronautics and Space Administration. Goddard Space Flight Center, Greenbelt, Md.

MAPPING STRUCTURES CHARACTERISTIC OF THE HIGHLAND BOUNDARY SCARP ON MARS Abstract Only

Herbert Frey and Ann Marie Semeniuk *In* NASA, Washington Repts. of Planetary Geol. and Geophys. Program, 1984 Apr. 1985 p 347-349 (For primary document see N85-23474 13-91)

Avail: NTIS HC A99/MF A01 CSCL 03B

In an effort to shed some light on the processes which have produced the highlands/lowlands boundary scrap on Mars, the global distributions of knobby terrain, detached and separated blocks and mesas, and craters larger than 10 km diameter were mapped. These data were represented as fractional areal percentages of the sample box, which is 2.5 deg high (latitude) along north-south profiles every 5 deg in longitude. The fractional area of crater interiors provides a way of quantitatively characterizing the boundary between cratered highlands and relatively uncratered plains. In the vicinity of the nomimal scarp there is generally good agreement between the dropoff in fractional area of craters and a drop-off in topography. Contoured versions of the fractional area of crater interiors, even at the low resolution imposed by the sample box, show good agreement with the geologic mapping. The most northerly occurrence of detached plateaus and knobby terrain were located in order to test the plausibility of the hypothesis that much of the present day highland boundary scrap is due to southward migration of a former boundary. M.G.

N85-23596*# National Air and Space Museum, Washington, D.C. Center for Earth and Planetary Studies.

INVESTIGATIONS OF THE MARS CRATERED TERRAIN:

SMOOTH PLAINS BOUNDARY IN THE EASTERN EQUATORIAL REGION Abstract Only

Ted. A. Maxwell and Jeffrey D. Corrigan (Texas Univ., Austin) *In* NASA, Washington Repts. of Geol. and Geophys. Program, 1984 Apr. 1985 p 350-351 refs (For primary document see N85-23474 13-91)

Avail: NTIS HC A99/MF A01 CSCL 03B

As part of an ongoing study to place geologic constraints on, and to interpret the origin of the ancient cratered terrain - smooth plains boundary on Mars, structural features in the eastern hemisphere were mapped, looking at wide-scale variations in aereal percentage of crater vocer and distinctive landforms. Maps and a digitized data set for graben, scarps, ridges and elongate plateaus in the eastern hemisphere were completed for 30 deg N to 30 deg. In the equatorial region, results indicate a marked change from the N oriented ridges north of the boundary to the NW orientations of those in the inter and intracrater plains south of the boundary. The WNW orientation of the boundary itself is matched by similar orientations of graben and scraps in the southern terrain. In order to determine whether outlying plateaus and isolated knobby hills found north of the boundary are formed from material of the ancient cratered terrain, the Viking 2 approach color data were used to discriminate surface materials in the eastern hemisphere. In the southern half of the Amenthes quadrange (MC-14), several correlations exist among surficial spectral reflectance and observed geologic units. Old terrain on the eastern rim of the Isidis basin is much redder than the smooth volcanic plains on either side of the rim, even though the plains unit east of the rim is located several kilometers higher than the plains on the floor of Isidis. Based on statistics derived from the color data, the plains within Isidis were found to differ from those north of the boundary zone. M.G.

N85-23597*# University of Southern Illinois, Carbondale. Dept. of Geology.

MARTIAN FRETTED TERRAIN MORPHOMETRY INTERPRETED USING PRINCIPAL COMPONENTS ANALYSIS Abstract Only

R. Craig Kochell *In* NASA, Washington Repts. of Planetary Geol. and Geophys. Program, 1984 Apr. 1985 p 352-354 refs (For primary document see N85-23474 13-91)

Avail: NTIS HC A99/MF A01 CSCL 03B

Martian fretted terrain is an extensive area of complex topography characterized by smooth, flat-floor valleys and mesas separated by abrupt escarpments along the boundary of heavily cratered uplands. The Deuteronilus-Protonilus region of the fretted terrain between latitude 35 degrees N and 50 degrees N and between 305 degrees W and 350 degrees W longitude was selected for quantitative landform study with the use of principal components analysis (PCA). The morphometry of upland mesa remnants and debris aprons was digitized with respect to latitude, longitude, and distance from the cratered terrain boundary (CTB). The PCA demonstrates that there are definable spatial variations in morphology with respect to longitude and latitude which suggest that the degradation along the CTB proceeded toward the southwest. The PCA also showed that there are organized relationships within the fretted landforms irrespective of their location. Finally, PCA indicated that an orientation of the degraded mesas exists which may be controlled by structure. M.G.

N85-23598*# National Aeronautics and Space Administration. Goddard Space Flight Center, Greenbelt, Md.

DISTRIBUTION AND PROPERTIES OF LARGE SYMMETRIC KNOBS ON MARS Abstract Only

Herbert Frey, Jennifer Middleton, and Ann Marie Semeniuk *In* NASA, Washington Repts. of Planetary Geol. and Geophys. Program, 1984 Apr. 1985 p 355-357 (For primary document see N85-23474 13-91)

Avail: NTIS HC A99/MF A01 CSCL 03B

Knobby terrain on Mars exists in a variety of forms from small closely spaced hills to widely separated large massifs. Fractional areal distributions of knobby terrain range from over 49% of the sampled area in regions of chaotic terrain to less than 5% along the cratered highland boundary in Amenthes and Aeolis. All symmetric knobs with long dimensions greater than or equal to 10 km were identified, mapped, and classified by shape. The spatial and dimensional distributions and shape characteristics of these features are discussed. The most common shape is elliptical: 79% of the knobs fall into this category, 11% were circular or round, 6% were triangular or wedge-shaped and the remaining 4% other shapes. All types show a roughly similar trend of rapidly decreasing number with increasing size, such that overall less than 10% of the knobs are larger than 20 km in long dimension. Circular knobs show the steepest fall-off in numbers with increasing diameter. Triangular knobs have a broader maximum with more than 65% falling in the 10 to 14 km range. M.G.

N85-23599*# Kansas State Univ., Manhattan. Dept. of Geology.

ENIGMATIC HILLS OF THE MOTTLED PLAINS, MARE ACIDALIUM QUADRANGLE (MC-4), MARS Abstract Only

Nanci E. Witbeck (Geological Survey, Flagstaff, Ariz.) and James R. Underwood, Jr. *In* NASA, Washington Repts. of Planetary Geol. and Geophys. Program, 1984 Apr. 1985 p 358-360 refs (For primary document see N85-23474 13-91)

Avail: NTIS HC A99/MF A01 CSCL 03B

Interpretations of Mariner 9 and Viking images of the mottled plains in Mare Acidalium are present and discussed. Although the boundaries between all the units are gradational, four subdivisions were recognized within the mottled plains region. One of these subdivisions was designated hummocky mottled plains. The unit is characterized by many small (<1 km), irregularly spaced dark hills surrounded by brighter material. One very poor-quality, high-resolution Viking strip (528B01-04) indicates that some of these dark hills have circular summit depressions. Possible interpretations of origin of these hills include: cinder cones, volcanic domes, maar volcanoes, pseudocraters, impact craters, or pingos. The uncratered hills or knobs may be igneous plugs, volcanic necks, or the dark remnants of a hummocky, cratered surface protruding through a relatively bright eolian blanket. The presence, however, of the small dark hills on the flow of the large (130 km diameter) C(2) crater Lomonosov, suggests that similar dark hills elsewhere also may be secondary. M.G.

N85-23600*# Jet Propulsion Lab., California Inst. of Tech., Pasadena.

GEOMORPHOLOGY AND GEOLOGY OF THE SOUTHWESTERN MARGARITIFER SINUS AND ARGYRE REGIONS OF MARS. PART 1: GEOLOGICAL AND GEOMORPHOLOGICAL OVERVIEW Abstract Only

Timothy J. Parker and David C. Pieri *In* NASA, Washington Repts. of Planetary Geol. and Geophys. Program, 1984 Apr. 1985 p 361-363 refs (For primary document see N85-23474 13-91)

Avail: NTIS HC A99/MF A01 CSCL 03B

Based upon Viking Orbiter 1 images of the southwestern portion of the Margaritifer Sinus Quadrangle, the northwestern portion of the Argyre Quadrangle, and a small portion of the southeastern Coprates Quadrangle, three major mountainous of plateau units, seven plains units, and six units related to valley forming processes were identified. The photomosaic is oriented such that it provides good areal coverage of the upper Chryse Trough from Argyre Planitia to just above Margaritifer Chaos as well as of plains units on either side of the Trough. The photomosaic was compiled from Viking Orbiter 1 images ranging in resolution from approximately 150 to 300 meters per pixel printed at a scale of about 1:2,000,000. The characteristics of each geomorphic unit are outlined. M.G.

N85-23601*# Jet Propulsion Lab., California Inst. of Tech., Pasadena.

GEOMORPHOLOGY AND GEOLOGY OF THE SOUTHWESTERN MARGARITIFER SINUS AND ARGYRE REGIONS OF MARS. PART 2: CRATER SIZE-FREQUENCY DISTRIBUTION CURVES AND GEOMORPHIC UNIT AGES Abstract Only

Timothy J. Parker and David C. Pieri *In* NASA, Washington Repts. of Planetary Geol. and Geophys. Program, 1984 Apr. 1985 p 364-366 refs (For primary document see N85-23474 13-91)

Avail: NTIS HC A99/MF A01 CSCL 03B

In assessing the relative ages of the geomorphic/geologic units, crater counts of the entire unit or nearly the entire unit were made and summed in order to get a more accurate value than obtainable by counts of isolated sections of each unit. Cumulative size-frequency counts show some interesting relationships. Most of the units show two distinct crater populations with a flattening out of the distribution curve at and below 10 km diameter craters. Above this crater size the curves for the different units diverge most notably. In general, the variance may reflect the relative ages of these units. At times, however, in the larger crater size range, these curves can overlap and cross on another. Also the error bars at these larger sizes are broader (and thus more suspect), since counts of larger craters show more scatter, whereas the unit areas remain constant. Occasional clusters of relatively large craters within a given unit, particularly one of limited areal extent, can affect the curve so that the unit might seem to be older than units which it overlies or cuts. M.G.

N85-23602*# Jet Propulsion Lab., California Inst. of Tech., Pasadena.
GEOMORPHOLOGY AND GEOLOGY OF THE SOUTHWESTERN MARGARITIFER SINUS AND ARGYRE REGIONS OF MARS. PART 3: VALLEY TYPES AND DISTRIBUTION Abstract Only
Timothy J. Parker and David C. Pieri *In* NASA, Washington Repts. of Planetary Geol. and Geophys. Program, 1984 Apr. 1985 p 367-368 refs (For primary document see N85-23474 13-91)
Avail: NTIS HC A99/MF A01 CSCL 03B

Three major valley tapes were identified in the SW Margaritefer Sinus and Argyre regions. Two are restricted to specific geologic units while the third is independent of the geology. The first type (the small valley networks) are found within the channeled and subdued plains unit in the eastern half of the map, in the grooved and channeled plains unit north of Nirgal Vallis, and in scattered instances in the cratered plateau unit north of Argyre. The even smaller valleys just inside Argyre's rim and on the inner slopes of many large craters are not directly related to the processes which formed the small valleys but are a result, instead, of post-impact modification of the crater walls. The second type of valley network is represented by Nirgal Vallis and the similar, shorter continuation of it to the west. This type is found only in the smooth plains material west of Uzboi Vallis in the map area. The third type of valley network is that of the Uzboi-Holden-Ladon valles system. This system is related to catastrophic outflow from Argyre Basin and is topographically rather than geologically controlled. M.G.

N85-23603*# Jet Propulsion Lab., California Inst. of Tech., Pasadena.
GEOMORPHOLOGY AND GEOLOGY OF THE SOUTHWESTERN MARGARITIFER SINUS AND ARGYRE REGIONS OF MARS. PART 4: FLOW EJECTA CRATER DISTRIBUTION Abstract Only
Timothy J. Parker and David C. Pieri *In* NASA, Washington Repts. of Planetary Geol. and Geophys. Program, 1984 Apr. 1985 p 369-370 (For primary document see N85-23474 13-91)
Avail: NTIS HC A99/MF A01 CSCL 03B

Flow ejecta craters - craters surrounded by lobate ejecta blankets - are found throughout the study area. The ratio of the crater's diameter to that of the flow ejecta in this region is approximately 40 to 45%. Flow ejecta craters are dominantly sharply defined craters, with slightly degraded craters being somewhat less common. This is probably indicative of the ejecta's relatively low resistence to weathering and susceptibility to burial. Flow ejecta craters here seem to occur within a narrow range of crater sizes - the smallest being about 4km in diameter and the largest being about 27km in diameter. Ejecta blankets of craters at 4km are easily seen and those of smaller craters are simply not seen even in images with better than average resolution for the region. This may be due to the depth of excavation of small impacting bodies being insufficient to reach volatile-rich material. Flow ejecta craters above 24km are rare, and those craters above 27km do not display flow ejecta blankets. This may be a result of an excavation depth so great that the volatile content of the ejecta is insufficient to form a fluid ejecta blanket. The geomorphic/geologic unit appears also to play an important role in the formation of flow ejecta craters. Given the typical size range for the occurrence of flow ejecta craters for most units, it can be seen that the percentage of flow ejecta craters to the total number of craters within this size range varies significantly from one unit to the next. The wide variance in flow ejecta crater density over this relatively small geographical area argues strongly for a lithologic control of their distribution. M.G.

N85-23604*# Arizona State Univ., Tempe. Dept. of Geology.
PLANETARY ANALOGS IN ANTARCTICA: MARS Abstract Only c46
Michael C. Malin *In* NASA, Washington Repts. of Planetary Geol. and Geophys. Program, 1984 Apr. 1985 p 371-373 refs (For primary document see N85-23474 13-91)
Avail: NTIS HC A99/MF A01 CSCL 08G

A study of chemical and physical weathering rates in Antarctic ice-free areas, sponsored by the National Science Foundation's Antarctic Research Program, permitted observations to be made that also have application other planetary surfaces. Four observations relevent to Mars are addressed: the effects of freezing on sand dune morphology (Mars polar dune field), chemical/physical weathering to create pits (Mars pitted rocks, Viking Lander 1 and 2 sites), armored surfaces (Mars lander sites), and mass movements (movement of Martian debris). M.G.

N85-23605*# Arizona State Univ., Tempe.
PLANETARY ANALOGS IN ANTARCTICA: ICY SATELLITES Abstract Only c46
Michael C. Malin *In* NASA, Washington Repts. of Planetary Geol. and Geophys. Program, 1984 Apr. 1985 p 374-375 refs (For primary document see N85-23474 13-91)
Avail: NTIS HC A99/MF A01 CSCL 08L

As part of a study to provide semi-quantitative techniques to date past Antarctic glaciations, sponsored by the Antarctic Research Program, field observations pertinent to other planets were also acquired. The extremely diverse surface conditions, marked by extreme cold and large amounts of ice, provide potential terrain and process analogs to the icy satellites of Jupiter and Saturn. Thin ice tectonic features and explosion craters (on sea ice) and deformation features on thicker ice (glaciers) are specifically addressed. M.G.

N85-23606*# Arizona State Univ., Tempe. Dept. of Geology.
THE GEOMORPHOLOGY OF RHEA Abstract Only
J. M. Moore, V. M. Horner, and R. Greeley *In* NASA, Washington Repts. of Planetary Geol. and Geophys. Program, 1984 Apr. 1985 p 376-378 refs (For primary document see N85-23474 13-91)
Avail: NTIS HC A99/MF A01 CSCL 03B

Rhea was imaged to a resolution of approximately 1 km/lp by the Voyager spacecraft, providing the most detailed view of any Saturnian satellite. A preliminary study of Rhea divided the northern hemisphere into population 1 cratered terrain (between 20 deg and 120 deg) and population 2 cratered terrain (between 300 deg and 360 deg). Population 1 includes craters that are $>$ 40 km and were formed before the termination of population 2 bombardment, which formed craters primarily $<$ 40 km. Several geomorphic features on Rhea are classified and interpreted including three physiographic provinces, multiringed basins, craters, megascarps, ridges and scarps, and troughs and coalescing pit chains. A generalized chronology for Rhea is constructed from an analysis of the superposition relationships among the landforms and physiographic provinces. M.G.

N85-23607*# Hawaii Univ., Honolulu. Planetary Geoscience Div.
MULTISPECTRAL ANALYSIS OF THE KASEI VALLIS-LANAE PLANUM REGION OF MARS Abstract Only
R. B. Singer, E. Cloutis, T. L. Roush, P. J. MouginisMark, B. R. Hawke, and P. R. Christensen (Arizona State Univ., Tempe) *In* NASA, Washington Repts. of Planetary Geol. and Geophys. Program, 1984 Apr. 1985 p 381-382 refs (For primary document see N85-23474 13-91)

Avail: NTIS HC A99/MF A01 CSCL 03B

The surficial geology of the Kasei Valles - Lunae Planum region of Mars was investigated using the three color Viking Orbiter 1 data. Spatial resolution is 820m and Ls = 100 deg, a season of low atmospheric and and surface dustiness. This region was chosen for high quality color and thermal inertia data as well as for the diversity of volcanic plains and fluvial landform. The data was reformatted to Mercator projection and calibrated to normal reflectance using in flight calibration parameters and observed photometric properties. Color properties from this image are displayed in two forms: the Red Albedo vs. Violet Albedo two dimensional histogram, and representative 3 point spectra. Virtually the full range of regolith color properties known from prior research is represented, plus some new characteristics. Interpretations of the data are presented which address general composition and formation processes of channel and intracrater deposits. M.G.

N85-23608*# Arizona State Univ., Tempe. Dept. of Geology.
GEOLOGIC INTERPRETATION OF REMOTE SENSING DATA FOR THE MARTIAN VOLCANO, ASCRAEUS MONS Abstract Only
J. Zimbelman and R. Greeley *In* NASA, Washington Repts. of Planetary Geol. and Geophys. Program, 1984 Apr. 1985 p 383-384 refs (For primary document see N85-23474 13-91)
Avail: NTIS HC A99/MF A01 CSCL 03B

Results of an investigation to relate remotely determined physical properties on Ascraeus Mons to the geologic history of the volcano are summarized. Products include a 1:2,000,000-scale photogeologic map of Ascraeus Mons and its environs; a 1:250,000-scale corrected thermal-inertia map of the summit caldera complex; four corrected thermal-inertia profiles across the volcano from high-resolution thermal data; fourteen low-resolution thermal sequences providing corrected thermal inertias for the volcano throughout half a Martian year; and a calibrated three-color photograph of the volcano. These data were combined with published spectral-reflectance, radar, and atmospheric water-vapor data relating to Acraeus Mons. Photogeologic mapping indicates that the sequence of events at Acraeus Mons is more complex than previously described. The plains surrounding the volcano include numerous flows, some of which can be traced to the flank of the volcano and some to different locations along the Tharsis Ridge. Surface morphology in the summit area is very distinct for features >100 m in scale, but the surface relief and tonal contrast steadily decrease toward the base of the shield, indicating modification by deposition or erosion. M.G.

N85-23609*# Washington Univ., St. Louis, Mo. Dept. of Earth and Planetary Sciences.
THE SEARCH FOR IGNEOUS MATERIALS AT THE VIKING LANDING SITES Abstract Only
R. E. Arvidson, M. Dale-Bannister, and E. A. Guinnes *In* NASA, Washington Repts. of Planetary Geol. and Geophys. Program, 1984 Apr. 1985 p 385-386 refs (For primary document see N85-23474 13-91)
Avail: NTIS HC A99/MF A01 CSCL 03B

The use of Viking Lander 6 channel (0.4 to 1.1 microns) images to identify igneous materials is discussed. Movies of synthetic image cubes demonstrate that there are a number of contrast reversals between soils and certain rocks. Typically, large, angular rocks are brighter than the surrounding soils in the shortest wavelengths, and much darker than the soils at longest wavelengths. These results, which seem difficult to explain solely on the basis of photometric effects related to local lighting and viewing, are consistent with the presence of Fe+2 bearing silicates at the rock surfaces, producing relatively moderate absorptions in the blue and green parts of the spectrum, but more significant absorptions near about 1.0 micrometer (e.g., Fe+2 bearing pyroxenes). The soils, on the other hand, have signatures consistent with strong Fe+3 related absorptions at shorter wavelengths (e.g., Fe+3 bearing oxides or hydroxides). M.G.

N85-23610*# Massachusetts Univ., Amherst. Dept. of Geology-Geography.
BASALTS OF MARS: CONSTRAINTS ON VOLATILE EVOLUTION Abstract Only
R. L. Huguenin *In* NASA, Washington Repts. of Planetary Geol. and Geophys. Program, 1984 Apr. 1985 p 387-388 (For primary document see N85-23474 13-91)
Avail: NTIS HC A99/MF A01 CSCL 03B

The mineralogy of relatively unweathered rocks on Mars place important constraints on models of planetary oxidation state, volcanism and associated outgassing, accretion and associated volatile inventory, and geochemical changes over time. Reflectance spectra (300 to 2500 nm) provide direct mineralogic information about the surface materials. Spectra measured using Earth-based telescopes were analyzed by a multiple high-order derivative spectroscopy technique. Nine areas, measured during the 1978 opposition, were analyzed by the technique. Each contained suites of well-defined absorption bands. These bands can be interpreted in terms of constituent mineralogy by the technique of Adams. Among the features extracted from the spectra were bands attributed to iron oxides. Other bands can be attributed to silicates within chemically unweathered rocks/fines. Absorption features suggest the presence of Mg-olivine and plagioclase feldspar. M.G.

N85-23611*# Arizona State Univ., Tempe. Dept. of Geology.
WATER-ICE CLOUDS ON MARS: LOCATION AND SEASONAL VARIATION Abstract Only
P. R. Christensen, L. Jaramillo, and R. Greeley *In* NASA, Washington Repts. of Planetary Geol. and Geophys. Program, 1984 Apr. 1985 p 389-390 refs (For primary document see N85-23474 13-91)
Avail: NTIS HC A99/MF A01 CSCL 03B

Water-ice clouds were located on Mars using Viking infrared thermal mapper (IRTM) broadband spectral observations. The IRTM instrument had 5 thermal bands centered at 7, 9, 11, 15, and 20 microns. Clouds and hazes were consistently observed in four northern hemisphere regions centered over Tharsis, Arabia, Elysium, and along the boundary between the crater uplands and the northern plains. During the northern spring and summer when the atmosphere is relatively free of dust, there is a distinct difference between the cloud abundance in the Northern and Southern Hemispheres, with clouds and hazes being rare in the south. A second important class of water-ice clouds are those observed along the boundary of the retreating north polar cap. These clouds occur at all longitudes around the cap and are generally confined to within +/- 5 deg of the cap boundary. The cloud opacities can be estimated using a delta-Eddington radiative transfer model which incorporates Mie scattering and the electrical properties of water-ice. Assuming realistic, but non-unique, values for the ice particle size and cloud temperature, the derived opacities range from near-zero to 1. M.G.

N85-23612*# Hawaii Univ., Honolulu.
FIRST DIRECT DETECTION OF CLAY MINERALS ON MARS Abstract Only
Robert B. Singer, Pamela D. Owensby, and Roger N. Clark (Geological Survey, Denver) *In* NASA, Washington Repts. of Planetary Geol. and Geophys. Program, 1984 Apr. 1985 p 391-392 refs (For primary document see N85-23474 13-91)
Avail: NTIS HC A99/MF A01 CSCL 03B

Magnesian clays or clay-type minerals were conclusively detected in the martian regolith. Near-IR spectral observations of Mars using the Mauna Kea 2.2-m telescope show weak but definite absorption bands near microns. The absorption band positions and widths match those produced by combined OH stretch and Mg-OH lattice modes and are diagnostic of minerals with structural OH such as clays and amphiboles. Likely candidate minerals include serpentine, talc, hectorite, and sponite. There is no spectral evidence for aluminous hydroxylated minerals. No distinct band occurs at 2.55 microns, as would be expected if carbonates were responsible for the 2.35 micron absorption. High-albedo regions such as Elysium and Utopia have the strongest bands near 2.35 microns, as would be expected for heavily weathered soils. Low-albedo regions such as Iapygia show weaker but distinct bands, consistent with moderate coatings, streaks, and splotches

of bright weathered material. In all areas observed, the 2.35-micron absorption is at least three times weaker than would be expected if well-crystallized clay minerals made up the bulk of bright soils on Mars. M.G.

N85-23613*# Massachusetts Univ., Amherst. Dept. of Geology-Geography.
IRON OXIDES OF MARS: EVIDENCE FOR CONTEMPORARY WEATHERING Abstract Only
R. L. Huguenin *In* NASA, Washington Repts. of Planetary Geol. and Geophys. Program, 1984 Apr. 1985 p 393-394 (For primary document see N85-23474 13-91)
Avail: NTIS HC A99/MF A01 CSCL 03B

Reflectance spectra of Mars were analyzed using a multiple high order derivative spectroscopy technique. Among the results of the analysis was the presence of suites of bands in each of the spectra that can be attributed to Fe(3e) phases. Several of the spectra contained bands that are very close to the band positions in the laboratory spectra of goethite, an hexagonal hydrated ferric oxide. Spectra of other areas showed absorption bands that were within 3% of the positions for hematite, and hexagonal close packed unhydrated Fe203. Remaining areas showed bands that are intermediate in position to the goethite and hematite bands, suggesting that there may be mixtures of goethite and hematite, and/or intermediate (partially dehydrated goethite) phases present in those areas. Both bright areas and dark areas showed suites of goethite bands and hematite bands, and there does not therefore appear to be a correlation with albedo. The areas that showed the goethite bands are, however, within zones of ongoing or historically frequent dust cloud activity, and the areas with the hematite bands were outside of the zones of frequent dust cloud activity. This suggests the possiblility that the more hydrated phase may occur within a mobile dust component. M.G.

N85-23614*# Massachusetts Inst. of Tech., Cambridge. Dept. of Earth, Atmospheric, and Planetary Sciences.
REASSIGNMENT OF THE IRON (3) ABSORPTION BANDS IN THE SPECTRA OF MARS Abstract Only
David M. Sherman *In* NASA, Washington Repts. of Planetary Geol. and Geophys. Program, 1984 Apr. 1985 p 395-396 refs (For primary document see N85-23474 13-91)
Avail: NTIS HC A99/MF A01 CSCL 03B

Absorption features in the near-infrared and visible region reflectance spectra of Mars have been assigned to specific Fe (3+) crystal-field and o(2-) yields Fe(3+) charge transfer transitions. Recently, near-ultraviolet absorption spectra of iron oxides were obtained and the energies of o(2-) yields Fe(3+) charge-transfer (LMCT) transitions were determined from accurate SCF-X # alpha-SW molecular orbital calculations on (FeO6)(9-) and (FeO4)(5-) clusters. Both the theoretical and experimental results, together with existing data in the literature, show that some of the previous Fe(3+) band assignments in the spectra of Mars need to be revised. The theory of Fe(3+) spectra in minerals is discussed and applied to the spectrum of Mars. M.G.

N85-23615*# Los Alamos Scientific Lab., N. Mex.
ZEOLITES ON MARS: PROSPECTS FOR REMOTE SENSING Abstract Only
E. S. Gaffney, R. B. Singer (Hawaii Univ., Honolulu), and T. D. Kunkle *In* NASA, Washington Repts. of Planetary Geol. and Geophys. Program, 1984 Apr. 1985 p 397 (For primary document see N85-23474 13-91)
Avail: NTIS HC A99/MF A01 CSCL 03B

The Martian surface composition measured by Viking can be represented by several combinations of minerals incorporating major fractions of zeolites known to occur in altered mafic rocks and polar soils on Earth. The abundant occurrence of zeolites on Mars is consistent with what is known about both the physical and chemical environment of that planet. The laboratory reflectance spectra (0.65 to 2.55 microns) of a number of relatively pure zeolite minerals and some naturally occurring zeolite-clay soils were measured. All of the spectra measured are dominated by strong absorption near 1.4 and 1.9 microns and a steep reflectance drop longward of about 2.2 microns, all of which are due to abundant H2O. Weaker water overtone bands are also apparent, and in most cases there is spectral evidence for minor Fe(3+). In these features the zeolite spectra are similar to spectra of smectite clays which have abundant interlayer water. The most diagnostic difference between clay and zeolite spectra is the total absence in the zeolites of the weak structural OH absorption. M.G.

N85-23616*# Hawaii Univ., Honolulu. Planetary Geosciences Div.
REMOTE SENSING ANALYSES OF LOCALIZED LUNAR DARK MANTLE DEPOSITS Abstract Only
L. R. Gaddis, P. Lucey, J. F. Bell, and B. R. Hawke *In* NASA, Washington Repts. of Planetary Geol. and Geophys. Program, 1984 Apr. 1985 p 399-401 refs (For primary document see N85-23474 13-91)
Avail: NTIS HC A99/MF A01 CSCL 03B

Near-infrared spectral reflectance data were obtained for 12 localized lunar dark mantle deposits. The dominant feature in these data is the Fe(+2) absorption band in the 1.0 micron wavelength region. In order to emphasize differences in the characteristics of this absorption band, a straight-line continuum was removed from these spectra. On the basis of the depth and shape of this 1.0 micron absorption band, these spectra can be separated into three groups. Group 1 includes spectra from Grimaldi pyroclastics, Franklin floor, Atlas dhc 1, and Archimedes south rim. Absorption band centers in this group are located near 0.93 to 0.95 microns, and depths are approximately 4 to 5%. The shape of the 1.0 micron band in these spectra can be described as check-like, with a straight, steep short-wavelength edge and a straight longer-wavelength edge with a shallower slope. Group 2 is comprised of spectra from Aristoteles East 1 and 2, Rima Fresnel and Atlas dhc 2. These 1.0 micron bands are centered near 0.96 micron, and are deeper (7%) and more symmetrical than those in Group 1. Spectra in group 3 are represented by that of J. Herschel; which have a moderately deep (7%), broad absorption band in the 1.0 micron wavelength region. M.G.

N85-23617*# Hawaii Univ., Honolulu. Planetary Geosciences Div.
SPECTRAL REFLECTANCE STUDIES OF THE ORIENTALE BASIN Abstract Only
B. R. Hawke, P. Lucey, J. F. Bell, and P. D. Spudis (Arizona State Univ., Tempe) *In* NASA, Washington Repts. of Planetary Geol. and Geophys. Program, 1984 Apr. 1985 p 402-403 refs (For primary document see N85-23474 13-91)
Avail: NTIS HC A99/MF A01 CSCL 03B

Twelve near-infrared spectra were obtained at the Mauna Kea Observatory 2.2-m telescopy using the Planetary Geosciences Division indium antimonide spectrometer. These include spectra obtained for two fresh surfaces on the inner Rook ring, two fresh craters in the outer Rook Mts., and two inner Rook ring, two fresh craters in the outer Rook Mts., and two fresh 11-km. craters (Eichstadt G and H) which are located between the outer Rook ring and the Cordillera ring and exposed material from within the knobby facies of the Montes Rook Formation. In addition, spectra were collected for portions of the Maunder Formation. Special attention was paid to the spectra collected for six immature features within the Cordillers ring. Analyses of the 1-micron band positions and shapes as well as continuum slopes indicate that the spectra for craters in the knobby facies and in the outer Rook Mts., while differing in detail, exhibit many common spectral characteristics. These spectra represent relatively fresh highlands rocks dominated by abundant Fe-bearing plagioclase feldspar and Ca-poor ortho-pyroxene. Compositions ranging between noritic anorthosite and anorthositic norite are indicated. M.G.

N85-23618*# Cornell Univ., Ithaca, N.Y. Lab. for Planetary Studies.
ACCURATE ALBEDOS OF THE BRIGHTEST REGIONS ON IO Abstract Only

Damon P. Simonelli and Joseph Veverka *In* NASA, Washington Repts. of Planetary Geol. and Geophys. Program, 1984 Apr. 1985 p 405-407 refs (For primary document see N85-23474 13-91)
(Grant NsG-7156)
Avail: NTIS HC A99/MF A01 CSCL 03B

The brightest, coldest areas on Io, the white regions, may act as cold traps for SO2 gas, and thus have an important role in governing the pressure, diurnal variation, and flow of the satellite's tenuous SO2 atmosphere. Therefore, it is essential to derive accurate albedos for the brightest regions, where the necessary albedos are those in the energy balance equation of the surface used to compute temperatures. Forty-one of the brightest of the white areas, each 60 to 120 km on a side were studied. The simplest way to estimate the required energy balance albedo for each region is to determine the Bond albedo of a planet covered with that type of material. This process is outlined and resulting albedos are given. with the exception of several darker regions on the poorly-resolved post eclipse face of Io, typical albedos are 0.6 to 0.7. The brightest areas studied are located in the cluster of white regions east of Prometheus (longitudes 90 to 40 deg W). It is possible using Voyager data and fits to Hapke's equation to derive albedos for the bright regions without making any assumptions about the phase integrals. M.G.

N85-23619*# Cornell Univ., Ithaca, N.Y. Lab. for Planetary Studies.
IO: PRECISE COMPARISON OF VOYAGER SPECTRAL CURVES WITH LABORATORY MEASUREMENTS Abstract Only
Damon P. Simonelli and Joseph Veverka *In* NASA, Washington Repts. of Planetary Geol. and Geophys. Program, 1984 Apr. 1985 p 408-410 refs (For primary document see N85-23474 13-91)
(Grant NsG-7156)
Avail: NTIS HC A99/MF A01 CSCL 03B

In order to derive more accurate normal reflectances of regions on Io, the near-opposition (alpha $<$ 10 deg) photometry of a set of regions on the 20 W face of the satellite, the face with the most complete near-opposition Voyager imaging coverage was analyzed. Sixty-eight regions were chosen for study, each approximately 120 km on a side, and divided into three coherent color classes: white, orange, and polar brown regions. Derived Minneart parameters, while generally consistent with previous limb darkening determinations, show that: (1) for the white regions, k rises linearly with increasing B(0), which is the trend to be expected for normal materials; (2) the white regions are slightly limb brightened ($k < 0.5$) at low wavelengths (low values of B(0)); and (3) k appears to drop with rising B(0) for the orange regions, contrary to the trend expected for most materials. Despite similar reflectances, there is one group of orange regions with large opposition surges and a second group showing significantly lower surges, possibly indicating differences in surface texture (porosity and/or particle size). A.R.H.

N85-23620*# Jet Propulsion Lab., California Inst. of Tech., Pasadena.
PHOTOMETRIC ANALYSIS OF JUPITER-ILLUMINATED IMAGES OF IO Abstract Only
B. J. Buratti and R. J. Terrile *In* NASA, Washington Repts. of Planetary Geol. and Geophys. Program, 1984 Apr. 1985 p 411-412 refs (For primary document see N85-23474 13-91)
Avail: NTIS HC A99/MF A01 CSCL 03B

Several sequences of the dark (Jupiter-illuminated) side of Io obtained during the Voyager 2 encounter present opporunity for understanding several problems relating to the surface composition of Io. The existence or absence of SO2 condensates on the night side is a sensitive indicator of an SO2 atmosphere. Preliminary analysis of the night side Io images suggests localized brightenings of approximately 25% may exist. Examination of the night side images represents an even more sensitive indicator for pure sulfur. Between 60 and 130 degrees (the minimum nighttime and maximum daytime temperatures, respectively), the relative spectral reflectance for yellow sulfur observed in the Voyager green and clear filters decreases by 25%. This decrease should be detectable on the nightside images. A search of the Voyager 2 Jupiter-illuminated images yielded a single pair of green and clear images. In these images one hemisphere of Io is Sun-illuminated and the other is Jupiter illuminated. Geologically similar regions of Io are being selected to obtain average color ratios of specific geologic units for both day and night sides. A.R.H.

N85-23621*# Jet Propulsion Lab., California Inst. of Tech., Pasadena. Inst. of Geophysics.
SPECTRAL UNITS ON EUROPA AND GANYMEDE Abstract Only
Thomas B. McCord, Marcia L. Nelson, Roger N. Clark, Torrence V. Johnson, Dennis L. Matson, Robert E. Johnson, and John Boring *In* NASA, Washington Repts. of Planetary Geol. and Geophys. Program, 1984 Apr. 1985 p 413-414 refs (For primary document see N85-23474 13-91)
Avail: NTIS HC A99/MF A01 CSCL 03B

Comparisons of Europa and Ganymede multispectral data show that Ganymede is less spectrally variable than Europa. Four major spectral units dominate Ganymede, corresponding to the ancient cratered terrain and the grooved terrain in the leading and trailing hemispheres. A hemispheric asymmetry in UV absorption definitely exists on Ganymede, although it is not so strong as that on Europa. Comparison of normalized spectra for the four major units shows that the sense of the asymmetry (more absoption toward shorter wavelengths on the trailing hemisphere) is also the same on the two bodies. This hemispheric asymmetry is interpreted as evidence of alteration of the surface by magnetospheric bombardment or micrometorite bombardment. It is concluded that the pattern observed represents a steady state involving both of these exogenic modifying agents. The spectral changes which could be produced by these two processes are grain size alteration and changes in composition. The spectral effects of variation in water ice grain size are fairly well known. Laboratory experiments are being conducted to study the spectral effects of sulfur irradiation on water ice. A.R.H.

N85-23622*# Washington Univ., Seattle. Dept. of Geological Sciences.
DETERMINING MINERAL TYPES AND ABUNDANCES FROM REFLECTANCE MEASUREMENTS Abstract Only. c43
Milton O. Smith and John B. Adams *In* NASA, Washington Repts. of Planetary Geol. and Geophys. Program, 1984 Apr. 1985 p 415-417 refs (For primary document see N85-23474 13-91)
Avail: NTIS HC A99/MF A01 CSCL 08G

Mineral types and their abundances were quantitatively determined from laboratory reflectance spectra using principal components analysis (PCA). PCA reduced the measured spectral dimensionality and allowed testing the uniqueness and validity of spectral mixing models. In addition to interpreting absorption bands, in this new approach we interpreted variations in the overall spectral curves in terms of physical processes, namely changes in mixtures of minerals, in particle size and in illumination geometry. Application of this approach to reflectances of planetary surfaces allows interpretation to be extended to quantitative determinations of mineral types and abundances. G.L.C.

N85-23623*# Geological Survey, Denver, Colo.
DETERMINATION OF MINERAL TYPE, ABUNDANCE, AND GRAIN SIZE WITH REMOTELY OBTAINED REFLECTANCE SPECTRA Abstract Only c43
Roger N. Clark *In* NASA, Washington Repts. of Planetary Geol. and Geophys. Program, 1984 Apr. 1985 p 418-420 refs (For primary document see N85-23474 13-91)
Avail: NTIS HC A99/MF A01 CSCL 08G

To derive the abundances of minerals in a surface composed of more then one mineral in an intimate mixture, the bidirectional reflectance spectrum must be measured at several angles of incidence and emission. From these measurements, the scattering parameters may be derived, and the effective single scattering albedo can be computed from the models. If the scattering parameters are not derived, and the particles scatter anisotropically, then the computed effective single scattering albedo has been computed, the solution to the model is a nonlinear least squares

problem with three unknowns per particle type. The solution is feasible when the complex indices of refraction and the densities of each mineral component are known. The unknowns are: the grain size of each particle type, the mass fraction of each particle type, and a grain internal scattering coefficient that describes grain imperfections. G.L.C.

N85-23624*# Massachusetts Univ., Amherst. Dept. of Geology-Geography.
AUTOMATED EXTRACTION OF ABSORPTION BANDS FROM REFLECTANCE SPECIAL Abstract Only c43
R. L. Huguenin, L. Vale, D. McIntire, and J. Jones *In* NASA, Washington Repts. of Planetary Geol. and Geophys. Program, 1984 Apr. 1985 p 421-428 (For primary document see N85-23474 13-91)
Avail: NTIS HC A99/MF A01 CSCL 20F

A multiple high order derivative spectroscopy technique has been developed for deriving wavelength positions, half widths, and heights of absorption bands in reflectance spectra. The technique is applicable to laboratory spectra as well as medium resolution (100-200/cm) telescope or spacecraft spectra with moderate (few percent) noise. The technique permits absorption band positions to be detected with an accuracy of better than 3%, and often better than 1%. The high complexity of radiative transfer processes in diffusely reflected spectra can complicate the determination of absorption band positions. Continuum reflections, random illumination geometries within the material, phase angle effects, composite overlapping bands, and calibration uncertainties can shift apparent band positions by 20% from their actual positions or mask them beyond detection. Using multiple high order derivative analysis, effects of scattering continua, phase angle, and calibration (smooth features) are suppressed. Inflection points that characterize the positions and half widths of constituent bands are enhanced by the process and directly detected with relatively high sensitivity. G.L.C.

N85-23625*# Wyoming Univ., Laramie.
QUANTITATIVE ANALYSES OF PLANETARY REFLECTANCE SPECTRA Abstract Only
Paul E. Johnson *In* NASA, Washington Repts. of Planetary Geol. and Geophys. Program, 1984 Apr. 1985 p 429-431 refs (For primary document see N85-23474 13-91)
Avail: NTIS HC A99/MF A01 CSCL 03B

The development of a set of quantitative models to analyze planetary reflectance spectra as a function of microscopic and macroscopic mineral mixtures, particle size, and illumination geometry is considered. The approach has been to simplify more sophisticated algorithms to include the smallest number of parameters possible, consistent with being able to use them to produce useful results. This means that they should be able to model the data to within the accuracy obtainable by laboratory, telescopic, and space instrumentation (roughly 1%). The algorithms are ideally given in terms of parameters that are directly measureable (such as spectral reflectance or particle size). G.L.C.

N85-23626*# Sul Ross State Univ., Alpine, Tex. Dept. of Geology.
ANALYSIS OF SMIRR DATA FOR VOLCANIC AND SEDIMENTARY TERRAINS OF THE TRANS-PECOS REGION, TEXAS Abstract Only c46
H. Grady Blount and James L. WhitfordStark *In* NASA, Washington Repts. of Planetary Geol. and Geophys. Program, 1984 Apr. 1985 p 432-433 refs (For primary document see N85-23474 13-91)
Avail: NTIS HC A99/MF A01 CSCL 08G

The Shuttle Multispectral Infrared Radiometer (SMIRR) carried on the second mission of the Space Shuttle produced spectral data for portions of Presidio and Jeff Davis Counties, Texas during the eighteenth orbit of the spacecraft in November of 1981. The data covers an area approximately 100 m in width and 100 km in length extending from the Rio Grande just north of Candelaria in the southwest to Fort Stockton in the northeast. The area is part of the Chihuahua Desert ecosystem. The purpose of the project is to provide groundtruth for the spectral data produced by the SMIRR scanner. The ten filters on the SMIRR scanner extend from 0.50 to 2.35 microns. It has been found that the bands from 2.0 to 2.35 microns are particularly useful for discriminating carbonate and clay minerals. G.L.C.

N85-23627*# Houston Univ., Tex. Dept. of Geosciences.
MONTE CARLO MODELING OF LUNAR MEGAREGOLITH DEVELOPMENT Abstract Only
Jac Cashore and Alex Woronow *In* NASA, Washington Repts. of Planetary Geol. and Geophys. Program, 1984 Apr. 1985 p 434-436 refs (For primary document see N85-23474 13-91)
Avail: NTIS HC A99/MF A01 CSCL 03B

A Monte Carlo model of lunar megaregolith development is proposed. Minimum megaregolith depths are obtained in the preliminary model. The model impacts a gridded, initially flat surface area randomly, with points not constrained to grid intersections. Information is recorded at grid points on evolving topography, deepest depth impacted to, and number of hits at that location. Two types of lunar surfaces ar simulated, maria and highlands. Crater production functions are after run to densities that are multiples of observed lunar crater densities for craters of 8 km in diameter and larger. all craters are considered to have formed in a gravity scaled regime. Edge effect problems are corrected in this model by allowing craters forming outside the grid area or along its edges to effect the gridded area. G.L.C.

N85-23628*# National Aeronautics and Space Administration. Lyndon B. Johnson Space Center, Houston, Tex.
CHEMICAL WEATHERING OF SOILS FROM THE DRY VALLEYS OF ANTARCTICA: A TERRESTRIAL ANALOG OF MARTIAN WEATHERING PROCESSES Abstract Only c46
Everett K. Gibson, Jr. *In* NASA, Washington Repts. of Planetary Geol. and Geophys. Program, 1984 Apr. 1985 p 437-439 refs (For primary document see N85-23474 13-91)
Avail: NTIS HC A99/MF A01 CSCL 08G

Martian soil subjected to chemical weathering processes could contain the following likely constituents: (1) fresh primary silicate material; (2) partially altered primary silicates; (3) secondary minerals, possibly including clay minerals, evaporites, carbonates, sulfates, hydrates, and zeolites; and (4) altered volcanic glass or impact glass. The soil may also include palogonite and other alteration products and secondary minerals. It is unlikely therefore that an equilibrium assemblage of minerals would be present. From the detailed study of the soils from the Dry Valleys of Antarctica, it is obvious that the complex processes in operation produce major changes in the parent materials, depending upon where the constituents reside and the degree to which weathering and diagenesis operates. It is clear that natural near surface environments, even in very cold and dry regions, may produce extremely complex soils. Extreme caution must be taken when interpreting the results and drawing conclusions, especially about possible processes operating in regoliths in cold, arid environments similar to those of the Dry Valleys or Mars. G.L.C.

N85-23629*# Jet Propulsion Lab., California Inst. of Tech., Pasadena.
PROPERTIES OF FILAMENTARY SUBLIMATION RESIDUES FROM DISPERSIONS OF CLAY IN ICE Abstract Only c46
James B. Stephens, Timothy J. Parker, R. Stephen Saunders, Eric G. Laue, and Fraser P. Fanale (Hawaii Univ., Honolulu) *In* NASA, Washington Repts. of Planetary Geol. and Geophys. Program, 1984 Apr. 1985 p 440-442 refs (For primary document see N85-23474 13-91)
Avail: NTIS HC A99/MF A01 CSCL 08L

The properties of sublimate residues are of considerable interest in studies of the thermal modeling of Martian and cometary ice surfaces. The study of the formation of sand grains from this mantle on Martian polar ice is also supported by these experiments. To understand these properties, a series of low temperature vacuum experiments were run during which dirty ices that might be expected to be found in Martian polar caps and in comet nuclei were made and then freeze dried. In addition to using particulate material of appropriate grain size and minerology,

particle nucleated ices were simulated by dispersing the particulates in the ice so that they did not contact one another. This noncontact dispersion was the most difficult requirement to achieve but the most rewarding in that it produced a new filamentary sublimate residue that was not a relic of the frozen dispersion. If the siliceous particles are allowed to touch one another in the ice the structure of the contacting particles in the ice will remain as a relic after the ice is sublimed away. G.L.C.

N85-23630*# Geological Survey, Flagstaff, Ariz.
PROGRESS IN PLANETARY RADARCLINOMETRY Abstract Only
Robert L. Wildey *In* NASA, Washington Repts. of Planetary Geol. and Geophys. Program, 1984 Apr. 1985 p 445-447 refs (For primary document see N85-23474 13-91)
Avail: NTIS HC A99/MF A01 CSCL 03B

Efforts have continued to improve radarclinometry in spite of the fact that the theory and algorithms still predate the development of the radiometrically calibrated radar upon which they must depend in order to achieve metric precision. Such efforts help to insure the availability of the technique for data returned by the Venus Radar Mapper. Even now, compensation for layover and production of synthesized stereo enhance geologic interpretability of radar images. The theory of radarclinometry utilizes a knowledge of the relation between pixel DN value and terrain surface orientation to produce a topographic map. The process may be conceived in terms of a surface integral which develops away from a topographic profile as available ground truth. Alternatively, in consideration of the unavailability of ground truth in extraterrestrial applications, radarclinometry may develop as a line integral developing from a single point, providing reasonable assumptions about the mathematical nature of local curvature. G.L.C.

N85-23631*# National Astronomy and Ionosphere Center, Arecibo, Puerto Rico.
MERCURY RADAR ALTIMETRY: A PRELIMINARY ANALYSIS Abstract Only
J. K. Harmon, D. B. Campbell, J. W. Head (Brown Univ.), D. L. Bindschadler (Brown Univ.), and I. I. Shapiro (Harvard-Smithsonian Center for Astrophysics) *In* NASA, Washington Repts. of Planetary Geol. and Geophys. Program, 1984 Apr. 1985 p 448-449 refs (For primary document see N85-23474 13-91)
Avail: NTIS HC A99/MF A01 CSCL 03B

Range-Doppler radar observations were made of the planet Mercury over the six year period 1978-1983. Approximately 30 continuous altitude profiles were obtained, each spanning between 20 and 90 degrees of longitude. The profiles are located in the equatorial zone of Mercury between 5 deg S and 12 deg N latitude. Approximately 40% of the total coverage is in the unimaged hemisphere. G.L.C.

N85-23632*# Geological Survey, Flagstaff, Ariz.
UNSUPERVISED CLASSIFICATION OF GLOBAL RADAR UNITS ON VENUS Abstract Only
Richard C. Kozak, Philip A. Davis, and Gerald G. Schaber *In* NASA, Washington Repts. of Planetary Geol. and Geophys. Program, 1984 Apr. 1985 p 450-452 refs (For primary document see N85-23474 13-91)
Avail: NTIS HC A99/MF A01 CSCL 03B

Characterization of the Venusian surface in terms of its radar properties was accomplished by application of an unsupervised, linear discriminant algorithm to two Pioneer-Venus (PV) Orbiter radar data sets: the RMS-slope (surface roughness) and reflectivity. Both databases were spatially filtered to the same effective resolution of 100 km prior to classification. A recent supervised classification study using these data was based on presupposed morphologic significance of selected data ranges. The knowledge of both Venusian geology and the geologic significance of the radar data is so limited that the data warrant a more unsupervised approach; for this study a linear discriminant classifier was chosen. This approach is purely statistical, thereby removing any observer bias. Statistical significance of the resulting clusters was evaluated by an ancillary program in which an F test utilizing the Mahalanobis' distance. G.L.C.

N85-23633*# Jet Propulsion Lab., California Inst. of Tech., Pasadena.
MAPPING AND GEOLOGICAL ANALYSIS OF MERCURY AND VENUS RADAR RANGING DATA Abstract Only
P. E. Clark, R. F. Jurgens, G. S. Downs, M. E. Strobell (Geological Survey), and G. G. Schaber (Geological Survey) *In* NASA, Washington Repts. of Planetary Geol. and Geophys. Program, 1984 Apr. 1985 p 453-455 refs (For primary document see N85-23474 13-91)
Avail: NTIS HC A99/MF A01 CSCL 03B

Although many radar profiles and images of the areas within 20 deg of Mercury's equator had been obtained from 1971, at both Goldstone and Arecibo radar facilities, surprisingly little geological analysis had been done with these data until recently. Topographic profiles and radar roughness reflectivity images which can be derived from these data will be crucial in completing the geological mapping of Mercury now underway at the U.S. Geological Survey. Earth based radar observations of Mercury and the other terrestrial planets as well are a potentially very valuable tool in the determination of the physical nature of their surfaces. Processing of available radar data must be completed to establish any systematic relationship between raar reflectivities and roughness, density, dielectric constant, and other related geological parameters. G.L.C.

N85-23634*# Jet Propulsion Lab., California Inst. of Tech., Pasadena.
CORRECTION AND GEOLOGICAL ANALYSIS OF LUNAR 3.8 cm RADAR DATA Abstract Only
P. E. Clark and T. W. Thompson *In* NASA, Washington Repts. of Planetary Geol. and Geophys. Program, 1984 Apr. 1985 p 456-457 refs Original document previously announced as N84-23531 (For primary document see N85-23474 13-91)
Avail: NTIS HC A99/MF A01 CSCL 03B

Earth based radar observations of the Moon have been taken at many wavelengths during the last ten years -- at 3.8, 70 cm, and most recently, 7.5 cm. Radar returns have been collected in both polarized and depolarized form so that is possible to derive both topographic and local surface roughness from the data. Until recently, work with 3.8 cm radar data had consisted of qualitative correlation of photographic and thermal IR data with individual depolarized radar data frames (local surface roughness) at different wavelengths. These studies provided results which demonstrated that the relationships between surface roughness (measured by either thermal emission or radar reflectivity) at different wavelengths can be used as an index of a crater's state of degradation (age). However, systematic studies of craters, or other local terrain features, as well as regional or global studies of major terrains (involving a number of data frames), cannot be done until individual frames are calibrated, geometric distortion is removed, and corrected frames are mosaicked. G.L.C.

N85-23635*# Jet Propulsion Lab., California Inst. of Tech., Pasadena.
LANDFORM IDENTIFICATION ON RADAR IMAGES Abstract Only
Henry J. Moore (Geological Survey, Menlo Park, Calif.) and T. W. Thompson *In* NASA, Washington Repts. of Planetary Geol. and Geophys. Program, 1984 Apr. 1985 p 458-460 refs (For primary document see N85-23474 13-91)
Avail: NTIS HC A99/MF A01 CSCL 03B

Polarized radar echo images of the Moon acquired using 3.8 and 70 cm wavelengths were examined to learn more about (1) the relationships between theoretical resolutions of the radars and the sizes of landforms that can be identified and (2) the factors that effect landform identification. G.L.C.

N85-23636*# Stanford Univ., Calif. Center for Radar Astronomy.
MARS RADAR CATALOG Abstract Only

Richard A. Simpson and G. Leonard Tyler *In* NASA, Washington Repts. of Planetary Geol. and Geophys. Program, 1984 Apr. 1985 p 461-462 (For primary document see N85-23474 13-91)
Avail: NTIS HC A99/MF A01 CSCL 03B

Radar observations of Mars have been conducted since 1963 using four Earth based facilities. Wavelengths have ranged from about 3 to about 70 cm. Experiments have been conducted in ranging, spectral, and mixed modes. Results include topographic profiles, estimates of dielectric constant and meter scale surface roughness, and qualtitative determinations of centimeter scale structure. G.L.C.

N85-23637*# Stanford Univ., Calif. Center for Radar Astronomy.
STATISTICS OF AEOLIAN SURFACE OF MARS Abstract Only
Richard A. Simpson, Frank Webb, and G. Leonard Tyler *In* NASA, Washington Repts. of Planetary Geol. and Geophys. Program, 1984 Apr. 1985 p 463 (For primary document see N85-23474 13-91)
Avail: NTIS HC A99/MF A01 CSCL 03B

Aeolian control of large scale surface texture is apparent in orbiter images from selected regions of Mars -- the polar areas, equatorial canyons, and some craters. At other locations on Mars there is evidence suggesting aeolian control on meter scales within a context provided by larger landforms. G.L.C.

N85-23638*# Jet Propulsion Lab., California Inst. of Tech., Pasadena.
RADAR AND THE DETECTION OF LIQUID WATER ON MARS Abstract Only
L. E. Roth and R. S. Saunders *In* NASA, Washington Repts. of Planetary Geol. and Geophys. Program, 1984 Apr. 1985 p 464-466 refs (For primary document see N85-23474 13-91)
Avail: NTIS HC A99/MF A01 CSCL 03B

Detection of the seasonally variable radar reflectivity in the Goldstone Mars data (the Solis Lacus radar anomaly and the proposed interpretation in terms of the near-surface presence of liquid water created a controversy in the planetary science community. Over the past year, skepticism was voiced about the reality of the phenomenon of a seasonally variable radar reflectivity anywhere on Mars. The necessary background information and the pertinent data are reviewed in a format perhaps more convincing than that employed in the original presentation of the discovery. A summary of the results and recommendations for future work are included. G.L.C.

N85-23639*# New Mexico Univ., Albuquerque. Dept. of Geology.
INTRA-ERUPTION GEOLOGIC MAP FROM AN X-BAND RADAR IMAGE DURING THE MAY 18, 1980 ERUPTION OF MOUNT ST. HELENS, WASHINGTON Abstract Only **c32**
C. W. Criswell and W. B. Elston *In* NASA, Washington Repts. of Planetary Geol. and Geophys. Program, 1984 Apr. 1985 p 466-469 refs (For primary document see N85-23474 13-91)
Avail: NTIS HC A99/MF A01 CSCL 17I

The use of side-looking airborne radar images for geologic interpretations has increased with the Vesuvian exploration projects. Interpretation of images without ground truth relies on examples in terrestrial environments for which geologic data are available. G.L.C.

N85-23640*# Arizona State Univ., Tempe. Dept. of Geology.
RADAR OBSERVATIONS OF FISSURE-FED BASALTIC LAVA FLOWS, CRATERS OF THE MOON, IDAHO Abstract Only **c32**
L. Martel and R. Greeley *In* NASA, Washington Repts. of Planetary Geol. and Geophys. Program, 1984 Apr. 1985 p 470 (For primary document see N85-23474 13-91)
Avail: NTIS, HC A99/MF A01 CSCL 17I

Changes in surface roughness of lava flows, estimated from dual polarization, synthetic aperture, X and L band side-looking airborne radar images, were tested as a means of locating fissure vent areas. If lava textures proess from smooth, near-vent shelly pahoehoe to hummocky pahoehoe to aa with distance from fissure vents, then radr images of the lava flows would show a progression from dark to brighter tones due to the flows' increasing radar back-scatter. G.L.C.

N85-23641*# Geological Survey, Flagstaff, Ariz.
LATE TERTIARY AND QUATERNARY RIVER SYSTEMS OF THE EASTERN SAHARA AS MAPPED ON SHUTTLE RADAR AND LANDSAT IMAGES Abstract Only **c43**
John F. McCauley, Carol S. Breed, and Gerald G. Schaber *In* NASA, Washington Repts. of Planetary Geol. and Geophys. Program, 1984 Apr. 1985 p 471-473 (For primary document see N85-23474 13-91)
Avail: NTIS HC A99/MF A01 CSCL 08H

SIR-A pictures of the Eastern Sahara show segments of what are interpreted as relics of once major Tertiary and Quaternary stream valleys. These previously unmapped features have a dark to very dark radar response and are generally concealed below a thin cover of flat to slightly undulating deposits, mostly of eolian origin. In most of the 150 pits and trenches we have studied to date, unconsolidated surface deposits range from a few centimeters to about a meter thick. The SIR-A system was able to 'see through' this loose, dry material, to a depth of about a meter or two. G.L.C.

N85-23642*# Arizona State Univ., Tempe. Dept. of Geology.
ANALYSES OF RADAR IMAGES OF SMALL CRATERS Abstract Only **c32**
R. Greeley, P. R. Christensen, and J. F. McHone *In* NASA, Washington Repts. of Planetary Geol. and Geophys. Program, 1984 Apr. 1985 p 474-475 refs (For primary document see N85-23474 13-91)
Avail: NTIS HC A99/MF A01 CSCL 17I

Clouds hide the surface of Venus from all but radar imaging systems, supplemented by limited views from land spacecraft. Among the surfaces features likely to be observed by radar are craters that have formed by a variety of processes. In order to assess the radar characteristics of craters, volcanic craters and impact structures on Earth are described as imaged by the Shuttle Imaging Radar (SIR-A) experiment. Although most of the craters are small, this analysis provides insight into the ability to discriminate craters of various origins and provides some basis for interpreting radar images returned from Venus. G.L.C.

N85-23643*# National Air and Space Museum, Washington, D.C. Center for Earth and Planetary Studies.
MECHANISMS OF BASALT-PLAINS RIDGE FORMATION Abstract Only
Thomas R. Watters and Ted A. Maxwell *In* NASA, Washington Repts. of Planetary Geol. and Geophys. Program, 1984 Apr. 1985 p 479-481 refs (For primary document see N85-23474 13-91)
Avail: NTIS HC A99/MF A01 CSCL 03B

The morphologic similarities between the Columbia Plateau ridges and ridges on the Moon, Mercury and Mars form a strong basis for the interpretation of basalt-plains ridges as compressional folds. The basalt-plains ridges appear to have formed on competent flood basalt units deformed at the surface with essentially no confining pressure. Estimates of compressive strain for planetary ridges range from a few tenths of a percent on the Moon to up to 0.4% on Mars, to as high as 35% for Columbia Plateau folds with associated thrust faults. Such values have strong implications for both deformational mechanisms as well as for the source of stress. Deformational mechanisms that will attempt to account for the morphology, fold geometry, possible associated thrust faulting and regular spacing of the basalt-plains ridges on the terrestrial planets are under investigation. G.L.C.

N85-23644*# Jet Propulsion Lab., California Inst. of Tech., Pasadena.
TERRESTRIAL ANALOGS FOR PLANETARY WRINKLE RIDGES Abstract Only **c46**
J. B. Plescia (Geological Survey, Flagstaff, Ariz.) and M. Golomobek *In* NASA, Washington Repts. of Planetary Geol. and Geophys. Program, 1984 Apr. 1985 p 482-484 refs (For primary document

see N85-23474 13-91)
Avail: NTIS HC A99/MF A01 CSCL 08G

Wrinkle ridges are common physiographic features on the terrestrial planets. Their origin has remained enigmatic, although two different types of models, volcanic and tectonic, have been proposed. The major impediment to deciphering the origin of wrinkle ridges has been the lack of a terrestrial analog. Seven terrestrial analogs were discussed, two in detail. Their implications for the origin for planetary wrinkle ridges were considered. All of the terrestrial analogs were formed in compressional environments and are the surface breaks of thrust faults. G.L.C.

N85-23645*# Jet Propulsion Lab., California Inst. of Tech., Pasadena.
ON THE ABSENCE OF STRIKE-SLIP FAULTS FROM THE PLANETS AND SATELLITES Abstract Only
Matthew P. Golombek *In* NASA, Washington Repts. of Planetary Geol. and Geophys. Program, 1984 Apr. 1985 p 485-487 refs (For primary document see N85-23474 13-91)
Avail: NTIS HC A99/MF A01 CSCL 03B

Lunar grabens are bounded by two downward converging 60 deg dipping normal faults. These faults intersect below the surface at a major mechanical discontinuity in the shallow crust between the megaregolith (total ejecta built up by repeated cratering) and the underlying in situ fractured rock. The ymmetry and simplicity of lunar grabens demands that the bounding faults initiate at this mechanical discontinuity and propagate up. Wrinkle ridges are though to result from thrust faulting or compressional folding of mare basalts. Identification and analysis of a number of terrestrial analogs that are morphologically similar to lunar and martian examples indicates that wrinkle ridges results from thrust faulting. The location of wrinkle ridges above suggested subsurface basin structures indicates that the trend and location of many wrinkle ridges are inherited from these pre-existing basin structures. This implies that the thrust faults responsible for wrinkle ridges initiate at the ase of the basalt-basin floor contact. This contact almost certainly represents a mechanical discontinuity in the shallow lunar crust because mare basalts are undoubtedly stronger than the underlying fall-back ejecta of the basin floor. G.L.C.

N85-23646*# Jet Propulsion Lab., California Inst. of Tech., Pasadena.
LUNAR MASCON LOADING: AN EXAMPLE OF THE IMPORTANCE OF FAULT INITIATION DEPTH ON FAULT TYPE PREDICTIONS FROM STRESSES ON PLANETARY SURFACES Abstract Only
Matthew P. Golombek *In* NASA, Washington Repts. of Planetary Geol. and Geophys. Program, 1984 Apr. 1985 p 488-490 refs (For primary document see N85-23474 13-91)
Avail: NTIS HC A99/MF A01 CSCL 03B

Geophysical models that predict fault type from stresses calculated at the planetary surface (zero depth) can be misleading because faults generally initiate at depth under a different stress regime and propagate to the surface. The generally accepted and most commonly employed criteria for fault prediction from calculated stresses on planetary surfaces points out problems in neglecting the effects of non-isotropic overburden stresses and the use of realistic material constants and shows a well known example (mascon loading on the moon) where neglecting this effect predicts a different type of fault than is actually observed. G.L.C.

N85-23647*# Massachusetts Inst. of Tech., Cambridge. Dept. of Earth, Atmospheric and Planetary Sciences.
THE DEEP STRUCTURE OF LUNAR BASINS: CLUES TO THE UNDERSTANDING OF BASIN FORMATION AND MODIFICATION Abstract Only
Steven R. Bratt, Sean C. Solomon, James W. Head (Brown Univ.), and Clifford H. Thurber (State Univ. of New York, Stony Brook) *In* NASA, Washington Repts. of Planetary Geol. and Geophys. Program, 1984 Apr. 1985 p 491-493 refs (For primary document see N85-23474 13-91)
Avail: NTIS HC A99/MF A01 CSCL 03B

Basin excavation has played a major role in shaping the surface and subsurface of the Moon. Though photogeologic observations provide estimates for the present volumes of lunar impact basins and their ejecta deposits, there is not sufficient information to describe completely either the geometry of the basins at the time of impact or their modification with time. Determination of the structure of the crust and upper mantle beneath large basins can provide important insight into the thermal and mechanical processes associated with basin formation and modification as well as the differences in these processes as functions of basin age and size. Using observed gravity and topography together with the seismically determined crustal thickness of the central nearside, a model for the structure of the crust and upper mantle of the nearside of the Moon is presented. With this model the deep structure of the largest lunar basins are compared. The implications for the processes of basin formation and modification at different stages in lunar history are explored. G.L.C.

N85-23648*# McDonnell Automation Co., St. Louis, Mo. Dept. of Earth and Planetary Sciences.
BOUGUER IMAGES OF THE NORTH AMERICAN CRATON Abstract Only **c46**
R. E. Arvidson, D. I. Bindschadler, S. Bowring, M. Eddy, E. Guinness, and C. Leff *In* NASA, Washington Repts. of Planetary Geo. and Geophys. Program, 1984 Apr. 1985 p 494-496 refs (For primary document see N85-23474 13-91)
Avail: NTIS HC A99/MF A01 CSCL 08G

Processing of existing gravity and aeromagnetic data with modern methods is providing new insights into crustal and mantle structures for large parts of the United States and Canada. More than three-quarters of a million ground station readings of gravity are now available for this region. These data offer a wealth of information on crustal and mantle structures when reduced and displayed as Bouguer anomalies, where lateral variations are controlled by the size, shape and densities of underlying materials. Digital image processing techniques were used to generate Bouguer images that display more of the granularity inherent in the data as compared with existing contour maps. A dominant NW-SE linear trend of highs and lows can be seen extending from South Dakota, through Nebaska, and into Missouri. This trend is probably related to features created during an early and perhaps initial episode of crustal assembly by collisional processes. The younger granitic materials are probably a thin cover over an older crust. G.L.C.

N85-23649*# Southern Methodist Univ., Dallas, Tex. Dept. of Geological Sciences.
PLANETARY INTERIOR MODELING AND TECTONIC IMPLICATIONS Abstract Only
R. J. Phillips *In* NASA, Washington Repts. of Planetary Geol. and Geophys. Program, 1984 Apr. 1985 p 497-499 refs (For primary document see N85-23474 13-91)
Avail: NTIS HC A99/MF A01 CSCL 03B

A technique is described for estimating spectral admittance functions using Pioneer Venus gravity and topography data. These admittance functions provide a convenient means to carry out systematic geophysical studies over much of the surface of Venus with a variety of interior density models. The admittance functions are calculated in the observation space of line-of-sight (LOS) gravity. Both closed and open system petrological models are considered for the Tharsis region of Mars. An analytic theory for isostatic compensation on one-plate planet is applied, including membrane stresses in the lithosphere, self gravitation, and rotational ellipticity. Crucial to this stress modeling and also to the petrological modeling is the observation that the earliest fracturing seen in the Tharsis region is associated with isostatic stresses. The radial fractures that extend far from Tharsis are associated with an additional and/or a completely different mechanism. A.R.H.

N85-23650*# Massachusetts Inst. of Tech., Cambridge. Dept. of Earth, Atmospheric and Planetary Sciences.
ELYSIUM REGION, MARS: TESTS OF LITHOSPHERIC LOADING MODELS FOR THE FORMATION OF TECTONIC FEA-

TURES Abstract Only
J. Lynn Hall, Sean C. Solomon, and James W. Head (Brown Univ.) *In* NASA, Washington Repts. of Planetary Geol. and Geophys. Program, 1984 Apr. 1985 p 500-502 refs (For primary document see N85-23474 13-91)
Avail: NTIS HC A99/MF A01 CSCL 03B

In an effort to constrain the tectonic history and mechanical properties of the lithosphere in the Elysium province, the stress fields predicted by different models are compared to the observed tectonic features of the region. The models are all products of volcanic loading of the Martian lithosphere, but at three different scales: global (Tharsis), regional (Elysium Planitia), and local (individual shields). Conclusions: The concentric graben surrounding Elysium Mons can be ascribed to the flexural response of an approximately 50-km-thick elastic lithosphere to loading by the volcano. No tectonic evidence for the support of larger-scale Elysium Planitia volcanic units by lithospheric flexure. The quasi-global loading of the Tharsis rise appears to have produced identifiable tectonic effects in the Elysium region. A.R.H.

N85-23651*# Wesleyan Univ., Middletown, Conn. Dept. of Earth and Environmental Sciences.
LITHOLOGIC AND STRUCTURAL CONTROL ON SLOPE MORPHOLOGY IN THE VALLES MARINERIS Abstract Only
Peter C. Patton *In* NASA, Washington Repts. of Planetary Geol. and Geophys. Program, 1984 Apr. 1985 p 503-505 refs (For primary document see N85-23474 13-91)
Avail: NTIS HC A99/MF A01 CSCL 03B

Throughout the Valles Marineris scarp morphology varies as a function of lithology, structure and scarp height. In addition lithology is an important control on permeability and the relative importance of spring sapping processes. Geomorphic mapping of distinct subareas can be used to define the characteristic scarp forms. Distinct morphologic zones defined on the basis of regional variations in lithology are described. Lithology and tectonic history are shown to be the two most important factors controlling slope development. Regional variation in scarp morphology can be correlated with the orientation and density of fracture systems; scarp height and the presence of rejuvenated fault scarps; and the thickness and degree of exposure of presumably less competent, more permeable, water saturated crated plateau material in the chasmata scarps. A.R.H.

N85-23652*# Geological Survey, Flagstaff, Ariz.
VALLES MARINERIS BASIN BEDS: A COMPLEX STORY Abstract Only
B. K. Lucchitta *In* NASA, Washington Repts. of Planetary Geol. and Geophys. Program, 1984 Apr. 1985 p 506-508 refs (For primary document see N85-23474 13-91)
Avail: NTIS HC A99/MF A01 CSCL 03B

High resolution stereoimages of the central Valles Marineris enabled detailed geologic mapping on Ophir and Candor Chasmata. Abundant light colored deposits, both layered and massive, fill the chasmata in this region. Units within these deposits were identified by their erosional characteristics and superposition and cross cutting relations. The Valles Marineris beds reflect a history of repeated faulting, volcanic eruptions, and deposition and erosion, resulting in stratigraphic sequences with several unconformities. Because of the preponderance of apparent volcanic deposits inside the troughs, the chasmata may not be simple grabens, but rather giant volcano tectonic depressions. Major events in chasmata development are examined. A.R.H.

N85-23653*# Geological Survey, Flagstaff, Ariz.
MARS: STRATIGRAPHY OF WESTERN HIGHLANDS AND POLAR REGIONS Abstract Only
Kenneth L. Tanaka, David H. Scott, and Marlene F. Tuesink *In* NASA, Washington Repts. of Planetary Geol. and Geophys. Program, 1984 Apr. 1985 p 509-511 refs (For primary document see N85-23474 13-91)
Avail: NTIS HC A99/MF A01 CSCL 03B

Geologic mapping and stratigraphic studies of Mars based on Viking images improved knowledge of the relative age and occurrence of geologic units on a global scale. Densities of geologic units or features during the Noarchian, Hesperian, and Amazonian periods are indicated for the North and South polar regions as well as the equatorial region of Mars. Cumulative counts of crater size frequencies for craters larger than 2 km in diameter on plateau units mapped in the western region of Mars counts indicate that the plateau terrain as a whole was thinly resurfaced during the Hesperian Period, and a large proportion of pre-existing craters less than 10 to 15 km in diameter was buried. The formation of northern plains, subpolar highlands, and both polar regions is also described. A.R.H.

N85-23654*# Massachusetts Univ., Amherst. Dept. of Geology/Geography.
KASEI VALLIS OF MARS: DATING THE INTERPLAY OF TECTONICS AND GEOMORPHOLOGY Abstract Only
Donald U. Wise *In* NASA, Washington Repts. of Planetary Geol. and Geophys. Program, 1984 Apr. 1985 p 512 (For primary document see N85-23474 13-91)
Avail: NTIS HC A99/MF A01 CSCL 03B

Crater density age dates on more than 250 small geomorphic surfaces in the Kasei Region of Mars show clusterings indicative of times of peak geomorphic and tectonic activity. Kasei Vallis is part of a 300 km wide channel system breaching a N-S trending ancient basement high (+50,000 crater age) separating the Chryse Basin from the Tharsis Volcanic Province of Mars. The basement high was covered by a least 3 groups of probable volcanic deposits. Major regional fracturing took place at age 4,000 to 5,000 and was immediately followed by deposition of regional volcanics of the Fesenkov Plains (age 3,000 to 4,200). Younger clusterings of dates in the 900 to 1,500 and 500 to 700 range represent only minor modification of the basic tectonic geomorphic landform. The data suggest that Kasei gap is a structurally controlled breach of a buried ridge by a rather brief episode of fluvial activity. A.R.H.

N85-23655*# California Univ., Livermore. Lawrence Livermore Lab.
CREEP OF ICE: FURTHER STUDIES Abstract Only **c43**
H. C. Heard, W. B. Durham, and S. H. Kirby *In* NASA, Washington Repts. of Planetary Geol. and Geophys. Program, 1984 Apr. 1985 p 513-515 refs (For primary document see N85-23474 13-91)
Avail: NTIS HC A99/MF A01 CSCL 08L

Frictional sliding experiments conducted to study crustal behavior on the icy Galilean satellites are described as well as the microstructural aspects of ice flow. An improved heat exchanger and computer control of temperature are being used to explore the lower regimes of strain rate. A preliminary measurement of the strengths of some of the higher pressure polymorphs of ice was obtained and is considered. A.R.H.

N85-23656*# McDonnell Aircraft Co., St. Louis, Mo. Dept. of Earth and Planetary Sciences.
FAULT OFFSETS AND LATERAL CRUSTAL MOVEMENT ON EUROPA Abstract Only
Paul M. Schenk *In* NASA, Washington Repts. of Planetary Geol. and Geophys. Program, 1984 Apr. 1985 p 516-518 refs (For primary document see N85-23474 13-91)
(Grant NAGw-432)
Avail: NTIS HC A99/MF A01 CSCL 03B

Structural evidence is presented for tension cracking associated with strike slip faulting and crustal movement in the bright ice covered Galilean satellite Europa. The structure and morphology of wedge shaped bands argues that they formed as a result of the rotation and lateral displacement of crustal units bounded by near vertical faults penetrating through the brittle crustal layer. The significant rotation and lateral motion of crustal blocks near the anti-jove point on Europa, without graben formation, also argues that the lithosphere in the fractured area is mechanically decoupled from the solid silicate interior, by either warm ice at depth or liquid water. Ice at depth and at a large fraction of its melting temperature is expected to behave as a fluid over geologically short time intervals due to its extremely low viscosity relative to the cold, brittle ice near the surface. One proposed convection

mechanism is thus considered unlikely as it would be difficult to transmit internal stress through a decoupling layer to the surface. A.R.H.

N85-23657*# McDonnell Aircraft Co., St. Louis, Mo. Dept. of Earth and Planetary Sciences.
THREE-LAYER GENERIC GANYMEDES: STRUCTURE AND EVOLUTION Abstract Only
S. W. Mueller and W. B. McKinnon *In* NASA, Washington Repts. of Planetary Geol. and Geophys. Program, 1984 Apr. 1985 p 519-521 refs (For primary document see N85-23474 13-91)
Avail: NTIS HC A99/MF A01 CSCL 03B

Accurate, three layered structural models were generated for Ganymede and Callisto. Three layered satellites consist of a rock core, a region of mixed rock and ice, and an outer shell of pure ice. This structure would result from either accretional melting of the outermost region of the satellite or differentiation subsequent to localized melting. A completely undifferentiated ice rock satellite possesses only the single, top boundary layer and, in this case, melting is also relatively difficult to initiate; this suggests that, if accretional melting results in a small degree of differentiation initially, subsequent melting may readily occur as the satellite warms due to radiogenic heating. Alternatively, if accretion is not accompanied by a small degree of differentiation, it may prove too difficult to initiate nonaccretional melting and the satellite might remain undifferentiated indefinitely. A.R.H.

N85-23658*# Arizona Univ., Tucson. Lunar and Planetary Lab.
LINEAMENTS ON GANYMEDE: NEW EVIDENCE FOR LATE TECTONIC ACTIVITY Abstract Only
Steven K. Croft *In* NASA, Washington Repts. of Planetary Geol. and Geophys. Program, 1984 Apr. 1985 p 522-524 refs (For primary document see N85-23474 13-91)
Avail: NTIS HC A99/MF A01 CSCL 03B

Families of lineaments in the Gilomesh and Ninki basins of Ganymede imply post impact tectonic activity. The grooves, previously considered the youngest tectonic features, are estimated to have formed between 3.8 and 3.1 Gyr ago. One rayed crater however, is probably less than 1 Gyr old, implying tectonic activity on Ganymede has extended nearly to the present. Like the grooves, the lineaments appear to be extensional. The parallel trends and nearly contiguous associations of the lineaments with the grooves imply that both are products of the same stress systems. The young inferred age of the lineaments implies that they (and presumably also the grooves) are not associated with stresses in the cooling of fresh deposits of bright terrain, but are probably associated with underlying convective stress patterns, the long implied duration of an extensional stress regime in Ganymede's lithosphere is consistent with the stress models of derived assuming a differentiated interior. A.R.H.

N85-23659*# Paris XI Univ., Orsay (France). Lab. de Geologie Dynamique Interne.
GLOBAL TECTONICS ON GANYMEDE Abstract Only
Pierre G. Thomas, Olivier P. Forni, and Philippe L. Masson *In* NASA, Washington Repts. of Planetary Geol. and Geophys. Program, 1984 Apr. 1985 p 525-527 refs Sponsored in part by CNRS (For primary document see N85-23474 13-91)
Avail: NTIS HC A99/MF A01 CSCL 03B

Three large basin surroundings on Ganymede located on grooved terrains, which are supposed to be intensely tectonized areas were studied. All rectilinear morphological elements such as ridges, block edges; and parts of scarps were mapped. The geometric properties (grid pattern) characteristics were determined and a history for the formation of the Ganymede basins studied is proposed. Results indicate that the grooved terrains are very surficial layers, and that their formation does not significantly affect, disturb or rotate the basement. This is in agreement with the conclusion obtained from completely different data (crosscutting relationships between groove sets and their basements). A.R.H.

N85-23660*# Paris XI Univ., Orsay (France). Lab. de Geologie Dynamique Interne.
TECTONICS OF THE GALILEO REGIO ON GANYMEDE Abstract Only
Pierre G. Thomas and Philippe L. Masson *In* NASA, Washington Repts. of Planetary Geol. and Geophys. Program, 1984 Apr. 1985 p 528-530 refs Sponsored in part by CNRS (For primary document see N85-23474 13-91)
Avail: NTIS HC A99/MF A01 CSCL 03B

The surface of Ganymede consists of dark cratered terrain, and groved terrain. The dark cratered terrains form polygonal units, the largest of which is Galileo Regio, the surface of which is transected by furrows, smooth floored valleys bounded by relatively sharp parallel ridges. The most apparent of them are grouped together and form an apparently arcuate system of subparallel furrows which was mapped using Voyager pictures and plotted on a map using a stereographic projection. With this kind of projection, the main furrow system is not arcuate, but rectilinear. Observations strongly suggest that the Galileo Regio furrow systems are not of impact origin and appear to be irrelevant to discussions about the basins' morphology or evolution of planetary lithosphere determined from multiring structures. A.R.H.

N85-23661*# Paris XI Univ., Orsay (France). Lab. de Geologie Dynamique Interne.
IMPORTANCE OF THE TECTONIC MOTIONS ON GANYMEDE Abstract Only
Olivier P. Forni, Pierre G. Thomas, and Philippe L. Masson *In* NASA, Washington Repts. of Planetary Geol. and Geophys. Program, 1984 Apr. 1985 p 531-534 refs Sponsored in part by CNRS (For primary document see N85-23474 13-91)
Avail: NTIS HC A99/MF A01 CSCL 03B

Voyager close up views of Ganymede reveal some provinces of old, cratered, dark terrains that are broken into polygons and cut through by light stripes of grooved terrains. The groove terrain unit and its relationships with the other units was studied at various scales because these features seem to relate at least to two main scales of processes. Minor displacements concerning only local features, i.e., large scale processes and major displacements concerning usually the major evolution of the surface, i.e., small scale processes. It appears that tectonic processes, at least in the studied areas, if playing a role in the formation of local or regional features, are very limited. The conclusions reached agree with those of Thomas et al. who show that post grooves basins reveal the presence of a primitive grid that is not disturbed by the grooved terrains. A.R.H.

N85-23662*# Paris XI Univ., Orsay (France). Lab. de Geologie Dynamique Interne.
TECTONICS OF THE VALHALLA STRUCTURE ON CALLISTO Abstract Only
Pierre G. Thomas and Philippe L. Masson *In* NASA, Washington Repts. of Planetary Geol. and Geophys. Program, 1984 Apr. 1985 p 535-539 refs Sponsored in part by CNRS (For primary document see N85-23474 13-91)
Avail: NTIS HC A99/MF A01 CSCL 03B

The surficial morphology of Callisto is dominated by large concentric patterns of ridges, scarps, and furrows. The largest one, Valhalla, shows a smooth central area 350 km in radius, surrounded by concentric sinuous ridges which extend as far as 600km from the center. Beyond the ridged area, scarps and furrows are observed as far as 2000 km. The global azimuthal distribution of the scarps and furrows of the outer ring (beyond 700 km from the center) was analyzed. It is proposed that the local geometry and the global distribution of scarps and furrows around Valhalla are the results of the reactivation of an old pattern by the Valhalla event. The coincidence of these local directions of a preexisting pattern (NW-SE and NE-SW) with the directions of the grids observed on most bodies observed so far in the solar system would indicate that this local pattern is a part of a global calistean grid. A.R.H.

N85-23663*# Geological Survey, Flagstaff, Ariz.
MARS GEOLOGIC MAPPING: A REVIEW AND NEW CONCEPTS Abstract Only

David H. Scott and Kenneth L. Tanaka *In* NASA, Washington Repts. of Planetary Geol. and Geophys. Program, 1984 Apr. 1985 p 541-543 refs (For primary document see N85-23474 13-91)
Avail: NTIS HC A99/MF A01 CSCL 03B

The final version of the 1.15 m scale geologic map of the western equatorial region of Mars based on Viking pictures has been completed in open file format. Geologic maps of the north and south polar regions were completed in provisional form. A map of the eastern equatorial region is in compilation. Evidences of erosion, water flooding, volcanic activity, and primary and satellite craters in these areas are discussed. A.R.H.

N85-23664*# Geological Survey, Flagstaff, Ariz.
THE GALILEAN SATELLITE GEOLOGICAL MAPPING PROGRAM, 1984 Abstract Only
B. K. Lucchitta *In* NASA, Washington Repts. of Planetary Geol. and Geophys. Program, 1984 Apr. 1985 p 544-545 (For primary document see N85-23474 13-91)
Avail: NTIS HC A99/MF A01 CSCL 03B

About 40 investigators from various universities, research institutes, and government offices in the United States, England, Germany, and Italy are compiling maps of the Galilean satellites. All maps are at a scale of 1:5 million except for three of the Io maps, where high resolution pictures permit compilation of selected areas at larger scales. Guidelines for mapping Ganymede are discussed. A.R.H.

N85-23665*# Geological Survey, Flagstaff, Ariz.
GEOLOGY OF THE GANYMEDE QUADRANGLE Jg7 Abstract Only
B. K. Lucchitta *In* NASA, Washington Repts. of Planetary Geol. and Geophys. Program, 1984 Apr. 1985 p 546-547 (For primary document see N85-23474 13-91)
Avail: NTIS HC A99/MF A01 CSCL 03B

The western half of Ganymede quadrangle Jg7 is covered by Voyager 2 images with resolution of .5 to 5 km/pixel. The imaged area includes dark terrain in the north underlying the southeastern part of Galileo Regio, and light terrain in the south underlying the southeastern extension of Uruk Sulcus. Several slivers and wedges of dark terrain occur within the light areas. Numerous craters are present, as well as three large palimsests (crater scars with little topographic expression) in the dark terrain and a basin in the light terrain. The boundary between dark and light materials on the south side of Galileo Regio is locally marked by a scarp that faces the light terrain. The scarp truncates several craters. The truncation and rotation of structures suggest that light material grew at the expense of dark material, and that the destruction, except for minor pivoting, was essentially in situ. The composition and structural properties of the palimsests and craters are examined. A.R.H.

N85-23666*# Geological Survey, Flagstaff, Ariz.
MARS PLANIMETRIC MAPPING Abstract Only
R. M. Batson, P. M. Bridges, and E. M. Lee *In* NASA, Washington Repts. of Planetary Geol. and Geophys. Program, 1984 Apr. 1985 p 548-549 refs (For primary document see N85-23474 13-91)
Avail: NTIS HC A99/MF A01 CSCL 03B

The 1:5,000,000 scale shaded relief maps of Mars originally compiled from Mariner 9 pictures are being upgraded by adding details visible on Viking Orbiter images. This work is done by modifying the original airbrush drawings; no attempt is made to reposition features according to the latest control nets. Thirteen of these maps have been published to date, two are in compilation, and two are in press. A hard cover atlas containing reduced scale versions of all Mars cartographic products will be published upon completion of the revisions of the 1:5,000,000 scale maps, the 1:2,000,000 scale photomosaics, and Mars color albedo mapping tasks. This atlas will supersede the existing Atlas of Mars prepared by Batson and others. A.R.H.

N85-23667*# Geological Survey, Flagstaff, Ariz.
VIKING LANDER MOSAICS OF MARS Abstract Only
E. C. Morris *In* NASA, Washington Repts. of Planetary Geol. and Geophys. Program, 1984 Apr. 1985 p 552-553 refs (For primary document see N85-23474 13-91)
Avail: NTIS HC A99/MF A01 CSCL 03B

The Viking Lander 1 and 2 cameras acquired many high-resolution pictures of the Chryse Planitia and Utopia Planitia landing sites. Based on computer-processed data of a selected number of these pictures, eight high-resolution mosaics were published by the U.S. Geological Survey as part of the Atlas of Mars, Miscellaneous Investigation Series. The mosaics are composites of the best picture elements (pixels) of all the Lander pictures used. Each complete mosaic extends 342.5 deg in azimuth, from approximately 5 deg above the horizon to 60 deg below, and incorporates approximately 15 million pixels. Each mosaic is shown in a set of five sheets. One sheet contains the full panorama from one camera taken in either morning or evening. The other four sheets show sectors of the panorama at an enlarged scale; when joined together they make a panorama approximately 2' X 9'. A.R.H.

N85-23668*# Geological Survey, Flagstaff, Ariz.
VOYAGER CARTOGRAPHY Abstract Only
R. M. Batson, P. M. Bridges, and K. F. Mullins *In* NASA, Washington Repts. of Planetary Geol. and Geophys. Program, 1984 Apr. 1985 p 554-555 refs (For primary document see N85-23474 13-91)
Avail: NTIS HC A99/MF A01 CSCL 03B

The Jovian and Saturnian satellites are being mapped at several scales from Voyager 1 and 2 data. The maps include specially formatted color mosaics, controlled photomosaics, and airbrush maps. More than 500 Voyager images of the Jovian and Saturnian satellites were radiometrically processed in preparation for cartographic processing. Of these images, 235 were geometrically transformed to map projections for base mosaic compilations. Special techniques for producing hybrid photomosaic/airbrush maps of Callisto are under investigation. The techniques involve making controlled computer mosaics of all available images with highest resolution images superimposed on lowest resolution images. The mosaics are then improved by airbrushing: seams and artifacts are removed, and image details enhanced that had been lost by saturation in some images. A controlled mosaic of the northern hemisphere of Rhea is complete, as is all processing for a similar mosaic of the equatorial region. Current plans and status of the various series are shown in a table. A.R.H.

N85-23669*# RAND Corp., Santa Monica, Calif.
A UNIFIED LUNAR CONTROL NETWORK Abstract Only
Merton E. Davies *In* NASA, Washington Repts. of Planetary Geol. and Geophys. Program, 1984 Apr. 1985 p 556-557 refs (For primary document see N85-23474 13-91)
Avail: NTIS HC A99/MF A01 CSCL 03B

A unified network program can tie independent regional networks into a single consistent planetwide control network. The Apollo 15, 16, and 17 ALSEP stations were identified on Apollo panorama photography and their locations transferred to Apollo mapping frames. Two primary control networks were computed based on the Apollo mapping pictures. Although these systems were computed relative to the center-of-mass, it was necessary to translate their origins to best-fit the ALSEP locations. The DMAAC/A15 system was translated 299 + or - 165 m and the NOS/USGS system was translated 2033 + or - 575 m. Many control networks have been computed based on pictures of the Moon taken through telescopes; these cover the Earth-facing region. Points common to the Apollo networks and to a telescopic network (Meyer, 1980) were selected. Using these points in the overlapping region of the two networks, best-fit translation, rotation, and scale parameters are computed to adjust the telescopic net to the Apollo net. As a start, ten well distributed points have been selected and parameters determined to adjust the telescopic network to the translated DMAAC/A15 system and the NOS/USGS system. The goodness of fit has not yet been examined. A.R.H.

N85-23670*# RAND Corp., Santa Monica, Calif.
THE CONTROL NETWORK OF MARS: OCTOBER 1984 Abstract Only

Merton E. Davies *In* NASA, Washington Repts. of Planetary Geol. and Geophys. Program, 1984 Apr. 1985 p 558 ref (For primary document see N85-23474 13-91)
Avail: NTIS HC A99/MF A01 CSCL 03B

Strips of Viking mapping pictures are being added to the planetwide control networks of Mars. These high resolution strips run from the Viking 1 lander site east to Airy-O, north along the 0 deg meridian to 60 deg latitude, southwest through the Viking 1 lander site to the equator, and along the equator encircling the planet. Everywhere along these strips, old points are incorporated in the measurements, thus assuring that the strips and planetwide net make a single large data set. The control points are much denser in the areas covered by the strips than in those regions not covered by strips and their coordinates of the control points is estimated to be less than 3 km and the error in longitude of a few points near Airy-O is less than 40 m. The horizontal coordinates of the control points on Mars have been updated with a single-block planetwide analytical triangulation. The standard error of measurement was 18.06 micron m. The longitude of the Viking 1 lander site was 47 deg.962 and the latitude 22 deg. 480. The latitude of Airy-O was -5 deg. 152. A.R.H.

N85-23671*# RAND Corp., Santa Monica, Calif.
THE CONTROL NETWORKS OF THE SATELLITES OF JUPITER AND SATURN Abstract Only
Merton E. Davies *In* NASA, Washington Repts. of Planetary Geol. and Geophys. Program, 1984 Apr. 1985 p 559 refs (For primary document see N85-23474 13-91)
Avail: NTIS HC A99/MF A01 CSCL 03B

Geodetic control networks are being computed photogrammetrically for the large satellites of Jupiter and many of the satellites of Saturn using pictures from the Voyager 1 and 2 encounters. Control points have been identified on the satellites and their coordinates computed by single-block analytical triangulations. Contents of data sets for Io, Europa, Ganymede, Callisto, and Rhea are summarized. A.R.H.

N85-23672*# Jet Propulsion Lab., California Inst. of Tech., Pasadena.
SHAPE OF IO Abstract Only
S. P. Synnott, J. E. Reidel, J. C. Callahan, and A. J. Donegan *In* NASA, Washington Repts. of Planetary Geol. and Geophys. Program, 1984 Apr. 1985 p 560-562 refs (For primary document see N85-23474 13-91)
Avail: NTIS HC A99/MF A01 CSCL 03B

An approach for measuring the triaxial shape of Io from Voyager images is described. Triaxial shape of a satellite is detrmined by comparing the theoretical shape and location of the body's limb and terminator curves with the actual curves observed in the two dimensional images. Limb or terminator points are found by matching a model for the limb profile with the actual appearance of the limb in the digital data. The theoretical model for the limb model depends on the viewing and illumination geometry, the satellite reflection characteristics and the camera 'point spread function'. The method is applied to imaging data taken of Io in the last 25 hours befor Voyager 1's closet approach to the satellite. A.R.H.

N85-23673*# Cornell Univ., Ithaca, N.Y. Center for Radiophysics and Space Research.
PARTICIPATION IN THE MARS DATA ANALYSIS PROGRAM: ANALYSIS OF CLOUD FORMS IN VIKING AND MARINER 9 IMAGES Final Technical Report, 1 Mar. 1983 - 28 Feb. 1985
Peter Gierasch and Ralph A. Kahn Apr. 1985 5 p
(Grant NsG-7612)
(NASA-CR-175604; NAS 1.26:175604) Avail: NTIS HC A02/MF A01 CSCL 03B

The first systematic account of the climate of Mars, based upon observations was produced. Cloud data were used to determine spatially and temporally varying near-surface wind direction, relative wind speed, static stability, and humidity conditions on a global scale. Existing models of meteorological processes were critically reexamined in light of the data, and more stringent constraints were set on global processes. Several discoveries were made, including the large extent and seasonal variability of the Mars equatorial Hadley cell, the failure of high latitude winds to reverse direction in early northern spring, the change in meridional wind component in southern midautum, and the almost constant cloud cover in the northern hemisphere, during spring and summer primarily by condensate clouds and in fall and winter by condensates and dust. The implications of these observations are discussed. B.G.

N85-23674# Library of Congress, Washington, D. C. Science and Technology Div.
HALLEY'S COMET, A BIBLIOGRAPHY
Ruth S. Fertig 1984 581 p
(LC-84-600109; ISBN-0-8444-0459-4) Avail: NTIS HC A25/MF A01

Included in the bibliography are references to publications on Halley's comet, its history, orbital motion, and physical characteristics, meteor streams associated with it, preparations for space missions in 1986, and popular reaction to it appearances. Also cited are a few papers that, although they devote little attention to Halley's Comet as such, are of importance to the present state of knowledge about comets in general. Author

N85-22410# Joint Publications Research Service, Arlington, Va.
EXPANSION OF FUNCTIONS DESCRIBING PLANETARY SURFACE AND GRAVITY FIELD Abstract Only
S. G. Valeyev *In its* USSR Rept.: Space (JPRS-USP-85-001) 4 Feb. 1985 p 33 Transl. into ENGLISH from Astronomicheskiy Vestnik (USSR), v. 18, no. 3, Jul.-Sep. 1984 p 208-214 (For primary document see N85-22403 13-12)
Avail: NTIS HC A07

N85-22411# Joint Publications Research Service, Arlington, Va.
AVERAGING OF EQUATIONS OF COMETARY ORBITAL MOTION WITH ALLOWANCE FOR NONGRAVITATIONAL EFFECTS Abstract Only
Y. N. Polyakhova *In its* USSR Rept.: Space (JPRS-USP-85-001) 4 Feb. 1985 p 33-34 Transl. into ENGLISH from Astronomicheskiy Vestnik (USSR), v. 18, no. 3, Jul.-Sep. 1984 p 235-239 (For primary document see N85-22403 13-12)
Avail: NTIS HC A07

N85-22427# Joint Publications Research Service, Arlington, Va.
COSMOGENIC Na-22 AND Al-26 IN LUNA-24 LUNAR DRILL CORE SOIL SAMPLES Abstract Only
A. K. Lavrukhina, P. Povinets, and G. K. Ustinova *In its* USSR Rept.: Space (JPRS-USP-85-001) 4 Feb. 1985 p 46 Transl. into ENGLISH from Kosmicheskiye Issled. (USSR), v. 22, no. 1, Jan.-Feb. 1984 p 110-119 Original language document announced as A84-26986 (For primary document see N85-22403 13-12)
Avail: NTIS HC A07

N85-22433# Joint Publications Research Service, Arlington, Va.
VOLCANISM ON VENUS AS CONNECTING LINK Abstract Only
L. V. Ksanfomaliti *In its* USSR Rept.: Space (JPRS-USP-85-001) 4 Feb. 1985 p 58 Transl. into ENGLISH from Pisma Astronomicheskiy Zh. (USSR), v. 10, no. 8, Aug. 1984 p 620-630 (For primary document see N85-22403 13-12)
Avail: NTIS HC A07

N85-22435# Joint Publications Research Service, Arlington, Va.
ANALYSIS OF SYSTEMATIC ERRORS IN SYSTEMS OF SELENODETIC COORDINATES Abstract Only
V. A. Nikonov *In its* USSR Rept.: Space (JPRS-USP-85-001) 4 Feb. 1985 p 59 Transl. into ENGLISH from Astronomicheskiy Vestnik (USSR), v. 18, no. 2, Apr.-Jun. 1984 p 107-116 (For primary document see N85-22403 13-12)
Avail: NTIS HC A07

N85-22436# Joint Publications Research Service, Arlington, Va.
MICROSTRUCTURE OF VENUS CLOUD LAYER BASED ON SPECTROPHOTOMETRIC DATA FROM VENERA-11 SPACE-

CRAFT Abstract Only
D. V. Titov *In its* USSR Rept.: Space (JPRS-USP-85-001) 4 Feb. 1985 p 60 Transl. into ENGLISH from Kosmicheskiye Issled. (USSR), v. 22, no. 1, Jan.-Feb. 1984 p 120-129 Original language document announced as A84-26987 (For primary document see N85-22403 13-12)
Avail: NTIS HC A07

N85-22437# Joint Publications Research Service, Arlington, Va.
VISUALIZATION OF RADAR ALTIMETRY DATA FOR VENUS Abstract Only
D. G. Stankevich, S. P. Redkin, Y. V. Korniyenko, A. T. Bazilevskiy, and Y. G. Shkuratov *In its* USSR Rept.: Space (JPRS-USP-85-001) 4 Feb. 1985 p 60-61 Transl. into ENGLISH from Kosmicheskiye Issled. (USSR), v. 22, no. 1, Jan.-Feb. 1984 p 138-140 Original language document announced as A84-26993 (For primary document see N85-22403 13-12)
Avail: NTIS HC A07

N85-22438# Joint Publications Research Service, Arlington, Va.
PRELIMINARY PHOTOMAPS OF VENUS SURFACE IN THE MAXWELL MOUNTAINS AND ADJACENT AREAS Abstract Only
A. F. Bogomolov and Y. S. Tyuflin *In its* USSR Rept.: Space (JPRS-USP-85-001) 4 Feb. 1985 p 61 Transl. into ENGLISH from Geodiziya i Kartografiya (USSR), no. 8, Aug. 1984 p 11-16 (For primary document see N85-22403 13-12)
Avail: NTIS HC A07

N85-22439# Joint Publications Research Service, Arlington, Va.
HYPSOMETRIC FEATURES ON VENUS Abstract Only
Z. F. Rodionova *In its* USSR Rept.: Space (JPRS-USP-85-001) 4 Feb. 1985 p 62 Transl. into ENGLISH from Astronomicheskiy Vestnik (USSR), v. 18, no. 2, Apr.-Jun. 1984 p 117-127 (For primary document see N85-22403 13-12)
Avail: NTIS HC A07

N85-22534# Air Force Rocket Propulsion Lab., Edwards AFB, Calif.
ACOUSTIC ENERGY EXCHANGE IN SHEARED MEAN FLOWS
J. D. Baum and J. N. Levine *In* APL 21st JANNAF Combust. Meeting, Vol. 1 Oct. 1984 p 83-90 refs (For primary document see N85-22526 13-20)
Avail: NTIS HC A21/MF A01 CSCL 20A

92 SOLAR PHYSICS

Includes solar activity, solar flares, solar radiation and sunspots.

N85-23675 Colorado Univ., Boulder.
ULTRAVIOLET SPECTRAL DIAGNOSTICS OF SOLAR FLARES AND HEATING EVENTS Ph.D. Thesis
Jason Garth Porter 1984 147 p
Avail: Univ. Microfilms Order No. DA8428675

Heating processes in the outer solar atmosphere manifest themselves in continuous and discrete phenomena ranging from te largest solar flares down to the smallest events discernible with present instruments. Two such phenomena are addressed as seen in ultraviolet observations of the solar transition zone; data obtained with the Solar maximum Mission (SMM) satellite are found to reveal the presence of frequent and rapid brightenings in ultraviolet line emission in active regions, and observations obtained with the NRL Slitless Spectroheliograph on Skylab are analyzed to determined the role of the helium resonance lines in the energy balance of a large class M flare. SMM observations with high spatial and temporal resolution at small bright sites in active regions show significant increases in intensity in spectral lines of Si IV and O IV on short time scales. Intensity increases of 20 to 100% are common and typically last 40 to 60 s. These characteristics suggest that topological dissipation of energy stored in the magnetic field is occurring more frequently and on smaller spatial scales than previously observed. Dissert. Abstr.

N85-23676*# Smithsonian Astrophysical Observatory, Cambridge, Mass.
SOLAR AND STELLAR CORONAL PLASMAS Semiannual Progress Report, 1 Nov. 1984 - 30 Apr. 1985
Leon Golub Apr. 1985 123 p refs
(Grant NAGw-112)
(NASA-CR-175623; NAS 1.26:175623; SAPR-9) Avail: NTIS HC A06/MF A01 CSCL 03B

Progress made in describing and interpreting coronal plasma processes and the relationship between the solar corona and its stellar counterparts is reported. Topics covered include: stellar X-ray emission, HEAO 2 X-ray survey of the Pleiades, closed coronal structures, X-ray survey of main-sequence stars with shallow convection zones, implications of the 1400 MHz flare emission, and magnetic field stochasticity. A.R.H.

N85-23677*# Smithsonian Astrophysical Observatory, Cambridge, Mass.
PHYSICS OF THE INNER HELIOSPHERE: MECHANISMS, MODELS AND OBSERVATIONAL SIGNATURES Semiannual Progress Report, 1 Nov. 1984 - 30 Apr. 1985
George L. Withbroe Apr. 1985 14 p refs
(Grant NAGw-249)
(NASA-CR-175632; NAS 1.26:175632; SAPR-7) Avail: NTIS HC A02/MF A01 CSCL 03B

The physics of the solar wind acceleration phenomena (e.g. effect of transient momentum deposition on the temporal and spatial variation of the temperature, density and flow speed of the solar wind, formation of shocks, etc.) and the resultant effects on observational signatures, particularly spectroscopic signature are studied. Phenomena under study include: (1) wave motions, particularly spectroscopic signatures are studied. Phenomena under study include:(1) wave motions, particularly Alfven and fast mode waves, (2) the formation of standing shocks in the inner heliosphere as a result of momentum and/or heat addition to the wind and (3) coronal transient phenomena where momentum and/or heat are deposited in the corona to produce transient plasma heating and/or mass ejections. Also included are the theoretical investigation of spectroscopic plasma diagnostics for the inner heliosphere and the analysis of existing Skylab and other relevant data. B.G.

N85-23678# Los Alamos Scientific Lab., N. Mex.
CONSTRAINTS OF OBSERVATIONS OF SOLAR OSCILLATIONS ON SOLAR MODELS WITH MIXING BY TURBULENT DIFFUSION
Arthur N. Cox, Russel B. Kidman, and Michael J. Newmen 1984 14 p refs Presented at the Conf. on Solar Neutrinos and Neutrino Astronomy, Lead, S.D., 23-25 Aug. 1984
(Contract W-7405-eng-36)
(DE85-003741; LA-UR-84-3583; CONF-8408132-5) Avail: NTIS HC A02/MF A01

The pulsational behavior of solar models with mixing produced by turbulent diffusion was investigated, for both p (pressure) modes and g (gravity) modes. It is found that while a small amount of mixing may be allowed by the large enough to reduce the predicted neutrino counting rate to the level seen by the (37)C1 experiment are in conflict with published solar oscillation data. DOE

N85-23679*# National Geophysical Data Center, Boulder, Colo.
SOLAR-GEOPHYSICAL DATA NUMBER 479, AUGUST 1981. PART 2: (COMPREHENSIVE REPORTS), DATA FOR JANUARY 1984 AND AUGUST 1981 AND MISCELLANEA. EXPLANATION OF DATA REPORTS ISSUED AS NUMBER 474 (SUPPLEMENT) FEBRUARY 1984
H. E. Coffey Jul. 1984 100 p
(NASA Order W-15519; Grant NSF ATM-83-1491)
(NASA-CR-175607; NAS 1.26:175607; PB85-115780; SGD-479-Pt-2; LC-79-640375) Avail: NTIS HC A05/MF A01 CSCL 03B

Various solar physical data are presented including: data for January 1984--(solar radio bursts af fixed frequencies, solar X-ray radiation from GOES satellite, Mass ejections from the sun); data for August 1981--solar flares; Miscellaneous data--(meudon carte synoptique, solar X-ray radiation from GOES satellite). GRA

N85-22412# Joint Publications Research Service, Arlington, Va.
CORRELATION OF INTERPLANETARY MEDIUM PARAMETERS IN TRANSITION REGION OF HIGH-VELOCITY SOLAR WIND STREAMS Abstract Only
N. V. Mymrina, L. I. Dorman, N. S. Kaminer, and A. Y. Kuzmicheva *In its* USSR Rept.: Space (JPRS-USP-85-001) 4 Feb. 1985 p 34-35 Transl. into ENGLISH from Geomagnetizm i Aeronomiya (USSR), v. 24, no. 3, May-Jun. 1984 p 376-380 (For primary document see N85-22403 13-12)
Avail: NTIS HC A07

93 SPACE RADIATION

Includes cosmic radiation; and inner and outer Earth's radiation belts.

For biological effects of radiation see *52 Aerospace Medicine*. For theory see *73 Nuclear and High-Energy Physics*.

N85-23680 California Univ., Berkeley.
MEASUREMENT OF THE LARGE-SCALE ANISOTROPY OF THE COSMIC BACKGROUND RADIATION AT 3 MM Ph.D. Thesis
Gerald Lewis Epstein 1984 150 p
Avail: Univ. Microfilms Order No. DA8426951

A balloon-borne differential radiometer has measured the large-scale anisotropy of the cosmic background radiation (CBR) with high sensitivity. The antenna temperature dipole anisotropy at 90 GHz (3mm wavelength) is 2.82 + or - 0.19 mK, corresponding to a thermodynamic anisotropy of 3.48 + or - 0.24 mK for a 2.7 K blackbody CBR. Since the magnitude of the dipole anisotropy induced by motion through the CBR depends on both the CBR intensity and its spectral index, anisotropy measurements at several frequencies provide information about the CBR spectrum. The ratio of the dipole magnitudes measured at 90 GHz by this experiment and at 24.5 GHz by another recent observation is consistent with a 2.7 K blackbody CBR but does not require such a spectrum. If the CBR spectrum is blackbody, the two measurements establish a 90% confidence-level lower limit of 2.2 K on its temperature. Dissert. Abstr.

N85-23681 California Univ., Berkeley.
A MEASUREMENT OF THE INTENSITY OF THE COSMIC BACKGROUND RADIATION AT 3.9 CM Ph.D. Thesis
Scott David Friedman 1984 134 p
Avail: Univ. Microfilms Order No. DA8426965

The intensity of the cosmic background radiation (CBR) was measured at a wavelength of 3.0 cm as part of a program to measure the Rayleigh-Jeans spectrum of the CBR at five wavelengths between 0.33 cm and 12 cm. The atmospheric emission was measured by rotating the radiometer. The CBR temperature is found by direct comparison with a liquid helium cooled absolute reference load. The weighted mean of five measurements is T sub cbr = 2.70 + or - 0.09 K. Fitting these five measurements to a Bose-Einstein spectrum yields a thermodynamic temperature of 2.75 or 0.15 K and a chemical potential micrometer = (2.30 or 5.29) x 10(3). These is no evidence for a bremsstrahlung repopulation of photons at long wavelengths. The data are consistent with a blackbody spectrum of the CBR. Dissert. Abstr.

N85-22413# Joint Publications Research Service, Arlington, Va.
CHARACTERISTICS OF LATITUDE EFFECT ON COSMIC RAY CHARGED COMPONENT IN ATMOSPHERE AT ALTITUDES 3-5 KM Abstract Only
A. M. Altukhov, P. N. Ageshin, A. F. Krasotkin, V. A. Rogoshin, V. M. Senchenok, A. N. Charakhchyan, and T. N. Charakhchyan *In its* USSR Rept.: Space (JPRS-USP-85-001) 4 Feb. 1985 p 35-36 Transl. into ENGLISH from Geomagnetizm i Aeronomiya (USSR), v. 24, no. 3, May-Jun. 1984 p 386-392 Original language document announced as A84-40082 (For primary document see N85-22403 13-12)
Avail: NTIS HC A07

N85-22415# Joint Publications Research Service, Arlington, Va.
LONGITUDE AND PITCH-ANGLE DISTRIBUTIONS OF STREAMS OF HIGH-ENERGY ELECTRONS UNDER EARTH'S RADIATION BELTS Abstract Only
S. A. Averin, A. M. Galper, V. M. Grachev, V. V. Dmitrenko, V. G. Kirillov-Ugryumov, and S. Y. Ulin *In its* USSR Rept.: Space (JPRS-USP-85-001) 4 Feb. 1985 p 37 Transl. into ENGLISH from Geomagnetizm i Aeronomiya (USSR), v. 24, no. 3, May-Jun. 1984 p 494-495 Original language document announced as A84-40102 (For primary document see N85-22403 13-12)
Avail: NTIS HC A07

N85-22430# Joint Publications Research Service, Arlington, Va.
OBSERVATION OF COSMIC RAY FLUX VARIATIONS IN STRATOSPHERE Abstract Only
Y. I. Barannikov, O. A. Barsukov, and P. F. Gavrilov *In its* USSR Rept.: Space (JPRS-USP-85-001) 4 Feb. 1985 p 47-48 Transl. into ENGLISH from Kosmicheskiye Issled. (USSR), v. 22, no. 1, Jan.-Feb. 1984 p 134-136 (For primary document see N85-22403 13-12)
Avail: NTIS HC A07

N85-22799# Joint Publications Research Service, Arlington, Va.
DIELECTRIC DETECTOR DEVICE FOR REGISTERING HEAVY COSMIC RADIATION PARTICLES Abstract Only
Ye. V. Gorchakov, N. L. Grigorov, V. A. Iozenas, R. A. Nymik, Yu. V. Trigubov, and G. G. Zenchev *In its* USSR Rept.: Eng. and Equipment (JPRS-UEQ-85-003) 12 Mar. 1985 p 17 Transl. into ENGLISH from Pribory i Tekhn. Eksperim. (Moscow), no. 2, Mar. - Apr. 1984 p 35 (For primary document see N85-22782 13-31)
Avail: NTIS HC A06

99 GENERAL

No abstracts in this category.

SUBJECT INDEX

Typical Subject Index Listing

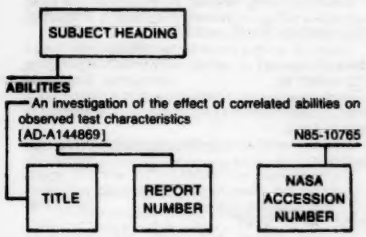

The subject heading is the key to the subject content of the document. Titles, report numbers, and accession numbers of pertinent documents are provided under each subject heading. When the title is insufficiently descriptive of the document content, a title extension has been added, separated from the title by three hyphens. The report number helps to indicate the type of document cited (e.g., NASA report, NASA translation, NASA contractor report). The NASA accession number is the number by which the document abstracts are arranged in this journal and by which the document is sold or requested. The titles, with title extensions if present, are arranged under each subject heading in ascending accession number order. The subject headings have been selected from the latest revision of the *NASA Thesaurus* (NASA SP-7051).

A

ABLATIVE MATERIALS
Adequacy of metal ablation process with laser radiation and a shock-compressed plasma N85-22708
Experimental study of enthalpy of quasimonocrystal of graphite and carbon glass in temperature range of 2890-3818 deg K N85-22751
ABRASION
A comparison of terrestrial saltation flux in the laboratory and the field N85-23582
ABRASION RESISTANCE
Effect of zero-wear in friction pairs operating in abrasive media N85-22601
ABSORBERS (MATERIALS)
Correctness of reflection characteristics of radio absorbent materials N85-22995
ABSORPTION SPECTRA
Below-room-temperature water-vapor continuum absorption within the 8- to 10 micron atmospheric transmission window
[TR-0084(4945-09)-1] N85-23268
Studies of galactic HI in 21-centimeter absorption N85-23466
First direct detection of clay minerals on Mars N85-23612
Reassignment of the iron (3) absorption bands in the spectra of Mars N85-23614
Determination of mineral type, abundance, and grain size with remotely obtained reflectance spectra N85-23623
AC GENERATORS
The ferrite permanent magnet AC motor: A technical and economical assessment
[DE85-002480] N85-22903
ACCELERATED LIFE TESTS
Life testing of rubber seals — aircraft hydraulic systems
[AD-A143193] N85-23086
Advanced life analysis methods. Volume 2: Crack growth analysis methods for attachment lugs
[AD-A150420] N85-23109
Parallel test method for LSI (Large Scale Integration) microprocessors
[AD-A150237] N85-23310
ACCELERATION (PHYSICS)
Averaging of equations of cometary orbital motion with allowance for nongravitational effects N85-22411
Physics of the inner heliosphere: Mechanisms, models and observational signatures
[NASA-CR-175632] N85-23677
ACCRETION DISKS
Evolution of grains in a turbulent solar nebula N85-23525
ACCURACY
Method for determining the number of correlative measurements required to validate the SBUV/2 ozone retrievals N85-23114
Measurement requirements for the detection of ozone trends N85-23115
Automated extraction of absorption bands from reflectance special N85-23624
ACID RAIN
Areas with forest soils sensitive to acidic deposition under alternative damage hypotheses
[DE85-005257] N85-23257
ACOUSTIC DUCTS
Investigations of reactive and non reactive acoustic boundary layers in porous walled ducts N85-22535
ACOUSTIC EMISSION
Use of acoustical emission method to study specifics of fracture of boron reinforced plastic structural elements N85-22696
Optimal synthesis of surface acoustic wave filters N85-22933
ACOUSTIC EXCITATION
Vibroacoustic study of the NASA Goddard Space Flight Center OSS-1 payload
[NASA-CR-175320] N85-22485
ACOUSTIC INSTABILITY
Acoustic energy balance method N85-22537
Investigation of the characteristics of the velocity-coupled response functions of solid propellants N85-22540
Measurements of distributed combustion N85-22542
Distributed combustion: A mechanism of acoustic suppression N85-22543
ACOUSTIC MEASUREMENT
Numerical results of acoustic radiation, transmission and reflection of steel plate in water
[AMTE(N)-TM-84037] N85-23378
Properties of materials using acoustic waves
[AD-A150465] N85-23382
ACOUSTIC PROPAGATION
Acoustic energy exchange in sheared mean flows — solid rocket motors N85-22534
ACOUSTIC SCATTERING
Surface scattering
[AD-A150252] N85-23366
Elastic wave scattering from cavities and sound inclusions analyzed by the resonance method
[AD-A150315] N85-23381
Properties of materials using acoustic waves
[AD-A150465] N85-23382
ACOUSTIC VELOCITY
Coupling between velocity oscillations and solid propellant combustion N85-22536
Coupled acoustic and hydrodynamic wave instabilities N85-22538
Investigation of the characteristics of the velocity-coupled response functions of solid propellants N85-22540
ACOUSTICS
Ice statistics and acoustic scattering in the Arctic basin
[AD-A150141] N85-23289
ACOUSTO-OPTICS
Acousto-optically addressed Fourier transform matched filters
[AD-A150298] N85-22889
USSR report: Electronics and electrical engineering
[JPRS-UEE-85-002] N85-22907
Space-time response characteristics of acoustooptic filter for compression of linearly frequency-modulated signal N85-22937
Integrated optical components utilizing acoustooptic and electrooptic diffraction in micro-waveguides N85-23044
Acoustooptic demodulation of frequency-modulated signals N85-23050
Acoustooptic cell as space-frequency filter N85-23051
Accuracy of random signal spectral parameter estimation against interference background in acoustooptical spectrum analyzers N85-23052
ACRYLATES
Chiral polymers
[AD-A150366] N85-22760
ACTIVATION
Activation of Si-N modes in silicon by pulsed laser annealing
[DE85-002988] N85-23082
ACTIVE CONTROL
Ground and flight testing for aircraft guidance and control
[AGARD-AG-282] N85-22350
Dynamic wind tunnel testing for active control research N85-22352
Dynamic wind-tunnel testing of active controls by the NASA Langley Research Center N85-22353
ACTUATORS
A quantitative comparison of active and passive damping for large space structures
[UTIAS-TN-249] N85-22524
Optimum design of electrical motors for multilink manipulators and automated manufacturing systems N85-22880
ADAPTIVE CONTROL
System dynamics and network control
[AD-A149420] N85-22953
Electronics Engineering Department EE Technical Review
[UCRL-50025-84-1] N85-22987
Adaptive control of airborne radar antennas N85-22989
ADAPTIVE FILTERS
Synthesis of optimum algorithms for secondary processing N85-22992
Methods of digital correction for channels of multichannel radar receivers N85-23005
ADDITIVES
Effects of HMX addition on the combustion of energetic binders N85-22580
The effects of lithium counterdoping on radiation damage and annealing in n(+)p silicon solar cells N85-22586
ADHESIVE BONDING
Study of character of adhesive interaction and breaking of polyimid-aluminum foil junction during process of hardening N85-22637
The characterisation of oxide films on treated aluminium alloys
[MOAD-R-849] N85-22667
Elasticity solution of an adhesively bonded joint
[NASA-CR-175591] N85-23097
ADHESIVES
Study of character of adhesive interaction and breaking of polyimid-aluminum foil junction during process of hardening N85-22637
ADSORPTION
Critical events in inelastic deformation of glassy polymers in adsorptive medium N85-22634
Adsorption behaviour of nitrogen compounds on to porous polymer beads and applications to atmospheric sampling
[BLL-DRIC-TRANS-7399-(3623.88)] N85-22753
Determining adsorption of surface-active substances by sea bottom deposits N85-23128
Adsorption site, adsorption energy and normal vibration frequency of H/Ni(100) via total energy calculations
[AD-A150555] N85-23388

ADVECTION
Two-dimensional numerical model of sensible and latent heat transport in an irrigated field under advective conditions N85-23261
Variation of Arctic cloud cover in summer [DE85-004507] N85-23285
AEOLIAN TONES
Statistics of Aeolian surface of Mars N85-23637
AERIAL PHOTOGRAPHY
Geoindication method for interpreting aerial and space photographs: Status and prospects N85-22445
Combined analysis of the dynamics of complex ecosystems based on repeated remote measurements N85-22450
Comprehensive, integrated, remote sensing at DOE sites [DE85-004857] N85-23240
Accomplishments of Institute of Cartography summarized N85-23435
AERIAL RECONNAISSANCE
1981 wC-130 airborne lightning characterization program data review [AD-A150230] N85-23275
AERODYNAMIC CHARACTERISTICS
Aerodynamic behavior of ventilated wind tunnel walls N85-22363
The application of some lifting-body reentry concepts to missile design [NASA-TM-86394] N85-22366
Calculation of vortex-flap aerodynamic characteristics [NASA-CR-175624] N85-22367
Large-scale Advanced Propfan (LAP) performance, acoustic and weight estimation, January, 1984 [NASA-CR-174782] N85-22368
Determination of aerodynamic and propulsion parameters of general aviation aircraft using steady state flight test data N85-22377
Redesign of fuselage compartments by method of special contours N85-22784
AERODYNAMIC CONFIGURATIONS
Calculation of vortex-flap aerodynamic characteristics [NASA-CR-175624] N85-22367
AERODYNAMIC DRAG
Investigations into the effects of scale and compressibility on lift and drag in the RAE 5m pressurised low-speed wind tunnel [RAE-TM-AERO-2006] N85-22372
Preliminary assessment of power-generating tethers in space and of propulsion for their orbit maintenance N85-22520
AERODYNAMIC FORCES
Flight dynamics of axisymmetrical rotating bodies in air medium N85-22791
AERODYNAMIC HEAT TRANSFER
Results of a M = 5.3 heat transfer test of the integrated vehicle using phase-change paint techniques on the 0.0175-scale model 56-OTS in the NASA/Ames Research Center 3.5-foot hypersonic wind tunnel [NASA-CR-167695] N85-22468
AERODYNAMIC HEATING
Aerodynamic heating rate distributions induced by trailing edge controls on hypersonic aircraft configurations at Mach 8 [NASA-TM-87453] N85-22370
Results of aeroheating DFI and ET design-data test on a 0.0175-scale model 60-OTS conducted in the Von Karman Gas Dynamics Facility (VKF) 40' supersonic and the 50' hypersonic wind tunnels A and C [NASA-CR-167693] N85-22466
AERODYNAMIC INTERFERENCE
Experimental study of main rotor tip geometry and tail rotor interactions in hover. Volume 1. Text and figures [NASA-CR-177336-VOL-1] N85-22344
Experimental study of main rotor tip geometry and tail rotor interactions in hover. Volume 2: Run log and tabulated data [NASA-CR-177336-VOL-2] N85-22345
Study for prediction of rotor/wake/fuselage interference, part 1 [NASA-CR-177340-VOL-1] N85-22346
Study for prediction of rotor/wake/fuselage interference. Part 2: Program users guide [NASA-CR-177340-VOL-2] N85-22347
AERODYNAMIC LOADS
Determination of stresses and deformations in linearly elastic conical shell subjected to aerodynamic loading and heating N85-22812
Preliminary study of inphase gusts and moment force wind loads over the first 150 meters at KSC, Florida [NASA-TM-86501] N85-23273
AERODYNAMIC NOISE
Large-scale Advanced Propfan (LAP) performance, acoustic and weight estimation, January, 1984 [NASA-CR-174782] N85-22368
Laboratory studies of spacecraft response to transient discharge pulses N85-22506
AERODYNAMICS
Aeronautical Engineering: A continuing bibliography with indexes, supplement 185 [NASA-SP-7037(185)] N85-22342
Aeronautical Engineering: A cumulative index to the 1984 issues of the continuing bibliography [NASA-SP-7037(183)] N85-22343
Absolute stability of unsteady movement of axisymmetrical rotating flight vehicle N85-22793
AEROELASTICITY
Study for the optimization of a transport aircraft wing for maximum fuel efficiency. Volume 1: Methodology, criteria, aeroelastic model definition and results [NASA-CR-172551] N85-22378
Simple theoretical models for composite rotor blades [NASA-CR-175620] N85-22382
Structural response of a rotating bladed disk to rotor whirl [NASA-CR-175605] N85-22391
AERONAUTICAL ENGINEERING
Aeronautical Engineering: A continuing bibliography with indexes, supplement 185 [NASA-SP-7037(185)] N85-22342
Aeronautical Engineering: A cumulative index to the 1984 issues of the continuing bibliography [NASA-SP-7037(183)] N85-22343
AEROSOLS
Microstructure of Venus cloud layer based on spectrophotometric data from Venera-11 spacecraft N85-22436
Effects of temperature variation among droplets in an evaporating fuel spray N85-22562
Multiple element neutron-activation analysis of atmospheric aerosols with X-ray and gamma-spectrometric recording of radionuclides formed N85-22631
One mechanism of formation of organic fraction in atmospheric aerosol N85-22632
Size and velocity distributions of particles and droplets in spray combustion systems [AD-A150355] N85-22648
The orientation distribution of nonspherical aerosol particles within a cloud [AD-A150600] N85-23061
Infrared aerosol absorption index N85-23147
The relationship between marine aerosol particles and satellite-detected radiance N85-23263
Cumulus cloud venting of mixed layer ozone [NASA-TM-87429] N85-23269
Analysis of biological particles by mass spectrometry [AD-A149952] N85-23291
AEROSPACE ENGINEERING
USSR report: Engineering and equipment [JPRS-UEQ-85-003] N85-22782
Authorizing appropriations to the National Aeronautics and Space Administration for fiscal year 1986 [H-REPT-99-32] N85-23452
AEROSPACE ENVIRONMENTS
Interactions between large space power systems and low-Earth-orbit plasmas N85-22490
AEROSPACE INDUSTRY
Aerospace Safety Advisory Panel [NASA-TM-87426] N85-22373
AEROSPACE MEDICINE
Lyakhov and Aleksandrov on 150-day flight N85-22405
China report: Science and technology [JPRS-CST-84-030] N85-22777
Research opportunities in human behavior and performances [NASA-CR-3886] N85-23299
AEROSPACE TECHNOLOGY TRANSFER
Authorizing appropriations to the National Aeronautics and Space Administration for fiscal year 1986 [H-REPT-99-32] N85-23452
Technology and Economics, Inc. Technology Application Team [NASA-CR-175630] N85-23454
AEROTHERMODYNAMICS
Results of aeroheating DFI and ET design-data test on a 0.0175-scale model 60-OTS conducted in the Von Karman Gas Dynamics Facility (VKF) 40' supersonic and the 50' hypersonic wind tunnels A and C [NASA-CR-167693] N85-22466
Results of a M = 5.3 heat transfer test of the integrated vehicle using phase-change paint techniques on the 0.0175-scale model 56-OTS in the NASA/Ames Research Center 3.5-foot hypersonic wind tunnel [NASA-CR-167695] N85-22468
AFTERBURNING
Some unique features in operation of two-stage turbojet engine with afterburner N85-22828
Effect of water injection into air for turbine cooling on economy of operation of gas turbine engine with afterburning N85-22830
AGGLOMERATION
Gasification of boron oxide drops and boron slurry agglomerates in combustion gases N85-22529
AGING (MATERIALS)
TEM/FIM study of modulated microstructures in the Fe-Be system [DE85-005379] N85-22678
Effect of alternative aging and accident simulations on polymer properties [DE85-002642] N85-22762
Stability of highly nonlinear oxide-zinc resistors under continuous voltage of industrial frequency N85-23030
AGING (METALLURGY)
Effects of neutron irradiation at 450(0)C and 16 dpa on the properties of various commercial copper alloys [DE85-005716] N85-22684
Decomposition of VTAN alloy solid solution upon irradiation and thermal aging N85-22712
AGRICULTURE
Moisture variation in northern hemisphere temperate latitudes N85-23119
Characterization of LANDSAT-4 TM and MSS image quality for the interpretation of California's agricultural resources --- Central Valley N85-23190
AGRISTARS PROJECT
Thematic Mapper data quality and performance assessment in renewable resources/agriculture/remote sensing N85-23201
AIR BREATHING ENGINES
Status of boron combustion research N85-22528
AIR CONDITIONING
Latent heat storage in cooling systems [DE85-005355] N85-23248
AIR COOLING
Effect of water injection into air for turbine cooling on economy of operation of gas turbine engine with afterburning N85-22830
effect of gas stream sweeping past the effluent of a perforated plate on heat transfer inside the perforations N85-22836
AIR FILTERS
Diffusion deposition in fibrous filters for parallel and transverse flow models [DE85-006149] N85-23066
AIR FLOW
Study for prediction of rotor/wake/fuselage interference, part 1 [NASA-CR-177340-VOL-1] N85-22346
Study for prediction of rotor/wake/fuselage interference. Part 2: Program users guide [NASA-CR-177340-VOL-2] N85-22347
Diffusion deposition in fibrous filters for parallel and transverse flow models [DE85-006149] N85-23066
The ASCOT Data Analysis Workshop [DE85-004407] N85-23283
AIR INTAKES
Selection of air intake parameters for supersonic-flow operation N85-22837
AIR MASSES
Variation of Arctic cloud cover in summer [DE85-004507] N85-23285
AIR POLLUTION
Adsorption behaviour of nitrogen compounds on to porous polymer beads and applications to atmospheric sampling [BLL-DRIC-TRANS-7399-(3623.66)] N85-22753
AIR TRAFFIC CONTROL
Civil avionics flight testing with the RAE(B) BAC1-11 N85-22354
A flight management algorithm and guidance for fuel-conservative descents in a time-based metered air traffic environment: Development and flight test results N85-22356
Planned office and facility consolidations: To improve system effectiveness and efficiency, FY 1985-87 [AD-A150441] N85-22376
Analysis of estimation algorithms for CDTI and CAS applications [NASA-CR-172444] N85-22387
AIR TRANSPORTATION
Assessing the behavior and performance of teams in organizations: The case of air transport crews [AD-A150359] N85-23302
AIR WATER INTERACTIONS
Modeling of mechanism of positive feedback between mean Earth surface temperature and atmospheric carbon dioxide in geologic time scale N85-23122
Numerical investigation of evolution of energy spectrum of slightly nonlinear Rossby waves N85-23124
Contribution to theory of ocean-atmosphere gas exchange N85-23134
AIRBORNE EQUIPMENT
Intra-eruption geologic map from an x-band radar image during the May 18, 1980 eruption of Mount St. Helens, Washington N85-23639

Radar observations of fissure-fed basaltic lava flows, Craters of the Moon, Idaho N85-23640

AIRBORNE/SPACEBORNE COMPUTERS
Feasibility of self-structured current accessed bubble devices in spacecraft recording systems [NASA-CR-172554] N85-22525

AIRCRAFT
Advanced life analysis methods. Volume 1: Cracking data survey and NDI (nondestructive inspection) assessment for attachment lugs [AD-A150419] N85-23108

AIRCRAFT ACCIDENTS
TCAS II: Design and validation of the high-traffic-density surveillance subsystem [DOT/FAA/PM-84/5] N85-22375

AIRCRAFT ANTENNAS
Coordinate determination errors in measuring characteristics of radiation field of airborne antennas N85-22919

AIRCRAFT CONFIGURATIONS
Study for prediction of rotor/wake/fuselage interference, part 1 [NASA-CR-177340-VOL-1] N85-22346
Study for prediction of rotor/wake/fuselage interference. Part 2: Program users guide [NASA-CR-177340-VOL-2] N85-22347

AIRCRAFT CONSTRUCTION MATERIALS
Corrosion of aircraft Al and Al-Zn ion plated steel fasteners N85-22666

AIRCRAFT CONTROL
Aeronautical Engineering: A continuing bibliography with indexes, supplement 185 [NASA-SP-7037(185)] N85-22342
Reference systems for the evaluation of dead-reckoning navigation equipment N85-22358

AIRCRAFT DESIGN
Aeronautical Engineering: A continuing bibliography with indexes, supplement 185 [NASA-SP-7037(185)] N85-22342
Dynamic wind-tunnel testing of active controls by the NASA Langley Research Center N85-22353
Study for the optimization of a transport aircraft wing for maximum fuel efficiency. Volume 1: Methodology, criteria, aeroelastic model definition and results [NASA-CR-172551] N85-22378
China report: Science and technology [JPRS-CST-84-008] N85-22384
Uses of composite materials N85-22698
Redesign of fuselage compartments by method of special contours N85-22784

AIRCRAFT ENGINES
Effects of inlet distortion on a static pressure probe mounted on the engine hub in an F-15 airplane [NASA-TP-2411] N85-22394
Hydrodynamic simulation of transient processes in injection system of aircraft engines during pump unswirling N85-22829
Effect of water injection into air for turbine cooling on economy of operation of gas turbine engine with afterburning N85-22830
T700 cutter life improvement program [AD-A150450] N85-23089

AIRCRAFT FUEL SYSTEMS
Hydrodynamic simulation of transient processes in injection system of aircraft engines during pump unswirling N85-22829

AIRCRAFT FUELS
A standard aircraft diffusion flame: Spectral characteristics and a feasibility study for developing an alternate calibration source for aircraft optical fire detection systems [AD-A150231] N85-22768

AIRCRAFT GUIDANCE
A flight management algorithm and guidance for fuel-conservative descents in a time-based metered air traffic environment: Development and flight test results N85-22356
Reference systems for the evaluation of dead-reckoning navigation equipment N85-22358

AIRCRAFT HAZARDS
Aircraft skin penetrator and agent applicator. Volume 1: Working model development and construction [AD-A150498] N85-22374

AIRCRAFT HYDRAULIC SYSTEMS
Life testing of rubber seals — aircraft hydraulic systems [AD-A143193] N85-23086

AIRCRAFT MAINTENANCE
Aviation maintenance computerized management information systems: Perspective for the future [AD-A150637] N85-22349

AIRCRAFT MANEUVERS
Coordinate determination errors in measuring characteristics of radiation field of airborne antennas N85-22919

AIRCRAFT MODELS
Structural design of the Sandia 34-M Vertical Axis Wind Turbine [DE85-002631] N85-23247

AIRCRAFT NOISE
A community survey of helicopter noise annoyance conducted under controlled noise exposure conditions [NASA-TM-86400] N85-23374
Research on the effect of noise at different times of day: Models, methods and findings [NASA-CR-3868] N85-23375
An experimental investigation of the chopping of helicopter main rotor tip vortices by the tail rotor [NASA-CR-177338] N85-23376
Wind tunnel acoustic study of a propeller installed behind an airplane empennage: Data report [NASA-CR-177335] N85-23377

AIRCRAFT PERFORMANCE
AIRLAB: A laboratory for flight-crucial-electronics system research N85-22362

AIRCRAFT STABILITY
Aeronautical Engineering: A continuing bibliography with indexes, supplement 185 [NASA-SP-7037(185)] N85-22342

AIRCRAFT STRUCTURES
Air Force technical objective document, Flight Dynamics Laboratory plans for fiscal year 1986. Air Force technical objective document [AD-A149648] N85-22348
Normal mode calculations for fuselage type intricate structures by regarding them as systems with superposed constraints N85-22817
Operational loads measurement: A philosophy and its implementation — aircraft structures [AD-A149445] N85-23308

AIRFOILS
Hypersonic flow about triangular airfoil at large angles of attack N85-22792
T700 cutter life improvement program [AD-A150450] N85-23089
Structural design of the Sandia 34-M Vertical Axis Wind Turbine [DE85-002631] N85-23247

AIRGLOW
Analysis and interpretation of observations of airglow at 297 nm in the Venus thermosphere N85-23473
A measurement of the intensity of the cosmic background radiation at 3.9 cm N85-23681

AIRPORT TOWERS
Planned office and facility consolidations: To improve system effectiveness and efficiency, FY 1985-87 [AD-A150441] N85-22376

ALBEDO
Snow reflectance from Thematic Mapper N85-23205
Seasonal and secular variation of the Solis Lacus albedo feature: Relation to the Martian dust-transport cycle N85-23576
Accurate albedos of the brightest regions on Io N85-23618
Determination of mineral type, abundance, and grain size with remotely obtained reflectance spectra N85-23623
Mars planimetric mapping N85-23666

ALCOHOLS
Trifunctional catalysts for conversion of syngas to alcohols [DE85-004577] N85-22771

ALFALFA
Two-dimensional numerical model of sensible and latent heat transport in an irrigated field under advective conditions N85-23261

ALGAE
Characteristic vector analysis of inflection ratio spectra: New technique for analysis of ocean color data [NASA-TP-2428] N85-23237

ALGORITHMS
A flight management algorithm and guidance for fuel-conservative descents in a time-based metered air traffic environment: Development and flight test results N85-22356
On the solution of the three-dimensional flowfield about a flow-through nacelle [NASA-TM-87448] N85-22371
Analysis of estimation algorithms for CDTI and CAS applications [NASA-CR-172444] N85-22387
Computation of elliptical functions in problems of celestial mechanics N85-22418
Algorithm for determining optimal three impulse point-to-orbit transfer with limited transfer time N85-22419
Assembly robot control algorithms N85-22808
Nonlinear behavior and stability of thin spherical shells subjected to non-axisymmetrical loading N85-22821
Efficiency of algorithms for gas-air channel diagnostics in gas turbine engines based on gas thermodynamic parameters N85-22823
Advanced mixed-mode simulation techniques N85-22883
Factorized algorithms for combined spatial and temporal processing of radar signals N85-22997
Algorithm in Walsh function basis for analysis of integrated microcircuits on MOS-structures N85-23006
Use of Bigaussian approximation to describe fading in scattering communications channel N85-23017
Computing convolution of multifrequency signal employing truncated fast Fourier transform algorithms N85-23019
Synthesis of quasi-optimum algorigthms for signal recognition against background of correlated noise employing discrete spectral transformations N85-23020
New convolution and discrete Fourier transformation algorithms based on rectangular transformations over field of roots of unity N85-23022
Discrimination of normal and anomalous magnetic and electric fields in geoelectromagnetic variations N85-23166
Polynomial parameterization in inverse gravimetric problem N85-23174
Primary processing of experimental magnetovariation sounding data using spline functions N85-23175
Orphan detection in the Argus system [AD-A150562] N85-23331
Implementation of some concurrent algorithms [DE85-004687] N85-23334
Algorithms for reconstruction of partially known, band limited Fourier transform pairs from noisy data [AD-A150194] N85-23347
Image data compression using uneven knots selection [AD-A150602] N85-23359
Algorithm for singular decomposition [DE85-016488] N85-23361
Motion planning with six degrees of freedom [AD-A150312] N85-23432
Quantitative analyses of planetary reflectance spectra N85-23625
Progress in planetary radarclinometry N85-23630

ALLOCATIONS
An analysis of a dynamic project cost problem [CSIR-TWISK-338] N85-23341

ALLOYS
Creep crack growth in ductile alloys [DE85-003937] N85-22678
New tooling for plasma cutting technology N85-22842

ALLUVIUM
Attenuation of seismic waves at regional distances [AD-A150196] N85-23267

ALPHA PARTICLES
Feasibility of alpha particle measurement by CO2 laser Thomson scattering [DE85-004938] N85-23081

ALPHANUMERIC CHARACTERS
Axial representations of shape [AD-A150387] N85-23356

ALTERNATING CURRENT
Power control for ac motor [NASA-CASE-MFS-25861-1] N85-22877

ALUMINUM
Measurements of distributed combustion N85-22542
Study of character of adhesive interaction and breaking of polyimid-aluminum foil junction during process of hardening N85-22637
Directional dependent engineering properties of aluminum-aramid-epoxy laminates [CCMS-85-02] N85-22638
An electrochemical study of the corrosion behavior of primer coated 2219-T87 aluminum [NASA-TP-2459] N85-22662
Dependence of superplastic flow on state of grain boundaries N85-22689
Method of calculating strength of joint produced by cold welding of aluminum under discrete loading N85-22743
AL-124 light-emitting diode in 30 Mbit/s fiber-optic communication line N85-22925

ALUMINUM ALLOYS
Ignition phenomena of bulk aluminum alloy as a function of oxygen pressure N85-22531
Structures of ordered linear dislocation multipoles in Cu-Al alloys [ISSN-0379-6906] N85-22664
The characterisation of oxide films on treated aluminium alloys [MOAD-R-849] N85-22667
Magnetic studies of Ni3Al(Fe) compounds [DE85-005262] N85-22686
USSR report: Materials science and metallurgy [JPRS-UMS-85-002] N85-22688
Dependence of superplastic flow on state of grain boundaries N85-22689

Fatigue and corrosion fatigue resistance of aluminum casting alloy VAL10 and forging alloy AK6 N85-22690
Structural strenght of strip D16T aluminum alloy with low copper and magnesium content N85-22691
Temperature effects of heterogenizated annealing on structure and properties of V95 aluminum alloy N85-22692
Anomalies of aluminum structure and properties N85-22693
New deformable secondary aluminum alloys N85-22694
Study of processes of modification of Al-Si alloys N85-22695
Aluminum alloy ATs5K5 (5% Zn + 5% Ca) for superplastic forming N85-22697
Segregation of silicon in silumin-carbon fiber composites N85-22706
Composition and thickness of oxide coatings on granule surfaces of aluminum alloys N85-22719
Basis and pyramidal slipping in single crystals of alpha-alloy Ti-Al-Sn N85-22730
Problem of pore formation mechanism in welded joints of aluminum alloys in the system aluminum-magnesium-lithium N85-22732
Analysis of strength and ductility of welded joints in AMtsS and AMg5 aluminum alloys N85-22737
Effect of moisture in inert gases on density of seam metal and on mechanical characteristics of welded joints of aluminum and aluminum alloys N85-22744
Characteristics of surface crack development in ATtsS aluminum alloy during slow-cycle loading N85-22745
China report: Science and technology [JPRS-CST-84-030] N85-22777
Experimental investigation of crippling strength of Chinese aluminum alloy (LY12CZ) sections N85-22779
Use of ferrofluids in machining of metals N85-22802

ALUMINUM BORON COMPOSITES
Influence of 3% NaCl solution on rate of accumulation of damage and residual strength of aluminum-boron composite N85-22699
Division boundary in Al-B composite material with boron in contact with solid and liquid aluminum N85-22704
Estimating degree of development of physical-chemical interaction among components in Al-B fiber composite material N85-22705
Effect of operating medium on cyclic durability of AD33-W composite N85-22716

ALUMINUM CARBIDES
Segregation of silicon in silumin-carbon fiber composites N85-22706

ALUMINUM COATINGS
Corrosion of aircraft Al and Al-Zn ion plated steel fasteners N85-22666

ALUMINUM ISOTOPES
Cosmogenic Na-22 and Al-26 in Luna-24 lunar drill core soil samples N85-22427

ALUMINUM OXIDES
Distributed combustion: A mechanism of acoustic suppression N85-22543
Formation of alumina layers on iron-base alloys [BLL-T6418/BG/LRS/LRST737/84] N85-22657
Composition and thickness of oxide coatings on granule surfaces of aluminum alloys N85-22719
Dispersed-metal-toughened alumina [NASA-CR-174687] N85-22758

AMBIENT TEMPERATURE
Portable Automated Mesonet (PAM) data from the 1980 experiment in Anderson Creek Valley [DE85-004361] N85-23282

AMERICIUM
Americium metal preparation on the multigram scale [DE85-003735] N85-22683

AMMONIUM PERCHLORATES
Mechanism of burning rate enhancement by ferric oxide N85-22546

AMORPHOUS MATERIALS
Corrosion-resistant amorphous alloys N85-22748
Structure of amorphous films of alloys based on Fe, condensed from laser erosion products N85-22749
Energy spectrum of processes of structural relaxation of amorphous alloy FeCo70Si15B10 N85-22750
Electronic transport in hydrogenated amorphous silicon films [DE85-002901] N85-23426

AMPLITUDE DISTRIBUTION ANALYSIS
Piezoelectric filter with low-Q inductances N85-22932

AMPLITUDE MODULATION
Parameters of amplitude-modulated signal upon reflections N85-22966

AMPLITUDES
Reduction of amplitude-phase distortions of movable microwave coupling circuit for antenna field measurements N85-22920
Programmable filter with fanned interdigital surface acoustic wave transducer N85-23008
Nature of seismic images with amplitude and time fluctuations of recorded oscillations N85-23156
A theoretical study of the ozone quasi-biennial oscillation in the tropical stratosphere N85-23264

ANAEROBES
Anaerobic digestion of biomass: status summary and research development needs, 1983 [PB85-161925] N85-22772

ANALOG COMPUTERS
Microcomputer: Controlled statistics analyzer [BLL-CE-TRANS-7971-(9022.09)] N85-23306

ANALOG TO DIGITAL CONVERTERS
The use of a high-speed 12-bit A/D converter for digital sampling of communication signal carriers [AD-A150578] N85-22872
Synthesis of quasi-optimum two-level signal discriminator with level changing at unknown point N85-23010

ANALOGIES
Terrestrial analogs for planetary wrinkle ridges N85-23644
On the absence of strike-slip faults from the planets and satellites N85-23645

ANALYSIS (MATHEMATICS)
Effects of assuming independent component failure times, if they are actually dependent, in a series system [AD-A150582] N85-23092
Interaction of metals and metalloids with biomembranes [DE85-004902] N85-23293

ANALYZERS
Microcomputer: Controlled statistics analyzer [BLL-CE-TRANS-7971-(9022.09)] N85-23306

ANGLE OF ATTACK
Hypersonic flow about triangular airfoil at large angles of attack N85-22792

ANGLES (GEOMETRY)
Mathematical model of discriminator for signals with fluctuations and thermal noise N85-22943
Examination of the contact wetting angle in the vicinity of critical temperature [BLL-T6416/BG/CRS/LR-ST735/84] N85-23054

ANGULAR MOMENTUM
Models of angular momentum input to a circum-terrestrial swarm from encounters with heliocentric planetesimals N85-23521

ANGULAR RESOLUTION
Determination of angular resolution of coded aperture gamma-ray telescope N85-22432

ANGULAR VELOCITY
Rotational motion of a satellite N85-22428
Status of and outlook for producing means of transmitting units of plane angle, angular velocity and acceleration with ring lasers N85-22955

ANISOTROPY
Correlation of interplanetary medium parameters in transition region of high-velocity solar wind streams N85-22412
Orientation and temperature dependence of some mechanical properties of the single-crystal nickel-base superalloy Rene N4. 3: Tension-compression anisotropy [NASA-TM-86982] N85-22660
Investigations of ultrasonic wave interactions at boundaries separating anisotropic materials [DE85-003506] N85-23384
Measurement of the large-scale anisotropy of the cosmic background radiation at 3 MM N85-23680

ANNEALING
The effects of lithium counterdoping on radiation damage and annealing in n(+)p silicon solar cells N85-22586
Temperature effects of heterogenizated annealing on structure and properties of V95 aluminum alloy N85-22692
Influence of annealing on cyclic and short-term strength of thin sheets of VT1-0 titanium and OTR4 alloy N85-22727
Thermal hardening of welded joints in titanium alloys with various structures N85-22734
Investigation of the effect of annealing on the dislocation and sub-grain boundary content of solvent-evaporation-grown CdTe [AD-A144087] N85-23415
Influence of substrate heating and thermal annealing on the surface crystallinity in single Si crystals implanted with high doses of (16)O [DE85-005264] N85-23428

ANNUAL VARIATIONS
Empirical and modeled synoptic cloud climatology of the Arctic Ocean [NASA-CR-175628] N85-23272
Seasonal and secular variation of the Solis Lacus albedo feature: Relation to the Martian dust-transport cycle N85-23576
Water-ice clouds on Mars: Location and seasonal variation N85-23611

ANNULAR DUCTS
High-pressure rocket engine turnaround duct computational fluid dynamics analysis N85-22556

ANODES
Application of modulated hydrodynamic voltammetry to the study of anodic electrocatalysis [DE85-004182] N85-22653
Molten carbonate fuel cell performance model update, draft [DE85-005423] N85-23252

ANOMALIES
Moisture variation in northern hemisphere temperate latitudes N85-23119
El Nino, the capricious child N85-23121

ANOXIA
Armed forces special Symposium on Medicine of Altitudes N85-23441

ANTARCTIC REGIONS
USSR report: Earth sciences [JPRS-UES-85-002] N85-23116
Antarctic glaciation, or what are catastrophes in Earth's history N85-23118
China report: Science and technology [JPRS-CST-85-003] N85-23433
Planetary analogs in Antarctica: Mars N85-23604
Planetary analogs in Antarctica: Icy satellites N85-23605
Chemical weathering of soils from the dry valleys of Antarctica: A terrestrial analog of Martian weathering processes N85-23628

ANTENNA ARRAYS
KAM-250 antenna switch N85-22916
Studies of galactic HI in 21-centimeter absorption N85-23466

ANTENNA DESIGN
Computer aided antenna design and frequency selection for HF communications [AD-A150485] N85-22869
Variational and moment method solutions of the fields in a parallel-plate waveguide-aperture system [DE85-006288] N85-22876
A generalized solution to a class of printed circuit antennas N85-22882
Experimental verification of beam deflection from hybrid reflector antenna within wide-angle sector N85-22984

ANTENNA FEEDS
KAM-250 antenna switch N85-22916

ANTENNA RADIATION PATTERNS
USSR report: Electronics and electrical engineering [JPRS-UEE-85-002] N85-22907
Coordinate determination errors in measuring characteristics of radiation field of airborne antennas N85-22919
Reduction of amplitude-phase distortions of movable microwave coupling circuit for antenna field measurements N85-22920
Experimental verification of beam deflection from hybrid reflector antenna within wide-angle sector N85-22984
Synthesis of multistep directional couplers with nonminimum-phase characteristics N85-22986
Scattering of waves by axisymmetrical edge N85-22987

ANTENNAS
USSR report: Electronics and electrical engineering [JPRS-UEE-85-002] N85-22907
KAM-250 antenna switch N85-22916

ANTHROPOMETRY
The application of anthropometric survey data to aircrew clothing sizing [AD-A150545] N85-23304

ANTIBODIES
Armed forces special Symposium on Medicine of Altitudes N85-23441

APERTURES
Determination of angular resolution of coded aperture gamma-ray telescope N85-22432
Variational and moment method solutions of the fields in a parallel-plate waveguide-aperture system [DE85-006288] N85-22876

APOLLO PROJECT
Feoktistov says manned lunar, Mars flights lack justification N85-22452

APOLLO SPACECRAFT
Analysis of systematic errors in systems of selenodetic coordinates N85-22435

APPROXIMATION
Preliminary development of an approximation procedure for supercritical wing design optimization applications [AD-A150177] N85-22383
Computing convolution of multifrequency signal employing truncated fast Fourier transform algorithms N85-23019
Significance of the thin-layer Navier-Stokes approximation [DE85-002630] N85-23063

Confidence intervals using the regenerative method for simulation output analysis
[AD-A150147] N85-23343
Approximation in optimal control and identification of large space structures
[AD-A150323] N85-23351
Accumulation of the terrestrial planets N85-23524

AQUIFERS
Determining deep heat flow and rate of horizontal percolation from temperature measurements in aquifer N85-23180

ARC DISCHARGES
An investigation of arc discharging on negatively biased dielectric conductor samples in a plasma N85-22496
Phenomenology of discharges in space: Application to a solar generator — SPOT satellite N85-22583
Electrostatic discharge testing on a carbon fiber solar panel structure N85-22584

ARC WELDING
Properties of welded joints in argon arc welding of titanium alloy using a protective coating N85-22733
Reliability of robotized welding apparatus N85-22741
Structure and mechanical characteristics of heterogeneous joints produced by laser welding N85-22742

ARCHITECTURE (COMPUTERS)
Feasibility of self-structured current accessed bubble devices in spacecraft recording systems
[NASA-CR-172554] N85-22525
Periodic binary sequence generators: VLSI circuits considerations
[NASA-CR-175649] N85-22886
Synthesis of tree-structured computing systems through use of closures
[AD-A150502] N85-23326
Performance evaluation of distributed systems with unbalanced flows: An analysis of the INFOPLEX data storage hierarchy
[AD-A150528] N85-23328
General design considerations of an Air Force information system
[AD-A150611] N85-23449

ARCTIC OCEAN
Ice statistics and acoustic scattering in the Arctic basin
[AD-A150141] N85-23289

ARCTIC REGIONS
USSR report: Earth sciences
[JPRS-UES-85-002] N85-23116
Arctic-North Atlantic rift megasystem N85-23117
Application of field X-ray: Radiometric analysis in exploratory geology and means for its improvement N85-23176
Empirical and modeled synoptic cloud climatology of the Arctic Ocean
[NASA-CR-175628] N85-23272
Variation of Arctic cloud cover in summer
[DE85-004507] N85-23285
Ice statistics and acoustic scattering in the Arctic basin
[AD-A150141] N85-23289
High-frequency acoustic variability in the arctic
[AD-A150550] N85-23363

ARGON
Argon ion pollution of the magnetosphere N85-22523
Properties of welded joints in argon arc welding of titanium alloy using a protective coating N85-22733
Threshold double photoionization of argon with synchrotron radiation
[AD-A150515] N85-23389

ARIZONA
The geology of Mt. Hope, a silicic volcanic center in West Central Arizona N85-23571

ARTIFICIAL INTELLIGENCE
Aviation maintenance computerized management information systems: Perspective for the future
[AD-A150637] N85-22349
Advancing automation and robotics technology for the Space Station and for the US economy. Volume 1: Executive overview
[NASA-TM-87566-VOL-1] N85-22460
Advancing automation and robotics technology for the Space Station and for the US economy, volume 2
[NASA-TM-87566-VOL-2] N85-22461
The potential for advanced computerized aids for comprehensible writing of technical documents
[AD-A150501] N85-22870
Artificial Intelligence and Bionics Workshop held at Stowe, Vermont on 11-15 June 1984
[AD-A150483] N85-23339

ARTIFICIAL SATELLITES
China report: Science and technology
[JPRS-CST-84-030] N85-22777
Nation said to rank high with 15 satellites N85-22778
Periodic movements of axisymmetrical satellite about center of mass due to gravitational moment N85-22783
Development, prospect of satellite dynamics discussed N85-22847

ASSEMBLIES
Development of a sintered shim
[DE85-006183] N85-22685

ASSEMBLING
Investigation of dynamics of manipulator with elastic sections N85-22819
Advanced life analysis methods. Volume 2: Crack growth analysis methods for attachment lugs
[AD-A150420] N85-23109

ASTEROIDS
Research in planetary studies and operation of Mauna Kea Observatory
[NASA-CR-175618] N85-23460
Study and estimation of planet-crossing asteroid populations: Discoveries and analysis N85-23498
The olivine asteroids: Discovery, mineralogy, and relationship to palasites N85-23500
Convex-profile inversion of asteroid lightcurves N85-23502
Surfaces of asteroids and cometary nuclei N85-23503

ASTRODYNAMICS
Method for prompt modeling of quasiperiodic movement of solid near-axisymmetrical body in atmosphere N85-22790

ASTRONAUTS
Astronaut hazard during free-flight polar EVA N85-22522

ASTRONOMICAL MODELS
Viking radio science data analysis and synthesis
[NASA-CR-175631] N85-23471
An idealized short period comet model: Surface insolation, H2O flux, dust flux and mantle evolution N85-23504

ASTRONOMICAL PHOTOGRAPHY
Evaluating accuracy in orientation of topographic photograph and satellite-centered direction from star photograph N85-22442

ASTRONOMICAL PHOTOMETRY
Convex-profile inversion of asteroid lightcurves N85-23502

ASTROPHYSICS
Theoretical and observational studies of stellar activity N85-23468
Giant planets and their satellites: Cosmochemistry, evolution and structure N85-23494
The structure and composition of Uranus and Neptune N85-23495

ASYMMETRY
Skewed stable variables and processes
[AD-A150549] N85-23372

ASYMPTOTIC METHODS
Investigation of dynamics of manipulator with elastic sections N85-22819
Domain of applicability of asymptotic description of radio pulse fields near critical frequency N85-22949
Scattering of waves by axisymmetrical edge N85-22987
Asymptotically optimum multialternative sequential procedures for discernment of processes minimizing average length of observations N85-23012
Confidence intervals using the regenerative method for simulation output analysis
[AD-A150147] N85-23343

ASYMPTOTIC PROPERTIES
Accuracy of approximation of Bayes estimates in presence of noninformative parameters N85-23015

ATLANTIC OCEAN
The imaging of internal waves by the SEASAT-A synthetic aperture radar
[ARE(PORTLAND)TN-720/84] N85-22860

ATMOSPHERIC ATTENUATION
Infrared aerosol absorption index N85-23147
Below-room-temperature water-vapor continuum absorption within the 8- to 10 micron atmospheric transmission window
[TR-0084(4945-09)-1] N85-23266

ATMOSPHERIC BOUNDARY LAYER
Radiosodar system for remote synchronous measurements of wind speed, temperature and its fluctuations N85-23145

ATMOSPHERIC CHEMISTRY
Multiple element neutron-activation analysis of atmospheric aerosols with X-ray and gamma-spectrometric recording of radionuclides formed N85-22631
One mechanism of formation of organic fraction in atmospheric aerosol N85-22632

ATMOSPHERIC CIRCULATION
Empirical and modeled synoptic cloud climatology of the Arctic Ocean
[NASA-CR-175628] N85-23272
Variation of Arctic cloud cover in summer
[DE85-004507] N85-23285

ATMOSPHERIC COMPOSITION
Multiple element neutron-activation analysis of atmospheric aerosols with X-ray and gamma-spectrometric recording of radionuclides formed N85-22631
One mechanism of formation of organic fraction in atmospheric aerosol N85-22632
Possible role of ocean biota in global carbon balance — phytoplankton production N85-23129
Sulfur oxygen processes on Io N85-23481
Photometric analysis of Jupiter-illuminated images of Io N85-23620

ATMOSPHERIC EFFECTS
Thematic Mapper data quality and performance assessment in renewable resources/agriculture/remote sensing N85-23201

ATMOSPHERIC ENTRY SIMULATION
Method for prompt modeling of quasiperiodic movement of solid near-axisymmetrical body in atmosphere N85-22790

ATMOSPHERIC MODELS
New atmospheric sensor analysis study
[NASA-CR-171426] N85-23069
Modeling of mechanism of positive feedback between mean Earth surface temperature and atmospheric carbon dioxide in geologic time scale N85-23122
Numerical experiments with simple model of ocean climate N85-23123
Possibility of determining atmospheric weather parameters by radio and radiooptical measurements of refraction of cosmic sources N85-23146
Stagnation zone impaction on a simple terrain feature in stable flow N85-23255

ATMOSPHERIC MOISTURE
Dependence of combustion of homogeneous kerosene-air mixtures on humidity of air N85-22635
Possibility of determining atmospheric weather parameters by radio and radiooptical measurements of refraction of cosmic sources N85-23146
Response of Earth's atmosphere to increases in solar flux and implications for loss of water from Venus N85-23518

ATMOSPHERIC OPTICS
Time spectra of intensity fluctuations along reflecting path N85-22981

ATMOSPHERIC PHYSICS
USSR report: Earth sciences
[JPRS-UES-85-002] N85-23116

ATMOSPHERIC PRESSURE
Portable Automated Mesonet (PAM) data from the 1980 experiment in Anderson Creek Valley
[DE85-004361] N85-23282

ATMOSPHERIC SOUNDING
Microstructure of Venus cloud layer based on spectrophotometric data from Venera-11 spacecraft N85-22436

ATMOSPHERIC TURBULENCE
A spatially incoherent and temporally coherent source
[AD-A151261] N85-23390

ATMOSPHERIC WINDOWS
Absorption of radiation by water vapor in windows of relative transparency of 95-145 micrometer range N85-22968
Below-room-temperature water-vapor continuum absorption within the 8- to 10 micron atmospheric transmission window
[TR-0084(4945-09)-1] N85-23266

ATOMIC COLLISIONS
Mean delta-ray energies in ion molecule collisions
[DE85-005524] N85-23395

ATOMIC SPECTRA
Sample introduction methods for improving the particle detection capability of the spectrometric oil analysis program
[AD-A150139] N85-23399

ATOMIZING
Atomization data requirements for rocket combustor modeling N85-22555

ATTACHMENT
Advanced life analysis methods. Volume 1: Cracking data survey and NDI (nondestructive inspection) assessment for attachment lugs
[AD-A150419] N85-23108
Advanced life analysis methods. Volume 2: Crack growth analysis methods for attachment lugs
[AD-A150420] N85-23109

ATTENUATION
Investigation of bimodal paramagnetic filter N85-23007

ATTENUATION COEFFICIENTS
Recommendation on use of series K157UL1 microcircuits N85-22936
Change of electrical characteristics of radio-frequency cables under thermal effect N85-22999

Fine structure of vertical distribution of light attenuation index of sea water N85-23140

ATTITUDE CONTROL
Space station systems technology study (add-on task). Volume 1: Executive summary
[NASA-CR-171415] N85-22459

AUDIO FREQUENCIES
Application of K176-series microcircuits N85-22973

AUDIOMETRY
The audiomat: An automatic audiometer for use in occupational audiometry
[DRIC-T-7138] N85-23294

AUDITORY PERCEPTION
The audiomat: An automatic audiometer for use in occupational audiometry
[DRIC-T-7138] N85-23294

AUDITORY SIGNALS
High-frequency acoustic variability in the arctic
[AD-A150550] N85-23383

AUGER SPECTROSCOPY
HREELS and Auger studies of conducting polymers
[DE85-004541] N85-22764
Threshold double photoionization of argon with synchrotron radiation
[AD-A150615] N85-23389

AURORAL ARCS
One-dimensional model of auroral magnetic force with longitudinal current and cyclotron heating of ions N85-22424

AURORAL ELECTROJETS
Polar orbit electrostatic charging of objects in shuttle wake N85-22487

AURORAS
Plans for Interbol satellite experiment N85-22407

AUSTENITIC STAINLESS STEELS
Hydrogen effects in austenitic stainless steels based on the Fe-Cr-Mn-N system
[DE85-003617] N85-22672

AUSTRALIA
MAGSAT anomaly field data of the crustal properties of Australia
[E85-10100] N85-23215
An investigation of the crustal properties of Australia and surrounding regions derived from interpretation of MAGSAT anomaly field data N85-23216
Data selection techniques in the interpretation of MAGSAT data over Australia N85-23218

AUTOCORRELATION
Method for approximating autocorrelation functions for describing areal photoimage features N85-22443
Regular synthesis of pairs of phase-keyed binary minimax signals N85-22923

AUTOMATA THEORY
Advancing automation and robotics technology for the Space Station and for the US economy. Volume 1: Executive overview
[NASA-TM-87566-VOL-1] N85-22460
Advancing automation and robotics technology for the Space Station and for the US economy, volume 2
[NASA-TM-87566-VOL-2] N85-22461
The hierarchical database decomposition approach to database concurrency control
[AD-A150612] N85-23450

AUTOMATED TRANSIT VEHICLES
Metrological support for remote transport vehicle speedometers N85-22963

AUTOMATIC CONTROL
Guidance and control research flight testing with HFB 320 test aircraft N85-22355
TASS update on unmanned flight of Salyut-7 N85-22404
Automatic charge control system for satellites N85-22508
Hydraulic brakes for industrial robots N85-22806

AUTOMATIC FLIGHT CONTROL
Air Force technical objective document, Flight Dynamics Laboratory plans for fiscal year 1986. Air Force technical objective document
[AD-A149648] N85-22348

AUTOMATION
Design of tightening device and calculation of forces in manipulator transmissions with base-drive mounted N85-22804
USSR report: Machine tools and metalworking equipment
[JPRS-UMM-85-005] N85-22839
Advances in cutting tool technology surveyed N85-22840
Motion planning with six degrees of freedom
[AD-A150312] N85-23432

AUTOMOBILES
Uses of composite materials N85-22698

AUTONOMY
Space station systems technology study (add-on task). Volume 1: Executive summary
[NASA-CR-171415] N85-22459

AVALANCHE DIODES
Investigations of the high frequency performance of impact avalanche transit-time diodes N85-22884

AVERAGE
Why do noninvertible estimated moving averages occur?
[AD-A150386] N85-23368

AVIONICS
Ground and flight testing for aircraft guidance and control
[AGARD-AG-262] N85-22350
Civil avionics flight testing with the RAE(B) BAC1-11 N85-22354
Guidance and control research flight testing with HFB 320 test aircraft N85-22355
Avionics Flight Evaluation System (AFES) N85-22357
AIRLAB: A laboratory for flight-crucial-electronics system research N85-22362
Reliability predictions for military avionics. Royal Signals and Radar Establishment reliability prediction method no. 250
[BR69221] N85-22388
Shuttle flight test of an advanced gamma-ray detection system
[AD-A150316] N85-22469

AXES OF ROTATION
Motion of symmetrical satellite with flexible viscoelastic rods about center of mass in circular orbit N85-22420
Axial representations of shape
[AD-A150387] N85-23356

AXIAL COMPRESSION LOADS
Stability of cylindrical shells with one-way constraints N85-22820

AXIAL FLOW
Flow-induced vibrations of a circular cylinder due to turbulent internal flows
[DE85-002766] N85-23110

AXIAL STRAIN
Dissipation of energy in composite material N85-22703

AXISYMMETRIC BODIES
Method for prompt modeling of quasiperiodic movement of solid near-axisymmetrical body in atmosphere N85-22790
Flight dynamics of axisymmetrical rotating bodies in air medium N85-22791
Absolute stability of unsteady movement of axisymmetrical rotating flight vehicle N85-22793
Steady-state reaction of three-layered cylindrical shell to effect of moving load N85-22811

AXISYMMETRIC FLOW
The low frequency behaviour of an immersed structure at a standstill in a high density fluid with free surface
[TP-1983-31] N85-23105

AZIMUTH
The effects of internal waves on acoustic normal modes
[AD-A150235] N85-23379

AZINES
Effects of triazine components on physicochemical properties of polybutadiene: urethane block copolymers N85-22635

B

BACKGROUND NOISE
Extraction of signals from background interference with unknown parameters in quantized sample N85-23013
Approximate rules for signal detection against background of Gaussian correlated interference N85-23027

BACKGROUND RADIATION
Measurement of the large-scale anisotropy of the cosmic background radiation at 3 MM N85-23680
A measurement of the intensity of the cosmic background radiation at 3.9 cm N85-23681

BACKSCATTERING
Reaction of amorphous NiNb films with crystalline metal overlayers
[DE85-005483] N85-22680
Optical reflectometer for multimode fiber lightpipes N85-22961
The microwave propagation and backscattering characteristics of vegetation --- wheat, sorghum, soybeans and corn fields in Kansas
[E85-10088] N85-23213
Microwave remote sensing of soil moisture N85-23235
Investigations of ultrasonic wave interactions at boundaries separating anisotropic materials
[DE85-003506] N85-23384

BACTERIA
Production and turnover of suspended organic detritus in the coastal water of the southeastern continental shelf
[DE85-003977] N85-23290

BALANCING
Development of a multiplane multispeed balancing system for turbine systems
[NASA-CR-174750] N85-22400

BALLOON-BORNE INSTRUMENTS
Calibration of solar cells outside the atmosphere N85-22603

BALMER SERIES
A model for eclipsing cataclysmic variables N85-23467

BALTIC SHIELD (EUROPE)
Study of stratigraphy of the Precambrian Soviet Baltic shield N85-23148

BANDPASS FILTERS
Investigation of bimodal paramagnetic filter N85-23007

BANDWIDTH
Beamwidth control in pyramidal horns
[R-NIAS-27] N85-22853
Gyrator frequency selectors with bandwidth independent of input signal level N85-23009

BARIUM TITANATES
Planar ferroelectric microcapacitors for microwave devices N85-23032

BARRED GALAXIES
Gas dynamics of the barred spiral galaxy NGC 3359 N85-23465

BASALT
Characteristics of basaltic lava flows on Venus N85-23508
Magmas as selective filters of volatiles between planetary mantles and surfaces N85-23557
Basaltic pressure ridges: Formation and relationship to flow emplacement N85-23567
Basalts of Mars: Constraints on volatile evolution N85-23610
Mechanisms of basalt-plains ridge formation N85-23643

BAYES THEOREM
Asymptotically optimum multialternative sequential procedures for discernment of processes minimizing average length of observations N85-23012
Accuracy of approximation of Bayes estimates in presence of noninformative parameters N85-23015

BEAM CURRENTS
SEM (Scanning Electron Microscope) investigation of silicon diodes using the electron beam induced current method
[AD-A150356] N85-22894

BEAM INTERACTIONS
System for forming and focusing high current beam of deuterium ions N85-22798

BEAM LEADS
Low capacitance e-beam fabricated beam-lead Schottky barrier diodes
[AD-A150238] N85-22888

BEAMS (RADIATION)
Beamwidth control in pyramidal horns
[R-NIAS-27] N85-22853
Experimental verification of beam deflection from hybrid reflector antenna within wide-angle sector N85-22984

BEARING (DIRECTION)
Helium atoms in interstellar and interplanetary space. II: Determination of direction of interstellar gas motion relative to Sun N85-22425

BENDING
Simple theoretical models for composite rotor blades
[NASA-CR-175620] N85-22382

BENZENE
Formation of high molecular weight products from benzene during boundary lubrication
[NASA-TM-86966] N85-22644

BERYLLIUM
TEM/FIM study of modulated microstructures in the Fe-Be system
[DE85-005379] N85-22678

BIBLIOGRAPHIES
Aeronautical Engineering: A continuing bibliography with indexes, supplement 185
[NASA-SP-7037(185)] N85-22342
Aeronautical Engineering: A cumulative index to the 1984 issues of the continuing bibliography
[NASA-SP-7037(183)] N85-22343
Cryogenic wind tunnels: A selected annotated bibliography
[NASA-TM-86346] N85-22401
Small business innovation research: Abstracts of 1984, Phase 1 awards
[NASA-TM-87427] N85-23431

NASA Patent Abstracts Bibliography. A continuing bibliography. Section 2: Indexes
[NASA-SP-7039(26)] N85-23445
BIMETALS
Microscopic magnetic structure of multiple bilayers of thin films of Fe and Ge
[DE85-004188] N85-22682
BINARY CODES
Error probability during optimal noncoherent reception of binary signals in multibeam channel N85-22922
BINARY DATA
Noise tolerance of digital demodulator for complex signal system employing binary quantization N85-22929
BINARY MIXTURES
Theoretical thermodynamics of mixtures at high pressures N85-23550
BINARY STARS
Theoretical and observational studies of stellar activity N85-23468
BINDERS (MATERIALS)
Development and study of two-matrix glass fiber composite with increased transverse deformation N85-22700
BIOINSTRUMENTATION
The audiomat: An automatic audiometer for use in occupational audiometry
[DRIC-T-7138] N85-23294
BIOLOGICAL EFFECTS
Interaction of metals and metalloids with biomembranes
[DE85-004902] N85-23293
BIOLOGICAL MODELS (MATHEMATICS)
Artificial Intelligence and Bionics Workshop held at Stowe, Vermont on 11-15 June 1984
[AD-A150463] N85-23339
BIOLUMINESCENCE
Luminescence in the ocean
[AD-B089136L] N85-23288
BIOMASS
Anaerobic digestion of biomass: status summary and research development needs, 1983
[PB85-161925] N85-22772
Remote sensing of coastal wetlands biomass using Thematic Mapper wavebands — Lewes, Delaware N85-23198
BIONICS
Artificial Intelligence and Bionics Workshop held at Stowe, Vermont on 11-15 June 1984
[AD-A150463] N85-23339
BIOSPHERE
Magmas as selective filters of volatiles between planetary mantles and surfaces N85-23557
BIPOLAR TRANSISTORS
Development of a planar heterojunction bipolar transistor for very high speed logic
[AD-A150374] N85-22895
BIPOLARITY
Drift fields and boundary conditions at grain boundaries in bipolar P/N junction silicon devices N85-22879
BISMUTH COMPOUNDS
Shuttle flight test of an advanced gamma-ray detection system
[AD-A150316] N85-22469
BLACK BODY RADIATION
Microwave blackbodies for spaceborne receivers
[NASA-CR-175847] N85-23068
Measurement of the large-scale anisotropy of the cosmic background radiation at 3 MM N85-23680
BLADE TIPS
An experimental investigation of the chopping of helicopter main rotor tip vortices by the tail rotor
[NASA-CR-177338] N85-23376
BLOCK DIAGRAMS
Dispersion of phase-shift keyed systems with fixed number of blocks N85-22928
BLOOD CIRCULATION
China report: Science and technology
[JPRS-CST-84-008] N85-22384
BODIES OF REVOLUTION
Average spacing for rings of individual multi-ring basins is 2.0(0.5)D N85-23541
BODY TEMPERATURE
China report: Science and technology
[JPRS-CST-84-030] N85-22777
Study of effective physiological temperature N85-22780
BOILING
Effects of temperature variation among droplets in an evaporating fuel spray N85-22562
BOILING WATER REACTORS
Steel containment buckling
[DE85-003744] N85-23111
BOLIVIA
A silicic shield volcano in Bolivia N85-23572
BOLOMETERS
BIG MAC: A bolometer array for mid-infrared astronomy, Center Director's Discretionary Fund
[NASA-TM-86502] N85-23463
BOLTS
Corrosion of aircraft Al and Al-Zn ion plated steel fasteners N85-22686
BONDING
Activation of Si-N modes in silicon by pulsed laser annealing
[DE85-002988] N85-23082
BONES
Distribution of radium and plutonium in human bone
[DE85-005025] N85-23298
BORON
Status of boron combustion research N85-22526
Gasification of boron oxide drops and boron slurry agglomerates in combustion gases N85-22529
Technological process effect on the carrier lifetime degradation of silicon solar cell base layer irradiated by 1 MeV electrons (boron doping case) N85-22585
Annealing of radiation damage in boron and gallium doped silicon solar cells N85-22624
BORON REINFORCED MATERIALS
Experiences with implanted Back Surface Field (BSF) solar cells N85-22571
Use of acoustical emission method to study specifics of fracture of boron reinforced plastic structural elements N85-22696
Effect of operating medium on cyclic durability of AD33-W composite N85-22716
BOSONS
Theoretical aspects of electroweak and other interactions in medium-energy nuclear physics
[DE85-003821] N85-23392
BOUGUER LAW
Bouguer images of the North American craton N85-23648
BOUNDARY LAYER EQUATIONS
Significance of the thin-layer Navier-Stokes approximation
[DE85-002630] N85-23063
BOUNDARY LAYER FLOW
Aerodynamic heating rate distributions induced by trailing edge controls on hypersonic aircraft configurations at Mach 8
[NASA-TM-87453] N85-22370
Preliminary study of inphase gusts and moment force wind loads over the first 150 meters at KSC, Florida
[NASA-TM-86501] N85-23273
BOUNDARY LAYER SEPARATION
Double and inverse Taylor-Hogg vortices in a stratified ocean N85-23137
BOUNDARY LAYERS
Investigations of reactive and non reactive acoustic boundary layers in porous walled ducts N85-22535
The relationship between marine aerosol particles and satellite-detected radiance N85-23263
H-division materials physics progress
[DE85-004990] N85-23430
Three-layer generic Ganymedes: Structure and evolution N85-23657
BOUNDARY LUBRICATION
Formation of high molecular weight products from benzene during boundary lubrication
[NASA-TM-86966] N85-22644
BOUNDARY VALUE PROBLEMS
Propagation of three-dimensional turbulent jet from lobar nozzle through surrounding stream N85-22785
Liquid moment on a filled coning cylinder during spin-up: Ad hoc model
[AD-A150280] N85-23060
BRAIN
Brain mechanisms underlying individual differences in reaction to stress: An animal model
[AD-A150195] N85-23301
BRAKES (FOR ARRESTING MOTION)
Hydraulic brakes for industrial robots N85-22806
BRAZING
Thermodynamics of copper-nickel alloys containing aluminum, silicon, titanium, and chromium relative to their use in ceramic brazing
[DE85-004787] N85-22674
BREADBOARD MODELS
Firefighters' communication transceiver test plan
[NASA-CR-171419] N85-22854
BRIGHTNESS
The relationship between marine aerosol particles and satellite-detected radiance N85-23263
Formation of bright terrain bands on Ganymede by unstable lithosphere extension N85-23485
BRIGHTNESS DISTRIBUTION
A posteriori increase of resolving power of optical system forming averaged monochromatic images N85-23003
Relationship between brightness spectrum of photographic image and spectrum of rises on a water surface with waves N85-23171
BRIGHTNESS TEMPERATURE
Calculations of microwave brightness temperature of rough soil surfaces: Bare field
[NASA-TM-86200] N85-23221
General report of the researches of snowpack properties, snowmelt runoff and evapotranspiration in Japan N85-23225
Microwave radiometer observations of snowpack properties and comparison of U.S. Japanese results — Hokkaido, Japan and Vermont and North Dakota test sites N85-23230
Studies on physical properties of snow based on multi channel microwave radiometer N85-23231
Analysis of NIMBUS-7 SMMR data — Hokkaido, Japan snow cover N85-23232
Estimation of regional evapotranspiration using remotely sensed land surface temperature. Part 1: Measurement of evapotranspiration at the Environmental Research Center and determination of Priestley-Taylor parameter N85-23233
Venus surface composition from radio/radar measurements N85-23509
BROADBAND
Efficiency of digital compensator of strong non-Gaussian interference N85-22942
Programmable filter with fanned interdigital surface acoustic wave transducer N85-23008
BROADCASTING
Electronic generation of text for television
[BBC-RD-1984/14] N85-22858
BRONZES
Microstructural study on the processing and properties of high-field A15 superconducting materials
[DE85-004652] N85-23423
BRUSHES (ELECTRICAL CONTACTS)
Thermal and thermoelastic effects in rolling/sliding contacts
[AD-A150435] N85-23429
BUBBLE MEMORY DEVICES
Feasibility of self-structured current accessed bubble devices in spacecraft recording systems
[NASA-CR-172554] N85-22525
BUCKLING
Steel containment buckling
[DE85-003744] N85-23111
BULK MODULUS
Research program on the effect of pressure on the mechanical properties of polymers, part 2
[DE85-000995] N85-22781
BURNING RATE
Mechanism of burning rate enhancement by ferric oxide N85-22546
Effect of variable solid phase thermal properties on propellant combustion N85-22547
Multiple reflection theory for microwave measurement of solid propellant burning rates N85-22549
In-situ burning rate determination using flash radiography N85-22550
Chemical kinetics of gas phase decomposition products of nitramine propellants N85-22558
A comprehensive review of black powder
[AD-A150455] N85-22769
BYPASSES
Problems with electrical interference between solar generators and shunt type regulators N85-22607

C

CADMIUM TELLURIDES
Investigation of the effect of annealing on the dislocation and sub-grain boundary content of solvent-evaporation-grown CdTe
[AD-A144087] N85-23415
CALCIUM
Aluminum alloy ATsSK5 (5% Zn + 5% Ca) for superplastic forming N85-22897
Effect of phase state of TiC-NiTi powder composite materials on nature of failure and mechanical properties N85-22702
CALCULATORS
Fibre composite laminated plate analysis using a card programmable calculator (HP41C/CV)
[NIAST-83/88] N85-23106
CALIBRATING
Determination of angular resolution of coded aperture gamma-ray telescope N85-22432
Calibration of solar cells outside the atmosphere N85-22603
Nonlinearity and spectral mismatch problems of solar cells N85-22606

A standard aircraft diffusion flame: Spectral characteristics and a feasibility study for developing an alternate calibration source for aircraft optical fire detection systems
[AD-A150231] N85-22768
Metrological support for remote transport vehicle speedometers N85-22963
Microwave blackbodies for spaceborne receivers
[NASA-CR-175647] N85-23068
Low temperature calibration fixture
[DE85-003969] N85-23071

CALIFORNIA
Summary of Meteorological Observations, Surface (SMOS) Camp Pendleton, California
[AD-A150482] N85-23277

CALLISTO
Ripple ring basins on Ganymede and Callisto N85-23547
Tectonics of the Valhalla structure on Callisto N85-23662

CAMERA SHUTTERS
High-resolution SIT TV tube for subnanosecond image shuttering
[DE85-005189] N85-23072

CAMERA TUBES
High-resolution SIT TV tube for subnanosecond image shuttering
[DE85-005189] N85-23072

CAMERAS
Electronics Engineering Department EE Technical Review
[UCRL-50025-84-1] N85-22887
A normal incidence, high resolution X-ray telescope for solar coronal observations
[NASA-CR-175622] N85-23461

CANOPIES (VEGETATION)
Remote sensing of coastal wetlands biomass using Thematic Mapper wavebands — Lewes, Delaware N85-23198
The microwave propagation and backscattering characteristics of vegetation — wheat, sorghum, soybeans and corn fields in Kansas
[E85-10068] N85-23213
Testing an energy balance model for estimating actual evapotranspiration using remotely sensed data — Hannover, West Germany barley and wheat fields N85-23236

CANTILEVER BEAMS
Stress intensity factor in a tapered specimen
[NASA-CR-175589] N85-23099

CANYONS
Lithologic and structural control on slope morphology in the Valles Marineris N85-23651
Valles Marineris basin beds: A complex story N85-23652

CAPACITANCE
Low capacitance e-beam fabricated beam-lead Schottky barrier diodes
[AD-A150238] N85-22888
On filter binary processes
[AD-A150328] N85-22890
Change of electrical characteristics of radio-frequency cables under thermal effect N85-22999

CAPACITORS
Control of cascaded induction generator systems
[AD-A150429] N85-22897
Planar ferroelectric microcapacitors for microwave devices N85-23032

CAPTURE EFFECT
Orbital resonances and planetary accretion in the solar nebula N85-23523

CARBON DIOXIDE
Modeling of mechanism of positive feedback between mean Earth surface temperature and atmospheric carbon dioxide in geologic time scale N85-23122
The evolution of CO2 on Mars N85-23558

CARBON DIOXIDE CONCENTRATION
Possible role of ocean biota in global carbon balance — phytoplankton production N85-23129

CARBON DIOXIDE LASERS
Near Field/Far Field (NF/FF) energy loss in Electric Discharge Lasers (EDL's): A mode-medium interaction
[AD-A150299] N85-23075
Feasibility of alpha particle measurement by CO2 laser Thomson scattering
[DE85-004936] N85-23081

CARBON FIBER REINFORCED PLASTICS
Electrostatic discharge testing on a carbon fiber solar panel structure N85-22584

CARBON FIBERS
Segregation of silicon in silumin-carbon fiber composites N85-22706

CARBONACEOUS CHONDRITES
Hibonite: Crystal chemistry and origin of blue coloration in meteoritic assemblages N85-23555

CARBONATES
Molten carbonate fuel cell performance model update, draft
[DE85-005423] N85-23252
Cathode materials for molten carbonate fuel cells
[DE85-004078] N85-23254
Analysis of SMIRR data for volcanic and sedimentary terrains of the trans-Pecos region, Texas N85-23626
Chemical weathering of soils from the dry valleys of Antarctica: A terrestrial analog of Martian weathering processes N85-23628

CARDIOGRAPHY
NDE methods for green ceramics
[DE85-004019] N85-22766

CARDS
Fibre composite laminated plate analysis using a card programmable calculator (HP41C/CV)
[NIAST-83/88] N85-23106

CARRIER DENSITY (SOLID STATE)
Investigations of radiation-induced and carrier-enhanced conductivity N85-22515
Technological process effect on the carrier lifetime degradation of silicon solar cell base layer irradiated by 1 MeV electrons (boron doping case) N85-22585

CARRIER FREQUENCIES
Experimental results on the application of convolutional coding and Viterbi decoding as a frequency diversity technique in HF data transmission
[CRC-1377] N85-22850

CASCADE RANGE (CA-OR-WA)
Morphologic evolution of the Mount St. Helens crater area, Washington N85-23568

CASPIAN SEA
Horizontal coherence of temperature microstructure in upper ocean layer N85-23139

CASSIOPEIA A
Absolute measurements of radiation intensity from Cassiopeia-A, Cygnus-A and crab nebula in 60-100 cm band N85-22978

CAST ALLOYS
Anomalies of aluminum structure and properties N85-22693

CASTINGS
Fatigue and corrosion fatigue resistance of aluminum casting alloy VAL10 and forging alloy AK6 N85-22690

CATACLYSMIC VARIABLES
A survey for galactic plane ultraviolet-excess objects: Space densities for white dwarfs, subdwarfs, and cataclysmic variables N85-23458
A model for eclipsing cataclysmic variables N85-23467

CATALOGS (PUBLICATIONS)
Crustal dynamics project: Catalogue of site information
[NASA-TM-87452] N85-23258

CATALYSIS
Application of modulated hydrodynamic voltammetry to the study of anodic electrocatalysis
[DE85-004182] N85-22653

CATALYSTS
Workshop report: Catalysis of Burn Rate of Energetic Binder propellants N85-22545
Mechanism of burning rate enhancement by ferric oxide N85-22546
USSR report: Chemistry
[JPRS-UCH-85-001] N85-22629
Trifunctional catalysts for conversion of syngas to alcohols
[DE85-004577] N85-22771

CATHODES
Molten carbonate fuel cell performance model update, draft
[DE85-005423] N85-23252
Cathode materials for molten carbonate fuel cells
[DE85-004078] N85-23254

CATS
Brain mechanisms underlying individual differences in reaction to stress: An animal model
[AD-A150195] N85-23301

CAVITATION CORROSION
Prediction of the resistance of structural materials to cavitation erosion
[BLL-DRIC-TRANS-7435-(3623.66)] N85-22659

CAVITATION FLOW
Properties of materials using acoustic waves
[AD-A150465] N85-23382

CAVITIES
Micromechanical modeling of microstructural damage in creeping alloys
[DE85-003925] N85-22671

CAVITY RESONATORS
Coupled-cavity gyrotrons with mode conversion N85-22967
Experimental study of high-stability oscillator with surface-acoustic-wave resonator in feedback loop N85-23053

CEILINGS (METEOROLOGY)
Summary of Meteorological Observations, Surface (SMOS), Beaufort, South Carolina
[AD-A150538] N85-23279

CELESTIAL MECHANICS
Lagrangian solutions in photogravitational restricted circular three-body problem N85-22416
Computation of elliptical functions in problems of celestial mechanics N85-22418
Feoktistov argues against U.S. space shuttle design concept N85-22453
China report: Science and technology
[JPRS-CST-85-005] N85-22843
Development, prospect of satellite dynamics discussed N85-22847
Dynamics of gas disks in triaxial galaxies N85-23469

CELLULOSE
Environmental cycling of cellulosic thermal insulation and its influence on fire performance
[DE85-004295] N85-22776

CENTER OF MASS
Motion of symmetrical satellite with flexible viscoelastic rods about center of mass in circular orbit N85-22420
Rotational motion of a satellite N85-22428
Evaluating accuracy in determining position of Earth's center of mass and elements of orientation of geodetic coordinate system N85-22441
Periodic movements of axisymmetrical satellite about center of mass due to gravitational moment N85-22783

CENTRAL PROCESSING UNITS
Research using a DISCUS based network emulator
[AD-A141294] N85-23338

CENTRIFUGING STRESS
Centrifuge impact cratering experiments N85-23533

CEPHEID VARIABLES
The color excesses of classical cepheids and the structure of our galaxy N85-23459

CERAMIC COATINGS
Metallic and metalloceramic coating by thermal decomposition
[NASA-TM-86992] N85-22755

CERAMIC MATRIX COMPOSITES
Film and interstitial formation of metals in plasma-sprayed ceramics
[NASA-TM-86993] N85-22756

CERAMICS
Thermodynamics of copper-nickel alloys containing aluminum, silicon, titanium, and chromium relative to their use in ceramic brazing
[DE85-004787] N85-22674
Densification and deformation in the presence of a liquid phase
[DE85-005101] N85-22763
NDE methods for green ceramics
[DE85-004019] N85-22766
Cathode materials for molten carbonate fuel cells
[DE85-004078] N85-23254

CERIUM COMPOUNDS
Anomalous magnetism of CeRh3B2 under pressure
[DE85-003069] N85-23425

CERMETS
Effect of zero-wear in friction pairs operating in abrasive media N85-22801

CHANNELS (DATA TRANSMISSION)
Data compression for noiseless channels N85-22651
Horizontal deflection TS-257 N85-22926
Dynamics of adaptive signal corrector N85-22940

CHARCOAL
A comprehensive review of black powder
[AD-A150455] N85-22769

CHARGE EFFICIENCY
Kapton charging characteristics: Effects of material thickness and electron-energy distribution N85-22513

CHARGE TRANSFER
Observation of a novel low-lying excited state in zinc complexes
[AD-A150188] N85-23385

CHARGED PARTICLES
Characteristics of latitude effect on cosmic ray charged component in atmosphere at altitudes 3-5 KM N85-22413
Observation of cosmic ray flux variations in stratosphere N85-22430
Suprathermal plasma observed on STS-3 Mission by plasma diagnostics package N85-22472
Discharges on a negatively biased solar cell array in a charged-particle environment N85-22499
EMI characteristics of a potential control system N85-22502
Spacecraft environmental interactions: A joint Air Force and NASA research and technology program N85-22517
Variable flexing device for targets in internal beams of charged particle accelerators N85-22797
Scattering of electromagnetic waves by charged particles N85-22913

Nonrelativistic Kapitza-Dirac scattering
[AD-A150622] N85-23405

CHARON
Research in planetary studies and operation of Mauna Kea Observatory
[NASA-CR-175618] N85-23460

CHEMICAL ANALYSIS
Structural distortions of ultra-dispersed titanium nitride powders N85-22717

CHEMICAL COMPOSITION
The influence of fuel quality upon flame-tube temperature and flame radiation in a model gas-turbine primary zone
[K233] N85-22396
Structural distortions of ultra-dispersed titanium nitride powders N85-22717
Composition and thickness of oxide coatings on granule surfaces of aluminum alloys N85-22719
Impurities in Kevlar 49 fibers
[DE85-004996] N85-22767
Composition and photochemical reactivity of turbine engine exhaust
[AD-A150559] N85-23256

CHEMICAL ENGINEERING
USSR report: Chemistry
[JPRS-UCH-85-001] N85-22629
Current plans for development of chemical industry N85-22633

CHEMICAL PROPERTIES
Sequential excitation preparation of molecular energy levels with special structural and chemical properties
[AD-A150301] N85-23386

CHEMICAL PROPULSION
Preliminary assessment of power-generating tethers in space and of propulsion for their orbit maintenance N85-22520

CHEMICAL REACTIONS
Sulfur oxygen processes on Io N85-23481

CHEMILUMINESCENCE
Luminescence in the ocean
[AD-B089136L] N85-23288

CHEMISORPTION
Dipole active surface vibrational resonances on clean and hydrogen covered Ni(110)
[AD-A150546] N85-23420

CHESAPEAKE BAY (US)
Comparison of MSS and TM data for landcover classification in the Chesapeake Bay area: A preliminary report — Taylor's Island, Maryland N85-23210

CHINA
China report: Science and technology
[JPRS-CST-84-030] N85-22777
China report: Science and technology
[JPRS-CST-85-003] N85-23433

CHLOROPHYLLS
Characteristic vector analysis of inflection ratio spectra: New technique for analysis of ocean color data
[NASA-TP-2428] N85-23237

CHROMIUM
Dispersed-metal-toughened alumina
[NASA-CR-174687] N85-22758

CHROMIUM ALLOYS
Orientation and temperature dependence of some mechanical properties of the single-crystal nickel-base superalloy Rene N4. 3: Tension-compression anisotropy
[NASA-TM-86982] N85-22660
Study of the effects of implantation on the high Fe-Ni-Cr and Ni-Cr-Al alloys
[NASA-CR-175625] N85-22661

CHROMIUM STEELS
Frictional and structural characterization of ion-nitrided low and high chromium steels
[NASA-TM-86991] N85-23085

CHRONOLOGY
Relative time-scale for channeling events within chaotic terrains, Margaritifer Sinus, Mars N85-23589

CIRCUIT BREAKERS
Optimization of overall dimensions of enclosures for low-voltage devices and equipment N85-23033

CIRCUIT PROTECTION
Electrical overstress protection of submicron devices
[AD-A150334] N85-22892
Requirements placed on information processing equipment
[BLL-CE-TRANS-7983-(9022.09)] N85-23307

CIRCUITS
Problems with electrical interference between solar generators and shunt type regulators N85-22607
Repetitive energy transfers from an inductive energy store N85-22881
USSR report: Electronics and electrical engineering
[JPRS-UEE-85-001] N85-22976

CIRCULAR POLARIZATION
Modern problems in polarimetry of solid surfaces of cosmic bodies N85-22409

CIRCULAR WAVEGUIDES
Scattering of waves by axisymmetrical edge N85-22987

CITIES
A comparison of metropolitan and non-metropolitan employment characteristics: Indications of the size of non-metropolitan mobile communication services user classes
[NASA-CR-175648] N85-22855
The use of Thematic Mapper data for land cover discrimination: Preliminary results from the UK SATMaP programme N85-23207
Technology and Economics, Inc. Technology Application Team
[NASA-CR-175630] N85-23454

CIVIL AVIATION
Ground and flight testing for aircraft guidance and control
[AGARD-AG-262] N85-22350
Civil avionics flight testing with the RAE(B) BAC1-11 N85-22354

CLAMPS
A clamped rectangular plate containing a crack
[NASA-CR-175590] N85-23098

CLASSIFICATIONS
Impact of Thematic Mapper sensor characteristics on classification accuracy — suburban Washington, D.C., Maryland, and the Chesapeake Bay N85-23188
Quick look analysis of TM data of the Washington, District of Columbia, area N85-23197
Microcomputer: Controlled statistics analyzer
[BLL-CE-TRANS-7971-(9022.09)] N85-23306
Geomorphic classification of lava flows on Io N85-23480
Classification of circular features on Venus N85-23511

CLAYS
First direct detection of clay minerals on Mars N85-23612
Analysis of SMIRR data for volcanic and sedimentary terrains of the trans-Pecos region, Texas N85-23626
Chemical weathering of soils from the dry valleys of Antarctica: A terrestrial analog of Martian weathering processes N85-23628

CLIMATE
Environmental cycling of cellulosic thermal insulation and its influence on fire performance
[DE85-004295] N85-22776

CLIMATOLOGY
Relationship of Indian monsoon intensity to time of onset N85-23120
Numerical experiments with simple model of ocean climate N85-23123
Summary of Meteorological Observations, Surface (SMOS), Fallon, Nevada
[AD-A150481] N85-23276
Summary of Meteorological Observations, Surface (SMOS) Camp Pendleton, California
[AD-A150482] N85-23277
Summary of Meteorological Observations, Surface (SMOS), Alameda, California
[AD-A150609] N85-23281

CLOCKS
Application of K176-series microcircuits N85-22973

CLOSURES
Synthesis of tree-structured computing systems through use of closures
[AD-A150502] N85-23326

CLOUD COVER
Summary of Meteorological Observations, Surface (SMOS), Alameda, California
[AD-A150609] N85-23281
Variation of Arctic cloud cover in summer
[DE85-004507] N85-23285

CLOUDS
The orientation distribution of nonspherical aerosol particles within a cloud
[AD-A150600] N85-23061
Snow reflectance from Thematic Mapper N85-23205
Water-ice clouds on Mars: Location and seasonal variation N85-23611
Participation in the Mars Data Analysis Program: Analysis of cloud forms in Viking and Mariner 9 images
[NASA-CR-175604] N85-23673

CLOUDS (METEOROLOGY)
Empirical and modeled synoptic cloud climatology of the Arctic Ocean
[NASA-CR-175628] N85-23272

CLUMPS
The chemistry of RDX and HMX cluster ions N85-22561
Relationship between topological and magnetic order in small metal clusters
[AD-A150547] N85-22651
Clustering and ordering in 3-5 alloys
[AD-A150604] N85-22670

COAGULATION
Evolution of grains in a turbulent solar nebula N85-23525

COAL GASIFICATION
USSR report: Chemistry
[JPRS-UCH-85-001] N85-22629

COASTAL WATER
Production and turnover of suspended organic detritus in the coastal water of the southeastern continental shelf
[DE85-003977] N85-23290

COATINGS
Experimental studies of low temperature surface interactions of atomic hydrogen using maser technique
[AD-A150218] N85-22647
USSR report: Materials science and metallurgy
[JPRS-UMS-85-002] N85-22668

COAXIAL CABLES
Change of electrical characteristics of radio-frequency cables under thermal effect N85-22999
Spectral evaluation of irregularity of superconducting coaxial cables N85-23000

COBALT ALLOYS
Corrosion-resistant amorphous alloys N85-22748

COCKPITS
Analysis of estimation algorithms for CDTI and CAS applications
[NASA-CR-172444] N85-22387

CODERS
Low-bit rate speech encoders based on Line-Spectrum Frequencies (LSF)
[AD-A150518] N85-22871

CODING
Determination of angular resolution of coded aperture gamma-ray telescope N85-22432
Experimental results on the application of convolutional coding and Viterbi decoding as a frequency diversity technique in HF data transmission
[CRC-1377] N85-22850
Code lock with microcircuit N85-22935
A perspective on multiaccess channels
[AD-A150183] N85-23322

COEFFICIENT OF FRICTION
Interaction of cylindrical shell with concentrated mass moving along its inner surface N85-22810

COGNITION
Human cognition and intelligence: Towards an integrated theoretical perspective
[CSIR-SR-PERS-350] N85-23300

COGNITIVE PSYCHOLOGY
Human cognition and intelligence: Towards an integrated theoretical perspective
[CSIR-SR-PERS-350] N85-23300

COHERENT LIGHT
A posteriori increase of resolving power of optical system forming averaged monochromatic images N85-23003

COHERENT RADIATION
A spatially incoherent and temporally coherent source
[AD-A151281] N85-23390

COHERENT SCATTERING
A spatially incoherent and temporally coherent source
[AD-A151281] N85-23390

COINCIDENCE CIRCUITS
A theoretical basis for the analysis of redundant software subject to coincident errors
[NASA-TM-86369] N85-23317

COLD PLASMAS
Direct measurements of severe spacecraft charging in auroral ionosphere N85-22480
Charging of DMSP/F6 spacecraft in aurora on 10 January 1983 N85-22481

COLD WELDING
Method of calculating strength of joint produced by cold welding of aluminum under discrete loading N85-22743

COLLIMATION
Intensity fluctuations of focused laser beam during reflection in turbulent atmosphere N85-22975

COLLISION AVOIDANCE
TCAS II: Design and validation of the high-traffic-density surveillance subsystem
[DOT/FAA/PM-84/5] N85-22375
Analysis of estimation algorithms for CDTI and CAS applications
[NASA-CR-172444] N85-22387

COLLISIONS
Experimental studies of low temperature surface interactions of atomic hydrogen using maser technique
[AD-A150218] N85-22647
Asteroid collisional evolution studies N85-23501
A circum-terrestrial compositional filter N85-23520

COLOR
A concept for the processing and display of Thematic Mapper data N85-23196

COLORADO
Volcanism of the Colorado Plateau (basin and range transition): Implications for crustal processes N85-23569

COMBAT
Air combat simulation: Methods, models, trends N85-22359

COMBINATORIAL ANALYSIS
Introduction to combinatorial geometry [DE85-003266] N85-23364

COMBUSTIBLE FLOW
Development of a three-phrase combustion code for modeling liquid rocket engines N85-22554

COMBUSTION
Size and velocity distributions of particles and droplets in spray combustion systems [AD-A150355] N85-22648
A comprehensive review of black powder [AD-A150455] N85-22769

COMBUSTION CHAMBERS
Deflected jet experiments in a turbulent combustor flowfield [NASA-CR-174863] N85-22390
Dilution jet configurations in a reverse flow combustor [NASA-CR-174868] N85-22392
Nonlinear interactions between vortices and acoustic waves in a rocket combustion chamber N85-22533
Exergetical analysis of turbojet engine cycle N85-22825

COMBUSTION EFFICIENCY
The influence of fuel quality upon flame-tube temperature and flame radiation in a model gas-turbine primary zone [K233] N85-22396
Dependence of combustion of homogeneous kerosene-air mixtures on humidity of air N85-22835

COMBUSTION PHYSICS
Gasification of boron oxide drops and boron slurry agglomerates in combustion gases N85-22529
Comprehensive mechanisms for combustion chemistry: An experimental and numerical study with emphasis on applied sensitivity analysis [DE85-000173] N85-22656

COMBUSTION PRODUCTS
Solid propellant combustion diagnostics and automated data retrieval from holograms N85-22527

COMBUSTION STABILITY
Twenty-first JANNAF Combustion Meeting, volume 1 [AD-A150981] N85-22526
Coupling between velocity oscillations and solid propellant combustion N85-22536
Acoustic energy balance method N85-22537
Coupled acoustic and hydrodynamic wave instabilities N85-22538
Characterization of heterogeneity of composite propellants and its effects on combustion behavior N85-22539
Investigation of the characteristics of the velocity-coupled response functions of solid propellants N85-22540
Comparisons of solid propellant with instability predictions and motor firing experience N85-22541
Measurements of distributed combustion N85-22542
Distributed combustion: A mechanism of acoustic suppression N85-22543
Workshop report: Catalysis of Burn Rate of Energetic Binder propellants N85-22545
An integral closed loop combustion stability model-status and review N85-22553

COMET NUCLEI
Studies of icy bodies: Uranian satellites and cometary nuclei N85-23496
Surfaces of asteroids and cometary nuclei N85-23503
An idealized short period comet model: Surface insolation, H2O flux, dust flux and mantle evolution N85-23504
Comet thermal modeling N85-23505
Dynamics of long-period comets N85-23506
Halley's Comet, a bibliography [LC-84-600109] N85-23674

COMET TAILS
Halley's Comet, a bibliography [LC-84-600109] N85-23674

COMETARY ATMOSPHERES
Averaging of equations of cometary orbital motion with allowance for nongravitational effects N85-22411
An idealized short period comet model: Surface insolation, H2O flux, dust flux and mantle evolution N85-23504
Comet thermal modeling N85-23505
Dynamics of long-period comets N85-23506
Halley's Comet, a bibliography [LC-84-600109] N85-23674

COMETS
Study and estimation of planet-crossing asteroid populations: Discoveries and analysis N85-23498

COMMAND AND CONTROL
Space station systems technology study (add-on task). Volume 1: Executive summary [NASA-CR-171415] N85-22459
Basic EMC (electromagnetic interference) technology advancement for c3 systems. Volume 3A: Probabilistic analysis of combinational circuits with random delays [AD-A150349] N85-22866

COMMAND LANGUAGES
Construction of a menu-based system [NASA-CR-172560] N85-23321

COMMUNICATION CABLES
Surge strength of symmetric cable with monolithic polyethylene insulation of quads N85-23001

COMMUNICATION NETWORKS
System dynamics and network control [AD-A149420] N85-22863
Integrated digital networks [AD-A150605] N85-22873
Satellite channels in packet-switching networks N85-22909
Satellite bridges in communications networks N85-22910

COMPARISON
Optimal designs for comparisons between two sets of treatments [AD-A150621] N85-23360

COMPENSATORS
Efficiency of digital compensator of strong non-Gaussian interference N85-22942

COMPILERS
Validation summary report, Burroughs Corporation, 820 FORTRAN release 4.0 [PB84-227792] N85-23316

COMPLEX COMPOUNDS
Observation of a novel low-lying excited state in zinc complexes [AD-A150188] N85-23385

COMPLEX SYSTEMS
Mean flow and turbulence in complex terrain NPS (Naval Postgraduate School)/Vandenberg measurement system [AD-A150184] N85-23274
Automatic symbolic solution of Markov chains [AD-A150476] N85-23369

COMPLEX VARIABLES
Computation of elliptical functions in problems of celestial mechanics N85-22418
Applicability of log-normal model to probabilistic description of quasi-pulse interference N85-23014

COMPONENT RELIABILITY
Reliability predictions for military avionics. Royal Signals and Radar Establishment reliability prediction method no. 250 [BR69221] N85-22388
Reliability bounds for fault-tolerant systems with competing responses to component failures [NASA-TP-2409] N85-23090
Automatic symbolic solution of Markov chains [AD-A150476] N85-23369

COMPOSITE MATERIALS
Simple theoretical models for composite rotor blades [NASA-CR-175620] N85-22382
Mechanism of strengthening plastics with rubbers N85-22636
USSR report: Materials science and metallurgy [JPRS-UMS-85-002] N85-22688
Uses of composite materials N85-22698
Dissipation of energy in composite material N85-22703
Possibility of producing monolithic composite materials based on niobium carbide N85-22707

COMPOSITE PROPELLANTS
Characterization of heterogeneity of composite propellants and its effects on combustion behavior N85-22539
Mechanism of burning rate enhancement by ferric oxide N85-22546

COMPOSITE STRUCTURES
Use of acoustical emission method to study specifics of fracture of boron reinforced plastic structural elements N85-22696
Axisymmetrical oscillations of shell systems subjected to impulse loads N85-22814

COMPOSITE WRAPPING
Testing of wound materials for strength with loading in the reinforcement plane N85-22701

COMPOSITION (PROPERTY)
Clustering and ordering in 3-5 alloys [AD-A150604] N85-22670

COMPRESSIBILITY EFFECTS
Investigations into the effects of scale and compressibility on lift and drag in the RAE 5m pressurised low-speed wind tunnel [RAE-TM-AERO-2006] N85-22372

COMPRESSION LOADS
Orientation and temperature dependence of some mechanical properties of the single-crystal nickel-base superalloy Rene N4. 3: Tension-compression anisotropy [NASA-TM-86982] N85-22660
Testing of wound materials for strength with loading in the reinforcement plane N85-22701
Impacts in ice: Commissions of solar system crater population N85-23536

COMPRESSION TESTS
Experimental investigation of crippling strength of Chinese aluminum alloy (LY12CZ) sections N85-22779

COMPRESSION WAVES
Shock compression of liquid helium to 56 GPa (560) kbar N85-23551

COMPRESSOR BLADES
Annular groove in compressor casing as device for control of air stream N85-22832

COMPRESSORS
Annular groove in compressor casing as device for control of air stream N85-22832

COMPUTATION
Rejection of anomalous observations when determining spacecraft trajectories N85-22421
Second thoughts on the mathematical software effort: A perspective [DE85-004831] N85-23333
Sparse matrix computations [DE85-004780] N85-23362

COMPUTATIONAL FLUID DYNAMICS
High-pressure rocket engine turnaround duct computational fluid dynamics analysis N85-22556
Grid generation for a pump collector [AD-A150217] N85-23059

COMPUTATIONAL GRIDS
Correcting depth line on nonlongitudinal seismic profile N85-23184

COMPUTER AIDED DESIGN
Study for the optimization of a transport aircraft wing for maximum fuel efficiency. Volume 1: Methodology, criteria, aeroelastic model definition and results [NASA-CR-172551] N85-22378
A description of the Langley wireframe geometry standard (LaWGS) format [NASA-TM-85767] N85-22380
Preliminary development of an approximation procedure for supercritical wing design optimization applications [AD-A150177] N85-22383
Computer aided engineering applied to the design and verification of the generic Advanced Rigid Array (ARA) --- solar array N85-22593
Redesign of fuselage compartments by method of special contours N85-22784
Computer aided antenna design and frequency selection for HF communications [AD-A150485] N85-22869
Optimum design of electrical motors for multilink manipulators and automated manufacturing systems N85-22880
Algorithm in Walsh function basis for analysis of integrated microcircuits on MOS-structures N85-23006
Grid generation for a pump collector [AD-A150217] N85-23059
Development of a single-family absorption chiller for use in a solar heating and cooling system, phase 3, volume 2 [DE85-003218] N85-23253
Motion planning with six degrees of freedom [AD-A150312] N85-23432

COMPUTER AIDED MAPPING
Assessment of computer based geologic mapping of rock units in the LANDSAT-4 scene of northern Death Valley, California N85-23195
An investigation of the crustal properties of Australia and surrounding regions derived from interpretation of MAGSAT anomaly field data N85-23216

COMPUTER GRAPHICS
A description of the Langley wireframe geometry standard (LaWGS) format [NASA-TM-85767] N85-22380
MAGSAT anomaly field data of the crustal properties of Australia [E85-10100] N85-23215
Data selection techniques in the interpretation of MAGSAT data over Australia N85-23216
Low altitude texture comparison data base and smooth shaded texture [AD-A150342] N85-23323

ROSS: An object-oriented language for constructing simulations
[AD-A150556] N85-23330
Introduction to CHART: A graphic analysis and display system, revision
[DE85-004612] N85-23335
COMPUTER NETWORKS
Satellite channels in packet-switching networks N85-22909
Exploiting parallel computing with limited program changes using a network of microcomputers
[NASA-TM-86387] N85-23318
Introduction to CHART: A graphic analysis and display system, revision
[DE85-004612] N85-23335
Research using a DISCUS based network emulator
[AD-A141294] N85-23338
COMPUTER PROGRAM INTEGRITY
A theoretical basis for the analysis of redundant software subject to coincident errors
[NASA-TM-86369] N85-23317
COMPUTER PROGRAMMING
Optimal allocation of components in parallel-series and series-parallel systems
[AD-A150169] N85-23309
FORTRAN in the 90's
[DE85-006154] N85-23332
The hierarchical database decomposition approach to database concurrency control
[AD-A150612] N85-23450
COMPUTER PROGRAMS
Method for the prediction of the installation aerodynamics of a propfan at subsonic speeds
[NASA-CR-3887] N85-22369
Two degree-of-freedom flutter solution for a personal computer
[NASA-TM-86381] N85-22379
Three-dimensional calculation of shuttle charging in polar orbit N85-22486
NASCAP simulation of PIX 2 experiments N85-22497
Investigations of radiation-induced and carrier-enhanced conductivity N85-22515
Development of a three-phrase combustion code for modeling liquid rocket engines N85-22554
Numerical/Electromagnetics Code (NEC)
[DE85-004999] N85-22874
Pre- and post-processing for stream-function eddy current calculations
[AD-A150417] N85-22896
New atmospheric sensor analysis study
[NASA-CR-171426] N85-23069
Use of three omega radionavigation system position lines for solving problems in marine geodesy N85-23131
ROSA: A computer model for optical power ratio calculations
[DE85-005174] N85-23251
A design analysis and implementation of a user-friendly interface for the UNIX operating system
[AD-A150558] N85-23312
Principles of software engineering environment design
[AD-A150352] N85-23324
ROSS: An object-oriented language for constructing simulations
[AD-A150556] N85-23330
Second thoughts on the mathematical software effort: A perspective
[DE85-004831] N85-23333
On a mathematical structure for an image algebra
[AD-A150228] N85-23348
Hexagonal data base study
[AD-A150176] N85-23448
Copyright law, computer software, and government acquisition
[AD-A150347] N85-23453
Comet thermal modeling N85-23505
COMPUTER STORAGE DEVICES
Fibre composite laminated plate analysis using a card programmable calculator (HP41C/CV)
[NIAST-83/88] N85-23106
COMPUTER SYSTEMS DESIGN
Construction of a menu-based system
[NASA-CR-172560] N85-23321
Measurement of SIFT operating system overhead
[NASA-TM-86322] N85-23337
The hierarchical database decomposition approach to database concurrency control
[AD-A150612] N85-23450
COMPUTER SYSTEMS PERFORMANCE
Bottleneckology: Evaluating supercomputers
[DE85-005574] N85-23315
COMPUTER SYSTEMS PROGRAMS
Computer aided engineering applied to the design and verification of the generic Advanced Rigid Array (ARA) — solar array N85-22593
Contribution of instrumentation and control software to system reliability
[DE85-004693] N85-23340
Numerical algorithms and software for matrix Riccati equations
[AD-A150148] N85-23344
COMPUTER SYSTEMS SIMULATION
Research using a DISCUS based network emulator
[AD-A141294] N85-23338
COMPUTER TECHNIQUES
Aviation maintenance computerized management information systems: Perspective for the future
[AD-A150637] N85-22349
Avionics Flight Evaluation System (AFES) N85-22357
The potential for advanced computerized aids for comprehensible writing of technical documents
[AD-A150501] N85-22870
Orphan detection in the Argus system
[AD-A150562] N85-23331
COMPUTERIZED SIMULATION
Space shuttle pilot-induced-oscillation research testing N85-22351
Dynamic wind tunnel testing for active control research N85-22352
Algorithm for determining optimal three impulse point-to-orbit transfer with limited transfer time N85-22419
Three-dimensional calculation of shuttle charging in polar orbit N85-22486
Self-consistent simulation of plasma interactions with secondary-emitting insulators N85-22492
NASCAP simulation of PIX 2 experiments N85-22497
Development of a three-phrase combustion code for modeling liquid rocket engines N85-22554
Method for prompt modeling of quasiperiodic movement of solid near-axisymmetrical body in atmosphere N85-22790
Research efforts in support of resonance extraction studies. Volume 1: Improvement and validation of TWFD (Thin-Wire Frequency-Domain): A thin-wire frequency-domain scattering code
[AD-A150296] N85-22864
Advanced mixed-mode simulation techniques N85-22883
Investigations of the high frequency performance of impact avalanche transit-time diodes N85-22884
Numerical simulation of inverters with I2L elements including effects of high doping level N85-23039
T700 cutter life improvement program
[AD-A150450] N85-23089
Effects of assuming independent component failure times, if they are actually dependent, in a series system
[AD-A150582] N85-23092
Structural design of the Sandia 34-M Vertical Axis Wind Turbine
[DE85-002631] N85-23247
ROSA: A computer model for optical power ratio calculations
[DE85-005174] N85-23251
Molten carbonate fuel cell performance model update, draft
[DE85-005423] N85-23252
ROSS: An object-oriented language for constructing simulations
[AD-A150556] N85-23330
SIGPI: A user's manual for the fast computation of the probabilistic performance of a complex system
[DE85-005447] N85-23336
Regenerative simulation of non-Markovian stochastic systems
[AD-A150344] N85-23367
Accumulation of the terrestrial planets N85-23524
A parmetric study of crater-saturation simulation N85-23540
COMPUTERS
Liquid mass flow rate computer N85-22962
China report: Science and technology
[JPRS-CST-85-003] N85-23433
CONCENTRATION (COMPOSITION)
Progress on studies of early intense cratering N85-23535
A parmetric study of crater-saturation simulation N85-23540
CONCENTRATORS
Concentrator technologies evaluation for large solar arrays and their application for space stations/platforms N85-22509
Study of concentration for space photovoltaic generators N85-22618
CONCENTRIC SPHERES
Average spacing for rings of individual multi-ring basins is 2.0(0.5)D N85-23541
Ring-diameter ratios for multi-ring basins average 2.0(0.5)D N85-23542
CONES (VOLCANOES)
The geology of Mt. Hope, a silicic volcanic center in West Central Arizona N85-23571
CONFERENCES
All-Union conference of radio astronomers N85-22408
Spacecraft Environmental Interactions Technology, 1983
[NASA-CP-2359] N85-22470
Twenty-first JANNAF Combustion Meeting, volume 1
[AD-A150981] N85-22526
Workshop report: Swirl Enhanced Combustion N85-22564
Photovoltaic Generators in Space — conferences
[ESA-SP-210] N85-22565
LANDSAT-4 Science Characterization Early Results. Volume 4: Applications — agriculture, soils land use, geology, hydrology, wetlands, water quality, biomass identification, and snow mapping
[E85-10070] N85-23186
Remote Sensing of Snow and Evapotranspiration
[NASA-CP-2363] N85-23223
Abstracts of 6th Annual Review Meeting on Photovoltaic Advanced Research and Development
[DE84-013047] N85-23246
Proceedings of the Geoscience Instrumentation Workshop
[DE85-004359] N85-23268
The ASCOT Data Analysis Workshop
[DE85-004407] N85-23283
Modulation of light energy transduction in photosynthesis
[DE85-004711] N85-23292
Technical Digest: Symposium on Optical Fiber measurements, 1984
[PB85-114700] N85-23407
CONFIDENCE LIMITS
Confidence intervals using the regenerative method for simulation output analysis
[AD-A150147] N85-23343
CONFORMAL MAPPING
Applications of the conformal mapping method to the solution of mechanical vibrations problems N85-23103
CONICAL SHELLS
Determination of stresses and deformations in linearly elastic conical shell subjected to aerodynamic loading and heating N85-22812
CONSISTENCY
Precedency control and other semantic integrity issues in a workbench database N85-23220
Consistency of smoothing with running linear fits
[AD-A150232] N85-23349
CONSTANTS
An integral representation of the generalized Euler-Mascheroni constants
[NASA-TP-2456] N85-23305
CONTINENTAL DRIFT
Antarctic glaciation, or what are catastrophes in Earth's history N85-23118
CONTINENTAL SHELVES
A tectonic model of an incipient spreading center and its margins: The Northern Red Sea and the Dead Sea rift N85-23286
CONTINGENCY
A model for large sparse contingency tables
[AD-A150320] N85-23350
CONTINUUM MECHANICS
Parallel processing for computational continuum dynamics
[AD-A150513] N85-23327
CONTINUUM MODELING
Spline-based Rayleigh-Ritz methods for the approximation of the natural modes of vibration for flexible beams with tip bodies
[NASA-CR-172566] N85-23100
CONTROL EQUIPMENT
Electronics Engineering Department EE Technical Review
[UCRL-50025-84-1] N85-22687
CONTROL SYSTEMS DESIGN
System dynamics and network control
[AD-A149420] N85-22803
CONTROL THEORY
Testing of the digital flight control system of the German CCV fighter experimental aircraft N85-22361
Model reduction for control system design
[NASA-CR-170417] N85-22398
CONTROLLERS
Model reduction for control system design
[NASA-CR-170417] N85-22398
CONVECTION
The role of convective perturbations in supercritical inlet oscillations N85-22563
Contribution to theory of ocean-atmosphere gas exchange N85-23134

Cumulus effects on the large-scale vorticity and momentum fields in the tropical atmosphere N85-23270
Implications of convection in the Moon and the terrestrial planets N85-23548

CONVECTION CURRENTS
Theoretical and observational studies of stellar activity N85-23468

CONVECTIVE HEAT TRANSFER
Theory of relaxation processes in decomposing polymer materials during high-intensity convective heating N85-22710
Natural convection during heat accumulation by substances with change of aggregate state N85-22787
A theoretical analysis of solar-driven natural convection energy conversion systems [DE84-004431] N85-23245
Cumulus cloud venting of mixed layer ozone [NASA-TM-87429] N85-23269

CONVERGENCE
A note about the strong convergence of the nonparametric estimation of a regression function [AD-A150325] N85-23353

CONVOLUTION INTEGRALS
New convolution and discrete Fourier transformation algorithms based on rectangular transformations over field of roots of unity N85-23022

COOLING
Energy losses at leading edge of turbine blade during multirow jet cooling N85-22626
Pressure drop and coefficients of internal heat transfer necessary for transpiration cooling N85-22631
Cooling performance improvement of a horizontal ground coupled heat pump [DE85-002470] N85-23065
Cooling of neutron stars with hyperons [DE85-004641] N85-23472
A measurement of the intensity of the cosmic background radiation at 3.9 cm N85-23681

COOLING SYSTEMS
Latent heat storage in cooling systems [DE85-005355] N85-23248

COORDINATES
Motion of symmetrical satellite with flexible viscoelastic rods about center of mass in circular orbit N85-22420
Analysis of systematic errors in systems of selenodetic coordinates N85-22435
Coordinate determination errors in measuring characteristics of radiation field of airborne antennas N85-22919
Zero-crossings on lines of curvature [AD-A150171] N85-23345
A unified lunar control network N85-23669
The control network of Mars: October 1984 N85-23670
The control networks of the satellites of Jupiter and Saturn N85-23671
Shape of Io N85-23672

COPOLYMERS
Effects of triazine components on physicochemical properties of polybutadiene: urethane block copolymers N85-22635
Influence of hydrogen bonding in block copolymers and their blends N85-22752
Exploratory development of foams from liquid crystal polymers [NASA-CR-172510] N85-22754
Chiral polymers [AD-A150366] N85-22760

COPPER
Mechanical properties of electrodeposited nickel and copper [DE85-005321] N85-22677
Effects of neutron irradiation at 450(0)C and 16 dpa on the properties of various commercial copper alloys [DE85-005716] N85-22684
Structural strenght of strip D16T aluminum alloy with low copper and magnesium content N85-22691
New deformable secondary aluminum alloys N85-22694
Possibility of producing monolithic composite materials based on niobium carbide N85-22707
Observation of surface vibrational resonances on (110) surfaces of FCC metals [AD-A150469] N85-23419

COPPER ALLOYS
Structures of ordered linear dislocation multipoles in Cu-Al alloys [ISSN-0379-6906] N85-22664
Thermodynamics of copper-nickel alloys containing aluminum, silicon, titanium, and chromium relative to their use in ceramic brazing [DE85-004787] N85-22674
First principles theory of Fermi-surface driven concentration waves in Cu/sub c/Pd/sub 1-c/ alloys [DE85-005367] N85-22681
Effects of neutron irradiation at 450(0)C and 16 dpa on the properties of various commercial copper alloys [DE85-005716] N85-22684

COPYRIGHTS
Copyright law, computer software, and government acquisition [AD-A150347] N85-23453

CORE SAMPLING
Cosmogenic Na-22 and Al-26 in Luna-24 lunar drill core soil samples N85-22427

CORONAL HOLES
Correlation of interplanetary medium parameters in transition region of high-velocity solar wind streams N85-22412

CORRECTION
Dynamics of adaptive signal corrector N85-22940

CORRELATION
Method for determining the number of correlative measurements required to validate the SBUV/2 ozone retrievals N85-23114
Calculations of microwave brightness temperature of rough soil surfaces: Bare field [NASA-TM-86200] N85-23221
Surface units on Venus derived from Pioneer-Venus altimetry, roughness, and reflectivity measurements N85-23510
Venus gravity: Global field results N85-23512

CORRELATION DETECTION
Theory of optimum M-filtration of signals against background of correlated interference N85-22927

CORRELATORS
Study of phase radiogeodetic systems with phase-locked loops N85-23172

CORROSION
Local electrochemistry of pitting corrosion in stainless steels [DE85-005207] N85-22673
Applications of the vibration probe to localized current measurements [DE85-004702] N85-22675

CORROSION PREVENTION
Formation of alumina layers on iron-base alloys [BLL-T6418/BG/LRS/LRST737/84] N85-22657

CORROSION RESISTANCE
Delayed cracking strength of experimental grades of 42 CD 4 steel in aqueous H2S surroundings [BLL-T6419/BG/LRS/LRST738/84] N85-22658
Study of the effects of implantation on the high Fe-Ni-Cr and Ni-Cr-Al alloys [NASA-CR-175625] N85-22661
Corrosion of aircraft Al and Al-Zn ion plated steel fasteners N85-22666
Influence of 3% NaCl solution on rate of accumulation of damage and residual strength of aluminum-boron composite N85-22699
Corrosion-resistant amorphous alloys N85-22748

CORROSION TESTS
An electrochemical study of the corrosion behavior of primer coated 2219-T87 aluminum [NASA-TP-2459] N85-22662
Change in microstructure of heat-resistant nickel alloys upon thermal cycling in a current of gas N85-22725

COSMIC DUST
Research in planetary studies and operation of Mauna Kea Observatory [NASA-CR-175618] N85-23460

COSMIC PLASMA
Hydromagnetic precursors of interplanetary plasma burst N85-22414

COSMIC RAY ALBEDO
Longitude and pitch-angle distributions of streams of high-energy electrons under Earth's radiation belts N85-22415

COSMIC RAY SHOWERS
Characteristics of latitude effect on cosmic ray charged component in atmosphere at altitudes 3-5 KM N85-22413
Longitude and pitch-angle distributions of streams of high-energy electrons under Earth's radiation belts N85-22415

COSMIC RAYS
Correlation of interplanetary medium parameters in transition region of high-velocity solar wind streams N85-22412
Observation of cosmic ray flux variations in stratosphere N85-22430
Dielectric detector device for registering heavy cosmic radiation particles N85-22799
Measurement of the large-scale anisotropy of the cosmic background radiation at 3 MM N85-23680
A measurement of the intensity of the cosmic background radiation at 3.9 cm N85-23681

COSMOCHEMISTRY
Implications of convection in the Moon and the terrestrial planets N85-23548
High pressure cosmochemistry of major planetary interiors: Laboratory studies of the water-rich region of the system ammonia-water N85-23549

COSMOLOGY
University of Cambridge Institute of Astronomy report of activities N85-23464
Measurement of the large-scale anisotropy of the cosmic background radiation at 3 MM N85-23680

COSMONAUTS
Feoktistov recalls period leading to Gagarin spaceflight N85-22451
Feoktistov says manned lunar, Mars flights lack justification N85-22452

COST ANALYSIS
An analysis of a dynamic project cost problem [CSIR-TWISK-338] N85-23341

COST REDUCTION
A low cost approach with larger diameter silicon wafer — solar cells N85-22572

COSTS
Advanced mixed-mode simulation techniques N85-22883

COULOMETERS
Portable electrochemical cell interrogator [DE85-005186] N85-22901

COUNTERS
Extraction of signals from background interference with unknown parameters in quantized sample N85-23013

COUPLED MODES
Coupled-cavity gyrotrons with mode conversion N85-22967

COUPLING
Coupling between velocity oscillations and solid propellant combustion N85-22536
Characterization of heterogeneity of composite propellants and its effects on combustion behavior N85-22539
Impacts in ice: Commissions of solar system crater population N85-23538

COUPLINGS
Cooling performance improvement of a horizontal ground coupled heat pump [DE85-002470] N85-23065

COVARIANCE
On limit of the largest eigenvalue of the large dimensional sample covariance matrix [AD-A150589] N85-23358

COVERINGS
Analysis of optimum front cover thickness for lightweight solar arrays N85-22606

CRAB NEBULA
Absolute measurements of radiation intensity from Cassiopeia-A, Cygnus-A and crab nebula in 60-100 cm band N85-22978

CRACK GEOMETRY
A clamped rectangular plate containing a crack [NASA-CR-175590] N85-23096

CRACK INITIATION
Fatigue life, crack initiation, and propagation of 304 stainless steel with non-proportional axialtorsional strain-paths N85-23094

CRACK PROPAGATION
Longitudinal splitting in unidirectional composites, analysis and experiments [NASA-CR-3881] N85-22639
Delayed cracking strength of experimental grades of 42 CD 4 steel in aqueous H2S surroundings [BLL-T6419/BG/LRS/LRST738/84] N85-22658
Micromechanical modeling of microstructural damage in creeping alloys [DE85-003925] N85-22671
Creep crack growth in ductile alloys [DE85-003937] N85-22676
Characteristics of surface crack development in ATtaS aluminum alloy during slow-cycle loading N85-22745
Fatigue life, crack initiation, and propagation of 304 stainless steel with non-proportional axialtorsional strain-paths N85-23094
Elastic wave scattering from an interface crack in a layered half space N85-23095
Fracture mechanics evaluation of GaAs [NASA-CR-175657] N85-23101
Advanced life analysis methods. Volume 1: Cracking data survey and NDI (nondestructive inspection) assessment for attachment lugs [AD-A150419] N85-23108
Advanced life analysis methods. Volume 2: Crack growth analysis methods for attachment lugs [AD-A150420] N85-23109

CRACK TIPS
Creep crack growth in ductile alloys [DE85-003937] N85-22676

CRACKING (FRACTURING)
Advanced life analysis methods. Volume 2: Crack growth analysis methods for attachment lugs [AD-A150420] N85-23109

Terrestrial analog studies for Martian patterned ground N85-23590

CRACKS
Experimental and numerical analysis of electric currents and electromagnetic blunting of cracks in thin plates [AD-A150418] N85-22689
Effects of fracture roughness on fluid flow through a single deformable fracture [DE85-004593] N85-23062
Stress intensity factor in a tapered specimen [NASA-CR-175589] N85-23099

CRATERING
Reports of the Planetary Geology and Geophysics Program, 1984 [NASA-TM-87563] N85-23474
Study and estimation of planet-crossing asteroid populations: Discoveries and analysis N85-23498
Impact and collisional processes in the solar system N85-23530
Centrifuge impact cratering experiments N85-23533
Progress on Experimental impact studies N85-23534
Progress on studies of early intense cratering N85-23535
Martian terrain ages N85-23537
Impacts in ice: Commissions of solar system crater population N85-23538
Problems in recovering crater production functions N85-23539
A parmetric study of crater-saturation simulation N85-23540
Ring-diameter ratios for multi-ring basins average 2.0(0.5)D N85-23542
Morphology and mechanics of terraces in lunar craters N85-23543
The nature of Martian flow ejecta craters N85-23545

CRATERS
Dark halo craters and the thickness of grooved terrain on Ganymede N85-23484
Average spacing for rings of individual multi-ring basins is 2.0(0.5)D N85-23541
Ring-diameter ratios for multi-ring basins average 2.0(0.5)D N85-23542
Ridged plains of Lunae Planum: Thickness distribution revised N85-23559
Planetary analogs in Antarctica: Icy satellites N85-23605
Analyses of radar images of small craters N85-23642

CREEP PROPERTIES
Creep crack growth in ductile alloys [DE85-003937] N85-22676
Some specifics of development of fatigue and creep in heat-resistant alloys with asymmetrical multicycle loading N85-22724
Densification and deformation in the presence of a liquid phase [DE85-005101] N85-22763

CRITERIA
Personal decision making: The influence of perceived locus of control and degree of rationality on information seeking strategies N85-23446

CRITICAL FREQUENCIES
Domain of applicability of asymptotic description of radio pulse fields near critical frequency N85-22949

CRITICAL LOADING
Spectral frequency of eigenvalues in optimal problems of stability of cylindrical shells of variable thickness N85-22815

CRITICAL TEMPERATURE
Examination of the contact wetting angle in the vicinity of critical temperature [BLL-T6416/BG/CRS/LR-ST735/84] N85-23054

CROP IDENTIFICATION
Characterization of LANDSAT-4 TM and MSS image quality for the interpretation of California's agricultural resources --- Central Valley N85-23190
An initial analysis of LANDSAT-4 Thematic Mapper data for the discrimination of agricultural, forested wetlands, and urban land cover --- Poinsett County, Arkansas; and Reelfoot Lake and Union City, Tennessee N85-23193
Preliminary evaluation of Thematic Mapper image data quality N85-23194

CROP INVENTORIES
Thematic Mapper data quality and performance assessment in renewable resources/agriculture/remote sensing N85-23201

CROSS CORRELATION
Regular synthesis of pairs of phase-keyed binary minimax signals N85-22923

CROSSOVERS
Interference immunity of fiber-optic communication lines with spectral multiplexing of channels N85-22924

CRUSTAL FRACTURES
On the absence of strike-slip faults from the planets and satellites N85-23645
Lunar mascon loading: An example of the importance of fault initiation depth on fault type predictions from stresses on planetary surfaces N85-23646
Fault offsets and lateral crustal movement on Europa N85-23656

CRUSTS
More precise curve of dependence between density and velocity of longitudinal waves in consolidated crust and top of mantle in oceanic structures N85-23143
Crustal and upper mantle density model of Owen fault zone N85-23144
Interrelationship of earthquake magnitude and lithospheric-asthenospheric thermodynamic parameters in seismically active zones N85-23183

CRYOGENIC COOLING
Experimental studies of low temperature surface interactions of atomic hydrogen using maser technique [AD-A150216] N85-22647

CRYOGENIC WIND TUNNELS
Cryogenic wind tunnels: A selected annotated bibliography [NASA-TM-86346] N85-22401

CRYOGENICS
Survey of the state-of-the-art of miniature cryocoolers for superconductive devices [AD-A150319] N85-22774

CRYSTAL DEFECTS
Fracture mechanics evaluation of GaAs [NASA-CR-175657] N85-23101

CRYSTAL DISLOCATIONS
Investigation of the effect of annealing on the dislocation and sub-grain boundary content of solvent-evaporation-grown CdTe [AD-A144087] N85-23415

CRYSTAL GROWTH
Basis and pyramidal slipping in single crystals of alpha-alloy Ti-Al-Sn N85-22730
Hibonite: Crystal chemistry and origin of blue coloration in meteoritic assemblages N85-23555

CRYSTAL LATTICES
The crystal and molecular structure of a new propellant compound: Triaminoguanidium Azide Nitrate (TAZN) N85-22551
Molecular dynamics studies of energy transfer processes in crystal systems [AD-A150161] N85-23416

CRYSTAL OPTICS
Research progress on laser crystals in China N85-23440

CRYSTAL OSCILLATORS
Externally compensated crystal oscillator (ECXO) study [AD-A150335] N85-22893

CRYSTAL STRUCTURE
Specifics of structure and mechanical properties of metastable beta-titanium alloys after deformation and aging N85-22731
H-division materials physics progress [DE85-004990] N85-23430

CRYSTALLINITY
Influence of substrate heating and thermal annealing on the surface crystallinity in single Si crystals implanted with high doses of (16)O [DE85-005264] N85-23428

CRYSTALLIZATION
Reaction of amorphous NiNb films with crystalline metal overlayers [DE85-005483] N85-22680
Study of processes of modification of Al-Si alloys N85-22695
Composition and thickness of oxide coatings on granule surfaces of aluminum alloys N85-22719
Thermodynamic and kinetic studies of pulsed laser annealing from transient conductivity measurements [DE85-003677] N85-23078
Modelling equilibrium and fractional crystallization in the system MgO-FeO-CaO-Al2O3-SiO2 N85-23552

CRYSTALLOGRAPHY
Crystal chemistry of meteoritic hibonites N85-23556

CRYSTALS
Molecular dynamics studies of energy transfer processes in crystal systems [AD-A150161] N85-23416

CUES
Low altitude texture comparison data base and smooth shaded texture [AD-A150342] N85-23323

CUMULATIVE DAMAGE
Influence of 3% NaCl solution on rate of accumulation of damage and residual strength of aluminum-boron composite N85-22699

CUMULUS CLOUDS
Cumulus cloud venting of mixed layer ozone [NASA-TM-87429] N85-23269
Cumulus effects on the large-scale vorticity and momentum fields in the tropical atmosphere N85-23270

CURIE TEMPERATURE
Magnetic studies of Ni3Al(Fe) compounds [DE85-005282] N85-22688

CURRENT DENSITY
Pre- and post-processing for stream-function eddy current calculations [AD-A150417] N85-22896
New high-efficiency silicon solar cells [NASA-CR-175643] N85-23244

CURVATURE
Zero-crossings on lines of curvature [AD-A150171] N85-23345

CURVES (GEOMETRY)
Reflected wave travel-time curves in stratified media with vertically heterogeneous layers and slightly sloping curved boundaries N85-23167

CUSHIONS
Blanket integrated cushioning of foldable and retractable solar arrays N85-22612

CUTTERS
Diamond cutters' grinders N85-22841
T700 cutter life improvement program [AD-A150450] N85-23089

CUTTING
Specifics of laser heat treatment of high steel tools N85-22714
USSR report: Machine tools and metalworking equipment [JPRS-UMM-85-005] N85-22839
T700 cutter life improvement program [AD-A150450] N85-23089

CYCLES
Exergetical analysis of turbojet engine cycle N85-22825

CYCLIC LOADS
Fatigue and corrosion fatigue resistance of aluminum casting alloy VAL10 and forging alloy AK6 N85-22690
Dissipation of energy in composite material N85-22703
Effect of operating medium on cyclic durability of AD33-W composite N85-22716
Cyclic industrial robots with mechanical energy storing devices: Multipositional system with one or several degrees of freedom N85-22803
Cyclic industrial robots with mechanical energy storing devices: Principles of drive design N85-22807

CYCLOTRON RESONANCE DEVICES
Design considerations for a 100 kW CW, 140 GHz gyrotron oscillator [DE85-005282] N85-22904
A 60 GHz 200 kW CW gyrotron with high output mode purity [DE85-005283] N85-22905
Coupled-cavity gyrotrons with mode conversion N85-22967

CYLINDRICAL ANTENNAS
Transient analysis of loaded thin-wire antennas and transmission lines N85-22852
Experimental verification of beam deflection from hybrid reflector antenna within wide-angle sector N85-22984

CYLINDRICAL SHELLS
Automatic multi-layer welding of thick cylindrical structures under flux N85-22746
Interaction of cylindrical shell with concentrated mass moving along its inner surface N85-22810
Steady-state reaction of three-layered cylindrical shell to effect of moving load N85-22811
Spectral frequency of eigenvalues in optimal problems of stability of cylindrical shells of variable thickness N85-22815
Stability of cylindrical shells with one-way constraints N85-22820

CZOCHRALSKI METHOD
Thermally stimulated conductivity in semi-insulating gallium arsenide N85-23036

D

DAMAGE
Advanced life analysis methods. Volume 1: Cracking data survey and NDI (nondestructive inspection) assessment for attachment lugs [AD-A150419] N85-23108
Advanced life analysis methods. Volume 2: Crack growth analysis methods for attachment lugs [AD-A150420] N85-23109

DAMPING
Distributed combustion: A mechanism of acoustic suppression N85-22543

DATA ACQUISITION
Development of a multiplane multispeed balancing system for turbine systems
[NASA-CR-174750] N85-22400
Measurement requirements for the detection of ozone trends N85-23115
Analysis of the inflow layer and air-sea interactions in Hurricane Frederic (1979)
[NASA-CR-175616] N85-23271
Mean flow and turbulence in complex terrain NPS (Naval Postgraduate School)/Vandenberg measurement system
[AD-A150184] N85-23274
Operational loads measurement: A philosophy and its implementation — aircraft structures
[AD-A149445] N85-23308

DATA BASE MANAGEMENT SYSTEMS
New atmospheric sensor analysis study
[NASA-CR-171426] N85-23069
GADB: A database facility for modelling naturally occurring geophysical fields N85-23217
Precedency control and other semantic integrity issues in a workbench database N85-23220
Presentation based user interfaces
[AD-A150311] N85-23311
Digital processing of mesoscale analysis and space sensor data
[NASA-CR-171429] N85-23319
Hexagonal data base study
[AD-A150176] N85-23448
The hierarchical database decomposition approach to database concurrency control
[AD-A150612] N85-23450

DATA BASES
Precedency control and other semantic integrity issues in a workbench database N85-23220
Low altitude texture comparison data base and smooth shaded texture
[AD-A150342] N85-23323
General design considerations of an Air Force information system
[AD-A150611] N85-23449
The hierarchical database decomposition approach to database concurrency control
[AD-A150612] N85-23450
Intel iDIS evaluation
[DE85-003748] N85-23451
Unsupervised classification of global radar units on Venus N85-23632

DATA COMPRESSION
Data compression for noiseless channels N85-22851
Image data compression using uneven knots selection
[AD-A150602] N85-23359

DATA CORRELATION
Ozone Correlative Measurements Workshop
[NASA-CP-2362] N85-23112

DATA LINKS
Satellite bridges in communications networks N85-22910
Optimum path selection in automated radio relay link design N85-22947
Investigation of influence of communications link and synchronization error on noise tolerence of group transmission of binary information based on orthogonal Walsh function N85-23026

DATA PROCESSING
Draftsman displays: A graphical technique for exploratory data analysis
[AD-A150515] N85-22775
Laser applications in last 10 years reviewed N85-22844
Liquid mass flow rate computer N85-22962
Efficiency of multitarget signal detection by digital radar data processing devices N85-22991
Application of field X-ray: Radiometric analysis in exploratory geology and means for its improvement N85-23176
Analysis and evaluation of the LANDSAT-4 MSS and TM sensors and ground data processing systems: Early results N85-23189
Geologic utility of LANSDAT-4 TM data — Death Valley, California and the Silver Bell area of southern Arizona N85-23192
Microcomputer: Controlled statistics analyzer
[BLL-CE-TRANS-7971-(9022.09)] N85-23306
Presentation based user interfaces
[AD-A150311] N85-23311
Measurement of SIFT operating system overhead
[NASA-TM-86322] N85-23337

DATA PROCESSING EQUIPMENT
Requirements placed on information processing equipment
[BLL-CE-TRANS-7983-(9022.09)] N85-23307
Parallel test method for LSI (Large Scale Integration) microprocessors
[AD-A150237] N85-23310

DATA REDUCTION
Draftsman displays: A graphical technique for exploratory data analysis
[AD-A150515] N85-22775
MAGSAT anomaly field data of the crustal properties of Australia
[E85-10100] N85-23215
An investigation of the crustal properties of Australia and surrounding regions derived from interpretation of MAGSAT anomaly field data N85-23216
Data selection techniques in the interpretation of MAGSAT data over Australia N85-23218

DATA RETRIEVAL
Solid propellant combustion diagnostics and automated data retrieval from holograms N85-22527

DATA SAMPLING
Measurement requirements for the detection of ozone trends N85-23115

DATA SIMULATION
Comparison of land cover information from LANDSAT Multispectral Scanner (MSS) and airborne Thematic Mapper simulator (TMS) data for hydrologic applications — Clinton River Basin, Michigan N85-23211

DATA STORAGE
Role of optical disk at computing centers
[DE85-005124] N85-23314
Performance evaluation of distributed systems with unbalanced flows: An analysis of the INFOPLEX data storage hierarchy
[AD-A150528] N85-23328
General design considerations of an Air Force information system
[AD-A150611] N85-23449

DATA STRUCTURES
GADB: A database facility for modelling naturally occurring geophysical fields N85-23217
Synthesis of tree-structured computing systems through use of closures
[AD-A150502] N85-23326

DATA SYSTEMS
General design considerations of an Air Force information system
[AD-A150611] N85-23449

DATA TRANSMISSION
Experimental results on the application of convolutional coding and Viterbi decoding as a frequency diversity technique in HF data transmission
[CRC-1377] N85-22850
Data compression for noiseless channels N85-22851
Integrated digital networks
[AD-A150805] N85-22873
Noise immunity of information transmission system with pseudorandom frequency switching under worst-case interference conditions N85-23029
Authorizing appropriations to the National Aeronautics and Space Administration for fiscal year 1986
[H-REPT-99-32] N85-23452

DEAD RECKONING
Reference systems for the evaluation of dead-reckoning navigation equipment N85-22358

DEATH VALLEY (CA)
Assessment of computer based geologic mapping of rock units in the LANDSAT-4 scene of northern Death Valley, California N85-23195

DEBRIS
On the latitudinal distribution of debris in the Northern Hemisphere of Mars N85-23579

DECISION MAKING
Rejection of anomalous observations when determining spacecraft trajectories N85-22421
Personal decision making: The influence of perceived locus of control and degree of rationality on information seeking strategies N85-23446

DECODERS
Stereo decoder without subcarrier restoration N85-22921

DECODING
Experimental results on the application of convolutional coding and Viterbi decoding as a frequency diversity technique in HF data transmission
[CRC-1377] N85-22850
A perspective on multiaccess channels
[AD-A150183] N85-23322

DECOMPOSITION
TEM/FIM study of modulated microstructures in the Fe-Be system
[DE85-005379] N85-22678
Decomposition of VTAN alloy solid solution upon irradiation and thermal aging N85-22712
Algorithm for singular decomposition
[DE85-016488] N85-23361

DEEP SPACE NETWORK
Activities of the Jet Propulsion Laboratory, 1 January - 31 December 1983
[NASA-CR-175555] N85-23447

DEFECTS
Influence of welding defects at melting boundary on static strength of welded joint in large-diameter pipe N85-22735
NDE methods for green ceramics
[DE85-004019] N85-22766
Shape optimization for minimal stress concentration N85-23093

DEFLECTION
Horizontal deflection TS-257 N85-22926

DEFORMATION
Structures of ordered linear dislocation multipoles in Cu-Al alloys
[ISSN-0379-6906] N85-22664
Temperature effects of heterogenizated annealing on structure and properties of V95 aluminum alloy N85-22692
High temperature antifriction properties of Ti sub 1-sub xNb sub x C sub 0.5N sub 0.5 alloys N85-22715
Specifics of structure and mechanical properties of metastable beta-titanium alloys after deformation and aging N85-22731
Densification and deformation in the presence of a liquid phase
[DE85-005101] N85-22763
On Hybrid and mixed finite element methods
[NASA-CR-175551] N85-23096
Normal-fault and fold development in sedimentary rocks above a pre-existing basement normal fault N85-23259

DEGASSING
Degassification of silicon nitride powders of various origins N85-22718

DEGREES OF FREEDOM
Two degree-of-freedom flutter solution for a personal computer
[NASA-TM-86381] N85-22379
Cyclic industrial robots with mechanical energy storing devices: Multipositional system with one or several degrees of freedom N85-22803
Design of tightening device and calculation of forces in manipulator transmissions with base-drive mounted N85-22804
Approximate rules for signal detection against background of Gaussian correlated interference N85-23027
Motion planning with six degrees of freedom
[AD-A150312] N85-23432

DELAY LINES
Dynamics of adaptive signal corrector N85-22940
Diffraction of periodic grounding system of finite length N85-22994

DEMODULATION
Acoustooptic demodulation of frequency-modulated signals N85-23050

DEMODULATORS
Noise tolerance of digital demodulator for complex signal system employing binary quantization N85-22929

DEMULTIPLEXING
Interference immunity of fiber-optic communication lines with spectral multiplexing of channels N85-22924

DENSE PLASMAS
Adequacy of metal ablation process with laser radiation and a shock-compressed plasma N85-22708

DENSIFICATION
Densification and deformation in the presence of a liquid phase
[DE85-005101] N85-22763

DENSITY (MASS/VOLUME)
More precise curve of dependence between density and velocity of longitudinal waves in consolidated crust and top of mantle in oceanic structures N85-23143
Crustal and upper mantle density model of Owen fault zone N85-23144
Determination of density of the crust and upper mantle from deep seismic sounding and gravimetry, 2 N85-23153
The effect of particle density on aeolian transport N85-23581

DENSITY DISTRIBUTION
Gas dynamics of the barred spiral galaxy NGC 3359 N85-23465
Problems in recovering crater production functions N85-23539
A parametric study of crater-saturation simulation N85-23540

DENSITY WAVE MODEL
Studies of planetary rings N85-23488

DEPLOYMENT
Concept for controlled fold by fold deployment and retraction of flexible, foldable solar generators N85-22613
Deployment analysis of the Olympus Astromast and comparison with test measurements — solar arrays N85-22616
Developments in deployable masts to support flexible solar arrays N85-22620

DEPOLARIZATION
Using fuel cells or anode depolarization to reduce electrowinning energy consumption
[DE85-006187] N85-23250
DEPOSITION
A simple model of electron beam initiated dielectric breakdown N85-22516
Diffusion deposition in fibrous filters for parallel and transverse flow models
[DE85-006149] N85-23066
Non-linear optical techniques for visible and UV lasers and thin film deposition
[AD-A150489] N85-23077
Electronic transport in hydrogenated amorphous silicon films
[DE85-002901] N85-23426
Lunar origin: Role of giant impacts N85-23519
Impact and collisional processes in the solar system N85-23530
Eolian erosion on Mars: Three scales N85-23577
The origin of regional dust deposits on Mars N85-23578
On the latitudinal distribution of debris in the Northern Hemisphere of Mars N85-23579
DEPTH
Microwave radiometer observations of snowpack properties and comparison of U.S. Japanese results — Hokkaido, Japan and Vermont and North Dakota test sites N85-23230
Studies on physical properties of snow based on multi channel microwave radiometer N85-23231
Analysis of NIMBUS-7 SMMR data — Hokkaido, Japan snow cover N85-23232
The effects of internal waves on acoustic normal modes
[AD-A150235] N85-23379
DEPTH MEASUREMENT
Variations in resistivity of upper crustal layer N85-23164
DESERTS
Analysis of SMIRR data for volcanic and sedimentary terrains of the trans-Pecos region, Texas N85-23626
DESICCANTS
Investigation of manganese dioxide as an improved solid desiccant
[DE85-004034] N85-22654
DESIGN ANALYSIS
Dynamic wind-tunnel testing of active controls by the NASA Langley Research Center N85-22353
Rational use of tatanium in nonferrous metallurgy N85-22728
Experimental determination of optimum ratio of runner blade height at exit to runner blade height at entrance of radial inward-flow microturbines N85-22827
Reluctance and doubly-excited reluctance motors
[DE85-003585] N85-22900
A 60 GHz 200 kW CW gyrotron with high output mode purity
[DE85-005283] N85-22905
Analysis and design of linear microwave transistor amplifiers N85-23036
Magnetic refrigeration and heat pumping design options
[DE85-003405] N85-23064
Optimum design and automated dynamic analysis of flexible mechanisms
[AD-A150152] N85-23066
A design analysis and implementation of a user-friendly interface for the UNIX operating system
[AD-A150558] N85-23312
DETECTION
Operational experience with ion concentration sensors in orientation systems N85-22422
Optimization of number of pulses in detection of fluctuating optical signals N85-22993
Orphan detection in the Argus system
[AD-A150562] N85-23331
Sample introduction methods for improving the particle detection capability of the spectrometric oil analysis program
[AD-A150139] N85-23399
DEUTERIUM
System for forming and focusing high current beam of deuterium ions N85-22796
DIAMETERS
A low cost approach with larger diameter silicon wafer — solar cells N85-22572
Spectral evaluation of irregularity of superconducting coaxial cables N85-23000
DIAMONDS
Diamond cutters/grinders N85-22641
DIAPHRAGMS (MECHANICS)
Experimentally determined characteristics of vortex heaters N85-22833
Theory of diaphragm light modulators with electrical input signal N85-23002
DIELECTRIC PERMEABILITY
Dielectric measurements in infralow-frequency band N85-23034
DIELECTRIC PROPERTIES
Investigations of radiation-induced and carrier-enhanced conductivity N85-22515
A simple model of electron beam initiated dielectric breakdown N85-22516
DIELECTRICS
Electric field effects on ion currents in satellite wakes N85-22485
Self-consistent simulation of plasma interactions with secondary-emitting insulators N85-22492
An investigation of arc discharging on negatively biased dielectric conductor samples in a plasma N85-22498
Characteristics of EMI generated by negative metal-positive dielectric voltage stresses due to spacecraft charging N85-22505
Discharge pulse phenomenology N85-22509
Discharge characteristics of dielectric materials examined in mono-, dual-, and spectral energy electron charging environments N85-22510
Electrical conduction in polymer dielectrics N85-22514
A simple model of electron beam initiated dielectric breakdown N85-22516
Dielectric detector device for registering heavy cosmic radiation particles N85-22799
Scattering of electromagnetic waves by charged particles N85-22913
Surge strength of symmetric cable with monolithic polyethylene insulation of quads N85-23001
DIESEL ENGINES
Sliding seal materials for adiabatic engines
[NASA-CR-174893] N85-22757
DIFFERENTIAL EQUATIONS
Nonlinear rotordynamics analysis
[NASA-CR-171425] N85-22364
Controlled movement of elastic manipulator with distributed parameters N85-22818
Mathematical modeling of transient performance of gas turbine engine N85-22834
DIFFERENTIAL GEOMETRY
Zero-crossings on lines of curvature
[AD-A150171] N85-23345
DIFFRACTION
Reflex attachment for line alignment in spectral diffraction devices N85-22794
Integrated optical components utilizing acoustooptic and electrooptic diffraction in micro-waveguides N85-23044
Acoustooptic cell as space-frequency filter N85-23051
DIFFRACTION PATTERNS
Structural characterization by intensity measurements of electron diffraction patterns
[DE85-004803] N85-23427
DIFFRACTION PROPAGATION
Intensity fluctuations of focused laser beam during reflection in turbulent atmosphere N85-22975
DIFFUSION
Diffusion deposition in fibrous filters for parallel and transverse flow models
[DE85-006149] N85-23066
Cathode materials for molten carbonate fuel cells
[DE85-004078] N85-23254
The ASCOT Data Analysis Workshop
[DE85-004407] N85-23283
DIFFUSION FLAMES
Laser diagnostic analyses of sooting flames
[AD-A150476] N85-22649
A standard aircraft diffusion flame: Spectral characteristics and a feasibility study for developing an alternate calibration source for aircraft optical fire detection systems
[AD-A150231] N85-22768
DIFFUSION WELDING
Mechanical properties and brittle fracture resistance of welded multilayer elements for high pressure vessels N85-22736
Effect of protective medium on durability and fracture structure on seam zones of thin-walled titanium articles produced by diffusion welding N85-22738
Technological parameters of diffusion welding processes in honeycomb titanium alloy structures N85-22739
Durability of VT16 alloy compounds obtained by diffusion welding N85-22740
DIGESTING
Anaerobic digestion of biomass: status summary and research development needs, 1983
[PB85-161925] N85-22772
DIGITAL DATA
Dynamics of adaptive signal corrector N85-22940
Ionospheric distortions of digital signals with wideband modulation N85-22945
Synthesis of quasi-optimum two-level signal discriminator with level changing at unknown point N85-23010
LANDSAT-4 Science Characterization Early Results. Volume 4: Applications — agriculture, soils land use, geology, hydrology, wetlands, water quality, biomass identification, and snow mapping
[E85-10070] N85-23186
Overview of TM applications research reports N85-23187
A preliminary comparison of the information content of data from the LANDSAT 4 Thematic Mapper and Multispectral Scanner — Arkansas N85-23199
Early results of investigations of LANDSAT 4 Thematic Mapper and Multispectral Scanner applications — Washington, D.C. N85-23200
Relative accuracy assessment of LANDSAT-4 MSS and TM data for level 1 land cover inventory — Washington, D.C. N85-23212
DIGITAL FILTERS
Optimal design efforts in Shanghai described N85-22386
Two-dimensional signal processing and storage and theory and applications of electromagnetic measurements
[AD-A150590] N85-22899
Optimal synthesis of surface acoustic wave filters N85-22933
Efficiency of digital compensator of strong non-Gaussian interference N85-22942
Methods of digital correction for channels of multichannel radar receivers N85-23005
Use of Walsh functions for calculating characteristics of digital filters with impulse response of finite duration N85-23011
DIGITAL RADAR SYSTEMS
Mathematical model of discriminator for signals with fluctuations and thermal noise N85-22943
Efficiency of multitarget signal detection by digital radar data processing devices N85-22991
Factorized algorithms for combined spatial and temporal processing of radar signals N85-22997
DIGITAL SYSTEMS
Testing of the digital flight control system of the German CCV fighter experimental aircraft N85-22381
The use of a high-speed 12-bit A/D converter for digital sampling of communication signal carriers
[AD-A150578] N85-22872
Noise tolerance of digital demodulator for complex signal system employing binary quantization N85-22929
Analysis of characteristics of digital discriminators for phase-shift keyed signals N85-22930
Interference immunity of binary systems with second-order phase-difference modulation in various reception modes N85-22944
Noise tolerance of diversity reception in frequency-adaptive digital transmission systems N85-23024
Use of importance sampling to investigate signal detection systems by simulated method N85-23028
Digital laser platemaker modifications
[AD-A150190] N85-23074
Optical memory research and its application to digital optical processing N85-23397
DIGITAL TECHNIQUES
Assessment of computer based geologic mapping of rock units in the LANDSAT-4 scene of northern Death Valley, California N85-23195
Comparative techniques used to evaluate Thematic Mapper data for land cover classification in Logan County, West Virginia N85-23209
Bouguer images of the North American craton N85-23648
DIMERS
Below-room-temperature water-vapor continuum absorption within the 8- to 10 micron atmospheric transmission window
[TR-0084(4945-09)-1] N85-23286
DIOXIDES
Investigation of manganese dioxide as an improved solid desiccant
[DE85-004034] N85-22654
DIPOLE ANTENNAS
Surface wave excitation study
[DE85-005301] N85-22875
Exact design formulas for field intensity of dipole deployed above flat homogeneous Earth with finite conductivity N85-22998
DIRECT CURRENT
Outlook for realization of proximity effect and Josephson direct current in helium-3 N85-22956
DIRECT POWER GENERATORS
Operational performance of the photovoltaic-powered grain mill and water pump at Tangaye, Burkina Faso (formerly Upper Volta)
[NASA-TM-86970] N85-23243

DIRECTIONAL COUPLERS
Synthesis of multistep directional couplers with nonminimum-phase characteristics N85-22986
DISCRETE FUNCTIONS
Computing convolution of multifrequency signal employing truncated fast Fourier transform algorithms N85-23019
DISCRIMINATION
Performance of time-position discriminator of composite signal N85-22941
Vertical discrimination in the sound channel [AD-A150254] N85-23380
DISCRIMINATORS
Mathematical model of discriminator for signals with fluctuations and thermal noise N85-22943
DISK GALAXIES
Dynamics of gas disks in triaxial galaxies N85-23469
The Formation of preplanetary disks from the collapse of rotating molecular cloud cores N85-23526
DISLOCATIONS (MATERIALS)
Structures of ordered linear dislocation multipoles in Cu-Al alloys [ISSN-0379-6906] N85-22664
DISPERSION
Dispersion characteristics of small-mode gradient optical fibers N85-23004
DISPERSIONS
Dispersion of phase-shift keyed systems with fixed number of blocks N85-22928
DISPLACEMENT
Fault offsets and lateral crustal movement on Europa N85-23656
Importance of the tectonic motions on Ganymede N85-23661
DISPLAY DEVICES
Analysis of estimation algorithms for CDTI and CAS applications [NASA-CR-172444] N85-22387
Draftsman displays: A graphical technique for exploratory data analysis [AD-A150515] N85-22775
Introduction to CHART: A graphic analysis and display system, revision [DE85-004612] N85-23335
DISTORTION
Reflex attachment for line alignment in spectral diffraction devices N85-22794
DISTRIBUTED PARAMETER SYSTEMS
Effect of space-charge field on output characteristics of O-type oscillators with distributed interaction N85-23043
DISTRIBUTED PROCESSING
Orphan detection in the Argus system [AD-A150562] N85-23331
DISTRIBUTION
Consistency of smoothing with running linear fits [AD-A150232] N85-23349
DISTRIBUTION (PROPERTY)
Distribution of radium and plutonium in human bone [DE85-005025] N85-23298
On the latitudinal distribution of debris in the Northern Hemisphere of Mars N85-23579
DISTRIBUTION FUNCTIONS
The orientation distribution of nonspherical aeroeol particles within a cloud [AD-A150600] N85-23061
DISULFIDES
The violet absorber on Io: Disulfur monoxide derivatives N85-23482
DIVERTERS
HPFTP flow diverter analysis [NASA-CR-171424] N85-23057
DOCUMENTS
M68000 RNF text formatter user's manual [NASA-TM-86327] N85-23320
DOMES (GEOLOGY)
Ridged plains of Lunae Planum: Thickness distribution revised N85-23559
DOPED CRYSTALS
Technological process effect on the carrier lifetime degradation of silicon solar cell base layer irradiated by 1 MeV electrons (boron doping case) N85-22585
Annealing of radiation damage in boron and gallium doped silicon solar cells N85-22624
High sheet resistance, arsenic implanted polycrystalline silicon for integrated circuit resistors [DE85-004355] N85-22902
Noise characteristics of sulfur-doped silicon diodes N85-22952
Numerical simulation of inverters with I2L elements including effects of high doping level N85-23039
DOPPLER EFFECT
Investigation of generation of oscillations using anomalous Doppler effect N85-22980
DOPPLER RADAR
Geophysical interpretation of Venus gravity data N85-23513
DOSIMETERS
The effect of the choice or response matrix on unfolded bonner sphere spectra [AD-A150462] N85-23404
DRAFTING (DRAWING)
Accomplishments of Institute of Cartography summarized N85-23435
DRAINAGE
The ASCOT Data Analysis Workshop [DE85-004407] N85-23283
A comparison of terrestrial saltation flux in the laboratory and the field N85-23582
Fluvial drainage basins and valley networks: Eastern Margaritifer Sinus, Mars N85-23586
DRAINAGE PATTERNS
Geologic utility of LANSDAT-4 TM data — Death Valley, California and the Silver Bell area of southern Arizona N85-23192
DRIFT (INSTRUMENTATION)
Drift fields and boundary conditions at grain boundaries in bipolar P/N junction silicon devices N85-22879
DROP SIZE
Effects of temperature variation among droplets in an evaporating fuel spray N85-22562
DROPS (LIQUIDS)
Gasification of boron oxide drops and boron slurry agglomerates in combustion gases N85-22529
Effects of temperature variation among droplets in an evaporating fuel spray N85-22562
Size and velocity distributions of particles and droplets in spray combustion systems [AD-A150355] N85-22648
DUCT GEOMETRY
Determination of boundary line between reverse jet and surrounding stream N85-22789
DUCTILITY
Creep crack growth in ductile alloys [DE85-003937] N85-22676
Analysis of strength and ductility of welded joints in AMtsS and AMg5 aluminum alloys N85-22737
DUNES
Microdunes and other aeolian bedforms on Venus: Wind tunnel simulations N85-23584
Planetary analogs in Antarctica: Mars N85-23604
DUPLEX OPERATION
Combined processing method and matched filter for discrete composite frequency phase-shift keyed signal N85-22931
DURABILITY
Prediction of the resistance of structural materials to cavitation erosion [BLL-DRIC-TRANS-7435-(3623.66)] N85-22659
Temperature effects of heterogenizated annealing on structure and properties of V95 aluminum alloy N85-22692
DUST
Seasonal and secular variation of the Solis Lacus albedo feature: Relation to the Martian dust-transport cycle N85-23576
Transformation of polar ice sublimate residue into Martian circumpolar sand N85-23580
DUST STORMS
Observed changes at Viking Lander 1 N85-23575
Seasonal and secular variation of the Solis Lacus albedo feature: Relation to the Martian dust-transport cycle N85-23576
The origin of regional dust deposits on Mars N85-23578
DYE LASERS
Chemical stabilization of laser dyes [AD-A150451] N85-23076
DYNAMIC CHARACTERISTICS
Comparison of dynamic-tension and constant-load strength characteristics of heat-resistant materials N85-22722
A parmetric study of crater-saturation simulation N85-23540
DYNAMIC PROGRAMMING
Normal mode calculations for fuselage type intricate structures by regarding them as systems with superposed constraints N85-22817
DYNAMIC RESPONSE
Vibroacoustic study of the NASA Goddard Space Flight Center OSS-1 payload [NASA-CR-175320] N85-22465
Use of importance sampling to investigate signal detection systems by simulated method N85-23026
Noise immunity of information transmission system with pseudorandom frequency switching under worst-case interference conditions N85-23029
DYNAMIC STABILITY
Optimum design and automated dynamic analysis of flexible mechanisms [AD-A150152] N85-23088
DYNAMIC STRUCTURAL ANALYSIS
Deployment analysis of the Olympus Astromast and comparison with test measurements — solar arrays N85-22616
Investigation of dynamics of manipulator with elastic sections N85-22819
DYNAMICAL SYSTEMS
Solar array dynamical simulation for illumination and temperature variation N85-22611

E

E REGION
Protons with energies above 30 KeV in Earth's radiation belt at low altitudes during magnetically quiet time close to geomagnetic equator N85-22423
EARTH (PLANET)
Evaluating accuracy in determining position of Earth's center of mass and elements of orientation of geodetic coordinate system N85-22441
Nature of seismic images with amplitude and time fluctuations of recorded oscillations N85-23156
Gravity field of Venus and comparison with Earth N85-23514
A circum-terrestrial compositional filter N85-23520
Models of angular momentum input to a circum-terrestrial swarm from encounters with heliocentric planetesimals N85-23521
Terrestrial analogs for planetary wrinkle ridges N85-23644
EARTH ALBEDO
Bifacial light sensitive space solar cell N85-22573
EARTH ATMOSPHERE
Response of Earth's atmosphere to increases in solar flux and implications for loss of water from Venus N85-23518
EARTH CORE
Magnetic location of Earth's core-mantle boundary and estimates of the adjacent fluid motion N85-23260
EARTH CRUST
Determination of density of the crust and upper mantle from deep seismic sounding and gravimetry, 2 N85-23153
Induction excitation of deep conducting zones N85-23154
Study of resolution of deep MT soundings by means of physical model N85-23155
Structure of Iceland and ocean floor spreading N85-23159
Variations in resistivity of upper crustal layer N85-23164
Boundary velocities of longitudinal seismic waves and lateral inhomogeneities of upper ocean mantle N85-23165
Solution of direct magnetometric problem on spherical Earth N85-23179
MAGSAT anomaly field data of the crustal properties of Australia [E85-10100] N85-23215
An investigation of the crustal properties of Australia and surrounding regions derived from interpretation of MAGSAT anomaly field data N85-23216
Remanent magnetization model for the broken ridge satellite magnetic anomaly N85-23219
Crustal dynamics project: Catalogue of site information [NASA-TM-87452] N85-23258
Volcanism of the Colorado Plateau (basin and range transition): Implications for crustal processes N85-23569
Bouguer images of the North American craton N85-23648
EARTH HYDROSPHERE
Drifting ice as mechanical factor in purifying and polluting hydrosphere N85-23132
World ocean level oscillations and their relationship to change in inflow of continental waters N85-23133
EARTH MANTLE
Determining degree of partial melting of asthenosphere from seismic data N85-23127
Determination of density of the crust and upper mantle from deep seismic sounding and gravimetry, 2 N85-23153
Induction excitation of deep conducting zones N85-23154
Study of resolution of deep MT soundings by means of physical model N85-23155
Boundary velocities of longitudinal seismic waves and lateral inhomogeneities of upper ocean mantle N85-23165

Magnetic location of Earth's core-mantle boundary and estimates of the adjacent fluid motion N85-23260
Bouguer images of the North American craton N85-23648

EARTH MOVEMENTS
Absolute movement of Pacific Ocean plate during last 120 million years N85-23126
Numerical modeling of plane stick-slip fault N85-23150
Crustal dynamics project: Catalogue of site information
[NASA-TM-87452] N85-23258

EARTH OBSERVATIONS (FROM SPACE)
NASA's land remote sensing plans for the 1980's N85-23224
A silicic shield volcano in Bolivia N85-23572

EARTH ORBITS
Nontraditional method for determining unperturbed orbits of unknown space objects using incomplete optical observational data N85-22417
Spacecraft Environmental Interactions Technology, 1983
[NASA-CP-2359] N85-22470
Argon ion pollution of the magnetosphere N85-22523
Nation said to rank high with 15 satellites N85-22778

EARTH PLANETARY STRUCTURE
Crustal dynamics studies in China
[NASA-CR-175617] N85-23265
Submarine volcanic eruptions and potential analogs for Venus N85-23573

EARTH RESOURCES
Remote sensing used for study of forest resources N85-22440
Characteristics of alumyte deposits discussed N85-23438

EARTH SATELLITES
Nontraditional method for determining unperturbed orbits of unknown space objects using incomplete optical observational data N85-22417

EARTHQUAKES
Observation of long-period oscillations of Earth N85-23149
Space and time distribtuion of aftershocks N85-23157
Magmatism in continent-ocean transition zone (development of ideas of A. N. Zavaritskiy) N85-23161
Study of geoingical media based on scattered earthquake waves N85-23168
Geomagnetic precursors of intensive earthquakes in the 1-0.-2 Hz frequency range of geomagnetic pulsations N85-23178
Attenuation of seismic waves at regional distances
[AD-A150198] N85-23267

ECCENTRIC ORBITS
Stability of the Galilean satellites in deep orbital resonance N85-23477
Studies of planetary rings N85-23488
Dynamical studies of Saturn's rings N85-23489

ECCENTRICITY
Studies of icy bodies: Uranian satellites and cometary nuclei N85-23496

ECLIPSES
A model for eclipsing cataclysmic variables N85-23467

ECONOMETRICS
Scientific, technical progress as factor of intensification of economy N85-23444

ECONOMIC FACTORS
USSR report: Science and technology policy
[JPRS-UST-85-002] N85-23442
Economic mechanism of integration of science, production N85-23443

ECONOMICS
USSR report: Science and technology policy
[JPRS-UST-85-002] N85-23442
Scientific, technical progress as factor of intensification of economy N85-23444

ECOSYSTEMS
Combined analysis of the dynamics of complex ecosystems based on repeated remote measurements N85-22450
Technologies to sustain tropical forest resources
[TI85-901085] N85-23241
Areas with forest soils sensitive to acidic deposition under alternative damage hypotheses
[DE85-005257] N85-23257

EDDY CURRENTS
Pre- and post-processing for stream-function eddy current calculations
[AD-A150417] N85-22896
Magnetic field interactions with material discontinuities
[AD-A150197] N85-23373

EDGES
Edge detection in SAR imagery using gradient operators — synthetic aperture radar (SAR)
[AD-A149411] N85-22862
Stress intensity factor in a tapered specimen
[NASA-CR-175589] N85-23099

EDITING
The potential for advanced computerized aids for comprehensible writing of technical documents
[AD-A150501] N85-22870

EFFECTS
The effects of internal waves on acoustic normal modes
[AD-A150235] N85-23379

EFFICIENCY
Methods of digital correction for channels of multichannel radar receivers N85-23005

EIGENVALUES
Spectral frequency of eigenvalues in optimal problems of stability of cylindrical shells of variable thickness N85-22815
On limit of the largest eigenvalue of the large dimensional sample covariance matrix
[AD-A150589] N85-23358

EIGENVECTORS
Analysis of interaction of dynamically adjustable gyroscopes on elastic platform by finite-element method N85-22822

EJECTA
Capture of planetesimals into a circumterrestrial swarm N85-23522
Impact cratering calculation N85-23531
Progress on Experimental impact studies N85-23534
The nature of Martian flow ejecta craters N85-23545
Interaction of Martian flow ejecta blankets with pre-existing impact craters: Morphological observations N85-23546
Geomorphology and geology of the Southwestern Margaritifer Sinus and Argyre regions of Mars. Part 4: Flow ejecta crater distribution N85-23603

EJECTION INJURIES
Tight Ribbon Arm Protection (TRAP) for aircrewman ejection
[AD-A150464] N85-23303

EJECTION SEATS
Tight Ribbon Arm Protection (TRAP) for aircrewman ejection
[AD-A150464] N85-23303

EL NIÑO
El Nino, the capricious child N85-23121

ELASTIC DAMPING
Controlled movement of elastic manipulator with distributed parameters N85-22818

ELASTIC DEFORMATION
Deployment analysis of the Olympus Astromast and comparison with test measurements — solar arrays N85-22616
Time dependent interaction of internal pressure wave with system of two spherical shells N85-22809
Determination of stresses and deformations in linearly elastic conical shell subjected to aerodynamic loading and heating N85-22812

ELASTIC PLATES
Investigation of dynamics of manipulator with elastic sections N85-22819

ELASTIC PROPERTIES
Elasticity formulas for thin-walled shells with piezoceramic layers N85-22816
Controlled movement of elastic manipulator with distributed parameters N85-22818
Attenuation of seismic waves at regional distances
[AD-A150198] N85-23267

ELASTIC SCATTERING
Elastic wave scattering from an interface crack in a layered half space N85-23095
Intensity vectors of sound scattering by a spherical shell
[AD-A147847] N85-23107
Elastic wave scattering from cavities and sound inclusions analyzed by the resonance method
[AD-A150315] N85-23381

ELASTIC WAVES
Scattering of elastic waves on fractures randomly distributed in a three-dimensional medium N85-23151
Elastic wave scattering from cavities and sound inclusions analyzed by the resonance method
[AD-A150315] N85-23381

ELASTOMERS
Effect of alternative aging and accident simulations on polymer properties
[DE85-002642] N85-22782

ELECTRIC BRIDGES
Piezoelectric filter with low-Q inductances N85-22932

ELECTRIC CONDUCTORS
An investigation of arc discharging on negatively biased dielectric conductor samples in a plasma N85-22498
Electrical conduction in polymer dielectrics N85-22514

ELECTRIC CONNECTORS
Magnetic field interactions with material discontinuities
[AD-A150197] N85-23373

ELECTRIC CONTACTS
Control of cascaded induction generator systems
[AD-A150429] N85-22897
Thermal and thermoelastic effects in rolling/sliding contacts
[AD-A150435] N85-23429

ELECTRIC CURRENT
Calculation of secondary-electron escape currents from inclined-spacecraft surfaces in a magnetic field N85-22491
Experimental and numerical analysis of electric currents and electromagnetic blunting of cracks in thin plates
[AD-A150418] N85-22669
Critical current measurements on an NbTi superconducting wire standard reference material
[PB85-118594] N85-22906
Noise characteristics of sulfur-doped silicon diodes N85-22952

ELECTRIC DIPOLES
High-field dipoles for future accelerators
[DE85-002315] N85-23391

ELECTRIC DISCHARGES
Galileo internal electrostatic discharge program N85-22504
Laboratory studies of spacecraft response to transient discharge pulses N85-22506
Discharge pulse phenomenology N85-22509
Discharge characteristics of dielectric materials examined in mono-, dual-, and spectral energy electron charging environments N85-22510
Mass spectra of neutral particles released during electrical breakdown of thin polymer films N85-22511
EOS (electrical overstress) protection for VLSI (Very Large Scale Integration) devices
[AD-A150333] N85-22891
Non-self-maintained high-voltage low-pressure discharge N85-23037
Near Field/Far Field (NF/FF) energy loss in Electric Discharge Lasers (EDL's): A mode-medium interaction
[AD-A150299] N85-23075

ELECTRIC FIELD STRENGTH
Method of separately determining electrophysical properties of bulky conductor N85-22951
Measuring intensity of electric field produced by electromagnetic pulse with aid of active probes N85-22958

ELECTRIC FIELDS
Galileo internal electrostatic discharge program N85-22504
Influence of external electric field on structural-mechanical properties of powdered materials N85-22630
Elasticity formulas for thin-walled shells with piezoceramic layers N85-22816
Analysis and optimization of parameters of fanned surface acoustic wave transducers N85-22934
Measuring intensity of electric field produced by electromagnetic pulse with aid of active probes N85-22958
Theory of diaphragm light modulators with electrical input signal N85-23002
Discrimination of normal and anomalous magnetic and electric fields in geoelectromagnetic variations N85-23166
1981 wC-130 airborne lightning characterization program data review
[AD-A150230] N85-23275

ELECTRIC FILTERS
On filter binary processes
[AD-A150328] N85-22890
Dynamics of adaptive signal corrector N85-22940
Synthesis of optimum single-channel discrete signals and filters N85-22990

ELECTRIC GENERATORS
Preliminary assessment of power-generating tethers in space and of propulsion for their orbit maintenance N85-22520
Control of cascaded induction generator systems
[AD-A150429] N85-22897

ELECTRIC HYBRID VEHICLES
Electric and hybrid vehicle demonstration project
[DE85-003939] N85-23455

ELECTRIC MOTOR VEHICLES
Electric vehicle test program: INEL transition qualification test plan
[DE85-005171] N85-23456

ELECTRIC MOTORS
Optimum design of electrical motors for multilink manipulators and automated manufacturing systems N85-22880
Reluctance and doubly-excited reluctance motors [DE85-003585] N85-22900
ELECTRIC NETWORKS
A Monte Carlo sampling plan for estimating network reliability [AD-A150511] N85-22898
ELECTRIC POTENTIAL
Discharges on a negatively biased solar cell array in a charged-particle environment N85-22499
EMI characteristics of a potential control system N85-22502
Characteristics of EMI generated by negative metal-positive dielectric voltage stresses due to spacecraft charging N85-22505
Space test program of high-voltage solar array-space plasma interactions N85-22519
Stability of highly nonlinear oxide-zinc resistors under continuous voltage of industrial frequency N85-23030
ELECTRIC PROPULSION
Preliminary assessment of power-generating tethers in space and of propulsion for their orbit maintenance N85-22520
ELECTRICAL CONDUCTIVITY METERS
Method of separately determining electrophysical properties of bulky conductor N85-22951
ELECTRICAL ENGINEERING
The DFS-Kopernikus solar generator electrical design N85-22590
The DFS-Kopernikus solar generator N85-22591
Electrical design of the Intelsat 6 solar generator N85-22592
Development and qualification of the electrical part of the Advanced Rigid Array (ARA) — solar array N85-22594
Design and qualification testing of the Olympus solar array blanket N85-22600
Electronics Engineering Department EE Technical Review [UCRL-50025-84-1] N85-22887
USSR report: Electronics and electrical engineering [JPRS-UEE-85-002] N85-22907
USSR report: Electronics and electrical engineering [JPRS-UEE-85-001] N85-22976
Microcomputers and the electrical engineer [AD-A150499] N85-23325
China report: Science and technology [JPRS-CST-85-003] N85-23433
ELECTRICAL FAULTS
Galileo internal electrostatic discharge program N85-22504
Mass spectra of neutral particles released during electrical breakdown of thin polymer films N85-22511
Electrical conduction in polymer dielectrics N85-22514
Breakdown of thin plates by radiation N85-22709
ELECTRICAL GROUNDING
Exact design formulas for field intensity of dipole deployed above flat homogeneous Earth with finite conductivity N85-22998
ELECTRICAL IMPEDANCE
Change of electrical characteristics of radio-frequency cables under thermal effect N85-22990
ELECTRICAL MEASUREMENT
The high voltage silicon cell: A comparative analysis N85-22569
Inverse behavior of silicon photovoltaic cells N85-22604
Comparing different theoretical designs of six-port reflectometer junctions [AD-A149419] N85-22861
Portable electrochemical cell interrogator [DE85-005186] N85-22901
Measuring intensity of electric field produced by electromagnetic pulse with aid of active probes N85-22958
ELECTRICAL PROPERTIES
Studies of electrical properties of surface films and localization during electrochemical dimensional working of titanium N85-22729
High sheet resistance, arsenic implanted polycrystalline silicon for integrated circuit resistors [DE85-004355] N85-22902
Electrical and thermal transport property studies of high-temperature thermoelectric materials [AD-A150167] N85-23417
ELECTRICAL RESISTANCE
On filter binary processes [AD-A150328] N85-22890
ELECTRICAL RESISTIVITY
Preliminary investigation of the electrodynamics of a conducting tether N85-22521
HREELS and Auger studies of conducting polymers [DE85-004541] N85-22764
Exact design formulas for field intensity of dipole deployed above flat homogeneous Earth with finite conductivity N85-22998
Induction excitation of deep conducting zones N85-23154
Variations in resistivity of upper crustal layer N85-23164
ELECTRO-OPTICAL EFFECT
Integrated optical components utilizing acoustooptic and electrooptic diffraction in micro-waveguides N85-23044
ELECTRO-OPTICS
USSR report: Engineering and equipment [JPRS-UEQ-85-003] N85-22782
Optoelectronic safety system for robotized technological complex N85-22805
Mathematical modeling of two-frequency laser sounding of scattering media N85-23045
Accuracy of random signal spectral parameter estimation against interference background in acoustooptical spectrum analyzers N85-23052
ELECTROACOUSTIC TRANSDUCERS
Electroacoustical imaging technique for encoding incoherent radiance fields as Gabor elementary signals [NASA-TM-86372] N85-23067
High-frequency acoustic variability in the arctic [AD-A150550] N85-23383
ELECTROACOUSTIC WAVES
Electroacoustical imaging technique for encoding incoherent radiance fields as Gabor elementary signals [NASA-TM-86372] N85-23067
ELECTROCHEMICAL CELLS
Portable electrochemical cell interrogator [DE85-005186] N85-22901
ELECTROCHEMICAL CORROSION
An electrochemical study of the corrosion behavior of primer coated 2219-T87 aluminum [NASA-TP-2459] N85-22662
ELECTROCHEMISTRY
Application of modulated hydrodynamic voltammetry to the study of anodic electrocatalysis [DE85-004182] N85-22653
Local electrochemistry of pitting corrosion in stainless steels [DE85-005207] N85-22673
Studies of electrical properties of surface films and localization during electrochemical dimensional working of titanium N85-22729
Raman structural studies of the nickel electrode [NASA-CR-175619] N85-23414
ELECTRODE FILM BARRIERS
Studies of electrical properties of surface films and localization during electrochemical dimensional working of titanium N85-22729
ELECTRODELESS DISCHARGES
Neodymium YAG laser pumped with radiation from high frequency electrodeless discharge N85-22796
ELECTRODEPOSITION
Mechanical properties of electrodeposited nickel and copper [DE85-005321] N85-22677
Film and interstitial formation of metals in plasma-sprayed ceramics [NASA-TM-86993] N85-22756
Demonstration of feasibility of depositing semiconductor layers using microwave enhanced plasma techniques [NASA-CR-174392] N85-23421
ELECTRODES
EXAFS of monolayers on silver electrodes: SSRL proposal number 717M [AD-A150623] N85-22652
Applications of the vibration probe to localized current measurements [DE85-004702] N85-22675
Electrodynamic stability of composite liquid-metal contacts N85-23031
Molten carbonate fuel cell performance model update, draft [DE85-005423] N85-23252
Raman structural studies of the nickel electrode [NASA-CR-175619] N85-23414
ELECTRODYNAMICS
Spacecraft Environmental Interactions Technology, 1983 [NASA-CP-2359] N85-22470
Preliminary investigation of the electrodynamics of a conducting tether N85-22521
Elasticity formulas for thin-walled shells with piezoceramic layers N85-22816
Electrodynamic stability of composite liquid-metal contacts N85-23031
Synthesis of optimum smooth transition in microstrip through line on microwave integrated circuit N85-23041
ELECTROJETS
Periodic substorm activity in the geomagnetic tail [NASA-CR-175629] N85-23409
ELECTROMAGNETIC COMPATIBILITY
Design guidelines for assessing and controlling spacecraft charging effects N85-22500
ELECTROMAGNETIC FIELDS
Models of discontinous random fields N85-22983
Problem of diffraction by wavy surface: Comparison of numerical methods of solution N85-22985
ELECTROMAGNETIC INTERACTIONS
Theoretical aspects of electroweak and other interactions in medium-energy nuclear physics [DE85-003821] N85-23392
ELECTROMAGNETIC INTERFERENCE
Shuttle electrical environment N85-22475
EMI characteristics of a potential control system N85-22502
Characteristics of EMI generated by negative metal-positive dielectric voltage stresses due to spacecraft charging N85-22505
Basic EMC (electromagnetic interference) technology advancement for c3 systems. Volume 3A: Probabilistic analysis of combinational circuits with random delays [AD-A150349] N85-22866
Efficiency of digital compensator of strong non-Gaussian interference N85-22942
Interference immunity of binary systems with second-order phase-difference modulation in various reception modes N85-22944
Spectra of incidental interference resulting from nonlinear conversion of signals from transmitters N85-22950
Interference flux during reflection of heterogeneous waves N85-22977
Models of discontinous random fields N85-22983
Applicability of log-normal model to probabilitistic description of quasi-pulse interference N85-23014
ELECTROMAGNETIC MEASUREMENT
Two-dimensional signal processing and storage and theory and applications of electromagnetic measurements [AD-A150590] N85-22899
Discrimination of normal and anomalous magnetic and electric fields in geoelectromagnetic variations N85-23166
ELECTROMAGNETIC NOISE
Prefiltration in Kalman filter with a priori indeterminacy N85-22939
Comparative analysis of noise tolerance of quasi-coherent phase shift keying signal demodulators N85-22946
Magnetic noise in single-machine rotating frequency converters N85-22969
Playback amplifier with high interference immunity N85-22970
ELECTROMAGNETIC PULSES
Design guidelines for assessing and controlling spacecraft charging effects N85-22500
Processing of signals in experiments with scattering of short radio pulses by conducting sphere N85-22917
Measuring intensity of electric field produced by electromagnetic pulse with aid of active probes N85-22958
Use of electronic coding-frequency meters to measure parameters of pulsed radio signals N85-22964
ELECTROMAGNETIC RADIATION
Numerical/Electromagnetics Code (NEC) [DE85-004999] N85-22874
Natural electromagnetic radiation in seismically active regions N85-23152
ELECTROMAGNETIC SCATTERING
Research efforts in support of resonance extraction studies. Volume 1: Improvement and validation of TWFD (Thin-Wire Frequency-Domain): A thin-wire frequency-domain scattering code [AD-A150296] N85-22864
Scattering of electromagnetic waves by charged particles N85-22913
Diffraction of plane TM-wave on continuously irregular elliptical plasma N85-22914
Extraction of surface-wave energy from plasma waveguide N85-22974
Scattering of waves by axisymmetrical edge N85-22987
ELECTROMAGNETIC SURFACE WAVES
Extraction of surface-wave energy from plasma waveguide N85-22974
ELECTROMAGNETIC WAVE FILTERS
Space-time response characteristics of acoustooptic filter for compression of linearly frequency-modulated signal N85-22937
ELECTROMAGNETISM
Magnetic location of Earth's core-mantle boundary and estimates of the adjacent fluid motion N85-23260

Magnetic field interactions with material discontinuities [AD-A150197] N85-23373

ELECTROMAGNETS
Code lock with microcircuit N85-22935

ELECTROMETERS
Dielectric measurements in infralow-frequency band N85-23034

ELECTRON ACCELERATION
Average and worst-case specifications of precipitating auroral electron environment N85-22482
Polar plasmas as observed by Dynamics Explorers 1 and 2 N85-22483

ELECTRON ACCELERATORS
High-field dipoles for future accelerators [DE85-002315] N85-23391

ELECTRON BEAM WELDING
Structure and mechanical characteristics of heterogeneous joints produced by laser welding N85-22742
Softening of metal near seam during welding of heat-resistant nickel alloys N85-22747

ELECTRON BEAMS
Electron beam charging of Space Shuttle thermal protection system tiles N85-22478
Sheath ionization model of beam emissions from large spacecraft N85-22489
Electron yields from spacecraft materials N85-22512
A simple model of electron beam initiated dielectric breakdown N85-22516
SEM (Scanning Electron Microscope) investigation of silicon diodes using the electron beam induced current method [AD-A150356] N85-22894
Design considerations for a 100 kW CW, 140 GHz gyrotron oscillator [DE85-005282] N85-22904
Investigation of generation of oscillations using anomalous Doppler effect N85-22980
Temperature dependence of propagation of high-current electron beam through drift space N85-22982
Effect of space-charge field on output characteristics of O-type oscillators with distributed interaction N85-23043
Los Alamos free electron laser: Accelerator performance [DE85-005722] N85-23084

ELECTRON BUNCHING
Los Alamos free electron laser: Accelerator performance [DE85-005722] N85-23084

ELECTRON CYCLOTRON HEATING
A 60 GHz 200 kW CW gyrotron with high output mode purity [DE85-005283] N85-22905
Investigation of generation of oscillations using anomalous Doppler effect N85-22980

ELECTRON DENSITY (CONCENTRATION)
Hartree-Fock interaction between a helium atom and lithium-metal: A test for the effective medium theory [AD-A150468] N85-23387

ELECTRON DIFFRACTION
HREELS and Auger studies of copducting polymers [DE85-004541] N85-22764
Structural characterization by intensity measurements of electron diffraction patterns [DE85-004803] N85-23427

ELECTRON DISTRIBUTION
Kapton charging characteristics: Effects of material thickness and electron-energy distribution N85-22513

ELECTRON EMISSION
Electron yields from spacecraft materials N85-22512
Non-self-maintained high-voltage low-pressure discharge N85-23037
Mean delta-ray energies in ion molecule collisions [DE85-005524] N85-23395

ELECTRON ENERGY
Kapton charging characteristics: Effects of material thickness and electron-energy distribution N85-22513

ELECTRON FLUX DENSITY
Average and worst-case specifications of precipitating auroral electron environment N85-22482
Three-dimensional calculation of shuttle charging in polar orbit N85-22486
Polar orbit electrostatic charging of objects in shuttle wake N85-22487

ELECTRON IRRADIATION
Discharge pulse phenomenology N85-22509
Technological process effect on the carrier lifetime degradation of silicon solar cell base layer irradiated by 1 MeV electrons (boron doping case) N85-22585
The effects of lithium counterdoping on radiation damage and annealing in n(+)p silicon solar cells N85-22586
Investigation of the degradation of GaAs photovoltaic cells by proton and electron irradiation N85-22587

ELECTRON MICROSCOPY
TEM/FIM study of modulated microstructures in the Fe-Be system [DE85-005379] N85-22678
Grain boundaries in NiO [DE85-006129] N85-22687
Decomposition of VTAN alloy solid solution upon irradiation and thermal aging N85-22712
Impurities in Kevlar 49 fibers [DE85-004996] N85-22767
A comprehensive review of black powder [AD-A150455] N85-22769
SEM (Scanning Electron Microscope) investigation of silicon diodes using the electron beam induced current method [AD-A150356] N85-22894
Structural characterization by intensity measurements of electron diffraction patterns [DE85-004803] N85-23427

ELECTRON OSCILLATIONS
Investigation of generation of oscillations using anomalous Doppler effect N85-22980

ELECTRON PLASMA
Charging of DMSP/F6 spacecraft in aurora on 10 January 1983 N85-22481
Average and worst-case specifications of precipitating auroral electron environment N85-22482

ELECTRON RADIATION
Periodic substorm activity in the geomagnetic tail [NASA-CR-175629] N85-23409

ELECTRON SOURCES
Development of a continuous broad-energy-spectrum electron source N85-22507

ELECTRON TRANSFER
Electronic transport in hydrogenated amorphous silicon films [DE85-002901] N85-23426

ELECTRON TUNNELING
Macroscopic quantum tunnelling in a current biased Josephson junction [DE85-004603] N85-23424

ELECTRON-HOLE DROPS
Investigations of radiation-induced and carrier-enhanced conductivity N85-22515

ELECTRONIC EQUIPMENT
Control of cascaded induction generator systems [AD-A150429] N85-22897
USSR report: Electronics and electrical engineering [JPRS-UEE-85-002] N85-22907
Simple detonation meter N85-22971
USSR report: Electronics and electrical engineering [JPRS-UEE-85-001] N85-22976

ELECTRONIC EQUIPMENT TESTS
Measurement of internal thermal resistance for quality control of semiconductor devices N85-22953

ELECTRONICS
USSR report: Electronics and electrical engineering [JPRS-UEE-85-002] N85-22907

ELECTRONS
Galileo internal electrostatic discharge program N85-22504
Discharge characteristics of dielectric materials examined in mono-, dual-, and spectral energy electron charging environments N85-22510

ELECTROPHYSIOLOGY
Brain mechanisms underlying individual differences in reaction to stress: An animal model [AD-A150195] N85-23301

ELECTROSTATIC CHARGE
Direct measurements of severe spacecraft charging in auroral ionosphere N85-22480
Average and worst-case specifications of precipitating auroral electron environment N85-22482
Galileo internal electrostatic discharge program N85-22504
Automatic charge control system for satellites N85-22508
Discharge characteristics of dielectric materials examined in mono-, dual-, and spectral energy electron charging environments N85-22510
Development and testing of a spacecraft surface potential monitor N85-22582
Electrostatic discharge testing on a carbon fiber solar panel structure N85-22584
EOS (electrical overstress) protection for VLSI (Very Large Scale Integration) devices [AD-A150333] N85-22891

ELECTROSTATIC PROBES
Ram-wake effects on plasma current collection of the PIX 2 Langmuir probe N85-22496

ELECTROSTATICS
Electrostatic forming and testing of polymer films on a 16-foot diameter test fixture [NASA-TM-86328] N85-22685

ELECTROWINNING
Using fuel cells or anode depolarization to reduce electrowinning energy consumption [DE85-006187] N85-23250

ELEMENTARY PARTICLE INTERACTIONS
Experimental studies of elementary particle interactions at high energies [DE85-004795] N85-23394

ELEVATION
Hypsometric features on Venus N85-22439
Mathematical modeling of results of geometric leveling in variable gravity field N85-23170
Surface units on Venus derived from Pioneer-Venus altimetry, roughness, and reflectivity measurements N85-23510

ELLIPSOMETERS
Time-resolved ellipsometry and reflectivity measurements of the optical properties of silicon during pulsed excimer laser irradiation [DE85-005091] N85-23079

ELLIPTIC FUNCTIONS
Computation of elliptical functions in problems of celestial mechanics N85-22418

ELLIPTICAL ORBITS
Averaging of equations of cometary orbital motion with allowance for nongravitational effects N85-22411
Satellite oscillations in elliptical orbit N85-22429
Periodic movements of axisymmetrical satellite about center of mass due to gravitational moment N85-22783

EMISSION
Increase in hydrogen emission of upper atmosphere following launches of space vehicles N85-22431

EMISSION SPECTRA
Impurities in Kevlar 49 fibers [DE85-004996] N85-22767
A standard aircraft diffusion flame: Spectral characteristics and a feasibility study for developing an alternate calibration source for aircraft optical fire detection systems [AD-A150231] N85-22768
Measurement of the large-scale anisotropy of the cosmic background radiation at 3 MM N85-23680

EMISSIVITY
Emissivity enhancement of fused silica for space applications — solar cells N85-22615

EMPLOYMENT
A comparison of metropolitan and non-metropolitan employment characteristics: Indications of the size of non-metropolitan mobile communication services user classes [NASA-CR-175648] N85-22855

ENERGY BUDGETS
Testing an energy balance model for estimating actual evapotranspiration using remotely sensed data — Hannover, West Germany barley and wheat fields N85-23236
Accurate albedos of the brightest regions on Io N85-23618

ENERGY CONSERVATION
Using fuel cells or anode depolarization to reduce electrowinning energy consumption [DE85-006187] N85-23250

ENERGY CONSUMPTION
Feoktistov discusses need for space colonization N85-22454
Using fuel cells or anode depolarization to reduce electrowinning energy consumption [DE85-006187] N85-23250

ENERGY CONVERSION
Modulation of light energy transduction in photosynthesis [DE85-004711] N85-23292

ENERGY CONVERSION EFFICIENCY
Nonlinearity and spectral mismatch problems of solar cells N85-22605
High output photovoltaic conversion: The quadrispectral project — spacecraft power supplies N85-22626
Reluctance and doubly-excited reluctance motors [DE85-003585] N85-22900
A theoretical analysis of solar-driven natural convection energy conversion systems [DE84-004431] N85-23245

ENERGY DISSIPATION
Dissipation of energy in composite material N85-22703
Energy losses at leading edge of turbine blade during multirow jet cooling N85-22826
Near Field/Far Field (NF/FF) energy loss in Electric Discharge Lasers (EDL's): A mode-medium interaction [AD-A150299] N85-23075
Special features of computations of vertical distribution of concentration of suspended sediments under marine conditions N85-23125
Seismic waves and dispersion relations N85-23181
Stability of the Galilean satellites in deep orbital resonance N85-23477

Capture of planetesimals into a circumterrestrial swarm N85-23522
ENERGY DISTRIBUTION
Acoustic energy balance method N85-22537
Breakdown of thin plates by radiation N85-22709
Theoretical thermodynamics of mixtures at high pressures N85-23550
ENERGY SPECTRA
Measured electron contribution to Shuttle plasma environment: Abbreviated update N85-22476
Development of a continuous broad-energy-spectrum electron source N85-22507
Discharge characteristics of dielectric materials examined in mono-, dual-, and spectral energy electron charging environments N85-22510
Nonlinearity and spectral mismatch problems of solar cells N85-22605
Energy spectrum of processes of structural relaxation of amorphous alloy FeCo70Si15B10 N85-22750
Numerical investigation of evolution of energy spectrum of slightly nonlinear Rossby waves N85-23124
Mean delta-ray energies in ion molecule collisions [DE85-005524] N85-23395
ENERGY STORAGE
Cyclic industrial robots with mechanical energy storing devices: Multipositional system with one or several degrees of freedom N85-22803
Cyclic industrial robots with mechanical energy storing devices: Principles of drive design N85-22807
ENERGY TECHNOLOGY
New high-efficiency silicon solar cells [NASA-CR-175643] N85-23244
ENERGY TRANSFER
Acoustic energy exchange in sheared mean flows — solid rocket motors N85-22534
Repetitive energy transfers from an inductive energy store N85-22681
Numerical investigation of evolution of energy spectrum of slightly nonlinear Rossby waves N85-23124
The effects of internal waves on acoustic normal modes [AD-A150235] N85-23379
Molecular dynamics studies of energy transfer processes in crystal systems [AD-A150161] N85-23416
ENGINE DESIGN
Experimental determination of optimum ratio of runner blade height at exit to runner blade height at entrance of radial inward-flow microturbines N85-22827
Hydrodynamic simulation of transient processes in injection system of aircraft engines during pump unswirling N85-22829
ENGINE FAILURE
Effects of inlet distortion on a static pressure probe mounted on the engine hub in an F-15 airplane [NASA-TP-2411] N85-22394
ENGINE INLETS
Selection of air intake parameters for supersonic-flow operation N85-22837
ENVIRONMENT EFFECTS
Areas with forest soils sensitive to acidic deposition under alternative damage hypotheses [DE85-005257] N85-23257
ENVIRONMENT POLLUTION
Feoktistov discusses need for space colonization N85-22454
ENVIRONMENT SIMULATION
Potential bedforms on Venus: Wind tunnel simulations N85-23583
Microdunes and other aeolian bedforms on Venus: Wind tunnel simulations N85-23584
ENVIRONMENTAL MONITORING
Combined analysis of the dynamics of complex ecosystems based on repeated remote measurements N85-22450
ENVIRONMENTAL QUALITY
China report: Science and technology [JPRS-CST-85-003] N85-23433
ENVIRONMENTS
Environmental cycling of cellulosic thermal insulation and its influence on fire performance [DE85-004295] N85-22776
Principles of software engineering environment design [AD-A150352] N85-23324
EPITAXY
Clustering and ordering in 3-5 alloys [AD-A150604] N85-22670
EPOXY MATRIX COMPOSITES
Directional dependent engineering properties of aluminum-aramid-epoxy laminates [CCMS-85-02] N85-22638
EQUATIONS OF STATE
H-division materials physics progress [DE85-004990] N85-23430
Cooling of neutron stars with hyperons [DE85-004641] N85-23472
Impact cratering calculation N85-23531
EQUATORIAL ATMOSPHERE
Kinetic Rayleigh-Taylor instability theory in the ionosphere near equator N85-22911
EQUATORIAL REGIONS
Investigations of the Mars cratered terrain: Smooth plains boundary in the eastern equatorial region N85-23596
EQUILIBRIUM
Exergetical analysis of turbojet engine cycle N85-22825
EQUILIBRIUM FLOW
Time-dependent flow of stream swirled in vortex chamber N85-22786
Interaction of cylindrical shell with concentrated mass moving along its inner surface N85-22810
EQUILIBRIUM METHODS
Modelling equilibriums and fractional crystallization in the system MgO-FeO-CaO-Al2O3-SiO2 N85-23552
ERROR ANALYSIS
Expansion of functions describing planetary surface and gravity field N85-22410
Analysis of systematic errors in systems of selenodetic coordinates N85-22435
Noise tolerance of digital demodulator for complex signal system employing binary quantization N85-22929
ERROR CORRECTING DEVICES
Methods of digital correction for channels of multichannel radar receivers N85-23005
ERROR DETECTION CODES
Error probability during optimal noncoherent reception of binary signals in multibeam channel N85-22922
ERROR SIGNALS
Reception of signal with unknown amplitude and duration submerged in white noise N85-23016
ERRORS
Rejection of anomalous observations when determining spacecraft trajectories N85-22421
Analysis of systematic errors in systems of selenodetic coordinates N85-22435
A Monte Carlo sampling plan for estimating network reliability [AD-A150511] N85-22898
Noise tolerance of diversity reception in frequency-adaptive digital transmission systems N85-23024
Investigation of influence of communications link and synchronization error on noise tolerence of group transmission of binary information based on orthogonal Walsh function N85-23026
Runge-Kutta formula with cheap error estimate [DE85-005674] N85-23363
ESCAPE SYSTEMS
Approach for service life extension of explosive devices for aircraft escape systems [NASA-TM-86323] N85-22381
ESCARPMENTS
Lithologic and structural control on slope morphology in the Valles Marineris N85-23651
ESTIMATES
Estimation of gas turbine engine boost provided by injecting water behind compressor N85-22838
Accuracy of approximation of Bayes estimates in presence of noninformative parameters N85-23015
A note about the strong convergence of the nonparametric estimation of a regression function [AD-A150325] N85-23353
Runge-Kutta formula with cheap error estimate [DE85-005674] N85-23363
ESTUARIES
Field-work report: Medway Estuary, 28 June - 18 July 1983 [RNC/NS/TR8] N85-22773
ETCHING
The characterisation of oxide films on treated aluminium alloys [MOAD-R-849] N85-22667
ETHYLENE OXIDE
Influence of hydrogen bonding in block copolymers and their blends N85-22752
EUCLIDEAN GEOMETRY
Schur-Ostrowski theorems for functionals on l1(0,1) [AD-A150193] N85-23346
EUROPA
Patterns of fracture and tidal stresses due to nonsynchronous rotation: Implications for fracturing on Europa N85-23483
Planetary analogs in Antarctica: Icy satellites N85-23605
Spectral units on Europa and Ganymede N85-23621
Fault offsets and lateral crustal movement on Europa N85-23656
EUTECTIC ALLOYS
Dependence of superplastic flow on state of grain boundaries N85-22689
Study of processes of modification of Al-Si alloys N85-22695
Aluminum alloy ATs5K5 (5% Zn + 5% Ca) for superplastic forming N85-22697
EUTROPHICATION
Geographic variation in the relationships of temperature, salinity or sigma sub t versus plant nutrient concentrations in the world ocean — silicic acid, nitrate, and phosphate concentration [NASA-CR-175621] N85-23287
EVALUATION
Operational performance of the photovoltaic-powered grain mill and water pump at Tangaye, Burkina Faso (formerly Upper Volta) [NASA-TM-86970] N85-23243
EVAPORATION
Effects of temperature variation among droplets in an evaporating fuel spray N85-22562
EVAPOTRANSPIRATION
Remote Sensing of Snow and Evapotranspiration [NASA-CP-2363] N85-23223
General report of the researches of snowpack properties, snowmelt runoff and evapotranspiration in Japan N85-23225
Estimation of regional evapotranspiration using remotely sensed land surface temperature. Part 1: Measurement of evapotranspiration at the Environmental Research Center and determination of Priestley-Taylor parameter N85-23233
Estimation of regional evapotranspiration using remotely sensed land surface temperature. Part 2: Application of equilibrium evaporation model to estimate evapotranspiration by remote sensing technique — Japan N85-23234
Testing an energy balance model for estimating actual evapotranspiration using remotely sensed data — Hannover, West Germany barley and wheat fields N85-23236
EVOKED RESPONSE (PSYCHOPHYSIOLOGY)
Brain mechanisms underlying individual differences in reaction to stress: An animal model [AD-A150195] N85-23301
EVOLUTION (DEVELOPMENT)
Asteroid collisional evolution studies N85-23501
EXCAVATION
Impacts in ice: Commissions of solar system crater population N85-23538
EXCIMER LASERS
Non-linear optical techniques for visible and UV lasers and thin film deposition [AD-A150489] N85-23077
Time-resolved ellipsometry and reflectivity measurements of the optical properties of silicon during pulsed excimer laser irradiation [DE85-005091] N85-23079
Low jitter trigger for an excimer laser [DE85-005732] N85-23080
EXCITATION
Large amplitude forcing of a high speed 2-dimensional jet [NASA-CR-175646] N85-22393
Use of markets to elucidate reacting sputtering processes [DE85-005723] N85-22655
Exitation of low-frequency resonance waves by moving conductor in space plasma N85-22912
Induction excitation of deep conducting zones N85-23154
Study of resolution of deep MT soundings by means of physical model N85-23155
Observation of a novel low-lying excited state in zinc complexes [AD-A150188] N85-23385
Sequential excitation preparation of molecular energy levels with special structural and chemical properties [AD-A150301] N85-23386
EXERCISE PHYSIOLOGY
Sleep deprivation and exercise tolerance [AD-A150566] N85-23296
EXHAUST EMISSION
Composition and photochemical reactivity of turbine engine exhaust [AD-A150559] N85-23256
EXISTENCE THEOREMS
The Chinese remainder theorem and multi-PRF radars [AD-A141375] N85-22858
EXPERIMENT DESIGN
Investigation of dynamics of radiation spectrum of injection lasers by infrared impulse Fourier spectroscopy N85-23047
EXPLORER 51 SATELLITE
Wakes and differential charging of large bodies in low Earth orbit N85-22488
EXPLOSIONS
Electric and hybrid vehicle demonstration project [DE85-003939] N85-23455

Centrifuge impact cratering experiments N85-23533
Hydrovolcanism N85-23574
EXPLOSIVE DEVICES
Approach for service life extension of explosive devices for aircraft escape systems
[NASA-TM-86323] N85-22381
EXPLOSIVES
A comprehensive review of black powder
[AD-A150455] N85-22769
IHE material qualification tests description and criteria
[DE85-004649] N85-22770
EXTERNAL SURFACE CURRENTS
Rocket body charge neutralization processes in ARAKS experiment (data from two launches) N85-22426
Electric field effects on ion currents in satellite wakes N85-22485
Calculation of secondary-electron escape currents from inclined-spacecraft surfaces in a magnetic field N85-22491
Surface interactions and high-voltage current collection N85-22493
Development of a continuous broad-energy-spectrum electron source N85-22507
Development and testing of a spacecraft surface potential monitor N85-22582
EXTERNAL TANKS
Results of aeroheating DFI and ET design-data test on a 0.0175-scale model 60-OTS conducted in the Von Karman Gas Dynamics Facility (VKF) 40° supersonic and the 50° hypersonic wind tunnels A and C
[NASA-CR-167693] N85-22466
Results of a M = 5.3 heat transfer test of the integrated vehicle using phase-change paint techniques on the 0.0175-scale model 56-OTS in the NASA/Ames Research Center 3.5-foot hypersonic wind tunnel
[NASA-CR-167695] N85-22468
EXTRAGALACTIC RADIO SOURCES
All-Union conference of radio astronomers N85-22408
EXTRAVEHICULAR ACTIVITY
Aerospace Safety Advisory Panel
[NASA-TM-87426] N85-22373
Astronaut hazard during free-flight polar EVA N85-22522
EXTREMELY LOW RADIO FREQUENCIES
Dielectric measurements in infralow-frequency band N85-23034

F

F-15 AIRCRAFT
Effects of inlet distortion on a static pressure probe mounted on the engine hub in an F-15 airplane
[NASA-TP-2411] N85-22394
F-16 AIRCRAFT
Dynamic wind-tunnel testing of active controls by the NASA Langley Research Center N85-22353
F-17 AIRCRAFT
Dynamic wind-tunnel testing of active controls by the NASA Langley Research Center N85-22353
F-104 AIRCRAFT
Testing of the digital flight control system of the German CCV fighter experimental aircraft N85-22361
FABRICATION
Low capacitance e-beam fabricated beam-lead Schottky barrier diodes
[AD-A150238] N85-22888
New high-efficiency silicon solar cells
[NASA-CR-175643] N85-23244
Structural design of the Sandia 34-M Vertical Axis Wind Turbine
[DE85-002631] N85-23247
A normal incidence, high resolution X-ray telescope for solar coronal observations
[NASA-CR-175622] N85-23481
FACE CENTERED CUBIC LATTICES
Observation of surface vibrational resonances on (110) surfaces of FCC metals
[AD-A150469] N85-23419
FACTORIZATION
Factorized algorithms for combined spatial and temporal processing of radar signals N85-22997
FAILURE
Reliability bounds for fault-tolerant systems with competing responses to component failures
[NASA-TP-2409] N85-23090
Effects of assuming independent component failure times, if they are actually dependent, in a series system
[AD-A150582] N85-23092
FAILURE ANALYSIS
Results of the AFRSI rewaterproofing systems screening test in the NASA/Ames Research Center (ARC) 2 x 2-foot transonic wind tunnel
[NASA-CR-167694] N85-22467
Reliability of robotized welding apparatus N85-22741
Characteristics of surface crack development in ATiS aluminum alloy during slow-cycle loading N85-22745
Advanced life analysis methods. Volume 1: Cracking data survey and NDI (nondestructive inspection) assessment for attachment lugs
[AD-A150419] N85-23108
A theoretical basis for the analysis of redundant software subject to coincident errors
[NASA-TM-86369] N85-23317
Contribution of instrumentation and control software to system reliability
[DE85-004693] N85-23340
FAILURE MODES
Use of acoustical emission method to study specifics of fracture of boron reinforced plastic structural elements N85-22696
FAR FIELDS
Near Field/Far Field (NF/FF) energy loss in Electric Discharge Lasers (EDL's): A mode-medium interaction
[AD-A150299] N85-23075
FARM CROPS
Characterization of LANDSAT-4 TM and MSS image quality for the interpretation of California's agricultural resources — Central Valley N85-23190
FARMLANDS
Characterization of LANDSAT-4 TM and MSS image quality for the interpretation of California's agricultural resources — Central Valley N85-23190
An initial analysis of LANDSAT-4 Thematic Mapper data for the discrimination of agricultural, forested wetlands, and urban land cover — Poinsett County, Arkansas; and Reelfoot Lake and Union City, Tennessee N85-23193
Preliminary evaluation of TM for soils information N85-23206
The use of Thematic Mapper data for land cover discrimination: Preliminary results from the UK SATMaP programme N85-23207
FAST FOURIER TRANSFORMATIONS
Computing convolution of multifrequency signal employing truncated fast Fourier transform algorithms N85-23019
FATIGUE (MATERIALS)
Experimental and numerical analysis of electric currents and electromagnetic blunting of cracks in thin plates
[AD-A150418] N85-22669
Long-term strength and fracture criteria for EI698VD alloy under complex stress conditions N85-22723
Some specifics of development of fatigue and creep in heat-resistant alloys with asymmetrical multicycle loading N85-22724
FATIGUE LIFE
Fatigue and corrosion fatigue resistance of aluminum casting alloy VAL10 and forging alloy AK6 N85-22690
Fatigue life, crack initiation, and propagation of 304 stainless steel with non-proportional axial/torsional strain-paths N85-23094
FATIGUE TESTS
Fatigue and corrosion fatigue resistance of aluminum casting alloy VAL10 and forging alloy AK6 N85-22690
Use of acoustical emission method to study specifics of fracture of boron reinforced plastic structural elements N85-22696
Advanced life analysis methods. Volume 1: Cracking data survey and NDI (nondestructive inspection) assessment for attachment lugs
[AD-A150419] N85-23108
FAULT TOLERANCE
AIRLAB: A laboratory for flight-crucial-electronics system research N85-22362
Reliability bounds for fault-tolerant systems with competing responses to component failures
[NASA-TP-2409] N85-23090
A theoretical basis for the analysis of redundant software subject to coincident errors
[NASA-TM-86369] N85-23317
Measurement of SIFT operating system overhead
[NASA-TM-86322] N85-23337
FAULT TREES
Contribution of instrumentation and control software to system reliability
[DE85-004693] N85-23340
FEASIBILITY ANALYSIS
A standard aircraft diffusion flame: Spectral characteristics and a feasibility study for developing an alternate calibration source for aircraft optical fire detection systems
[AD-A150231] N85-22768
Multifunctional elements for integrated optics N85-22918
FEEDBACK CONTROL
Testing of the digital flight control system of the German CCV fighter experimental aircraft N85-22361
Periodic binary sequence generators: VLSI circuits considerations
[NASA-CR-175649] N85-22886
Control of cascaded induction generator systems
[AD-A150429] N85-22897
FEEDERS
New technique for fluid feed in simultaneous multisurface grinding N85-22800
FERMI SURFACES
First principles theory of Fermi-surface driven concentration waves in Cu/sub c/Pd/sub 1-c/ alloys
[DE85-005367] N85-22681
FERRITES
Quenching effects on iron site partitioning in the Apollo 17 orange glass composition N85-23553
FERRITIC STAINLESS STEELS
The ferrite permanent magnet AC motor: A technical and economical assessment
[DE85-002480] N85-22903
FERROFLUIDS
Use of ferrofluids in machining of metals N85-22902
FERROMAGNETISM
Magnetovolume effects in some Y-Ni intermetallic compounds
[ISSN-0066-2003] N85-22663
Anomalous magnetism of CeRh3B2 under pressure
[DE85-003069] N85-23425
FEVER
China report: Science and technology
[JPRS-CST-84-008] N85-22384
FIBER COMPOSITES
Estimating degree of development of physical-chemical interaction among components in Al-B fiber composite material N85-22705
Segregation of silicon in silumin-carbon fiber composites N85-22706
FIBER OPTICS
Analysis of fiber-gyroscopes discussed N85-22845
Interference immunity of fiber-optic communication lines with spectral multiplexing of channels N85-22924
AL-124 light-emitting diode in 30 Mbit/s fiber-optic communication line N85-22925
Optical reflectometer for multimode fiber lightpipes N85-22961
Dispersion characteristics of small-mode gradient optical fibers N85-23004
Technical Digest: Symposium on Optical Fiber measurements, 1984
[PB85-114700] N85-23407
FIBER ORIENTATION
The orientation distribution of nonspherical aerosol particles within a cloud
[AD-A150600] N85-23081
Technical Digest: Symposium on Optical Fiber measurements, 1984
[PB85-114700] N85-23407
FIBER REINFORCED COMPOSITES
Behavior of fiber-reinforced composites under dynamic tension
[AD-A150619] N85-22641
Fibre composite laminated plate analysis using a card programmable calculator (HP41C/CV)
[NIAST-83/86] N85-23106
FIBERS
Impurities in Kevlar 49 fibers
[DE85-004996] N85-22767
FIELD STRENGTH
Exact design formulas for field intensity of dipole deployed above flat homogeneous Earth with finite conductivity N85-22998
FILAMENT WINDING
Testing of wound materials for strength with loading in the reinforcement plane N85-22701
FILTERS
Theory of optimum M-filtration of signals against background of correlated interference N85-22927
FINANCIAL MANAGEMENT
An analysis of a dynamic project cost problem
[CSIR-TWISK-338] N85-23341
FINITE DIFFERENCE THEORY
Machine analysis of resonance characteristics of plate-type radio electronic equipment constructions N85-23018
Calculation of level surface in problems of large-scale ocean circulation N85-23136
Parallel processing for computational continuum dynamics
[AD-A150513] N85-23327
FINITE ELEMENT METHOD
Experimental and numerical analysis of electric currents and electromagnetic blunting of cracks in thin plates
[AD-A150418] N85-22669
Micromechanical modeling of microstructural damage in creeping alloys
[DE85-003925] N85-22671
Analysis of interaction of dynamically adjustable gyroscopes on elastic platform by finite-element method N85-22822

Pre- and post-processing for stream-function eddy current calculations
[AD-A150417] N85-22896
HPFTP flow diverter analysis
[NASA-CR-171424] N85-23057
On Hybrid and mixed finite element methods
[NASA-CR-175551] N85-23096
Advanced life analysis methods. Volume 2: Crack growth analysis methods for attachment lugs
[AD-A150420] N85-23109
Exploiting parallel computing with limited program changes using a network of microcomputers
[NASA-TM-86387] N85-23318
User's and programmer's guide to the mechanics of moving finite element code
[DE85-006165] N85-23365
Magnetic field interactions with material discontinuities
[AD-A150197] N85-23373

FIR FILTERS
Use of Walsh functions for calculating characteristics of digital filters with impulse response of finite duration N85-23011

FIRE CONTROL
Ground evaluation of helicopter air-to-air warfare N85-22360

FIRE EXTINGUISHERS
Aircraft skin penetrator and agent applicator. Volume 1: Working model development and construction
[AD-A150496] N85-22374

FIRE FIGHTING
Firefighters' communication transceiver test plan
[NASA-CR-171419] N85-22854

FIREPROOFING
Environmental cycling of cellulosic thermal insulation and its influence on fire performance
[DE85-004295] N85-22776

FIRES
Aircraft skin penetrator and agent applicator. Volume 1: Working model development and construction
[AD-A150496] N85-22374
Environmental cycling of cellulosic thermal insulation and its influence on fire performance
[DE85-004295] N85-22776

FISSURES (GEOLOGY)
Radar observations of fissure-fed basaltic lava flows, Craters of the Moon, Idaho N85-23640

FIXTURES
Electrostatic forming and testing of polymer films on a 16-foot diameter test fixture
[NASA-TM-86328] N85-22885

FLAME TEMPERATURE
The influence of fuel quality upon flame-tube temperature and flame radiation in a model gas-turbine primary zone
[K233] N85-22396
The influence of fuel molecular composition upon flame-tube temperature and flame radiation in a model gas-turbine primary zone
[K234] N85-22646
Laser diagnostic analyses of sooting flames
[AD-A150478] N85-22649

FLEXIBILITY
Effects of triazine components on physicochemical properties of polybutadiene: urethane block copolymers N85-22635
Optimum design and automated dynamic analysis of flexible mechanisms
[AD-A150152] N85-23088

FLEXIBLE BODIES
Developments in deployable masts to support flexible solar arrays N85-22620
Spline-based Rayleigh-Ritz methods for the approximation of the natural modes of vibration for flexible beams with tip bodies
[NASA-CR-172566] N85-23100

FLEXING
Variable flexing device for targets in internal beams of charged particle accelerators N85-22797
Machine analysis of resonance characteristics of plate-type radio electronic equipment constructions N85-23018

FLIGHT CLOTHING
The application of anthropometric survey data to aircrew clothing sizing
[AD-A150545] N85-23304

FLIGHT CREWS
Assessing the behavior and performance of teams in organizations: The case of air transport crews
[AD-A150359] N85-23302
The application of anthropometric survey data to aircrew clothing sizing
[AD-A150545] N85-23304

FLIGHT MANAGEMENT SYSTEMS
Ground and flight testing for aircraft guidance and control
[AGARD-AG-262] N85-22350
Civil avionics flight testing with the RAE(B) BAC1-11 N85-22354
A flight management algorithm and guidance for fuel-conservative descents in a time-based metered air traffic environment: Development and flight test results N85-22356

FLIGHT MECHANICS
Dynamic wind tunnel testing for active control research N85-22352

FLIGHT TESTS
Civil avionics flight testing with the RAE(B) BAC1-11 N85-22354
Guidance and control research flight testing with HFB 320 test aircraft N85-22355
A flight management algorithm and guidance for fuel-conservative descents in a time-based metered air traffic environment: Development and flight test results N85-22356
Avionics Flight Evaluation System (AFES) N85-22357
Improved Y-11 general-purpose transport designated Y-12 N85-22385
Operational loads measurement: A philosophy and its implementation --- aircraft structures
[AD-A149445] N85-23308

FLOODS
Catastrophic-flood features in Swedish Lapland as a terrestrial analog for Martian channel flows N85-23587

FLOW CHARACTERISTICS
Calibration of wind tunnel flow quality N85-22399
Hydraulic brakes for industrial robots N85-22606

FLOW DIRECTION INDICATORS
Determination of boundary line between reverse jet and surrounding stream N85-22789

FLOW DISTRIBUTION
Aerodynamic behavior of ventilated wind tunnel walls N85-22363
On the solution of the three-dimensional flowfield about a flow-through nacelle
[NASA-TM-87448] N85-22371
Results of the AFRSI rewaterproofing systems screening test in the NASA/Ames Research Center (ARC) 2 x 2-foot transonic wind tunnel
[NASA-CR-167694] N85-22467
HPFTP flow diverter analysis
[NASA-CR-171424] N85-23057
Centrifuge impact cratering experiments N85-23533
The nature of Martian flow ejecta craters N85-23545
Interaction of Martian flow ejecta blankets with pre-existing impact craters: Morphological observations N85-23546

FLOW GEOMETRY
Grid generation for a pump collector
[AD-A150217] N85-23059

FLOW MEASUREMENT
Liquid mass flow rate computer N85-22962
Turbulent flows of surfacant solutions
[AD-B089137L] N85-23058
Mean flow and turbulence in complex terrain NPS (Naval Postgraduate School)/Vandenberg measurement system
[AD-A150184] N85-23274
Field measurements of the 1983 Royal Gardens lava flows, Kilauea Volcano, and 1984 Mauna Loa lava flows, Hawaii N85-23565

FLOW RESISTANCE
Turbulent flows of surfacant solutions
[AD-B089137L] N85-23058

FLOW STABILITY
Acoustic energy balance method N85-22537

FLOW VELOCITY
Liquid mass flow rate computer N85-22962
Turbulence measurements in shock induced flows N85-23055

FLOW VISUALIZATION
Deflected jet experiments in a turbulent combustor flowfield
[NASA-CR-174863] N85-22390
An experimental investigation of the chopping of helicopter main rotor tip vortices by the tail rotor
[NASA-CR-177338] N85-23376

FLOWMETERS
Field-work report: Medway Estuary, 28 June - 18 July 1983
[RNC/NS/TR8] N85-22773

FLUID DYNAMICS
Current problems in turbomachinery fluid dynamics
[AD-A150533] N85-22397
The low frequency behaviour of an immersed structure at a standstill in a high density fluid with free surface
[TP-1983-31] N85-23105

FLUID FLOW
Results of the AFRSI rewaterproofing systems screening test in the NASA/Ames Research Center (ARC) 2 x 2-foot transonic wind tunnel
[NASA-CR-167694] N85-22467
Workshop report: Swirl Enhanced Combustion N85-22584
HPFTP flow diverter analysis
[NASA-CR-171424] N85-23057
Effects of fracture roughness on fluid flow through a single deformable fracture
[DE85-004593] N85-23062
Emplacement of long lava flows on Mauna Loa (Hawaii) and Alba (Mars) N85-23563
Thermal infrared observations of lava flows during the 1984 Mauna Loa eruption N85-23564
Surface structures of Hawaiian lavas N85-23566
Basaltic pressure ridges: Formation and relationship to flow emplacement N85-23567

FLUID MECHANICS
USSR report: Engineering and equipment
[JPRS-UEQ-85-003] N85-22782

FLUORESCENCE
Application of fluorescence to measurement of surface temperature in solid propellants N85-22548
Luminescence in the ocean
[AD-B089136L] N85-23288
Ion transport in beam-plasma interactions
[AD-A150145] N85-23410

FLUORIDES
Synthesis and characterization of poly(vinylidene fluoride)
[AD-A150291] N85-22759

FLUTTER ANALYSIS
Dynamic wind-tunnel testing of active controls by the NASA Langley Research Center N85-22353
Two degree-of-freedom flutter solution for a personal computer
[NASA-TM-86381] N85-22379

FLUX (RATE)
Absolute measurements of radiation intensity from Cassiopeia-A, Cygnus-A and crab nebula in 60-100 cm band N85-22978

FLUXES
Automatic multi-layer welding of thick cylindrical structures under flux N85-22746

FLY BY WIRE CONTROL
Guidance and control research flight testing with HFB 320 test aircraft N85-22355

FLYBY MISSIONS
The violet absorber on Io: Disulfur monoxide derivatives N85-23482
Dark halo craters and the thickness of grooved terrain on Ganymede N85-23484
Formation of bright terrain bands on Ganymede by unstable lithosphere extension N85-23485
Dynamical studies of Saturn's rings N85-23489

FOAMS
Exploratory development of foams from liquid crystal polymers
[NASA-CR-172510] N85-22754

FOCUSING
Axial focusing of signal from distant point radiator reflected twice in deep paraboloid N85-22979
Effects of focusing on HRS focal-plane polarimeter measurements
[DE85-004627] N85-23406

FOKKER-PLANCK EQUATION
On filter binary processes
[AD-A150328] N85-22880

FOLDING STRUCTURES
SPOT solar array N85-22595
Retractable Rigid Solar Generator (GSR) N85-22597
Blanket integrated cushioning of foldable and retractable solar arrays N85-22612

FOLDS (GEOLOGY)
Normal-fault and fold development in sedimentary rocks above a pre-existing basement normal fault N85-23259
Mechanisms of basalt-plains ridge formation N85-23643
Terrestrial analogs for planetary wrinkle ridges N85-23644

FORECASTING
Bootstrapping the Kalman filter
[AD-A150509] N85-23370

FOREST MANAGEMENT
Remote sensing used for study of forest resources N85-22440
Technologies to sustain tropical forest resources
[TI85-901085] N85-23241

FORESTS
The use of Thematic Mapper data for land cover discrimination: Preliminary results from the UK SATMaP programme N85-23207
Areas with forest soils sensitive to acidic deposition under alternative damage hypotheses
[DE85-005257] N85-23257

FORGING
USSR report: Machine tools and metalworking equipment
[JPRS-UMM-85-005] N85-22839

FORMAT
M68000 RNF text formatter user's manual [NASA-TM-86327] N85-23320
FORMATIONS
Morphology and mechanics of terraces in lunar craters N85-23543
FORMING TECHNIQUES
Aluminum alloy ATs5K5 (5% Zn + 5% Ca) for superplastic forming N85-22697
Electrostatic forming and testing of polymer films on a 16-foot diameter test fixture [NASA-TM-86328] N85-22885
FORTRAN
Validation summary report, Burroughs Corporation, 820 FORTRAN release 4.0 [PB84-227792] N85-23316
FORTRAN in the 90's [DE85-006154] N85-23332
FOURIER ANALYSIS
Nonlinear behavior and stability of thin spherical shells subjected to non-axisymmetrical loading N85-22821
FOURIER TRANSFORMATION
Acousto-optically addressed Fourier transform matched filters [AD-A150298] N85-22889
Processing of signals in experiments with scattering of short radio pulses by conducting sphere N85-22917
Synthesis of quasi-optimum algorithms for signal recognition against background of correlated noise employing discrete spectral transformations N85-23020
New convolution and discrete Fourier transformation algorithms based on rectangular transformations over field of roots of unity N85-23022
Algorithms for reconstruction of partially known, band limited Fourier transform pairs from noisy data [AD-A150194] N85-23347
Optical processing in radon space [AD-A150289] N85-23402
FRACTURE MECHANICS
Longitudinal splitting in unidirectional composites, analysis and experiments [NASA-CR-3881] N85-22639
Behavior of fiber-reinforced composites under dynamic tension [AD-A150619] N85-22641
Creep crack growth in ductile alloys [DE85-003937] N85-22676
Long-term strength and fracture criteria for EI698VD alloy under complex stress conditions N85-22723
Advanced life analysis methods. Volume 2: Crack growth analysis methods for attachment lugs [AD-A150420] N85-23109
Scattering of elastic waves on fractures randomly distributed in a three-dimensional medium N85-23151
Patterns of fracture and tidal stresses due to nonsynchronous rotation: Implications for fracturing on Europa N85-23483
FRACTURE STRENGTH
Interlaminar fracture toughness in resin matrix composites [AD-A150565] N85-22640
Particulate toughened silicon carbide [DE85-004797] N85-22643
Prediction of the resistance of structural materials to cavitation erosion [BLL-DRIC-TRANS-7435-(3623.66)] N85-22659
Fatigue and corrosion fatigue resistance of aluminum casting alloy VAL10 and forging alloy AK6 N85-22690
Structural strenght of strip D16T aluminum alloy with low copper and magnesium content N85-22691
Use of acoustical emission method to study specifics of fracture of boron reinforced plastic structural elements N85-22696
Mechanical properties and brittle fracture resistance of welded multilayer elements for high pressure vessels N85-22736
Analysis of strength and ductility of welded joints in AMtsS and AMg5 aluminum alloys N85-22737
Effect of protective medium on durability and fracture structure on seam zones of thin-walled titanium articles produced by diffusion welding N85-22738
Dispersed-metal-toughened alumina [NASA-CR-174667] N85-22758
Fracture mechanics evaluation of GaAs [NASA-CR-175657] N85-23101
FRACTURES (MATERIALS)
Effects of fracture roughness on fluid flow through a single deformable fracture [DE85-004593] N85-23062
Scattering of elastic waves on fractures randomly distributed in a three-dimensional medium N85-23151
Study of resolution of deep MT soundings by means of physical model N85-23155
FRACTURING
Hydrogen effects in austenitic stainless steels based on the Fe-Cr-Mn-N system [DE85-003617] N85-22672
Hydrovolcanism N85-23574
FRAGMENTATION
Hydrovolcanism N85-23574
FREE CONVECTION
Natural convection during heat accumulation by substances with change of aggregate state N85-22787
FREE ELECTRON LASERS
Los Alamos free electron laser: Accelerator performance [DE85-005722] N85-23084
FREE JETS
Time-dependent flow of stream swirled in vortex chamber N85-22786
FREQUENCIES
Externally compensated crystal oscillator (ECXO) study [AD-A150335] N85-22893
Programmable filter with fanned interdigital surface acoustic wave transducer N85-23008
Adsorption site, adsorption energy and normal vibration frequency of H/Ni(100) via total energy calculations [AD-A150555] N85-23388
FREQUENCY ANALYZERS
Use of electronic coding-frequency meters to measure parameters of pulsed radio signals N85-22964
FREQUENCY CONTROL
Stereo decoder without subcarrier restoration N85-22921
Gyrator frequency selectors with bandwidth independent of input signal level N85-23009
FREQUENCY CONVERTERS
Magnetic noise in single-machine rotating frequency converters N85-22969
FREQUENCY DISCRIMINATORS
Analysis of characteristics of digital discriminators for phase-shift keyed signals N85-22930
FREQUENCY DISTRIBUTION
Noise immunity of information transmission system with pseudorandom frequency switching under worst-case interference conditions N85-23029
A statistical treatment of the regional slope characteristics of Venus and Earth N85-23517
FREQUENCY MEASUREMENT
Use of electronic coding-frequency meters to measure parameters of pulsed radio signals N85-22964
FREQUENCY MODULATION
Space-time response characteristics of acoustooptic filter for compression of linearly frequency-modulated signal N85-22937
Simple detonation meter N85-22971
Synthesis of optimum single-channel discrete signals and filters N85-22990
Analysis of interference caused by interfering radio signals in communications systems with frequency separation of telephone channels and frequency modulation N85-23025
FREQUENCY SHIFT
Experimental studies of low temperature surface interactions of atomic hydrogen using maser technique [AD-A150216] N85-22647
FREQUENCY SHIFT KEYING
Ionospheric distortions of digital signals with wideband modulation N85-22945
FREQUENCY STABILITY
Coupled acoustic and hydrodynamic wave instabilities N85-22538
Spectral frequency of eigenvalues in optimal problems of stability of cylindrical shells of variable thickness N85-22815
Effect of variance of photoreceiver frequency characteristics on characteristics of measuring instruments N85-22965
Experimental study of high-stability oscillator with surface-acoustic-wave resonator in feedback loop N85-23053
FREQUENCY STANDARDS
Experimental studies of low temperature surface interactions of atomic hydrogen using maser technique [AD-A150216] N85-22647
FREQUENCY SYNTHESIZERS
Regular synthesis of pairs of phase-keyed binary minimax signals N85-22923
Theory of optimum M-filtration of signals against background of correlated interference N85-22927
Optimal synthesis of surface acoustic wave filters N85-22933
Simple sweep frequency generator N85-22960
FRESH WATER
Operational performance of the photovoltaic-powered grain mill and water pump at Tangaye, Burkina Faso (formerly Upper Volta) [NASA-TM-86970] N85-23243
FRICTION
Dissipation of energy in composite material N85-22703
High temperature antifriction properties of Ti sub 1-sub xNb sub x C sub 0.5N sub 0.5 alloys N85-22715
Effect of zero-wear in friction pairs operating in abrasive media N85-22901
FROST
The violet absorber on Io: Disulfur monoxide derivatives N85-23482
FUEL CELLS
Using fuel cells or anode depolarization to reduce electrowinning energy consumption [DE85-006187] N85-23250
Molten carbonate fuel cell performance model update, draft [DE85-005423] N85-23252
Cathode materials for molten carbonate fuel cells [DE85-004078] N85-23254
FUEL COMBUSTION
Ignition of mixtures of SiH sub 4, CH sub 4, O sub 2, and Ar or N sub 2 behind reflected shock waves [NASA-TP-2415] N85-22395
The influence of fuel quality upon flame-tube temperature and flame radiation in a model gas-turbine primary zone [K233] N85-22396
Workshop report: Swirl Enhanced Combustion N85-22564
The influence of fuel molecular composition upon flame-tube temperature and flame radiation in a model gas-turbine primary zone [K234] N85-22646
Laser diagnostic analyses of sooting flames [AD-A150478] N85-22649
Dependence of combustion of homogeneous kerosene-air mixtures on humidity of air N85-22835
FUEL CONSUMPTION
Effect of water injection into air for turbine cooling on economy of operation of gas turbine engine with afterburning N85-22830
FUEL PRODUCTION
Trifunctional catalysts for conversion of syngas to alcohols [DE85-004577] N85-22771
Anaerobic digestion of biomass: status summary and research development needs, 1983 [PB85-161925] N85-22772
FUEL PUMPS
Hydrodynamic simulation of transient processes in injection system of aircraft engines during pump unswirling N85-22829
HPFTP flow diverter analysis [NASA-CR-171424] N85-23057
FUEL-AIR RATIO
Dependence of combustion of homogeneous kerosene-air mixtures on humidity of air N85-22835
FUNCTIONAL ANALYSIS
Schur-Ostrowski theorems for functionals on l1(0,1) [AD-A150193] N85-23346
FUNCTIONS (MATHEMATICS)
A note about the strong convergence of the nonparametric estimation of a regression function [AD-A150325] N85-23353
FUSELAGES
Study for prediction of rotor/wake/fuselage interference, part 1 [NASA-CR-177340-VOL-1] N85-22346
Study for prediction of rotor/wake/fuselage interference. Part 2: Program users guide [NASA-CR-177340-VOL-2] N85-22347
Redesign of fuselage compartments by method of special contours N85-22784
Normal mode calculations for fuselage type intricate structures by regarding them as systems with superposed constraints N85-22817

G

GALACTIC COSMIC RAYS
Characteristics of latitude effect on cosmic ray charged component in atmosphere at altitudes 3-5 KM N85-22413
GALACTIC EVOLUTION
Research on the early history of the solar system N85-23527
GALACTIC NUCLEI
All-Union conference of radio astronomers N85-22408
GALACTIC RADIO WAVES
All-Union conference of radio astronomers N85-22408
GALACTIC STRUCTURE
The color excesses of classical cepheids and the structure of our galaxy N85-23459

Gas dynamics of the barred spiral galaxy NGC 3359 N85-23465
Dynamics of gas disks in triaxial galaxies N85-23469

GALAXIES
University of Cambridge Institute of Astronomy report of activities N85-23464
Studies of galactic HI in 21-centimeter absorption N85-23466

GALERKIN METHOD
Spline-based Rayleigh-Ritz methods for the approximation of the natural modes of vibration for flexible beams with tip bodies [NASA-CR-172566] N85-23100

GALILEAN SATELLITES
Stability of the Galilean satellites in deep orbital resonance N85-23477
Creep of ice: Further studies N85-23655
The Galilean Satellite Geological Mapping Program, 1984 N85-23664
Voyager cartography N85-23668
The control networks of the satellites of Jupiter and Saturn N85-23671

GALILEO SPACECRAFT
Galileo internal electrostatic discharge program N85-22504

GALLIUM
Annealing of radiation damage in boron and gallium doped silicon solar cells N85-22624
Improvement in magnetic field properties of vanadium-gallium superconductors by enhancement of spin-orbit scattering [DE85-002893] N85-23422

GALLIUM ARSENIDES
Gallium arsenide arrays versus silicon arrays for space application N85-22574
Space qualified AlGaAs/GaAs solar cells N85-22575
Availability of AlGaAs/GaAs solar cells in space N85-22576
Comparative study of GaAs solar cell potentialities for space applications N85-22577
Investigation of high output gallium arsenide solar cells N85-22578
Development of very thin large area GaAs solar cells for space application N85-22579
GaAs and 3-5 compound solar cells status and prospects for use in space N85-22580
GaAlAs-GaAs solar cell development: Prospective for space applications under concentration N85-22581
Investigation of the degradation of GaAs photovoltaic cells by proton and electron irradiation N85-22587
Isotropic proton irradiation of GaAs solar cells N85-22622
High output photovoltaic conversion: The quadrispectral project — spacecraft power supplies N85-22626
Thermally stimulated conductivity in semi-insulating gallium arsenide N85-23036
Fracture mechanics evaluation of GaAs [NASA-CR-175657] N85-23101

GALVANOMAGNETIC EFFECTS
Study of resolution of deep MT soundings by means of physical model N85-23155

GAMMA RAY ASTRONOMY
Shuttle flight test of an advanced gamma-ray detection system [AD-A150316] N85-22469

GAMMA RAY TELESCOPES
Determination of angular resolution of coded aperture gamma-ray telescope N85-22432

GANYMEDE
Dark halo craters and the thickness of grooved terrain on Ganymede N85-23484
Formation of bright terrain bands on Ganymede by unstable lithosphere extension N85-23485
Polar cap formation on Ganymede N85-23486
Giant planets and their satellites: Cosmochemistry, evolution and structure N85-23494
Ripple ring basins on Ganymede and Callisto N85-23547
Planetary analogs in Antarctica: Icy satellites N85-23605
Spectral units on Europa and Ganymede N85-23621
Three-layer generic Ganymedes: Structure and evolution N85-23657
Lineaments on Ganymede: New evidence for late tectonic activity N85-23658
Global tectonics on Ganymede N85-23659
Tectonics of the Galileo Regio on Ganymede N85-23660
Importance of the tectonic motions on Ganymede N85-23661
Geology of the Ganymede quadrangle Jg7 N85-23665

GAPS (GEOLOGY)
Ridged plains of Lunae Planum: Thickness distribution revised N85-23559
Mechanisms of basalt-plains ridge formation N85-23643
Terrestrial analogs for planetary wrinkle ridges N85-23644

GAS DYNAMICS
Internal fluid mechanism of solid propellant rocket motors N85-22544
Hypersonic flow about triangular airfoil at large angles of attack N85-22792
Gas dynamics of the barred spiral galaxy NGC 3359 N85-23465
Dynamics of gas disks in triaxial galaxies N85-23469

GAS EXCHANGE
Contribution to theory of ocean-atmosphere gas exchange N85-23134

GAS FLOW
Some unique features of isentrophic flow of gas under high pressures N85-22788
Efficiency of algorithms for gas-air channel diagnostics in gas turbine engines based on gas thermodynamic parameters N85-22823
Mathematical modeling of transient performance of gas turbine engine N85-22834

GAS GIANT PLANETS
Shock compression of liquid helium to 56 GPa (560) kbar N85-23551

GAS GUNS
Behavior of fiber-reinforced composites under dynamic tension [AD-A150619] N85-22641

GAS HEATING
Experimentally determined characteristics of vortex heaters N85-22833

GAS IONIZATION
Frictional and structural characterization of ion-nitrided low and high chromium steels [NASA-TM-86991] N85-23085

GAS PRESSURE
Ignition phenomena of bulk aluminum alloy as a function of oxygen pressure N85-22531
Molecular dynamics of propellant gases, part 2 N85-22552

GAS STREAMS
Discharge pulse phenomenology N85-22509

GAS TURBINE ENGINES
Current problems in turbomachinery fluid dynamics [AD-A150533] N85-22397
Development of a multiplane multispeed balancing system for turbine systems [NASA-CR-174750] N85-22400
The influence of fuel molecular composition upon flame-tube temperature and flame radiation in a model gas-turbine primary zone [K2S4] N85-22646
Efficiency of algorithms for gas-air channel diagnostics in gas turbine engines based on gas thermodynamic parameters N85-22823
Effect of water injection into air for turbine cooling on economy of operation of gas turbine engine with afterburning N85-22830
effect of gas stream sweeping past the effluent of a perforated plate on heat transfer inside the perforations N85-22836
Estimation of gas turbine engine boost provided by injecting water behind compressor N85-22838

GAS TURBINES
Optimal design efforts in Shanghai described N85-22386
Oxidation resistant materials for hot gas turbines and jet engines [AD-B087399L] N85-22389
Composition and photochemical reactivity of turbine engine exhaust [AD-A150559] N85-23256

GAS-METAL INTERACTIONS
Change in microstructure of heat-resistant nickel alloys upon thermal cycling in a current of gas N85-22725
Hartree-Fock interaction between a helium atom and lithium-metal: A test for the effective medium theory [AD-A150468] N85-23387

GAS-SOLID INTERACTIONS
High pressure cosmochemistry of major planetary interiors: Laboratory studies of the water-rich region of the system ammonia-water N85-23549

GASIFICATION
Gasification of boron oxide drops and boron slurry agglomerates in combustion gases N85-22529

GATES (CIRCUITS)
Basic EMC (electromagnetic interference) technology advancement for c3 systems. Volume 3A: Probabilistic analysis of combinational circuits with random delays [AD-A150349] N85-22666

GEOBOTANY
NASA's land remote sensing plans for the 1980's N85-23224

GEOCHEMISTRY
Reports of the Planetary Geology and Geophysics Program, 1984 [NASA-TM-87563] N85-23474
Hibonite: Crystal chemistry and origin of blue coloration in meteoritic assemblages N85-23555
Basalts of Mars: Constraints on volatile evolution N85-23610

GEOCHRONOLOGY
Crustal dynamics studies in China [NASA-CR-175617] N85-23265
Why not a constant early lunar impact rate? N85-23536
Martian terrain ages N85-23537
The geology of Mt. Hope, a silicic volcanic center in West Central Arizona N85-23571
Geomorphology and geology of the Southwestern Margaritifer Sinus and Argyre regions of Mars. Part 2: Crater size-frequency distribution curves and geomorphic unit ages N85-23601

GEODESIC LINES
Reflected wave travel-time curves in stratified media with vertically heterogeneous layers and slightly sloping curved boundaries N85-23167
Informative geometry of probability spaces [AD-A150510] N85-23371

GEODESY
Use of three omega radionavigation system position lines for solving problems in marine geodesy N85-23131
Determining vector of radiointerferometer base from observations of natural radio emission with narrow spectrum N85-23158
Development, achievements in China's cartography work N85-23434
A unified lunar control network N85-23669
The control network of Mars: October 1984 N85-23670
The control networks of the satellites of Jupiter and Saturn N85-23671
Shape of Io N85-23672

GEODETIC ACCURACY
An investigation of several aspects of LANDSAT-5 data quality — Palmer County, Shelby, mt; White sands, NM; Great Salt Lake, UT; San Matted Bridge and Sacramento, California [E85-10096] N85-23214

GEODETIC COORDINATES
Evaluating accuracy in determining position of Earth's center of mass and elements of orientation of geodetic coordinate system N85-22441
Determining vector of radiointerferometer base from observations of natural radio emission with narrow spectrum N85-23158
Study of phase radiogeodetic systems with phase-locked loops N85-23172

GEODETIC SURVEYS
Consideration of heterogeneity of gravity fields in local high precision geodetic constructions N85-23169
Mathematical modeling of results of geometric leveling in variable gravity field N85-23170
Crustal dynamics project: Catalogue of site information [NASA-TM-87452] N85-23258

GEODYNAMICS
Absolute movement of Pacific Ocean plate during last 120 million years N85-23126
Crustal dynamics project: Catalogue of site information [NASA-TM-87452] N85-23258
Crustal dynamics studies in China [NASA-CR-175617] N85-23265

GEOELECTRICITY
Discrimination of normal and anomalous magnetic and electric fields in geoelectromagnetic variations N85-23166

GEOGRAPHY
Hexagonal data base study [AD-A150176] N85-23448

GEOLOGICAL FAULTS
Arctic-North Atlantic rift megasystem N85-23117
Crustal and upper mantle density model of Owen fault zone N85-23144
Numerical modeling of plane stick-slip fault N85-23150
Study of geological media based on scattered earthquake waves N85-23168
Crustal dynamics project: Catalogue of site information [NASA-TM-87452] N85-23258
Normal-fault and fold development in sedimentary rocks above a pre-existing basement normal fault N85-23259
Crustal dynamics studies in China [NASA-CR-175617] N85-23265
Volcanism and rift formation in Beta Regio, Venus: New radar results N85-23507

Volcanic debris flows in the Elysium region of Mars N85-23560
Geomorphology and geology of the Southwestern Margaritifer Sinus and Argyre regions of Mars. Part 1: Geological and geomorphological overview N85-23600
On the absence of strike-slip faults from the planets and satellites N85-23645
Lunar mascon loading: An example of the importance of fault initiation depth on fault type predictions from stresses on planetary surfaces N85-23646
Elysium region, Mars: Tests of lithospheric loading models for the formation of tectonic features N85-23650
Creep of ice: Further studies N85-23655
Fault offsets and lateral crustal movement on Europa N85-23656

GEOLOGICAL SURVEYS
GADB: A database facility for modelling naturally occurring geophysical fields N85-23217
NASA's land remote sensing plans for the 1980's N85-23224

GEOLOGY
Geological remote sensing develops rapidly, finds broad applications N85-22848
Application of field X-ray: Radiometric analysis in exploratory geology and means for its improvement N85-23176
Possibilities of aerial electric prospecting by long cable method for detecting poorly conducting strata N85-23177
Proceedings of the Geoscience Instrumentation Workshop
[DE85-004359] N85-23268
China report: Science and technology
[JPRS-CST-85-003] N85-23433
Rapid advances in geological work N85-23437
Dark halo craters and the thickness of grooved terrain on Ganymede N85-23484
Polar cap formation on Ganymede N85-23486
Studies of planetary rings N85-23488
Mapping and geological analysis of Mercury and Venus radar ranging data N85-23633
Bouguer images of the North American craton N85-23648

GEOMAGNETIC LATITUDE
Characteristics of latitude effect on cosmic ray charged component in atmosphere at altitudes 3-5 KM N85-22413

GEOMAGNETIC TAIL
Periodic substorm activity in the geomagnetic tail
[NASA-CR-175629] N85-23409

GEOMAGNETISM
One-dimensional model of auroral magnetic force with longitudinal current and cyclotron heating of ions N85-22424
Auroral-polar cap environment and its impact on spacecraft plasma interactions N85-22484
Calculation of secondary-electron escape currents from inclined-spacecraft surfaces in a magnetic field N85-22491
Geomagnetic precursors of intensive earthquakes in the 1-0.-2 Hz frequency range of geomagnetic pulsations N85-23178
Solution of direct magnetometric problem on spherical Earth N85-23179
Geomagnetic field dynamics N85-23182
MAGSAT anomaly field data of the crustal properties of Australia
[E85-10100] N85-23215
GADB: A database facility for modelling naturally occurring geophysical fields N85-23217
Data selection techniques in the interpretation of MAGSAT data over Australia N85-23218

GEOMETRIC RECTIFICATION (IMAGERY)
Analysis and evaluation of the LANDSAT-4 MSS and TM sensors and ground data processing systems: Early results N85-23189
Correction and geological analysis of lunar 3.8 cm radar data N85-23634

GEOMETRICAL THEORY OF DIFFRACTION
Scattering of waves by axisymmetrical edge N85-22987

GEOMETRY
Experimental study of main rotor tip geometry and tail rotor interactions in hover. Volume 1. Text and figures
[NASA-CR-177336-VOL-1] N85-22344
Experimental study of main rotor tip geometry and tail rotor interactions in hover. Volume 2: Run log and tabulated data
[NASA-CR-177336-VOL-2] N85-22345
Magnetostatic-wave propagation in a finite YIG-Loaded rectangular waveguide
[AD-A150332] N85-22665
Mathematical modeling of results of geometric leveling in variable gravity field N85-23170
Introduction to combinatorial geometry
[DE85-003266] N85-23364
Informative geometry of probability spaces
[AD-A150510] N85-23371
Quantitative analyses of planetary reflectance spectra N85-23625

GEOMORPHOLOGY
Planetary geology in the 1980s
[NASA-SP-467] N85-23457
Geomorphic classification of lava flows on Io N85-23480
Martian terrain ages N85-23537
Average spacing for rings of individual multi-ring basins is 2.0(0.5)D N85-23541
Ring-diameter ratios for multi-ring basins average 2.0(0.5)D N85-23542
Morphology and mechanics of terraces in lunar craters N85-23543
Interaction of Martian flow ejecta blankets with pre-existing impact craters: Morphological observations N85-23546
Ripple ring basins on Ganymede and Callisto N85-23547
Morphologic evolution of the Mount St. Helens crater area, Washington N85-23568
The geology of Mt. Hope, a silicic volcanic center in West Central Arizona N85-23571
A silicic shield volcano in Bolivia N85-23572
Martian fretted terrain morphometry interpreted using principal components analysis N85-23597
Distribution and properties of large symmetric knobs on Mars N85-23598
Enigmatic hills of the mottled plains, Mare Acidalium quadrangle (MC-4), Mars N85-23599
Geomorphology and geology of the Southwestern Margaritifer Sinus and Argyre regions of Mars. Part 1: Geological and geomorphological overview N85-23600
Geomorphology and geology of the Southwestern Margaritifer Sinus and Argyre regions of Mars. Part 2: Crater size-frequency distribution curves and geomorphic unit ages N85-23601
Geomorphology and geology of the Southwestern Margaritifer Sinus and Argyre regions of Mars. Part 3: Valley types and distribution N85-23602
Geomorphology and geology of the Southwestern Margaritifer Sinus and Argyre regions of Mars. Part 4: Flow ejecta crater distribution N85-23603
The geomorphology of Rhea N85-23606
Kasei Vallis of Mars: Dating the interplay of tectonics and geomorphology N85-23654

GEOPHYSICAL FLUIDS
Magnetic location of Earth's core-mantle boundary and estimates of the adjacent fluid motion N85-23260

GEOPHYSICS
Aeronautical Engineering: A continuing bibliography with indexes, supplement 185
[NASA-SP-7037(185)] N85-22342
USSR report: Earth sciences
[JPRS-UES-85-002] N85-23116
Application of field X-ray: Radiometric analysis in exploratory geology and means for its improvement N85-23176
Reports of the Planetary Geology and Geophysics Program, 1984
[NASA-TM-87563] N85-23474
Planetary interior modeling and tectonic implications N85-23649

GEOPOTENTIAL
Approximate perturbing part of geopotential by polynomials of stipulated form N85-22448

GEOSYNCHRONOUS ORBITS
Design guidelines for assessing and controlling spacecraft charging effects N85-22500
Development of a continuous broad-energy-spectrum electron source N85-22507
Automatic charge control system for satellites N85-22508

GEOTEMPERATURE
Determining deep heat flow and rate of horizontal percolation from temperature measurements in aquifer N85-23180

GEOTHERMAL ENERGY EXTRACTION
Thermohydrodynamic model: Hydrothermal system, shallowly seated magma chamber N85-23173

GEOTHERMAL RESOURCES
Normal and anomalous geothermal fields and their relationship to hierarchy of geological bodies N85-23163
Thermohydrodynamic model: Hydrothermal system, shallowly seated magma chamber N85-23173

GERMANIUM
Shuttle flight test of an advanced gamma-ray detection system
[AD-A150316] N85-22469
Time resolved X-ray studies during pulsed laser irradiation of Ge
[DE85-005263] N85-23083

GIOTTO MISSION
Giotto solar array: Design, manufacture and test N85-22589

GLACIERS
Catastrophic-flood features in Swedish Lapland as a terrestrial analog for Martian channel flows N85-23587

GLACIOLOGY
Antarctic glaciation, or what are catastrophes in Earth's history N85-23118
Numerical experiments with simple model of ocean climate N85-23123
Reports of the Planetary Geology and Geophysics Program, 1984
[NASA-TM-87563] N85-23474

GLANDS (SEALS)
Life testing of rubber seals — aircraft hydraulic systems
[AD-A143193] N85-23086

GLASS
Densification and deformation in the presence of a liquid phase
[DE85-005101] N85-22763
Experimental methds for quenching structures in lunar-analog silicate melts: Variations as a function of quench media and composition N85-23554

GLASS FIBER REINFORCED PLASTICS
Stability of three-layer glass-reinforced plastic shells of rotation N85-22813

GLASS FIBERS
Development and study of two-matrix glass fiber composite with increased transverse deformation N85-22700

GLASS LASERS
Research, development of laser glasses in China N85-23439

GLASSY CARBON
Experimental study of enthalpy of quasimonocrystal of graphite and carbon glass in temperature range of 2890-3818 deg K N85-22751

GLOW DISCHARGES
Frictional and structural characterization of ion-nitrided low and high chromium steels
[NASA-TM-86891] N85-23085

GOVERNMENT PROCUREMENT
Copyright law, computer software, and government acquisition
[AD-A150347] N85-23453

GRADIENTS
Edge detection in SAR imagery using gradient operators — synthetic aperture radar (SAR)
[AD-A149411] N85-22662
Method for processing broad-profile data N85-23185

GRAIN BOUNDARIES
Micromechanical modeling of microstructural damage in creeping alloys
[DE85-003925] N85-22671
Grain boundaries in NiO
[DE85-006129] N85-22687
Dependence of superplastic flow on state of grain boundaries N85-22689
Drift fields and boundary conditions at grain boundaries in bipolar P/N junction silicon devices N85-22879
Investigation of the effect of annealing on the dislocation and sub-grain boundary content of solvent-evaporation-grown CdTe
[AD-A144087] N85-23415

GRAINS (FOOD)
Operational performance of the photovoltaic-powered grain mill and water pump at Tangaye, Burkina Faso (formerly Upper Volta)
[NASA-TM-86970] N85-23243

GRAMMARS
Construction of a menu-based system
[NASA-CR-172560] N85-23321

GRANTS
Small business innovation research: Abstracts of 1984. Phase 1 awards
[NASA-TM-87427] N85-23431

GRAPHIC ARTS
Draftsman displays: A graphical technique for exploratory data analysis
[AD-A150515] N85-22775
Digital laser platemaker modifications
[AD-A150190] N85-23074

GRAPHITE
Experimental study of enthalpy of quasimonocrystal of graphite and carbon glass in temperature range of 2890-3818 deg K N85-22751

GRAPHITE-EPOXY COMPOSITES
Longitudinal splitting in unidirectional composites, analysis and experiments
[NASA-CR-3881] N85-22639

Development of epoxy matrices for filament-wound graphite structures
[DE85-003674] N85-22642

GRAPHS (CHARTS)
Introduction to CHART: A graphic analysis and display system, revision
[DE85-004612] N85-23335

GRATINGS (SPECTRA)
Reflex attachment for line alignment in spectral diffraction devices N85-22794

GRAVIMETRY
Determination of density of the crust and upper mantle from deep seismic sounding and gravimetry, 2 N85-23153
Polynomial parameterization in inverse gravimetric problem N85-23174

GRAVITATION
Venus gravity: Global field results N85-23512

GRAVITATIONAL EFFECTS
Averaging of equations of cometary orbital motion with allowance for nongravitational effects N85-22411
Lagrangian solutions in photogravitational restricted circular three-body problem N85-22416
Periodic movements of axisymmetrical satellite about center of mass due to gravitational moment N85-22783

GRAVITATIONAL FIELDS
Consideration of heterogeneity of gravity fields in local high precision geodetic constructions N85-23169
Mathematical modeling of results of geometric leveling in variable gravity field N85-23170
Polynomial parameterization in inverse gravimetric problem N85-23174
Gravity field of Venus and comparison with Earth N85-23514
The support of long wavelength loads on Venus N85-23515
Gravity field of the Jovian system from Pioneer and Voyager tracking data N85-23529

GRAVITATIONAL LENSES
University of Cambridge Institute of Astronomy report of activities N85-23464

GRAVITY ANOMALIES
Polynomial parameterization in inverse gravimetric problem N85-23174
Gravity field of Venus and comparison with Earth N85-23514
The support of long wavelength loads on Venus N85-23515
Impacts in ice: Commissions of solar system crater population N85-23538

GRAVITY WAVES
Analysis and interpretation of observations of airglow at 297 nm in the Venus thermosphere N85-23473

GREEN'S FUNCTIONS
Elastic wave scattering from an interface crack in a layered half space N85-23095
Surface scattering
[AD-A150252] N85-23366

GREENHOUSE EFFECT
Modeling of mechanism of positive feedback between mean Earth surface temperature and atmospheric carbon dioxide in geologic time scale N85-23122

GRIDS
Grid generation for a pump collector
[AD-A150217] N85-23059

GRINDING (MATERIAL REMOVAL)
New technique for fluid feed in simultaneous multisurface grinding N85-22800

GRINDING MACHINES
Diamond cutters' grinders N85-22841

GRINDING MILLS
Operational performance of the photovoltaic-powered grain mill and water pump at Tangaye, Burkina Faso (formerly Upper Volta)
[NASA-TM-86970] N85-23243

GROOVES
Annular groove in compressor casing as device for control of air stream N85-22832

GROUND BASED CONTROL
Planned office and facility consolidations: To improve system effectiveness and efficiency, FY 1985-87
[AD-A150441] N85-22376

GROUND TESTS
Spacecraft environmental interactions: A joint Air Force and NASA research and technology program N85-22517
Scientific requirements for ozone measurements N85-23113

GROUND TRUTH
Intra-eruption geologic map from an x-band radar image during the May 18, 1980 eruption of Mount St. Helens, Washington N85-23639

GROUND WIND
Preliminary study of inphase gusts and moment force wind loads over the first 150 meters at KSC, Florida
[NASA-TM-86501] N85-23273
Summary of Meteorological Observations, Surface (SMOS), Bermuda
[AD-A150537] N85-23278
Summary of Meteorological Observations, Surface (SMOS), Beaufort, South Carolina
[AD-A150538] N85-23279

GROUP VELOCITY
Dispersion characteristics of small-mode gradient optical fibers N85-23004

GUN PROPELLANTS
Twenty-first JANNAF Combustion Meeting, volume 1
[AD-A150981] N85-22526

GUST LOADS
Dynamic wind tunnel testing for active control research N85-22352

GYRATORS
Gyrator frequency selecters with bandwidth independent of input signal level N85-23009

GYROSCOPES
Analysis of interaction of dynamically adjustable gyroscopes on elastic platform by finite-element method N85-22822

GYROSCOPIC STABILITY
Flight dynamics of axisymmetrical rotating bodies in air medium N85-22791

H

H ALPHA LINE
Increase in hydrogen emission of upper atmosphere following launches of space vehicles N85-22431

HABITABILITY
NASA's land remote sensing plans for the 1980's N85-23224

HALF SPACES
Elastic wave scattering from an interface crack in a layered half space N85-23095

HALLEY'S COMET
Averaging of equations of cometary orbital motion with allowance for nongravitational effects N85-22411
History and future views on solar cells of Japanese scientific satellites N85-22566
Giotto solar array: Design, manufacture and test N85-22589
Development of Halley's Comet explorer PLANET-A solar array N85-22608
Research in planetary studies and operation of Mauna Kea Observatory
[NASA-CR-175618] N85-23460
Halley's Comet, a bibliography
[LC-84-600109] N85-23674

HALOS
Dark halo craters and the thickness of grooved terrain on Ganymede N85-23484

HARDENING (MATERIALS)
Thermal hardening of welded joints in titanium alloys with various structures N85-22734

HARMONIC OSCILLATORS
Coupled-cavity gyrotrons with mode conversion N85-22967

HARMONICS
The effects of internal waves on acoustic normal modes
[AD-A150235] N85-23379

HARNESSES
Tight Ribbon Arm Protection (TRAP) for aircrewman ejection
[AD-A150464] N85-23303

HARTREE APPROXIMATION
Hartree-Fock interaction between a helium atom and lithium-metal: A test for the effective medium theory
[AD-A150468] N85-23387

HAWAII
Emplacement of long lava flows on Mauna Loa (Hawaii) and Alba (Mars) N85-23563
Thermal infrared observations of lava flows during the 1984 Mauna Loa eruption N85-23564
Field measurements of the 1983 Royal Gardens lava flows, Kilauea Volcano, and 1984 Mauna Loa lava flows, Hawaii N85-23565
Surface structures of Hawaiian lavas N85-23566

HAZARDS
Astronaut hazard during free-flight polar EVA N85-22522
Electric and hybrid vehicle demonstration project
[DE85-003939] N85-23455

HAZE
Water-ice clouds on Mars: Location and seasonal variation N85-23611

HEAT BALANCE
Breakdown of thin plates by radiation N85-22709
Accurate albedos of the brightest regions on Io N85-23618

HEAT EXCHANGERS
Development of a single-family absorption chiller for use in a solar heating and cooling system, phase 3, volume 2
[DE85-003218] N85-23253

HEAT OF FUSION
Natural convection during heat accumulation by substances with change of aggregate state N85-22787

HEAT PUMPS
Magnetic refrigeration and heat pumping design options
[DE85-003405] N85-23064
Cooling performance improvement of a horizontal ground coupled heat pump
[DE85-002470] N85-23065

HEAT RESISTANT ALLOYS
Orientation and temperature dependence of some mechanical properties of the single-crystal nickel-base superalloy Rene N4. 3: Tension-compression anisotropy
[NASA-TM-86982] N85-22660
USSR report: Materials science and metallurgy
[JPRS-UMS-85-002] N85-22688
Comparison of dynamic-tension and constant-load strength characteristics of heat-resistant materials N85-22722
Some specifics of development of fatigue and creep in heat-resistant alloys with asymmetrical multicycle loading N85-22724
Change in microstructure of heat-resistant nickel alloys upon thermal cycling in a current of gas N85-22725
Softening of metal near seam during welding of heat-resistant nickel alloys N85-22747
Effect of zero-wear in friction pairs operating in abrasive media N85-22801

HEAT STORAGE
Natural convection during heat accumulation by substances with change of aggregate state N85-22787
Latent heat storage in cooling systems
[DE85-005355] N85-23248
Overview of latent storage for passive solar applications
[DE85-005354] N85-23249

HEAT TRANSFER
Coupling between velocity oscillations and solid propellant combustion N85-22536
Pressure drop and coefficients of internal heat transfer necessary for transpiration cooling N85-22831
effect of gas stream sweeping past the effluent of a perforated plate on heat transfer inside the perforations N85-22836
Two-dimensional numerical model of sensible and latent heat transport in an irrigated field under advective conditions N85-23261
H-division materials physics progress
[DE85-004990] N85-23430
Classification of circular features on Venus N85-23511
Hydrovolcanism N85-23574
Physics of the inner heliosphere: Mechanisms, models and observational signatures
[NASA-CR-175832] N85-23677

HEAT TRANSMISSION
Normal and anomalous geothermal fields and their relationship to hierarchy of geological bodies N85-23163
Determining deep heat flow and rate of horizontal percolation from temperature measurements in aquifer N85-23180

HEAT TREATMENT
Influence of laser treatment of structure and mechanical properties if MA21 alloy N85-22713
Specifics of laser heat treatment of high steel tools N85-22714
Specifics of kinetics of polymorphous conversion upon heating of low carbon steels N85-22721
Effect of zero-wear in friction pairs operating in abrasive media N85-22801
Stability of three-layer glass-reinforced plastic shells of rotation N85-22813
Microstructural study on the processing and properties of high-field A15 superconducting materials
[DE85-004652] N85-23423

HEATERS
Experimentally determined characteristics of vortex heaters N85-22833

HEATING
Influence of substrate heating and thermal annealing on the surface crystallinity in single Si crystals implanted with high doses of (16)O
[DE85-005264] N85-23428
Thermal and thermoelastic effects in rolling/sliding contacts
[AD-A150435] N85-23429

HEIGHT
Analysis of the inflow layer and air-sea interactions in Hurricane Frederic (1979)
[NASA-CR-175616] N85-23271
HELICOPTER TAIL ROTORS
Experimental study of main rotor tip geometry and tail rotor interactions in hover. Volume 1. Text and figures
[NASA-CR-177336-VOL-1] N85-22344
Experimental study of main rotor tip geometry and tail rotor interactions in hover. Volume 2: Run log and tabulated data
[NASA-CR-177336-VOL-2] N85-22345
HELICOPTER WAKES
Study for prediction of rotor/wake/fuselage interference, part 1
[NASA-CR-177340-VOL-1] N85-22346
Study for prediction of rotor/wake/fuselage interference. Part 2: Program users guide
[NASA-CR-177340-VOL-2] N85-22347
HELICOPTERS
Study for prediction of rotor/wake/fuselage interference, part 1
[NASA-CR-177340-VOL-1] N85-22346
Study for prediction of rotor/wake/fuselage interference. Part 2: Program users guide
[NASA-CR-177340-VOL-2] N85-22347
Ground evaluation of helicopter air-to-air warfare N85-22360
A community survey of helicopter noise annoyance conducted under controlled noise exposure conditions
[NASA-TM-86400] N85-23374
An experimental investigation of the chopping of helicopter main rotor tip vortices by the tail rotor
[NASA-CR-177338] N85-23376
HELIUM ATOMS
Helium atoms in interstellar and interplanetary space. II: Determination of direction of interstellar gas motion relative to Sun N85-22425
Hartree-Fock interaction between a helium atom and lithium-metal: A test for the effective medium theory
[AD-A150468] N85-23387
HELIUM HYDROGEN ATMOSPHERES
Shock compression of liquid helium to 56 GPa (560) kbar N85-23551
HELIUM ISOTOPES
Outlook for realization of proximity effect and Josephson direct current in helium-2 N85-22956
HETEROGENEITY
Temperature effects of heterogenizated annealing on structure and properties of V95 aluminum alloy N85-22692
Consideration of heterogeneity of gravity fields in local high precision geodetic constructions N85-23169
HETEROJUNCTION DEVICES
Comparative study of GaAs solar cell potentialities for space applications N85-22577
GaAs and 3-5 compound solar cells status and prospects for use in space N85-22580
HETEROJUNCTIONS
Development of a planar heterojunction bipolar transistor for very high speed logic
[AD-A150374] N85-22895
HIERARCHIES
Normal and anomalous geothermal fields and their relationship to hierarchy of geological bodies N85-23163
The hierarchical database decomposition approach to database concurrency control
[AD-A150612] N85-23450
HIGH ALTITUDE BALLOONS
Observation of cosmic ray flux variations in stratosphere N85-22430
HIGH ALTITUDE ENVIRONMENTS
Armed forces special Symposium on Medicine of Altitudes N85-23441
HIGH CURRENT
Surface interactions and high-voltage current collection N85-22493
Collective acceleration of ions using high current relativistic electron beams
[DE85-004889] N85-23393
HIGH ENERGY ELECTRONS
Longitude and pitch-angle distributions of streams of high-energy electrons under Earth's radiation belts N85-22415
HIGH ENERGY INTERACTIONS
Experimental studies of elementary particle interactions at high energies
[DE85-004795] N85-23394
HIGH FREQUENCIES
Computer aided antenna design and frequency selection for HF communications
[AD-A150485] N85-22869
Coupled-cavity gyrotrons with mode conversion N85-22967
HIGH POWER LASERS
Research, development of laser glasses in China N85-23439
HIGH PRESSURE
High-pressure rocket engine turnaround duct computational fluid dynamics analysis N85-22556
Possibility of producing monolithic composite materials based on niobium carbide N85-22707
Some unique features of isentrophic flow of gas under high pressures N85-22788
High pressure cosmochemistry of major planetary interiors: Laboratory studies of the water-rich region of the system ammonia-water N85-23549
Theoretical thermodynamics of mixtures at high pressures N85-23550
HIGH RESOLUTION
HREELS and Auger studies of conducting polymers
[DE85-004541] N85-22764
Hot spots on Io: Correlation of infrared emission and visible reflectance N85-23475
Surfaces of asteroids and cometary nuclei N85-23503
Venus surface composition from radio/radar measurements N85-23509
Automated extraction of absorption bands from reflectance special N85-23624
Viking Lander mosaics of Mars N85-23667
HIGH SPEED
Development of a multiplane multispeed balancing system for turbine systems
[NASA-CR-174750] N85-22400
Specifics of laser heat treatment of high steel tools N85-22714
HIGH TEMPERATURE
High temperature antifriction properties of Ti sub 1-sub xNb sub x C sub 0.5N sub 0.5 alloys N85-22715
Degassification of silicon nitride powders of various origins N85-22718
HIGH TEMPERATURE GASES
Molecular dynamics of propellant gases, part 2 N85-22552
HIGH TEMPERATURE PLASMAS
Spacecraft-environment interaction: The environmental plasma aspect N85-22479
Ruby wavefront-conjugation laser for obtaining high temperature plasma N85-22795
HIGH TEMPERATURE TESTS
Experimental study of enthalpy of quasimonocrystal of graphite and carbon glass in temperature range of 2890-3818 deg K N85-22751
HIGH VOLTAGES
Spacecraft Environmental Interactions Technology, 1983
[NASA-CP-2359] N85-22470
Non-self-maintained high-voltage low-pressure discharge N85-23037
HIGHLANDS
Mapping structures characteristic of the highland boundary scarp on Mars N85-23595
Mars: Stratigraphy of western highlands and polar regions N85-23653
HIGHWAYS
Optimal design efforts in Shanghai described N85-22386
HILSCH TUBES
Experimentally determined characteristics of vortex heaters N85-22833
HISTOGRAMS
Normal and anomalous geothermal fields and their relationship to hierarchy of geological bodies N85-23163
HISTORIES
Feoktistov recalls period leading to Gagarin spaceflight N85-22451
HMX
Effects of HMX addition on the combustion of energetic binders N85-22560
The chemistry of RDX and HMX cluster ions N85-22561
HOLOGRAPHY
Solid propellant combustion diagnostics and automated data retrieval from holograms N85-22527
Laser applications in last 10 years reviewed N85-22844
HOMOGENEITY
Surface scattering
[AD-A150252] N85-23366
HOMOJUNCTIONS
Comparative study of GaAs solar cell potentialities for space applications N85-22577
Investigation of high output gallium arsenide solar cells N85-22578
GaAs and 3-5 compound solar cells status and prospects for use in space N85-22580
HONEYCOMB STRUCTURES
Technological parameters of diffusion welding processes in honeycomb titanium alloy structures N85-22739
HORIZONTAL ORIENTATION
Horizontal deflection TS-257 N85-22926
HORN ANTENNAS
Beamwidth control in pyramidal horns
[R-NIAS-27] N85-22853
HOT PRESSING
Particulate toughened silicon carbide
[DE85-004797] N85-22643
Dispersed-metal-toughened alumina
[NASA-CR-174687] N85-22758
HOT SURFACES
Problems with electrical interference between solar generators and shunt type regulators N85-22607
HOUSEHOLDER TRANSFORMATIONS
Implementation of some concurrent algorithms
[DE85-004687] N85-23334
HOVERING
Experimental study of main rotor tip geometry and tail rotor interactions in hover. Volume 1. Text and figures
[NASA-CR-177336-VOL-1] N85-22344
Experimental study of main rotor tip geometry and tail rotor interactions in hover. Volume 2: Run log and tabulated data
[NASA-CR-177336-VOL-2] N85-22345
HTPB PROPELLANTS
Effect of variable solid phase thermal properties on propellant combustion N85-22547
HUBBLE SPACE TELESCOPE
Innovative research in the design and operation of large telescopes for space: Aspects of giant telescopes in space
[NASA-CR-175626] N85-23462
HUMAN BEHAVIOR
Assessing the behavior and performance of teams in organizations: The case of air transport crews
[AD-A150359] N85-23302
HUMAN BEINGS
Human cognition and intelligence: Towards an integrated theoretical perspective
[CSIR-SR-PERS-350] N85-23300
HUMAN BODY
Study of effective physiological temperature N85-22780
Distribution of radium and plutonium in human bone
[DE85-005025] N85-23298
HUMAN FACTORS ENGINEERING
TASS update on unmanned flight of Salyut-7 N85-22404
Construction of a menu-based system
[NASA-CR-172560] N85-23321
Principles of software engineering environment design
[AD-A150352] N85-23324
HUMAN PERFORMANCE
Assessing the behavior and performance of teams in organizations: The case of air transport crews
[AD-A150359] N85-23302
Personal decision making: The influence of perceived locus of control and degree of rationality on information seeking strategies N85-23446
HUMAN TOLERANCES
Research on the effect of noise at different times of day: Models, methods and findings
[NASA-CR-3888] N85-23375
HUMIDITY
Study of effective physiological temperature N85-22780
Two-dimensional numerical model of sensible and latent heat transport in an irrigated field under advective conditions N85-23261
Portable Automated Mesonet (PAM) data from the 1980 experiment in Anderson Creek Valley
[DE85-004361] N85-23262
HURRICANES
Analysis of the inflow layer and air-sea interactions in Hurricane Frederic (1979)
[NASA-CR-175616] N85-23271
HYDRATES
Chemical weathering of soils from the dry valleys of Antarctica: A terrestrial analog of Martian weathering processes N85-23628
HYDRAULIC ANALOGIES
Catastrophic-flood features in Swedish Lapland as a terrestrial analog for Martian channel flows N85-23587
HYDRAULIC CONTROL
Hydraulic brakes for industrial robots N85-22806
HYDROCARBON COMBUSTION
Comprehensive mechanisms for combustion chemistry: An experimental and numerical study with emphasis on applied sensitivity analysis
[DE85-000173] N85-22656
HYDRODYNAMIC COEFFICIENTS
Hydraulic brakes for industrial robots N85-22806

HYDRODYNAMICS
Coupled acoustic and hydrodynamic wave instabilities N85-22538
Application of modulated hydrodynamic voltammetry to the study of anodic electrocatalysis [DE85-004182] N85-22653
Turbulent flows of surfacant solutions [AD-B069137L] N85-23058
Calculation of level surface in problems of large-scale ocean circulation N85-23136
Double and inverse Taylor-Hogg vortices in a stratified ocean N85-23137
HYDROELASTICITY
Time dependent interaction of internal pressure wave with system of two spherical shells N85-22809
Thermal and thermoelastic effects in rolling/sliding contacts [AD-A150435] N85-23429
HYDROGEN
Increase in hydrogen emission of upper atmosphere following launches of space vehicles N85-22431
Adsorption site, adsorption energy and normal vibration frequency of H/Ni(100) via total energy calculations [AD-A150555] N85-23388
Gas dynamics of the barred spiral galaxy NGC 3359 N85-23465
HYDROGEN ATOMS
Dipole active surface vibrational resonances on clean and hydrogen covered Ni(110) [AD-A150546] N85-23420
HYDROGEN BONDS
Influence of hydrogen bonding in block copolymers and their blends N85-22752
HYDROGEN EMBRITTLEMENT
Delayed cracking strength of experimental grades of 42 CD 4 steel in aqueous H2S surroundings [BLL-T6419/BG/LRS/LRST738/84] N85-22658
Hydrogen effects in austenitic stainless steels based on the Fe-Cr-Mn-N system [DE85-003617] N85-22672
HYDROGEN IONS
Three-dimensional calculation of shuttle charging in polar orbit N85-22486
HYDROGEN MASERS
Experimental studies of low temperature surface interactions of atomic hydrogen using maser technique [AD-A150216] N85-22647
HYDROGEN PLASMA
Frictional and structural characterization of ion-nitrided low and high chromium steels [NASA-TM-86991] N85-23085
HYDROGEOLOGY
Mars: Long term changes in the state and distribution of H2O N85-23593
HYDROLOGY
Effects of fracture roughness on fluid flow through a single deformable fracture [DE85-004593] N85-23062
Snow reflectance from Thematic Mapper N85-23205
Hydrovolcanism N85-23574
Paleohydrologic implications of valley networks of Mars N85-23585
Catastrophic-flood features in Swedish Lapland as a terrestrial analog for Martian channel flows N85-23587
HYDROLOGY MODELS
World ocean level oscillations and their relationship to change in inflow of continental waters N85-23133
Remote Sensing of Snow and Evapotranspiration [NASA-CP-2363] N85-23223
Snowmelt-runoff model utilizing remotely-sensed data N85-23226
Snowmelt runoff model in Japan N85-23227
Application of Martinec-Rango model to river basin in Japan N85-23228
HYDROTHERMAL SYSTEMS
Thermohydrodynamic model: Hydrothermal system, shallowly seated magma chamber N85-23173
Determining deep heat flow and rate of horizontal percolation from temperature measurements in aquifer N85-23180
HYPERONS
Cooling of neutron stars with hyperons [DE85-004641] N85-23472
HYPERSONIC AIRCRAFT
Aerodynamic heating rate distributions induced by trailing edge controls on hypersonic aircraft configurations at Mach 8 [NASA-TM-87453] N85-22370
HYPERSONIC FLOW
Hypersonic flow about trianguler airfoil at large angles of attack N85-22792
HYPERVELOCITY IMPACT
Plasma production by meteoroid impact N85-23492
Progress on studies of early intense cratering N85-23535
Martian terrain ages N85-23537
Morphology and mechanics of terraces in lunar craters N85-23543
Newly discovered Martian impact basins N85-23544
HYPSOGRAPHY
Hypsometric features on Venus N85-22439

I

ICE
Latent heat storage in cooling systems [DE85-005355] N85-23248
Variation of Arctic cloud cover in summer [DE85-004507] N85-23285
Patterns of fracture and tidal stresses due to nonsynchronous rotation: Implications for fracturing on Europa N85-23483
Comet thermal modelleg N85-23505
High pressure cosmochemistry of major planetary interiors: Laboratory studies of the water-rich region of the system ammonia-water N85-23549
Transformation of polar ice sublimate residue into Martian circumpolar sand N85-23580
Mars: Long term changes in the state and distribution of H2O N85-23593
Creep of ice: Further studies N85-23655
ICE ENVIRONMENTS
Planetary analogs in Antarctica: Icy satellites N85-23605
ICELAND
Structure of Iceland and ocean floor spreading N85-23159
IDAHO
The geology of East Butte, a rhyolitic volcanic dome on the Eastern Snake River Plain, Idaho N85-23570
IDENTIFYING
Approximation in optimal control and identification of large space structures [AD-A150323] N85-23351
IGNEOUS ROCKS
The search for igneous materials at the Viking landing sites N85-23609
Bouguer images of the North American craton N85-23648
IGNITION
Ignition of mixtures of SiH sub 4, CH sub 4, O sub 2, and Ar or N sub 2 behind reflected shock waves [NASA-TP-2415] N85-22395
Ignition phenomena of bulk aluminum alloy as a function of oxygen pressure N85-22531
Combustion of zirconium carbide N85-22532
ILLUMINANCE
Quantitative analyses of planetary reflectance spectra N85-23625
IMAGE ANALYSIS
Method for approximating autocorrelation functions for describing areal photoimage features N85-22443
Experience in automated interpretation of aerospace photographs N85-22444
Geoindication method for interpreting aerial and space photographs: Status and prospects N85-22445
Edge detection in SAR imagery using gradient operators — synthetic aperture radar (SAR) [AD-A149411] N85-22662
An investigation of several aspects of LANDSAT-5 data quality — Palmer County, Shelby, mt; White sands, NM; Great Salt Lake, UT; San Matted Bridge and Sacramento, California [E85-10096] N85-23214
Photometric analysis of Jupiter-illuminated images of Io N85-23620
IMAGE ENHANCEMENT
A concept for the processing and display of Thematic Mapper data N85-23196
IMAGE INTENSIFIERS
Research in the optical sciences [AD-A150196] N85-23401
IMAGE PROCESSING
Method for approximating autocorrelation functions for describing areal photoimage features N85-22443
Electronic generation of text for television [BBC-RD-1984/14] N85-22856
Nature of seismic images with amplitude and time fluctuations of recorded oscillations N85-23156
LANDSAT-4 Science Characterization Early Results. Volume 4: Applications — agriculture, soils land use, geology, hydrology, wetlands, water quality, biomass identification, and snow mapping [E85-10070] N85-23186
A concept for the processing and display of Thematic Mapper data N85-23196
Early results of investigations of LANDSAT 4 Thematic Mapper and Multispectral Scanner applications — Washington, D.C. N85-23200
Comparative techniques used to evaluate Thematic Mapper data for land cover classification in Logan County, West Virginia N85-23209
Comparison of MSS and TM data for landcover classification in the Chesapeake Bay area: A preliminary report — Taylor's Island, Maryland N85-23210
Distribution of snow and maximum snow water equivalent obtained by LANDSAT data and degree day method N85-23229
Feature extraction assessment study [AD-A150189] N85-23239
On a mathematical structure for an image algebra [AD-A150228] N85-23348
Image data compression using uneven knots selection [AD-A150602] N85-23359
Hexagonal data base study [AD-A150176] N85-23448
Hot spots on Io: Correlation of infrared emission and visible reflectance N85-23475
Bouguer images of the North American craton N85-23648
Participation in the Mars Data Analysis Program: Analysis of cloud forms in Viking and Mariner 9 images [NASA-CR-175604] N85-23673
IMAGE RECONSTRUCTION
Image data compression using uneven knots selection [AD-A150602] N85-23359
IMAGE RESOLUTION
Overview of TM applications research reports N85-23187
Analysis and evaluation of the LANDSAT-4 MSS and TM sensors and ground data processing systems: Early results N85-23189
Characterization of LANDSAT-4 TM and MSS image quality for the interpretation of California's agricultural resources — Central Valley N85-23190
Preliminary evaluation of Thematic Mapper image data quality N85-23194
IMAGERY
Relationship between brightness spectrum of photographic image and spectrum of rises on a water surface with waves N85-23171
IMAGES
A posteriori increase of resolving power of optical system forming averaged monochromatic images N85-23003
IMAGING TECHNIQUES
Grain boundaries in NiO [DE85-006129] N85-22687
A posteriori increase of resolving power of optical system forming averaged monochromatic images N85-23003
Electroacoustical imaging technique for encoding incoherent radiance fields as Gabor elementary signals [NASA-TM-86372] N85-23067
Image data compression using uneven knots selection [AD-A150602] N85-23359
Optical system [NASA-CASE-NPO-15801-1] N85-23396
IMPACT
Stagnation zone impaction on a simple terrain feature in stable flow N85-23255
Lunar origin: Role of giant impacts N85-23519
Impact cratering calculation N85-23531
Impact crater scaling laws N85-23532
IMPACT MELTS
Centrifuge impact cratering experiments N85-23533
Progress on studies of early intense cratering N85-23535
Why not a constant early lunar impact rate? N85-23536
IMPACT STRENGTH
Prediction of the resistance of structural materials to cavitation erosion [BLL-DRIC-TRANS-7435-(3623.66)] N85-22659
IMPACT TESTS
Behavior of fiber-reinforced composites under dynamic tension [AD-A150619] N85-22641
IHE material qualification tests description and criteria [DE85-004649] N85-22770
Progress on Experimental impact studies N85-23534
IMPACTORS
Progress on studies of early intense cratering N85-23535
Why not a constant early lunar impact rate? N85-23536
Martian terrain ages N85-23537
Interaction of Martian flow ejecta blankets with pre-existing impact craters: Morphological observations N85-23546
IMPLOSIONS
Prediction of the resistance of structural materials to cavitation erosion [BLL-DRIC-TRANS-7435-(3623.66)] N85-22659
IMPULSES
Axisymmetrical oscillations of shell systems subjected to impulse loads N85-22814

IMPURITIES
Americium metal preparation on the multigram scale [DE85-003735] N85-22683
Impurities in Kevlar 49 fibers [DE85-004996] N85-22767
INCOHERENT SCATTERING
Error probability during optimal noncoherent reception of binary signals in multibeam channel N85-22922
A spatially incoherent and temporally coherent source [AD-A151281] N85-23390
INDIA
Relationship of Indian monsoon intensity to time of onset N85-23120
INDIAN OCEAN
Remanent magnetization model for the broken ridge satellite magnetic anomaly N85-23219
INDUCTANCE
Piezoelectric filter with low-Q inductances N85-22932
INDUCTION MOTORS
Power control for ac motor [NASA-CASE-MFS-25861-1] N85-22877
Magnetic noise in single-machine rotating frequency converters N85-22969
INDUSTRIAL PLANTS
Optoelectronic safety system for robotized technological complex N85-22805
INDUSTRIAL SAFETY
The audiomat: An automatic audiometer for use in occupational audiometry [DRIC-T-7138] N85-23294
INDUSTRIES
Current plans for development of chemical industry N85-22633
INELASTIC COLLISIONS
Capture of planetesimals into a circumterrestrial swarm N85-23522
Accumulation of the terrestrial planets N85-23524
INEQUALITIES
Schur-Ostrowski theorems for functionals on l1(0,1) [AD-A150193] N85-23346
INERTIAL NAVIGATION
Avionics Flight Evaluation System (AFES) N85-22357
INFERENCE
Multivariate analysis and its applications [AD-A150324] N85-23352
INFORMATION
Accomplishments of Institute of Cartography summarized N85-23435
INFORMATION DISSEMINATION
Electronics Engineering Department EE Technical Review [UCRL-50025-84-1] N85-22887
INFORMATION RETRIEVAL
Precedency control and other semantic integrity issues in a workbench database N85-23220
General design considerations of an Air Force information system [AD-A150611] N85-23449
INFORMATION SYSTEMS
Performance evaluation of distributed systems with unbalanced flows: An analysis of the INFOPLEX data storage hierarchy [AD-A150528] N85-23328
Intel iDIS evaluation [DE85-003748] N85-23451
INFORMATION THEORY
Investigation of influence of communications link and synchronization error on noise tolerence of group transmission of binary information based on orthogonal Walsh function N85-23026
A preliminary comparison of the information content of data from the LANDSAT 4 Thematic Mapper and Multispectral Scanner — Arkansas N85-23199
A perspective on multiaccess channels [AD-A150163] N85-23322
INFRARED ABSORPTION
Infrared aerosol absorption index N85-23147
INFRARED ASTRONOMY
BIG MAC: A bolometer array for mid-infrared astronomy, Center Director's Discretionary Fund [NASA-TM-86502] N85-23463
INFRARED ASTRONOMY SATELLITE
Dynamics of long-period comets N85-23506
INFRARED DETECTORS
Performance estimate of a reflecting light pipe for infrared detectors [AD-A141269] N85-23398
BIG MAC: A bolometer array for mid-infrared astronomy, Center Director's Discretionary Fund [NASA-TM-86502] N85-23463
INFRARED RADIATION
Below-room-temperature water-vapor continuum absorption within the 8- to 10 micron atmospheric transmission window [TR-0084(4945-09)-1] N85-23266
INFRARED RADIOMETERS
Analysis of SMIRR data for volcanic and sedimentary terrains of the trane-Pecos region, Texas N85-23626
INFRARED SCANNERS
Thermal infrared observations of lava flows during the 1984 Mauna Loa eruption N85-23564
INFRARED SPECTRA
A method for estimating soil moisture availability [NASA-CR-175606] N85-23238
Water-ice clouds on Mars: Location and seasonal variation N85-23611
Reassignment of the iron (3) absorption bands in the spectra of Mars N85-23614
Participation in the Mars Data Analysis Program: Analysis of cloud forms in Viking and Mariner 9 images [NASA-CR-175604] N85-23673
INFRARED SPECTROMETERS
Hot spots on Io: Correlation of infrared emission and visible reflectance N85-23475
INFRARED SPECTROSCOPY
Investigation of dynamics of radiation spectrum of injection lasers by infrared impulse Fourier spectroscopy N85-23047
INHOMOGENEITY
Boundary velocities of longitudinal seismic waves and lateral inhomogeneities of upper ocean mantle N85-23165
INJECTION LASERS
Investigation of dynamics of radiation spectrum of injection lasers by infrared impulse Fourier spectroscopy N85-23047
INJURIES
Interaction of metals and metalloids with biomembranes [DE85-004902] N85-23293
INLET FLOW
Effects of inlet distortion on a static pressure probe mounted on the engine hub in an F-15 airplane [NASA-TP-2411] N85-22394
Experimentally determined characteristics of vortex heaters N85-22833
INPUT
Theory of diaphragm light modulators with electrical input signal N85-23002
Gyrator frequency selectors with bandwidth independent of input signal level N85-23009
INSTRUMENT ORIENTATION
Operational experience with ion concentration sensors in orientation systems N85-22422
Evaluating accuracy in orientation of topographic photograph and satellite-centered direction from star photograph N85-22442
INSULATION
Optimization of overall dimensions of enclosures for low-voltage devices and equipment N85-23033
INSULATORS
Self-consistent simulation of plasma interactions with secondary-emitting insulators N85-22492
INTAKE SYSTEMS
The role of convective perturbations in supercritical inlet oscillations N85-22563
INTEGRAL EQUATIONS
Magnetostatic-wave propagation in a finite YIG-Loaded rectangular waveguide [AD-A150332] N85-22865
INTEGRALS
An integral representation of the generalized Euler-Mascheroni constants [NASA-TP-2456] N85-23305
INTEGRATED CIRCUITS
X-ray lithography and VLSI circuits N85-22848
Basic EMC (electromagnetic interference) technology advancement for c3 systems. Volume 3A: Probabilistic analysis of combinational circuits with random delays [AD-A150349] N85-22868
Advanced mixed-mode simulation techniques N85-22883
Low capacitance e-beam fabricated beam-lead Schottky barrier diodes [AD-A150238] N85-22888
EOS (electrical overstress) protection for VLSI (Very Large Scale Integration) devices [AD-A150333] N85-22891
High sheet resistance, arsenic implanted polycrystalline silicon for integrated circuit resistors [DE85-004355] N85-22902
Algorithm in Walsh function basis for analysis of integrated microcircuits on MOS-structures N85-23006
Synthesis of optimum smooth transition in microstrip through line on microwave integrated circuit N85-23041
Parallel test method for LSI (Large Scale Integration) microprocessors [AD-A150237] N85-23310
INTEGRATED OPTICS
Multifunctional elements for integrated optics N85-22918
Integrated optical components utilizing acoustooptic and electrooptic diffraction in micro-waveguides N85-23044
INTELLIGENCE
Human cognition and intelligence: Towards an integrated theoretical perspective [CSIR-SR-PERS-350] N85-23300
INTELSAT SATELLITES
Electrical design of the Intelsat 6 solar generator N85-22592
INTERCEPTION
Space interception guidance with uncertain factors N85-22781
INTERDIGITAL TRANSDUCERS
Experimental study of high-stability oscillator with surface-acoustic-wave resonator in feedback loop N85-23053
INTERFACES
Problems with electrical interference between solar generators and shunt type regulators N85-22607
Presentation based user interfaces [AD-A150311] N85-23311
A design analysis and implementation of a user-friendly interface for the UNIX operating system [AD-A150558] N85-23312
INTERFACIAL TENSION
Properties of materials using acoustic waves [AD-A150465] N85-23382
INTERFERENCE GRATING
Extraction of signals from background interference with unknown parameters in quantized sample N85-23013
Probability of detection of pulsed signals employing zero-gating interference suppression N85-23021
INTERFEROMETERS
Comparison reference etalon of unit laser radiation power N85-22957
INTERGRANULAR CORROSION
Role of segregated P and S in intergranular stress corrosion cracking of nickel [DE85-004547] N85-22679
INTERIOR BALLISTICS
Molecular dynamics of propellant gases, part 2 N85-22552
INTERMETALLICS
Magnetic studies of Ni3Al(Fe) compounds [DE85-005262] N85-22686
INTERMOLECULAR FORCES
Some unique features of isentrophic flow of gas under high pressures N85-22788
INTERNAL COMBUSTION ENGINES
Laboratory tests of reciprocating internal combustion engines [AD-A150143] N85-23087
INTERNAL FRICTION
Interaction of cylindrical shell with concentrated mass moving along its inner surface N85-22810
Steady-state reaction of three-layered cylindrical shell to effect of moving load N85-22811
INTERNAL WAVES
The imaging of internal waves by the SEASAT-A synthetic aperture radar [ARE(PORTLAND)TN-720/84] N85-22980
The effects of internal waves on acoustic normal modes [AD-A150235] N85-23379
INTERNATIONAL COOPERATION
INMARSAT marine satellite organization N85-22456
INTERNATIONAL SUN EARTH EXPLORER 1
Anomalously high potentials observed on ISEE N85-22503
INTERPLANETARY DUST
Evolution of grains in a turbulent solar nebula N85-23525
INTERPLANETARY MAGNETIC FIELDS
Plans for Interbol satellite experiment N85-22407
INTERPLANETARY MEDIUM
Hydromagnetic precursors of interplanetary plasma burst N85-22414
Interplanetary shock waves during April and May of 1981 N85-22434
INTERPOLATION
Digital standards conversion: Interpolation theory and aperture synthesis [BBC-RD-1984/20] N85-22957
INTERSTELLAR EXTINCTION
Dynamics of long-period comets N85-23506
INTERSTELLAR GAS
Helium atoms in interstellar and interplanetary space. II: Determination of direction of interstellar gas motion relative to Sun N85-22425

INTERSTELLAR MATTER
Dynamics of long-period comets N85-23506
INTERVALS
Confidence intervals using the regenerative method for simulation output analysis
[AD-A150147] N85-23343
INVERSIONS
Inverse behavior of silicon photovoltaic cells N85-22604
Algorithms for reconstruction of partially known, band limited Fourier transform pairs from noisy data
[AD-A150194] N85-23347
INVERTERS
Numerical simulation of inverters with I2L elements including effects of high doping level N85-23039
IO
Research in planetary studies and operation of Mauna Kea Observatory
[NASA-CR-175618] N85-23460
Hot spots on Io: Correlation of infrared emission and visible reflectance N85-23475
Io: Generation of silicate magma by shear melting at the base of a basaltic lithosphere N85-23476
Topographic evidence for shield volcanism on Io N85-23478
Sulfur volcanoes on Io? N85-23479
Sulfur oxygen processes on Io N85-23481
The violet absorber on Io: Disulfur monoxide derivatives N85-23482
Emplacement of long lava flows on Mauna Loa (Hawaii) and Alba (Mars) N85-23563
Accurate albedos of the brightest regions on Io N85-23618
Io: Precise comparison of Voyager spectral curves with laboratory measurements N85-23619
Photometric analysis of Jupiter-illuminated images of Io N85-23620
Shape of Io N85-23672
ION BEAMS
Sheath ionization model of beam emissions from large spacecraft N85-22489
System for forming and focusing high current beam of deuterium ions N85-22798
Collective acceleration of ions using high current relativistic electron beams
[DE85-004889] N85-23393
Ion transport in beam-plasma interactions
[AD-A150145] N85-23410
ION CYCLOTRON RADIATION
Lower hybrid heating and current drive, and ion cyclotron heating experiments on the Alcator C and the Versator II Tokamaks
[DE85-004918] N85-23412
ION EXCHANGING
Ion transport in beam-plasma interactions
[AD-A150145] N85-23410
ION IMPLANTATION
Experiences with implanted Back Surface Field (BSF) solar cells N85-22571
Use of markets to elucidate reacting sputtering processes
[DE85-005723] N85-22655
Study of the effects of implantation on the high Fe-Ni-Cr and Ni-Cr-Al alloys
[NASA-CR-175625] N85-22661
High sheet resistance, arsenic implanted polycrystalline silicon for integrated circuit resistors
[DE85-004355] N85-22902
Activation of Si-N modes in silicon by pulsed laser annealing
[DE85-002968] N85-23082
Influence of substrate heating and thermal annealing on the surface crystallinity in single Si crystals implanted with high doses of (16)O
[DE85-005264] N85-23428
ION INJECTION
Argon ion pollution of the magnetosphere N85-22523
ION PLATING
Corrosion of aircraft Al and Al-Zn ion plated steel fasteners N85-22666
IONIC COLLISIONS
Mean delta-ray energies in ion molecule collisions
[DE85-005524] N85-23395
IONIC REACTIONS
Use of markets to elucidate reacting sputtering processes
[DE85-005723] N85-22655
IONIZATION
Sheath ionization model of beam emissions from large spacecraft N85-22489
A simple model of electron beam initiated dielectric breakdown N85-22516
Mean delta-ray energies in ion molecule collisions
[DE85-005524] N85-23395
IONIZATION POTENTIALS
Relationship between topological and magnetic order in small metal clusters
[AD-A150547] N85-22651
IONIZING RADIATION
Periodic substorm activity in the geomagnetic tail
[NASA-CR-175629] N85-23409
IONOSPHERE
Direct measurements of severe spacecraft charging in auroral ionosphere N85-22480
Polar plasmas as observed by Dynamics Explorers 1 and 2 N85-22483
Ionospheric distortions of digital signals with wideband modulation N85-22945
IONOSPHERIC CURRENTS
One-dimensional model of auroral magnetic force with longitudinal current and cyclotron heating of ions N85-22424
Direct measurements of severe spacecraft charging in auroral ionosphere N85-22480
Three-dimensional calculation of shuttle charging in polar orbit N85-22486
IONOSPHERIC DISTURBANCES
Kinetic Rayleigh-Taylor instability theory in the ionosphere near equator N85-22911
IONOSPHERIC ION DENSITY
One-dimensional model of auroral magnetic force with longitudinal current and cyclotron heating of ions N85-22424
IONS
Operational experience with ion concentration sensors in orientation systems N85-22422
The chemistry of RDX and HMX cluster ions N85-22561
Interaction of the magnetospheric ions with the surfaces of the icy satellites of Saturn N85-23491
IRAS-ARAKI-ALCOCK COMET
Research in planetary studies and operation of Mauna Kea Observatory
[NASA-CR-175618] N85-23460
IRON
A circum-terrestrial compositional filter N85-23520
Reassignment of the iron (3) absorption bands in the spectra of Mars N85-23614
IRON ALLOYS
Formation of alumina layers on iron-base alloys
[BLL-T6418/BG/LRS/LRST737/84] N85-22657
Study of the effects of implantation on the high Fe-Ni-Cr and Ni-Cr-Al alloys
[NASA-CR-175625] N85-22661
TEM/FIM study of modulated microstructures in the Fe-Be system
[DE85-005379] N85-22678
Corrosion-resistant amorphous alloys N85-22748
Structure of amorphous films of alloys based on Fe, condensed from laser erosion products N85-22749
Energy spectrum of processes of structural relaxation of amorphous alloy FeCo70Si15B10 N85-22750
IRON OXIDES
Mechanism of burning rate enhancement by ferric oxide N85-22546
Iron oxides of Mars: Evidence for contemporary weathering N85-23613
IRRADIATION
Decomposition of VTAN alloy solid solution upon irradiation and thermal aging N85-22712
Specifics of laser heat treatment of high steel tools N85-22714
Time-resolved ellipsometry and reflectivity measurements of the optical properties of silicon during pulsed excimer laser irradiation
[DE85-005091] N85-23079
Time resolved X-ray studies during pulsed laser irradiation of Ge
[DE85-005263] N85-23063
Time-resolved reflectivity measurement of extrinsic silicon during pulsed laser irradiation
[AD-A150350] N85-23403
IRREGULARITIES
Spectral evaluation of irregularity of superconducting coaxial cables N85-23000
ISLAND ARCS
Magmatism in continent-ocean transition zone (development of ideas of A. N. Zavaritskiy) N85-23161
ITERATION
On an iterative scheme for the solution of constrained variational equations
[CSIR-TWISK-341] N85-23342
ITERATIVE SOLUTION
On an iterative scheme for the solution of constrained variational equations
[CSIR-TWISK-341] N85-23342

J

JAPAN
Interrelationship of earthquake magnitude and lithospheric-asthenospheric thermodynamic parameters in seismically active zones N85-23183
General report of the researches of snowpack properties, snowmelt runoff and evapotranspiration in Japan N85-23225
Snowmelt runoff model in Japan N85-23227
Application of Martinec-Rango model to river basin in Japan N85-23228
Analysis of NIMBUS-7 SMMR data — Hokkaido, Japan snow cover N85-23232
Estimation of regional evapotranspiration using remotely sensed land surface temperature. Part 2: Application of equilibrium evaporation model to estimate evapotranspiration by remote sensing technique — Japan N85-23234
JAPANESE SPACE PROGRAM
History and future views on solar cells of Japanese scientific satellites N85-22586
JAPANESE SPACECRAFT
Development of Halley's Comet explorer PLANET-A solar array N85-22608
JET ENGINES
Oxidation resistant materials for hot gas turbines and jet engines
[AD-B087399L] N85-22389
JET FLOW
Large amplitude forcing of a high speed 2-dimensional jet
[NASA-CR-175646] N85-22393
JET MIXING FLOW
Determination of boundary line between reverse jet and surrounding stream N85-22789
JOINTS (JUNCTIONS)
Elasticity solution of an adhesively bonded joint
[NASA-CR-175591] N85-23097
Scattering of elastic waves on fractures randomly distributed in a three-dimensional medium N85-23151
JOSEPHSON JUNCTIONS
Macroscopic quantum tunnelling in a current biased Josephson junction
[DE85-004603] N85-23424
JP-4 JET FUEL
Effects of temperature variation among droplets in an evaporating fuel spray N85-22562
JP-8 JET FUEL
Effects of temperature variation among droplets in an evaporating fuel spray N85-22562
JUPITER (PLANET)
Investigations of planetary ring phenomena N85-23487
Studies of planetary rings N85-23488
Orbital resonances and planetary accretion in the solar nebula N85-23523
JUPITER SATELLITES
Gravity field of the Jovian system from Pioneer and Voyager tracking data N85-23529

K

KALMAN FILTERS
Reference systems for the evaluation of dead-reckoning navigation equipment N85-22358
Prefiltration in Kalman filter with a priori indeterminacy N85-22939
Numerical algorithms and software for matrix Riccati equations
[AD-A150148] N85-23344
Bootstrapping the Kalman filter
[AD-A150509] N85-23370
Geophysical interpretation of Venus gravity data N85-23513
KAPTON (TRADEMARK)
Laboratory studies of Kapton degradation in an oxygen ion beam N85-22477
Kapton charging characteristics: Effects of material thickness and electron-energy distribution N85-22513
KEPLER LAWS
Averaging of equations of cometary orbital motion with allowance for nongravitational effects N85-22411
Nontraditional method for determining unperturbed orbits of unknown space objects using incomplete optical observational data N85-22417
KEROSENE
Dependence of combustion of homogeneous kerosene-air mixtures on humidity of air N85-22635
KEVLAR (TRADEMARK)
Impurities in Kevlar 49 fibers
[DE85-004996] N85-22767
KINEMATICS
Assembly robot control algorithms N85-22808

On Hybrid and mixed finite element methods [NASA-CR-175551] N85-23096

KINETIC EQUATIONS
Theoretical thermodynamics of mixtures at high pressures N85-23550

KINETIC THEORY
Kinetic Rayleigh-Taylor instability theory in the ionosphere near equator N85-22911

KRYPTON FLUORIDE LASERS
Time-resolved studies of rapid solidification in highly undercooled molten silicon [DE85-004857] N85-22765

L

L-SAT
Derivation of the Olympus solar array requirements N85-22598
The Olympus solar array development and test program N85-22599
Design and qualification testing of the Olympus solar array blanket N85-22600
The performance of the Olympus power subsystem with its solar array N85-22601

LABORATORIES
Air Force technical objective document, Flight Dynamics Laboratory plans for fiscal year 1986. Air Force technical objective document [AD-A149648] N85-22348
Accomplishments of Institute of Cartography summarized N85-23435

LAGRANGE MULTIPLIERS
On an iterative scheme for the solution of constrained variational equations [CSIR-TWISK-341] N85-23342

LAGRANGIAN EQUILIBRIUM POINTS
Lagrangian solutions in photogravitational restricted circular three-body problem N85-22416

LAKES
A first evaluation of LANDSAT TM data to monitor suspended sediments in lakes — Lake Chicot, Arkansas N85-23204

LAMINAR FLOW
Diffusion deposition in fibrous filters for parallel and transverse flow models [DE85-006149] N85-23066

LAMINATES
Directional dependent engineering properties of aluminum-aramid-epoxy laminates [CCMS-85-02] N85-22638
Longitudinal splitting in unidirectional composites, analysis and experiments [NASA-CR-3881] N85-22639
Interlaminar fracture toughness in resin matrix composites [AD-A150565] N85-22640
Mechanical properties and brittle fracture resistance of welded multilayer elements for high pressure vessels N85-22736
Fibre composite laminated plate analysis using a card programmable calculator (HP41C/CV) [NIAST-83/88] N85-23106

LAND MANAGEMENT
Combined analysis of the dynamics of complex ecosystems based on repeated remote measurements N85-22450

LAND MOBILE SATELLITE SERVICE
A comparison of metropolitan and non-metropolitan employment characteristics: Indications of the size of non-metropolitan mobile communication services user classes [NASA-CR-175648] N85-22855

LAND USE
Characterization of LANDSAT-4 TM and MSS image quality for the interpretation of California's agricultural resources — Central Valley N85-23190
An initial analysis of LANDSAT-4 Thematic Mapper data for the discrimination of agricultural, forested wetlands, and urban land cover — Poinsett County, Arkansas; and Reelfoot Lake and Union City, Tennessee N85-23193
Quick look analysis of TM data of the Washington, District of Columbia, area N85-23197
Thematic Mapper data quality and performance assessment in renewable resources/agriculture/remote sensing N85-23201
Preliminary comparisons of the information content and utility of TM versus MSS data N85-23202
The use of Thematic Mapper data for land cover discrimination: Preliminary results from the UK SATMaP programme N85-23207
Preliminary study of information extraction of LANDSAT TM data for a suburban/regional test site N85-23208
Comparative techniques used to evaluate Thematic Mapper data for land cover classification in Logan County, West Virginia N85-23209
Comparison of MSS and TM data for landcover classification in the Chesapeake Bay area: A preliminary report — Taylor's Island, Maryland N85-23210

LANDFORMS
Newly discovered Martian impact basins N85-23544
Thickness of ridged plains materials in Hesperia Planum, Mars N85-23561
Submarine volcanic eruptions and potential analogs for Venus N85-23573
Transformation of polar ice sublimate residue into Martian circumpolar sand N85-23580
Potential bedforms on Venus: Wind tunnel simulations N85-23583
Experiments and analyses of the formation of erosional scour marks with implications to the origin of the Martian outflow channels N85-23588
Distribution and properties of large symmetric knobs on Mars N85-23598
Enigmatic hills of the mottled plains, Mare Acidalium quadrangle (MC-4), Mars N85-23599
Geomorphology and geology of the Southwestern Margaritifer Sinus and Argyre regions of Mars. Part 3: Valley types and distribution N85-23602
The geomorphology of Rhea N85-23606

LANDING SITES
The search for igneous materials at the Viking landing sites N85-23609

LANDSAT SATELLITES
Thematic Mapper data quality and performance assessment in renewable resources/agriculture/remote sensing N85-23201

LANDSAT 4
LANDSAT-4 Science Characterization Early Results. Volume 4: Applications — agriculture, soils land use, geology, hydrology, wetlands, water quality, biomass identification, and snow mapping [E85-10070] N85-23186
Overview of TM applications research reports N85-23187
Impact of Thematic Mapper sensor characteristics on classification accuracy — suburban Washington, D.C., Maryland, and the Chesapeake Bay N85-23188
Analysis and evaluation of the LANDSAT-4 MSS and TM sensors and ground data processing systems: Early results N85-23189
Characterization of LANDSAT-4 TM and MSS image quality for the interpretation of California's agricultural resources — Central Valley N85-23190
Evaluation of Thematic Mapper performance as applied to hydrocarbon exploration — Ontario, Canada; Cement, Oklahoma; and Death Valley, California N85-23191
An initial analysis of LANDSAT-4 Thematic Mapper data for the discrimination of agricultural, forested wetlands, and urban land cover — Poinsett County, Arkansas; and Reelfoot Lake and Union City, Tennessee N85-23193
A preliminary comparison of the information content of data from the LANDSAT 4 Thematic Mapper and Multispectral Scanner — Arkansas N85-23199
Early results of investigations of LANDSAT 4 Thematic Mapper and Multispectral Scanner applications — Washington, D.C. N85-23200
Preliminary comparisons of the information content and utility of TM versus MSS data N85-23202
Snow reflectance from Thematic Mapper N85-23205
The use of Thematic Mapper data for land cover discrimination: Preliminary results from the UK SATMaP programme N85-23207
Relative accuracy assessment of LANDSAT-4 MSS and TM data for level 1 land cover inventory — Washington, D.C. N85-23212

LANDSAT 5
An investigation of several aspects of LANDSAT-5 data quality — Palmer County, Shelby, mt; White sands, NM; Great Salt Lake, UT; San Mattied Bridge and Sacramento, California [E85-10096] N85-23214

LANTHANUM
Americium metal preparation on the multigram scale [DE85-003735] N85-22683

LAPLACE EQUATION
Computation of elliptical functions in problems of celestial mechanics N85-22418
Applications of the conformal mapping method to the solution of mechanical vibrations problems N85-23103

LAPLACE TRANSFORMATION
Time dependent interaction of internal pressure wave with system of two spherical shells N85-22809

LARGE SCALE INTEGRATION
Parallel test method for LSI (Large Scale Integration) microprocessors [AD-A150237] N85-23310

LARGE SPACE STRUCTURES
Report on final recommendations for IMPS engineering-science payload [NASA-CR-175659] N85-22484
Spacecraft environmental interactions: A joint Air Force and NASA research and technology program N85-22517
Interactions measurement payload for Shuttle N85-22518
A quantitative comparison of active and passive damping for large space structures [UTIAS-TN-249] N85-22524
Approximation in optimal control and identification of large space structures [AD-A150323] N85-23351

LASER ANNEALING
In-orbit laser regeneration of the radiation damaged solar arrays N85-22588
Thermodynamic and kinetic studies of pulsed laser annealing from transient conductivity measurements [DE85-003677] N85-23078
Activation of Si-N modes in silicon by pulsed laser annealing [DE85-002988] N85-23082

LASER APPLICATIONS
Solid propellant combustion diagnostics and automated data retrieval from holograms N85-22527
A 2 x 6 Back Surface Reflection (BSR) silicon solar cell N85-22570
Effect of transparent coatings on generation of laser-induced shock waves in metals N85-22711
China report: Science and technology [JPRS-CST-85-005] N85-22843
Laser applications in last 10 years reviewed N85-22844
Status of and outlook for producing means of transmitting units of plane angle, angular velocity and acceleration with ring lasers N85-22955
Digital laser platemaker modifications [AD-A150190] N85-23074

LASER CAVITIES
Mode control and wavelength tuning in open ended Michelson interferometric semiconductor laser N85-23073

LASER DAMAGE
Time-resolved reflectivity measurement of extrinsic silicon during pulsed laser irradiation [AD-A150350] N85-23403

LASER DRILLING
Laser applications in last 10 years reviewed N85-22844

LASER HEATING
Influence of laser treatment of structure and mechanical properties if MA21 alloy N85-22713
Specifics of laser heat treatment of high steel tools N85-22714
Structure of amorphous films of alloys based on Fe, condensed from laser erosion products N85-22749

LASER INTERFEROMETRY
Geophysical laser interferometer with 12.5 meter base N85-23046

LASER MATERIALS
Research progress on laser crystals in China N85-23440

LASER OUTPUTS
Adequacy of metal ablation process with laser radiation and a shock-compressed plasma N85-22708
Neodymium YAG laser pumped with radiation from high frequency electrodeless discharge N85-22796
Comparison reference etalon of unit laser radiation power N85-22957
Invariance of probability characteristics of detector to shape of optical pulse signals N85-23048
Near Field/Far Field (NF/FF) energy loss in Electric Discharge Lasers (EDL's): A mode-medium interaction [AD-A150299] N85-23075
Chemical stabilization of laser dyes [AD-A150451] N85-23076
A spatially incoherent and temporally coherent source [AD-A151281] N85-23390
Ion transport in beam-plasma interactions [AD-A150145] N85-23410

LASER PLASMA INTERACTIONS
Increased hot-electron production at quarter-critical density in long-scalelength, laser-plasma interactions [AD-A150519] N85-23411

LASER WELDING
Structure and mechanical characteristics of heterogeneous joints produced by laser welding N85-22742

LASERS
Intensity fluctuations of focused laser beam during reflection in turbulent atmosphere N85-22975
China report: Science and technology [JPRS-CST-85-003] N85-23433

LATTICE VIBRATIONS
Observation of surface vibrational resonances on (110) surfaces of FCC metals [AD-A150469] N85-23419

LAUNCH DATES
List of recent Soviet space launches N85-22457
LAVA
Geomorphic classification of lava flows on Io N85-23480
Characteristics of basaltic lava flows on Venus N85-23508
Magmas as selective filters of volatiles between planetary mantles and surfaces N85-23557
Estimates of lava eruption rates at Alba Patera, Mars N85-23562
Emplacement of long lava flows on Mauna Loa (Hawaii) and Alba (Mars) N85-23563
Surface structures of Hawaiian lavas N85-23566
Basaltic pressure ridges: Formation and relationship to flow emplacement N85-23567
Radar observations of fissure-fed basaltic lava flows, Craters of the Moon, Idaho N85-23640
LAW (JURISPRUDENCE)
Microcomputers and the electrical engineer [AD-A150499] N85-23325
LEAD (METAL)
EXAFS of monolayers on silver electrodes: SSRL proposal number 717M [AD-A150623] N85-22652
Spectral evaluation of irregularity of superconducting coaxial cables N85-23000
LEADING EDGE SLATS
Effects of leading-edge devices on the low-speed aerodynamic characteristics of a highly-swept arrow-wing [NASA-CR-172531] N85-22365
LEADING EDGES
Energy losses at leading edge of turbine blade during multirow jet cooling N85-22826
LEAKAGE
Magnetic field interactions with material discontinuities [AD-A150197] N85-23373
LEAST SQUARES METHOD
Efficiency of algorithms for gas-air channel diagnostics in gas turbine engines based on gas thermodynamic parameters N85-22823
Consistency of smoothing with running linear fits [AD-A150232] N85-23349
LEGAL LIABILITY
Microcomputers and the electrical engineer [AD-A150499] N85-23325
LEVEL (HORIZONTAL)
Mathematical modeling of results of geometric leveling in variable gravity field N85-23170
LIFE (DURABILITY)
Technological process effect on the carrier lifetime degradation of silicon solar cell base layer irradiated by 1 MeV electrons (boron doping case) N85-22585
Low thrust bipropellant engine/redundant seat valve assembly [AD-A150293] N85-22628
Some specifics of development of fatigue and creep in heat-resistant alloys with asymmetrical multicycle loading N85-22724
Developing procedures for thermomechanical processing of high-durability VT22 titanium alloy N85-22726
Durability of VT16 alloy compounds obtained by diffusion welding N85-22740
LIFE SCIENCES
Aerospace Safety Advisory Panel [NASA-TM-87426] N85-22373
China report: Science and technology [JPRS-CST-85-003] N85-23433
LIFT
Investigations into the effects of scale and compressibility on lift and drag in the RAE 5m pressurised low-speed wind tunnel [RAE-TM-AERO-2006] N85-22372
LIFTING REENTRY VEHICLES
The application of some lifting-body reentry concepts to missile design [NASA-TM-86394] N85-22366
LIGHT (VISIBLE RADIATION)
Acoustooptic cell as space-frequency filter N85-23051
LIGHT BEAMS
Intensity fluctuations of focused laser beam during reflection in turbulent atmosphere N85-22975
Time spectra of intensity fluctuations along reflecting path N85-22981
LIGHT CURVE
Convex-profile inversion of asteroid lightcurves N85-23502
LIGHT EMITTING DIODES
AL-124 light-emitting diode in 30 Mbit/s fiber-optic communication line N85-22925
LIGHT MODULATION
Space-time response characteristics of acoustooptic filter for compression of linearly frequency-modulated signal N85-22937
Theory of diaphragm light modulators with electrical input signal N85-23002
LIGHT SCATTERING
A systematic study of light scattering by irregularly shaped particles [AD-A150192] N85-23400
Nonrelativistic Kapitza-Dirac scattering [AD-A150622] N85-23405
LIGHT TRANSMISSION
Fine structure of vertical distribution of light attenuation index of sea water N85-23140
LIGHTNING
Surge-strength of symmetric cable with monolithic polyethylene insulation of quads N85-23001
1981 wCJ30 airborne lightning characterization program data review [AD-A150230] N85-23275
LIMITS (MATHEMATICS)
On limit of the largest eigenvalue of the large dimensional sample covariance matrix [AD-A150589] N85-23358
LINE SPECTRA
An atlas of nitrogen-broadened water vapor spectra from 500 to 5000 cm(-1), volume 1 [AD-A150527] N85-22650
LINEAR ACCELERATORS
Los Alamos free electron laser: Accelerator performance [DE85-005722] N85-23084
Collective acceleration of ions using high current relativistic electron beams [DE85-004889] N85-23393
LINEAR FILTERS
Piezoelectric filter with low-Q inductances N85-22932
Acoustooptic cell as space-frequency filter N85-23051
LINEAR PROGRAMMING
Approaches and algorithms for robust signal processing N85-22878
Optimal allocation of components in parallel-series and series-parallel systems [AD-A150169] N85-23309
LEXICON: A structured modeling system for optimization [AD-A150536] N85-23329
LINEAR SYSTEMS
Analysis and design of linear microwave transistor amplifiers N85-23038
LINEARITY
Absolute stability of unsteady movement of axisymmetrical rotating flight vehicle N85-22793
Approaches and algorithms for robust signal processing N85-22878
Consistency of smoothing with running linear fits [AD-A150232] N85-23349
LINES (GEOMETRY)
A description of the Langley wireframe geometry standard (LaWGS) format [NASA-TM-85767] N85-22380
LIQUEFIED GASES
Electronics Engineering Department EE Technical Review [UCRL-50025-84-1] N85-22887
LIQUID CRYSTALS
Exploratory development of foams from liquid crystal polymers [NASA-CR-172510] N85-22754
LIQUID FLOW
Liquid mass flow rate computer N85-22962
Radiation-dominated snowmelt on Mars N85-23592
LIQUID FUELS
The influence of fuel quality upon flame-tube temperature and flame radiation in a model gas-turbine primary zone [K233] N85-22396
The influence of fuel molecular composition upon flame-tube temperature and flame radiation in a model gas-turbine primary zone [K234] N85-22646
LIQUID HELIUM
Shock compression of liquid helium to 56 GPa (560) kbar N85-23551
A measurement of the intensity of the cosmic background radiation at 3.9 cm N85-23681
LIQUID HELIUM 2
Outlook for realization of proximity effect and Josephson direct current in helium-2 N85-22956
LIQUID INJECTION
Effect of water injection into air for turbine cooling on economy of operation of gas turbine engine with afterburning N85-22830
LIQUID METALS
Anomalies of aluminum structure and properties N85-22693
Division boundary in Al-B composite material with boron in contact with solid and liquid aluminum N85-22704
Electrodynamic stability of composite liquid-metal contacts N85-23031
LIQUID OXYGEN
Nonlinear rotordynamics analysis [NASA-CR-171425] N85-22364
LIQUID PHASES
Densification and deformation in the presence of a liquid phase [DE85-005101] N85-22763
LIQUID PROPELLANT ROCKET ENGINES
An integral closed loop combustion stability model-status and review N85-22553
Development of a three-phrase combustion code for modeling liquid rocket engines N85-22554
Atomization data requirements for rocket combustor modeling N85-22555
Effect of compliability of hot walls in liquid-propellant engine on low frequency instability N85-22824
LIQUID ROCKET PROPELLANTS
Atomization data requirements for rocket combustor modeling N85-22555
Low thrust bipropellant engine/redundant seat valve assembly [AD-A150293] N85-22628
LIQUID-GAS MIXTURES
Mathematical-cartographic model for study of distribution of hydrochemical elements in sea water (using dissolved oxygen in the Pacific Ocean as an example) N85-23138
LIQUID-LIQUID INTERFACES
Properties of materials using acoustic waves [AD-A150465] N85-23382
LIQUID-SOLID INTERFACES
Time resolved X-ray studies during pulsed laser irradiation of Ge [DE85-005263] N85-23083
Surface scattering [AD-A150252] N85-23366
LIQUID-VAPOR INTERFACES
Surface scattering [AD-A150252] N85-23366
LIQUIDS
Examination of the contact wetting angle in the vicinity of critical temperature [BLL-T6416/BG/CRS/LR-ST735/84] N85-23054
LITHIUM
The effects of lithium counterdoping on radiation damage and annealing in n(+)p silicon solar cells N85-22586
Relationship between topological and magnetic order in small metal clusters [AD-A150547] N85-22651
Hartree-Fock interaction between a helium atom and lithium-metal: A test for the effective medium theory [AD-A150468] N85-23367
LITHIUM ALLOYS
Problem of pore formation mechanism in welded joints of aluminum alloys in the system aluminum-magnesium-lithium N85-22732
LITHOGRAPHY
China report: Science and technology [JPRS-CST-85-005] N85-22843
X-ray lithography and VLSI circuits N85-22846
LITHOLOGY
Review of problems in lithology N85-23160
Geologic utility of LANSDAT-4 TM data --- Death Valley, California and the Silver Bell area of southern Arizona N85-23192
Lithologic and structural control on slope morphology in the Valles Marineris N85-23651
LITHOSPHERE
Use of paleomagnetic data in tectonic analysis of oceanic structures N85-23135
Interrelationship of earthquake magnitude and lithospheric-asthenospheric thermodynamic parameters in seismically active zones N85-23183
Io: Generation of silicate magma by shear melting at the base of a basaltic lithosphere N85-23478
Formation of bright terrain bands on Ganymede by unstable lithosphere extension N85-23485
Venus chasmata: A lithosphere stretching model N85-23516
Elysium region, Mars: Tests of lithospheric loading models for the formation of tectonic features N85-23650
LOAD DISTRIBUTION (FORCES)
Controlled movement of elastic manipulator with distributed parameters N85-22818
LOADING OPERATIONS
Advanced life analysis methods. Volume 2: Crack growth analysis methods for attachment lugs [AD-A150420] N85-23109

LOADS (FORCES)
Study for prediction of rotor/wake/fuselage interference, part 1
[NASA-CR-177340-VOL-1] N85-22346
Study for prediction of rotor/wake/fuselage interference. Part 2: Program users guide
[NASA-CR-177340-VOL-2] N85-22347
Prediction of the resistance of structural materials to cavitation erosion
[BLL-DRIC-TRANS-7435-(3623.66)] N85-22659
Development of a sintered shim
[DE85-006183] N85-22685
Comparison of dynamic-tension and constant-load strength characteristics of heat-resistant materials N85-22722
Characteristics of surface crack development in ATiaS aluminum alloy during slow-cycle loading N85-22745
Steady-state reaction of three-layered cylindrical shell to effect of moving load N85-22811
Axisymmetrical oscillations of shell systems subjected to impulse loads N85-22814
Nonlinear behavior and stability of thin spherical shells subjected to non-axisymmetrical loading N85-22821
Elysium region, Mars: Tests of lithospheric loading models for the formation of tectonic features N85-23650

LOCKS (FASTENERS)
Code lock with microcircuit N85-22935

LOGARITHMS
Applicability of log-normal model to probabilitistic description of quasi-pulse interference N85-23014
Parallel update of minimum spanning trees in logarithmic time
[AD-A150497] N85-23357

LOGIC CIRCUITS
Basic EMC (electromagnetic interference) technology advancement for c3 systems. Volume 3A: Probabilistic analysis of combinational circuits with random delays
[AD-A150349] N85-22868
Development of a planar heterojunction bipolar transistor for very high speed logic
[AD-A150374] N85-22895

LONG DURATION SPACE FLIGHT
Comments on Salyut-7 150-day flight N85-22406
Research opportunities in human behavior and performances
[NASA-CR-3886] N85-23299

LONG TERM EFFECTS
Long-term strength and fracture criteria for EI698VD alloy under complex stress conditions N85-22723
Influence of annealing on cyclic and short-term strength of thin sheets of VT1-0 titanium and OTR4 alloy N85-22727

LONGITUDINAL WAVES
Generation of longitudinal acoustic waves by modulated helicon waves — nonlinear steady state waves in metals N85-23049

LOOPS
Normal mode calculations for fuselage type intricate structures by regarding them as systems with superposed constraints N85-22617

LOSSES
Optical reflectometer for multimode fiber lightpipes N85-22961

LOW ALTITUDE
Low altitude texture comparison data base and smooth shaded texture
[AD-A150342] N85-23323

LOW CARBON STEELS
Specifics of kinetics of polymorphous conversion upon heating of low carbon steels N85-22721

LOW COST
Aspects of low cost module technology — spacecraft solar arrays N85-22614

LOW FREQUENCIES
Effect of compliability of hot walls in liquid-propellant engine on low frequency instability N85-22824
Exitation of low-frequency resonance waves by moving conductor in space plasma N85-22912
The low frequency behaviour of an immersed structure at a standstill in a high density fluid with free surface
[TP-1983-31] N85-23105

LOW PASS FILTERS
Synthesis of low-pass filters using coupled lines with unmatched loads N85-22938
Efficiency of digital compensator of strong non-Gaussian interference N85-22942

LOW PRESSURE
Non-self-maintained high-voltage low-pressure discharge N85-23037

LOW SPEED
Effects of leading-edge devices on the low-speed aerodynamic characteristics of a highly-swept arrow-wing
[NASA-CR-172531] N85-22365

LOW SPEED WIND TUNNELS
Investigations into the effects of scale and compressibility on lift and drag in the RAE 5m pressurised low-speed wind tunnel
[RAE-TM-AERO-2006] N85-22372
China report: Science and technology
[JPRS-CST-85-005] N85-22843
CARD's low-speed wind tunnel described N85-22849

LOW TEMPERATURE
Experimental studies of low temperature surface interactions of atomic hydrogen using maser technique
[AD-A150216] N85-22647
Low temperature calibration fixture
[DE85-003969] N85-23071

LOW TEMPERATURE ENVIRONMENTS
Properties of filamentary sublimation residues from dispersions of clay in ice N85-23629

LOW TEMPERATURE TESTS
Geomagnetic field dynamics N85-23182

LOW THRUST
Low thrust bipropellant engine/redundant seat valve assembly
[AD-A150293] N85-22628

LOW VOLTAGE
Optimization of overall dimensions of enclosures for low-voltage devices and equipment N85-23033

LOWER ATMOSPHERE
Characteristics of latitude effect on cosmic ray charged component in atmosphere at altitudes 3-5 KM N85-22413

LUBRICANTS
Formation of high molecular weight products from benzene during boundary lubrication
[NASA-TM-86966] N85-22644
Use of ferrofluids in machining of metals N85-22802

LUBRICATING OILS
New technique for fluid feed in simultaneous multisurface grinding N85-22800

LUBRICATION
Development of a multiplane multispeed balancing system for turbine systems
[NASA-CR-174750] N85-22400
Thermal and thermoelastic effects in rolling/sliding contacts
[AD-A150435] N85-23429

LUGS
Advanced life analysis methods. Volume 1: Cracking data survey and NDI (nondestructive inspection) assessment for attachment lugs
[AD-A150419] N85-23108
Advanced life analysis methods. Volume 2: Crack growth analysis methods for attachment lugs
[AD-A150420] N85-23109

LUMINESCENCE
EXAFS of monolayers on silver electrodes: SSRL proposal number 717M
[AD-A150623] N85-22652

LUMINOUS INTENSITY
A posteriori increase of resolving power of optical system forming averaged monochromatic images N85-23003

LUNAR COMPOSITION
Remote sensing analyses of localized lunar dark mantle deposits N85-23616
Spectral reflectance studies of the Orientale basin N85-23617
Landform identification on radar images N85-23635

LUNAR CORE
Cosmogenic Na-22 and Al-26 in Luna-24 lunar drill core soil samples N85-22427
Implications of convection in the Moon and the terrestrial planets N85-23548
Modeling equilibrium and fractional crystallization in the system MgO-FeO-CaO-Al2O3-SiO2 N85-23552
Quenching effects on iron site partitioning in the Apollo 17 orange glass composition N85-23553

LUNAR CRATERS
Monte Carlo modeling of lunar megaregolith development N85-23627
Radar observations of fissure-fed basaltic lava flows, Craters of the Moon, Idaho N85-23640

LUNAR CRUST
The deep structure of lunar basins: Clues to the understanding of basin formation and modification N85-23647

LUNAR EVOLUTION
Lunar origin: Role of giant impacts N85-23519
Implications of convection in the Moon and the terrestrial planets N85-23548
Modeling equilibrium and fractional crystallization in the system MgO-FeO-CaO-Al2O3-SiO2 N85-23552

LUNAR GEOLOGY
Why not a constant early lunar impact rate? N85-23536
Correction and geological analysis of lunar 3.8 cm radar data N85-23634

LUNAR MANTLE
Remote sensing analyses of localized lunar dark mantle deposits N85-23616
The deep structure of lunar basins: Clues to the understanding of basin formation and modification N85-23647

LUNAR MAPS
A unified lunar control network N85-23669

LUNAR PHOTOGRAPHY
A unified lunar control network N85-23669

LUNAR RADAR ECHOES
Landform identification on radar images N85-23635

LUNAR ROCKS
Quenching effects on iron site partitioning in the Apollo 17 orange glass composition N85-23553
Experimental methds for quenching structures in lunar-analog silicate melts: Variations as a function of quench media and composition N85-23554

LUNAR SOIL
Cosmogenic Na-22 and Al-26 in Luna-24 lunar drill core soil samples N85-22427

LUNAR SURFACE
Why not a constant early lunar impact rate? N85-23536
Morphology and mechanics of terraces in lunar craters N85-23543
Quenching effects on iron site partitioning in the Apollo 17 orange glass composition N85-23553
Remote sensing analyses of localized lunar dark mantle deposits N85-23616
Spectral reflectance studies of the Orientale basin N85-23617
Monte Carlo modeling of lunar megaregolith development N85-23627
Mechanisms of basalt-plains ridge formation N85-23643
On the absence of strike-slip faults from the planets and satellites N85-23645
The deep structure of lunar basins: Clues to the understanding of basin formation and modification N85-23647

LUNAR TOPOGRAPHY
Monte Carlo modeling of lunar megaregolith development N85-23627

LUNIK LUNAR PROBES
Cosmogenic Na-22 and Al-26 in Luna-24 lunar drill core soil samples N85-22427

M

MACHINE TOOLS
Development of a sintered shim
[DE85-006183] N85-22685
Rational use of tatanium in nonferrous metallurgy N85-22728
New technique for fluid feed in simultaneous multisurface grinding N85-22800
USSR report: Machine tools and metalworking equipment
[JPRS-UMM-85-005] N85-22839
Diamond cutters' grinders N85-22841
Machine tool vibrations: A review N85-23104

MACHINING
Use of ferrofluids in machining of metals N85-22802
USSR report: Machine tools and metalworking equipment
[JPRS-UMM-85-005] N85-22839
T700 cutter life improvement program
[AD-A150450] N85-23089

MAGELLANIC CLOUDS
All-Union conference of radio astronomers N85-22408

MAGMA
Magmatism in continent-ocean transition zone (development of ideas of A. N. Zavaritskiy) N85-23161
Thermohydrodynamic model: Hydrothermal system, shallowly seated magma chamber N85-23173
Io: Generation of silicate magma by shear melting at the base of a basaltic lithosphere N85-23476
Characteristics of basaltic lava flows on Venus N85-23508
Modeling equilibrium and fractional crystallization in the system MgO-FeO-CaO-Al2O3-SiO2 N85-23552
Magmas as selective filters of volatiles between planetary mantles and surfaces N85-23557
Volcanism of the Colorado Plateau (basin and range transition): Implications for crustal processes N85-23560
A silicic shield volcano in Bolivia N85-23572
Hydrovolcanism N85-23574

MAGNESIUM
Structural strenght of strip D16T aluminum alloy with low copper and magnesium content N85-22691
New deformable secondary aluminum alloys N85-22694

MAGNESIUM ALLOYS
Rapid solidification processing of magnesium alloys [AD-A150270] N85-22668
Influence of laser treatment of structure and mechanical properties if MA21 alloy N85-22713
Problem of pore formation mechanism in welded joints of aluminum alloys in the system aluminum-magnesium-lithium N85-22732
MAGNETIC ANOMALIES
Structure of Iceland and ocean floor spreading N85-23159
MAGSAT anomaly field data of the crustal properties of Australia [E85-10100] N85-23215
An investigation of the crustal properties of Australia and surrounding regions derived from interpretation of MAGSAT anomaly field data N85-23216
Remanent magnetization model for the broken ridge satellite magnetic anomaly N85-23219
MAGNETIC COILS
Mathematical model of electromagnetic suspension device with two control windings N85-22954
MAGNETIC COOLING
Magnetic refrigeration and heat pumping design options [DE85-003405] N85-23084
MAGNETIC DISTURBANCES
Plans for Interbol satellite experiment N85-22407
MAGNETIC EFFECTS
Calculation of secondary-electron escape currents from inclined-spacecraft surfaces in a magnetic field N85-22491
Magnetovolume effects in some Y-Ni intermetallic compounds [ISSN-0066-2003] N85-22663
MAGNETIC FIELD CONFIGURATIONS
Magnetostatic-wave propagation in a finite YIG-Loaded rectangular waveguide [AD-A150332] N85-22665
MAGNETIC FIELDS
Use of ferrofluids in machining of metals N85-22602
Exitation of low-frequency resonance waves by moving conductor in space plasma N85-22912
Magnetic noise in single-machine rotating frequency converters N85-22969
Study of resolution of deep MT soundings by means of physical model N85-23155
Discrimination of normal and anomalous magnetic and electric fields in geoelectromagnetic variations N85-23166
1981 wC-130 airborne lightning characterization program data review [AD-A150230] N85-23275
High-field dipoles for future accelerators [DE85-002315] N85-23391
Improvement in magnetic field properties of vanadium-gallium superconductors by enhancement of spin-orbit scattering [DE85-002893] N85-23422
MAGNETIC FLUX
Observation of cosmic ray flux variations in stratosphere N85-22430
Method of separately determining electrophysical properties of bulky conductor N85-22951
MAGNETIC MATERIALS
Relationship between topological and magnetic order in small metal clusters [AD-A150547] N85-22651
MAGNETIC MEASUREMENT
Solution of direct magnetometric problem on spherical Earth N85-23179
Rapid advances in geological work N85-23437
MAGNETIC MOMENTS
Microscopic magnetic structure of multiple bilayers of thin films of Fe and Ge [DE85-004188] N85-22682
MAGNETIC PERMEABILITY
Method of separately determining electrophysical properties of bulky conductor N85-22951
MAGNETIC PROPERTIES
Magnetic studies of Ni3Al(Fe) compounds [DE85-005262] N85-22686
Primary processing of experimental magnetovariation sounding data using spline functions N85-23175
Improvement in magnetic field properties of vanadium-gallium superconductors by enhancement of spin-orbit scattering [DE85-002893] N85-23422
MAGNETIC STORMS
Periodic substorm activity in the geomagnetic tail [NASA-CR-175629] N85-23409
MAGNETIC SURVEYS
GADB: A database facility for modelling naturally occurring geophysical fields N85-23217
Data selection techniques in the interpretation of MAGSAT data over Australia N85-23218
MAGNETIC SUSPENSION
Mathematical model of electromagnetic suspension device with two control windings N85-22954
MAGNETIC TAPES
Simple detonation meter N85-22971
MAGNETICALLY TRAPPED PARTICLES
Longitude and pitch-angle distributions of streams of high-energy electrons under Earth's radiation belts N85-22415
MAGNETIZATION
Remanent magnetization model for the broken ridge satellite magnetic anomaly N85-23219
MAGNETOHYDRODYNAMIC FLOW
Wakes and differential charging of large bodies in low Earth orbit N85-22488
MAGNETOHYDRODYNAMIC STABILITY
Discharges on a negatively biased solar cell array in a charged-particle environment N85-22499
Increased hot-electron production at quarter-critical density in long-scalelength, laser-plasma interactions [AD-A150519] N85-23411
Lower hybrid heating and current drive, and ion cyclotron heating experiments on the Alcator C and the Versator II Tokamaks [DE85-004918] N85-23412
Theoretical and observational studies of stellar activity N85-23468
MAGNETOHYDRODYNAMIC WAVES
Hydromagnetic precursors of interplanetary plasma burst N85-22414
Excitation of low-frequency plasma waves by a conducting, tethered satellite N85-23470
MAGNETOHYDRODYNAMICS
Physics of the inner heliosphere: Mechanisms, models and observational signatures [NASA-CR-175632] N85-23677
MAGNETOSPHERE
Plans for Interbol satellite experiment N85-22407
Aerospace spacecraft-charging guidelines document N85-22501
Argon ion pollution of the magnetosphere N85-22523
Excitation of low-frequency plasma waves by a conducting, tethered satellite N85-23470
Interaction of the magnetospheric ions with the surfaces of the icy satellites of Saturn N85-23491
MAGNETOSTATICS
Magnetostatic-wave propagation in a finite YIG-Loaded rectangular waveguide [AD-A150332] N85-22665
MAGNETS
The ferrite permanent magnet AC motor: A technical and economical assessment [DE85-002480] N85-22903
MAN MACHINE SYSTEMS
USSR report: Space [JPRS-USP-85-001] N85-22403
TASS update on unmanned flight of Salyut-7 N85-22404
A design analysis and implementation of a user-friendly interface for the UNIX operating system [AD-A150558] N85-23312
MANAGEMENT ANALYSIS
Aviation maintenance computerized management information systems: Perspective for the future [AD-A150637] N85-22349
MANAGEMENT INFORMATION SYSTEMS
Aviation maintenance computerized management information systems: Perspective for the future [AD-A150637] N85-22349
General design considerations of an Air Force information system [AD-A150611] N85-23449
MANGANESE
Investigation of manganese dioxide as an improved solid desiccant [DE85-004034] N85-22654
MANIPULATORS
Cyclic industrial robots with mechanical energy storing devices: Multipositional system with one or several degrees of freedom N85-22803
Design of tightening device and calculation of forces in manipulator transmissions with base-drive mounted N85-22804
Hydraulic brakes for industrial robots N85-22806
Controlled movement of elastic manipulator with distributed parameters N85-22818
Investigation of dynamics of manipulator with elastic sections N85-22819
Optimum design of electrical motors for multilink manipulators and automated manufacturing systems N85-22880
MANNED SPACE FLIGHT
USSR report: Space [JPRS-USP-85-001] N85-22403
TASS update on unmanned flight of Salyut-7 N85-22404
Feoktistov recalls period leading to Gagarin spaceflight N85-22451
Feoktistov says manned lunar, Mars flights lack justification N85-22452
Research opportunities in human behavior and performances [NASA-CR-3886] N85-23299
MANUFACTURING
A 2 x 6 Back Surface Reflection (BSR) silicon solar cell N85-22570
Optimum design of electrical motors for multilink manipulators and automated manufacturing systems N85-22880
MANY BODY PROBLEM
Capture of planetesimals into a circumterrestrial swarm N85-23522
MAPPING
Geological remote sensing develops rapidly, finds broad applications N85-22848
Possibility of mapping active tectonic structures from mercury gas aureoles over sea surface N85-23162
Possibilities of aerial electric prospecting by long cable method for detecting poorly conducting strata N85-23177
China report: Science and technology [JPRS-CST-85-003] N85-23433
Development, achievements in China's cartography work N85-23434
Accomplishments of Institute of Cartography summarized N85-23435
Geophysical interpretation of Venus gravity data N85-23513
Newly discovered Martian impact basins N85-23544
Mapping and geological analysis of Mercury and Venus radar ranging data N85-23633
Mars radar catalog N85-23636
Late Tertiary and Quaternary river systems of the eastern Sahara as mapped on shuttle radar and LANDSAT images N85-23641
MAPS
Digital laser platemaker modifications [AD-A150190] N85-23074
An investigation of the crustal properties of Australia and surrounding regions derived from interpretation of MAGSAT anomaly field data N85-23216
Development, achievements in China's cartography work N85-23434
Accomplishments of Institute of Cartography summarized N85-23435
Hexagonal data base study [AD-A150176] N85-23448
Mars geologic mapping: A review and new concepts N85-23663
The Galilean Satellite Geological Mapping Program, 1984 N85-23664
MARINE BIOLOGY
Production and turnover of suspended organic detritus in the coastal water of the southeastern continental shelf [DE85-003977] N85-23290
MARINE ENVIRONMENTS
Special features of computations of vertical distribution of concentration of suspended sediments under marine conditions N85-23125
Contribution to theory of ocean-atmosphere gas exchange N85-23134
The relationship between marine aerosol particles and satellite-detected radiance N85-23263
MARINE METEOROLOGY
Science opportunities using the NASA scatterometer on N-ROSS [NASA-CR-175639] N85-23222
MARINER 9 SPACE PROBE
Participation in the Mars Data Analysis Program: Analysis of cloud forms in Viking and Mariner 9 images [NASA-CR-175604] N85-23673
MARITIME SATELLITES
INMARSAT marine satellite organization N85-22456
MARKOV CHAINS
Reliability bounds for fault-tolerant systems with competing responses to component failures [NASA-TP-2409] N85-23090
Regenerative simulation of non-Markovian stochastic systems [AD-A150344] N85-23367
Automatic symbolic solution of Markov chains [AD-A150476] N85-23369
MARS
Volcanic debris flows in the Elysium region of Mars N85-23560
Estimates of lava eruption rates at Alba Patera, Mars N85-23562

MARS (PLANET)
Viking radio science data analysis and synthesis [NASA-CR-175631] N85-23471
Study and estimation of planet-crossing asteroid populations: Discoveries and analysis N85-23498
Viking radio science data analysis and synthesis N85-23528
Estimates of lava eruption rates at Alba Patera, Mars N85-23562
Observed changes at Viking Lander 1 N85-23575
Seasonal and secular variation of the Solis Lacus albedo feature: Relation to the Martian dust-transport cycle N85-23576
Eolian erosion on Mars: Three scales N85-23577
The origin of regional dust deposits on Mars N85-23578
On the latitudinal distribution of debris in the Northern Hemisphere of Mars N85-23579
Transformation of polar ice sublimate residue into Martian circumpolar sand N85-23580
The effect of particle density on aeolian transport N85-23581
Paleohydrologic implications of valley networks of Mars N85-23585
Fluvial drainage basins and valley networks: Eastern Margaritifer Sinus, Mars N85-23586
Catastrophic-flood features in Swedish Lapland as a terrestrial analog for Martian channel flows N85-23587
Experiments and analyses of the formation of erosional scour marks with implications to the origin of the Martian outflow channels N85-23588
Relative time-scale for channeling events within chaotic terrains, Margaritifer Sinus, Mars N85-23589
Terrestrial analog studies for Martian patterned ground N85-23590
Origin of Martian polygonal terrain: Preliminary results N85-23591
Radiation-dominated snowmelt on Mars N85-23592
Chemical weathering of soils from the dry valleys of Antarctica: A terrestrial analog of Martian weathering processes N85-23628
Mars radar catalog N85-23636
Statistics of Aeolian surface of Mars N85-23637
Radar and the detection of liquid water on Mars N85-23638
Planetary interior modeling and tectonic implications N85-23649
Elysium region, Mars: Tests of lithospheric loading models for the formation of tectonic features N85-23650
Mars: Stratigraphy of western highlands and polar regions N85-23653
Participation in the Mars Data Analysis Program: Analysis of cloud forms in Viking and Mariner 9 images [NASA-CR-175604] N85-23673

MARS ATMOSPHERE
The effect of particle density on aeolian transport N85-23581
Mars: Long term changes in the state and distribution of H2O N85-23593
Water-ice clouds on Mars: Location and seasonal variation N85-23611

MARS CRATERS
The nature of Martian flow ejecta craters N85-23545
Paleohydrologic implications of valley networks of Mars N85-23585
Geomorphology and geology of the Southwestern Margaritifer Sinus and Argyre regions of Mars. Part 2: Crater size-frequency distribution curves and geomorphic unit ages N85-23601
Geomorphology and geology of the Southwestern Margaritifer Sinus and Argyre regions of Mars. Part 4: Flow ejecta crater distribution N85-23603

MARS ENVIRONMENT
Properties of filamentary sublimation residues from dispersions of clay in ice N85-23629
Statistics of Aeolian surface of Mars N85-23637

MARS PHOTOGRAPHS
Viking Lander mosaics of Mars N85-23667
The control network of Mars: October 1984 N85-23670

MARS SURFACE
Viking radio science data analysis and synthesis N85-23528
Martian terrain ages N85-23537
The evolution of CO2 on Mars N85-23558
Ridged plains of Lunae Planum: Thickness distribution revised N85-23559
Thickness of ridged plains materials in Hesperia Planum, Mars N85-23561
Observed changes at Viking Lander 1 N85-23575
Seasonal and secular variation of the Solis Lacus albedo feature: Relation to the Martian dust-transport cycle N85-23576
Eolian erosion on Mars: Three scales N85-23577
The origin of regional dust deposits on Mars N85-23578
On the latitudinal distribution of debris in the Northern Hemisphere of Mars N85-23579
Transformation of polar ice sublimate residue into Martian circumpolar sand N85-23580
Paleohydrologic implications of valley networks of Mars N85-23585
Fluvial drainage basins and valley networks: Eastern Margaritifer Sinus, Mars N85-23586
Catastrophic-flood features in Swedish Lapland as a terrestrial analog for Martian channel flows N85-23587
Experiments and analyses of the formation of erosional scour marks with implications to the origin of the Martian outflow channels N85-23588
Mars: Long term changes in the state and distribution of H2O N85-23593
Mapping structures characteristic of the highland boundary scarp on Mars N85-23595
Investigations of the Mars cratered terrain: Smooth plains boundary in the eastern equatorial region N85-23596
Martian fretted terrain morphometry interpreted using principal components analysis N85-23597
Distribution and properties of large symmetric knobs on Mars N85-23598
Enigmatic hills of the mottled plains, Mare Acidalium quadrangle (MC-4), Mars N85-23599
Geomorphology and geology of the Southwestern Margaritifer Sinus and Argyre regions of Mars. Part 1: Geological and geomorphological overview N85-23600
Geomorphology and geology of the Southwestern Margaritifer Sinus and Argyre regions of Mars. Part 2: Crater size-frequency distribution curves and geomorphic unit ages N85-23601
Geomorphology and geology of the Southwestern Margaritifer Sinus and Argyre regions of Mars. Part 3: Valley types and distribution N85-23602
Geomorphology and geology of the Southwestern Margaritifer Sinus and Argyre regions of Mars. Part 4: Flow ejecta crater distribution N85-23603
Planetary analogs in Antarctica: Mars N85-23604
Multispectral analysis of the Kasei Vallis-Lunae Planum region of Mars N85-23607
Geologic interpretation of remote sensing data for the Martian volcano, Ascraeus Mons N85-23608
The search for igneous materials at the Viking landing sites N85-23609
Basalts of Mars: Constraints on volatile evolution N85-23610
First direct detection of clay minerals on Mars N85-23612
Iron oxides of Mars: Evidence for contemporary weathering N85-23613
Reassignment of the iron (3) absorption bands in the spectra of Mars N85-23614
Zeolites on Mars: Prospects for remote sensing N85-23615
Mars radar catalog N85-23636
Statistics of Aeolian surface of Mars N85-23637
Radar and the detection of liquid water on Mars N85-23638
Mechanisms of basalt-plains ridge formation N85-23643
On the absence of strike-slip faults from the planets and satellites N85-23645
Lithologic and structural control on slope morphology in the Valles Marineris N85-23651
Valles Marineris basin beds: A complex story N85-23652
Kasei Vallis of Mars: Dating the interplay of tectonics and geomorphology N85-23654
Mars geologic mapping: A review and new concepts N85-23663
Mars planimetric mapping N85-23666

MARS VOLCANOES
Emplacement of long lava flows on Mauna Loa (Hawaii) and Alba (Mars) N85-23563
Geologic interpretation of remote sensing data for the Martian volcano, Ascraeus Mons N85-23608

MARSHLANDS
Remote sensing of coastal wetlands biomass using Thematic Mapper wavebands — Lewes, Delaware N85-23198

MARTENSITIC TRANSFORMATION
Effect of phase state of TiC-NiTi powder composite materials on nature of failure and mechanical properties N85-22702

MASS DISTRIBUTION
Dynamics of gas disks in triaxial galaxies N85-23469

MASS FLOW
Mathematical modeling of transient performance of gas turbine engine N85-22834
Turbulence measurements in shock induced flows N85-23055

MASS SPECTRA
Analysis of biological particles by mass spectrometry [AD-A149952] N85-23291

MASS SPECTROMETERS
Mass spectra of neutral particles released during electrical breakdown of thin polymer films N85-22511

MASS SPECTROSCOPY
Analysis of biological particles by mass spectrometry [AD-A149952] N85-23291

MASS TRANSFER
A survey for galactic plane ultraviolet-excess objects: Space densities for white dwarfs, subdwarfs, and cataclysmic variables N85-23458
Seasonal and secular variation of the Solis Lacus albedo feature: Relation to the Martian dust-transport cycle N85-23576
Eolian erosion on Mars: Three scales N85-23577
The effect of particle density on aeolian transport N85-23581
A comparison of terrestrial saltation flux in the laboratory and the field N85-23582

MASSIFS
Geomorphology and geology of the Southwestern Margaritifer Sinus and Argyre regions of Mars. Part 1: Geological and geomorphological overview N85-23600

MATCHED FILTERS
Acousto-optically addressed Fourier transform matched filters [AD-A150298] N85-22869

MATERIALS
Electrostatic forming and testing of polymer films on a 16-foot diameter test fixture [NASA-TM-86328] N85-22885

MATHEMATICAL MODELS
Simple theoretical models for composite rotor blades [NASA-CR-175620] N85-22382
Model reduction for control system design [NASA-CR-170417] N85-22398
Expansion of functions describing planetary surface and gravity field N85-22410
Nontraditional method for determining unperturbed orbits of unknown space objects using incomplete optical observational data N85-22417
An integral closed loop combustion stability model-status and review N85-22553
Improved modeling of the open circuit voltage of solar cells N85-22619
Some unique features of isentrophic flow of gas under high pressures N85-22788
Mathematical modeling of transient performance of gas turbine engine N85-22834
Research efforts in support of resonance extraction studies. Volume 1: Improvement and validation of TWFD (Thin-Wire Frequency-Domain): A thin-wire frequency-domain scattering code [AD-A150296] N85-22864
Mathematical model of discriminator for signals with fluctuations and thermal noise N85-22943
Mathematical model of electromagnetic suspension device with two control windings N85-22954
Problem of diffraction by wavy surface: Comparison of numerical methods of solution N85-22985
Mathematical modeling of two-frequency laser sounding of scattering media N85-23045
Investigation of parabolic computational techniques for internal high-speed viscous flows [NASA-CR-172555] N85-23056
Numerical experiments with simple model of ocean climate N85-23123
Numerical modeling of plane stick-slip fault N85-23150
Mathematical modeling of results of geometric leveling in variable gravity field N85-23170
The microwave propagation and backscattering characteristics of vegetation — wheat, sorghum, soybeans and corn fields in Kansas [E85-10088] N85-23213
Remanent magnetization model for the broken ridge satellite magnetic anomaly N85-23219
Estimation of regional evapotranspiration using remotely sensed land surface temperature. Part 1: Measurement of evapotranspiration at the Environmental Research Center and determination of Priestley-Taylor parameter N85-23233
Estimation of regional evapotranspiration using remotely sensed land surface temperature. Part 2: Application of equilibrium evaporation model to estimate evapotranspiration by remote sensing technique — Japan N85-23234
Testing an energy balance model for estimating actual evapotranspiration using remotely sensed data — Hannover, West Germany barley and wheat fields N85-23236
ROSS: An object-oriented language for constructing simulations [AD-A150556] N85-23330

On a mathematical structure for an image algebra [AD-A150228] N85-23348
The design of a unified package for the solution of stochastic petri net models [AD-A150326] N85-23354
Magnetic field interactions with material discontinuities [AD-A150197] N85-23373
A model for eclipsing cataclysmic variables N85-23467
Impact crater scaling laws N85-23532
Planetary interior modeling and tectonic implications N85-23649
Elysium region, Mars: Tests of lithospheric loading models for the formation of tectonic features N85-23650

MATRICES (MATHEMATICS)
Implementation of some concurrent algorithms [DE85-004687] N85-23334
On limit of the largest eigenvalue of the large dimensional sample covariance matrix [AD-A150589] N85-23358
Algorithm for singular decomposition [DE85-016488] N85-23361
Sparse matrix computations [DE85-004780] N85-23362

MATRIX MATERIALS
Development of epoxy matrices for filament-wound graphite structures [DE85-003674] N85-22642

MAXIMUM LIKELIHOOD ESTIMATES
Accuracy of approximation of Bayes estimates in presence of noninformative parameters N85-23015
Reception of signal with unknown amplitude and duration submerged in white noise N85-23016
Why do noninvertible estimated moving averages occur? [AD-A150368] N85-23368

MEAN
Motion of symmetrical satellite with flexible viscoelastic rods about center of mass in circular orbit N85-22420
Microcomputer: Controlled statistics analyzer [BLL-CE-TRANS-7971-(9022.09)] N85-23306

MEASURING INSTRUMENTS
Dielectric measurements in infralow-frequency band N85-23034
Proceedings of the Geoscience Instrumentation Workshop [DE85-004359] N85-23268

MECHANICAL DEVICES
Cyclic industrial robots with mechanical energy storing devices: Principles of drive design N85-22807
Optimum design and automated dynamic analysis of flexible mechanisms [AD-A150152] N85-23088

MECHANICAL DRIVES
Design of tightening device and calculation of forces in manipulator transmissions with base-drive mounted N85-22804
Cyclic industrial robots with mechanical energy storing devices: Principles of drive design N85-22807
Assembly robot control algorithms N85-22808

MECHANICAL ENGINEERING
Design and qualification testing of the Olympus solar array blanket N85-22600
The Olympus solar array structure and mechanisms N85-22623
Advances in cutting tool technology surveyed N85-22840

MECHANICAL PROPERTIES
Kapton charging characteristics: Effects of material thickness and electron-energy distribution N85-22513
Influence of external electric field on structural-mechanical properties of powdered materials N85-22630
Rapid solidification processing of magnesium alloys [AD-A150270] N85-22668
Mechanical properties of electrodeposited nickel and copper [DE85-005321] N85-22677
Influence of laser treatment of structure and mechanical properties if MA21 alloy N85-22713
Influence of annealing on cyclic and short-term strength of thin sheets of VT1-0 titanium and OTR4 alloy N85-22727
Method of calculating strength of joint produced by cold welding of aluminum under discrete loading N85-22743
Effect of moisture in inert gases on density of seam metal and on mechanical characteristics of welded joints of aluminum and aluminum alloys N85-22744
Characteristics of surface crack development in AT1sS aluminum alloy during slow-cycle loading N85-22745
Research program on the effect of pressure on the mechanical properties of polymers, part 2 [DE85-000995] N85-22761
Diamond cutters' grinders N85-22841
The ferrite permanent magnet AC motor: A technical and economical assessment [DE85-002480] N85-22903
The Shock and Vibration Digest, volume 16, no. 12 [AD-A150594] N85-23102

MECHANICAL SHOCK
The Shock and Vibration Digest, volume 16, no. 12 [AD-A150584] N85-23102

MECHANICS (PHYSICS)
User's and programmer's guide to the mechanics of moving finite element code [DE85-006165] N85-23365

MEDICAL SCIENCE
Armed forces special Symposium on Medicine of Altitudes N85-23441

MELT SPINNING
Rapid solidification processing of magnesium alloys [AD-A150270] N85-22668
Apparatus for producing amorphous and microcrystalline metal powders N85-22720

MELTING
Experimental and numerical analysis of electric currents and electromagnetic blunting of cracks in thin plates [AD-A150418] N85-22669
Determining degree of partial melting of asthenosphere from seismic data N85-23127
Hydrovolcanism N85-23574
Radiation-dominated snowmelt on Mars N85-23592

MELTS (CRYSTAL GROWTH)
Experimental methds for quenching structures in lunar-analog silicate melts: Variations as a function of quench media and composition N85-23554

MEMBRANES
Interaction of metals and metalloids with biomembranes [DE85-004902] N85-23293

MENTAL PERFORMANCE
Human cognition and intelligence: Towards an integrated theoretical perspective [CSIR-SR-PERS-350] N85-23300

MERCURY (PLANET)
Mercury radar altimetry: A preliminary analysis N85-23631
Mapping and geological analysis of Mercury and Venus radar ranging data N85-23633
Mechanisms of basalt-plains ridge formation N85-23643

MESOSCALE PHENOMENA
Digital processing of mesoscale analysis and space sensor data [NASA-CR-171429] N85-23319

MESSAGE PROCESSING
A perspective on multiaccess channels [AD-A150183] N85-23322
Orphan detection in the Argus system [AD-A150562] N85-23331

METAL BONDING
Study of character of adhesive interaction and breaking of polyimid-aluminum foil junction during process of hardening N85-22637

METAL COATINGS
Metallic and metalloceramic coating by thermal decomposition [NASA-TM-86992] N85-22755
Film and interstitial formation of metals in plasma-sprayed ceramics [NASA-TM-86993] N85-22756

METAL COMBUSTION
Status of boron combustion research N85-22528
Ignition phenomena of bulk aluminum alloy as a function of oxygen pressure N85-22531

METAL CRYSTALS
Observation of surface vibrational resonances on (110) surfaces of FCC metals [AD-A150469] N85-23419

METAL FATIGUE
Structural strenght of strip D16T aluminum alloy with low copper and magnesium content N85-22691
Fatigue life, crack initiation, and propagation of 304 stainless steel with non-proportional axial/torsional strain-paths N85-23094

METAL FILMS
Reaction of amorphous NiNb films with crystalline metal overlayers [DE85-005483] N85-22680

METAL FOILS
Study of character of adhesive interaction and breaking of polyimid-aluminum foil junction during process of hardening N85-22637

METAL MATRIX COMPOSITES
Effect of operating medium on cyclic durability of AD33-W composite N85-22716

METAL OXIDE SEMICONDUCTORS
Metal-semiconductor phase transition and its application [DRIC-T-7149] N85-22665
Electrical overstress protection of submicron devices [AD-A150334] N85-22892
Algorithm in Walsh function basis for analysis of integrated microcircuits on MOS-structures N85-23006

METAL PARTICLES
Sample introduction methods for improving the particle detection capability of the spectrometric oil analysis program [AD-A150139] N85-23399

METAL PLATES
Numerical results of acoustic radiation, transmission and reflection of steel plate in water [AMTE(N)-TM-84037] N85-23378

METAL POWDER
Structural distortions of ultra-dispersed titanium nitride powders N85-22717
Degassification of silicon nitride powders of various origins N85-22718
Apparatus for producing amorphous and microcrystalline metal powders N85-22720

METAL SURFACES
Formation of alumina layers on iron-base alloys [BLL-T6418/BG/LRS/LRST737/84] N85-22657
Study of the effects of implantation on the high Fe-Ni-Cr and Ni-Cr-Al alloys [NASA-CR-175625] N85-22661

METAL VAPORS
Combustion kinetics of metal atoms and metallic radicals over wide temperature ranges N85-22530

METAL WORKING
Use of ferrofluids in machining of metals N85-22802
USSR report: Machine tools and metalworking equipment [JPRS-UMM-85-005] N85-22839
Advances in cutting tool technology surveyed N85-22840
New tooling for plasma cutting technology N85-22842

METALLIC GLASSES
Quenching effects on iron site partitioning in the Apollo 17 orange glass composition N85-23553

METALLIZING
Electrostatic forming and testing of polymer films on a 16-foot diameter test fixture [NASA-TM-86328] N85-22885

METALLOIDS
Interaction of metals and metalloids with biomembranes [DE85-004902] N85-23293

METALS
Characteristics of EMI generated by negative metal-positive dielectric voltage stresses due to spacecraft charging N85-22505
Adequacy of metal ablation process with laser radiation and a shock-compressed plasma N85-22708
Effect of transparent coatings on generation of laser-induced shock waves in metals N85-22711
Generation of longitudinal acoustic waves by modulated helicon waves — nonlinear steady state waves in metals N85-23049

METASTABLE STATE
Specifics of structure and mechanical properties of metastable beta-titanium alloys after deformation and aging N85-22731

METEOR TRAILS
Calculation of amplitude-phase characteristics of signal scattered obliquely on meteor trail N85-22948

METEORITE CRATERS
Martian terrain ages N85-23537
Interaction of Martian flow ejecta blankets with pre-existing impact craters: Morphological observations N85-23546

METEORITIC COMPOSITION
Hibonite: Crystal chemistry and origin of blue coloration in meteoritic assemblages N85-23555
Crystal chemistry of meteoritic hibonites N85-23556

METEORITIC MICROSTRUCTURES
Crystal chemistry of meteoritic hibonites N85-23556

METEOROIDS
Plasma production by meteoroid impact N85-23492

METEOROLOGICAL CHARTS
Digital processing of mesoscale analysis and space sensor data [NASA-CR-171429] N85-23319

METEOROLOGICAL PARAMETERS
Slow motions in the tropical troposphere N85-23262
Summary of Meteorological Observations, Surface (SMOS) Camp Pendleton, California [AD-A150482] N85-23277
Summary of Meteorological Observations, Surface (SMOS), Bermuda [AD-A150537] N85-23278
Summary of Meteorological Observations Surface (SMOS), Sigonella, Sicily/Navy [AD-A150539] N85-23280

Summary of Meteorological Observations, Surface (SMOS), Alameda, California
[AD-A150609] N85-23281

METEOROLOGICAL RADAR
Radiosodar system for remote synchronous measurements of wind speed, temperature and its fluctuations N85-23145

METEOROLOGICAL SATELLITES
Remote sensing used for study of forest resources N85-22440

METEOROLOGY
USSR report: Earth sciences
[JPRS-UES-85-002] N85-23116
Mean flow and turbulence in complex terrain NPS (Naval Postgraduate School)/Vandenberg measurement system
[AD-A150184] N85-23274

METHANE
Ignition of mixtures of SiH sub 4, CH sub 4, O sub 2, and Ar or N sub 2 behind reflected shock waves
[NASA-TP-2415] N85-22395
Anaerobic digestion of biomass: status summary and research development needs, 1983
[PB85-161925] N85-22772

METHOD OF MOMENTS
Variational and moment method solutions of the fields in a parallel-plate waveguide-aperture system
[DE85-006288] N85-22876

MICHELSON INTERFEROMETERS
Geophysical laser interferometer with 12.5 meter base N85-23046
Mode control and wavelength tuning in open ended Michelson interferometric semiconductor laser N85-23073

MICROCOMPUTERS
Microcomputer: Controlled statistics analyzer
[BLL-CE-TRANS-7971-(9022.09)] N85-23306
Exploiting parallel computing with limited program changes using a network of microcomputers
[NASA-TM-86387] N85-23318
Microcomputers and the electrical engineer
[AD-A150499] N85-23325

MICROCRACKS
Change in microstructure of heat-resistant nickel alloys upon thermal cycling in a current of gas N85-22725

MICROELECTRONICS
Electrical overstress protection of submicron devices
[AD-A150334] N85-22892
Code lock with microcircuit N85-22935
Recommendation on use of series K157UL1 microcircuits N85-22936
Application of K176-series microcircuits N85-22973
Parallel test method for LSI (Large Scale Integration) microprocessors
[AD-A150237] N85-23310

MICROHARDNESS
Structure and mechanical characteristics of heterogeneous joints produced by laser welding N85-22742
Frictional and structural characterization of ion-nitrided low and high chromium steels
[NASA-TM-86991] N85-23085

MICROORGANISMS
Analysis of biological particles by mass spectrometry
[AD-A149952] N85-23291

MICROPROCESSORS
NDE methods for green ceramics
[DE85-004019] N85-22766
The audiomat: An automatic audiometer for use in occupational audiometry
[DRIC-T-7138] N85-23294

MICROSTRIP TRANSMISSION LINES
A generalized solution to a class of printed circuit antennas N85-22862
Synthesis of optimum smooth transition in microstrip through line on microwave integrated circuit N85-23041

MICROSTRUCTURE
Micromechanical modeling of microstructural damage in creeping alloys
[DE85-003925] N85-22671
TEM/FIM study of modulated microstructures in the Fe-Be system
[DE85-005379] N85-22678
Influence of laser treatment of structure and mechanical properties if MA21 alloy N85-22713
Electrodynamic stability of composite liquid-metal contacts N85-23031
Microstructural study on the processing and properties of high-field A15 superconducting materials
[DE85-004652] N85-23423

MICROWAVE AMPLIFIERS
Analysis and design of linear microwave transistor amplifiers N85-23038

MICROWAVE ATTENUATION
Absorption of radiation by water vapor in windows of relative transparency of 95-145 micrometer range N85-22968
The microwave propagation and backscattering characteristics of vegetation — wheat, sorghum, soybeans and corn fields in Kansas
[E85-10088] N85-23213

MICROWAVE CIRCUITS
Reduction of amplitude-phase distortions of movable microwave coupling circuit for antenna field measurements N85-22920

MICROWAVE COUPLING
Reduction of amplitude-phase distortions of movable microwave coupling circuit for antenna field measurements N85-22920
Synthesis of multistep directional couplers with nonminimum-phase characteristics N85-22986

MICROWAVE EMISSION
Remote Sensing of Snow and Evapotranspiration
[NASA-CP-2363] N85-23223
Microwave radiometer observations of snowpack properties and comparison of U.S. Japanese results — Hokkaido, Japan and Vermont and North Dakota test sites N85-23230
Microwave remote sensing of soil moisture N85-23235

MICROWAVE EQUIPMENT
Planar ferroelectric microcapacitors for microwave devices N85-23032
Demonstration of feasibility of depositing semiconductor layers using microwave enhanced plasma techniques
[NASA-CR-174392] N85-23421

MICROWAVE FILTERS
Synthesis of low-pass filters using coupled lines with unmatched loads N85-22938
Investigation of bimodal paramagnetic filter N85-23007

MICROWAVE OSCILLATORS
Effect of space-charge field on output characteristics of O-type oscillators with distributed interaction N85-23043

MICROWAVE PROBES
Mutiple reflection theory for microwave measurement of solid propellant burning rates N85-22549

MICROWAVE RADIOMETERS
Studies on physical properties of snow based on multi channel microwave radiometer N85-23231

MICROWAVE REFLECTOMETERS
Comparing different theoretical designs of six-port reflectometer junctions
[AD-A149419] N85-22861

MICROWAVE SCATTERING
The microwave propagation and backscattering characteristics of vegetation — wheat, sorghum, soybeans and corn fields in Kansas
[E85-10088] N85-23213

MICROWAVE SENSORS
Short-range radiotechnical point sensor N85-22996

MICROWAVE TRANSMISSION
Millimeter-wave range masers: A review N85-23042

MICROWAVES
Microwave blackbodies for spaceborne receivers
[NASA-CR-175647] N85-23088
Calculations of microwave brightness temperature of rough soil surfaces: Bare field
[NASA-TM-86200] N85-23221

MIDAIR COLLISIONS
TCAS II: Design and validation of the high-traffic-density surveillance subsystem
[DOT/FAA/PM-84/5] N85-22375

MIE SCATTERING
A systematic study of light scattering by irregularly shaped particles
[AD-A150192] N85-23400

MILITARY AIRCRAFT
Reliability predictions for military avionics. Royal Signals and Radar Establishment reliability prediction method no. 250
[BR69221] N85-22388

MILITARY OPERATIONS
Testing of the digital flight control system of the German CCV fighter experimental aircraft N85-22361

MILITARY TECHNOLOGY
U.S., Soviet space program aims contrasted N85-22455
Low-bit rate speech encoders based on Line-Spectrum Frequencies (LSF)
[AD-A150518] N85-22871

MILKY WAY GALAXY
The color excesses of classical cepheids and the structure of our galaxy N85-23459

MILLIMETER WAVES
Effect of space-charge field on output characteristics of O-type oscillators with distributed interaction N85-23043

MILLING MACHINES
New tooling for plasma cutting technology N85-22842
T700 cutter life improvement program
[AD-A150450] N85-23089

MINERAL DEPOSITS
Geologic utility of LANSDAT-4 TM data — Death Valley, California and the Silver Bell area of southern Arizona N85-23192
Characteristics of alumyte deposits discussed N85-23438

MINERAL EXPLORATION
Arctic-North Atlantic rift megasystem N85-23117
Possibilities of aerial electric prospecting by long cable method for detecting poorly conducting strata N85-23177
Evaluation of Thematic Mapper performance as applied to hydrocarbon exploration — Ontario, Canada; Cement, Oklahoma; and Death Valley, California N85-23191

MINERALOGY
Characteristics of alumyte deposits discussed N85-23438
The olivine asteroids: Discovery, mineralogy, and relationship to palasites N85-23500
Crystal chemistry of meteoritic hibonites N85-23556
Determining mineral types and abundances from reflectance measurements N85-23622
Determination of mineral type, abundance, and grain size with remotely obtained reflectance spectra N85-23623
Quantitative analyses of planetary reflectance spectra N85-23625
Analysis of SMIRR data for volcanic and sedimentary terrains of the trans-Pecos region, Texas N85-23626

MINERALS
Review of problems in lithology N85-23160
Rapid advances in geological work N85-23437
Characteristics of alumyte deposits discussed N85-23438
Impact and collisional processes in the solar system N85-23530
First direct detection of clay minerals on Mars N85-23612
Iron oxides of Mars: Evidence for contemporary weathering N85-23613
Zeolites on Mars: Prospects for remote sensing N85-23615

MINES (EXCAVATIONS)
Comparative techniques used to evaluate Thematic Mapper data for land cover classification in Logan County, West Virginia N85-23209
Rapid advances in geological work N85-23437

MINIMAX TECHNIQUE
Regular synthesis of pairs of phase-keyed binary minimax signals N85-22923

MINING
China report: Science and technology
[JPRS-CST-85-003] N85-23433
Rapid advances in geological work N85-23437

MIRRORS
Three-mirror open resonator for millimeter wave band N85-22972
ROSA: A computer model for optical power ratio calculations
[DE85-005174] N85-23251
Innovative research in the design and operation of large telescopes for space: Aspects of giant telescopes in space
[NASA-CR-175626] N85-23462

MISMATCH (ELECTRICAL)
Nonlinearity and spectral mismatch problems of solar cells N85-22605

MISSILE CONTROL
Space interception guidance with uncertain factors N85-22781

MISSILE DESIGN
The application of some lifting-body reentry concepts to missile design
[NASA-TM-86394] N85-22366

MISSILE TRAJECTORIES
Technical manual: Description and operation Slaved Tracking System
[DE85-004807] N85-23070

MISSION PLANNING
Activities of the Jet Propulsion Laboratory, 1 January - 31 December 1983
[NASA-CR-175555] N85-23447

MIXING
Constraints of observations of solar oscillations on solar models with mixing by turbulent diffusion
[DE85-003741] N85-23678

MODELS
Protons with energies above 30 KeV in Earth's radiation belt at low altitudes during magnetically quiet time close to geomagnetic equator N85-22423
Auroral-polar cap environment and its impact on spacecraft plasma interactions N85-22484
Three-dimensional calculation of shuttle charging in polar orbit N85-22486

Acoustic energy balance method N85-22537
Measurement requirements for the detection of ozone trends N85-23115
Study of resolution of deep MT soundings by means of physical model N85-23155
LEXICON: A structured modeling system for optimization [AD-A150536] N85-23329
Monte Carlo modeling of lunar megaregolith development N85-23627
Analyses of radar images of small craters N85-23642
Terrestrial analogs for planetary wrinkle ridges N85-23644

MODES
The effects of internal waves on acoustic normal modes [AD-A150235] N85-23379

MODULATION
Generation of longitudinal acoustic waves by modulated helicon waves — nonlinear steady state waves in metals N85-23049
Modulation of light energy transduction in photosynthesis [DE85-004711] N85-23292

MODULATION TRANSFER FUNCTION
An investigation of several aspects of LANDSAT-5 data quality — Palmer County, Shelby, mt; White sands, NM; Great Salt Lake, UT; San Matted Bridge and Sacramento, California [E85-10096] N85-23214

MODULUS OF ELASTICITY
Development and study of two-matrix glass fiber composite with increased transverse deformation N85-22700
Fracture mechanics evaluation of GaAs [NASA-CR-175657] N85-23101

MOISTURE
The evolution of CO2 on Mars N85-23558

MOISTURE CONTENT
Effect of moisture in inert gases on density of seam metal and on mechanical characteristics of welded joints of aluminum and aluminum alloys N85-22744
Dependence of combustion of homogeneous kerosene-air mixtures on humidity of air N85-22835
Distribution of snow and maximum snow water equivalent obtained by LANDSAT data and degree day method N85-23229
Microwave radiometer observations of snowpack properties and comparison of U.S. Japanese results — Hokkaido, Japan and Vermont and North Dakota test sites N85-23230
Studies on physical properties of snow based on multi channel microwave radiometer N85-23231

MOLDING MATERIALS
Exploratory development of foams from liquid crystal polymers [NASA-CR-172510] N85-22754

MOLECULAR CLOUDS
The Formation of preplanetary disks from the collapse of rotating molecular cloud cores N85-23526

MOLECULAR DIFFUSION
Contribution to theory of ocean-atmosphere gas exchange N85-23134

MOLECULAR ENERGY LEVELS
Sequential excitation preparation of molecular energy levels with special structural and chemical properties [AD-A150301] N85-23386

MOLECULAR EXCITATION
Threshold double photoionization of argon with synchrotron radiation [AD-A150615] N85-23389

MOLECULAR FLOW
Structure of amorphous films of alloys based on Fe, condensed from laser erosion products N85-22749

MOLECULAR INTERACTIONS
Combustion kinetics of metal atoms and metallic radicals over wide temperature ranges N85-22530
Molecular dynamics of propellant gases, part 2 N85-22552
Molecular dynamics studies of energy transfer processes in crystal systems [AD-A150161] N85-23416

MOLECULAR OSCILLATIONS
Sequential excitation preparation of molecular energy levels with special structural and chemical properties [AD-A150301] N85-23386

MOLECULAR RELAXATION
Theory of relaxation processes in decomposing polymer materials during high-intensity convective heating N85-22710

MOLECULAR STRUCTURE
The crystal and molecular structure of a new propellant compound: Triaminoguanidium Azide Nitrate (TAZN) N85-22551
The chemistry of RDX and HMX cluster ions N85-22561
The influence of fuel molecular composition upon flame-tube temperature and flame radiation in a model gas-turbine primary zone [K234] N85-22646
Sequential excitation preparation of molecular energy levels with special structural and chemical properties [AD-A150301] N85-23386

MOLECULES
Mean delta-ray energies in ion molecule collisions [DE85-005524] N85-23395

MOLTEN SALTS
Cathode materials for molten carbonate fuel cells [DE85-004078] N85-23254

MOMENTUM
Mathematical modeling of transient performance of gas turbine engine N85-22834

MOMENTUM TRANSFER
Physics of the inner heliosphere: Mechanisms, models and observational signatures [NASA-CR-175632] N85-23677

MONOCHROMATIZATION
A posteriori increase of resolving power of optical system forming averaged monochromatic images N85-23003

MONOMERS
Chiral polymers [AD-A150366] N85-22760

MONOPOLE ANTENNAS
Surface wave excitation study [DE85-005301] N85-22875

MONSOONS
Relationship of Indian monsoon intensity to time of onset N85-23120

MONTE CARLO METHOD
A Monte Carlo sampling plan for estimating network reliability [AD-A150511] N85-22898
Introduction to combinatorial geometry [DE85-003266] N85-23364
Problems in recovering crater production functions N85-23539
Monte Carlo modeling of lunar megaregolith development N85-23627

MOON
Giant planets and their satellites: Cosmochemistry, evolution and structure N85-23494
A circum-terrestrial compositional filter N85-23520
Models of angular momentum input to a circum-terrestrial swarm from encounters with heliocentric planetesimals N85-23521
Landform identification on radar images N85-23635
Radar observations of fissure-fed basaltic lava flows, Craters of the Moon, Idaho N85-23640

MORPHOLOGY
Origin of Martian polygonal terrain: Preliminary results N85-23591

MOSAICS
Viking Lander mosaics of Mars N85-23667
Voyager cartography N85-23668

MOSSBAUER EFFECT
Quenching effects on iron site partitioning in the Apollo 17 orange glass composition N85-23553
Hibonite: Crystal chemistry and origin of blue coloration in meteoritic assemblages N85-23555

MOTION SIMULATION
Method for prompt modeling of quasiperiodic movement of solid near-axisymmetrical body in atmosphere N85-22790

MOTION STABILITY
Absolute stability of unsteady movement of axisymmetrical rotating flight vehicle N85-22793
Electronics Engineering Department EE Technical Review [UCRL-50025-84-1] N85-22887

MOUNTAINS
Preliminary photomaps of Venus surface in the Maxwell Mountains and adjacent areas N85-22438
The geology of Mt. Hope, a silicic volcanic center in West Central Arizona N85-23571
Geomorphology and geology of the Southwestern Margaritifer Sinus and Argyre regions of Mars. Part 1: Geological and geomorphological overview N85-23600

MOUNTING
Advanced life analysis methods. Volume 1: Cracking data survey and NDI (nondestructive inspection) assessment for attachment lugs [AD-A150419] N85-23108
Advanced life analysis methods. Volume 2: Crack growth analysis methods for attachment lugs [AD-A150420] N85-23109

MOVING TARGET INDICATORS
Moving target detection N85-22915

MULTIBEAM ANTENNAS
Synthesis of multistep directional couplers with nonminimum-phase characteristics N85-22986

MULTICHANNEL COMMUNICATION
Error probability during optimal noncoherent reception of binary signals in multibeam channel N85-22922
Asymptotically optimum multialternative sequential procedures for discernment of processes minimizing average length of observations N85-23012
A perspective on multiaccess channels [AD-A150183] N85-23322

MULTIMODE RESONATORS
Coupled-cavity gyrotrons with mode conversion N85-22967
Investigation of generation of oscillations using anomalous Doppler effect N85-22980

MULTIPHASE FLOW
Development of a three-phrase combustion code for modeling liquid rocket engines N85-22554

MULTIPLE ACCESS
A perspective on multiaccess channels [AD-A150183] N85-23322

MULTIPLEXING
Integrated digital networks [AD-A150605] N85-22873
Interference immunity of fiber-optic communication lines with spectral multiplexing of channels N85-22924

MULTIPLIERS
Efficiency of digital compensator of strong non-Gaussian interference N85-22942

MULTIPOLES
Structures of ordered linear dislocation multipoles in Cu-Al alloys [ISSN-0379-6906] N85-22664

MULTIPROCESSING (COMPUTERS)
Exploiting multiprocessors: Issues and options [DE85-003144] N85-23313
Synthesis of tree-structured computing systems through use of closures [AD-A150502] N85-23326

MULTIPROGRAMMING
Exploiting multiprocessors: Issues and options [DE85-003144] N85-23313

MULTISPECTRAL BAND SCANNERS
Preliminary comparisons of the information content and utility of TM versus MSS data N85-23202
The use of Thematic Mapper data for land cover discrimination: Preliminary results from the UK SATMaP programme N85-23207

MULTISPECTRAL PHOTOGRAPHY
Feature extraction assessment study [AD-A150189] N85-23239
Comprehensive, integrated, remote sensing at DOE sites [DE85-004867] N85-23240
Multispectral analysis of the Kasei Vallis-Lanae Planum region of Mars N85-23607

MULTIVARIATE STATISTICAL ANALYSIS
Draftsman displays: A graphical technique for exploratory data analysis [AD-A150515] N85-22775
Effects of assuming independent component failure times, if they are actually dependent, in a series system [AD-A150582] N85-23092
Multivariate analysis and its applications [AD-A150324] N85-23352
On limit of the largest eigenvalue of the large dimensional sample covariance matrix [AD-A150589] N85-23358

N

N-TYPE SEMICONDUCTORS
Thermally stimulated conductivity in semi-insulating gallium arsenide N85-23036

NAP-OF-THE-EARTH NAVIGATION
Ground evaluation of helicopter air-to-air warfare N85-22360

NASA PROGRAMS
U.S., Soviet space program aims contrasted N85-22455
NASA photovoltaic research and technology development program for space applications N85-22617
NASA's land remote sensing plans for the 1980's N85-23224
Small business innovation research: Abstracts of 1984. Phase 1 awards [NASA-TM-87427] N85-23431
NASA Patent Abstracts Bibliography. A continuing bibliography. Section 2: Indexes [NASA-SP-7039(26)] N85-23445
Authorizing appropriations to the National Aeronautics and Space Administration for fiscal year 1986 [H-REPT-99-32] N85-23452

NATURAL GAS
New method of reconstructing conditions of recent differentiation of oil and gas in the Amudarya Basin (based on results of interpretation of space photographs) N85-22446

NATURAL GAS EXPLORATION
New method of reconstructing conditions of recent differentiation of oil and gas in the Amudarya Basin (based on results of interpretation of space photographs) N85-22446
Evaluation of Thematic Mapper performance as applied to hydrocarbon exploration — Ontario, Canada; Cement, Oklahoma; and Death Valley, California N85-23191

NATURAL SATELLITES
Interaction of the magnetospheric ions with the surfaces of the icy satellites of Saturn N85-23491
Origin and evolution of the Saturn system N85-23493
Studies of icy bodies: Uranian satellites and cometary nuclei N85-23496
Small solar system bodies N85-23499
Impact and collisional processes in the solar system N85-23530

NAVIER-STOKES EQUATION
Internal fluid mechanism of solid propellant rocket motors N85-22544
Liquid moment on a filled coning cylinder during spin-up: Ad hoc model [AD-A150280] N85-23060
Significance of the thin-layer Navier-Stokes approximation [DE85-002630] N85-23063

NAVIGATION AIDS
Reference systems for the evaluation of dead-reckoning navigation equipment N85-22358
Operational experience with ion concentration sensors in orientation systems N85-22422

NAVIGATION INSTRUMENTS
Reference systems for the evaluation of dead-reckoning navigation equipment N85-22358

NEAR FIELDS
Near Field/Far Field (NF/FF) energy loss in Electric Discharge Lasers (EDL's): A mode-medium interaction [AD-A150299] N85-23075

NEGATIVE FEEDBACK
Playback amplifier with high interference immunity N85-22970

NEODYMIUM LASERS
Neodymium YAG laser pumped with radiation from high frequency electrodeless discharge N85-22796
Research, development of laser glasses in China N85-23439

NEPTUNE (PLANET)
The structure and composition of Uranus and Neptune N85-23495

NETWORK ANALYSIS
A fully distributed approach to the design of a 16 K bit/sec VHF packet radio network [AD-A141282] N85-22859
Research using a DISCUS based network emulator [AD-A141294] N85-23338

NETWORK CONTROL
System dynamics and network control [AD-A149420] N85-22663

NEUMANN PROBLEM
The low frequency behaviour of an immersed structure at a standstill in a high density fluid with free surface [TP-1983-31] N85-23105

NEUTRAL PARTICLES
Mass spectra of neutral particles released during electrical breakdown of thin polymer films N85-22511

NEUTRON ACTIVATION ANALYSIS
Multiple element neutron-activation analysis of atmospheric aerosols with X-ray and gamma-spectrometric recording of radionuclides formed N85-22631

NEUTRON COUNTERS
Ultrahigh-sensitivity threshold neutron detector for plasma diagnostics [DE85-005270] N85-23413

NEUTRON DIFFRACTION
Microscopic magnetic structure of multiple bilayers of thin films of Fe and Ge [DE85-004188] N85-22682

NEUTRON IRRADIATION
Effects of neutron irradiation at 450(0)C and 16 dpa on the properties of various commercial copper alloys [DE85-005716] N85-22684

NEUTRON SPECTRA
The effect of the choice or response matrix on unfolded bonner sphere spectra [AD-A150462] N85-23404

NEUTRON SPECTROMETERS
The effect of the choice or response matrix on unfolded bonner sphere spectra [AD-A150462] N85-23404

NEUTRON STARS
Cooling of neutron stars with hyperons [DE85-004841] N85-23472

NEVADA
Summary of Meteorological Observations, Surface (SMOS), Fallon, Nevada [AD-A150481] N85-23276

NICKEL
Mechanical properties of electrodeposited nickel and copper [DE85-005321] N85-22677
Role of segregated P and S in intergranular stress corrosion cracking of nickel [DE85-004547] N85-22679
Apparatus for producing amorphous and microcrystalline metal powders N85-22720
Molten carbonate fuel cell performance model update, draft [DE85-005423] N85-23252
Adsorption site, adsorption energy and normal vibration frequency of H/Ni(100) via total energy calculations [AD-A150555] N85-23388
Observation of surface vibrational resonances on (110) surfaces of FCC metals [AD-A150469] N85-23419
Dipole active surface vibrational resonances on clean and hydrogen covered Ni(110) [AD-A150546] N85-23420

NICKEL ALLOYS
Study of the effects of implantation on the high Fe-Ni-Cr and Ni-Cr-Al alloys [NASA-CR-175625] N85-22661
Thermodynamics of copper-nickel alloys containing aluminum, silicon, titanium, and chromium relative to their use in ceramic brazing [DE85-004787] N85-22674
Reaction of amorphous NiNb films with crystalline metal overlayers [DE85-005483] N85-22680
Effect of phase state of TiC-NiTi powder composite materials on nature of failure and mechanical properties N85-22702
Long-term strength and fracture criteria for EI698VD alloy under complex stress conditions N85-22723
Change in microstructure of heat-resistant nickel alloys upon thermal cycling in a current of gas N85-22725

NICKEL COMPOUNDS
Magnetovolume effects in some Y-Ni intermetallic compounds [ISSN-0066-2003] N85-22663
Raman structural studies of the nickel electrode [NASA-CR-175619] N85-23414

NICKEL OXIDES
Grain boundaries in NiO [DE85-006129] N85-22687

NIGHTGLOW
Increase in hydrogen emission of upper atmosphere following launches of space vehicles N85-22431

NIOBIUM
Spectral evaluation of irregularity of superconducting coaxial cables N85-23000

NIOBIUM ALLOYS
Reaction of amorphous NiNb films with crystalline metal overlayers [DE85-005483] N85-22680
Decomposition of VTAN alloy solid solution upon irradiation and thermal aging N85-22712
High temperature antifriction properties of Ti sub 1-sub xNb sub x C sub 0.5N sub 0.5 alloys N85-22715

NIOBIUM CARBIDES
Possibility of producing monolithic composite materials based on niobium carbide N85-22707

NIOBIUM COMPOUNDS
Critical current measurements on an NbTi superconducting wire standard reference material [PB85-118594] N85-22906

NITRAMINE PROPELLANTS
Chemical kinetics of gas phase decomposition products of nitramine propellants N85-22558
Kinetics of mechanism of the thermal decomposition of dimethylnitramine and dimethylnitrosamine N85-22559

NITRATES
The crystal and molecular structure of a new propellant compound: Triaminoguanidium Azide Nitrate (TAZN) N85-22551
Geographic variation in the relationships of temperature, salinity or sigma sub t versus plant nutrient concentrations in the world ocean — silicic acid, nitrate, and phosphate concentration [NASA-CR-175621] N85-23287

NITROGEN
Molecular dynamics of propellant gases, part 2 N85-22552
An atlas of nitrogen-broadened water vapor spectra from 500 to 5000 cm(-1), volume 1 [AD-A150527] N85-22650

NITROGEN COMPOUNDS
Adsorption behaviour of nitrogen compounds on to porous polymer beads and applications to atmospheric sampling [BLL-DRIC-TRANS-7399-(3623.66)] N85-22753

NITROGEN PLASMA
Frictional and structural characterization of ion-nitrided low and high chromium steels [NASA-TM-86991] N85-23085

NOAA SATELLITES
Scientific requirements for ozone measurements N85-23113

NOISE (SOUND)
Machine tool vibrations: A review N85-23104

NOISE PREDICTION (AIRCRAFT)
Wind tunnel acoustic study of a propeller installed behind an airplane empennage: Data report [NASA-CR-177335] N85-23377

NOISE SPECTRA
Shuttle electrical environment N85-22475
Noise characteristics of sulfur-doped silicon diodes N85-22952

NOISE TOLERANCE
Investigation of influence of communications link and synchronization error on noise tolerance of group transmission of binary information based on orthogonal Walsh function N85-23026
A community survey of helicopter noise annoyance conducted under controlled noise exposure conditions [NASA-TM-86400] N85-23374

NONDESTRUCTIVE TESTS
Investigation of steel structures using ultrasonic waves [BR93258] N85-23091
Magnetic field interactions with material discontinuities [AD-A150197] N85-23373

NONFERROUS METALS
Rational use of tatanium in nonferrous metallurgy N85-22728

NONLINEAR FILTERS
Prefiltration in Kalman filter with a priori indeterminacy N85-22939

NONLINEAR SYSTEMS
Nonlinear rotordynamics analysis [NASA-CR-171425] N85-22364
Nonlinear interactions between vortices and acoustic waves in a rocket combustion chamber N85-22533
A model for large sparse contingency tables [AD-A150320] N85-23350

NONLINEARITY
Seismic waves and dispersion relations N85-23181

NONSTABILIZED OSCILLATION
Coupled acoustic and hydrodynamic wave instabilities N85-22538

NONUNIFORM PLASMAS
Diffraction of plane TM-wave on continuously irregular elliptical plasma N85-22914

NONUNIFORMITY
Spectral evaluation of irregularity of superconducting coaxial cables N85-23000

NORTH AMERICA
Arctic-North Atlantic rift megasystem N85-23117
El Nino, the capricious child N85-23121

NORTHERN HEMISPHERE
Moisture variation in northern hemisphere temperate latitudes N85-23119

NOZZLE GEOMETRY
Some unique features of isentrophic flow of gas under high pressures N85-22788

NOZZLES
Pressure drop and coefficients of internal heat transfer necessary for transpiration cooling N85-22831

NUCLEAR EXPLOSIONS
Attenuation of seismic waves at regional distances [AD-A150198] N85-23257

NUCLEAR INTERACTIONS
Theoretical aspects of electroweak and other interactions in medium-energy nuclear physics [DE85-003821] N85-23392

NUCLEAR PHYSICS
Theoretical aspects of electroweak and other interactions in medium-energy nuclear physics [DE85-003821] N85-23392

NUCLEAR REACTORS
Comprehensive, integrated, remote sensing at DOE sites [DE85-004867] N85-23240

NUMERICAL ANALYSIS
China report: Science and technology [JPRS-CST-84-008] N85-22384
Elasticity solution of an adhesively bonded joint [NASA-CR-175591] N85-23097
A clamped rectangular plate containing a crack [NASA-CR-175590] N85-23098

Evolution of set of Rossby waves toward anisotropic equilibrium state N85-23141
Two-dimensional numerical model of sensible and latent heat transport in an irrigated field under advective conditions N85-23261
Second thoughts on the mathematical software effort: A perspective
[DE85-004831] N85-23333

NUMERICAL CONTROL
Reliability of robotized welding apparatus N85-22741
Assembly robot control algorithms N85-22808

NUMERICAL INTEGRATION
Problem of diffraction by wavy surface: Comparison of numerical methods of solution N85-22985

NUMERICAL WEATHER FORECASTING
Summary of Meteorological Observations, Surface (SMOS), Bermuda
[AD-A150537] N85-23278
Summary of Meteorological Observations, Surface (SMOS), Beaufort, South Carolina
[AD-A150538] N85-23279

O

OCEAN BOTTOM
Determining degree of partial melting of asthenosphere from seismic data N85-23127
Determining adsorption of surface-active substances by sea bottom deposits N85-23128
Use of paleomagnetic data in tectonic analysis of oceanic structures N85-23135
More precise curve of dependence between density and velocity of longitudinal waves in consolidated crust and top of mantle in oceanic structures N85-23143
Crustal and upper mantle density model of Owen fault zone N85-23144
Structure of Iceland and ocean floor spreading N85-23159
Assessing LANDSAT TM and MSS data for detecting submerged plant communities N85-23203
Remanent magnetization model for the broken ridge satellite magnetic anomaly N85-23219
Submarine volcanic eruptions and potential analogs for Venus N85-23573

OCEAN COLOR SCANNER
Characteristic vector analysis of inflection ratio spectra: New technique for analysis of ocean color data
[NASA-TP-2428] N85-23237

OCEAN CURRENTS
Calculation of level surface in problems of large-scale ocean circulation N85-23136
Double and inverse Taylor-Hogg vortices in a stratified ocean N85-23137

OCEAN DYNAMICS
Characteristic vector analysis of inflection ratio spectra: New technique for analysis of ocean color data
[NASA-TP-2428] N85-23237

OCEAN MODELS
Calculation of level surface in problems of large-scale ocean circulation N85-23136
Mathematical-cartographic model for study of distribution of hydrochemical elements in sea water (using dissolved oxygen in the Pacific Ocean as an example) N85-23138

OCEAN SURFACE
Calculation of level surface in problems of large-scale ocean circulation N85-23136
Possibility of mapping active tectonic structures from mercury gas aureoles over sea surface N85-23162

OCEAN TEMPERATURE
Horizontal coherence of temperature microstructure in upper ocean layer N85-23139
Geographic variation in the relationships of temperature, salinity or sigma sub t versus plant nutrient concentrations in the world ocean — silicic acid, nitrate, and phosphate concentration
[NASA-CR-175621] N85-23287

OCEANOGRAPHY
USSR report: Earth sciences
[JPRS-UES-85-002] N85-23116
World ocean level oscillations and their relationship to change in inflow of continental waters N85-23133
Fine structure of vertical distribution of light attenuation index of sea water N85-23140
Science opportunities using the NASA scatterometer on N-ROSS
[NASA-CR-175639] N85-23222

OCEANS
Numerical experiments with simple model of ocean climate N85-23123
Boundary velocities of longitudinal seismic waves and lateral inhomogeneities of upper ocean mantle N85-23165
Assessing LANDSAT TM and MSS data for detecting submerged plant communities N85-23203
Luminescence in the ocean
[AD-B069136L] N85-23288

OIL EXPLORATION
New method of reconstructing conditions of recent differentiation of oil and gas in the Amudarya Basin (based on results of interpretation of space photographs) N85-22446
Evaluation of Thematic Mapper performance as applied to hydrocarbon exploration — Ontario, Canada; Cement, Oklahoma; and Death Valley, California N85-23191

OIL FIELDS
New method of reconstructing conditions of recent differentiation of oil and gas in the Amudarya Basin (based on results of interpretation of space photographs) N85-22446

OIL POLLUTION
Drifting ice as mechanical factor in purifying and polluting hydrosphere N85-23132

OLIVINE
The olivine asteroids: Discovery, mineralogy, and relationship to palasites N85-23500

OMEGA NAVIGATION SYSTEM
Use of three omega radionavigation system position lines for solving problems in marine geodesy N85-23131

ONBOARD EQUIPMENT
Adaptive control of airborne radar antennas N85-22989

OPEN CIRCUIT VOLTAGE
Improved modeling of the open circuit voltage of solar cells N85-22619
New high-efficiency silicon solar cells
[NASA-CR-175643] N85-23244

OPERATIONAL PROBLEMS
Electric and hybrid vehicle demonstration project
[DE85-003939] N85-23455

OPTICAL COMMUNICATION
Optimization of number of pulses in detection of fluctuating optical signals N85-22993
Technical Digest: Symposium on Optical Fiber measurements, 1984
[PB85-114700] N85-23407

OPTICAL DATA PROCESSING
Electronic generation of text for television
[BBC-RD-1984/14] N85-22856
Two-dimensional signal processing and storage and theory and applications of electromagnetic measurements
[AD-A150590] N85-22899
Optical memory research and its application to digital optical processing N85-23397
Optical processing in radon space
[AD-A150289] N85-23402

OPTICAL DISKS
Role of optical disk at computing centers
[DE85-005124] N85-23314

OPTICAL EQUIPMENT
Optical system
[NASA-CASE-NPO-15801-1] N85-23396

OPTICAL GYROSCOPES
Analysis of fiber-gyroscopes discussed N85-22845

OPTICAL MEASUREMENT
Parameters of amplitude-modulated signal upon reflections N85-22966

OPTICAL MEMORY (DATA STORAGE)
Acousto-optically addressed Fourier transform matched filters
[AD-A150296] N85-22889
Two-dimensional signal processing and storage and theory and applications of electromagnetic measurements
[AD-A150590] N85-22899

OPTICAL PATHS
Time spectra of intensity fluctuations along reflecting path N85-22981

OPTICAL PROPERTIES
Time-resolved ellipsometry and reflectivity measurements of the optical properties of silicon during pulsed excimer laser irradiation
[DE85-005091] N85-23079
Assessing LANDSAT TM and MSS data for detecting submerged plant communities N85-23203
Research in the optical sciences
[AD-A150196] N85-23401

OPTICAL RADAR
Time spectra of intensity fluctuations along reflecting path N85-22981

OPTICAL REFLECTION
Parameters of amplitude-modulated signal upon reflections N85-22966
Time spectra of intensity fluctuations along reflecting path N85-22981
Performance estimate of a reflecting light pipe for infrared detectors
[AD-A141269] N85-23396

OPTICAL WAVEGUIDES
Dispersion characteristics of small-mode gradient optical fibers N85-23004
Integrated optical components utilizing acoustooptic and electrooptic diffraction in micro-waveguides N85-23044
Acoustooptic demodulation of frequency-modulated signals N85-23050
Technical Digest: Symposium on Optical Fiber measurements, 1984
[PB85-114700] N85-23407

OPTIMAL CONTROL
Synthesis of quasi-optimum two-level signal discriminator with level changing at unknown point N85-23010
Approximation in optimal control and identification of large space structures
[AD-A150323] N85-23351
Optimal designs for comparisons between two sets of treatments
[AD-A150621] N85-23360

OPTIMIZATION
Preliminary development of an approximation procedure for supercritical wing design optimization applications
[AD-A150177] N85-22383
China report: Science and technology
[JPRS-CST-84-008] N85-22384
Optimal design efforts in Shanghai described N85-22386
Model reduction for control system design
[NASA-CR-170417] N85-22398
Analysis and optimization of parameters of fanned surface acoustic wave transducers N85-22934
Optimization of number of pulses in detection of fluctuating optical signals N85-22993
Asymptotically optimum multialternative sequential procedures for discernment of processes minimizing average length of observations N85-23012
Shape optimization for minimal stress concentration N85-23093
Optimal allocation of components in parallel-series and series-parallel systems
[AD-A150169] N85-23309

ORBIT CALCULATION
On the origin of Triton and Pluto N85-23497

ORBIT MANEUVERING ENGINE (SPACE SHUTTLE)
Space station systems technology study (add-on task). Volume 1: Executive summary
[NASA-CR-171415] N85-22459
Selected tether applications in space: Phase 2. Executive summary
[NASA-CR-171421] N85-22462
Selected tether applications in space: Phase 2
[NASA-CR-171422] N85-22463

ORBIT TRANSFER VEHICLES
Space station systems technology study (add-on task). Volume 1: Executive summary
[NASA-CR-171415] N85-22459
Selected tether applications in space: Phase 2. Executive summary
[NASA-CR-171421] N85-22462
Selected tether applications in space: Phase 2
[NASA-CR-171422] N85-22463
Space Station technology planning N85-22471

ORBITAL MECHANICS
Algorithm for determining optimal three impulse point-to-orbit transfer with limited transfer time N85-22419
Satellite oscillations in elliptical orbit N85-22429
Satellite-to-satellite orbit determination using minimum, discrete range and range-rate data only N85-22458
Halley's Comet, a bibliography
[LC-84-600109] N85-23674

ORBITAL SPACE STATIONS
Concentrator technologies evaluation for large solar arrays and their application for space stations/platforms N85-22609
Space Station solar array N85-22610

ORBITS
Improvement in magnetic field properties of vanadium-gallium superconductors by enhancement of spin-orbit scattering
[DE85-002893] N85-23422

ORDER-DISORDER TRANSFORMATIONS
First principles theory of Fermi-surface driven concentration waves in Cu/sub c/Pd/sub 1-c/ alloys
[DE85-005367] N85-22681

ORGANIC COMPOUNDS
One mechanism of formation of organic fraction in atmospheric aerosol N85-22632
Analysis of biological particles by mass spectrometry
[AD-A149952] N85-23291

ORGANIC MATERIALS
Production and turnover of suspended organic detritus in the coastal water of the southeastern continental shelf
[DE85-003977] N85-23290

ORGANIC PHOSPHORUS COMPOUNDS
USSR report: Chemistry
[JPRS-UCH-85-001] N85-22629
ORTHOGONAL FUNCTIONS
Noise tolerance of digital demodulator for complex signal system employing binary quantization N85-22929
OSCILLATING FLOW
Large amplitude forcing of a high speed 2-dimensional jet
[NASA-CR-175646] N85-22393
The role of convective perturbations in supercritical inlet oscillations N85-22563
OSCILLATION DAMPERS
Controlled movement of elastic manipulator with distributed parameters N85-22818
OSCILLATIONS
Space shuttle pilot-induced-oscillation research testing N85-22351
Satellite oscillations in elliptical orbit N85-22429
Measurements of distributed combustion N85-22542
Distributed combustion: A mechanism of acoustic suppression N85-22543
Interaction of cylindrical shell with concentrated mass moving along its inner surface N85-22810
Stereo decoder without subcarrier restoration N85-22921
Machine analysis of resonance characteristics of plate-type radio electronic equipment constructions N85-23018
Regions of propagation of short-wave perturbations in spherical layer of rotating fluid N85-23130
Observation of long-period oscillations of Earth N85-23149
Nature of seismic images with amplitude and time fluctuations of recorded oscillations N85-23156
OSCILLATORS
Design considerations for a 100 kW CW, 140 GHz gyrotron oscillator
[DE85-005282] N85-22904
Square-pulse generator N85-22959
Experimental study of high-stability oscillator with surface-acoustic-wave resonator in feedback loop N85-23053
OSS-1 PAYLOAD
Vibroacoustic study of the NASA Goddard Space Flight Center OSS-1 payload
[NASA-CR-175320] N85-22465
Vehicle charging on STS-3 Mission N85-22473
OUTER SPACE TREATY
U.S., Soviet space program aims contrasted N85-22455
OUTLET FLOW
effect of gas stream sweeping past the effluent of a perforated plate on heat transfer inside the perforations N85-22836
OUTPUT
Confidence intervals using the regenerative method for simulation output analysis
[AD-A150147] N85-23343
OVERVOLTAGE
Stability of highly nonlinear oxide-zinc resistors under continuous voltage of industrial frequency N85-23030
Requirements placed on information processing equipment
[BLL-CE-TRANS-7983-(9022.09)] N85-23307
OXAZOLE
Chiral polymers
[AD-A150366] N85-22760
OXIDATION
Combustion kinetics of metal atoms and metallic radicals over wide temperature ranges N85-22530
Combustion of zirconium carbide N85-22532
Interaction of metals and metalloids with biomembranes
[DE85-004902] N85-23283
OXIDATION RESISTANCE
Oxidation resistant materials for hot gas turbines and jet engines
[AD-B087399L] N85-22389
OXIDE FILMS
The characterisation of oxide films on treated aluminium alloys
[MOAD-R-849] N85-22667
OXIDES
Gasification of boron oxide drops and boron slurry agglomerates in combustion gases N85-22529
Electrical and thermal transport property studies of high-temperature thermoelectric materials
[AD-A150167] N85-23417
OXYGEN
Ignition phenomena of bulk aluminum alloy as a function of oxygen pressure N85-22531
Sulfur oxygen processes on Io N85-23481
OXYGEN IONS
Three-dimensional calculation of shuttle charging in polar orbit N85-22486
OXYGENATION
Mathematical-cartographic model for study of distribution of hydrochemical elements in sea water (using dissolved oxygen in the Pacific Ocean as an example) N85-23138
OZONE
Ozone Correlative Measurements Workshop
[NASA-CP-2362] N85-23112
Scientific requirements for ozone measurements N85-23113
Method for determining the number of correlative measurements required to validate the SBUV/2 ozone retrievals N85-23114
Measurement requirements for the detection of ozone trends N85-23115
A theoretical study of the ozone quasi-biennial oscillation in the tropical stratosphere N85-23264
Cumulus cloud venting of mixed layer ozone
[NASA-TM-87429] N85-23269

P

P-N JUNCTIONS
Improved modeling of the open circuit voltage of solar cells N85-22619
PACIFIC OCEAN
El Nino, the capricious child N85-23121
Absolute movement of Pacific Ocean plate during last 120 million years N85-23126
Mathematical-cartographic model for study of distribution of hydrochemical elements in sea water (using dissolved oxygen in the Pacific Ocean as an example) N85-23138
PACKET SWITCHING
Satellite channels in packet-switching networks N85-22909
PACKET TRANSMISSION
A fully distributed approach to the design of a 16 K bit/sec VHF packet radio network
[AD-A141282] N85-22859
PACKETS (COMMUNICATION)
Satellite channels in packet-switching networks N85-22909
PALEOMAGNETISM
Use of paleomagnetic data in tectonic analysis of oceanic structures N85-23135
Geomagnetic field dynamics N85-23182
PALLADIUM ALLOYS
First principles theory of Fermi-surface driven concentration waves in Cu/sub c/Pd/sub 1-c/ alloys
[DE85-005367] N85-22681
PARABOLIC ANTENNAS
Experimental verification of beam deflection from hybrid reflector antenna within wide-angle sector N85-22984
PARABOLIC REFLECTORS
Axial focusing of signal from distant point radiator reflected twice in deep parsboloid N85-22979
PARALLEL FLOW
Diffusion deposition in fibrous filters for parallel and transverse flow models
[DE85-006149] N85-23066
PARALLEL PLATES
Variational and moment method solutions of the fields in a parallel-plate waveguide-aperture system
[DE85-006288] N85-22876
PARALLEL PROCESSING (COMPUTERS)
Optimal allocation of components in parallel-series and series-parallel systems
[AD-A150169] N85-23309
Exploiting parallel computing with limited program changes using a network of microcomputers
[NASA-TM-86387] N85-23318
Parallel processing for computational continuum dynamics
[AD-A150513] N85-23327
PARALLEL PROGRAMMING
Implementation of some concurrent algorithms
[DE85-004687] N85-23334
Optical memory research and its application to digital optical processing N85-23397
PARAMAGNETISM
Investigation of bimodal paramagnetic filter N85-23007
PARAMETER IDENTIFICATION
Air combat simulation: Methods, models, trends N85-22359
Determination of aerodynamic and propulsion parameters of general aviation aircraft using steady state flight test data N85-22377
Use of Walsh functions for calculating characteristics of digital filters with impulse response of finite duration N85-23011
PARAMETERIZATION
Polynomial parameterization in inverse gravimetric problem N85-23174
PARAMETRIC AMPLIFIERS
Millimeter-wave range masers: A review N85-23042
PARSING ALGORITHMS
Construction of a menu-based system
[NASA-CR-172560] N85-23321
PARTIAL DIFFERENTIAL EQUATIONS
Effect of compliability of hot walls in liquid-propellant engine on low frequency instability N85-22824
Models of discontinous random fields N85-22983
PARTICLE ACCELERATORS
Variable flexing device for targets in internal beams of charged particle accelerators N85-22797
Experimental studies of elementary particle interactions at high energies
[DE85-004795] N85-23394
PARTICLE COLLISIONS
Adequacy of metal ablation process with laser radiation and a shock-compressed plasma N85-22708
PARTICLE DENSITY (CONCENTRATION)
Properties of materials using acoustic waves
[AD-A150485] N85-23382
PARTICLE INTERACTIONS
Ion transport in beam-plasma interactions
[AD-A150145] N85-23410
PARTICLE SIZE DISTRIBUTION
Microstructure of Venus cloud layer based on spectrophotometric data from Venera-11 spacecraft N85-22436
Solid propellant combustion diagnostics and automated data retrieval from holograms N85-22527
Characterization of heterogeneity of composite propellants and its effects on combustion behavior N85-22539
Recent trends in particle size analysis techniques
[NASA-TM-77735] N85-22845
Size and velocity distributions of particles and droplets in spray combustion systems
[AD-A150355] N85-22648
Laser diagnostic analyses of sooting flames
[AD-A150478] N85-22649
Infrared aerosol absorption index N85-23147
Potential bedforms on Venus: Wind tunnel simulations N85-23583
Quantitative analyses of planetary reflectance spectra N85-23625
PARTICLE THEORY
A systematic study of light scattering by irregularly shaped particles
[AD-A150192] N85-23400
PARTICLES
The orientation distribution of nonspherical aerosol particles within a cloud
[AD-A150600] N85-23061
Sample introduction methods for improving the particle detection capability of the spectrometric oil analysis program
[AD-A150139] N85-23399
The effect of particle density on aeolian transport N85-23581
PATENT POLICY
NASA Patent Abstracts Bibliography. A continuing bibliography. Section 2: Indexes
[NASA-SP-7039(26)] N85-23445
PATTERN RECOGNITION
Acousto-optically addressed Fourier transform matched filters
[AD-A150298] N85-22589
Electroacoustical imaging technique for encoding incoherent radiance fields as Gabor elementary signals
[NASA-TM-86372] N85-23067
Preliminary evaluation of Thematic Mapper image data quality N85-23194
Comparative techniques used to evaluate Thematic Mapper data for land cover classification in Logan County, West Virginia N85-23209
Relative accuracy assessment of LANDSAT-4 MSS and TM data for level 1 land cover inventory — Washington, D.C. N85-23212
Feature extraction assessment study
[AD-A150189] N85-23239
Multivariate analysis and its applications
[AD-A150324] N85-23352
Terrestrial analog studies for Martian patterned ground N85-23590
PENETRATION
Aircraft skin penetrator and agent applicator. Volume 1: Working model development and construction
[AD-A150498] N85-22374
PERCOLATION
Determining deep heat flow and rate of horizontal percolation from temperature measurements in aquifer N85-23180
PERFORATED PLATES
effect of gas stream sweeping past the effluent of a perforated plate on heat transfer inside the perforations N85-22836

PERFORMANCE PREDICTION
Surface wave excitation study [DE85-005301] N85-22875
Investigations of the high frequency performance of impact avalanche transit-time diodes N85-22884
PERFORMANCE TESTS
The Olympus solar array development and test program N85-22599
Surge strength of symmetric cable with monolithic polyethylene insulation of quads N85-23001
Algorithm in Walsh function basis for analysis of integrated microcircuits on MOS-structures N85-23006
Laboratory tests of reciprocating internal combustion engines [AD-A150143] N85-23087
PERIHELIONS
Comet thermal modeling N85-23505
PERIODICALS
D-1 report: The first German spacelab mission [NASA-TM-77637] N85-22402
PERMAFROST
Permafrost and subsurface ice in the solar system N85-23594
PERMITTIVITY
Electric field effects on ion currents in satellite wakes N85-22485
Extraction of surface-wave energy from plasma waveguide N85-22974
Change of electrical characteristics of radio-frequency cables under thermal effect N85-22999
Dielectric measurements in infralow-frequency band N85-23034
Microwave remote sensing of soil moisture N85-23235
Mars radar catalog N85-23636
PERSONAL COMPUTERS
Two degree-of-freedom flutter solution for a personal computer [NASA-TM-86381] N85-22379
PERTURBATION THEORY
Surface scattering [AD-A150252] N85-23366
Nonrelativistic Kapitza-Dirac scattering [AD-A150622] N85-23405
PETRI NETS
The design of a unified package for the solution of stochastic petri net models [AD-A150326] N85-23354
Regenerative stochastic Petri nets [AD-A150343] N85-23355
PETROGRAPHY
Assessment of computer based geologic mapping of rock units in the LANDSAT-4 scene of northern Death Valley, California N85-23195
PETROLOGY
Reports of the Planetary Geology and Geophysics Program, 1984 [NASA-TM-87563] N85-23474
Io: Generation of silicate magma by shear melting at the base of a basaltic lithosphere N85-23476
Modelling equilibrium and fractional crystallization in the system MgO-FeO-CaO-Al2O3-SiO2 N85-23552
Quenching effects on iron site partitioning in the Apollo 17 orange glass composition N85-23553
PHASE CHANGE MATERIALS
Natural convection during heat accumulation by substances with change of aggregate state N85-22787
Latent heat storage in cooling systems [DE85-005355] N85-23248
Overview of latent storage for passive solar applications [DE85-005354] N85-23249
PHASE COHERENCE
Comparative analysis of noise tolerance of quasi-coherent phase shift keying signal demodulators N85-22946
Reception noise immunity of multiposition signals N85-23023
PHASE CONTRAST
Synthesis of multistep directional couplers with nonminimum-phase characteristics N85-22986
PHASE DEMODULATORS
Interference immunity of binary systems with second-order phase-difference modulation in various reception modes N85-22944
Comparative analysis of noise tolerance of quasi-coherent phase shift keying signal demodulators N85-22946
PHASE DEVIATION
Error in compensating phase fluctuations of wave field by means of adaptive reflectors with continuous or compound surface N85-22988
Investigation of bimodal paramagnetic filter N85-23007
PHASE LOCKED SYSTEMS
Stereo decoder without subcarrier restoration N85-22921
Study of phase radiogeodetic systems with phase-locked loops N85-23172
PHASE MODULATION
Interference immunity of binary systems with second-order phase-difference modulation in various reception modes N85-22944
Synthesis of optimum single-channel discrete signals and filters N85-22990
Reception noise immunity of multiposition signals N85-23023
PHASE SHIFT
Use of electronic coding-frequency meters to measure parameters of pulsed radio signals N85-22964
Change of electrical characteristics of radio-frequency cables under thermal effect N85-22999
PHASE SHIFT CIRCUITS
USSR report: Electronics and electrical engineering [JPRS-UEE-85-002] N85-22907
PHASE SHIFT KEYING
Regular synthesis of pairs of phase-keyed binary minimax signals N85-22923
Dispersion of phase-shift keyed systems with fixed number of blocks N85-22928
Analysis of characteristics of digital discriminators for phase-shift keyed signals N85-22930
Combined processing method and matched filter for discrete composite frequency phase-shift keyed signal N85-22931
Ionospheric distortions of digital signals with wideband modulation N85-22945
Comparative analysis of noise tolerance of quasi-coherent phase shift keying signal demodulators N85-22946
PHASE TRANSFORMATIONS
Metal-semiconductor phase transition and its application [DRIC-T-7149] N85-22665
Influence of hydrogen bonding in block copolymers and their blends N85-22752
PHONEMES
Research in continuous speech recognition [AD-A150474] N85-22868
PHONETICS
Research in continuous speech recognition [AD-A150474] N85-22868
PHOSPHATES
Geographic variation in the relationships of temperature, salinity or sigma sub t versus plant nutrient concentrations in the world ocean --- silicic acid, nitrate, and phosphate concentration [NASA-CR-175621] N85-23287
PHOSPHORUS
Study of processes of modification of Al-Si alloys N85-22695
PHOTOCATHODES
High-resolution SIT TV tube for subnanosecond image shuttering [DE85-005189] N85-23072
PHOTOCHEMICAL REACTIONS
Chemical stabilization of laser dyes [AD-A150451] N85-23076
Composition and photochemical reactivity of turbine engine exhaust [AD-A150559] N85-23256
A theoretical study of the ozone quasi-biennial oscillation in the tropical stratosphere N85-23264
PHOTOCONDUCTIVITY
Optical memory research and its application to digital optical processing N85-23397
PHOTOGEOLOGY
Evaluation of Thematic Mapper performance as applied to hydrocarbon exploration --- Ontario, Canada; Cement, Oklahoma; and Death Valley, California N85-23191
Geologic utility of LANSDAT-4 TM data --- Death Valley, California and the Silver Bell area of southern Arizona N85-23192
Assessment of computer based geologic mapping of rock units in the LANDSAT-4 scene of northern Death Valley, California N85-23195
Geologic interpretation of remote sensing data for the Martian volcano, Ascraeus Mons N85-23608
The deep structure of lunar basins: Clues to the understanding of basin formation and modification N85-23647
Mars geologic mapping: A review and new concepts N85-23663
PHOTOGONIOMETERS
Status of and outlook for producing means of transmitting units of plane angle, angular velocity and acceleration with ring lasers N85-22955
PHOTOGRAMMETRY
Evaluating accuracy in orientation of topographic photograph and satellite-centered direction from star photograph N85-22442
A unified lunar control network N85-23669
The control network of Mars: October 1984 N85-23670
The control networks of the satellites of Jupiter and Saturn N85-23671
Shape of Io N85-23672
PHOTOGRAPHIC PLATES
Digital laser platemaker modifications [AD-A150190] N85-23074
PHOTOGRAPHY
Relationship between brightness spectrum of photographic image and spectrum of rises on a water surface with waves N85-23171
PHOTOINTERPRETATION
Method for approximating autocorrelation functions for describing areal photoimage features N85-22443
Experience in automated interpretation of aerospace photographs N85-22444
Geoindication method for interpreting aerial and space photographs: Status and prospects N85-22445
Experience in combined special mapping using space information N85-22449
Combined analysis of the dynamics of complex ecosystems based on repeated remote measurements N85-22450
Overview of TM applications research reports N85-23187
Preliminary study of information extraction of LANDSAT TM data for a suburban/regional test site N85-23208
PHOTOIONIZATION
Threshold double photoionization of argon with synchrotron radiation [AD-A150615] N85-23389
PHOTOMAPS
Preliminary photomaps of Venus surface in the Maxwell Mountains and adjacent areas N85-22438
PHOTOMETERS
Effect of variance of photoreceiver frequency characteristics on characteristics of measuring instruments N85-22965
Invariance of probability characteristics of detector to shape of optical pulse signals N85-23048
PHOTOMETRY
Photometric analysis of Jupiter-illuminated images of Io N85-23620
PHOTOSYNTHESIS
Modulation of light energy transduction in photosynthesis [DE85-004711] N85-23292
PHOTOVOLTAIC CELLS
History and future views on solar cells of Japanese scientific satellites N85-22566
Thin and ultrathin silicon solar cells for space use N85-22567
Space solar cells: Adjusting to new demands N85-22568
The high voltage silicon cell: A comparative analysis N85-22569
A 2 x 6 Back Surface Reflection (BSR) silicon solar cell N85-22570
Experiences with implanted Back Surface Field (BSF) solar cells N85-22571
A low cost approach with larger diameter silicon wafer --- solar cells N85-22572
Bifacial light sensitive space solar cell N85-22573
Gallium arsenide arrays versus silicon arrays for space application N85-22574
Space qualified AlGaAs/GaAs solar cells N85-22575
Availability of AlGaAs/GaAs solar cells in space N85-22576
Comparative study of GaAs solar cell potentialities for space applications N85-22577
Investigation of high output gallium arsenide solar cells N85-22578
Development of very thin large area GaAs solar cells for space application N85-22579
GaAs and 3-5 compound solar cells status and prospects for use in space N85-22580
GaAlAs-GaAs solar cell development: Prospective for space applications under concentration N85-22581
Investigation of the degradation of GaAs photovoltaic cells by proton and electron irradiation N85-22587
Electrical design of the Intelsat 6 solar generator N85-22592
Survival testing of silicon solar modules N85-22602
Calibration of solar cells outside the atmosphere N85-22603
Inverse behavior of silicon photovoltaic cells N85-22604
NASA photovoltaic research and technology development program for space applications N85-22617

High output photovoltaic conversion: The quadrispectral project — spacecraft power supplies N85-22626
Operational performance of the photovoltaic-powered grain mill and water pump at Tangaye, Burkina Faso (formerly Upper Volta)
[NASA-TM-86970] N85-23243
PHOTOVOLTAIC CONVERSION
Photovoltaic Generators in Space — conferences
[ESA-SP-210] N85-22565
NASA photovoltaic research and technology development program for space applications N85-22617
Study of concentration for space photovoltaic generators N85-22618
High output photovoltaic conversion: The quadrispectral project — spacecraft power supplies N85-22626
PHOTOVOLTAIC EFFECT
Abstracts of 6th Annual Review Meeting on Photovoltaic Advanced Research and Development
[DE84-013047] N85-23246
PHYSICAL CHEMISTRY
Estimating degree of development of physical-chemical interaction among components in Al-B fiber composite material N85-22705
PHYSICAL EXERCISE
Sleep deprivation and exercise tolerance
[AD-A150180] N85-23295
Sleep deprivation and exercise tolerance
[AD-A150566] N85-23296
Sleep deprivation and exercise tolerance
[AD-A150626] N85-23297
PHYSIOLOGICAL RESPONSES
Sleep deprivation and exercise tolerance
[AD-A150180] N85-23295
Sleep deprivation and exercise tolerance
[AD-A150566] N85-23296
Sleep deprivation and exercise tolerance
[AD-A150626] N85-23297
PIEZOELECTRIC CERAMICS
Elasticity formulas for thin-walled shells with piezoceramic layers N85-22816
PIEZOELECTRIC TRANSDUCERS
Piezoelectric filter with low-Q inductances N85-22932
PILOT PERFORMANCE
Space shuttle pilot-induced-oscillation research testing N85-22351
Air combat simulation: Methods, models, trends N85-22359
PIONEER VENUS SPACECRAFT
Analysis and interpretation of observations of airglow at 297 nm in the Venus thermosphere N85-23473
Venus gravity: Global field results N85-23512
Geophysical interpretation of Venus gravity data N85-23513
Venus chasmata: A lithosphere stretching model N85-23516
PIONEER 11 SPACE PROBE
Investigations of planetary ring phenomena N85-23487
PIPELINING (COMPUTERS)
Exploiting multiprocessors: Issues and options
[DE85-003144] N85-23313
Implementation of some concurrent algorithms
[DE85-004687] N85-23334
PIPES (TUBES)
Influence of welding defects at melting boundary on static strength of welded joint in large-diameter pipe N85-22735
Cooling performance improvement of a horizontal ground coupled heat pump
[DE85-002470] N85-23065
PISTONS
Sliding seal materials for adiabatic engines
[NASA-CR-174893] N85-22757
PITCH (INCLINATION)
Protons with energies above 30 KeV in Earth's radiation belt at low altitudes during magnetically quiet time close to geomagnetic equator N85-22423
PITTING
Local electrochemistry of pitting corrosion in stainless steels
[DE85-005207] N85-22673
PLAINS
Thickness of ridged plains materials in Hesperia Planum, Mars N85-23561
Investigations of the Mars cratered terrain: Smooth plains boundary in the eastern equatorial region N85-23596
Enigmatic hills of the mottled plains, Mare Acidalium quadrangle (MC-1), Mars N85-23599
Geomorphology and geology of the Southwestern Margaritifer Sinus and Argyre regions of Mars. Part 1: Geological and geomorphological overview N85-23600
Mechanisms of basalt-plains ridge formation N85-23643
PLANAR STRUCTURES
Axial representations of shape
[AD-A150387] N85-23356
The structure and composition of Uranus and Neptune N85-23495
PLANE STRAIN
Elastic wave scattering from an interface crack in a layered half space N85-23095
Elasticity solution of an adhesively bonded joint
[NASA-CR-175591] N85-23097
PLANETARY ATMOSPHERES
Impact and collisional processes in the solar system N85-23530
Magmas as selective filters of volatiles between planetary mantles and surfaces N85-23557
PLANETARY COMPOSITION
Multispectral analysis of the Kasei Vallis-Lunae Planum region of Mars N85-23607
The search for igneous materials at the Viking landing sites N85-23609
Basalts of Mars: Constraints on volatile evolution N85-23610
First direct detection of clay minerals on Mars N85-23612
Iron oxides of Mars: Evidence for contemporary weathering N85-23613
Reassignment of the iron (3) absorption bands in the spectra of Mars N85-23614
Zeolites on Mars: Prospects for remote sensing N85-23615
PLANETARY CRATERS
Impact cratering calculation N85-23531
Impact crater scaling laws N85-23532
Problems in recovering crater production functions N85-23539
PLANETARY EVOLUTION
Planetary geology in the 1980s
[NASA-SP-467] N85-23457
Studies of planetary rings N85-23488
Origin and evolution of the Saturn system N85-23493
Giant planets and their satellites: Cosmochemistry, evolution and structure N85-23494
The structure and composition of Uranus and Neptune N85-23495
On the origin of Triton and Pluto N85-23497
The Formation of preplanetary disks from the collapse of rotating molecular cloud cores N85-23526
The evolution of CO2 on Mars N85-23558
Three-layer generic Ganymedes: Structure and evolution N85-23657
PLANETARY GEOLOGY
Planetary geology in the 1980s
[NASA-SP-467] N85-23457
Reports of the Planetary Geology and Geophysics Program, 1984
[NASA-TM-87563] N85-23474
A statistical treatment of the regional slope characteristics of Venus and Earth N85-23517
Centrifuge impact cratering experiments N85-23533
Progress on Experimental impact studies N85-23534
Progress on studies of early intense cratering N85-23535
Why not a constant early lunar impact rate? N85-23536
Martian terrain ages N85-23537
Impacts in Ice: Commissions of solar system crater population N85-23538
Problems in recovering crater production functions N85-23539
A parmetric study of crater-saturation simulation N85-23540
Average spacing for rings of individual multi-ring basins is 2.0(0.5)D N85-23541
Ring-diameter ratios for multi-ring basins average 2.0(0.5)D N85-23542
Morphology and mechanics of terraces in lunar craters N85-23543
Newly discovered Martian impact basins N85-23544
The nature of Martian flow ejecta craters N85-23545
Interaction of Martian flow ejecta blankets with pre-existing impact craters: Morphological observations N85-23546
Ripple ring basins on Ganymede and Callisto N85-23547
Implications of convection in the Moon and the terrestrial planets N85-23548
High pressure cosmochemistry of major planetary interiors: Laboratory studies of the water-rich region of the system ammonia-water N85-23549
Modelling equilibrium and fractional crystallization in the system MgO-FeO-CaO-Al2O3-SiO2 N85-23552
Ridged plains of Lunae Planum: Thickness distribution revised N85-23559
Volcanic debris flows in the Elysium region of Mars N85-23560
Thickness of ridged plains materials in Hesperia Planum, Mars N85-23561
Mapping structures characteristic of the highland boundary scarp on Mars N85-23595
Investigations of the Mars cratered terrain: Smooth plains boundary in the eastern equatorial region N85-23596
Martian fretted terrain morphometry interpreted using principal components analysis N85-23597
Enigmatic hills of the mottled plains, Mare Acidalium quadrangle (MC-4), Mars N85-23599
Geomorphology and geology of the Southwestern Margaritifer Sinus and Argyre regions of Mars. Part 1: Geological and geomorphological overview N85-23600
Geomorphology and geology of the Southwestern Margaritifer Sinus and Argyre regions of Mars. Part 2: Crater size-frequency distribution curves and geomorphic unit ages N85-23601
Geomorphology and geology of the Southwestern Margaritifer Sinus and Argyre regions of Mars. Part 3: Valley types and distribution N85-23602
Geomorphology and geology of the Southwestern Margaritifer Sinus and Argyre regions of Mars. Part 4: Flow ejecta crater distribution N85-23603
Multispectral analysis of the Kasei Vallis-Lunae Planum region of Mars N85-23607
Io: Precise comparison of Voyager spectral curves with laboratory measurements N85-23619
Determining mineral types and abundances from reflectance measurements N85-23622
Determination of mineral type, abundance, and grain size with remotely obtained reflectance spectra N85-23623
Quantitative analyses of planetary reflectance spectra N85-23625
Terrestrial analogs for planetary wrinkle ridges N85-23644
On the absence of strike-slip faults from the planets and satellites N85-23645
Lunar mascon loading: An example of the importance of fault initiation depth on fault type predictions from stresses on planetary surfaces N85-23648
Planetary interior modeling and tectonic implications N85-23649
Elysium region, Mars: Tests of lithospheric loading models for the formation of tectonic features N85-23650
Lithologic and structural control on slope morphology in the Valles Marineris N85-23651
Valles Marineris basin beds: A complex story N85-23652
Mars: Stratigraphy of western highlands and polar regions N85-23653
Kasei Vallis of Mars: Dating the interplay of tectonics and geomorphology N85-23654
Creep of ice: Further studies N85-23655
Fault offsets and lateral crustal movement on Europa N85-23656
Three-layer generic Ganymedes: Structure and evolution N85-23657
Lineaments on Ganymede: New evidence for late tectonic activity N85-23658
Global tectonics on Ganymede N85-23659
Tectonics of the Galileo Regio on Ganymede N85-23660
Importance of the tectonic motions on Ganymede N85-23661
Tectonics of the Valhalla structure on Callisto N85-23662
Mars geologic mapping: A review and new concepts N85-23663
PLANETARY GRAVITATION
Expansion of functions describing planetary surface and gravity field N85-22410
Viking radio science data analysis and synthesis N85-23528
Gravity field of the Jovian system from Pioneer and Voyager tracking data N85-23529
PLANETARY MAGNETIC FIELDS
Hydromagnetic precursors of interplanetary plasma burst N85-22414
PLANETARY MANTLES
Magmas as selective filters of volatiles between planetary mantles and surfaces N85-23557
PLANETARY MAPPING
Visualization of radar altimetry data for Venus N85-22437
Mapping structures characteristic of the highland boundary scarp on Mars N85-23595
Tectonics of the Galileo Regio on Ganymede N85-23660
Mars geologic mapping: A review and new concepts N85-23663
The Galilean Satellite Geological Mapping Program, 1984 N85-23664

Geology of the Ganymede quadrangle Jg7 N85-23665
Mars planimetric mapping N85-23666
Viking Lander mosaics of Mars N85-23667
Voyager cartography N85-23668
The control network of Mars: October 1984 N85-23670
The control networks of the satellites of Jupiter and Saturn N85-23671

PLANETARY ORBITS
Small solar system bodies N85-23499

PLANETARY RINGS
Investigations of planetary ring phenomena N85-23487
Studies of planetary rings N85-23488
Dynamical studies of Saturn's rings N85-23489
Meteoroidal impacts, plasma, fine structure of ringlets and spokes on Saturn's ring B N85-23490
Plasma production by meteoroid impact N85-23492
Origin and evolution of the Saturn system N85-23493

PLANETARY ROTATION
Viking radio science data analysis and synthesis [NASA-CR-175631] N85-23471
Viking radio science data analysis and synthesis N85-23528

PLANETARY STRUCTURE
Giant planets and their satellites: Cosmochemistry, evolution and structure N85-23494
Studies of icy bodies: Uranian satellites and cometary nuclei N85-23496
Viking radio science data analysis and synthesis N85-23528

PLANETARY SURFACES
Expansion of functions describing planetary surface and gravity field N85-22410
Evaluating accuracy in orientation of topographic photograph and satellite-centered direction from star photograph N85-22442
Planetary geology in the 1980s [NASA-SP-467] N85-23457
A parmetric study of crater-saturation simulation N85-23540
Relative time-scale for channeling events within chaotic terrains, Margaritifer Sinus, Mars N85-23589
Permafrost and subsurface ice in the solar system N85-23594
Terrestrial analogs for planetary wrinkle ridges N85-23644
Lunar mascon loading: An example of the importance of fault initiation depth on fault type predictions from stresses on planetary surfaces N85-23648

PLANETARY WAVES
Numerical investigation of evolution of energy spectrum of slightly nonlinear Rossby waves N85-23124

PLANETS
Impact and collisional processes in the solar system N85-23530

PLANKTON
Possible role of ocean biota in global carbon balance — phytoplankton production N85-23129
Geographic variation in the relationships of temperature, salinity or sigma sub t versus plant nutrient concentrations in the world ocean — silicic acid, nitrate, and phosphate concentration [NASA-CR-175621] N85-23287
Production and turnover of suspended organic detritus in the coastal water of the southeastern continental shelf [DE85-003977] N85-23290

PLANNING
Air Force technical objective document, Flight Dynamics Laboratory plans for fiscal year 1986. Air Force technical objective document [AD-A149648] N85-22348

PLANTS (BOTANY)
Assessing LANDSAT TM and MSS data for detecting submerged plant communities N85-23203

PLASMA ARC CUTTING
USSR report: Machine tools and metalworking equipment [JPRS-UMM-85-005] N85-22839
New tooling for plasma cutting technology N85-22842

PLASMA COMPRESSION
Adequacy of metal ablation process with laser radiation and a shock-compressed plasma N85-22708

PLASMA CONDUCTIVITY
Exitation of low-frequency resonance waves by moving conductor in space plasma N85-22912

PLASMA CONTROL
Winding insulation in electromagnetic systems for Tokamak reactor plants N85-23035
Confinement properties of high energy density plasmas in the Wisconsin levitated octupole N85-23408
Lower hybrid heating and current drive, and ion cyclotron heating experiments on the Alcator C and the Versator II Tokamaks [DE85-004918] N85-23412

PLASMA CURRENTS
Direct measurements of severe spacecraft charging in auroral ionosphere N85-22480
Ram-wake effects on plasma current collection of the PIX 2 Langmuir probe N85-22496

PLASMA CYLINDERS
Diffraction of plane TM-wave on continuously irregular elliptical plasma N85-22914

PLASMA DENSITY
Vehicle charging on STS-3 Mission N85-22473
Ram-wake effects on plasma current collection of the PIX 2 Langmuir probe N85-22496
NASCAP simulation of PIX 2 experiments N85-22497
Confinement properties of high energy density plasmas in the Wisconsin levitated octupole N85-23408
Increased hot-electron production at quarter-critical density in long-scalelength, laser-plasma interactions [AD-A150519] N85-23411

PLASMA DIAGNOSTICS
Plans for Interbol satellite experiment N85-22407
Suprathermal plasma observed on STS-3 Mission by plasma diagnostics package N85-22472
Vehicle charging on STS-3 Mission N85-22473
Electron and ion density depletions measured in the STS-3 orbiter wake N85-22474
Measured electron contribution to Shuttle plasma environment: Abbreviated update N85-22476
Ram-wake effects on plasma current collection of the PIX 2 Langmuir probe N85-22496
Feasibility of alpha particle measurement by CO2 laser Thomson scattering [DE85-004936] N85-23081
Confinement properties of high energy density plasmas in the Wisconsin levitated octupole N85-23408
Ion transport in beam-plasma interactions [AD-A150145] N85-23410
Ultrahigh-sensitivity threshold neutron detector for plasma diagnositcs [DE85-005270] N85-23413
Physics of the inner heliosphere: Mechanisms, models and observational signatures [NASA-CR-175632] N85-23677

PLASMA DISPLAY DEVICES
Frictional and structural characterization of ion-nitrided low and high chromium steels [NASA-TM-86991] N85-23085

PLASMA GENERATORS
EMI characteristics of a potential control system N85-22502

PLASMA HEATING
Ruby wavefront-conjugation laser for obtaining high temperature plasma N85-22795
Lower hybrid heating and current drive, and ion cyclotron heating experiments on the Alcator C and the Versator II Tokamaks [DE85-004918] N85-23412

PLASMA INTERACTION EXPERIMENT
The PIX-2 experiment: An overview N85-22494
Plasma interaction experiment 2 (PIX 2): Laboratory and flight results N85-22495
Ram-wake effects on plasma current collection of the PIX 2 Langmuir probe N85-22496

PLASMA INTERACTIONS
Plans for Interbol satellite experiment N85-22407
Spacecraft Environmental Interactions Technology, 1983 [NASA-CP-2359] N85-22470
Measured electron contribution to Shuttle plasma environment: Abbreviated update N85-22476
Self-consistent simulation of plasma interactions with secondary-emitting insulators N85-22492
Surface interactions and high-voltage current collection N85-22493
The PIX-2 experiment: An overview N85-22494
Plasma interaction experiment 2 (PIX 2): Laboratory and flight results N85-22495
Discharges on a negatively biased solar cell array in a charged-particle environment N85-22499
Spacecraft environmental interactions: A joint Air Force and NASA research and technology program N85-22517
Space test program of high-voltage solar array-space plasma interactions N85-22519

PLASMA OSCILLATIONS
Spacecraft-environment interaction: The environmental plasma aspect N85-22479

PLASMA PHYSICS
University of Cambridge Institute of Astronomy report of activities N85-23464

PLASMA POTENTIALS
Anomalously high potentials observed on ISEE N85-22503

PLASMA RESONANCE
Exitation of low-frequency resonance waves by moving conductor in space plasma N85-22912
Scattering of electromagnetic waves by charged particles N85-22913

PLASMA SHEATHS
Direct measurements of severe spacecraft charging in auroral ionosphere N85-22480
Polar plasmas as observed by Dynamics Explorers 1 and 2 N85-22483
Sheath ionization model of beam emissions from large spacecraft N85-22489

PLASMA SPRAYING
Film and interstitial formation of metals in plasma-sprayed ceramics [NASA-TM-86993] N85-22756

PLASMA-ELECTROMAGNETIC INTERACTION
Hydromagnetic precursors of interplanetary plasma burst N85-22414
Report on final recommendations for IMPS engineering-science payload [NASA-CR-175659] N85-22484
Spacecraft-environment interaction: The environmental plasma aspect N85-22479
Scattering of electromagnetic waves by charged particles N85-22913
Diffraction of plane TM-wave on continuously irregular elliptical plasma N85-22914

PLASMA-PARTICLE INTERACTIONS
Spacecraft-environment interaction: The environmental plasma aspect N85-22479

PLASMAS (PHYSICS)
Use of markets to elucidate reacting sputtering processes [DE85-005723] N85-22655
System for forming and focusing high current beam of deuterium ions N85-22798
Calculation of amplitude-phase characteristics of signal scattered obliquely on meteor trail N85-22948
Domain of applicability of asymptotic description of radio pulse fields near critical frequency N85-22949
Meteoroidal impacts, plasma, fine structure of ringlets and spokes on Saturn's ring B N85-23490
Interaction of the magnetospheric ions with the surfaces of the icy satellites of Saturn N85-23491
Plasma production by meteoroid impact N85-23492
Solar and stellar coronal plasmas [NASA-CR-175623] N85-23676

PLASMONS
Research in the optical sciences [AD-A150196] N85-23401

PLASTIC DEFORMATION
Critical events in inelastic deformation of glassy polymers in adsorptive medium N85-22634
Development and study of two-matrix glass fiber composite with increased transverse deformation N85-22700
Fatigue life, crack initiation, and propagation of 304 stainless steel with non-proportional axial/torsional strain-paths N85-23094

PLASTIC FLOW
Dependence of superplastic flow on state of grain boundaries N85-22689

PLASTICS
Mechanism of strengthening plastics with rubbers N85-22636

PLATE THEORY
Numerical results of acoustic radiation, transmission and reflection of steel plate in water [AMTE(N)-TM-84037] N85-23378

PLATEAUS
Basaltic pressure ridges: Formation and relationship to flow emplacement N85-23567
Volcanism of the Colorado Plateau (basin and range transition): Implications for crustal processes N85-23569

PLATES (STRUCTURAL MEMBERS)
Machine analysis of resonance characteristics of plate-type radio electronic equipment constructions N85-23016

PLATES (TECTONICS)
Absolute movement of Pacific Ocean plate during last 120 million years N85-23126
Crustal dynamics studies in China [NASA-CR-175617] N85-23265
A tectonic model of an incipient spreading center and its margins: The Northern Red Sea and the Dead Sea rift N85-23286

PLATFORMS
Analysis of interaction of dynamically adjustable gyroscopes on elastic platform by finite-element method N85-22822

PLAYBACKS
Playback amplifier with high interference immunity N85-22970

PLUMES
Stagnation zone impaction on a simple terrain feature in stable flow N85-23255
PLUTO (PLANET)
Research in planetary studies and operation of Mauna Kea Observatory [NASA-CR-175618] N85-23460
On the origin of Triton and Pluto N85-23497
PLUTONIUM
Distribution of radium and plutonium in human bone [DE85-005025] N85-23298
POINTS (MATHEMATICS)
A description of the Langley wireframe geometry standard (LaWGS) format [NASA-TM-85767] N85-22380
POISSON RATIO
Development and study of two-matrix glass fiber composite with increased transverse deformation N85-22700
Research program on the effect of pressure on the mechanical properties of polymers, part 2 [DE85-000995] N85-22761
POLAR CAPS
Polar cap formation on Ganymede N85-23486
Properties of filamentary sublimation residues from dispersions of clay in ice N85-23629
POLAR ORBITS
Direct measurements of severe spacecraft charging in auroral ionosphere N85-22480
Charging of DMSP/F6 spacecraft in aurora on 10 January 1983 N85-22481
Average and worst-case specifications of precipitating auroral electron environment N85-22482
Auroral-polar cap environment and its impact on spacecraft plasma interactions N85-22484
Three-dimensional calculation of shuttle charging in polar orbit N85-22486
Polar orbit electrostatic charging of objects in shuttle wake N85-22487
POLAR REGIONS
Polar plasmas as observed by Dynamics Explorers 1 and 2 N85-22483
Mars: Stratigraphy of western highlands and polar regions N85-23653
POLARIMETERS
Effects of focusing on HRS focal-plane polarimeter measurements [DE85-004627] N85-23406
POLARIMETRY
Modern problems in polarimetry of solid surfaces of cosmic bodies N85-22409
POLARITY
Characteristics of EMI generated by negative metal-positive dielectric voltage stresses due to spacecraft charging N85-22505
POLARIZATION (SPIN ALIGNMENT)
Effects of focusing on HRS focal-plane polarimeter measurements [DE85-004627] N85-23406
POLARIZATION (WAVES)
Modern problems in polarimetry of solid surfaces of cosmic bodies N85-22409
Interference flux during reflection of heterogeneous waves N85-22977
POLARIZATION CHARACTERISTICS
Modern problems in polarimetry of solid surfaces of cosmic bodies N85-22409
POLARIZED ELECTROMAGNETIC RADIATION
Modern problems in polarimetry of solid surfaces of cosmic bodies N85-22409
POLICIES
USSR report: Space [JPRS-USP-85-001] N85-22403
INMARSAT marine satellite organization N85-22456
USSR report: Science and technology policy [JPRS-UST-85-002] N85-23442
POLLUTION TRANSPORT
Drifting ice as mechanical factor in purifying and polluting hydrosphere N85-23132
POLYBUTADIENE
Effects of triazine components on physicochemical properties of polybutadiene: urethane block copolymers N85-22635
POLYCRYSTALS
High sheet resistance, arsenic implanted polycrystalline silicon for integrated circuit resistors [DE85-004355] N85-22902
POLYGONS
Origin of Martian polygonal terrain: Preliminary results N85-23591
POLYIMIDE RESINS
Development and study of two-matrix glass fiber composite with increased transverse deformation N85-22700
Adsorption behaviour of nitrogen compounds on to porous polymer beads and applications to atmospheric sampling [BLL-DRIC-TRANS-7399-(3623.66)] N85-22753
POLYIMIDES
Study of character of adhesive interaction and breaking of polyimid-aluminum foil junction during process of hardening N85-22637
POLYMER CHEMISTRY
USSR report: Chemistry [JPRS-UCH-85-001] N85-22629
Effect of alternative aging and accident simulations on polymer properties [DE85-002642] N85-22762
POLYMER MATRIX COMPOSITES
Electrical conduction in polymer dielectrics N85-22514
Interlaminar fracture toughness in resin matrix composites [AD-A150565] N85-22640
POLYMER PHYSICS
Critical events in inelastic deformation of glassy polymers in adsorptive medium N85-22634
Effects of triazine components on physicochemical properties of polybutadiene: urethane block copolymers N85-22635
Theory of relaxation processes in decomposing polymer materials during high-intensity convective heating N85-22710
POLYMERIC FILMS
Optimal design efforts in Shanghai described N85-22386
Mass spectra of neutral particles released during electrical breakdown of thin polymer films N85-22511
Study of character of adhesive interaction and breaking of polyimid-aluminum foil junction during process of hardening N85-22637
Electrostatic forming and testing of polymer films on a 16-foot diameter test fixture [NASA-TM-86326] N85-22885
POLYMERIZATION
Synthesis and characterization of poly(vinylidene fluoride) [AD-A150291] N85-22759
Chiral polymers [AD-A150366] N85-22760
POLYMERS
Research program on the effect of pressure on the mechanical properties of polymers, part 2 [DE85-000995] N85-22761
HREELS and Auger studies of conducting polymers [DE85-004541] N85-22764
POLYMETHYL METHACRYLATE
Theory of relaxation processes in decomposing polymer materials during high-intensity convective heating N85-22710
POLYMORPHISM
Synthesis and characterization of poly(vinylidene fluoride) [AD-A150291] N85-22759
POLYNOMIALS
Approximate perturbing part of geopotential by polynomials of stipulated form N85-22448
Polynomial parameterization in inverse gravimetric problem N85-23174
POLYPHENYL ETHER
Formation of high molecular weight products from benzene during boundary lubrication [NASA-TM-86966] N85-22644
POPULATIONS
Feoktistov discusses need for space colonization N85-22454
Study and estimation of planet-crossing asteroid populations: Discoveries and analysis N85-23498
POROSITY
Problem of pore formation mechanism in welded joints of aluminum alloys in the system aluminum-magnesium-lithium N85-22732
NDE methods for green ceramics [DE85-004019] N85-22766
POROUS MATERIALS
Adsorption behaviour of nitrogen compounds on to porous polymer beads and applications to atmospheric sampling [BLL-DRIC-TRANS-7399-(3623.66)] N85-22753
Molten carbonate fuel cell performance model update, draft [DE85-005423] N85-23252
Impact crater scaling laws N85-23532
POROUS WALLS
Investigations of reactive and non reactive acoustic boundary layers in porous walled ducts N85-22535
PORTABLE EQUIPMENT
Portable electrochemical cell interrogator [DE85-005186] N85-22901
Technical manual: Description and operation Slaved Tracking System [DE85-004807] N85-23070
PORTS (OPENINGS)
Comparing different theoretical designs of six-port reflectometer junctions [AD-A149419] N85-22861
POSITION (LOCATION)
Performance of time-position discriminator of composite signal N85-22941
Use of three omega radionavigation system position lines for solving problems in marine geodesy N85-23131
POSITION INDICATORS
Short-range radiotechnical point sensor N85-22906
POSITIVE IONS
Mean delta-ray energies in ion molecule collisions [DE85-005524] N85-23395
POTENTIOMETERS (INSTRUMENTS)
Development and testing of a spacecraft surface potential monitor N85-22582
POWDER (PARTICLES)
Influence of external electric field on structural-mechanical properties of powdered materials N85-22630
Recent trends in particle size analysis techniques [NASA-TM-77735] N85-22645
A comprehensive review of black powder [AD-A150455] N85-22769
POWDER METALLURGY
USSR report: Materials science and metallurgy [JPRS-UMS-85-002] N85-22688
Effect of phase state of TiC-NiTi powder composite materials on nature of failure and mechanical properties N85-22702
Apparatus for producing amorphous and microcrystalline metal powders N85-22720
POWER EFFICIENCY
Estimation of gas turbine engine boost provided by injecting water behind compressor N85-22838
The ferrite permanent magnet AC motor: A technical and economical assessment [DE85-002480] N85-22903
POWER FACTOR CONTROLLERS
Power control for ac motor [NASA-CASE-MFS-25861-1] N85-22877
POWER LINES
Numerical/Electromagnetics Code (NEC) [DE85-004999] N85-22874
PREAMPLIFIERS
Recommendation on use of series K157UL1 microcircuits N85-22936
PRECIPITATION (CHEMISTRY)
Microstructural study on the processing and properties of high-field A15 superconducting materials [DE85-004652] N85-23423
PRECIPITATION (METEOROLOGY)
Moisture variation in northern hemisphere temperate latitudes N85-23119
Relationship of Indian monsoon intensity to time of onset N85-23120
Summary of Meteorological Observations, Surface (SMOS), Bermuda [AD-A150537] N85-23278
Summary of Meteorological Observations, Surface (SMOS), Beaufort, South Carolina [AD-A150538] N85-23279
Summary of Meteorological Observations Surface (SMOS), Sigonella, Sicily/Navy [AD-A150539] N85-23280
Summary of Meteorological Observations, Surface (SMOS), Alameda, California [AD-A150609] N85-23281
PRECIPITATION HARDENING
Anomalies of aluminum structure and properties N85-22693
PRECISION
Operational experience with ion concentration sensors in orientation systems N85-22422
Method for determining the number of correlative measurements required to validate the SBUV/2 ozone retrievals N85-23114
PREDICTION ANALYSIS TECHNIQUES
Method for the prediction of the installation aerodynamics of a propfan at subsonic speeds [NASA-CR-3687] N85-22369
Reliability predictions for military avionics. Royal Signals and Radar Establishment reliability prediction method no. 250 [BR69221] N85-22388
Snowmelt runoff model in Japan N85-23227
Thermal and thermoelastic effects in rolling/sliding contacts [AD-A150435] N85-23429
PRESSES
Automatic multi-layer welding of thick cylindrical structures under flux N85-22746

PRESSURE EFFECTS
Ignition phenomena of bulk aluminum alloy as a function of oxygen pressure N85-22531
PRESSURE GRADIENTS
Fine structure of vertical distribution of light attenuation index of sea water N85-23140
PRESSURE MEASUREMENT
Liquid moment on a filled coning cylinder during spin-up: Ad hoc model
[AD-A150280] N85-23060
PRESSURE OSCILLATIONS
Nonlinear interactions between vortices and acoustic waves in a rocket combustion chamber N85-22533
Comparisons of solid propellant with instability predictions and motor firing experience N85-22541
PRESSURE VESSELS
Mechanical properties and brittle fracture resistance of welded multilayer elements for high pressure vessels N85-22736
PREVENTION
Tight Ribbon Arm Protection (TRAP) for aircrewman ejection
[AD-A150464] N85-23303
PRIMERS (COATINGS)
An electrochemical study of the corrosion behavior of primer coated 2219-T87 aluminum
[NASA-TP-2459] N85-22662
PRINCIPAL COMPONENTS ANALYSIS
Martian fretted terrain morphometry interpreted using principal components analysis N85-23597
Determining mineral types and abundances from reflectance measurements N85-23622
PRINTED CIRCUITS
A generalized solution to a class of printed circuit antennas N85-22682
PRISMS
Reflex attachment for line alignment in spectral diffraction devices N85-22794
Three-mirror open resonator for millimeter wave band N85-22972
PROBABILITY DENSITY FUNCTIONS
On filter binary processes
[AD-A150328] N85-22890
Invariance of probability characteristics of detector to shape of optical pulse signals N85-23048
PROBABILITY DISTRIBUTION FUNCTIONS
Analysis of characteristics of digital discriminators for phase-shift keyed signals N85-22930
Informative geometry of probability spaces
[AD-A150510] N85-23371
PROBABILITY THEORY
Rejection of anomalous observations when determining spacecraft trajectories N85-22421
A Monte Carlo sampling plan for estimating network reliability
[AD-A150511] N85-22898
Error probability during optimal noncoherent reception of binary signals in multibeam channel N85-22922
Probability of detection of pulsed signals employing zero-gating interference suppression N85-23021
Noise tolerance of diversity reception in frequency-adaptive digital transmission systems N85-23024
SIGPI: A user's manual for the fast computation of the probabilistic performance of a complex system
[DE85-005447] N85-23336
Why do noninvertible estimated moving averages occur?
[AD-A150388] N85-23368
PROBLEM SOLVING
Satellite-to-satellite orbit determination using minimum, discrete range and range-rate data only N85-22458
Sparse matrix computations
[DE85-004780] N85-23362
Personal decision making: The influence of perceived locus of control and degree of rationality on information seeking strategies N85-23446
PROCESSING
Edge detection in SAR imagery using gradient operators — synthetic aperture radar (SAR)
[AD-A149411] N85-22862
PRODUCT DEVELOPMENT
Improved Y-11 general-purpose transport designated Y-12 N85-22385
Giotto solar array: Design, manufacture and test N85-22589
The Olympus solar array development and test program N85-22599
Possibility of producing monolithic composite materials based on niobium carbide N85-22707
PRODUCTION COSTS
A low cost approach with larger diameter silicon wafer — solar cells N85-22572
PRODUCTION ENGINEERING
A 2 x 6 Back Surface Reflection (BSR) silicon solar cell N85-22570
Development of very thin large area GaAs solar cells for space application N85-22579
Economic mechanism of integration of science, production N85-23443
PRODUCTION MANAGEMENT
USSR report: Science and technology policy
[JPRS-UST-85-002] N85-23442
PRODUCTION PLANNING
USSR report: Science and technology policy
[JPRS-UST-85-002] N85-23442
PRODUCTIVITY
Advances in cutting tool technology surveyed N85-22840
Scientific, technical progress as factor of intensification of economy N85-23444
PROFILES
Study of geological media based on scattered earthquake waves N85-23168
PROGRAMMING LANGUAGES
Principles of software engineering environment design
[AD-A150352] N85-23324
LEXICON: A structured modeling system for optimization
[AD-A150536] N85-23329
ROSS: An object-oriented language for constructing simulations
[AD-A150556] N85-23330
Orphan detection in the Argus system
[AD-A150562] N85-23331
PROGRESS
Scientific, technical progress as factor of intensification of economy N85-23444
PROJECT MANAGEMENT
Space Station technology planning N85-22471
PROJECT PLANNING
Space Station technology planning N85-22471
PROP-FAN TECHNOLOGY
Large-scale Advanced Propfan (LAP) performance, acoustic and weight estimation, January, 1984
[NASA-CR-174782] N85-22368
PROPELLANT ADDITIVES
Workshop report: Catalysis of Burn Rate of Energetic Binder propellants N85-22545
Mechanism of burning rate enhancement by ferric oxide N85-22546
PROPELLANT BINDERS
Workshop report: Catalysis of Burn Rate of Energetic Binder propellants N85-22545
Effects of HMX addition on the combustion of energetic binders N85-22560
PROPELLANT CHEMISTRY
The crystal and molecular structure of a new propellant compound: Triaminoguanidium Azide Nitrate (TAZN) N85-22551
PROPELLANT COMBUSTION
Twenty-first JANNAF Combustion Meeting, volume 1
[AD-A150981] N85-22526
Status of boron combustion research N85-22528
Development of a three-phrase combustion code for modeling liquid rocket engines N85-22554
Atomization data requirements for rocket combustor modeling N85-22555
Effects of HMX addition on the combustion of energetic binders N85-22560
PROPELLANT GRAINS
Status of boron combustion research N85-22528
PROPELLANT SENSITIVITY
Effect of variable solid phase thermal properties on propellant combustion N85-22547
PROPELLANT TESTS
Characterization standards for solid propellant rocket motors
[AD-A150250] N85-22627
PROPELLANTS
Measurements of distributed combustion N85-22542
PROPELLER BLADES
Determination of aerodynamic and propulsion parameters of general aviation aircraft using steady state flight test data N85-22377
PROPELLER FANS
Large-scale Advanced Propfan (LAP) performance, acoustic and weight estimation, January, 1984
[NASA-CR-174782] N85-22368
PROPELLERS
Method for the prediction of the installation aerodynamics of a propfan at subsonic speeds
[NASA-CR-3887] N85-22369
Wind tunnel acoustic study of a propeller installed behind an airplane empennage: Data report
[NASA-CR-177335] N85-23377
PROPULSION
Characterization standards for solid propellant rocket motors
[AD-A150250] N85-22627
PROPULSION SYSTEM PERFORMANCE
Determination of aerodynamic and propulsion parameters of general aviation aircraft using steady state flight test data N85-22377
PROTECTION
EOS (electrical overstress) protection for VLSI (Very Large Scale Integration) devices
[AD-A150333] N85-22891
PROTECTIVE CLOTHING
The application of anthropometric survey data to aircrew clothing sizing
[AD-A150545] N85-23304
PROTECTIVE COATINGS
Formation of alumina layers on iron-base alloys
[BLL-T6418/BG/LRS/LRST737/84] N85-22657
Properties of welded joints in argon arc welding of titanium alloy using a protective coating N85-22733
PROTECTORS
Optoelectronic safety system for robotized technological complex N85-22805
PROTON ENERGY
Protons with energies above 30 KeV in Earth's radiation belt at low altitudes during magnetically quiet time close to geomagnetic equator N85-22423
PROTON IRRADIATION
Investigation of the degradation of GaAs photovoltaic cells by proton and electron irradiation N85-22587
Isotropic proton irradiation of GaAs solar cells N85-22622
PROTONS
Effects of focusing on HRS focal-plane polarimeter measurements
[DE85-004627] N85-23406
PROTOPLANETS
Lunar origin: Role of giant impacts N85-23519
A circum-terrestrial compositional filter N85-23520
Models of angular momentum input to a circum-terrestrial swarm from encounters with heliocentric planetesimals N85-23521
Capture of planetesimals into a circumterrestrial swarm N85-23522
Orbital resonances and planetary accretion in the solar nebula N85-23523
Accumulation of the terrestrial planets N85-23524
Evolution of grains in a turbulent solar nebula N85-23525
The Formation of preplanetary disks from the collapse of rotating molecular cloud cores N85-23526
PROTOTYPES
Improved Y-11 general-purpose transport designated Y-12 N85-22385
PROVING
Validation summary report, Burroughs Corporation, 820 FORTRAN release 4.0
[PB84-227792] N85-23316
PROXIMITY EFFECT (ELECTRICITY)
Outlook for realization of proximity effect and Josephson direct current in helium-2 N85-22956
PSYCHOLOGICAL EFFECTS
Sleep deprivation and exercise tolerance
[AD-A150626] N85-23297
PSYCHOMETRICS
Human cognition and intelligence: Towards an integrated theoretical perspective
[CSIR-SR-PERS-350] N85-23300
PULSE AMPLITUDE
Reception of signal with unknown amplitude and duration submerged in white noise N85-23016
PULSE COMMUNICATION
Use of electronic coding-frequency meters to measure parameters of pulsed radio signals N85-22964
PULSE DURATION
Square-pulse generator N85-22959
Use of electronic coding-frequency meters to measure parameters of pulsed radio signals N85-22964
PULSE FREQUENCY MODULATION
Applicability of log-normal model to probabilistic description of quasi-pulse interference N85-23014
PULSE GENERATORS
Square-pulse generator N85-22959
Accuracy of approximation of Bayes estimates in presence of noninformative parameters N85-23015
PULSE REPETITION RATE
Repetitive energy transfers from an inductive energy store N85-22881
Square-pulse generator N85-22959
PULSED LASERS
Mathematical modeling of two-frequency laser sounding of scattering media N85-23045
Time-resolved ellipsometry and reflectivity measurements of the optical properties of silicon during pulsed excimer laser irradiation
[DE85-005091] N85-23079
Activation of Si-N modes in silicon by pulsed laser annealing
[DE85-002988] N85-23082

Time resolved X-ray studies during pulsed laser irradiation of Ge
[DE85-005263] N85-23083
Time-resolved reflectivity measurement of extrinsic silicon during pulsed laser irradiation
[AD-A150350] N85-23403

PULSED RADIATION
Invariance of probability characteristics of detector to shape of optical pulse signals N85-23048

PULSES
Domain of applicability of asymptotic description of radio pulse fields near critical frequency N85-22949
Optimization of number of pulses in detection of fluctuating optical signals N85-22993
Probability of detection of pulsed signals employing zero-gating interference suppression N85-23021

PUMPS
Operational performance of the photovoltaic-powered grain mill and water pump at Tangaye, Burkina Faso (formerly Upper Volta)
[NASA-TM-86970] N85-23243

PURSUIT TRACKING
Space interception guidance with uncertain factors N85-22781

PYRAMIDS
Beamwidth control in pyramidal horns
[R-NIAS-27] N85-22853

Q

Q FACTORS
Piezoelectric filter with low-Q inductances N85-22932

Q SWITCHED LASERS
Low jitter trigger for an excimer laser
[DE85-005732] N85-23080

QUALIFICATIONS
IHE material qualification tests description and criteria
[DE85-004649] N85-22770

QUALITY CONTROL
Characterization standards for solid propellant rocket motors
[AD-A150250] N85-22627
Measurement of internal thermal resistance for quality control of semiconductor devices N85-22953

QUANTITATIVE ANALYSIS
Interlaminar fracture toughness in resin matrix composites
[AD-A150565] N85-22640

QUANTUM COUNTERS
Noise tolerance of digital demodulator for complex signal system employing binary quantization N85-22929

QUANTUM MECHANICS
Macroscopic quantum tunnelling in a current biased Josephson junction
[DE85-004603] N85-23424

QUANTUM STATISTICS
A measurement of the intensity of the cosmic background radiation at 3.9 cm N85-23681

QUASARS
University of Cambridge Institute of Astronomy report of activities N85-23484

QUENCHING (COOLING)
Quenching effects on iron site partitioning in the Apollo 17 orange glass composition N85-23553
Experimental methds for quenching structures in lunar-analog silicate melts: Variations as a function of quench media and composition N85-23554

R

RADAR ANTENNAS
Adaptive control of airborne radar antennas N85-22969

RADAR APPROACH CONTROL
Planned office and facility consolidations: To improve system effectiveness and efficiency, FY 1985-87
[AD-A150441] N85-22376

RADAR CROSS SECTIONS
Research efforts in support of resonance extraction studies. Volume 1: Improvement and validation of TWFD (Thin-Wire Frequency-Domain): A thin-wire frequency-domain scattering code
[AD-A150296] N85-22684

RADAR DATA
Visualization of radar altimetry data for Venus N85-22437

RADAR ECHOES
Mars radar catalog N85-23636

RADAR GEOLOGY
Volcanism and rift formation in Beta Regio, Venus: New radar results N85-23507
Classification of circular features on Venus N85-23511

RADAR IMAGERY
The imaging of internal waves by the SEASAT-A synthetic aperture radar
[ARE(PORTLAND)TN-720/84] N85-22660
Edge detection in SAR imagery using gradient operators — synthetic aperture radar (SAR)
[AD-A149411] N85-22662
Surfaces of asteroids and cometary nuclei N85-23503
Volcanism and rift formation in Beta Regio, Venus: New radar results N85-23507
Venus surface composition from radio/radar measurements N85-23509
Classification of circular features on Venus N85-23511
Correction and geological analysis of lunar 3.8 cm radar data N85-23634
Landform identification on radar images N85-23635
Mars radar catalog N85-23636
Radar and the detection of liquid water on Mars N85-23638
Intra-eruption geologic map from an x-band radar image during the May 18, 1980 eruption of Mount St. Helens, Washington N85-23639
Radar observations of fissure-fed basaltic lava flows, Craters of the Moon, Idaho N85-23640
Late Tertiary and Quaternary river systems of the eastern Sahara as mapped on shuttle radar and LANDSAT images N85-23641

RADAR MAPS
Progress in planetary radarclinometry N85-23630
Mercury radar altimetry: A preliminary analysis N85-23631

RADAR MEASUREMENT
Progress in planetary radarclinometry N85-23630
Mercury radar altimetry: A preliminary analysis N85-23631
Mapping and geological analysis of Mercury and Venus radar ranging data N85-23633
Landform identification on radar images N85-23635

RADAR RECEIVERS
Methods of digital correction for channels of multichannel radar receivers N85-23005

RADAR RESOLUTION
Landform identification on radar images N85-23635

RADAR SCANNING
Mathematical model of discriminator for signals with fluctuations and thermal noise N85-22943

RADAR TRACKING
Synthesis of optimum algorithms for secondary processing N85-22992

RADAR TRANSMISSION
Factorized algorithms for combined spatial and temporal processing of radar signals N85-22997

RADAR TRANSMITTERS
The Chinese remainder theorem and multi-PRF radars
[AD-A141375] N85-22658

RADIAL VELOCITY
Experimental determination of optimum ratio of runner blade height at exit to runner blade height at entrance of radial inward-flow microturbines N85-22627

RADIANCE
Remote sensing of coastal wetlands biomass using Thematic Mapper wavebands — Lewes, Delaware N85-23198
The relationship between marine aerosol particles and satellite-detected radiance N85-23263

RADIANT FLUX DENSITY
Performance estimate of a reflecting light pipe for infrared detectors
[AD-A141269] N85-23398

RADIATION ABSORPTION
Correctness of reflection characteristics of radio absorbent materials N85-22995

RADIATION BELTS
Longitude and pitch-angle distributions of streams of high-energy electrons under Earth's radiation belts N85-22415
Protons with energies above 30 KeV in Earth's radiation belt at low altitudes during magnetically quiet time close to geomagnetic equator N85-22423

RADIATION DAMAGE
Technological process effect on the carrier lifetime degradation of silicon solar cell base layer irradiated by 1 MeV electrons (boron doping case) N85-22585
The effects of lithium counterdoping on radiation damage and annealing in n(+)p silicon solar cells N85-22586
Investigation of the degradation of GaAs photovoltaic cells by proton and electron irradiation N85-22587
In-orbit laser regeneration of the radiation damaged solar arrays N85-22588
Analysis of optimum front cover thickness for lightweight solar arrays N85-22606
Annealing of radiation damage in boron and gallium doped silicon solar cells N85-22624

RADIATION DETECTORS
Dielectric detector device for registering heavy cosmic radiation particles N85-22799

RADIATION DOSAGE
Distribution of radium and plutonium in human bone
[DE85-005025] N85-23208

RADIATION EFFECTS
Solar array dynamical simulation for illumination and temperature variation N85-22611
Breakdown of thin plates by radiation N85-22709
Effect of alternative aging and accident simulations on polymer properties
[DE85-002642] N85-22762
Radiation-dominated snowmelt on Mars N85-23592

RADIATION MEASUREMENT
Operational experience with ion concentration sensors in orientation systems N85-22422
Two-dimensional signal processing and storage and theory and applications of electromagnetic measurements
[AD-A150590] N85-22899
Comprehensive, integrated, remote sensing at DOE sites
[DE85-004867] N85-23240

RADIATION SOURCES
Possibility of mapping active tectonic structures from mercury gas aureoles over sea surface N85-23162

RADIATION SPECTRA
Investigation of dynamics of radiation spectrum of injection lasers by intrared impulse Fourier spectroscopy N85-23047

RADIATION TRANSPORT
Introduction to combinatorial geometry
[DE85-003266] N85-23364

RADIO ALTIMETERS
Visualization of radar altimetry data for Venus N85-22437

RADIO ASTRONOMY
USSR report: Space
[JPRS-USP-85-001] N85-22403
All-Union conference of radio astronomers N85-22408
Studies of galactic HI in 21-centimeter absorption N85-23466
Venus surface composition from radio/radar measurements N85-23509

RADIO COMMUNICATION
INMARSAT marine satellite organization N85-22456
Firefighters' communication transceiver test plan
[NASA-CR-171419] N85-22854
A comparison of metropolitan and non-metropolitan employment characteristics: Indications of the size of non-metropolitan mobile communication services user classes
[NASA-CR-175648] N85-22855
Use of Bigaussian approximation to describe fading in scattering communications channel N85-23017

RADIO DIRECTION FINDERS
Natural electromagnetic radiation in seismically active regions N85-23152

RADIO ELECTRONICS
USSR report: Electronics and electrical engineering
[JPRS-UEE-85-002] N85-22907

RADIO EMISSION
Determining vector of radiointerferometer base from observations of natural radio emission with narrow spectrum N85-23158

RADIO EQUIPMENT
Machine analysis of resonance characteristics of plate-type radio electronic equipment constructions N85-23018

RADIO FILTERS
Theory of optimum M-filtration of signals against background of correlated interference N85-22927
Combined processing method and matched filter for discrete composite frequency phase-shift keyed signal N85-22931
Programmable filter with fanned interdigital surface acoustic wave transducer N85-23008

RADIO FREQUENCIES
Horizontal deflection TS-257 N85-22926
Combined processing method and matched filter for discrete composite frequency phase-shift keyed signal N85-22931

RADIO FREQUENCY INTERFERENCE
Interference immunity of fiber-optic communication lines with spectral multiplexing of channels N85-22924
Probability of detection of pulsed signals employing zero-gating interference suppression N85-23021
Analysis of interference caused by interfering radio signals in communications systems with frequency separation of telephone channels and frequency modulation N85-23025
Approximate rules for signal detection against background of Gaussian correlated interference N85-23027

Noise immunity of information transmission system with pseudorandom frequency switching under worst-case interference conditions N85-23029

RADIO INTERFEROMETERS

Determining vector of radiointerferometer base from observations of natural radio emission with narrow spectrum N85-23158

RADIO NAVIGATION

INMARSAT marine satellite organization N85-22456

RADIO PHYSICS

Millimeter-wave range masers: A review N85-23042

RADIO RELAY SYSTEMS

Optimum path selection in automated radio relay link design N85-22947

RADIO SCATTERING

Correctness of reflection characteristics of radio absorbent materials N85-22995

RADIO SIGNALS

The use of a high-speed 12-bit A/D converter for digital sampling of communication signal carriers [AD-A150578] N85-22872

Space-time response characteristics of acoustooptic filter for compression of linearly frequency-modulated signal N85-22937

Domain of applicability of asymptotic description of radio pulse fields near critical frequency N85-22949

Reception noise immunity of multiposition signals N85-23023

Analysis of interference caused by interfering radio signals in communications systems with frequency separation of telephone channels and frequency modulation N85-23025

Investigation of influence of communications link and synchronization error on noise tolerence of group transmission of binary information based on orthogonal Walsh function N85-23026

Approximate rules for signal detection against background of Gaussian correlated interference N85-23027

Use of importance sampling to investigate signal detection systems by simulated method N85-23028

RADIO SOURCES (ASTRONOMY)

Absolute measurements of radiation intensity from Cassiopeia-A, Cygnus-A and crab nebula in 60-100 cm band N85-22978

RADIO TELESCOPES

Error in compensating phase fluctuations of wave field by means of adaptive reflectors with continuous or compound surface N85-22988

RADIO WAVE REFRACTION

Possibility of determining atmospheric weather parameters by radio and radiooptical measurements of refraction of cosmic sources N85-23146

RADIO WAVES

Calculation of amplitude-phase characteristics of signal scattered obliquely on meteor trail N85-22948

RADIOACTIVE ISOTOPES

Multiple element neutron-activation analysis of atmospheric aerosols with X-ray and gamma-spectrometric recording of radionuclides formed N85-22631

RADIOGRAPHY

In-situ burning rate determination using flash radiography N85-22550

RADIOMETERS

Application of field X-ray: Radiometric analysis in exploratory geology and means for its improvement N85-23176

RADIOMETRIC CORRECTION

Analysis and evaluation of the LANDSAT-4 MSS and TM sensors and ground data processing systems: Early results N85-23189

RADIOMETRIC RESOLUTION

Impact of Thematic Mapper sensor characteristics on classification accuracy — suburban Washington, D.C., Maryland, and the Chesapeake Bay N85-23188

Assessing LANDSAT TM and MSS data for detecting submerged plant communities N85-23203

The use of Thematic Mapper data for land cover discrimination: Preliminary results from the UK SATMaP programme N85-23207

RADIUM

Distribution of radium and plutonium in human bone [DE85-005025] N85-23298

RAILGUN ACCELERATORS

H-division materials physics progress [DE85-004990] N85-23430

RAMAN SPECTRA

Mathematical modeling of two-frequency laser sounding of scattering media N85-23045

RAMAN SPECTROSCOPY

Laser diagnostic analyses of sooting flames [AD-A150478] N85-22649

Raman structural studies of the nickel electrode [NASA-CR-175619] N85-23414

RAMJET ENGINES

Twenty-first JANNAF Combustion Meeting, volume 1 [AD-A150981] N85-22526

Nonlinear interactions between vortices and acoustic waves in a rocket combustion chamber N85-22533

Selection of air intake parameters for supersonic-flow operation N85-22837

RANDOM ACCESS MEMORY

Parallel update of minimum spanning trees in logarithmic time [AD-A150497] N85-23357

RANDOM NOISE

Interference immunity of binary systems with second-order phase-difference modulation in various reception modes N85-22944

Synthesis of quasi-optimum two-level signal discriminator with level changing at unknown point N85-23010

Use of Bigaussian approximation to describe fading in scattering communications channel N85-23017

RANDOM PROCESSES

Models of discontinous random fields N85-22983

RANDOM SIGNALS

Accuracy of random signal spectral parameter estimation against interference background in acoustooptical spectrum analyzers N85-23052

RANDOM VARIABLES

Skewed stable variables and processes [AD-A150549] N85-23372

RANGE AND RANGE RATE TRACKING

Satellite-to-satellite orbit determination using minimum, discrete range and range-rate data only N85-22458

RAPID QUENCHING (METALLURGY)

Rapid solidification processing of magnesium alloys [AD-A150270] N85-22668

Time-resolved studies of rapid solidification in highly undercooled molten silicon [DE85-004857] N85-22765

RARE GASES

Effect of moisture in inert gases on density of seam metal and on mechanical characteristics of welded joints of aluminum and aluminum alloys N85-22744

RATS

Brain mechanisms underlying individual differences in reaction to stress: An animal model [AD-A150195] N85-23301

RAYLEIGH DISTRIBUTION

Spline-based Rayleigh-Ritz methods for the approximation of the natural modes of vibration for flexible beams with tip bodies [NASA-CR-172566] N85-23100

RAYLEIGH SCATTERING

A measurement of the intensity of the cosmic background radiation at 3.9 cm N85-23681

RDX

The chemistry of RDX and HMX cluster ions N85-22561

REACTION KINETICS

Ignition of mixtures of SiH sub 4, CH sub 4, O sub 2, and Ar or N sub 2 behind reflected shock waves [NASA-TP-2415] N85-22395

Gasification of boron oxide drops and boron slurry agglomerates in combustion gases N85-22529

Combustion kinetics of metal atoms and metallic radicals over wide temperature ranges N85-22530

Combustion of zirconium carbide N85-22532

Chemical kinetics of gas phase decomposition products of nitramine propellants N85-22558

Kinetics of mechanism of the thermal decomposition of dimethylnitramine and dimethylnitrosamine N85-22559

The chemistry of RDX and HMX cluster ions N85-22561

Comprehensive mechanisms for combustion chemistry: An experimental and numerical study with emphasis on applied sensitivity analysis [DE85-000173] N85-22656

Estimating degree of development of physical-chemical interaction among components in Al-B fiber composite material N85-22705

Segregation of silicon in silumin-carbon fiber composites N85-22706

Specifics of kinetics of polymorphous conversion upon heating of low carbon steels N85-22721

Thermodynamic and kinetic studies of pulsed laser annealing from transient conductivity measurements [DE85-003677] N85-23078

REACTOR SAFETY

Steel containment buckling [DE85-003744] N85-23111

REACTOR TECHNOLOGY

USSR report: Engineering and equipment [JPRS-UEQ-85-003] N85-22782

Winding insulation in electromagnetic systems for Tokamak reactor plants N85-23035

RECEIVERS

Programmable filter with fanned interdigital surface acoustic wave transducer N85-23008

Invariance of probability characteristics of detector to shape of optical pulse signals N85-23048

Microwave blackbodies for spaceborne receivers [NASA-CR-175647] N85-23068

RECTANGULAR PLATES

A clamped rectangular plate containing a crack [NASA-CR-175590] N85-23098

RECTANGULAR WAVEGUIDES

Magnetostatic-wave propagation in a finite YIG-Loaded rectangular waveguide [AD-A150332] N85-22865

RED SEA

A tectonic model of an incipient spreading center and its margins: The Northern Red Sea and the Dead Sea rift N85-23286

REDUCTION (CHEMISTRY)

Americium metal preparation on the multigram scale [DE85-003735] N85-22683

REDUNDANCY

Low thrust bipropellant engine/redundant seat valve assembly [AD-A150293] N85-22628

A theoretical basis for the analysis of redundant software subject to coincident errors [NASA-TM-86369] N85-23317

REFLECTANCE

Correctness of reflection characteristics of radio absorbent materials N85-22995

Zero-crossings on lines of curvature [AD-A150171] N85-23345

Time-resolved reflectivity measurement of extrinsic silicon during pulsed laser irradiation [AD-A150350] N85-23403

Surface units on Venus derived from Pioneer-Venus altimetry, roughness, and reflectivity measurements N85-23510

Unsupervised classification of global radar units on Venus N85-23632

REFLECTED WAVES

Intensity fluctuations of focused laser beam during reflection in turbulent atmosphere N85-22975

Reflected wave travel-time curves in stratified media with vertically heterogeneous layers and slightly sloping curved boundaries N85-23167

Correcting depth line on nonlongitudinal seismic profile N85-23184

REFLECTING TELESCOPES

Error in compensating phase fluctuations of wave field by means of adaptive reflectors with continuous or compound surface N85-22988

REFLECTION

Mutiple reflection theory for microwave measurement of solid propellant burning rates N85-22549

REFLECTOMETERS

Optical reflectometer for multimode fiber lightpipes N85-22961

REFLECTORS

Intensity fluctuations of focused laser beam during reflection in turbulent atmosphere N85-22975

Error in compensating phase fluctuations of wave field by means of adaptive reflectors with continuous or compound surface N85-22988

Innovative research in the design and operation of large telescopes for space: Aspects of giant telescopes in space [NASA-CR-175626] N85-23462

REFRACTION

Acoustic energy exchange in sheared mean flows — solid rocket motors N85-22534

Reflected wave travel-time curves in stratified media with vertically heterogeneous layers and slightly sloping curved boundaries N85-23167

REFRACTIVITY

Multifunctional elements for integrated optics N85-22918

Dispersion characteristics of small-mode gradient optical fibers N85-23004

Possibility of determining atmospheric weather parameters by radio and radiooptical measurements of refraction of cosmic sources N85-23146

REFRACTORY MATERIALS

Experimental study of enthalpy of quasimonocrystal of graphite and carbon glass in temperature range of 2690-3818 deg K N85-22751

REFRIGERATING

Magnetic refrigeration and heat pumping design options [DE85-003405] N85-23064

REGENERATION (ENGINEERING)

In-orbit laser regeneration of the radiation damaged solar arrays N85-22588

Regenerative stochastic Petri nets [AD-A150343] N85-23355

Regenerative simulation of non-Markovian stochastic systems
[AD-A150344] N85-23367
REGOLITH
Progress on Experimental impact studies N85-23534
Multispectral analysis of the Kasei Vallis-Lunae Planum region of Mars N85-23607
REGRESSION ANALYSIS
Expansion of functions describing planetary surface and gravity field N85-22410
Approaches and algorithms for robust signal processing N85-22878
Ozone Correlative Measurements Workshop
[NASA-CP-2362] N85-23112
Measurement requirements for the detection of ozone trends N85-23115
Consistency of smoothing with running linear fits
[AD-A150232] N85-23349
A model for large sparse contingency tables
[AD-A150320] N85-23350
A note about the strong convergence of the nonparametric estimation of a regression function
[AD-A150325] N85-23353
REINFORCED SHELLS
Testing of wound materials for strength with loading in the reinforcement plane N85-22701
REINFORCING MATERIALS
Mechanism of strengthening plastics with rubbers N85-22636
RELATIVISTIC EFFECTS
Viking radio science data analysis and synthesis
[NASA-CR-175631] N85-23471
RELATIVISTIC ELECTRON BEAMS
Collective acceleration of ions using high current relativistic electron beams
[DE85-004689] N85-23393
RELATIVISTIC PLASMAS
Spacecraft-environment interaction: The environmental plasma aspect N85-22479
RELATIVISTIC THEORY
Viking radio science data analysis and synthesis
[NASA-CR-175631] N85-23471
RELAXATION (MECHANICS)
Energy spectrum of processes of structural relaxation of amorphous alloy FeCo70Si15B10 N85-22750
Numerical simulation of inverters with I2L elements including effects of high doping level N85-23039
RELEASING
Theoretical thermodynamics of mixtures at high pressures N85-23550
RELIABILITY
Effects of assuming independent component failure times, if they are actually dependent, in a series system
[AD-A150582] N85-23092
Parallel test method for LSI (Large Scale Integration) microprocessors
[AD-A150237] N85-23310
Contribution of instrumentation and control software to system reliability
[DE85-004693] N85-23340
Electric and hybrid vehicle demonstration project
[DE85-003939] N85-23455
RELIABILITY ENGINEERING
AIRLAB: A laboratory for flight-crucial-electronics system research N85-22362
RELIEF MAPS
Expansion of functions describing planetary surface and gravity field N85-22410
Visualization of radar altimetry data for Venus N85-22437
Mars planimetric mapping N85-23666
Voyager cartography N85-23668
RELIEVING
Theory of diaphragm light modulators with electrical input signal N85-23002
REMOTE SENSING
USSR report: Space
[JPRS-USP-85-001] N85-22403
Remote sensing used for study of forest resources N85-22440
China report: Science and technology
[JPRS-CST-85-005] N85-22843
Geological remote sensing develops rapidly, finds broad applications N85-22848
Radiosodar system for remote synchronous measurements of wind speed, temperature and its fluctuations N85-23145
Remote Sensing of Snow and Evapotranspiration
[NASA-CP-2363] N85-23223
NASA's land remote sensing plans for the 1990's N85-23224
General report of the researches of snowpack properties, snowmelt runoff and evapotranspiration in Japan N85-23225
Snowmelt-runoff model utilizing remotely-sensed data N85-23226
Microwave radiometer observations of snowpack properties and comparison of U.S. Japanese results — Hokkaido, Japan and Vermont and North Dakota test sites N85-23230
Estimation of regional evapotranspiration using remotely sensed land surface temperature. Part 1: Measurement of evapotranspiration at the Environmental Research Center and determination of Priestley-Taylor parameter N85-23233
Estimation of regional evapotranspiration using remotely sensed land surface temperature. Part 2: Application of equilibrium evaporation model to estimate evapotranspiration by remote sensing technique — Japan N85-23234
Characteristic vector analysis of inflection ratio spectra: New technique for analysis of ocean color data
[NASA-TP-2428] N85-23237
Feature extraction assessment study
[AD-A150189] N85-23239
Comprehensive, integrated, remote sensing at DOE sites
[DE85-004867] N85-23240
Accomplishments of Institute of Cartography summarized N85-23435
Zeolites on Mars: Prospects for remote sensing N85-23615
Analysis of SMIRR data for volcanic and sedimentary terrains of the trans-Pecos region, Texas N85-23626
REMOTE SENSORS
Digital processing of mesoscale analysis and space sensor data
[NASA-CR-171429] N85-23319
REPORTS
Activities of the Jet Propulsion Laboratory, 1 January - 31 December 1983
[NASA-CR-175555] N85-23447
RESEARCH
University of Cambridge Institute of Astronomy report of activities N85-23464
RESEARCH AIRCRAFT
Civil avionics flight testing with the RAE(B) BAC1-11 N85-22354
RESEARCH AND DEVELOPMENT
China report: Science and technology
[JPRS-CST-84-030] N85-22777
Physicists' role in new technological development discussed N85-23436
RESEARCH FACILITIES
Activities of the Jet Propulsion Laboratory, 1 January - 31 December 1983
[NASA-CR-175555] N85-23447
RESEARCH MANAGEMENT
Research in the optical sciences
[AD-A150196] N85-23401
Activities of the Jet Propulsion Laboratory, 1 January - 31 December 1983
[NASA-CR-175555] N85-23447
Authorizing appropriations to the National Aeronautics and Space Administration for fiscal year 1986
[H-REPT-99-32] N85-23452
RESIDUES
Transformation of polar ice sublimate residue into Martian circumpolar sand N85-23580
RESILIENCE
New deformable secondary aluminum alloys N85-22694
RESIN MATRIX COMPOSITES
Interlaminar fracture toughness in resin matrix composites
[AD-A150565] N85-22640
RESISTORS
High sheet resistance, arsenic implanted polycrystalline silicon for integrated circuit resistors
[DE85-004355] N85-22902
Stability of highly nonlinear oxide-zinc resistors under continuous voltage of industrial frequency N85-23030
RESOLUTION
Study of resolution of deep MT soundings by means of physical model N85-23155
RESONANCE
Dipole active surface vibrational resonances on clean and hydrogen covered Ni(110)
[AD-A150546] N85-23420
Stability of the Galilean satellites in deep orbital resonance N85-23477
Studies of planetary rings N85-23488
Orbital resonances and planetary accretion in the solar nebula N85-23523
RESONATORS
Three-mirror open resonator for millimeter wave band N85-22972
Effect of space-charge field on output characteristics of O-type oscillators with distributed interaction N85-23043
RESOURCES MANAGEMENT
Technologies to sustain tropical forest resources
[TI85-901065] N85-23241
RETRACTABLE EQUIPMENT
Blanket integrated cushioning of foldable and retractable solar arrays N85-22612
Concept for controlled fold by fold deployment and retraction of flexible, foldable solar generators N85-22613
Growth capabilities of European retractable solar arrays N85-22625
REUSABLE HEAT SHIELDING
Electron beam charging of Space Shuttle thermal protection system tiles N85-22478
REVERSED FLOW
Dilution jet configurations in a reverse flow combustor
[NASA-CR-174886] N85-22392
Determination of boundary line between reverse jet and surrounding stream N85-22789
REYNOLDS NUMBER
Cryogenic wind tunnels: A selected annotated bibliography
[NASA-TM-86346] N85-22401
RHEOLOGY
Thermal and thermoelastic effects in rolling/sliding contacts
[AD-A150435] N85-23429
Sulfur volcanoes on Io? N85-23479
Geomorphic classification of lava flows on Io N85-23480
Emplacement of long lava flows on Mauna Loa (Hawaii) and Alba (Mars) N85-23563
Field measurements of the 1983 Royal Gardens lava flows, Kilauea Volcano, and 1984 Mauna Loa lava flows, Hawaii N85-23565
Surface structures of Hawaiian lavas N85-23566
Submarine volcanic eruptions and potential analogs for Venus N85-23573
Creep of ice: Further studies N85-23655
RHODIUM COMPOUNDS
Anomalous magnetism of CeRh3B2 under pressure
[DE85-003069] N85-23425
RHOMBIC ANTENNAS
Surface wave excitation study
[DE85-005301] N85-22875
RICCATI EQUATION
Numerical algorithms and software for matrix Riccati equations
[AD-A150148] N85-23344
RIGID STRUCTURES
Computer aided engineering applied to the design and verification of the generic Advanced Rigid Array (ARA) — solar array N85-22593
Development and qualification of the electrical part of the Advanced Rigid Array (ARA) — solar array N85-22594
Rigid Solar Generator (GSR) solar arrays N85-22596
Retractable Rigid Solar Generator (GSR) N85-22597
Generic design and verification of an Advanced Rigid Array (ARA) — solar array N85-22621
RING LASERS
Status of and outlook for producing means of transmitting units of plane angle, angular velocity and acceleration with ring lasers N85-22955
RIPPLES
Ripple ring basins on Ganymede and Callisto N85-23547
RITZ AVERAGING METHOD
Spline-based Rayleigh-Ritz methods for the approximation of the natural modes of vibration for flexible beams with tip bodies
[NASA-CR-172566] N85-23100
RIVER BASINS
Comparison of land cover information from LANDSAT Multispectral Scanner (MSS) and airborne Thematic Mapper simulator (TMS) data for hydrologic applications — Clinton River Basin, Michigan N85-23211
General report of the researches of snowpack properties, snowmelt runoff and evapotranspiration in Japan N85-23225
Snowmelt-runoff model utilizing remotely-sensed data N85-23226
Snowmelt runoff model in Japan N85-23227
Application of Martinec-Rango model to river basin in Japan N85-23228
Distribution of snow and maximum snow water equivalent obtained by LANDSAT data and degree day method N85-23229
The geology of East Butte, a rhyolitic volcanic dome on the Eastern Snake River Plain, Idaho N85-23570
RIVERS
A comparison of terrestrial saltation flux in the laboratory and the field N85-23582

ROBOTICS
Advancing automation and robotics technology for the Space Station and for the US economy. Volume 1: Executive overview
[NASA-TM-87566-VOL-1] N85-22460
Advancing automation and robotics technology for the Space Station and for the US economy, volume 2
[NASA-TM-87566-VOL-2] N85-22461
Reliability of robotized welding apparatus N85-22741
Optoelectronic safety system for robotized technological complex N85-22805
Optimum design of electrical motors for multilink manipulators and automated manufacturing systems N85-22880
Motion planning with six degrees of freedom
[AD-A150312] N85-23432

ROBOTS
Cyclic industrial robots with mechanical energy storing devices: Multipositional system with one or several degrees of freedom N85-22803
Hydraulic brakes for industrial robots N85-22806
Cyclic industrial robots with mechanical energy storing devices: Principles of drive design N85-22807
Assembly robot control algorithms N85-22808
Optimum design and automated dynamic analysis of flexible mechanisms
[AD-A150152] N85-23088

ROBUSTNESS (MATHEMATICS)
Approaches and algorithms for robust signal processing N85-22878
Bootstrapping the Kalman filter
[AD-A150509] N85-23370

ROCKET ENGINE CASES
Characterization standards for solid propellant rocket motors
[AD-A150250] N85-22627

ROCKET ENGINES
Twenty-first JANNAF Combustion Meeting, volume 1
[AD-A150981] N85-22526
Minimizing plume contamination production in bipropellant thrusters N85-22557

ROCKET EXHAUST
Minimizing plume contamination production in bipropellant thrusters N85-22557
Technical manual: Description and operation Slaved Tracking System
[DE85-004807] N85-23070

ROCKET LAUNCHING
Rocket body charge neutralization processes in ARAKS experiment (data from two launches) N85-22426

ROCKET NOZZLES
Characterization standards for solid propellant rocket motors
[AD-A150250] N85-22627

ROCKET PROPELLANTS
Twenty-first JANNAF Combustion Meeting, volume 1
[AD-A150981] N85-22526

ROCKS
Effects of fracture roughness on fluid flow through a single deformable fracture
[DE85-004593] N85-23062
Geomagnetic field dynamics N85-23182
Assessment of computer based geologic mapping of rock units in the LANDSAT-4 scene of northern Death Valley, California N85-23195

ROLL FORMING
Division boundary in Al-B composite material with boron in contact with solid and liquid aluminum N85-22704

ROOTS OF EQUATIONS
Zero-crossings on lines of curvature
[AD-A150171] N85-23345

ROSSBY REGIMES
Evolution of set of Rossby waves toward anisotropic equilibrium state N85-23141
Stability of Rossby waves within framework of three-component analysis N85-23142

ROTARY STABILITY
Structural response of a rotating bladed disk to rotor whirl
[NASA-CR-175605] N85-22391
Rotational motion of a satellite N85-22428

ROTARY WINGS
Experimental study of main rotor tip geometry and tail rotor interactions in hover. Volume 1. Text and figures
[NASA-CR-177336-VOL-1] N85-22344
Experimental study of main rotor tip geometry and tail rotor interactions in hover. Volume 2: Run log and tabulated data
[NASA-CR-177336-VOL-2] N85-22345
Study for prediction of rotor/wake/fuselage interference, part 1
[NASA-CR-177340-VOL-1] N85-22346
Study for prediction of rotor/wake/fuselage interference. Part 2: Program users guide
[NASA-CR-177340-VOL-2] N85-22347
Simple theoretical models for composite rotor blades
[NASA-CR-175620] N85-22362

ROTATING BODIES
Flight dynamics of axisymmetrical rotating bodies in air medium N85-22791
Axisymmetrical oscillations of shell systems subjected to impulse loads N85-22814

ROTATING FLUIDS
Regions of propagation of short-wave perturbations in spherical layer of rotating fluid N85-23130

ROTATING LIQUIDS
Double and inverse Taylor-Hogg vortices in a stratified ocean N85-23137

ROTATION
Absolute stability of unsteady movement of axisymmetrical rotating flight vehicle N85-22793

ROTOR AERODYNAMICS
Study for prediction of rotor/wake/fuselage interference, part 1
[NASA-CR-177340-VOL-1] N85-22346
Study for prediction of rotor/wake/fuselage interference. Part 2: Program users guide
[NASA-CR-177340-VOL-2] N85-22347
Flight dynamics of axisymmetrical rotating bodies in air medium N85-22791

ROTOR BLADES (TURBOMACHINERY)
Structural response of a rotating bladed disk to rotor whirl
[NASA-CR-175605] N85-22391
Experimental determination of optimum ratio of runner blade height at exit to runner blade height at entrance of radial inward-flow microturbines N85-22827
An experimental investigation of the chopping of helicopter main rotor tip vortices by the tail rotor
[NASA-CR-177338] N85-23376

ROTOR SPEED
Experimental study of main rotor tip geometry and tail rotor interactions in hover. Volume 1. Text and figures
[NASA-CR-177336-VOL-1] N85-22344

RUBBER
Mechanism of strengthening plastics with rubbers N85-22636

RUBY LASERS
Effect of transparent coatings on generation of laser-induced shock waves in metals N85-22711
Ruby wavefront-conjugation laser for obtaining high temperature plasma N85-22795

RUN TIME (COMPUTERS)
Exploiting multiprocessors: Issues and options
[DE85-003144] N85-23313

RUNGE-KUTTA METHOD
Runge-Kutta formula with cheap error estimate
[DE85-005674] N85-23363

RURAL AREAS
A comparison of metropolitan and non-metropolitan employment characteristics: Indications of the size of non-metropolitan mobile communication services user classes
[NASA-CR-175648] N85-22855

S

SAFETY DEVICES
Optoelectronic safety system for robotized technological complex N85-22805

SAHARA DESERT (AFRICA)
Late Tertiary and Quaternary river systems of the eastern Sahara as mapped on shuttle radar and LANDSAT images N85-23641

SALINITY
Geographic variation in the relationships of temperature, salinity or sigma sub t versus plant nutrient concentrations in the world ocean — silicic acid, nitrate, and phosphate concentration
[NASA-CR-175821] N85-23287

SALT SPRAY TESTS
Influence of 3% NaCl solution on rate of accumulation of damage and residual strength of aluminum-boron composite N85-22699

SALYUT SPACE STATION
Lyakhov and Aleksandrov on 150-day flight N85-22405
Comments on Salyut-7 150-day flight N85-22406
Remote sensing used for study of forest resources N85-22440

SAMPLING
The use of a high-speed 12-bit A/D converter for digital sampling of communication signal carriers
[AD-A150578] N85-22872
A Monte Carlo sampling plan for estimating network reliability
[AD-A150511] N85-22898
Use of importance sampling to investigate signal detection systems by simulated method N85-23028

SANDS
Transformation of polar ice sublimate residue into Martian circumpolar sand N85-23580
A comparison of terrestrial saltation flux in the laboratory and the field N85-23582
Potential bedforms on Venus: Wind tunnel simulations N85-23583

SATELLITE ATTITUDE CONTROL
Minimizing plume contamination production in bipropellant thrusters N85-22557

SATELLITE GROUND TRACKS
Scientific requirements for ozone measurements N85-23113

SATELLITE IMAGERY
Nation said to rank high with 15 satellites N85-22778
LANDSAT-4 Science Characterization Early Results. Volume 4: Applications — agriculture, soils land use, geology, hydrology, wetlands, water quality, biomass identification, and snow mapping
[E85-10070] N85-23186
Overview of TM applications research reports N85-23187
Characterization of LANDSAT-4 TM and MSS image quality for the interpretation of California's agricultural resources — Central Valley N85-23190
Preliminary evaluation of Thematic Mapper image data quality N85-23194
A concept for the processing and display of Thematic Mapper data N85-23196
Quick look analysis of TM data of the Washington, District of Columbia, area N85-23197
A preliminary comparison of the information content of data from the LANDSAT 4 Thematic Mapper and Multispectral Scanner — Arkansas N85-23199
Thematic Mapper data quality and performance assessment in renewable resources/agriculture/remote sensing N85-23201
Preliminary evaluation of TM for soils information N85-23206
Comparison of MSS and TM data for landcover classification in the Chesapeake Bay area: A preliminary report — Taylor's Island, Maryland N85-23210
An investigation of several aspects of LANDSAT-5 data quality — Palmer County, Shelby, mt; White sands, NM; Great Salt Lake, UT; San Matted Bridge and Sacramento, California
[E85-10096] N85-23214
Distribution of snow and maximum snow water equivalent obtained by LANDSAT data and degree day method N85-23229
Analysis of NIMBUS-7 SMMR data — Hokkaido, Japan snow cover N85-23232
The relationship between marine aerosol particles and satellite-detected radiance N85-23263
Analysis of the inflow layer and air-sea interactions in Hurricane Frederic (1979)
[NASA-CR-175616] N85-23271

SATELLITE INSTRUMENTS
Development and testing of a spacecraft surface potential monitor N85-22582

SATELLITE NETWORKS
Assessment of effectiveness of signal-code constructions in time division-multi-access satellite systems N85-22908
Satellite bridges in communications networks N85-22910

SATELLITE OBSERVATION
Evaluating accuracy in determining position of Earth's center of mass and elements of orientation of geodetic coordinate system N85-22441
New method of reconstructing conditions of recent differentiation of oil and gas in the Amudarya Basin (based on results of interpretation of space photographs) N85-22446
MAGSAT anomaly field data of the crustal properties of Australia
[E85-10100] N85-23215
A method for estimating soil moisture availability
[NASA-CR-175606] N85-23238

SATELLITE ORBITS
Nontraditional method for determining unperturbed orbits of unknown space objects using incomplete optical observational data N85-22417
Satellite oscillations in elliptical orbit N85-22429
Satellite-to-satellite orbit determination using minimum, discrete range and range-rate data only N85-22458
Method for determining the number of correlative measurements required to validate the SBUV/2 ozone retrievals N85-23114
Small solar system bodies N85-23499

SATELLITE PERTURBATION
Approximate perturbing part of geopotential by polynomials of stipulated form N85-22448

SATELLITE ROTATION
Motion of symmetrical satellite with flexible viscoelastic rods about center of mass in circular orbit N85-22420

Rotational motion of a satellite N85-22428
Electric field effects on ion currents in satellite wakes N85-22485
Patterns of fracture and tidal stresses due to nonsynchronous rotation: Implications for fracturing on Europa N85-23483

SATELLITE SURFACES
The violet absorber on Io: Disulfur monoxide derivatives N85-23482
Polar cap formation on Ganymede N85-23486
Interaction of the magnetospheric ions with the surfaces of the icy satellites of Saturn N85-23491
Plasma production by meteoroid impact N85-23492
Ripple ring basins on Ganymede and Callisto N85-23547
Permafrost and subsurface ice in the solar system N85-23594
Planetary analogs in Antarctica: Icy satellites N85-23605
The geomorphology of Rhea N85-23606
Io: Precise comparison of Voyager spectral curves with laboratory measurements N85-23619
Photometric analysis of Jupiter-illuminated images of Io N85-23620
Spectral units on Europa and Ganymede N85-23621
Fault offsets and lateral crustal movement on Europa N85-23656
Lineaments on Ganymede: New evidence for late tectonic activity N85-23658
Global tectonics on Ganymede N85-23659
Tectonics of the Galileo Regio on Ganymede N85-23660
Importance of the tectonic motions on Ganymede N85-23661
Tectonics of the Valhalla structure on Callisto N85-23662
The Galilean Satellite Geological Mapping Program, 1984 N85-23664
Geology of the Ganymede quadrangle Jg7 N85-23665
Voyager cartography N85-23668

SATELLITE TRACKING
China report: Science and technology [JPRS-CST-85-005] N85-22843
Development, prospect of satellite dynamics discussed N85-22847

SATELLITE TRANSMISSION
Assessment of effectiveness of signal-code constructions in time division-multi-access satellite systems N85-22908
Satellite bridges in communications networks N85-22910

SATELLITE-BORNE INSTRUMENTS
Dielectric detector device for registering heavy cosmic radiation particles N85-22799
Scientific requirements for ozone measurements N85-23113

SATELLITE-BORNE PHOTOGRAPHY
Evaluating accuracy in orientation of topographic photograph and satellite-centered direction from star photograph N85-22442
New method of reconstructing conditions of recent differentiation of oil and gas in the Amudarya Basin (based on results of interpretation of space photographs) N85-22446

SATURN (PLANET)
Investigations of planetary ring phenomena N85-23487
Studies of planetary rings N85-23488
Dynamical studies of Saturn's rings N85-23489
Meteoroidal impacts, plasma, fine structure of ringlets and spokes on Saturn's ring B N85-23490
Interaction of the magnetospheric ions with the surfaces of the icy satellites of Saturn N85-23491
Plasma production by meteoroid impact N85-23492
Origin and evolution of the Saturn system N85-23493

SATURN SATELLITES
Voyager cartography N85-23668
The control networks of the satellites of Jupiter and Saturn N85-23671

SCALE (RATIO)
Mars radar catalog N85-23636

SCALE EFFECT
Investigations into the effects of scale and compressibility on lift and drag in the RAE 5m pressurised low-speed wind tunnel [RAE-TM-AERO-2006] N85-22372

SCALING LAWS
Impact crater scaling laws N85-23532

SCANNING
NDE methods for green ceramics [DE85-004019] N85-22766

SCATHA SATELLITE
Aerospace spacecraft-charging guidelines document N85-22501
Automatic charge control system for satellites N85-22508

SCATTERING
Mathematical modeling of two-frequency laser sounding of scattering media N85-23045
Improvement in magnetic field properties of vanadium-gallium superconductors by enhancement of spin-orbit scattering [DE85-002893] N85-23422

SCATTERING AMPLITUDE
Calculation of amplitude-phase characteristics of signal scattered obliquely on meteor trail N85-22948

SCATTERING FUNCTIONS
Scattering of waves by axisymmetrical edge N85-22987

SCATTEROMETERS
Science opportunities using the NASA scatterometer on N-ROSS [NASA-CR-175639] N85-23222

SCENE ANALYSIS
Preliminary study of information extraction of LANDSAT TM data for a suburban/regional test site N85-23208

SCHOTTKY DIODES
Low capacitance e-beam fabricated beam-lead Schottky barrier diodes [AD-A150238] N85-22888

SCIENTISTS
China report: Science and technology [JPRS-CST-85-003] N85-23433
Physicists' role in new technological development discussed N85-23436

SCINTILLATION COUNTERS
The effect of the choice or response matrix on unfolded bonner sphere spectra [AD-A150462] N85-23404

SCORING
A 2 x 6 Back Surface Reflection (BSR) silicon solar cell N85-22570

SEA ICE
Drifting ice as mechanical factor in purifying and polluting hydrosphere N85-23132

SEA LEVEL
Calculation of level surface in problems of large-scale ocean circulation N85-23136

SEA WATER
Possible role of ocean biota in global carbon balance — phytoplankton production N85-23129
Mathematical-cartographic model for study of distribution of hydrochemical elements in sea water (using dissolved oxygen in the Pacific Ocean as an example) N85-23138
Geographic variation in the relationships of temperature, salinity or sigma sub t versus plant nutrient concentrations in the world ocean — silicic acid, nitrate, and phosphate concentration [NASA-CR-175621] N85-23267
Luminescence in the ocean [AD-B089136L] N85-23288

SEALS (STOPPERS)
Sliding seal materials for adiabatic engines [NASA-CR-174893] N85-22757

SEAMS (JOINTS)
Softening of metal near seam during welding of heat-resistant nickel alloys N85-22747

SEASAT 1
The imaging of internal waves by the SEASAT-A synthetic aperture radar [ARE(PORTLAND)TN-720/84] N85-22860

SEATS
Low thrust bipropellant engine/redundant seat valve assembly [AD-A150293] N85-22628

SECONDARY EMISSION
Calculation of secondary-electron escape currents from inclined-spacecraft surfaces in a magnetic field N85-22491
Self-consistent simulation of plasma interactions with secondary-emitting insulators N85-22492
Electron yields from spacecraft materials N85-22512

SECONDARY RADAR
Synthesis of optimum algorithms for secondary processing N85-22992

SEDIMENTARY ROCKS
Normal-fault and fold development in sedimentary rocks above a pre-existing basement normal fault N85-23259

SEDIMENTS
Special features of computations of vertical distribution of concentration of suspended sediments under marine conditions N85-23125
Determining adsorption of surface-active substances by sea bottom deposits N85-23128
Review of problems in lithology N85-23160
A first evaluation of LANDSAT TM data to monitor suspended sediments in lakes — Lake Chicot, Arkansas N85-23204

SEISMIC ENERGY
Interrelationship of earthquake magnitude and lithospheric-asthenospheric thermodynamic parameters in seismically active zones N85-23183

SEISMIC WAVES
Two-and-one-half dimensional in-plane wave propagation [AD-A150467] N85-22867
Determining degree of partial melting of asthenosphere from seismic data N85-23127
More precise curve of dependence between density and velocity of longitudinal waves in consolidated crust and top of mantle in oceanic structures N85-23143
Nature of seismic images with amplitude and time fluctuations of recorded oscillations N85-23158
Magmatism in continent-ocean transition zone (development of ideas of A. N. Zavaritskiy) N85-23161
Boundary velocities of longitudinal seismic waves and lateral inhomogeneities of upper ocean mantle N85-23165
Seismic waves and dispersion relations N85-23181
Interrelationship of earthquake magnitude and lithospheric-asthenospheric thermodynamic parameters in seismically active zones N85-23183
Correcting depth line on nonlongitudinal seismic profile N85-23184
Attenuation of seismic waves at regional distances [AD-A150198] N85-23267

SEISMOGRAPHS
Use of mobile surface station for synchronous satellite measurements in seismological research N85-22447

SEISMOLOGY
Use of mobile surface station for synchronous satellite measurements in seismological research N85-22447
Geophysical laser interferometer with 12.5 meter base N85-23046
Crustal and upper mantle density model of Owen fault zone N85-23144
Observation of long-period oscillations of Earth N85-23149
Natural electromagnetic radiation in seismically active regions N85-23152
Determination of density of the crust and upper mantle from deep seismic sounding and gravimetry, 2 N85-23153
Geomagnetic precursors of intensive earthquakes in the 1-0.-2 Hz frequency range of geomagnetic pulsations N85-23178
Correcting depth line on nonlongitudinal seismic profile N85-23184
Method for processing broad-profile data N85-23185
Attenuation of seismic waves at regional distances [AD-A150198] N85-23267

SELECTORS
Gyrator frequency selectors with bandwidth independent of input signal level N85-23009

SELENOGRAPHY
Analysis of systematic errors in systems of selenodetic coordinates N85-22435

SELENOLOGY
A unified lunar control network N85-23669

SELF ADAPTIVE CONTROL SYSTEMS
Adaptive control of airborne radar antennas N85-22989

SEMANTICS
Precedency control and other semantic integrity issues in a workbench database N85-23220

SEMICONDUCTING FILMS
Non-linear optical techniques for visible and UV lasers and thin film deposition [AD-A150489] N85-23077

SEMICONDUCTOR DEVICES
Drift fields and boundary conditions at grain boundaries in bipolar P/N junction silicon devices N85-22879
Electrical overstress protection of submicron devices [AD-A150334] N85-22892
Measurement of internal thermal resistance for quality control of semiconductor devices N85-22953
Requirements placed on information processing equipment [BLL-CE-TRANS-7983-(9022.09)] N85-23307

SEMICONDUCTOR DIODES
SEM (Scanning Electron Microscope) investigation of silicon diodes using the electron beam induced current method [AD-A150356] N85-22894

SEMICONDUCTOR JUNCTIONS
Drift fields and boundary conditions at grain boundaries in bipolar P/N junction silicon devices N85-22879

SEMICONDUCTOR LASERS
Mode control and wavelength tuning in open ended Michelson interferometric semiconductor laser N85-23073

SEMICONDUCTOR PLASMAS
Demonstration of feasibility of depositing semiconductor layers using microwave enhanced plasma techniques [NASA-CR-174392] N85-23421
SEMICONDUCTORS (MATERIALS)
Clustering and ordering in 3-5 alloys [AD-A150604] N85-22670
Noise characteristics of sulfur-doped silicon diodes N85-22952
Numerical simulation of inverters with I2L elements including effects of high doping level N85-23039
Electronic transport in hydrogenated amorphous silicon films [DE85-002901] N85-23426
SENSITIVITY
Comprehensive mechanisms for combustion chemistry: An experimental and numerical study with emphasis on applied sensitivity analysis [DE85-000173] N85-22656
SENSORS
New atmospheric sensor analysis study [NASA-CR-171426] N85-23069
Technical Digest: Symposium on Optical Fiber measurements, 1984 [PB85-114700] N85-23407
SEPARATED FLOW
Annular groove in compressor casing as device for control of air stream N85-22832
SEQUENTIAL CONTROL
Asymptotically optimum multialternative sequential procedures for discernment of processes minimizing average length of observations N85-23012
SERIES (MATHEMATICS)
Effects of assuming independent component failure times, if they are actually dependent, in a series system [AD-A150582] N85-23092
An integral representation of the generalized Euler-Mascheroni constants [NASA-TP-2456] N85-23305
SERIES EXPANSION
Transient analysis of loaded thin-wire antennas and transmission lines N85-22852
SERVICE LIFE
Approach for service life extension of explosive devices for aircraft escape systems [NASA-TM-86323] N85-22381
Survival testing of silicon solar modules N85-22602
SERVICES
A comparison of metropolitan and non-metropolitan employment characteristics: Indications of the size of non-metropolitan mobile communication services user classes [NASA-CR-175648] N85-22855
SET THEORY
Optimal designs for comparisons between two sets of treatments [AD-A150621] N85-23360
SHAPES
A description of the Langley wireframe geometry standard (LaWGS) format [NASA-TM-85767] N85-22380
Shape optimization for minimal stress concentration N85-23093
Surfaces of asteroids and cometary nuclei N85-23503
SHEAR FLOW
Acoustic energy exchange in sheared mean flows --- solid rocket motors N85-22534
SHEAR LAYERS
Variations in resistivity of upper crustal layer N85-23164
SHEAR STRESS
Influence of external electric field on structural-mechanical properties of powdered materials N85-22630
Longitudinal splitting in unidirectional composites, analysis and experiments [NASA-CR-3681] N85-22639
SHELLS (STRUCTURAL FORMS)
USSR report: Engineering and equipment [JPRS-UEQ-85-003] N85-22782
Stability of three-layer glass-reinforced plastic shells of rotation N85-22813
Axisymmetrical oscillations of shell systems subjected to impulse loads N85-22814
SHIPS
INMARSAT marine satellite organization N85-22456
Uses of composite materials N85-22698
SHOCK LOADS
Molecular dynamics studies of energy transfer processes in crystal systems [AD-A150161] N85-23416
SHOCK RESISTANCE
Prediction of the resistance of structural materials to cavitation erosion [BLL-DRIC-TRANS-7435-(3623.66)] N85-22659
Dispersed-metal-toughened alumina [NASA-CR-174687] N85-22758
SHOCK TUBES
Turbulence measurements in shock induced flows N85-23055
SHOCK WAVE CONTROL
Selection of air intake parameters for supersonic-flow operation N85-22837
SHOCK WAVE GENERATORS
Flow-induced vibrations of a circular cylinder due to turbulent internal flows [DE85-002766] N85-23110
Shock compression of liquid helium to 56 GPa (560) kbar N85-23551
SHOCK WAVE INTERACTION
Study of geological media based on scattered earthquake waves N85-23168
SHOCK WAVE PROPAGATION
Interplanetary shock waves during April and May of 1981 N85-22434
SHOCK WAVES
Aerodynamic heating rate distributions induced by trailing edge controls on hypersonic aircraft configurations at Mach 8 [NASA-TM-87453] N85-22370
Ignition of mixtures of SiH sub 4, CH sub 4, O sub 2, and Ar or N sub 2 behind reflected shock waves [NASA-TP-2415] N85-22395
Effect of transparent coatings on generation of laser-induced shock waves in metals N85-22711
Space and time distribtuion of aftershocks N85-23157
Study of geological media based on scattered earthquake waves N85-23168
Physics of the inner heliosphere: Mechanisms, models and observational signatures [NASA-CR-175632] N85-23677
SHORT CIRCUIT CURRENTS
New high-efficiency silicon solar cells [NASA-CR-175643] N85-23244
SIDE-LOOKING RADAR
Intra-eruption geologic map from an x-band radar image during the May 18, 1980 eruption of Mount St. Helens, Washington N85-23639
SIGNAL ANALYSIS
Performance of time-position discriminator of composite signal N85-22941
Synthesis of quasi-optimum two-level signal discriminator with level changing at unknown point N85-23010
Accuracy of approximation of Bayes estimates in presence of noninformative parameters N85-23015
SIGNAL DETECTION
Theory of optimum M-filtration of signals against background of correlated interference N85-22927
Effect of variance of photoreceiver frequency characteristics on characteristics of measuring instruments N85-22965
Asymptotically optimum multialternative sequential procedures for discernment of processes minimizing average length of observations N85-23012
Extraction of signals from background interference with unknown parameters in quantized sample N85-23013
Reception of signal with unknown amplitude and duration submerged in white noise N85-23016
Synthesis of quasi-optimum algorigthms for signal recognition against background of correlated noise employing discrete spectral transformations N85-23020
Probability of detection of pulsed signals employing zero-gating interference suppression N85-23021
Approximate rules for signal detection against background of Gaussian correlated interference N85-23027
Use of importance sampling to investigate signal detection systems by simulated method N85-23028
SIGNAL DETECTORS
Efficiency of multitarget signal detection by digital radar data processing devices N85-22991
Short-range radiotechnical point sensor N85-22996
Synthesis of quasi-optimum two-level signal discriminator with level changing at unknown point N85-23010
SIGNAL DISTORTION
Ionospheric distortions of digital signals with wideband modulation N85-22945
Simple detonation meter N85-22971
Nature of seismic images with amplitude and time fluctuations of recorded oscillations N85-23156
SIGNAL GENERATORS
Application of K176-series microcircuits N85-22973
Computing convolution of multifrequency signal employing truncated fast Fourier transform algorithms N85-23019
SIGNAL MIXING
Error probability during optimal noncoherent reception of binary signals in multibeam channel N85-22922
SIGNAL PROCESSING
Approaches and algorithms for robust signal processing N85-22878
Acousto-optically addressed Fourier transform matched filters [AD-A150298] N85-22689
Two-dimensional signal processing and storage and theory and applications of electromagnetic measurements [AD-A150590] N85-22899
USSR report: Electronics and electrical engineering [JPRS-UEE-85-002] N85-22907
Assessment of effectiveness of signal-code constructions in time division-multi-access satellite systems N85-22908
Processing of signals in experiments with scattering of short radio pulses by conducting sphere N85-22917
Dispersion of phase-shift keyed systems with fixed number of blocks N85-22928
Noise tolerance of digital demodulator for complex signal system employing binary quantization N85-22929
Combined processing method and matched filter for discrete composite frequency phase-shift keyed signal N85-22931
Space-time response characteristics of acoustooptic filter for compression of linearly frequency-modulated signal N85-22937
Dynamics of adaptive signal corrector N85-22940
Spectra of incidental interference resulting from nonlinear conversion of signals from transmitters N85-22950
Models of discontinous random fields N85-22983
Synthesis of optimum single-channel discrete signals and filters N85-22990
Synthesis of optimum algorithms for secondary processing N85-22992
Factorized algorithms for combined spatial and temporal processing of radar signals N85-22997
Electrothermal transducer with short time constant N85-23040
Acoustooptic demodulation of frequency-modulated signals N85-23050
Optical processing in radon space [AD-A150289] N85-23402
SIGNAL RECEPTION
Error probability during optimal noncoherent reception of binary signals in multibeam channel N85-22922
Regular synthesis of pairs of phase-keyed binary minimax signals N85-22923
Interference immunity of binary systems with second-order phase-difference modulation in various reception modes N85-22944
Reception of signal with unknown amplitude and duration submerged in white noise N85-23016
Reception noise immunity of multiposition signals N85-23023
SIGNAL REFLECTION
Parameters of amplitude-modulated signal upon reflections N85-22956
Axial focusing of signal from distant point radiator reflected twice in deep paraboloid N85-22979
SIGNAL TO NOISE RATIOS
Shuttle flight test of an advanced gamma-ray detection system [AD-A150316] N85-22469
Moving target detection N85-22915
Theory of optimum M-filtration of signals against background of correlated interference N85-22927
Performance of time-position discriminator of composite signal N85-22941
Effect of variance of photoreceiver frequency characteristics on characteristics of measuring instruments N85-22965
Accuracy of approximation of Bayes estimates in presence of noninformative parameters N85-23015
Reception of signal with unknown amplitude and duration submerged in white noise N85-23016
Synthesis of quasi-optimum algorigthms for signal recognition against background of correlated noise employing discrete spectral transformations N85-23020
Noise tolerance of diversity reception in frequency-adaptive digital transmission systems N85-23024
Algorithms for reconstruction of partially known, band limited Fourier transform pairs from noisy data [AD-A150194] N85-23347
SIGNAL TRANSMISSION
The use of a high-speed 12-bit A/D converter for digital sampling of communication signal carriers [AD-A150578] N85-22872
Analysis and design of linear microwave transistor amplifiers N85-23038
SILANES
Ignition of mixtures of SiH sub 4, CH sub 4, O sub 2, and Ar or N sub 2 behind reflected shock waves [NASA-TP-2415] N85-22395

SILICA GLASS
Emissivity enhancement of fused silica for space applications — solar cells N85-22615
SILICATES
A circum-terrestrial compositional filter N85-23520
Quenching effects on iron site partitioning in the Apollo 17 orange glass composition N85-23553
Experimental methds for quenching structures in lunar-analog silicate melts: Variations as a function of quench media and composition N85-23554
SILICON
Gallium arsenide arrays versus silicon arrays for space application N85-22574
Availability of AlGaAs/GaAs solar cells in space N85-22576
Technological process effect on the carrier lifetime degradation of silicon solar cell base layer irradiated by 1 MeV electrons (boron doping case) N85-22585
The effects of lithium counterdoping on radiation damage and annealing in n(+)p silicon solar cells N85-22586
Study of processes of modification of Al-Si alloys N85-22695
Segregation of silicon in silumin-carbon fiber composites N85-22706
Time-resolved studies of rapid solidification in highly undercooled molten silicon
[DE85-004857] N85-22765
Drift fields and boundary conditions at grain boundaries in bipolar P/N junction silicon devices N85-22879
SEM (Scanning Electron Microscope) investigation of silicon diodes using the electron beam induced current method
[AD-A150356] N85-22894
High sheet resistance, arsenic implanted polycrystalline silicon for integrated circuit resistors
[DE85-004355] N85-22902
Noise characteristics of sulfur-doped silicon diodes N85-22952
Thermodynamic and kinetic studies of pulsed laser annealing from transient conductivity measurements
[DE85-003677] N85-23078
Time-resolved ellipsometry and reflectivity measurements of the optical properties of silicon during pulsed excimer laser irradiation
[DE85-005091] N85-23079
Time-resolved reflectivity measurement of extrinsic silicon during pulsed laser irradiation
[AD-A150350] N85-23403
Transport properties of silica thermally grown on silicon
[AD-A150304] N85-23418
Demonstration of feasibility of depositing semiconductor layers using microwave enhanced plasma techniques
[NASA-CR-174392] N85-23421
Electronic transport in hydrogenated amorphous silicon films
[DE85-002901] N85-23426
Influence of substrate heating and thermal annealing on the surface crystallinity in single Si crystals implanted with high doses of (16)O
[DE85-005264] N85-23428
SILICON CARBIDES
Particulate toughened silicon carbide
[DE85-004797] N85-22643
SILICON DIOXIDE
Transport properties of silica thermally grown on silicon
[AD-A150304] N85-23418
A silicic shield volcano in Bolivia N85-23572
SILICON NITRIDES
Degassification of silicon nitride powders of various origins N85-22718
SILICON POLYMERS
EOS (electrical overstress) protection for VLSI (Very Large Scale Integration) devices
[AD-A150333] N85-22891
SILVER
EXAFS of monolayers on silver electrodes: SSRL proposal number 717M
[AD-A150623] N85-22652
SIMULATION
Air combat simulation: Methods, models, trends N85-22359
Microwave blackbodies for spaceborne receivers
[NASA-CR-175647] N85-23066
Markov method for simulating non-Gaussian wind speed time series
[DE85-003450] N85-23284
SINGLE CRYSTALS
Orientation and temperature dependence of some mechanical properties of the single-crystal nickel-base superalloy Rene N4. 3: Tension-compression anisotropy
[NASA-TM-86862] N85-22660
Basis and pyramidal slipping in single crystals of alpha-alloy Ti-Al-Sn N85-22730
Fracture mechanics evaluation of GaAs
[NASA-CR-175657] N85-23101
Influence of substrate heating and thermal annealing on the surface crystallinity in single Si crystals implanted with high doses of (16)O
[DE85-005264] N85-23428
SINGLE SIDEBAND TRANSMISSION
Study of phase radiogeodetic systems with phase-locked loops N85-23172
SINGULARITY (MATHEMATICS)
Transient analysis of loaded thin-wire antennas and transmission lines N85-22852
SINKS
Evolution of set of Rossby waves toward anisotropic equilibrium state N85-23141
SINTERING
Development of a sintered shim
[DE85-006183] N85-22685
Densification and deformation in the presence of a liquid phase
[DE85-005101] N85-22763
SITE SELECTION
Optimum path selection in automated radio relay link design N85-22947
SITES
Adsorption site, adsorption energy and normal vibration frequency of H/Ni(100) via total energy calculations
[AD-A150555] N85-23388
SIZE DETERMINATION
Recent trends in particle size analysis techniques
[NASA-TM-77735] N85-22645
SIZE DISTRIBUTION
Asteroid collisional evolution studies N85-23501
SIZING (SURFACE TREATMENT)
The application of anthropometric survey data to aircrew clothing sizing
[AD-A150545] N85-23304
SKEWNESS
Skewed stable variables and processes
[AD-A150549] N85-23372
SLEEP DEPRIVATION
Sleep deprivation and exercise tolerance
[AD-A150180] N85-23295
Sleep deprivation and exercise tolerance
[AD-A150566] N85-23296
Sleep deprivation and exercise tolerance
[AD-A150826] N85-23297
SLIDING FRICTION
Sliding seal materials for adiabatic engines
[NASA-CR-174893] N85-22757
SLOPES
Relationship between brightness spectrum of photographic image and spectrum of rises on a water surface with waves N85-23171
A statistical treatment of the regional slope characteristics of Venus and Earth N85-23517
Lithologic and structural control on slope morphology in the Valles Marineris N85-23651
SLURRIES
Gasification of boron oxide drops and boron slurry agglomerates in combustion gases N85-22529
SMOOTHING
Consistency of smoothing with running linear fits
[AD-A150232] N85-23349
SNOW
Snow reflectance from Thematic Mapper N85-23205
Remote Sensing of Snow and Evapotranspiration
[NASA-CP-2363] N85-23223
General report of the researches of snowpack properties, snowmelt runoff and evapotranspiration in Japan N85-23225
Snowmelt-runoff model utilizing remotely-sensed data N85-23226
Snowmelt runoff model in Japan N85-23227
Studies on physical properties of snow based on multi channel microwave radiometer N85-23231
Radiation-dominated snowmelt on Mars N85-23592
SNOW COVER
Application of Martinec-Rango model to river basin in Japan N85-23228
Distribution of snow and maximum snow water equivalent obtained by LANDSAT data and degree day method N85-23229
Microwave radiometer observations of snowpack properties and comparison of U.S. Japanese results — Hokkaido, Japan and Vermont and North Dakota test sites N85-23230
Analysis of NIMBUS-7 SMMR data — Hokkaido, Japan snow cover N85-23232
Estimation of regional evapotranspiration using remotely sensed land surface temperature. Part 2: Application of equilibrium evaporation model to estimate evapotranspiration by remote sensing technique — Japan N85-23234
SOCIAL FACTORS
Aeronautical Engineering: A continuing bibliography with indexes, supplement 185
[NASA-SP-7037(185)] N85-22342
SODAR
Radioacoustic sounding system for remote synchronous measurements of wind speed, temperature and its fluctuations N85-23145
SODIUM
Study of processes of modification of Al-Si alloys N85-22695
SODIUM ISOTOPES
Cosmogenic Na-22 and Al-26 in Luna-24 lunar drill core soil samples N85-22427
SOFTENING
Softening of metal near seam during welding of heat-resistant nickel alloys N85-22747
SOFTWARE ENGINEERING
Validation summary report, Burroughs Corporation, B20 FORTRAN release 4.0
[PB84-227792] N85-23316
Principles of software engineering environment design
[AD-A150352] N85-23324
Measurement of SIFT operating system overhead
[NASA-TM-86322] N85-23337
SOFTWARE TOOLS
Microcomputers and the electrical engineer
[AD-A150499] N85-23325
SOIL MAPPING
Preliminary evaluation of TM for soils information N85-23206
SOIL MOISTURE
Estimation of regional evapotranspiration using remotely sensed land surface temperature. Part 1: Measurement of evapotranspiration at the Environmental Research Center and determination of Priestley-Taylor parameter N85-23233
Microwave remote sensing of soil moisture N85-23235
Testing an energy balance model for estimating actual evapotranspiration using remotely sensed data — Hannover, West Germany barley and wheat fields N85-23236
A method for estimating soil moisture availability
[NASA-CR-175606] N85-23238
SOILS
Characterization of LANDSAT-4 TM and MSS image quality for the interpretation of California's agricultural resources — Central Valley N85-23190
Preliminary comparisons of the information content and utility of TM versus MSS data N85-23202
Calculations of microwave brightness temperature of rough soil surfaces: Bare field
[NASA-TM-86200] N85-23221
Areas with forest soils sensitive to acidic deposition under alternative damage hypotheses
[DE85-005257] N85-23257
Chemical weathering of soils from the dry valleys of Antarctica: A terrestrial analog of Martian weathering processes N85-23528
SOLAR ACTIVITY
Auroral-polar cap environment and its impact on spacecraft plasma interactions N85-22484
SOLAR ACTIVITY EFFECTS
Interplanetary shock waves during April and May of 1981 N85-22434
SOLAR ARRAYS
Interactions between large space power systems and low-Earth-orbit plasmas N85-22490
The PIX-2 experiment: An overview N85-22494
Plasma interaction experiment 2 (PIX 2): Laboratory and flight results N85-22495
Discharges on a negatively biased solar cell array in a charged-particle environment N85-22499
Space test program of high-voltage solar array-space plasma interactions N85-22519
Photovoltaic Generators in Space — conference
[ESA-SP-210] N85-22585
Thin and ultrathin silicon solar cells for space use N85-22587
Space solar cells: Adjusting to new demands N85-22588
Bifacial light sensitive space solar cell N85-22573
Gallium arsenide arrays versus silicon arrays for space application N85-22574
Availability of AlGaAs/GaAs solar cells in space N85-22576
Comparative study of GaAs solar cell potentialities for space applications N85-22577
Investigation of high output gallium arsenide solar cells N85-22578
Development of very thin large area GaAs solar cells for space application N85-22579
GaAs and 3-5 compound solar cells status and prospects for use in space N85-22580

Development and testing of a spacecraft surface potential monitor N85-22582
Electrostatic discharge testing on a carbon fiber solar panel structure N85-22584
In-orbit laser regeneration of the radiation damaged solar arrays N85-22588
Giotto solar array: Design, manufacture and test N85-22589
The DFS-Kopernikus solar generator electrical design N85-22590
The DFS-Kopernikus solar generator N85-22591
Electrical design of the Intelsat 6 solar generator N85-22592
Computer aided engineering applied to the design and verification of the generic Advanced Rigid Array (ARA) — solar array N85-22593
Development and qualification of the electrical part of the Advanced Rigid Array (ARA) — solar array N85-22594
SPOT solar array N85-22595
Rigid Solar Generator (GSR) solar arrays N85-22596
Retractable Rigid Solar Generator (GSR) N85-22597
Derivation of the Olympus solar array requirements N85-22598
The Olympus solar array development and test program N85-22599
The performance of the Olympus power subsystem with its solar array N85-22601
Survival testing of silicon solar modules N85-22602
Analysis of optimum front cover thickness for lightweight solar arrays N85-22606
Problems with electrical interference between solar generators and shunt type regulators N85-22607
Development of Halley's Comet explorer PLANET-A solar array N85-22608
Concentrator technologies evaluation for large solar arrays and their application for space stations/platforms N85-22609
Space Station solar array N85-22610
Solar array dynamical simulation for illumination and temperature variation N85-22611
Aspects of low cost module technology — spacecraft solar arrays N85-22614
Deployment analysis of the Olympus Astromast and comparison with test measurements — solar arrays N85-22616
NASA photovoltaic research and technology development program for space applications N85-22617
Study of concentration for space photovoltaic generators N85-22618
Developments in deployable masts to support flexible solar arrays N85-22620
Generic design and verification of an Advanced Rigid Array (ARA) — solar array N85-22621
Growth capabilities of European retractable solar arrays N85-22625

SOLAR ATMOSPHERE
Ultraviolet spectral diagnostics of solar flares and heating events N85-23675

SOLAR BLANKETS
Design and qualification testing of the Olympus solar array blanket N85-22600
Blanket integrated cushioning of foldable and retractable solar arrays N85-22612
Concept for controlled fold by fold deployment and retraction of flexible, foldable solar generators N85-22613
The Olympus solar array structure and mechanisms N85-22623

SOLAR CELLS
An investigation of arc discharging on negatively biased dielectric conductor samples in a plasma N85-22498
Discharges on a negatively biased solar cell array in a charged-particle environment N85-22499
Photovoltaic Generators in Space — conferences [ESA-SP-210] N85-22565
History and future views on solar cells of Japanese scientific satellites N85-22566
Thin and ultrathin silicon solar cells for space use N85-22567
Space solar cells: Adjusting to new demands N85-22568
The high voltage silicon cell: A comparative analysis N85-22569
A 2 x 6 Back Surface Reflection (BSR) silicon solar cell N85-22570
Experiences with implanted Back Surface Field (BSF) solar cells N85-22571
A low cost approach with larger diameter silicon wafer — solar cells N85-22572
Bifacial light sensitive space solar cell N85-22573
Gallium arsenide arrays versus silicon arrays for space application N85-22574
Space qualified AlGaAs/GaAs solar cells N85-22575
Availability of AlGaAs/GaAs solar cells in space N85-22576
Development of very thin large area GaAs solar cells for space application N85-22579
GaAlAs-GaAs solar cell development: Prospective for space applications under concentration N85-22581
Phenomenology of discharges in space: Application to a solar generator — SPOT satellite N85-22583
Technological process effect on the carrier lifetime degradation of silicon solar cell base layer irradiated by 1 MeV electrons (boron doping case) N85-22585
The effects of lithium counterdoping on radiation damage and annealing in n(+)p silicon solar cells N85-22586
Investigation of the degradation of GaAs photovoltaic cells by proton and electron irradiation N85-22587
The DFS-Kopernikus solar generator electrical design N85-22590
The DFS-Kopernikus solar generator N85-22591
Electrical design of the Intelsat 6 solar generator N85-22592
Development and qualification of the electrical part of the Advanced Rigid Array (ARA) — solar array N85-22594
Survival testing of silicon solar modules N85-22602
Calibration of solar cells outside the atmosphere N85-22603
Inverse behavior of silicon photovoltaic cells N85-22604
Nonlinearity and spectral mismatch problems of solar cells N85-22605
Emissivity enhancement of fused silica for space applications — solar cells N85-22615
NASA photovoltaic research and technology development program for space applications N85-22617
Improved modeling of the open circuit voltage of solar cells N85-22619
Isotropic proton irradiation of GaAs solar cells N85-22622
Annealing of radiation damage in boron and gallium doped silicon solar cells N85-22624
Fracture mechanics evaluation of GaAs [NASA-CR-175657] N85-23101
New high-efficiency silicon solar cells [NASA-CR-175643] N85-23244
Demonstration of feasibility of depositing semiconductor layers using microwave enhanced plasma techniques [NASA-CR-174392] N85-23421

SOLAR COLLECTORS
ROSA: A computer model for optical power ratio calculations [DE85-005174] N85-23251

SOLAR COOLING
Development of a single-family absorption chiller for use in a solar heating and cooling system, phase 3, volume 2 [DE85-003218] N85-23253

SOLAR CORONA
A normal incidence, high resolution X-ray telescope for solar coronal observations [NASA-CR-175622] N85-23461
Orbital resonances and planetary accretion in the solar nebula N85-23523
Evolution of grains in a turbulent solar nebula N85-23525
Research on the early history of the solar system N85-23527
Physics of the inner heliosphere: Mechanisms, models and observational signatures [NASA-CR-175632] N85-23677

SOLAR ENERGY
ROSA: A computer model for optical power ratio calculations [DE85-005174] N85-23251

SOLAR ENERGY ABSORBERS
Development of a single-family absorption chiller for use in a solar heating and cooling system, phase 3, volume 2 [DE85-003218] N85-23253

SOLAR ENERGY CONVERSION
A theoretical analysis of solar-driven natural convection energy conversion systems [DE84-004431] N85-23245

SOLAR FLARES
Ultraviolet spectral diagnostics of solar flares and heating events N85-23675
Solar-geophysical data number 479, August 1981. Part 2: (Comprehensive reports), data for January 1984 and August 1981 and miscellanea. Explanation of data reports issued as number 474 (supplement) February 1984 [NASA-CR-175607] N85-23679

SOLAR FLUX
Response of Earth's atmosphere to increases in solar flux and implications for loss of water from Venus N85-23518

SOLAR HEATING
Overview of latent storage for passive solar applications [DE85-005354] N85-23249
Development of a single-family absorption chiller for use in a solar heating and cooling system, phase 3, volume 2 [DE85-003218] N85-23253

SOLAR MAXIMUM MISSION
Ultraviolet spectral diagnostics of solar flares and heating events N85-23675

SOLAR OBSERVATORIES
A normal incidence, high resolution X-ray telescope for solar coronal observations [NASA-CR-175622] N85-23461

SOLAR ORBITS
Models of angular momentum input to a circum-terrestrial swarm from encounters with heliocentric planetesimals N85-23521

SOLAR OSCILLATIONS
Constraints of observations of solar oscillations on solar models with mixing by turbulent diffusion [DE85-003741] N85-23678

SOLAR PLANETARY INTERACTIONS
Response of Earth's atmosphere to increases in solar flux and implications for loss of water from Venus N85-23518

SOLAR POWER SATELLITES
Argon ion pollution of the magnetosphere N85-22523

SOLAR RADIO BURSTS
Solar-geophysical data number 479, August 1981. Part 2: (Comprehensive reports), data for January 1984 and August 1981 and miscellanea. Explanation of data reports issued as number 474 (supplement) February 1984 [NASA-CR-175607] N85-23679

SOLAR SIMULATION
Isotropic proton irradiation of GaAs solar cells N85-22622

SOLAR SYSTEM
Planetary geology in the 1980s [NASA-SP-467] N85-23457
Viking radio science data analysis and synthesis [NASA-CR-175631] N85-23471
On the origin of Triton and Pluto N85-23497
Small solar system bodies N85-23499
Asteroid collisional evolution studies N85-23501
Impacts in ice: Commissions of solar system crater population N85-23538

SOLAR TERRESTRIAL INTERACTIONS
Interplanetary shock waves during April and May of 1981 N85-22434
World ocean level oscillations and their relationship to change in inflow of continental waters N85-23133

SOLAR WIND
Plans for Interbol satellite experiment N85-22407
Correlation of interplanetary medium parameters in transition region of high-velocity solar wind streams N85-22412
Polar plasmas as observed by Dynamics Explorers 1 and 2 N85-22483
Physics of the inner heliosphere: Mechanisms, models and observational signatures [NASA-CR-175632] N85-23677

SOLAR WIND VELOCITY
Correlation of interplanetary medium parameters in transition region of high-velocity solar wind streams N85-22412

SOLAR X-RAYS
Solar and stellar coronal plasmas [NASA-CR-175623] N85-23676
Solar-geophysical data number 479, August 1981. Part 2: (Comprehensive reports), data for January 1984 and August 1981 and miscellanea. Explanation of data reports issued as number 474 (supplement) February 1984 [NASA-CR-175607] N85-23679

SOLID PHASES
Effect of variable solid phase thermal properties on propellant combustion N85-22547

SOLID PROPELLANT COMBUSTION
Solid propellant combustion diagnostics and automated data retrieval from holograms N85-22527
Combustion of zirconium carbide N85-22532
Coupling between velocity oscillations and solid propellant combustion N85-22536
Mechanism of burning rate enhancement by ferric oxide N85-22546
Effect of variable solid phase thermal properties on propellant combustion N85-22547
Multiple reflection theory for microwave measurement of solid propellant burning rates N85-22549
In-situ burning rate determination using flash radiography N85-22550
Molecular dynamics of propellant gases, part 2 N85-22552

SOLID PROPELLANT ROCKET ENGINES
Nonlinear interactions between vortices and acoustic waves in a rocket combustion chamber N85-22533
Acoustic energy exchange in sheared mean flows — solid rocket motors N85-22534
Investigations of reactive and non reactive acoustic boundary layers in porous walled ducts N85-22535
Comparisons of solid propellant with instability predictions and motor firing experience N85-22541
Internal fluid mechanism of solid propellant rocket motors N85-22544
Characterization standards for solid propellant rocket motors
[AD-A150250] N85-22627
SOLID PROPELLANTS
Application of fluorescence to measurement of surface temperature in solid propellants N85-22548
The crystal and molecular structure of a new propellant compound: Triaminoguanidium Azide Nitrate (TAZN) N85-22551
SOLID ROCKET PROPELLANTS
Investigation of the characteristics of the velocity-coupled response functions of solid propellants N85-22540
Comparisons of solid propellant with instability predictions and motor firing experience N85-22541
Distributed combustion: A mechanism of acoustic suppression N85-22543
Chemical kinetics of gas phase decomposition products of nitramine propellants N85-22558
SOLID STATE DEVICES
Research in the optical sciences
[AD-A150196] N85-23401
SOLID STATE LASERS
Low jitter trigger for an excimer laser
[DE85-005732] N85-23080
Research progress on laser crystals in China N85-23440
SOLID-SOLID INTERFACES
Segregation of silicon in silumin-carbon fiber composites N85-22706
SOLIDIFICATION
Rapid solidification processing of magnesium alloys
[AD-A150270] N85-22668
Time-resolved studies of rapid solidification in highly undercooled molten silicon
[DE85-004857] N85-22765
SOLIDS
Division boundary in Al-B composite material with boron in contact with solid and liquid aluminum N85-22704
USSR report: Engineering and equipment
[JPRS-UEQ-85-003] N85-22782
SOOT
Laser diagnostic analyses of sooting flames
[AD-A150478] N85-22649
A standard aircraft diffusion flame: Spectral characteristics and a feasibility study for developing an alternate calibration source for aircraft optical fire detection systems
[AD-A150231] N85-22768
SORPTION
Drifting ice as mechanical factor in purifying and polluting hydrosphere N85-23132
SOUND FIELDS
The effects of internal waves on acoustic normal modes
[AD-A150235] N85-23379
SOUND INTENSITY
Research on the effect of noise at different times of day: Models, methods and findings
[NASA-CR-3888] N85-23375
High-frequency acoustic variability in the arctic
[AD-A150550] N85-23383
SOUND PRESSURE
Wind tunnel acoustic study of a propeller installed behind an airplane empennage: Data report
[NASA-CR-177335] N85-23377
SOUND PROPAGATION
Intensity vectors of sound scattering by a spherical shell
[AD-A147847] N85-23107
SOUND RANGING
High-frequency acoustic variability in the arctic
[AD-A150550] N85-23383
SOUND TRANSDUCERS
Analysis and optimization of parameters of fanned surface acoustic wave transducers N85-22934
SOUND TRANSMISSION
Simple detonation meter N85-22971
Ice statistics and acoustic scattering in the Arctic basin
[AD-A150141] N85-23269
SOUND WAVES
Nonlinear interactions between vortices and acoustic waves in a rocket combustion chamber N85-22533
Generation of longitudinal acoustic waves by modulated helicon waves — nonlinear steady state waves in metals N85-23049
Intensity vectors of sound scattering by a spherical shell
[AD-A147847] N85-23107
Numerical results of acoustic radiation, transmission and reflection of steel plate in water
[AMTE(N)-TM-84037] N85-23378
Properties of materials using acoustic waves
[AD-A150465] N85-23382
SOUNDING
Mathematical modeling of two-frequency laser sounding of scattering media N85-23045
Induction excitation of deep conducting zones N85-23154
Study of resolution of deep MT soundings by means of physical model N85-23155
Primary processing of experimental magnetovariation sounding data using spline functions N85-23175
SOUTH AMERICA
El Nino, the capricious child N85-23121
SOVIET SPACECRAFT
List of recent Soviet space launches N85-22457
SOYUZ SPACECRAFT
Feoktistov says manned lunar, Mars flights lack justification N85-22452
SPACE CHARGE
Discharge pulse phenomenology N85-22509
Effect of space-charge field on output characteristics of O-type oscillators with distributed interaction N85-23043
SPACE COLONIES
Feoktistov discusses need for space colonization N85-22454
SPACE ENVIRONMENT SIMULATION
Giotto solar array: Design, manufacture and test N85-22589
Survival testing of silicon solar modules N85-22602
SPACE EXPLORATION
Activities of the Jet Propulsion Laboratory, 1 January - 31 December 1983
[NASA-CR-175555] N85-23447
Planetary geology in the 1980s
[NASA-SP-467] N85-23457
SPACE HEATING (BUILDINGS)
Overview of latent storage for passive solar applications
[DE85-005354] N85-23249
SPACE MAINTENANCE
In-orbit laser regeneration of the radiation damaged solar arrays N85-22588
SPACE MISSIONS
D-1 report: The first German spacelab mission
[NASA-TM-77637] N85-22402
SPACE PLASMAS
Hydromagnetic precursors of interplanetary plasma burst N85-22414
One-dimensional model of auroral magnetic force with longitudinal current and cyclotron heating of ions N85-22424
Interplanetary shock waves during April and May of 1981 N85-22434
Spacecraft-environment interaction: The environmental plasma aspect N85-22479
Direct measurements of severe spacecraft charging in auroral ionosphere N85-22480
Polar plasmas as observed by Dynamics Explorers 1 and 2 N85-22483
Auroral-polar cap environment and its impact on spacecraft plasma interactions N85-22484
Three-dimensional calculation of shuttle charging in polar orbit N85-22486
Interactions between large space power systems and low-Earth-orbit plasmas N85-22490
Self-consistent simulation of plasma interactions with secondary-emitting insulators N85-22492
Surface interactions and high-voltage current collection N85-22493
The PIX-2 experiment: An overview N85-22494
Plasma interaction experiment 2 (PIX 2): Laboratory and flight results N85-22495
Ram-wake effects on plasma current collection of the PIX 2 Langmuir probe N85-22496
NASCAP simulation of PIX 2 experiments N85-22497
An investigation of arc discharging on negatively biased dielectric conductor samples in a plasma N85-22498
Space test program of high-voltage solar array-space plasma interactions N85-22519
Preliminary investigation of the electrodynamics of a conducting tether N85-22521
Exitation of low-frequency resonance waves by moving conductor in space plasma N85-22912
SPACE SHUTTLE MAIN ENGINE
Nonlinear rotordynamics analysis
[NASA-CR-171425] N85-22364
High-pressure rocket engine turnaround duct computational fluid dynamics analysis N85-22556
HPFTP flow diverter analysis
[NASA-CR-171424] N85-23057
SPACE SHUTTLE ORBITERS
Aerospace Safety Advisory Panel
[NASA-TM-87426] N85-22373
Results of a M = 5.3 heat transfer test of the integrated vehicle using phase-change paint techniques on the 0.0175-scale model 56-OTS in the NASA/Ames Research Center 3.5-foot hypersonic wind tunnel
[NASA-CR-167695] N85-22488
Wakes and differential charging of large bodies in low Earth orbit N85-22488
SPACE SHUTTLE PAYLOADS
Report on final recommendations for IMPS engineering-science payload
[NASA-CR-175659] N85-22464
Suprathermal plasma observed on STS-3 Mission by plasma diagnostics package N85-22472
Electron and ion density depletions measured in the STS-3 orbiter wake N85-22474
Shuttle electrical environment N85-22475
Interactions measurement payload for Shuttle N85-22518
Electrostatic forming and testing of polymer films on a 16-foot diameter test fixture
[NASA-TM-86328] N85-22885
SPACE SHUTTLES
Ground and flight testing for aircraft guidance and control
[AGARD-AG-262] N85-22350
Feoktistov argues against U.S. space shuttle design concept N85-22453
Selected tether applications in space: Phase 2. Executive summary
[NASA-CR-171421] N85-22462
Selected tether applications in space: Phase 2
[NASA-CR-171422] N85-22463
Vibroacoustic study of the NASA Goddard Space Flight Center OSS-1 payload
[NASA-CR-175320] N85-22465
Results of aeroheating DFI and ET design-data test on a 0.0175-scale model 60-OTS conducted in the Von Karman Gas Dynamics Facility (VKF) 40° supersonic and the 50° hypersonic wind tunnels A and C
[NASA-CR-167693] N85-22466
Spacecraft Environmental Interactions Technology, 1983
[NASA-CP-2359] N85-22470
Space Station technology planning N85-22471
Vehicle charging on STS-3 Mission N85-22473
Measured electron contribution to Shuttle plasma environment: Abbreviated update N85-22476
Laboratory studies of Kapton degradation in an oxygen ion beam N85-22477
Electron beam charging of Space Shuttle thermal protection system tiles N85-22478
Interactions measurement payload for Shuttle N85-22518
Preliminary investigation of the electrodynamics of a conducting tether N85-22521
Astronaut hazard during free-flight polar EVA N85-22522
Research opportunities in human behavior and performances
[NASA-CR-3886] N85-23299
SPACE STATIONS
Aerospace Safety Advisory Panel
[NASA-TM-87426] N85-22373
Feoktistov argues against U.S. space shuttle design concept N85-22453
Space station systems technology study (add-on task). Volume 1: Executive summary
[NASA-CR-171415] N85-22459
Advancing automation and robotics technology for the Space Station and for the US economy. Volume 1: Executive overview
[NASA-TM-87566-VOL-1] N85-22460
Advancing automation and robotics technology for the Space Station and for the US economy, volume 2
[NASA-TM-87566-VOL-2] N85-22461
Selected tether applications in space: Phase 2. Executive summary
[NASA-CR-171421] N85-22462
Selected tether applications in space: Phase 2
[NASA-CR-171422] N85-22463
Space Station technology planning N85-22471
Space test program of high-voltage solar array-space plasma interactions N85-22519
Research opportunities in humin behavior and performances
[NASA-CR-3886] N85-23299
SPACE TRANSPORTATION SYSTEM
Aerospace Safety Advisory Panel
[NASA-TM-87426] N85-22373

SPACE TRANSPORTATION SYSTEM 4 FLIGHT
Shuttle electrical environment N85-22475
SPACEBORNE EXPERIMENTS
Lyakhov and Aleksandrov on 150-day flight N85-22405
Comments on Salyut-7 150-day flight N85-22406
SPACEBORNE PHOTOGRAPHY
Lyakhov and Aleksandrov on 150-day flight N85-22405
Experience in automated interpretation of aerospace photographs N85-22444
Geoindication method for interpreting aerial and space photographs: Status and prospects N85-22445
Experience in combined special mapping using space information N85-22449
SPACECRAFT CHARGING
Rocket body charge neutralization processes in ARAKS experiment (data from two launches) N85-22426
Spacecraft Environmental Interactions Technology, 1983 [NASA-CP-2359] N85-22470
Vehicle charging on STS-3 Mission N85-22473
Electron and ion density depletions measured in the STS-3 orbiter wake N85-22474
Shuttle electrical environment N85-22475
Measured electron contribution to Shuttle plasma environment: Abbreviated update N85-22476
Laboratory studies of Kapton degradation in an oxygen ion beam N85-22477
Electron beam charging of Space Shuttle thermal protection system tiles N85-22478
Charging of DMSP/F6 spacecraft in aurora on 10 January 1983 N85-22481
Average and worst-case specifications of precipitating auroral electron environment N85-22482
Auroral-polar cap environment and its impact on spacecraft plasma interactions N85-22484
Electric field effects on ion currents in satellite wakes N85-22485
Three-dimensional calculation of shuttle charging in polar orbit N85-22486
Polar orbit electrostatic charging of objects in shuttle wake N85-22487
Wakes and differential charging of large bodies in low Earth orbit N85-22488
Sheath ionization model of beam emissions from large spacecraft N85-22489
Interactions between large space power systems and low-Earth-orbit plasmas N85-22490
Calculation of secondary-electron escape currents from inclined-spacecraft surfaces in a magnetic field N85-22491
Self-consistent simulation of plasma interactions with secondary-emitting insulators N85-22492
Surface interactions and high-voltage current collection N85-22493
The PIX-2 experiment: An overview N85-22494
Plasma interaction experiment 2 (PIX 2): Laboratory and flight results N85-22495
Design guidelines for assessing and controlling spacecraft charging effects N85-22500
Aerospace spacecraft-charging guidelines document N85-22501
EMI characteristics of a potential control system N85-22502
Anomalously high potentials observed on ISEE N85-22503
Characteristics of EMI generated by negative metal-positive dielectric voltage stresses due to spacecraft charging N85-22505
Laboratory studies of spacecraft response to transient discharge pulses N85-22506
Development of a continuous broad-energy-spectrum electron source N85-22507
Automatic charge control system for satellites N85-22508
Discharge pulse phenomenology N85-22509
Discharge characteristics of dielectric materials examined in mono-, dual-, and spectral energy electron charging environments N85-22510
Electron yields from spacecraft materials N85-22512
Electrical conduction in polymer dielectrics N85-22514
Spacecraft environmental interactions: A joint Air Force and NASA research and technology program N85-22517
Interactions measurement payload for Shuttle N85-22518
Astronaut hazard during free-flight polar EVA N85-22522
Development and testing of a spacecraft surface potential monitor N85-22582
Phenomenology of discharges in space: Application to a solar generator — SPOT satellite N85-22583
Electrostatic discharge testing on a carbon fiber solar panel structure N85-22584
SPACECRAFT COMMUNICATION
Ionospheric distortions of digital signals with wideband modulation N85-22945
SPACECRAFT CONTAMINATION
Minimizing plume contamination production in bipropellant thrusters N85-22557
SPACECRAFT DESIGN
Feoktistov recalls period leading to Gagarin spaceflight N85-22451
Feoktistov argues against U.S. space shuttle design concept N85-22453
Feoktistov discusses need for space colonization N85-22454
Report on final recommendations for IMPS engineering-science payload [NASA-CR-175659] N85-22464
Design guidelines for assessing and controlling spacecraft charging effects N85-22500
Uses of composite materials N85-22698
SPACECRAFT ENVIRONMENTS
Vibroacoustic study of the NASA Goddard Space Flight Center OSS-1 payload [NASA-CR-175320] N85-22465
SPACECRAFT EQUIPMENT
Automated extraction of absorption bands from reflectance special N85-23624
SPACECRAFT INSTRUMENTS
Microwave blackbodies for spaceborne receivers [NASA-CR-175647] N85-23068
Optical system [NASA-CASE-NPO-15801-1] N85-23396
SPACECRAFT LANDING
Feoktistov recalls period leading to Gagarin spaceflight N85-22451
Small solar system bodies N85-23499
SPACECRAFT LAUNCHING
Increase in hydrogen emission of upper atmosphere following launches of space vehicles N85-22431
Feoktistov argues against U.S. space shuttle design concept N85-22453
List of recent Soviet space launches N85-22457
China report: Science and technology [JPRS-CST-84-030] N85-22777
SPACECRAFT ORBITS
Models of angular momentum input to a circum-terrestrial swarm from encounters with heliocentric planetesimals N85-23521
Orbital resonances and planetary accretion in the solar nebula N85-23523
SPACECRAFT POSITION INDICATORS
Operational experience with ion concentration sensors in orientation systems N85-22422
SPACECRAFT POWER SUPPLIES
Interactions between large space power systems and low-Earth-orbit plasmas N85-22490
Photovoltaic Generators in Space — conferences [ESA-SP-210] N85-22565
History and future views on solar cells of Japanese scientific satellites N85-22566
Thin and ultrathin silicon solar cells for space use N85-22567
Space solar cells: Adjusting to new demands N85-22568
Bifacial light sensitive space solar cell N85-22573
Space qualified AlGaAs/GaAs solar cells N85-22575
Availability of AlGaAs/GaAs solar cells in space N85-22576
Comparative study of GaAs solar cell potentialities for space applications N85-22577
Investigation of high output gallium arsenide solar cells N85-22578
Development of very thin large area GaAs solar cells for space application N85-22579
GaAs and 3-5 compound solar cells status and prospects for use in space N85-22580
GaAlAs-GaAs solar cell development: Prospective for space applications under concentration N85-22581
Phenomenology of discharges in space: Application to a solar generator — SPOT satellite N85-22583
In-orbit laser regeneration of the radiation damaged solar arrays N85-22588
The DFS-Kopernikus solar generator electrical design N85-22590
The DFS-Kopernikus solar generator N85-22591
Electrical design of the Intelsat 6 solar generator N85-22592
Computer aided engineering applied to the design and verification of the generic Advanced Rigid Array (ARA) — solar array N85-22593
Development and qualification of the electrical part of the Advanced Rigid Array (ARA) — solar array N85-22594
SPOT solar array N85-22595
Rigid Solar Generator (GSR) solar arrays N85-22596
Retractable Rigid Solar Generator (GSR) N85-22597
Derivation of the Olympus solar array requirements N85-22598
The Olympus solar array development and test program N85-22599
Design and qualification testing of the Olympus solar array blanket N85-22600
The performance of the Olympus power subsystem with its solar array N85-22601
Analysis of optimum front cover thickness for lightweight solar arrays N85-22606
Development of Halley's Comet explorer PLANET-A solar array N85-22608
Concentrator technologies evaluation for large solar arrays and their application for space stations/platforms N85-22609
Space Station solar array N85-22610
Solar array dynamical simulation for illumination and temperature variation N85-22611
Blanket integrated cushioning of foldable and retractable solar arrays N85-22612
Concept for controlled fold by fold deployment and retraction of flexible, foldable solar generators N85-22613
Aspects of low cost module technology — spacecraft solar arrays N85-22614
Emissivity enhancement of fused silica for space applications — solar cells N85-22615
NASA photovoltaic research and technology development program for space applications N85-22617
Study of concentration for space photovoltaic generators N85-22618
Developments in deployable masts to support flexible solar arrays N85-22620
Generic design and verification of an Advanced Rigid Array (ARA) — solar array N85-22621
Growth capabilities of European retractable solar arrays N85-22625
High output photovoltaic conversion: The quadrispectral project — spacecraft power supplies N85-22626
SPACECRAFT STABILITY
Rotational motion of a satellite N85-22428
SPACECRAFT TRACKING
Space interception guidance with uncertain factors N85-22781
SPACECRAFT TRAJECTORIES
Rejection of anomalous observations when determining spacecraft trajectories N85-22421
SPACELAB
D-1 report: The first German spacelab mission [NASA-TM-77637] N85-22402
SPALLING
Impact and collisional processes in the solar system N85-23530
SPARK GAPS
Low jitter trigger for an excimer laser [DE85-005732] N85-23080
SPATIAL DISTRIBUTION
Space and time distribtuion of aftershocks N85-23157
Motion planning with six degrees of freedom [AD-A150312] N85-23432
Distribution and properties of large symmetric knobs on Mars N85-23598
SPATIAL FILTERING
Acoustooptic cell as space-frequency filter N85-23051
SPATIAL RESOLUTION
High-resolution SIT TV tube for subnanosecond image shuttering [DE85-005189] N85-23072
Impact of Thematic Mapper sensor characteristics on classification accuracy — suburban Washington, D.C., Maryland, and the Chesapeake Bay N85-23188
Quick look analysis of TM data of the Washington, District of Columbia, area N85-23197
Preliminary comparisons of the information content and utility of TM versus MSS data N85-23202
Assessing LANDSAT TM and MSS data for detecting submerged plant communities N85-23203
The use of Thematic Mapper data for land cover discrimination: Preliminary results from the UK SATMaP programme N85-23207
Preliminary study of information extraction of LANDSAT TM data for a suburban/regional test site N85-23208
Comparison of land cover information from LANDSAT Multispectral Scanner (MSS) and airborne Thematic Mapper simulator (TMS) data for hydrologic applications — Clinton River Basin, Michigan N85-23211
Surface units on Venus derived from Pioneer-Venus altimetry, roughness, and reflectivity measurements N85-23510
SPECIFIC HEAT
Effect of variable solid phase thermal properties on propellant combustion N85-22547

SPECIFICATIONS
Spacecraft environmental interactions: A joint Air Force and NASA research and technology program N85-22517
SPECIMEN GEOMETRY
Stress intensity factor in a tapered specimen [NASA-CR-175589] N85-23099
SPECTRAL BANDS
Snow reflectance from Thematic Mapper N85-23205
Relative accuracy assessment of LANDSAT-4 MSS and TM data for level 1 land cover inventory — Washington, D.C. N85-23212
Reassignment of the iron (3) absorption bands in the spectra of Mars N85-23614
Determination of mineral type, abundance, and grain size with remotely obtained reflectance spectra N85-23623
SPECTRAL EMISSION
Interference immunity of fiber-optic communication lines with spectral multiplexing of channels N85-22924
SPECTRAL LINE WIDTH
Spectral frequency of eigenvalues in optimal problems of stability of cylindrical shells of variable thickness N85-22815
SPECTRAL METHODS
Synthesis of quasi-optimum algorigthms for signal recognition against background of correlated noise employing discrete spectral transformations N85-23020
Automated extraction of absorption bands from reflectance special N85-23624
SPECTRAL RECONNAISSANCE
Feature extraction assessment study [AD-A150189] N85-23239
SPECTRAL REFLECTANCE
Snow reflectance from Thematic Mapper N85-23205
Multispectral analysis of the Kasei Vallis-Lunae Planum region of Mars N85-23607
Geologic interpretation of remote sensing data for the Martian volcano, Ascraeus Mons N85-23608
The search for igneous materials at the Viking landing sites N85-23609
Basalts of Mars: Constraints on volatile evolution N85-23610
Zeolites on Mars: Prospects for remote sensing N85-23615
Remote sensing analyses of localized lunar dark mantle deposits N85-23616
Spectral reflectance studies of the Orientale basin N85-23617
Io: Precise comparison of Voyager spectral curves with laboratory measurements N85-23619
Spectral units on Europa and Ganymede N85-23621
Determining mineral types and abundances from reflectance measurements N85-23622
Determination of mineral type, abundance, and grain size with remotely obtained reflectance spectra N85-23623
Automated extraction of absorption bands from reflectance special N85-23624
Quantitative analyses of planetary reflectance spectra N85-23625
SPECTRAL RESOLUTION
Impact of Thematic Mapper sensor characteristics on classification accuracy — suburban Washington, D.C., Maryland, and the Chesapeake Bay N85-23188
Quick look analysis of TM data of the Washington, District of Columbia, area N85-23197
Preliminary comparisons of the information content and utility of TM versus MSS data N85-23202
Assessing LANDSAT TM and MSS data for detecting submerged plant communities N85-23203
The use of Thematic Mapper data for land cover discrimination: Preliminary results from the UK SATMaP programme N85-23207
Preliminary study of information extraction of LANDSAT TM data for a suburban/regional test site N85-23208
Comparison of land cover information from LANDSAT Multispectral Scanner (MSS) and airborne Thematic Mapper simulator (TMS) data for hydrologic applications — Clinton River Basin, Michigan N85-23211
Automated extraction of absorption bands from reflectance special N85-23624
SPECTRAL SENSITIVITY
LANDSAT-4 Science Characterization Early Results. Volume 4: Applications — agriculture, soils land use, geology, hydrology, wetlands, water quality, biomass identification, and snow mapping [E85-10070] N85-23186
A first evaluation of LANDSAT TM data to monitor suspended sediments in lakes — Lake Chicot, Arkansas N85-23204
Preliminary evaluation of TM for soils information N85-23206
Comparison of MSS and TM data for landcover classification in the Chesapeake Bay area: A preliminary report — Taylor's Island, Maryland N85-23210
SPECTRAL SIGNATURES
Overview of TM applications research reports N85-23187
A concept for the processing and display of Thematic Mapper data N85-23198
Early results of investigations of LANDSAT 4 Thematic Mapper and Multispectral Scanner applications — Washington, D.C. N85-23200
Experimental methds for quenching structures in lunar-analog silicate melts: Variations as a function of quench media and composition N85-23554
SPECTROMETERS
Protons with energies above 30 KeV in Earth's radiation belt at low altitudes during magnetically quiet time close to geomagnetic equator N85-22423
Rocket body charge neutralization processes in ARAKS experiment (data from two launches) N85-22426
Reflex attachment for line alignment in spectral diffraction devices N85-22794
Possibility of mapping active tectonic structures from mercury gas aureoles over sea surface N85-23162
Effects of focusing on HRS focal-plane polarimeter measurements [DE85-004627] N85-23406
SPECTROPHOTOMETRY
Microstructure of Venus cloud layer based on spectrophotometric data from Venera-11 spacecraft N85-22436
Determining adsorption of surface-active substances by sea bottom deposits N85-23128
SPECTROSCOPIC ANALYSIS
Multiple element neutron-activation analysis of atmospheric aerosols with X-ray and gamma-spectrometric recording of radionuclides formed N85-22631
SPECTROSCOPY
Research in the optical sciences [AD-A150196] N85-23401
SPECTRUM ANALYSIS
Spectra of incidental interference resulting from nonlinear conversion of signals from transmitters N85-22950
Efficiency of multitarget signal detection by digital radar data processing devices N85-22991
Accuracy of random signal spectral parameter estimation against interference background in acoustooptical spectrum analyzers N85-23052
Determining vector of radiointerferometer base from observations of natural radio emission with narrow spectrum N85-23158
Relationship between brightness spectrum of photographic image and spectrum of rises on a water surface with waves N85-23171
Sulfur oxygen processes on Io N85-23481
Photometric analysis of Jupiter-illuminated images of Io N85-23620
SPEECH
Low-bit rate speech encoders based on Line-Spectrum Frequencies (LSF) [AD-A150518] N85-22871
SPEECH RECOGNITION
Research in continuous speech recognition [AD-A150474] N85-22868
SPEED INDICATORS
Metrological support for remote transport vehicle speedometers N85-22963
SPHERICAL COORDINATES
Solution of direct magnetometric problem on spherical Earth N85-23179
SPHERICAL HARMONICS
Time dependent interaction of internal pressure wave with system of two spherical shells N85-22809
Venus gravity: Global field results N85-23512
SPHERICAL SHELLS
Time dependent interaction of internal pressure wave with system of two spherical shells N85-22809
Nonlinear behavior and stability of thin spherical shells subjected to non-axisymmetrical loading N85-22821
Intensity vectors of sound scattering by a spherical shell [AD-A147847] N85-23107
SPIN DYNAMICS
Liquid moment on a filled coning cylinder during spin-up: Ad hoc model [AD-A150280] N85-23060
Observation of a novel low-lying excited state in zinc complexes [AD-A150188] N85-23365
SPLINE FUNCTIONS
Spline-based Rayleigh-Ritz methods for the approximation of the natural modes of vibration for flexible beams with tip bodies [NASA-CR-172566] N85-23100
Primary processing of experimental magnetovariation sounding data using spline functions N85-23175
SPLITTING
Longitudinal splitting in unidirectional composites, analysis and experiments [NASA-CR-3681] N85-22639
SPOT (FRENCH SATELLITE)
SPOT solar array N85-22595
SPRAYERS
Size and velocity distributions of particles and droplets in spray combustion systems [AD-A150355] N85-22648
SPREAD F
Kinetic Rayleigh-Taylor instability theory in the ionosphere near equator N85-22911
SPUTTERING
Use of markets to elucidate reacting sputtering processes [DE85-005723] N85-22655
SQUARE WAVES
Square-pulse generator N85-22959
STABILITY
Stability of cylindrical shells with one-way constraints N85-22820
Nonlinear behavior and stability of thin spherical shells subjected to non-axisymmetrical loading N85-22821
Effect of compliability of hot walls in liquid-propellant engine on low frequency instability N85-22824
Stability of highly nonlinear oxide-zinc resistors under continuous voltage of industrial frequency N85-23030
Electrodynamic stability of composite liquid-metal contacts N85-23031
STAGNATION FLOW
Stagnation zone impaction on a simple terrain feature in stable flow N85-23255
STAINLESS STEELS
Local electrochemistry of pitting corrosion in stainless steels [DE85-005207] N85-22673
Development of a sintered shim [DE85-006183] N85-22685
Use of ferrofluids in machining of metals N85-22802
Fatigue life, crack initiation, and propagation of 304 stainless steel with non-proportional axial/torsional strain-paths N85-23094
STANDARDS
A description of the Langley wireframe geometry standard (LaWGS) format [NASA-TM-85767] N85-22380
Characterization standards for solid propellant rocket motors [AD-A150250] N85-22627
Digital standards conversion: Interpolation theory and aperture synthesis [BBC-RD-1984/20] N85-22857
Critical current measurements on an NbTi superconducting wire standard reference material [PB85-118594] N85-22908
Validation summary report, Burroughs Corporation, 820 FORTRAN release 4.0 [PB84-227792] N85-23316
STANDING WAVES
Nonrelativistic Kapitza-Dirac scattering [AD-A150622] N85-23405
STAR DISTRIBUTION
The color excesses of classical cepheids and the structure of our galaxy N85-23459
STARS
University of Cambridge Institute of Astronomy report of activities N85-23464
STATIC CHARACTERISTICS
Electrothermal transducer with short time constant N85-23040
STATIC PRESSURE
Effects of inlet distortion on a static pressure probe mounted on the engine hub in an F-15 airplane [NASA-TP-2411] N85-22394
STATIONS
Use of mobile surface station for synchronous satellite measurements in seismological research N85-22447
STATISTICAL ANALYSIS
Motion of symmetrical satellite with flexible viscoelastic rods about center of mass in circular orbit N85-22420
Ice statistics and acoustic scattering in the Arctic basin [AD-A150141] N85-23289
Microcomputer: Controlled statistics analyzer [BLL-CE-TRANS-7971-(9022.09)] N85-23306
Bootstrapping the Kalman filter [AD-A150609] N85-23370
Informative geometry of probability spaces [AD-A150510] N85-23371
Unsupervised classification of global radar units on Venus N85-23632
STATISTICAL CORRELATION
More precise curve of dependance between density and velocity of longitudinal waves in consolidated crust and top of mantle in oceanic structures N85-23143

STATISTICAL DISTRIBUTIONS
Skewed stable variables and processes
[AD-A150549] N85-23372
Average spacing for rings of individual multi-ring basins is 2.0(0.5)D N85-23541
STATORS
Magnetic noise in single-machine rotating frequency converters N85-22969
STEADY FLOW
Internal fluid mechanism of solid propellant rocket motors N85-22544
STEADY STATE
A simple model of electron beam initiated dielectric breakdown N85-22519
Internal fluid mechanism of solid propellant rocket motors N85-22544
Confidence intervals using the regenerative method for simulation output analysis
[AD-A150147] N85-23343
STEADY STATE CREEP
Steady-state reaction of three-layered cylindrical shell to effect of moving load N85-22811
STEEL STRUCTURES
Investigation of steel structures using ultrasonic waves
[BR93258] N85-23091
STEELS
Delayed cracking strength of experimental grades of 42 CD 4 steel in aqueous H2S surroundings
[BLL-T8419/BG/LRS/LRST738/84] N85-22658
USSR report: Materials science and metallurgy
[JPRS-UMS-85-002] N85-22688
Specifics of laser heat treatment of high steel tools N85-22714
Comparison of dynamic-tension and constant-load strength characteristics of heat-resistant materials N85-22722
Mechanical properties and brittle fracture resistance of welded multilayer elements for high pressure vessels N85-22736
Structure and mechanical characteristics of heterogeneous joints produced by laser welding N85-22742
New tooling for plasma cutting technology N85-22842
STELLAR ACTIVITY
Solar and stellar coronal plasmas
[NASA-CR-175623] N85-23676
STELLAR COLOR
The color excesses of classical cepheids and the structure of our galaxy N85-23459
STELLAR CORONAS
Solar and stellar coronal plasmas
[NASA-CR-175623] N85-23676
STELLAR EVOLUTION
All-Union conference of radio astronomers N85-22408
Dynamics of long-period comets N85-23506
The Formation of preplanetary disks from the collapse of rotating molecular cloud cores N85-23526
Research on the early history of the solar system N85-23527
STELLAR MASS
The Formation of preplanetary disks from the collapse of rotating molecular cloud cores N85-23526
STELLAR MASS ACCRETION
Orbital resonances and planetary accretion in the solar nebula N85-23523
Research on the early history of the solar system N85-23527
STELLAR MODELS
Theoretical and observational studies of stellar activity N85-23468
Constraints of observations of solar oscillations on solar models with mixing by turbulent diffusion
[DE85-003741] N85-23678
STELLAR SPECTRA
Solar and stellar coronal plasmas
[NASA-CR-175623] N85-23676
STELLAR STRUCTURE
Research on the early history of the solar system N85-23527
STELLAR TEMPERATURE
Cooling of neutron stars with hyperons
[DE85-004641] N85-23472
STOCHASTIC PROCESSES
An analysis of a dynamic project cost problem
[CSIR-TWISK-336] N85-23341
The design of a unified package for the solution of stochastic petri net models
[AD-A150326] N85-23354
Regenerative stochastic Petri nets
[AD-A150343] N85-23355
Regenerative simulation of non-Markovian stochastic systems
[AD-A150344] N85-23367
STORAGE RINGS (PARTICLE ACCELERATORS)
Electronics Engineering Department EE Technical Review
[UCRL-50025-84-1] N85-22887
STRAIN MEASUREMENT
Fibre composite laminated plate analysis using a card programmable calculator (HP41C/CV)
[NIAST-83/88] N85-23106
STRAIN RATE
Behavior of fiber-reinforced composites under dynamic tension
[AD-A150619] N85-22641
STRATA
Regions of propagation of short-wave perturbations in spherical layer of rotating fluid N85-23130
STRATIFICATION
Horizontal coherence of temperature microstructure in upper ocean layer N85-23139
STRATIGRAPHY
Study of stratigraphy of the Precambrian Soviet Baltic shield N85-23148
Reflected wave travel-time curves in stratified media with vertically heterogeneous layers and slightly sloping curved boundaries N85-23167
Assessment of computer based geologic mapping of rock units in the LANDSAT-4 scene of northern Death Valley, California N85-23195
Dark halo craters and the thickness of grooved terrain on Ganymede N85-23484
Valles Marineris basin beds: A complex story N85-23652
Mars: Stratigraphy of western highlands and polar regions N85-23653
STRATOSPHERE
Observation of cosmic ray flux variations in stratosphere N85-22430
Calibration of solar cells outside the atmosphere N85-22603
A theoretical study of the ozone quasi-biennial oscillation in the tropical stratosphere N85-23264
STREAMS
Late Tertiary and Quaternary river systems of the eastern Sahara as mapped on shuttle radar and LANDSAT images N85-23641
STRESS (PHYSIOLOGY)
Brain mechanisms underlying individual differences in reaction to stress: An animal model
[AD-A150195] N85-23301
STRESS CONCENTRATION
Shape optimization for minimal stress concentration N85-23093
On Hybrid and mixed finite element methods
[NASA-CR-175551] N85-23096
Elasticity solution of an adhesively bonded joint
[NASA-CR-175591] N85-23097
Advanced life analysis methods. Volume 2: Crack growth analysis methods for attachment lugs
[AD-A150420] N85-23109
STRESS CORROSION CRACKING
Role of segregated P and S in intergranular stress corrosion cracking of nickel
[DE85-004547] N85-22679
Advanced life analysis methods. Volume 1: Cracking data survey and NDI (nondestructive inspection) assessment for attachment lugs
[AD-A150419] N85-23108
STRESS INTENSITY FACTORS
Effect of phase state of TiC-NiTi powder composite materials on nature of failure and mechanical properties N85-22702
A clamped rectangular plate containing a crack
[NASA-CR-175590] N85-23098
Stress intensity factor in a tapered specimen
[NASA-CR-175589] N85-23099
STRESS-STRAIN RELATIONSHIPS
Behavior of fiber-reinforced composites under dynamic tension
[AD-A150619] N85-22641
Dissipation of energy in composite material N85-22703
Method of calculating strength of joint produced by cold welding of aluminum under discrete loading N85-22743
Determination of stresses and deformations in linearly elastic conical shell subjected to aerodynamic loading and heating N85-22812
STRESSES
Characteristics of EMI generated by negative metal-positive dielectric voltage stresses due to spacecraft charging N85-22505
STRETCHING
Critical events in inelastic deformation of glassy polymers in adsorptive medium N85-22634
STRONTIUM TITANATES
Planar ferroelectric microcapacitors for microwave devices N85-23032
STRUCTURAL ANALYSIS
Air Force technical objective document, Flight Dynamics Laboratory plans for fiscal year 1986. Air Force technical objective document
[AD-A149648] N85-22348
Simple theoretical models for composite rotor blades
[NASA-CR-175620] N85-22382
Specifics of kinetics of polymorphous conversion upon heating of low carbon steels N85-22721
Machine analysis of resonance characteristics of plate-type radio electronic equipment constructions N85-23018
Operational loads measurement: A philosophy and its implementation — aircraft structures
[AD-A149445] N85-23308
Raman structural studies of the nickel electrode
[NASA-CR-175619] N85-23414
Meteoroidal impacts, plasma, fine structure of ringlets and spokes on Saturn's ring B N85-23490
The olivine asteroids: Discovery, mineralogy, and relationship to palasites N85-23500
STRUCTURAL BASINS
Review of problems in lithology N85-23160
Average spacing for rings of individual multi-ring basins is 2.0(0.5)D N85-23541
Ring-diameter ratios for multi-ring basins average 2.0(0.5)D N85-23542
Ripple ring basins on Ganymede and Callisto N85-23547
Fluvial drainage basins and valley networks: Eastern Margaritifer Sinus, Mars N85-23586
Spectral reflectance studies of the Orientale basin N85-23617
The deep structure of lunar basins: Clues to the understanding of basin formation and modification N85-23647
Valles Marineris basin beds: A complex story N85-23652
Global tectonics on Ganymede N85-23659
STRUCTURAL DESIGN
Developments in deployable masts to support flexible solar arrays N85-22620
Generic design and verification of an Advanced Rigid Array (ARA) — solar array N85-22621
The Olympus solar array structure and mechanisms N85-22623
Experimental investigation of crippling strength of Chinese aluminum alloy (LY12CZ) sections N85-22779
Shape optimization for minimal stress concentration N85-23093
STRUCTURAL DESIGN CRITERIA
Study for the optimization of a transport aircraft wing for maximum fuel efficiency. Volume 1: Methodology, criteria, aeroelastic model definition and results
[NASA-CR-172551] N85-22378
STRUCTURAL FAILURE
Steel containment buckling
[DE85-003744] N85-23111
STRUCTURAL PROPERTIES (GEOLOGY)
Review of problems in lithology N85-23160
Normal and anomalous geothermal fields and their relationship to hierarchy of geological bodies N85-23163
Planetary geology in the 1980s
[NASA-SP-467] N85-23457
Io: Generation of silicate magma by shear melting at the base of a basaltic lithosphere N85-23476
Topographic evidence for shield volcanism on Io N85-23478
Sulfur volcanoes on Io? N85-23479
Patterns of fracture and tidal stresses due to nonsynchronous rotation: Implications for fracturing on Europa N85-23483
Formation of bright terrain bands on Ganymede by unstable lithosphere extension N85-23485
Progress on studies of early intense cratering N85-23535
Impacts in ice: Commissions of solar system crater population N85-23538
Problems in recovering crater production functions N85-23539
The nature of Martian flow ejecta craters N85-23545
Distribution and properties of large symmetric knobs on Mars N85-23598
Planetary analogs in Antarctica: Icy satellites N85-23605
Lithologic and structural control on slope morphology in the Valles Marineris N85-23651
Three-layer generic Ganymedes: Structure and evolution N85-23657
Lineaments on Ganymede: New evidence for late tectonic activity N85-23658
Tectonics of the Valhalla structure on Callisto N85-23662
Mars geologic mapping: A review and new concepts N85-23663

Geology of the Ganymede quadrangle Jg7 N85-23665

STRUCTURAL VIBRATION
A quantitative comparison of active and passive damping for large space structures [UTIAS-TN-249] N85-22524
Spline-based Rayleigh-Ritz methods for the approximation of the natural modes of vibration for flexible beams with tip bodies [NASA-CR-172586] N85-23100
Applications of the conformal mapping method to the solution of mechanical vibrations problems N85-23103

STYRENES
Influence of hydrogen bonding in block copolymers and their blends N85-22752

SUBMERGED BODIES
The low frequency behaviour of an immersed structure at a standstill in a high density fluid with free surface [TP-1983-31] N85-23105

SUBMILLIMETER WAVES
Absorption of radiation by water vapor in windows of relative transparency of 95-145 micrometer range N85-22968

SUBSONIC FLOW
Aerodynamic behavior of ventilated wind tunnel walls N85-22363
Investigation of parabolic computational techniques for internal high-speed viscous flows [NASA-CR-172555] N85-23056

SUBSTRATES
Influence of substrate heating and thermal annealing on the surface crystallinity in single Si crystals implanted with high doses of (16)O [DE85-005264] N85-23428

SUBURBAN AREAS
A comparison of metropolitan and non-metropolitan employment characteristics: Indications of the size of non-metropolitan mobile communication services user classes [NASA-CR-175648] N85-22855

SULFATES
Chemical weathering of soils from the dry valleys of Antarctica: A terrestrial analog of Martian weathering processes N85-23628

SULFUR
Sulfur volcanoes on Io? N85-23479
Sulfur oxygen processes on Io N85-23481

SUMMER
Variation of Arctic cloud cover in summer [DE85-004507] N85-23285

SUN
Helium atoms in interstellar and interplanetary space. II: Determination of direction of interstellar gas motion relative to Sun N85-22425

SUPERCOMPUTERS
Bottleneckology: Evaluating supercomputers [DE85-005574] N85-23315

SUPERCONDUCTING MAGNETS
Design considerations for a 100 kW CW, 140 GHz gyrotron oscillator [DE85-005282] N85-22904
High-field dipoles for future accelerators [DE85-002315] N85-23391

SUPERCONDUCTIVITY
Critical current measurements on an NbTi superconducting wire standard reference material [PB85-118594] N85-22906
Outlook for realization of proximity effect and Josephson direct current in helium-2 N85-22956
Microstructural study on the processing and properties of high-field A15 superconducting materials [DE85-004652] N85-23423

SUPERCONDUCTORS
Survey of the state-of-the-art of miniature cryocoolers for superconductive devices [AD-A150319] N85-22774
Critical current measurements on an NbTi superconducting wire standard reference material [PB85-118594] N85-22906
Spectral evaluation of irregularity of superconducting coaxial cables N85-23000
Winding insulation in electromagnetic systems for Tokamak reactor plants N85-23035
Improvement in magnetic field properties of vanadium-gallium superconductors by enhancement of spin-orbit scattering [DE85-002893] N85-23422

SUPERCRITICAL WINGS
Preliminary development of an approximation procedure for supercritical wing design optimization applications [AD-A150177] N85-22383

SUPERFLUIDITY
Outlook for realization of proximity effect and Josephson direct current in helium-2 N85-22956

SUPERHEATING
Anomalies of aluminum structure and properties N85-22693

SUPERPLASTICITY
Dependence of superplastic flow on state of grain boundaries N85-22689
Aluminum alloy ATs5K5 (5% Zn + 5% Ca) for superplastic forming N85-22697

SUPERPOSITION (MATHEMATICS)
Normal mode calculations for fuselage type intricate structures by regarding them as systems with superposed constraints N85-22817

SUPERSONIC COMBUSTION RAMJET ENGINES
Investigation of parabolic computational techniques for internal high-speed viscous flows [NASA-CR-172555] N85-23056

SUPERSONIC DIFFUSERS
The role of convective perturbations in supercritical inlet oscillations N85-22563

SUPERSONIC FLIGHT
Selection of air intake parameters for supersonic-flow operation N85-22837

SUPERSONIC FLOW
Investigation of parabolic computational techniques for internal high-speed viscous flows [NASA-CR-172555] N85-23056

SUPERSONIC TRANSPORTS
Effects of leading-edge devices on the low-speed aerodynamic characteristics of a highly-swept arrow-wing [NASA-CR-172531] N85-22365

SUPERSONIC WAKES
Wakes and differential charging of large bodies in low Earth orbit N85-22488

SUPPRESSORS
Measurements of distributed combustion N85-22542
Distributed combustion: A mechanism of acoustic suppression N85-22543

SURFACE ACOUSTIC WAVE DEVICES
Optimal synthesis of surface acoustic wave filters N85-22933
Analysis and optimization of parameters of fanned surface acoustic wave transducers N85-22934
Experimental study of high-stability oscillator with surface-acoustic-wave resonator in feedback loop N85-23053
Optical processing in radon space [AD-A150289] N85-23402

SURFACE FINISHING
Innovative research in the design and operation of large telescopes for space: Aspects of giant telescopes in space [NASA-CR-175626] N85-23462

SURFACE NAVIGATION
Use of three omega radionavigation system position lines for solving problems in marine geodesy N85-23131

SURFACE PROPERTIES
Problem of diffraction by wavy surface: Comparison of numerical methods of solution N85-22985
Method for processing broad-profile data N85-23185
Dipole active surface vibrational resonances on clean and hydrogen covered Ni(110) [AD-A150546] N85-23420
Study and estimation of planet-crossing asteroid populations: Discoveries and analysis N85-23498
The olivine asteroids: Discovery, mineralogy, and relationship to palasites N85-23500
Surfaces of asteroids and cometary nuclei N85-23503
Venus surface composition from radio/radar measurements N85-23509
Surface structures of Hawaiian lavas N85-23566

SURFACE REACTIONS
Three-dimensional calculation of shuttle charging in polar orbit N85-22486
Confinement properties of high energy density plasmas in the Wisconsin levitated octupole N85-23408

SURFACE ROUGHNESS
A posteriori increase of resolving power of optical system forming averaged monochromatic images N85-23003
Effects of fracture roughness on fluid flow through a single deformable fracture [DE85-004593] N85-23062
Calculations of microwave brightness temperature of rough soil surfaces: Bare field [NASA-TM-86200] N85-23221
Microwave remote sensing of soil moisture N85-23235
A systematic study of light scattering by irregularly shaped particles [AD-A150192] N85-23400
Unsupervised classification of global radar units on Venus N85-23632
Mapping and geological analysis of Mercury and Venus radar ranging data N85-23633
Mars radar catalog N85-23636
Statistics of Aeolian surface of Mars N85-23637

SURFACE TEMPERATURE
Application of fluorescence to measurement of surface temperature in solid propellants N85-22548
Estimation of regional evapotranspiration using remotely sensed land surface temperature. Part 1: Measurement of evapotranspiration at the Environmental Research Center and determination of Priestley-Taylor parameter N85-23233
Estimation of regional evapotranspiration using remotely sensed land surface temperature. Part 2: Application of equilibrium evaporation model to estimate evapotranspiration by remote sensing technique --- Japan N85-23234
Testing an energy balance model for estimating actual evapotranspiration using remotely sensed data --- Hannover, West Germany barley and wheat fields N85-23236
A method for estimating soil moisture availability [NASA-CR-175606] N85-23238

SURFACE WAVES
Surface wave excitation study [DE85-005301] N85-22875

SURFACTANTS
Turbulent flows of surfacant solutions [AD-B089137L] N85-23058
Determining adsorption of surface-active substances by sea bottom deposits N85-23128

SURGES
Surge strength of symmetric cable with monolithic polyethylene insulation of quads N85-23001

SURVEILLANCE
TCAS II: Design and validation of the high-traffic-density surveillance subsystem [DOT/FAA/PM-84/5] N85-22375

SURVEYS
A community survey of helicopter noise annoyance conducted under controlled noise exposure conditions [NASA-TM-86400] N85-23374
Research on the effect of noise at different times of day: Models, methods and findings [NASA-CR-3888] N85-23375
Development, achievements in China's cartography work N85-23434

SWEDEN
Catastrophic-flood features in Swedish Lapland as a terrestrial analog for Martian channel flows N85-23587

SWEEP FREQUENCY
Simple sweep frequency generator N85-22980

SWEPT WINGS
Effects of leading-edge devices on the low-speed aerodynamic characteristics of a highly-swept arrow-wing [NASA-CR-172531] N85-22365
Calculation of vortex-flap aerodynamic characteristics [NASA-CR-175624] N85-22367

SWIRLING
Workshop report: Swirl Enhanced Combustion N85-22564

SWITCHES
KAM-250 antenna switch N85-22916

SWITCHING
Stereo decoder without subcarrier restoration N85-22921

SYMBOLS
Automatic symbolic solution of Markov chains [AD-A150476] N85-23369

SYNCHRONISM
Investigation of influence of communications link and synchronization error on noise tolerence of group transmission of binary information based on orthogonal Walsh function N85-23026

SYNCHRONOUS PLATFORMS
Concentrator technologies evaluation for large solar arrays and their application for space stations/platforms N85-22609

SYNCHRONOUS SATELLITES
In-orbit laser regeneration of the radiation damaged solar arrays N85-22588
The DFS-Kopernikus solar generator electrical design N85-22590
The DFS-Kopernikus solar generator N85-22591

SYNCHROTRON RADIATION
EXAFS of monolayers on silver electrodes: SSRL proposal number 717M [AD-A150623] N85-22652
Threshold double photoionization of argon with synchrotron radiation [AD-A150615] N85-23389

SYNOPTIC MEASUREMENT
Empirical and modeled synoptic cloud climatology of the Arctic Ocean [NASA-CR-175626] N85-23272

SYNTHESIS (CHEMISTRY)
Synthesis and characterization of poly(vinylidene fluoride)
[AD-A150291] N85-22759
Geomagnetic field dynamics N85-23182
SYNTHESIZERS
Optimal design efforts in Shanghai described N85-22386
SYNTHETIC APERTURE RADAR
The imaging of internal waves by the SEASAT-A synthetic aperture radar
[ARE(PORTLAND)TN-720/84] N85-22860
Edge detection in SAR imagery using gradient operators — synthetic aperture radar (SAR)
[AD-A149411] N85-22862
SYNTHETIC APERTURES
Digital standards conversion: Interpolation theory and aperture synthesis
[BBC-RD-1984/20] N85-22857
SYNTHETIC FIBERS
Diamond cutters' grinders N85-22841
SYNTHETIC FUELS
Trifunctional catalysts for conversion of syngas to alcohols
[DE85-004577] N85-22771
SYSTEM FAILURES
EOS (electrical overstress) protection for VLSI (Very Large Scale Integration) devices
[AD-A150333] N85-22891
Parallel test method for LSI (Large Scale Integration) microprocessors
[AD-A150237] N85-23310
Contribution of instrumentation and control software to system reliability
[DE85-004693] N85-23340
SYSTEM GENERATED ELECTROMAGNETIC PULSES
Laboratory studies of spacecraft response to transient discharge pulses N85-22506
Discharge pulse phenomenology N85-22509
Electron yields from spacecraft materials N85-22512
SYSTEMS ANALYSIS
Reluctance and doubly-excited reluctance motors
[DE85-003585] N85-22900
Cooling performance improvement of a horizontal ground coupled heat pump
[DE85-002470] N85-23065
SIGPI: A user's manual for the fast computation of the probabilistic performance of a complex system
[DE85-005447] N85-23336
Automatic symbolic solution of Markov chains
[AD-A150476] N85-23369
SYSTEMS ENGINEERING
Derivation of the Olympus solar array requirements N85-22598
Optimal allocation of components in parallel-series and series-parallel systems
[AD-A150169] N85-23309
Performance evaluation of distributed systems with unbalanced flows: An analysis of the INFOPLEX data storage hierarchy
[AD-A150528] N85-23328
LEXICON: A structured modeling system for optimization
[AD-A150536] N85-23329
SYSTEMS INTEGRATION
Integrated digital networks
[AD-A150605] N85-22873
SYSTEMS SIMULATION
Solar array dynamical simulation for illumination and temperature variation N85-22611

T

TABLES (DATA)
Experimental study of main rotor tip geometry and tail rotor interactions in hover. Volume 2: Run log and tabulated data
[NASA-CR-177336-VOL-2] N85-22345
A model for large sparse contingency tables
[AD-A150320] N85-23350
TAIL ASSEMBLIES
Wind tunnel acoustic study of a propeller installed behind an airplane empennage: Data report
[NASA-CR-177335] N85-23377
TAIL ROTORS
An experimental investigation of the chopping of helicopter main rotor tip vortices by the tail rotor
[NASA-CR-177338] N85-23376
TAIWAN
Crustal dynamics studies in China
[NASA-CR-175617] N85-23265
TANKS (COMBAT VEHICLES)
Ground evaluation of helicopter air-to-air warfare N85-22360
TAPE RECORDERS
Playback amplifier with high interference immunity N85-22970
TARGET ACQUISITION
Efficiency of multitarget signal detection by digital radar data processing devices N85-22991
TARGET RECOGNITION
Moving target detection N85-22915
TARGETS
Variable flexing device for targets in internal beams of charged particle accelerators N85-22797
Microwave blackbodies for spaceborne receivers
[NASA-CR-175647] N85-23068
TAYLOR INSTABILITY
Kinetic Rayleigh-Taylor instability theory in the ionosphere near equator N85-22911
TAYLOR SERIES
Efficiency of algorithms for gas-air channel diagnostics in gas turbine engines based on gas thermodynamic parameters N85-22823
TEAMS
Assessing the behavior and performance of teams in organizations: The case of air transport crews
[AD-A150359] N85-23302
TECHNICAL WRITING
The potential for advanced computerized aids for comprehensible writing of technical documents
[AD-A150501] N85-22870
TECHNOLOGICAL FORECASTING
GaAlAs-GaAs solar cell development: Prospective for space applications under concentration N85-22581
Growth capabilities of European retractable solar arrays N85-22625
FORTRAN in the 90's
[DE85-006154] N85-23332
TECHNOLOGY ASSESSMENT
The high voltage silicon cell: A comparative analysis N85-22569
Gallium arsenide arrays versus silicon arrays for space application N85-22574
Availability of AlGaAs/GaAs solar cells in space N85-22576
Comparative study of GaAs solar cell potentialities for space applications N85-22577
Survival testing of silicon solar modules N85-22602
Aspects of low cost module technology — spacecraft solar arrays N85-22614
Study of concentration for space photovoltaic generators N85-22618
Isotropic proton irradiation of GaAs solar cells N85-22622
Recent trends in particle size analysis techniques
[NASA-TM-77735] N85-22645
Survey of the state-of-the-art of miniature cryocoolers for superconductive devices
[AD-A150319] N85-22774
Nation said to rank high with 15 satellites N85-22778
USSR report: Machine tools and metalworking equipment
[JPRS-UMM-85-005] N85-22839
Technologies to sustain tropical forest resources
[TI85-901085] N85-23241
TECHNOLOGY TRANSFER
China report: Science and technology
[JPRS-CST-85-003] N85-23433
TECHNOLOGY UTILIZATION
Space solar cells: Adjusting to new demands N85-22568
Metal-semiconductor phase transition and its application
[DRIC-T-7149] N85-22665
Role of optical disk at computing centers
[DE85-005124] N85-23314
Physicists' role in new technological development discussed N85-23436
Economic mechanism of integration of science, production N85-23443
Technology and Economics, Inc. Technology Application Team
[NASA-CR-175630] N85-23454
TECTONICS
Use of paleomagnetic data in tectonic analysis of oceanic structures N85-23135
Review of problems in lithology N85-23160
Possibility of mapping active tectonic structures from mercury gas aureoles over sea surface N85-23162
Geomagnetic precursors of intensive earthquakes in the 1-0.-2 Hz frequency range of geomagnetic pulsations N85-23178
A tectonic model of an incipient spreading center and its margins: The Northern Red Sea and the Dead Sea rift N85-23288
Venus chasmata: A lithosphere stretching model N85-23516
Terrestrial analog studies for Martian patterned ground N85-23590
Terrestrial analogs for planetary wrinkle ridges N85-23644
Planetary interior modeling and tectonic implications N85-23649
Elysium region, Mars: Tests of lithospheric loading models for the formation of tectonic features N85-23650
Kasei Vallis of Mars: Dating the interplay of tectonics and geomorphology N85-23654
Creep of ice: Further studies N85-23655
Lineaments on Ganymede: New evidence for late tectonic activity N85-23658
Global tectonics on Ganymede N85-23659
Tectonics of the Galileo Regio on Ganymede N85-23660
Importance of the tectonic motions on Ganymede N85-23661
Tectonics of the Valhalla structure on Callisto N85-23662
TEFLON (TRADEMARK)
Spectral evaluation of irregularity of superconducting coaxial cables N85-23000
TELECOMMUNICATION
Integrated digital networks
[AD-A150605] N85-22873
USSR report: Electronics and electrical engineering
[JPRS-UEE-85-001] N85-22976
Analysis of interference caused by interfering radio signals in communications systems with frequency separation of telephone channels and frequency modulation N85-23025
TELEOPERATORS
Investigation of dynamics of manipulator with elastic sections N85-22819
TELEVISION RECEPTION
Horizontal deflection TS-257 N85-22926
TELEVISION SYSTEMS
Electronic generation of text for television
[BBC-RD-1984/14] N85-22856
TELEVISION TRANSMISSION
Digital standards conversion: Interpolation theory and aperture synthesis
[BBC-RD-1984/20] N85-22857
Horizontal deflection TS-257 N85-22926
TEMPERATURE
Externally compensated crystal oscillator (ECXO) study
[AD-A150335] N85-22893
TEMPERATURE DEPENDENCE
Combustion kinetics of metal atoms and metallic radicals over wide temperature ranges N85-22530
Orientation and temperature dependence of some mechanical properties of the single-crystal nickel-base superalloy Rene N4. 3: Tension-compression anisotropy
[NASA-TM-86982] N85-22660
Magnetic studies of Ni3Al(Fe) compounds
[DE85-005262] N85-22686
Division boundary in Al-B composite material with boron in contact with solid and liquid aluminum N85-22704
Temperature dependence of propagation of high-current electron beam through drift space N85-22962
Change of electrical characteristics of radio-frequency cables under thermal effect N85-22999
TEMPERATURE DISTRIBUTION
Dilution jet configurations in a reverse flow combustor
[NASA-CR-174888] N85-22392
Effects of temperature variation among droplets in an evaporating fuel spray N85-22562
Horizontal coherence of temperature microstructure in upper ocean layer N85-23139
Analysis of NIMBUS-7 SMMR data — Hokkaido, Japan snow cover N85-23232
Thermal and thermoelastic effects in rolling/sliding contacts
[AD-A150435] N85-23429
TEMPERATURE EFFECTS
Effects of temperature variation among droplets in an evaporating fuel spray N85-22562
Solar array dynamical simulation for illumination and temperature variation N85-22611
Study of effective physiological temperature N85-22780
Cooling performance improvement of a horizontal ground coupled heat pump
[DE85-002470] N85-23065
Thermal and thermoelastic effects in rolling/sliding contacts
[AD-A150435] N85-23429
Io: Generation of silicate magma by sheer melting at the base of a basaltic lithosphere N85-23478
Characteristics of basaltic lava flows on Venus N85-23508
Terrestrial analog studies for Martian patterned ground N85-23590

TEMPERATURE GRADIENTS
Turbulence measurements in shock induced flows N85-23055
Fine structure of vertical distribution of light attenuation index of sea water N85-23140
Characteristics of basaltic lava flows on Venus N85-23508

TEMPERATURE MEASUREMENT
Dilution jet configurations in a reverse flow combustor [NASA-CR-174888] N85-22392
Application of fluorescence to measurement of surface temperature in solid propellants N85-22548
Radiosodar system for remote synchronous measurements of wind speed, temperature and its fluctuations N85-23145
Modulation of light energy transduction in photosynthesis [DE85-004711] N85-23282
Analysis and interpretation of observations of airglow at 297 nm in the Venus thermosphere N85-23473

TEMPERATURE PROFILES
Two-dimensional numerical model of sensible and latent heat transport in an irrigated field under advective conditions N85-23261
Radiation-dominated snowmelt on Mars N85-23592

TEMPORAL DISTRIBUTION
Space and time distribtuion of aftershocks N85-23157

TEMPORAL RESOLUTION
Time-resolved studies of rapid solidification in highly undercooled molten silicon [DE85-004857] N85-22765

TENSILE PROPERTIES
Effects of neutron irradiation at 450(0)C and 16 dpa on the properties of various commercial copper alloys [DE85-005716] N85-22684

TENSILE STRENGTH
Structural strenght of strip D16T aluminum alloy with low copper and magneeium content N85-22691
New deformable secondary aluminum alloys N85-22694
Effect of operating medium on cyclic durability of AD33-W composite N85-22716
Analysis of strength and ductility of welded joints in AMtsS and AMg5 aluminum alloys N85-22737
Experimental investigation of crippling strength of Chinese aluminum alloy (LY12CZ) sections N85-22779

TENSILE STRESS
Longitudinal splitting in unidirectional composites, analysis and experiments [NASA-CR-3881] N85-22639
Orientation and temperature dependence of some mechanical properties of the single-crystal nickel-base superalloy Rene N4. 3: Tension-compression anisotropy [NASA-TM-86982] N85-22660
Origin of Martian polygonal terrain: Preliminary results N85-23591

TERNARY ALLOYS
Clustering and ordering in 3-5 alloys [AD-A150604] N85-22670

TERRACES (LANDFORMS)
Morphology and mechanics of terraces in lunar craters N85-23543
Newly discovered Martian impact basins N85-23544
Interaction of Martian flow ejecta blankets with pre-existing impact craters: Morphological observations N85-23546

TERRAIN
Mean flow and turbulence in complex terrain NPS (Naval Postgraduate School)/Vandenberg measurement system [AD-A150184] N85-23274
The ASCOT Data Analysis Workshop [DE85-004407] N85-23283
Low altitude texture comparison data base and smooth shaded texture [AD-A150342] N85-23323
Dark halo craters and the thickness of grooved terrain on Ganymede N85-23484
Formation of bright terrain bands on Ganymede by unstable lithosphere extension N85-23485
Basaltic pressure ridges: Formation and relationship to flow emplacement N85-23587
Paleohydrologic implications of valley networks of Mars N85-23585
Relative time-scale for channeling events within chaotic terrains, Margaritifer Sinus, Mars N85-23589
Terrestrial analog studies for Martian patterned ground N85-23590
Origin of Martian polygonal terrain: Preliminary results N85-23591
Investigations of the Mars cratered terrain: Smooth plains boundary in the eastern equatorial region N85-23596
Martian fretted terrain morphometry interpreted using principal components analysis N85-23597
Distribution and properties of large symmetric knobs on Mars N85-23598
Enigmatic hills of the mottled plains, Mare Acidalium quadrangle (MC-4), Mars N85-23599
Importance of the tectonic motions on Ganymede N85-23661

TERRAIN ANALYSIS
Stagnation zone impaction on a simple terrain feature in stable flow N85-23255

TERRESTRIAL PLANETS
Accumulation of the terrestrial planets N85-23524
Implications of convection in the Moon and the terrestrial planets N85-23548

TEST FACILITIES
AIRLAB: A laboratory for flight-crucial-electronics system research N85-22362
Activities of the Jet Propulsion Laboratory, 1 January - 31 December 1983 [NASA-CR-175555] N85-23447
Electric vehicle test program: INEL transition qualification test plan [DE85-005171] N85-23456

TETHERED BALLOONS
Preliminary investigation of the electrodynamics of a conducting tether N85-22521

TETHERED SATELLITES
Excitation of low-frequency plasma waves by a conducting, tethered satellite N85-23470

TETHERING
Selected tether applications in space: Phase 2. Executive summary [NASA-CR-171421] N85-22482
Selected tether applications in space: Phase 2 [NASA-CR-171422] N85-22483
Preliminary assessment of power-generating tethers in space and of propulsion for their orbit maintenance N85-22520
Preliminary investigation of the electrodynamics of a conducting tether N85-22521

TEXAS
Analysis of SMIRR data for volcanic and sedimentary terrains of the trans-Pecos region, Texas N85-23626

TEXTS
Electronic generation of text for television [BBC-RD-1984/14] N85-22856

TEXTURES
Microwave remote sensing of soil moisture N85-23235
Low altitude texture comparison data base and smooth shaded texture [AD-A150342] N85-23323

THEMATIC MAPPING
Experience in combined special mapping using space information N85-22449
LANDSAT-4 Science Characterization Early Results. Volume 4: Applications — agriculture, soils land use, geology, hydrology, wetlands, water quality, biomass identification, and snow mapping [E85-10070] N85-23186
Overview of TM applications research reports N85-23187
Impact of Thematic Mapper sensor characteristics on classification accuracy — suburban Washington, D.C., Maryland, and the Chesapeake Bay N85-23188
Analysis and evaluation of the LANDSAT-4 MSS and TM sensors and ground data processing systems: Early results N85-23189
Characterization of LANDSAT-4 TM and MSS image quality for the interpretation of California's agricultural resources — Central Valley N85-23190
Evaluation of Thematic Mapper performance as applied to hydrocarbon exploration — Ontario, Canada; Cement, Oklahoma; and Death Valley, California N85-23191
Geologic utility of LANSDAT-4 TM data — Death Valley, California and the Silver Bell area of southern Arizona N85-23192
An initial analysis of LANDSAT-4 Thematic Mapper data for the discrimination of agricultural, forested wetlands, and urban land cover — Poinsett County, Arkansas; and Reelfoot Lake and Union City, Tennessee N85-23193
Preliminary evaluation of Thematic Mapper image data quality N85-23194
Assessment of computer based geologic mapping of rock units in the LANDSAT-4 scene of northern Death Valley, California N85-23195
A concept for the processing and display of Thematic Mapper data N85-23196
Quick look analysis of TM data of the Washington, District of Columbia, area N85-23197
Remote sensing of coastal wetlands biomass using Thematic Mapper wavebands — Lewes, Delaware N85-23198
A preliminary comparison of the information content of data from the LANDSAT 4 Thematic Mapper and Multispectral Scanner — Arkansas N85-23199
Early results of investigations of LANDSAT 4 Thematic Mapper and Multispectral Scanner applications — Washington, D.C. N85-23200
Thematic Mapper data quality and performance assessment in renewable resources/agriculture/remote sensing N85-23201
Preliminary comparisons of the information content and utility of TM versus MSS data N85-23202
A first evaluation of LANDSAT TM data to monitor suspended sediments in lakes — Lake Chicot, Arkansas N85-23204
Snow reflectance from Thematic Mapper N85-23205
Preliminary evaluation of TM for soils information N85-23206
Preliminary study of information extraction of LANDSAT TM data for a suburban/regional test site N85-23208
Comparative techniques used to evaluate Thematic Mapper data for land cover classification in Logan County, West Virginia N85-23209
Comparison of MSS and TM data for landcover classification in the Chesapeake Bay area: A preliminary report — Taylor's Island, Maryland N85-23210
Comparison of land cover information from LANDSAT Multispectral Scanner (MSS) and airborne Thematic Mapper simulator (TMS) data for hydrologic applications — Clinton River Basin, Michigan N85-23211
Relative accuracy assessment of LANDSAT-4 MSS and TM data for level 1 land cover inventory — Washington, D.C. N85-23212
An investigation of several aspects of LANDSAT-5 data quality — Palmer County, Shelby, mt; White sands, NM; Great Salt Lake, UT; San Matted Bridge and Sacramento, California [E85-10096] N85-23214
Studies on physical properties of snow based on multi channel microwave radiometer N85-23231
Analysis of NIMBUS-7 SMMR data — Hokkaido, Japan snow cover N85-23232

THEOREM PROVING
The Chinese remainder theorem and multi-PRF radars [AD-A141375] N85-22858

THEORETICAL PHYSICS
Theoretical aspects of electroweak and other interactions in medium-energy nuclear physics [DE85-003821] N85-23392

THERMAL CONDUCTIVITY
Effect of variable solid phase thermal properties on propellant combustion N85-22547
Thermally stimulated conductivity in semi-insulating gallium arsenide N85-23036
Time resolved X-ray studies during pulsed laser irradiation of Ge [DE85-005263] N85-23083
Electrical and thermal transport property studies of high-temperature thermoelectric materials [AD-A150167] N85-23417
H-division materials physics progress [DE85-004990] N85-23430

THERMAL CYCLING TESTS
Change in microstructure of heat-resistant nickel alloys upon thermal cycling in a current of gas N85-22725

THERMAL DECOMPOSITION
Kinetics of mechanism of the thermal decomposition of dimethylnitramine and dimethylnitrosamine N85-22559
Theory of relaxation processes in decomposing polymer materials during high-intensity convective heating N85-22710
Metallic and metallocermic coating by thermal decompositon [NASA-TM-86992] N85-22755

THERMAL DEGRADATION
Laboratory studies of Kapton degradation in an oxygen ion beam N85-22477

THERMAL EMISSION
Hot spots on Io: Correlation of infrared emission and visible reflectance N85-23475

THERMAL EXPANSION
Fracture mechanics evaluation of GaAs [NASA-CR-175657] N85-23101

THERMAL INSULATION
Environmental cycling of cellulosic thermal insulation and its influence on fire performance [DE85-004295] N85-22778

THERMAL MAPPING
Geologic interpretation of remote sensing data for the Martian volcano, Ascraeus Mons N85-23606
Water-ice clouds on Mars: Location and seasonal variation N85-23611

THERMAL NOISE
Mathematical model of discriminator for signals with fluctuations and thermal noise N85-22943

THERMAL PROTECTION
Electron beam charging of Space Shuttle thermal protection system tiles N85-22475

THERMAL RESISTANCE
Possibility of producing monolithic composite materials based on niobium carbide N85-22707
System for forming and focusing high current beam of deuterium ions N85-22798
Measurement of internal thermal resistance for quality control of semiconductor devices N85-22953

THERMAL SHOCK
Possibility of producing monolithic composite materials based on niobium carbide N85-22707
Dispersed-metal-toughened alumina [NASA-CR-174687] N85-22758

THERMAL STABILITY
Stability of three-layer glass-reinforced plastic shells of rotation N85-22813

THERMAL STRESSES
Optimization of overall dimensions of enclosures for low-voltage devices and equipment N85-23033

THERMOCHEMISTRY
Combustion kinetics of metal atoms and metallic radicals over wide temperature ranges N85-22530

THERMOCOUPLES
Results of aeroheating DFI and ET design-data test on a 0.0175-scale model 60-OTS conducted in the Von Karman Gas Dynamics Facility (VKF) 40' supersonic and the 50' hypersonic wind tunnels A and C [NASA-CR-167693] N85-22466
Low temperature calibration fixture [DE85-003969] N85-23071

THERMODYNAMIC PROPERTIES
Efficiency of algorithms for gas-air channel diagnostics in gas turbine engines based on gas thermodynamic parameters N85-22823
Thermodynamic and kinetic studies of pulsed laser annealing from transient conductivity measurements [DE85-003677] N85-23078

THERMODYNAMICS
Clustering and ordering in 3-5 alloys [AD-A150604] N85-22670
Thermodynamics of copper-nickel alloys containing aluminum, silicon, titanium, and chromium relative to their use in ceramic brazing [DE85-004787] N85-22674
Some unique features of isentrophic flow of gas under high pressures N85-22788
Impact and collisional processes in the solar system N85-23530
Theoretical thermodynamics of mixtures at high pressures N85-23550

THERMOELASTICITY
Effects of triazine components on physicochemical properties of polybutadiene: urethane block copolymers N85-22635

THERMOELECTRIC MATERIALS
Electrical and thermal transport property studies of high-temperature thermoelectric materials [AD-A150167] N85-23417

THERMOELECTRICITY
Electrothermal transducer with short time constant N85-23040
Electrical and thermal transport property studies of high-temperature thermoelectric materials [AD-A150167] N85-23417

THERMOHYDRAULICS
Thermohydrodynamic model: Hydrothermal system, shallowly seated magma chamber N85-23173

THERMOMECHANICAL TREATMENT
Developing procedures for thermomechanical processing of high-durability VT22 titanium alloy N85-22726

THERMOMETERS
Low temperature calibration fixture [DE85-003969] N85-23071

THERMOPLASTIC RESINS
Stability of three-layer glass-reinforced plastic shells of rotation N85-22813

THERMOREGULATION
Sleep deprivation and exercise tolerance [AD-A150566] N85-23296

THERMOSPHERE
Analysis and interpretation of observations of airglow at 297 nm in the Venus thermosphere N85-23473

THICK PLATES
Method of separately determining electrophysical properties of bulky conductor N85-22951

THICKNESS
Analysis of optimum front cover thickness for lightweight solar arrays N85-22606
Composition and thickness of oxide coatings on granule surfaces of aluminum alloys N85-22719
Spectral frequency of eigenvalues in optimal problems of stability of cylindrical shells of variable thickness N85-22815
Thickness of ridged plains materials in Hesperia Planum, Mars N85-23561

THIN FILMS
Mass spectra of neutral particles released during electrical breakdown of thin polymer films N85-22511
Microscopic magnetic structure of multiple bilayers of thin films of Fe and Ge [DE85-004188] N85-22682
Structure of amorphous films of alloys based on Fe, condensed from laser erosion products N85-22749
Planar ferroelectric microcapacitors for microwave devices N85-23032
Non-linear optical techniques for visible and UV lasers and thin film deposition [AD-A150489] N85-23077

THIN PLATES
Experimental and numerical analysis of electric currents and electromagnetic blunting of cracks in thin plates [AD-A150418] N85-22669
Breakdown of thin plates by radiation N85-22709
Pre- and post-processing for stream-function eddy current calculations [AD-A150417] N85-22896

THIN WALLED SHELLS
Elasticity formulas for thin-walled shells with piszoceramic layers N85-22816

THIN WALLS
Effect of protective medium on durability and fracture structure on seam zones of thin-walled titanium articles produced by diffusion welding N85-22738
Theory of diaphragm light modulators with electrical input signal N85-23002

THIOLS
Formation of high molecular weight products from benzene during boundary lubrication [NASA-TM-86966] N85-22644

THOMAS-FERMI MODEL
Theoretical thermodynamics of mixtures at high pressures N85-23550

THOMSON SCATTERING
Feasibility of alpha particle measurement by CO2 laser Thomson scattering [DE85-004938] N85-23081

THREE BODY PROBLEM
Lagrangian solutions in photogravitational restricted circular three-body problem N85-22416
Computation of elliptical functions in problems of celestial mechanics N85-22418

THREE DIMENSIONAL FLOW
On the solution of the three-dimensional flowfield about a flow-through nacelle [NASA-TM-87448] N85-22371
Preliminary development of an approximation procedure for supercritical wing design optimization applications [AD-A150177] N85-22383

THREE DIMENSIONAL MOTION
Cyclic industrial robots with mechanical energy storing devices: Multipositional system with one or several degrees of freedom N85-22803
Stability of Rossby waves within framework of three-component analysis N85-23142

THYRATRONS
Non-self-maintained high-voltage low-pressure discharge N85-23037

TIDES
Field-work report: Medway Estuary, 28 June - 18 July 1983 [RNC/NS/TR8] N85-22773
Stability of the Galilean satellites in deep orbital resonance N85-23477

TILES
Electron beam charging of Space Shuttle thermal protection system tiles N85-22478

TIMBER IDENTIFICATION
An initial analysis of LANDSAT-4 Thematic Mapper data for the discrimination of agricultural, forested wetlands, and urban land cover — Poinsett County, Arkansas; and Reelfoot Lake and Union City, Tennessee N85-23193

TIME DEPENDENCE
Research program on the effect of pressure on the mechanical properties of polymers, part 2 [DE85-000995] N85-22761
Time-dependent flow of stream swirled in vortex chamber N85-22786
Time dependent interaction of internal pressure wave with system of two spherical shells N85-22809
Time-resolved ellipsometry and reflectivity measurements of the optical properties of silicon during pulsed excimer laser irradiation [DE85-005091] N85-23079
Nonrelativistic Kapitza-Dirac scattering [AD-A150622] N85-23405

TIME DIVISION MULTIPLE ACCESS
Assessment of effectiveness of signal-code constructions in time division-multi-access satellite systems N85-22908

TIME FUNCTIONS
Reflected wave travel-time curves in stratified media with vertically heterogeneous layers and slightly sloping curved boundaries N85-23167

TIME SERIES ANALYSIS
Approaches and algorithms for robust signal processing N85-22878
Markov method for simulating non-Gaussian wind speed time series [DE85-003450] N85-23284

TIN ALLOYS
Basis and pyramidal slipping in single crystals of alpha-alloy Ti-Al-Sn N85-22730

TIP DRIVEN ROTORS
Experimental study of main rotor tip geometry and tail rotor interactions in hover. Volume 1. Text and figures [NASA-CR-177336-VOL-1] N85-22344
Experimental study of main rotor tip geometry and tail rotor interactions in hover. Volume 2: Run log and tabulated data [NASA-CR-177336-VOL-2] N85-22345

TITAN
Research in planetary studies and operation of Mauna Kea Observatory [NASA-CR-175618] N85-23460
Giant planets and their satellites: Cosmochemistry, evolution and structure N85-23494

TITANIUM
Rational use of tatanium in nonferrous metallurgy N85-22728
Studies of electrical properties of surface films and localization during electrochemical dimensional working of titanium N85-22729

TITANIUM ALLOYS
Effect of phase state of TiC-NiTi powder composite materials on nature of failure and mechanical properties N85-22702
Decomposition of VTAN alloy solid solution upon irradiation and thermal aging N85-22712
High temperature antifriction properties of Ti sub 1-sub xNb sub x C sub 0.5N sub 0.5 alloys N85-22715
Developing procedures for thermomechanical processing of high-durability VT22 titanium alloy N85-22726
Influence of annealing on cyclic and short-term strength of thin sheets of VT1-0 titanium and OTR4 alloy N85-22727
Basis and pyramidal slipping in single crystals of alpha-alloy Ti-Al-Sn N85-22730
Specifics of structure and mechanical properties of metastable beta-titanium alloys after deformation and aging N85-22731
Properties of welded joints in argon arc welding of titanium alloy using a protective coating N85-22733
Thermal hardening of welded joints in titanium alloys with various structures N85-22734
Effect of protective medium on durability and fracture structure on seam zones of thin-walled titanium articles produced by diffusion welding N85-22738
Technological parameters of diffusion welding processes in honeycomb titanium alloy structures N85-22739

TITANIUM CARBIDES
Particulate toughened silicon carbide [DE85-004797] N85-22643

TITANIUM COMPOUNDS
Critical current measurements on an NbTi superconducting wire standard reference material [PB85-118594] N85-22906

TITANIUM NITRIDES
Structural distortions of ultra-dispersed titanium nitride powders N85-22717

TOKAMAK DEVICES
Winding insulation in electromagnetic systems for Tokamak reactor plants N85-23035
Lower hybrid heating and current drive, and ion cyclotron heating experiments on the Alcator C and the Versator II Tokamaks [DE85-004918] N85-23412

TOLERANCES (MECHANICS)
Advanced life analysis methods. Volume 1: Cracking data survey and NDI (nondestructive inspection) assessment for attachment lugs [AD-A150419] N85-23108
Advanced life analysis methods. Volume 2: Crack growth analysis methods for attachment lugs [AD-A150420] N85-23109

TOLERANCES (PHYSIOLOGY)
Sleep deprivation and exercise tolerance [AD-A150180] N85-23295
Sleep deprivation and exercise tolerance [AD-A150566] N85-23296
Sleep deprivation and exercise tolerance [AD-A150626] N85-23297

TOMOGRAPHY
NDE methods for green ceramics [DE85-004019] N85-22766
Optical processing in radon space [AD-A150289] N85-23402
TOOLING
New tooling for plasma cutting technology N85-22842
TOPOGRAPHY
Hypsometric features on Venus N85-22439
Evaluating accuracy in orientation of topographic photograph and satellite-centered direction from star photograph N85-22442
Development, achievements in China's cartography work N85-23434
Topographic evidence for shield volcanism on Io N85-23478
The support of long wavelength loads on Venus N85-23515
Newly discovered Martian impact basins N85-23544
Mapping structures characteristic of the highland boundary scarp on Mars N85-23595
Mercury radar altimetry: A preliminary analysis N85-23631
Unsupervised classification of global radar units on Venus N85-23632
Mapping and geological analysis of Mercury and Venus radar ranging data N85-23633
Correction and geological analysis of lunar 3.8 cm radar data N85-23634
Mars radar catalog N85-23636
The deep structure of lunar basins: Clues to the understanding of basin formation and modification N85-23647
Mars: Stratigraphy of western highlands and polar regions N85-23653
The Galilean Satellite Geological Mapping Program, 1984 N85-23664
TOPOLOGY
Relationship between topological and magnetic order in small metal clusters [AD-A150547] N85-22651
Method for processing broad-profile data N85-23185
TORSIONAL STRESS
Steady-state reaction of three-layered cylindrical shell to effect of moving load N85-22611
TOUGHNESS
Interlaminar fracture toughness in resin matrix composites [AD-A150565] N85-22640
Particulate toughened silicon carbide [DE85-004797] N85-22643
TOXICITY
Interaction of metals and metalloids with biomembranes [DE85-004902] N85-23293
TRACKING (POSITION)
Technical manual: Description and operation Slaved Tracking System [DE85-004807] N85-23070
TRACKING FILTERS
Synthesis of optimum algorithms for secondary processing N85-22992
TRACKING RADAR
Avionics Flight Evaluation System (AFES) N85-22357
TRAILING EDGES
Aerodynamic heating rate distributions induced by trailing edge controls on hypersonic aircraft configurations at Mach 8 [NASA-TM-87453] N85-22370
TRAJECTORY ANALYSIS
Rejection of anomalous observations when determining spacecraft trajectories N85-22421
TRAJECTORY CONTROL
Space interception guidance with uncertain factors N85-22781
TRAJECTORY MEASUREMENT
Rejection of anomalous observations when determining spacecraft trajectories N85-22421
TRAJECTORY OPTIMIZATION
Algorithm for determining optimal three impulse point-to-orbit transfer with limited transfer time N85-22419
Synthesis of optimum algorithms for secondary processing N85-22992
TRANSDUCERS
Rocket body charge neutralization processes in ARAKS experiment (data from two launches) N85-22426
Programmable filter with fanned interdigital surface acoustic wave transducer N85-23008
Electrothermal transducer with short time constant N85-23040
TRANSFER OF TRAINING
China report: Science and technology [JPRS-CST-85-003] N85-23433
TRANSFER ORBITS
Algorithm for determining optimal three impulse point-to-orbit transfer with limited transfer time N85-22419
TRANSIENT RESPONSE
Laboratory studies of spacecraft response to transient discharge pulses N85-22506
Hydrodynamic simulation of transient processes in injection system of aircraft engines during pump unswirling N85-22629
Transient analysis of loaded thin-wire antennas and transmission lines N85-22852
Research efforts in support of resonance extraction studies. Volume 1: Improvement and validation of TWFD (Thin-Wire Frequency-Domain): A thin-wire frequency-domain scattering code [AD-A150296] N85-22864
TRANSISTOR AMPLIFIERS
Playback amplifier with high interference immunity N85-22970
TRANSISTOR CIRCUITS
Recommendation on use of series K157UL1 microcircuits N85-22936
TRANSISTOR LOGIC
Development of a planar heterojunction bipolar transistor for very high speed logic [AD-A150374] N85-22895
TRANSISTORS
Code lock with microcircuit N85-22935
TRANSLATIONAL MOTION
Absolute movement of Pacific Ocean plate during last 120 million years N85-23126
TRANSMISSION
Temperature dependence of propagation of high-current electron beam through drift space N85-22982
TRANSMISSION EFFICIENCY
Recommendation on use of series K157UL1 microcircuits N85-22936
TRANSMISSION LINES
Transient analysis of loaded thin-wire antennas and transmission lines N85-22852
Interference immunity of fiber-optic communication lines with spectral multiplexing of channels N85-22924
AL-124 light-emitting diode in 30 Mbit/s fiber-optic communication line N85-22925
Synthesis of low-pass filters using coupled lines with unmatched loads N85-22938
Possibilities of aerial electric prospecting by long cable method for detecting poorly conducting strata N85-23177
TRANSMISSION LOSS
Optical reflectometer for multimode fiber lightpipes N85-22961
Ice statistics and acoustic scattering in the Arctic basin [AD-A150141] N85-23289
TRANSMISSIONS (MACHINE ELEMENTS)
Design of tightening device and calculation of forces in manipulator transmissions with base-drive mounted N85-22804
TRANSMISSIVITY
Fine structure of vertical distribution of light attenuation index of sea water N85-23140
TRANSMITTER RECEIVERS
Firefighters' communication transceiver test plan [NASA-CR-171419] N85-22854
TRANSONIC FLOW
Preliminary development of an approximation procedure for supercritical wing design optimization applications [AD-A150177] N85-22383
TRANSONIC WIND TUNNELS
Calibration of wind tunnel flow quality N85-22399
TRANSPARENCE
Effect of transparent coatings on generation of laser-induced shock waves in metals N85-22711
TRANSPIRATION
Pressure drop and coefficients of internal heat transfer necessary for transpiration cooling N85-22831
TRANSPORT AIRCRAFT
Guidance and control research flight testing with HFB 320 test aircraft N85-22355
Study for the optimization of a transport aircraft wing for maximum fuel efficiency. Volume 1: Methodology, criteria, aeroelastic model definition and results [NASA-CR-172551] N85-22378
China report: Science and technology [JPRS-CST-84-008] N85-22384
Improved Y-11 general-purpose transport designated Y-12 N85-22385
Assessing the behavior and performance of teams in organizations: The case of air transport crews [AD-A150359] N85-23302
TRANSPORT PROPERTIES
The ASCOT Data Analysis Workshop [DE85-004407] N85-23283
Electrical and thermal transport property studies of high-temperature thermoelectric materials [AD-A150167] N85-23417
Transport properties of silica thermally grown on silicon [AD-A150304] N85-23418
TRANSPORT THEORY
Polar cap formation on Ganymede N85-23486
TRANSVERSE ACCELERATION
Axisymmetrical oscillations of shell systems subjected to impulse loads N85-22814
TRAVELING WAVE MASERS
Millimeter-wave range masers: A review N85-23042
TRAVELING WAVES
Reflected wave travel-time curves in stratified media with vertically heterogeneous layers and slightly sloping curved boundaries N85-23187
TREES (MATHEMATICS)
Synthesis of tree-structured computing systems through use of closures [AD-A150502] N85-23326
Parallel update of minimum spanning trees in logarithmic time [AD-A150497] N85-23357
TREES (PLANTS)
Areas with forest soils sensitive to acidic deposition under alternative damage hypotheses [DE85-005257] N85-23257
TRIAMINOGUANIDINIUM AZIDE
The crystal and molecular structure of a new propellant compound: Triaminoguanidium Azide Nitrate (TAZN) N85-22551
TRIBOLOGY
Thermal and thermoelastic effects in rolling/sliding contacts [AD-A150435] N85-23429
TRIGGER CIRCUITS
Low jitter trigger for an excimer laser [DE85-005732] N85-23080
TRITON
Research in planetary studies and operation of Mauna Kea Observatory [NASA-CR-175618] N85-23460
On the origin of Triton and Pluto N85-23497
TROPICAL REGIONS
Slow motions in the tropical troposphere N85-23262
A theoretical study of the ozone quasi-biennial oscillation in the tropical stratosphere N85-23264
Cumulus effects on the large-scale vorticity and momentum fields in the tropical atmosphere N85-23270
TROPOSPHERE
Slow motions in the tropical troposphere N85-23262
Cumulus cloud venting of mixed layer ozone [NASA-TM-87429] N85-23269
Cumulus effects on the large-scale vorticity and momentum fields in the tropical atmosphere N85-23270
TTL INTEGRATED CIRCUITS
AL-124 light-emitting diode in 30 Mbit/s fiber-optic communication line N85-22925
TURBINE BLADES
Energy losses at leading edge of turbine blade during multirow jet cooling N85-22826
effect of gas stream sweeping past the effluent of a perforated plate on heat transfer inside the perforations N85-22836
TURBINE ENGINES
Pressure drop and coefficients of internal heat transfer necessary for transpiration cooling N85-22831
Composition and photochemical reactivity of turbine engine exhaust [AD-A150559] N85-23256
TURBOCOMPRESSORS
Some unique features in operation of two-stage turbojet engine with afterburner N85-22828
HPFTP flow diverter analysis [NASA-CR-171424] N85-23057
T700 cutter life improvement program [AD-A150450] N85-23089
TURBOFAN ENGINES
On the solution of the three-dimensional flowfield about a flow-through nacelle [NASA-TM-87448] N85-22371
Effects of inlet distortion on a static pressure probe mounted on the engine hub in an F-15 airplane [NASA-TP-2411] N85-22394
TURBOFANS
Structural response of a rotating bladed disk to rotor whirl [NASA-CR-175605] N85-22391
TURBOJET ENGINES
Propagation of three-dimensional turbulent jet from lobar nozzle through surrounding stream N85-22785
Exergetical analysis of turbojet engine cycle N85-22825

Some unique features in operation of two-stage turbojet engine with afterburner N85-22828

TURBOMACHINE BLADES
Current problems in turbomachinery fluid dynamics [AD-A150533] N85-22397

TURBOMACHINERY
Current problems in turbomachinery fluid dynamics [AD-A150533] N85-22397

TURBULENCE
Intensity fluctuations of focused laser beam during reflection in turbulent atmosphere N85-22975
Mean flow and turbulence in complex terrain NPS (Naval Postgraduate School)/Vandenberg measurement system [AD-A150194] N85-23274
Evolution of grains in a turbulent solar nebula N85-23525

TURBULENCE METERS
Turbulence measurements in shock induced flows N85-23055

TURBULENT DIFFUSION
Constraints of observations of solar oscillations on solar models with mixing by turbulent diffusion [DE85-003741] N85-23678

TURBULENT FLOW
Turbulent flows of surfacant solutions [AD-B089137L] N85-23058
Flow-induced vibrations of a circular cylinder due to turbulent internal flows [DE85-002766] N85-23110
Evolution of set of Rossby waves toward anisotropic equilibrium state N85-23141

TURBULENT JETS
Deflected jet experiments in a turbulent combustor flowfield [NASA-CR-174863] N85-22390

TURBULENT MIXING
Propagation of three-dimensional turbulent jet from lobar nozzle through surrounding stream N85-22785
Time-dependent flow of stream swirled in vortex chamber N85-22786

TURBULENT WAKES
Method for the prediction of the installation aerodynamics of a propfan at subsonic speeds [NASA-CR-3687] N85-22369

TWO BODY PROBLEM
Accumulation of the terrestrial planets N85-23524

TWO DIMENSIONAL FLOW
Propagation of three-dimensional turbulent jet from lobar nozzle through surrounding stream N85-22785
Evolution of set of Rossby waves toward anisotropic equilibrium state N85-23141
Stability of Rossby waves within framework of three-component analysis N85-23142

TWO DIMENSIONAL JETS
Large amplitude forcing of a high speed 2-dimensional jet [NASA-CR-175646] N85-22393

U

U.S.S.R.
New method of reconstructing conditions of recent differentiation of oil and gas in the Amudarya Basin (based on results of interpretation of space photographs) N85-22446
Current plans for development of chemical industry N85-22633
USSR report: Electronics and electrical engineering [JPRS-UEE-85-002] N85-22907
Possibilities of aerial electric prospecting by long cable method for detecting poorly conducting strata N85-23177

U.S.S.R. SPACE PROGRAM
Feoktistov says manned lunar, Mars flights lack justification N85-22452
U.S., Soviet space program aims contrasted N85-22455

ULTRASONIC RADIATION
Investigations of ultrasonic wave interactions at boundaries separating anisotropic materials [DE85-003506] N85-23384

ULTRASONIC TESTS
Investigation of steel structures using ultrasonic waves [BR93256] N85-23091

ULTRASONICS
Elastic wave scattering from cavities and sound inclusions analyzed by the resonance method [AD-A150315] N85-23381

ULTRAVIOLET ABSORPTION
Cumulus cloud venting of mixed layer ozone [NASA-TM-87429] N85-23269

ULTRAVIOLET LASERS
Non-linear optical techniques for visible and UV lasers and thin film deposition [AD-A150489] N85-23077

ULTRAVIOLET SPECTRA
A survey for galactic plane ultraviolet-excess objects: Space densities for white dwarfs, subdwarfs, and cataclysmic variables N85-23458
Ultraviolet spectral diagnostics of solar flares and heating events N85-23675

ULTRAVIOLET SPECTROMETERS
Ozone Correlative Measurements Workshop [NASA-CP-2362] N85-23112
Scientific requirements for ozone measurements N85-23113
Method for determining the number of correlative measurements required to validate the SBUV/2 ozone retrievals N85-23114

UNDERWATER ACOUSTICS
Numerical results of acoustic radiation, transmission and reflection of steel plate in water [AMTE(N)-TM-84037] N85-23378
Vertical discrimination in the sound channel [AD-A150254] N85-23380

UPPER ATMOSPHERE
Increase in hydrogen emission of upper atmosphere following launches of space vehicles N85-22431

URANUS (PLANET)
Research in planetary studies and operation of Mauna Kea Observatory [NASA-CR-175618] N85-23480
Giant planets and their satellites: Cosmochemistry, evolution and structure N85-23494
The structure and composition of Uranus and Neptune N85-23495
Studies of icy bodies: Uranian satellites and cometary nuclei N85-23496

URBAN RESEARCH
An initial analysis of LANDSAT-4 Thematic Mapper data for the discrimination of agricultural, forested wetlands, and urban land cover — Poinsett County, Arkansas; and Reelfoot Lake and Union City, Tennessee N85-23193

USER MANUALS (COMPUTER PROGRAMS)
ROSA: A computer model for optical power ratio calculations [DE85-005174] N85-23251
M68000 RNF text formatter user's manual [NASA-TM-86327] N85-23320
SIGPI: A user's manual for the fast computation of the probabilistic performance of a complex system [DE85-005447] N85-23336
User's and programmer's guide to the mechanics of moving finite element code [DE85-006165] N85-23365

V

VACUUM
High temperature antifriction properties of Ti sub 1-sub xNb sub x C sub 0.5N sub 0.5 alloys N85-22715

VALLEYS
Paleohydrologic implications of valley networks of Mars N85-23585
Geomorphology and geology of the Southwestern Margaritifer Sinus and Argyre regions of Mars. Part 1: Geological and geomorphological overview N85-23600
Geomorphology and geology of the Southwestern Margaritifer Sinus and Argyre regions of Mars. Part 3: Valley types and distribution N85-23602
Late Tertiary and Quaternary river systems of the eastern Sahara as mapped on shuttle radar and LANDSAT images N85-23641

VANADIUM
Improvement in magnetic field properties of vanadium-gallium superconductors by enhancement of spin-orbit scattering [DE85-002893] N85-23422

VANADIUM ALLOYS
Decomposition of VTAN alloy solid solution upon irradiation and thermal aging N85-22712

VANADIUM OXIDES
Metal-semiconductor phase transition and its application [DRIC-T-7149] N85-22665

VAPOR PHASES
Chemical kinetics of gas phase decomposition products of nitramine propellants N85-22558

VARIABILITY
Ozone Correlative Measurements Workshop [NASA-CP-2362] N85-23112
Scientific requirements for ozone measurements N85-23113

VARIABLE STARS
A model for eclipsing cataclysmic variables N85-23467

VARIANCE (STATISTICS)
Optimal designs for comparisons between two sets of treatments [AD-A150621] N85-23360

VARIATIONAL PRINCIPLES
On Hybrid and mixed finite element methods [NASA-CR-175551] N85-23096
On an iterative scheme for the solution of constrained variational equations [CSIR-TWISK-341] N85-23342

VARIATIONS
Observation of cosmic ray flux variations in stratosphere N85-22430
Variations in resistivity of upper crustal layer N85-23164
Method for processing broad-profile data N85-23185
The relationship between marine aerosol particles and satellite-detected radiance N85-23263

VARIOMETERS
Primary processing of experimental magnetovariation sounding data using spline functions N85-23175

VECTOR ANALYSIS
Characteristic vector analysis of inflection ratio spectra: New technique for analysis of ocean color data [NASA-TP-2428] N85-23237

VECTORS (MATHEMATICS)
Determining vector of radiointerferometer base from observations of natural radio emission with narrow spectrum N85-23158
Schur-Ostrowski theorems for functionals on l1(0,1) [AD-A150193] N85-23346

VEGA PROJECT
USSR report: Space [JPRS-USP-85-001] N85-22403

VEGETATION
Preliminary comparisons of the information content and utility of TM versus MSS data N85-23202
The microwave propagation and backscattering characteristics of vegetation — wheat, sorghum, soybeans and corn fields in Kansas [E85-10088] N85-23213
Microwave remote sensing of soil moisture N85-23235

VEGETATIVE INDEX
Remote sensing of coastal wetlands biomass using Thematic Mapper wavebands — Lewes, Delaware N85-23198

VELOCITY COUPLING
Coupling between velocity oscillations and solid propellant combustion N85-22536
Coupled acoustic and hydrodynamic wave instabilities N85-22538
Investigation of the characteristics of the velocity-coupled response functions of solid propellants N85-22540

VELOCITY DISTRIBUTION
Dilution jet configurations in a reverse flow combustor [NASA-CR-174888] N85-22392
Size and velocity distributions of particles and droplets in spray combustion systems [AD-A150355] N85-22648
More precise curve of dependence between density and velocity of longitudinal waves in consolidated crust and top of mantle in oceanic structures N85-23143
Progress on Experimental impact studies N85-23534
Ring-diameter ratios for multi-ring basins average 2.0(0.5)D N85-23542

VELOCITY MEASUREMENT
Dilution jet configurations in a reverse flow combustor [NASA-CR-174888] N85-22392

VENERA 11 SATELLITE
Microstructure of Venus cloud layer based on spectrophotometric data from Venera-11 spacecraft N85-22436

VENTING
Cumulus cloud venting of mixed layer ozone [NASA-TM-87429] N85-23269

VENUS (PLANET)
Volcanism on Venus as connecting link N85-22433
Preliminary photomaps of Venus surface in the Maxwell Mountains and adjacent areas N85-22438
Analysis and interpretation of observations of airglow at 297 nm in the Venus thermosphere N85-23473
Characteristics of basaltic lava flows on Venus N85-23508
Venus surface composition from radio/radar measurements N85-23509
Surface units on Venus derived from Pioneer-Venus altimetry, roughness, and reflectivity measurements N85-23510
Classification of circular features on Venus N85-23511
Venus gravity: Global field results N85-23512
Geophysical interpretation of Venus gravity data N85-23513
Gravity field of Venus and comparison with Earth N85-23514
The support of long wavelength loads on Venus N85-23515

Venus chasmata: A lithosphere stretching model N85-23516
A statistical treatment of the regional slope characteristics of Venus and Earth N85-23517
The effect of particle density on aeolian transport N85-23581
Potential bedforms on Venus: Wind tunnel simulations N85-23583
Analyses of radar images of small craters N85-23642
Planetary interior modeling and tectonic implications N85-23649

VENUS ATMOSPHERE
Response of Earth's atmosphere to increases in solar flux and implications for loss of water from Venus N85-23518
The effect of particle density on aeolian transport N85-23581

VENUS CLOUDS
Microstructure of Venus cloud layer based on spectrophotometric data from Venera-11 spacecraft N85-22436

VENUS RADAR ECHOES
Progress in planetary radarclinometry N85-23630

VENUS SURFACE
Visualization of radar altimetry data for Venus N85-22437
Preliminary photomaps of Venus surface in the Maxwell Mountains and adjacent areas N85-22438
Hypsometric features on Venus N85-22439
Volcanism and rift formation in Beta Regio, Venus: New radar results N85-23507
Characteristics of basaltic lava flows on Venus N85-23508
Venus surface composition from radio/radar measurements N85-23509
Surface units on Venus derived from Pioneer-Venus altimetry, roughness, and reflectivity measurements N85-23510
Classification of circular features on Venus N85-23511
Venus gravity: Global field results N85-23512
Geophysical interpretation of Venus gravity data N85-23513
The support of long wavelength loads on Venus N85-23515
Venus chasmata: A lithosphere stretching model N85-23516
A statistical treatment of the regional slope characteristics of Venus and Earth N85-23517
Potential bedforms on Venus: Wind tunnel simulations N85-23583
Microdunes and other aeolian bedforms on Venus: Wind tunnel simulations N85-23584
Unsupervised classification of global radar units on Venus N85-23632
Analyses of radar images of small craters N85-23642

VERTICAL DISTRIBUTION
Special features of computations of vertical distribution of concentration of suspended sediments under marine conditions N85-23125

VERTICAL ORIENTATION
Vertical discrimination in the sound channel [AD-A150254] N85-23360
High-frequency acoustic variability in the arctic [AD-A150550] N85-23363

VERY HIGH FREQUENCIES
A fully distributed approach to the design of a 16 K bit/sec VHF packet radio network [AD-A141282] N85-22859

VERY LARGE SCALE INTEGRATION
X-ray lithography and VLSI circuits N85-22846
Periodic binary sequence generators: VLSI circuits considerations [NASA-CR-175649] N85-22886
EOS (electrical overstress) protection for VLSI (Very Large Scale Integration) devices [AD-A150333] N85-22891

VERY LONG BASE INTERFEROMETRY
Studies of galactic HI in 21-centimeter absorption N85-23466

VESTA ASTEROID
Asteroid collisional evolution studies N85-23501

VIBRATION
Nonlinear rotordynamics analysis [NASA-CR-171425] N85-22364
Normal mode calculations for fuselage type intricate structures by regarding them as systems with superposed constraints N85-22817
The Shock and Vibration Digest, volume 16, no. 12 [AD-A150594] N85-23102
Machine tool vibrations: A review N85-23104
Flow-induced vibrations of a circular cylinder due to turbulent internal flows [DE85-002766] N85-23110

VIBRATION DAMPING
A quantitative comparison of active and passive damping for large space structures [UTIAS-TN-249] N85-22524

VIBRATION MEASUREMENT
Applications of the vibration probe to localized current measurements [DE85-004702] N85-22675

VIBRATION MODE
Spline-based Rayleigh-Ritz methods for the approximation of the natural modes of vibration for flexible beams with tip bodies [NASA-CR-172566] N85-23100

VIBRATION TESTS
Vibroacoustic study of the NASA Goddard Space Flight Center OSS-1 payload [NASA-CR-175320] N85-22485

VIBRATIONAL SPECTRA
Adsorption site, adsorption energy and normal vibration frequency of H/Ni(100) via total energy calculations [AD-A150555] N85-23388
Observation of surface vibrational resonances on (110) surfaces of FCC metals [AD-A150469] N85-23419
Dipole active surface vibrational resonances on clean and hydrogen covered Ni(110) [AD-A150546] N85-23420

VIDEO COMMUNICATION
Combined processing method and matched filter for discrete composite frequency phase-shift keyed signal N85-22931

VIDEO DATA
Performance of time-position discriminator of composite signal N85-22941

VIKING LANDER SPACECRAFT
The search for igneous materials at the Viking landing sites N85-23609

VIKING LANDER 1
Observed changes at Viking Lander 1 N85-23575

VIKING SPACECRAFT
Participation in the Mars Data Analysis Program: Analysis of cloud forms in Viking and Mariner 9 images [NASA-CR-175604] N85-23673

VINYL POLYMERS
Chiral polymers [AD-A150366] N85-22760

VINYLIDENE
Synthesis and characterization of poly(vinylidene fluoride) [AD-A150291] N85-22759

VISCOELASTIC DAMPING
A quantitative comparison of active and passive damping for large space structures [UTIAS-TN-249] N85-22524

VISIBLE SPECTRUM
Non-linear optical techniques for visible and UV lasers and thin film deposition [AD-A150489] N85-23077
Spectral units on Europa and Ganymede N85-23621

VISUAL FLIGHT RULES
Analysis of estimation algorithms for CDTI and CAS applications [NASA-CR-172444] N85-22387

VOICE COMMUNICATION
Low-bit rate speech encoders based on Line-Spectrum Frequencies (LSF) [AD-A150518] N85-22871

VOLATILITY
Magmas as selective filters of volatiles between planetary mantles and surfaces N85-23557

VOLCANOES
Volcanism on Venus as connecting link N85-22433
Sulfur volcanoes on Io? N85-23479
Geomorphic classification of lava flows on Io N85-23480
Volcanism and rift formation in Beta Regio, Venus: New radar results N85-23507
Volcanic debris flows in the Elysium region of Mars N85-23560
Estimates of lava eruption rates at Alba Patera, Mars N85-23562
Thermal infrared observations of lava flows during the 1984 Mauna Loa eruption N85-23564
Field measurements of the 1983 Royal Gardens lava flows, Kilauea Volcano, and 1984 Mauna Loa lava flows, Hawaii N85-23565
Surface structures of Hawaiian lavas N85-23566
Morphologic evolution of the Mount St. Helens crater area, Washington N85-23568
Volcanism of the Colorado Plateau (basin and range transition): Implications for crustal processes N85-23569
The geology of East Butte, a rhyolitic volcanic dome on the Eastern Snake River Plain, Idaho N85-23570
A silicic shield volcano in Bolivia N85-23572
Submarine volcanic eruptions and potential analogs for Venus N85-23573
Terrestrial analogs for planetary wrinkle ridges N85-23644

VOLCANOLOGY
Structure of Iceland and ocean floor spreading N85-23159
Magmatism in continent-ocean transition zone (development of ideas of A. N. Zavaritskiy) N85-23161
Planetary geology in the 1980s [NASA-SP-467] N85-23457
Reports of the Planetary Geology and Geophysics Program, 1984 [NASA-TM-87563] N85-23474
Topographic evidence for shield volcanism on Io N85-23476
Estimates of lava eruption rates at Alba Patera, Mars N85-23562
Emplacement of long lava flows on Mauna Loa (Hawaii) and Alba (Mars) N85-23563
Thermal infrared observations of lava flows during the 1984 Mauna Loa eruption N85-23564
Volcanism of the Colorado Plateau (basin and range transition): Implications for crustal processes N85-23569
The geology of Mt. Hope, a silicic volcanic center in West Central Arizona N85-23571
Hydrovolcanism N85-23574

VOLT-AMPERE CHARACTERISTICS
Planar ferroelectric microcapacitors for microwave devices N85-23032

VOLTAGE REGULATORS
Problems with electrical interference between solar generators and shunt type regulators N85-22607

VOLTMETERS
Application of modulated hydrodynamic voltammetry to the study of anodic electrocatalysis [DE85-004182] N85-22653

VORTEX FLAPS
Calculation of vortex-flap aerodynamic characteristics [NASA-CR-175624] N85-22367

VORTEX SHEDDING
Nonlinear interactions between vortices and acoustic waves in a rocket combustion chamber N85-22533
Acoustic energy exchange in sheared mean flows — solid rocket motors N85-22534

VORTICES
Study for prediction of rotor/wake/fuselage interference, part 1 [NASA-CR-177340-VOL-1] N85-22346
Study for prediction of rotor/wake/fuselage interference. Part 2: Program users guide [NASA-CR-177340-VOL-2] N85-22347
Method for the prediction of the installation aerodynamics of a propfan at subsonic speeds [NASA-CR-3687] N85-22369
Deflected jet experiments in a turbulent combustor flowfield [NASA-CR-174863] N85-22390
Propagation of three-dimensional turbulent jet from lobar nozzle through surrounding stream N85-22785
Time-dependent flow of stream swirled in vortex chamber N85-22786
Experimentally determined characteristics of vortex heaters N85-22833
Grid generation for a pump collector [AD-A150217] N85-23059
Double and inverse Taylor-Hogg vortices in a stratified ocean N85-23137
An experimental investigation of the chopping of helicopter main rotor tip vortices by the tail rotor [NASA-CR-177338] N85-23376

VORTICITY
Cumulus effects on the large-scale vorticity and momentum fields in the tropical atmosphere N85-23270

VOYAGER PROJECT
Sulfur volcanoes on Io? N85-23479
Geomorphic classification of lava flows on Io N85-23480
Sulfur oxygen processes on Io N85-23481
The violet absorber on Io: Disulfur monoxide derivatives N85-23482
Dark halo craters and the thickness of grooved terrain on Ganymede N85-23484
Formation of bright terrain bands on Ganymede by unstable lithosphere extension N85-23485
Investigations of planetary ring phenomena N85-23487
Dynamical studies of Saturn's rings N85-23489

VOYAGER 1 SPACECRAFT
Hot spots on Io: Correlation of infrared emission and visible reflectance N85-23475

VOYAGER 2 SPACECRAFT
Patterns of fracture and tidal stresses due to nonsynchronous rotation: Implications for fracturing on Europa N85-23483

W

WAFERS
A low cost approach with larger diameter silicon wafer — solar cells N85-22572
Multifunctional elements for integrated optics N85-22918
Time-resolved reflectivity measurement of extrinsic silicon during pulsed laser irradiation [AD-A150350] N85-23403
WAKES
Electron and ion density depletions measured in the STS-3 orbiter wake N85-22474
Polar orbit electrostatic charging of objects in shuttle wake N85-22487
Ram-wake effects on plasma current collection of the PIX 2 Langmuir probe N85-22496
WALLS
Experimental studies of low temperature surface interactions of atomic hydrogen using maser technique [AD-A150216] N85-22647
Optimization of overall dimensions of enclosures for low-voltage devices and equipment N85-23033
Overview of latent storage for passive solar applications [DE85-005354] N85-23249
Confinement properties of high energy density plasmas in the Wisconsin levitated octupole N85-23408
WALSH FUNCTION
Algorithm in Walsh function basis for analysis of integrated microcircuits on MOS-structures N85-23006
Use of Walsh functions for calculating characteristics of digital filters with impulse response of finite duration N85-23011
Investigation of influence of communications link and synchronization error on noise tolerence of group transmission of binary information based on orthogonal Walsh function N85-23026
WARFARE
Ground evaluation of helicopter air-to-air warfare N85-22360
WARNING SYSTEMS
Extraction of signals from background interference with unknown parameters in quantized sample N85-23013
WATER
Polar cap formation on Ganymede N85-23486
The evolution of CO2 on Mars N85-23558
Hydrovolcanism N85-23574
Mars: Long term changes in the state and distribution of H2O N85-23593
Radar and the detection of liquid water on Mars N85-23638
WATER CURRENTS
Field-work report: Medway Estuary, 28 June - 18 July 1983 [RNC/NS/TR8] N85-22773
WATER EROSION
Experiments and analyses of the formation of erosional scour marks with implications to the origin of the Martian outflow channels N85-23588
WATER FLOW
World ocean level oscillations and their relationship to change in inflow of continental waters N85-23133
WATER INJECTION
Estimation of gas turbine engine boost provided by injecting water behind compressor N85-22838
WATER POLLUTION
Determining adsorption of surface-active substances by sea bottom deposits N85-23128
WATER PRESSURE
Fine structure of vertical distribution of light attenuation index of sea water N85-23140
WATER QUALITY
Drifting ice as mechanical factor in purifying and polluting hydrosphere N85-23132
A first evaluation of LANDSAT TM data to monitor suspended sediments in lakes — Lake Chicot, Arkansas N85-23204
WATER RUNOFF
Remote Sensing of Snow and Evapotranspiration [NASA-CP-2363] N85-23223
General report of the researches of snowpack properties, snowmelt runoff and evapotranspiration in Japan N85-23225
Snowmelt-runoff model utilizing remotely-sensed data N85-23226
Snowmelt runoff model in Japan N85-23227
Distribution of snow and maximum snow water equivalent obtained by LANDSAT data and degree day method N85-23229
WATER TEMPERATURE
Fine structure of vertical distribution of light attenuation index of sea water N85-23140
A first evaluation of LANDSAT TM data to monitor suspended sediments in lakes — Lake Chicot, Arkansas N85-23204
WATER VAPOR
An atlas of nitrogen-broadened water vapor spectra from 500 to 5000 cm(-1), volume 1 [AD-A150527] N85-22650
Absorption of radiation by water vapor in windows of relative transparency of 95-145 micrometer range N85-22968
Below-room-temperature water-vapor continuum absorption within the 8- to 10 micron atmospheric transmission window [TR-0084(4945-09)-1] N85-23266
WATER WAVES
Relationship between brightness spectrum of photographic image and spectrum of rises on a water surface with waves N85-23171
WATERPROOFING
Results of the AFRSI rewaterproofing systems screening test in the NASA/Ames Research Center (ARC) 2 x 2-foot transonic wind tunnel [NASA-CR-167694] N85-22467
WAVE ATTENUATION
Applicability of log-normal model to probabilitistic description of quasi-pulse interference N85-23014
WAVE DIFFRACTION
Diffraction of plane TM-wave on continuously irregular elliptical plasma N85-22914
Calculation of amplitude-phase characteristics of signal scattered obliquely on meteor trail N85-22948
Intensity fluctuations of focused laser beam during reflection in turbulent atmosphere N85-22975
Problem of diffraction by wavy surface: Comparison of numerical methods of solution N85-22985
Diffraction of periodic grounding system of finite length N85-22994
Accuracy of random signal spectral parameter estimation against interference background in acoustooptical spectrum analyzers N85-23052
WAVE DISPERSION
Magnetostatic-wave propagation in a finite YIG-Loaded rectangular waveguide [AD-A150332] N85-22865
Intensity fluctuations of focused laser beam during reflection in turbulent atmosphere N85-22975
WAVE EXCITATION
Surface wave excitation study [DE85-005301] N85-22875
WAVE FRONT RECONSTRUCTION
Algorithms for reconstruction of partially known, band limited Fourier transform pairs from noisy data [AD-A150194] N85-23347
WAVE FRONTS
Ruby wavefront-conjugation laser for obtaining high temperature plasma N85-22795
WAVE GENERATION
Generation of longitudinal acoustic waves by modulated helicon waves — nonlinear steady state waves in metals N85-23049
WAVE INTERACTION
Coupling between velocity oscillations and solid propellant combustion N85-22536
Measurements of distributed combustion N85-22542
Stability of Rossby waves within framework of three-component analysis N85-23142
WAVE PROPAGATION
Magnetostatic-wave propagation in a finite YIG-Loaded rectangular waveguide [AD-A150332] N85-22865
Two-and-one-half dimensional in-plane wave propagation [AD-A150467] N85-22867
USSR report: Electronics and electrical engineering [JPRS-UEE-85-002] N85-22907
Mode control and wavelength tuning in open ended Michelson interferometric semiconductor laser N85-23073
Applications of the conformal mapping method to the solution of mechanical vibrations problems N85-23103
Regions of propagation of short-wave perturbations in spherical layer of rotating fluid N85-23130
Geomagnetic precursors of intensive earthquakes in the 1-0.-2 Hz frequency range of geomagnetic pulsations N85-23178
Seismic waves and dispersion relations N85-23181
Vertical discrimination in the sound channel [AD-A150254] N85-23360
Investigations of ultrasonic wave interactions at boundaries separating anisotropic materials [DE85-003506] N85-23364
WAVE REFLECTION
Three-mirror open resonator for millimeter wave band N85-22972
Interference flux during reflection of heterogeneous waves N85-22977
Axial focusing of signal from distant point radiator reflected twice in deep paraboloid N85-22979
Experimental verification of beam deflection from hybrid reflector antenna within wide-angle sector N85-22984
WAVE SCATTERING
Calculation of amplitude-phase characteristics of signal scattered obliquely on meteor trail N85-22948
Use of Bigaussian approximation to describe fading in scattering communications channel N85-23017
Elastic wave scattering from an interface crack in a layered half space N85-23095
Scattering of elastic waves on fractures randomly distributed in a three-dimensional medium N85-23151
WAVEFORMS
The use of a high-speed 12-bit A/D converter for digital sampling of communication signal carriers [AD-A150578] N85-22872
Invariance of probability characteristics of detector to shape of optical pulse signals N85-23048
Generation of longitudinal acoustic waves by modulated helicon waves — nonlinear steady state waves in metals N85-23049
WAVEGUIDE FILTERS
Optimal synthesis of surface acoustic wave filters N85-22933
WAVEGUIDES
Variational and moment method solutions of the fields in a parallel-plate waveguide-aperture system [DE85-006288] N85-22876
A 60 GHz 200 kW CW gyrotron with high output mode purity [DE85-005263] N85-22905
Diffraction of periodic grounding system of finite length N85-22994
WAVELENGTHS
Regions of propagation of short-wave perturbations in spherical layer of rotating fluid N85-23130
WAVES
Special features of computations of vertical distribution of concentration of suspended sediments under marine conditions N85-23125
WEAK ENERGY INTERACTIONS
Theoretical aspects of electroweak and other interactions in medium-energy nuclear physics [DE85-003821] N85-23392
WEAPON SYSTEMS
Air combat simulation: Methods, models, trends N85-22359
WEAR
Rational use of tatanium in nonferrous metallurgy N85-22728
Durability of VT16 alloy compounds obtained by diffusion welding N85-22740
Sliding seal materials for adiabatic engines [NASA-CR-174893] N85-22757
WEAR INHIBITORS
Effect of zero-wear in friction pairs operating in abrasive media N85-22801
WEATHER
El Nino, the capricious child N85-23121
Possibility of determining atmospheric weather parameters by radio and radiooptical measurements of refraction of cosmic sources N85-23146
Summary of Meteorological Observations, Surface (SMOS), Fallon, Nevada [AD-A150481] N85-23276
Summary of Meteorological Observations, Surface (SMOS) Camp Pendleton, California [AD-A150482] N85-23277
Summary of Meteorological Observations, Surface (SMOS), Bermuda [AD-A150537] N85-23278
Summary of Meteorological Observations, Surface (SMOS), Alameda, California [AD-A150609] N85-23281
WEATHER FORECASTING
New atmospheric sensor analysis study [NASA-CR-171426] N85-23069
Summary of Meteorological Observations Surface (SMOS), Sigonella, Sicily/Navy [AD-A150539] N85-23280
WEATHERING
Planetary analogs in Antarctica: Mars N85-23604
Iron oxides of Mars: Evidence for contemporary weathering N85-23613
WEIGHT REDUCTION
Development of Halley's Comet explorer PLANET-A solar array N85-22608

WELD STRENGTH
Influence of welding defects at melting boundary on static strength of welded joint in large-diameter pipe N85-22735
Technological parameters of diffusion welding processes in honeycomb titanium alloy structures N85-22739
WELDED JOINTS
Problem of pore formation mechanism in welded joints of aluminum alloys in the system aluminum-magnesium-lithium N85-22732
Properties of welded joints in argon arc welding of titanium alloy using a protective coating N85-22733
Thermal hardening of welded joints in titanium alloys with various structures N85-22734
Influence of welding defects at melting boundary on static strength of welded joint in large-diameter pipe N85-22735
Mechanical properties and brittle fracture resistance of welded multilayer elements for high pressure vessels N85-22736
Analysis of strength and ductility of welded joints in AMtsS and AMg5 aluminum alloys N85-22737
Effect of protective medium on durability and fracture structure on seam zones of thin-walled titanium articles produced by diffusion welding N85-22738
Durability of VT16 alloy compounds obtained by diffusion welding N85-22740
Structure and mechanical characteristics of heterogeneous joints produced by laser welding N85-22742
Method of calculating strength of joint produced by cold welding of aluminum under discrete loading N85-22743
Effect of moisture in inert gases on density of seam metal and on mechanical characteristics of welded joints of aluminum and aluminum alloys N85-22744
Automatic multi-layer welding of thick cylindrical structures under flux N85-22746
Softening of metal near seam during welding of heat-resistant nickel alloys N85-22747
WELDING
Automatic multi-layer welding of thick cylindrical structures under flux N85-22746
WELDING MACHINES
Automatic multi-layer welding of thick cylindrical structures under flux N85-22746
WEST GERMANY
D-1 report: The first German spacelab mission [NASA-TM-77837] N85-22402
WETLANDS
An initial analysis of LANDSAT-4 Thematic Mapper data for the discrimination of agricultural, forested wetlands, and urban land cover — Poinsett County, Arkansas; and Reelfoot Lake and Union City, Tennessee N85-23193
Remote sensing of coastal wetlands biomass using Thematic Mapper wavebands — Lewes, Delaware N85-23196
Comparison of MSS and TM data for landcover classification in the Chesapeake Bay area: A preliminary report — Taylor's Island, Maryland N85-23210
WETTING
Examination of the contact wetting angle in the vicinity of critical temperature [BLL-T6416/BG/CRS/LR-ST735/84] N85-23054
WHISTLERS
Excitation of low-frequency plasma waves by a conducting, tethered satellite N85-23470
WHITE DWARF STARS
A survey for galactic plane ultraviolet-excess objects: Space densities for white dwarfs, subdwarfs, and cataclysmic variables N85-23458
WHITE NOISE
Methods of digital correction for channels of multichannel radar receivers N85-23005
WIDEBAND COMMUNICATION
Ionospheric distortions of digital signals with wideband modulation N85-22945
WIND (METEOROLOGY)
Summary of Meteorological Observations Surface (SMOS), Sigonella, Sicily/Navy [AD-A150630] N85-23280
Summary of Meteorological Observations, Surface (SMOS), Alameda, California [AD-A150609] N85-23281
WIND DIRECTION
Portable Automated Mesonet (PAM) data from the 1980 experiment in Anderson Creek Valley [DE85-004361] N85-23282
WIND EFFECTS
Portable Automated Mesonet (PAM) data from the 1980 experiment in Anderson Creek Valley [DE85-004361] N85-23282
Seasonal and secular variation of the Solis Lacus albedo feature: Relation to the Martian dust-transport cycle N85-23576
The effect of particle density on aeolian transport N85-23581
A comparison of terrestrial saltation flux in the laboratory and the field N85-23582
Statistics of Aeolian surface of Mars N85-23637
WIND EROSION
Observed changes at Viking Lander 1 N85-23575
Seasonal and secular variation of the Solis Lacus albedo feature: Relation to the Martian dust-transport cycle N85-23576
Eolian erosion on Mars: Three scales N85-23577
Planetary analogs in Antarctica: Mars N85-23604
WIND PROFILES
Preliminary study of inphase gusts and moment force wind loads over the first 150 meters at KSC, Florida [NASA-TM-86501] N85-23273
WIND TUNNEL CALIBRATION
Calibration of wind tunnel flow quality N85-22399
WIND TUNNEL TESTS
Dynamic wind tunnel testing for active control research N85-22352
Dynamic wind-tunnel testing of active controls by the NASA Langley Research Center N85-22353
Effects of leading-edge devices on the low-speed aerodynamic characteristics of a highly-swept arrow-wing [NASA-CR-172531] N85-22365
Investigations into the effects of scale and compressibility on lift and drag in the RAE 5m pressurised low-speed wind tunnel [RAE-TM-AERO-2006] N85-22372
Deflected jet experiments in a turbulent combustor flowfield [NASA-CR-174863] N85-22390
Cryogenic wind tunnels: A selected annotated bibliography [NASA-TM-86346] N85-22401
Results of aeroheating DFI and ET design-data test on a 0.0175-scale model 60-OTS conducted in the Von Karman Gas Dynamics Facility (VKF) 40' supersonic and the 50' hypersonic wind tunnels A and C [NASA-CR-167693] N85-22466
Results of the AFRSI rewaterproofing systems screening test in the NASA/Ames Research Center (ARC) 2 x 2-foot transonic wind tunnel [NASA-CR-167694] N85-22467
Results of a M = 5.3 heat transfer test of the integrated vehicle using phase-change paint techniques on the 0.0175-scale model 56-OTS in the NASA/Ames Research Center 3.5-foot hypersonic wind tunnel [NASA-CR-167695] N85-22468
CARD's low-speed wind tunnel described N85-22849
Wind tunnel acoustic study of a propeller installed behind an airplane empennage: Data report [NASA-CR-177335] N85-23377
The effect of particle density on aeolian transport N85-23581
Potential bedforms on Venus: Wind tunnel simulations N85-23583
Microdunes and other aeolian bedforms on Venus: Wind tunnel simulations N85-23584
WIND TUNNEL WALLS
Aerodynamic behavior of ventilated wind tunnel walls N85-22363
WIND TURBINES
Development of large, horizontal-axis wind turbines [NASA-TM-86950] N85-23242
Structural design of the Sandia 34-M Vertical Axis Wind Turbine [DE85-002631] N85-23247
WIND VELOCITY
Study of effective physiological temperature N85-22780
Preliminary study of inphase gusts and moment force wind loads over the first 150 meters at KSC, Florida [NASA-TM-86501] N85-23273
Portable Automated Mesonet (PAM) data from the 1980 experiment in Anderson Creek Valley [DE85-004361] N85-23282
Markov method for simulating non-Gaussian wind speed time series [DE85-003450] N85-23284
WIND VELOCITY MEASUREMENT
Radiosodar system for remote synchronous measurements of wind speed, temperature and its fluctuations N85-23145
Science opportunities using the NASA scatterometer on N-ROSS [NASA-CR-175639] N85-23222
WINDPOWERED GENERATORS
Development of large, horizontal-axis wind turbines [NASA-TM-86950] N85-23242
WINGS
Study for the optimization of a transport aircraft wing for maximum fuel efficiency. Volume 1: Methodology, criteria, aeroelastic model definition and results [NASA-CR-172551] N85-22378
WORD PROCESSING
M68000 RNF text formatter user's manual [NASA-TM-86327] N85-23320
WORKING FLUIDS
Effect of operating medium on cyclic durability of AD33-W composite N85-22716

X

X RAY ANALYSIS
In-situ burning rate determination using flash radiography N85-22550
EXAFS of monolayers on silver electrodes: SSRL proposal number 717M [AD-A150823] N85-22652
Application of field X-ray: Radiometric analysis in exploratory geology and means for its improvement N85-23176
X RAY ASTRONOMY
Solar and stellar coronal plasmas [NASA-CR-175623] N85-23676
X RAY DIFFRACTION
Microscopic magnetic structure of multiple bilayers of thin films of Fe and Ge [DE85-004188] N85-22682
X RAY LASERS
Time resolved X-ray studies during pulsed laser irradiation of Ge [DE85-005263] N85-23083
X RAY TELESCOPES
A normal incidence, high resolution X-ray telescope for solar coronal observations [NASA-CR-175622] N85-23481
X RAYS
X-ray lithography and VLSI circuits N85-22848

Y

YAG LASERS
Neodymium YAG laser pumped with radiation from high frequency electrodeless discharge N85-22798
YAWING MOMENTS
Liquid moment on a filled coning cylinder during spin-up: Ad hoc model [AD-A150280] N85-23060
YIELD
Electron yields from spacecraft materials N85-22512
YIELD STRENGTH
Structural strenght of strip D16T aluminum alloy with low copper and magnesium content N85-22691
New deformable secondary aluminum alloys N85-22694
Experimental investigation of crippling strength of Chinese aluminum alloy (LY12CZ) sections N85-22779
YTTRIUM
Magnetovolume effects in some Y-Ni intermetallic compounds [ISSN-0066-2003] N85-22683

Z

ZEOLITES
Zeolites on Mars: Prospects for remote sensing N85-23615
Chemical weathering of soils from the dry valleys of Antarctica: A terrestrial analog of Martian weathering processes N85-23628
ZINC
New deformable secondary aluminum alloys N85-22694
Aluminum alloy ATs5K5 (5% Zn + 5% Ca) for superplastic forming N85-22697
Observation of a novel low-lying excited state in zinc complexes [AD-A150188] N85-23385
ZINC COATINGS
Corrosion of aircraft Al and Al-Zn ion plated steel fasteners N85-22666
ZINC OXIDES
Stability of highly nonlinear oxide-zinc resistors under continuous voltage of industrial frequency N85-23030
ZIRCONIUM CARBIDES
Combustion of zirconium carbide N85-22532
Measurements of distributed combustion N85-22542

PERSONAL AUTHOR INDEX

Typical Personal Author Index Listing

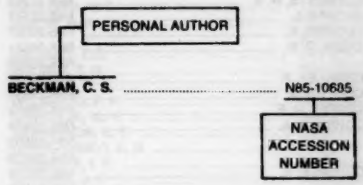

Listings in this index are arranged alphabetically by personal author. The NASA accession number denotes the number by which the citation is identified.

A

ABEL, I. N85-22353
ABEL, J. F. N85-22669
N85-22896
ABERG, T. N85-23389
ABRAMOV, I. I. N85-23039
ABRAMOVICH, B. S. N85-22912
ABRAMOVICH, Y. I. N85-23005
ABRAMS, M. N85-23192
ABU-MOSTAFA, A. S. N85-22399
ABU-ZEID, O. A. N85-22666
ACKERMAN, J. P. N85-23254
ACKERMAN, T. P. N85-23518
ACKLESON, S. G. N85-23203
ADAM, V. N85-22355
ADAMO, R. C. N85-22506
N85-22507
ADAMS, J. B. N85-23622
ADLER, L. N85-23384
AEBY, I. N85-23072
AFEFYEV, B. A. N85-22704
AGEEVIN, P. N. N85-22413
AGEYEV, N. V. N85-22730
AGEYEV, V. P. N85-22709
AGON, A. S. N85-22671
AGUIRRE-MARTINEZ, M. N85-22620
AGULTO, M. E. N85-23281
AHMADI, A. R. N85-23376
AHRENS, T. J. N85-23530
N85-23531
AINSWORTH, O. R. N85-23305
AKHMEDZYANOV, A. M. N85-22823
AKIMOV, A. A. N85-23047
AKSEL, G. M. N85-23097
AKSENOV, V. V. N85-23166
ALBA, C. N85-22762
ALBIN, E. F. N85-23478
ALCURILLA, R. N85-22581
ALEKHIN, Y. N. N85-22994
ALEKSANDROV, A. P. N85-22405
ALEKSANDROV, V. A. N85-22728
ALEKSEYEV, S. N85-22973
ALEMAR, J. D. N85-23381
ALEYNIKOV, V. S. N85-22749
ALEYNIKOVA, I. N. N85-22630
ALFEROV, Z. I. N85-22985
ALLEMBY, R. J. N85-23258
ALLIN, G. N85-23413
ALTHOUSE, E. L. N85-22672
ALTUKHOV, A. M. N85-22413
ALYABYEV, S. P. N85-22939
AMUNDSEN, D. L. N85-22525
AMURSKIY, G. I. N85-22446
ANAMIN, S. N. N85-22994
ANDERS, C. N85-22589
ANDERSON, D. M. N85-23584
ANDERSON, J. R. N85-23282
ANDERSON, O. L. N85-23056
ANDERSON, P. B. N85-22475
ANDERSON, R. M. N85-23251
ANDERSON, T. W. N85-23368
ANDERSON, W. H. N85-23200
ANDREYEV, Y. G. N85-22717
ANDRIYEVSKIY, R. A. N85-22718
ANGEL, J. R. P. N85-23462
ANISIMOVA, L. I. N85-22726
ANKENEY, L. A. N85-23348
ANKUDINOV, D. R. N85-22908
ANOSHIN, V. Y. N85-22456
ANTINONE, R. J. N85-22692
ANTIPIN, O. P. N85-22720
ANTIPIN, V. P. N85-22719
ANTONOVA, N. M. N85-23128
ANTOV, N. N. N85-22962
APFEL, R. E. N85-23362
APGAR, S. A., III N85-22683
APLIN, J. E. N85-23304
ARAI, H. N85-22608
AREFYEV, B. S. N85-23150
ARGON, A. S. N85-22676
ARIKHIPOV, I. K. N85-22703
ARKIMOV, L. A. N85-22409
ARMANIOS, E. A. N85-22640
ARMEN, G. B. N85-23389
ARMSTRONG, T. P. N85-22492
ARMYAGOV, A. A. N85-22697
ARRIZABALAGA, F. N85-22577
ARUTYUNYAN, V. M. N85-22952
ARVIDSON, R. E. N85-23579
N85-23609
N85-23648
ASKINAZI, G. B. N85-22910
ASLAM, S. N85-23365
ASLANOV, P. B. N85-23058
ASTAKHOVA, V. A. N85-22449
AUCOUTURIER, M. N85-22658
AUSTIN, D. S. N85-22853
AUTON, J. R. N85-22984
AVDEYEV, V. V. N85-22942
AVERILL, W. P. N85-22969
AVERIN, S. A. N85-22415
AXE, J. D. N85-22682
AXELROD, T. S. N85-23313
AYTACER, E., JR. N85-23449

B

BABEY, Y. I. N85-22748
BABKIN, V. I. N85-23133
BACA, L. S. N85-23363
BAER, D. R. N85-22679
BAGG, M. T. N85-22980
BAI, Z. D. N85-23358
BAKER, J. R. N85-23207
BAKER, N. E. N85-23111
BAKER, V. R. N85-23585
BAKEYEV, N. F. N85-22634
BAKINOVSKIY, K. N. N85-22977
BAKUT, P. A. N85-23003
BALAKSHIY, V. I. N85-23061
BALCH, D. T. N85-22344
N85-22345
BALDWIN, D. H. N85-23342
BALICK, L. K. N85-23200
BALL, J. R. N85-23486
BALLARD, T. N85-23454
BALOGA, S. M. N85-23548
N85-23562
N85-23564
BALTZER, O. J. N85-22993
BALYKINA, O. N. N85-23175
BANKS, D. O. N85-23066
BANKS, P. M. N85-22473
BARAKAT, R. N85-23347
BARANNIKOV, Y. I. N85-22430
BARE, S. R. N85-23419
N85-23420
BARFIELD, J. N85-22483
BARKER, J. L. N85-23186
BARKHATOV, D. B. N85-23176
BARKHATOVA, V. Y. N85-23133
BARLOW, N. G. N85-23537
BARR, H. S. N85-23397
BARR, S. N85-23283
BARRETT, H. H. N85-23402
BARRIEY, R. N85-23490
BARRY, R. G. N85-23272
BARSEGYAN, R. S. N85-22662
BARSUKOV, O. A. N85-22430
BASTARD, J. L. N85-22596
BATES, J. L. N85-23417
BATRAKOV, S. G. N85-22805
BATSON, R. M. N85-23666
N85-23668
BAUGH, R. N. N85-23065
BAUGHER, C. N85-23463
BAUHS, K. C. N85-23070
BAUM, J. D. N85-22534
BAYKOVA, A. T. N85-23022
BAZHANOV, V. I. N85-22837
BAZHENOV, V. V. N85-22733
BAZILEVSKIY, A. T. N85-22437
BEACH, G. L. N85-23568
BEAUCHAMP, W. T. N85-22615
BEAUMONT, B. N85-22626
BEBERMEIER, H. N85-22614
BEBYAKOV, A. P. N85-22768
BECKSTEAD, M. W. N85-22542
N85-22543
BEERS, B. L. N85-22516
BEHRENS, G. N85-22613
BEKYASHEV, K. A. N85-22456
BELETSKIY, V. M. N85-22690
BELENKIY, A. V. N85-23045
BELL, J. F. N85-23500
N85-23618
N85-23617
BELOKONOV, I. V. N85-22790
BELOKONOV, V. M. N85-22790
BELOUSOV, N. N. N85-22946
BELOV, A. A. N85-23034
BELOV, A. S. N85-22798
BELYAYEV, V. L. N85-23031
BELYAYEV, V. S. N85-22931
BEMENT, L. J. N85-22581
BENARFA, H. N85-22604
BENERDT, W. B. N85-23515
BENNETT, J. N85-23292
BENNETT, J. G. N85-23111
BENTLEY, J. N85-23427
BENTLEY, J. H. N85-23075
BERBYUK, V. Y. N85-22818
BERDICHEVSKIY, M. N. N85-23154
N85-23155
BERESTOV, A. L. N85-23136
BEREZHNAYA, G. I. N85-22681
BEREZHNAYA, N. D. N85-23139
BERG, D. E. N85-23247
BERGER, H. N85-22708
BERNAL, L. N85-22393
BERNARD, J. N85-22587
N85-22604
N85-22622
BERNSTEIN, R. N85-23189
BERTO, Z. L. N85-22425
BERTOTTI, L. N85-22579
BESSALOV, A. V. N85-22929
BESSE, A. L. N85-22481
BESSONOVA, N. P. N85-22635
BHAVNANI, K. H. N85-22489
BICHUN, G. N85-22848
BIELLE-DASPET, D. N85-22581
N85-22585
BIER, R. N85-22904
N85-22905
BIERMANN, W. J. N85-23253
BIJETINA, R. N85-22772
BILINSKIY, A. I. N85-23154
N85-23155
BILLS, B. G. N85-23512
BINDSCHADLER, D. L. N85-23648
BINDSCHADLER, D. L. N85-23631
BINGHTOK, V. B. N85-22943
BISCHOFF, K. B. N85-22771
BIZZELL, R. M. N85-23194
N85-23201

BJORKMAN, M. D. N85-23533
BLACKNER, A. M. N85-22536
BLACKWELL, B. N85-23412
BLANTER, B. E. N85-22955
BLEISTEIN, N. N85-22867
BLODGET, H. W. N85-23209
BLOOMFIELD, F. S. N85-22547
BLOTTNER, F. G. N85-23063
BLOUNT, H. G. N85-23626
BLUM, L. N85-22652
BLYAS, E. A. N85-23167
BOATWRIGHT, G. O. N85-23204
BOBBIO, A. N85-23354
BOBO, P. N85-22597
N85-22618
BOEDEKER, L. R. N85-22649
BOENI, P. N85-22682
BOGAR, T. J. N85-22563
BOGATIKOV, O. A. N85-23161
BOGDANOV, S. G. N85-23040
BOGDANOV, Y. B. N85-23148
BOGDANOVA, L. K. N85-23040
BOGOMOLOV, A. F. N85-22436
BOKK, O. F. N85-22941
BOLDASOV, V. S. N85-23037
BOLOTIN, L. M. N85-22607
BOLOTINA, N. Y. N85-22420
BONCELET, C. G., JR. N85-22878
BOND, L. J. N85-23091
BONDARENKO, Y. F. N85-22749
BONDARYUK, N. N. N85-22726
BONOLI, P. N85-23412
BOOTHROYD, J. C. N85-23586
BORGES, G. L. N85-22652
BORING, J. N85-23621
BORISENOK, I. T. N85-22791
BORISOV, V. N85-22695
N85-22817
BORODKOVA, N. L. N85-22434
BORONOYEV, V. V. N85-22975
BOUGAN, S. J. N85-23583
BOURRIEAU, J. N85-22587
BOVENKO, V. G. N85-23168
BOWDEN, T. T. N85-22396
N85-22646
BOWIN, C. N85-23514
BOWRING, S. N85-23648
BOYKO, V. A. N85-22795
BOYLES, R. A. N85-23066
BRACUTI, A. J. N85-22551
BRAGER, H. R. N85-22684
BRAITHWAITE, P. C. N85-22542
BRANCH, M. C. N85-22531
N85-22556
BRANDHORST, H. W., JR. N85-22586
N85-22617
BRANDON, S. T. N85-22492
BRANSFORD, J. W. N85-22531
BRASS, A. M. N85-22658
BRATT, S. R. N85-23647
BREAKALL, J. K. N85-22874
BRECKINRIDGE, J. B. N85-23396
BREED, C. S. N85-23641
BRENNEAR, S. S. N85-22678
BRETCHES, J. E. N85-23570
BREWER, D. A. N85-23269
BRIDGES, P. M. N85-23666
N85-23668
BRINKER, D. J. N85-22580
BRON, O. B. N85-23031
BROWELL, E. V. N85-23269
BROWN, G. N85-23369
BROWN, R. S. N85-22536
BRUMFIELD, J. O. N85-23209
BRUNNER, O. N85-22616
BRUSSAT, T. R. N85-23108
N85-23109
BRYKSIN, V. V. N85-23017
BUCHNEV, L. M. N85-22751
BUGAEV, A. A. N85-22665
BURATTI, B. J. N85-23620
BURBEA, J. N85-23371
BURCH, J. N85-22483
BURENKOV, V. I. N85-23140
BURGESS, E. T. N85-23060
BURKE, G. J. N85-22674
N85-22675
BURKE, M. G. N85-22678
BURKE, W. J. N85-22480
N85-22482
N85-22502
BURKE, W. R. N85-22505
BURNS, J. A. N85-23487
BURNS, R. G. N85-23555
N85-23556
BURNS, V. M. N85-23555
N85-23556
BUROV, A. A. N85-22429
BURSON, Z. G. N85-23240
BUSTARD, L. D. N85-22762
BUTERA, K. M. N85-23224
BUTEYKO, V. K. N85-23016
BUTLER, R. W. N85-23337
BUTOMO, N. I. N85-23176
BUTTRY, D. A. N85-22652
BUYANOV, Y. I. N85-22958

C

CABESTANY, J. N85-22577
CALDERER, J. N85-22577
CALLAHAN, J. C. N85-23672
CAMBIAGGIO, M. C. N85-23342
CAMERON, A. G. W. N85-23527
CAMILLO, P. J. N85-23236
CAMPANA, J. E. N85-22561
CAMPBELL, D. B. N85-23507
N85-23631
CAMPBELL, J. K. N85-23529
CARLIN, F. N85-22762
CARLOTTO, M. J. N85-23239
CARLSON, T. N. N85-23238
CARNES, J. N85-23194
CARPENTER, R. W. N85-22765
CARR, M. H. N85-23476
CARRUTH, M. R., JR. N85-22519
CASE, K. M. N85-23366
CASHORE, J. N85-23627
CASKEY, G. R., JR. N85-22672
CASSEN, P. N85-23526
CASTANER, L. N85-22577
CATANI, G. N85-22360
CATHEY, S. G. N85-22851
CHABAN, V. N. N85-22814
CHAKY, R. C. N85-22505
CHALYKH, A. Y. N85-22637
CHAN, W. N85-23346
CHANDRASEKARAN, B. N85-22369
CHANG, A. T. C. N85-23230
CHANG, Y. M. N85-22554
CHAPLYGIN, V. A. N85-22925
CHAPMAN, B. M. N85-23509
CHAPMAN, C. R. N85-23501
N85-23520
CHARAKHCHYAN, A. N. N85-22413
CHARAKHCHYAN, T. N. N85-22413
CHARBONNIER, J. C. N85-22658
CHAYKOVSKIY, V. I. N85-22997
CHEADLE, J. M. N85-23451
CHEN, C. P. N85-23101
CHEN, F. L. N85-22535
CHEN, M. H. N85-23389
CHEN, Y. H. N85-22879
CHENG, P. N85-22780
CHENION, J. N85-22762
CHENOWETH, E. L. N85-23403
CHERNOWAZ, V. Y. N85-22630
CHERNOMORDIK, V. V. N85-22709
CHERNYSHOVA, T. A. N85-22706
CHERPAK, N. T. N85-23042
CHERTKOV, B. M. N85-22605
CHERVAKOV, V. V. N85-22629
CHEYSHVILI, O. D. N85-22956
CHIKOUCHE, A. N85-22581
N85-22585
CHING, J. K. S. N85-23269
CHISTYAKOV, F. K. N85-22784
CHOBAN, Y. M. N85-23041
CHOI, T. N85-22680
CHOTTINER, G. S. N85-22764
CHOUDHURY, P. R. N85-22562
CHOW, C. C. N85-22458
CHOW, Y. L. N85-22668
CHRISTENSEN, J. M. N85-23299
CHRISTENSEN, P. R. N85-23572
N85-23578
N85-23607
N85-23611
N85-23642
CHRISTIANSEN, E. H. N85-23560
CHUDNOV, A. M. N85-23029
CHUDNOVSKY, F. A. N85-22665
CHUGUNOVA, N. F. N85-22637
CHUKAYEV, A. G. N85-22787
CHUKHLOMLIN, A. Y. N85-22702
CHUNG, H. N85-23110
CHUNG, T. J. N85-22538
CHUNG, T. S. N85-22754
CHYNOWETH, D. P. N85-22772
CIARDO, G. N85-23354
CICARELLI, E. C. I. N85-23311
CLARK, A. F. N85-22906
CLARK, D. R. N85-22346
N85-22347
CLARK, P. E. N85-23633
N85-23634
CLARK, R. N. N85-23612
N85-23621
N85-23623
CLARKE, C. K. P. N85-22657
CLARKE, J. N85-22658
N85-23424
CLAY, W. T. N85-23413
CLEMENCE, R. D., JR. N85-23329
CLEMENT, E. J. N85-23378
CLEMENTS, W. E. N85-23263
CLOSAS, L. N85-22577
CLOUTIS, E. N85-23607
CLOW, G. D. N85-23541
N85-23592
COAKLEY, P. N85-22510
CODY, W. J. N85-23333
COFFEY, H. E. N85-23679
COHEN, H. A. N85-22489
N85-22502
N85-22508
COHEN, N. S. N85-22539
N85-22560
COHEN, S. N85-22368
COLLINS, W. R. N85-23321
COLWELL, R. N. N85-23190
COMINS, N. R. N85-22664
COMPTON, W. B., III N85-22371
CONDIT, C. D. N85-23569
CONEL, J. N85-23192
CONNELLY, R. N85-23502
CONNELLY, T. G. N85-23338
CONNER, F. N85-22378
CONTOUR, J. P. N85-22626
COOK, A. F. N85-23490
COOK, G. M. N85-23250
COOKE, D. L. N85-22486
N85-22487
COOL, R. L. N85-23394
CORDI, R. C. N85-22655
CORNILSEN, B. C. N85-23414
CORRIGAN, J. D. N85-23598
COTTS, D. B. N85-22514
COUTSIAS, E. A. N85-23405
COWEY, K. N85-22667
COX, A. N. N85-23678
COX, G. B., JR. N85-22556
CRABB, R. L. N85-22622
N85-22624
N85-22625
CRAIDON, C. B. N85-23380
CRANE, R. G. N85-23272
CRASEMANN, B. N85-23389
CRAWLEY, E. F. N85-22391
CREAMER, B. A. N85-23258
CRISWELL, C. W. N85-23639
CROFT, S. K. N85-23543
N85-23547
N85-23658
CROSBY, G. A. N85-23385
CROTTY, G. T. N85-23244
CROWLEY, J. C. N85-22560
CUQUEL, A. N85-22578
CUTHBERTSON, R. H. N85-22374
CUZZI, J. N85-23488

D

DABNEY, R. W. N85-22877
DAGUANG, S. N85-23437
DALE-BANNISTER, M. N85-23609
DALE, C. B. N85-22549
DALODYE, F. N85-22425
DAMON, E. K. N85-22650
DAMPNEY, C. N. G. N85-23216
N85-23217
N85-23218
N85-23220
DANFORD, M. D. N85-22662
DANIEL, B. R. N85-22540
DANIELL, R. E. N85-22516
DANIELSON, M. J. N85-22679
DANILCHENKO, V. P. N85-22830
DANILKIN, V. A. N85-22719
DANILOVICH, O. S. N85-22947
DASHENKOV, V. M. N85-22933
DASHNIMAYEV, V. D. N85-22975
DAUD, T. N85-23244
DAUPHINAS, P. R. N85-23453
DAVIES, B. H. N85-22859
DAVIES, M. A. H. N85-22606
DAVIES, M. E. N85-23669
N85-23670

N85-23671
DAVIS, D. R. N85-23501
N85-23521
N85-23523
N85-23534
DAVIS, P. A. N85-23632
DAVIS, R. F. N85-23428
DAVIS, W. T. N85-22885
DAY, W. B. N85-22364
DEAN, R. H. N85-22525
DECHER, R. N85-23463
DECRAMER, L. N85-22595
DEGAETANO, E. A. N85-22557
N85-22628
DEGLORIA, S. D. N85-23190
DEHON, R. A. N85-23559
N85-23561
DELANEY, I. C. N85-22677
DELMER, T. N. N85-22516
DELOREY, D. N85-22476
DELSANTO, P. P. N85-23381
DEMIDYUK, M. V. N85-22818
DEMIRANDA, C. T. N85-23359
DEMYANENKO, K. B. N85-23030
DENISOVA, I. P. N85-22962
DERRICK, J. F. N85-22349
DERYUGINA, A. I. N85-23003
DETTLAFF, K. N85-22589
DEVORET, M. H. N85-23424
DEZIDERYEV, S. G. N85-22831
DICKINSON, A. N85-22598
DIESSNER, F. N85-22591
DMITRENKO, V. V. N85-22415
DMITRIYENKO, A. N. N85-23013
DMITRIYEV, I. A. N85-22751
DMITRIYEV, V. N. N85-22720
DOBBS, G. M. N85-22649
DOBERSHTEYN, S. A. N85-23008
DOBISZ, E. A. N85-22680
DOBROVOLSKIY, Y. V. N85-22696
DOBRUNOV, Y. V. N85-22728
DOELP, G. R. N85-22669
DOGGETT, R. V. N85-22353
DOLLERY, A. A. N85-22624
DOMBROWSKI, D. M. N85-23089
DONALD, B. R. N85-23432
DONATELLI, D. E. N85-22502
DONEGAN, A. J. N85-23672
DONGARRA, J. J. N85-23334
DORMAN, L. I. N85-22412
DOSS, J. D. N85-22901
DOVBISHCHENKO, I. V. N85-22744
DOVIDENAS, V. N85-22698
DOW, T. A. N85-23429
DOWNES, R. A. N85-23458
DOWNS, G. S. N85-23633
DOYLE, B. L. N85-22680
DOYLE, R. J., JR. N85-22561
DOZIER, J. N85-23205
DRAISEY, S. N85-22599
DREIM, D. N85-22378
DRYER, F. L. N85-22658
DUBANOV, A. A. N85-22784
DUBROV, M. N. N85-23046
DUDIK, V. N85-22970
DUGAN, J. B. N85-23354
DULGEROFF, C. R. N85-22513
DUNBAR, D. L. N85-23072
DUNBAR, R. S. N85-23498
DUNLAP, R. N85-22536
DURHAM, W. B. N85-23655
DURKEE, P. A. N85-23263
DUTRIEU, E. N85-22604
DYACHENKO, V. S. N85-22714
DYAR, M. D. N85-23553
N85-23554
DYKSTRA, J. N85-23191

E

EASTMAN, T. E. N85-23409
ECHOLS, W. E. N85-22891
ECKBRETH, A. C. N85-22649
ECKHARDT, D. E., JR. N85-23317
EDDY, M. N85-23648
EDEN, J. G. N85-23077
EGGLESTON, D. S. N85-22526
EIDEN, M. N85-22616
EKIN, J. W. N85-22906
EL-ANTABLY, A. M. N85-22900
EL-NEWEHY, E. N85-23309
ELDIWANY, B. H. N85-23093
ELEZKI, M. N85-22599
ELLINGSON, W. A. N85-22786
ELSTON, W. B. N85-23639
ELSTON, W. E. N85-23569
EMBLETON, B. J. J. N85-23216
EMMETT, M. B. N85-23364
ENGLAND, P. N85-22354
ENGLISH, R. E. N85-22520
ENNS, D. N85-22398
ENOCH, J. N85-22492
EPHRATH, A. N85-22666
EPSTEIN, A. H. N85-22397
EPSTEIN, G. L. N85-23680
ERDOGAN, F. N85-23097
N85-23098
N85-23099
EVERETT, J. R. N85-23191
EVIATAR, A. N85-23492
EZ, V. V. N85-23159

F

FAETH, G. M. N85-22528
N85-22529
FAKLIS, D. N85-23080
FALES, C. L. N85-23067
FANALE, F. P. N85-23504
N85-23580
N85-23593
N85-23629
FANG, Z. N85-23353
FANNIN, K. F. N85-22772
FATHY, D. N85-23428
FATTAH, I. H. A. N85-23073
FAYENOV, A. Y. N85-22795
FAYNGAOLD, M. I. N85-22979
FAYZULLIN, I. Y. N85-22713
FEDDERS, P. A. N85-22670
FEDOROV, A. G. N85-22742
FEDOROV, K. N. N85-23121
FEDOROV, N. N. N85-22949
FEDOROVA, O. V. N85-22740
FEDOSEYEV, V. A. N85-22732
FEDOSIMOV, A. I. N85-22795
FEHRENZ, H. P. N85-23359
FEIFAN, D. N85-22845
FELCH, K. N85-22904
N85-22905
FELINSKIY, G. S. N85-23044
FENNELL, J. F. N85-22501
FEOKTISTOV, K. P. N85-22406
N85-22451
N85-22452
N85-22453
N85-22454
FERGERSON, R. W. N85-23406
FERGUSON, D. C. N85-22477
N85-22496
FERRELL, G. B. N85-22390
FERRENBERG, A. J. N85-22555
FERTIG, R. S. N85-23674
FEUQUAY, J. W. N85-23200
FIDDES, S. P. N85-22372
FIELD, R. W. N85-23386
FIELDS, J. M. N85-23374
N85-23375
FIJUN, S. N85-23436
FILATOV, Y. V. N85-22955
FILIPPOVA, M. G. N85-23120
FILLIPYCHEV, D. S. N85-23037
FILONENKO, V. P. N85-22707
FINK, J. N85-23479
N85-23565
FINK, L. M. N85-22944
FINLAYSON, P. A. N85-22533
FINNEGAN, P. M. N85-22520
FIRSOV, V. S. N85-23048
FISCHER, J. W. N85-22767
FISHBEYN, B. D. N85-22828
FISHER, A. T. N85-23427
FISHKOVA, L. M. N85-22431
FISHMAN, G. S. N85-22898
FISHMAN, M. M. N85-23012
FLANDRO, G. A. N85-22533
N85-22537
FLATTE, S. M. N85-23380
FLEMINGS, M. C. N85-22668
FLOOD, D. J. N85-22580
N85-22617
FLORES, C. N85-22579
FLY, G. W. N85-23111
FOMCHENKOV, A. T. N85-22737
FOMIN, A. I. N85-22922
FONTIJN, A. N85-22530
FORD, P. G. N85-23509
FORD, W. T. N85-23251
FORESTIERI, A. F. N85-22610
FORNI, O. P. N85-23659
N85-23661
FOSTER, R. L. N85-22545
FOX, L. N85-22904
N85-22905
FRAIOLI, A. V. N85-22654
FRANK, C. W. N85-22759
FRANK, L. A. N85-22472
N85-23409
FRANK, W. M. N85-23271
FRANSEN, L. J. N85-22871
FRASER, J. S. N85-23084
FREDERICK, J. E. N85-23114
N85-23115
FREDERICKSON, A. R. N85-22509
FREILICH, M. H. N85-23222
FRENKEL, L. A. N85-23004
FREY, H. N85-23595
N85-23596
FRIEDMAN, S. D. N85-23681
FRIEDRICH, G. N85-22573
FROLOVA, T. M. N85-22720
FROLUSHKIN, V. M. N85-22015
N85-23027
FROST, J. R. N85-23324
FRYER, M. O. N85-23340
FRYER, P. N85-23573
FUBAO, Z. N85-22779
FURASHOV, N. I. N85-22968
FUSEV, P. S. N85-22796
FUSKOV, V. P. N85-22796
FUXI, G. N85-23439

G

GAAB, T. P. N85-22660
GABELKO, L. B. N85-23147
GABRIEL, T. A. N85-23364
GADDIS, L. R. N85-23563
N85-23573
N85-23616
GAFFEY, M. J. N85-23500
GAFFNEY, E. S. N85-23615
GALIULLIN, K. F. N85-22823
GALLAGER, R. G. N85-23322
GALLILY, I. N85-23061
GALPER, A. M. N85-22415
GALPERIN, Y. I. N85-22424
GALPEROVICH, D. Y. N85-23000
GANEYEV, A. A. N85-23162
GANICHEV, A. I. N85-22824
GARCIA, J. N85-22577
GARCIAMORENO, E. N85-22577
GARDNER, J. H. N85-23411
GARNER, F. A. N85-22684
GARNIER, J. E. N85-23417
GARRETT, H. B. N85-22464
N85-22484
N85-22500
GARRISON, G. R. N85-23383
GARVIN, J. B. N85-23506
N85-23510
GASKELBERG, V. G. N85-23148
GASSANOV, L. G. N85-23044
GATAULLIN, I. G. N85-22789
GAUSSENS, G. N85-22762
GAVRILOV, P. F. N85-22430
GAVRILOV, V. V. N85-22443
GAYDA, J. N85-22660
GAYKOVICH, K. P. N85-23146
GAYLER, J. E. N85-23207
GAZAZYAN, E. D. N85-22919
GELB, A. N85-23252
GELBWACHS, J. A. N85-23286
GERASIMOV, I. A. N85-22418
GERBER, N. N85-23060
GERLACH, L. N85-22600
GERSHMAN, B. N. N85-22911
GERSTEIN, M. N85-22562
GERVIN, J. C. N85-23210
N85-23211
GEVORKYAN, V. K. N85-23135
GIBART, P. N85-22626
GIBELING, H. J. N85-22544
GIBSON, E. K., JR. N85-23628
GIBSON, J. N85-23499
GIBSON, J. S. N85-23351
GIBSON, L. N85-23448
GIERASCH, P. N85-23673
GIESS, S. C. N85-22662
GILBERT, E. N. N85-22631
GILLESPIE, A. N85-23192
GILLESPIE, R. N85-23564
GIROUARD, D. N85-22475
GIRSHOV, V. S. N85-23023
GLASSMIRE, M. E. N85-23451
GLENN, J. M. N85-22527

GLICK, R. L. N85-22550
GLUMOV, V. P. N85-23172
GLYNN, P. W. N85-23343
GMELIN, B. N85-23352
GNATYUK, A. D. N85-22690
GODLEWSKI, M. P. N85-22569
GODOVSKIY, Y. K. N85-22635
GOERGENS, B. N85-22594
GOGATISHVILI, Y. M. N85-23176
GOKA, T. N85-22387
GOLDBUKHT, G. Y. N85-22694
GOLIKOV, V. S. N85-22927
GOLIKOVA, S. N. N85-22796
GOLOD, O. S. N85-23172
GOLOLOBOV, V. I. N85-22616
GOLOMBEK, M. P. N85-23645
N85-23646
GOLOMOBEK, M. N85-23644
GOLOVIN, S. A. N85-22703
GOLUB, L. N85-23481
N85-23676
GOLUB, M. V. N85-22801
GOLUB, V. P. N85-22724
GOLUBKIN, V. N. N85-22792
GOLUBOVSKIY, Y. R. N85-22723
GOMER, W. N85-23448
GONCHAROVA, N. V. N85-23165
GOODRICH, L. F. N85-22906
GORBACHEV, A. P. N85-22986
GORBATOV, N. A. N85-22925
GORCHAKOV, Y. V. N85-22799
GORDEYEV, Y. N85-22407
GORDON, J. G., II N85-22652
GORDON, W. L. N85-22512
GOREE, J. G. N85-22639
GORELOV, G. M. N85-22830
GORITSKIY, V. M. N85-22736
GOROZHANIN, D. V. N85-22980
GORSHKOV, A. S. N85-23046
GORSHKOV, V. G. N85-23129
GORSKIY, V. A. N85-22909
GOSLEE, J. W. N85-22885
GOSS, L. F. N85-22548
GOSTISHCHEV, E. A. N85-22958
GOTO, M. N85-22576
GOVERNO, G. K. N85-23551
GOVOR, I. N. N85-22957
GRABIS, Y. P. N85-22717
GRABKE, H. J. N85-22657
GRACHEV, V. M. N85-22415
GRAHAM, K. J. N85-22527
GRANT, J. A. N85-23586
GRANTHAM, C. N85-23320
GRAYZER, V. M. N85-23150
GREELEY, R. N85-23478
N85-23479
N85-23545
N85-23572
N85-23581
N85-23582
N85-23583
N85-23584
N85-23606
N85-23608
N85-23611
N85-23640
N85-23642
GREENBERG, R. N85-23477
N85-23501
N85-23520
N85-23521
GREENE, R. R. N85-23289
GREGORY, D. A. N85-22689
GREGORY, L. J. N85-22767
GREITZER, E. M. N85-22397
GREW, G. W. N85-23237
GREZEV, A. N. N85-22742
GRIER, N. T. N85-22495
GRIEVE, R. N85-23511
GRIFFIN, C. W. N85-23417
GRIFFIN, D. N85-23412
GRIFFIN, E. J. N85-22861
GRIFFITH, W. N85-23085
GRIFFITHS, M. P. N85-23338
GRIGORKINA, T. Y. N85-23133
GRIGOROV, N. L. N85-22799
GRIGORYANT, A. G. N85-22742
GRIGORYEVA, M. A. N85-22909
GRIGORYEVSKIY, V. I. N85-23053
GRISHINA, Y. P. N85-22729
GROENERT, F. E., JR. N85-23312
GROH, K. H. N85-22584
GRUDZINSKIY, B. V. N85-22737
GRYAZNOV, Y. M. N85-22961
GUANGQING, Y. N85-22848
GUBLER, M. I. N85-23032
GUDOVSKIKH, S. S. N85-23177
GUIDICE, D. A. N85-22518
GUILLAUME, J. C. N85-22626
GUINNES, E. A. N85-23609
GUINNESS, E. N85-23648
GUINNESS, E. A. N85-23579
GULYAYEV, Y. V. N85-23053
GULYELMI, A. V. N85-22414
GURGIOLO, C. N85-22483
GURNEY, R. J. N85-23236
GUSEV, S. I. N85-22738
N85-22739
GUSHCHO, Y. P. N85-23002
GUSSENHOVEN, M. S. N85-22482
GYORFFY, B. L. N85-22681

H

HAAS, P. J. N85-23355
HACKMAN, J. R. N85-23302
HAFF, P. K. N85-23492
HAGNUSON, J. A. N85-23467
HAGUE, J. R. N85-23325
HALL, D. F. N85-22501
HALL, D. N. B. N85-23460
HALL, F. G. N85-23194
HALL, J. L. N85-23650
HALL, W. N. N85-22522
HAPKE, B. N85-23482
HARDIN, C. D., JR. N85-23372
HARDING, J. N85-22641
HARDISKY, M. A. N85-23198
HARDY, D. A. N85-22480
N85-22481
N85-22482
HARDY, J. R. N85-23207
HARMON, J. K. N85-23507
N85-23631
HARRIS, R. B. A. N85-22601
HARRIS, R. K. N85-22527
HART, R. E. N85-22569
HARTMANN, W. K. N85-23519
N85-23534
N85-23535
HAUFFE, K. N85-22389
HAUN, J. E. N85-23339
HAWKE, B. R. N85-23500
N85-23607
N85-23616
N85-23617
HAWKINS, R. L. N85-22768
HAYDN, R. N85-23196
HAZELL, M. S. N85-22859
HAZELTON, R. C. N85-22515
HEAD, J. W. N85-23507
N85-23508
N85-23510
N85-23511
N85-23516
N85-23517
N85-23631
N85-23647
N85-23650
HEARD, H. C. N85-23655
HEATH, M. T. N85-23362
HEBERT, F. N85-23521
HEGDE, U. G. N85-22535
HEINISCH, H. L. N85-22684
HEISELMANN, H. W. N85-23456
HELFENSTEIN, P. N85-23483
HELIN, E. F. N85-23498
HELMREICH, R. L. N85-23302
HEMKER, K. J. N85-22660
HENDERSON, K. E. N85-23206
HENDRICKS, R. C. N85-22755
N85-22756
HENRICKS, W. N85-22465
HERAKOVICH, C. T. N85-22638
HERBERT, F. N85-23552
HERBIG, J. N85-23335
HERBST, M. J. N85-23411
HERMAN, W. H. N85-22375
HEYNE, C. J. N85-22900
HICKEY, J. S. N85-23319
HICKS, D. L. N85-23327
HIGG, H. C. N85-23224
HIGGINS, R. H. N85-22662
HILLS, C. R. N85-23082
HILLS, R. N85-22476
HILSENRATH, E. N85-23112
HINE, A. A. N85-23507
HINSON, W. F. N85-22685
HINTERMANN, A. N85-23387
HIRANO, T. N85-22566
N85-22567
HIRLEMAN, E. D. N85-22648
HIRSCHFELD, D. A. N85-22638
HO, W. N85-23419
N85-23420
HODGETTS, T. E. N85-22861
HOFFMAN, G. H. N85-23059
HOFFMAN, R. W. N85-22512
N85-22764
HOLDEN, D. G. N85-22362
HOLDREN, M. W. N85-23256
HOLEMAN, E. N85-22482
HOLFORD, D. M. N85-23308
HOLL, J. T. N85-22529
HOLLAND, O. W. N85-23428
HOLLOWAY, J. R. N85-23557
HOLMES, N. C. N85-23551
HOLSAPPLE, K. A. N85-23532
HOLT, H. E. N85-23474
HOLT, H. M. N85-22362
HONIG, E. M. N85-22881
HOORFAR, A. N85-22852
HORNER, V. M. N85-23545
N85-23606
HOUSEN, K. R. N85-23533
HOUSTON, A. G. N85-23206
HOWELL, L. W. N85-23305
HSIEH, S. J. N85-22670
HSING, C. C. N85-22367
HSU, D. S. Y. N85-22559
HSU, M. N85-23450
HSU, T. M. N85-23108
N85-23109
HUANG, C. Y. N85-23409
HUBBARD, W. B. N85-23550
HUCK, F. O. N85-23067
HUCKABEE, L. L. N85-22889
HUDSON, T. L. N85-22903
HUDSON, W. R. N85-22517
HUEY, H. N85-22904
N85-22905
HUGHES, D. L. N85-22394
HUGUENIN, R. L. N85-23610
N85-23613
N85-23624
HUNT, G. E. N85-23490
HURICK, M. N85-23546
HURRASS, K. N85-22357
HUTCHINSON, D. P. N85-23081
HYMANN, J. N85-22513

I

ICE, G. E. N85-23389
IGLEHART, D. L. N85-23343
N85-23367
ILES, P. A. N85-22568
ILYENKO, V. M. N85-22697
IMBRIE, P. K. N85-22365
IMURA, N. N85-22576
INOUE, M. N85-23228
INOUYE, G. T. N85-22505
IORDANSKIY, I. A. N85-23131
IOZENAS, V. A. N85-22799
IRONS, J. R. N85-23188
N85-23197
ISAACS, H. S. N85-22673
N85-22675
ISAKOV, G. N. N85-22710
ISAKOV, M. V. N85-22709
ISHIHARA, K. N85-23227
ISHIKAWA, Y. N85-22675
ISKAKOV, K. M. N85-22836
ISKHAKOV, Z. S. N85-22836
IVANITSKIY, A. M. N85-22932
IVANOV, B. I. N85-22980
IVANOV, K. G. N85-22414
IVANOV, L. I. N85-22712
IVANOV, O. N. N85-22813
IVANOV, V. V. N85-22742
IVANOV, Y. D. N85-23021
IVANOV, Y. N. N85-22749
IVASHKIN, V. V. N85-22419
IVES, L. N85-22904
N85-22905
IWASA, Y. N85-22774
IZMAYLOV, V. V. N85-23132

J

JACHIMOWSKI, C. J. N85-22395
JACKSON, M. J. N85-23207
JACKSON, N. S. F. N85-23446
JACOBS, E. W. N85-23245
JAKOBSSON, S. N85-23557

JAMES, J. H. N85-23107
JANKE, D. N85-23589
JANNEY, M. A. N85-22643
JARAMILLO, L. N85-23611
JARAMILLO, S. A. N85-23072
JAREM, J. M. N85-22876
JELLISON, G. E., JR. N85-22765
N85-23079
JENA, P. N85-22651
N85-23387
JENNINGS, W. D. N85-22764
JERGER, D. E. N85-22772
JOHNSON, B. D. N85-23216
N85-23218
N85-23219
JOHNSON, C. B. N85-22370
JOHNSON, G. D. N85-23403
JOHNSON, K. I. N85-22860
JOHNSON, M. N85-23549
JOHNSON, M. D., JR. N85-22775
JOHNSON, P. E. N85-23625
JOHNSON, R. E. N85-23491
N85-23621
JOHNSON, T. L. N85-23404
JOHNSON, T. V. N85-23475
N85-23621
JOHNSON, W. S. N85-23085
JONES, J. N85-23624
JONES, R. H. N85-22679
JORY, H. N85-22904
N85-22905
JURGENS, R. F. N85-23633

K

KAASE, H. N85-22605
KABANOV, S. Y. N85-22719
KABANOV, V. S. N85-22736
KACHUR, V. G. N85-23005
KAHLE, A. B. N85-23192
N85-23564
KAHLE, J. N85-23564
KAHN, R. N85-23558
KAHN, R. A. N85-23673
KAI, K. N85-23233
N85-23234
KALABIN, I. V. N85-22804
KALASHNIKOV, N. I. N85-23025
KALEGANOV, V. F. N85-22965
KALIMULLIN, R. K. N85-22713
KALNIBOLOTSKIY, Y. M. N85-23006
KALOSHIN, V. A. N85-22987
KAMINER, N. S. N85-22412
KAMYKOWSKI, D. N85-23287
KANAVETS, I. P. N85-22720
KANAYEV, Y. M. N85-22805
KANG, G. S. N85-22671
KANG, S. H. N85-22645
KAPCHINSKIY, M. I. N85-22980
KAPLINSKIY, A. L. N85-22745
KAPTSOV, A. N. N85-22450
KARABASHEV, G. S. N85-23288
KARIM, K. R. N85-23389
KARIMOVA, A. G. N85-22831
KARITANI, S. N85-23319
KARLASHOV, A. V. N85-22690
KARO, A. M. N85-23416
KASTING, J. F. N85-23518
KATEHI-TSEREGOUNIS, P. B. N85-22882
KATHIRESAN, K. N85-23108
N85-23109
KATSNELSON, H. N85-22926
KATZ, I. N85-22485
N85-22486
N85-22487
N85-22493
KAUFFMAN, R. E. N85-23399
KAUFMAN, J. W. N85-23273
KAUFMAN, L. G., II N85-22370
KAVALYAUSKENE, G. S. N85-23036
KAWAKAMI, A. N85-22575
KAYBYSHEV, O. A. N85-22689
KAZAKOV, N. F. N85-22740
KAZANSKIY, L. P. N85-22637
KEARSE, A. J. N85-23086
KEIL-SIMON, G. N85-22578
KEKALO, I. B. N85-22750
KELMAN, V. M. N85-22794
KEMP, N. H. N85-23252
KENDALL, B. R. F. N85-22511
KENNARD, J. N85-23242
KENNEDY, R. S. N85-22375
KERCHNER, H. R. N85-22686
KERNOV, Y. P. N85-22906
KERREBROCK, J. L. N85-22397
KERSHNER, C. J. N85-23080
KEYS, V. N. N85-23032
KHARLAMENKO, V. I. N85-22801
KHAUSTOVA, S. G. N85-22725
KHAYTUN, F. I. N85-22993
KHENTOV, A. A. N85-22426
KHEVROLIN, V. Y. N85-22923
KHKHLOV, E. N. N85-23020
KHOREV, M. A. N85-22734
KHOZIN, G. S. N85-22455
KHRENKOV, N. N. N85-22999
KHROMOV, A. A. N85-23152
KHUZYASHEV, R. G. N85-22948
KICHIGIN, V. N. N85-22947
KIDMAN, R. B. N85-23678
KIEFFER, H. H. N85-23505
KIERAS, D. E. N85-22870
KIKNADZE, L. V. N85-22956
KILGORE, R. A. N85-22401
KIM, C. N85-23459
KIMBALL, O. N85-22868
KIMSTACH, G. M. N85-22695
KINBER, B. Y. N85-22984
KING, J. S. N85-23570
N85-23571
KING, N. S. P. N85-23072
KING, R. N85-23326
KING, R. J. N85-22875
KING, T. E. G. N85-22863
KINGSLAND, R. B. N85-22467
KINSEY, J. L. N85-23386
KIRBY, D. A. N85-22372
KIRBY, S. H. N85-23655
KIRILENKO, A. I. N85-22977
KIRILLOV-UGRYUMOV, V. G. N85-22415
KIROL, L. D. N85-23064
KIRYUKHIN, A. V. N85-23173
KISELEV, Y. S. N85-22800
KITTERER, B. N85-22510
KIVMAN, G. A. N85-23130
KLAHR, P. N85-23330
KLASSEN, V. I. N85-22984
KLAVINS, P. N85-23425
KLECKNER, J. E. N85-22883
KLEIN, J. P. N85-23092
KLEMAS, V. N85-23198
N85-23203
KLIGER, J. J. N85-22549
KLIMENKO, B. V. N85-23033
KLIMOV, S. A. N85-22736
KLYUYEV, Y. I. N85-22821
KMITA, A. M. N85-23053
KNAUTS, H. E. N85-23456
KNOWLTON, S. N85-23412
KNOX, C. E. N85-22356
KNYAZEV, B. N. N85-22423
KNYSH, P. I. N85-22806
KNYSH, Y. A. N85-22786
KOBELEVA, L. I. N85-22706
KOBZOVA, V. M. N85-23154
N85-23155
KOCH, J. N85-22589
N85-22612
KOCH, T. H. N85-23076
KOCHELL, R. C. N85-23597
KOCHESHKOV, I. V. N85-22705
KOENENKAMP, R. N85-23426
KOENIG, R. M., JR. N85-23310
KOHBATA, M. N85-22568
N85-22608
KOLACHEV, B. A. N85-22727
KOLDASHOV, G. A. N85-22795
KOLESNICHENKO, G. D. N85-22941
KOLESNICHENKO, V. A. N85-22705
KOLOMENSKIY, A. B. N85-22727
KOMAR, P. D. N85-23588
KONDRASHOV, N. S. N85-22810
KONDRATENKO, A. N. N85-22974
KONG, F. M. N85-22642
KONONOV, A. A. N85-22990
KONONOV, M. V. N85-23126
KONOPIKHIN, A. A. N85-23169
KONTOROVICH, V. M. N85-22408
KONTROVICH, V. Y. N85-22983
KOONS, H. C. N85-22501
N85-22502
KOPP, D. M. N85-22872
KOPP, M. K. N85-23413
KORENDYASEV, A. I. N85-22803
N85-22807
KORIGODSKIY, A. R. N85-22635
KORNIYENKO, V. V. N85-22437
KOROBKA, A. N85-22935
KOROSTELEVA, A. A. N85-22714
KOROTKIKH, M. T. N85-22842
KORTE, U. N85-22361
KOSHEVOY, V. M. N85-22990
KOSTIKOV, V. I. N85-22751
KOSTINA, S. S. N85-23028
KOSTYLEV, A. A. N85-22917
KOSYAN, R. D. N85-23125
KOTADA, K. N85-23233
KOTIKOVA, T. D. N85-22725
KOTODA, K. N85-23234
KOTOV, Y. D. N85-22432
KOUMVAKALIS, A. S. N85-23549
KOVALENKO, V. I. N85-23161
KOVALEVA, V. N. N85-22730
KOVTYUKH, A. S. N85-22423
KOZAI, K. N85-23232
KOZAK, R. C. N85-23632
KOZHEVNIKOV, Y. V. N85-22713
KOZLOV, A. G. N85-22423
KOZLOV, V. V. N85-22449
KOZYREV, N. D. N85-22918
KRAHN, D. R. N85-22525
KRANKOTA, J. L. N85-22677
KRASHENINNIKOV, S. Y. N85-22786
KRASKOVSKIY, A. Y. N85-23010
KRASNER, M. N85-22868
KRASOTKIN, A. F. N85-22413
KRATS, K. O. N85-23148
KRAVCHENKO, N. I. N85-22927
KRAVCHUK, L. V. N85-22725
KRAWCZYK, R. N85-22595
KRINSKY, I. S. N85-22503
KRISHNAIAH, P. R. N85-23352
N85-23358
KRIVTSOV, Y. P. N85-22955
KRUEGER, M. N85-22570
KRUSHENKO, G. G. N85-22693
KRUTKO, P. D. N85-22808
KSANFOMALITI, L. V. N85-22433
KSENZENKO, A. Y. N85-22963
KUBAREV, A. V. N85-22957
KUCERA, G. H. N85-23254
KUDOH, M. N85-22608
KUECHLER, G. N85-22600
KUHLMAN, B. P. N85-23275
KUKLA, G. J. N85-23285
KUKLIN, V. M. N85-22974
KUKS, A. M. N85-22787
KUKUSHKIN, Y. N. N85-22692
KULAGIN, D. P. N85-22743
KULEZNEV, V. N. N85-22636
KULKARNI, S. R. N85-23466
KULKOV, S. N. N85-22702
KUNDIN, A. P. N85-23053
KUNIN, N. Y. N85-23165
KUNKLE, T. D. N85-23615
KUPPERMAN, D. S. N85-22766
KURIAT, R. I. N85-22725
KUROWSKI, G. J. N85-23066
KURT, V. G. N85-22425
KUTEPOV, D. F. N85-22635
KUTEYNIKOV, A. F. N85-22751
KUYI, H. N85-22847
KUZMICHEV, A. I. N85-23037
KUZMICHEVA, A. Y. N85-22412
KUZMIN, S. Z. N85-23028
KUZMINOV, V. A. N85-22448
KVASOV, D. N85-23118

L

LACKEY, J. G. N85-23240
LAFRAMBOISE, J. G. N85-22491
LAGET, R. N85-22506
LAGOUIN, M. N85-22585
LAI, S. T. N85-22489
LAISER, D. D. N85-23245
LAKOTA, N. A. N85-22808
LAN, C. E. N85-22367
LANDO, V. S. N85-23026
LANG, H. N85-23192
LANKFORD, J. N85-22757
LAPORTE, A. N85-22603
LAPTEV, A. A. N85-23000
LARIN, N. V. N85-22719
LAROCHE, G. N85-22592
LARRY, T. L. N85-22664
LARSON, B. C. N85-23083
LARUE, J. C. N85-22582
N85-22602
LATTY, R. S. N85-23188
N85-23197
LAU, C. W. N85-22676
LAUB, A. J. N85-23344
LAUE, E. G. N85-23580
N85-23629
LAUER, D. T. N85-23200

LAURA, P. A. A. N85-23103
LAURENT, A. N85-23105
LAVRUKHINA, A. K. N85-22427
LAWSON, D. K. N85-23429
LAWSON, J. R. N85-22776
LAZAR, A. N85-22873
LAZAREV, A. M. N85-22940
LAZAREV, S. A. N85-22432
LAZORENKO, V. M. N85-22712
LEACH, R. N. N85-23584
LEBEDEV, V. I. N85-23134
LEBEDEV, Y. V. N85-23443
LECHNER, W. N85-22355
LECOMPTE, M. A. N85-23473
LEDNEV, M. M. N85-22901
LEE, E. M. N85-23066
LEE, L. D. N85-23090
N85-23317
LEE, N. S. T. N85-22884
LEE, S. W. N85-23576
LEE, Y. N85-22527
LEE, Y. A. N85-22465
LEEF, C. R. N85-22466
LEFF, C. N85-23648
LEFF, C. E. N85-23579
LEGOTAYEV, V. P. N85-22422
LEHMAN, G. L. N85-23427
LEHTINEN, M. N85-22663
LEMEUR, M. N85-22762
LEONTYEV, M. A. N85-22718
LERINMAN, R. M. N85-22731
LESMAN, M. Y. N85-23024
LETNOV, L. A. N85-22920
LEUNG, P. L. N85-22504
LEVENTOURI, T. N85-22686
LEVIN, J. C. N85-23389
LEVIN, V. Y. N85-22788
LEVINE, J. N. N85-22534
LEVY, L. N85-22582
N85-22583
LI, S. N85-22845
LIANG, P. Y. N85-22554
LIDHOLM, U. S. N85-22888
LIEBROCK, L. M. N85-23327
LIKHATSKIY, S. I. N85-22686
LILLEY, D. G. N85-22390
LILLEY, J. R., JR. N85-22486
LIM, R. N85-22767
LIN, C. N85-22483
LIN, M. C. N85-22559
LINDER, H. G. N85-23258
LING, X. N85-23264
LINKOV, Y. M. N85-23149
LINNER, L. N85-22378
LIPPY, L. J. N85-22462
N85-22463
LISKIN, A. M. N85-22697
LISTOV, V. N85-22633
LITVINOVICH, V. V. N85-22994
LLOYD, B. N85-23412
LLOYD, S. A. N85-22559
LO, D. S. N85-22525
LO, G. A. N85-22560
LOBANOV, A. V. N85-22999
LOBANOV, S. V. N85-22695
LOEB, H. W. N85-22584
LOGGINOV, A. S. N85-23047
LOGINOV, V. M. N85-22938
LOGINOV, V. P. N85-23444
LOGOVOY, P. Z. N85-22814
LOKSHIN, B. Y. N85-22791
LOMAKIN, I. E. N85-23135
LOMBARDI, J. N85-22344
N85-22345
LONG, R. K. N85-22650
LONG, S. I. N85-22895
LONGOV, A. A. N85-22406
LOPER, G. L. N85-23266
LOPEZ, N. N85-22905
LOPEZ, R. E. N85-22523
LORCH, D. N85-23303
LORD, W. N85-23373
LOTSPIECH, J. B. N85-23189
LOWNDES, D. H. N85-22765
N85-23079
LOWRY, K. A. N85-23404
LOZINSKIY, V. M. N85-22916
LU, P. J. N85-22363
LU, Y. C. N85-23210
N85-23211
N85-23212
LUBITSKIY, A. A. N85-23139
LUCAS, D. N85-23448
LUCCHITTA, B. K. N85-23652
N85-23664
N85-23665
LUCEY, P. N85-23616
N85-23617
LUCHANSKAYA, K. I. N85-22923
LUCHKOV, B. I. N85-22432
LUKOVKIN, G. M. N85-22634
LUKYANOV, D. P. N85-22955
LUKYANOV, L. G. N85-22416
LUNDSTROM, I. N85-22764
LUPIN, V. A. N85-22735
LUPTON, A. O. N85-22362
LURYE, I. K. N85-22444
LUSHNIKOV, A. A. N85-22913
LYAKHOV, S. B. N85-22426
LYAKHOV, V. A. N85-22405
LYNCH, M. T. N85-23084
LYNN, N. M. N85-22773
LYON, T. F. N85-23256
LYSYNCHUK, D. V. N85-23184
LYUBOVTSEVA, Y. S. N85-23147
LYUBTSEVA, Y. F. N85-23177

M

MACDONALD, R. B. N85-23194
MACFADYEN, D. J. N85-23454
MACKALL, K. G. N85-22394
MADNICK, S. E. N85-23328
MAJKRZAK, C. F. N85-22682
MAJUMDAR, D. N85-23360
MAKAROV, P. P. N85-22631
MAKHOUL, J. N85-22868
MAKLAKOV, D. V. N85-22789
MAKOV, I. P. N85-22826
MAKSIMENKO, V. V. N85-22913
MAKSYUTENKO, S. N. N85-23058
MALETS, K. V. N85-22441
MALIN, M. C. N85-23503
N85-23604
N85-23605
MALINOVSKIY, K. A. N85-22825
MALTSEV, O. A. N85-23053
MALYGIN, S. A. N85-22967
MALYSHEV, M. N. N85-23032
MALYSHEV, V. N. N85-22801
MAMALADZE, Y. G. N85-22956
MANAGADZE, G. G. N85-22426
MANCA, J. N85-22905
MANDELL, M. J. N85-22486
N85-22487
N85-22493
N85-22497
MANDROSOV, V. I. N85-23003
MANKA, C. K. N85-23411
MANNINEN, M. N85-22651
N85-23387
MANOGUE, W. N85-22771
MANSOUR, I. R. M. N85-22619
MANUKYAN, A. G. N85-23179
MAOXUN, W. N85-22849
MARCELL, R. F. N85-23209
N85-23211
MARCHENKO, S. N. N85-22925
MARCHENKO, Y. Y. N85-23017
MARDIROSYN, G. K. N85-22447
MARGOT-MARETTE, H. N85-22658
MARHOUL, J. C. N85-23349
N85-23350
MARIE, R. N85-23369
MARION, J. E., II N85-22763
MARKHAM, B. L. N85-23188
N85-23197
N85-23202
MARKOVSKIY, V. S. N85-23135
MARKS, G. W. N85-22599
MARROQUIN, J. N85-22466
N85-22467
N85-22468
MARSHALL, J. R. N85-23583
N85-23584
MART, J. N85-23286
MARTEL, L. N85-23640
MARTIN, B. J. N85-23295
N85-23296
N85-23297
MARTIN, G. A. N85-22596
MARTIN, J. N85-23332
MARTIN, M. R. N85-22400
MARTINIS, J. M. N85-23424
MARTIROSOV, V. Y. N85-22946
MARTSVALADZE, N. M. N85-22431
MARTYNOV, V. A. N85-22709
MARTZ, J. E. N85-23243
MASHIMOV, M. M. N85-22441
MASHIN, V. S. N85-22744
MASHKOVA, N. A. N85-22740
MASHYANOV, N. R. N85-23162
MASKEW, B. N85-22346
N85-22347
MASKHULIYA, L. G. N85-22715
MASLOV, V. V. N85-23035
MASLOVA, N. B. N85-23130
MASSON, P. L. N85-23659
N85-23660
N85-23661
N85-23662
MATHES, H. B. N85-22541
MATSON, D. L. N85-23475
N85-23621
MATSUDA, S. N85-22567
N85-22575
N85-22576
MATSUTANI, T. N85-22566
N85-22567
MATTISON, E. M. N85-22647
MATVEYEV, V. I. N85-22963
MATVEYEV, V. N. N85-22627
MAWIRA, D. N85-22621
MAXWELL, O. V. N85-23472
MAXWELL, T. A. N85-23596
N85-23643
MAY, I. N85-22935
MCARTHUR, D. N85-23330
MCCABE, C. W. N85-22901
MCCAULEY, J. F. N85-23641
MCCORD, T. B. N85-23621
MCCOY, T. J. N85-22896
MCCREARU, W. J. N85-22655
MCCUNE, J. E. N85-22397
MCDONALD, G. N85-22755
N85-22756
MCDONALD, H. N85-22544
MCEWEN, A. S. N85-23475
MCGILL, G. E. N85-23591
MCGRATH, J. F. N85-23327
MCGRAW, B. A. N85-23065
MCGRAW, J. R. N85-23313
MCGUIRE, P. D. N85-22401
MCHONE, J. F. N85-23642
MCINTIRE, D. N85-23624
MCIVER, J. K. N85-23405
MCKEE, P. N85-22667
MCKINNON, W. B. N85-23484
N85-23497
N85-23538
N85-23657
MCLAIN, A. G. N85-22395
MCLARNON, B. D. N85-22850
MCMAHON, W. N85-22476
MCMILLAN, D. J. N85-22773
MCNERNEY, G. M. N85-23264
MEAD, G. D. N85-23258
MEDVEDEV, N. G. N85-22815
MEHLHORN, R. J. N85-23293
MEHREZ, A. N85-23341
MEHTA, S. N85-22586
MELNICHUK, V. I. N85-23122
MELO, A. V. N85-22764
MELROY, O. R. N85-22652
MERKISHIN, G. V. N85-22966
MERKLE, K. L. N85-22687
MESERVY, R. N85-23422
MESHCHANINOVA, L. S. N85-22731
MESHCHANOV, V. P. N85-22938
MESIAS, S. N85-22872
METALNIKOV, A. N85-22440
METZDORF, J. N85-22605
MEULENBERG, A., JR. N85-22515
MEYERS, A. I. N85-22760
MEZHEVICH, V. V. N85-22922
MICHEL, A. N85-22604
MIDDLETON, E. M. N85-23212
MIDDLETON, J. N85-23598
MIGUNOV, N. I. N85-23152
MIKEROV, A. G. N85-22989
MIKHAYLOV, S. A. N85-22819
MILLER, B. K. N85-22874
MILLER, E. K. N85-22875
MILLER, H. G. N85-23342
MILLER, M. K. N85-22678
MILLER, M. Y. N85-22976
MILLER, T. A. N85-22349
MILLER, T. J. E. N85-22903
MILLER, T. N. N85-22717
MILLER, V. C. N85-23413
MILLER, W. L. N85-22496
MILLS, D. M. N85-23083
MILLS, G. A. N85-22771
MILYUTIN, V. N. N85-22738
MIMPEN, A. M. N85-23294
MINAYEVA, I. A. N85-22942
MINER, R. V. N85-22660

MINH, N. Q. N85-23254
MIRABEL, A. P. N85-23142
MIRONOVA, Y. N. N85-22425
MIROSHNICHENKO, V. K. N85-23001
MISHEV, D. N. N85-22447
MITCHELL, A. C. N85-23551
MITCHELL, B. J. N85-23267
MITCHELL, C. E. N85-22553
MITNIK, M. M. N85-23180
MITSELMAGER, E. Y. N85-22928
MIZERA, P. F. N85-22501
MKHITARYAN, Z. O. N85-22952
MO, T. N85-23221
MOCCI, G. N85-22611
MOCHALOVA, O. S. N85-23128
MOESCHBERGER, M. L. N85-23092
MOISEYEV, Y. N. N85-22800
MONAKHOV, V. A. N85-23131
MONASTYRNYY, Y. A. N85-22981
MONES, E. T. N85-22642
MONIN, M. A. N85-22995
MOODY, J. N85-23412
MOON, F. C. N85-22669
N85-22896
MOORE, H. J. N85-23575
N85-23635
MOORE, J. M. N85-23478
N85-23606
MOORHEAD, A. J. N85-22758
MORACHEVSKIY, V. G. N85-22632
MORALES, W. N85-22644
MORE, K. N85-23428
MORGAN, R. J. N85-22642
N85-22767
MORIARTY, J. A. N85-23430
MOROZ, A. V. N85-22914
MOROZ, I. P. N85-23154
N85-23155
MOROZ, P. N85-22440
MOROZOV, V. V. N85-22709
MORRIS, E. C. N85-23667
MORTENSEN, A. N85-22668
MOSOLOVA, G. I. N85-23119
MOTTINGER, N. A. N85-23512
MOUGINISMARK, P. J. N85-23563
N85-23573
N85-23607
MOZEYKO, B. Y. N85-22733
MOZHAYEV, B. N. N85-22445
MUCHNAYA, V. I. N85-23157
MUELLER, S. W. N85-23657
MUKERJI, P. K. N85-22752
MUKHAMEDYAROV, R. D. N85-22926
MUKHINA, N. P. N85-23119
MUKHOPADHYAY, N. C. N85-23392
MUKHOVETSKIY, Y. P. N85-22695
MULLEN, R. L. N85-22756
MULLER, M. W. N85-22670
MULLIGAN, P. J. N85-23210
MULLIN, J. P. N85-22617
MULLINS, K. F. N85-23668
MULLINS, L. J. N85-22683
MURAVSKIY, I. G. N85-22812
MURAVYEV, I. I. N85-22727
MURKINA, N. G. N85-22737
MURPHY, G. B. N85-22472
N85-22474
MYERS, L. P. N85-22394
MYMRINA, N. V. N85-22412
MYSYK, D. A. N85-22813

N

NACHTIGALL, P. E. N85-23339
NAGLE-ESHLEMAN, J. N85-23102
NAKAGAWA, S. N85-23233
N85-23234
NAKHMANSON, G. S. N85-23052
NANEVICZ, J. E. N85-22506
N85-22507
NAPPO, C. J. N85-23282
N85-23283
NARAIN, S. N85-23330
NARAYANASWAMI, L. L. N85-22540
NATARAJAN, C. N85-22764
NAYKHANOV, V. V. N85-22784
NEFF, W. N85-23283
NEGRUTSA, T. F. N85-23148
NEGRUTSA, V. A. N85-23148
NELIN, Y. A. N85-22934
NELLIS, W. J. N85-23551
NELSON, G. L. N85-22525
NELSON, M. L. N85-23621
NELSON, R. F. N85-23188
N85-23197
NELSON, R. M. N85-23481
NEMTSOV, B. Y. N85-22912
NESHPOR, G. S. N85-22691
NESMELOV, V. V. N85-22710
NESTEROVA, M. P. N85-23129
NETZER, D. W. N85-22527
NEVEROV, S. G. N85-22986
NEVSKIY, O. I. N85-22729
NEWBERY, R. R. N85-22354
NEWMAN, R. C. N85-22673
NEWMANN, T. W. N85-22903
NEWMEN, M. J. N85-23678
NEWSOM, J. R. N85-22353
NEZYM, V. Y. N85-22832
NGUYEN, K. N85-22531
NICHOLSON, P. D. N85-23489
NICKS, O. W. N85-22365
NICOL, M. N85-23549
NIKOLAIZIG, N. K. N85-22584
NIKOLAYEV, V. N85-22422
N85-22701
NIKONOV, S. V. N85-22982
NIKONOV, V. A. N85-22435
NISHIMURA, Y. N85-23227
NOEL, B. W. N85-23072
NOLL, C. E. N85-23258
NOONAN, R. E. N85-23321
NOVIKOV, N. N. N85-22833
NOVOSELTSEV, L. Y. N85-22915
NSHANYAN, M. A. N85-22924
NUTTLI, O. W. N85-23267
NYMIK, R. A. N85-22799

O

OBENSCHAIN, S. P. N85-23411
OBESNYUK, V. F. N85-22711
OBIKHVOST, N. M. N85-22916
OBRIEN, W. F. N85-22549
OCHIAI, H. N85-23229
OGORODOVA, L. V. N85-23169
OGRADY, W. E. N85-22764
OKEEFE, D. A. N85-22378
OKEEFE, J. L. N85-23531
OKUNEV, Y. B. N85-22944
OLISOV, A. N. N85-22722
OLSEN, L. C. N85-23417
OLSEN, R. C. N85-22503
ONEILL, M. A. N85-23266
ONKEN, R. N85-22350
ORDANYAN, S. S. N85-22715
ORLOV, Y. I. N85-22949
ORLOVSKIY, L. S. N85-22813
ORTMEYER, T. H. N85-22897
OSASYUK, V. V. N85-22722
OSBORN, J. R. N85-22547
OSTRO, S. J. N85-23502
OSTSEMIN, A. A. N85-22735
OTODA, M. N85-22575
OVAKIMOV, A. G. N85-22804
OVSYANNIKOV, B. V. N85-22829
OWEN, A. B. N85-23349
OWENS, H. N85-22472
OWENS, R. N85-22685
OWENSBY, P. D. N85-23612
OZMAT, B. N85-22676
OZOLIN, V. V. N85-22957

P

PAGE, N. A. N85-23396
PALUMBO, D. L. N85-23337
PANASYUK, M. I. N85-22423
PANCHENKO, V. G. N85-22919
PANIN, V. Y. N85-22702
PANTELEYEV, I. B. N85-22715
PANYAM, R. R. N85-22532
PARAMZIN, A. V. N85-22448
PARIS, D. T. N85-22899
PARK, C. J. N85-22532
PARKER, K. G. N85-23069
PARKER, L. W. N85-22488
N85-22515
PARKER, T. J. N85-23580
N85-23600
N85-23601
N85-23602
N85-23603
N85-23629
PARKS, D. E. N85-22485
N85-22487
PARKS, D. M. N85-22676
PARMENTIER, E. M. N85-23483
N85-23485
PARSHIN, Y. N. N85-22942
PARTYKA, E. N85-22659
PARVIANEN, S. N85-22663
PARZYCH, D. N85-22368
PASHUK, M. G. N85-23183
PATENAUDE, C. J. N85-23336
PATERSON, W. N85-22472
PATHAK, S. K. N85-22378
PATRUSHEV, G. Y. N85-22981
PATTEN, E. A. N85-22670
PATTON, P. C. N85-23651
PATTON, T. L., III N85-23259
PAUL, M. C. N85-22525
PAVELYEV, V. G. N85-22987
PAVLOV, L. N. N85-23006
PAVLOV, P. P. N85-22999
PAWAGI, S. N85-23357
PAWULA, R. F. N85-22890
PEARSON, J. H. N85-22396
N85-22646
PECHENEGOV, S. M. N85-22796
PECKHAM, D. H. N85-22372
PEERCY, P. S. N85-22680
N85-23078
N85-23082
PELENC, L. N85-22574
PENLAND, M. C. N85-23379
PENNYCOOK, S. J. N85-22765
PEREPEZKO, J. H. N85-22680
PERLMAN, M. N85-22886
PEROV, N. I. N85-22417
PERSSON, M. N85-23419
N85-23420
PESHKOV, V. V. N85-22738
N85-22739
PESKIN, A. M. N85-23314
PETENKO, I. V. N85-23145
PETERFREUND, A. R. N85-23510
PETERS, J. N85-22657
PETERSON, J. S. N85-23390
PETROSYAN, A. K. N85-22924
PETROV, A. I. N85-22981
PETROV, G. V. N85-23038
PETROV, K. N85-22936
PETRUNIN, V. F. N85-22717
PETRUSHIN, G. D. N85-22703
PETTENGILL, G. H. N85-23509
PHELPS, M. N85-23323
PHILLIPS, R. J. N85-23649
PIAN, T. H. H. N85-23098
PICKETT, J. S. N85-22472
N85-22474
PIERCE, R. D. N85-23254
PIERI, D. C. N85-23480
N85-23546
N85-23562
N85-23584
N85-23600
N85-23601
N85-23602
N85-23603
PIGGOTT, R. E. N85-22667
PIKE, C. P. N85-22517
N85-22518
PIKE, R. J. N85-23541
N85-23542
PILCHER, C. B. N85-23486
PILIPENKO, N. V. N85-22746
PIRALISHVILI, S. A. N85-22833
PITTMAN, E. S. N85-22906
PITTS, D. E. N85-23194
N85-23206
PLAKHOV, Y. V. N85-22448
PLAMP, G. H. N85-22504
PLATOV, Y. M. N85-22712
PLEKIN, V. Y. N85-22991
PLESCIA, J. B. N85-23644
PLOSHKIN, V. V. N85-22707
PODGORKOV, V. V. N85-22802
PODOLAK, M. N85-23495
PODOLNYY, I. A. N85-22699
PODSHIVALOV, A. Y. N85-23000
POECK, D. N85-22504
POKASOV, V. V. N85-22981
POKHILYUK, A. P. N85-22984
POL, C. N85-22577
POLETIKA, T. M. N85-22702
POLISHCHUK, V. M. N85-22690
POLLACK, J. B. N85-23493
POLLOCK, J. G. N85-23518
POLYAKHOV, N. D. N85-22989
POLYAKHOVA, Y. N. N85-22411
POMEROY, L. R. N85-23290
POHOMAREV, V. B. N85-22958
PONYATOVSKAYA, V. I. N85-23151
POPENKO, N. A. N85-22972

POPKOV, Y. P. N85-22972
POPLAUKHIN, V. N. N85-22975
POPOV, A. A. N85-22726
POPOV, A. P. N85-22987
POPOV, V. D. N85-22701
POPOV, V. I. N85-22969
PORCH, W. N85-23283
PORCO, C. C. N85-23489
PORKOLAB, M. N85-23412
POROKHNYUK, A. N85-22921
PORTER, J. G. N85-23675
PORTNOY, S. L. N85-22908
PORTNOY, V. K. N85-22697
POSTAWKO, S. E. N85-23593
POTEMKIN, V. V. N85-23034
POULEK, V. N85-22586
POVINETS, P. N85-22427
POVKH, I. L. N85-23058
POWELL, C. A. N85-23374
POWER, G. D. N85-23056
POWERS, B. G. N85-22351
POWERS, J. P. N85-22527
POZHUYEV, V. I. N85-22811
PRAT, L. N85-22577
PRESSLEY, H. M., JR. N85-22550
PREUSS, L. N85-22590
PRICE, E. W. N85-22532
N85-22546
PRICE, J. C. N85-23199
PRIDO, R. N85-22607
PRIOR, H. L. N85-23201
PRISTAVAKINA, Y. I. N85-23127
PRIVALOV, V. A. N85-22791
PROKHUR, N. Z. N85-23185
PROKOFYEV, A. N. N85-22838
PROSCHAN, F. N85-23309
N85-23346
PRUNEDA, C. O. N85-22767
PUNJANI, M. N85-23091
PURVIS, C. K. N85-22494
N85-22500
N85-22517
N85-22519
PUSHKIN, S. G. N85-22631
PUTOV, V. V. N85-22989

Q

QUATTROCHI, D. A. N85-23193

R

RABKIN, D. M. N85-22744
RADMANESH, M. N85-22865
RADOVCICH, N. A. N85-22378
RAITT, W. J. N85-22473
RAITT, W. S. N85-22474
RAMAKRISHNAN, I. V. N85-23357
RAMAMURTI, V. N85-23104
RANCOURT, J. N85-22615
RANGO, A. N85-23226
RAO, B. K. N85-22651
N85-23387
RAO, C. R. N85-23352
RAO, D. G. N85-23104
RAO, K. N. N85-22768
RASCH, K. D. N85-22571
N85-22572
N85-22573
RASMUSSEN, C. E. N85-23470
RATH, J. N85-22609
RAUN, R. L. N85-22542
REASENBERG, R. D. N85-23513
N85-23526
REASER, J. S. N85-22378
REAVIS, J. G. N85-22683
REAZER, M. J. N85-23275
REBIAI, S. N85-22585
REBROV, A. N85-22704
N85-22706
REDDY, A. D. N85-22640
REDDY, J. F. N85-22687
REDIESS, H. A. N85-22350
REDKIN, S. P. N85-22437
REHFIELD, L. W. N85-22382
N85-22640
REIBMAN, A. N85-23369
REIDEL, J. E. N85-23672
REIMANN, R. C. N85-23253
REISNER, D. E. N85-22652
REMPEL, G. G. N85-23174
RESTER, A. C., JR. N85-22469
RETICCIOLI, M. N85-22611
REULET, R. N85-22581
N85-22587
N85-22622
REYNA, E. N85-23194
REYNOLDS, R. T. N85-23495
N85-23496
REYZMAN, S. Y. N85-22423
REZNIK, G. M. N85-23124
N85-23141
REZNIK, V. Y. N85-22830
RHINE, W. E. N85-23399
RHODES, D. D. N85-23587
RIBARSKY, M. W. N85-22661
RICE, S. O. N85-22890
RICH, F. J. N85-22480
RICHARDSON, D. N85-22378
RICHTER, E. N85-22903
RIGGIN, R. M. N85-23256
RINKYAVICHYUS, V. S. N85-23036
RITCHIE, J. C. N85-23204
ROBERTS, A. F. N85-23243
ROBINSON, G. Y., JR. N85-22774
ROBINSON, P. A., JR. N85-22504
ROBINSON, R. J. N85-22753
ROCHE, J. C. N85-22497
RODIONOVA, Z. F. N85-22439
RODNIKOVA, I. V. N85-22794
ROG, A. I. N85-23020
ROGERS, J. L., JR. N85-23318
ROGERS, R. C. N85-22395
ROGOSHIN, V. A. N85-22413
ROMANOV, B. F. N85-22841
ROMANYUK, T. V. N85-23153
ROSARIO, E. N85-23381
ROSEN, I. G. N85-23100
ROSENFELD, A. N85-23356
ROSS, D. C. N85-23361
ROSS, M. N85-23551
ROSSBACHER, L. A. N85-23587
N85-23590
ROSSI, M. G. N85-22891
ROTE, D. M. N85-23268
ROTH, L. E. N85-23638
ROULLE, C. N85-22582
ROUSH, T. L. N85-23607
ROUSSEL, M. N85-22603
N85-22604
ROUX, M. N85-22581
N85-22587
ROUZIES, C. N85-22607
ROWLAND, S. N85-23563
ROWLAND, S. K. N85-23566
ROY, K. N85-22570
N85-22572
ROZENBERG, A. D. N85-23139
ROZHDESTVENSKIY, A. N. N85-23008
ROZUM, Y. I. N85-22797
RUBIN, A. G. N85-22480
N85-22481
RUBIN, A. J. N85-22486
N85-22487
RUBINA, Y. B. N85-22730
RUBTSOV, A. Y. N85-22637
RUBTSOV, V. D. N85-23014
RUDENKO, Y. N. N85-22746
RUDI, Y. A. N85-22785
RUDNITSKIY, V. P. N85-23181
RUIKANG, P. N85-22849
RUKHLENKO, A. S. N85-22933
RUMYANTSEV, K. Y. N85-23048
RUMYANTSEV, V. V. N85-22826
RUMYANTSEV, Y. M. N85-22729
RUSAKOV, O. M. N85-23143
RUSK, R. L. N85-22492
RUSTAN, P. L. N85-23275
RYABCHIKOV, I. D. N85-23161
RYABCHIKOVA, V. I. N85-22449
RYAN, M. P. N85-23560
RYAZANTSEV, V. I. N85-22732

S

SABNIS, J. S. N85-22544
SABZEHBARVAR, M. N85-22377
SACHS, I. N85-22615
SACKUVICH, R. N85-23071
SADEGHI, F. N85-23429
SADOWSKI, F. G. N85-23200
SAFLEKOS, N. A. N85-22480
N85-22483
SAGA, T. N85-22566
N85-22567
SAJBEN, M. N85-22563
SAKA, K. N85-22641
SAKHAROV, V. V. N85-22716
SALAMANDRA, B. L. N85-22803
N85-22807
SALANECK, W. R. N85-22784
SALIBEKOV, S. Y. N85-22716
SALOV, V. A. N85-22700
SALTER, R. N85-22476
SALVAIL, J. R. N85-23504
N85-23593
SALZMAN, K. A. N85-22670
SAMBAMURTHI, J. K. N85-22532
N85-22546
SAMEH, A. H. N85-23334
SAMIR, U. N85-22479
SAMOYLIK, A. V. N85-22958
SANCHEZ, J. N85-22615
SANDFORD, M. N85-22353
SAPRYKIN, Y. V. N85-22809
SARAPULOV, S. A. N85-22822
SARDAROV, S. S., JR. N85-23163
SARGENT, W. N85-22564
SAROHIA, V. N85-22393
SARRAIL, D. N85-22582
N85-22583
SASSE, R. A. N85-22769
SATTERFIELD, L. C. N85-23282
SAULIN, K. I. N85-22422
SAUNDERS, R. S. N85-23515
N85-23580
N85-23629
N85-23638
SAVENKO, V. S. N85-23134
SAVIN, A. V. N85-23163
SAVINA, N. G. N85-23149
SAVITSKIY, Y. M. N85-22720
SAVRASOV, Y. S. N85-22421
SAVVINOV, A. M. N85-22941
SAXTON, P. M. N85-23301
SAZHAYEV, V. D. N85-22796
SAZONOV, V. V. N85-22783
SCHABER, G. G. N85-23632
N85-23633
N85-23641
SCHACHER, G. E. N85-23274
SCHAFER, R. W. N85-22899
SCHENK, P. M. N85-23484
N85-23656
SCHIEBE, F. R. N85-23204
SCHILLADY, D. N85-23387
SCHILLING, J. S. N85-23425
SCHILLING, R. N85-22570
SCHIMMEL, M. L. N85-22381
SCHLENKER, R. A. N85-23298
SCHMIDT, R. M. N85-23533
SCHMIDT, W. N85-22571
SCHMITT, J. H. M. M. N85-23468
SCHMUGGE, T. N85-23223
SCHMUGGE, T. J. N85-23221
N85-23235
SCHOENBERGER, W. N85-23306
SCHUBERT, W. K. N85-22902
SCHULKIN, M. N85-23383
SCHULTZ, M. N85-23303
SCHUSS, J. J. N85-23412
SCHWARTZ, M. N85-22873
SCHWARTZ, R. N85-22868
SCOTT, D. H. N85-23653
N85-23663
SCOTT, S. J. N85-22365
SEEVERS, P. M. N85-23200
SEKHON, R. S. N85-23212
SEKI, K. N85-23233
N85-23234
SEKULA, S. T. N85-22686
SEMENIUK, A. M. N85-23595
N85-23598
SEMENOV, G. R. N85-22725
SEMENOV, V. N. N85-22821
SEMENOV, Y. G. N85-22953
SEMENOVA, G. I. N85-23165
SEMIKHATOV, M. A. N85-23148
SENATOROV, K. Y. N85-23047
SENCHENOK, V. M. N85-22413
SERDYUKOV, P. N. N85-22922
SERGEYEV, A. S. N85-23030
SERVENYUK, S. N. N85-23138
SETHURAMAN, J. N85-23309
N85-23346
SETTLE, M. N85-23224
SHACK, R. V. N85-23396
SHAHEEN, S. A. N85-23425
SHAKHMATOV, M. V. N85-22735
SHAMPINE, L. F. N85-23363
SHANNON, R. R. N85-23396
N85-23401
SHANUROV, G. A. N85-23158
SHAPIRO, I. I. N85-23471
N85-23528
N85-23631

SHAPIRO, V. I. N85-23517
SHAPOVALOV, L. A. N85-22821
SHASHKOV, O. D. N85-22731
SHATERIN, M. A. N85-22842
SHAWHAN, S. D. N85-22472
N85-22474
SHAYA, E. J. N85-23486
SHCHERBAKOV, M. I. N85-22442
SHCHERBAKOVA, B. Y. N85-23168
SHCHERBINA, G. I. N85-22830
SHCHETININ, M. V. N85-23034
SHEDLER, G. S. N85-23355
N85-23367
SHEFFIELD, C. N85-23191
SHEFFIELD, J. N85-23081
SHEFFIELD, R. L. N85-23084
SHELTON, R. N. N85-23425
SHELUKHIN, O. I. N85-22939
N85-22996
SHELUKHIN, V. I. N85-22996
SHEMSHEDINOV, R. B. N85-22965
N85-22993
SHEN, F. N85-22524
SHENGOI, L. N85-23438
SHENKMAN, A. N85-22368
SHERIDAN, M. F. N85-23574
SHERMAN, D. M. N85-23614
SHERNOUSKO, F. L. N85-22819
SHESTOPALOV, Y. N. N85-22955
SHEVCHENKO, A. N. N85-22911
SHEVCHENKO, V. V. N85-22727
SHEVCHENKO, Y. V. N85-22940
SHEVENKOVA, N. V. N85-22749
SHEYKHZADE, E. R. N85-23165
SHIKOVA, L. V. N85-22938
SHIMING, L. N85-23435
SHIPLEY, S. T. N85-23269
SHIQING, S. N85-22781
SHISHLOV, A. V. N85-22984
SHITOV, A. N. N85-22834
SHIVELY, J. N85-22905
SHKABAROV, L. V. N85-22722
SHKURATOV, Y. G. N85-22409
N85-22437
SHLOMA, A. M. N85-22992
SHMATKO, A. A. N85-23043
SHOLUPOV, S. Y. N85-23162
SHORSHOROV, M. K. N85-22705
N85-22738
SHORT, N. M. N85-23195
SHOWALTER, M. R. N85-23487
SHPILMAN, Y. N85-22926
SHTERIN, V. B. N85-22842
SHU, F. H. N85-23526
SHUMAN, B. M. N85-22508
SHURKIN, K. A. N85-23148
SHURYGIN, Y. A. N85-23145
SHVEDE, U. A. N85-22450
SHVETS, V. V. N85-22748
SIDORIN, A. Y. N85-23164
SIDOROV, V. A. N85-22719
SIDORYUK, M. Y. N85-22783
SIEGEL, J. N85-23301
SIGMAN, R. K. N85-22532
SIGMAR, D. J. N85-23081
SIGOV, A. S. N85-23002
SIKYAK, V. A. N85-23009
SIMAKOV, S. V. N85-22712
SIMMONS, A. M. N85-23571
SIMONELLI, D. P. N85-23618
N85-23619
SIMONENKO, A. P. N85-23058
SIMONOV, A. Y. N85-22913
SIMPSON, R. A. N85-23636
N85-23637
SINCOVEC, R. F. N85-23365
SINELNIKOV, A. Y. N85-22955
SINGER, R. B. N85-23607
N85-23612
N85-23615
SINHA, M. P. N85-23291
SINITSYN, A. B. N85-22798
SIROTA, A. A. N85-23020
SIZOV, V. V. N85-23172
SJOGREN, W. L. N85-23512
SJOREEN, T. P. N85-23428
SKAKOV, Y. A. N85-22749
SKORODINSKIY, V. I. N85-22793
SKOROKHODOV, A. P. N85-22419
SKOROV, V. G. N85-22920
SKORTSOV, Y. A. N85-22834
SLAPE, R. J. N85-22770
SMEDDY, M. N85-22475
SMIRNOV, L. V. N85-23117
SMIRNOV, Y. V. N85-22432
SMITH, A. A. N85-22548
SMITH, J. L. N85-23254
SMITH, J. L., JR. N85-22774
SMITH, M. O. N85-23622
SMITH, S. G. N85-22358
SMOORENBURG, G. F. N85-23294
SMYLIE, R. E. N85-22471
SMYLSOV, A. I. N85-22751
SMYSHLYAYEV, S. P. N85-22632
SMYTHE, W. D. N85-23481
SNIEDOVICH, M. N85-23341
SNYDER, D. B. N85-22499
SNYDER, M. E. N85-22894
SOBIESZCZANSKI-SOBIESKI, J. N85-23318
SOBOLEV, G. A. N85-23152
SODERBLOM, L. A. N85-23475
SOFFA, W. A. N85-22678
SOHN, J. L. N85-22536
SOLNTSEV, V. I. N85-22808
SOLOMON, A. S. P. N85-22529
SOLOMON, S. C. N85-23516
N85-23647
N85-23650
SOLOVYEV, N. N. N85-22446
SOOMERE, T. E. N85-23124
N85-23141
SORENSEN, C. N85-23194
SORENSEN, D. C. N85-23334
SOSNOVETS, E. N. N85-22423
SOTNIKOV, V. C. N85-22962
SPADLEY, L. W. N85-23057
SPALVINS, T. N85-23085
SPANG, S. N85-22904
N85-22905
SPANGLER, T. C. N85-23255
SPEARMAN, M. L. N85-22366
SPICER, C. W. N85-23256
SPIRICHEV, Y. Y. N85-22961
SPRINGER, B. W. N85-22655
SPUDIS, P. D. N85-23541
N85-23542
N85-23617
SQUYRES, S. W. N85-23496
SRIVASTAVA, V. J. N85-22772
STACEY, J. M. N85-23068
STAHARA, S. S. N85-22383
STAM, M. N85-23544
STANKEVICH, D. G. N85-22437
STANT, R. S. N85-23071
STANTON, T. P. N85-23274
STAROSTENKO, V. I. N85-23179
STARTSEV, V. M. N85-22637
STARVRINIDIS, C. N85-22616
STASKUS, J. V. N85-22478
STAUFFER, M. L. N85-23186
N85-23197
STEBLEV, Y. I. N85-22951
STEELS, R. N85-22598
STEFANTSEV, L. A. N85-23140
STEIMAN-CAMERON, T. Y. N85-23469
STEIN, G. A. N85-22525
STEIN, H. J. N85-23082
STEIN, W. E. N85-23084
STELLER, K. N85-22659
STENHOLM, H. N85-22663
STEPANOV, A. P. N85-23025
STEPANOV, B. N. N85-22697
STEPCHKOV, A. A. N85-22837
STEPHENS, J. B. N85-23580
N85-23629
STEPHENS, W. D. N85-22627
STERN, R. A. N85-23410
STERN, T. N85-22873
STEVENS, N. J. N85-22490
N85-22500
STEVENSON, D. J. N85-23494
STILLE, J. K. N85-22760
STOCKS, G. M. N85-22681
STOFAN, E. R. N85-23511
STOFFER, D. S. N85-23370
STOKES, R. F. N85-22358
STONE, C. S. N85-22893
STOREY, L. R. O. N85-22473
STRAKHOV, V. N. N85-23153
STRAND, L. D. N85-22539
STRIZHALOV, V. A. N85-22696
STRIZHKIN, I. I. N85-23171
STRIZHKOV, S. A. N85-23151
STROBELL, M. E. N85-23633
STROBL, G. N85-22571
N85-22573
STROM, R. G. N85-23537
STROSCIO, J. A. N85-23419
N85-23420
STRUCHEV, V. F. N85-23005
STUPIN, A. B. N85-23058
STURDEVANT, J. A. N85-23300
STURGEON, J. R. N85-23308
SUDAREVA, S. V. N85-22731
SUGAWARA, K. N85-22587
SUI, C. H. N85-23270
SUKHOV, N. N85-22971
SUKHOVOY, M. B. N85-22422
SUKOV, A. I. N85-22995
SULLIVAN, W. P. N85-22475
SULTANOV, M. A. N85-22708
SURKOV, V. S. N85-23117
SUROVTSEV, A. P. N85-22721
SUSHKOVA, L. T. N85-23017
SUTHERLAND, A. P. N. N85-23106
SUTUGIN, A. G. N85-22913
SUZUKI, A. N85-22566
N85-22567
N85-22587
SVENTEK, V. N85-23335
SVERDLOV, B. A. N85-22968
SVESHNIKOV, G. B. N85-23162
SWARTZ, C. K. N85-22569
N85-22586
SWEERS, J. N85-22378
SYCHENKOV, V. A. N85-22835
SYNNOTT, S. P. N85-23529
N85-23672
SYSOYEV, V. U. N85-23019

T

TADJBAKHSH, I. G. N85-23088
TAKAHASHI, K. N85-22566
N85-22608
TAKASE, Y. N85-23412
TAKEDA, K. N85-23225
N85-23227
N85-23228
N85-23229
N85-23231
N85-23232
N85-23233
N85-23234
TAKEMURA, A. N85-23368
TAKEUCHI, S. N85-23229
TALBOT, J. M. N85-23299
TANAKA, K. L. N85-23653
N85-23663
TANG, R. N85-23098
TANTON, N. E. N85-22656
N85-22657
TARANENKO, V. G. N85-22988
TARANICHEV, V. Y. N85-22750
TARAPOV, S. I. N85-22972
TARATUTA, A. S. N85-22741
TARTAKOVSKIY, A. M. N85-23018
TARTAKOVSKIY, L. S. N85-22996
TASTET, P. N85-22607
TATKOV, G. I. N85-23174
TAUTZ, M. N85-22489
TAUTZ, M. F. N85-22480
TEDROW, P. M. N85-23422
TELESCO, C. M. N85-23463
TELEZHNYY, B. G. N85-22950
TENTSCHER, K. H. N85-22571
N85-22573
TEPLYAKOV, I. M. N85-22945
TER-SAAKOV, E. I. N85-23172
TERAMOT, K. N85-22575
TERDOKHLEBOV, G. N. N85-22714
TEREBY, S. N85-23526
TERMARTIROSYAN, L. T. N85-23032
TERRILE, R. J. N85-23620
TESLENKO, L. N85-22959
TETEREV, N. V. N85-22796
TEXTER, S. N85-23412
THAYER, N. N. N85-23072
THEILIG, E. N85-23567
THEREZ, F. N85-22581
N85-22585
THOMAS, P. G. N85-23577
N85-23659
N85-23660
N85-23661
N85-23662
THOMAS, P. L. N85-22677
THOMPKINS, W. T. N85-22397
THOMPSON, D. R. N85-23206
THOMPSON, J. R. N85-22686
THOMPSON, M. O. N85-23078
THOMPSON, R. L. N85-23071
THOMPSON, T. W. N85-23634
N85-23635
THOMPSON, W. B. N85-22521
THORSEN, M. H. N85-22463
THORSON, M. H. N85-22462

THURBER, C. H. N85-23647
TIEGS, T. N. N85-22758
TIKHONOV, A. N. N85-22827
TIKHONOV, N. T. N85-22827
TIMCHENKO, V. A. N85-22741
TIMOFEYEV, I. A. N85-22804
TIMOFEYEV, P. P. N85-23160
TIPISEV, S. Y. N85-23149
TISCHLER, J. Z. N85-23083
TISHKOVETS, V. P. N85-22400
TITOV, A. D. N85-22977
TITOV, A. V. N85-23011
TITOV, D. V. N85-22436
TKACHENKO, Y. G. N85-22715
TOBOLEV, A. K. N85-22984
TOLL, D. L. N85-23188
N85-23197
N85-23208
TOM, V. T. N85-23239
TOMLINSON, J. J. N85-23248
N85-23249
TOPOROV, Y. P. N85-22630
TORBERT, R. B. N85-22503
TORSHILOVA, S. I. N85-22693
TOTSKIY, N. P. N85-22815
TOWNSHEND, J. R. G. N85-23207
TRAINOR, R. J. N85-23551
TREADWAY, M. N85-22510
TRETYACHENKO, G. N. N85-22725
TRETYAKOV, O. A. N85-23043
TRIFONOV, A. P. N85-23015
N85-23016
TRIGUBOV, Y. V. N85-22799
TRINCHUK, B. F. N85-22796
TRIVEDI, K. S. N85-23354
N85-23369
TROLIER, J. W. N85-23055
TROUGHTON, N. N85-23415
TROUP, J. M. N85-22551
TROYNIKOV, V. A. N85-22962
TRUBACHEV, S. G. N85-23035
TRUBACHEYEV, E. A. N85-22975
TRUESDELL, K. A. N85-23385
TRUSHIN, V. A. N85-22836
TSANG, Y. W. N85-23062
TSCHOEGL, N. W. N85-22761
TSENEV, N. K. N85-22689
TSHIHARA, K. N85-23228
TSIGLER, I. N. N85-22795
TSIMRING, S. E. N85-22967
TSUCHIYA, K. N85-23231
N85-23232
TSVETKOV, A. A. N85-23161
TSVETKOV, V. Y. N85-22750
TUESINK, M. F. N85-23653
TUKH, G. S. N85-23024
TUKHVATULIN, V. V. N85-23020
TULIANI, L. I. N85-23183
TURCOTTE, D. L. N85-23548
TURNER, R. S. N85-23257
TURNOCK, D. L. N85-22379
TURNS, S. R. N85-22529
TUTTLE, M. H. N85-22401
TWICHELL, J. C. N85-23408
TYAPKIN, Y. K. N85-23156
TYLER, G. L. N85-23636
N85-23637
TYLKINA, M. I. N85-22706
TYUFLIN, Y. S. N85-22438
TYVES, L. I. N85-22803
N85-22807

U

ULABY, F. T. N85-23213
ULIN, S. Y. N85-22415
ULYANINA, I. Y. N85-22707
ULYANOV, Y. G. N85-22422
UMRIGAR, C. N85-23388
UMSTEAD, M. E. N85-22559
UNDERWOOD, J. R., JR. N85-23599
UNYAHIN, A. N. N85-22800
URBAIN, G. N85-22506
URBANSKI, K. N85-23306
URBINA, C. N85-23424
URQUHART, H. N. N85-23348
URYEV, N. B. N85-22630
URYVSKIY, A. F. N85-22786
USENKO, S. V. N85-23165
USHIROKAWA, A. N85-22566
N85-22608
USTINOVA, G. K. N85-22427
UTKIN, V. S. N85-22699
N85-22716

V

VALE, L. N85-23624
VALENTIAN, D. N85-22582
VALENTINE, K. H. N85-23413
VALEYEV, S. G. N85-22410
VALISETTY, R. R. N85-22382
VALIYEV, R. Z. N85-22689
VALUYEV, V. V. N85-22713
VAMPOLA, A. F. N85-22501
VANBLARICUM, M. L. N85-22864
VANDERNEUT, C. A. N85-22853
VANDERSLUIS, K. L. N85-23081
VANRAAIJ, J. L. N85-23294
VARMA, M. S. N85-22555
VARYAHITSA, V. Y. N85-22740
VASILKOV, A. P. N85-23140
VASILYEV, M. P. N85-23050
VASILYEV, V. I. N85-22785
VASILYEV, V. V. N85-22700
VASILYEV, Y. A. N85-23185
VASILYEV, Y. G. N85-22937
VAVRIV, D. M. N85-23043
VAYNSHTEYN, L. A. N85-22985
VECCHIA, D. A. N85-22906
VEERS, P. S. N85-23284
VERBITSKIY, M. Y. N85-23123
VERIE, C. N85-22626
VERKHOVSKIY, Y. M. N85-23009
VERSHININ, V. A. N85-23026
VERSTER, J. M. N85-23300
VERTIY, A. A. N85-22972
VESELOV, G. I. N85-22994
VESHEV, A. V. N85-23177
VESSOT, R. F. C. N85-22647
VEVERKA, J. N85-23457
N85-23618
N85-23619
VIGDORCHIK, N. Y. N85-23049
VIGILYANSKAYA, L. I. N85-23182
VILISOV, A. A. N85-22925
VILKE, V. G. N85-22420
VINE, B. H. N85-23072
VINING, C. B. N85-23425
VINOGRADOV, B. V. N85-22450
VISHNEVSKIY, G. Y. N85-22710
VISWANATHAN, R. N85-22513
VLADIMIROFF, T. N85-22552
VLASOV, M. A. N85-22962
VLASOVA, N. A. N85-22423
VOLKOV, M. A. N85-22424
VOLKOV, V. I. N85-22729
VOLMAN, V. I. N85-22918
VOLONKOV, V. P. N85-22992
VOLOSEVICH, A. V. N85-22424
VOLYNSKIY, A. L. N85-22634
VOLYNSKIY, V. V. N85-22728
VOORHIES, C. V. N85-23260
VORONOVA, M. I. N85-22749
VOSKRESENSKIY, K. P. N85-23133
VOVK, I. G. N85-23170
VOZNESENSKIY, V. A. N85-23044
VVEDENSKIY, Y. V. N85-22961
VYSHKOV, Y. D. N85-22954

W

WADSWORTH, J. N85-22681
WAFELBAKKER, C. K. N85-22593
WAGNER, J. B., JR. N85-23418
WAHRBURG, J. N85-23306
WALKDEN, M. W. N85-22606
WALKER, E. F. N85-23331
WALKER, F. E. N85-23416
WALKER, G. P. L. N85-23563
N85-23566
WALKUP, C. M. N85-22642
WALLACE, G. K. N85-23239
WALLACE, R. J. N85-22854
WALTZ, F. A. N85-23200
WANG, J. R. N85-23221
WANG, R. T. N85-23400
WANG, Y. Y. R. N85-23328
WARNER, J. N85-23398
WARREN, R. W. N85-23084
WATTERS, T. R. N85-23474
N85-23643
WEBB, F. N85-23637
WEBBER, W. T. N85-22557
WEIDENSCHILLING, S. J. N85-23501
N85-23522
N85-23523
N85-23525
N85-23534
WEINBERG, I. N85-22586
WEINER, D. D. N85-22866
WEIQING, J. N85-22780
WEISSMAN, P. R. N85-23505
N85-23506
WEIZER, V. G. N85-22569
WEN, T. N85-23383
WENJIE, X. N85-22385
WESTPHAL, W. N85-22609
WETHERILL, G. W. N85-23524
WHIPPLE, E. C. N85-22503
WHITE, P. A. N85-22606
WHITFORDSTARK, J. L. N85-23626
WHITTLESEY, A. N85-22500
WILBY, E. G. N85-23377
WILBY, J. F. N85-23377
WILCOX, R. E. N85-22855
WILD, N. N85-22510
WILDEY, R. L. N85-23630
WILEMSKI, G. N85-23252
WILEY, C. L. N85-22687
WILEY, J. D. N85-22680
WILHELM, K. N85-22352
WILHELMS, D. E. N85-23536
WILKINS, J. W. N85-23388
WILL, R. W. N85-23320
WILLIAMS, D. J. N85-23409
WILLIAMS, D. L. N85-23187
N85-23188
N85-23197
WILLIAMS, J. G. N85-23499
WILLIAMS, R. O. N85-22674
WILLIAMS, S. H. N85-23581
N85-23582
WILLIAMSON, P. R. N85-22473
WILLIAMSON, W. S. N85-22513
WILLOUGHY, P. G. N85-22536
WILSON, D. D. N85-22891
WILSON, E. A. N85-23213
WILSON, L. N85-23508
N85-23563
N85-23573
WILSON, W. E. N85-23395
WINNINGHAM, D. N85-22483
WIPF, S., L. N85-23391
WISE, D. U. N85-23654
WITBECK, N. E. N85-23599
WITHBROE, G. L. N85-23677
WITHERSPOON, P. A. N85-23062
WITT, R. G. N85-23209
N85-23212
WODKE, B. N85-22589
WOHLETZ, K. H. N85-23574
WOLFE, C. M. N85-22670
WOLLA, J. M. N85-22639
WOOD, H. L. N85-22549
WOOD, R. F. N85-22765
WOODWARD, D. S. N85-22372
WORLTON, J. N85-23315
WORONOW, A. N85-23539
N85-23540
N85-23627
WRIGLEY, R. C. N85-23214
WRIXON, G. T. N85-22886
WU, F. T. N85-23265
WU, I. W. D. N85-23423
WUNDERLICH, G. N85-22359

X

XIANMING, C. N85-23438
XUE-HUI, L. N85-23099

Y

YADLOWSKI, E. J. N85-22515
YAGUSHKIN, N. I. N85-22958
YAKOVLEV, A. V. N85-22989
YAKUSHIN, B. F. N85-22747
YAMADA, T. N85-23283
YANG, C. C. N85-23094
YANG, H. J. P. N85-23095
YANG, K. N85-22512
YANKOVSKIY, V. M. N85-22835
YANOVSKAYA, T. B. N85-23149
YAO, S. N85-23194
YAROVOY, V. V. N85-22721
YASHIN, A. A. N85-23041
YASTREB, A. N. N85-22746
YATES, G. J. N85-23072
YEDNERAL, N. V. N85-22749
YEFIMENKO, A. P. N85-22832
YEFIMOV, Y. V. N85-22720
YEFREMOV, S. A. N85-23136

YEGOROV, I. N85-22960
YEH, H. C. N85-22480
N85-22482
YELKINA, O. A. N85-22731
YENINA, Y. P. N85-23015
YEREMEYEV, A. N. N85-22737
YEREMICHEV, A. N. N85-22820
YERGIYEV, G. N. N85-22932
YERMAKOVA, N. V. N85-22740
YERMOLAYEV, A. G. N85-22717
YEROFEYEV, V. V. N85-22735
YERSHOV, N. S. N85-22829
YERSHOV, V. N. N85-22832
YEZHKOV, V. N85-22440
YIN, Y. Q. N85-23358
YINGXIA, Z. N85-23440
YOSHIDA, S. N85-22575
N85-22576
YOSHINO, M. M. N85-23233
N85-23234
YOUNG, D. A. N85-23551
YOUNG, F. C. N85-23411
YOUNG, P. A. N85-22892
YRUCHENKO, D. Z. N85-22715
YUILLE, A. N85-23345
YULYUGIN, V. K. N85-22715
YUNG, K. N85-23441
YUROV, V. N. N85-22432
YUZEFOVICH, A. P. N85-23169

Z

ZABOLOTNOV, Y. M. N85-22790
ZADORINA, Y. N. N85-22710
ZAGINAYLOV, G. I. N85-22974
ZAGORODNYY, V. G. N85-23148
ZAKHARCHENYA, B. P. N85-22665
ZAKHARENKO, S. K. N85-22953
ZAKHAROV, V. V. N85-22692
ZANDANOVA, G. I. N85-22975
ZAPEVALOV, V. Y. N85-22967
ZASTENKER, G. N. N85-22434
ZAYTSEV, A. N. N85-23014
ZAYTSEV, V. G. N85-23007
ZBRUTSKIY, A. V. N85-22822
ZEKTSER, D. M. N85-23033
ZELENKOV, G. S. N85-22989
ZELENYUK, F. M. N85-22717
ZEMTSOV, M. P. N85-22696
ZENCHEV, G. G. N85-22799
ZENGQI, X. N85-23438
ZENT, A. P. N85-23593
ZENTARA, S. J. N85-23287
ZHALKOVSKIY, N. D. N85-23157
ZHELEZNYI, V. P. N85-23054
ZHERO, O. G. N85-23117
ZHIGUO, L. N85-22844
ZHIRYAKOV, B. M. N85-22711
ZHOD, V. P. N85-22840
ZHUCHENKO, A. G. N85-22445
ZHUKOV, V. A. N85-22796
ZHUMAGAZIN, B. A. N85-22954
ZHURKOVA, T. B. N85-22704
ZIMBELMAN, J. N85-23565
N85-23608
ZINKOVSKIY, Y. F. N85-22934
ZINN, B. T. N85-22535
N85-22540
ZISK, S. A. N85-23510
ZIZELMAN, J. N85-22392
ZOLOTIV, A. A. N85-23138
ZORINA, Y. G. N85-23165
ZUBE, B. N85-23307
ZUBER, M. T. N85-23485
ZUYEV, A. B. N85-22961
ZVENIGORODSKIY, S. G. N85-22632
ZWANENBURG, R. N85-22623
ZYRYANOV, V. N. N85-23137

Typical Corporate Source Index Listing

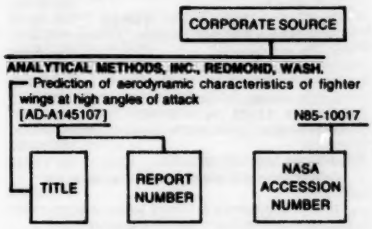

Listings in this index are arranged alphabetically by corporate source. The title of the document provides the user with a brief description of the subject matter. The report number helps to indicate the type of document cited (e.g., NASA report, translation, NASA contractor report). The NASA accession number denotes the number by which the citation is identified. The titles are arranged under each corporate source in ascending accession number order.

A

ADMIRALTY MARINE TECHNOLOGY ESTABLISHMENT, TEDDINGTON (ENGLAND).
Intensity vectors of sound scattering by a spherical shell
[AD-A147847] N85-23107
Numerical results of acoustic radiation, transmission and reflection of steel plate in water
[AMTE(N)-TM-84037] N85-23378

ADMIRALTY UNDERWATER WEAPONS ESTABLISHMENT, PORTLAND (ENGLAND).
The imaging of internal waves by the SEASAT-A synthetic aperture radar
[ARE(PORTLAND)TN-720/84] N85-22860

ADVISORY GROUP FOR AEROSPACE RESEARCH AND DEVELOPMENT, NEUILLY-SUR-SEINE (FRANCE).
Ground and flight testing for aircraft guidance and control
[AGARD-AG-262] N85-22350

AEG-TELEFUNKEN, WEDEL (WEST GERMANY).
Glotto solar array: Design, manufacture and test N85-22589
Development and qualification of the electrical part of the Advanced Rigid Array (ARA) N85-22594
Design and qualification testing of the Olympus solar array blanket N85-22600
Concentrator technologies evaluation for large solar arrays and their application for space stations/platforms N85-22609
Blanket integrated cushioning of foldable and retractable solar arrays N85-22612
Concept for controlled fold by fold deployment and retraction of flexible, foldable solar generators N85-22613
Aspects of low cost module technology N85-22614

AERONAUTICAL RESEARCH LABS., MELBOURNE (AUSTRALIA).
Below-room-temperature water-vapor continuum absorption within the 8- to 10 micron atmospheric transmission window
[TR-0084(4945-09)-1] N85-23266

AEROSPACE CORP., LOS ANGELES, CALIF.
Aerospace spacecraft-charging guidelines document N85-22501

AGRICULTURAL RESEARCH SERVICE, BELTSVILLE, MD.
A preliminary comparison of the information content of data from the LANDSAT 4 Thematic Mapper and Multispectral Scanner N85-23199
A first evaluation of LANDSAT TM data to monitor suspended sediments in lakes N85-23204
Snowmelt-runoff model utilizing remotely-sensed data N85-23226

AGRICULTURAL RESEARCH SERVICE, DURANT, OKLA.
A first evaluation of LANDSAT TM data to monitor suspended sediments in lakes N85-23204

AGRICULTURAL RESEARCH SERVICE, HOUSTON, TEX.
A first evaluation of LANDSAT TM data to monitor suspended sediments in lakes N85-23204

AIR FORCE ARMAMENT LAB., EGLIN AFB, FLA.
On a mathematical structure for an image algebra
[AD-A150226] N85-23348

AIR FORCE GEOPHYSICS LAB., HANSCOM AFB, MASS.
Spacecraft Environmental Interactions Technology, 1983
[NASA-CP-2359] N85-22470
Shuttle electrical environment N85-22475
Measured electron contribution to Shuttle plasma environment: Abbreviated update N85-22476
Direct measurements of severe spacecraft charging in auroral ionosphere N85-22480
Charging of DMSP/F6 spacecraft in aurora on 10 January 1983 N85-22481
Average and worst-case specifications of precipitating auroral electron environment N85-22482
Sheath ionization model of beam emissions from large spacecraft N85-22489
Automatic charge control system for satellites N85-22508
Interactions measurement payload for Shuttle N85-22518
Astronaut hazard during free-flight polar EVA N85-22522

AIR FORCE HUMAN RESOURCES LAB., WILLIAMS AFB, ARIZ.
Low altitude texture comparison data base and smooth shaded texture
[AD-A150342] N85-23323

AIR FORCE LOGISTICS COMMAND, WRIGHT-PATTERSON AFB, OHIO.
Electric and hybrid vehicle demonstration project
[DE85-003939] N85-23455

AIR FORCE ROCKET PROPULSION LAB., EDWARDS AFB, CALIF.
Acoustic energy exchange in sheared mean flows N85-22534
In-situ burning rate determination using flash radiography N85-22550

AIR FORCE WEAPONS LAB., KIRTLAND AFB, N. MEX.
SEM (Scanning Electron Microscope) investigation of silicon diodes using the electron beam induced current method
[AD-A150356] N85-22894

AIR FORCE WRIGHT AERONAUTICAL LABS., WRIGHT-PATTERSON AFB, OHIO.
Air Force technical objective document, Flight Dynamics Laboratory plans for fiscal year 1986. Air Force technical objective document
[AD-A149648] N85-22348
1981 wC-130 airborne lightning characterization program data review
[AD-A150230] N85-23275

ALABAMA UNIV., HUNTSVILLE.
Twenty-first JANNAF Combustion Meeting, volume 1
[AD-A150981] N85-22526
Coupled acoustic and hydrodynamic wave instabilities N85-22538

ALFATEH UNIV., TRIPOLI (LIBYA).
Improved modeling of the open circuit voltage of solar cells N85-22619

ALUMINUM CO. OF AMERICA, ALCOA CENTER, PA.
Directional dependent engineering properties of aluminum-aramid-epoxy laminates
[CCMS-85-02] N85-22638

AMES LAB., IOWA.
Application of modulated hydrodynamic voltammetry to the study of anodic electrocatalysis
[DE85-004182] N85-22653
Anomalous magnetism of CeFth3B2 under pressure
[DE85-003069] N85-23425

AMETEK, SANTA BARBARA, CALIF.
Aircraft skin penetrator and agent applicator. Volume 1: Working model development and construction
[AD-A150498] N85-22374

ANALYTIC SCIENCES CORP., READING, MASS.
Feature extraction assessment study
[AD-A150189] N85-23239

ANALYTICAL MECHANICS ASSOCIATES, INC., MOUNTAIN VIEW, CALIF.
Analysis of estimation algorithms for CDTI and CAS applications
[NASA-CR-172444] N85-22387

ANALYTICAL METHODS, INC., REDMOND, WASH.
Study for prediction of rotor/wake/fuselage interference, part 1
[NASA-CR-177340-VOL-1] N85-22346
Study for prediction of rotor/wake/fuselage interference. Part 2: Program users guide
[NASA-CR-177340-VOL-2] N85-22347

APPLIED SOLAR ENERGY CORP., CITY OF INDUSTRY, CALIF.
Space solar cells: Adjusting to new demands N85-22568

ARGONNE NATIONAL LAB., ILL.
Investigation of manganese dioxide as an improved solid desiccant
[DE85-004034] N85-22654
Grain boundaries in NiO
[DE85-006129] N85-22687
NDE methods for green ceramics
[DE85-004019] N85-22766
Flow-induced vibrations of a circular cylinder due to turbulent internal flows
[DE85-002766] N85-23110
Using fuel cells or anode depolarization to reduce electrowinning energy consumption
[DE85-006167] N85-23250
Cathode materials for molten carbonate fuel cells
[DE85-004078] N85-23254
Proceedings of the Geoscience Instrumentation Workshop
[DE85-004359] N85-23268
Distribution of radium and plutonium in human bone
[DE85-005025] N85-23298
Second thoughts on the mathematical software effort: A perspective
[DE85-004831] N85-23333
Implementation of some concurrent algorithms
[DE85-004687] N85-23334

ARIZONA STATE UNIV., TEMPE.
Size and velocity distributions of particles and droplets in spray combustion systems
[AD-A150355] N85-22648
Transport properties of silica thermally grown on silicon
[AD-A150304] N85-23418
Topographic evidence for shield volcanism on Io N85-23478
Sulfur volcanoes on Io? N85-23479
Surfaces of asteroids and cometary nuclei N85-23503
The nature of Martian flow ejecta craters N85-23545
Magmas as selective filters of volatiles between planetary mantles and surfaces N85-23557
Field measurements of the 1983 Royal Gardens lava flows, Kilauea Volcano, and 1984 Mauna Loa lava flows, Hawaii N85-23565
Basaltic pressure ridges: Formation and relationship to flow emplacement N85-23567
A silicic shield volcano in Bolivia N85-23572
Hydrovolcanism N85-23574
The origin of regional dust deposits on Mars N85-23578
The effect of particle density on aeolian transport N85-23581
A comparison of terrestrial saltation flux in the laboratory and the field N85-23582
Potential bedforms on Venus: Wind tunnel simulations N85-23583
Microdunes and other aeolian bedforms on Venus: Wind tunnel simulations N85-23584

Relative time-scale for channeling events within chaotic terrains, Margaritifer Sinus, Mars N85-23589
Planetary analogs in Antarctica: Mars N85-23604
Planetary analogs in Antarctica: Icy satellites N85-23605
The geomorphology of Rhea N85-23606
Geologic interpretation of remote sensing data for the Martian volcano, Ascraeus Mons N85-23608
Water-ice clouds on Mars: Location and seasonal variation N85-23611
Radar observations of fissure-fed basaltic lava flows, Craters of the Moon, Idaho N85-23640
Analyses of radar images of small craters N85-23642

ARIZONA UNIV., TUCSON.
An investigation of several aspects of LANDSAT-5 data quality
[E85-10096] N85-23214
Research in the optical sciences
[AD-A150196] N85-23401
Optical processing in radon space
[AD-A150289] N85-23402
Innovative research in the design and operation of large telescopes for space: Aspects of giant telescopes in space
[NASA-CR-175626] N85-23462
Martian terrain ages N85-23537
Morphology and mechanics of terraces in lunar craters N85-23543
Ripple ring basins on Ganymede and Callisto N85-23547
Theoretical thermodynamics of mixtures at high pressures N85-23550
Modelling equilibrium and fractional crystallization in the system MgO-FeO-CaO-Al2O3-SiO2 N85-23552
Paleohydrologic implications of valley networks of Mars N85-23585
Lineaments on Ganymede: New evidence for late tectonic activity N85-23658

ARMY MISSILE COMMAND, REDSTONE ARSENAL, ALA.
Characterization standards for solid propellant rocket motors
[AD-A150250] N85-22627
Acousto-optically addressed Fourier transform matched filters
[AD-A150298] N85-22889
Near Field/Far Field (NF/FF) energy loss in Electric Discharge Lasers (EDL's): A mode-medium interaction
[AD-A150299] N85-23075

ARMY RESEARCH AND DEVELOPMENT COMMAND, DOVER, N.J.
The crystal and molecular structure of a new propellant compound: Triaminoguanidium Azide Nitrate (TAZN) N85-22551
Molecular dynamics of propellant gases, part 2 N85-22552

ARMY TEST AND EVALUATION COMMAND, ABERDEEN PROVING GROUND, MD.
Laboratory tests of reciprocating internal combustion engines
[AD-A150143] N85-23087

ATLANTIC RESEARCH CORP., GAINESVILLE, VA.
Workshop report: Swirl Enhanced Combustion N85-22564

ATSUKO COMPUTING INTERNATIONAL, HUNTSVILLE, ALA.
Digital processing of mesoscale analysis and space sensor data
[NASA-CR-171429] N85-23319

AUBURN UNIV., ALA.
Nonlinear rotordynamics analysis
[NASA-CR-171425] N85-22364

B

BALLISTIC RESEARCH LABS., ABERDEEN PROVING GROUND, MD.
A comprehensive review of black powder
[AD-A150455] N85-22769
Liquid moment on a filled coning cylinder during spin-up: Ad hoc model
[AD-A150260] N85-23060

BATTELLE COLUMBUS LABS., OHIO.
Composition and photochemical reactivity of turbine engine exhaust
[AD-A150559] N85-23256

BATTELLE PACIFIC NORTHWEST LABS., RICHLAND, WASH.
Electrical and thermal transport property studies of high-temperature thermoelectric materials
[AD-A150167] N85-23417

BDM CORP., ALBUQUERQUE, N. MEX.
Electrical overstress protection of submicron devices
[AD-A150334] N85-22692

BEERS ASSOCIATES, INC., RESTON, VA.
A simple model of electron beam initiated dielectric breakdown N85-22516

BENDIX CORP., KANSAS CITY, MO.
Development of a sintered shim
[DE85-006183] N85-22685

BIONETICS CORP., HAMPTON, VA.
Research on the effect of noise at different times of day: Models, methods and findings
[NASA-CR-3888] N85-23375

BOEING AEROSPACE CO., HUNTSVILLE, ALA.
Space station systems technology study (add-on task). Volume 1: Executive summary
[NASA-CR-171415] N85-22459

BOEING AEROSPACE CO., SEATTLE, WASH.
Centrifuge impact cratering experiments N85-23533

BOLT, BERANEK, AND NEWMAN, INC., CAMBRIDGE, MASS.
Research in continuous speech recognition
[AD-A150474] N85-22868
An experimental investigation of the chopping of helicopter main rotor tip vortices by the tail rotor
[NASA-CR-177338] N85-23376

BOLT, BERANEK, AND NEWMAN, INC., CANOGA PARK, CALIF.
Wind tunnel acoustic study of a propeller installed behind an airplane empennage: Data report
[NASA-CR-177335] N85-23377

BOSTON COLL., CHESTNUT HILL, MASS.
EMI characteristics of a potential control system N85-22502

BRIGHAM YOUNG UNIV., PROVO, UTAH.
Measurements of distributed combustion N85-22542
Distributed combustion: A mechanism of acoustic suppression N85-22543
The color excesses of classical cepheids and the structure of our galaxy N85-23459

BRISTOL UNIV. (ENGLAND).
First principles theory of Fermi-surface driven concentration waves in Cu/sub c/Pd/sub 1-c/ alloys
[DE85-005367] N85-22681

BRITISH AEROSPACE DYNAMICS GROUP, STEVENAGE (ENGLAND).
The performance of the Olympus power subsystem with its solar array N85-22601

BRITISH BROADCASTING CORP., KINGSWOOD (ENGLAND).
Electronic generation of text for television
[BBC-RD-1984/14] N85-22656
Digital standards conversion: Interpolation theory and aperture synthesis
[BBC-RD-1984/20] N85-22657

BRITISH LIBRARY LENDING DIV., BOSTON SPA (ENGLAND).
Formation of alumina layers on iron-base alloys
[BLL-T6418/BG/LRS/LRST737/84] N85-22657
Delayed cracking strength of experimental grades of 42 CD 4 steel in aqueous H2S surroundings
[BLL-T6419/BG/LRS/LRST738/84] N85-22658
Examination of the contact wetting angle in the vicinity of critical temperature
[BLL-T6416/BG/CRS/LR-ST735/84] N85-23054
Microcomputer: Controlled statistics analyzer
[BLL-CE-TRANS-7971-(9022.09)] N85-23306
Requirements placed on information processing equipment
[BLL-CE-TRANS-7983-(9022.09)] N85-23307

BROOKHAVEN NATIONAL LAB., UPTON, N. Y.
Local electrochemistry of pitting corrosion in stainless steels
[DE85-005207] N85-22673
Applications of the vibration probe to localized current measurements
[DE85-004702] N85-22675
Microscopic magnetic structure of multiple bilayers of thin films of Fe and Ge
[DE85-004188] N85-22682
HREELS and Auger studies of conducting polymers
[DE85-004541] N85-22764
Modulation of light energy transduction in photosynthesis
[DE85-004711] N85-23292
Role of optical disk at computing centers
[DE85-005124] N85-23314

BROWN UNIV., PROVIDENCE, R. I.
Patterns of fracture and tidal stresses due to nonsynchronous rotation: Implications for fracturing on Europa N85-23483
Formation of bright terrain bands on Ganymede by unstable lithosphere extension N85-23485
Characteristics of basaltic lava flows on Venus N85-23508
Surface units on Venus derived from Pioneer-Venus altimetry, roughness, and reflectivity measurements N85-23510
Classification of circular features on Venus N85-23511
A statistical treatment of the regional slope characteristics of Venus and Earth N85-23517

C

CALIFORNIA INST. OF TECH., PASADENA.
Research program on the effect of pressure on the mechanical properties of polymers, part 2
[DE85-000995] N85-22761
Plasma production by meteoroid impact N85-23492
Giant planets and their satellites: Cosmochemistry, evolution and structure N85-23494
Impact and collisional processes in the solar system N85-23530
Impact cratering calculation N85-23531

CALIFORNIA STATE POLYTECHNIC UNIV., POMONA.
Terrestrial analog studies for Martian patterned ground N85-23590

CALIFORNIA UNIV., BERKELEY.
Advanced mixed-mode simulation techniques N85-22883
Mode control and wavelength tuning in open ended Michelson interferometric semiconductor laser N85-23073
Elastic wave scattering from an interface crack in a layered half space N85-23095
Characterization of LANDSAT-4 TM and MSS image quality for the interpretation of California's agricultural resources N85-23190
Studies of galactic HI in 21-centimeter absorption N85-23466
Measurement of the large-scale anisotropy of the cosmic background radiation at 3 MM N85-23680
A measurement of the intensity of the cosmic background radiation at 3.9 cm N85-23681

CALIFORNIA UNIV., BERKELEY. LAWRENCE BERKELEY LAB.
Densification and deformation in the presence of a liquid phase
[DE85-005101] N85-22763
Effects of fracture roughness on fluid flow through a single deformable fracture
[DE85-004593] N85-23062
Interaction of metals and metalloids with biomembranes
[DE85-004902] N85-23293
Introduction to CHART: A graphic analysis and display system, revision
[DE85-004612] N85-23335
Microstructural study on the processing and properties of high-field A15 superconducting materials
[DE85-004652] N85-23423
Macroscopic quantum tunnelling in a current biased Josephson junction
[DE85-004603] N85-23424
Cooling of neutron stars with hyperons
[DE85-004841] N85-23472

CALIFORNIA UNIV., DAVIS.
Diffusion deposition in fibrous filters for parallel and transverse flow models
[DE85-006149] N85-23066

CALIFORNIA UNIV., LIVERMORE. LAWRENCE LIVERMORE LAB.
Development of epoxy matrices for filament-wound graphite structures
[DE85-003674] N85-22642
Impurities in Kevlar 49 fibers
[DE85-004996] N85-22767
Numerical/Electromagnetics Code (NEC)
[DE85-004999] N85-22874
Surface wave excitation study
[DE85-005301] N85-22875
Electronics Engineering Department EE Technical Review
[UCRL-50025-84-1] N85-22887
The ASCOT Data Analysis Workshop
[DE85-004407] N85-23283
Exploiting multiprocessors: Issues and options
[DE85-003144] N85-23313
FORTRAN in the 90's
[DE85-006154] N85-23332
SIGPI: A user's manual for the fast computation of the probabilistic performance of a complex system
[DE85-005447] N85-23336
Molecular dynamics studies of energy transfer processes in crystal systems
[AD-A150161] N85-23416
H-division materials physics progress
[DE85-004990] N85-23430
Shock compression of liquid helium to 56 GPa (560) kbar N85-23551
Creep of ice: Further studies N85-23655

CALIFORNIA UNIV., LOS ANGELES.
A generalized solution to a class of printed circuit antennas N85-22882
Investigations of the high frequency performance of impact avalanche transit-time diodes N85-22884
Cumulus effects on the large-scale vorticity and momentum fields in the tropical atmosphere N85-23270
Approximation in optimal control and identification of large space structures [AD-A150323] N85-23351
A survey for galactic plane ultraviolet-excess objects: Space densities for white dwarfs, subdwarfs, and cataclysmic variables N85-23458
High pressure cosmochemistry of major planetary interiors: Laboratory studies of the water-rich region of the system ammonia-water N85-23549

CALIFORNIA UNIV., SAN DIEGO.
Optical memory research and its application to digital optical processing N85-23397

CALIFORNIA UNIV., SAN DIEGO, LA JOLLA.
Anomalously high potentials observed on ISEE N85-22503
Preliminary investigation of the electrodynamics of a conducting tether N85-22521

CALIFORNIA UNIV., SANTA BARBARA.
Development of a planar heterojunction bipolar transistor for very high speed logic [AD-A150374] N85-22895
Snow reflectance from Thematic Mapper N85-23205

CAMBRIDGE UNIV. (ENGLAND).
University of Cambridge Institute of Astronomy report of activities N85-23464

CARNEGIE INSTITUTION OF WASHINGTON, D. C.
Accumulation of the terrestrial planets N85-23524

CARRIER CORP., SYRACUSE, N.Y.
Development of a single-family absorption chiller for use in a solar heating and cooling system, phase 3, volume 2 [DE85-003218] N85-23253

CASE WESTERN RESERVE UNIV., CLEVELAND, OHIO.
Dilution jet configurations in a reverse flow combustor [NASA-CR-174888] N85-22392
Electron yields from spacecraft materials N85-22512
HREELS and Auger studies of conducting polymers [DE85-004541] N85-22764

CELANESE RESEARCH CORP., SUMMIT, N.J.
Exploratory development of foams from liquid crystal polymers [NASA-CR-172510] N85-22754

CENTRE NATIONAL D'ETUDES SPATIALES, TOULOUSE (FRANCE).
Investigation of high output gallium arsenide solar cells N85-22578
Calibration of solar cells outside the atmosphere N85-22603
Inverse behavior of silicon photovoltaic cells N85-22604
Problems with electrical interference between solar generators and shunt type regulators N85-22607

CENTRE NATIONAL DE LA RECHERCHE SCIENTIFIQUE, TOULOUSE (FRANCE).
GaAlAs-GaAs solar cell development: Prospective for space applications under concentration N85-22581
Technological process effect on the carrier lifetime degradation of silicon solar cell base layer irradiated by 1 MeV electrons (boron doping case) N85-22585

CENTRE NATIONAL DE LA RECHERCHE SCIENTIFIQUE, VALBONNE (FRANCE).
High output photovoltaic conversion: The quadrispectral project N85-22626

CENTRO INFORMAZIONI STUDI ESPERIENZE, MILAN (ITALY).
Development of very thin large area GaAs solar cells for space application N85-22579

CESKOSLOVENSKA AKADEMIE VED, PRAQUE.
In-orbit laser regeneration of the radiation damaged solar arrays N85-22588

CHIBA UNIV. (JAPAN).
Studies on physical properties of snow based on multi channel microwave radiometer N85-23231
Analysis of NIMBUS-7 SMMR data N85-23232

CHRYSLER CORP., NEW ORLEANS, LA.
Results of aeroheating DFI and ET design-data test on a 0.0175-scale model 60-OTS conducted in the Von Karman Gas Dynamics Facility (VKF) 40° supersonic and the 50° hypersonic wind tunnels A and C [NASA-CR-167693] N85-22466
Results of the AFRSI rewaterproofing systems screening test in the NASA/Ames Research Center (ARC) 2 x 2-foot transonic wind tunnel [NASA-CR-167694] N85-22467
Results of a M = 5.3 heat transfer test of the integrated vehicle using phase-change paint techniques on the 0.0175-scale model 58-OTS in the NASA/Ames Research Center 3.5-foot hypersonic wind tunnel [NASA-CR-167695] N85-22468

CLARKSON COLL. OF TECHNOLOGY, POTSDAM, N.Y.
Control of cascaded induction generator systems [AD-A150429] N85-22897

CLEMSON UNIV., S.C.
Longitudinal splitting in unidirectional composites, analysis and experiments [NASA-CR-3881] N85-22639
Data compression for noiseless channels N85-22851

COLORADO SCHOOL OF MINES, GOLDEN.
Two-and-one-half dimensional in-plane wave propagation [AD-A150467] N85-22867

COLORADO STATE UNIV., FORT COLLINS.
An integral closed loop combustion stability model-status and review N85-22553
Chiral polymers [AD-A150366] N85-22760
Slow motions in the tropical troposphere N85-23262
The relationship between marine aerosol particles and satellite-detected radiance N85-23263
A theoretical study of the ozone quasi-biennial oscillation in the tropical stratosphere N85-23264
Magnetic field interactions with material discontinuities [AD-A150197] N85-23373

COLORADO UNIV., BOULDER.
Satellite-to-satellite orbit determination using minimum, discrete range and range-rate data only N85-22458
Ignition phenomena of bulk aluminum alloy as a function of oxygen pressure N85-22531
Chemical kinetics of gas phase decomposition products of nitramine propellants N85-22558
Transient analysis of loaded thin-wire antennas and transmission lines N85-22852
Chemical stabilization of laser dyes [AD-A150451] N85-23076
Magnetic location of Earth's core-mantle boundary and estimates of the adjacent fluid motion N85-23260
Empirical and modeled synoptic cloud climatology of the Arctic Ocean [NASA-CR-175628] N85-23272
User's and programmer's guide to the mechanics of moving finite element code [DE85-006165] N85-23365
Ion transport in beam-plasma interactions [AD-A150145] N85-23410
Personal decision making: The influence of perceived locus of control and degree of rationality on information seeking strategies N85-23446
Analysis and interpretation of observations of airglow at 297 nm in the Venus thermosphere N85-23473
Ultraviolet spectral diagnostics of solar flares and heating events N85-23675

COLUMBIA UNIV., NEW YORK.
Integrated digital networks [AD-A150605] N85-22873

COMMITTEE ON SCIENCE AND TECHNOLOGY (U. S. HOUSE).
Authorizing appropriations to the National Aeronautics and Space Administration for fiscal year 1986 [H-REPT-99-32] N85-23452

COMMUNICATIONS RESEARCH CENTRE, OTTAWA (ONTARIO).
Experimental results on the application of convolutional coding and Viterbi decoding as a frequency diversity technique in HF data transmission [CRC-1377] N85-22850

COMMUNICATIONS SATELLITE CORP., CLARKSBURG, MD.
Investigations of radiation-induced and carrier-enhanced conductivity N85-22515

CORNELL UNIV., ITHACA, N.Y.
Relationship between topological and magnetic order in small metal clusters [AD-A150547] N85-22651
Experimental and numerical analysis of electric currents and electromagnetic blunting of cracks in thin plates [AD-A150418] N85-22669
Pre- and post-processing for stream-function eddy current calculations [AD-A150417] N85-22806
Time resolved X-ray studies during pulsed laser irradiation of Ge [DE85-005263] N85-23083
Hartree-Fock interaction between a helium atom and lithium-metal: A test for the effective medium theory [AD-A150468] N85-23387
Adsorption site, adsorption energy and normal vibration frequency of H/Ni(100) via total energy calculations [AD-A150555] N85-23388
Collective acceleration of ions using high current relativistic electron beams [DE85-004889] N85-23393
Observation of surface vibrational resonances on (110) surfaces of FCC metals [AD-A150469] N85-23419
Dipole active surface vibrational resonances on clean and hydrogen covered Ni(110) [AD-A150548] N85-23420
Planetary geology in the 1980s [NASA-SP-467] N85-23457
Investigations of planetary ring phenomena N85-23487
Dynamical studies of Saturn's rings N85-23489
Convex-profile inversion of asteroid lightcurves N85-23502
Implications of convection in the Moon and the terrestrial planets N85-23548
Seasonal and secular variation of the Solis Lacus albedo feature: Relation to the Martian dust-transport cycle N85-23576
Eolian erosion on Mars: Three scales N85-23577
Accurate albedos of the brightest regions on Io N85-23618
Io: Precise comparison of Voyager spectral curves with laboratory measurements N85-23619
Participation in the Mars Data Analysis Program: Analysis of cloud forms in Viking and Mariner 9 images [NASA-CR-175604] N85-23673

COUNCIL FOR SCIENTIFIC AND INDUSTRIAL RESEARCH, PRETORIA (SOUTH AFRICA).
Structures of ordered linear dislocation multipoles in Cu-Al alloys [ISSN-0379-6906] N85-22664
Human cognition and intelligence: Towards an integrated theoretical perspective [CSIR-SR-PERS-350] N85-23300

D

DARTMOUTH COLL., HANOVER, N.H.
A model for eclipsing cataclysmic variables N85-23467

DAYTON UNIV., OHIO.
Sample introduction methods for improving the particle detection capability of the spectrometric oil analysis program [AD-A150139] N85-23309

DEFENCE RESEARCH INFORMATION CENTRE, ORPINGTON (ENGLAND).
Oxidation resistant materials for hot gas turbines and jet engines [AD-B087399L] N85-22389
Prediction of the resistance of structural materials to cavitation erosion [BLL-DRIC-TRANS-7435-(3623.66)] N85-22659
Metal-semiconductor phase transition and its application [DRIC-T-7149] N85-22665
Adsorption behaviour of nitrogen compounds on to porous polymer beads and applications to atmospheric sampling [BLL-DRIC-TRANS-7399-(3623.66)] N85-22753
Turbulent flows of surfacant solutions [AD-B089137L] N85-23058
Luminescence in the ocean [AD-B089136L] N85-23288
The audiomat: An automatic audiometer for use in occupational audiometry [DRIC-T-7138] N85-23294

DELAWARE UNIV., NEWARK.
Trifunctional catalysts for conversion of syngas to alcohols [DE85-004577] N85-22771
Remote sensing of coastal wetlands biomass using Thematic Mapper wavebands N85-23198
Assessing LANDSAT TM and MSS data for detecting submerged plant communities N85-23203
Brain mechanisms underlying individual differences in reaction to stress: An animal model [AD-A150195] N85-23301

DEPARTEMENT D'ETUDES ET DE RECHERCHES EN TECHNOLOGIE SPATIALE, TOULOUSE (FRANCE).
Isotropic proton irradiation of GaAs solar cells N85-22622

DEUTSCHE FORSCHUNGS- UND VERSUCHSANSTALT FUER LUFT- UND RAUMFAHRT, BONN (WEST GERMANY).
The DFS-Kopernikus solar generator N85-22591

DEUTSCHE FORSCHUNGS- UND VERSUCHSANSTALT FUER LUFT- UND RAUMFAHRT, BRUNSWICK (WEST GERMANY).
Dynamic wind tunnel testing for active control research N85-22352

Guidance and control research flight testing with HFB 320 test aircraft N85-22355
Avionics Flight Evaluation System (AFES) N85-22357

DU PONT DE NEMOURS (E. I.) AND CO., AIKEN, S.C.
Hydrogen effects in austenitic stainless steels based on the Fe-Cr-Mn-N system [DE85-003617] N85-22672

DUKE UNIV., DURHAM, N. C.
The design of a unified package for the solution of stochastic petri net models [AD-A150326] N85-23354
Automatic symbolic solution of Markov chains [AD-A150476] N85-23369

E

EARTH SATELLITE CORP., CHEVY CHASE, MD.
Evaluation of Thematic Mapper performance as applied to hydrocarbon exploration N85-23191

EDGERTON, GERMESHAUSEN AND GRIER, INC., IDAHO FALLS, IDAHO.
Contribution of instrumentation and control software to system reliability [DE85-004693] N85-23340

EDGERTON, GERMESHAUSEN AND GRIER, INC., LAS VEGAS, NEV.
Comprehensive, integrated, remote sensing at DOE sites [DE85-004667] N85-23240

EUROPEAN SPACE AGENCY, PARIS (FRANCE).
Photovoltaic Generators in Space [ESA-SP-210] N85-22565
Emissivity enhancement of fused silica for space applications N85-22615

EUROPEAN SPACE AGENCY. EUROPEAN SPACE RESEARCH AND TECHNOLOGY CENTER, ESTEC, NOORDWIJK (NETHERLANDS).
Derivation of the Olympus solar array requirements N85-22598
Survival testing of silicon solar modules N85-22602
Deployment analysis of the Olympus Astromast and comparison with test measurements N85-22616
Developments in deployable masts to support flexible solar arrays N85-22620
Annealing of radiation damage in boron and gallium doped silicon solar cells N85-22624
Growth capabilities of European retractable solar arrays N85-22625

F

FEDERAL AVIATION ADMINISTRATION, WASHINGTON, D.C.
Planned office and facility consolidations: To improve system effectiveness and efficiency, FY 1985-87 [AD-A150441] N85-22376

FEDERAL COMPILER TESTING CENTER, FALLS CHURCH, VA.
Validation summary report, Burroughs Corporation, 820 FORTRAN release 4.0 [PB84-227792] N85-23316

FEDERATION OF AMERICAN SOCIETIES FOR EXPERIMENTAL BIOLOGY, BETHESDA, MD.
Research opportunities in human behavior and performances [NASA-CR-3886] N85-23299

FLORIDA STATE UNIV., TALLAHASSEE.
Schur-Ostrowski theorems for functionals on l1(0,1) [AD-A150193] N85-23346

FLORIDA UNIV., GAINESVILLE.
Shuttle flight test of an advanced gamma-ray detection system [AD-A150316] N85-22469
Drift fields and boundary conditions at grain boundaries in bipolar P/N junction silicon devices N85-22879
Optimum design of electrical motors for multilink manipulators and automated manufacturing systems N85-22880
A systematic study of light scattering by irregularly shaped particles [AD-A150192] N85-23400
Gas dynamics of the barred spiral galaxy NGC 3359 N85-23465

G

GENERAL ELECTRIC CO., LYNN, MASS.
T700 cutter life improvement program [AD-A150450] N85-23089

GENERAL ELECTRIC CO., SCHENECTADY, N. Y.
The ferrite permanent magnet AC motor: A technical and economical assessment [DE85-002480] N85-22903

GENERAL RESEARCH CORP., SANTA BARBARA, CALIF.
Research efforts in support of resonance extraction studies. Volume 1: Improvement and validation of TWFD (Thin-Wire Frequency-Domain): A thin-wire frequency-domain scattering code [AD-A150296] N85-22864

GEOLOGICAL SURVEY, DENVER, COLO.
Determination of mineral type, abundance, and grain size with remotely obtained reflectance spectra N85-23623

GEOLOGICAL SURVEY, FLAGSTAFF, ARIZ.
Progress in planetary radarclinometry N85-23630
Unsupervised classification of global radar units on Venus N85-23632
Late Tertiary and Quaternary river systems of the eastern Sahara as mapped on shuttle radar and LANDSAT images N85-23641
Valles Marineris basin beds: A complex story N85-23652
Mars: Stratigraphy of western highlands and polar regions N85-23653
Mars geologic mapping: A review and new concepts N85-23663
The Galilean Satellite Geological Mapping Program, 1984 N85-23664
Geology of the Ganymede quadrangle Jg7 N85-23665
Mars planimetric mapping N85-23666
Viking Lander mosaics of Mars N85-23667
Voyager cartography N85-23668

GEOLOGICAL SURVEY, MENLO PARK, CALIF.
Io: Generation of silicate magma by shear melting at the base of a basaltic lithosphere N85-23476
Why not a constant early lunar impact rate? N85-23536
Average spacing for rings of individual multi-ring basins is 2.0(0.5)D N85-23541
Ring-diameter ratios for multi-ring basins average 2.0(0.5)D N85-23542
Observed changes at Viking Lander 1 N85-23575
Radiation-dominated snowmelt on Mars N85-23592

GEORGE WASHINGTON UNIV., WASHINGTON, D.C.
On the solution of the three-dimensional flowfield about a flow-through nacelle [NASA-TM-87448] N85-22371

GEORGIA INST. OF TECH., ATLANTA.
Simple theoretical models for composite rotor blades [NASA-CR-175620] N85-22382
Combustion of zirconium carbide N85-22532
Investigations of reactive and non reactive acoustic boundary layers in porous walled ducts N85-22535
Investigation of the characteristics of the velocity-coupled response functions of solid propellants N85-22540
Mechanism of burning rate enhancement by ferric oxide N85-22546
Interlaminar fracture toughness in resin matrix composites [AD-A150565] N85-22640
Study of the effects of implantation on the high Fe-Ni-Cr and Ni-Cr-Al alloys [NASA-CR-175625] N85-22661
Two-dimensional signal processing and storage and theory and applications of electromagnetic measurements [AD-A150590] N85-22899

GEORGIA UNIV., ATHENS.
Production and turnover of suspended organic detritus in the coastal water of the southeastern continental shelf [DE85-003977] N85-23290

GIESSEN UNIV. (WEST GERMANY).
Electrostatic discharge testing on a carbon fiber solar panel structure N85-22584

H

HAMILTON STANDARD, WINDSOR LOCKS, CONN.
Large-scale Advanced Propfan (LAP) performance, acoustic and weight estimation, January, 1984 [NASA-CR-174782] N85-22368

HANFORD ENGINEERING DEVELOPMENT LAB., RICHLAND, WASH.
Effects of neutron irradiation at 450(0)C and 16 dpa on the properties of various commercial copper alloys [DE85-005716] N85-22684

HARVARD-SMITHSONIAN CENTER FOR ASTROPHYSICS, CAMBRIDGE, MASS.
Research on the early history of the solar system N85-23527
Viking radio science data analysis and synthesis N85-23528

HARVARD UNIV., CAMBRIDGE, MASS.
Theoretical and observational studies of stellar activity N85-23468

HAWAII INST. OF GEOPHYSICS, HONOLULU.
The olivine asteroids: Discovery, mineralogy, and relationship to palasites N85-23500
An idealized short period comet model: Surface insolation, H2O flux, dust flux and mantle evolution N85-23504

HAWAII UNIV., HILO.
Polar cap formation on Ganymede N85-23486

HAWAII UNIV., HONOLULU.
Research in planetary studies and operation of Mauna Kea Observatory [NASA-CR-175618] N85-23460
Emplacement of long lava flows on Mauna Loa (Hawaii) and Alba (Mars) N85-23563
Surface structures of Hawaiian lavas N85-23566
Submarine volcanic eruptions and potential analogs for Venus N85-23573
Mars: Long term changes in the state and distribution of H2O N85-23593
Multispectral analysis of the Kasei Vallis-Lanae Planum region of Mars N85-23607
First direct detection of clay minerals on Mars N85-23612
Remote sensing analyses of localized lunar dark mantle deposits N85-23616
Spectral reflectance studies of the Orientale basin N85-23617

HEBREW UNIV., JERUSALEM (ISRAEL).
The orientation distribution of nonspherical aerosol particles within a cloud [AD-A150600] N85-23061

HERCULES, INC., CUMBERLAND, MD.
Workshop report: Catalysis of Burn Rate of Energetic Binder propellants N85-22545

HERZBERG INST. OF ASTROPHYSICS, OTTAWA (ONTARIO).
Meteoroidal impacts, plasma, fine structure of ringlets and spokes on Saturn's ring B N85-23490

HOUSTON UNIV., TEX.
Shape optimization for minimal stress concentration N85-23093
Problems in recovering crater production functions N85-23539
A parmetric study of crater-saturation simulation N85-23540
Monte Carlo modeling of lunar megaregolith development N85-23627

HUGHES AIRCRAFT CO., EL SEGUNDO, CALIF.
Interactions between large space power systems and low-Earth-orbit plasmas N85-22490

HUGHES RESEARCH LABS., MALIBU, CALIF.
Kapton charging characteristics: Effects of material thickness and electron-energy distribution N85-22513

I

IBM RESEARCH LAB., SAN JOSE, CALIF.
EXAFS of monolayers on silver electrodes: SSRL proposal number 717M [AD-A150623] N85-22652

IDAHO NATIONAL ENGINEERING LAB., IDAHO FALLS.
Magnetic refrigeration and heat pumping design options [DE85-003405] N85-23064
Electric vehicle test program: INEL transition qualification test plan [DE85-005171] N85-23456

ILLINOIS UNIV., CHICAGO.
Optimal allocation of components in parallel-series and series-parallel systems [AD-A150169] N85-23309
Optimal designs for comparisons between two sets of treatments [AD-A150621] N85-23360

ILLINOIS UNIV., URBANA.
Non-linear optical techniques for visible and UV lasers and thin film deposition [AD-A150489] N85-23077

INDIANA UNIV., BLOOMINGTON.
Sleep deprivation and exercise tolerance [AD-A150180] N85-23295
Sleep deprivation and exercise tolerance [AD-A150566] N85-23296
Sleep deprivation and exercise tolerance [AD-A150626] N85-23297
Dynamics of gas disks in triaxial galaxies N85-23469

INDUSTRIEANLAGEN-BETRIEBSGESELLSCHAFT M.B.H., OTTOBRUNN (WEST GERMANY).
Air combat simulation: Methods, models, trends N85-22359

INSTITUTE OF ELECTRICAL AND ELECTRONICS ENGINEERS, NEW YORK, N.Y.
Technical Digest: Symposium on Optical Fiber measurements, 1984 [PB85-114700] N85-23407
INSTITUTE OF GAS TECHNOLOGY, CHICAGO, ILL.
Anaerobic digestion of biomass: status summary and research development needs, 1983 [PB85-161925] N85-22772
INSTITUTE OF SPACE AND ASTRONAUTICAL SCIENCE, TOKYO (JAPAN).
History and future views on solar cells of Japanese scientific satellites N85-22566
Development of Halley's Comet explorer PLANET-A solar array N85-22608
INTERACTIVE SYSTEMS CORP., LITTLETON, COLO.
Hexagonal data base study [AD-A150176] N85-23448
INTERNATIONAL BUSINESS MACHINES CORP., PALO ALTO, CALIF.
Analysis and evaluation of the LANDSAT-4 MSS and TM sensors and ground data processing systems: Early results N85-23189
IOWA UNIV., IOWA CITY.
Suprathermal plasma observed on STS-3 Mission by plasma diagnostics package N85-22472
Fatigue life, crack initiation, and propagation of 304 stainless steel with non-proportional axialtorsional strain-paths N85-23094
Periodic substorm activity in the geomagnetic tail [NASA-CR-175629] N85-23409
Volcanic debris flows in the Elysium region of Mars N85-23560

J

JAYCOR, SAN DIEGO, CALIF.
Discharge characteristics of dielectric materials examined in mono-, dual-, and spectral energy electron charging environments N85-22510
JET PROPULSION LAB., CALIFORNIA INST. OF TECH., PASADENA.
Large amplitude forcing of a high speed 2-dimensional jet [NASA-CR-175646] N85-22393
Repair on final recommendations for IMPS engineering-science payload [NASA-CR-175659] N85-22464
Auroral-polar cap environment and its impact on spacecraft-plasma interactions N85-22484
Galileo internal electrostatic discharge program N85-22504
Characterization of heterogeneity of composite propellants and its effects on combustion behavior N85-22539
A comparison of metropolitan and non-metropolitan employment characteristics: Indications of the size of non-metropolitan mobile communication services user classes [NASA-CR-175648] N85-22855
Periodic binary sequence generators: VLSI circuits considerations [NASA-CR-175649] N85-22886
Microwave blackbodies for spaceborne receivers [NASA-CR-175647] N85-23068
Fracture mechanics evaluation of GaAs [NASA-CR-175657] N85-23101
Geologic utility of LANSDAT-4 TM data N85-23192
Science opportunities using the NASA scatterometer on N-ROSS [NASA-CR-175639] N85-23222
New high-efficiency silicon solar cells [NASA-CR-175643] N85-23244
Analysis of biological particles by mass spectrometry [AD-A149952] N85-23291
Optical system [NASA-CASE-NPO-15801-1] N85-23396
Activities of the Jet Propulsion Laboratory, 1 January - 31 December 1983 [NASA-CR-175555] N85-23447
Hot spots on Io: Correlation of infrared emission and visible reflectance N85-23475
Geomorphic classification of lava flows on Io N85-23480
Sulfur oxygen processes on Io N85-23481
Study and estimation of planet-crossing asteroid populations: Discoveries and analysis N85-23498
Small solar system bodies N85-23499
Comet thermal modeling N85-23505
Dynamics of Idhg-period comets N85-23506
Venus gravity: Global field results N85-23512
The support of long wavelength loads on Venus N85-23515
Gravity field of the Jovian system from Pioneer and Voyager tracking data N85-23529
Interaction of Martian flow ejecta blankets with pre-existing impact craters: Morphological observations N85-23546
Estimates of lava eruption rates at Alba Patera, Mars N85-23562
Thermal infrared observations of lava flows during the 1984 Mauna Loa eruption N85-23564
Transformation of polar ice sublimate residue into Martian circumpolar sand N85-23580
Geomorphology and geology of the Southwestern Margaritifer Sinus and Argyre regions of Mars. Part 1: Geological and geomorphological overview N85-23600
Geomorphology and geology of the Southwestern Margaritifer Sinus and Argyre regions of Mars. Part 2: Crater size-frequency distribution curves and geomorphic unit ages N85-23601
Geomorphology and geology of the Southwestern Margaritifer Sinus and Argyre regions of Mars. Part 3: Valley types and distribution N85-23602
Geomorphology and geology of the Southwestern Margaritifer Sinus and Argyre regions of Mars. Part 4: Flow ejecta crater distribution N85-23603
Photometric analysis of Jupiter-illuminated images of Io N85-23620
Spectral units on Europa and Ganymede N85-23621
Properties of filamentary sublimation residues from dispersions of clay in ice N85-23629
Mapping and geological analysis of Mercury and Venus radar ranging data N85-23633
Correction and geological analysis of lunar 3.8 cm radar data N85-23634
Landform identification on radar images N85-23635
Radar and the detection of liquid water on Mars N85-23638
Terrestrial analogs for planetary wrinkle ridges N85-23644
On the absence of strike-slip faults from the planets and satellites N85-23645
Lunar mascon loading: An example of the importance of fault initiation depth on fault type predictions from stresses on planetary surfaces N85-23646
Shape of Io N85-23672
JOINT PUBLICATIONS RESEARCH SERVICE, ARLINGTON, VA.
China report: Science and technology [JPRS-CST-84-008] N85-22384
Improved Y-11 general-purpose transport designated Y-12 N85-22385
Optimal design efforts in Shanghai described N85-22386
USSR report: Space [JPRS-USP-85-001] N85-22403
TASS update on unmanned flight of Salyut-7 N85-22404
Lyakhov and Aleksandrov on 150-day flight N85-22405
Comments on Salyut-7 150-day flight N85-22406
Plans for Interbol satellite experiment N85-22407
All-Union conference of radio astronomers N85-22408
Modern problems in polarimetry of solid surfaces of cosmic bodies N85-22409
Expansion of functions describing planetary surface and gravity field N85-22410
Averaging of equations of cometary orbital motion with allowance for nongravitational effects N85-22411
Correlation of interplanetary medium parameters in transition region of high-velocity solar wind streams N85-22412
Characteristics of latitude effect on cosmic ray charged component in atmosphere at altitudes 3-5 KM N85-22413
Hydromagnetic precursors of interplanetary plasma burst N85-22414
Longitude and pitch-angle distributions of streams of high-energy electrons under Earth's radiation belts N85-22415
Lagrangian solutions in photogravitational restricted circular three-body problem N85-22416
Nontraditional method for determining unperturbed orbits of unknown space objects using incomplete optical observational data N85-22417
Computation of elliptical functions in problems of celestial mechanics N85-22418
Algorithm for determining optimal three impulse point-to-orbit transfer with limited transfer time N85-22419
Motion of symmetrical satellite with flexible viscoelastic rods about center of mass in circular orbit N85-22420
Rejection of anomalous observations when determining spacecraft trajectories N85-22421
Operational experience with ion concentration sensors in orientation systems N85-22422
Protons with energies above 30 KeV in Earth's radiation belt at low altitudes during magnetically quiet time close to geomagnetic equator N85-22423
One-dimensional model of auroral magnetic force with longitudinal current and cyclotron heating of ions N85-22424
Helium atoms in interstellar and interplanetary space. II: Determination of direction of interstellar gas motion relative to Sun N85-22425
Rocket body charge neutralization processes in ARAKS experiment (data from two launches) N85-22426
Cosmogenic Na-22 and Al-26 in Luna-24 lunar drill core soil samples N85-22427
Rotational motion of a satellite N85-22428
Satellite oscillations in elliptical orbit N85-22429
Observation of cosmic ray flux variations in stratosphere N85-22430
Increase in hydrogen emission of upper atmosphere following launches of space vehicles N85-22431
Determination of angular resolution of coded aperture gamma-ray telescope N85-22432
Volcanism on Venus as connecting link N85-22433
Interplanetary shock waves during April and May of 1981 N85-22434
Analysis of systematic errors in systems of selenodetic coordinates N85-22435
Microstructure of Venus cloud layer based on spectrophotometric data from Venera-11 spacecraft N85-22436
Visualization of radar altimetry data for Venus N85-22437
Preliminary photomaps of Venus surface in the Maxwell Mountains and adjacent areas N85-22438
Hypsometric features on Venus N85-22439
Remote sensing used for study of forest resources N85-22440
Evaluating accuracy in determining position of Earth's center of mass and elements of orientation of geodetic coordinate system N85-22441
Evaluating accuracy in orientation of topographic photograph and satellite-centered direction from star photograph N85-22442
Method for approximating autocorrelation functions for describing areal photoimage features N85-22443
Experience in automated interpretation of aerospace photographs N85-22444
Geoindication method for interpreting aerial and space photographs: Status and prospects N85-22445
New method of reconstructing conditions of recent differentiation of oil and gas in the Amudarya Basin (based on results of interpretation of space photographs) N85-22446
Use of mobile surface station for synchronous satellite measurements in seismological research N85-22447
Approximate perturbing part of geopotential by polynomials of stipulated form N85-22448
Experience in combined special mapping using space information N85-22449
Combined analysis of the dynamics of complex ecosystems based on repeated remote measurements N85-22450
Feoktistov recalls period leading to Gagarin spaceflight N85-22451
Feoktistov says manned lunar, Mars flights lack justification N85-22452
Feoktistov argues against U.S. space shuttle design concept N85-22453
Feoktistov discusses need for space colonization N85-22454
U.S., Soviet space program aims contrasted N85-22455
INMARSAT marine satellite organization N85-22456
List of recent Soviet space launches N85-22457
USSR report: Chemistry [JPRS-UCH-85-001] N85-22629
Influence of external electric field on structural-mechanical properties of powdered materials N85-22630
Multiple element neutron-activation analysis of atmospheric aerosols with X-ray and gamma-spectrometric recording of radionuclides formed N85-22631
One mechanism of formation of organic fraction in atmospheric aerosol N85-22632
Current plans for development of chemical industry N85-22633
Critical events in inelastic deformation of glassy polymers in adsorptive medium N85-22634
Effects of triazine components on physicochemical properties of polybutadiene: urethane block copolymers N85-22635
Mechanism of strengthening plastics with rubbers N85-22636
Study of character of adhesive interaction and breaking of polyimid-aluminum foil junction during process of hardening N85-22637
USSR report: Materials science and metallurgy [JPRS-UMS-85-002] N85-22688
Dependence of superplastic flow on state of grain boundaries N85-22689

Fatigue and corrosion fatigue resistance of aluminum casting alloy VAL10 and forging alloy AK6 N85-22690
Structural strenght of strip D16T aluminum alloy with low copper and magnesium content N85-22691
Temparature effects of heterogenizated annealing on structure and properties of V95 aluminum alloy N85-22692
Anomalies of aluminum structure and properties N85-22693
New deformable secondary aluminum alloys N85-22694
Study of processes of modification of Al-Si alloys N85-22695
Use of acoustical emission method to study specifics of fracture of boron reinforced plastic structural elements N85-22696
Aluminum alloy ATs5K5 (5% Zn + 5% Ca) for superplastic forming N85-22697
Uses of composite materials N85-22698
Influence of 3% NaCl solution on rate of accumulation of damage and residual strength of aluminum-boron composite N85-22699
Development and study of two-matrix glass fiber composite with increased transverse deformation N85-22700
Testing of wound materials for strength with loading in the reinforcement plane N85-22701
Effect of phase state of TiC-NiTi powder composite materials on nature of failure and mechanical properties N85-22702
Dissipation of energy in composite material N85-22703
Division boundary in Al-B composite material with boron in contact with solid and liquid aluminum N85-22704
Estimating degree of development of physical-chemical interaction among components in Al-B fiber composite material N85-22705
Segregation of silicon in silumin-carbon fiber composites N85-22706
Possibility of producing monolithic composite materials based on niobium carbide N85-22707
Adequacy of metal ablation process with laser radiation and a shock-compressed plasma N85-22708
Breakdown of thin plates by radiation N85-22709
Theory of relaxation processes in decomposing polymer materials during high-intensity convective heating N85-22710
Effect of transparent coatings on generation of laser-induced shock waves in metals N85-22711
Decomposition of VTAN alloy solid solution upon irradiation and thermal aging N85-22712
Influence of laser treatment of structure and mechanical properties if MA21 alloy N85-22713
Specifics of laser heat treatment of high steel tools N85-22714
High temperature antifriction properties of Ti sub 1-sub xNb sub x C sub 0.5N sub 0.5 alloys N85-22715
Effect of operating medium on cyclic durability of AD33-W composite N85-22716
Structural distortions of ultra-dispersed titanium nitride powders N85-22717
Degasification of silicon nitride powders of various origins N85-22718
Composition and thickness of oxide coatings on granule surfaces of aluminum alloys N85-22719
Apparatus for producing amorphous and microcrystalline metal powders N85-22720
Specifics of kinetics of polymorphous conversion upon heating of low carbon steels N85-22721
Comparison of dynamic-tension and constant-load strength characteristics of heat-resistant materials N85-22722
Long-term strength and fracture criteria for EI698VD alloy under complex stress conditions N85-22723
Some specifics of development of fatigue and creep in heat-resistant alloys with asymmetrical multicycle loading N85-22724
Change in microstructure of heat-resistant nickel alloys upon thermal cycling in a current of gas N85-22725
Developing procedures for thermomechanical processing of high-durability VT22 titanium alloy N85-22726
Influence of annealing on cyclic and short-term strength of thin sheets of VT1-0 titanium and OTR4 alloy N85-22727
Rational use of tatanium in nonferrous metallurgy N85-22728
Studies of electrical properties of surface films and localization during electrochemical dimensional working of titanium N85-22729
Basis and pyramidal slipping in single crystals of alpha-alloy Ti-Al-Sn N85-22730
Specifics of structure and mechanical properties of metastable beta-titanium alloys after deformation and aging N85-22731
Problem of pore formation mechanism in welded joints of aluminum alloys in the system aluminum-magnesium-lithium N85-22732
Properties of welded joints in argon arc welding of titanium alloy using a protective coating N85-22733
Thermal hardening of welded joints in titanium alloys with various structures N85-22734
Influence of welding defects at melting boundary on static strength of welded joint in large-diameter pipe N85-22735
Mechanical properties and brittle fracture resistance of welded multilayer elements for high pressure vessels N85-22736
Analysis of strength and ductility of welded joints in AMtsS and AMg5 aluminum alloys N85-22737
Effect of protective medium on durability and fracture structure on seam zones of thin-walled titanium articles produced by diffusion welding N85-22738
Technological parameters of diffusion welding processes in honeycomb titanium alloy structures N85-22739
Durability of VT16 alloy compounds obtained by diffusion welding N85-22740
Reliability of robotized welding apparatus N85-22741
Structure and mechanical characteristics of heterogeneous joints produced by laser welding N85-22742
Method of calculating strength of joint produced by cold welding of aluminum under discrete loading N85-22743
Effect of moisture in inert gases on density of seam metal and on mechanical characteristics of welded joints of aluminum and aluminum alloys N85-22744
Characteristics of surface crack development in ATtsS aluminum alloy during slow-cycle loading N85-22745
Automatic multi-layer welding of thick cylindrical structures under flux N85-22746
Softening of metal near seam during welding of heat-resistant nickel alloys N85-22747
Corrosion-resistant amorphous alloys N85-22748
Structure of amorphous films of alloys based on Fe, condensed from laser erosion products N85-22749
Energy spectrum of processes of structural relaxation of amorphous alloy FeCo70Si15B10 N85-22750
Experimental study of enthalpy of quasimonocrystal of graphite and carbon glass in temperature range of 2890-3818 deg K N85-22751
China report: Science and technology [JPRS-CST-84-030] N85-22777
Nation said to rank high with 15 satellites N85-22778
Experimental investigation of crippling strength of Chinese aluminum alloy (LY12CZ) sections N85-22779
Study of effective physiological temperature N85-22780
Space interception guidance with uncertain factors N85-22781
USSR report: Engineering and equipment [JPRS-UEQ-85-003] N85-22782
Periodic movements of axisymmetrical satellite about center of mass due to gravitational moment N85-22783
Redesign of fuselage compartments by method of special contours N85-22784
Propagation of three-dimensional turbulent jet from lobar nozzle through surrounding stream N85-22785
Time-dependent flow of stream swirled in vortex chamber N85-22786
Natural convection during heat accumulation by substances with change of aggregate state N85-22787
Some unique features of isentrophic flow of gas under high pressures N85-22788
Determination of boundary line between reverse jet and surrounding stream N85-22789
Method for prompt modeling of quasiperiodic movement of solid near-axisymmetrical body in atmosphere N85-22790
Flight dynamics of axisymmetrical rotating bodies in air medium N85-22791
Hypersonic flow about triangular airfoil at large angles of attack N85-22792
Absolute stability of unsteady movement of axisymmetrical rotating flight vehicle N85-22793
Reflex attachment for line alignment in spectral diffraction devices N85-22794
Ruby wavefront-conjugation laser for obtaining high temperature plasma N85-22795
Neodymium YAG laser pumped with radiation from high frequency electrodeless discharge N85-22796
Variable flexing device for targets in internal beams of charged particle accelerators N85-22797
System for forming and focusing high current beam of deuterium ions N85-22798
Dielectric detector device for registering heavy cosmic radiation particles N85-22799
New technique for fluid feed in simultaneous multisurface grinding N85-22800
Effect of zero-wear in friction pairs operating in abrasive media N85-22801
Use of ferrofluids in machining of metals N85-22802
Cyclic industrial robots with mechanical energy storing devices: Multipositional system with one or several degrees of freedom N85-22803
Design of tightening device and calculation of forces in manipulator transmissions with base-drive mounted N85-22804
Optoelectronic safety system for robotized technological complex N85-22805
Hydraulic brakes for industrial robots N85-22806
Cyclic industrial robots with mechanical energy storing devices: Principles of drive design N85-22807
Assembly robot control algorithms N85-22808
Time dependent interaction of internal pressure wave with system of two spherical shells N85-22809
Interaction of cylindrical shell with concentrated mass moving along its inner surface N85-22810
Steady-state reaction of three-layered cylindrical shell to effect of moving load N85-22811
Determination of stresses and deformations in linearly elastic conical shell subjected to aerodynamic loading and heating N85-22812
Stability of three-layer glass-reinforced plastic shells of rotation N85-22813
Axisymmetrical oscillations of shell systems subjected to impulse loads N85-22814
Spectral frequency of eigenvalues in optimal problems of stability of cylindrical shells of variable thickness N85-22815
Elasticity formulas for thin-walled shells with piezoceramic layers N85-22816
Normal mode calculations for fuselage type intricate structures by regarding them as systems with superposed constraints N85-22817
Controlled movement of elastic manipulator with distributed parameters N85-22818
Investigation of dynamics of manipulator with elastic sections N85-22819
Stability of cylindrical shells with one-way constraints N85-22820
Nonlinear behavior and stability of thin spherical shells subjected to non-axisymmetrical loading N85-22821
Analysis of interaction of dynamically adjustable gyroscopes on elastic platform by finite-element method N85-22822
Efficiency of algorithms for gas-air channel diagnostics in gas turbine engines based on gas thermodynamic parameters N85-22823
Effect of compliability of hot walls in liquid-propellant engine on low frequency instability N85-22824
Exergetical analysis of turbojet engine cycle N85-22825
Energy losses at leading edge of turbine blade during multirow jet cooling N85-22826
Experimental determination of optimum ratio of runner blade height at exit to runner blade height at entrance of radial inward-flow microturbines N85-22827
Some unique features in operation of two-stage turbojet engine with afterburner N85-22828
Hydrodynamic simulation of transient processes in injection system of aircraft engines during pump unswirling N85-22829
Effect of water injection into air for turbine cooling on economy of operation of gas turbine engine with afterburning N85-22830
Pressure drop and coefficients of internal heat transfer necessary for transpiration cooling N85-22831
Annular groove in compressor casing as device for control of air stream N85-22832
Experimentally determined characteristics of vortex heaters N85-22833
Mathematical modeling of transient performance of gas turbine engine N85-22834
Dependence of combustion of homogeneous kerosene-air mixtures on humidity of air N85-22835
effect of gas stream sweeping past the effluent of a perforated plate on heat transfer inside the perforations N85-22836
Selection of air intake parameters for supersonic-flow operation N85-22837
Estimation of gas turbine engine boost provided by injecting water behind compressor N85-22838
USSR report: Machine tools and metalworking equipment [JPRS-UMM-85-005] N85-22839
Advances in cutting tool technology surveyed N85-22840
Diamond cutters' grinders N85-22841
New tooling for plasma cutting technology N85-22842
China report: Science and technology [JPRS-CST-85-005] N85-22843
Laser applications in last 10 years reviewed N85-22844
Analysis of fiber-gyroscopes discussed N85-22845
X-ray lithography and VLSI circuits N85-22846

Development, prospect of satellite dynamics discussed N85-22847
Geological remote sensing develops rapidly, finds broad applications N85-22848
CARD's low-speed wind tunnel described N85-22849
USSR report: Electronics and electrical engineering [JPRS-UEE-85-002] N85-22907
Assessment of effectiveness of signal-code constructions in time division-multi-access satellite systems N85-22908
Satellite channels in packet-switching networks N85-22909
Satellite bridges in communications networks N85-22910
Kinetic Rayleigh-Taylor instability theory in the ionosphere near equator N85-22911
Exitation of low-frequency resonance waves by moving conductor in space plasma N85-22912
Scattering of electromagnetic waves by charged particles N85-22913
Diffraction of plane TM-wave on continuously irregular elliptical plasma N85-22914
Moving target detection N85-22915
KAM-250 antenna switch N85-22916
Processing of signals in experiments with scattering of short radio pulses by conducting sphere N85-22917
Multifunctional elements for integrated optics N85-22918
Coordinate determination errors in measuring characteristics of radiation field of airborne antennas N85-22919
Reduction of amplitude-phase distortions of movable microwave coupling circuit for antenna field measurements N85-22920
Stereo decoder without subcarrier restoration N85-22921
Error probability during optimal noncoherent reception of binary signals in multibeam channel N85-22922
Regular synthesis of pairs of phase-keyed binary minimax signals N85-22923
Interference immunity of fiber-optic communication lines with spectral multiplexing of channels N85-22924
AL-124 light-emitting diode in 30 Mbit/s fiber-optic communication line N85-22925
Horizontal deflection TS-257 N85-22926
Theory of optimum M-filtration of signals against background of correlated interference N85-22927
Dispersion of phase-shift keyed systems with fixed number of blocks N85-22928
Noise tolerance of digital demodulator for complex signal system employing binary quantization N85-22929
Analysis of characteristics of digital discriminators for phase-shift keyed signals N85-22930
Combined processing method and matched filter for discrete composite frequency phase-shift keyed signal N85-22931
Piezoelectric filter with low-Q inductances N85-22932
Optimal synthesis of surface acoustic wave filters N85-22933
Analysis and optimization of parameters of fanned surface acoustic wave transducers N85-22934
Code lock with microcircuit N85-22935
Recommendation on use of „series K157UL1 microcircuits N85-22936
Space-time response characteristics of acoustooptic filter for compression of linearly frequency-modulated signal N85-22937
Synthesis of low-pass filters using coupled lines with unmatched loads N85-22938
Prefiltration in Kalman filter with a priori indeterminacy N85-22939
Dynamics of adaptive signal corrector N85-22940
Performance of time-position discriminator of composite signal N85-22941
Efficiency of digital compensator of strong non-Gaussian interference N85-22942
Mathematical model of discriminator for signals with fluctuations and thermal noise N85-22943
Interference immunity of binary systems with second-order phase-difference modulation in various reception modes N85-22944
Ionospheric distortions of digital signals with wideband modulation N85-22945
Comparative analysis of noise tolerance of quasi-coherent phase shift keying signal demodulators N85-22946
Optimum path selection in automated radio relay link design N85-22947
Calculation of amplitude-phase characteristics of signal scattered obliquely on meteor trail N85-22948
Domain of applicability of asymptotic description of radio pulse fields near critical frequency N85-22949
Spectra of incidental interference resulting from nonlinear conversion of signals from transmitters N85-22950
Method of separately determining electrophysical properties of bulky conductor N85-22951
Noise characteristics of sulfur-doped silicon diodes N85-22952
Measurement of internal thermal resistance for quality control of semiconductor devices N85-22953
Mathematical model of electromagnetic suspension device with two control windings N85-22954
Status of and outlook for producing means of transmitting units of plane angle, angular velocity and acceleration with ring lasers N85-22955
Outlook for realization of proximity effect and Josephson direct current in helium-2 N85-22956
Comparison reference etalon of unit laser radiation power N85-22957
Measuring intensity of electric field produced by electromagnetic pulse with aid of active probes N85-22958
Square-pulse generator N85-22959
Simple sweep frequency generator N85-22960
Optical reflectometer for multimode fiber lightpipes N85-22961
Liquid mass flow rate computer N85-22962
Metrological support for remote transport vehicle speedometers N85-22963
Use of electronic coding-frequency meters to measure parameters of pulsed radio signals N85-22964
Effect of variance of photoreceiver frequency characteristics on characteristics of measuring instruments N85-22965
Parameters of amplitude-modulated signal upon reflections N85-22966
Coupled-cavity gyrotrons with mode conversion N85-22967
Absorption of radiation by water vapor in windows of relative transparency of 95-145 micrometer range N85-22968
Magnetic noise in single-machine rotating frequency converters N85-22969
Playback amplifier with high interference immunity N85-22970
Simple detonation meter N85-22971
Three-mirror open resonator for millimeter wave band N85-22972
Application of K176-series microcircuits N85-22973
Extraction of surface-wave energy from plasma waveguide N85-22974
Intensity fluctuations of focused laser beam during reflection in turbulent atmosphere N85-22975
USSR report: Electronics and electrical engineering [JPRS-UEE-85-001] N85-22976
Interference flux during reflection of heterogeneous waves N85-22977
Absolute measurements of radiation intensity from Cassiopeia-A, Cygnus-A and crab nebula in 60-100 cm band N85-22978
Axial focusing of signal from distant point radiator reflected twice in deep paraboloid N85-22979
Investigation of generation of oscillations using anomalous Doppler effect N85-22980
Time spectra of intensity fluctuations along reflecting path N85-22981
Temperature dependence of propagation of high-current electron beam through drift space N85-22982
Models of discontinous random fields N85-22983
Experimental verification of beam deflection from hybrid reflector antenna within wide-angle sector N85-22984
Problem of diffraction by wavy surface: Comparison of numerical methods of solution N85-22985
Synthesis of multistep directional couplers with nonminimum-phase characteristics N85-22986
Scattering of waves by axisymmetrical edge N85-22987
Error in compensating phase fluctuations of wave field by means of adaptive reflectors with continuous or compound surface N85-22988
Adaptive control of airborne radar antennas N85-22989
Synthesis of optimum single-channel discrete signals and filters N85-22990
Efficiency of multitarget signal detection by digital radar data processing devices N85-22991
Synthesis of optimum algorithms for secondary processing N85-22992
Optimization of number of pulses in detection of fluctuating optical signals N85-22993
Diffraction of periodic grounding system of finite length N85-22994
Correctness of reflection characteristics of radio absorbent materials N85-22995
Short-range radiotechnical point sensor N85-22996
Factorized algorithms for combined spatial and temporal processing of radar signals N85-22997
Exact design formulas for field intensity of dipole deployed above flat homogeneous Earth with finite conductivity N85-22998
Change of electrical characteristics of radio-frequency cables under thermal effect N85-22999
Spectral evaluation of irregularity of superconducting coaxial cables N85-23000
Surge strength of symmetric cable with monolithic polyethylene insulation of quads N85-23001
Theory of diaphragm light modulators with electrical input signal N85-23002
A posteriori increase of resolving power of optical system forming averaged monochromatic images N85-23003
Dispersion characteristics of small-mode gradient optical fibers N85-23004
Methods of digital correction for channels of multichannel radar receivers N85-23005
Algorithm in Walsh function basis for analysis of integrated microcircuits on MOS-structures N85-23006
Investigation of bimodal paramagnetic filter N85-23007
Programmable filter with fanned interdigital surface acoustic wave transducer N85-23008
Gyrator frequency selectors with bandwidth independent of input signal level N85-23009
Synthesis of quasi-optimum two-level signal discriminator with level changing at unknown point N85-23010
Use of Walsh functions for calculating characteristics of digital filters with impulse response of finite duration N85-23011
Asymptotically optimum multialternative sequential procedures for discernment of processes minimizing average length of observations N85-23012
Extraction of signals from background interference with unknown parameters in quantized sample N85-23013
Applicability of log-normal model to probabilistic description of quasi-pulse interference N85-23014
Accuracy of approximation of Bayes estimates in presence of noninformative parameters N85-23015
Reception of signal with unknown amplitude and duration submerged in white noise N85-23016
Use of Bigaussian approximation to describe fading in scattering communications channel N85-23017
Machine analysis of resonance characteristics of plate-type radio electronic equipment constructions N85-23018
Computing convolution of multifrequency signal employing truncated fast Fourier transform algorithms N85-23019
Synthesis of quasi-optimum algorigthms for signal recognition against background of correlated noise employing discrete spectral transformations N85-23020
Probability of detection of pulsed signals employing zero-gating interference suppression N85-23021
New convolution and decrete Fourier transformation algorithms based on rectangular transformations over field of roots of unity N85-23022
Reception noise immunity of multiposition signals N85-23023
Noise tolerance of diversity reception in frequency-adaptive digital transmission systems N85-23024
Analysis of interference caused by interfering radio signals in communications systems with frequency separation of telephone channels and frequency modulation N85-23025
Investigation of influence of communiczations link and synchronization error on noise tolerence of group transmission of binary information based on orthogonal Walsh function N85-23026
Approximate rules for signal detection against background of Gaussian correlated interference N85-23027
Use of importance sampling to investigate signal detection systems by simulated method N85-23028
Noise immunity of information transmission system with pseudorandom frequency switching under worst-case interference conditions N85-23029
Stability of highly nonlinear oxide-zinc resistors under continuous voltage of industrial frequency N85-23030
Electrodynamic stability of composite liquid-metal contacts N85-23031
Planar ferroelectric microcapacitors for microwave devices N85-23032
Optimization of overall dimensions of enclosures for low-voltage devices and equipment N85-23033
Dielectric measurements in infralow-frequency band N85-23034
Winding insulation in electromagnetic systems for Tokamak reactor plants N85-23035
Thermally stimulated conductivity in semi-insulating gallium arsenide N85-23036
Non-self-maintained high-voltage low-pressure discharge N85-23037
Analysis and design of linear microwave transistor amplifiers N85-23038
Numerical simulation of inverters with I2L elements including effects of high doping level N85-23039

Electrothermal transducer with short time constant N85-23040
Synthesis of optimum smooth transition in microstrip through line on microwave integrated circuit N85-23041
Millimeter-wave range masers: A review N85-23042
Effect of space-charge field on output characteristics of O-type oscillators with distributed interaction N85-23043
Integrated optical components utilizing acoustooptic and electrooptic diffraction in micro-waveguides N85-23044
Mathematical modeling of two-frequency laser sounding of scattering media N85-23045
Geophysical laser interferometer with 12.5 meter base N85-23046
Investigation of dynamics of radiation spectrum or injection lasers by infrared impulse Fourier spectroscopy N85-23047
Invariance of probability characteristics of detector to shape of optical pulse signals N85-23048
Generation of longitudinal acoustic waves by modulated helicon waves N85-23049
Acoustooptic demodulation of frequency-modulated signals N85-23050
Acoustooptic cell as space-frequency filter N85-23051
Accuracy of random signal spectral parameter estimation against interference background in acoustooptical spectrum analyzers N85-23052
Experimental study of high-stability oscillator with surface-acoustic-wave resonator in feedback loop N85-23053
USSR report: Earth sciences [JPRS-UES-85-002] N85-23116
Arctic-North Atlantic rift megasystem N85-23117
Antarctic glaciation, or what are catastrophes in Earth's history N85-23118
Moisture variation in northern hemisphere temperate latitudes N85-23119
Relationship of Indian monsoon intensity to time of onset N85-23120
El Nino, the capricious child N85-23121
Modeling of mechanism of positive feedback between mean Earth surface temperature and atmospheric carbon dioxide in geologic time scale N85-23122
Numerical experiments with simple model of ocean climate N85-23123
Numerical investigation of evolution of energy spectrum of slightly nonlinear Rossby waves N85-23124
Special features of computations of vertical distribution of concentration of suspended sediments under marine conditions N85-23125
Absolute movement of Pacific Ocean plate during last 120 million years N85-23126
Determining degree of partial melting of asthenosphere from seismic data N85-23127
Determining adsorption of surface-active substances by sea bottom deposits N85-23128
Possible role of ocean biota in global carbon balance N85-23129
Regions of propagation of short-wave perturbations in spherical layer of rotating fluid N85-23130
Use of three omega radionavigation system position lines for solving problems in marine geodesy N85-23131
Drifting ice as mechanical factor in purifying and polluting hydrosphere N85-23132
World ocean level oscillations and their relationship to change in inflow of continental waters N85-23133
Contribution to theory of ocean-atmosphere gas exchange N85-23134
Use of paleomagnetic data in tectonic analysis of oceanic structures N85-23135
Calculation of level surface in problems of large-scale ocean circulation N85-23136
Double and inverse Taylor-Hogg vortices in a stratified ocean N85-23137
Mathematical-cartographic model for study of distribution of hydrochemical elements in sea water (using dissolved oxygen in the Pacific Ocean as an example) N85-23138
Horizontal coherence of temperature microstructure in upper ocean layer N85-23139
Fine structure of vertical distribution of light attenuation index of sea water N85-23140
Evolution of set of Rossby waves toward anisotropic equilibrium state N85-23141
Stability of Rossby waves within framework of three-component analysis N85-23142
More precise curve of dependence between density and velocity of longitudinal waves in consolidated crust and top of mantle in oceanic structures N85-23143
Crustal and upper mantle density model of Owen fault zone N85-23144
Radiosodar system for remote synchronous measurements of wind speed, temperature and its fluctuations N85-23145
Possibility of determining atmospheric weather parameters by radio and radiooptical measurements of refraction of cosmic sources N85-23146
Infrared aerosol absorption index N85-23147
Study of stratigraphy of the Precambrian Soviet Baltic shield N85-23148
Observation of long-period oscillations of Earth N85-23149
Numerical modeling of plane stick-slip fault N85-23150
Scattering of elastic waves on fractures randomly distributed in a three-dimensional medium N85-23151
Natural electromagnetic radiation in seismically active regions N85-23152
Determination of density of the crust and upper mantle from deep seismic sounding and gravimetry, 2 N85-23153
Induction excitation of deep conducting zones N85-23154
Study of resolution of deep MT soundings by means of physical model N85-23155
Nature of seismic images with amplitude and time fluctuations of recorded oscillations N85-23156
Space and time distribtuion of aftershocks N85-23157
Determining vector of radiointerferometer base from observations of natural radio emission with narrow spectrum N85-23158
Structure of Iceland and ocean floor spreading N85-23159
Review of problems in lithology N85-23160
Magmatism in continent-ocean transition zone (development of ideas of A. N. Zavaritskiy) N85-23161
Possibility of mapping active tectonic structures from mercury gas aureoles over sea surface N85-23162
Normal and anomalous geothermal fields and their relationship to hierarchy of geological bodies N85-23163
Variations in resistivity of upper crustal layer N85-23164
Boundary velocities of longitudinal seismic waves and lateral inhomogeneities of upper ocean mantle N85-23165
Discrimination of normal and anomalous magnetic and electric fields in geoelectromagnetic variations N85-23166
Reflected wave travel-time curves in stratified media with vertically heterogeneous layers and slightly sloping curved boundaries N85-23167
Study of geological media based on scattered earthquake waves N85-23168
Consideration of heterogeneity of gravity fields in local high precision geodetic constructions N85-23169
Mathematical modeling of results of geometric leveling in variable gravity field N85-23170
Relationship between brightness spectrum of photographic image and spectrum of rises on a water surface with waves N85-23171
Study of phase radiogeodetic systems with phase-locked loops N85-23172
Thermohydrodynamic model: Hydrothermal system, shallowly seated magma chamber N85-23173
Polynomial parameterization in inverse gravimetric problem N85-23174
Primary processing of experimental magnetovariation sounding data using spline functions N85-23175
Application of field X-ray: Radiometric analysis in exploratory geology and means for its improvement N85-23176
Possibilities of aerial electric prospecting by long cable method for detecting poorly conducting strata N85-23177
Geomagnetic precursors of intensive earthquakes in the 1-0.-2 Hz frequency range of geomagnetic pulsations N85-23178
Solution of direct magnetometric problem on spherical Earth N85-23179
Determining deep heat flow and rate of horizontal percolation from temperature measurements in aquifer N85-23180
Seismic waves and dispersion relations N85-23181
Geomagnetic field dynamics N85-23182
Interrelationship of earthquake magnitude and lithospheric-asthenospheric thermodynamic parameters in seismically active zones N85-23183
Correcting depth line on nonlongitudinal seismic profile N85-23184
Method for processing broad-profile data N85-23185
China report: Science and technology [JPRS-CST-85-003] N85-23433
Development, achievements in China's cartography work N85-23434
Accomplishments of Institute of Cartography summarized N85-23435
Physicists' role in new technological development discussed N85-23436
Rapid advances in geological work N85-23437
Characteristics of alumyte deposits discussed N85-23438
Research, development of laser glasses in China N85-23439
Research progress on laser crystals in China N85-23440
Armed forces special Symposium on Medicine of Altitudes N85-23441
USSR report: Science and technology policy [JPRS-UST-85-002] N85-23442
Economic mechanism of integration of science, production N85-23443
Scientific, technical progress as factor of intensification of economy N85-23444

K

KANSAS STATE UNIV., MANHATTAN.
Enigmatic hills of the mottled plains, Mare Acidalium quadrangle (MC-4), Mars N85-23599
KANSAS UNIV., LAWRENCE.
Calculation of vortex-flap aerodynamic characteristics [NASA-CR-175624] N85-22367
Self-consistent simulation of plasma interactions with secondary-emitting insulators N85-22492
KANSAS UNIV. CENTER FOR RESEARCH, INC., LAWRENCE.
The microwave propagation and backscattering characteristics of vegetation [E85-10088] N85-23213
KESTREL INST., PALO ALTO, CALIF.
Synthesis of tree-structured computing systems through use of closures [AD-A150502] N85-23326
KMS FUSION, INC., ANN ARBOR, MICH.
Parallel processing for computational continuum dynamics [AD-A150513] N85-23327

L

LAMONT-DOHERTY GEOLOGICAL OBSERVATORY, PALISADES, N. Y.
Variation of Arctic cloud cover in summer [DE85-004507] N85-23285
LEHIGH UNIV., BETHLEHEM, PA.
Elasticity solution of an adhesively bonded joint [NASA-CR-175591] N85-23097
A clamped rectangular plate containing a crack [NASA-CR-175590] N85-23098
Stress intensity factor in a tapered specimen [NASA-CR-175589] N85-23099
LIBRARY OF CONGRESS, WASHINGTON, D. C.
Halley's Comet, a bibliography [LC-84-600109] N85-23674
LINCOLN LAB., MASS. INST. OF TECH., LEXINGTON.
TCAS II: Design and validation of the high-traffic-density surveillance subsystem [DOT/FAA/PM-84/5] N85-22375
LINKOEPING UNIV. (SWEDEN).
HREELS and Auger studies of conducting polymers [DE85-004541] N85-22764
LOCKHEED-CALIFORNIA CO., BURBANK.
Study for the optimization of a transport aircraft wing for maximum fuel efficiency. Volume 1: Methodology, criteria, aeroelastic model definition and results [NASA-CR-172551] N85-22378
LOCKHEED ENGINEERING AND MANAGEMENT SERVICES CO., INC., HOUSTON, TEX.
Preliminary evaluation of Thematic Mapper image data quality N85-23194
LOCKHEED-GEORGIA CO., MARIETTA.
Advanced life analysis methods. Volume 1: Cracking data survey and NDI (nondestructive inspection) assessment for attachment lugs [AD-A150419] N85-23108
Advanced life analysis methods. Volume 2: Crack growth analysis methods for attachment lugs [AD-A150420] N85-23109
LOCKHEED MISSILES AND SPACE CO., HUNTSVILLE, ALA.
HPFTP flow diverter analysis [NASA-CR-171424] N85-23057
LOCKHEED MISSILES AND SPACE CO., PALO ALTO, CALIF.
Effects of HMX addition on the combustion of energetic binders N85-22560
LOCKHEED MISSILES AND SPACE CO., SUNNYVALE, CALIF.
Vibroacoustic study of the NASA Goddard Space Flight Center OSS-1 payload [NASA-CR-175320] N85-22485

LOS ALAMOS SCIENTIFIC LAB., N. MEX.
Use of markets to elucidate reacting sputtering processes
[DE85-005723] N85-22655
Americium metal preparation on the multigram scale
[DE85-003735] N85-22683
Portable electrochemical cell interrogator
[DE85-005186] N85-22901
High-resolution SIT TV tube for subnanosecond image shuttering
[DE85-005189] N85-23072
Los Alamos free electron laser: Accelerator performance
[DE85-005722] N85-23084
Steel containment buckling
[DE85-003744] N85-23111
The ASCOT Data Analysis Workshop
[DE85-004407] N85-23283
Bottleneckology: Evaluating supercomputers
[DE85-005574] N85-23315
Algorithm for singular decomposition
[DE85-016488] N85-23361
High-field dipoles for future accelerators
[DE85-002315] N85-23391
Effects of focusing on HRS focal-plane polarimeter measurements
[DE85-004627] N85-23406
Intel iDIS evaluation
[DE85-003748] N85-23451
Zeolites on Mars: Prospects for remote sensing N85-23615
Constraints of observations of solar oscillations on solar models with mixing by turbulent diffusion
[DE85-003741] N85-23678

M

MACQUARIE UNIV., NORTH RYDE (AUSTRALIA).
MAGSAT anomaly field data of the crustal properties of Australia
[E85-10100] N85-23215
An investigation of the crustal properties of Australia and surrounding regions derived from interpretation of MAGSAT anomaly field data N85-23216
GADB: A database facility for modelling naturally occurring geophysical fields N85-23217
Data selection techniques in the interpretation of MAGSAT data over Australia N85-23218
Precedence control and other semantic integrity issues in a workbench database N85-23220
MARTIN MARIETTA AEROSPACE, DENVER, COLO.
EOS (electrical overstress) protection for VLSI (Very Large Scale Integration) devices
[AD-A150333] N85-22891
MARTIN MARIETTA CORP., DENVER, COLO.
Selected tether applications in space: Phase 2. Executive summary
[NASA-CR-171421] N85-22462
Selected tether applications in space: Phase 2
[NASA-CR-171422] N85-22463
MARYLAND UNIV., COLLEGE PARK.
Testing an energy balance model for estimating actual evapotranspiration using remotely sensed data N85-23236
Axial representations of shape
[AD-A150387] N85-23356
Parallel update of minimum spanning trees in logarithmic time
[AD-A150497] N85-23357
MASSACHUSETTS INST. OF TECH., CAMBRIDGE.
Structural response of a rotating bladed disk to rotor whirl
[NASA-CR-175605] N85-22391
Current problems in turbomachinery fluid dynamics
[AD-A150533] N85-22397
Rapid solidification processing of magnesium alloys
[AD-A150270] N85-22668
Micromechanical modeling of microstructural damage in creeping alloys
[DE85-003925] N85-22671
Creep crack growth in ductile alloys
[DE85-003937] N85-22676
IHE material qualification tests description and criteria
[DE85-004849] N85-22770
On Hybrid and mixed finite element methods
[NASA-CR-175551] N85-23096
Presentation based user interfaces
[AD-A150311] N85-23311
A perspective on multiaccess channels
[AD-A150183] N85-23322
Performance evaluation of distributed systems with unbalanced flows: An analysis of the INFOPLEX data storage hierarchy
[AD-A150528] N85-23328
Orphan detection in the Argus system
[AD-A150562] N85-23331
Zero-crossings on lines of curvature
[AD-A150171] N85-23345
Sequential excitation preparation of molecular energy levels with special structural and chemical properties
[AD-A150301] N85-23386
Lower hybrid heating and current drive, and ion cyclotron heating experiments on the Alcator C and the Versator II Tokamaks
[DE85-004918] N85-23412
Improvement in magnetic field properties of vanadium-gallium superconductors by enhancement of spin-orbit scattering
[DE85-002893] N85-23422
Motion planning with six degrees of freedom
[AD-A150312] N85-23432
The hierarchical database decomposition approach to database concurrency control
[AD-A150612] N85-23450
Venus surface composition from radio/radar measurements N85-23509
Venus chasmata: A lithosphere stretching model N85-23516
Quenching effects on iron site partitioning in the Apollo 17 orange glass composition N85-23553
Experimental methds for quenching structures in lunar-analog silicate melts: Variations as a function of quench media and composition N85-23554
Hibonite: Crystal chemistry and origin of blue coloration in meteoritic assemblages N85-23555
Crystal chemistry of meteoritic hibonites N85-23556
Reassignment of the iron (3) absorption bands in the spectra of Mars N85-23614
The deep structure of lunar basins: Clues to the understanding of basin formation and modification N85-23647
Elysium region, Mars: Tests of lithospheric loading models for the formation of tectonic features N85-23650
MASSACHUSETTS UNIV., AMHERST.
Newly discovered Martian impact basins N85-23544
Origin of Martian polygonal terrain: Preliminary results N85-23591
Basalts of Mars: Constraints on volatile evolution N85-23610
Iron oxides of Mars: Evidence for contemporary weathering N85-23613
Automated extraction of absorption bands from reflectance special N85-23624
Kasei Vallis of Mars: Dating the interplay of tectonics and geomorphology N85-23654
MATERIALS QUALITY ASSURANCE DIRECTORATE, LONDON (ENGLAND).
The characterisation of oxide films on treated aluminium alloys
[MOAD-R-849] N85-22667
MCDONNELL AIRCRAFT CO., ST. LOUIS, MO.
Fault offsets and lateral crustal movement on Europa N85-23656
Three-layer generic Ganymedes: Structure and evolution N85-23657
MCDONNELL AUTOMATION CO., ST. LOUIS, MO.
Bouguer images of the North American craton N85-23648
MCDONNELL-DOUGLAS CORP., ST. LOUIS, MO.
Parallel test method for LSI (Large Scale Integration) microprocessors
[AD-A150237] N85-23310
MCDONNELL-DOUGLAS RESEARCH LABS., ST. LOUIS, MO.
The role of convective perturbations in supercritical inlet oscillations N85-22563
MECHANICAL TECHNOLOGY, INC., LATHAM, N. Y.
Development of a multiplane multispeed balancing system for turbine systems
[NASA-CR-174750] N85-22400
MESSERSCHMITT-BOELKOW-BLOHM G.M.B.H., MUNICH (WEST GERMANY).
Testing of the digital flight control system of the German CCV fighter experimental aircraft N85-22361
MESSERSCHMITT-BOELKOW-BLOHM G.M.B.H., OTTOBRUNN (WEST GERMANY).
The DFS-Kopernikus solar generator electrical design N85-22590
Electrical design of the Intelsat 6 solar generator N85-22592
MICHIGAN TECHNOLOGICAL UNIV., HOUGHTON.
Raman structural studies of the nickel electrode
[NASA-CR-175619] N85-23414
MICHIGAN UNIV., ANN ARBOR.
Spacecraft-environment interaction: The environmental plasma aspect N85-22479
Magnetostatic-wave propagation in a finite YIG-Loaded rectangular waveguide
[AD-A150332] N85-22665
The potential for advanced computerized aids for comprehensible writing of technical documents
[AD-A150501] N85-22670
MICROELECTRONICS CENTER OF NORTH CAROLINA, RESEARCH TRIANGLE PARK.
Influence of substrate heating and thermal annealing on the surface crystallinity in single Si crystals implanted with high doses of (16)O
[DE85-005264] N85-23428
MIDWEST RESEARCH INST., GOLDEN, COLO.
A theoretical analysis of solar-driven natural convection energy conversion systems
[DE84-004431] N85-23245
Abstracts of 6th Annual Review Meeting on Photovoltaic Advanced Research and Development
[DE84-013047] N85-23248
MISSISSIPPI STATE UNIV., MISSISSIPPI STATE.
Determination of aerodynamic and propulsion parameters of general aviation aircraft using steady state flight test data N85-22377
MITRE CORP., MCLEAN, VA.
Surface scattering
[AD-A150252] N85-23366
Vertical discrimination in the sound channel
[AD-A150254] N85-23380
MITSUBISHI ELECTRIC CORP., HYOGO (JAPAN).
Availability of AlGaAs/GaAs solar cells in space N85-22576
MONSANTO RESEARCH CORP., DAYTON, OHIO.
Low jitter trigger for an excimer laser
[DE85-005732] N85-23080

N

NATIONAL AERONAUTICS AND SPACE ADMINISTRATION, WASHINGTON, D. C.
Aeronautical Engineering: A continuing bibliography with indexes, supplement 185
[NASA-SP-7037(185)] N85-22342
Aeronautical Engineering: A cumulative index to the 1984 issues of the continuing bibliography
[NASA-SP-7037(183)] N85-22343
Aerospace Safety Advisory Panel
[NASA-TM-87426] N85-22373
D-1 report: The first German spacelab mission
[NASA-TM-77637] N85-22402
Advancing automation and robotics technology for the Space Station and for the US economy. Volume 1: Executive overview
[NASA-TM-87566-VOL-1] N85-22460
Advancing automation and robotics technology for the Space Station and for the US economy, volume 2
[NASA-TM-87566-VOL-2] N85-22461
Space Station technology planning N85-22471
Suprathermal plasma observed on STS-3 Mission by plasma diagnostics package N85-22472
Electron and ion density depletions measured in the STS-3 orbiter wake N85-22474
Space Station solar array N85-22610
NASA photovoltaic research and technology development program for space applications N85-22617
Recent trends in particle size analysis techniques
[NASA-TM-77735] N85-22645
NASA's land remote sensing plans for the 1990's N85-23224
Small business innovation research: Abstracts of 1984. Phase 1 awards
[NASA-TM-87427] N85-23431
NASA Patent Abstracts Bibliography. A continuing bibliography. Section 2: Indexes
[NASA-SP-7039(26)] N85-23445
Reports of the Planetary Geology and Geophysics Program, 1984
[NASA-TM-87563] N85-23474
NATIONAL AERONAUTICS AND SPACE ADMINISTRATION. AMES RESEARCH CENTER, MOFFETT FIELD, CALIF.
Space shuttle pilot-induced-oscillation research testing N85-22351
Effects of inlet distortion on a static pressure probe mounted on the engine hub in an F-15 airplane
[NASA-TP-2411] N85-22394
Studies of planetary rings N85-23486
Origin and evolution of the Saturn system N85-23493
The structure and composition of Uranus and Neptune N85-23495
Studies of icy bodies: Uranian satellites and cometary nuclei N85-23496
Response of Earth's atmosphere to increases in solar flux and implications for loss of water from Venus N85-23518
The Formation of preplanetary disks from the collapse of rotating molecular cloud cores N85-23526

NATIONAL AERONAUTICS AND SPACE ADMINISTRATION. EARTH RESOURCES LABS., BAY ST. LOUIS, MISS.
An initial analysis of LANDSAT-4 Thematic Mapper data for the discrimination of agricultural, forested wetlands, and urban land cover N85-23193

NATIONAL AERONAUTICS AND SPACE ADMINISTRATION. GODDARD SPACE FLIGHT CENTER, GREENBELT, MD.
Ozone Correlative Measurements Workshop
[NASA-CP-2362] N85-23112
Scientific requirements for ozone measurements N85-23113
Method for determining the number of correlative measurements required to validate the SBUV/2 ozone retrievals N85-23114
Measurement requirements for the detection of ozone trends N85-23115
LANDSAT-4 Science Characterization Early Results. Volume 4: Applications
[E85-10070] N85-23186
Overview of TM applications research reports N85-23187
Impact of Thematic Mapper sensor characteristics on classification accuracy N85-23188
Assessment of computer based geologic mapping of rock units in the LANDSAT-4 scene of northern Death Valley, California N85-23195
Quick look analysis of TM data of the Washington, District of Columbia, area N85-23197
Preliminary comparisons of the information content and utility of TM versus MSS data N85-23202
Preliminary study of information extraction of LANDSAT TM data for a suburban/regional test site N85-23208
Comparative techniques used to evaluate Thematic Mapper data for land cover classification in Logan County, West Virginia N85-23209
Comparison of MSS and TM data for landcover classification in the Chesapeake Bay area: A preliminary report N85-23210
Comparison of land cover information from LANDSAT Multispectral Scanner (MSS) and airborne Thematic Mapper simulator (TMS) data for hydrologic applications N85-23211
Relative accuracy assessment of LANDSAT-4 MSS and TM data for level 1 land cover inventory N85-23212
Remanent magnetization model for the broken ridge satellite magnetic anomaly N85-23219
Calculations of microwave brightness temperature of rough soil surfaces: Bare field
[NASA-TM-86200] N85-23221
Remote Sensing of Snow and Evapotranspiration
[NASA-CP-2363] N85-23223
Microwave radiometer observations of snowpack properties and comparison of U.S. Japanese results N85-23230
Microwave remote sensing of soil moisture N85-23235
Crustal dynamics project: Catalogue of site information
[NASA-TM-87452] N85-23258
Mapping structures characteristic of the highland boundary scarp on Mars N85-23595
Distribution and properties of large symmetric knobs on Mars N85-23598

NATIONAL AERONAUTICS AND SPACE ADMINISTRATION. LYNDON B. JOHNSON SPACE CENTER, HOUSTON, TEX.
Preliminary evaluation of Thematic Mapper image data quality N85-23194
Thematic Mapper data quality and performance assessment in renewable resources/agriculture/remote sensing N85-23201
Preliminary evaluation of TM for soils information N85-23206
Chemical weathering of soils from the dry valleys of Antarctica: A terrestrial analog of Martian weathering processes N85-23626

NATIONAL AERONAUTICS AND SPACE ADMINISTRATION. LANGLEY RESEARCH CENTER, HAMPTON, VA.
Dynamic wind-tunnel testing of active controls by the NASA Langley Research Center N85-22353
A flight management algorithm and guidance for fuel-conservative descents in a time-based metered air traffic environment: Development and flight test results N85-22356
AIRLAB: A laboratory for flight-crucial-electronics system research N85-22362
The application of some lifting-body reentry concepts to missile design
[NASA-TM-86394] N85-22366
Aerodynamic heating rate distributions induced by trailing edge controls on hypersonic aircraft configurations at Mach 8
[NASA-TM-87453] N85-22370
Two degree-of-freedom flutter solution for a personal computer
[NASA-TM-86381] N85-22378
A description of the Langley wireframe geometry standard (LaWGS) format
[NASA-TM-85767] N85-22380
Approach for service life extension of explosive devices for aircraft escape systems
[NASA-TM-86323] N85-22381
Ignition of mixtures of SiH sub 4, CH sub 4, O sub 2, and Ar or N sub 2 behind reflected shock waves
[NASA-TP-2415] N85-22395
Cryogenic wind tunnels: A selected annotated bibliography
[NASA-TM-86346] N85-22401
Electrostatic forming and testing of polymer films on a 16-foot diameter test fixture
[NASA-TM-86328] N85-22885
Electroacoustical imaging technique for encoding incoherent radiance fields as Gabor elementary signals
[NASA-TM-86372] N85-23067
Reliability bounds for fault-tolerant systems with competing responses to component failures
[NASA-TP-2409] N85-23090
Spline-based Rayleigh-Ritz methods for the approximation of the natural modes of vibration for flexible beams with tip bodies
[NASA-CR-172566] N85-23100
Characteristic vector analysis of inflection ratio spectra: New technique for analysis of ocean color data
[NASA-TP-2428] N85-23237
Cumulus cloud venting of mixed layer ozone
[NASA-TM-87429] N85-23269
A theoretical basis for the analysis of redundant software subject to coincident errors
[NASA-TM-86369] N85-23317
Exploiting parallel computing with limited program changes using a network of microcomputers
[NASA-TM-86387] N85-23318
M68000 RNF text formatter user's manual
[NASA-TM-86327] N85-23320
Construction of a menu-based system
[NASA-CR-172560] N85-23321
Measurement of SIFT operating system overhead
[NASA-TM-86322] N85-23337
A community survey of helicopter noise annoyance conducted under controlled noise exposure conditions
[NASA-TM-86400] N85-23374

NATIONAL AERONAUTICS AND SPACE ADMINISTRATION. LEWIS RESEARCH CENTER, CLEVELAND, OHIO.
Spacecraft Environmental Interactions Technology, 1983
[NASA-CP-2359] N85-22470
Laboratory studies of Kapton degradation in an oxygen ion beam N85-22477
Electron beam charging of Space Shuttle thermal protection system tiles N85-22478
Three-dimensional calculation of shuttle charging in polar orbit N85-22486
Polar orbit electrostatic charging of objects in shuttle wake N85-22487
The PIX-2 experiment: An overview N85-22494
Plasma interaction experiment 2 (PIX 2): Laboratory and flight results N85-22495
Ram-wake effects on plasma current collection of the PIX 2 Langmuir probe N85-22496
NASCAP simulation of PIX 2 experiments N85-22497
An investigation of arc discharging on negatively biased dielectric conductor samples in a plasma N85-22498
Discharges on a negatively biased solar cell array in a charged-particle environment N85-22499
Design guidelines for assessing and controlling spacecraft charging effects N85-22500
Spacecraft environmental interactions: A joint Air Force and NASA research and technology program N85-22517
Preliminary assessment of power-generating tethers in space and of propulsion for their orbit maintenance N85-22520
The high voltage silicon cell: A comparative analysis N85-22569
GaAs and 3-5 compound solar cells status and prospects for use in space N85-22580
The effects of lithium counterdoping on radiation damage and annealing in n(+)p silicon solar cells N85-22586
Formation of high molecular weight products from benzene during boundary lubrication
[NASA-TM-86966] N85-22644
Orientation and temperature dependence of some mechanical properties of the single-crystal nickel-base superalloy Rene N4. 3: Tension-compression anisotropy
[NASA-TM-86982] N85-22660
Metallic and metalloceramic coating by thermal decomposition
[NASA-TM-86992] N85-22755
Film and interstitial formation of metals in plasma-sprayed ceramics
[NASA-TM-86993] N85-22756
Frictional and structural characterization of ion-nitrided low and high chromium steels
[NASA-TM-86991] N85-23085
Development of large, horizontal-axis wind turbines
[NASA-TM-86950] N85-23242
Operational performance of the photovoltaic-powered grain mill and water pump at Tangaye, Burkina Faso (formerly Upper Volta)
[NASA-TM-86970] N85-23243

NATIONAL AERONAUTICS AND SPACE ADMINISTRATION. MARSHALL SPACE FLIGHT CENTER, HUNTSVILLE, ALA.
Space test program of high-voltage solar array-space plasma interactions N85-22519
An electrochemical study of the corrosion behavior of primer coated 2219-T87 aluminum
[NASA-TP-2459] N85-22662
Power control for ac motor
[NASA-CASE-MFS-25861-1] N85-22877
Preliminary study of inphase gusts and moment force wind loads over the first 150 meters at KSC, Florida
[NASA-TM-86501] N85-23273
An integral representation of the generalized Euler-Mascheroni constants
[NASA-TP-2456] N85-23305
BIG MAC: A bolometer array for mid-infrared astronomy, Center Director's Discretionary Fund
[NASA-TM-86502] N85-23463

NATIONAL AERONAUTICS AND SPACE ADMINISTRATION. PASADENA OFFICE, CALIF.
Optical system
[NASA-CASE-NPO-15801-1] N85-23396

NATIONAL AIR AND SPACE MUSEUM, WASHINGTON, D.C.
Investigations of the Mars cratered terrain: Smooth plains boundary in the eastern equatorial region N85-23596
Mechanisms of basalt-plains ridge formation N85-23643

NATIONAL ASTRONOMY AND IONOSPHERE CENTER, ARECIBO, PUERTO RICO.
Volcanism and rift formation in Beta Regio, Venus: New radar results N85-23507
Mercury radar altimetry: A preliminary analysis N85-23631

NATIONAL BUREAU OF STANDARDS, BOULDER, COLO.
Critical current measurements on an NbTi superconducting wire standard reference material
[PB85-118594] N85-22906

NATIONAL BUREAU OF STANDARDS, GAITHERSBURG, MD.
Technical Digest: Symposium on Optical Fiber measurements, 1984
[PB85-114700] N85-23407

NATIONAL BUREAU OF STANDARDS, WASHINGTON, D.C.
Environmental cycling of cellulosic thermal insulation and its influence on fire performance
[DE85-004295] N85-22776

NATIONAL GEOPHYSICAL DATA CENTER, BOULDER, COLO.
Solar-geophysical data number 479, August 1981. Part 2: (Comprehensive reports), data for January 1984 and August 1981 and miscellanea. Explanation of data reports issued as number 474 (supplement) February 1984
[NASA-CR-175607] N85-23679

NATIONAL INST. FOR AERONAUTICS AND SYSTEMS TECHNOLOGY, PRETORIA (SOUTH AFRICA).
Beamwidth control in pyramidal horns
[R-NIAS-27] N85-22853
Fibre composite laminated plate analysis using a card programmable calculator (HP41C/CV)
[NIAST-83/88] N85-23106

NATIONAL OCEANIC AND ATMOSPHERIC ADMINISTRATION, OAK RIDGE, TENN.
Portable Automated Mesonet (PAM) data from the 1980 experiment in Anderson Creek Valley
[DE85-004361] N85-23282
The ASCOT Data Analysis Workshop
[DE85-004407] N85-23283

NATIONAL RESEARCH INST. FOR MATHEMATICAL SCIENCES, PRETORIA (SOUTH AFRICA).
An analysis of a dynamic project cost problem
[CSIR-TWISK-338] N85-23341
On an iterative scheme for the solution of constrained variational equations
[CSIR-TWISK-341] N85-23342

NATIONAL SPACE DEVELOPMENT AGENCY, IBARAKI (JAPAN).
Thin and ultrathin silicon solar cells for space use N85-22567
Space qualified AlGaAs/GaAs solar cells N85-22575
NATURAL ENVIRONMENT RESEARCH COUNCIL, LONDON (ENGLAND).
The use of Thematic Mapper data for land cover discrimination: Preliminary results from the UK SATMaP programme N85-23207
NAVAL AIR DEVELOPMENT CENTER, WARMINSTER, PA.
Tight Ribbon Arm Protection (TRAP) for aircrewman ejection
[AD-A150464] N85-23303
NAVAL OCEAN SYSTEMS CENTER, SAN DIEGO, CALIF.
Artificial Intelligence and Bionics Workshop held at Stowe, Vermont on 11-15 June 1984
[AD-A150463] N85-23339
NAVAL OCEANOGRAPHY COMMAND DETACHMENT, ASHEVILLE, N.C.
Summary of Meteorological Observations, Surface (SMOS), Fallon, Nevada
[AD-A150481] N85-23276
Summary of Meteorological Observations, Surface (SMOS) Camp Pendleton, California
[AD-A150482] N85-23277
Summary of Meteorological Observations, Surface (SMOS), Bermuda
[AD-A150537] N85-23278
Summary of Meteorological Observations, Surface (SMOS), Beaufort, South Carolina
[AD-A150538] N85-23279
Summary of Meteorological Observations Surface (SMOS), Sigonella, Sicily/Navy
[AD-A150539] N85-23280
Summary of Meteorological Observations, Surface (SMOS), Alameda, California
[AD-A150609] N85-23281
NAVAL POSTGRADUATE SCHOOL, MONTEREY, CALIF.
Aviation maintenance computerized management information systems: Perspective for the future
[AD-A150637] N85-23349
Solid propellant combustion diagnostics and automated data retrieval from holograms N85-22527
Draftsman displays: A graphical technique for exploratory data analysis
[AD-A150515] N85-22775
Computer aided antenna design and frequency selection for HF communications
[AD-A150485] N85-22869
Mean flow and turbulence in complex terrain NPS (Naval Postgraduate School)/Vandenberg measurement system
[AD-A150184] N85-23274
A design analysis and implementation of a user-friendly interface for the UNIX operating system
[AD-A150558] N85-23312
Principles of software engineering environment design
[AD-A150352] N85-23324
Microcomputers and the electrical engineer
[AD-A150499] N85-23325
LEXICON: A structured modeling system for optimization
[AD-A150536] N85-23329
Image data compression using uneven knots selection
[AD-A150602] N85-23359
A spatially incoherent and temporally coherent source
[AD-A151281] N85-23390
Time-resolved reflectivity measurement of extrinsic silicon during pulsed laser irradiation
[AD-A150350] N85-23403
General design considerations of an Air Force information system
[AD-A150611] N85-23449
Copyright law, computer software, and government acquisition
[AD-A150347] N85-23453
NAVAL RESEARCH LAB., WASHINGTON, D. C.
Kinetics of mechanism of the thermal decomposition of dimethylnitramine and dimethylnitrosamine N85-22559
The chemistry of RDX and HMX cluster ions N85-22561
Survey of the state-of-the-art of miniature cryocoolers for superconductive devices
[AD-A150319] N85-22774
Low-bit rate speech encoders based on Line-Spectrum Frequencies (LSF)
[AD-A150518] N85-22871
The use of a high-speed 12-bit A/D converter for digital sampling of communication signal carriers
[AD-A150578] N85-22872
The effect of the choice or response matrix on unfolded bonner sphere spectra
[AD-A150462] N85-23404
Increased hot-electron production at quarter-critical density in long-scalelength, laser-plasma interactions
[AD-A150519] N85-23411
NAVAL WEAPONS CENTER, CHINA LAKE, CALIF.
Comparisons of solid propellant with instability predictions and motor firing experience N85-22541
NEW MEXICO UNIV., ALBUQUERQUE.
Nonrelativistic Kapitza-Dirac scattering
[AD-A150622] N85-23405
Volcanism of the Colorado Plateau (basin and range transition): Implications for crustal processes N85-23569
Intra-eruption geologic map from an x-band radar image during the May 18, 1980 eruption of Mount St. Helens, Washington N85-23639
NEW TECHNOLOGY, INC., HUNTSVILLE, ALA.
New atmospheric sensor analysis study
[NASA-CR-171426] N85-23069
NIELSEN ENGINEERING AND RESEARCH, INC., MOUNTAIN VIEW, CALIF.
Preliminary development of an approximation procedure for supercritical wing design optimization applications
[AD-A150177] N85-22383
NORTH CAROLINA STATE UNIV., RALEIGH.
Geographic variation in the relationships of temperature, salinity or sigma sub t versus plant nutrient concentrations in the world ocean
[NASA-CR-175621] N85-23287
Influence of substrate heating and thermal annealing on the surface crystallinity in single Si crystals implanted with high doses of (16)O
[DE85-005264] N85-23428
Thermal and thermoelastic effects in rolling/sliding contacts
[AD-A150435] N85-23429
NORTH CAROLINA UNIV., CHAPEL HILL.
A Monte Carlo sampling plan for estimating network reliability
[AD-A150511] N85-22898
Skewed stable variables and processes
[AD-A150549] N85-23372
NORTHEAST LOUISIANA STATE COLL., MONROE.
Ridged plains of Lunae Planum: Thickness distribution revised N85-23559
Thickness of ridged plains materials in Hesperia Planum, Mars N85-23561

O

OAK RIDGE ASSOCIATED UNIVERSITIES, TENN.
Structural characterization by intensity measurements of electron diffraction patterns
[DE85-004803] N85-23427
OAK RIDGE NATIONAL LAB., TENN.
Particulate toughened silicon carbide
[DE85-004797] N85-22643
Thermodynamics of copper-nickel alloys containing aluminum, silicon, titanium, and chromium relative to their use in ceramic brazing
[DE85-004787] N85-22674
TEM/FIM study of modulated microstructures in the Fe-Be system
[DE85-005379] N85-22678
First principles theory of Fermi-surface driven concentration waves in Cu/sub c/Pd/sub 1-c/ alloys
[DE85-005367] N85-22681
Magnetic studies of Ni3Al(Fe) compounds
[DE85-005262] N85-22686
Dispersed-metal-toughened alumina
[NASA-CR-174687] N85-22758
Time-resolved studies of rapid solidification in highly undercooled molten silicon
[DE85-004857] N85-22765
Time-resolved ellipsometry and reflectivity measurements of the optical properties of silicon during pulsed excimer laser irradiation
[DE85-005091] N85-23079
Feasibility of alpha particle measurement by CO2 laser Thomson scattering
[DE85-004938] N85-23081
Time resolved X-ray studies during pulsed laser irradiation of Ge
[DE85-005263] N85-23083
Latent heat storage in cooling systems
[DE85-005355] N85-23248
Overview of latent storage for passive solar applications
[DE85-005354] N85-23249
Areas with forest soils sensitive to acidic deposition under alternative damage hypotheses
[DE85-005257] N85-23257
Sparse matrix computations
[DE85-004780] N85-23362
Introduction to combinatorial geometry
[DE85-003266] N85-23364
Ultrahigh-sensitivity threshold neutron detector for plasma diagnositcs
[DE85-005270] N85-23413
Structural characterization by intensity measurements of electron diffraction patterns
[DE85-004803] N85-23427
Influence of substrate heating and thermal annealing on the surface crystallinity in single Si crystals implanted with high doses of (16)O
[DE85-005264] N85-23428
OFFICE NATIONAL D'ETUDES ET DE RECHERCHES AEROSPATIALES, PARIS (FRANCE).
The low frequency behaviour of an immersed structure at a standstill in a high density fluid with free surface
[TP-1983-31] N85-23105
OFFICE NATIONAL D'ETUDES ET DE RECHERCHES AEROSPATIALES, TOULOUSE (FRANCE).
Phenomenology of discharges in space: Application to a solar generator N85-22583
Investigation of the degradation of GaAs photovoltaic cells by proton and electron irradiation N85-22587
OFFICE OF TECHNOLOGY ASSESSMENT, WASHINGTON, D.C.
Technologies to sustain tropical forest resources
[TI85-901085] N85-23241
OHIO STATE UNIV., COLUMBUS.
An atlas of nitrogen-broadened water vapor spectra from 500 to 5000 cm(-1), volume 1
[AD-A150527] N85-22650
A standard aircraft diffusion flame: Spectral characteristics and a feasibility study for developing an alternate calibration source for aircraft optical fire detection systems
[AD-A150231] N85-22768
Effects of assuming independent component failure times, if they are actually dependent, in a series system
[AD-A150582] N85-23092
Investigations of ultrasonic wave interactions at boundaries separating anisotropic materials
[DE85-003506] N85-23384
OKLAHOMA STATE UNIV., STILLWATER.
Deflected jet experiments in a turbulent combustor flowfield
[NASA-CR-174863] N85-22390
Calibration of wind tunnel flow quality N85-22399
OPTICAL SOCIETY OF AMERICA, WASHINGTON, D. C.
Technical Digest: Symposium on Optical Fiber measurements, 1984
[PB85-114700] N85-23407
OREGON STATE UNIV., CORVALLIS.
Morphologic evolution of the Mount St. Helens crater area, Washington N85-23568
Experiments and analyses of the formation of erosional scour marks with implications to the origin of the Martian outflow channels N85-23588
OREGON UNIV., EUGENE.
Threshold double photoionization of argon with synchrotron radiation
[AD-A150615] N85-23389
OXFORD UNIV. (ENGLAND).
Behavior of fiber-reinforced composites under dynamic tension
[AD-A150619] N85-22641

P

PACIFIC NORTHWEST LAB., RICHLAND, WASH.
Role of segregated P and S in intergranular stress corrosion cracking of nickel
[DE85-004547] N85-22679
Mean delta-ray energies in ion molecule collisions
[DE85-005524] N85-23395
PARIS XI UNIV., ORSAY (FRANCE).
Global tectonics on Ganymede N85-23659
Tectonics of the Galileo Regio on Ganymede N85-23660
Importance of the tectonic motions on Ganymede N85-23661
Tectonics of the Valhalla structure on Callisto N85-23662
PARKER (LEE W.), INC., CONCORD, MASS.
Wakes and differential charging of large bodies in low Earth orbit N85-22488
PENNSYLVANIA STATE UNIV., UNIVERSITY PARK.
Mass spectra of neutral particles released during electrical breakdown of thin polymer films N85-22511
Status of boron combustion research N85-22528
Gasification of boron oxide drops and boron slurry agglomerates in combustion gases N85-22529
Grid generation for a pump collector
[AD-A150217] N85-23059

A method for estimating soil moisture availability
[NASA-CR-175606] N85-23238
Analysis of the inflow layer and air-sea interactions in Hurricane Frederic (1979)
[NASA-CR-175616] N85-23271
PHYSICAL SCIENCES, INC., ANDOVER, MASS.
Molten carbonate fuel cell performance model update, draft
[DE85-005423] N85-23252
PHYSIKALISCH-TECHNISCHE BUNDESANSTALT, BRUNSWICK (WEST GERMANY).
Nonlinearity and spectral mismatch problems of solar cells N85-22605
PITTSBURGH UNIV., PA.
Multivariate analysis and its applications
[AD-A150324] N85-23352
A note about the strong convergence of the nonparametric estimation of a regression function
[AD-A150325] N85-23353
On limit of the largest eigenvalue of the large dimensional sample covariance matrix
[AD-A150589] N85-23358
Bootstrapping the Kalman filter
[AD-A150509] N85-23370
Informative geometry of probability spaces
[AD-A150510] N85-23371
The violet absorber on Io: Disulfur monoxide derivatives N85-23482
PLANETARY SCIENCE INST., TUCSON, ARIZ.
Stability of the Galilean satellites in deep orbital resonance N85-23477
Asteroid collisional evolution studies N85-23501
Lunar origin: Role of giant impacts N85-23519
A circum-terrestrial compositional filter N85-23520
Models of angular momentum input to a circum-terrestrial swarm from encounters with heliocentric planetesimals N85-23521
Capture of planetesimals into a circumterrestrial swarm N85-23522
Orbital resonances and planetary accretion in the solar nebula N85-23523
Evolution of grains in a turbulent solar nebula N85-23525
Progress on Experimental impact studies N85-23534
Progress on studies of early intense cratering N85-23535
POLYTECHNIC INST. OF NEW YORK, BROOKLYN.
Influence of hydrogen bonding in block copolymers and their blends N85-22752
PRATT AND WHITNEY AIRCRAFT, WEST PALM BEACH, FLA.
High-pressure rocket engine turnaround duct computational fluid dynamics analysis N85-22556
PRINCETON UNIV., N. J.
Aerodynamic behavior of ventilated wind tunnel walls N85-22363
Laser diagnostic analyses of sooting flames
[AD-A150478] N85-22649
Comprehensive mechanisms for combustion chemistry: An experimental and numerical study with emphasis on applied sensitivity analysis
[DE85-000173] N85-22656
Approaches and algorithms for robust signal processing N85-22878
PUERTO RICO UNIV., MAYAGUEZ.
Elastic wave scattering from cavities and sound inclusions analyzed by the resonance method
[AD-A150315] N85-23381
PURDUE UNIV., LAFAYETTE, IND.
Effect of variable solid phase thermal properties on propellant combustion N85-22547

R

RAND CORP., SANTA MONICA, CALIF.
ROSS: An object-oriented language for constructing simulations
[AD-A150556] N85-23330
A unified lunar control network N85-23669
The control network of Mars: October 1984 N85-23670
The control networks of the satellites of Jupiter and Saturn N85-23671
RANDOM APPLICATIONS, INC., MONTROSE, COLO.
On filter binary processes
[AD-A150328] N85-22890
RENSSELAER POLYTECHNIC INST., TROY, N. Y.
Combustion kinetics of metal atoms and metallic radicals over wide temperature ranges N85-22530
Turbulence measurements in shock induced flows N85-23055
Optimum design and automated dynamic analysis of flexible mechanisms
[AD-A150152] N85-23088
Theoretical aspects of electroweak and other interactions in medium-energy nuclear physics
[DE85-003821] N85-23392
RESEARCH TRIANGLE INST., RESEARCH TRIANGLE PARK, N.C.
Firefighters' communication transceiver test plan
[NASA-CR-171419] N85-22854
RGB ASSOCIATES, INC., WAYLAND, MASS.
Algorithms for reconstruction of partially known, band limited Fourier transform pairs from noisy data
[AD-A150194] N85-23347
RHODE ISLAND UNIV., KINGSTON.
Fluvial drainage basins and valley networks: Eastern Margaritifer Sinus, Mars N85-23586
RICE UNIV., HOUSTON, TEX.
Argon ion pollution of the magnetosphere N85-22523
ROCKEFELLER UNIV., NEW YORK.
Experimental studies of elementary particle interactions at high energies
[DE85-004795] N85-23394
ROCKETDYNE, CANOGA PARK, CALIF.
Development of a three-phrase combustion code for modeling liquid rocket engines N85-22554
Atomization data requirements for rocket combustor modeling N85-22555
Minimizing plume contamination production in bipropellant thrusters N85-22557
ROCKWELL INTERNATIONAL CORP., CANOGA PARK, CALIF.
Low thrust bipropellant engine/redundant seat valve assembly
[AD-A150293] N85-22628
ROCKWELL INTERNATIONAL CORP., GOLDEN, COLO.
Mechanical properties of electrodeposited nickel and copper
[DE85-005321] N85-22677
Low temperature calibration fixture
[DE85-003969] N85-23071
ROME AIR DEVELOPMENT CENTER, HANSCOM AFB, MASS.
Discharge pulse phenomenology N85-22509
ROYAL AIRCRAFT ESTABLISHMENT, BEDFORD (ENGLAND).
Civil avionics flight testing with the RAE(B) BAC1-11 N85-22354
ROYAL AIRCRAFT ESTABLISHMENT, FARNBOROUGH (ENGLAND).
Reference systems for the evaluation of dead-reckoning navigation equipment N85-22358
Investigations into the effects of scale and compressibility on lift and drag in the RAE 5m pressurised low-speed wind tunnel
[RAE-TM-AERO-2006] N85-22372
Analysis of optimum front cover thickness for lightweight solar arrays N85-22606
Life testing of rubber seals
[AD-A143193] N85-23086
The application of anthropometric survey data to aircrew clothing sizing
[AD-A150545] N85-23304
Operational loads measurement: A philosophy and its implementation
[AD-A149445] N85-23308
ROYAL NAVAL COLL., GREENWICH, LONDON (ENGLAND).
Field-work report: Medway Estuary, 28 June - 18 July 1983
[RNC/NS/TR8] N85-22773
ROYAL NETHERLANDS AIRCRAFT FACTORIES FOKKER, SCHIPHOL-OOST.
Computer aided engineering applied to the design and verification of the generic Advanced Rigid Array (ARA) N85-22593
Generic design and verification of an Advanced Rigid Array (ARA) N85-22621
The Olympus solar array structure and mechanisms N85-22623
ROYAL SIGNALS AND RADAR ESTABLISHMENT, MALVERN (ENGLAND).
Reliability predictions for military avionics. Royal Signals and Radar Establishment reliability prediction method no. 250
[BR69221] N85-22368
The Chinese remainder theorem and multi-PRF radars
[AD-A141375] N85-22858
A fully distributed approach to the design of a 16 K bit/sec VHF packet radio network
[AD-A141282] N85-22859
Comparing different theoretical designs of six-port reflectometer junctions
[AD-A149419] N85-22861
Edge detection in SAR imagery using gradient operators
[AD-A149411] N85-22862
System dynamics and network control
[AD-A149420] N85-22863
Research using a DISCUS based network emulator
[AD-A141294] N85-23338
Performance estimate of a reflecting light pipe for infrared detectors
[AD-A141269] N85-23398
Investigation of the effect of annealing on the dislocation and sub-grain boundary content of solvent-evaporation-grown CdTe
[AD-A144087] N85-23415

S

SAINT LOUIS UNIV., MO.
Attenuation of seismic waves at regional distances
[AD-A150198] N85-23267
SALFORD UNIV. (ENGLAND).
Corrosion of aircraft Al and Al-Zn ion plated steel fasteners N85-22666
SANDIA CORP., ALBUQUERQUE, N. MEX.
Effect of alternative aging and accident simulations on polymer properties
[DE85-002642] N85-22762
Thermodynamic and kinetic studies of pulsed laser annealing from transient conductivity measurements
[DE85-003677] N85-23078
SANDIA LABS., ALBUQUERQUE, N. MEX.
Reaction of amorphous NiNb films with crystalline metal overlayers
[DE85-005483] N85-22680
Variational and moment method solutions of the fields in a parallel-plate waveguide-aperture system
[DE85-006288] N85-22876
High sheet resistance, arsenic implanted polycrystalline silicon for integrated circuit resistors
[DE85-004355] N85-22902
Significance of the thin-layer Navier-Stokes approximation
[DE85-002630] N85-23063
Technical manual: Description and operation Slaved Tracking System
[DE85-004807] N85-23070
Activation of Si-N modes in silicon by pulsed laser annealing
[DE85-002988] N85-23082
Structural design of the Sandia 34-M Vertical Axis Wind Turbine
[DE85-002631] N85-23247
Markov method for simulating non-Gaussian wind speed time series
[DE85-003450] N85-23284
Runge-Kutta formula with cheap error estimate
[DE85-005674] N85-23363
SCIENCE AND TECHNOLOGY AGENCY, TOKYO (JAPAN).
General report of the researches of snowpack properties, snowmelt runoff and evapotranspiration in Japan N85-23225
Snowmelt runoff model in Japan N85-23227
Application of Martinec-Rango model to river basin in Japan N85-23228
Distribution of snow and maximum snow water equivalent obtained by LANDSAT data and degree day method N85-23229
SCIENCE APPLICATIONS, INC., MCLEAN, VA.
Ice statistics and acoustic scattering in the Arctic basin
[AD-A150141] N85-23289
SCIENTIFIC RESEARCH ASSOCIATES, INC., GLASTONBURY, CONN.
Internal fluid mechanism of solid propellant rocket motors N85-22544
SHELL RESEARCH LTD., CHESTER (ENGLAND).
The influence of fuel quality upon flame-tube temperature and flame radiation in a model gas-turbine primary zone
[K233] N85-22396
The influence of fuel molecular composition upon flame-tube temperature and flame radiation in a model gas-turbine primary zone
[K234] N85-22648
SHOCK AND VIBRATION INFORMATION CENTER (DEFENSE), WASHINGTON, D. C.
The Shock and Vibration Digest, volume 16, no. 12
[AD-A150594] N85-23102
Applications of the conformal mapping method to the solution of mechanical vibrations problems N85-23103
Machine tool vibrations: A review N85-23104
SIKORSKY AIRCRAFT, STRATFORD, CONN.
Experimental study of main rotor tip geometry and tail rotor interactions in hover. Volume 1. Text and figures
[NASA-CR-177336-VOL-1] N85-22344

Experimental study of main rotor tip geometry and tail rotor interactions in hover. Volume 2: Run log and tabulated data
[NASA-CR-177336-VOL-2] N85-22345

SMITHSONIAN ASTROPHYSICAL OBSERVATORY, CAMBRIDGE, MASS.
Experimental studies of low temperature surface interactions of atomic hydrogen using maser technique
[AD-A150216] N85-22647
A normal incidence, high resolution X-ray telescope for solar coronal observations
[NASA-CR-175622] N85-23461
Viking radio science data analysis and synthesis
[NASA-CR-175631] N85-23471
Geophysical interpretation of Venus gravity data N85-23513
Viking radio science data analysis and synthesis N85-23528
Solar and stellar coronal plasmas
[NASA-CR-175623] N85-23676
Physics of the inner heliosphere: Mechanisms, models and observational signatures
[NASA-CR-175632] N85-23677

SOCIETE EUROPEENNE DE PROPULSION, VERNON (FRANCE).
Development and testing of a spacecraft surface potential monitor N85-22582

SOCIETE NATIONALE INDUSTRIELLE AEROSPATIALE, CANNES (FRANCE).
Gallium arsenide arrays versus silicon arrays for space application N85-22574
SPOT solar array N85-22595
Rigid Solar Generator (GSR) solar arrays N85-22596
Retractable Rigid Solar Generator (GSR) N85-22597
Study of concentration for space photovoltaic generators N85-22618

SOCIETE NATIONALE INDUSTRIELLE AEROSPATIALE, MARIGNANE (FRANCE.)
Ground evaluation of helicopter air-to-air warfare N85-22360

SOUTHEASTERN CENTER FOR ELECTRICAL ENGINEERING EDUCATION, INC., ST. CLOUD, FLA.
Basic EMC (electromagnetic interference) technology advancement for c3 systems. Volume 3A: Probabilistic analysis of combinational circuits with random delays
[AD-A150349] N85-22866

SOUTHERN METHODIST UNIV., DALLAS, TEX.
Planetary interior modeling and tectonic implications N85-23649

SOUTHWEST RESEARCH INST., SAN ANTONIO, TEX.
Polar plasmas as observed by Dynamics Exporers 1 and 2 N85-22483
Sliding seal materials for adiabatic engines
[NASA-CR-174893] N85-22757

SPAR AEROSPACE LTD., TORONTO (ONTARIO).
The Olympus solar array development and test program N85-22599

SPECTRA RESEARCH SYSTEMS, INC., HUNTSVILLE, ALA.
Space station systems technology study (add-on task). Volume 1: Executive summary
[NASA-CR-171415] N85-22459

SPERRY RAND CORP., ST. PAUL, MINN.
Feasibility of self-structured current accessed bubble devices in spacecraft recording systems
[NASA-CR-172554] N85-22525

SRI INTERNATIONAL CORP., MENLO PARK, CALIF.
Laboratory studies of spacecraft response to transient discharge pulses N85-22506
Development of a continuous broad-energy-spectrum electron source N85-22507
Electrical conduction in polymer dielectrics N85-22514

STANFORD UNIV., CALIF.
Model reduction for control system design
[NASA-CR-170417] N85-22398
Vehicle charging on STS-3 Mission N85-22473
Synthesis and characterization of poly(vinylidene fluoride)
[AD-A150291] N85-22759
Confidence intervals using the regenerative method for simulation output analysis
[AD-A150147] N85-23343
Consistency of smoothing with running linear fits
[AD-A150232] N85-23349
A model for large sparse contingency tables
[AD-A150320] N85-23350
Regenerative stochastic Petri nets
[AD-A150343] N85-23355
Regenerative simulation of non-Markovian stochastic systems
[AD-A150344] N85-23367
Why do noninvertible estimated moving averages occur?
[AD-A150388] N85-23368
Mars radar catalog N85-23636
Statistics of Aeolian surface of Mars N85-23637

STATE UNIV. OF NEW YORK, BINGHAMTON.
Crustal dynamics studies in China
[NASA-CR-175617] N85-23285

STATE UNIV. OF NEW YORK, BUFFALO.
The geology of East Butte, a rhyolitic volcanic dome on the Eastern Snake River Plain, Idaho N85-23570
The geology of Mt. Hope, a silicic volcanic center in West Central Arizona N85-23571

SUL ROSS STATE UNIV., ALPINE, TEX.
Analysis of SMIRR data for volcanic and sedimentary terrains of the trans-Pecos region, Texas N85-23626

SUPERWAVE TECHNOLOGY, INC., SANTA CLARA, CALIF.
Demonstration of feasibility of depositing semiconductor layers using microwave enhanced plasma techniques
[NASA-CR-174392] N85-23421

SYSTEMS RESEARCH LABS., INC., DAYTON, OHIO.
Application of fluorescence to measurement of surface temperature in solid propellants N85-22548

SYSTEMS SCIENCE AND SOFTWARE, LA JOLLA, CALIF.
Electric field effects on ion currents in satellite wakes N85-22485
Surface interactions and high-voltage current collection N85-22493

T

TECHNICOLOR GOVERNMENT SERVICES, INC., SIOUX FALLS, S. DAK.
Early results of investigations of LANDSAT 4 Thematic Mapper and Multispectral Scanner applications N85-23200

TECHNISCHE UNIV., MUNICH (WEST GERMANY).
A concept for the processing and display of Thematic Mapper data N85-23196

TECHNOLOGY AND ECONOMICS, INC., CAMBRIDGE, MASS.
Technology and Economics, Inc. Technology Application Team
[NASA-CR-175630] N85-23454

TECHNOLOGY APPLICATIONS, INC., FALLS CHURCH, VA.
Digital laser platemaker modifications
[AD-A150190] N85-23074

TEKWORLD CO., HAMPTON, VA.
Effects of leading-edge devices on the low-speed aerodynamic characteristics of a highly-swept arrow-wing
[NASA-CR-172531] N85-22365

TELEFUNKEN ELECTRONIC G.M.B.H., HEILBRONN (WEST GERMANY).
A 2 x 6 Back Surface Reflection (BSR) silicon solar cell N85-22570
Experiences with implanted Back Surface Field (BSF) solar cells N85-22571
A low cost approach with larger diameter silicon wafer N85-22572
Bifacial light sensitive space solar cell N85-22573

TELESPAZIO, S.P.A., ROME (ITALY).
Solar array dynamical simulation for illumination and temperature variation N85-22611

TENNESSEE UNIV., KNOXVILLE.
Cooling performance improvement of a horizontal ground coupled heat pump
[DE85-002470] N85-23065

TEXAS A&M UNIV., COLLEGE STATION.
Normal-fault and fold development in sedimentary rocks above a pre-existing basement normal fault N85-23259
A tectonic model of an incipient spreading center and its margins: The Northern Red Sea and the Dead Sea rift N85-23286
Permafrost and subsurface ice in the solar system N85-23594

TEXAS TECHNOLOGICAL UNIV., LUBBOCK.
Repetitive energy transfers from an inductive energy store N85-22881
ROSA: A computer model for optical power ratio calculations
[DE85-005174] N85-23251

TEXAS UNIV., AUSTIN.
The effects of internal waves on acoustic normal modes
[AD-A150235] N85-23379

TORONTO UNIV., DOWNSVIEW (ONTARIO).
A quantitative comparison of active and passive damping for large space structures
[UTIAS-TN-249] N85-22524

TRACOR, INC., AUSTIN, TEX.
Externally compensated crystal oscillator (ECXO) study
[AD-A150335] N85-22893

TRW SPACE TECHNOLOGY LABS., REDONDO BEACH, CALIF.
Characteristics of EMI generated by negative metal-positive dielectric voltage stresses due to spacecraft charging N85-22505

TSUKUBA UNIV. (JAPAN).
Estimation of regional evapotranspiration using remotely sensed land surface temperature. Part 1: Measurement of evapotranspiration at the Environmental Research Center and determination of Priestley-Taylor parameter N85-23233
Estimation of regional evapotranspiration using remotely sensed land surface temperature. Part 2: Application of equilibrium evaporation model to estimate evapotranspiration by remote sensing technique N85-23234

TULANE UNIV., NEW ORLEANS, LA.
Electronic transport in hydrogenated amorphous silicon films
[DE85-002901] N85-23426

TURKU UNIV. (FINLAND).
Magnetovolume effects in some Y-Ni intermetallic compounds
[ISSN-0066-2003] N85-22663

U

UNITED TECHNOLOGIES CORP., SAN JOSE, CALIF.
Coupling between velocity oscillations and solid propellant combustion N85-22536

UNITED TECHNOLOGIES OF NEW MEXICO, INC., EAST HARTFORD, CONN.
Investigation of parabolic computational techniques for internal high-speed viscous flows
[NASA-CR-172555] N85-23056

UNITED TECHNOLOGIES RESEARCH CENTER, EAST HARTFORD, CONN.
Laser diagnostic analyses of sooting flames
[AD-A150478] N85-22649

UNIVERSIDAD POLITECNICA DE BARCELONA (SPAIN).
Comparative study of GaAs solar cell potentialities for space applications N85-22577

UNIVERSITY COLL., CORK (IRELAND).
Low capacitance e-beam fabricated beam-lead Schottky barrier diodes
[AD-A150238] N85-22868

UNIVERSITY COLL., LONDON (ENGLAND).
Investigation of steel structures using ultrasonic waves
[BR93258] N85-23091

UNIVERSITY OF SOUTHERN CALIFORNIA, LOS ANGELES.
Effects of temperature variation among droplets in an evaporating fuel spray N85-22562
Numerical algorithms and software for matrix Riccati equations
[AD-A150148] N85-23344

UNIVERSITY OF SOUTHERN ILLINOIS, CARBONDALE.
Martian fretted terrain morphometry interpreted using principal components analysis N85-23597

UTAH STATE UNIV., LOGAN.
Stagnation zone impaction on a simple terrain feature in stable flow N85-23255
Two-dimensional numerical model of sensible and latent heat transport in an irrigated field under advective conditions N85-23261
Excitation of low-frequency plasma waves by a conducting, tethered satellite N85-23470

UTAH UNIV., SALT LAKE CITY.
Nonlinear interactions between vortices and acoustic waves in a rocket combustion chamber N85-22533
Acoustic energy balance method N85-22537

V

VARIAN ASSOCIATES, PALO ALTO, CALIF.
Design considerations for a 100 kW CW, 140 GHz gyrotron oscillator
[DE85-005282] N85-22904
A 60 GHz 200 kW CW gyrotron with high output mode purity
[DE85-005283] N85-22905

VIGYAN RESEARCH ASSOCIATES, INC., HAMPTON, VA.
Method for the prediction of the installation aerodynamics of a propfan at subsonic speeds
[NASA-CR-3867] N85-22360

VIRGINIA COMMONWEALTH UNIV., RICHMOND.
Relationship between topological and magnetic order in small metal clusters
[AD-A150547] N85-22651

VIRGINIA POLYTECHNIC INST. AND STATE UNIV., BLACKSBURG.
Multiple reflection theory for microwave measurement of solid propellant burning rates N85-22549

Directional dependent engineering properties of aluminum-aramid-epoxy laminates
[CCMS-85-02] N85-22638
VIRGINIA UNIV., CHARLOTTESVILLE.
Interaction of the magnetospheric ions with the surfaces of the icy satellites of Saturn N85-23491

W

WASHINGTON STATE UNIV., PULLMAN.
Observation of a novel low-lying excited state in zinc complexes
[AD-A150188] N85-23365
WASHINGTON UNIV., SEATTLE.
High-frequency acoustic variability in the arctic
[AD-A150550] N85-23383
Impact crater scaling laws N85-23532
Determining mineral types and abundances from reflectance measurements N85-23622
WASHINGTON UNIV., ST. LOUIS, MO.
Clustering and ordering in 3-5 alloys
[AD-A150604] N85-22670
Dark halo craters and the thickness of grooved terrain on Ganymede N85-23484
On the origin of Triton and Pluto N85-23497
Impacts in ice: Commissions of solar system crater population N85-23538
The evolution of CO2 on Mars N85-23558
On the latitudinal distribution of debris in the Northern Hemisphere of Mars N85-23579
The search for igneous materials at the Viking landing sites N85-23609
WESLEYAN UNIV., MIDDLETOWN, CONN.
Lithologic and structural control on slope morphology in the Valles Marineris N85-23651
WESTINGHOUSE ELECTRIC CORP., PITTSBURGH, PA.
Reluctance and doubly-excited reluctance motors
[DE85-003585] N85-22900
WHITTIER COLL., CALIF.
Catastrophic-flood features in Swedish Lapland as a terrestrial analog for Martian channel flows N85-23587
WISCONSIN UNIV., MADISON.
Reaction of amorphous NiNb films with crystalline metal overlayers
[DE85-005483] N85-22680
Confinement properties of high energy density plasmas in the Wisconsin levitated octupole N85-23408
WOODS HOLE OCEANOGRAPHIC INSTITUTION, MASS.
Gravity field of Venus and comparison with Earth N85-23514
WYOMING UNIV., LARAMIE.
Quantitative analyses of planetary reflectance spectra N85-23625

Y

YALE UNIV., NEW HAVEN, CONN.
Assessing the behavior and performance of teams in organizations: The case of air transport crews
[AD-A150359] N85-23302
Properties of materials using acoustic waves
[AD-A150465] N85-23382
YORK UNIV., TORONTO (ONTARIO).
Calculation of secondary-electron escape currents from inclined-spacecraft surfaces in a magnetic field N85-22491

Typical Contract Number Index Listing

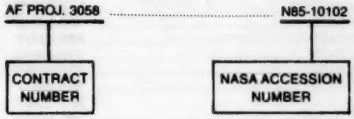

Listings in this index are arranged alphanumerically by contract number. Under each contract number the NASA accession numbers denoting documents that have been produced as a result of research done under that contract are arranged in ascending order. The NASA accession number denotes the number by which the citation is identified.

AF PROJ. C85-5 ..... N85-23347
AF PROJ. ILI-R N85-22894
AF PROJ. 112-3 ..... N85-23323
AF PROJ. 230-9 ..... N85-22469
AF PROJ. 2301 ..... N85-23389
AF PROJ. 2304 ..... N85-23092
N85-23358
N85-23360
N85-23372
AF PROJ. 2306 ..... N85-22670
AF PROJ. 2307 ..... N85-22640
N85-22641
AF-AFOSR-0006-84 ..... N85-22558
AF-AFOSR-0056-83 ..... N85-22640
AF-AFOSR-0073-82 ..... N85-22530
AF-AFOSR-0084-83 ..... N85-22538
AF-AFOSR-0132-84 ..... N85-23354
N85-23369
AF-AFOSR-0140-84 ..... N85-22898
AF-AFOSR-0157-83 ..... N85-22542
N85-22543
AF-AFOSR-0170-80 ..... N85-23309
N85-23360
AF-AFOSR-0231-82 ..... N85-22670
AF-AFOSR-0249-82 ..... N85-23402
AF-AFOSR-0268-83 ..... N85-22897
AF-AFOSR-0277-82 ..... N85-23405
AF-AFOSR-0307-82 ..... N85-23092
AF-AFOSR-0317-83 ..... N85-23351
AF-AFOSR-0325-83 ..... N85-23410
AF-AFOSR-0344-82 ..... N85-22895
AF-AFOSR-0346-82 ..... N85-22641
AF-AFOSR-0356-83 ..... N85-22532
N85-22546
AF-AFOSR-0393-84 ..... N85-23100
AFOSR-ISSA-81-00019 ..... N85-22539
AFOSR-ISSA-82-00030 ..... N85-22539
AFOSR-ISSA-83-00052 ..... N85-22539
AFOSR-82-K-0007 ..... N85-23309
ARPA ORDER 3655 ..... N85-23347
ARPA ORDER 4067 ..... N85-23369
ARPA ORDER 4311 ..... N85-22868
ARPA ORDER 4397 ..... N85-23267
ARPA ORDER 4565 ..... N85-22469
CNRS-3870.01 ..... N85-22581
DA PROJ. 1L1-62662-A-552 ..... N85-23061
DA PROJ. 3E1-62777-A-879 ..... N85-23295
N85-23296
N85-23297
DAAG29-80-K-0015 ..... N85-23301
DAAG29-80-K-0096 ..... N85-23088
DAAG29-81-G-0016 ..... N85-23381
DAAG29-81-K-0084 ..... N85-22650
DAAG29-81-K-0104 ..... N85-23400
DAAG29-81-K-0115 ..... N85-23373
DAAG29-81-K-0131 ..... N85-23344
DAAG29-81-K-0146 ..... N85-23076
DAAG29-81-K-0170 ..... N85-22760
DAAG29-82-K-0052 ..... N85-23418
DAAG29-82-K-0056 ..... N85-23350
DAAG29-82-K-0156 ..... N85-23368
DAAG29-82-K-0168 ..... N85-23309
N85-23348
DAAG29-84-K-0024 ..... N85-22899
DAAG29-84-K-0030 ..... N85-23343
N85-23355
N85-23367
DAAG46-82-K-0051 ..... N85-22668
DAAK50-81-C-0029 ..... N85-23089
DAAK70-82-C-0133 ..... N85-23448
DAAK70-83-C-0165 ..... N85-23074
DACA76-82-C-0004 ..... N85-23239
DAJA37-81-C-0261 ..... N85-22888
DAJA45-83-C-0004 ..... N85-23061
DAMD17-81-C-1023 ..... N85-23295
N85-23296
N85-23297
DARPA ORDER 3045 ..... N85-23322
DE-AC02-74ER-04461 ..... N85-22671
DE-AC02-76CH-00016 ..... N85-22673
N85-22675
N85-22682
N85-22784
N85-23292
N85-23314
DE-AC02-77ER-04461 ..... N85-22676
DE-AC02-80ER-10569 ..... N85-23393
DE-AC02-81ER-40033 ..... N85-23394
DE-AC02-81EV-10665 ..... N85-23285
DE-AC02-83CH-10093 ..... N85-23245
N85-23246
N85-23426
DE-AC02-83ER-13045 ..... N85-22658
DE-AC02-83ER-40114 ..... N85-23392
DE-AC02-83ER-45026 ..... N85-23422
DE-AC03-76SF-00098 ..... N85-22763
N85-23062
N85-23293
N85-23335
N85-23423
N85-23424
N85-23472
DE-AC03-77CS-31587 ..... N85-23253
DE-AC04-76DP-00053 ..... N85-23060
DE-AC04-76DP-00487 ..... N85-22770
DE-AC04-76DP-00613 ..... N85-22685
DE-AC04-76DP-00789 ..... N85-22680
N85-22762
N85-22902
N85-23063
N85-23070
N85-23078
N85-23082
N85-23247
N85-23284
N85-23363
DE-AC04-76DP-03533 ..... N85-22677
N85-23071
DE-AC04-83AL-21557 ..... N85-23251
DE-AC05-84OR-21400 ..... N85-22643
N85-22674
N85-22678
N85-22681
N85-22686
N85-22758
N85-22765
N85-22900
N85-22903
N85-22904
N85-22905
N85-23065
N85-23079
N85-23081
N85-23083
N85-23248
N85-23249
N85-23257
N85-23362
N85-23364
N85-23413
N85-23427
N85-23428
DE-AC06-76FF-02170 ..... N85-22684
DE-AC06-76RL-01830 ..... N85-22679
DE-AC07-76ID-01570 ..... N85-23395
N85-23084
N85-23340
N85-23456
DE-AC08-83NV-10282 ..... N85-23240
DE-AC09-76SR-00001 ..... N85-22672
DE-AC21-81FE-15078 ..... N85-23252
DE-AI01-76ET-20320 ..... N85-23242
DE-AI01-80CS-50194 ..... N85-22757
DE-AI05-78CR-06113 ..... N85-22776
DE-AI08-80CS-50208 ..... N85-23455
DE-AS09-76EV-00639 ..... N85-23290
DE-AT03-76ER-75016 ..... N85-22761
DE-FG02-84ER-45057 ..... N85-23384
DE-FG02-84ER-45096 ..... N85-22680
DE-FG22-84PC-70780 ..... N85-22771
DEN3-352 ..... N85-22757
DNA001-81-C-0267 ..... N85-22507
DOT-FA77-WAI-817 ..... N85-22375
ESTEC-5413/83/NL-PB N85-22584
ESTEC-5491/83/NL-PB(SC) N85-22572
ESTEC-5589/83/NL-PB(SC) N85-22577
FY7121-83-N-001 ..... N85-22483
F82-582 ..... N85-22774
F04611-81-C-0007 ..... N85-22537
F04611-82-C-0084 ..... N85-22628
F04611-83-C-0003 ..... N85-22533
N85-22544
F04611-84-X-0001 ..... N85-22527
F04701-83-C-0084 ..... N85-23268
F08636-82-C-0131 ..... N85-23256
F08635-82-C-0472 ..... N85-22374
F19601-82-C-0023 ..... N85-22516
F19628-81-C-0076 ..... N85-22514
F19628-81-C-0087 ..... N85-22893
F19628-81-K-0011 ..... N85-22502
F19628-82-C-0081 ..... N85-22495
N85-22486
N85-22487
F19628-82K-0024 ..... N85-22483
F19628-83-K-0028 ..... N85-22491
F19628-84-C-0001 ..... N85-23366
N85-23380
F29601-82-C-0015 ..... N85-22510
F30602-81-C-0082 ..... N85-22866
F30602-81-C-0269 ..... N85-23310
F30602-82-C-0110 ..... N85-22892
F30602-82-C-0111 ..... N85-22691
F30602-82-C-0146 ..... N85-23347
F33615-80-C-3211 ..... N85-23108
N85-23109
F33615-81-K-1429 ..... N85-22865
F33615-83-K-2306 ..... N85-22768
F49620-80-C-0022 ..... N85-23401
F49620-81-C-0027 ..... N85-22536
F49620-82-C-0007 ..... N85-23326
F49620-82-C-0009 ..... N85-23372
F49620-82-C-0013 ..... N85-22540
F49620-82-C-0018 ..... N85-23330
F49620-82-K-0001 ..... N85-23352
N85-23353
N85-23358
N85-23370
F49620-82-K-0002 ..... N85-22397
F49620-82-K-0007 ..... N85-23346
F49620-83-C-0003 ..... N85-23077
F49620-83-C-0010 ..... N85-23386
F49620-83-C-0015 ..... N85-23267
F49620-83-C-0082 ..... N85-23356
N85-23357
F49620-83-C-0085 ..... N85-22890
F49620-83-C-0109 ..... N85-23417
F49620-83-C-0131 ..... N85-22469
F49620-83-C-0138 ..... N85-22548
F49620-84-C-0039 ..... N85-23389
F49620-84-C-0111 ..... N85-23327
F49620-85-C-0008 ..... N85-23371
MIN-DEF-A45A/578 ..... N85-22396
N85-22648
MIPR-ARO-103-83 ..... N85-23401
MIPR-50-81 ..... N85-23291
MIPR-119-84 ..... N85-23291
MOD-2047/090-AMTE-13 ..... N85-23091

MOD-2047/091-AMTE-13 ..... N85-23091
NAG-320 ..... N85-22503
NAGW-112 ..... N85-23676
NAGW-192 ..... N85-23550
NAGW-221 ..... N85-23462
NAGW-235 ..... N85-22473
NAGW-249 ..... N85-23677
NAGW-367 ..... N85-23287
NAGW-397 ..... N85-23461
NAGW-411 ..... N85-23471
NAGW-432 ..... N85-23484
N85-23497
N85-23656
NAGW-517 ..... N85-23590
NAG1-396 ..... N85-22367
NAG1-398 ..... N85-22382
NAG1-534 ..... N85-23321
NAG2-223 ..... N85-22398
NAG3-33 ..... N85-23096
NAG3-200 ..... N85-22391
NAG3-255 ..... N85-22661
NAG3-449 ..... N85-22472
N85-22474
NAG3-519 ..... N85-23414
NAG3-549 ..... N85-22390
NAG5-184 ..... N85-23238
NAG5-240 ..... N85-23265
NAG5-272 ..... N85-23213
NAG5-398 ..... N85-23271
NAG5-417 ..... N85-23272
NASA ORDER C-72801-D N85-22758
NASA ORDER DSB-5710-2-79 ..... N85-23243
NASA ORDER W-15519 ..... N85-23679
NASA PURCHASE ORDER L-69215B N85-22365
NASW-3336 ..... N85-23454
NASW-3924 ..... N85-23299
NASW-4004 ..... N85-22402
NAS1-16135 ..... N85-22387
NAS1-16742 ..... N85-22369
NAS1-16794 ..... N85-22378
NAS1-16911 ..... N85-22525
NAS1-16978 ..... N85-23374
N85-23375
NAS1-17070 ..... N85-23100
N85-23321
NAS1-17290 ..... N85-22754
NAS1-17561 ..... N85-23056
NAS2-10620 ..... N85-22346
N85-22347
NAS2-11085 ..... N85-23377
NAS2-11266 ..... N85-22344
N85-22345
NAS2-11313 ..... N85-23376
NAS3-20609 ..... N85-22400
NAS3-23051 ..... N85-22368
NAS3-23058 ..... N85-22493
NAS5-24455 ..... N85-22473
NAS5-25156 ..... N85-22465
NAS5-25683 ..... N85-22483
NAS5-26363 ..... N85-22483
NAS5-27355 ..... N85-23189
NAS5-27377 ..... N85-23190
NAS5-27580 ..... N85-23198
NAS7-100 ..... N85-23421
NAS7-918 ..... N85-22393
N85-22464
N85-22484
N85-22855
N85-22886
N85-23068
N85-23101
N85-23222
N85-23244
NAS8-34504 ..... N85-22555
NAS8-34893 ..... N85-22459
NAS8-34928 ..... N85-22554
NAS8-35499 ..... N85-22462
N85-22463
NAS8-35816 ..... N85-22854
NAS8-35917 ..... N85-23319
NAS8-35984 ..... N85-23057
NAS8-35992 ..... N85-22364
NAS8-36179 ..... N85-23069
NAS9-17179 ..... N85-22466
N85-22467
N85-22468
NGL-12-001-057 ..... N85-23460
NGR-39-007-011 ..... N85-23097
N85-23098
N85-23099
NSF ATM-83-1491 ..... N85-23679
NSF DAR-80-17836 ..... N85-23198
NSF DMR-80-22225 ..... N85-22678
NSF DMR-82-17227 ..... N85-23420
NSF MCS-82-03483 ..... N85-23343
N85-23355
NSF MEA-84-14477 ..... N85-23367
N85-23098
N85-23099
NSF PCM-77-01133 ..... N85-22682
NSG-1297 ..... N85-22639
NSG-3197 ..... N85-22512
NSG-3206 ..... N85-22392
NSG-3301 ..... N85-22511
NSG-7156 ..... N85-23457
N85-23618
N85-23619
NSG-7612 ..... N85-23673
N00014-75-C-0522 ..... N85-23311
N00014-76-C-0527 ..... N85-23382
N00014-77-C-0309 ..... N85-23383
N00014-77-C-0777 ..... N85-22647
N00014-79-C-0224 ..... N85-22669
N85-22896
N00014-79-C-0363 ..... N85-22648
N00014-79-C-0764 ..... N85-22546
N00014-80-C-0299 ..... N85-22864
N00014-80-C-0490 ..... N85-23379
N00014-80-C-0505 ..... N85-23345
N85-23432
N00014-80-C-0555 ..... N85-23302
N00014-81-C-0046 ..... N85-22649
N00014-81-C-0557 ..... N85-22383
N00014-81-C-0699 ..... N85-22870
N00014-81-C-0738 ..... N85-22868
N00014-81-C-0776 ..... N85-22652
N00014-81-K-0494 ..... N85-23432
N00014-81-K-0505 ..... N85-23419
N85-23420
N00014-81-K-0683 ..... N85-22759
N00014-82-K-0334 ..... N85-23432
N00014-82-K-0508 ..... N85-22873
N00014-82-K-0551 ..... N85-23429
N00014-82-K-0576 ..... N85-22651
N85-23367
N85-23368
N85-23419
N85-23420
N00014-83-G-0121 ..... N85-23350
N00014-83-K-0125 ..... N85-23331
N00014-83-K-0472 ..... N85-23349
N85-23350
N00014-83-K-0609 ..... N85-23365
N00014-84-C-0180 ..... N85-23289
N00014-84-F-0094 ..... N85-23416
N00014-84-K-0049 ..... N85-22867
N00014-84-K-0357 ..... N85-23322
N00014-84-K-0530 ..... N85-23357
N00024-79-C-6043 ..... N85-23059
N00024-81-C-6042 ..... N85-23383
N00024-83-C-5301 ..... N85-22526
N00039-83-C-0463 ..... N85-23328
N85-23450
N00174-82-C-0039 ..... N85-22549
N68335-83-C-0625 ..... N85-23399
PROJ. AGRISTARS N85-23201
RR0-1103 ..... N85-22647
RR0-1108 ..... N85-23382
S15-80 ..... N85-23404
W-31-109-ENG-33 ..... N85-23334
W-31-109-ENG-38 ..... N85-22654
N85-22687
N85-22768
N85-23110
N85-23250
N85-23254
N85-23268
N85-23298
N85-23333
W-7405-ENG-36 ..... N85-22655
N85-22683
N85-22901
N85-23072
N85-23084
N85-23111
N85-23315
N85-23361
N85-23391
N85-23406
N85-23451
N85-23678
W-7405-ENG-48 ..... N85-22642
N85-22767
N85-22874
N85-22875
N85-22887
N85-23066
N85-23282
N85-23283
N85-23313
N85-23332
N85-23336
N85-23365
N85-23430
W-7405-ENG-82 ..... N85-22653
N85-23425
W05-84 ..... N85-23303
307-04-02 ..... N85-23067
505-31-53-01 ..... N85-22401
505-31-83-01 ..... N85-23100
N85-23321
505-32-01 ..... N85-23377
505-33-1A N85-22660
505-33-33 ..... N85-22754
505-33-33-05 ..... N85-22639
505-33-43-07 ..... N85-22379
505-33-53 ..... N85-23318
505-33-53-12 ..... N85-22378
505-33-62 ..... N85-22644
505-34-01 ..... N85-22396
505-34-13 ..... N85-23317
N85-23337
505-34-13-40 ..... N85-23090
505-35-13-03 ..... N85-22387
505-35-13-52 ..... N85-23374
505-35-13-53 ..... N85-23375
505-37-03-01 ..... N85-23320
505-37-23-01 ..... N85-22380
505-40-90-01 ..... N85-22369
505-42-11 ..... N85-22344
N85-22345
N85-22346
N85-22347
N85-23376
505-42-23-56 ..... N85-22381
505-43-43 ..... N85-22366
505-43-43-01 ..... N85-22365
506-53-1B N85-23085
506-60-12 ..... N85-22755
N85-22756
506-62-23 ..... N85-22685
533-02-21 ..... N85-22394
533-04-1A N85-22390
535-03-12 ..... N85-22368
535-05-12 ..... N85-22392
618-32-33-01 ..... N85-23237
776-31-41 ..... N85-23242
776-54-01 ..... N85-23243

REPORT / ACCESSION NUMBER INDEX

Typical Report / Accession Number Index Listing

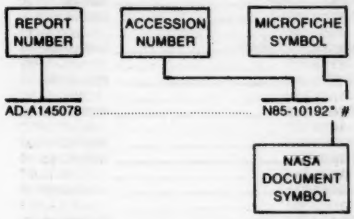

Listings in this index are arranged alphanumerically by report number. The NASA accession number denotes the number by which the citation is identified. An asterisk (*) indicates that the item is a NASA report. A pound sign (#) indicates that the item is available on microfiche.

ACI-021185-FR ..... N85-23319* #

AD-A141269 ..... N85-23398
AD-A141282 ..... N85-22859 #
AD-A141294 ..... N85-23338 #
AD-A141375 ..... N85-22858 #
AD-A143193 ..... N85-23086 #
AD-A144087 ..... N85-23415 #
AD-A147847 ..... N85-23107 #
AD-A149411 ..... N85-22862 #
AD-A149419 ..... N85-22861 #
AD-A149420 ..... N85-22863 #
AD-A149445 ..... N85-23306 #
AD-A149648 ..... N85-22348 #
AD-A149952 ..... N85-23291 #
AD-A150139 ..... N85-23399 #
AD-A150141 ..... N85-23289 #
AD-A150143 ..... N85-23087 #
AD-A150145 ..... N85-23410 #
AD-A150147 ..... N85-23343 #
AD-A150148 ..... N85-23344 #
AD-A150152 ..... N85-23088 #
AD-A150161 ..... N85-23416 #
AD-A150167 ..... N85-23417 #
AD-A150169 ..... N85-23309 #
AD-A150171 ..... N85-23345 #
AD-A150176 ..... N85-23448 #
AD-A150177 ..... N85-22383 #
AD-A150180 ..... N85-23295 #
AD-A150183 ..... N85-23322 #
AD-A150184 ..... N85-23274 #
AD-A150188 ..... N85-23385 #
AD-A150189 ..... N85-23239 #
AD-A150190 ..... N85-23074 #
AD-A150192 ..... N85-23400 #
AD-A150193 ..... N85-23346 #
AD-A150194 ..... N85-23347 #
AD-A150195 ..... N85-23301 #
AD-A150196 ..... N85-23401 #
AD-A150197 ..... N85-23373 #
AD-A150198 ..... N85-23267 #
AD-A150216 ..... N85-22647 #
AD-A150217 ..... N85-23059 #
AD-A150226 ..... N85-23348 #
AD-A150230 ..... N85-23275 #
AD-A150231 ..... N85-22768 #
AD-A150232 ..... N85-23349 #
AD-A150235 ..... N85-23379 #
AD-A150237 ..... N85-23310 #
AD-A150238 ..... N85-22888 #
AD-A150250 ..... N85-22627 #
AD-A150252 ..... N85-23366 #
AD-A150254 ..... N85-23380 #
AD-A150270 ..... N85-22666 #
AD-A150280 ..... N85-23060 #
AD-A150289 ..... N85-23402 #
AD-A150291 ..... N85-22759 #
AD-A150293 ..... N85-22628 #
AD-A150296 ..... N85-22864 #
AD-A150298 ..... N85-22889 #
AD-A150299 ..... N85-23075 #

AD-A150301 ..... N85-23386 #
AD-A150304 ..... N85-23418 #
AD-A150311 ..... N85-23311 #
AD-A150312 ..... N85-23432 #
AD-A150315 ..... N85-23381 #
AD-A150316 ..... N85-22469 #
AD-A150319 ..... N85-22774 #
AD-A150320 ..... N85-23350 #
AD-A150323 ..... N85-23351 #
AD-A150324 ..... N85-23352 #
AD-A150325 ..... N85-23353 #
AD-A150326 ..... N85-23354 #
AD-A150328 ..... N85-22890 #
AD-A150332 ..... N85-22865 #
AD-A150333 ..... N85-22891 #
AD-A150334 ..... N85-22892 #
AD-A150335 ..... N85-22893 #
AD-A150342 ..... N85-23323 #
AD-A150343 ..... N85-23355 #
AD-A150344 ..... N85-23367 #
AD-A150347 ..... N85-23453 #
AD-A150349 ..... N85-22866 #
AD-A150350 ..... N85-23403 #
AD-A150352 ..... N85-23324 #
AD-A150355 ..... N85-22648 #
AD-A150356 ..... N85-22894 #
AD-A150359 ..... N85-23302 #
AD-A150366 ..... N85-22760 #
AD-A150374 ..... N85-22895 #
AD-A150387 ..... N85-23356 #
AD-A150388 ..... N85-23368 #
AD-A150417 ..... N85-22896 #
AD-A150418 ..... N85-22669 #
AD-A150419 ..... N85-23108 #
AD-A150420 ..... N85-23109 #
AD-A150429 ..... N85-22897 #
AD-A150435 ..... N85-23429 #
AD-A150441 ..... N85-22376 #
AD-A150450 ..... N85-23089 #
AD-A150451 ..... N85-23076 #
AD-A150455 ..... N85-22769 #
AD-A150462 ..... N85-23404 #
AD-A150463 ..... N85-23339 #
AD-A150464 ..... N85-23303 #
AD-A150465 ..... N85-23382 #
AD-A150467 ..... N85-22867 #
AD-A150468 ..... N85-23387 #
AD-A150469 ..... N85-23419 #
AD-A150474 ..... N85-22868 #
AD-A150476 ..... N85-23369 #
AD-A150478 ..... N85-22649 #
AD-A150481 ..... N85-23276 #
AD-A150482 ..... N85-23277 #
AD-A150485 ..... N85-22869 #
AD-A150489 ..... N85-23077 #
AD-A150497 ..... N85-23357 #
AD-A150498 ..... N85-22374 #
AD-A150499 ..... N85-23325 #
AD-A150501 ..... N85-22870 #
AD-A150502 ..... N85-23326 #
AD-A150509 ..... N85-23370 #
AD-A150510 ..... N85-23371 #
AD-A150511 ..... N85-22898 #
AD-A150513 ..... N85-23327 #
AD-A150515 ..... N85-22775 #
AD-A150518 ..... N85-22871 #
AD-A150519 ..... N85-23411 #
AD-A150527 ..... N85-22650 #
AD-A150528 ..... N85-23328 #
AD-A150533 ..... N85-22397 #
AD-A150536 ..... N85-23329 #
AD-A150537 ..... N85-23278 #
AD-A150538 ..... N85-23279 #
AD-A150539 ..... N85-23280 #
AD-A150545 ..... N85-23304 #
AD-A150546 ..... N85-23420 #
AD-A150547 ..... N85-22651 #
AD-A150549 ..... N85-23372 #
AD-A150550 ..... N85-23383 #
AD-A150555 ..... N85-23388 #
AD-A150556 ..... N85-23330 #
AD-A150558 ..... N85-23312 #
AD-A150559 ..... N85-23256 #

AD-A150562 ..... N85-23331 #
AD-A150565 ..... N85-22640 #
AD-A150566 ..... N85-23296 #
AD-A150578 ..... N85-22872 #
AD-A150582 ..... N85-23092 #
AD-A150589 ..... N85-23358 #
AD-A150590 ..... N85-22899 #
AD-A150594 ..... N85-23102 #
AD-A150600 ..... N85-23081 #
AD-A150602 ..... N85-23359 #
AD-A150604 ..... N85-22670 #
AD-A150605 ..... N85-22873 #
AD-A150609 ..... N85-23281 #
AD-A150611 ..... N85-23449 #
AD-A150612 ..... N85-23450 #
AD-A150615 ..... N85-23389 #
AD-A150619 ..... N85-22641 #
AD-A150621 ..... N85-23360 #
AD-A150622 ..... N85-23405 #
AD-A150623 ..... N85-22652 #
AD-A150626 ..... N85-23297 #
AD-A150637 ..... N85-22349 #
AD-A150981 ..... N85-22526 #
AD-A151281 ..... N85-23390 #

AD-B087399L N85-22389
AD-B089136L ..... N85-23288 #
AD-B089137L ..... N85-23058 #

AD-E950650 ..... N85-23075 #
AD-E950655 ..... N85-22627 #
AD-E950657 ..... N85-22889 #

AD-F300559 ..... N85-22684 #
AD-F300562 ..... N85-23060 #
AD-F300568 ..... N85-22769 #

AFATL-TR-85-04 ..... N85-23348 #

AFESC/ESL-TR-84-12 ..... N85-22374 #
AFESC/ESL-TR-84-28 ..... N85-23256 #

AFGL-TR-0018 ..... N85-22470* #

AFHRL-TP-84-33 ..... N85-23323 #

AFOSR-84-173TR ..... N85-23309 #
AFOSR-84-1210TR ..... N85-23417 #
AFOSR-84-1231TR ..... N85-23386 #
AFOSR-84-1236TR ..... N85-22895 #
AFOSR-84-1245TR ..... N85-23346 #
AFOSR-84-1256TR ..... N85-22469 #
AFOSR-84-1257TR ..... N85-23410 #
AFOSR-84-1259TR ..... N85-22897 #
AFOSR-84-1263TR ..... N85-23077 #
AFOSR-84-1267TR ..... N85-23402 #
AFOSR-84-1272TR ..... N85-23267 #
AFOSR-84-1273TR ..... N85-23372 #
AFOSR-84-1276TR ..... N85-22670 #
AFOSR-85-0001TR ..... N85-23092 #
AFOSR-85-0005TR ..... N85-23353 #
AFOSR-85-0006TR ..... N85-23358 #
AFOSR-85-0008TR ..... N85-23360 #
AFOSR-85-0009TR ..... N85-23352 #
AFOSR-85-0012TR ..... N85-23399 #
AFOSR-85-0013TR ..... N85-23354 #
AFOSR-85-0014TR ..... N85-23370 #
AFOSR-85-0015TR ..... N85-23371 #
AFOSR-85-0016TR ..... N85-22397 #
AFOSR-85-0045TR ..... N85-23327 #
AFOSR-85-0046TR ..... N85-22898 #
AFOSR-85-0047TR ..... N85-23356 #
AFOSR-85-0049TR ..... N85-23351 #
AFOSR-85-0055TR ..... N85-22890 #
AFOSR-85-0059TR ..... N85-23389 #
AFOSR-85-0061TR ..... N85-22640 #
AFOSR-85-0063TR ..... N85-22641 #
AFOSR-85-0065TR ..... N85-23326 #
AFOSR-85-0068TR ..... N85-23405 #
AFOSR-85-0069TR ..... N85-23357 #
AFOSR-85-0132TR ..... N85-23401 #

AFRPL-TR-84-066 ..... N85-22629 #

AFWAL-TR-83-3000 ..... N85-22348 #
AFWAL-TR-84-1174 ..... N85-22665 #
AFWAL-TR-84-2060 ..... N85-22768 #
AFWAL-TR-84-3000 ..... N85-22348 #
AFWAL-TR-84-3024 ..... N85-23275 #
AFWAL-TR-84-3080-VOL-1 ..... N85-23108 #
AFWAL-TR-84-3080-VOL-2 ..... N85-23109 #

AFWL-TR-84-13 ..... N85-22894 #

AGARD-AG-262 ..... N85-22350 #

AI-M-718 ..... N85-23345 #

AI-TR-791 ..... N85-23432 #
AI-TR-794 ..... N85-23311 #

AIAA-85-0497 ..... N85-22366* #

AMMRC-TR-84-37 ..... N85-22668 #

AMSMI/RH-84-5-TR ..... N85-23075 #

AMSMI/RK-85-1-TR ..... N85-22627 #

AMSMI/RR-84-8-TR ..... N85-22689 #

AMTE(N)-TM-84037 ..... N85-23378 #
AMTE(N)-TM-84080 ..... N85-23107 #

ANL-84-83 ..... N85-23333 #

ANL/EES-TM-266 ..... N85-23268 #

ANL/MCS-TM-25 ..... N85-23334 #

APL-UW-8312 ..... N85-23383 #

AR-3 ..... N85-23296 #

ARE(PORTLAND)TN-720/84 ..... N85-22860 #

ARL-TR-84-14 ..... N85-23379 #

ARL/PSU/TM-85-12 ..... N85-23059 #

ARO-15412.20-PH ..... N85-23401 #
ARO-17085.3-LS ..... N85-23301 #
ARO-17575.6-EG ..... N85-23088 #
ARO-17803.5-GS-VOL-1 ..... N85-22650 #
ARO-17888.3-MS ..... N85-23418 #
ARO-17923.1-MS ..... N85-23373 #
ARO-18100.6-GS ..... N85-23400 #
ARO-18135.4-CH ..... N85-23076 #
ARO-18137.5-CH ..... N85-23291 #
ARO-18289.15-MA ..... N85-23344 #
ARO-18630.2-CH ..... N85-22760 #
ARO-18757.8-MA-H ..... N85-23381 #
ARO-19065.13-MA ..... N85-23368 #
ARO-19367.21-MA ..... N85-23346 #
ARO-19367.22-MA ..... N85-23309 #
ARO-20927.2-MA ..... N85-23367 #
ARO-20927.3-MA ..... N85-23343 #
ARO-20927.4-MA ..... N85-23355 #

ASCOT-84-4 ..... N85-23282 #
ASCOT-84-7 ..... N85-23283 #

ASR-2 ..... N85-23295 #
ASR-4 ..... N85-23297 #

ATC-126 ..... N85-22375 #

ATR-2 ..... N85-22895 #

BBC-RD-1984/14 ..... N85-22856
BBC-RD-1984/20 ..... N85-22857

BBN-5658 ..... N85-23377* #
BBN-5756 ..... N85-23376* #
BBN-5799 ..... N85-22868 #

BDM/A-84-114-TR-R1 ..... N85-22892 #

BDX-613-3166 ..... N85-22685 #

BLL-CE-TRANS-7971-(9022.09) ..... N85-23306 #
BLL-CE-TRANS-7983-(9022.09) ..... N85-23307 #

BLL-DRIC-TRANS-7399-(3623.66) ..... N85-22753 #
BLL-DRIC-TRANS-7435-(3623.66) ..... N85-22659 #

BLL-T8416/BG/CRS/LR-ST735/84 ..... N85-23054 #
BLL-T8418/BG/LRS/LRST737/84 ..... N85-22657 #
BLL-T8419/BG/LRS/LRST738/84 ..... N85-22658 #

BNL-35432 ..... N85-22673 #
BNL-35481 ..... N85-22682 #
BNL-35534 ..... N85-22764 #
BNL-35551 ..... N85-23314 #
BNL-35568 ..... N85-22675 #
BNL-35577 ..... N85-23292 #

BRL-TR-2628 ..... N85-23060 #
BRL-TR-2630 ..... N85-22769 #

BR69221 ..... N85-22388 #
BR90541 ..... N85-23086 #
BR91055 ..... N85-22396 #
BR91161 ..... N85-23378 #
BR91266 ..... N85-22665 #
BR91414 ..... N85-23338 #
BR91490 ..... N85-23398
BR91491 ..... N85-22858 #
BR91513 ..... N85-22859 #
BR91695 ..... N85-22667 #
BR91771 ..... N85-23294 #
BR92218 ..... N85-23415 #
BR92219 ..... N85-22773 #
BR93043 ..... N85-23308 #
BR93111 ..... N85-22372 #
BR93176 ..... N85-23107 #
BR93258 ..... N85-23091 #
BR93288 ..... N85-22389
BR93397 ..... N85-22660 #
BR93573 ..... N85-22661 #
BR93577 ..... N85-22663 #
BR93642 ..... N85-22662 #
BR93714 ..... N85-23058 #
BR93715 ..... N85-23288 #
BR93796 ..... N85-22646 #

CAR-TR-97 ..... N85-23357 #
CAR-TR-102 ..... N85-23356 #

CCMS-85-02 ..... N85-22638 #

CISR-TR-15 ..... N85-23328 #
CISR-TR-16 ..... N85-23450 #

CONF-840767-11 ..... N85-22678 #
CONF-840767-12 ..... N85-23427 #
CONF-840783-4 ..... N85-23292 #
CONF-840872-14-REV ..... N85-23361 #
CONF-840876-4 ..... N85-23425 #
CONF-840910-20 ..... N85-23412 #
CONF-841007-52 ..... N85-23413 #
CONF-841021-ABSTS ..... N85-23246 #
CONF-841117-36 ..... N85-23428 #
CONF-841122-3 ..... N85-23340 #
CONF-841157-23 ..... N85-23078 #
CONF-841157-27 ..... N85-22672 #
CONF-841157-36 ..... N85-23082 #
CONF-841157-43 ..... N85-22681 #
CONF-841157-45 ..... N85-23079 #
CONF-841157-47 ..... N85-22765 #
CONF-841157-51 ..... N85-23083 #
CONF-841157-53 ..... N85-22680 #
CONF-841157-58 ..... N85-22686 #
CONF-841157-66 ..... N85-22687 #
CONF-841184-27 ..... N85-22682 #
CONF-841187-27 ..... N85-23240 #
CONF-841210-6 ..... N85-22683 #
CONF-841218-20 ..... N85-22655 #
CONF-841234-4 ..... N85-22905 #
CONF-841234-6 ..... N85-22904 #
CONF-841246-18 ..... N85-22684 #
CONF-841247-3 ..... N85-23424 #
CONF-841255-1 ..... N85-23362 #
CONF-850101-4 ..... N85-23062 #
CONF-850137-1 ..... N85-23314 #
CONF-850139-1 ..... N85-23063 #
CONF-850140-1 ..... N85-23364 #
CONF-850211-3 ..... N85-23250 #
CONF-850218-1 ..... N85-23247 #
CONF-850218-2 ..... N85-23284 #
CONF-850219-2 ..... N85-23110 #
CONF-850255-1 ..... N85-23315 #
CONF-850311-4 ..... N85-23254 #
CONF-850311-6 ..... N85-22675 #
CONF-850323-1 ..... N85-22642 #
CONF-850323-2 ..... N85-22767 #
CONF-850392-1 ..... N85-22674 #
CONF-8311213-SUMM ..... N85-23283 #
CONF-8404216 ..... N85-23268 #
CONF-8404219-1 ..... N85-22676 #
CONF-8406187-2 ..... N85-22764 #
CONF-8406132-5 ..... N85-23678 #
CONF-8406133-2 ..... N85-22766 #
CONF-8409108-6 ..... N85-22903 #
CONF-8409144-3 ..... N85-23084 #
CONF-8409186-1 ..... N85-23064 #

CONF-8409199-1 ..... N85-23293 #
CONF-8410103-4 ..... N85-22643 #
CONF-8410142-35 ..... N85-22762 #
CONF-8410142-67 ..... N85-23111 #
CONF-8410153-5 ..... N85-23065 #
CONF-8410161-3 ..... N85-23298 #
CONF-8410207-1 ..... N85-22673 #
CONF-8410208-2 ..... N85-22679 #
CONF-8410219-1 ..... N85-23332 #
CONF-8411114-2 ..... N85-23451 #
CONF-8411126-1 ..... N85-23313 #
CONF-8411137-1 ..... N85-23257 #

CPIA-PUBL-412-VOL-1 ..... N85-22526 #

CRC-1377 ..... N85-22850

CRDC-CR-84118 ..... N85-23061 #

CS-TR-1452 ..... N85-23357 #
CS-TR-1462 ..... N85-23356 #

CS-1984-23 ..... N85-23369 #

CSIR-SR-PERS-350 ..... N85-23300 #

CSIR-TWISK-338 ..... N85-23341 #
CSIR-TWISK-341 ..... N85-23342 #

CWP-014 ..... N85-22867 #

DE84-004431 ..... N85-23245 #
DE84-013047 ..... N85-23246 #
DE85-000173 ..... N85-22656 #
DE85-000625 ..... N85-23421* #
DE85-000995 ..... N85-22761 #
DE85-002315 ..... N85-23391 #
DE85-002470 ..... N85-23085 #
DE85-002480 ..... N85-22903 #
DE85-002630 ..... N85-23083 #
DE85-002631 ..... N85-23247 #
DE85-002642 ..... N85-22762 #
DE85-002766 ..... N85-23110 #
DE85-002893 ..... N85-23422 #
DE85-002901 ..... N85-23426 #
DE85-002988 ..... N85-23082 #
DE85-003069 ..... N85-23425 #
DE85-003144 ..... N85-23313 #
DE85-003218 ..... N85-23253 #
DE85-003266 ..... N85-23364 #
DE85-003405 ..... N85-23064 #
DE85-003450 ..... N85-23284 #
DE85-003506 ..... N85-23384 #
DE85-003585 ..... N85-22900 #
DE85-003617 ..... N85-22672 #
DE85-003674 ..... N85-22642 #
DE85-003677 ..... N85-23076 #
DE85-003735 ..... N85-22683 #
DE85-003741 ..... N85-23678 #
DE85-003744 ..... N85-23111 #
DE85-003748 ..... N85-23451 #
DE85-003821 ..... N85-23392 #
DE85-003925 ..... N85-22671 #
DE85-003937 ..... N85-22676 #
DE85-003939 ..... N85-23455 #
DE85-003969 ..... N85-23071 #
DE85-003977 ..... N85-23290 #
DE85-004019 ..... N85-22766 #
DE85-004034 ..... N85-22654 #
DE85-004078 ..... N85-23254 #
DE85-004182 ..... N85-22653 #
DE85-004188 ..... N85-22682 #
DE85-004295 ..... N85-22776 #
DE85-004355 ..... N85-22902 #
DE85-004359 ..... N85-23268 #
DE85-004361 ..... N85-23282 #
DE85-004407 ..... N85-23283 #
DE85-004507 ..... N85-23285 #
DE85-004541 ..... N85-22764 #
DE85-004547 ..... N85-22679 #
DE85-004577 ..... N85-22771 #
DE85-004593 ..... N85-23062 #
DE85-004603 ..... N85-23424 #
DE85-004612 ..... N85-23335 #
DE85-004627 ..... N85-23406 #
DE85-004641 ..... N85-23472 #
DE85-004649 ..... N85-22770 #
DE85-004652 ..... N85-23423 #
DE85-004687 ..... N85-23334 #
DE85-004693 ..... N85-23340 #
DE85-004702 ..... N85-22675 #
DE85-004711 ..... N85-23292 #
DE85-004780 ..... N85-23362 #
DE85-004787 ..... N85-22674 #
DE85-004795 ..... N85-23394 #
DE85-004797 ..... N85-22643 #

DE85-004803 ..... N85-23427 #
DE85-004807 ..... N85-23070 #
DE85-004831 ..... N85-23333 #
DE85-004857 ..... N85-22765 #
DE85-004867 ..... N85-23240 #
DE85-004889 ..... N85-23393 #
DE85-004902 ..... N85-23293 #
DE85-004918 ..... N85-23412 #
DE85-004938 ..... N85-23081 #
DE85-004990 ..... N85-23430 #
DE85-004996 ..... N85-22767 #
DE85-004999 ..... N85-22874 #
DE85-005025 ..... N85-23298 #
DE85-005091 ..... N85-23079 #
DE85-005101 ..... N85-22763 #
DE85-005124 ..... N85-23314 #
DE85-005171 ..... N85-23456 #
DE85-005174 ..... N85-23251 #
DE85-005186 ..... N85-22901 #
DE85-005189 ..... N85-23072 #
DE85-005207 ..... N85-22673 #
DE85-005257 ..... N85-23257 #
DE85-005262 ..... N85-22686 #
DE85-005263 ..... N85-23083 #
DE85-005264 ..... N85-23428 #
DE85-005270 ..... N85-23413 #
DE85-005282 ..... N85-22904 #
DE85-005283 ..... N85-22905 #
DE85-005301 ..... N85-22875 #
DE85-005321 ..... N85-22677 #
DE85-005354 ..... N85-23249 #
DE85-005355 ..... N85-23248 #
DE85-005367 ..... N85-22681 #
DE85-005379 ..... N85-22678 #
DE85-005423 ..... N85-23252 #
DE85-005447 ..... N85-23336 #
DE85-005483 ..... N85-22680 #
DE85-005524 ..... N85-23395 #
DE85-005574 ..... N85-23315 #
DE85-005674 ..... N85-23363 #
DE85-005716 ..... N85-22684 #
DE85-005722 ..... N85-23084 #
DE85-005723 ..... N85-22655 #
DE85-005732 ..... N85-23080 #
DE85-006129 ..... N85-22687 #
DE85-006149 ..... N85-23066 #
DE85-006154 ..... N85-23332 #
DE85-006165 ..... N85-23365 #
DE85-006183 ..... N85-22685 #
DE85-006187 ..... N85-23250 #
DE85-006288 ..... N85-22876 #
DE85-016488 ..... N85-23361 #

DMS-DR-2520 ..... N85-22466* #
DMS-DR-2521 ..... N85-22467* #
DMS-DR-2524 ..... N85-22468* #

DOE/AL-21557/T1 ..... N85-23251 #

DOE/CS-31587/T3-VOL-2 ..... N85-23253 #
DOE/CS-50208/1 ..... N85-23455 #

DOE/ER-04461/7 ..... N85-22671 #
DOE/ER-10569/T3 ..... N85-23393 #
DOE/ER-13045/2 ..... N85-22656 #
DOE/ER-40033/70 ..... N85-23394 #
DOE/ER-40114/3 ..... N85-23392 #
DOE/ER-45026/2 ..... N85-23422 #
DOE/ER-45057/T1 ..... N85-23384 #
DOE/ER-75016/T4 ..... N85-22761 #

DOE/ET-51013/131 ..... N85-23412 #

DOE/EV-00639/26 ..... N85-23290 #
DOE/EV-10665/5 ..... N85-23285 #

DOE/JPL-956828/2 ..... N85-23421* #

DOE/MC-15078/7-3 ..... N85-23252 #

DOE/NASA/0352-1 ..... N85-22757* #
DOE/NASA/2801-1 ..... N85-22758* #
DOE/NASA/20320-62 ..... N85-23242* #

DOE/NBM-5004/34 ..... N85-22654 #

DOE/OR-21400/T81 ..... N85-23249 #
DOE/OR-21400/T82 ..... N85-23248 #

DOE/PC-70780/1 ..... N85-22771 #

DOE/TIC-4500-REV-73 ..... N85-23071 #

DOT/FAA/PM-84/5 ..... N85-22375 #

DP-MS-84-74 ..... N85-22672 #

DRIC-BR-93752 ..... N85-23304 #

DRIC-T-7138 ..... N85-23294 #
DRIC-T-7145 ..... N85-22389
DRIC-T-7149 ..... N85-22685 #
DRIC-T-7375 ..... N85-23288 #
DRIC-T-7376 ..... N85-23056 #

D483-10012-1 ..... N85-22459* #

E-2186 ..... N85-22470* #
E-2433 ..... N85-22644* #
E-2471 ..... N85-23242* #
E-2487 ..... N85-23085* #
E-2496 ..... N85-23243* #
E-2525 ..... N85-22660* #
E-2538 ..... N85-22755* #
E-2539 ..... N85-22758* #

EGG-M-21984 ..... N85-23064 #
EGG-M-25484 ..... N85-23340 #

EGG-SE-6746 ..... N85-23456 #

EGG-10282-1070 ..... N85-23240 #

EPA-600/D-84-299 ..... N85-23269* #

ESA-SP-210 ..... N85-22565 #

ESL-713774-4-VOL-1 ..... N85-22650 #

ETL-0360 ..... N85-23448 #
ETL-0377 ..... N85-23239 #
ETL-0379 ..... N85-23074 #

E85-10070 ..... N85-23186* #
E85-10088 ..... N85-23213* #
E85-10096 ..... N85-23214* #
E85-10100 ..... N85-23215* #

FSU-STATISTICS-M684 ..... N85-23346 #

FSU-TR-M690 ..... N85-23309 #

GPO-44-360 ..... N85-23452 #

GRC-CR-84-1309 ..... N85-22664 #

GRI-84/0133.1 ..... N85-22772 #

H-REPT-99-32 ..... N85-23452 #

H-1182 ..... N85-22394* #

HEDL-SA-3174-FP ..... N85-22684 #

ICASE-85-16 ..... N85-23321* #
ICASE-85-22 ..... N85-23100* #

IS-M-522 ..... N85-23425 #

IS-T-1129 ..... N85-22653 #

ISBN-0-7986-2339-9 ..... N85-23300 #
ISBN-0-7986-3020-4 ..... N85-23106 #
ISBN-0-8330-0608-8 ..... N85-23330 #
ISBN-0-8444-0459-4 ..... N85-23674 #
ISBN-92-835-1482-3 ..... N85-22350 #
ISBN-951-41-0479-X ..... N85-22663 #

ISSN-0066-2003 ..... N85-22663 #
ISSN-0082-5263 ..... N85-22524 #
ISSN-0379-6566 ..... N85-22565 #
ISSN-0379-6906 ..... N85-22664 #

JPL-PUB-84-56 ..... N85-22464* #
JPL-PUB-84-57 ..... N85-23222* #
JPL-PUB-84-91 ..... N85-22393* #
JPL-PUB-85-6 ..... N85-23244* #
JPL-PUB-85-7 ..... N85-22666* #
JPL-PUB-85-9 ..... N85-22655* #
JPL-PUB-85-10 ..... N85-23068* #

JPL-84-81 ..... N85-23101* #

JPRS-CST-84-008 ..... N85-22384 #
JPRS-CST-84-030 ..... N85-22777 #
JPRS-CST-85-003 ..... N85-23433 #
JPRS-CST-85-005 ..... N85-22843 #

JPRS-UCH-85-001 ..... N85-22629 #

JPRS-UEE-85-001 ..... N85-22976 #
JPRS-UEE-85-002 ..... N85-22907 #

JPRS-UEQ-85-003 ..... N85-22762 #

JPRS-UES-85-002 ..... N85-23116 #

JPRS-UMM-85-005 ..... N85-22839 #

JPRS-UMS-85-002 ..... N85-22688 #

JPRS-USP-85-001 ..... N85-22403 #

JPRS-UST-85-002 ..... N85-23442 #

JSR-83-211 ..... N85-23366 #
JSR-83-216 ..... N85-23360 #

KES-U-84-6 ..... N85-23326 #

KMSF-U1539 ..... N85-23327 #

K233 ..... N85-22396 #
K234 ..... N85-22646 #

L-15853 ..... N85-23090* #
L-15855 ..... N85-23337* #
L-15881 ..... N85-22395* #
L-15885 ..... N85-23237* #
L-15915 ..... N85-22401* #

LA-UR-84-2336-REV ..... N85-23361 #
LA-UR-84-3483 ..... N85-23111 #
LA-UR-84-3537 ..... N85-23451 #
LA-UR-84-3583 ..... N85-23678 #
LA-UR-84-3755 ..... N85-22683 #
LA-UR-84-3793 ..... N85-23084 #
LA-UR-84-3805 ..... N85-22655 #
LA-UR-84-3942 ..... N85-23315 #

LA-9771-MS ..... N85-23072 #
LA-10153-MS ..... N85-23406 #
LA-10219-MS ..... N85-23391 #
LA-10274-MS ..... N85-22901 #

LBL-PUB-3034-REV ..... N85-23335 #

LBL-16999 ..... N85-23423 #
LBL-17514 ..... N85-23062 #
LBL-17925 ..... N85-23293 #
LBL-18411 ..... N85-22763 #
LBL-18681 ..... N85-23424 #
LBL-18703 ..... N85-23472 #

LC-79-640375 ..... N85-23679* #
LC-84-22879 ..... N85-23330 #
LC-84-600109 ..... N85-23674 #
LC-84-601018 ..... N85-23241 #
LC-84-601092 ..... N85-23407 #
LC-84-601108 ..... N85-22906 #

LCS-TR-8 ..... N85-23349 #
LCS-TR-13 ..... N85-23350 #

LG82ER0117-1 ..... N85-23108 #
LG82ER0117-2 ..... N85-23109 #

LIDS-P-1428 ..... N85-23322 #

LMSC-D980796 ..... N85-22465* #

LMSC-HREC-PR-F042316 ..... N85-23057* #

MCR-84-506 ..... N85-22891 #
MCR-85-1306 ..... N85-22463* #
MCR-85-1309 ..... N85-22462* #

MHSMP-84-22 ..... N85-22770 #

MIT/LCS/TR-326 ..... N85-23331 #

MLM-3213 ..... N85-23060 #

MQAD-R-849 ..... N85-22667 #

MTI-84TR39 ..... N85-22400* #

MTP-2-2-700 ..... N85-23087 #

M010-8312-16 ..... N85-23450 #

NADC-84115-60 ..... N85-23303 #

NAEC-92-185 ..... N85-23399 #

NAS 1.15:77637 ..... N85-22402* #
NAS 1.15:77735 ..... N85-22645* #
NAS 1.15:85767 ..... N85-22380* #
NAS 1.15:86200 ..... N85-23221* #

NAS 1.15:86322 ..... N85-23337* #
NAS 1.15:86323 ..... N85-22361* #
NAS 1.15:86327 ..... N85-23320* #
NAS 1.15:86328 ..... N85-22885* #
NAS 1.15:86346 ..... N85-22401* #
NAS 1.15:86369 ..... N85-23317* #
NAS 1.15:86372 ..... N85-23067* #
NAS 1.15:86381 ..... N85-22379* #
NAS 1.15:86387 ..... N85-23318* #
NAS 1.15:86394 ..... N85-22366* #
NAS 1.15:86400 ..... N85-23374* #
NAS 1.15:86501 ..... N85-23273* #
NAS 1.15:86502 ..... N85-23463* #
NAS 1.15:86950 ..... N85-23242* #
NAS 1.15:86966 ..... N85-22644* #
NAS 1.15:86970 ..... N85-23243* #
NAS 1.15:86982 ..... N85-22660* #
NAS 1.15:86991 ..... N85-23085* #
NAS 1.15:86992 ..... N85-22755* #
NAS 1.15:86993 ..... N85-22756* #
NAS 1.15:87426 ..... N85-22373* #
NAS 1.15:87427 ..... N85-23431* #
NAS 1.15:87429 ..... N85-23269* #
NAS 1.15:87448 ..... N85-22371* #
NAS 1.15:87452 ..... N85-23258*
NAS 1.15:87453 ..... N85-22370* #
NAS 1.15:87563 ..... N85-23474* #
NAS 1.15:87566-VOL-1 ..... N85-22460* #
NAS 1.15:87566-VOL-2 ..... N85-22461* #
NAS 1.21:467 ..... N85-23457* #
NAS 1.21:7037(183) N85-22343*
NAS 1.21:7037(185) N85-22342*
NAS 1.21:7039(26) N85-23445*
NAS 1.26:3881 ..... N85-22639* #
NAS 1.26:3886 ..... N85-23299* #
NAS 1.26:3887 ..... N85-22369* #
NAS 1.26:3888 ..... N85-23375* #
NAS 1.26:167693 ..... N85-22466* #
NAS 1.26:167694 ..... N85-22467* #
NAS 1.26:167695 ..... N85-22468* #
NAS 1.26:170417 ..... N85-22398* #
NAS 1.26:171415 ..... N85-22459* #
NAS 1.26:171419 ..... N85-22854* #
NAS 1.26:171421 ..... N85-22462* #
NAS 1.26:171422 ..... N85-22463* #
NAS 1.26:171424 ..... N85-23057* #
NAS 1.26:171425 ..... N85-22364* #
NAS 1.26:171426 ..... N85-23069* #
NAS 1.26:171429 ..... N85-23319* #
NAS 1.26:172444 ..... N85-22387* #
NAS 1.26:172510 ..... N85-22754* #
NAS 1.26:172531 ..... N85-22365* #
NAS 1.26:172551 ..... N85-22378* #
NAS 1.26:172554 ..... N85-22525* #
NAS 1.26:172555 ..... N85-23056* #
NAS 1.26:172560 ..... N85-23321* #
NAS 1.26:172566 ..... N85-23100* #
NAS 1.26:174392 ..... N85-23421* #
NAS 1.26:174687 ..... N85-22758* #
NAS 1.26:174750 ..... N85-22400* #
NAS 1.26:174782 ..... N85-22368* #
NAS 1.26:174863 ..... N85-22390* #
NAS 1.26:174888 ..... N85-22392* #
NAS 1.26:174893 ..... N85-22757* #
NAS 1.26:175320 ..... N85-22465* #
NAS 1.26:175523 ..... N85-23213* #
NAS 1.26:175531 ..... N85-23214* #
NAS 1.26:175551 ..... N85-23096* #
NAS 1.26:175555 ..... N85-23447* #
NAS 1.26:175589 ..... N85-23099* #
NAS 1.26:175590 ..... N85-23098* #
NAS 1.26:175591 ..... N85-23097* #
NAS 1.26:175604 ..... N85-23673* #
NAS 1.26:175605 ..... N85-22391* #
NAS 1.26:175606 ..... N85-23238* #
NAS 1.26:175607 ..... N85-23679* #
NAS 1.26:175615 ..... N85-23215* #
NAS 1.26:175616 ..... N85-23271* #
NAS 1.26:175617 ..... N85-23265* #
NAS 1.26:175618 ..... N85-23460* #
NAS 1.26:175619 ..... N85-23414* #
NAS 1.26:175620 ..... N85-22382* #
NAS 1.26:175621 ..... N85-23287* #
NAS 1.26:175622 ..... N85-23461* #
NAS 1.26:175623 ..... N85-23676* #
NAS 1.26:175624 ..... N85-22367* #
NAS 1.26:175625 ..... N85-22661* #
NAS 1.26:175626 ..... N85-23462* #
NAS 1.26:175628 ..... N85-23272* #
NAS 1.26:175629 ..... N85-23409* #
NAS 1.26:175630 ..... N85-23454* #
NAS 1.26:175631 ..... N85-23471* #
NAS 1.26:175632 ..... N85-23677* #
NAS 1.26:175639 ..... N85-23222* #
NAS 1.26:175643 ..... N85-23244* #
NAS 1.26:175646 ..... N85-22393* #
NAS 1.26:175647 ..... N85-23068* #
NAS 1.26:175648 ..... N85-22855* #
NAS 1.26:175649 ..... N85-22886* #
NAS 1.26:175657 ..... N85-23101* #
NAS 1.26:175659 ..... N85-22464* #
NAS 1.26:177335 ..... N85-23377* #
NAS 1.26:177336-VOL-1 ..... N85-22344* #
NAS 1.26:177336-VOL-2 ..... N85-22345* #
NAS 1.26:177338 ..... N85-23376* #
NAS 1.26:177340-VOL-1 ..... N85-22346* #
NAS 1.26:177340-VOL-2 ..... N85-22347* #
NAS 1.55:2355-VOL-4 ..... N85-23186* #
NAS 1.55:2359 ..... N85-22470* #
NAS 1.55:2362 ..... N85-23112* #
NAS 1.55:2363 ..... N85-23223* #
NAS 1.60:2409 ..... N85-23090* #
NAS 1.60:2411 ..... N85-22394* #
NAS 1.60:2415 ..... N85-22395* #
NAS 1.60:2428 ..... N85-23237* #
NAS 1.60:2456 ..... N85-23305* #
NAS 1.60:2459 ..... N85-22662* #
NAS 1.71:MFS-25861-1 ..... N85-22877*
NAS 1.71:NPO-15801-1 ..... N85-23396*

NASA-CASE-MFS-25861-1 ..... N85-22877*

NASA-CASE-NPO-15801-1 ..... N85-23396*

NASA-CP-2355-VOL-4 ..... N85-23186* #
NASA-CP-2359 ..... N85-22470* #
NASA-CP-2362 ..... N85-23112* #
NASA-CP-2363 ..... N85-23223* #

NASA-CR-3881 ..... N85-22639* #
NASA-CR-3886 ..... N85-23299* #
NASA-CR-3887 ..... N85-22369* #
NASA-CR-3888 ..... N85-23375* #
NASA-CR-167693 ..... N85-22466* #
NASA-CR-167694 ..... N85-22467* #
NASA-CR-167695 ..... N85-22468* #
NASA-CR-170417 ..... N85-22398* #
NASA-CR-171415 ..... N85-22459* #
NASA-CR-171419 ..... N85-22854* #
NASA-CR-171421 ..... N85-22462* #
NASA-CR-171422 ..... N85-22463* #
NASA-CR-171424 ..... N85-23057* #
NASA-CR-171425 ..... N85-22364* #
NASA-CR-171426 ..... N85-23069* #
NASA-CR-171429 ..... N85-23319* #
NASA-CR-172444 ..... N85-22387* #
NASA-CR-172510 ..... N85-22754* #
NASA-CR-172531 ..... N85-22365* #
NASA-CR-172551 ..... N85-22378* #
NASA-CR-172554 ..... N85-22525* #
NASA-CR-172555 ..... N85-23056* #
NASA-CR-172560 ..... N85-23321* #
NASA-CR-172566 ..... N85-23100* #
NASA-CR-174392 ..... N85-23421* #
NASA-CR-174687 ..... N85-22758* #
NASA-CR-174750 ..... N85-22400* #
NASA-CR-174782 ..... N85-22368* #
NASA-CR-174863 ..... N85-22390* #
NASA-CR-174888 ..... N85-22392* #
NASA-CR-174893 ..... N85-22757* #
NASA-CR-175320 ..... N85-22465* #
NASA-CR-175523 ..... N85-23213* #
NASA-CR-175531 ..... N85-23214* #
NASA-CR-175551 ..... N85-23096* #
NASA-CR-175555 ..... N85-23447* #
NASA-CR-175589 ..... N85-23099* #
NASA-CR-175590 ..... N85-23098* #
NASA-CR-175591 ..... N85-23097* #
NASA-CR-175604 ..... N85-23673* #
NASA-CR-175605 ..... N85-22391* #
NASA-CR-175606 ..... N85-23238* #
NASA-CR-175607 ..... N85-23679* #
NASA-CR-175615 ..... N85-23215* #
NASA-CR-175616 ..... N85-23271* #
NASA-CR-175617 ..... N85-23265* #
NASA-CR-175618 ..... N85-23460* #
NASA-CR-175619 ..... N85-23414* #
NASA-CR-175620 ..... N85-22382* #
NASA-CR-175621 ..... N85-23287* #
NASA-CR-175622 ..... N85-23461* #
NASA-CR-175623 ..... N85-23676* #
NASA-CR-175624 ..... N85-22367* #
NASA-CR-175625 ..... N85-22661* #
NASA-CR-175626 ..... N85-23462* #
NASA-CR-175628 ..... N85-23272* #
NASA-CR-175629 ..... N85-23409* #
NASA-CR-175630 ..... N85-23454* #
NASA-CR-175631 ..... N85-23471* #
NASA-CR-175632 ..... N85-23677* #
NASA-CR-175639 ..... N85-23222* #
NASA-CR-175643 ..... N85-23244* #
NASA-CR-175646 ..... N85-22393* #
NASA-CR-175647 ..... N85-23068* #
NASA-CR-175648 ..... N85-22855* #
NASA-CR-175649 ..... N85-22886* #
NASA-CR-175657 ..... N85-23101* #
NASA-CR-175659 ..... N85-22464* #
NASA-CR-177335 ..... N85-23377* #
NASA-CR-177336-VOL-1 ..... N85-22344* #
NASA-CR-177336-VOL-2 ..... N85-22345* #
NASA-CR-177338 ..... N85-23376* #
NASA-CR-177340-VOL-1 ..... N85-22346* #
NASA-CR-177340-VOL-2 ..... N85-22347* #

NASA-SP-467 ..... N85-23457* #
NASA-SP-7037(183) N85-22343*
NASA-SP-7037(185) N85-22342*
NASA-SP-7039(26) N85-23445*

NASA-TM-77637 ..... N85-22402* #
NASA-TM-77735 ..... N85-22645* #
NASA-TM-85767 ..... N85-22380* #
NASA-TM-86200 ..... N85-23221* #
NASA-TM-86322 ..... N85-23337* #
NASA-TM-86323 ..... N85-22361* #
NASA-TM-86327 ..... N85-23320* #
NASA-TM-86328 ..... N85-22885* #
NASA-TM-86346 ..... N85-22401* #
NASA-TM-86369 ..... N85-23317* #
NASA-TM-86372 ..... N85-23067* #
NASA-TM-86381 ..... N85-22379* #
NASA-TM-86387 ..... N85-23318* #
NASA-TM-86394 ..... N85-22366* #
NASA-TM-86400 ..... N85-23374* #
NASA-TM-86501 ..... N85-23273* #
NASA-TM-86502 ..... N85-23463* #
NASA-TM-86950 ..... N85-23242* #
NASA-TM-86966 ..... N85-22644* #
NASA-TM-86970 ..... N85-23243* #
NASA-TM-86982 ..... N85-22660* #
NASA-TM-86991 ..... N85-23085* #
NASA-TM-86992 ..... N85-22755* #
NASA-TM-86993 ..... N85-22756* #
NASA-TM-87426 ..... N85-22373* #
NASA-TM-87427 ..... N85-23431* #
NASA-TM-87429 ..... N85-23269* #
NASA-TM-87448 ..... N85-22371* #
NASA-TM-87452 ..... N85-23258*
NASA-TM-87453 ..... N85-22370* #
NASA-TM-87563 ..... N85-23474* #
NASA-TM-87566-VOL-1 ..... N85-22460* #
NASA-TM-87566-VOL-2 ..... N85-22461* #

NASA-TP-2409 ..... N85-23090* #
NASA-TP-2411 ..... N85-22394* #
NASA-TP-2415 ..... N85-22395* #
NASA-TP-2428 ..... N85-23237* #
NASA-TP-2456 ..... N85-23305* #
NASA-TP-2459 ..... N85-22662* #

NBS/SP-260/91 ..... N85-22906 #
NBS/SP-683 ..... N85-23407 #

NBSIR-84-2917 ..... N85-22776 #

NEAR-TR-337 ..... N85-22383 #

NIAST-83/88 ..... N85-23106 #

NOSC/TR-1003 ..... N85-23339 #

NPS-61-84-005 ..... N85-23274 #

NRL-MR-5484 ..... N85-23411 #
NRL-MR-5490 ..... N85-22774 #
NRL-MR-5493 ..... N85-23404 #
NRL-MR-5518 ..... N85-22872 #

NRL-8857 ..... N85-22871 #

ORNL-6072 ..... N85-22674 #

ORNL/SUB-81-95013/1 ..... N85-22900 #

ORNL/TM-9090 ..... N85-23081 #
ORNL/TM-9518 ..... N85-22758* #

OTA-F-214 ..... N85-23241 #

PB84-227792 ..... N85-23316 #
PB85-114700 ..... N85-23407 #
PB85-115780 ..... N85-23679* #
PB85-118594 ..... N85-22906 #
PB85-144137 ..... N85-23269* #
PB85-161925 ..... N85-22772 #

PEL-005 ..... N85-23429 #

PFC/CP-84-14 ..... N85-23412 #

PNL-SA-11484 ..... N85-23395 #
PNL-SA-12341 ..... N85-22679 #

PR1359 ..... N85-23069* #

PSI-TR-455 ..... N85-23252 #

QR-1 ..... N85-22771 #

R-NIAS-27 ..... N85-22853

RADC-TR-82-286-VOL-3A ..... N85-22866 #
RADC-TR-84-32 ..... N85-23310 #
RADC-TR-84-72 ..... N85-23347 #
RADC-TR-84-166 ..... N85-22893 #
RADC-TR-84-179 ..... N85-22892 #
RADC-TR-84-183 ..... N85-22891 #

RAE-FS(F)-207 ..... N85-23086 #

RAE-MATER/STRUCT-76 ..... N85-23308 #

RAE-TM-AERO-2006 ..... N85-22372 #

RAE-TR-83069 ..... N85-23086 #
RAE-TR-84031 ..... N85-23308 #
RAE-TR-84050 ..... N85-23304 #

RAND/R-3160-AF ..... N85-23330 #

REPT-6 ..... N85-23419 #
REPT-8 ..... N85-23388 #
REPT-9 ..... N85-23420 #
REPT-10 ..... N85-23387 #
REPT-11 ..... N85-22651 #
REPT-84B0036 ..... N85-23223* #
REPT-85B0115-VOL-4 ..... N85-23186* #
REPT-85B0183 ..... N85-23112* #
REPT-153-3223 ..... N85-23410 #
REPT-8304-I-VOL-1 ..... N85-22346* #
REPT-8304-I-VOL-2 ..... N85-22347* #

RF-763265/714837 ..... N85-23092 #

RFP-3607 ..... N85-23071 #
RFP-3715 ..... N85-22677 #

RI/RD84-196 ..... N85-22628 #

RM-799 ..... N85-22370* #

RNC/NS/TR8 ..... N85-22773 #

RSRE-MEMO-3539 ..... N85-23338 #
RSRE-MEMO-3650 ..... N85-22858 #
RSRE-MEMO-3661 ..... N85-23398
RSRE-MEMO-3680 ..... N85-23415 #
RSRE-MEMO-3684 ..... N85-22861 #
RSRE-MEMO-3743 ..... N85-22862 #
RSRE-MEMO-3755 ..... N85-22863 #

RSRE-84003 ..... N85-22859 #

R84-956611 ..... N85-23056* #
R84AEB010 ..... N85-23089 #

SAIC-84/1132 ..... N85-23289 #

SAND-80-2050 ..... N85-23070 #
SAND-84-1227C ..... N85-23284 #
SAND-84-1230C ..... N85-23078 #
SAND-84-1254C ..... N85-23082 #
SAND-84-1267C ..... N85-23247 #
SAND-84-1292C ..... N85-22680 #
SAND-84-1642 ..... N85-22876 #
SAND-84-1759C ..... N85-22762 #
SAND-84-2022 ..... N85-22902 #
SAND-84-2190 ..... N85-23363 #
SAND-84-2345C ..... N85-23063 #

SAPR-5 ..... N85-23461* #
SAPR-7 ..... N85-23677* #
SAPR-9 ..... N85-23676* #

SAR-28 ..... N85-23460* #
SAR-29 ..... N85-23460* #

SD-TR-84-14 ..... N85-23266 #

SERI/CP-211-2507 ..... N85-23246 #

SERI/STR-211-2469 ..... N85-23426 #

SERI/TR-211-1950 ..... N85-23245 #

SGD-479-PT-2 ..... N85-23679* #

SOM-WP-62 ..... N85-23302 #

SP-06A83 ..... N85-22368* #

SRI-06-7963 ..... N85-22757* #

TI85-901085 ..... N85-23241 #

TOP-2-2-700 ..... N85-23087 #

TP-1983-31 ..... N85-23105 #

TR-D-69-ARO ..... N85-23346 #
TR-D-73-ARO ..... N85-23309 #

TR-2 ..... N85-23367 #
TR-2-ONR ..... N85-23385 #
TR-3 ..... N85-22888 #
TR-3 ..... N85-23343 #
TR-4 ..... N85-23355 #
TR-5 ..... N85-23302 #
TR-13 ..... N85-23368 #
TR-16 ..... N85-22652 #
TR-79 ..... N85-23372 #
TR-84-7 ..... N85-23360 #
TR-84-12 ..... N85-22669 #
TR-84-13 ..... N85-22896 #
TR-84-44 ..... N85-23358 #
TR-84-45 ..... N85-23353 #
TR-84-51 ..... N85-23370 #
TR-84-52 ..... N85-23371 #
TR-85/ONR-17 ..... N85-22870 #
TR-170 ..... N85-22865 #
TR-0084(4945-09)-1 ..... N85-23266 #

TRACOR-T84-AE-9124U ..... N85-22893 #

U-OF-IOWA-83-6 ..... N85-23409* #

UCID-18574-84-2 ..... N85-23430 #
UCID-20214 ..... N85-22875 #
UCID-20227 ..... N85-23282 #
UCID-20279 ..... N85-23336 #

UCRL-15637 ..... N85-23066 #
UCRL-15645 ..... N85-23365 #
UCRL-50025-84-1 ..... N85-22887 #
UCRL-90560 ..... N85-22874 #
UCRL-90946 ..... N85-22642 #
UCRL-90947 ..... N85-22767 #
UCRL-91634 ..... N85-23332 #
UCRL-91734 ..... N85-23313 #

UDR-TR-84-37 ..... N85-23399 #

UNC/ORSA/TR-84/8 ..... N85-22898 #

US-PATENT-APPL-SN-478130 ..... N85-23396*
US-PATENT-APPL-SN-504345 ..... N85-22877*

US-PATENT-CLASS-318-729 ..... N85-22877*
US-PATENT-CLASS-318-812 ..... N85-22877*
US-PATENT-CLASS-350-168 ..... N85-23396*
US-PATENT-CLASS-350-505 ..... N85-23396*
US-PATENT-CLASS-350-619 ..... N85-23396*
US-PATENT-CLASS-356-323 ..... N85-23396*
US-PATENT-CLASS-356-330 ..... N85-23396*
US-PATENT-CLASS-356-331 ..... N85-23396*

US-PATENT-4,489,264 ..... N85-22877*
US-PATENT-4,497,540 ..... N85-23396*

UTIAS-TN-249 ..... N85-22524 #

UTRC/R84-955388-F ..... N85-22649 #

VPI-E-85-03 ..... N85-22638 #

VSR-OIT/FSTC-84/139 ..... N85-23316 #

WU/SRL-59583A-3 ..... N85-22670 #

X-601-85-6 ..... N85-23258*

Y-1 ..... N85-22853

Z-2 ..... N85-22380* #

☆U.S. GOVERNMENT PRINTING OFFICE: 1985-461-597/20017

THE UNIVERSITY OF MICHIGAN

BUILDING

DATE DUE 8/88

USE ONLY

FEDERAL DEPOSITORY LIBRARY PROGRAM

The Federal Depository Library Program provides Government publications to designated libraries throughout the United States. The Regional Depository Libraries listed below receive and retain at least one copy of nearly every Federal Government publication, either in printed or microfilm form, for use by the general public. These libraries provide reference services and inter-library loans; however, they are *not* sales outlets. You may wish to ask your local library to contact a Regional Depository to help you locate specific publications, or you may contact the Regional Depository yourself.

ARKANSAS STATE LIBRARY
One Capitol Mall
Little Rock, AR 72201
(501) 371-2326

AUBURN UNIV. AT MONTGOMERY LIBRARY
Documents Department
Montgomery, AL 36193
(205) 279-9110, ext. 253

UNIV. OF ALABAMA LIBRARY
Documents Dept.—Box S
University, AL 35486
(205) 348-7369

DEPT. OF LIBRARY, ARCHIVES AND PUBLIC RECORDS
Third Floor—State Cap.
1700 West Washington
Phoenix, AZ 85007
(602) 255-4121

UNIVERSITY OF ARIZONA LIB.
Government Documents Dept.
Tucson, AZ 85721
(602) 626-5233

CALIFORNIA STATE LIBRARY
Govt. Publications Section
P.O. Box 2037
Sacramento, CA 95809
(916) 322-4572

UNIV. OF COLORADO LIB.
Government Pub. Division
Campus Box 184
Boulder, CO 80309
(303) 492-8834

DENVER PUBLIC LIBRARY
Govt. Pub. Department
1357 Broadway
Denver, CO 80203
(303) 571-2131

CONNECTICUT STATE LIBRARY
Government Documents Unit
231 Capitol Avenue
Hartford, CT 06106
(203) 566-4971

UNIV. OF FLORIDA LIBRARIES
Library West
Documents Department
Gainesville, FL 32611
(904) 392-0367

UNIV. OF GEORGIA LIBRARIES
Government Reference Dept.
Athens, Ga 30602
(404) 542-8951

UNIV. OF HAWAII LIBRARY
Govt. Documents Collection
2550 The Mall
Honolulu, HI 96822
(808) 948-8230

UNIV. OF IDAHO LIBRARY
Documents Section
Moscow, ID 83843
(208) 885-6344

ILLINOIS STATE LIBRARY
Information Services Branch
Centennial Building
Springfield, IL 62706
(217) 782-5185

INDIANA STATE LIBRARY
Serials Documents Section
140 North Senate Avenue
Indianapolis, IN 46204
(317) 232-3686

UNIV. OF IOWA LIBRARIES
Govt. Documents Department
Iowa City, IA 52242
(319) 353-3318

UNIVERSITY OF KANSAS
Doc. Collect—Spencer Lib.
Lawrence, KS 66045
(913) 864-4662

UNIV. OF KENTUCKY LIBRARIES
Govt. Pub. Department
Lexington, KY 40506
(606) 257-3139

LOUISIANA STATE UNIVERSITY
Middleton Library
Govt. Docs. Dept.
Baton Rouge, LA 70803
(504) 388-2570

LOUISIANA TECHNICAL UNIV. LIBRARY
Documents Department
Ruston, LA 71272
(318) 257-4962

UNIVERSITY OF MAINE
Raymond H. Fogler Library
Tri-State Regional Documents Depository
Orono, ME 04469
(207) 581-1680

UNIVERSITY OF MARYLAND
McKeldin Lib.—Doc. Div.
College Park, MD 20742
(301) 454-3034

BOSTON PUBLIC LIBRARY
Government Docs. Dept.
Boston, MA 02117
(617) 536-5400 ext. 226

DETROIT PUBLIC LIBRARY
Sociology Department
5201 Woodward Avenue
Detroit, MI 48202
(313) 833-1409

MICHIGAN STATE LIBRARY
P.O. Box 30007
Lansing, MI 48909
(517) 373-0640

UNIVERSITY OF MINNESOTA
Government Pubs. Division
409 Wilson Library
309 19th Avenue South
Minneapolis, MN 55455
(612) 373-7813

UNIV. OF MISSISSIPPI LIB.
Documents Department
University, MS 38677
(601) 232-5857

UNIV. OF MONTANA
Mansfield Library
Documents Division
Missoula, MT 59812
(406) 243-6700

NEBRASKA LIBRARY COMM.
Federal Documents
1420 P Street
Lincoln, NE 68508
(402) 471-2045
In cooperation with University of Nebraska-Lincoln

UNIVERSITY OF NEVADA LIB.
Govt. Pub. Department
Reno, NV 89557
(702) 784-6579

NEWARK PUBLIC LIBRARY
5 Washington Street
Newark, NJ 07101
(201) 733-7812

UNIVERSITY OF NEW MEXICO
Zimmerman Library
Government Pub. Dept.
Albuquerque, NM 87131
(505) 277-5441

NEW MEXICO STATE LIBRARY
Reference Department
325 Don Gaspar Avenue
Santa Fe, NM 87501
(505) 827-2033, ext. 22

NEW YORK STATE LIBRARY
Empire State Plaza
Albany, NY 12230
(518) 474-5563

UNIVERSITY OF NORTH CAROLINA AT CHAPEL HILL
Wilson Library
BA/SS Documents Division
Chapel Hill, NC 27515
(919) 962-1321

UNIVERSITY OF NORTH DAKOTA
Chester Fritz Library
Documents Department
Grand Forks, ND 58202
(701) 777-2617, ext. 27
(In cooperation with North Dakota State Univ. Library)

STATE LIBRARY OF OHIO
Documents Department
65 South Front Street
Columbus, OH 43215
(614) 462-7051

OKLAHOMA DEPT. OF LIB.
Government Documents
200 NE 18th Street
Oklahoma City, OK 73105
(405) 521-2502

OKLAHOMA STATE UNIV. LIB.
Documents Department
Stillwater, OK 74078
(405) 624-6546

PORTLAND STATE UNIV. LIB.
Documents Department
P.O. Box 1151
Portland, OR 97207
(503) 229-3673

STATE LIBRARY OF PENN.
Government Pub. Section
P.O. Box 1601
Harrisburg, PA 17105
(717) 787-3752

TEXAS STATE LIBRARY
Public Services Department
P.O. Box 12927—Cap. Sta.
Austin, TX 78753
(512) 471-2996

TEXAS TECH UNIV. LIBRARY
Govt. Documents Department
Lubbock, TX 79409
(806) 742-2268

UTAH STATE UNIVERSITY
Merrill Library, U.M.C. 30
Logan, UT 84322
(801) 750-2682

UNIVERSITY OF VIRGINIA
Alderman Lib.—Public Doc.
Charlottesville, VA 22901
(804) 924-3133

WASHINGTON STATE LIBRARY
Documents Section
Olympia, WA 98504
(206) 753-4027

WEST VIRGINIA UNIV. LIB.
Documents Department
Morgantown, WV 26506
(304) 293-3640

MILWAUKEE PUBLIC LIBRARY
814 West Wisconsin Avenue
Milwaukee, WI 53233
(414) 278-3000

ST. HIST LIB. OF WISCONSIN
Government Pub. Section
816 State Street
Madison, WI 53706
(608) 262-4347

WYOMING STATE LIBRARY
Supreme Ct. & Library Bld.
Cheyenne, WY 82002
(307) 777-6344

National Aeronautics and
Space Administration
Code NIT - 4
Washington, D.C.
20546
Official Business
Penalty for Private Use, $300

SPECIAL FOURTH CLASS MAIL
Book

Postage and Fees Paid
National Aeronautics and
Space Administration
NASA-451

U.S. MAIL

6 T STAR, 850626 S00606HU
UNIV OF MICHIGAN
ENG TRANSPORATION LIBRARY
ATTN: SERIALS UNIT
312 UNDERGRADUATE LIBRARY BLDG
ANN ARBOR MI 48109

NASA

POSTMASTER: If Undeliverable (Section 158
Postal Manual) Do Not Return